ISSI

Period.

VOL. 640 NOS. 1 + 2 JUNE 25, 1993

COMPLETE IN ONE ISSUE

Int. Ion Chromatography Symp. 1992
Linz, September 21–24, 1992

NAL OF HROMATOGRAPHY

UDING ELECTROPHORESIS AND OTHER SEPARATION METHODS

SYMPOSIUM VOLUMES

JOURNAL OF CHROMATOGRAPHY

INCLUDING ELECTROPHORESIS AND OTHER SEPARATION METHODS

Scope. The *Journal of Chromatography* publishes papers on all aspects of **chromatography, electrophoresis** and related methods. Contributions consist mainly of research papers dealing with chromatographic theory, instrumental developments and their applications. The section *Biomedical Applications*, which is under separate editorship, deals with the following aspects: developments in and applications of chromatographic and electrophoretic techniques related to clinical diagnosis or alterations during medical treatment; screening and profiling of body fluids or tissues related to the analysis of active substances and to metabolic disorders; drug level monitoring and pharmacokinetic studies; clinical toxicology; forensic medicine; veterinary medicine; occupational medicine; results from basic medical research with direct consequences in clinical practice. In *Symposium volumes*, which are under separate editorship, proceedings of symposia on chromatography, electrophoresis and related methods are published.

Submission of Papers. The preferred medium of submission is on disk with accompanying manuscript (see *Electronic manuscripts* in the Instructions to Authors, which can be obtained from the publisher, Elsevier Science Publishers B.V., P.O. Box 330, 1000 AH Amsterdam, Netherlands). Manuscripts (in English; *four* copies are required) should be submitted to: Editorial Office of *Journal of Chromatography*, P.O. Box 681, 1000 AR Amsterdam, Netherlands, Telefax (+31-20) 5862 304, or to: The Editor of *Journal of Chromatography, Biomedical Applications*, P.O. Box 681, 1000 AR Amsterdam, Netherlands. Review articles are invited or proposed in writing to the Editors who welcome suggestions for subjects. An outline of the proposed review should first be forwarded to the Editors for preliminary discussion prior to preparation. Submission of an article is understood to imply that the article is original and unpublished and is not being considered for publication elsewhere. For copyright regulations, see below.

Publication. The *Journal of Chromatography* (incl. *Biomedical Applications*) has 40 volumes in 1993. The subscription prices for 1993 are:

J. Chromatogr. (incl. *Cum. Indexes, Vols. 601–650*) + *Biomed. Appl.* (Vols. 612–651):
Dfl. 8520.00 plus Dfl. 1320.00 (p.p.h.) (total *ca.* US$ 5466.75)

J. Chromatogr. (incl. *Cum. Indexes, Vols. 601–650*) only (Vols. 623–651):
Dfl. 7047.00 plus Dfl. 957.00 (p.p.h.) (total *ca.* US$ 4446.75)

Biomed. Appl. only (Vols. 612–622):
Dfl. 2783.00 plus Dfl. 363.00 (p.p.h.) (total *ca.* US$ 1747.75).

Subscription Orders. The Dutch guilder price is definitive. The US$ price is subject to exchange-rate fluctuations and is given as a guide. Subscriptions are accepted on a prepaid basis only, unless different terms have been previously agreed upon. Subscriptions orders can be entered only by calender year (Jan.–Dec.) and should be sent to Elsevier Science Publishers, Journal Department, P.O. Box 211, 1000 AE Amsterdam, Netherlands, Tel. (+31-20) 5803 642, Telefax (+31-20) 5803 598, or to your usual subscription agent. Postage and handling charges include surface delivery except to the following countries where air delivery via SAL (Surface Air Lift) mail is ensured: Argentina, Australia, Brazil, Canada, China, Hong Kong, India, Israel, Japan*, Malaysia, Mexico, New Zealand, Pakistan, Singapore, South Africa, South Korea, Taiwan, Thailand, USA. *For Japan air delivery (SAL) requires 25% additional charge of the normal postage and handling charge. For all other countries airmail rates are available upon request. Claims for missing issues must be made within six months of our publication (mailing) date, otherwise such claims cannot be honoured free of charge. Back volumes of the *Journal of Chromatography* (Vols. 1–611) are available at Dfl. 230.00 (plus postage). Customers in the USA and Canada wishing information on this and other Elsevier journals, please contact Journal Information Center, Elsevier Science Publishing Co. Inc., 655 Avenue of the Americas, New York, NY 10010, USA, Tel. (+1-212) 633 3750, Telefax (+1-212) 633 3764.

Abstracts/Contents Lists published in Analytical Abstracts, Biochemical Abstracts, Biological Abstracts, Chemical Abstracts, Chemical Titles, Chromatography Abstracts, Current Awareness in Biological Sciences (CABS), Current Contents/Life Sciences, Current Contents/Physical, Chemical & Earth Sciences, Deep-Sea Research/Part B: Oceanographic Literature Review, Excerpta Medica. Index Medicus, Mass Spectrometry Bulletin, PASCAL-CNRS, Referativnyi Zhurnal, Research Alert and Science Citation Index.

US Mailing Notice. *Journal of Chromatography* (ISSN 0021-9673) is published weekly (total 52 issues) by Elsevier Science Publishers (Sara Burgerhartstraat 25, P.O. Box 211, 1000 AE Amsterdam, Netherlands). Annual subscription price in the USA US$ 4446.75 (subject to change), including air speed delivery. Second class postage paid at Jamaica, NY 11431. **USA POSTMASTERS:** Send address changes to *Journal of Chromatography*, Publications Expediting, Inc., 200 Meacham Avenue, Elmont, NY 11003. Airfreight and mailing in the USA by Publication Expediting.

See inside back cover for Publication Schedule, Information for Authors and information on Advertisements.

0021-9673/93/$06.00

This issue is printed on acid-free paper.

Printed in the Netherlands

For Contents, see p. VII

Compared To Other Ion Analysis Techniques, Our New Capillary Ion Analysis System Is Five Times Faster, Delivers Superior Reproducibility, Uses 90% Fewer Chemicals, Requires Substantially Less Maintenance And Literally Pays For Itself In Two Years.[1]

Other Than That, There's Not Much To Say.

For the definitive word on ion analysis by CIA, send for our brochure today.

St. Quentin, France (1) 30127000 Hong Kong (852) 803 9111
Tokyo, Japan 03-3471-7191 Marlborough, MA, USA (508) 624-8400
Vienna, Austria 43/1/8778926

MILLIPORE

Waters Chromatography

[1] Turnet, A., Toy, D., *Using Capillary Electrophoresis to Measure Ions*, PI Quality, 3[1], 22-23.

JOURNAL OF CHROMATOGRAPHY

VOL. 640 (1993)

JOURNAL of CHROMATOGRAPHY

INCLUDING ELECTROPHORESIS AND OTHER SEPARATION METHODS

SYMPOSIUM VOLUMES

ELSEVIER
AMSTERDAM — LONDON — NEW YORK — TOKYO

J. Chromatogr., Vol. 640 (1993)

Linz (1792)

0021-9673/93/$06.00

Printed in the Netherlands

SYMPOSIUM VOLUME

INTERNATIONAL ION CHROMATOGRAPHY SYMPOSIUM 1992

Linz (Austria), September 21–24, 1992

Guest Editor

G. K. BONN

(Linz)

VOL. 640 NOS. 1+2 JOURNAL OF CHROMATOGRAPHY JUNE 25, 1993

CONTENTS

Journal of Chromatography, 640 (1993) 1
Elsevier Science Publishers B.V., Amsterdam

CHROM. 25 149

Foreword

The *International Ion Chromatography Symposium 1992* (IICS'92) was held at the Johannes Kepler University in Linz, Austria, September 21–24, 1992. IICS'92 was attended by over 240 scientists from 24 countries and featured more than 130 technical presentations covering both theoretical and practical applications of ion chromatography (IC) and capillary electrophoresis of small organic and inorganic ions. IICS'92 was the third in this series of symposia and was designed to serve ion chromatographers worldwide by covering a wide variety of topics, including all aspects of the technique.

The symposium opened with an impressive ceremony of music and welcoming speeches from government and university officials. Immediately thereafter, the Ion Chromatography Achievement Award was presented to Joachim Weiss of Dionex Corporation, Idstein, Germany. He opened the technical program with a lecture on "Separation concepts for ion analysis at the turn of the century" which reviewed IC technology of the past 17 years. The remainder of the symposium agenda was organized around the following session topics: Fundamental principles and general applications of IC, Novel instrumentation and phases, Clinical and pharmaceutical applications, Capillary electrophoresis, Applications in the nuclear and power generation industry, Industrial applications, and Environmental applications.

The success of IICS'92 was primarily due to the quality of the technical presentations and to the diverse perspectives and experience provided by the participants. This symposium provided a forum that had not existed since the Sils-Maria meetings organized by the late Professor Roland Frei for European scientists to focus on this important technology. The symposium will rotate between Europe (even years) and North America (odd years).

Thanks are due to the members of the scientific committee (R. M. Cassidy, J. S. Fritz, D. T. Gjerde, P. R. Haddad, P. Jandik, J. D. Lamb, D. J. Pietrzyk, G. Schmuckler, H. Small and J. R. Stillian) and to the members of the organizing committee (W. Buchberger, P. Hajos, K. Hammond, J. Inczedy, F. Marçenac, C. Sarzanini, A. Timerbaev, and J. Weiss) for their valuable contributions to the design of the symposium. Special recognition is also due to my colleague Wolfgang Buchberger and to Janet Strimaitis of Century International for the superb manner in which the meeting was organized, and to Dr. Erich Heftmann of the *Journal of Chromatography* for serving as editor of this proceedings volume. The symposium attendees express special appreciation to the joint corporate sponsors, Dionex Corporation and Waters Chromatography Division of Millipore, for financial support. We look forward to IICS'93 which will be held at the Hyatt Regency Inner Harbor Hotel in Baltimore, MD, USA on September 12–15, 1993 under the chairmanship of Richard M. Cassidy of the University of Saskatchewan.

Linz (Austria)

Günther K. Bonn
Symposium Chairman

Journal of Chromatography, 640 (1993) 3–14
Elsevier Science Publishers B.V., Amsterdam

CHROMSYMP. 2745

Computer-assisted predictions of resolution, peak height and retention time for the separation of inorganic anions by ion chromatography

Q. Xianren*

Department of Analytical Chemistry, Vrije Universiteit Brussel, Pleinlaan 2, 1050 Brussels (Belgium)

X. Chong-Yu

Laboratory of Hydrology, Vrije Universiteit Brussel, Pleinlaan 2, 1050 Brussels (Belgium)

W. Baeyens

Department of Analytical Chemistry, Vrije Universiteit Brussel, Pleinlaan 2, 1050 Brussels (Belgium)

ABSTRACT

A computer-assisted method, designed to determine the combined effects of mobile phase variables, was applied in an experimental study in which both an inorganic anion-exchange chromatographic system and a reversed-phase ion-interaction chromatographic system were tested. A Hamilton PRP-X100 anion-exchange column and a Partisil 10 ODS-3 reversed-phase column were used in these studies. Direct resolution, sensitivity (peak height) and retention time modelling were used to predict the total analysis time and the resolutions and peak heights of some critical peaks in the search area of the mobile phase composition. The relationship between resolution, retention time and peak height and the mobile phase variables was approximated by a quadratic polynomial function. In this work, the results of computer plotting of some three-dimensional response surfaces are presented. These graphical illustrations not only helped us to provide a detailed understanding of the chromatographic processes, but also enabled us to define more precisely the location of the optimum conditions.

INTRODUCTION

Computer optimization procedures, using computer programs to select chromatographic conditions leading to the achievement of a desired separation, have found extensive application in liquid chromatography [1,2]. One of the most successful of these applications is the selection of mobile phase composition for reversed-phase liquid chromatography (RPLC). Despite the success experienced with RPLC the knowledge gained has found only limited application to ion chromatography (IC) for the separation of inorganic anions within both ion exchange [3,4] and reversed phase ion-pair or ion-interaction chromatography [5]. Likely reasons are as follows: (1) The retention mechanism involved in ion-exchange and ion-interaction chromatography is more complex than the binary or ternary solvent mixture system in HPLC. As a consequence, an empirical, mathematical relationship between solute retention and mobile phase composition may be required. (2) Lack of facilities to control optimization with respect to the real analytical importance of individual peaks and/or the time of analysis. The aim of optimization of eluent composition in some particular cases cannot simply be defined as the maximization of the resolution (R_s) of all adjacent solute peaks and consideration of a reasonable analysis

* Corresponding author.

0021-9673/93/$06.00

time. Under this circumstance, the choice of a general quality criterion is fraught with problems, since the requirements are often ambiguous and difficult to express in quantitative terms. (3) Furthermore, attempting to optimize many criteria when dealing with a complex sample often complicates the process. An example was given in a previous optimization problem, where the objective was to achieve a global optimum [5]. This required the maximization of the separation of the pair of peaks NO_2^- and Br^-, which is currently the most difficult to resolve, but simultaneously this optimization also required minimization of the resolution of peaks NO_3^- and SO_4^{2-} in order to reduce the total analysis time, and to increase the detection sensitivity (peak height) as much as possible. Three criteria were thus used in this optimization exercise. Such a typical optimization example occurs in practical chromatographic separation problems and, thus, a method such as the widely used "mixture design statistical technique" (MDST) [6], or a method involving composite criteria such as the overlapping resolution map (ORM) concept [7] or the chromatographic optimization function (COF) [8,9] describing the quality of the chromatogram as a whole, might be difficult to apply here.

Most computer-assisted optimization procedures are based on retention modelling [4,10,11]. The retention model that describes the relationship between retention time (t_R) (or capacity factor) and mobile phase composition allows retention times to be predicted for any mobile phase in the search area. The reliability of these predicted retention times is dependent on the suitability of the retention model used. Mechanistic, semiempirical or fully empirical retention models are frequently used to tackle a specific separation problem [12]. Owing to the complex nature of inter- and intramolecular interactions encountered in retention phenomena, a multidimensional empirical modelling technique based on polynomial regression will be the method of choice. This technique is very adaptable to different retention mechanisms and enables several variables to be handled simultaneously. In addition, it can deal with irregularly spaced variable data. In this paper, we present the computer-assisted results of some experimental studies dealing with both inorganic anion-exchange chromatography and reversed-phase ion-interaction chromatography designed to determine the combined effects of mobile phase variables. A Hamilton PRP-X100 anion-exchange column and a Partisil 10 ODS-3 reversed-phase column were used in these studies. Direct resolution, detectability (peak height) and retention time modelling were used to predict the total analysis time and the resolutions and the peak heights of some critical peaks in the search area of the mobile phase composition. The relationship between resolution, retention time and peak height and the mobile phase variables was approximated by a quadratic polynomial function. The computer plotting of some three-dimensional response surfaces not only helped to provide a detailed understanding of the chromatographic process but also led to a more precise definition of the location of the optimum conditions.

EXPERIMENTAL

Apparatus

A DuPont 870 HPLC pump, a Valco injection valve equipped with a 100-ml loop, a Perkin-Elmer LC-21 conductivity detector and an Ommiscribe B5 217-5 strip chart recorder were used. One 250 × 3.9 mm I.D. PRP-X100 anion-exchange column (Hamilton) with a cartridge guard column and one 250 × 4.6 mm I.D. Partisil 10 ODS-3 RP column (Whatman) with a 60 × 2.1 mm I.D. guard column were used in the experiments.

Reagents

Methanol, chromatographic quality, was obtained from Merck (Germany). Hydroxybenzoic acid (HBA, analytical-reagent grade) was from Aldrich-Chemie (Germany). Tetrabutylammonium iodide (TBAI), potassium hydrogen phthalate (KHP) and other reagents are similar to the description in ref. 5.

All separations were carried out at room temperature, and the separation column, guard column and detector cell were thermally isolated in a wooden box to minimize short-term temperature variations. Each retention time (t_R) and peak height (h) is the mean from two experiments.

Statistical optimization methods

The mobile phase optimization we applied can be considered as a stochastic statistical procedure. The

essential steps of this approach, the choice of the optimization criteria and the choice of the factors have been discussed in a previous publication [5].

In this work an anion-exchange chromatographic mode and a reversed-phase ion-interaction mode were chosen to investigate the effect of mobile phase variables on the chromatographic response (resolution, peak height and/or retention time). Both regular and irregular experimental data were fitted by a statistical model.

Anion-exchange chromatography

The original separation method, recommended by the PRP-X100 column manufacturer, allows the separation of F^-, CO_3^{2-}, Cl^-, NO_2^-, Br^-, NO_3^-, HPO_4^{2-} and SO_4^{2-} using an eluent of 4 m*M* HBA at pH 8.6; it needs about 16 min to complete the total elution with a mobile phase flow-rate of 3 ml/min. The aim of the optimization is to reduce the total elution time with the objective of baseline separation of all the anions mentioned before. By slightly increasing or decreasing the hydroxybenzoic acid (HBA) concentration and the pH value based on the mobile phase composition prescribed by the manufacturer, the aim of optimization might be achieved since we found that the retention of all these anions, and in particular of the last three relatively strongly retained species, NO_3^-, HPO_4^{2-} and SO_4^{2-}, is very sensitive to changes in the HBA concentration and pH. In addition, the peaks of HPO_4^{2-} and NO_3^-, which are the first two peaks, tend to overlap and thus form a critical part of the optimization.

A small amount of organic modifier (methanol) was added to the mobile phase to optimize the retention selectivity of the above-mentioned anions, because we found that the organic modifiers are also very sensitive to the retention behaviour of all these anions. It is known that PRP-X100 is a low-capacity, strong-base anion-exchange phase derived from a macroporous poly(styrene–divinylbenzene) reversed phase, PRP-1. It has retained some of the original reversed-phase characteristics of its parent to function in that mode [16].

A two-factor, three-level factorial design (3^2) was adopted as the optimization strategy. A set of nine experimental points was used to investigate the effect of the pH and methanol content of the mobile phase on the resolution and the total elution time. A second set of eleven experimental points was used to investigate the effect of the HBA concentration and pH on the resolution and the total elution time. These results were used for the construction of the three-dimentional plots of resolution and retention time surfaces. The compositions of the mobile phase that were used in this work are given in Table I.

Ion-interaction chromatography

ODS-3 packing is an octadecyl-bonded reversed phase. It can be applied to separate common inorganic anions when the packing is coated or dynamically coated with a hydrophobic quaternary ammonium salt. The quaternary ammonium salt is commonly presented together with a competing anion (such as phthalate) in the mobile phase. In this case, the ion-interaction reversed-phase chromatographic system has some ion-exchange characteristics. However, the ion-exchange capacity is very low and organic modifiers must not be used to optimize the retention selectivity of inorganic anions. The concentrations of TBAI and KHP and the pH of the mobile phase were selected as the factors that will be used to optimize the selected criteria [14].

Two sets of thirteen and nine experimental points were selected from a series of evolutionary experiments. The first set of thirteen experimental points covered two factors, each at six levels (TBAI concentration, 0.5, 1.0, 2.0, 4.0, 8.0 and 16.0 m*M*; and pH, 4.0, 4.5, 5.0, 5.5, 6.0 and 6.5). The second set of nine experimental points covered two factors at four and five levels (TBAI concentration 2, 4, 6 and 8 m*M*; and KHP concentration 0, 0.5, 1.0, 1.5 and 2.0 m*M*). These experimental points represented almost the whole factor space in which we were interested, but by a limited number of experimental points. Furthermore, most of these selected mobile phase compositions resulted in a reasonable separation of the two critical peak pairs (NO_2^-–Br^- and NO_3^-–SO_4^{2-}), as well as in a measurable peak height. These results were used for the construction of the three-dimensional plots of the resolution and peak-height surface.

For the ion-interaction chromatography, we used two sets of experimental data which existed from "one factor at a time" experiments without any previous factorial design. In addition, (1) a two-factor,

TABLE I

THE RESULTS OF THE COMBINED EFFECT OF TWO FACTORS IN ANION-EXCHANGE CHROMATOGRAPHY ON THE RESOLUTION AND THE RETENTION TIME CALCULATION OF THE OPTIMUM REGRESSION COEFFICIENTS USING EQN. 2

	HBA[a] (mM)	pH[a]	R_s (HPO_4^{2-}–NO_3^-)	t_R(SO_4^{2-})	Methanol[b]	pH[b]	R_s (HPO_4^{2-}–NO_3^-)	t_R(SO_4^{2-})
1	3.0	8.2	11.04	24.0	1.8	7.5	10.95	23.3
2	3.0	8.8	8.07	18.6	2.4	7.5	11.60	22.0
3	3.0	9.4	5.44	14.7	3.0	7.5	10.36	21.9
4	4.0	8.2	9.95	19.5	1.8	8.5	5.46	13.6
5	4.0	8.8	5.71	13.4	2.4	8.5	4.86	12.4
6	4.0	9.4	2.35	9.5	3.0	8.5	3.29	10.8
7	5.0	8.2	5.91	13.5	1.8	9.5	0.56	7.8
8	5.0	8.8	3.60	10.0	2.4	9.5	1.05	8.3
9	5.0	9.4	1.87	8.1	3.0	9.5	1.28	7.6
10	4.0	9.8	1.28	7.2				
11	4.0	7.5	10.36	22.0				
a_0			−12.28	0.25			−3.39	6.39
a_1			6.30	−0.72			−3.53	0.51
a_2			3.07	0.55			1.65	−1.03
a_3			−0.66	0.16			−5.03	−1.50
a_4			−0.17	−0.04			−0.15	0.05
a_5			−0.81	−0.07			0.87	0.04

[a] The mobile phase has a constant methanol content of 3%.
[b] The mobile phase has a constant HBA concentration of 4 mM.

six-level or five-level design would lead to a much too large number of experiments (36 or 25) to be carried out and (2) also, among these experiments, too many useless results (bad separation results) could be expected. The compositions of the mobile phase that were used in this work are given in Table II.

The response function

The mathematical form of the response functions, f, relating the observed response, y (the resolution factors, peak heights and retention time), to the chromatographic variables, x_n, is unknown:

$$y = f(x_n) \quad (1)$$

In order to describe the response surface in the region where the optimum is to be found by means of a graphic plotting method, the response surface was approximated by a generalized polynomial equation of the second order. When the responses are expressed as a function of two independent variables, the polynomial equations can be described by a quadratic equation:

$$y = a_0 + a_1x_1 + a_2x_2 + a_3x_1^2 + a_4x_2^2 + a_5x_1x_2 \quad (2)$$

In the case of the ion-exchange chromatography, $y = \log R_s$ (or $\log t_R$), $x_1 = \log [M]$, M = HBA, x_2 = pH, when the fitting was carried out on eleven experimental data points and $y = \log R_s$ (or t_R), x_1 = log(MeOH%), x_2 = pH, when the fitting was performed on the nine experimental data points. In the case of the ion-interaction chromatography, $y = \log R_s$ (or $\log h$), $x_1 = \log [M]$, M = TBAI, x_2 = pH, when the fitting was carried out on thirteen experimental data points and $y = R_s$ (or h), x_1 = (TBAI), x_2 = (KHP), when the fitting was performed on the nine experimental data points.

The optimization and estimation of the coefficients of the polynomial equation

The optimization procedure deals with the esti-

TABLE II

THE RESULTS OF THE COMBINED EFFECT OF TWO FACTORS IN REVERSED-PHASE ION-INTERACTION CHROMATOGRAPHY ON THE RESOLUTION AND THE PEAK-HEIGHT CALCULATION OF THE OPTIMUM REGRESSION COEFFICIENTS USING EQN. 2

	[TBAI] (mM)	pH	[KHP] (mM)	$R_{s1}(NO_2^-$–$Br^-)$	$R_{s2}(NO_3^-$–$SO_4^{2-})$	$h_1(Cl^-)$ (cm)	$h_2(NO_3^-)$ (cm)	$h_3(SO_4^{2-})$ (cm)
1	0.50	5.00	1	0.60	7.20	7.8	6.2	3.0
2	1.00	5.50		0	5.52	4.3	4.3	11.5
3	1.00	4.00		0	3.1	3.3	3.2	5.2
4	2.00	4.00		0.74	7.87	10.2	8.2	4.5
5	2.00	5.50		1.10	6.41	9.3	7.1	5.9
6	4.00	4.00		0.81	7.23	14.0	5.5	5.4
7	4.00	5.00		1.03	4.98	8.8	8.2	12.5
8	4.00	6.00		1.33	3.57	8.5	4.0	7.5
9	8.00	4.00		0.73	3.34	11.3	6.8	9.0
10	8.00	4.50		1.06	3.19	11.6	11.3	15.2
11	8.00	6.00		1.38	1.52	10.2	11.7	19.4
12	8.00	6.50		1.35	1.25	6.3	8.2	15.8
13	16.00	5.00		1.11	2.10	10.1	14.9	13.2
a_0				−3.75	−1.52	−0.17	−2.30	−1.33
a_1				0.98	1.45	1.25	−0.62	0.24
a_2				1.18	0.87	0.33	1.30	0.75
a_3				0.38	−0.46	−0.14	0.18	−0.08
a_4				−0.11	−0.08	−0.03	−0.14	−0.07
a_5				0.02	−0.28	−0.18	0.16	0.05
1	2.00	6	1.00	1.05	4.79	8.1	5.8	5.6
2	4.00		0	1.25	–	6.5	3.5	–
3	4.00		1.00	1.33	3.57	8.5	4.0	7.5
4	4.00		2.00	1.00	0.97	10.0	3.5	6.0
5	6.00		0.50	1.00	5.11	7.4	3.4	16.1
6	6.00		1.50	1.06	0.77	11.9	5.1	9.7
7	8.00		1.00	1.38	1.52	10.2	11.7	19.4
8	8.00		1.00	1.13	1.60	9.9	5.2	11.0
9	8.00		2.00	1.10	0	11.5	3.3	6.5
a_0				1.25	2.25	4.11	4.99	0.92
a_1				−0.01	0.30	0.72	−1.82	3.23
a_2				−0.55	5.31	3.40	6.53	−0.52
a_3				0	0.02	−0.07	0.30	0
a_4				−0.10	−2.27	−1.28	−1.36	1.46
a_5				0.03	−0.21	−0.31	−0.84	−1.57

mation of the coefficients in the polynomial equation in order to describe as well as possible the responses of a chromatographic experiment. By using the information contained in the optimized equation the analyst can alter the dependent variables in the desired fashion and calculate wherever he wants, respecting the boundaries of the response value.

The polynomial eqn. 2 is an example of an expression describing the chromatographic dependence of the dependent variables (resolution factor, peak height , retention time, etc.) on the independent variables (concentration of the competing ions, percentage of organic modifiers, pH of the mobile phase, etc.). However, the relation between the response y and variables x_1 and x_2 in this model, obviously, is not a causal relation since it is based not on a theoretical (thermodynamic or mechanic)

derivation but on the assumption that the resolution factor of two adjacent peaks or the peak height or retention time of any analyte within a LC system depends not only on each individual mobile phase variable but also on the interactions between these variables. It is clear that the validity and the quality of this model are highly dependent on how well the real but unknown coefficients of the equation can be estimated. In other words, the coefficients of the polynomial equation must be estimated using statistical methods before the optimal mobile phase composition can be calculated in the global optimization process. Since the accuracy of the chromatographic response prediction using this model is highly dependent on the quality of the estimation of the coefficients in eqn. 2, it is thus highly dependent on the algorithms and the computing program chosen. The coefficients in eqn. 2 have been estimated and optimized employing the least-squares approach with a relatively small set of experiments and using a computer program that involves a most important subroutine called VAO5A.

The subroutine VAO5A

Since the key to the global optimization process of the mobile phase composition is to optimize the coefficients of eqn. 2, the subroutine VAO5A was employed in order to obtain the optimum coefficients. The original VAO5A program was obtained from the Harwell Subroutine Library (Hopper, 1978) [15], and it is now running on the CDC-6500 computer of the Vrije Universiteit Brussel — Universite Libre de Bruxelles (V.U.B.–U.L.B.) computer centre. It can be used in cases where minimization of a sum of squares is required. The program is a compromise between three different algorithms for minimizing a sum of squares, namely the Newton–Raphson, the steepest descent and the Marquadt algorithms. It automatically obtains and improves an approximation of the Jacobian J (the first-derivative matrix), following the ideas of Broyden. The VAO5A algorithm is unable to deal with constraints, but a reasonable choice of the parameter DSTEP and of the initial values of the parameters prevents the program from leaving the feasible parameter space region.

The standard output of VAO5A provides only the values of the residuals (functions) and the parameters (a_0, a_1, a_2, a_3, a_4 and a_5 in eqn. 2). In order to provide valuable elements for the statistical evaluation of the coefficients' optimization, the VAO5A program was supplemented with a program called ERROR 11, allowing the computation of the correlation matrix and confidence regions. The Jacobian and Hessian matrices, as well as the 95% confidence limits of the parameters, may also be obtained. Detailed discussions concerning these algorithms and the computer programs can be found in ref. 16.

After the coefficients in eqn. 2 have been estimated, a three-dimensional response surface can be plotted using "Mathematical" software on a Macintosh II computer. The optimum mobile phase composition can then, be either calculated with a small program using BASIC language or visualized graphically using the Macintosh computer.

RESULTS AND DISCUSSION

Based on the experimental results and the discussion reported in a previous publication [5], the simultaneous effects of two factors in the mobile phase on the resolutions of some critical peak pairs, on the retention time of the last peak and on the peak heights were investigated. Table I shows the compositions of the mobile phase with anion-exchange chromatography that have been used in the two-factor, three-level experimental design. Eleven (9 + 2) and nine experimental points were evaluated chromatographically. The duplicated experimental results of the measured retention time of the last peak SO_4^{2-} and the calculated resolution factors, R_s, for the critical peak pair of HPO_4^{2-} and NO_3^- were also reported in Table I for the eleven- and nine-point experiments, respectively. The variables in the eleven point experiments were the HBA concentration and the pH of the mobile phase, but the methanol content was kept constant. The two variables in the case of the nine-point experiments were the percentage of methanol and the pH value, but the HBA concentration in the mobile phase was constant. In order to predict the resolution factors and the retention times of some particular peaks, the visualized three-dimensional response surfaces and the ultimate global chromatographic optimal mobile phase composition, polynomial regressions were performed on the data from Table I according to eqn. 2. The best model was selected: a logarithmic form was used in the case of both [HBA]–pH

TABLE III

COMPARISON BETWEEN THE EXPERIMENTALLY DETERMINED AND THE PREDICTED RESOLUTION, R_s, (NO_3^-–HPO_4^{2-}) AND RETENTION TIME t_R (SO_4^{2-}) VALUES IN ELEVEN- AND NINE-POINT EXPERIMENTAL, RESPECTIVELY

	Resolution prediction (HPO_4^{2-}–NO_3^-)						Retention prediction (SO_4^{2-} peak)					
	[HBA]–pH			MeOH%–pH			[HBA]–pH			MeOH%–pH		
	Exptl.	Pred.	Deviation	Exptl.	Pred.	Deviation	Exptl.	Pred.	Deviation	Exptl.	Pred.	Deviation
1	11.04	11.75	0.71	10.95	12.59	1.64	24.00	24.65	0.65	23.30	23.99	0.58
2	8.07	8.63	0.56	11.60	11.85	0.25	18.60	19.15	0.55	22.00	22.86	0.86
3	5.44	4.78	−0.66	10.36	8.82	−1.54	14.70	13.90	−0.80	21.85	20.52	−1.33
4	9.95	8.61	−1.34	5.46	4.04	−1.42	19.50	17.75	−1.75	13.60	12.59	−1.01
5	5.70	5.50	−0.20	4.86	4.89	0.03	13.40	13.62	0.22	12.35	12.19	−0.16
6	2.35	2.65	0.30	3.29	4.42	1.13	9.50	9.77	0.27	10.08	11.03	0.75
7	5.91	6.55	0.64	0.56	0.66	0.10	13.50	13.87	0.37	7.80	8.22	0.42
8	3.60	3.75	0.15	1.05	1.02	−0.03	10.00	10.54	0.54	8.25	8.05	−0.20
9	1.87	1.62	−0.25	1.28	1.12	−0.16	8.10	7.48	−0.62	7.55	7.35	−0.20
10	1.28	1.39	0.11				7.20	7.54	0.34			
11	10.36	10.16	−0.20				22.10	22.20	0.10			

and % MeOH–pH regression. Table I shows the best non-linear least-squares estimated coefficients of the corresponding polynomial eqn. 2.

Table II contains duplicated results of measured peak heights of Cl^- (h_1), NO_3^- (h_2) and SO_4^{2-} (h_3), and calculated resolution factors (R_s) for two critical peak pairs (NO_2^-–Br^- and NO_3^-–SO_4^{2-}) corresponding to each of the irregular designed experi-

TABLE IV

COMPARISON OF THE PREDICTION QUALITY BETWEEN THE DIFFERENT EXPERIMENTAL STRATEGIES USING THE POLYNOMIAL REGRESSION MODELS

Experimental strategy	Prediction quality (R.S.D., %)						
	Resolution			Peak Height			Retention time Peak of SO_4^{2-} (last)
	R_{s1}[a]	R_{s2}[b]	R_{s3}[c]	Cl^-	NO_3^-	SO_4^{2-}	
Two-factor, three level design (9 + 2 exptl. data)			7.5 (out of 9 data)				4.1 (out of 11 data)
Two-factor, three level design (9 exptl. data)			9.18 (out of 7 data)				4.6 (out of 9 data)
Three-factor central composite design (15 + 6 exptl. data[d])	6.5 (17 data)	7.0 (16 data)		10.7 (15 data)	11.5 (15 data)	13.2 (14 data)	
Irregular exptl. data (13 points)	18.2 (9 data)	14.8 (9 data)		12.0 (9 data)	11.4 (10 data)	18.8 (9 data)	
Irregular exptl. data (9 poins)	9.2 (8 data)	>25 (7 data)		6.4 (8 data)	18.0 (7 data)	12.1 (8 data)	

[a] NO_2^-–Br^-.
[b] NO_3^-–SO_4^{2-}.
[c] HPO_4^{2-}–NO_3^-.
[d] R.S.D. (%) data taken from ref. 5.

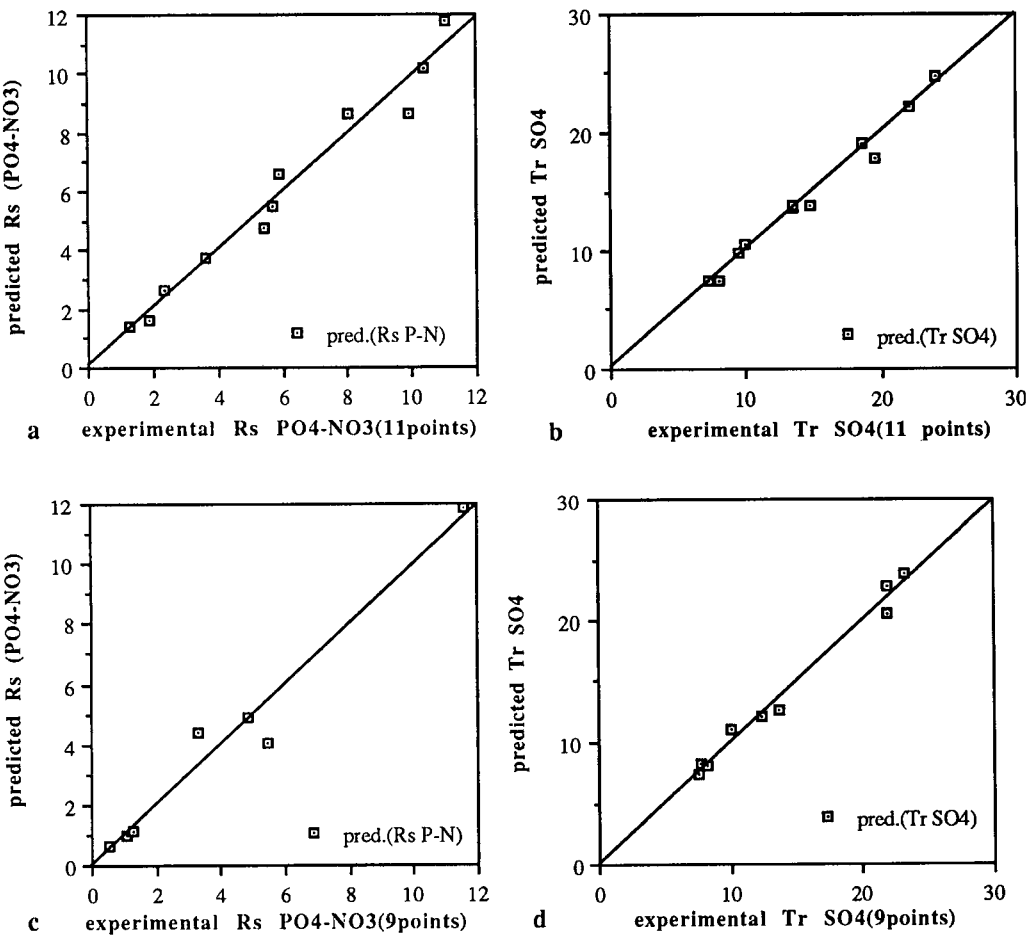

Fig. 1. The actual resolution factors of HPO_4^{2-}–NO_3^- and retention time of SO_4^{2-} obtained from the eleven- and nine-points experiments using the two-factor, three-level design plotted against the predicted resolution factors (a and c) and retention times (b and d). Lines: (a) $y = 8.07 \cdot 10^{-2} + 0.99x$, $R^2 = 0.97$; (b) $y = 0.10 + 0.99x$, $R^2 = 0.98$; (c) $y = 2.03 \cdot 10^{-2} + 0.99x$, $R^2 = 0.96$; (d) $y = 4.66 \cdot 10^{-2} + 1.00x$, $R^2 = 0.99$.

ments for the thirteen combinations of the variables [TBAI] and pH, and for the nine combinations of the variables [TBAI] and [KHP]. In these cases, a reversed-phase ion-interaction chromatographic system was used. Table II also shows the optimal non-linear least-squares estimated coefficients a_0, a_1, ... a_5. A logarithmic form of eqn. 2 in the case of variables [TBAI] and pH (thirteen experimental points) and the normal form of eqn. 2 in the case of variables [TBAI] and [KHP] (nine experimental points) was applied for the polynomial regressions.

Table III shows the resolution (R_s) and retention time (t_R) computer predictions based on the two-factor, three-level experimental design in an ion-exchange chromatographic system. In this table, the computer-predicted resolution R_s (HPO_4^{2-}–NO_3^-) and retention time t_R (SO_4^{2-}) values are compared with the experimentally determined values. In all cases, the deviations between experimental and predicted value are rather small. They vary between 1.9 and 13.5% for the HBA–pH effect on the resolution prediction, between 0.6 and 26% for the % MeOH–pH effect on the resolution prediction, between 0.5 and 9.0% for the HBA–pH effect on the retention time prediction and between 1.3 and 7.4% for the % MeOH–pH effect on the retention time predic-

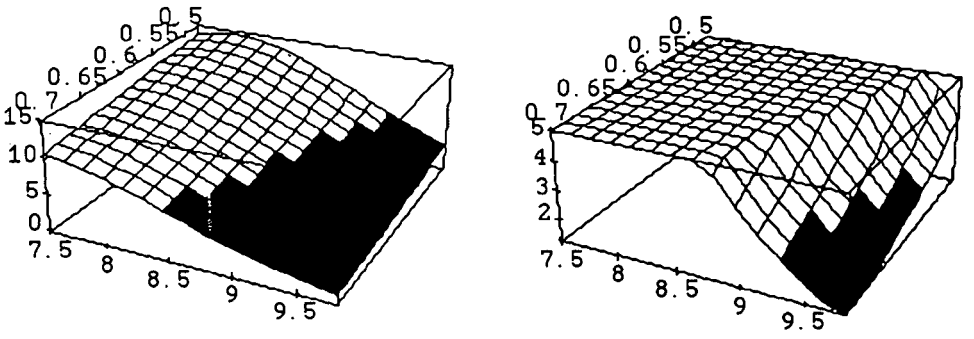

a b

Fig. 2. (a) The resolution factor of the peak pair HPO_4^{2-}–NO_3^- as a function of HBA concentration and pH of the mobile phase with constant methanol content (3%). Separation column: anion-exchange Hamilton PRP-X100. Regression and plotting model: logarithmic form of eqn. 2. (b) Three-dimensional plot of resolution factor surface, R_s (HPO_4^{2-}–NO_3^-) with R_s ranging from 1.2 to 5.0. Other conditions are the same as in (a).

tion. This achievement of computer prediction is also shown in Table IV. Table IV compares the prediction qualities of the results when different experimental strategies are used. In all cases of the two-factor three-level experimental design (nine plus two experimental points and nine experimental points), the average relative standard deviation (R.S.D.) between the computer-predicted and the experimental values is rather low, and the retention time prediction is the best (R.S.D. < 5%).

Fig. 1a–1d shows the plots of the predicted resolution factors and retention times against the actual resolution factors of HPO_4^{2-}–NO_3^- and retention times of SO_4^{2-} based on the factor-designed eleven- and nine-point chromatographic evaluations. Linear correlations were obtained. Slopes of the regression lines are in the range 0.99–1.0. Their intercepts are in the range 0.02–0.1 and the correlation coeffi-

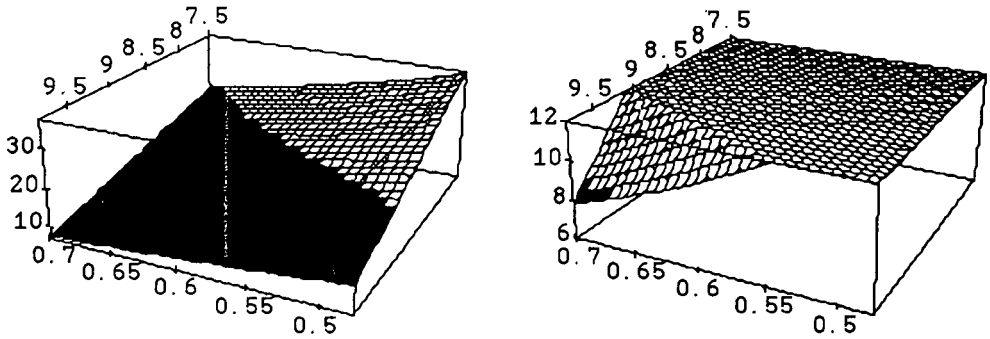

a b

Fig. 3. (a) The retention time of the last peak, SO_4^{2-} as a function of HBA concentration and pH of the mobile phase with constant methanol content (3%). Separation column: anion-exchange Hamilton PRP-X100. Regression and plotting model: logarithmic form of eqn. 2. (b) Three-dimensional plot of retention time (t_R) of SO_4^{2-} with t_R ranging from 6 to 12 (min). Other conditions are the same as in (a).

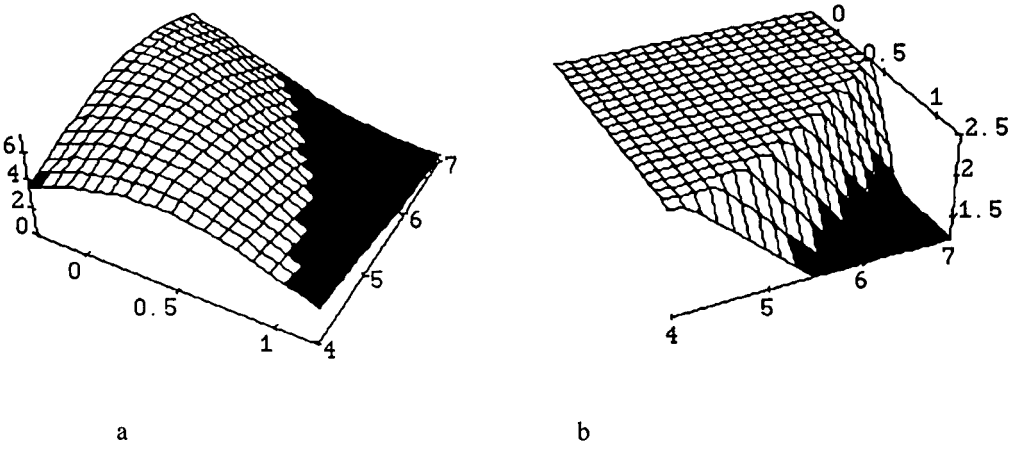

a b

Fig. 4. (a) The resolution surface of the peak pair R_s(NO_3^-–SO_4^{2-}) as a function of TBAI concentration and pH of the mobile phase with constant KHP concentration (1 m*M*). Separation column: Whatman Partisil 10 ODS-3 RP. Regression and plotting model: logarithmic form of eqn. 2. (b) Three-dimensional plot of resolution surface R_s (NO_3^-–SO_4^{2-}) with R_s ranging from 1.2 to 2.5. Other conditions are the same as in (a).

cients are very close to unity.

When an irregular experimental design was used, quite good agreement was obtained between the experimental and the predicted results: for example R_s NO_3^-–SO_4^{2-} and peak heights Cl^- and NO_3^- with TBAI and pH as variables (thirteen experimental points), and R_s NO_2^-–Br^- and peak heights Cl^- and SO_4^{2-} with TBAI and KHP as variables (nine experimental points). However, in the remaining cases using irregular experimental design, the differences between experimental results and predicted data were much larger. The reasons for the uncertainty of the predictions are (1) the experimental sets we used were not organized in a proper factorial design and (2) the number of experimental points used was too small to obtain a good least-squares estimation of the coefficients corresponding to eqn. 2. There are several advantages of organizing the experiments in a factorial design [17]: (i) When there are no interactions the factorial design

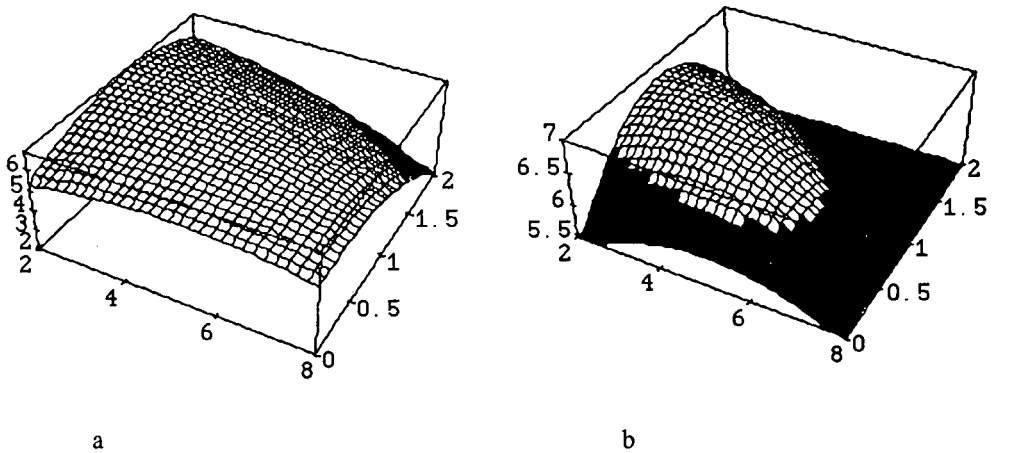

a b

Fig. 5. (a) The peak height of Cl^- as a function of TBAI and KHP concentrations in the mobile phase with constant pH (5). Separation column: Whatman Partisil 10 ODS-3 RP. Regression and plotting model: normal form of eqn. 2. (b) Three-dimensional plot of peak height surface h (Cl^-) with h range from 5.5 to 7.0 (cm). Other conditions are the same as in (a).

gives the maximum efficiency in the estimation of the effects. (ii) When interactions exist, and their nature is unknown, a factorial design is necessary to avoid misleading conclusions. (iii) In the factorial design the effect of a factor is estimated at several levels of the other factors, and the conclusions hold over a wide range of conditions.

Figs. 2a–5a show some typical computer predicted chromatographic response surfaces. In these figures, the estimated resolution factors, retention times and peak heights as a function of HBA concentration and pH, methanol content and pH, TBAI concentration and pH and/or TBAI and KHP concentrations are shown. With the use of these visualized three-dimensioned plots, it is possible to determine the optimum mobile phase conditions by restricting the optimization criteria within a required range. After rearranging R_s, t_R and/or h, Figs. 2b–5b show the relevant chromatographic response surfaces and acceptable mobile phase conditions that can be used in the practice.

Obviously, the simultaneous effects of mobile phase variables on the separation and detection of inorganic anions are not as simple as in the case of single-factor effects. This is because both the resolution factor (R_s) and the peak height (h) are not direct functions (or could at least be very complex functions) of the mobile phase variables and, in particular, the interactions between factors can play an important role, as we can see from these figures. Information obtained from these response surfaces may not be easy to obtain with the normally used "one factor at a time" method. Developing a multifactor and simultaneous method for estimating the interactions of the variables in the mobile phase, leading to the optimization of the mobile phase composition, is certainly necessary. In this work, some of the experimental sets we used were not organized in a proper factorial design, which diminishes the quality of the computer predictions and reduces the possibility of finding the optimal conditions for the eluent to achieve the selected criteria: maximum (or minimum) separation of critical peak pairs, reduction in total analysis time, maximum peak heights for the various components, etc. However, the present approach is valuable not only in terms of the visualization of the response surface as a function of two variables using a very limited number of experiments, but also in terms of the methodology, which provides a simple, straightforward way to achieve multifactor mobile phase optimization for the prediction of resolution factor and the prediction of the peak height (or peak area) in a complex inorganic ion separation problem in which both ion-exchange and ion-interaction chromatographic systems were employed.

With the optimization procedure described in this paper, we obtained, in the case of ion-exchange chromatography, baseline separation for eight anions (F^-, CO_3^{2-}, Cl^-, NO_2^-, Br^-, NO_3^-, HPO_4^{2-}, SO_4^{2-}) with a total elution time of less than 10 min (Fig. 6). The mobile phase composition for HBA is

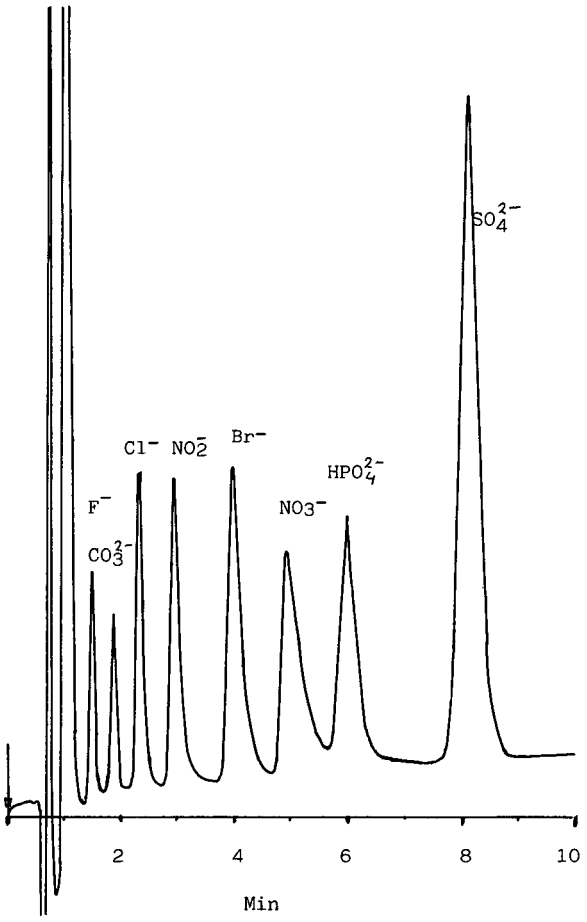

Fig. 6. Separation of eight anions —fluoride, carbonate, chloride, nitrite, bromide, nitrate, phosphate and sulphate— at 3 ml/min and 5 m*M* *p*-hydroxybenzoic acid, 3% methanol, pH 9.5, on a 250 × 3.9 mm I.D. PRP-X100 column. Conductivity detection was used.

5 m*M* and pH is 9.5–9.8 with addition of 3% methanol. In the case of ion-interaction chromatography baseline separation was obtained for five anions (Cl^-, NO_2^-, Br^-, NO_3^-, SO_4^{2-}) with a total elution time of less than 9 min. The mobile phase composition for TBAI is 8–8.5 m*M*, for KHP is 1 m*M*, pH of 6–6.5.

REFERENCES

1 G. D'Agostino and L. Castagnetta, *J. Chromatogr.*, 338 (1985) 1–23.
2 J. L. Glajch and J.J. Kirkland, *J. Chromatogr.*, 485 (1989) 51–63.
3 P.R. Haddad and C. E. Cowie, *J. Chromatogr.*, 303 (1984) 321–330.
4 P.R. Haddad and A. D. Sosimenko, *J. Chromatogr. Sci.*, 27 (1989) 456–461.
5 Q. Xianren, W. Baeyens and Y. Michotte, *J. Chromatogr.*, 467 (1989) 15–30.
6 J. L. Glajch and J.J. Kirkland and J. M. Minor, *J. Liq. Chromatogr.*, 10 (1987) 1727–1747.
7 S. N. Deming and L. R. Parker, *Anal. Chem.*, 7 (1978) 187–202.
8 J. L. Glajch and J.J. Kirkland, K. M. Squire and J. M. Minor, *J. Chromatogr.*, 199 (1980) 57–79.
9 M. W. Watson and P. W. Carr, *Anal Chem.*, 51 (1979) 1835–1842.
10 Y. Baba, N. Yoza and S. Ohashi, *J. Chromatogr.*, 350 (1985) 461–467.
11 S. N. Deming, J. M. Palasota, J. Lee and Lifang Sun, *J. Chromatogr.*, 485 (1989) 15–25.
12 W. Lindberg, E. Johansson and K. Johansson, *J. Chromatogr.*, 211 (1981) 201–212.
13 D. Peter Lee, *J. Chromatogr. Sci.*, 22 (1984) 327–331.
14 Q. Xianren and W. Baeyens, *J. Chromatogr.*, 456 (1988) 267–285.
15 M. J. Hopper, *A Catalogue of Subroutines, Harwell Subroutine Library*, UK Atomic Energy Authority, Harwell, 1978, p. 69.
16 Vandewiele G.L., *Decision Analysis in Water Management*, Vrije Universiteit Brussels, Brussels, 1986.
17 O.L. Davies, *The Design and Analysis of Industrial Experiments*, Oliver & Boyd, London, 1967 pp. 253 and 534.

Journal of Chromatography, 640 (1993) 15–25
Elsevier Science Publishers B.V., Amsterdam

CHROMSYMP. 2730

Retention model for the separation of anionic metal–EDTA complexes in ion chromatography

Peter Hajos* and Gabriella Revesz

Department of Analytical Chemistry, University of Veszprem, P.O. Box 158, 8201 Veszprem (Hungary)

Corrado Sarzanini, Giovanni Sacchero and Edoardo Mentasti

Department of Analytical Chemistry, University of Turin, Via P. Giuria 5, Turin (Italy)

ABSTRACT

A retention model is derived for complex anions eluted from an anion-exchange column with multiple ionic eluents containing hydrogencarbonate, carbonate, and hydroxyl species and the sample solution, containing transition metals, anions and complexing ligand. The theory is based on the generalized ion-exchange equilibrium, protonation and complex-formation equilibria. The unknown parameters of chromatographic ion-exchange equilibrium constants for sample and eluent species are determined from the experimental retention data by iterative minimization, using a non-linear regression algorithm. The model was utilized to predict the retention behaviour of $CdEDTA^{2-}$, $CoEDTA^{2-}$, $MnEDTA^{2-}$ and $NiEDTA^{2-}$ ions. The capacity factors of complex ions were determined for wide ranges of pH values and eluent concentrations. Good agreement was obtained between the observed and predicted retentions.

INTRODUCTION

Complexing eluents have been used to improve the selectivity of the chromatographic separation of metal ions [1]. When a basic solution contains an excess of a strong complexing anion of high charge such as ethylenediaminetetraacetate (EDTA) ion, most metal ions will occur as anionic complexes. The metal–EDTA complexes ($MEDTA^{2-}$, $MHEDTA^{-}$) are anions and can be separated by anion exchange. Hence this method provides simultaneous metal and anion separation [2–4].

Multidentate chelating ligands can form strong complexes with alkaline earth metal, transition metal and lanthanide ions and have an important role in ion chromatography. The chromatographic separation will depend on the charge of the complexes, the stability of the complexes, the ion-exchange behaviour on the ion exchanger [5] and the eluent type and concentration.

The problem of the prediction of retention and the optimization of eluent composition can be solved on the basis of valid models of retention [6,7]. If the eluent contains only a single competing anion, a relatively straightforward model can be derived [1,8–10]. A system that contains several ionic species, such as CO_3^{2-}, HCO_3^{-} and OH^{-} in the eluent and different complex forms of analytes in the sample is very complicated. This is probably due to its theoretical complexity and the lack of a commonly accepted model of simultaneous equilibria. At the eluent pHs used, three eluent species will be present and simultaneous ion-exchange equilibria will take place. In order to have a reliable retention model all the eluent species in the system must be considered.

The aim of this work was to develop a theoretical model for the retention of complex anions. Until some definitive study of retention behaviour has

* Corresponding author. Present address: Department of Chemistry, Swiss Federal Institute of Technology, 1015 Lausanne, Switzerland.

0021-9673/93/$06.00

been made, much of the chromatography of metal complexes and other difficult ionic separations will remain unpredictable. In this paper we provide a detailed description and evaluation of a new model as a predictive tool for retention. This will be a rigorous method that takes into consideration all of the relevant equilibria.

THEORY

Understanding the chromatographic behaviour in this system requires a modelling of interplay between ion-exchange and complexation reactions. We shall consider the equilibrium distribution and chromatography of Cd^{2+}, Co^{2+}, Mn^{2+} and Ni^{2+} on anion exchangers with EDTA ions as the complexing ligand using a carbonate eluent for separation.

Ion-exchange equilibria and complexation of sample ions

The ion-exchange equilibrium for binding of a solute anion A^{y-} to a stationary phase that has been conditioned with an eluent containing a competing anion E^{x-} is given by

$$y\,R_x\text{–}E + x\,A^{y-} \overset{K_{A/E}}{\rightleftharpoons} x\,R_y\text{–}A + y\,E^{x-} \quad (1)$$

where R represents the stationary phase. The equilibrium constant for this reaction is given by [1]

$$K_{A/E} = \frac{(A^{y-})^x\,[E^{x-}]^y}{[A^{y-}]^x\,(E^{x-})^y} \quad (2)$$

where the parentheses and square brackets refer to molar concentrations in the stationary and the mobile phase, respectively. In ion chromatography, activity effects could be ignored because of the low concentrations of the sample and the eluent that are used. The volumetric distribution coefficient of A^{y-} can be obtained from eqn. 2

$$D_A = \frac{(A^{y-})}{[A^{y-}]} = K_{A/E}^{1/x}\left(\frac{(E^{x-})}{[E^{x-}]}\right)^{y/x} \quad (3)$$

We can assume that the eluent ion, E^{x-}, occupies x ion-exchange sites on the stationary phase. The molar concentration of solid phase can be defined through the ion-exchange capacity, Q, of the column, $(E^{x-}) = Q/x$, and eqn. 3 can be rewritten as

$$D_A = K_{A/E}^{1/x}\left(\frac{Q}{x}\right)^{y/x}[E^{x-}]^{-y/x} \quad (4)$$

The logarithmic form provides the relationship

$$\log D_A = \frac{1}{x}\log K_{A/E} + \frac{y}{x}\log\left(\frac{Q}{x}\right) - \frac{y}{x}\log[E^{x-}] \quad (5)$$

In the formation of anionic metal complexes with EDTA ligand, pH-dependent side-reactions occur. Multivalent metal ions tend to form protonated complexes, basic complexes and other mixed-ligand complexes. In the pH range of interest the forms of complex anions of the metals examined are $CdEDTA^{2-}$, $CdHEDTA^{-}$, $Cd(OH)_3^-$, $Cd(OH)_4^{2-}$, $CoEDTA^{2-}$, $CoHEDTA^{-}$, $Co(OH)_3^-$, $MnEDTA^{2-}$, $MnHEDTA^{-}$, $NiEDTA^{2-}$ and $NiHEDTA^{-}$

The anion-exchange processes for metal–EDTA complexes underlying the separation are given by the following equilibria

$$2\,R\text{–}E + MEDTA^{2-} \overset{K_{MEDTA/E}}{\rightleftharpoons} R_2\text{–}MEDTA + 2\,E^{-} \quad (6)$$

$$R\text{–}E + MHEDTA^{-} \overset{K_{MHEDTA/E}}{\rightleftharpoons} R\text{–}MHEDTA + E^{-} \quad (7)$$

The ion-exchange equilibrium constants of sample ions can be written as

$$K_{MEDTA/E} = \frac{(MEDTA^{2-})\,[E]^2}{[MEDTA^{2-}]\,(E)^2} \quad (8)$$

$$K_{MHEDTA/E} = \frac{(MHEDTA^{-})\,[E]}{[MHEDTA^{-}]\,(E)} \quad (9)$$

Eqns. 8 and 9 can be rearranged to obtain the concentrations of $MEDTA^{2-}$ and $MHEDTA^{-}$ in the stationary phase

$$(MEDTA^{2-}) = K_{MEDTA/E}\cdot\frac{[MEDTA^{2-}]\,(E)^2}{[E]^2} \quad (10)$$

$$(MHEDTA^{-}) = K_{MHEDTA/E}\cdot\frac{[MHEDTA^{-}]\,(E)}{[E]} \quad (11)$$

In this case the volumetric distribution coefficient is expressed as follows

$$D_M = \frac{(MEDTA^{2-}) + (MHEDTA^{-})}{[M^{2+}] + [MHEDTA^{-}] + [MEDTA^{2-}] + \sum_{i=1}^{n} [M(OH)_i^{2-i}]} \quad (1$$

In the numerator there are the M species bound to the stationary phase and in the denominator all the species present in the mobile phase. Substitution of eqns. 10 and 11 in eqn. 12 gives

$$D_M = \frac{K_{MEDTA/E} \cdot \frac{[MEDTA^{2-}]\,(E)^2}{[E]^2} + K_{MHEDTA/E} \cdot \frac{[MHEDTA^{-}]\,(E)}{[E]}}{[M^{2+}] + [MHEDTA^{-}] + [MEDTA^{2-}] + \sum_{i=1}^{n} [M(OH)_i^{2-i}]} \quad (1$$

We can define Φ as the molar fraction of the total concentration of metal–anion complex in the eluent. Then eqn. 13 can be rewritten as

$$D_M = \frac{K_{MEDTA/E}\,(E)^2}{[E]^2} \cdot \Phi_{MEDTA} + \frac{K_{MHEDTA/E}\,(E)}{[E]} \cdot \Phi_{MHEDTA} \quad (14)$$

Ion-exchange equilibria of eluent ions

The carbonate eluent contains three competing anions, CO_3^{2-}, HCO_3^- and OH^-. The molar concentrations of these species can be calculated from the two protonation constants of carbonate at the pH of the mobile phase. In the presence of eluent species simultaneous ion-exchange equilibria take place. The ion-exchange capacity of the separator column is given by

$$Q = 2\,(CO_3^{2-}) + (HCO_3^-) + (OH^-) \quad (15)$$

Taking into account ion-exchange equilibria for the eluent species

$$CO_3^{2-} + 2\,R\text{–}HCO_3 \overset{K_{CO_3/HCO_3}}{\rightleftharpoons} R_2\text{–}CO_3 + 2\,HCO_3^- \quad (16)$$

$$OH^- + R\text{–}HCO_3 \overset{K_{OH/HCO_3}}{\rightleftharpoons} R\text{–}OH + HCO_3^- \quad (17)$$

The inter-eluent ion-exchange equilibrium constants are

$$K_{CO_3/HCO_3} = \frac{(CO_3^{2-})\,[HCO_3^-]^2}{[CO_3^{2-}]\,(HCO_3^-)^2} \quad (18)$$

and

$$K_{OH/HCO_3} = \frac{(OH^-)\,[HCO_3^-]}{[OH^-]\,(HCO_3^-)} \quad (19)$$

From eqns. 18 and 19, we can write

$$(CO_3^{2-}) = K_{CO_3/HCO_3}\,[CO_3^{2-}] \cdot \frac{(HCO_3^-)^2}{[HCO_3^-]^2} \quad (2$$

and

$$(OH^-) = K_{OH/HCO_3}\,[OH^-] \cdot \frac{(HCO_3^-)}{[HCO_3^-]} \quad (2$$

The concentrations of CO_3^{2-} and OH^- on the stationary phase are now expressed in terms of (HCO_3^-) through the corresponding equilibrium constants, eqns. 18 and 19. By combination of eqns. 15, 20 and 21, the following quadratic equation is obtained

$$Q = \frac{2\,K_{CO_3/HCO_3}\,[CO_3^{2-}]}{[HCO_3^-]^2} \cdot (HCO_3^-)^2 + \left(1 + \frac{K_{OH/HCO_3}\,[OH^-]}{[HCO_3^-]}\right)(HCO_3^-) \quad (2$$

Solution of eqn. 22 gives

$$(HCO_3^-) = \frac{\sqrt{b^2 + 4aQ} - b}{2a} \quad (2$$

where

$$a = \frac{2\,K_{CO_3/HCO_3}\,[CO_3^{2-}]}{[HCO_3^-]^2}$$

and

$$b = 1 + \frac{K_{OH/HCO_3}\,[OH^-]}{[HCO_3^-]}$$

and the value of (HCO_3^-) can be substituted in eqn. 14

$$D_M = \frac{K_{MEDTA/HCO_3^-}(\sqrt{b^2+4aQ}-b)^2}{4a^2[HCO_3^-]^2}\cdot\Phi_{MEDTA} + \frac{K_{MHEDTA/HCO_3^-}(\sqrt{b^2+4aQ}-b)}{2a[HCO_3^-]}\cdot\Phi_{MHEDTA} \quad (24)$$

Calculation of molar fractions of complex anions (Φ)

We now have to determine the ratio of the concentration of the effective complex formed by metal ions, which take part in ion-exchange equilibrium, and the total metal ion concentration. They are considered in terms of the above-mentioned Φ function. The value of Φ depends on the molar concentrations of ions that are present in the solution and react with the metal ions. The values of Φ can be calculated as follows

$$\Phi_{MEDTA} = \frac{K_{MEDTA}[EDTA]}{1 + K_{MEDTA}[EDTA] + K_{MHEDTA}K_{EDTA(H)_1}[H][EDTA] + \sum_{i=1}^{n}\gamma_i[OH]^i} \quad (25)$$

and

$$\Phi_{MHEDTA} = \frac{K_{MHEDTA}K_{EDTA(H)_1}[H][EDTA]}{1 + K_{MEDTA}[EDTA] + K_{MHEDTA}K_{EDTA(H)_1}[H][EDTA] + \sum_{i=1}^{n}\gamma_i[OH]^i} \quad (26)$$

where K_{MEDTA} and K_{MHEDTA} are the stability constants of metal–anion complexes, $K_{EDTA(H)_1}$ is the first protonation constant of EDTA, [EDTA] is the concentration of the free form of EDTA and γ is the complex formation constant of metal–hydroxo complexes.

The concentration of the free form of EDTA can be obtained by the following equation for the average number of ligand units per metal

$$\bar{n} = \frac{C_{EDTA} - [EDTA]\alpha_{EDTA(H)}}{C_M} = \frac{K_{MEDTA}[EDTA] + K_{MHEDTA}K_{EDTA(H)_1}[H][EDTA]}{1 + K_{MEDTA}[EDTA] + K_{MHEDTA}K_{EDTA(H)_1}[H][EDTA] + \sum_{i=1}^{n}\gamma_i[OH]^i} = \Phi_{MEDTA} + \Phi_{MHEDTA} \quad (27)$$

where C_{EDTA} is the total concentration of EDTA in the sample and

$$\alpha_{EDTA(H)} = 1 + [H^+]K_{EDTA(H)_1} + [H^+]^2K_{EDTA(H)_1}K_{EDTA(H)_2} + [H^+]^3K_{EDTA(H)_1}K_{EDTA(H)_2}K_{EDTA(H)_3} + [H^+]^4K_{EDTA(H)_1}K_{EDTA(H)_2}K_{EDTA(H)_3}K_{EDTA(H)_4}$$

The numerator in eqn. 27 gives the concentration of EDTA in MEDTA complexes and the denominator gives the total metal concentration. Eqn. 27 is a quadratic equation in [EDTA].

By solution of eqn. 27 one can obtain the concentration of the free ionic species of EDTA in the following form (where $n_{OH^-} = 1$)

$$[EDTA] = \frac{-e + \sqrt{e^2 - 4df}}{2d} \quad (28)$$

where

$$d = K_{MEDTA}\alpha_{EDTA(H)} + K_{MHEDTA}K_{EDTA(H_1)}[H]\alpha_{EDTA(H)}$$

$$e = C_M K_{MHEDTA}K_{EDTA(H_1)}[H] + C_M K_{MEDTA} + \gamma_1[OH]\alpha_{EDTA(H_1)} + \alpha_{EDTA(H)} - C_{EDTA}K_{MEDTA} - C_{EDTA}K_{MHEDTA}K_{EDTA(H_1)}[H]$$

$$f = -C_{EDTA} - \gamma_1[OH]C_{EDTA}$$

We now can substitute the values of Φ into eqn. 24 to obtain one of the final forms of the model

$$D_M = ml + pq \tag{29}$$

where

$$m = \frac{K_{MEDTA/HCO_3}(\sqrt{b^2+4aQ}-b)^2}{4a^2[HCO_3^-]^2}$$

$$l = \frac{K_{MEDTA}\cdot\frac{-e+\sqrt{e^2-4df}}{2d}}{1+K_{MEDTA}\cdot\frac{-e+\sqrt{e^2-4df}}{2d}+K_{MHEDTA}K_{EDTA(H)_1}[H]\cdot\frac{-e+\sqrt{e^2-4df}}{2d}+\gamma_1[OH]}$$

$$p = \frac{K_{MHEDTA/HCO_3}(\sqrt{b^2+4aQ}-b)}{2a[HCO_3^-]}$$

$$q = \frac{K_{MEDTA}K_{EDTA[H]_1}[H]\cdot\frac{-e+\sqrt{e^2-4df}}{2d}}{1+K_{MEDTA}\cdot\frac{-e+\sqrt{e^2-4df}}{2d}+K_{MHEDTA}K_{EDTA(H)_1}[H]\cdot\frac{-e+\sqrt{e^2-4df}}{2d}+\gamma_1[OH]}$$

Ion-exchange equilibria of metal–hydroxo complexes

For Co and Cd, hydroxo species must also be considered. Taking into account the anion-exchange equilibrium

$$R\text{–}HCO_3 + M(OH)_3^- \overset{K_{M(OH)_3/HCO_3}}{\rightleftharpoons} R\text{–}M(OH)_3 + HCO_3^- \tag{30}$$

following the same derivation as above, eqn. 24 becomes

$$D_M = \frac{K_{MEDTA/HCO_3}(\sqrt{b^2+4aQ}-b)^2}{4a^2[HCO_3^-]^2}\cdot\Phi_{MEDTA} + \frac{K_{MHEDTA/HCO_3}\sqrt{b^2+4aQ}-b}{2a[HCO_3^-]}\cdot\Phi_{MHEDTA} + \frac{K_{M(OH)_3/HCO_3}\sqrt{b^2+4aQ}-b}{2a[HCO_3^-]}\cdot\Phi_{M(OH)_3^-} \tag{31}$$

where

$$\Phi_{M(OH)_3^-} = \frac{\gamma_3[OH]^3}{1+K_{MEDTA}[EDTA]+K_{MHEDTA}K_{EDTA(H)_1}[H][EDTA]+\sum_{i=1}^{3}\gamma_i[OH]^i} \tag{32}$$

For Co there are four hydroxo ligands and a similar derivation can be obtained.

In general, the volume distribution coefficient for solute M is designated as D_M and is related to the capacity factor k'_M by the expression

$$D_M = \frac{V_0 k'_M}{V_{stat}} \tag{33}$$

where V_0, the void volume of the column, and V_{stat}, the volume of stationary phase, are known or easily evaluated.

EXPERIMENTAL

Reagents and solutions

The anion eluents ($NaHCO_3$, Na_2CO_3 and NaOH mixtures) were prepared by dissolving analytical-reagent grade salts (Merck, Darmstadt, Germany) in high-purity water obtained using a Milli-Q system (Millipore, Bedford, MA, USA) filtered through a 0.45-μm filter. Standard solutions of metal ions, namely Co(II), Ni(II), Cd(II), Mn(II), were prepared by dilution of concentrated stock solutions (Merck). Standard solutions of fluoride, chloride, nitrate and sulphate anions were prepared by dissolution of analytical-reagent grade salts (Fluka, Buchs, Switzerland) and the chelating agent EDTA (Carlo Erba, Milan, Italy).

Unless stated otherwise, all samples (injection volume 100 μl) were $5.0 \cdot 10^{-5}$ *M* in metal ion and $1.5 \cdot 10^{-4}$ *M* in EDTA; the sample pH was adjusted to the appropriate value using NaOH.

Instrumentation

A Dionex Series 4000i ion chromatograph was used with a conductivity detector equipped with an AMMS1 anion suppressor (Dionex, Synnyvale, CA, USA). The chromatograms were recorded with an SP 4270 data module integrator (Carlo Erba).

The separation column (Dionex AS9, 250 × 4 mm) was based on a 15-μm polystyrene–divinylbenzene substrate agglomerated with anion-exchange latex that had been completely aminated. The latex has a polyacrylate backbone and carries the actual ion-exchange sites. Ion-exchange capacity was determined empirically (26 μequiv. per column). All chromatograms were obtained at room temperature. The flow-rate was 2.0 ml/min. Retention times were the means of triplicate injections of single samples.

RESULTS AND DISCUSSION

The retention behaviour of the four analytes considered (NiEDTA, MnEDTA, CoEDTA and CdEDTA) was evaluated for different pH values and various eluent concentrations of the investigated system as shown in Table I. Figs. 1 and 2 show typical chromatograms obtained with different eluent compositions. Modelling of retention requires, as described above, evaluation of the analyte–eluent

TABLE I

CONCENTRATIONS OF ELUENT SPECIES (CO_3^{2-} + HCO_3^-)

C_{eluent} (m*M*)	pH	$C_{CO_3^{2-}}$ (10^{-2} m*M*)	$C_{HCO_3^-}$ (10^{-2} m*M*)	C_{OH^-} (10^{-2} m*M*)
2.0	9.10	18.2	181.6	1.26
2.0	9.57	45.6	154.4	3.71
2.0	9.92	79.6	120.4	8.32
2.0	10.35	128.0	72.0	22.39
2.0	11.07	180.6	19.3	117.5
2.5	9.93	100.1	149.1	8.51
3.0	9.63	75.9	224.0	4.26
3.0	10.30	183.9	116.0	20.00
3.0	10.80	250.1	49.9	63.10
3.5	9.40	58.2	291.6	2.51
5.0	9.80	166.9	333.0	6.31
5.0	10.76	410.2	89.7	57.54
7.0	9.40	116.4	583.2	2.51
7.0	9.87	259.4	440.5	7.41
7.0	10.25	409.8	290.2	17.78
7.0	10.60	531.8	168.2	39.81
7.0	11.10	636.4	63.6	125.9

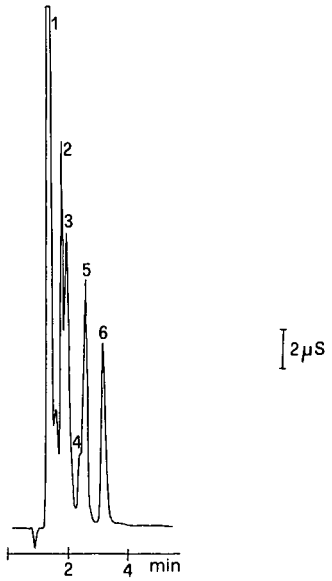

Fig. 1. Chromatogram of (1) Cl^-, (2) Mn–EDTA, (3) Cd–EDTA, (4) Al–EDTA, (5) Ni–EDTA and (6) Co–EDTA. Chromatographic conditions: $C_{eluent} = 2.0$ m*M*; pH = 11.07; sample (100 μl), 1.0 m*M* EDTA; detection, conductivity.

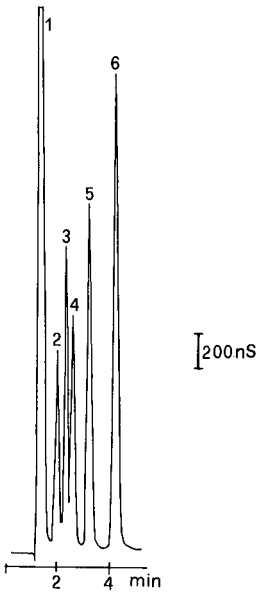

Fig. 2. Chromatogram of (1) Cl^-, (2) Cd–EDTA, (3) NO_3^-, (4) Al–EDTA, (5) Co–EDTA and (6) SO_4^{2-}. Chromatographic conditions: $C_{eluent} = 3.0$ mM; pH = 10.80; sample (100 μl), 1.0 mM EDTA; detection, conductivity.

and inter-eluent ion-exchange equilibrium constants. These unknown parameters, K_{MEDTA/HCO_3}, K_{MHEDTA/HCO_3}, K_{CO_3/HCO_3}, K_{OH/HCO_3} and $K_{M(OH)_n/HCO_3}$, can be determined from the experimental retention data by iterative minimization using a non-linear regression algorithm. In particular, a Nelder and Mead simplex algorithm, which compares observed and predicted retentions for different concentrations and pH, was successfully used.

The chemical equilibrium constants used for these calculations were taken from the literature [5,11]. Calculated values of the ion-exchange equilibrium constants, from experimental data, for complex forms of metal ions and for eluent species are given in Tables II–V. It can be seen that the values of the ion-exchange equilibrium constants obtained are reliable and independent of the experimental conditions. It is noteworthy that these constants are sufficient to determine the position of the simultaneous ion-exchange processes.

A comparison of predicted and observed retention volume is given in Tables VI–IX and Fig. 3

TABLE II

CHROMATOGRAPHIC ION-EXCHANGE EQUILIBRIUM CONSTANTS FOR COMPLEX FORMS OF Co IONS AND FOR ELUENT SPECIES CALCULATED FROM EXPERIMENTAL DATA

Ion-exchange constant	Eluent concentration ($CO_3^{2-} + HCO_3^-$) (mM)						Mean ± S.D.
	2.0	2.5	3.0	3.5	5.0	7.0	
$K_{CoHEDTA/HCO_3}$	1.000	0.967	0.936	0.962	1.000	0.988	0.98 ± 0.04
K_{CoEDTA/HCO_3}	8.250	8.567	8.114	8.500	8.502	8.500	8.41 ± 0.30
K_{OH/HCO_3}	10.612	10.713	10.821	10.716	10.611	10.705	10.70 ± 0.13
K_{CO_3/HCO_3}	13.498	13.723	13.997	13.761	13.986	13.000	13.66 ± 0.61
$K_{Co(OH)_3/HCO_3}$	9.888	9.703	9.999	9.764	9.894	9.745	9.83 ± 0.20

TABLE III

CHROMATOGRAPHIC ION-EXCHANGE EQUILIBRIUM CONSTANTS FOR COMPLEX FORMS OF Mn IONS AND FOR ELUENT SPECIES CALCULATED FROM EXPERIMENTAL DATA

Ion-exchange constant	Eluent concentration ($CO_3^{2-} + HCO_3^-$) (mM)						Mean ± S.D.
	2.0	2.5	3.0	3.5	5.0	7.0	
$K_{MnHEDTA/HCO_3}$	0.387	0.383	0.400	0.370	3.990	0.311	0.38 ± 0.05
K_{MnEDTA/HCO_3}	4.471	4.344	3.305	4.374	4.068	4.567	4.40 ± 0.28
K_{OH/HCO_3}	11.477	11.017	11.405	11.312	10.500	11.487	11.20 ± 0.63
K_{CO_3/HCO_3}	13.994	13.824	14.000	13.608	13.983	13.948	13.89 ± 0.25

TABLE IV

CHROMATOGRAPHIC ION-EXCHANGE EQUILIBRIUM CONSTANTS FOR COMPLEX FORMS OF Ni IONS AND FOR ELUENT SPECIES CALCULATED FROM EXPERIMENTAL DATA

Ion-exchange constant	Eluent concentration ($CO_3^{2-} + HCO_3^-$) (mM)						Mean ± S.D.
	2.0	2.5	3.0	3.5	5.0	7.0	
$K_{NiHEDTA/HCO_3}$	0.609	0.678	0.699	0.675	0.694	0.658	0.67 ± 0.05
K_{NiEDTA/HCO_3}	7.866	7.800	7.990	7.961	7.550	7.990	7.86 ± 0.28
K_{OH/HCO_3}	10.995	10.633	10.600	10.547	10.000	11.496	10.71 ± 0.80
K_{CO_3/HCO_3}	13.993	13.578	13.998	13.425	13.972	13.000	13.66 ± 0.60

TABLE V

CHROMATOGRAPHIC ION-EXCHANGE EQUILIBRIUM CONSTANTS FOR COMPLEX FORMS OF Cd IONS AND FOR ELUENT SPECIES CALCULATED FROM EXPERIMENTAL DATA

Ion-exchange constant	Eluent concentration ($CO_3^{2-} + HCO_3^-$) (mM)						Mean ± S.D.
	2.0	2.5	3.0	3.5	5.0	7.0	
$K_{CdHEDTA/HCO_3}$	0.562	0.568	0.575	0.580	0.579	0.570	0.572 ± 0.01
K_{CdEDTA/HCO_3}	4.746	4.669	4.509	4.830	4.500	4.907	4.70 ± 0.27
K_{OH/HCO_3}	11.610	11.685	11.852	11.793	11.910	11.998	11.81 ± 0.24
K_{CO_3/HCO_3}	14.000	13.652	13.992	13.836	13.998	13.999	13.91 ± 0.23
$K_{Cd(OH)_3/HCO_3}$	3.574	3.652	3.940	3.714	3.841	3.111	3.64 ± 0.48
$K_{Cd(OH)_4/HCO_3}$	5.639	5.665	5.935	5.750	5.848	5.080	5.65 ± 0.50

TABLE VI

COMPARISON OF PREDICTED AND OBSERVED RETENTION VOLUMES OF CoEDTA

Eluent		Retention volume (ml)		Difference (%)[a]
$C_{(CO_3^{2-} + HCO_3^-)}$ (mM)	pH	Measured	Calculated	
2.0	9.10	41.80	41.92	0.28
2.0	9.57	19.72	19.36	1.83
2.0	9.92	11.38	12.19	7.12
2.0	10.35	8.46	8.18	3.31
2.0	11.07	6.38	5.06	20.69
2.5	9.93	10.42	10.3	1.15
3.0	9.63	12.00	12.65	5.42
3.0	10.30	6.34	6.51	2.68
3.0	10.80	6.50	4.94	24.00
3.5	9.40	15.20	15.15	0.33
5.0	9.80	6.30	6.80	7.9
5.0	10.76	4.34	3.87	10.83
7.0	9.40	8.64	8.05	6.83
7.0	9.87	5.16	5.04	2.33
7.0	10.25	4.04	3.99	1.24
7.0	10.60	3.50	3.50	0
7.0	11.10	3.16	3.05	3.48

[a] Mean of standard deviations = 5.85%.

TABLE VII

COMPARISON OF PREDICTED AND OBSERVED RETENTION VOLUMES OF MnEDTA

Eluent		Retention volume (ml)		Difference (%)[a]
$C_{(CO_3^{2-}+HCO_3^-)}$ (mM)	pH	Measured	Calculated	
2.0	9.10	23.8	23.3	2.10
2.0	9.57	11.22	11.22	0
2.0	9.92	6.70	7.39	10.3
2.0	10.35	5.10	5.25	2.94
2.0	11.07	3.56	3.56	0
2.5	9.93	6.20	6.23	0.48
3.0	9.63	7.20	7.45	3.5
3.0	10.30	4.08	4.28	4.9
3.0	10.80	3.92	3.47	11.48
3.5	9.40	8.82	8.74	0.91
5.0	9.80	4.14	4.44	7.25
5.0	10.76	3.10	2.92	5.81
7.0	9.40	5.40	5.08	5.93
7.0	9.87	3.50	3.53	0.86
7.0	10.25	2.86	2.99	4.55
7.0	10.60	2.56	2.74	7.03
7.0	11.10	2.30	2.50	8.70

[a] Mean of standard deviations = 4.51%.

TABLE VIII

COMPARISON OF PREDICTED AND OBSERVED RETENTION VOLUMES OF NiEDTA

Eluent		Retention volume (ml)		Difference (%)[a]
$C_{(CO_3^{2-}+HCO_3^-)}$ (mM)	pH	Measured	Calculated	
2.0	9.10	40.00	40.69	1.73
2.0	9.57	18.76	18.81	0.27
2.0	9.92	10.66	11.87	11.35
2.0	10.35	7.74	7.98	3.10
2.0	11.07	5.04	4.95	1.79
2.5	9.93	9.74	9.75	0.10
3.0	9.63	11.80	11.95	1.27
3.0	10.30	5.82	6.21	6.70
3.0	10.80	5.62	4.74	15.66
3.5	9.40	14.64	14.28	2.46
5.0	9.80	6.02	6.48	7.64
5.0	10.76	4.16	3.75	9.86
7.0	9.40	8.34	7.65	8.27
7.0	9.87	5.00	4.84	3.20
7.0	10.25	3.88	3.86	0.52
7.0	10.60	3.32	3.40	2.41
7.0	11.10	2.86	2.98	4.20

[a] Mean of standard deviations = 4.74%.

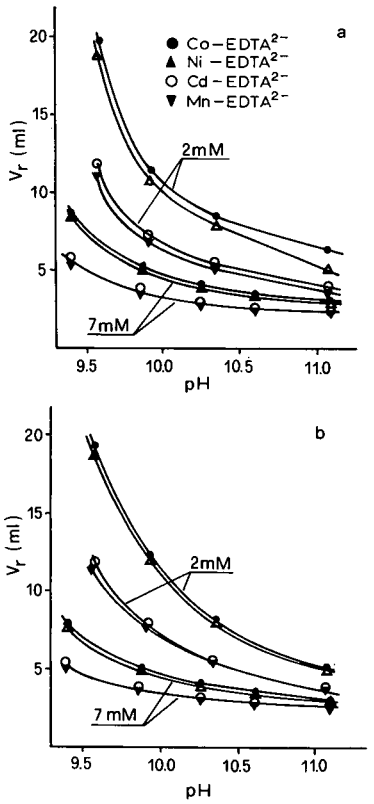

Fig. 3. Effect of pH on retention volumes (V_r) for two eluent concentrations (2 and 7 mM). (a) Experimental and (b) predicted values.

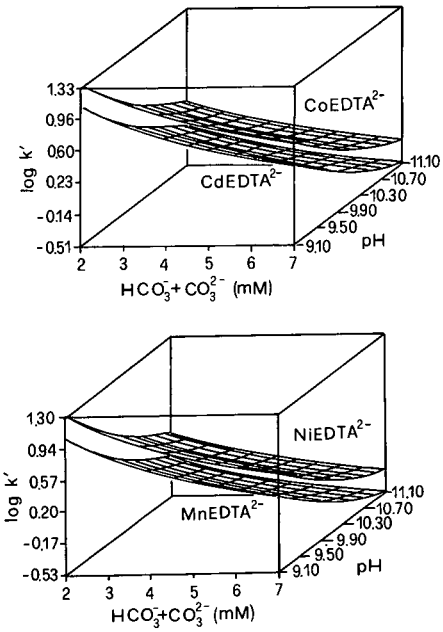

Fig. 4. Calculated retention surface for metal–EDTA complexes.

shows the good agreement between the two sets of data. The mean relative differences (%) between the evaluated and computed retention volumes confirm the good suitability of the proposed model. Calculated retention surfaces for metal–EDTA com-

TABLE IX

COMPARISON OF PREDICTED AND OBSERVED RETENTION VOLUMES OF CdEDTA

Eluent		Retention volume (ml)		Difference (%)[a]
$C_{(CO_3^{2-}+HCO_3^-)}$ (mM)	pH	Measured	Calculated	
2.0	9.10	25.00	24.70	1.20
2.0	9.57	11.82	11.83	0.08
2.0	9.92	7.06	7.74	9.63
2.0	10.35	5.38	5.45	1.30
2.0	11.07	3.92	3.63	7.40
2.5	9.93	6.56	6.51	0.76
3.0	9.63	7.36	7.80	5.98
3.0	10.30	4.24	4.43	4.48
3.0	10.80	4.16	3.55	14.66
3.5	9.40	9.42	9.18	2.55
5.0	9.80	4.32	4.60	6.48
5.0	10.76	3.22	2.98	7.45
7.0	9.40	5.58	5.29	5.20
7.0	9.87	3.62	3.64	0.55
7.0	10.25	3.96	3.06	3.38
7.0	10.60	2.64	2.79	5.68
7.0	11.10	2.40	2.53	5.42

[a] Mean of standard deviations = 4.83%.

plexes, obtained through eqns. 24, 29, 31 and 33, are also shown in Fig. 4 and according to the above data validate the proposed model.

ACKNOWLEDGEMENTS

We acknowledge financial support from OTKA-2562 (Hungary) and the Consiglio Nazionale delle Ricerche (CNR, Italy).

REFERENCES

1 G. J. Sevenich and J. S. Fritz, *Anal. Chem.*, 55 (1983) 12.
2 S. Matsushita, *J. Chromatogr.*, 312 (1984) 327.
3 G. Schwedt and B. Kondratjonok, *Fresenius' Z. Anal. Chem.*, 332 (1989) 855.
4 C. Sarzanini, O. Abollino, E. Mentasti and V. Porta, *Chromatographia*, 30 (1990) 293.
5 J. Inczedy, *Analytical Application of Complex Equilibria*, Ellis Horwood, Chichester, and Akadémiai Kiadó, Budapest, 1976.
6 P. Hajos and J. Inczedy, presented at the *15th International Symposium on Column Liquid Chromatography, Basel, June 3–7, 1991*, poster P 146/2.
7 P. R. Haddad and P. E. Jackson, *Ion Chromatography —Principles and Applications*, Elsevier, Amsterdam, 1990, Ch. 5, p. 133.
8 P. Hajos and J. Inczedy, in D. Naden and M. Streat (Editors), *Ion Exchange Technology*, Ellis Horwood, Chichester, 1984, p. 450.
9 T. B. Hoover, *Sep. Sci. Technol.*, 17 (1982) 295.
10 P. Hajos, T. Kecskemeti and J. Inczedy, *React. Polym.*, 7 (1988) 239.
11 L. G. Sillen, *Stability Constants of Metal Complexes*, Chemical Society, London, 1971.

Journal of Chromatography, 640 (1993) 27–31
Elsevier Science Publishers B.V., Amsterdam

CHROMSYMP. 2772

Determination of inorganic and organic anions in one run by ion chromatography with column switching

C. Umile* and J. F. K. Huber

Institute of Analytical Chemistry, University of Vienna, Währingerstrasse 38, A-1090 Vienna (Austria)

ABSTRACT

A method for the simultaneous determination of low-molecular-mass organic and inorganic anions in aqueous solutions was developed using isocratic ion chromatography (IC) with suppressed conductimetric detection and column switching. Owing to the large differences in distribution coefficients between sulphate, nitrate and phosphate and the other species, these ions are separated in the first stage on a medium-capacity anion exchanger, whereas the other anions are led through a second column packed with a high-capacity anion-exchange resin via a column-switching valve. After optimization of the switching procedure a spiked drinking water sample was analysed. Fluoride, acetate, butyrate, formate, nitrate, nitrite and phosphate could be determined in addition to the main anions (chloride and sulphate). The time for a complete analysis is less than 20 min and the method can easily be automated. The precision and detection limit are as usual in IC with background suppression.

INTRODUCTION

In the last decade, ion chromatography (IC) has undergone significant changes. Initially IC was focused primarily on the determination of inorganic anions [1]. Nowadays it has a much wider scope, which ranges from the determination of inorganic and organic cations to that of inorganic and organic anions [1,2].

The introduction of a membrane suppressor [3] with improved suppression capacity and reduced void volume permitted the use of high concentrations of hydroxide as eluent and therefore the elution of more strongly retained anions. The high suppression capacity also opened the door to gradient elution in IC using suppressed conductivity detection [4]. This is one way to separate species with widely varying affinities (capacity factors, k') for the stationary phase in a reasonable time. Gradient elution starts with an eluent of low ionic elution strength for the resolution of the most weakly retained species. Increasing the concentration of the eluent during the run leads to the elution of the more strongly retained ions in a reasonable time. Using sodium hydroxide as an eluent component results in water as the suppression product. One example of the benefit of an ion strength gradient is the resolution of fluoride and early-eluting organic anions (most notably acetate and formate) under isocratic conditions, which caused serious problems in the routine determination of anions in environmental and power industrial samples [5,6].

Gradient elution is not without problems. One is the build-up of eluent impurities (mostly carbonate) in the separation column and their subsequent release as the eluent strength is increased. This problem can be minimized by using a trap column and very pure reagents (carbonate free sodium hydroxide and 18 MΩ cm water). Nevertheless, there remains a baseline drift caused by these impurities which complicates the integration of the peaks. Another drawback in gradient elution is that the column must be returned to its initial state, which leads to a longer analysis time.

An alternative to this technique resulted from the

* Corresponding author.

0021-9673/93/$06.00

introduction of a new high-capacity macroporous resin for anion exchange, which made it possible to separate fluoride from the early-eluting organic acids and to elute the more strongly retained anions isocratically. One drawback of this method is the long time of 40 min for the elution of nitrate and phosphate with a wide time window of non-used baseline. A final solution of the problem can be expected by applying column switching, combining this new high-capacity column with the low-capacity column used in previous work.

Column switching was first used in liquid chromatography in the low-pressure mode [7,8] and later in the high-pressure mode [9–21]. In IC one of the approaches to cation determination uses column switching to determine mono- and divalent ions in one isocratic run [22]. Another application of this technique in IC is the rapid analysis of pulping liquors [23].

This paper discusses the use of the column-switching technique for the determination of inorganic and organic anions by IC. After optimization of the system the method was tested with drinking water samples.

EXPERIMENTAL

Chemicals

All chemicals were of analytical-reagent grade: 50% sodium hydroxide (J. T. Baker, Deventer, Netherlands), sodium carbonate, sodium nitrate, sodium nitrite, 96% sulphuric acid, formic acid, acetic acid, butyric acid and sulphate, chloride, phosphate and fluoride Titrisol standards of 1000 mg/l (E. Merck, Darmstadt, Germany). All working standard solutions were prepared by appropriate dilutions of stock standard solutions. The eluents, regenerants and standards were prepared using ultra-pure 18 MΩ cm HPLC-grade water.

Apparatus

A Model 4500i ion chromatograph (Dionex, Sunnyvale, CA, USA) was used, equipped with an electrical conductivity detector with integrated background suppression via an anion micro membrane suppressor (Dionex). The instrument was modified by the plumbing of an additional high-pressure multi-port valve (Dionex) allowing column switching.

In position 1 of the switching valve the effluent is first led through the first column C_1 and then via the switching valve to the second column C_2 and finally, after suppression of the ion background, to the conductivity detector cell. In position 2 of the column switching valve the column sequence is reversed, maintaining the direction of flow within the columns. The chromatograms were monitored and processed by a Model AI-450 data station (Dionex). The injector and the switching valve were activated by the pump control.

The conditions for analysis were as follows: eluent, 75 m*M* NaOH solution; flow-rate, 1 ml/min; columns, C_1 = AS4A anion exchanger (Dionex) (250 × 4.6 mm I.D.) and C_2 AS10 anion exchanger (Dionex) (250 × 4.6 mm I.D.); column switching, 3 min after injection; injection volume, 50 μl; detector, electrical conductivity with chemical ion suppression; micro membrane suppressor continuously regenerated with 25 m*M* H_2SO_4 at 4 ml/min.

RESULTS AND DISCUSSION

Retention characteristics of columns C_1 and C_2

Table I compares the properties of the packing materials in the two columns. Owing to the higher capacity of column C_2 compared with C_1 the anions are generally eluted later under the same chromatographic conditions. Compared with the elution sequence with column C_2, there is a difference in selectivity. On column C_1 carbonate co-elutes with nitrite whereas on column C_2 there is co-elution of carbonate with chloride.

Column-switching sequence

Fig. 1 shows schematically the principle of separation. (a) The sample is injected on to column C_1 and the flow is directed from C_1 to C_2. (b) After a certain time the different species start to separate according to their differential retention. All inorganic anions, except fluoride, chloride and carbonate, have a higher affinity than the low-molecular-mass organic species for the anion exchanger. Therefore, they move slowly in column C_1, whereas the other anions elute from column C_1 and are directed via the switching valve to column C_2, where separation continues. (c) Now the switching valve is activated and the column sequence is reversed. The eluent flows first through column C_2

TABLE I

COMPARISON OF THE PROPERTIES OF THE PACKING MATERIALS IN COLUMNS C_1 AND C_2

Property	AS4A(C_1)	AS10(C_2)
Support	Pellicular	Macroporous
	Poly(styrene–divinylbenzene)	Ethylvinylbenzene–divinylbenzene
Diameter	15 μm	8.5 μm
Cross-Link	4%	55%
Pore Size	<1 Å	2000 Å
Layer	Latex	Latex
Diameter	200 nm	65 nm
Cross-Link	0.5%	5%
Functional group	Alkanol	Alkanol
	Quaternary amine	Quaternary amine
Ion-exchange capacity	20 μequiv.	170 μequiv.
Column dimensions	250 mm × 4.6 mm I.D.	250 mm × 4.6 mm I.D.

and then through column C_1 without changing the flow direction within the columns. At first the more strongly retained anions, sulphate and nitrate, are eluted from column C_1 and detected (peaks 7 and 8 in Fig. 2). These species are separated only on column C_1. Phosphate as the most retained anion of the sample is passed by fluoride and the low-molecular-mass organic acids coming from column C_2 (peaks 1–3 in Fig. 2). The situation before the elution of phosphate is shown in Fig. 1d. Phosphate elutes from C_1, followed by chloride, carbonate and nitrite, which, like the organics, first pass through column C_1, then through C_2 and finally once again via the switching valve through column C_2.

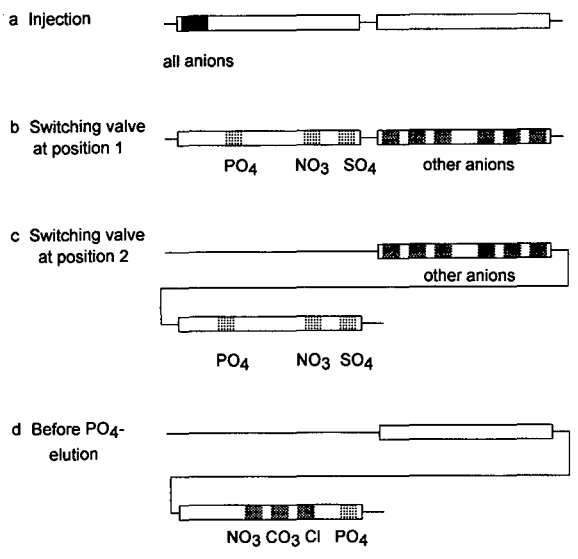

Fig. 1. Elution sequence during column switching

Switching time optimization

To find the optimum switching point first a chromatogram was monitored by injecting a nine-anion standard solution only using column C_1 (AS4A)

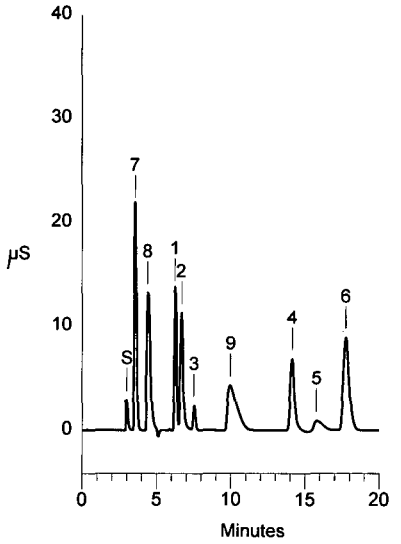

Fig. 2. Chromatogram of a nine-anion standard solution using column switching. Peaks: 1 = 2 mg/l fluoride; 2 = 10 mg/l acetate; 3 = 10 mg/l formate; 4 = 3 mg/l chloride; 5 = 100 mg/l carbonate; 6 = 10 mg/l nitrite; 7 = 5 mg/l sulphate; 8 = 10 mg/l nitrate; 9 = 15 mg/l phosphate; S = switching peak.

under the optimized mobile phase conditions for column C_2 (AS10). Compared with the conditions optimized for column C_1 ($NaHCO_3$–Na_2CO_3 eluent), different sensitivities and a different elution sequence can be observed. The inorganic anions elute in the order fluoride, chloride, nitrite, sulphate, nitrate, phosphate. Acetate and formate coelute with fluoride and carbonate interferes with nitrite. The complete elution of nitrite from column C_1 marks the earliest switching point, whereas the start of the elution of sulphate indicates the latest switching point.

The chromatograms obtained during the optimization of the switching point are shown in Fig. 3. Choosing the switching point between 3.1 and 2.8 min after injection (b to e), nitrite as the last-switched peak is transferred quantitatively on to C_2. Fig. 3a shows a decreased nitrite peak and an increase in the switching peak due to a non-quantitative transfer of the nitrite peak. The optimum switching point in this case is 3.00 min after injection.

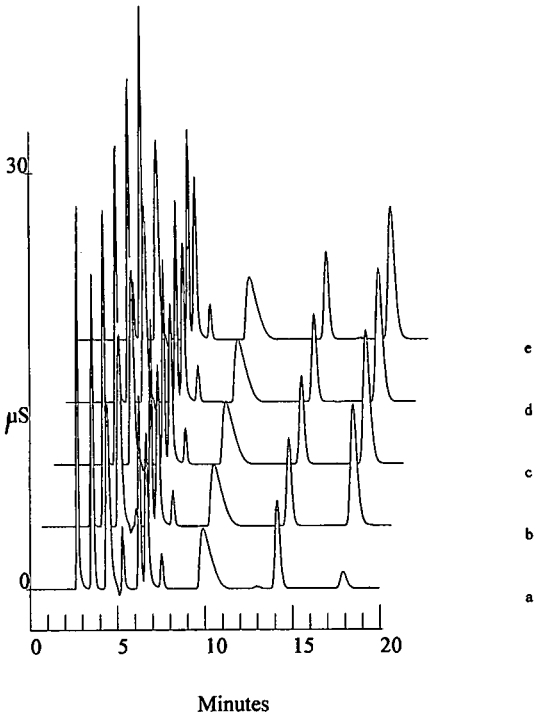

Fig. 3. Chromatograms of a nine-anion standard solution using column switching at different times. Switching point after (a) 2.7, (b) 2.8, (c) 2.9, (d) 3.0 and (e) 3.1 min.

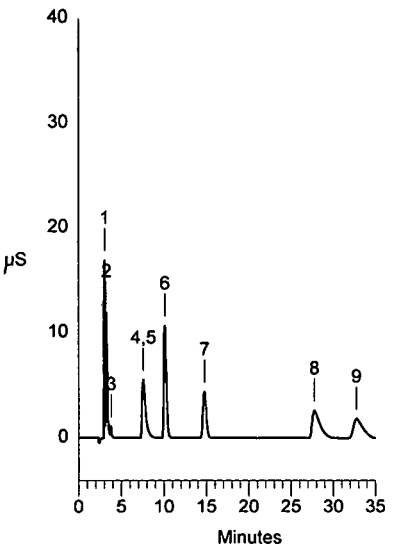

Fig. 4. Chromatogram of a nine-anion standard solution on column C_2. Peaks 1–9 as in Fig. 2.

One of the advantages of this method is that observing these limits there normally is a wide time window where the switching action can take place. Hence the control of this command does not need

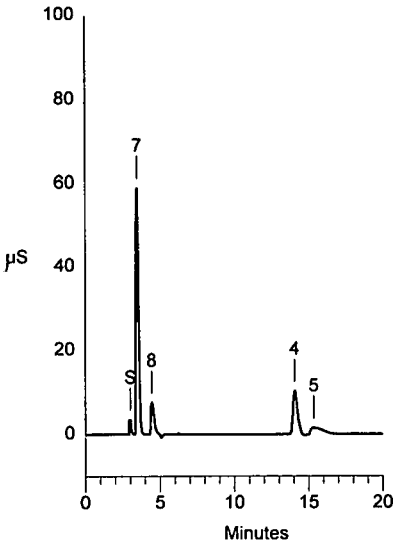

Fig. 5. Chromatogram of a drinking water sample using column switching. Peaks: 7 = sulphate; 8 = nitrate; 4 = chloride; 5 = carbonate; S = switching peak.

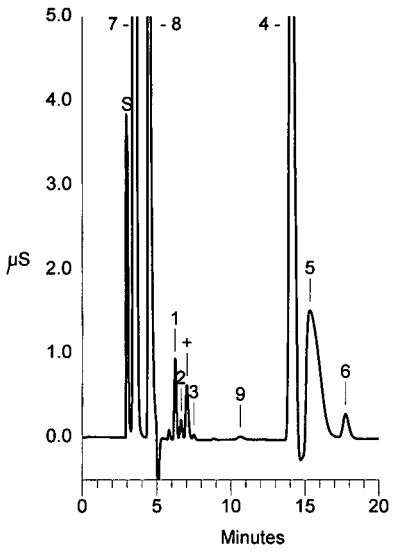

Fig. 6. Chromatogram of a spiked drinking water sample using column switching. Peaks: 7 = sulphate; 8 = nitrate; 4 = chloride; 5 = carbonate; S = switching peak. Spikes: 1 = 0.1 mg/l fluoride; 2 = 0.1 mg/l acetate; + = 0.1 mg/l butyrate; 3 = 0.1 mg/l formate; 6 = 0.3 mg/l nitrite; 9 = 0.1 mg/l phosphate.

to be very exact and can also be done manually just using a watch.

Compared with the separation on column C_2 alone (Fig. 4), there is a time saving of almost 50% and additionally the separation of chloride and carbonate, which may be very important, *e.g.*, in the application discussed in the following section.

Application

After optimization of the switching procedure, several drinking water samples were analysed. A representative sample is shown in Fig. 5. There is no interference between chloride (peak 4) and carbonate (peak 5). The spiked sample (Fig. 6) shows a good separation of fluoride (peak 1, 0.1 mg/l spike) from the organic acids acetate (peak 2, 0.1 mg/l spike), formate (peak 3, 0.1 mg/l spike) and butyrate (peak 2*, 0.1 mg/l spike). Phosphate (peak 9, 0.1 mg/l spike) and nitrite (peak 6, 0.3 mg/l spike) can also be measured with no problems in less than 20 min.

CONCLUSIONS

The example shown in this paper demonstrates the usefulness of column switching in ion chromatography. There are no significant adverse effects from the additional switching device and the very easy set-up, optimization and automation make this method very practical.

REFERENCES

1 H. Small, T. S. Stevens and W. C. Baumann, *Anal. Chem.*, 47 (1975) 1801.
2 H. Small, *Ion Chromatography*, Plenum Press, New York, 1989.
3 J. Stillian, *LC Mag.*, 3 (9) (1985) 802.
4 J. Weiss, *Ionenchromatographie*, VCH, Weinheim, 1991.
5 *Dionex Technical Note, No. 19*, Dionex, Sunnyvale, CA, 1986.
6 S. Harvey, *J. Chromatogr.*, 546 (1991) 125.
7 L. R. Snyder, *J. Chromatogr. Sci.*, 8 (1970) 692.
8 J. J. Lijama and A. A. Hallen, *J. Chromatogr.*, 57 (1971) 153.
9 J. F. K. Huber, R. van der Linden, E. Ecker und M. Oreans, *J. Chromatogr.*, 83 (1973) 267.
10 H. Oster and E. Ecker, *Chromatographia*, 3 (1970) 220.
11 I. Fogy, E. R. Schmid and J. F. K. Huber, *Z. Lebensm.-Unters.-Forsch.*, 173 (1981) 268.
12 I. Fogy, E. R. Schmid und J. F. K. Huber, *Z. Lebensm.-Unters.-Forsch.*, 169 (1979) 438.
13 I. Fogy, E. R. Schmid und J. F. K. Huber, *Z. Lebensm.-Unters.-Forsch.*, 170 (1980) 184.
14 J. F. K. Huber, I. Fogy and C. Fioresi, *Chromatographia*, 13 (1980) 408.
15 J. F. K. Huber and F. Eisenbeiss, *J. Chromatogr.*, 149 (1978) 127.
16 R. J. Dolphin, F. W. Willmott, A. D. Mills and L. P. J. Hoogeveen, *J. Chromatogr.*, 122 (1976) 259.
17 F. M. Willmott, I. Mackenzie and R. J. Dolphin, *J. Chromatogr.*, 167 (1979) 31.
18 F. Erni and R. W. Frei, *J. Chromatogr.*, 149 (1978) 561.
19 E. L. Johnson, R. Gloor and R. E. Majors, *J. Chromatogr.*, 149 (1978) 571.
20 H. Hulpke and U. Werthmann, *Chromatographia*, 12 (1979) 390.
21 H. Hulpke and U. Werthmann, *Chromatographia*, 13 (1980) 395.
22 *Dionex Product Information, Fast Cation*, Dionex, Sunnyvale, CA, 1986
23 S. Utzmann and D. Campbell, *LC · GC*, 9 (1991) 300.

Journal of Chromatography, 640 (1993) 33–40
Elsevier Science Publishers B.V., Amsterdam

CHROMSYMP. 2652

Anion chromatography with a crown ether-based stationary phase and an organic modifier in the eluent

John D. Lamb* and Robert G. Smith

Department of Chemistry, Brigham Young University, Provo, UT 84602 (USA)

Jacek Jagodzinski

Dionex Corporation, Sunnyvale, CA 90488 (USA)

ABSTRACT

The unique ability of macrocyclic ligands, such as the crown ethers and cryptands, to selectively complex alkali metal cations can be used as the basis for chromatographic separations of anions. Specifically, macrocycles which are adsorbed onto a reversed-phase column, form positively charged anion-exchange sites when they combine with eluent cations. Previously we have demonstrated gradient anion separations based on changing the column capacity during the course of the separation by altering the eluent cation, temperature, or organic modifier content using cryptand-based columns. Herein we report that excellent separations can also be achieved using 18-crown-6 based columns. In this column, anion retention increases with increasing eluent strength and organic modifier content. This observation is in keeping with the relatively moderate affinity of crown ethers for alkali metals when compared to cryptands. The separation of anions achieved by optimizing mobile phase variables shows that isocratic separations of anions on the crown-based column are almost as good as separations achieved only under gradient conditions on cryptand-based columns. Cation gradients provide additional improvements on the separations using the crown-based column.

INTRODUCTION

Since their discovery, macrocyclic ligands such as the crown ethers and cryptands have been noted for their ability to selectively complex cations [1,2]. This unique selectivity has been used to perform chromatographic and other types of separations [3–8]. The selectivity of macrocycles for cations is often based on the ability of the cation to fit into the central cavity of the macrocycle, *i.e.*, those cations that fit most closely into the macrocyclic cavity are bound more strongly than those cations that are too small or too large to fit into the cavity. In chromatographic separations, cations that are bound most tightly by the macrocycle are retained longer than the more loosely bound cations [3,4].

Macrocycle-based columns have also been used to separate anions chromatographically with the macrocycle–cation complex serving as the anion-exchange site. This is possible because most macrocycles are uncharged, and thus an anion must be associated with the complex to maintain electrical neutrality. Since the macrocycle is also generally hydrophobic and is associated with the hydrophobic environment of the column, those anions which are more hydrophobic are retained longer. Thus, anions with a common cation can be separated, as well as cations with common anion.

Most macrocycle-based separations have involved a ligand-exchange mechanism. We have explored the use of macrocycle-based anion separations which are based rather on an ion-exchange mechanism. An alkali metal hydroxide solution is used as eluent. The eluent metal ions complex with the stationary phase macrocycles, creating positively charged anion-

* Corresponding author.

0021-9673/93/$06.00

exchange sites. The hydroxide ion elutes sample anions from the column [9].

Using columns of the type described above, gradient separations can be achieved by changing the column capacity during the course of the separation. The column anion-exchange capacity can be varied in several ways, including changing (i) the eluent cation, (ii) the temperature, or (iii) the organic modifier concentration [10]. Gradients of the first type are performed by changing the eluent cation from one which has a high affinity for the macrocycle to one which has a lower affinity. This change results in fewer macrocycle–cation complexes on the column, decreasing the ion-exchange capacity [11, 12]. Gradient separations of the second type are performed by increasing the column temperature during the separation. Since the complexation reaction between cations and macrocycles is generally quite exothermic, increasing the temperature results in fewer column complexes, decreasing the column capacity [12,13]. Gradients of the third type have been used in separations of nucleosides and nucleotides [10]. These capacity gradients enjoy some advantages over conventional gradients in ion chromatography which are carried out by increasing eluent strength, resulting in baseline drift when using conductivity detection. Capacity gradients are carried out with very little or no change in the eluent ionic strength, yielding a stable baseline.

We have previously reported capacity gradient separations on columns based on cryptand-type macrocycles [9–13]. In this work we report anion separations on chromatography columns based on crown ether macrocycles and introduce capacity gradients based on organic modifier concentration.

EXPERIMENTAL

Materials

Reagent-grade cryptands *n*-decyl-2.2.2 (D-2.2.2) and *n*-decyl-2.2.1 (D-2.2.1) (Fig. 1) were obtained from EM Science (Gibbstown, NJ, USA). The *n*-decyl-18-crown-6 and *n*-tetradecyl-18-crown-6 crown ethers were synthesized by the procedure reported by Ikeda *et al.* [14]. Reagent-grade compounds were used in making all standards and eluents. HPLC-grade methanol and acetonitrile were obtained from Fisher Scientific (Fair Lawn, NJ, USA). Water used in making eluents and standards was purified to 18 MΩ resistivity with a Milli-Q water purification system (Millipore) and all eluents were degassed by sparging with helium.

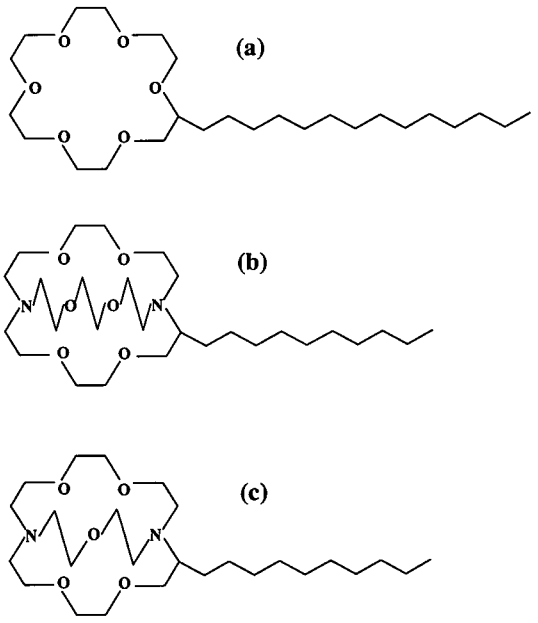

Fig. 1. Structures of (a) *n*-tetradecyl-18-crown-6 (TD-18-crown-6), (b) *n*-decyl-2.2.2 (D-2.2.2) and (c) *n*-decyl-2.2.1 (D-2.2.1).

Instrumentation

A Dionex 4000i series ion chromatograph was used to perform all chromatographic separations. Dionex anion micromembrane (AMMS) suppressors were used for eluent suppression prior to conductometric detection with a Dionex conductivity detector. Suppressant was 25 m*M* H_2SO_4 flowing at 3–5 ml/min. Macrocycle columns were prepared from Dionex MPIC NS-1 columns. The chromatograph was controlled and the data collected on a personal computer using the Dionex AI400 control software.

Column preparation

Macrocycle-based columns were prepared as previously described [8] by recirculating a solution of the macrocycle in a methanol–water (60:40) solution through the column for a period of 12 h.

RESULTS AND DISCUSSION

Factors affecting anion retention

In traditional ion chromatography, the anion retention is mainly a function of the eluent strength, with other factors playing a lesser role. With macrocycle-based chromatography the retention is determined not only by the eluent strength but also by the column capacity, a factor that is usually fixed in traditional ion chromatography. The column capacity in macrocycle-based chromatography is not only a function of the amount of ligand on the column, but also the number of cation–macrocycle complexes formed. The number of complexes formed can be affected by the identity of the eluent cation, the cation concentration, and the amount of organic modifier added to the eluent. The effect of each of these factors will be discussed.

Eluent cation

The ability of the macrocycle to bind cations is expressed by the binding constant for the reaction between the macrocycle adsorbed on the column and the cation in the eluent. In our previous work we used the cryptands D-2.2.1 and D-2.2.2 as the basis for columns to separate anions. In Fig. 2, the log of the binding constants for these macrocycles with the alkali metal cations are compared to those of 18-crown-6, the type of macrocycle used in this study. The 18-crown-6 and 2.2.2 ligands show similar selectivities, each binding K^+ strongest, followed by Rb^+, Na^+, Cs^+ an Li^+. One significant difference between these two ligands is that the crown has a higher affinity for Cs^+ than Na^+ while D-2.2.2 binds Na^+ better than Cs^+. On the other hand, D-2.2.1 shows the highest affinity for Na^+, followed by K^+, Rb^+, Li^+ and Cs^+.

The dependence of anion retention on eluent cation is demonstrated by measuring anion retention with different cations in the eluent. The effect of eluent cation on the retention of chloride is demonstrated in Fig. 3. In these experiments, approximately the same amount of macrocycle was loaded on each column and the eluents are all 20 m*M* alkali metal hydroxides. The amount of retention is clearly related to the binding constant of the cation in the eluent with the macrocycle on the column. For all three ligands the order of retention directly mirrors the order of the binding constants of the ligands for the eluent cations shown in Fig. 2. The 18-crown-6 and D-2.2.2 columns show the most retention with the KOH eluent, while the D-2.2.1 columns retains anions longest with the NaOH eluent.

The most significant difference between cryp-

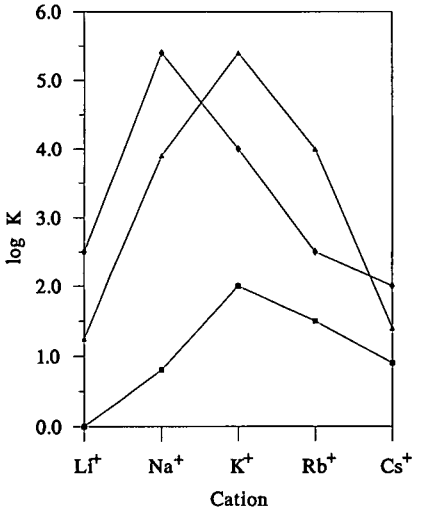

Fig. 2. Variation in log *K*, the stability constant for alkali metal ion complexes, in water for the cryptands D-2.2.2 (▲) and D-2.2.1 (◆) and the crown ether 18-crown-6 (■) at 25°C. From ref. 1.

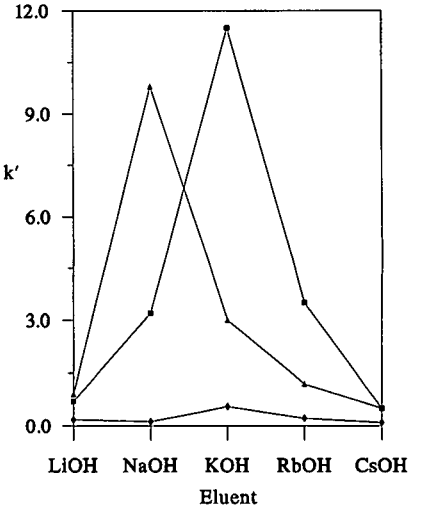

Fig. 3. Variation in Cl^- capacity factor, *k'*, with eluent alkali metal cation (20 m*M*) on D-2.2.2 (■), D-2.2.1 (▲) and TD-18-crown-6 (◆) columns.

tands and crown ethers is that the cryptands show a much higher affinity for all of the alkali metals [1,2]. This implies that for a given amount of macrocycle loaded on the column, cryptand columns should show higher column capacities than crown columns for a given cation in the eluent. This expectation is indeed realized, as shown by Fig. 3. The retention of chloride is much greater for the cryptand columns with all of the eluents.

Eluent concentration

In traditional ion chromatography the retention of anions decreases with increasing eluent strength. With macrocycle-based chromatography, there are two separate and opposing effects of changing eluent concentration. As the eluent concentration is increased: (i) the eluting power of the eluent is increased and (ii) the column capacity increases. In order to understand these two opposing effects we can consider the reactions responsible for anion retention taking place in the column. The first reaction is the formation of the cation–macrocycle exchange site:

$$M_m^+ + OH_m^- + L_s \rightleftarrows (ML^+OH^-)_s$$

where ML^+ is the cation–macrocycle complex, OH^- is the hydroxide ion, and L is the macrocyclic ligand, the subscript m refers to the species in the mobile phase and the subscript s refers to the species in the stationary phase. The associated formation constant is:

$$K_C = \frac{[(ML^+OH^-)_s]}{[M_m^+][OH_m^-][L_s - (ML^+OH^-)_s]}$$

The second reaction is the ion-exchange reaction described by the equation:

$$(ML^+OH^-)_s + A_m^- \rightleftarrows ML^+A_s^- + OH_m^-$$

where M^+, OH^-, and L have the same meaning as above and A^- is the analyte anion. The equilibrium constant for this reaction can be written:

$$K_A = \frac{[(ML^+A^-)_s][OH_m^-]}{[(ML^+OH^-)_s][A_m^-]}$$

We can rearrange the expression for K_C to solve for $[(ML^+OH^-)_s]$ to find the result:

$$[(ML^+OH^-)_s] = \frac{K_A[L_s][M_m^+]^2}{1 + K_A[M_m^+]^2}$$

This result can then be sustituted in the equation for K_A and solved to yield:

$$\frac{[(ML^+A^-)_s]}{[A_m^-]} = \frac{\dfrac{K_A K_C[L_s][M_m^+]^2}{1 + K_C[M_m^+]^2}}{[M_m^+]} = K_D$$

The factor on the left side of the equation is the distribution coefficient, K_D, for the anion between the stationary and mobile phases, which is directly proportional to retention as expressed in the capacity factor k'.

If the product $K_C[M_m^+]^2$ is much less than 1, then the distribution coefficient K_D approaches being directly proportional to the eluent concentration, $[M_m^+]$, and analyte retention should increase with increasing eluent concentration. On the other hand, if the product is much greater than 1 then K_D is inversely proportional to the eluent concentration $[M_m^+]$ and retention should decrease as the eluent concentration is increased. Thus, if we perform separations at a variety of eluent MOH concentrations, we should observe that retention increases with MOH concentration in the low concentration region, reaches a maximum, then decreases with increasing [MOH] at high concentration. The experimental results that we have previously reported with the cryptand columns [9] agree with this

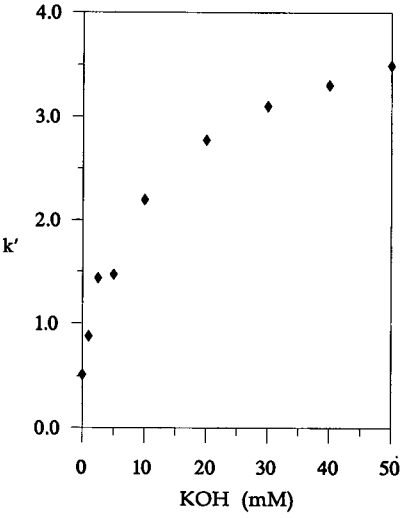

Fig. 4. Variation in NO_3^- capacity factor with eluent KOH concentration in 20% (v/v) aqueous acetonitrile on D-18-crown-6 column.

prediction. With the D-2.2.2 column we observed that anion retention increased with eluent KOH concentrations below 0.75 m*M*, where retention reached a maximum, with retention decreasing at eluent KOH concentrations greater than 0.75 m*M*.

Fig. 4 shows the effect of eluent concentration on the retention of nitrate ion using the crown-based column. As KOH concentration is increased, the capacity factor of nitrate is increased. In this case, the effect of the increasing the population of ion-exchange sites outweighs the effect of increasing the eluting power of the eluent. This is to be expected because the binding constants for the alkali metal cations with the crown are significantly lower than for the cryptands.

Organic modifier

The use of organic modifiers on ion chromatography has been limited until the recent development of solvent compatible columns. For common inorganic anions, the use of organic solvents in the eluent has a limited effect. However, the effect of solvent on the strength of binding of cations by crown ethers has been well documented, with the binding constants being several orders of magnitude higher in solvents such as methanol and acetonitrile than in pure aqueous systems [1,2]. Thus, it was anticipated that the column capacity of macrocycle columns would be increased by incorporation of an organic modifier in the eluent system. This effect is demonstrated in Fig. 5, which summarizes experiments in which the retention of nitrate ion on the crown column was measured *versus* the acetonitrile content of the mobile phase. The eluent was 50 m*M* KOH and the acetonitrile content was varied from 0 to 20% (v/v). The retention of nitrate is affected only slightly until the acetonitrile content reaches 10%, above which retention increases rapidly as the content of acetonitrile is increased. Column capacity, and thus anion retention can be significantly increased by increasing the amount of organic modifier in the eluent.

One concern with the use of organic solvents in the eluent in macrocycle-based chromatography of the type described herein is column stability. In our studies, the crown was adsorbed onto the reversed-phase column by hydrophobic interactions between the hydrophobic tail of the crown ether and the polystyrene resin. The addition of an organic solvent can affect the column stability since it can serve to elute the crown from the column. It was therefore necessary to determine the effect of organic solvent on column stability. We first studied the use of the C_{10} derivative of 18-crown-6 (Fig. 1). Column stability was checked first with a purely aqueous eluent by repeatedly injecting a 250 μM nitrate standard onto a column equilibrated with 20 m*M*

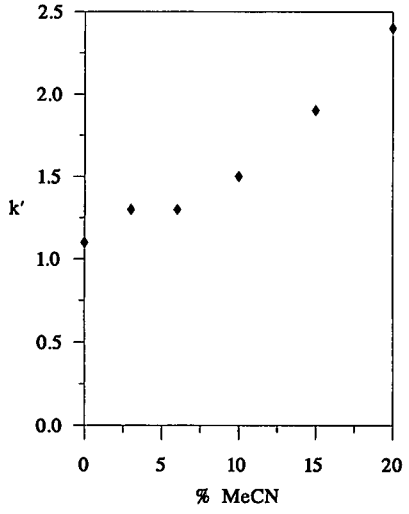

Fig. 5. Variation in NO_3^- capacity factor with acetonitrile content in 20 m*M* KOH eluent using TD-18-crown-6 column.

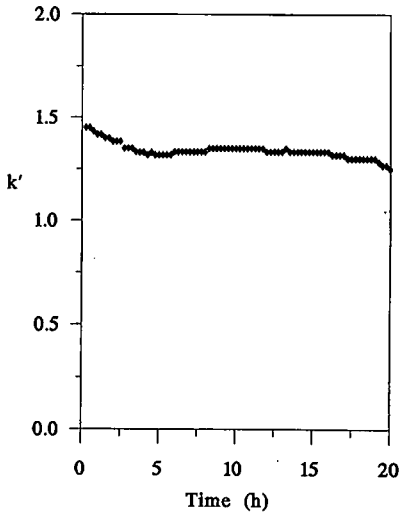

Fig. 6. Retention of NO_3^- on TD-18-crown-6 column *versus* time with 20 m*M* KOH eluent.

KOH eluent. A plot of the nitrate capacity factor over 20 h (Fig. 6) shows that crown was slowly eluted from the column by the purely aqueous eluent. It was concluded that the decyl derivative was insufficiently hydrophobic to provide a stable column even with water eluent. We therefore incorporated a longer aliphatic sidechain onto the crown ether functionality to provide better column stability. Aromatic substitution of the crown ether to increase hydrophobicity was avoided because the addition of an aromatic moiety to the macrocyclic ring results in lower binding stability and selectivity. The C_{14} derivative of 18-crown-6 provided a much more stable column than the C_{10} substituted crown. When a similar experiment was carried out with the tetradecyl crown column, no macrocycle loss was observed. The tetradecyl-18-crown-6 column was then evaluated by a similar experiment, but this time using an eluent containing 20% acetonitrile. The column was stable over 15 h even with 20% organic modifier in the eluent, as shown in Fig. 7. However, at higher concentrations of acetonitrile the crown was stripped from the column, as indicated by loss of column capacity.

Anion separations

The factors that affect anion retention in macrocycle-based chromatography can be combined to perform successful separations. In the past we have demonstrated successful gradient separations using cryptand-based columns. The crown ether columns useful characteristics as compared to the cryptand and traditional ion chromatography columns.

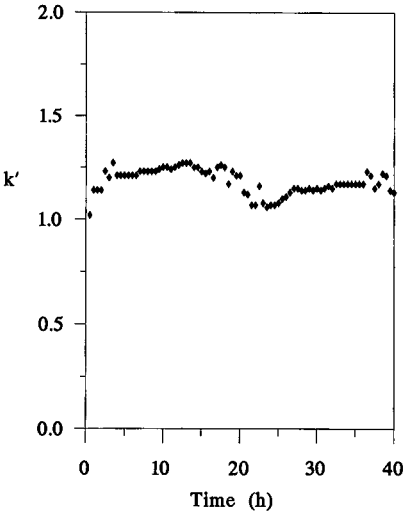

Fig. 7. Retention of NO_3^- on TD-18-crown-6 column *versus* time with 20 m*M* aqueous KOH–acetonitrile (80:20, v/v) eluent.

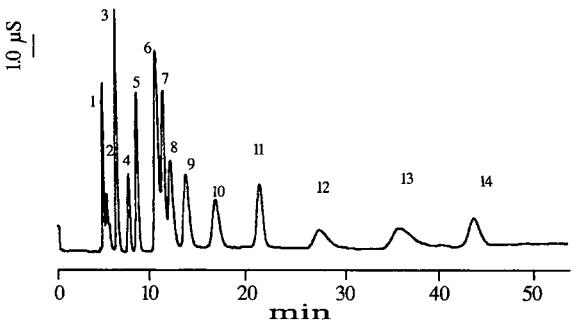

Fig. 8. Separation of 14 anions: 1 = F^-, 1.5 ppm (w/w); 2 = acetate, 10 ppm; 3 = Cl^-, 2.5 ppm; 4 = NO_2^-, 10 ppm; 5 = Br^-, 10 ppm; 6 = SO_4^{2-}, 10 ppm; 7 = NO_3^-, 10 ppm; 8 = oxalate, 10 ppm; 9 = CrO_4^{2-}, 10 ppm; 10 = phthalate, 10 ppm; 11 = I^-, 10 ppm; 12 = PO_4^{3-}, 10 ppm; 13 = citrate, 10 ppm; 14 = SCN^-, 10 ppm; on TD-18-crown-6 column with 50 m*M* aqueous KOH–acetonitrile (80:20) eluent.

The separation of a 14-anion standard on two tetradecyl-18-crown-6 columns joined in series with an eluent consisting of 50 m*M* aqueous KOH–acetonitrile (80:20) is shown in Fig. 8. Two columns were used because a single column showed insufficient capacity to effectively separate the anions. All 14 anions were well separated in less than 45 min. This separation shows several interesting differences from the separations of the same anions carried out using cryptand-based columns. Specifically, on the cryptand columns weakly retained species such as fluoride and chloride and strongly retained anions such as phthalate and thiocyanate were effectively separated only by performing capacity gradients, as shown in Fig. 9. The crown column on the other hand achieves similar separations in approximately the same time period under isocratic conditions. The column shows a lower selectivity for divalent anions as compared to the cryptand-based and traditional ion-exchange columns. This effect may be due to a lower density of exchange sites on the crown column, permitting interaction with only one monovalent exchange site at a time. The effect results in changes in elution order of the anions, with sulphate eluting before nitrate, a reversal from the usual

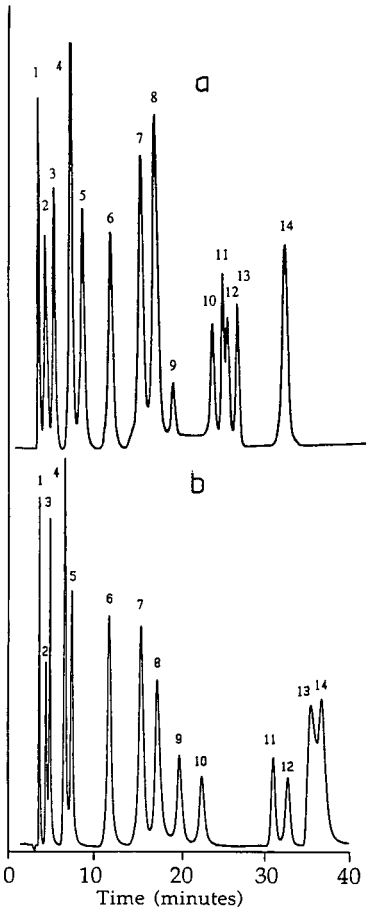

Fig. 9. Capacity gradient separation of 14 anions: 1 = F^-, 1.5 ppm (w/w); 2 = acetate, 10 ppm; 3 = Cl^-, 2.5 ppm; 4 = NO_2^-, 10 ppm; 5 = Br^-, 10 ppm; 6 = NO_3^-, 10 ppm; 7 = SO_4^{2-}, 10 ppm; 8 = oxalate, 10 ppm; 9 = CrO_4^{2-}, 10 ppm; 10 = I^-, 10 ppm; 11 = PO_4^{3-}, 10 ppm; 12 = phthalate, 10 ppm; 13 = citrate, 10 ppm; 14 = SCN^-, 10 ppm; on (a) D-2.2.2 column, with 30 m*M* NaOH–30 m*M* LiOH linear gradient for 20 min; (b) D-2.2.1 column, with 30 m*M* KOH–30 m*M* LiOH linear gradient for 20 min. From ref. 11.

elution order on the cryptand column and on traditional ion-exchange columns. The retention of the more hydrophobic anions such as thiocyanate is lower on the crown column than on the cryptand column due to the presence of acetonitrile in the eluent of the former.

Cation gradient separations are possible with the crown-based column, as with the cryptand-based columns. Such gradients, as shown in Fig. 10, result

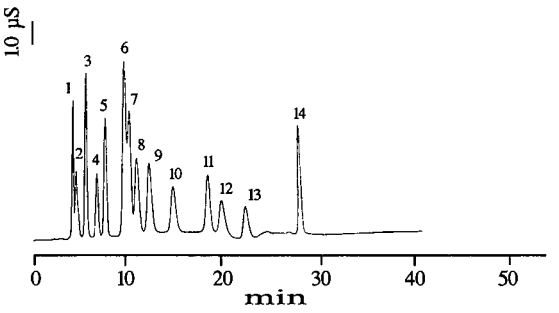

Fig. 10. Capacity gradient separation of 14 anions: 1 = F^-, 1.5 ppm (w/w); 2 = acetate, 10 ppm; 3 = Cl^-, 2.5 ppm; 4 = NO_2^-, 10 ppm; 5 = Br^-, 10 ppm; 6 = SO_4^{2-}, 10 ppm; 7 = NO_3^-, 10 ppm; 8 = oxalate, 10 ppm; 9 = CrO_4^{2-}, 10 ppm; 10 = phthalate, 10 ppm; 11 = I^-, 10 ppm; 12 = PO_4^{3-}, 10 ppm; 13 = citrate, 10 ppm; 14 = SCN^-, 10 ppm; on TD-18-crown-6 column with 50 m*M* KOH–50 m*M* NaOH (each in 20% aqueous acetonitrile) 20-min linear gradient starting at 5 min.

in faster separations than can be achieved under isocratic conditions. In this case, the eluent was changed from 50 m*M* KOH to 50 m*M* NaOH during the separation, decreasing the column capacity and speeding the elution of the anions from the column.

CONCLUSIONS

We have demonstrated the ability of an anion separator column, formed by the adsorption of a hydrophobic crown ether onto a reversed-phase column, to separate anions with widely varying anion-exchange affinities under isocratic conditions. This is possible because of the lower density of exchange sites, resulting in lower selectivity for divalent anions, and the use of an organic modifier in the eluent, speeding the elution of hydrophobic anions from the column. This system has some possible advantages over gradient systems. Gradient separations require pumps with gradient capabilities, making separations more complicated and expensive. Also, most gradients involve a change in eluent conditions, resulting in some baseline disturbance. Eluent gradients speed elution of strongly retained species from the column. However, some of this speed of elution is wasted because of the time required to re-equilibrate the column with the original eluent in preparation for the next separation. The separation on the crown column suffers none of these disadvantages, making the separations

of anions from fluoride to thiocyanate possible under isocratic conditions.

ACKNOWLEDGEMENTS

The authors would like to thank Richard Garrick for his help in obtaining experimental results and Dionex Corporation for providing funding for this research.

REFERENCES

1 R. M. Izatt, J. S. Bradshaw, S. A. Nielsen, J. D. Lamb and J. J. Christensen, *Chem. Rev.*, 85 (1985) 271.
2 R. M. Izatt, K. Pawlak, J. S. Bradshaw and R. L. Bruening, *Chem. Rev.*, 91 (1991) 1721.
3 K. Kimura, H. Harino, E. Hayata and T. Shono, *Anal. Chem.*, 58 (1986) 2233.
4 E. Blasius and K. P. Janzen, *Top. Curr. Chem.*, 98 (1981) 163.
5 E. Blasius, K. P. Janzen, W. Klein, H. Klotz, V. B. Nguyen, T. Nguyen-Tien, R. Pfieffer, G. Scholten, H. Simon, H. Stockemer and A. Toussaint, *J. Chromatogr.*, 201 (1980) 147.
6 M. Nakajima, K. Kimura and T. Shono, *Bull. Chem. Soc. Jpn.*, 56 (1983) 3052.
7 T. Iwachido, H. Naito, F. Samukawa, K. Ishimaru and K. Toei, *Bull. Chem. Soc. Jpn.*, 59 (1986) 1475.
8 M. Lauth and P. Gramain, *J. Chromatogr.*, 395 (1987) 153.
9 J. D. Lamb and P. A. Drake, *J. Chromatogr.*, 482 (1989) 367.
10 J. D. Lamb and Y. K. Ye, *J. Chromatogr.*, 602 (1992) 189.
11 J. D. Lamb, P. A. Drake and K. Woolley, in P. Jandik and R. M. Cassidy (Editors), *Advances in Ion Chromatography*, Vol. 2, Century International, Medfield, MA, 1990, p. 197.
12 J. D. Lamb and R. G. Smith, *Talanta*, 39 (1992) 923.
13 R. G. Smith, P. A. Drake and J. D. Lamb, *J. Chromatogr.*, 546 (1991) 139.
14 I. Ikeda, S. Yamamura, Y. Nakatsuji and M. Okahara, *J. Org. Chem.*, 45 (1980) 5355.

Journal of Chromatography, 640 (1993) 41–48
Elsevier Science Publishers B.V., Amsterdam

CHROMSYMP. 2706

Simultaneous separation of alkali and alkaline-earth cations on polybutadiene–maleic acid-coated stationary phase by mineral acid eluents

Lakshmy M. Nair*, Raaidah Saari-Nordhaus and James M. Anderson, Jr.

Alltech Associates, Inc., 2051 Waukegan Road, Deerfield, IL 60015 (USA)

ABSTRACT

The simultaneous separation of alkali and alkaline-earth cations on polybutadiene–maleic acid-coated silica columns can be achieved with mineral acid eluents. Simple ion-exchange retention mechanisms and the high selectivity of eluent hydronium ions towards the carboxylate group are the basis for the separation. Use of mineral acid eluents allows using this column in both single column and suppressor-based IC systems. Both types of ion chromatography systems provide detection limits in the low-ng/ml range with excellent linearity.

INTRODUCTION

Since the introduction of ion chromatography (IC) in 1975, the technique has been widely applied for analyzing various aqueous samples such as waste and drinking water, food and beverages, pharmaceuticals, metal plating solutions, etc. Alkali, alkaline earth, and ammonium cations are often found together in these samples and the demand for determining these species is increasing. Conventional IC methods for the analysis of these cations are time consuming and complicated. Alkali metal ions, ammonium and cations of several monovalent amines are separated by low capacity sulfonic acid cation-exchange columns along with dilute solutions of inorganic acids such as nitric acid or hydrochloric acid [1]. The divalent and trivalent cations, due to their affinity to the resin, will not be eluted with monovalent acid eluents. Divalent cations are separated by divalent cations such as *m*-phenylenediamine or ethylenediamine [1]. An effective, isocratic separation of both monovalent and divalent cations in one run by single column IC was not established until recently [2].

In suppressor-based IC, a gradient separation has been shown to be useful for the simultaneous separation of monovalent and divalent cations [3]. A gradient of 7 to 100% of the 40 m*M* HCl–20 m*M* DAP (2,3-diaminopropionic acid) · HCl eluent and water is able to separate monovalent lithium, sodium, ammonium and potassium, and divalent magnesium, calcium and ethylenediammonium in one run. Even though gradient elution is useful for the initial investigation of unknown samples, it faces disadvantages such as the need for a scavenger column to remove the impurities from the eluent, baseline shift due to changing eluent composition, long retention times and lengthy re-equilibration periods between runs. The overall operational cost is also higher because of the expensive eluents, regenerants and gradient pumps. Stillian *et al.* [4] reported an isocratic separation of mono/divalent cations on a sulfonic acid cation-exchange column using 60 m*M* hydrochloric aicd–6 m*M* DAP eluent by suppressed conductivity. This method simplifies the mono- and divalent cation analysis by suppressor-based IC.

A column switching (dual column) technique was

* Corresponding author.

0021-9673/93/$06.00

also reported for the simultaneous separation of both mono- and divalent cations [3]. Samples are eluted through two separate columns each optimized for the chromatography of one group of cations. The separation is accomplished by switching the eluent flowpaths between the columns. This method has several advantages compared to the gradient technique including: isocratic operation, shorter run times and no re-equilibration period between runs. However this technique requires sophisticated instrumentation and sensitivity for divalent cations is poor.

Other approaches use inorganic eluents followed by indirect UV detection. Small and Miller [5] first developed an IC system consisted of two separate columns with different cation-exchange capacities for the separation of sodium, potassium, magnesium, and calcium using copper sulfate eluent and indirect UV detection. Mayazaki *et al.* [6] reported the separation of alkali earth cations as well as magnesium and calcium on a Zipax cation-exchange column with copper sulfate eluent. However, lithium, barium and strontium are not separated using this method. Sherman and Danielson [7] used a styrene–divinylbenzene (ST-DVB)-based sulfonic acid cation exchanger along with cerium(III) as the eluent. This method is effective for the separation of sodium, potassium, magnesium and calcium. However ammonium and potassium coelute and a system peak due to cerium(III) interferes with the magnesium peak. A combination of benzylamine–citric acid–N-hydroxyethylenediamine-N,N′,N′-triacetic acid (EDTA-OH) and a combination of 1,1′-di-*n*-heptyl-4,5′-bipyridimium (DHBP) ion–citric acid along with indirect UV detection was developed by Sato [8] for the separation of mono/divalent cations. With these eluents no interference was reported, but the sensitivity for divalent cations was poor.

A new cation-exchange stationary phase made of polybutadiene–maleic acid (PBDMA) coated on silica was developed by Schomburg *et al.* [2] for the isocratic and simultaneous separation of monovalent and divalent cations by single column IC (SCIC). The separation was accomplished using different organic acid eluents and indirect electrical conductivity detection. The eluents used for the separation such as citric acid, phthalic acid, tartaric acid, salicylic acid, and pyridine-2,6-dicarboxylic acid, were all capable of complexing divalent cations. The authors report that the separation takes place due to ion-exchange and complex formation mechanisms, both of which reportedly have an important and sometimes opposing effect on the separation of cations. Yan and Schwedt [9] reported the influence of eluents containing organic complexing acids such as 1-hydroxyisobutyric, tartaric, oxalic, pyridine-2,6-dicarboxylic acid and EDTA with this column.

These authors report that the elution of monovalent ions depends on the hydronium concentration in the eluent while the elution of divalent ions is greatly influenced by the type and concentration of organic acid counter ion. The use of an EDTA–nitric acid eluent on the PBDMA-coated silica column is also reported [10]. Monovalent cations are reportedly separated through an ion-exchange mechanism while divalent cations are reportedly separated through the formation of coordination complexes with the eluent and stationary phase.

This paper focuses on the applications of PBDMA-coated silica stationary phase using non-complexing mineral acid eluents, such as hydrochloric acid and nitric acid. Contrary to previous work with this type of column, the separation appears to take place by ion-exchange mechanisms only, with no contribution from complexation mechanisms. The column's compatibility with mineral acid eluents allows it's use on both single-column and suppressor-based IC systems.

EXPERIMENTAL

Instrumentation

SCIC was performed on an Alltech modular ion chromatography system (Alltech, Deerfield, IL, USA) which consists of a Model 325 metal-free pump, Model 320 conductivity detector, Model 330 column heater and Model 9125 Rheodyne injection valve (Rheodyne, Cotati, CA, USA). The temperature of the column heater and the detector cell were maintained at 35°C. For suppressor-based IC, a Dionex BioLC System (Dionex, Sunnyvale, CA, USA) was used. A cation micromembrane suppressor (Model CMMS-11, Dionex) was used to suppress the background conductance of the eluent. All the data were recorded with a Model SP 4400 Chromjet integrator (Spectra Physics, Santa Clara, CA, USA).

Columns

Two types of carboxylic-acid based ion-exchange columns were used in this work. PBDMA coated on silica (Alltech universal cation column, 100 mm × 4.6 mm I.D.) was used to investigate retention mechanisms with a stationary phase capable of forming coordination complexes with divalent cations. A second column packed with a methacrylate-based mono-functional carboxylic acid ion-exchange material (Alltech HEMA CM, 10 μm, 150 mm × 4.6 mm I.D.) was used to investigate the separation of magnesium and calcium on a non-chelating stationary phase. A cation scavenger column (30 mm × 4.6 mm I.D.) (Alltech), packed with a high capacity sulfonic acid cation-exchange material, was connected between the pump and the injector. The scavenger column is needed only when mineral acid eluents are used. Traces of transition metals from the eluent will irreversibly retain on the analytical column causing deactivation of the column. The symptom can be identified as a decrease in retention time as the column exchange sites are tied up by the strongly bound ions. The scavenger column traps the transition metals from entering the analytical column.

Reagents

All eluents were prepared from 99.99% pure chemicals (Aldrich, Milwaukee, WI, USA) and deionized (18 mΩ) water. A Barnstead Nanopure 11 system (Sybron Barnstead, Boston, MA, USA) was used to produce the water used for eluent and sample preparation. A stock solution of 100 m*M* hydrochloric acid was prepared by diluting 99.99% hydrochloric acid in deionized water. This solution was diluted with deionized water to make 5 m*M* hydrochloric acid eluent. The 3 m*M* nitric acid eluent was prepared by diluting 99.99% nitric acid with deionized water. The suppressor regenerant (50 m*M* tetrabutyl ammonium hydroxide [TBAOH]) was prepared by diluting a 55% aqueous solution of TBAOH (Sachem, Austin, TX, USA) with deionized water. The eluents and the regenerant were prepared daily and filtered through a 0.45-μm nylon filter (Alltech).

Sample preparation

All samples except coffee and soil extracts were diluted 10 times with deionized water before injection. The coffee and the soil extracts were filtered through a 0.2-μm Anotop IC syringe filter (Alltech) before injection.

RESULTS AND DISCUSSION

Conventional cation chromatography using sulfonic acid cation-exchange columns requires either two separate conditions or addition of diamino propionic acid to mineral acid eluent for the analysis of mono/divalent cations. A low capacity cation-exchange column along with a dilute acid eluent containing hydrogen (hydronium) ions is used for the separation of monovalent cations and an eluent containing a divalent cation such as ethylenediamine or *m*-phenylenediamine, is used for the separation of divalent cations. An eluent containing hydrochloric acid and diamino propionic acid has been found successful to separate both groups of cations in one run using these columns [4].

The cation-exchange stationary phase, made of PBDMA-coated silica, is capable of achieving the simultaneous, isocratic separation of lithium, sodium, ammonium, potassium, rubidium, magnesium, calcium and barium [2]. The eluents used for the separation are citric acid, tartaric acid, phthalic acid, salicylic acid, 1-hydroxyisobutyric acid, pyridine-2,6-dicarboxylic acid, oxalic acid and ethylene diamine tetraacetic acid, all of which are capable of forming coordination complexes with divalent cations. The monovalent cations are reportedly separated by IC mechanism while the divalent cations are reportedly separated by ion exchange and the formation of coordination complexes with the maleic acid stationary phase and the organic acid eluent.

In this report we will show the separation of mono/divalent cations using mineral acid eluents such as nitric and hydrochloric acid. Because the anionic counter ions of these mineral acids do not form coordination complexes with the divalent cations in this study, we believe the separation is based only on ion-exchange. Complexing eluents are not required. The compatibility of this column with mineral acid eluents opens the possibility of using the column with suppressor-based IC.

Separation by SCIC

Nitric acid eluent. The column performance with

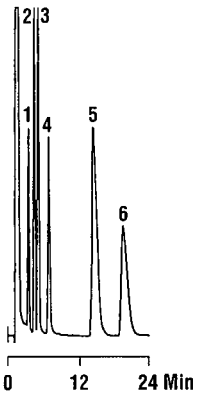

Fig. 1. Simultaneous SCIC separation of mono/divalent cations using 3 m*M* nitric acid. Flow-rate: 1.0 ml/min; column: Alltech universal cation (100 mm × 4.6 mm I.D.); detector: conductivity (negative polarity), 1.0 μS full scale; injection volume: 100 μl. Peak identification: 1 = lithium (0.2 μg/ml), 2 = sodium (1.5 μg/ml), 3 = ammonium (1.5 μg/ml), 4 = potassium (2.5 μg/ml), 5 = magnesium (2 μg/ml), 6 = calcium (2 μg/ml).

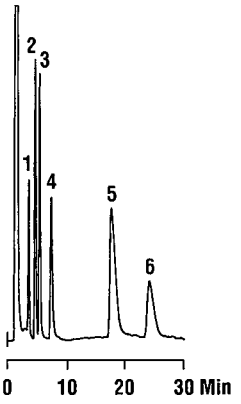

Fig. 2. Simultaneous SCIC separation of mono/divalent cations using 5 m*M* hydrochloric acid. Flow-rate: 1.0 ml/min; column: Alltech universal cation (100 mm × 4.6 mm I.D.); detector: conductivity (negative polarity), 1.0 μS full scale; injection volume: 100 μl. Peak identification: 1 = lithium (0.2 μg/ml), 2 = sodium (1.5 μg/ml), 3 = ammonium (1.5 μg/ml), 4 = potassium (2.5 μg/ml), 5 = magnesium (2 μg/ml), 6 = calcium (2 μg/ml).

nitric acid eluent and SCIC is demonstrated in Fig. 1. Nitric acid is the most common eluent used for the monovalent cation analysis by SCIC when sulfonic acid cation-exchange columns are used. However, the separation of divalent cations on these columns is not possible with this eluent due to the strong affinity of the divalent cations towards the sulfonic acid functional groups. By using a carboxylate-functionalized PBDMA-coated silica column, both groups of cations can be separated isocratically with nitric acid eluents.

Hydrochloric acid eluent. Fig. 2 shows the separation of lithium, sodium, ammonium, potassium, magnesium and calcium on a silica based PBDMA stationary phase using 5 m*M* hydrochloric acid eluent by SCIC. The separation of mono/divalent cations including rubidium and barium are shown in Fig. 3. The sensitivity for monovalent rubidium and divalent barium are quite good. The separation of ethanolamines using PBDMA-coated silica is shown in Fig. 4. Chromatograms of some real world samples are shown in Fig. 5A–C.

In SCIC, indirect conductivity is used for cation analysis. The equivalent conductance of the sample cations are lower than the equivalent conductance of the hydronium ion in the eluent, hence the sample ions are detected as a decrease in conductance. This decrease in conductance is proportional to the concentration of the sample solute cations. The peaks appear positive in the figures by reversing the polarity of the detector.

Separation by suppressor-based IC

Hydrochloric acid is the most common eluent used for monovalent cation analysis by suppressor-

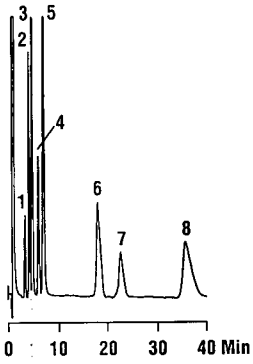

Fig. 3. Simultaneous SCIC separation of mono/divalent cations including rubidium and barium using hydrochloric acid. Chromatographic conditions as in Fig. 2. Peak identification: 1 = lithium (0.2 μg/ml), 2 = sodium (1.5 μg/ml), 3 = ammonium (1.5 μg/ml), 4 = potassium (2.5 μg/ml), 5 = rubidium (2 μg/ml), 6 = magnesium (2 μg/ml), 7 = calcium (2 μg/ml), 8 = barium (5 μg/ml).

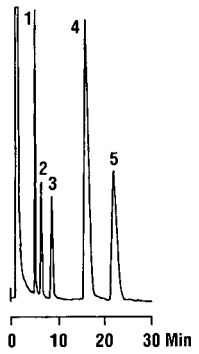

Fig. 4. SCIC separation of ethanolamines using hydrochloric acid. Chromatographic conditions as in Fig. 2. Peak identification: 1 = monoethanolamine, 2 = diethanolamine, 3 = triethanolamine, 4 = magnesium, 5 = calcium.

based IC. However, this eluent is not capable of eluting the divalent cations when conventional sulfonic acid cation-exchange columns are used. With the PBDMA-coated silica stationary phase, hydrochloric acid eluent is able to separate both mono- and divalent cations in one isocratic run.

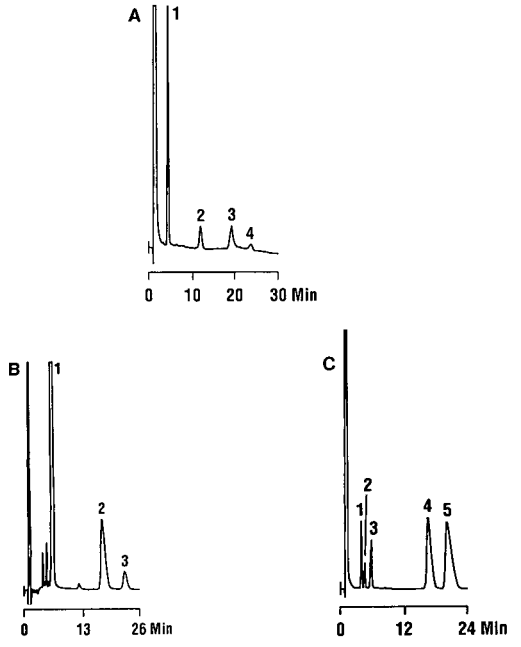

Fig. 5. Cation separations using hydrochloric acid eluent by SCIC. Chromatographic conditions are as in Fig. 2. (A) L-Carnitine and choline in vitamins. Peak identification: 1 = sodium, 2 = L-carnitine, 3 = choline, 4 = calcium. (B) Cations in coffee extract. Peak identification: 1 = potassium, 2 = magnesium, 3 = calcium. (C) Cations in soil extract. Peak identification: 1 = sodium, 2 = ammonium, 3 = potassium, 4 = magnesium, 5 = calcium.

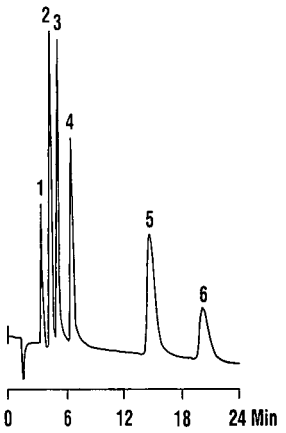

Fig. 6. Simultaneous separation of mono- and divalent cations by suppressor-based IC. Eluent: 5 m*M* hydrochloric acid; flow-rate: 1.0 ml/min; column: Alltech (100 mm × 4.6 mm I.D.); detector: suppressed conductivity, 1.0 μS full scale; injection volume: 100 μl; regenerant: 50 m*M* TBAOH; flow-rate: 7 ml/min. Peak identification: 1 = lithium (0.2 μg/ml), 2 = sodium (1.5 μg/ml), 3 = ammonium (1.5 μg/ml), 4 = potassium (2.5 μg/ml), 5 = magnesium (2 μg/ml), 6 = calcium (2 μg/ml).

The separation of mono/divalent cations on PBDMA-coated silica column using a suppressor-based IC system is shown in Fig. 6. The suppressor-based cation IC system consists of a suppressible eluent, a column that is capable of separating the cations, a micromembrane suppressor in the hydroxide form and a regenerant solution to regenerate the suppressor. The cation micromembrane suppressor is used to suppress the background conductivity and to enhance the sensitivity of the analytes. 5 m*M* hydrochloric acid is used as the eluent and 50 m*M* TBAOH is used for regenerating the suppressor. When the hydrochloric acid eluent passes through the suppressor, chloride in the eluent is exchanged with hydroxide which reacts with hydronium ions to form water. Conversion of eluent to water reduces background conductivity to near zero. The sample ions are converted to corresponding aqueous hydroxide salt solutions which have much higher conductance than the suppressed eluent; hence they are detected as positive peaks.

Analysis of some real samples such as tap water, well water, lemonade and cola using suppressor-

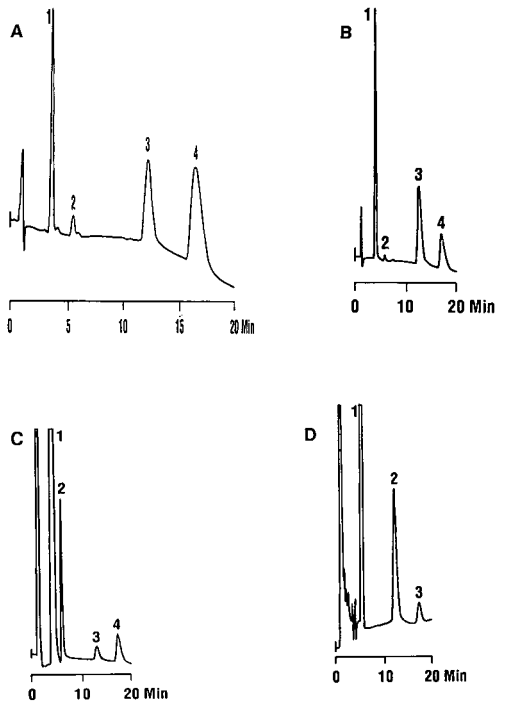

Fig. 7. Cation separations using hydrochloric acid eluent by suppressor-based IC. Chromatographic conditions as in Fig. 6. (A) Cations in tap water. Peak identification: 1 = sodium, 2 = potassium, 3 = magnesium, 4 = calcium. (B) Cations in well water. Peak identification: 1 = sodium, 2 = potassium, 3 = magnesium, 4 = calcium. (C) Cations in lemonade. Peak identification: 1 = sodium, 2 = potassium, 3 = magnesium, 4 = calcium. (D) Cations in cola. Peak identification: 1 = potassium, 2 = magnesium, 3 = calcium.

based IC are shown in Fig. 7A–D respectively. No chromatographic interferences were observed and filtering the samples was not necessary.

The background conductance on the suppressor-based system was not stable from day to day. This problem could be due to the quality of the regenerant and the deionized water used for the eluent preparation. The background conductance of the eluent was greatly influenced by the flow-rate of the regenerant through the micromembrane suppressor and the concentration of the regenerant solution. If the flow-rate and the concentration are too low suppression will not be quantitative and background conductance will increase. However, if the flow-rate or concentration is too high permeation of the regenerant solution through the micromembrane may occur [11]. A concentration of 50 m*M* TBAOH solution, at a flow-rate of 7 ml/min was adequate for the work presented here.

Detection limits and detection linearity of cations by SCIC and suppressor-based IC

The detection limits (calculated as a signal-to-noise ratio of 3) obtained for mono/divalent cations using both types of IC systems (hydrochloric acid eluent) based on a 100-μl injection volume are listed in Table I. SCIC gave slightly better detection limits; however, both types of IC are capable of separating and detecting cations at a very low concentration levels. The higher detection limits for cations for SCIC can be explained by the greater change in conductance for SCIC than for the suppressor-based IC [1]. For example, the equivalent conductance for eluent is $H^+ + Cl^- = 350 + 76 = 426$ and for sample peak is $Li^+ + Cl^- = 39 + 76 = 115$, a net signal of 311. In suppressor-based IC, hydroxide is the counter ion that accompanies the cations. Based on an equivalent concentration, the lithium peak will have an equivalent conductance of 237 ($Li^+ + OH^- = 39 + 198$). A net signal of 237 is observed against water, with equivalent conductance near zero. The higher signal observed in SCIC is partially offset by increased noise associated with high-conductivity of the mineral acid eluent. Close linear dependence between the peak area and the concentration of the ions over a wide range of concentrations are observed for both SCIC and suppressor-based IC.

TABLE I

DETECTION LIMITS (ng/ml) FOR MONO/DIVALENT CATIONS USING SCIC AND SUPPRESSOR-BASED IC

Column: universal cation (100 mm × 4.6 mm I.D.).

Cations	SCIC (HCl eluent)	Suppressor-based IC (HCl eluent)
Lithium	1	3
Sodium	2	3
Ammonium	3	4
Potassium	8	8
Magnesium	4	7
Calcium	3	9

When inorganic acid eluents are used, traces of transition metals from the eluent may irreversibly retain on the analytical column causing column deactivation. The symptom can be identified by a gradual decrease in retention time with each run. In order to protect the colum from deactivation, a cation scavenger column packed with a high capacity sulfonic acid cation-exchange material was connected between the pump and the injector. This column traps traces of transition metals in the eluent before they reach the separator column. Column deactivation due to transition metals in the eluent does not occur when complexing eluents are used. Complexing eluents interact with the metals and elute them from the column. This is one advantage of using complexing eluents for cation analysis on this stationary phase.

Separation mechanisms on PBDMA stationary phase

Earlier studies on PBDMA stationary phases report that the separation of divalent cations on this column using complexing eluents are based on both ion-exchange and complex formation with the stationary phase and eluent anions. Monovalent cations are reportedly separated by ion exchange.

The data presented in this report shows that complexation between the divalent cations and the eluent anion is not necessary to elute divalent cations from the column. The separation of divalent cations using nitric and hydrochloric acid is an example for this. We believe that ion-exchange retention mechanisms coupled with the high selectivity of the hydronium ions towards the carboxylate group provides the significant driving force for the separation [12]. The ion-exchange selectivity for carboxylic acid ion exchangers is significantly different than for sulfonic acid ion exchangers traditionally employed for cation analysis. More specifically, hydronium ions have very high affinity for carboxylic acid ion exchangers, even exceeding the affinity of divalent magnesium and calcium. By contrast, hydronium ions are only weekly attracted to sulfonic acid ion-exchange groups with far less affinity for the support than the divalent cations. The order of selectivity of the analyte cations is identical on both carboxylic and sulfonic acid stationary phases. The high ion-exchange affinity of hydronium ions for the PBDMA stationary phase allows elution of divalent cations from this type of column using dilute acid eluents. Complexation with eluent anions is not necessary. Elution of divalent cations from sulfonic acid ion-exchange columns by dilute acid eluents is not possible due to the low selectivity of hydronium ions with this support.

The successful use of mineral acid eluents demonstrates conclusively that complex formation with eluent anions is not necessary to elute divalent cations from PBDMA stationary phases. However, it does not address the question of whether formation of coordination complexes between divalent cations and the PBDMA stationary phase is necessary for retention of divalent cations on PBDMA columns. Because the maleic acid functional group on the PBDMA polymer can act as both an ion exchanger and a metal chelator, ion exchange and/or chelation may be responsible for retention of those cations capable of forming complexes with maleic acid. Ion exchange alone must be responsible for retention of the alkali metal cations and ammonium because these cations do not form complexes with maleic acid.

A second type of carboxylate-based ion-exchange column (HEMA CM, 150 mm × 4.6 mm I.D.) was used to investigate the importance of chelation as a retention mechanism for divalent cations. The HEMA packing material consists of highly cross-linked hydroxyethylmethacrylate particles functionalized with carboxymethyl (CM) ion-exchange groups. Unlike the maleic acid ion-exchange groups on the PBDMA support, the carboxymethyl ion-exchange groups on the HEMA support will not form stable metal complexes with calcium or magnesium. As demonstrated in Fig. 8, calcium and magnesium are retained and well resolved on the HEMA CM column using dilute hydrochloric acid as the eluent. Consequently, retention of magnesium and calcium on the HEMA CM column must be due to ion exchange alone. While this result does not rule out the possibility that coordination complexes are formed between divalent cations and the PBDMA stationary phase, it does demonstrate that formation of such complexes is not critical to the separation.

We believe the above data strongly suggests that the separation of alkali and alkaline earth cations on PBDMA stationary phases takes place predominantly, if not entirely, by ion-exchange mecha-

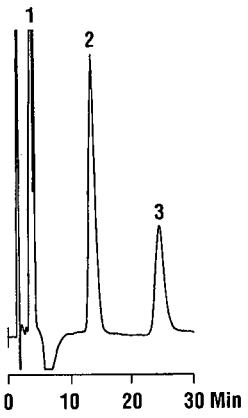

Fig. 8. Analysis of cations on HEMA CM stationary phase. Eluent: 2 m*M* hydrochloric acid; flow-rate: 1 ml/min; column: HEMA CM 10 μm (150 mm × 4.6 mm I.D.); detector: conductivity (negative polarity), 1.0 μS full scale; injection volume: 100 μl. Peak identification: 1 = monovalent cations, 2 = magnesium, 3 = calcium.

nisms, fueled by the high selectivity of hydronium ions for the carboxylic acid functional groups.

ACKNOWLEDGEMENT

The authors greatly appreciate Dr. Ravichandran (Boehringer Mannheim, Indianapolis, IN, USA) for his work on the suppressor-based IC system.

REFERENCES

1 D. T. Gjerde and J. S. Fritz, *Ion Chromatography*, Huthig, New York, 2nd ed., 1987, Ch. 9.
2 G. Schomburg, P. Kolla and M. W. Laubli, *Am. Lab.*, 21 (1989) 92.
3 R. D. Rocklin, M. A. Rey, J. R. Stillian and D. L. Campbell, *J. Chromatogr. Sci.*, 27 (1989) 474.
4 J. Stillian, C. Phol, A. Woodruff and C. R. Devasa, presented at the *Pittsburgh Conference on Analytical Chemistry, New York, 1990*, paper No. 628.
5 H. Small and T. E. Miller, *Anal. Chem.*, 59 (1982) 490.
6 M. Mayazaki, K. Hayakawa and S. Choi, *J. Chromatogr. Sci.*, 323 (1985) 443.
7 J. H. Sherman and N. D. Danielson, *Anal. Chem.*, 59 (1987) 490.
8 H. Sato, *J. Chromatogr. Sci.*, 469 (1989) 339.
9 D. Yan and G. Schwedt, *Anal. Chem.*, 338 (1990) 149.
10 *Ion Analysis Notes*, Vol. 3, No. 1, Millipore Corporation, Waters Chromatography, Milford, MA, 1990, p. 11.
11 P. Pastore, A. Boaretto, I. Lavagnini and A. Diop, *J. Chromatogr. Sci.*, 591 (1992) 219.
12 *Bio-Rex 70 Weakly Acidic Cation Exchange Resin Instruction Manual*, Bio-Rad Laboratories, Herculies, CA, 1990.

Journal of Chromatography, 640 (1993) 49–56
Elsevier Science Publishers B.V., Amsterdam

CHROMSYMP. 2666

Anion chromatography on hydroxyethyl methacrylate-based sorbents

Ivan Vinš*

Tessek Ltd. Prague, Křižovnická 3, 110 00 Prague 1 (Czech Republic)

Raaidah Saari-Nordhaus

Alltech Associates, Inc., 2051 Waukegan Road, Deerfield, IL (USA)

ABSTRACT

The selectivity of sorbents plays an important role in the design of ion chromatographic separations. The selectivity of the hydroxyethylmethacrylate-based sorbent Tessek Separon HEMA-S 1000 Q-L was compared with those of other commonly used sorbents and the role of the eluent charge was investigated. The selectivity of this sorbent was found to be satisfactory for most commonly used ion chromatographic detection modes, including indirect photometry and both suppressed and non-suppressed conductivity detection.

INTRODUCTION

Ion chromatography (IC) is a widely used technique and the methods used and applications are described in several books [1–3] and reviews [4–6]. An interesting aspect of anion chromatography is the selectivity of separation. An understanding of the rules that influence selectivity is essential for optimizing the conditions for difficult separations. The most important factors influencing selectivity are eluent anion, its charge, eluent concentration and pH, as well as sorbent matrix, functional group and its content.

The selectivity of separations in anion chromatography was shown to be determined essentially by the above factors. The influence of the character of the functional group [7–9], spacer length [10] and character of the support [11] on selectivity has been studied earlier. Retention models for ion chromatography were evaluated and only partial agreement was found between theoretical models and experimental data [12,13]. There is still much to be investigated, the problem of the selectivity of mono- and divalent anions having been neglected so far.

The potential of the hydroxyethyl methacrylate-based Tessek Separon HEMA-S 1000 Q-L sorbent (Tessek, Prague, Czech Republic) in Alltech universal anion columns for both suppressed and single-column ion chromatography has been extensively studied by Saari-Nordhaus and co-workers [14–16]. During the development and production of this sorbent, an extreme dependence of sorbent selectivity on minor variations in the matrix properties was observed. In this work, the selectivity of this sorbent was compared with those of other common sorbents based on published data [12]. The influence of the matrix surface character and eluent charge on selectivity was also studied. Utilization of selectivity changes is demonstrated in several applications.

THEORY

Equations describing retention and selectivity in IC can be derived from ion-exchange equilibrium and chromatographic theory [8,17,18] for separa-

* Corresponding author.

0021-9673/93/$06.00

tion of anions A^{x-} and B^{y-} on a sorbent with functional groups R^+ with eluent anion E^{z-}:

$$\overline{x(-R_z^+E^{z-})} + zA^{x-} \rightleftharpoons \overline{z(-R_x^+A^{x-})} + xE^{z-} \quad (1)$$

$$\overline{y(-R_z^+E^{z-})} + zB^{y-} \rightleftharpoons \overline{z(-R_y^+B^{y-})} + yE^{z-} \quad (2)$$

where the overbars refer to species bound in the stationary phase. The capacity factor, k_A, with certain assumptions, can be expressed in the form

$$k_A = K_{xE}^{zA\,1/x}\left(\frac{Q_g/z}{c_E}\right)^{x/z}\frac{m_s}{V_m} \quad (3)$$

After combining eqns. 1 and 2, an equation for the dependence of the separation factor on the capacity factor can be derived [8]:

$$\alpha_{A,B} = (K_{xB}^{yA})^{1/x} k_A^{(x-y)/x}\left(\frac{V_m}{m_s}\right)^{(x-y)/x} \quad (4)$$

where K_{xB}^{yA} and K_{xE}^{zA} are selectivity coefficients, $\alpha_{A,B}$ is the separation factor, Q_g is the specific ion-exchange capacity of the sorbent, c_E is the eluent concentration and m_s and V_m are the mass of sorbent and mobile phase volume in column, respectively.

In logarithmic coordinates, linear dependences of capacity factor on eluent concentration or sorbent capacity and of selectivity factor on capacity factor can be derived from eqn. 3. Based on eqn. 4, diagrams for the dependence of selectivity coefficient on chloride capacity factor are well suited for comparison of the selectivities of different sorbents. The slopes of these dependences should be related to the charges of the eluting and eluted anions. Nevertheless, these models do not consider the common situation where both eluent and analyte anions can be present in different ionic states. For the situation where multiple eluent anions are present, equations were derived by Hoover [19] and used by Jenke and Pagenkopf [13,20] and Maruo *et al.* [21]. However, simplifying assumptions had to be made and the fit of the models was usually unsatisfactory. Consideration of all the equilibria present (dissociation of eluent anion, dissociation of analyte anion, dissociation of sorbent) will give a very complicated system of equations. For this reason, only a qualitative approach was adopted in this study.

EXPERIMENTAL

Instrumentation

The liquid chromatograph used for selectivity measurements consisted from Model 1350 soft start pump (Bio-Rad Labs., Richmond, CA, USA), a Model 7125 injection valve (Rheodyne, Cotati, CA, USA), and a Model 731.87 spectrophotometer (Knauer, Berlin, Germany). An APEX version 2.0 PC computer-based chromatographyic integrator (DataApex, Prague, Czech Republic) was used for data collection and evaluation. A modular IC system, consisting of Model 325 HPLC pump, Model 330 column heater and Model 320 conductivity detector (Alltech, Deerfield, IL, USA), a Model 9125RV injection valve (Rheodyne) and a Model 4400 ChromJet integrator (Spectra-Physics, Santa Clara, CA, USA), was employed.

Columns

Compact glass cartridge (CGC) columns (70 or 150 × 3.3 mm I.D.) were packed by an aqueous slurry technique in the laboratory and used with an appropriate column holder (Tessek). The sorbents used were Tessek Separon HEMA-S 1000 Q-L (10 μm) (Tessek) with a 0.15 mmol/g ion-exchange capacity and an experimental batch of Tessek Separon HEMA-BIO 1000 Q-L (Tessek) with a 0.1 mmol/g ion-exchange capacity. PEEK Alltech Universal Anion columns (150 × 4.6 mm I.D.) (Alltech) packed with the first sorbent were used in applications.

Eluents and analytes

Potassium hydrogenphthalate (analytical-reagent grade) (Merck, Darmstadt, Germany) and distilled, deionized water were used for the preparation of eluents. Phthalic acid was used for the preparation of eluents with pH 4.0. The pH was adjusted with sodium hydroxide (analytical-reagent grade) (Merck) with the use of an Acidimeter 333 (Druopta, Prague, Czech Republic) equipped with a Crytur 01-29 combined glass pH electrode (Monokrystaly, Turnov, Czech Republic) unless stated otherwise. The eluents were filtered before use through a Schleicher & Schüll (Dassel, Germany) ME 25 membrane filter with 0.45-μm pores. Each column was equilibrated with eluent for several hours. EZ-LUTE buffer concentrates (Alltech) were used for the preparation

of other eluents; the pH was adjusted with lithium hydroxide.

As analytes, typical inorganic anions were selected. Fluoride, chloride, bromide and iodide represented the halides, nitrite and nitrate monovalent oxoanions, sulphate and thiosulphate divalent ions and sulphite and phosphate ions with charge dependent on pH.

Analytical-reagent grade salts were used. Stock standard solutions containing 1000 mg/l of anion were prepared and appropriate working standard solutions were prepared by dilution with distilled, deionized water. Sodium hydrogensulphite was dissolved in 0.2% formaldehyde solution owing to its instability in aqueous solution [22].

RESULTS AND DISCUSSION

Two types of selectivity can be distinguished in IC [10]: selectivity for anions of the same charge and that for anions with different charges. The selectivity of a sorbent for the separation of anions with the same charge can be compared on the basis of the separation factor (proportional to the selectivity coefficient). The elution sequence of monovalent anions $F^- < Cl^- < NO_2^- < Br^- < NO_3^- < I^-$ does not vary, with only slight shifts in the relative retentions of the halides and oxoanions. The sorbents studied did not show the problems with the resolution of the NO_2^-–Br^- and Br^-–NO_3^- pairs that sometimes occur on agglomerated sorbents. The various sorbents are compared on basis of their separation factors for nitrate–chloride in Fig. 1.

For the separation of anions with different charges, the separation factor is a function of retention and therefore it could not be directly compared. The graphs of dependences according to eqn. 4 can serve for an illuminating comparison of the selectivities of mono- and divalent ions.

Five commercially available and one research sample sorbent (Table I) were compared for selectivity in phthalate eluent, based on measured [HEMA-S 1000 Q-L (Table II) and HEMA-BIO 1000 Q-L (Table III)] and literature [12,20] data. Relative retentions at pH 6.0 are plotted in Fig. 2 against the capacity factor of chloride to provide a correction for different sorbent capacities. At pH 6.0 with 65% phthalate as divalent anion [20] the silica-based Vydac 302 IC shows very low selectivity for

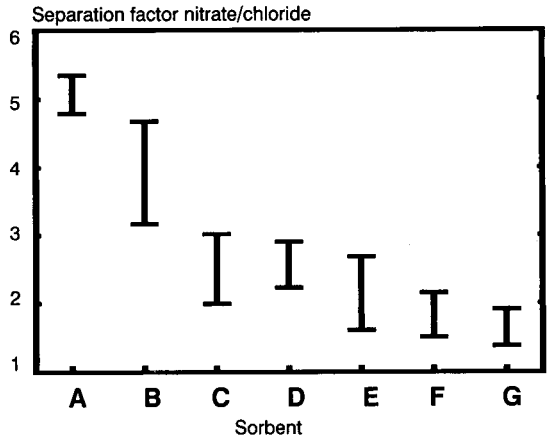

Fig. 1. Comparison of separation factors of nitrate and chloride on different sorbents. The data based on refs. 12 and 20 and this work were measured in phthalate eluents at concentrations from 1 to 4 mmol/l and pH 4.0–6.0 (for the Dionex column pH 8.5 was adjusted with 4 m*M* borate). (A) Dionex AS-1 agglomerated sorbent; (B) HEMA-BIO 1000 Q-L; (C) HEMA-S 1000 Q-L; (D) Waters IC Pak A; (E) Hamilton PRP-X-100; (F) Wescan 269-001 silica-based sorbent; (G) Vydac 302 IC.

monovalent and a high affinity for divalent anions. The sulphate is eluted after iodide even at very low capacity factors of chloride, where fluoride is incompatible with the silica matrix. The polystyrene-based PRP-X 100 resin has a similar character, but the selectivity for monovalent ions is higher and sulphate is usually eluted between nitrate and iodide. The IC Pak A and HEMA-S 1000 Q-L hydroxyethyl methacrylate-based sorbents behave in an almost identical manner with high selectivity for monovalent anions and sulphate eluting before or after nitrate. HEMA-BIO 1000 Q-L shows an extremely high selectivity for monovalent anions and a low retention for sulphate. The agglomerated sorbent AS-1 shows a high selectivity for nitrate, but sulphate is eluted before or after nitrate. Limited data were available for this column; the pH was adjusted by addition of 4 m*M* borate. The published hydrogensulphite retention times [12] are almost identical with those reported for sulphate, and so are not labelled in Fig. 2. Extreme care must be used to avoid the oxidation of hydrogensulphite to sulphate.

The character of the matrix exhibited a larger effect than different substituents on the amino functional group. When an additionally hydrophilized HEMA-BIO matrix was used, the retention of

TABLE I

COMPARISON OF SORBENT PROPERTIES

Sorbent	Matrix	Capacity
Hamilton PRP-X 100	Styrene–divinylbenzene	0.19 mmol/g
Vydac 302 IC	Silica	0.1 mmol/g
Waters IC Pak A	Methacrylate	0.03 mmol/ml
HEMA-S 1000 Q-L	Hydroxyethyl methacrylate	0.15 mmol/g
HEMA-BIO 1000 Q-L	Hydroxyethyl methacrylate	0.1 mmol/g
Dionex AS-1	Styrene–divinylbenzene (agglomerated)	0.05 mmol/g

TABLE II

DEPENDENCE OF RETENTION TIMES (min) ON ELUENT CONCENTRATION AND pH

Column, HEMA-S 1000 Q-L (10 μm) (70 × 3.3 mm I.D.); eluent, hydrogenphthalate; flow-rate, 0.5 ml/min; indirect UV detection.

Ion	Eluent concentration (mmol/l)								
	1 (pH 4)	2 (pH 4)	4 (pH 4)	1 (pH 5)	2 (pH 5)	4 (pH 5)	1 (pH 6)	2 (pH 6)	4 (pH 6)
Fluoride	3.76	2.76	2.00	2.45	1.80	1.48	2.05	1.75	1.28
Chloride	7.58	5.14	3.45	4.75	3.35	2.46	3.81	3.21	2.18
Bromide	13.36	8.68	5.53	8.51	5.78	4.06	6.78	5.65	3.63
Iodide	41.06	26.01	15.16	27.76	18.48	12.45	21.52	18.97	10.86
Nitrite	10.19	6.65	4.04	7.03	4.76	3.38	5.76	4.57	3.25
Nitrate	17.13	11.01	6.85	11.23	7.51	5.27	9.09	7.30	4.91
Sulphite	5.38	3.71	2.52	3.31	2.31	1.81	2.74	2.18	1.64
Sulphate	79.91	30.16	13.76	23.30	10.49	5.43	12.77	7.22	3.71
Thiosulphate	148.00	64.26	24.87	43.32	20.10	9.70	25.36	14.42	6.75
Phosphate	3.85	2.78	1.94	2.44	1.76		2.54	1.98	1.36
Void	0.66	0.69	0.68	0.66	0.72	0.74	0.68	0.79	0.75
System	52.32	29.76	16.05	43.06	26.16	15.54			19.66

TABLE III

DEPENDENCE OF RETENTION TIMES (min) ON ELUENT CONCENTRATION AND pH

Column, HEMA-BIO 1000 Q-L (10 μm) (70 × 3.3 mm I.D.); eluent, hydrogenphthalate; flow-rate, 0.5 ml/min; indirect UV detection.

Ion	Eluent concentration (mmol/l)								
	1 (pH 4)	2 (pH 4)	4 (pH 4)	1 (pH 5)	2 (pH 5)	4 (pH 5)	1 (pH 6)	2 (pH 6)	4 (pH 6)
Fluoride	2.83	2.07	1.50	1.88	1.48	1.23	1.71	1.43	1.18
Chloride	6.60	4.41	2.84	4.35	3.03	2.24	4.03	3.03	2.27
Bromide	14.70	9.53	5.66	10.37	6.72	4.61	10.02	7.71	4.46
Iodide	70.99	46.43	25.41	58.30	33.60	22.75	57.36	46.85	24.21
Nitrite	9.43	6.06	3.98	6.93	4.54	3.20	6.59	5.04	3.34
Nitrate	21.09	13.01	7.53	15.40	9.52	6.40	16.00	11.59	6.68
Sulphite	3.98	2.76	1.88	2.50	1.91	1.50	2.22	1.55	1.47
Sulphate	55.11	24.84	8.77	15.61	7.55	4.02	9.74	5.32	2.88
Thiosulphate		92.05	24.98	60.10	27.53		40.48	21.59	9.31
Phosphate	2.97	2.12	1.53	1.93	1.51	1.21	2.05	1.48	1.23
Void	0.67	0.69	0.68	0.65	0.72	0.73	0.67	0.74	0.74
System	31.36	17.73	10.39		17.80	9.88	45.72		16.60

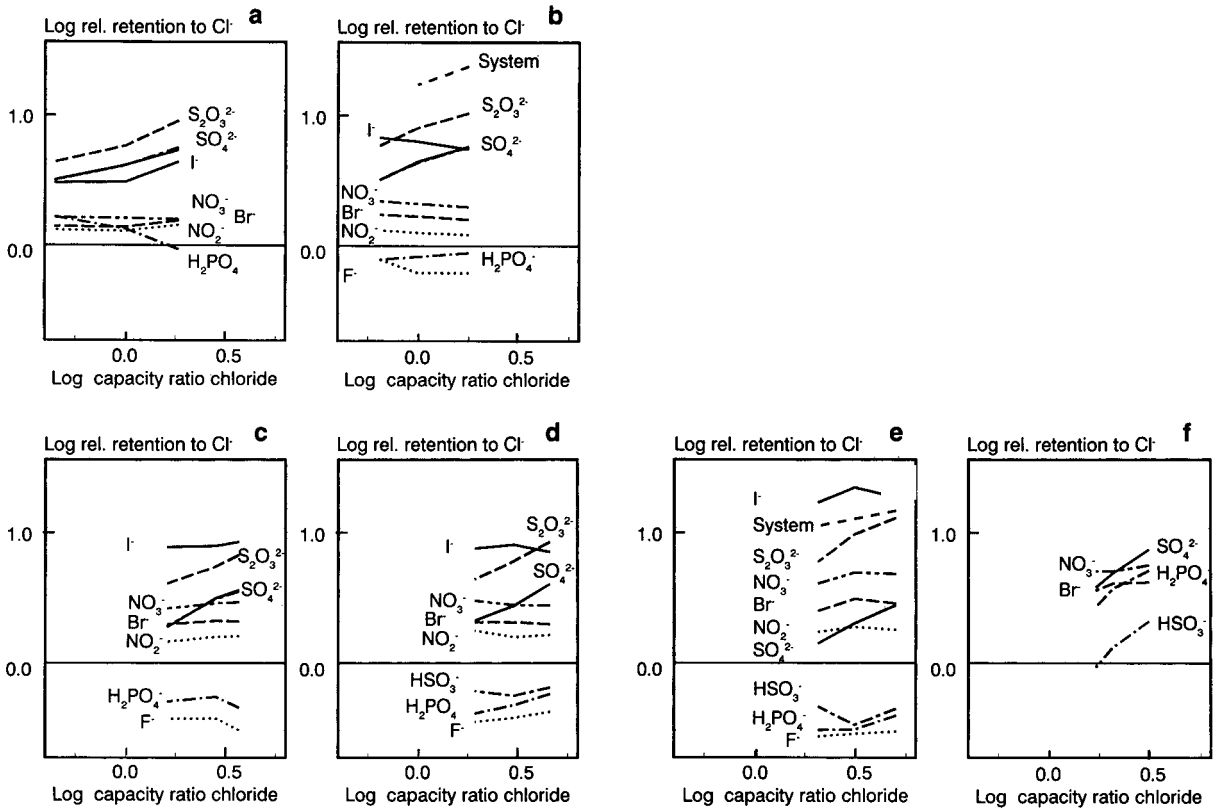

Fig. 2. Relative retention of anions to chloride plotted against capacity factor of chloride in phthalate eluent (pH 6.0) (concentrations 1.0, 2.0 and 4.0 mmol/l). (a) Vydac 302 IC; (b) Hamilton PRP-X-100; (c) Waters IC Pak A; (d) HEMA-S 1000 Q-L; (e) HEMA-BIO 1000 Q-L; (f) Dionex AS-1 (pH 8.5, adjusted with 4 m*M* borate).

divalent (sulphate) anions decreased dramatically, so sulphate eluted before nitrate and sometimes even with chloride. Both the HEMA Q-L have the same functional group and differ only in the matrix treatment. The HEMA-S matrix is additionally cross-linked with monomers, whereas HEMA-BIO is treated with epichlorohydrin and hydrolysed. HEMA-BIO exhibits a higher hydrophilicity towards proteins, but the increase in polarity for small molecules such as toluene (in methanol–water) or benzyl alcohol (in water) is very small when compared with the difference from hydrophilized silica sorbents. Also, one would expect doubling of the content of hydroxyl groups due to the hydrophilization, but in reality there is a decrease of about 30%. The explanation probably lies in the polymer structure of HEMA surface: epichlorohydrin apparently causes some cross-linking of the polymer chains, resulting in more hydroxyl groups oriented to the solvent (increasing the hydrophilicity for proteins) but not changing significantly the polarity for small molecules, which penetrate into the polymer matrix.

The influence of pH is demonstrated in Fig. 3, where the separation factors of nitrate–chloride and sulphate–chloride are plotted against the capacity factor of chloride. Similar pictures are obtained with all the other sorbents compared. The selectivity for monovalent ions increases and the retention of divalent anions decreases in all instances with increasing pH (increase in the ratio of divalent phthalate to monovalent hydrogenphthalate). It can be seen from Fig. 3 that at the same k_{Cl^-} the retention of sulphate will decrease with increase in pH and thus in proportion to the divalent phthalate in the eluent. The divalent phthalate is therefore more efficient eluent for divalent sulphate than for monovalent ions.

This can be confirmed by the difference in selec-

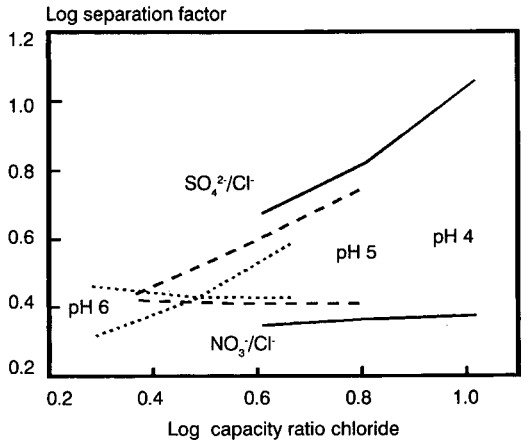

Fig. 3. Separation factor of nitrate and sulphate to chloride plotted against capacity factor of chloride in phthalate eluent at different pH values on a HEMA-S 1000 Q-L (10 μm) column (70 × 3.3 mm I.D.).

tivity observed when using mono- and divalent eluents of comparable eluting power, *e.g.*, with the same retention for the nitrate anion. The retention of divalent anions increased substantially with the use of monovalent eluents, so the resulting selectivity approached that commonly encountered with silica-based sorbents, where the monovalent anions are either not resolved or sulphate elutes very late (Fig. 4).

Two factors are considered to influence the selectivity: loss of free energy on the formation of a functional group–analyte anion pair and an electroselectivity, where the ion with higher charge is more strongly bound. The electroselectivity, however, needs two sites on the sorbent to interact with divalent ions simultaneously. The electroselectivity theory [23] supposes that the lower affinity of some sorbents to divalent anions is caused by hindered access to the formation of an ion pair with two sites simultaneously. From the electroselectivity theory in IC one could expect that the selectivities for ions with the same and with different charges would be independent, so a sorbent can show a high selectivity both for monovalent and for mono- and divalent anions. With the exception of the Dionex sorbent, the results compared here do not support this conclusion, however. The reason may be that this sorbent has a high density of ion-exchange groups concentrated in small latex particles, attached to an inert core, whereas the other sorbents have a low content of functional groups distributed on a large surface.

The rules of the influence of pH are complicated, as the pH influences the dissociation of the eluent anion, sorbent functional group and analyte anion. The effective concentration and charge of these anions change with pH in different manners according to their dissociation constants. In addition to the known shift in the retention of phosphate from a position before chloride at pH < 6 to a position after

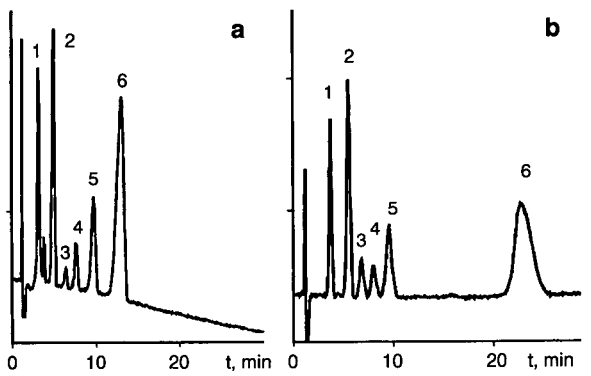

Fig. 4. Comparison of selectivity in divalent and monovalent eluents. Column, HEMA-S 1000 Q-L (10 μm), PEEK (150 × 4.6 mm I.D.); flow-rate, 1 ml/min; detection, indirect spectrophotometry at 254 nm. Eluent: (a) 0.5 m*M* sulphosalicylate (pH 5.4); (b) 3.0 m*M* salicylate (pH 5.8). Peaks: 1 = fluoride; 2 = chloride; 3 = nitrite; 4 = bromide; 5 = nitrate; 6 = sulphate.

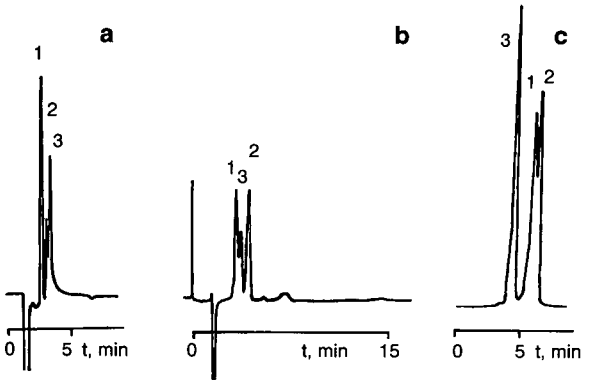

Fig. 5. Separation of fluoride in the presence of acetate and formate. Column, HEMA-S 1000 Q-L (10 μm) (150 × 3.3 mm I.D.); flow-rate, 0.5 ml/min. (a, b) Indirect spectrophotometry detection at 254 nm, eluent 0.5 m*M* sulphosalicylate–5% MeOH at (a) pH 3.1 and (b) pH 4.5; (c) suppressed conductivity detection, eluent 1.5 m*M* sodium carbonate. Peaks: 1 = acetate; 2 = formate; 3 = fluoride.

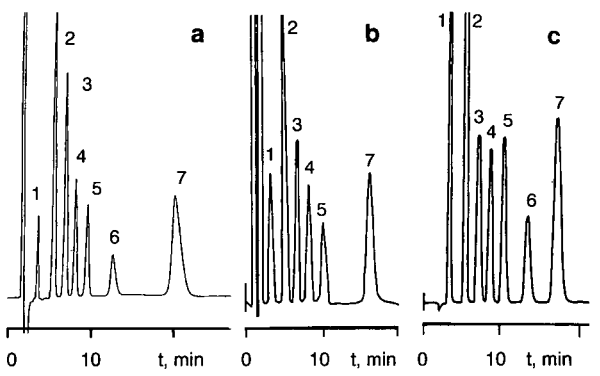

Fig. 6. Comparison of commonly used eluents on an Alltech universal anion PEEK column (150 × 4.6 mm I.D.). Flow-rate, 1.0 ml/min; conductivity detection. Eluent: (a) 5 m*M* *p*-hydroxybenzoate (pH 7.9); (b) 4 m*M* phthalate (pH 4.5); (c) 2.8 m*M* hydrogencarbonate–2.2 m*M* carbonate (suppressed conductivity detection). Peaks: 1 = fluoride; 2 = chloride; 3 = nitrite; 4 = bromide; 5 = nitrate; 6 = phosphate; 7 = sulphate.

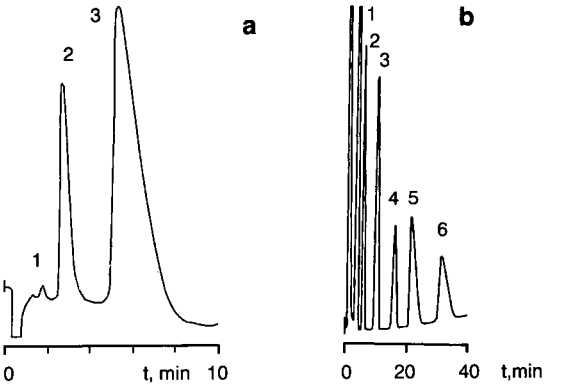

Fig. 7. Separations of late-eluting anions. (a) Column, Alltech universal anion PEEK (150 × 4.6 mm I.D.); eluent, 8 m*M* ethylenediaminetetraacetic acid, disodium salt; flow-rate, 0.5 ml/min; conductivity detection. Peaks: 1 = phosphate; 2 = pyrophosphate; 3 = tripolyphosphate. (b) Column, Alltech universal anion PEEK (150 × 2.1 mm I.D.); eluent, 1.5 m*M* sodium octanesulphonate; flow-rate, 0.5 ml/min; conductivity detection. Peaks: 1 = chloride; 2 = nitrate; 3 = iodide; 4 = thiocyanate; 5 = sulphate; 6 = thiosulphate.

nitrate at pH > 7.5, caused by its transition from mono- to divalent form, as another example Fig. 5 shows the separation of fluoride from formate and acetate peaks. At high pH fluoride is eluted before acetate and formate, whereas on decreasing the pH to 4.5 fluoride elutes between them and at pH 3.1 elutes after them, as the dissociation of weaker organic acids is suppressed.

The selectivity of HEMA-S 1000 Q-L sorbent was found to be acceptable in all commonly used IC systems [14], as is shown in Fig. 6. With the selection of a suitable eluent, the selectivity can be influenced to separate even difficult mixtures such as late-eluting anions or polyphosphates. The divalent ethylenediaminetetraacetate disodium salt eluent proved to be an efficient eluent for polyphosphate in food additives (Fig. 7a), whereas monovalent octanesulphonate permitted the elution of late-eluting monovalent iodide and thiocyanate before sulphate and thiosulphate (Fig. 7b).

CONCLUSIONS

Some dependences of retention on chromatographic conditions have been evaluated and the matrix character and eluent charge were shown to play significant roles in the selectivity of IC separations. The selectivities of commonly used sorbents were compared for the separations of mono- and divalent anions on the basis of the separation factor–capacity factor dependence. The selectivity for monovalent ions increases from silica-based through non-polar and polar polymers to agglomerated sorbents. A higher selectivity for monovalent ions seems to be connected with a lower affinity for divalent anions. Monovalent eluents seem to give a lower selectivity for monovalent and a higher retention for divalent anions. The influence of pH can be estimated from dissociation constants of eluent and analyte anions.

REFERENCES

1 D. T. Gjerde and J. S. Fritz, *Ion Chromatography*, Hüthig, New York, 2nd ed., 1987.
2 P. R. Haddad and P. E. Jackson, *Ion Chromatography*, Elsevier, Amsterdam, 1990.
3 R. E. Smith, *Ion Chromatography*, CRC Press, Boca Raton, FL, 1988.
4 G. D. Franklin, *Int. Lab.*, 15 (1985) 56.
5 P. R. Haddad and A. L. Heckenberg, *J. Chromatogr.*, 300 (1984) 357.
6 H. Small, *J. Chromatogr.*, 546 (1990) 3.

7 R. E. Barron and J. S. Fritz, *J. Chromatogr.*, 284 (1984) 13.
8 F. Vláčil and I. Vinš, *J. Chromatogr.*, 391 (1987) 133.
9 R. W. Slingsby and Ch. A. Pohl, *J. Chromatogr.*, 458 (1988) 241.
10 L. D. Warth and J. S. Fritz, *J. Chromatogr. Sci.*, 29 (1988) 630.
11 D. L. DuVal and J. S. Fritz, *J. Chromatogr.*, 295 (1984) 89.
12 A. D. Sosimenko and P. R. Haddad, *J. Chromatogr.*, 546 (1991) 37.
13 D. R. Jenke and G. K. Pagenkopf, *Anal. Chem.*, 56 (1984) 88.
14 R. Saari-Nordhaus, I. R. Henderson and J. M. Anderson, Jr., *J. Chromatogr.*, 546 (1991) 89.
15 R. Saari-Nordhaus, J. M. Anderson, Jr. and K. Ravichandran, *J. Chromatogr.*, 602 (1992) 15.
16 R. Saari-Nordhaus, J. M. Anderson, Jr. and K. Ravichandran, *Am. Lab.*, (1992) 501.
17 D. T. Gjerde, G. Schmuckler and J. S. Fritz, *J. Chromatogr.*, 187 (1980) 35.
18 P. R. Haddad and C. E. Cowie, *J. Chromatogr.*, 303 (1984) 321.
19 T. B. Hoover, *Sep. Sci. Technol.*, 17 (1982) 295.
20 D. R. Jenke and G. K. Pagenkopf, *Anal. Chem.*, 56 (1984) 2674.
21 M. Maruo, H. Naoki and T. Kuwamoto, *J. Chromatogr.*, 481 (1989) 315.
22 D. R. Jenke, *Anal. Chem.*, 56 (1984) 2764.
23 D. Clifford and W. J. Weber, *React. Polym.*, 1 (1983) 77.

Journal of Chromatography, 640 (1993) 57–64
Elsevier Science Publishers B.V., Amsterdam

CHROMSYMP. 2836

Polymer-coated cation exchangers in high-performance ion chromatography: preparation and application

Gernot Huhn☆ and Helmut Müller*

University of Halle, Department of Chemistry, Institute of Analytical and Environmental Chemistry, O-4200 Merseburg (Germany)

ABSTRACT

Low-capacity cation-exchange stationary phases for ion chromatography were prepared by coating a vinyl-modified silica gel with polystyrene or poly(glycidyl methacrylate). Strong acid ion-exchange groups were formed by sulphonation with concentrated sulphuric acid or by ring opening of the polymer-coated silica gels with sulphite solution. Carbon–sulphur elemental analyses of the polymer-coated cation exchangers (PCCEs) were applied to determine the average polymer film thickness. The pH stability depended on the polymer film thickness. The PCCEs were stable in the pH range 0.5–9. The low-capacity PCCEs (capacities 18–91 μmol/g) were applied to determine alkali and alkaline earth metal ions in tap and mineral waters.

INTRODUCTION

Most stationary phases used in ion chromatography are based on polymer or silica gel materials [1–3]. Silica particles possess favourable properties, such as a homogeneous matrix, good porosity and excellent stability to solvents and pressure. The advantage of polymer-based stationary phases is their stability over en broad pH range, commonly from 0 to 12. Silica gel phases are stable only from pH 2 to 8. Polymer-coated silica gel phases should combine good pH stability with the good chromatographic properties of silica gel carriers.

The preparation of a sulphonated polystyrene-coated cation exchanger (PS-PCCE) and its application to heavy metal separations have been described [4]. The preparation of poly(glycidyl methacrylate)-coated cation exchangers (PGMA-PCCEs) and separations of alkali and alkaline earth metal ions by using PS- and PGMA-PCCE columns have been reported previously [5]. This paper describes the preparation, properties and applications of PCCE columns in high-performance ion chromatography (HPIC), together with aspects such as the polymer film thickness, pH stability and examples of rapid separations of alkali and alkaline earth matel ions.

EXPERIMENTAL

Preparation of stationary phases

The synthesis of the PCCEs is a three-step procedure (see Fig. 1):

(1) The silica gel surface was modified with triethoxyvinylsilane.

(2) The thermal decomposition of an incorporated peroxide started the polymerization of styrene or glycidyl methacrylate and divinylbenzene to form a cross-linked polymer network.

(3a) The polystyrene-coated silica gels were sulphonated with concentrated sulphuric acid.

(3b) The PGMA-coated silica gels were sulphonated with 1 mol/l sodium sulphite solution in the presence of tetrabutylammonium bromide as catalyst.

* Corresponding author.

☆ Present address: Centre for Environmental Research, Department of Environmental Chemistry and Ecotoxicology, Hallesche Strasse 44, O-4204 Bad Lauchstädt, Germany.

0021-9673/93/$06.00

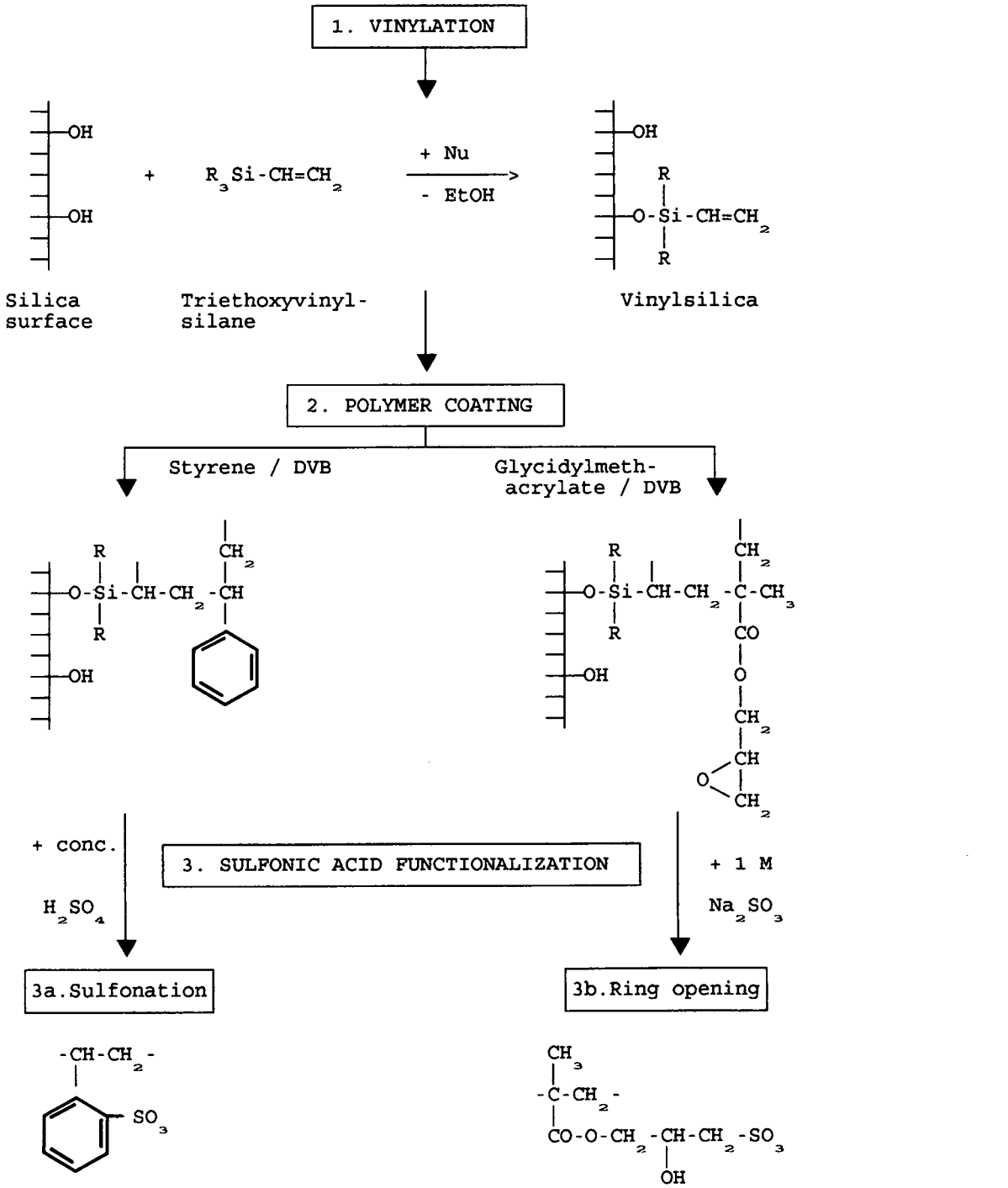

Fig. 1. Preparation of polymer-coated cation exchangers (PCCE). Nucleophil (Nu): triethylamine, pyridine, imidazole.

TABLE I

CHARACTERIZATION OF UNMODIFIED SILICA GELS

A_s = specific surface area by the BET method; D_{part} = average particle diameter; d_p = average pore diameter; V_p = pore volume.

Silica gel[a]	PCCE No.	A_s (m^2/g)	D_{part} (μm)	V_p (ml/g)	d_p (nm)
LI 60-5	VI	650	5	0.95	6
ES 360-4	VII	120	4.5	1.09	13
ES 210-7	VIII	177	7	0.93	21

[a] LI = LiChrospher (Merck); ES = ES-gel (Leuna).

The columns were slurry packed with a mixture of cyclohexanol and toluene as dispergent. The capacities of the filled columns were determined by a breakthrough experiment with conductivity detection of the effluent as described previously [5].

Instrumentation

IC analyses were performed on a modular HPLC system (Knauer, Berlin, Germany) consisting of an analytical pump (Model 64 HPLC pump), an injection valve, a conductivity detector and a recorder. The sample volumes injected were 20 μl.

For carbon–sulphur elemental analyses, a C–N–S 932 Analyser (LECO, St. Joseph, MI, USA) was used.

Materials and reagents

The mobile phases for the separation of alkaline earth metal ions were prepared by mixing analytical-reagent grade ethylenediamine and oxalic acid solutions. For pH adjustment, nitric acid was used. The mobile phases for the separation of alkali metal ions was dilute nitric acid. The mobile phases were filtered and degassed.

Stock solutions of 1 g/l of alkali and alkaline earth metals were prepared from potassium nitrate, sodium chloride, calcium chloride and magnesium sulphate and diluted to the desired concentrations with deionized water. All reagents were of analytical reagent-grade quality.

Table I shows some characteristics of the silica gel supports used. ES-Gels were obtained from Leuna (Leuna, Germany) and LiChrospher from Merck (Darmstadt, Germany).

RESULTS AND DISCUSSION

The composition and concentration of the mobile phases depend on the chemical properties and ion-exchange capacities of the stationary phases used. Table II shows the measured column capacities and the calculated mass capacities (column capacity divided by the mass of stationary phase per column). The ion-exchange capacities are influenced by the

TABLE II

CAPACITIES OF THE POLYMER-COATED CATION EXCHANGERS

Column	Dimensions (mm)[a]	Li^+ capacity[b] (μmol per column)	Mass capacity[c] (μmol/g)
PCCE VI	30 × 4	11	50
PCCE VII	30 × 4	8	36
PCCE VIII	30 × 4	17	91

[a] Stainless-steel columns, length × I.D.

[b] Determined by recording the effluent conductivity change.

[c] Column capacity divided by dry mass of stationary phase per column.

TABLE III

ELEMENTAL ANALYSIS OF THE POLYMER-COATED SILICA GELS

Column	Polymer coating[a]	Elemental analysis		Average polymer film thickness[b] (nm)	C/S ratio
		C (%)	S (%)		
PCCE VI	PS	3.9	1.4	0.12	2.8
PCCE VII	PGMA	2.2	0.15	0.33	15
PCCE VIII	PGMA	2.5	0.42	0.27	5.9

[a] PS = polystyrene; PGMA = poly(glycidyl methacrylate).

[b] Average polymer film thickness = $[(x/y) \cdot 1000]/[(1 - x/y) A_s d]$, where x = carbon content (%) of the PCCE stationary phase, y = average carbon content (%) of the monomer mixture (styrene–divinylbenzene), A_s = specific surface area (m^2/g) and d = polymer film density (1 g/cm^3 was assumed).

amount of the bonded-polymer coating and the degree of sulphonation of anion-exchange syntheses (third step in Fig. 1: sulphonation with sulphuric acid or ring opening with sodium sulphite solution).

The sulphonation of the PS-coated silica gels gave nearly completely monosulphonated PS-PCCEs, as calculated from the results of carbon–sulphur elemental analyses. The C/S ratio (Table III) gave a value close to the theoretical value (3 for styrene monosulphonic acid). This degree of sulphonation was obtained by using concentrated sulphuric acid with short reaction times (10–15 min) and temperatures of 80–90°C. The duration and the temperature of sulphonation must be limited in order to avoid PS networks on the silica gel surface as much as possible. The opening of the epoxy rings showed lower degrees of sulphonation (theoretical C/S ratio = 3). In this instance, longer reaction times were necessary to obtain higher degrees of sulphonation and higher ion-exchange capacities.

The average polymer film thickness [6], calculated from the results of elemental analyses (Table III) was used as a practical value for the characterization of the polymer coating bonded to the silica gel surface. After polymer coating, the average polymer film thickness was 0.25–0.5 nm (Table IV). Comparison of the polymer film thickness of the PCCEs after polymer coating and after ion-exchange syntheses (sulphonation) showed that the degradation of the PS-PCCE was greater than that of the PGMA-PCCE. It can be assumed that part of the PS coating decomposed during the sulphonation. The polymer network was partly oxidized, or the covalent Si–C bond linking the polymer network to the silica substrate was partly broken. By this means, the PGMA-PCCE showed a higher polymer film thickness and therefore higher pH stability (Fig. 2).

In Fig. 2, the square root of the number of theoretical plates per column is plotted against the volume of alkaline buffer solution as the number of column volumes. The number of theoretical plates per column was calculated with a 10 mg/l Mg standard sample by using the same chromatographic conditions for each measurement. The pH stabilities of PCCE VI and PCCE VIII were determined by pumping buffer solutions of pH 9.5 and 11, re-

TABLE IV

COMPARISON OF THE AVERAGE POLYMER FILM THICKNESS AFTER POLYMER COATING AND AFTER SULPHONIC ACID FUNCTIONALIZATION

Column	Average polymer film thickness (nm)[a]		B/A (%)
	A	B	
PCCE VI	0.24	0.12	50
PCCE VII	0.49	0.34	69
PCCE VIII	0.39	0.28	71

[a] A = Average polymer film thickness after polymer coating; B = average polymer film thickness after sulphonic acid functionalization.

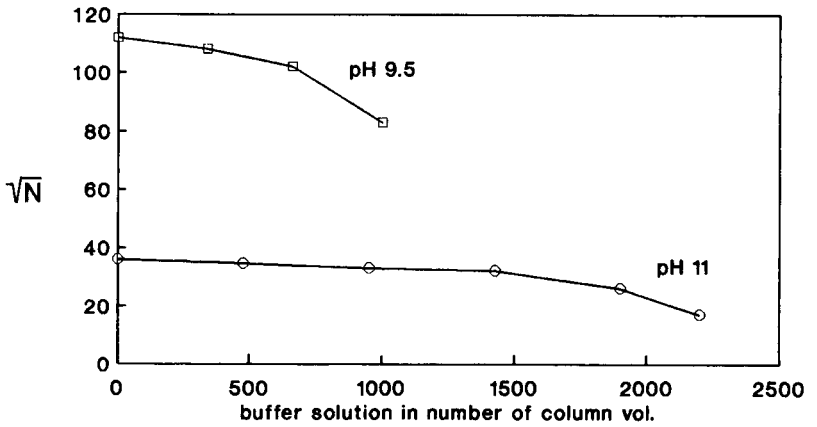

Fig. 2. pH stability of the PCCE. Plots of the square root of the number of theoretical plates against the alkaline buffer solution as number of column volumes. ○ = PCCE VIII; □ = PCCE VI.

spectively, through the columns. With degradation of the silica core, the column bed decreased, producing a dead volume on the head of the column and the efficiencies of the columns decreased. The PCCE VIII material, with the greater polymer film thickness, was much more stable, indicating that pH stability is strongly dependent on the thickness of the polymer coating.

On the other hand, a thin layer (partly) surrounding the impervious silica core gives rise to a rapid radial mass transfer of the solute in the polymer network (c parameter of the Knox equation [7]). The best comparative measure of the kinetic performance of a column packing material is a plot of the reduced plate height (h) against the reduced velocity (v) along with a measure of the column resistance parameter (φ) [7]. An efficient column must have both a low reduced plate height and a low resistance factor. In practice, φ is found to lie within the range 500–800 for silica phases, depending on the method of packing the column and the porosity of the packing material. The values of φ (Table V) fall in the upper part of the acceptable range, indicating that the materials showed good flow properties.

A summary of the additionally reduced column parameters (v and h) of the PCCE columns used is given in Table V. All parameters lie in the region that are typical for silica-based materials with the

TABLE V

REDUCED COLUMN PARAMETERS OF THE POLYMER-COATED CATION EXCHANGERS

D_{part} = mean particle diameter; φ = column resistance parameter = $\Delta p D_{part}^2/u\eta L$, where u = eluent linear velocity, η = eluent viscosity, L = column length, and Δp = pressure drop across column; h = reduced plate height = H/D_{part}, where H = plate height; v = reduced velocity = uD_{part}/D_m, where D_m = diffusion coefficient of solute in eluent.

Column[a]	D_{part} (μm)	φ	v	h			
				Mg	Ca	Na	K
PCCE VI	5	790	16	10	8.5	16	61
PCCE VII	4	890	25	9.5	7.8	8.5	9.8
PCCE VIII	7	850	30	7.5	5.8	5	5.5

[a] For dimensions, see Table I.

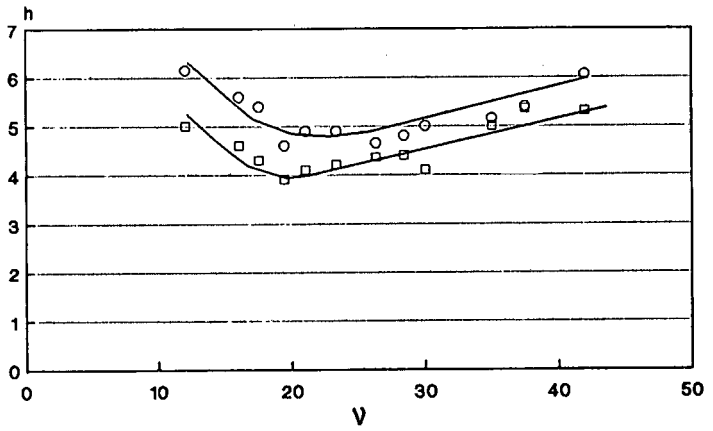

Fig. 3. *h versus v* plots for the PCCE VIII. Injection of 20 μl of standard (□) 6 mg/l Na^+ and (○) 8 mg/l K^+ samples. Column, 30 mm × 4 mm I.D.; eluent, 3 m*M* nitric acid.

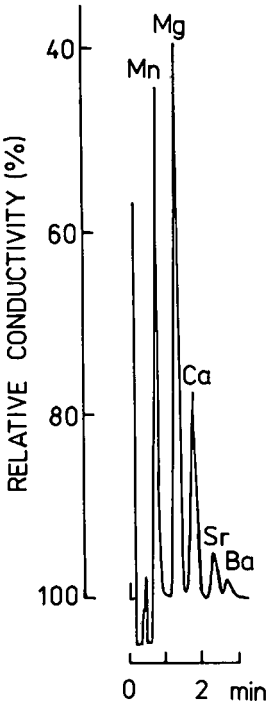

Fig. 4. IC analysis of a standard sample on PS-PCCE VI. Eluent, 0.85 m*M* ethylenediamine–1.2 m*M* oxalic acid–5 vol.% acetone; pH, 4.0; flow-rate, 1.5 ml/min; concentration of each metal ion, 10 mg/l.

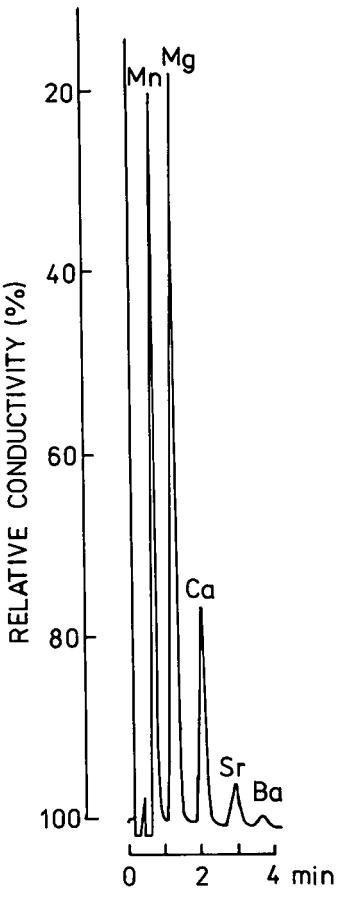

Fig. 5. IC analysis of a standard sample on PGMA-PCCE VIII. Eluent, 1.2 m*M* ethylenediamine–1.7 m*M* oxalic acid–5 vol.% acetone; pH, 4.0; flow-rate, 1.5 ml/min; concentration of each metal ion 10 mg/l.

exception of alkali metals on the PCCE VI column (PS coated). The number of theoretical plates (N) calculated for the short columns (30 mm length) was 600–850. These good N values were due to the excellent chromatographic efficiencies of the silica gels, which had small particle size and pore-size diameter distributions.

These results can also be seen in Fig. 3, which shows a plot of the reduced plate height against reduced velocity for sodium and potassium on the PCCE III column. The minimum values of h were 4 for sodium and 5 for potassium, and indicated good efficiencies of the polymer-coated silica gel columns. Of greatest interest are the shapes of the plots above the minimum values, which correspond to the c-values of the Van Deemter equation and reflect the resistance to mass transfer within the particles. The h *versus* v plots rise gradually with increasing velocity above the minimum values, showing good resistance to mass transfer within the thin polymer-coated particles, which is an advantage of the PCCE columns over the polymer phases. These characterized polymer-coated cation exchangers were tested for rapid separations of alkali and alkaline earth metal ions by using short columns. Other applications have been published previously [4,5]. As the capacity is low, rapid separations can be achieved with relatively weak eluents, which is favourable in single-column IC, particularly when conductivity detection is applied.

Figs. 4–7 shows alkali and alkaline earth metal ion separations on PS- and PGMA-coated silica gels. For alkali metal ion separations nitric acid was used and for alkaline earth metal ion separations

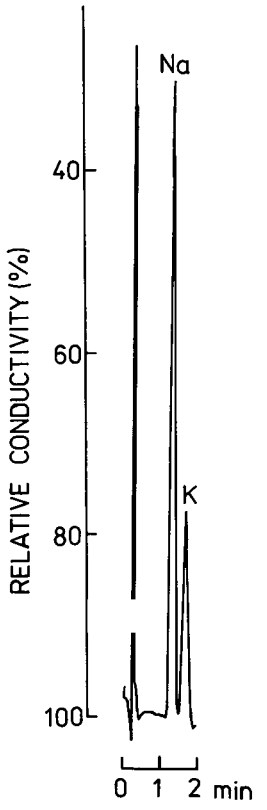

Fig. 6. Determination of alkali metal ions in drinking water (Kemberg) on PGMA-PCCE VIII. Eluent, 3 mM nitric acid; flow-rate, 1.5 ml/min; sample, 1:10 dilution, Na^+ 83 mg/l, K^+ 71 mg/l.

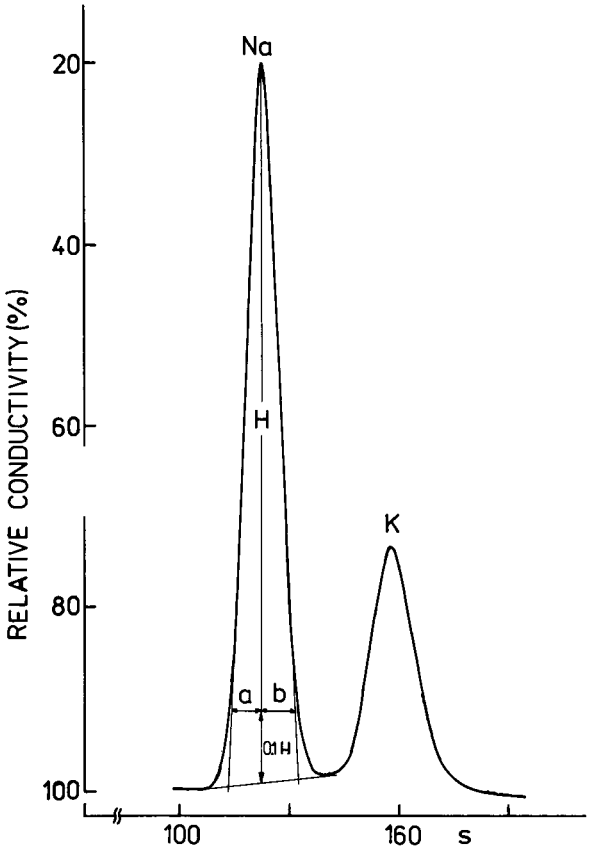

Fig. 7. IC analysis of a standard sample on PGMA-PCCE VIII. Eluent, 3 mM nitric acid; sample, Na^+ 6 mg/l, K^+ 8 mg/l. Peak symmetry factors (b/a): Na^+ = 1.18; K^+ = 1.13.

mixtures of ethylenediamine and oxalic acid were used as the eluent.

With the PCCE columns tested, all alkaline earth metals (Mg, Ca, Sr and Ba) and manganese were separated in at least 4 min. Sodium and potassium were separated in only 2–3 min using the PGMA phases (Figs. 5 and 6). The good chromatographic and flow properties of the PCCE columns produced very symmetrical signals (Fig. 6). The peak symmetry factor (b/a) [8] is 1.0 for an ideal symmetrical signal.

The columns were used to determine alkali and alkaline earth metal ions in mineral, drinking and tap waters. The results were in agreement with those obtained by flame atomic absorption spectrometry and EDTA titration.

The disadvantage of the short columns is the small loading capacity. Especially for alkali metal ion separations, the analyses had to be stopped when the retention times became too short. Under the conditions used for alkali metal ion separations, the alkaline earth metal ions were accumulated on the stationary phase and therefore had to be eluted by injection of 0.1 M nitric acid from time to time.

CONCLUSIONS

Polymer-coated cation exchangers with a silica core are very suitable for ion chromatography. The described procedure provides a reproducible means of preparing low-capacity polymer-coated cation exchangers. The average polymer film thickness was 0.12–0.33 nm. The ion-exchange capacities (30–90 μmol/g) and the pH stabilities (0.5–9.5) were limited. The pH stability of pure polymer phase were not achieved with polymer-coated materials based on silica gels. Good mass transfer properties were advantageous and were discernible from the *h versus v* plots. The PCCE columns showed good chromatographic and flow properties and were applicable to rapid separations of alkali and alkaline earth metals by using short columns.

REFERENCES

1 D. T. Gjerde and J. S. Fritz, *Ion Chromatography*, Hüthig, Heidelberg, 1987, Ch. 3, p. 47.
2 J. G. Dorsey, J. P. Foley, W. T. Cooper, R. A. Barford and H. G. Barth, *Anal. Chem.*, 64 (1992) 367R.
3 P. R. Haddad and P. E. Jackson, *Ion Chromatography — Principles and Applications* (*Journal of Chromatography Library*, Vol. 46), Elsevier, Amsterdam, 1990.
4 G. Huhn, H. Müller and G. Eppert, *React. Polym.*, 170 (1992) 109.
5 G. Huhn, G. Schwedt and H. Müller, *Fresenius' J. Anal. Chem.*, 342 (1992) 678.
6 H. Engelhardt, H. Löw, W. Eberhardt and M. Mauss, *Chromatographia*, 27 (1989) 535.
7 J. H. Knox and A. Pryde, *J. Chromatogr.*, 112 (1975) 171.
8 G. Eppert, *Einführung in die Schnelle Flüssigchromatographie*, Akademie-Verlag, Berlin, 1988, p. 45.

Journal of Chromatography, 640 (1993) 65–71
Elsevier Science Publishers B.V., Amsterdam

CHROMSYMP. 2801

Novel weak acid cation-exchange column

Detlef Jensen and Joachim Weiss*

Dionex GmbH, Am Wörtzgarten 10, W-6270 Idstein (Germany)

Maria A. Rey and Christopher A. Pohl

Dionex Corporation, 1228 Titan Way, Sunnyvale, CA 94086 (USA)

ABSTRACT

A cation-exchange column with carboxylate cation-exchange sites was developed. Compared with conventional surface-sulfonated or latex agglomerated resins, this weak acid cation exchanger has a high selectivity for hydronium ions. Mono- and divalent cations such as alkali and alkaline earth metals can therefore be determined simultaneously in less than 10 min using a weakly acidic eluent under isocratic conditions. Because the ethylvinylbenzene–divinylbenzene substrate is highly cross-linked, the new separator is solvent compatible, thus allowing the use of organic solvents to alter the selectivity of the separation and to remove organic contaminants from the column. The separation characteristics of this column are presented and various applications are discussed.

INTRODUCTION

Since the introduction of ion chromatography in 1975 [1], there have been numerous publications on chromatographic methods suitable for alkali and alkaline earth metals in which conductimetric detection is applied to the column effluent [2–6]. At first, the large differences in ion-exchange selectivities of alkali *versus* alkaline earth metals necessitated sequential determinations of the two cation classes using surface-sulfonated polystyrene–divinylbenzene resins. While monovalent cations such as alkali metals, ammonium and small aliphatic amines are easily eluted with dilute mineral acids [7], the separation of alkaline earth metals required the use of divalent eluent ions such as *m*-phenylenediamine or ethylenediamine [5]. However, the aim of the inorganic analytical chemist has always been the simultaneous determination of alkali metal, alkaline earth metal and ammonium cations, and various column materials and eluents have been tested for this purpose. Kolla *et al.* [8] were the first to report on an isocratic elution of both cation classes within a reasonable time period using a silica-based weak cation exchanger coated with poly(butadiene–maleic acid) as the stationary phase and mildly acidic complexing agents as the eluent. Thus, cation-exchange and chelating processes take place, the latter being strongly dependent on sample pH. Although the eluent composition occasionally has to be adjusted when using columns from different production batches to compensate for the variations in the coating process, the concept of using a stationary phase with a carboxylate functionality results in an analysis time of *ca.* 20 min for the above-mentioned mono- and divalent cations.

As an alternative concept, a column-switching technique was proposed based on two latex agglomerated strong acid cation exchangers of different dimensions and capacities and switching them to change the flow direction during the elution for the simultaneous determination of alkali and alkaline earth metals [9]. Although the resulting resolution between the monovalent cations was sufficient, the major drawback of this technique was the poor effi-

* Corresponding author.

0021-9673/93/$06.00

ciency for divalent cations. This limitation was overcome with the introduction of a more efficient strong acid latex agglomerated cation-exchange column, IonPac CS10 [10]. In contrast to a conventional latex agglomerated cation exchanger of the IonPac CS3 type, an ethylvinylbenzene–divinylbenzene copolymer was used as the substrate material to ensure solvent compatibility. Thus, it is possible either to alter the selectivity of the separation by adding organic solvents to the eluent or to remove organic contaminants by rinsing the packing material with acetonitrile or methanol. Also, two different monomers have been used to polymerize the latex material, one of which is not readily sulfonated, thus producing a lower charge density ion-exchange material. This, in turn, is important for the ion-exchange process of divalent metal separation. Owing to this lower charge density, the interaction of the divalent cations with the stationary phase is significantly reduced. With a mixture of hydrochloric acid and 2,3-diaminopropionic acid as the eluent, sodium, ammonium, potassium, magnesium and calcium are eluted within 15 min. As shown in the chromatogram in Fig. 1, all ions are separated to the baseline. On the other hand, the tremendous resolution between calcium and magnesium is unnecessary for routine water analysis. Nevertheless, this column concept is well understood, and a good column-to-column reproducibility is obtained [11].

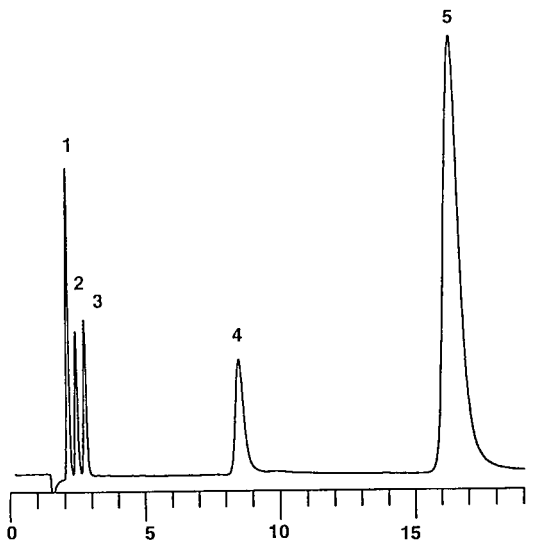

Fig. 1. Simultaneous separation of alkali and alkaline earth metals on IonPac CS10. Eluent, 0.04 mol/l hydrochloric acid + 0.004 mol/l, 2,3-diaminopropionic acid; flow-rate, 1 ml/min; detection, suppressed conductivity; injection volume, 25 μl; solute concentrations, (1) 1 ppm sodium, (2) 0.5 ppm ammonium, (3) 1 ppm potassium, (4) 1 ppm magnesium and (5) 10 ppm calcium.

The major effort during the past 2 years was to combine the benefits of both column concepts, *i.e.*, to develop a polymeric solvent-compatible stationary phase with a carboxylate functionality. The work presented in this paper focuses on the chromatographic properties and the applicability of such a packing material. In order to study this new separation material, chromatographic parameters such as eluent composition, eluent concentration and flow-rate were varied.

EXPERIMENTAL

Apparatus

All experiments were carried out with a DX-300 ion chromatographic system (Dionex, Sunnyvale, CA, USA) consisting of a quaternary gradient pump, a chromatographic module and a conductivity detector. Eluents were degassed by purging them with helium using the eluent degas module. Separations were performed on an IonPac CS12 cation exchanger. A guard column (IonPac CG12) was used at all times. Conductivity detection was carried out in the recycle mode using a cation self-regenerating suppressor (CSRS-1). A chromatographic data system (Al-450; Dionex) was used for instrument control and for data collection and processing.

Reagents

Ultrapure water (18 MΩ cm resistivity at 25°C), used for the preparation of the eluents, was obtained from a water purification system (SERAL, Ransbach-Baumbach, Germany). Methanesulfonic acid (Ventron Alfa Products, Karlsruhe, Germany) was of analytical-reagent grade. Tetrabutylammonium hydroxide (1.5 mol/l in water) was purchased from Riedel-de Haën (Seelze, Germany) and acetonitrile (Chrom AR grade) from Promochem (Wesel, Germany).

Dilute working standards solutions of all the cations under investigation were prepared daily from 1000 ppm stock standard solutions. All standard solutions were stored in polyethylene containers.

RESULTS AND DISCUSSION

The new cation exchanger is commercially available under the trade name IonPac CS12. Its structural and physical properties are summarized in Table I.

In order to overcome the stability problem of polymer-coated silica phases, we used a highly cross-linked, macroporous ethylvinylbenzene–divinylbenzene polymer with a bead diameter of 8 μm, a pore size of 6 nm and a specific surface area of 300 m^2/g as substrate material. In a second step, this substrate material was grafted with another polymer, containing carboxylate groups, resulting in a relatively high ion-exchange capacity of 2.8 mequiv. per column. In contrast to conventional latex agglomerated strong acid cation exchangers such as IonPac CS10, very simple eluents such as hydrochloric acid or methanesulfonic acid can be used to elute mono- and divalent cations rapidly and efficiently under isocratic conditions. As can be seen from Fig. 2, sodium, ammonium, potassium, magnesium and calcium are separated to the baseline in less than 10 min.

Experiments were carried out to investigate the maximum sodium-to-ammonium ratio that still allows a separation of these two ions on the IonPac CS12. Under isocratic conditions, using an eluent concentration of 0.01 mol/l methanesulfonic acid (MSA) and a flow-rate of 2 ml/min, it is possible to analyze samples containing a 250–500-fold excess of sodium in comparison with ammonium (Fig. 3). As can be seen from Fig. 3, even samples with a sodium-to-ammonium ratio of 1000:1 can be analyzed for ammonium. However, the resolution between sodium and ammonium is less than 1.3 at this concentration ratio, and quantification is therefore only possible using the corrected peak height for ammonium. To improve the resolution between sodium and ammonium, a step gradient can be used, as shown in Fig. 4. Starting the analysis with an MSA concentration of 0.004 mol/l and switching it to 0.016 mol/l after 5.1 min, a baseline-resolved separation between sodium and ammonium, even with a 1000-fold excess of sodium, can be obtained. The total analysis time including the re-equilibration step is less than 20 min, thus this technique is suitable for routine water analysis.

A major problem with weak acid cation exchangers is that the dissociation of the carboxylate

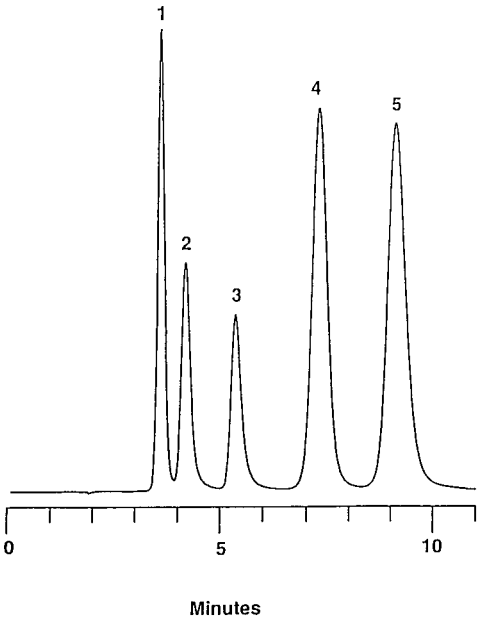

Fig. 2. Simultaneous separation of alkali and alkaline earth metals on IonPac CS12. Eluent, 0.02 mol/l methanesulfonic acid; flow-rate; 1 ml/min; detection, suppressed conductivity; injection volume, 25 μl; solute concentrations, 5 ppm (1) sodium, (2) ammonium, (3) potassium and (4) magnesium and (5) 10 ppm calcium.

TABLE I

STRUCTURAL AND PHYSICAL PROPERTIES OF THE IONPAC CS12 SEPARATOR

Parameter	Valve
Column dimensions	(A) 250 mm × 4 mm I.D. (B) 250 mm × 2 mm I.D.
Substrate	Ethylvinylbenzene cross-linked with 55% divinylbenzene
Bead diameter	8 μm
Pore size	6 nm
Surface area	300 m^2/g
Ion-exchange group	Carboxylic acid ($pK_a < 3$)
Capacity	(A) 2.8 mequiv. per column (B) 0.7 mequiv. per column
Mobile phase compatibility	Acidic eluents; compatible with HPLC solvents. Alcohols should be avoided

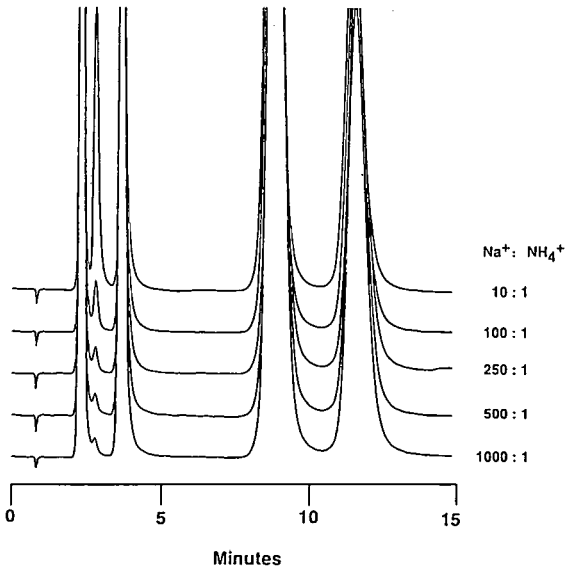

Fig. 3. Separation of sodium and ammonium at different concentration ratios using IonPac CS12. Eluent, 0.01 mol/l methanesulfonic acid; flow-rate, 2 ml/min; detection, suppressed conductivity; injection volume, 25 μl; solute concentrations, 20 ppm sodium, potassium, magnesium and calcium.

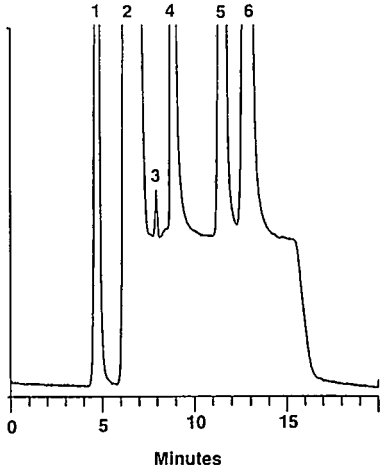

Fig. 4. Determination of ammonium in presence of large amounts of sodium. Separator, IonPac CS12; eluent, 0.004 mol/l methanesulfonic acid with step change at 5.1 min to 0.016 mol/l; flow-rate, 2 ml/min; detection, suppressed conductivity; injection volume, 25 μl; solute concentrations, (1) 0.5 ppm lithium, (2) 52 ppm sodium, (3) 0.05 ppm ammonium, (4) 5 ppm potassium, (5) 2.5 ppm magnesium and (6) 5 ppm calcium.

functional groups is strongly affected by the sample pH. Polymer-coated silica phases, for instance, such as that according to Kolla *et al.* [8], require an adjustment of the sample pH with either nitric acid or sodium hydroxide. This is time consuming and prone to interferences as the chemicals could contain other cationic impurities. Therefore, experiments with IonPac CS12 were carried out to investigate the influence of the sample pH on the separation of cations. As shown in Table I, the pK_a value of the carboxylate functionality that was chosen for this material is less than 3. This was done to allow the analysis of strongly acidic samples in much the same way as it was possible with sulfonated strong acid cation-exchange columns. A representative chromatogram of an acid soil digest is shown in Fig. 5. The sample was diluted 20-fold, having a final pH of about 2 after dilution. Methanesulfonic acid (0.02 mol/l) at a flow-rate of 1 ml/min was used as the eluent. Suppressed conductivity detection was carried out utilizing the CSRS-1 in the auto-suppression mode [12]. As can be seen from Fig. 5, the baseline performance is not affected by the acid sample matrix and the peak shapes for the divalent metal ions are absolutely symmetrical.

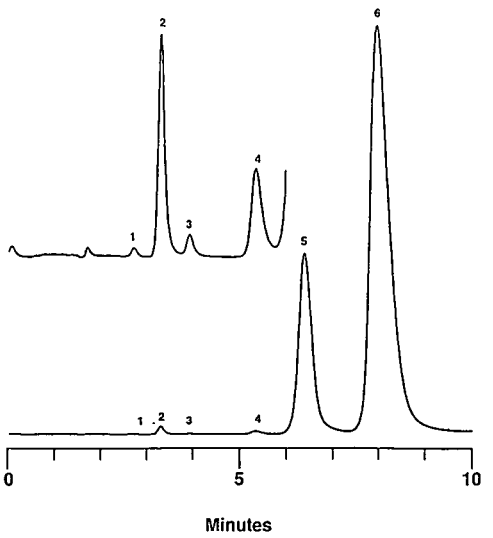

Fig. 5. Determination of inorganic cations in an acid soil digest. Separator, IonPac CS12; eluent, 0.02 mol/l methanesulfonic acid; flow-rate, 1 ml/min; detection, suppressed conductivity; injection volume, 10 μl; sample, acid soil digest (diluted 20-fold) with (1) 0.01 ppm lithium, (2) 1 ppm sodium, (3) 0.1 ppm ammonium (4) 0.9 ppm potassium, (5) 25 ppm magnesium and (6) 130 ppm calcium.

In many European countries, including Germany, there is an increasing demand for the ability to determine simultaneously alkali and alkaline earth metals, including barium, in a variety of water samples. Whereas the required detection limit for barium is in the low mg/l range, the concentrations of the other metal cations are usually several orders of magnitude higher. As is commonly known, barium, the least stable of the alkaline earth elements, is strongly retained on conventional cation-exchange resins, resulting in significant peak broadening which, in turn, leads to a lower sensitivity in comparison with the earlier eluting alkaline earth metals. However, using IonPac CS12 with 0.02 mol/l MSA at a flow-rate of 1 ml/min under isocratic conditions, barium elutes after 13 min (Fig. 6). With suppressed conductivity detection and a larger injection loop (100 μl), barium can be detected down to 0.1 mg/l. Other alkali and alkaline earth metals in higher concentrations do not interfere. Another approach to lowering the detection limit for barium is to use a step gradient starting with an MSA concentration of 0.016 mol/l until calcium is eluted, and than switching to 0.04 mol/l MSA to elute barium. With this procedure, a sharper peak for barium is obtained, resulting in a lower detection limit.

A high sensitivity for barium can also be obtained by applying gradient elution. As shown in Fig. 7, elution of all the alkali and alkaline earth metal cations of interest and ammonium is completed in about 10 min by increasing the MSA concentration in the mobile phase from 0.004 to 0.04 mol/l during the run. Similar gradients have already been tried with conventional strong acid cation exchangers such as IonPac CS10 [13]. The major problem with this method is the magnesium and calcium impurities in the eluent used. These ions are concentrated on the column while equilibrating it with the weak eluent. When starting the gradient, they are eluted at their expected retention times. With a cation trap column between the pump and the injection valve, this problem could be partly solved. When running linear gradients on an IonPac CS12 column with methanesulfonic acid, a cation trap column is no longer necessary.

IonPac CS12 can also be used in combination with non-suppressed conductivity detection. In this mode, the eluent used (0.0025 mol/l HNO_3 + 100

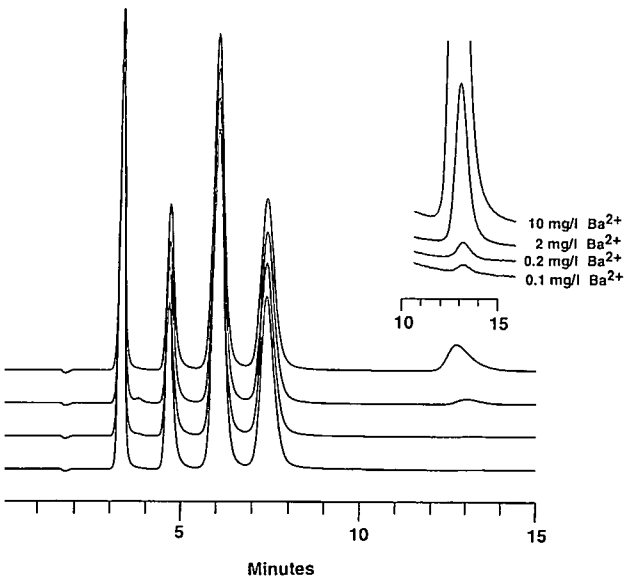

Fig. 6. Determination of barium on IonPac CS12. Chromatographic conditions as in Fig. 5 except injection volume, 100 μl; solute concentrations, 20 ppm sodium, potassium, magnesium and calcium.

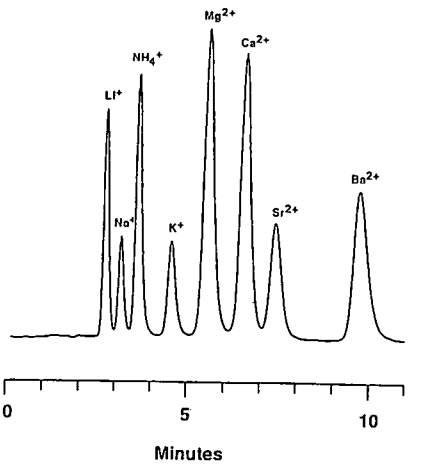

Fig. 7. Gradient elution of alkali and alkaline earth metals on IonPac CS12. Eluent, methanesulfonic acid; gradient, 0.004 mol/l isocratic for 1 min then linear to 0.04 mol/l in 10 min; flow-rate, 1 ml/min; detection, suppressed conductivity; injection volume, 25 μl; solute concentrations, 2.5 ppm lithium and sodium, 5 ppm ammonium and potassium, 10 ppm calcium and strontium and 25 ppm barium.

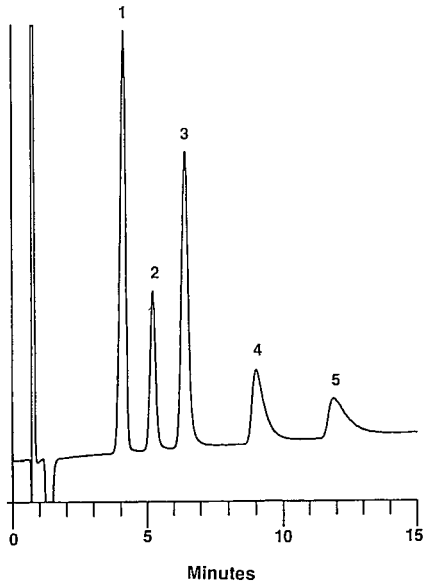

Fig. 8. Separation of alkali metal ions on IonPac CS12. Eluent, 0.0025 mol/l nitric acid; flow-rate, 2 ml/min; detection, non-suppressed conductivity; injection volume, 25 μl; solute concentrations, (1) 5 ppm lithium, (2) 5 ppm sodium, (3) 10 ppm ammonium, (4) 10 ppm potassium and (5) 20 ppm rubidium.

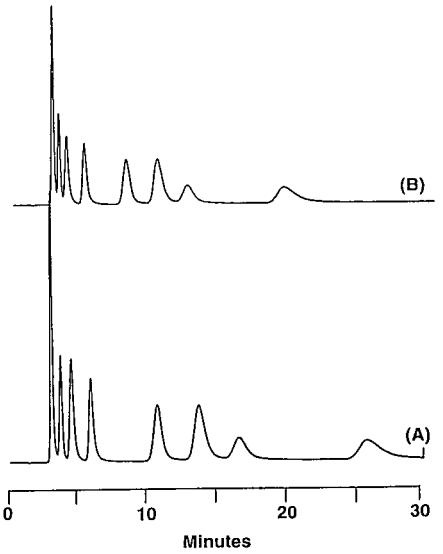

Fig. 9. Effect of acetonitrile on the retention of alkali and alkaline earth metals on IonPac CS12. Eluent, (A) 0.018 mol/l methanesulfonic acid and (B) 0.018 mol/l methanesulfonic acid–acetonitrile (95:5, v/v), flow-rate, 1 ml/min; detection, suppressed conductivity; injection volume, 25 μl; solute concentrations, 20 ppm lithium, sodium, ammonium, potassium, magnesium, calcium, strontium and barium.

ml/l acetonitrile) exhibits a high background conductivity so that the metal cations are detected as negative signals. In Fig. 8, a typical chromatogram for the separation of alkali metals is shown. Whereas lithium, sodium, ammonium and potassium are eluted within 10 min, divalent cations such as alkaline earth metals cannot be eluted with a dilute mineral acid because the column capacity is too high. As is typical for non-suppressed conductivity work, the temperatures of the eluent, the column and the detector cell have to be closely controlled.

As mentioned above, the support material of IonPac CS12 is a highly cross-linked ethylvinylbenzene–divinylbenzene copolymer ensuring solvent compatibility. Whereas organic solvents as eluent modifiers can alter the selectivity of the stationary phase for organic cations such as organic amines [11,14,15], the retention behavior of inorganic cations is not significantly influenced, especially when using strong acid cation exchangers such as IonPac CS10. On the other hand, for a weak acid cation exchanger such as IonPac CS12, one should expect an influence of aprotic solvents (*e.g.*, acetonitrile) on retention, because aprotic solvents diminish the

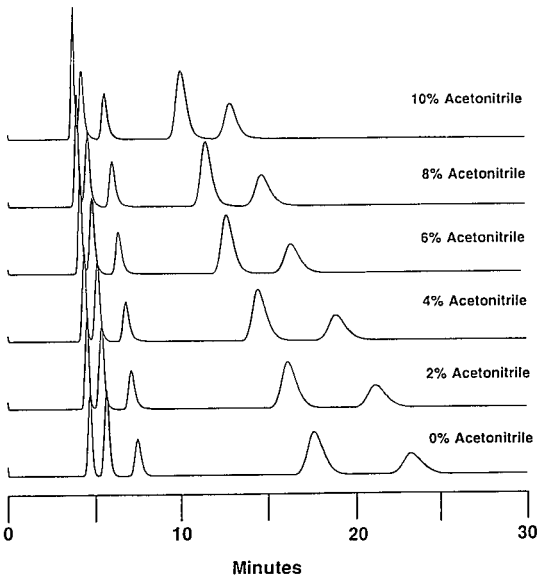

Fig. 10. Effect of acetonitrile on the retention of alkali and alkaline earth metals on IonPac CS12. Eluent, 0.01 mol/l methanesulfonic acid–acetonitrile; flow-rate, 1 ml/min; detection, suppressed conductivity; injection volume, 25 μl; solute concentrations, 10 ppm sodium, ammonium, potassium, magnesium and calcium.

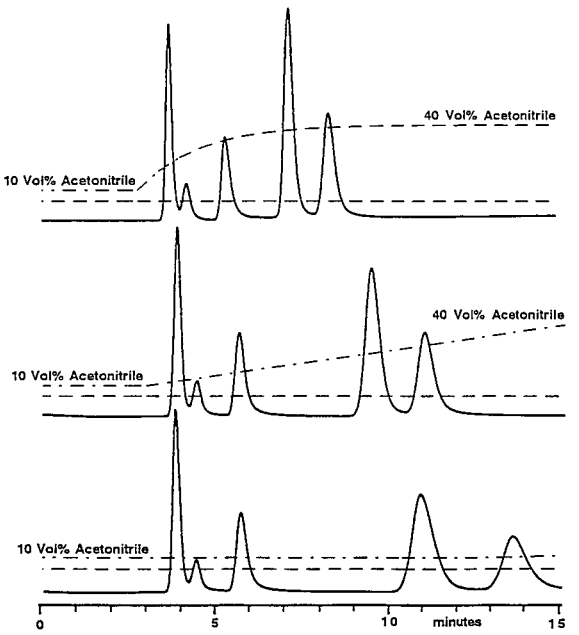

Fig. 11. Effect of different acetonitrile gradients on the resolution of alkali and alkaline earth metals on IonPac CS12. Eluent, 0.01 mol/l methanesulfonic acid–acetonitrile; flow-rate, 1 ml/min; detection, suppressed conductivity; injection volume and solute concentrations as in Fig. 10.

dissociation of the carboxylate ion-exchange groups, thus reducing the effective capacity of the resin. To confirm this assumption, a set of experiments were carried out keeping the MSA concentration in the mobile phase constant 0.01 mol/l and increasing the acetonitrile content in steps of 2% (v/v). As can be seen in Fig. 9, the retention times, especially for the divalent cations, decrease with increasing content of acetonitrile in the mobile phase. Acetonitrile seems to reduce the dissociation of the carboxylate functionality, resulting in a lower effective capacity of the resin. This means that if an organic solvent is added to the mobile phase, the concentration of the acid eluent has to be decreased to obtain the same separation as without organic solvents in the mobile phase. Fig. 10 shows the resulting chromatograms of isocratic alkali and alkaline earth metal separations with different acetonitrile contents in the mobile phase. From Fig. 10, it can be concluded that adding 10% acetonitrile to the eluent reduces the retention times of magnesium and calcium by 45%. In this case, the MSA concentration should be half the starting concentration in order to maintain a constant retention time. As shown in Fig. 11, acetonitrile gradients of different shapes (linear, convex, concave) have also been investigated. The results of these experiments suggest the use of acetonitrile gradients to generate separations for sodium, ammonium, potassium, magnesium, and calcium that look similar to isocratic separations. This application can be used to analyze samples containing large amounts of organic contaminants, because the column is continuously cleaned with acetonitrile during the ongoing separation of the inorganic compounds.

REFERENCES

1 H. Small, T. S. Stevens and W. C. Bauman, *Anal. Chem.*, 47 (1975) 1801.
2 D. T. Gjerde and J. Fritz, *Ion Chromatography*, Hüthig, Heidelberg, 2nd ed., 1987.
3 H. Small, *Ion Chromatography*, Plenum Press, New York, 1989.
4 J. Weiss, *Ionenchromatographie*, VCH, Weinheim, 2nd ed., 1991.
5 G. J. Sevenich and J. S. Fritz, *J. Chromatogr.*, 347 (1985) 147.
6 R. D. Rocklin, M. A. Rey, J. R. Stillian and D. L. Campbell, *J. Chromatogr. Sci.*, 27 (1989) 474.
7 J. S. Fritz, D. T. Gjerde and R. M. Becker, *Anal. Chem.*, 52 (1980) 519.
8 P. Kolla, J. Köhler and G. Schomburg, *Chromatographia*, 23 (1987) 465.
9 D. L. Campbell, J. R. Stillian, S. Carson, R. Joyce and S. Heberling, *J. Chromatogr.*, 546 (1991) 229.
10 J. Weiss, *GIT Spezial, Chromatographie*, No. 2 (1992) 67.
11 D. Jensen, *Labo*, 4 (1992) 64.
12 J. R. Stillian, V. Barreto, K. Friedman, S. Rabin, M. Toofan, J. Statler and H. Dhillon, presented at the *3rd International Symposium on Ion Chromatography, Linz, Austria, 1992.*
13 E. Dabek-Zlotorzynska and J. F. Dlouhy, *J. Chromatogr.*, 638 (1993) 35.
14 *Application Report No. 04/91/06*, Dionex, Idstein, 1991.
15 *Application Report No. 01/92/02*, Dionex, Idstein, 1992.

Journal of Chromatography, 640 (1993) 73–78
Elsevier Science Publishers B.V., Amsterdam

CHROMSYMP. 2705

Metal speciation by means of microbore columns with direct-injection nebulization by inductively coupled plasma atomic emission spectroscopy

Douglas T. Gjerde*

Sarasep, Inc., 1600 Wyatt Drive, Suite 10, Santa Clara, CA 95054 (USA)

Daniel R. Wiederin and Fred G. Smith

Cetac Technologies, Inc., 5600 South 42nd Street, Omaha, NE 68107 (USA)

Bruce M. Mattson

Department of Chemistry, Creighton University, Omaha, NE 68178 (USA)

ABSTRACT

Ion chromatography can be used to perform speciation of several elements. This paper examines the use of ion chromatography with inductively coupled plasma atomic emission spectroscopy detection. A new type of nebulizer, the direct-injection nebulizer, was used to introduce the sample into the plasma. Columns were developed to interface with the direct-injection nebulizer at a flow-rate of 80–100 μl/min. The speciation of arsenic, selenium and chromium is discussed.

INTRODUCTION

Inductively coupled plasma atomic emission spectroscopy (ICP-AES) is often used to determine the concentrations of elements in a sample. However, the total elemental concentration is not a complete description because an element is often present in a variety of chemical forms or species. Different species of an element may possess quite different biological, medicinal or toxicological properties. For example, Cr(VI) is extremely toxic, but a trace amount of Cr(III) is essential for human health. Other elements exhibit similar characteristics. Measuring the concentration of the different chemical forms of a particular element can be important to determine the hazards of a particular sample.

* Corresponding author.

The work presented here describes general methods for elemental speciation using microbore columns. Ion chromatography has been successful in separating the various species of particular elements. Because sample matrices are often complex and the elements present in low concentrations, selective detection may be needed to achieve the desired sensitivity.

ICP-AES has been interfaced with liquid chromatography for elemental detection [1]. A nebulizer introduces the column effluent into the ICP. Conventional pneumatic nebulizers operate at about 1 ml/min sample flow. This is compatible with conventional ion chromatography columns. However, this type of nebulizer may introduce as little as 1% of the sample into the plasma.

This work utilizes the direct-injection nebulizer (DIN) developed by workers at Iowa State Univer-

0021-9673/93/$06.00

sity [2–8]. This nebulizer operates at much lower sample flow-rates (5–10% of that normally used for conventional pneumatic nebulizers). By design, 100% of the sample is introduced into the ICP. This results in significant advantages including superior precision, elimination of memory effects, higher sample throughput, improved detection limits and elimination of speciation effects. Another advantage of the DIN interface with chromatographic columns is that a large range of separation conditions can be used without any need to adjust the nebulizing conditions. Anion-exchange, cation-exchange, reversed-phase, size-exclusion columns, etc. are easily switched without changing nebulizer interface parameters. For conventional nebulizers, each eluent may require a modification of the sample introduction conditions to maintain a stable plasma. Chromatographic buffer gradients are difficult to perform with conventional nebulizers. Moreover, special conditions must be used to introduce organic solvents with conventional nebulizers, otherwise the plasma could extinguish [9]. The DIN will tolerate eluent gradients up to 100% organic solvents with no change in operating conditions. This is due to the low flow-rates used and the fineness of the DIN aerosol.

Where possible, the separation conditions were based on those developed for standard bore columns (4.0–4.6 mm I.D.) [10]. However, the DIN was designed to accommodate a column effluent input rate of 10–100 μl/min. The microbore columns developed for this work require eluent flow-rates of about 100 μl/min. Eluent flow-rates of *ca.* 100 μl/min rather than 10 μl/min were used in order to introduce the maximum amount of sample to the plasma and gain the greatest sensitivity. Typical column diameters ranged from 1.6 to 2.0 mm I.D. and column lengths ranged from 2 to 15 cm.

EXPERIMENTAL

Ultrex-II-grade nitric acid was from J. T. Baker. Trace metal-grade ammonium hydroxide was from Fisher, and the organoarsenic species were from Aldrich. All other chemicals used were reagent grade or better.

All columns (Sarasep) were manufactured using polyether ether ketone (PEEK) or polyethylene frits, tubes and endfittings. All columns were packed with macroporous, strong-base anion exchangers with an exchange capacity of 0.05 mequiv./g. Column lengths were chosen based on the efficiency needed to separate a particular mixture. If only two species were to be separated, then the shortest possible column was selected to give a 1–2-min separation. If more species were to be separated or the sample matrix contained a high concentration of ions, then a longer column was used. The column hardware was connected directly to the inlet of the DIN–ICP-AES via a short length of 0.3 mm I.D. PEEK tubing. The columns used are summarized in Table I.

TABLE I

SUMMARY OF MICROCOLUMNS USED FOR SPECIATION

Mercury, lead, tin and some arsenic speciation work performed by Shum and co-workers [11,12] on Sarasep-supplied columns.

Species	Column
As(III), As(V)	ANX1705
As(III), DMA, MMA, As(V)	ANX1710, RPX1710
Hg^{2+}	RPX1705
Hg^{2+}, methyl-Hg^{+}, ethyl-Hg^{+}	RPX1715
Pb^{2+}, trimethyl-Pb^{+}, triethyl-Pb^{+}	RPX1705, C181705
Alkyl tin species	RPX1710
Se(IV), Se(VI)	ANX1705
Cr(III), Cr(VI)	ANX1710

In cases where few components in a mixture were to be separated and high sensitivity was desired, large injections of 5–20 μl were used. In cases where the sample contained a high ionic matrix or several species to be separated, smaller injection volumes of 0.2–0.5 μl can be used to gain the greatest column resolution. A Rheodyne Model 9010 injector was used in all work.

The DIN used was a System 3 from Cetac Technologies, and the HPLC pump used was a Model 222D from Scientific Systems. Sample traveled through a fused-silica capillary of 50 μm I.D. (Fig. 1). A concentric tube was used to introduce argon gas which nebulized the sample into the plasma. The ICP spectrometer used was a Thermo Jarrell Ash ICAP 61. Operating conditions for the DIN and the ICP spectrometer are given in Table II.

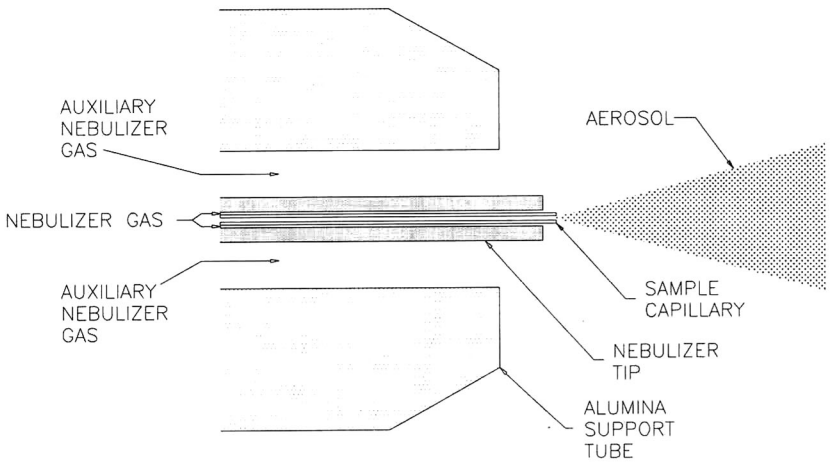

Fig. 1. Schematic of direct-injection nebulizer (DIN). The complete aerosol is directed into the ICP.

RESULTS AND DISCUSSION

Arsenic

Arsenic is very common and is found in soil, preservatives, coal, etc. As(III) and As(V) are particularly toxic. Organoarsenic species appear to be less toxic. Previous DIN interface work performed by Shum and co-workers [11,12] demonstrated that reversed-phase microbore columns and eluents containing ion-pairing reagents could be coupled with mass spectrometric (MS) detection for arsenic speciation.

Much of the previous speciation work with standard columns has been with anion-exchange type columns [13–17]. In this work, a microbore column (10 cm × 1.7 mm I.D.) packed with low-capacity anion-exchange material (0.05 mequiv./g capacity) was used for the speciation of As(III), monomethylarsonate and As(V) (Fig. 2) The eluent contained 5 m*M* ammonium carbonate and 5 m*M* ammonium bicarbonate at pH 8.6. The ammonium salts were used to prevent salt formation and plugging of the DIN tip. A relatively large injection volume (10 μl) was used to obtain higher sensitivity. Dimethylarsinate (DMA), if present, would elute directly after As(III) and not be completely resolved. A smaller injection volume (0.5 μl) or a longer column would be needed to resolve DMA and As(III). If the pK_a values of the species to be separated differ, adjusting the eluent buffer pH can improve the resolution of

TABLE II

DIN AND ICP OPERATING CONDITIONS

ICP torch	DT-B20 (Cetac Technologies)
Argon outer flow-rates	17 l/min
Argon intermediate flow-rate	0.7 l/min
Nebulizer gas pressure	550 kPa (80 p.s.i.)
Plasma forward power	1.5 kW
Sample flow-rate	80 μl/min
Integration time	3.0 s

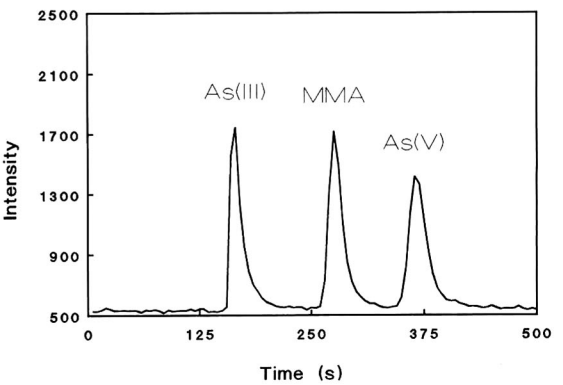

Fig. 2. Anion-exchange separation of arsenic species. Column ANX1710 was used with a 5.0 m*M* NH_4HCO_3–$(NH_4)_2CO_3$ eluent. Eluent flow-rate was 80 μl/min with a 10-μl sample injection volume.

TABLE III

RESPONSE DATA FOR ARSENIC SPECIES

Species	Conventional Nebulizer –ICP-MS detection[a]	DIN–ICP-MS detection[b]	DIN-ICP-AES detection[c]
Arsenite	5.9	240	4170
Dimethylarsinate	11.2	220	
Monomethylarsonate	5.0	260	4740
Arsenate	2.4	230	4430

[a] Data in counts per picogram from ref. 18.
[b] Data in counts per picogram from ref. 12.
[c] Relative intensity for 10-μl injection, present work.

the species. The detection limit for arsenic is 10 μg/l, and the minimum detectable quantity is 100 pg.

Table III gives a comparison of detector response data for various forms of arsenic. The results in the first two columns were obtained with a conventional column with a pneumatic nebulizer and a microbore column with DIN–ICP-MS detection [12,18]. The last column shows data obtained with a microbore column and DIN–ICP-AES detection. Because different organoarsenic species have different volatilities, transport efficiency of the species into the plasma with conventional pneumatic nebulizers will vary. The DIN nebulizes all of the sample into the plasma, so the amount of a particular species entering the ICP is independent of its volatility. Therefore, introduction of all of the sample into the plasma by the DIN provides relatively uniform sensitivity for both ICP-AES and ICP-MS. Separate speciation experiments of Cr(III) and Cr(VI) and Se(IV) and Se(VI) also resulted in uniform AES sensitivity.

Besides direct calibration, another advantage of uniform response is the ability to mass balance the various species with the total elemental content of a sample. A sample may be separated into various elemental species. However, because of column selectivity differences, it is not known if all species eluted from the chromatographic column. The total elemental content of a sample can be determined by performing a second injection without the column present and keeping all other conditions constant. Elemental concentration without the column can be compared to the total concentration of the various species measured from the column separation.

Selenium

Selenium has been reported in the media for years. It has caused widespread poisoning of water fowl in several watershed areas of central California. Selenium has been washed or leached into these areas, mainly due to the widespread irrigation of selenium-containing farm soil. Selenite is roughly twice as toxic as selenate. At very low levels, selenium is recognized as an essential trace element in human and animal nutrition. In fact, vitamins often contain selenium.

Selenium has been speciated previously by anion-exchange chromatography [1,19–21]. The selenite and selenate speciation was achieved using identical column and eluent conditions as used in the arsenic speciation described above. A simultaneous separation of arsenic and selenium species is given in Fig. 3. Individual injections of the various oxidation

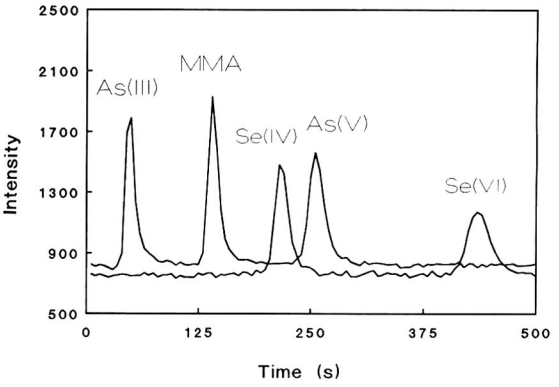

Fig. 3. Simultaneous separation of arsenic and selenium species. Column ANX1710 was used with a 5.0 m*M* NH_4HCO_3–$(NH_4)_2CO_3$ eluent. Eluent flow-rate was 80 μl/min with a 10-μl sample injection volume.

states of selenium and arsenic showed that no oxidation or reduction of the various species occurred in the sample mixture. The selenium detection limit is 4 μg/l (40 pg for a 10-μl injection).

Chromium

Cr(III) is an essential micronutrient. However, Cr(VI) is extremely toxic. Current methods for chromium speciation of environmental samples are lengthy and complex. Total chromium is determined by stabilizing a sample at pH 2 and then analyzing it by ICP-AES. Using US Environmental Protection Agency (EPA) Method 218.6 [22], Cr(VI) is determined by stabilizing a sample at pH 9, filtering it [which removes precipitated Cr(III)] and then using an anion-exchange ion chromatography method to measure chromate. The amount of Cr(III) in the sample is calculated by subtracting the Cr(VI) concentration from the total chromium concentration.

Our strategy for performing chromium speciation was to develop an anion-exchange method that could be carried out under acidic pH conditions so that both Cr(III) and Cr(VI) are soluble. Only a few methods with standard-bore anion-exchange columns have been reported [23,24]. Cr(III) is a cation and should travel unretained through an anion-exchange column. However, Cr(VI) is an anion and should be retained and eluted later. The major difficulty in this strategy is the possible precipitation of Cr(III) either prior to injection or during injection on the column. Because of this possibility a low-pH eluent was developed to prevent Cr(III) precipitation. No other sample preservation procedures were employed. Fig. 4 shows an unretained Cr(III) peak using a pH 2 eluent. A matrix up to 500 ppm sulfate with a 10-μl injection volume was tolerated without affecting the retention times. (In a similar study with arsenic and selenium, a background matrix of 500 ppm sulfate did have a small effect on the retention times and peak shapes. This is possibly due to the relatively low concentration of buffer eluent used in the arsenic–selenium studies.) The detection limit for chromium is 2 μg/l (20 pg for a 10 μl injection).

There is concern that low pH could convert Cr (VI) to Cr(III) [25]. In our experience, this was never observed. Experiments of individual species at a pH range of 2–9 showed that the lower pH keeps

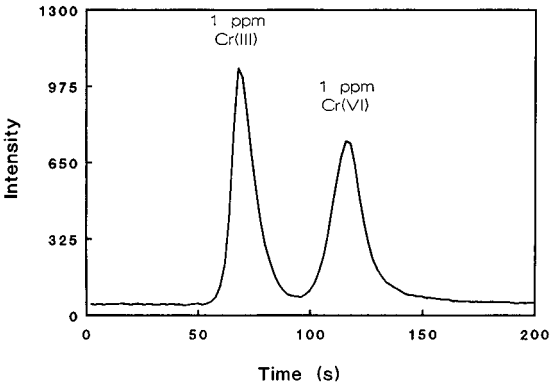

Fig. 4. Simultaneous separation of 1 mg/l each of Cr(III) and Cr(VI) in the presence of 500 mg/l of sulfate matrix. Column ANX1705 was used with a 110 m*M* NH_4NO_3 eluent (pH 2). Eluent flow-rate was 80 μl/min with a 10-μl sample injection volume.

Cr(III) dissolved, but does not facilitate conversion of Cr(VI) to Cr(III). The eluent was prepared by making up a solution of 110 m*M* nitric acid and adjusting the pH to 2 with ammonium hydroxide. Samples that are acidified give nicely shaped Cr(III) and Cr(VI) peaks. At pH 7, the Cr(VI) peak is well shaped; however, the Cr(III) peak is split. Even if the Cr(III) peak is poorly shaped, the concentration of Cr(III) will correspond to the peak area if analyzed promptly. Upon storage at pH 7, the Cr(III) precipitates over the course of a few days. If the sample is even more basic, Cr(III) is insoluble.

If a strong reducing agent is present under acidic conditions, Cr(VI) may be reduced to Cr(III) [25]. However, storage and stabilization of the sample at pH 9 is not acceptable because chromate will precipitate with cations such as lead. If EPA Method 218.6 is used, the sample is filtered, the pH adjusted to 9.0–9.5, and the sample refiltered. Partial or complete loss of Cr^{6+} may occur if Pb^{2+} or similar ions are present that form insoluble chromate salts under basic conditions.

The sample pH, not the eluent pH, may be the important factor with regard to conversion of Cr (VI) to Cr(III). In order to test this hypothesis, a number of reducing agents were added to Cr(VI) and the solution was analyzed for Cr(III) and Cr (VI). First a mixture of Se(IV) and As(III) was added to Cr(VI) at both pH 2 and pH 9. In neither case was Cr(III) generated. Next, excess Fe(II) was added to 1 mg/l of chromate and was found to reduce the Cr(VI) to Cr(III) over a period of 1 h.

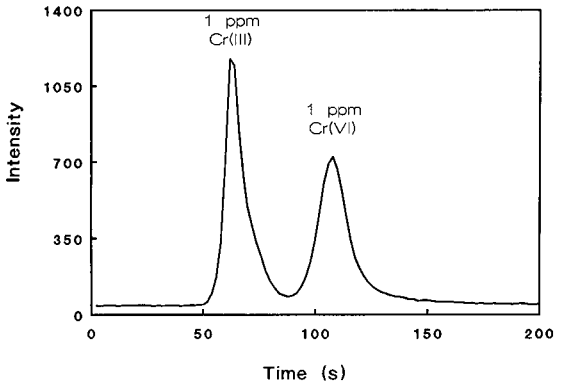

Fig. 5. Separation of 1 mg/l each of Cr(III) and Cr(VI) spiked into Omaha creek water. The unspiked sample did not contain detectable chromium. There was no oxidation or reduction of the chromium species in the creek water matrix. Column ANX1705 was used with a 110 m*M* NH_4NO_3 eluent (pH 2). Eluent flow-rate was 80 μl/min with a 10-μl sample injection volume.

Environmental water samples were spiked with 1.0 mg/l each of Cr(III) and Cr(VI). The samples were stabilized by mixing 50:50 with the acidic buffer eluent. A separation of the two chromium species spiked into Papio Creek water (Omaha, NE, USA) is given in Fig. 5. No species interconversion was noted over an eight-day period, indicating that these species are stable under acidic conditions.

CONCLUSIONS

Phase 1 of this work was to establish a family of columns that can interface with a DIN–ICP-AES detection scheme and separate a variety of elemental species. The separation conditions were chosen to operate with a variety of samples. The specific column, eluent, injection volume, etc. depend on the type and number of species to be separated, the sample matrix, sample stability and detection limits required. In general, conditions were chosen based on methods developed for standard columns so that published sample preparation procedures can be used.

Phase 2 of this work is to develop specific methods for particular samples. This is an ongoing process. Verification of the chromatographic conditions depends on making certain that the relative concentration of the particular species does not change during the course of sampling, sample preparation and analysis.

REFERENCES

1 I. S. Krull (Editor), *Trace Metal Analysis and Speciation (Journal of Chromatography Library*, Vol. 47), Elsevier, Amsterdam, 1991.
2 K. E. Lawrence, G. W. Rice and V. A. Fassel, *Anal. Chem.*, 56 (1984) 289.
3 K. E. LaFreniere, G. W. Rice and V. A. Fassel, *Spectrochim. Acta*, 40B (1985) 1495.
4 K. E. LaFreniere, V. A. Fassel and D. E. Eckels, *Anal. Chem.*, 59 (1987) 879.
5 T. W. Avery, C. Chakrabarty and J. J. Thompson, *Appl. Spectrosc.*, 44 (1990) 1690.
6 D. R. Wiederin, F. G. Smith and R. S. Houk, *Anal. Chem.*, 63 (1991) 219.
7 D. R. Wiederin, R. E. Smyczek and R. S. Houk, *Anal. Chem.*, 63 (1991) 1626.
8 F. G. Smith, D. R. Wiederin, R. S. Houk, C. B. Egan and R. E. Serfass, *Anal. Chim. Acta*, 248 (1991) 229.
9 A. W. Boorn and R. F. Browner, in P. W. J. M. Boumans (Editor), *Inductively Coupled Plasma Emission Spectroscopy, Part II: Applications and Fundamentals*, Wiley, New York, 1987 pp. 151–216.
10 D. T. Gjerde and H. Mehra, in I.S. Krull (Editor), *Trace Metal Analysis and Speciation (Journal of Chromatography Library*, Vol. 47), Elsevier, Amsterdam, 1991 pp. 213–239.
11 S. Shum, H. Pang and R. S. Houk, *Anal. Chem.*, 64 (1992) 2444.
12 S. Shum, R. Neddersen and R. S. Houk, *Analyst*, 117 (1992) 577.
13 R. J. Williams, *Anal. Chem.*, 55 (1983) 851.
14 G. K.-C. Low, G. E. Batley and S. J. Buchanan, *Anal. Chim. Acta*, 197 (1987) 327.
15 G. K.-C. Low, G. E. Batley and S. J. Buchanan, *Chromatographia*, 22 (1986) 292.
16 L. K. Tan and J. E. Durtizac, *Anal. Chem.*, 58 (1986) 1383.
17 F. E. Brinckman, K. L. Jewett, W. P. Iverson, K. J. Irgolic, K. C. Ehrhardt and R. A. Stockton, *J. Chromatogr.*, 191 (1980) 31.
18 D. T. Heitkemper, J. Creed, J. Caruso and F. L. Fricke, *J. Anal. At. Spectrom.*, 4 (1989) 279.
19 I. T. Urasa and F. Ferede, *Anal. Chem.*, 59 (1987) 1563.
20 F. Noguchi, H. Ito, T. Bakamura, Y. Ueda and K. Ota, *Anal. Sci.*, 4 (1988) 398.
21 H. C. Mehra and W. T. Frankenberger, Jr., *Chromatographia*, 25 (1988) 585.
22 *Methods for the Determination of Metals in Environmental Samples*, United States Environmental Protection Agency, EPA/600 4-91/010, Office of Research and Development, Washington, DC, June, 1991.
23 F. Makata, S. Hara, H. Matsuo, T. Kumamaru and S. Matsushita *Anal. Sci.*, 1 (1985) 157.
24 I. T. Urasa and S. H. Nam, *J. Chromatogr. Sci.*, 127 (1989) 30.
25 F. A. Cotton and G. Wilkinson, *Advanced Inorganic Chemistry*, Wiley, New York, 3rd ed., 1972.

Journal of Chromatography, 640 (1993) 79–96
Elsevier Science Publishers B.V., Amsterdam

CHROMSYMP. 2643

Review

Pulsed amperometric detection of carbohydrates, amines and sulfur species in ion chromatography —the current state of research

Dennis C. Johnson*, David Dobberpuhl, Richard Roberts and Peter Vandeberg

Department of Chemistry, Iowa State University, Ames, IA 50011 (USA)

ABSTRACT

A review is given of so-called pulsed amperometric detection at Au and Pt electrodes. Of greatest interest is the application of pulsed amperometric detection for polar aliphatic compounds not easily detected by conventional photometric or fluorometric techniques. The anodic detection mechanisms are electrocatalytic in nature under the control of potential-dependent surface states. Oxidations of carbohydrates at Au electrodes in alkaline media occur in a potential region where a submonolayer of adsorbed hydroxyl radicals (OH_{ads}) is formed and speculation is offered on the role of this species in the anodic mechanisms. Very little anodic signal is obtained at Au electrodes for low-molecular-mass *n*-alcohols; however, a large response is obtained from oxidation of the alcohol moiety of *n*-alkanolamines. This is attributed to the beneficial effect of adsorption via the amine moiety with the result that the residence time of the molecules at the electrode surface is increased to give a high probability for ultimate oxidation. Amines and sulfur compounds with non-bonded electrons on the N and S atom, respectively, are adsorbed at Au electrodes and are oxidatively desorbed concomitantly with formation of inert surface oxide (AuO). The simultaneous formation of surface oxide produces a large background signal in pulsed amperometric detection. Hence, a modification of the pulsed waveform is described whose application is called integrated pulsed amperometric detection. Applications are shown for pulsed amperometric detection and integrated pulsed amperometric detection in ion chromatography to illustrate strengths of these combined technologies.

CONTENTS

* Corresponding author.

0021-9673/93/$24.00

1. CONCEPTS OF ELECTROCATALYTIC DETECTION

1.1. Introduction

The development of ion chromatography (IC) in both the suppressed and non-suppressed forms has relied heavily on electrochemical detection [1–4]. At its inception, IC utilized conductance detection (CD) and, because of its simplicity and reliability for both inorganic and organic ions, CD continues as the most common detection technique in IC. Potentiometric detection also has been used in IC. Applications have included complexing agents at Cu electrodes, and halides and pseudo-halides at Ag electrodes. More recently, much interest has been directed to amperometric detection in IC as a result of successful separations of organic compounds [5–8].

This review is focused on anodic detection of aliphatic compounds based on electrocatalytic mechanisms at Pt and Au electrodes under the control of multi-step potential–time (E–t) waveforms [5–8]. Applications of these detection mechanisms have included simple alcohols, polyalcohols, carbohydrates, amines and some sulfur compounds. A description of the voltammetric basis of this detection technology is given here with examples of chromatographic applications.

1.2. Background

Many polar aromatic compounds are detected in aqueous media by oxidation at conventional anodes (*e.g.*, Au, Pt and C in its various forms) using constant (d.c.) applied potentials. Included are phenol, aminophenols and catecholamines, and numerous applications have appeared for liquid chromatography (LC) [9]. In contrast, d.c. detection is consistently ineffective for aliphatic alcohols and amines at these same electrodes. The reactivity of aromatic compounds is believed to benefit from conjugated bonding which stabilizes free-radical oxidation products and, thereby, lowers the activation barrier. However, a similar mechanism does not exist in aliphatic compounds and their oxidations are typically slow or non-existent at inert electrodes.

Absence of π-bonding in aliphatic compounds also has the consequence of low sensitivity for photometric (UV–Vis) detection. Hence, development of detection procedures for polar aliphatic compounds separated by various forms of LC has represented a major challenge to analytical chemistry. Many ad-

vances have been reported in the use of pre-injection and post-column chemical derivatizations to generate photometrically as well as electrochemically active adducts [10,11]. Nevertheless, the authors believe there will always be preference for the simplicity of direct detection, whenever available with sufficient sensitivity.

1.3. Electrocatalytic oxidation mechanisms

A premise of the detection strategy reviewed here is that activation barriers for oxidation of polar aliphatic compounds can be decreased at clean Au and Pt electrodes which have unsaturated surface d-orbitals. These surfaces stabilize free-radical oxidation products by adsorption and, thereby, can promote faradaic reactions of numerous polar aliphatic compounds. However, a consequence of adsorption can be extensive fouling of surfaces by accumulated detection products. Hence, historical consensus of non-reactivity for many aliphatic compounds at Au and Pt electrodes is actually a consequence of the high but short-lived activity of these electrode surfaces.

Faradaic processes are described as *electrocatalytic* when the electrode surface interacts beneficially within the reaction mechanisms. A characteristic of electrocatalytic mechanisms is that the voltammetric response of members within a family of compounds is controlled primarily by the potential dependence of the requisite catalytic surface state. Hence, mixtures of compounds reacting by the same electrocatalytic mechanism cannot possibly be resolved on the basis of their voltammetric response. Therefore, the greatest analytical utility of electrocatalytic detection mechanisms is obtained when they are coupled with chromatographic systems to achieve *a priori* separations.

1.4. Renewal of electrode surface activity

A serious consequence of strong adsorption of organic molecules and free radicals on Au and Pt electrodes can be the attenuation of surface reactivity. However, these adsorbates are usually oxidatively desorbed quite efficiently by application of a large positive potential step to achieve anodic formation of surface oxides (AuO and PtO) [12,13]. A subsequent large negative potential step quickly achieves cathodic dissolution of the oxides to restore the native reactivity of the clean surfaces.

Large positive and/or negative potential pulses have long been used for activation of solid electrodes. Table 1 contains a brief historical review of the associated literature. Of greatest significance to this review are multi-step waveforms which alternate amperometric detection with surface cleaning and reactivation to achieve continuous monitoring of chromatographic effluents.

1.5. pH Requirements

The heterogeneous rate constants for electrocatalytic oxidations of polar aliphatic compounds at clean Au and Pt surfaces are generally observed to increase with increasing pH. This pH effect is undoubtedly the result of H^+ production in the anodic mechanisms. Nevertheless, the minimum pH for satisfactory analytical response is dependent on the choice of electrode material. For example, high sensitivity for anodic detection of carbohydrates at Au electrodes requires pH $\geqslant$ *ca.* 12, whereas detection at Pt electrodes is satisfactory even at pH <1. This dramatic difference in the minimal useful pH is attributed to the lower electronic occupancy of the surface d-orbitals at Pt and, therefore, a greater ability to promote reactions by stabilization of free-radical oxidation products. Nevertheless, Au electrodes are more popular than Pt. One reason is that dissolved O_2 contributes a cathodic response at Pt over the entire potential range useful for anodic detection, whereas careful selection of detection potential at Au can avoid serious O_2 interference.

1.6. Selection of chromatographic phases

The need for pH control in chromatographic applications of electrocatalytic anodic detections at Au and Pt electrodes can be achieved by post-column additions of an appropriate buffer solution. However, greatest convenience and economy is achieved whenever separation phases are available that are tolerant of the conditions of pH and ionic strength desired for optimum detector response. Hence, polymeric separation phases developed for IC are highly preferred over silica-based phases developed for reversed-phase LC because of their greater stability over an extended pH range.

TABLE 1

HISTORICAL OVERVIEW OF APPLICATIONS OF MULTISTEP POTENTIAL–TIME WAVEFORMS FOR THE CLEANING AND REACTIVATION OF SOLID ELECTRODE SURFACES

Pos. = Positive; neg. = negative; C = glassy carbon electrode.

Author(s)	Year	Electrode	Summary	Ref.
Hammett	1924	Pt	Pos. pulses applied for pretreatment of electrode prior to oxidation of H_2	14
Armstrong *et al.*	1934	Pt	Pos. pulses applied for pretreatment of electrode prior to reduction of O_2	15
Gilman	1963	Pt	Pos./neg. pulses applied for electrode pretreatment in study of oxidation of simple alcohols	16
Breiter	1963	Pt and others	Pos./neg. pulses applied for electrode pretreatment in study of methanol oxidation	17
Giner	1964	Pt	Pos./neg. pulses applied for electrode pretreatment in study of alcohol oxidation	18
Adams	1969	Pt and C	Application of pos./neg. pulses recommended as general procedure for pretreatment for solid electrodes	19
Clark *et al.*	1972	Pt	Pos./neg. pulses applied for reactivation of electrodes during oxidation of ethylene	20
MacDonald and Duke	1973	Pt	Pos./neg. pulses applied for reactivation of electrodes during oxidation of *p*-aminophenol	21
Fleet and Little	1974	C	Use of two-step waveform decreased rate of electrode fouling in flow-through cell	22
Stulik and Hora	1976	Pt	Pos./neg. pulses for periodic reactivation of electrode during cathodic detection of Fe^{3+} and Cu^{2+}	23
Van der Linden and Diekes	1980	C	Pos./neg. pulses recommended as general means of electrode pretreatment	24
Van Rooijen and Poppe	1981	C	Periodic application of square-wave pulse train for electrode reactivation	25
Ewing *et al.*	1981	C	Application of two-step waveform for pulse voltammetry at microelectrodes to decrease rate of electrode fouling	26
Hughes *et al.*	1981	Pt	Pos./neg. pulses used in a three-step waveform for anodic detection of simple alcohols	27
Hughes and Johnson	1983	Pt	Three-step waveform for anodic detection of carbohydrates following chromatographic separation	28
Edwards and Haak	1983	Au	Three-step waveform for anodic detection of carbohydrates following chromatographic separation	29
Polta and Johnson	1983	Pt	Three-step waveform for anodic detection of amino acids following chromatographic separation	30
Polta and Johnson	1986	Au	Three-step waveform for anodic detection of sulfur compounds	31
Neuburger and Johnson	1987	Pt and Au	Three-step waveform for pulsed voltammetric comparison of carbohydrate response	32
Neuburger and Johnson	1988	Au	Multi-step waveform for oxide-catalyzed detection with automatic background rejection	33
Chen *et al.*	1992	Pt	Three-step waveform for pulse voltammetry at microelectrode in intracellular fluid	34
LaCourse and Johnson	1992	Au	Automated optimization of three-step waveforms for carbohydrate detection	35

2. EXPERIMENTAL

Voltammetric data were obtained at rotated disk electrodes (RDEs) using Models MSR rotators and RDE4 potentiostats (Pine Instrument Co). Analog waveforms at slow scan rates (50–100 mV/s) were generated within the RDE4. Staircase waveforms were generated external to the RDE4 by an IBM-compatible PC using Asyst 2.0 software (Asyst Technologies). Studies with fast scans ($\gg$ 50 mV/s) used analog waveforms generated by a Model 175 programmer connected to a Model 173 potentiostat (EG&G Princeton Applied Research). Digital recording of electrode response was achieved using IBM-compatible PCs with Asyst software. Interface boards were the DT-2800 (Data Translation) or DAS-1602 (MetraByte).

Counter electrodes in all voltammetric studies were Pt wires separated from the test solutions by fritted-glass junctions. Reference electrodes were saturated calomel electrodes (SCEs) separated from the test solutions by fritted-glass junctions.

Solutions were prepared from reagent-grade chemicals (Fisher Scientific) with water that had been purified by passage through two D-45 demineralizing cartridges (Culligan) and further treatment in a Milli-Q system (Millipore). When desired, solutions were deaerated by dispersed N_2 and an inert atmosphere was maintained over the solutions.

Chromatographic data shown for sulfur compounds were obtained using a Model GPM-2 pump (Dionex). All other chromatographic data are reproduced from earlier publications and the associated experimental details can be found in the references cited.

3. RESIDUAL VOLTAMMETRIC RESPONSE OF ELECTRODES

A complete description of amperometric detection must begin with the voltammetric response observed in the absence of analyte for an electrode potential applied according to the triangular waveform in Fig. 1A. That response is discussed here for Au in alkaline media and Pt in acidic media.

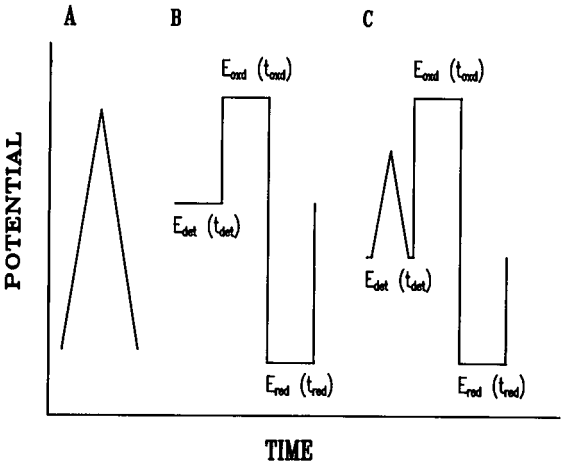

Fig. 1. Potential–time (E–t) waveforms. Curves: (A) voltammetric detection, (B) pulsed amperometric detection, (C) integrated pulsed amperometric detection. E_{det} = Detection potential; E_{red} = reduction potential; E_{oxd} = oxidation potential; t_{det} = detection period; t_{red} = reduction period; t_{oxd} = oxidation period.

3.1. Gold

Residual current–potential (i–E) curves obtained for a Au rotated disk electrode (RDE; 16.4 mm^2) in 0.1 M NaOH are shown in Fig. 2 for the absence (A and C) and presence (B) of dissolved O_2. The waveform (Fig. 1A) producing curves A and B was generated by analog instrumentation. Therefore, potential was a continuous function of time and elec-

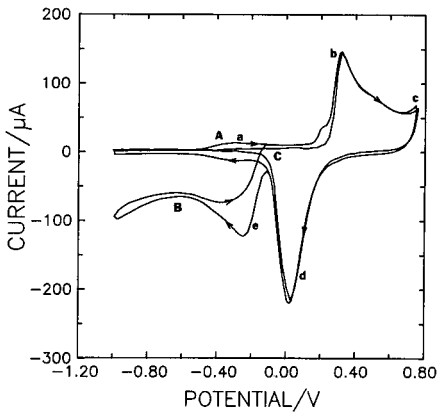

Fig. 2. Voltammetric response for a Au RDE in 0.10 M NaOH. Conditions: 400 rpm rotation, 500 mV/s scan. Solution: (A and C) deaerated, (B) aerated. Waveform generation (Fig. 1A): (A and B) analog, (C) digital. For a–e, see text.

trode current (i) was recorded as a continuous function of potential. Wave a, observed on the positive scan in the region *ca.* −0.6 to +0.1 V, is believed to correspond to anodic discharge of H_2O with formation of a submonolayer of adsorbed hydroxyl radicals ($^{\bullet}OH_{ads}$), frequently designated AuOH, perhaps at dislocated Au atoms or small atomic clusters. A monolayer of inert surface oxide (AuO) is formed during the positive scan for $E >$ *ca.* +0.2 V (wave b) and solvent breakdown with O_2 evolution occurs for $E >$ *ca.* +0.6 V (wave c). Evolution of O_2 and formation of AuO cease with scan reversal at +0.75 V and cathodic dissolution of AuO occurs in the region +0.2 to −0.1 V (peak d). Dissolved O_2, if present (curve B), is cathodically detected at $E <$ *ca.* −0.2 V (wave e).

Curve C was obtained using a waveform generated by digital instrumentation in which potential was advanced by 25-mV increments (ΔE) applied at 50-ms intervals (Δt). This so-called *staircase* waveform is a good approximation of the analog waveform when ΔE and Δt are very small. In obtaining curve C, current was sampled digitally after a 15-ms delay following each application of ΔE. Hence, contribution from double-layer charging is negligible. Also minimized are contributions from fast faradaic transformations of the electrode. Hence, there is almost no signal in curve C corresponding to wave a in curves A and B for anodic generation of $^{\bullet}OH_{ads}$. The remaining features of curve C are identical to curve A.

3.2. Platinum

Typically, Pt electrodes are chosen only when the sensitivity of Au electrodes is not sufficient. Specifically, this corresponds to detection of low-molecular-mass *n*-alcohols and glycols. These compounds can be detected with high sensitivity at Pt even in acidic media. Residual voltammetric curves obtained using a triangular analog waveform (Fig. 1A) are shown in Fig. 3 for a Pt RDE (16.4 mm^2) in 0.1 *M* $HClO_4$. Dissolved O_2 was present only for curve B. During the positive scan, a submonolayer of $^{\bullet}OH_{ads}$ is believed to form in the regions *ca.* +0.2 to +0.5 V (wave a), inert surface oxide (PtO) is generated at $E >$ *ca.* +0.5 V (wave b) and rapid discharge of H_2O with evolution of O_2 occurs for $E >$ *ca.* +1.2 V (wave c). Scan reversal at +1.3 V

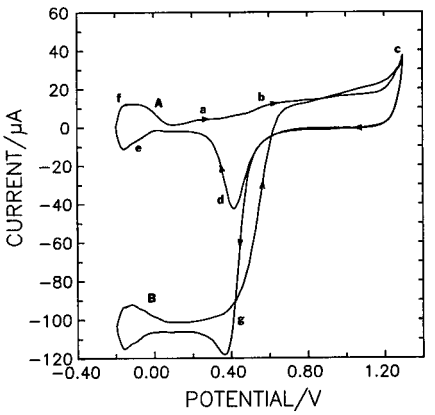

Fig. 3. Voltammetric response of a Pt RDE in 0.10 *M* NaOH. Conditions: 400 rpm, 50 mV/s. Solution: (A) deaerated, (B) aerated. Waveform generation (Fig. 1A): analog. For a–f, see text.

causes O_2 evolution and PtO formation to cease, and the current remains at virtually zero until cathodic dissolution of PtO occurs in the region +0.5 to +0.2 V (wave d). Continuation of the negative scan results in cathodic production of adsorbed hydrogen atoms ($^{\bullet}H_{ads}$) at $E <$ *ca.* 0.0 V (wave e) and evolution of H_2 at $E <$ −0.2 V (not shown). Upon scan reversal at −0.2 V, anodic desorption of $^{\bullet}H_{ads}$ occurs in the region −0.2 to 0.0 V (wave f). Dissolved O_2, when present (curve B), is cathodically detected at $E <$ *ca.* +0.4 V (wave g).

4. DETECTION STRATEGIES

4.1. Reaction modes

There are two unique modes of anodic electrocatalytic detection that are available at Au and Pt electrodes [5,8,36]. These are described for Au in 0.1 *M* NaOH.

4.1.1. Mode I detection

This detection mode corresponds to anodic mechanisms that occur with production of a submonolayer of $^{\bullet}OH_{ads}$ but virtually no inert oxide (AuO), *i.e.*, *ca.* $-0.6 < E < +0.2$ V *vs.* SCE for Au in 0.1 *M* NaOH. The residual current in this potential region is small and decays quickly to a negligible value during a brief delay period following a step to the detection potential. Applications of

mode I detection at Au have been in alkaline media for carbohydrates and polyalcohols [29,37–45], and *n*-alkanolamines [46]. Mode I detection at Pt electrodes has included carbohydrates and polyalcohols in alkaline media [28], and alcohols and glycols in acidic media [47].

4.1.2. Mode II detection

This detection mode corresponds to anodic mechanisms catalyzed by formation of inert surface oxide (AuO) for $E > +0.2$ V *vs.* SCE in 0.1 *M* NaOH. We conclude that the monolayer of $^{\bullet}OH_{ads}$ (AuOH) generated as an intermediate product in the production of AuO is the source of oxygen being transferred to the oxidation products of mode II detection mechanisms. Contributions to the analytical signal originate both from oxidation of adsorbed analyte and analyte being transported to the electrode surface simultaneously with AuO formation. Generally, the anodic response is quickly terminated with scan reversal when formation of AuO (and $^{\bullet}OH_{ads}$) ceases. Therefore, detection requires current measurement simultaneously with AuO formation and, hence, a large background signal can be obtained. A unique approach will be described to minimize problems originating from the background signal. Applications of mode II detection at Au have been in alkaline media for amines and amino acids [48], and some sulfur compounds [49,50].

4.2. Pulsed amperometric detection

The amperometric detection of carbohydrates and polyalcohols in alkaline media based on mode I mechanisms can be managed successfully by multi-step *E–t* waveforms of the type illustrated by Fig. 1B. The detection potential (E_{det}) is chosen to give the maximum desired response and the faradaic signal is sampled by digital integration for a short time period (t_{int}) following a brief delay (t_{del}) in the detection period (*i.e.*, $t_{det} = t_{del} + t_{int}$). Subsequently, the electrode is oxidatively cleaned by a positive step to $E_{oxd} \gg E_{det}$ (t_{oxd}) and then reductively reactivated by a negative step to $E_{red} \ll E_{det}$ (t_{red}) prior to repetition of the waveform. Amperometric detection under control of multi-step waveforms is called pulsed amperometric detection. Optimization of pulsed amperometric detection waveforms has been discussed [35,42,43,51].

The value of t_{int} in pulsed amperometric detection is chosen to maximize the signal-to-noise ratio (*S/N*). A major noise component is sinusoidal and is correlated with the 60-Hz line frequency. Hence, it is common to integrate the electrode current over an integral number (*m*) of 60-Hz cycles (*i.e.*, $t_{int} = 16.7m$ ms) [52]. Accordingly, a large *m* value results in increased signal strength without a significant increase in noise. Typically, $m = 12$ (*i.e.*, $t_{int} = 200$ ms). Signal output in pulsed amperometric detection can be the integral of current ($\int i\partial t$) or the average current ($\int i\partial t/t_{int}$).

4.3. Integrated pulsed amperometric detection

A large baseline signal from formation of surface oxide is obtained when the pulsed amperometric detection waveform in Fig. 1B is applied for mode II detection mechanisms. Furthermore, the baseline signal is commonly observed to drift to more anodic values, especially for new for freshly polished electrodes, because of the slow increase in electrode area as a consequence of surface reconstruction from the repeated formation/dissolution cycles for the surface oxide.

The problem of baseline offset and drift in mode II detections is diminished significantly by use of the waveform in Fig. 1C [33]. In this waveform, the electrode current is integrated during the entirety of a rapid cyclic scan of E_{det} within the detection period. Oxidative detection of analyte occurs concomitantly with oxide formation during the positive scan and the oxide is reduced during the subsequent negative scan. Because the charge for oxide reduction (negative scan) is approximately equal but with opposite polarity to the charge for oxide formation (positive scan), the signal on the electronic integrator at the conclusion of t_{det} can be virtually zero. Furthermore, the background signal is relatively unaffected by gradual changes in electrode area and less time is required for baseline stabilization during start-up of IC–integrated pulsed amperometric detection systems [33]. This detection strategy is referred to as IPAD.

The following guidelines apply for application of IPAD at Au electrodes in 0.1 *M* NaOH [33,53]: (i) the cyclic scan of E_{det} must begin and end at a value for which the electrode is free of surface oxide, *i.e.*, $\leqslant$ *ca.* -0.1 V *vs.* SCE; (ii) the positive scan of E_{det}

should not extend to values > *ca.* +0.6 V *vs.* SCE corresponding to solvent breakdown and O_2 evolution ; (iii) if dissolved O_2 is present, the negative scan of E_{det} should not extend to values < −0.1 V *vs.* SCE corresponding to detection of O_2. Incorrect choice of the negative scan limit for E_{det} can result in a substantial baseline when dissolved O_2 is present. When possible, it is preferable to deaerate the mobile phase with dispersed He and to use O_2-impermeable connective tubing for assembly of IC–IPAD systems.

5. CARBOHYDRATES AND POLYALCOHOLS

5.1. Voltammetric response at Au electrodes

The mode I response of carbohydrates is represented in Fig. 4 by that for glucose (curve B) obtained using the analog *E–t* waveform (Fig. 1A) at a Au RDE (16.4 mm^2) in 0.1 *M* NaOH. Curve A shows the residual response for Au in this media. During the positive scan, oxidation of the aldehyde moiety of glucose to produce the gluconate anion (number of electrons in reaction, n = 2 equiv./mol) occurs for E > *ca.* −0.6 V (wave a) coincident with formation of the submonolayer of $^{\bullet}OH_{ads}$ [54]. The heterogeneous rate constant for this oxidation is fast and the anodic current at *ca.* −0.35 V in the plateau region is limited by the rate of convective-diffusional transport of glucose to the Au RDE surface. The $^{\bullet}OH_{ads}$ is believed to play an important

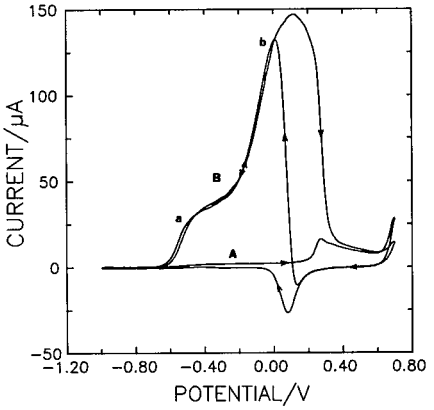

Fig. 4. Voltammetric response of glucose at an Au RDE in 0.10 *M* NaOH. Conditions: 400 rpm, 50 mV/s. Glucose (m*M*): (A) 0.0, (B) 0.5. For a and b, see text.

role in anodic reactions that occur with transfer of oxygen from H_2O to the oxidation products [55]. Evidence for this is the observation that half-wave potentials ($E_{1/2}$) for numerous O-transfer reactions are virtually identical and coincident with the onset of wave a in the residual *i–E* curve. According to this mechanism, $^{\bullet}OH_{ads}$ generated by anodic discharge of H_2O is the intermediate form of oxygen to be transferred from H_2O to the oxidation product. It is also possible that an adsorption step in the oxidation mechanism for polyalcohols and carbohydrates is facilitated by the presence of $^{\bullet}OH_{ads}$.

All carbohydrates (aldoses and ketoses) and polyalcohols produce a large anodic peak response at *ca.* +0.15 V similar to wave b for glucose in Fig. 4. The peak for glucose corresponds to an overall reaction with n approaching 10 equiv./mol for fluid velocities typical of flow-through detection cells [54]. This n value is consistent with an overall oxidation of glucose in alkaline media corresponding to oxidative cleavage of the C_1–C_2 and C_5–C_6 bonds with production of two moles of formate and one mole of dicarboxylate dianion. It is tentatively concluded that oxidations of all carbohydrates and polyalcohols proceed from the terminal carbons. Accordingly, mass sensitivity in pulsed amperometric detection is observed to decrease with increasing molecular mass.

It is significant that the anodic mode I response for glucose is sharply attenuated during the positive scan at E > +0.2 V (see Fig. 4). Whereas the Au surface would become fouled during d.c. detection at +0.15 V over an extended time period, the attenuation shown in Fig. 4 results from oxide formation and not from adsorption of detection products. Oxidation of glucose resumes on the negative scan almost immediately following the onset of cathodic dissolution of surface oxide at E < *ca.* +0.1 V. This behavior is true for all carbohydrates and polyalcohols. We interpret these results to indicate that mode I oxidation of carbohydrates and polyalcohols occurs only at highly reactive sites on the Au surface representing a small fraction of the total area (*i.e.*, <0.2). It is at these sites that oxide (AuO) is first produced during the positive scan and from which the oxide is first to be removed during the negative scan. This conclusion is supported by the observation that scan reversal at +0.30 V results in the return of the current to an anodic value on the

negative scan almost equal to the peak current at +0.15 V observed on the preceding positive scan. These observations indicate that the catalytic sites for oxidation of carbohydrates and polyalcohols are those sites at which the submonolayer of $^{\bullet}OH_{ads}$ is formed during the positive scan for $E > -0.6$ V *vs.* SCE. Furthermore, we conclude these sites correspond to Au atoms with low coordination number in the metal surface, *i.e.*, dislocated atoms, and, possibly, small clusters of Au atoms.

5.2. Chromatographic separations

Carbohydrates and polyalcohols are weakly acidic with $pK_a > 12$ [56]. Hence, separations are easily achieved from alkaline mobile phase (pH > 12) using low-capacity anion-exchange columns [38,42, 57]. These alkaline media are also appropriate for pulsed amperometric detection by the mode I mechanism at Au electrodes. Retention time is inversely correlated with pK_a value and increases dramatically with increasing molecular mass. Retention time can be decreased conveniently by addition of acetate ion (OAc^-). Olechno *et al.* [38] demonstrated the separation of 43 components of a partially hydrolyzed sample of corn starch within a 35-min period using a linear solvent gradient form 0.1 *M* NaOH to 0.1 *M* NaOH + 0.6 *M* NaOAc.

Shown in Fig. 5 is the separation of a mixture of polyalcohols, monosaccharides and small oligosaccharides [5]. Initially, the small polyalcohols are eluted isocratically with 50 m*M* NaOH (0–6 min). Next, the elution of xylose, fructose, sucrose and maltose is achieved by a linear solvent gradient that brings the mobile phase to 75 m*M* NaOH + 250 m*M* NaOAc (6–15 min). Finally, members of the oligosaccharides, ranging from maltotriaose to maltoheptaose (degree of polymerization, DP = 3–7), are eluted isocratically by 75 m*M* NaOH + 250 m*M* NaOAc (15–21 min). The detection limit for glucose is well below 1 ng ($S/N = 3$) with a linear response over more than four decades in concentration.

Larew and co-workers [58,59] considered the challenge of quantification of chromatographic peaks for glucose polymers with DP = 2–7. A short (1.5 cm) reactor column containing immobilized glucoamylase was placed between the chromatographic column and the detector to achieve conversion of polyglucose compounds to the equivalent amount of glucose. For 100% conversion to glucose, a single glucose calibration curve suffices for peak quantification. Conversion efficiency of the short reactor column was *ca.* >95% for DP = 4–7 but <90% for DP = 2 (maltose). Hence, longer reactor columns are recommended to achieve uniformly quantitative conversion of all oligosaccharides. The reactor column was refrigerated when not in use and conversion efficiency did not decrease during a 1-year period of use.

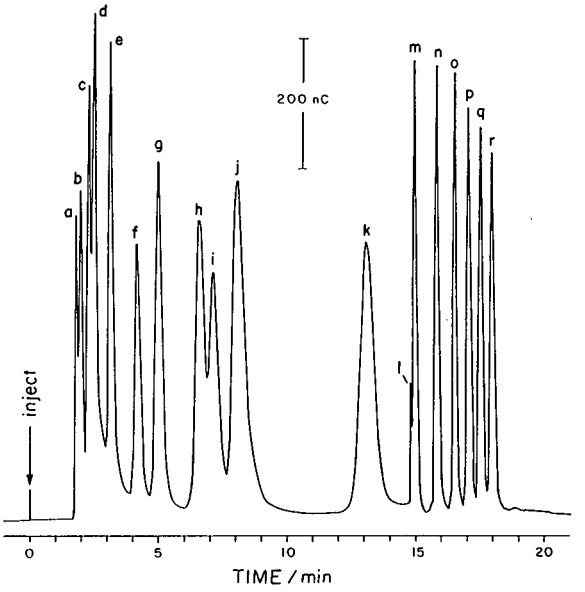

Fig. 5. Separation of carbohydrate mixture. Pulsed amperometric detection (mode I) at Au; Ag/AgCl reference; $E_{det} = +0.10$ V ($t_{det} = 610$ ms, $t_{del} = 400$ ms, $t_{int} = 200$ ms); $E_{oxd} = +0.80$ V ($t_{oxd} = 120$ ms); $E_{red} = -0.60$ V ($t_{red} = 200$ ms). Column: Dionex AS-6 Carbopac. Solvents: (A) 100 m*M* NaOH, (B) 50 m*M* NaOH + 0.5 *M* NaOAc, (C) H_2O. Elution: isocratic (0–6 min) with A–C (50:50); linear gradient (6–15 min) to A–B (50:50); isocratic (15–21 min) with A–B (50:50). Post-column addition: 0.4 *M* NaOH. Peaks: a = inositol; b = xylitol; c = sorbitol; d = mannitol; e = fucose; f = rhamnose; g = arabinose; h = glucose; i = xylose; j = fructose; k = sucrose; l = unknown; m = maltose; n = maltotriose; o = maltotetraose; p = maltopentaose; q = maltohexaose; r = maltopheptaose. From ref. 5 by permission from the American Chemical Society.

Anodic response of sugar amines can be based either on detection of the carbohydrate moiety (mode I) or the amine group (mode II). However, mode I detection yields greater sensitivity.

6. SIMPLE ALCOHOLS AND GLYCOLS

6.1. Voltammetric response at Pt electrodes

The mode I response of low-molecular-mass *n*-alcohols and glycols at Pt in acidic media is adequately represented by the *i–E* curve in Fig. 6 for ethylene glycol. During the positive scan, a peak response is observed at *ca.* +0.4 V corresponding to formation of a submonolayer of $^{\bullet}OH_{ads}$ on Pt. The anodic signal is sharply attenuated by formation of surface oxide (PtO) at $E > +0.5$ V. Cathodic dissolution of the surface oxide during the negative scan allows resumption of the oxidation of ethylene glycol and the current swings to a net anodic value in the region *ca.* +0.3 to +0.1 V.

6.2. Chromatography

Whereas simple *n*-alcohols are volatile and their separations and quantitative determinations can easily be achieved by gas chromatography (GC), glycols are sufficiently polar so that they are not readily determined by GC without *a priori* derivatization. Furthermore, the absence of conjugated bonding in these compounds has greatly restricted the use of photometric detection in the development of LC separations for their quantitative determinations.

Simple alcohols and glycols are easily detected by pulsed amperometric detection at Pt electrodes based on electrocatalytic mechanisms (mode I). Fig. 7 shows results for 13 alcohols and glycols separated by ion exclusion chromatography using an anion-exchange column with 0.050 *M* $HClO_4$ as the mobile phase [60]. This is a prime example of the utility of IC columns for separation of polar nonionic organic compounds. Detection limits for ethylene glycol by this method are typically *ca.* 10 ppb (w/w) ($S/N = 3$).

Results are shown in Fig. 8 for 13 alcohols separated by a mixed-mode IC column using a linear acetonitrile gradient [60]. Post-column addition of NaOH brought the chromatographic effluent to an alkaline pH to facilitate pulsed amperometric detection (mode I) at a Au electrode. The detection sensitivity for these compounds was diminished somewhat as a result of the competitive adsorption of acetonitrile at the catalytic reaction sites of the electrode.

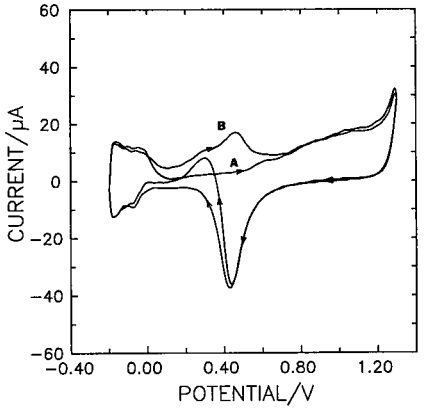

Fig. 6. Voltammetric response of ethylene glycol at a Pt RDE in 0.10 *M* $HClO_4$. Conditions: 400 rpm, 50 mV/s. Ethylene glycol (m*M*): (A) 0.0, (B) 0.5.

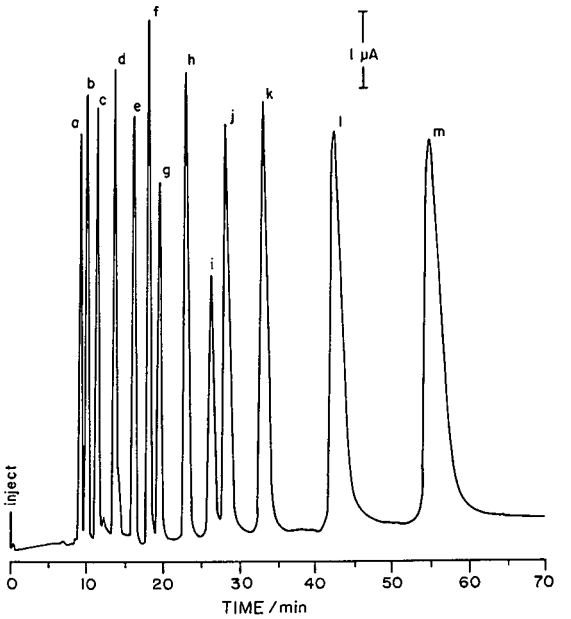

Fig. 7. Separation of alcohol mixture. Pulsed amperometric detection (mode I) at Pt; Ag/AgCl reference; $E_{det} = +0.30$ V ($t_{det} = 300$ ms, $t_{del} = 280$ ms, $t_{int} = ca.$ 20 ms); $E_{oxd} = +1.40$ V ($t_{oxd} = 120$ ms); $E_{red} = -0.40$ V ($t_{red} = 420$ ms). Column: Dionex AS-1. Elution: isocratic, 50 m*M* $HClO_4$. Sample: 50 μl. Peaks: a = adonitol, 45 ppm; b = erythritol, 36 ppm; c = glycerol, 9 ppm; d = ethylene glycol, 10 ppm; e = methanol, 30 ppm; f = ethanol, 45 ppm; g = 2-propanol, 177 ppm; h = 1-propanol, 202 ppm; i = 2-butanol, 202 ppm; j = 2-methyl-1-propanol, 120 ppm; k = 1-butanol, 122 ppm; l = 3-methyl-1-butanol, 364 ppm; m = 1-pentanol, 365 ppm. From ref. 60 by permission from the American Chemical Society.

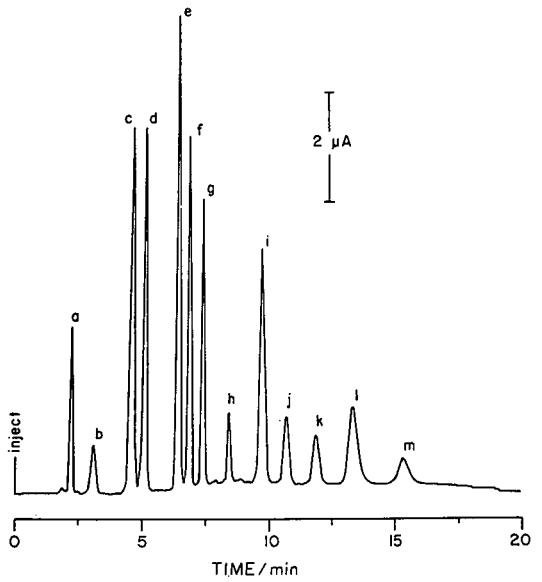

Fig. 8. Separation of alcohol mixture. Pulsed amperometric detection (mode I) at Au; Ag/AgCl reference; E_{det} = +0.10 V (t_{det} = 720 ms, t_{del} = 520 ms, t_{int} = *ca.* 200 ms); E_{oxd} = +1.00 V (t_{oxd} = 120 ms); E_{red} = −0.80 V (t_{red} = 300 ms). Column: Dionex OmniPAC PCX-500. Elution: gradient, 18–85.5% acetonitrile in water. Post-column addition: 0.3 *M* NaOH. Sample: 50 μl. Peaks: a = ethanol, 1840 ppm; b = 1-propanol, 460 ppm; c = 2-methyl-2-propen-1-ol, 46 ppm; d = cyclopentanol, 460 ppm; e = phenylmethanol, 69 ppm; f = 1-phenylethanol, 115 ppm; g = 3-phenyl-1-propanol, 115 ppm; h = 2-ethyl-1-hexanol, 460 ppm; i = 1-decanol, 460 ppm; j = 1-undecanol, 920 ppm; k = 1-dodecanol, 920 ppm; l = 1-tridecanol, 920 ppm; m = 1-tetradecanol, 920 ppm. From ref. 60 by permission from the American Chemical Society.

7. ALKANOLAMINES AND AMINO ACIDS

7.1. Voltammetric response at Au electrodes

Amines can be detected by anodic oxidation at Au electrodes in alkaline media [46,61,62]. This response is illustrated in Fig. 9 by *i–E* curves for ethylamine (curve B), glycine (curve C) and ethanolamine (curve D), in comparison with the residual response for Au (curve A). Oxidation of amines that are adsorbed and being transported to the electrode occurs by the mode II mechanism in the region +0.1 to +0.6 V (positive scan) concomitantly with formation of surface oxide. Oxidation terminates with cessation of oxide formation as the result

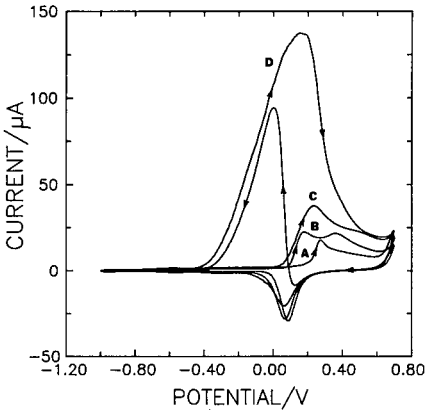

Fig. 9. Voltammetric response of amines at Au RDE in 0.10 *M* NaOH. Conditions: 400 rpm, 50 mV/s. Curves: (A) residual, (B) 0.5 m*M* glycine, (C) 0.5 m*M* ethylamine, (D) 0.5 m*M* ethanolamine.

of scan reversal at +0.7 V. Products of amine oxidation have not yet been identified.

A unique response is observed for *n*-alkanolamines, as illustrated by curve D for ethanolamine (Fig. 9). The large peak response at *ca.* +0.15 V is characteristic of the oxidation of terminal alcohol groups in polyalcohols and carbohydrates (mode I). Hence, this peak for ethanolamine is attributed to oxidation of the $-CH_2OH$ moiety with production of the glycinate anion (n = 4 equiv./mol) [62]. The remarkable aspect of this observation is the fact that the anodic response for ethanol is very small at Au in 0.1 *M* NaOH. The large reactivity of the $-CH_2OH$ group in ethanolamine is attributed to the effect of adsorption of the N atom in the amine moiety with the consequence of retention of the neutral molecule at the electrode surface. Hence, even though the inherent rate constant is small for oxidation of $-CH_2OH$, the increased residence time at the electrode surface results in ultimate oxidation. The anionic oxidation product in this alkaline media is hydrophilic and, therefore, is rapidly desorbed to allow the adsorption site to be recycled in the electrocatalytic mechanism. This mechanism is sufficiently rapid to cause the peak response at +0.15 V to be virtually limited by the rate of mass transport. This mechanism is believed to apply for all *n*-alkanolamines.

7.2. Chromatography of alkanolamines

Alkanolamines are used extensively in chemical industry as emulsifying agents and corrosion inhibitors. They lack natural chromophores and fluorophores for photometric and fluorometric detection, and, furthermore, their high polarity virtually excludes quantitative determination by GC.

The separation of a mixture of linear and branched alkanolamines by reversed-phase paired-ion chromatography is shown in Fig. 10 with pulsed amperometric detection (mode I) at a Au electrode [46]. The mobile phase contained acetonitrile and sodium dodecyl sulfonate, as the ion-pairing agent. The peaks for monoethanolamine and triethanolamine are well resolved; however, monoethanolamine and diethylamine are co-eluted. The requirement of alkalinity for pulsed amperometric detection was achieved by post-column addition of NaOH. The detection limit (S/N = 3) for ethanolamine by this method is *ca.* 40 ppb (*i.e.*, 8 ng/200 μl sample) with a linear response to 10 ppm.

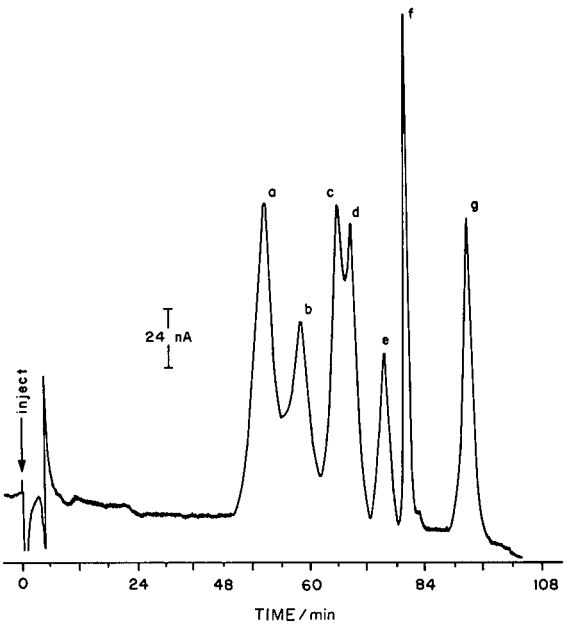

Fig. 10. Separation of alkanolamines. Pulsed amperometric detection (mode I) at Au; Ag/AgCl reference; E_{det} = +0.20 V *vs.* SCE (t_{del} = 280 ms, t_{int} = 17 ms, t_{det} = 300 ms), E_{oxd} = +1.00 V *vs.* SCE (t_{oxd} = 400 ms), E_{red} = −0.40 V *vs.* SCE (t_{red} = 350 ms). Column: Hamilton PRP-1 C_{18}. Solvents: (A) 0.75 m*M* dodecanesulfonate in acetonitrile–water (15:85), (B) 0.75 m*M* dodecanesulfonate and 10 m*M* $NaNO_3$ in acetonitrile–water (15:85). Elution: isocratic (0–50 min), 100% A; linear ramp (50–70 min) to A–B (90:10); linear ramp (70–71 min) to 100% B; isocratic (>71 min), 100% B. Post-column addition: 0.3 *M* NaOH. Sample: 200 μl. Peaks: a = 2-amino-1-ethanol, 3 ppm; b = 4-amino-1-butanol, 4 ppm; c = 5-amino-1-pentanol, 4 ppm; d = 2-amino-1-butanol, 3 ppm; e = 6-amino-1-hexanol, 2 ppm; f = 2-amino-1-pentanol, 2 ppm; g = 2-amino-1-hexanol, 4 ppm. From ref. 46 by permission from the American Chemical Society.

7.3. Chromatography of amino acids

The majority of amino acids in biological materials have been perceived historically as being electroinactive [63,64]. Nevertheless, all amino acids can be detected directly by the mode II mechanism at Au electrodes in alkaline media (see curve C in Fig. 9).

Chromatographic results are shown in Fig. 11 for a mixture of 20 amino acids in a protein hydrolyzate [61]. This separation required the use of a complex pH gradient described in ref. 61. In spite of post-column addition of NaOH, small fluctuations of pH were evident in the detector cell. Changes in pH cause a shift in the onset potential for the anodic wave resulting from oxide formation (wave b in Fig. 1) by the amount −59 mV/pH. Hence, for an increase in pH, the baseline obtained for pulsed amperometric detection (mode II) increases anodically.

The use of IPAD decreases significantly the baseline fluctuation caused by changes in pH; however, optimum potential values for the IPAD waveform also shift with change in pH. To eliminate this problem, a glass-membrane, H^+-selective electrode was used as the potential reference in the detector cell in place of the conventional pH-independent reference electrode, *e.g.*, Ag/AgCl(s) electrode [65,66]. Because the pH dependence of the glass-membrane electrode is the same as that for the anodic processes at the Au electrode, the voltammetric response at Au obtained using this reference appears to be independent of pH. Hence, results in Fig. 11 were obtained using a glass-membrane reference electrode.

Detection limits (S/N = 3) for essential amino acids by IPAD are *ca.* 3–5 pmol. It is especially significant that the sensitivity of IPAD is nearly the same for primary and secondary amino acids.

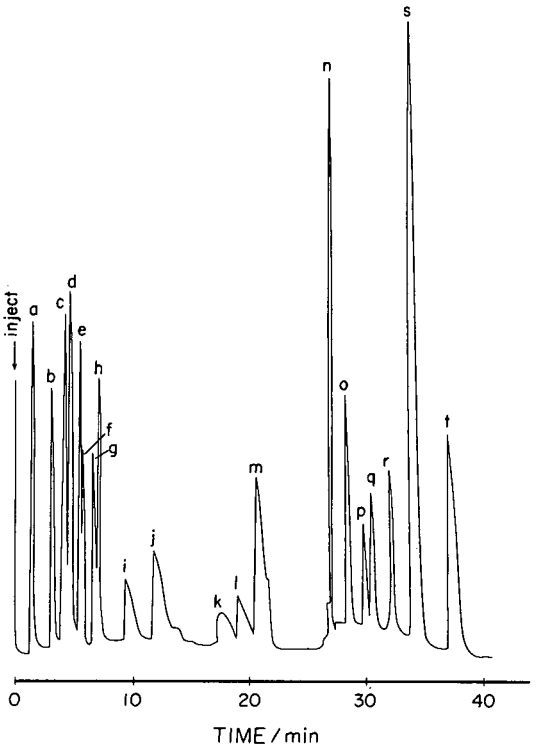

Fig. 11. Separation of amino acids in protein hydrolyzate. Detection: IPAD (mode II) at Au; glass-membrane reference; see waveform in Table III of ref. 48. Column: Dionex AS-8. Elution: gradient, see Table II of ref. 48. Sample: 50 μl. Peaks: a = arginine; b = lysine; c = glutamine; d = asparagine; e = threonine; f = alanine; g = glycine; h = serine; i = valine; j = proline; k = isoleucine; l = leucine; m = methionine; n = histidine; o = phenylalanine; p = glutamic acid; q = aspartic acid; r = cysteine; s = cystine; t = tyrosine. From ref. 48 by permission from the American Chemical Society.

8. SULFUR COMPOUNDS

8.1. Voltammetric response at Au electrodes

Numerous sulfur compounds are detected by mode II mechanisms at Au and Pt [31,50]. Detected are compounds having at least one non-bonded pair of electrons on the S atom. Examples include thioalcohols, thiophenes, thiocarbamates and organic thiophosphates. Sulfones and sulfonic acid derivatives are not detected.

The voltammetric response of thiourea is shown in Fig. 12 (curve B) obtained at a Au RDE (0.20 cm^2) in 0.1 *M* NaOH. The residual response is

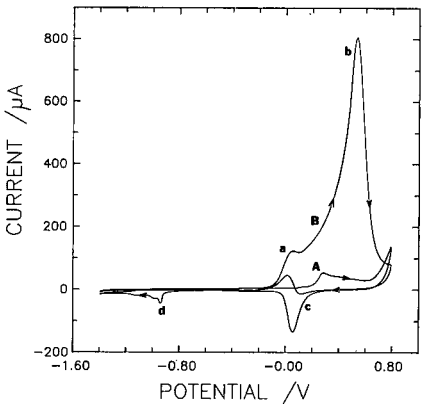

Fig. 12. Voltammetric response of thiourea at Au RDE in 0.10 *M* NaOH. Conditions: 1000 rpm, 100 mV/s. Curves: (A) residual, (B) 1.0 *M* thiourea. For a–d, see text.

shown by curve A [67]. Wave a starting at *ca.* −0.1 V (positive scan) occurs just prior to the onset of AuO formation and is attributed to the one-electron oxidation of the S atom with subsequent dimerization of the product to form formamidine disulfide [67,68]. Anodic peak b in the region *ca.* +0.2 to +0.7 V (positive scan) occurs concomitantly with oxide formation and corresponds to oxidative desorption of adsorbed formamidine disulfide as well as oxidation of thiourea transported to the electrode surface. Sulfate was identified as a major product of the anodic reactions contributing to peak b and these oxidation processes are concluded to occur by a catalytic O-transfer mechanism (mode II) [67]. The anodic O-transfer mechanism is severely attenuated for $E >$ *ca.* +0.5 V because the electrode surface becomes covered by the inert oxide layer (AuO).

With scan reversal at +0.8 V, further formation of oxide ceases and the current remains at zero until cathodic dissolution of AuO commences at *ca.* +0.1 V (peak c). Almost immediately, the net current swings to anodic values as a result of the oxidation of thiourea on the reduced portions of the electrode. Continued negative scan yields cathodic peaks d at $E <$ −0.9 V. These peaks have been identified as resulting from cathodic desorption of S^0 formed at $E >$ +0.2 V by incomplete oxidation of thiourea without oxygen transfer. If the negative scan is reversed at values > −0.9 V, S^0 accumulates with repeated cyclic scans to produce a visible film which causes severe attenuation of wave a and peak

b (positive scan). Conversely, if the negative scan is reversed at values < *ca.* −1.0 V, the electrode surface is cathodically cleaned of adsorbed S^0 within each consecutive cyclic scan, and wave a and peak b are large and reproducible [67].

It is apparent from Figs. 9 and 12 that both amines and sulfur compounds are detected concomitantly with oxide formation (mode II) at Au electrodes. There are situations in which selective detection of S compounds is desired without interference from the presence of amines, *e.g.*, chromatographic determination of cysteine, cystine and/or methionine in the presence of other amino acids. Fig. 13 compares the voltammetric response for 0.005 m*M* cysteine (curve B) and 0.5 m*M* glycine (curve C) at a Au RDE in 0.1 *M* $HClO_4$; the residual curve for Au is shown by curve A. Clearly, under these acidic conditions, the sensitivity for cysteine detection far exceeds that for glycine. Addition of 10% acetonitrile results in virtual elimination of the glycine signal. This occurs because acetonitrile is adsorbed on Au more strongly than amines in acidic media and blocks the electrocatalytic mechanism for anodic detection. Presence of the acetonitrile has virtually no effect on the detection of the more strongly adsorbed cysteine.

8.2. Chromatography

Chromatographic results using PAD (mode II) are shown in Fig. 14 for a beer sample spiked with 1 ppm ethylenethiourea (ETU). No sample clean-up was employed and separation was by a Dionex MPIC-NS1 column (20 cm) using 0.1 *M* NaOH as the mobile phase. The ETU is well resolved from the other beer components. The detection limit (S/N = 3) for ETU by this method is *ca.* 5 ppb.

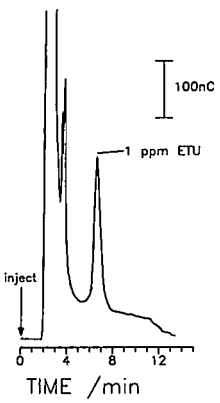

Fig. 14. Separation of 1 ppm ethylenethiourea (ETU) from other components of beer. Pulsed amperometric detection (mode II) at Au; Ag/AgCl reference; E_{det} = +0.50 V (t_{det} = 440 ms, t_{int} = 100 ms, t_{det} = 540 ms), E_{oxd} = +0.80 V (t_{oxd} = 60 ms), E_{red} = −1.30 V (t_{red} = 300 ms). Column: Dionex MPIC-NS1. Elution: isocratic, 100 m*M* NaOH, 1.0 ml/min. Sample: 50 μl.

Chromatographic results are shown in Fig. 15 for a mixture of 10 μ*M* cysteine, methionine and cystine containing 1 m*M* alanine, glycine, serine and threo-

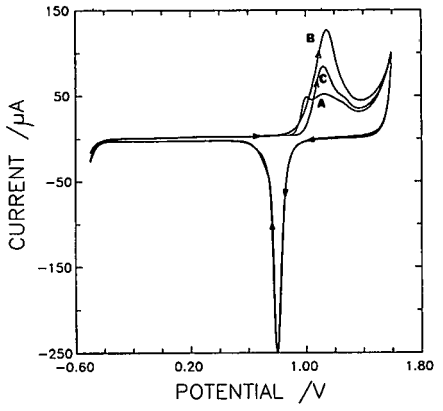

Fig. 13. Comparison of voltammetric response of cysteine and glycine at Au RDE in 0.10 *M* $HClO_4$. Conditions: 1000 rpm, 100 mV/s. Curves: (A) residual, (B) 0.005 m*M* cysteine, (C) 0.5 m*M* glycine.

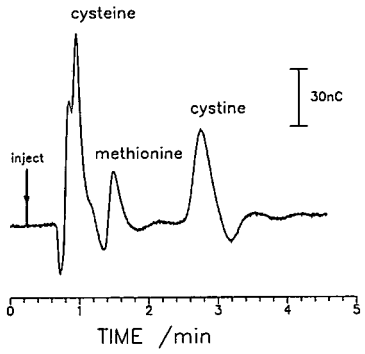

Fig. 15. Separation of 10 μ*M* cysteine, methionine and cystine in the presence of 1 m*M* alanine, glycine, serine and threonine. Pulsed amperometric detection (mode II) at Au; Ag/AgCl reference; E_{det} = +1.60 V (t_{det} = 250 ms, t_{int} = 50 ms, t_{det} = 300 ms), E_{oxd} = +2.00 V (t_{oxd} = 30 ms), E_{red} = −0.50 V (t_{red} = 120 ms). Column: Dionex OmniPAC PCX-500 guard (5 mm length). Elution: isocratic, 0.5 *M* phosphate buffer–acetonitrile (95:5) (pH 1.6), 0.8 ml/min.

nine. A Dionex OmniPAC-PCX-500 guard column (5 mm) was used with 0.5 *M* phosphate buffer–acetonitrile (95:5) (pH 1.6) and pulsed amperometric detection (mode II) at a Au electrode in the acidic effluent. Under these conditions, peaks are obtained only for the S-containing amino acids.

9. FUTURE DEVELOPMENTS

9.1. Faster waveforms

Typical applications of pulsed amperometric detection and IPAD using mode I and II reaction mechanisms have utilized waveform frequencies in the range *ca.* 0.5 to 1 Hz for maximum *S/N*. However, recent improvements to column efficiencies and separation velocities, and the development of capillary columns, are providing motivation for the use of higher waveform frequencies to guarantee acceptable correlation between apparent and actual peak shapes. Because of the essential role of oxide formation and dissolution in the maintenance of reactive Au and Pt surfaces, it is expected that the kinetics of these processes will be a significant factor when increasing the frequency of pulsed amperometric detection and IPAD waveforms [69].

Fig. 16 contains an instructive illustration of the effect of finite kinetics on the residual voltammetric response at a Au RDE (0.78 mm^2) in 0.1 *M* NaOH. The *i–E* curves were obtained using a triangular analog *E–t* waveform (Fig. 1A) with values of scan rate (ϕ) increasing from 0.2 to 200 V/s. The current response was recorded digitally so the curves are not distorted by the slow response of an analog recorder. The basis of this illustration is the fact that, for a linear potential scan, the potential axis is a linear time (*t*) axis. Hence, increases in ϕ can cause the *i–E* response for a slow electrode process to be shifted along the potential axis in the direction of longer *t*.

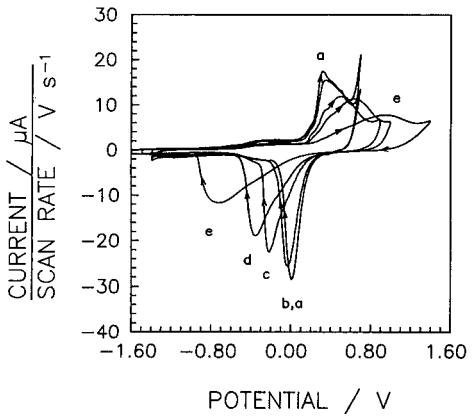

Fig. 16. Residual voltammetric response at a Au RDE in 0.10 *M* NaOH as a function of scan rate. Conditions: 1000 rpm. Scan rate (V/s): (a) 0.20, (b) 1.0, (c) 20, (d) 50, (e) 200.

During the positive scan at low ϕ values ($\leq$1 V/s), the amount of oxide (AuO) formed at $E \geq$ *ca.* +0.2 V is virtually at an equilibrium value and, hence, the current for oxide formation is observed to be proportional to ϕ. Therefore, the current scale in Fig. 16 has been normalized with respect to ϕ. As a consequence, the normalized currents at *ca.* +0.2 V (positive scan) for ϕ = 0.2 and 1 V/s are virtually identical and no shift of the oxide-formation wave is observed. For ϕ > 1 V/s, however, the anodic wave for oxide formation is shifted to higher potential values (longer *t*) and the maximum normalized current decreases as ϕ is increased. These observations are evidence that the oxide coverage lags behind its equilibrium value for fast scan rates (> 1 V/s) due to slow heterogeneous kinetics. The behavior of the cathodic peak (negative scan) corresponding to oxide dissolution is similar to that of the anodic wave for oxide formation, except that the peak shift is to more negative potentials. It is significant in Fig. 16 that the anodic wave for formation of $^{\cdot}OH_{ads}$ (wave a in Fig. 2) is not shifted over the range of ϕ values tested and this anodic process is concluded to be very fast.

The effect of increased ϕ on the voltammetric response of glucose at the Au RDE used in Fig. 16 is shown in Fig. 17. Clearly, the anodic wave for the aldehyde moiety (E > *ca.* −0.6 V), a process believed to be promoted by formation of $^{\cdot}OH_{ads}$, is not shifted along the potential axis over the range of ϕ values tested. Likewise the anodic peak response at *ca.* +0.15 V, characteristic of all carbohydrates and polyalcohols, is not shifted as a consequence of increased ϕ. This is indicative of fast oxidation mechanisms.

In contrast to the response of carbohydrates and polyalcohols, the voltammetric response for amines and S compounds is dependent on formation of AuO. Hence, the anodic response for these compounds obtained using fast scan rates is shifted to higher potentials (longer *t*).

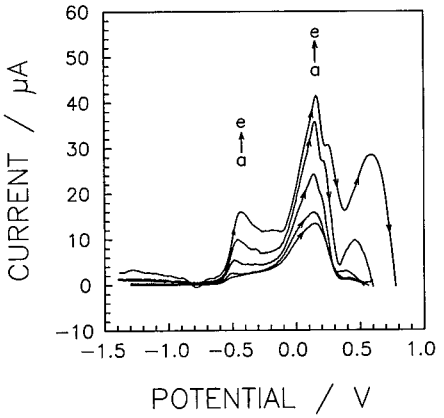

Fig. 17. Voltammetric response of 0.50 m*M* glucose at a Au RDE in 0.10 *M* NaOH as a function of scan rate. Conditions: 1000 rpm. Scan rate (V/s): (a) 0.20, (b) 1.0, (c) 5.0, (d) 20, (e) 50.

9.2. *Voltammetric detection*

The application of voltammetric detection in chromatographic separations has been reviewed [2,70]. The technique produces so-called chromatovoltammograms (*i–E–t* curves) which can be useful in the deconvolution of unresolved chromatographic peaks. Voltammetric detection under pulsed waveforms, including staircase waveforms, can be called pulsed voltammetric detection (PVD). PVD has been applied to capillary LC columns by Kennedy and Jorgenson [71].

Application of PVD to conventional LC columns was described by Owens *et al.* [72] using staircase Pt electrodes with cleaning and reactivation pulses between staircase scans. PVD with cleaning and reactivation pulses applied prior to each potential step can, in principle, be achieved by use of a pulsed amperometric detection waveform (Fig. 1B) in which E_{det} is varied according to a staircase waveform [32,34,35,52]. Accordingly, the electrode has a uniform activity for all potential values in the voltammetric response (*i–E*) curve. Whereas the use of small ΔE values in the staircase waveform increases voltammetric resolution, the time required for formation and dissolution of surface oxide with each cycle of the pulsed amperometric detection waveform necessitates a low rate of voltammetric scan. Hence, applications of this version of PVD in LC can be problematic because of the likelihood that the time to complete a scan of the staircase waveform will be greater than the chromatographic peak width.

The trend in chromatographic development is toward smaller injection volumes to improve chromatographic resolution with emphasis on highly diluted samples. These factors decrease the extent of electrode fouling and, as a result, it might not be necessary to apply a cleaning–reactivation cycle prior to each application of ΔE in the staircase waveform. We observe for dilute carbohydrate solutions (<1 m*M*) that electrode reactivity is maintained at a reproducible level provided the positive and negative scan limits in the staircase waveform are sufficient to permit the requisite processes of oxidation cleaning and reductive reactivation once within the execution of each waveform. The choice of scan limits for fast voltammetric waveforms must be made with consideration of the relatively slow kinetics for oxide formation and dissolution (see Fig. 16).

10. CONCLUSIONS

Numerous aliphatic compounds are detected with high sensitivity based on electrocatalytic oxidation mechanisms at Au and Pt electrodes under the control of multi-step potential–time waveforms. These waveforms alternate the processes of amperometric detection with oxidative cleaning and reductive reactivation of the electrodes to maintain high catalytic surface activity without the undesired effects of fouling as the result of accumulation of adsorbed detection products and/or solution impurities.

The high sensitivity and convenience of pulsed amperometric detection and IPAD at Au and Pt serve as further motivation to extend applications of IC columns for separations of non-ionic aliphatic compounds not detected by conductance and photometric measurements. A useful example is the ion-exclusion separation of alcohols and glycols.

The frequencies of pulsed amperometric detection and IPAD waveforms can be increased for applications to capillary columns, albeit not without some sacrifice to *S/N*. However, it is projected that the slow kinetics of oxide formation and dissolution at Au and Pt will limit the useful upper frequency to *ca.* 5–10 Hz.

Voltammetric resolution is not possible within classes of compounds whose anodic response is based on a common electrocatalytic mechanism. However, differences in voltammetric response for aldoses (reducing sugars) and all other carbohydrates might be useful in the deconvolution of poorly resolved chromatographic peaks. It is essential, however, that dissolved O_2 be maintained at a near-zero level if the voltammetric technique is to be applied for carbohydrates at low levels (<1 ppm).

11. ACKNOWLEDGEMENTS

This research is supported by grants form Dionex Corp., Sunnyvale, CA, USA, and the US National Science Foundation (grant CHE-8914700).

REFERENCES

1 D. T. Gjerde and J. S. Fritz, *Ion Chromatography*, Hüthig, Mamaroneck, NY, 2nd ed., 1987.
2 P. Jandik, P. R. Haddad and P. E. Sturrock, *CRC Crit. Rev. Anal. Chem.*, 20 (1988) 1.
3 H. Small, *J. Chromatogr.*, 546 (1991) 3.
4 R. D. Rocklin, *J. Chromatogr.*, 546 (1991) 175.
5 D. C. Johnson and W. R. LaCourse, *Anal. Chem.*, 62 (1990) 589A.
6 P. Luo, F. Zhang and R. P. Baldwin, *Anal. Chim. Acta*, 244 (1991) 169.
7 P. Luo, F. Zhang and R. P. Baldwin, *Anal. Chem.*, 63 (1991) 1702.
8 D. C. Johnson and W. R. LaCourse, *Electroanal.*, 4 (1992) 367.
9 R. E. Shoup, *Recent Reports on Liquid Chromatography–Electrochemistry*, Bioanalytical Systems Press, West Lafayette, IN, 1982. (*Note:* a recent listing can be obtained on database by contacting R.E.S.)
10 I. S. Krull (Editor), *Post-Column Reaction Detectors in HPLC*, Marcel Dekker, New York, 1986.
11 P. K. Dasgupta, *J. Chromatogr. Sci.*, 27 (1989) 422.
12 R. Woods, in A. J. Bard (Editor), *Electroanalytical Chemistry*, Vol. 9, Marcel Dekker, New York, 1976, p. 20.
13 S. Gilman, in A. J. Bard (Editor), *Electroanalytical Chemistry*, Vol. 2, Marcell Dekker, New York, 1967, p. 111.
14 L. P. Hammett, *J. Am. Chem. Soc.*, 46 (1924) 7.
15 G. Armstrong, F. R. Himsworth and J. A. V. Butler, *Proc. Roy. Soc. London (A)*, 143 (1934) 89.
16 S. Gilman, *J. Phys. Chem.*, 67 (1963) 78.
17 M. W. Breiter, *Electrochim. Acta*, 8 (1963) 973.
18 J. Giner, *Electrochim. Acta*, 9 (1964) 63.
19 R. N. Adams, *Electrochemistry at Solid Electrodes*, Marcel Dekker, New York, 1969, p. 206.
20 D. Clark, M. Fleishman and D. Pletcher, *J. Electroanal. Chem.*, 36 (1972) 137.
21 A. MacDonald and P. D. Duke, *J. Chromatogr.*, 83 (1973) 331.
22 B. Fleet and C. J. Little, *J. Chromatogr. Sci*, 12 (1974) 747.
23 W. Stulik and V. Hora, *J. Electroanal. Chem.*, 70 (1976) 253.
24 W. E. van der Linden and J. W. Diekes, *Anal. Chim. Acta*, 119 (1980) 1.
25 H. W. van Rooijen and H. Poppe, *Anal. Chim. Acta*, 130 (1981) 9.
26 A. G. Ewing, M. A. Dayton and R. M. Wightman, *Anal. Chem.*, 53 (1981) 1842.
27 S. Hughes, P. L. Meschi and D. C. Johnson, *Anal. Chim. Acta*, 132 (1981) 1.
28 S. Hughes and D. C. Johnson, *Anal. Chim. Acta*, 149 (1983) 1.
29 P. Edwards and K. K. Haak, *Am. Lab.*, April (1983) 28.
30 J. A. Polta and D. C. Johnson, *J. Liq. Chromatogr.*, 6 (1983) 1727.
31 T. Z. Polta and D. C. Johnson, *J. Electroanal. Chem.*, 209 (1986) 159.
32 G. C. Neuburger and D. C. Johnson, *Anal. Chem.*, 59 (1987) 203.
33 G. C. Neuburger and D. C. Johnson, *Anal. Chem.*, 60 (1988) 2288.
34 T. K. Chen, Y. Y. Lau, D. K. Y. Wong and A. G. Ewing, *Anal. Chem.*, 64 (1992) 1264.
35 W. R. LaCourse and D. C. Johnson, *Anal. Chem.*, 65 (1993) 50.
36 D. S. Austin-Harrison and D. C. Johnson, *Electroanal.*, 1 (1989) 189.
37 R. D. Rocklin and C. A. Pohl, *J. Liq. Chromatogr.*, 6 (1983) 1577.
38 J. Olechno, S. R. Carter, W. T. Edwards and D. G. Gillen, *Am. Biotech. Lab.*, 5 (1987) 38.
39 M. R. Hardy and R. R. Townsend, *Proc. Natl. Acad. Sci. U.S.A.*, 85 (1988) 3289.
40 M. R. Hardy, R. R. Townsend and Y. C. Lee, *Anal. Biochem.*, 170 (1988) 54.
41 R. R. Townsend, M. R. Hardy, O. Hindsgaul and Y. C. Lee, *Anal. Biochem.*, 174 (1988) 459.
42 W. R. LaCourse and D. C. Johnson, *Carbohydr. Res.*, 215 (1991) 159.
43 R. W. Andrews and R. M. King, *Anal. Chem.*, 62 (1990) 2130.
44 D. A. Martens and W. T. Frankenberger, Jr., *J. Chromatogr.*, 546 (1991) 297.
45 D. A. Roston and R. R. Rhinebarger, *J. Liq. Chromatogr.*, 13 (1991) 539.
46 W. R. LaCourse, W. A. Jackson and D. C. Johnson, *Anal. Chem.*, 61 (1989) 2466.
47 W. R. LaCourse, D. C. Johnson, M. A. Rey and R. W. Slingsby, *Anal. Chem.*, 63 (1991) 134.
48 L. E. Welch, W. R. LaCourse, D. A. Mead, Jr., D. C. Johnson and T. Hu, *Anal. Chem.*, 61 (1989) 555.
49 T. Z. Polta and D. C. Johnson, *Chromatogr. Forum*, 1 (1986) 37.
50 A. Ngoviwatchai and D. C. Johnson, *Anal. Chim. Acta*, 215 (1988) 1.
51 R. Rocklin, *Conductivity and Amperometry: Electrochemical Detection in Ion Chromatography*, Dionex, Sunnyvale, CA, 1991.
52 G. G. Neuburger and D. C. Johnson, *Anal. Chim. Acta*, 192 (1987) 205.

53 W. R. LaCourse and D. C. Johnson, in P. Jandik and R. M. Cassidy (Editors), *Advances in Ion Chromatography*, Vol. 2, Century International, Medfield, MA, 1990, p. 353.
54 L. A. Larew and D. C. Johnson, *J. Electroanal. Chem.*, 262 (1989) 167.
55 J. E. Vitt, L. A. Larew and D. C. Johnson, *Electroanal.*, 2 (1990) 21.
56 J. A. Rendleman, in H. S. Isbell (Editor), *Carbohydrates in Solution (Advances in Chemistry Series*, No. 117), American Chemical Society, Washington, DC, 1973, p. 51.
57 T. J. Paskach, H. P. Lieker, P. J. Reilley and K. Thielecke, *Carbohydr. Res.*, 215 (1991) 1.
58 L. A. Larew, D. A. Mead, Jr. and D. C. Johnson, *Anal. Chim. Acta*, 204 (1988) 43.
59 L. A. Larew and D. C. Johnson, *Anal. Chem.*, 60 (1988) 1867.
60 W. R. LaCourse, D. C. Johnson, M. A. Rey and R. W. Slingsby, *Anal. Chem.*, 63 (1991) 134.
61 L. E. Welch, W. R. LaCourse, D. A. Mead, Jr., D. C. Johnson and T. Hu, *Anal. Chem.*, 61 (1989) 555.
62 W. A. Jackson, W. R. LaCourse, D. A. Dobberpuhl and D. C. Johnson, *Electroanal.*, 3 (1991) 607.
63 M. Malfoy and J. A. Reynaud, *J. Electroanal. Chem.*, 114 (1980) 213.
64 H. M. Joseph and P. Davies, *Curr. Sep.*, 4 (1982) 62.
65 D. A. Mead, L. A. Larew and D. C. Johnson, in P. Jandik and R. M. Cassidy (Editors), *Advances in Ion Chromatography*, Century International, Franklin, MA, 1989, p. 13.
66 W. R. LaCourse, D. A. Mead and D. C. Johnson, *Anal. Chem.*, 62 (1990) 220.
67 P. J. Vandeberg, J. L. Kawagoe and D. C. Johnson, *Anal. Chim. Acta*, 260 (1992) 1.
68 V. A. Zakharov, I. M. Bessarabova, O. A. Songina and M. A. Timoshkin, *Elektrokhim.*, 7 (1971) 1215.
69 R. Roberts and D. C. Johnson, *Electroanal.*, 4 (1992) 741.
70 P. R. Haddad and P. Jandik, in J. G. Tarter (Editor), *Ion Chromatography*, Marcel Dekker, New York, 1987, p. 87.
71 R. T. Kennedy and J. W. Jorgenson, *Anal. Chem.*, 61 (1989) 436.
72 D. S. Owens, C. M. Johnson, P. E. Sturrock and A. Jaramillo, *Anal. Chim. Acta*, 197 (1987) 249.

Journal of Chromatography, 640 (1993) 97–109
Elsevier Science Publishers B.V., Amsterdam

CHROMSYMP. 2800

New membrane-based electrolytic suppressor device for suppressed conductivity detection in ion chromatography

Steve Rabin*, John Stillian, Victor Barreto, Keith Friedman and Mahmood Toofan

Dionex Corporation, 1228 Titan Way, Sunnyvale, CA 94088 (USA)

ABSTRACT

This paper discusses the newest advancement in chemical suppression preceding conductivity detection. The new suppressor uses electrolysis of deionized water to generate the required acid or base for the suppression neutralization reaction and utilizes the electrical field to enhance, through electrodialysis, the suppressor's capacity for neutralization. The suppressor is able to accommodate eluents as high as 150 m*M* NaOH, without the need for a separate regenerant solution, by recycling the conductivity detector cell waste to the regenerant and electrolyzing the water in the waste stream to the required acid or base. The device is able to use deionized water as regenerant and neutralize the eluent stream to deionized water without the expected increase in resistance by employing ion exchange material in intimate contact with the electrodes and the membranes. The current is carried with low resistance through the ion-exchange material via ion transport from one ion-exchange site to another.

INTRODUCTION

Ion chromatography (IC) has developed into a strong analytical technique from its meager beginnings as a method to determine chloride and sulfate. Today IC uses a variety of detectors and a variety of separation modes to analyze for inorganic and organic ions in a broad range of matrices. The common thread for ion chromatography is the use of ion-exchange media to separate the ions of interest in the matrix. The original detection scheme, chemically suppressed conductance detection, is still the mainstay method of detection for IC.

Chemically suppressed conductance involves the use of weak acid or weak base salts as eluents for the elution of anion and cations, respectively, followed by chemically exchanging eluent ions, by means of an ion-exchange resin or membrane, for hydronium ions (anion determination) or hydroxide ions (cation determination). This causes decreased conductance from the eluent because the eluent is a weak acid or base and therefore weakly ionized, and increases the detector conductance signal for the strong acid or strong base analytes by pairing them with highly conducting hydronium ions (anion determination) or hydroxide ions (cation determination). It has been said that the suppressor turns the bulk property conductivity detector into a solute specific detector.

Suppressors have developed from the first, so called, packed-bed suppressor, described by Small *et al.* [1] to continuously regenerated membrane based suppressors. The first membrane-based suppressor was the fiber suppressor [2], a tubular shaped ion-exchange membrane continuously bathed with dilute sulfuric acid regenerant. This was followed by the MicroMembrane suppressor [3], which was composed of a thin (< 0.075 mm) flat ion-exchange membrane in intimate contact with ion-exchange screens in the eluent and regenerant chambers to maximize suppression capacity and minimize dispersion.

This paper describes an electrochemical suppressor which takes advantage of the evolution of suppressors and combines electrodialysis and electroly-

* Corresponding author.

0021-9673/93/$06.00

sis to create the best-performance lowest-maintenance suppressor for IC with suppressed conductance detection. General construction, theory of operation, modes of operation and performance are discussed.

EXPERIMENTAL

Chromatography system

The chromatography systems used in this study were Dionex DX-300 and System 4500i ion chromatographs. The DX-300 uses a Dionex AGP quaternary gradient pump fitted with pistons to generate flow-rates compatible with either 2 or 4 mm I.D. columns. The System 4500i is equipped with a Dionex GPM-2 quaternary gradient pump. Detectors for these systems were a Dionex CDM-II conductivity detector and a Dionex pulsed electrochemical detector operating in the conductivity mode. All data were collected and processed on Dionex AI-450 software.

Columns

Separation columns for this work included the Dionex IonPac CS12 for cation determinations and Dionex IonPac AS4A-SC, AS5A and AS9-SC columns for anion separations.

Chemicals

Methanesulfonic acid (MSA) eluents for cation determinations were prepared from the 99+% puriss. acid (Fluka, Ronkonkoma, NY, USA). Hydroxide eluents for anion separations were prepared by dilution from the certified grade 50% solution (Fisher, Pittsburgh, PA, USA). Carbonate–hydrogencarbonate eluents were prepared from a commercially available mixed concentrate (Dionex, Sunnyvale, CA, USA). Deionized water (18 MΩ) was obtained from a Millipore (Bedford, MA, USA) Milli-Q water purifier.

RESULTS AND DISCUSSION

Mechanism of suppression

Chemical suppression for IC serves two purposes. The first is the most familiar, lowering the background conductance to a low level, which reduces the system noise. Equally important is enhancement of the overall conductance of the analyte. These two factors together serve to greatly enhance the signal-to-noise ratio for suppressed IC.

The general mechanism of suppression is outlined in Fig. 1. This is shown for the anion separation case, although the cation case is completely analogous. The highly conductive eluent (NaOH) passes through the column, then encounters hydronium ions on the ion-exchange sites in the suppressor. The hydronium ion neutralizes the eluent, forming a weakly conducting species (water) and the counterion form of the ion-exchange site. Analytes passing through the suppressor interact similarly. The analyte counterions exchange for hydronium ions, forming very highly conducting species as hydronium ions have the highest specific conductance of all ions. The net result is a very strong signal superimposed on a low-noise background, giving a very favorable signal-to-noise ratio. For cations, the analogous situation uses hydroxide neutralizing an acidic eluent as well as exchanging for the anionic portion of the analyte.

History of chemical suppression

Packed bed suppressors

Chemical suppression for IC was first conceived by Small *et al.* [1] at Dow Chemical Company in 1975. To reduce the background conductance due to the eluent, they placed a second ion-exchange column between the separator column and the conductivity cell. This second column, originally called the "stripper" column by the inventors, was a simple, yet elegant solution to a difficult problem.

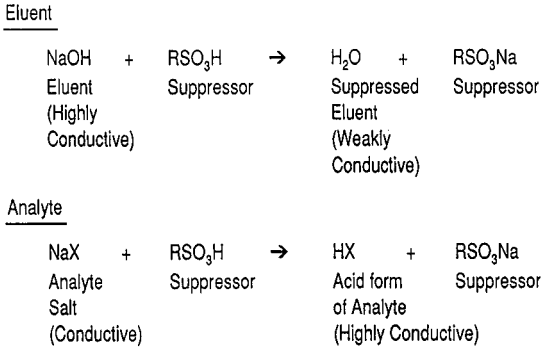

Fig. 1. General mechanism of suppression for anion determinations.

These original suppressors consisted of large columns containing strong acid cation-exchange resin in the hydronium ion form. For anion analysis, alkali metal salts of weak bases were chosen as eluents. As the eluent entered the suppressor, the weak base anion reacted with hydronium, neutralizing the species. Simultaneously, the alkali metal counterion would occupy the ion-exchange sites freed by the hydronium. This served to greatly reduce the conductometric background. As with all suppression, the analyte counterions also exchange for hydronium, serving to greatly enhance the conductivity signal. Cation analysis was completely analogous, using mineral acid eluents and anion exchange resin in the suppressor.

The advent of the packed bed suppressor allowed the use of detection specifically geared toward ions, namely, conductivity. Before chemical suppression, conductivity was seldom used because it is a bulk property detector, subject to being "swamped out" by the background signal due to the ionic eluent. With the first suppressors, conductivity became a sensitive and specific detection scheme for ions of all types.

The original packed bed suppressors had some major drawbacks. To contain enough resin to be feasible, the suppressors had a very large dead volume, on the order of 1500 μl. This in turn caused considerable peak dispersion and broadening. At the time, however, this was not a major problem because the separation columns available had low efficiency thus were not greatly affected by the dead volume of the suppressor. The other problem was regeneration of the bed. After several hours of analyses, the bed became expended, *i.e.* all of the ion-exchange sites were in the counterion form rather than hydronium or hydroxide. The column had to be regenerated off-line with acid or base (depending on the type of suppressor), flushed with water, and then placed back on-line. While this process could be automated to some degree, it was still a source of annoyance and did not allow around the clock operation. Another problem was the analysis of weakly ionized species such as organic acids. These neutral organic acids (that have been neutralized in the suppressor) could penetrate the Donnan membrane (which excludes ionic species) of the protonated ion-exchange sites and interact by inclusion in the suppressor resin phase with the stationary phase. As the suppressor became expended, the organic acids would deprotonate, thus causing a change in peak height and shorter retention times [4].

Despite these problems, the packed bed suppressor made IC a viable commercial technique. The first commercial IC with packed bed suppression was sold by Dionex in 1975. IC proved to be a very valuable analytical technique, especially for anion analysis. Previously, the wet methods for inorganic anions such as chloride, nitrate, and sulfate were time consuming, labor intensive and not particularly sensitive. These methods were based largely on such techniques as titration, colorimetry and gravimetry. No methods existed that had detection specific to the analytes of interest; most of these techniques used bulk properties such as pH or precipitation reactions that are highly subject to interference. IC immediately improved this situation by being able to do all of the ions in a single run, was sensitive, specific and amenable to automation. The cation version originally required runs of the monovalent ions separately from the divalents, however, both were reasonably rapid and sensitive.

Fiber suppressors

To combat some of the drawbacks with the packed bed suppressors, Stevens *et al.* [2] at Dow developed the hollow-fiber suppressor in 1981. This was the first membrane-based suppression device. The fiber suppressor consisted of a long, hollow fiber made of semi-permeable ion-exchange material. Eluent passed through the hollow center of the fiber, while a regenerating solution bathed the outside of the fiber, allowing for continual replacement of the regenerant ion as the eluent passed through. The main advantage of this design was that it allowed for continuous operation of the chromatography system. There was no need to take the suppressor off-line for regeneration as with the packed bed devices.

Operation of the fiber suppressors is as follows. The eluent, for this example sodium carbonate, passes through the center of the fiber, which is bathed with a sulfuric acid solution counter-current to the eluent to provide hydronium ions for the suppression reaction. The cation-exchange sites in the fiber permit the transfer of hydronium ions to neutralize the carbonate to the weakly ionized carbonic acid. Sodium ions from the eluent are transported out

through the cation-exchange sites in the fiber to the regenerant solution, forming a sodium hydrogen-sulfate solution. The regenerant solution constantly flows at several ml/min to remove the sodium ions. Operation of the cation version used anion-exchange fibers, mineral acid eluents and hydroxide as the regenerant solution.

Fiber suppressors offered several advantages over the packed beds beside continuous operation. Dead volumes for these devices were on the order of 300 μl, considerably lower than the packed bed types. This gave more efficient chromatographic peaks, which was useful because column technology had advanced significantly in the six years since the advent of IC. As columns became more efficient, the need for more efficient suppressors arose. Also, Donnan forces which wreaked havoc with weakly ionized species were greatly reduced, thus determination of these analytes became more reliable.

Fiber suppressors were limited in their ability to suppress fast flow-rates (>2 ml/min) or high concentration (>0.005 *M*) eluents. Their suppression capacity relative to packed beds was considerably lower. It had been found that laminar flow in the hollow fiber prevented good mass transport of the eluent ions to the walls of the fiber, resulting in significant band broadening. A solution to this problem was to pack the fiber with neutral resin beads to promote tortuous flow to the walls, with much improved band broadening [5].

Membrane suppressors

The drawbacks with the fiber suppressors proved limiting to the growth of IC. Separation column technology was advancing rapidly; there was a strong desire to perform different analyses in more varied matrices. At the time, gradient IC was not possible due to the lack of suitable suppression. To take advantage of these advances, a new suppression device with much higher capacity and lower dead volume would be necessary, yet still able to operate around the clock with minimal supervision. A flat membrane suppressor, known by the trade name MicroMembrane suppressor (MMS) from Dionex, proved to have all of these attributes upon introduction in 1985 [3].

Design of the MicroMembrane incorporates two semi-permeable ion-exchange membranes sandwiched in between three sets of ion-exchange screens as depicted in Fig. 2. The eluent screen is a fine-mesh ion-exchange screen that promotes the suppression reaction while occupying very little volume. Ion-exchange membranes on either side of the eluent screen define the eluent chamber. These membranes allow passage of the regenerating ion in and the eluent counterion out of the eluent chamber in much the same manner as described for the fiber suppressor. There are two regenerant screens, both ion-exchange functionalized, that permit tortuous flow of the regenerant solution towards the membranes. These screens provide a reservoir for suppressing ions, essentially at molar concentrations, directly at the membrane without having counterions present. One of the drawbacks of the fiber suppressor was that the regenerating medium directly bathed the membrane, which led to counterion leakage into the eluent chamber, causing higher background and noise. With functionalized ion-exchange screens in the membrane suppressor, counterion leakage is greatly reduced and suppression capacity is increased to more than 25 times that of a fiber device.

The flow pattern for the anion suppressor is shown in Fig. 3. The eluent, the sodium salt of a weak acid (in this example, sodium hydroxide) flows into the eluent chamber. A mineral acid such as dilute sulfuric acid is flowing counter-current to the eluent at approximately 3–10 times the chromatographic flow-rate. Cation-exchange membranes permit the flow of hydronium ions from the

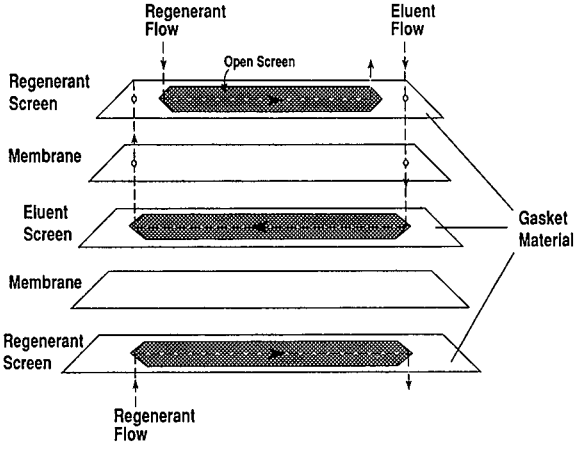

Fig. 2. Internal design of the MicroMembrane Suppressor.

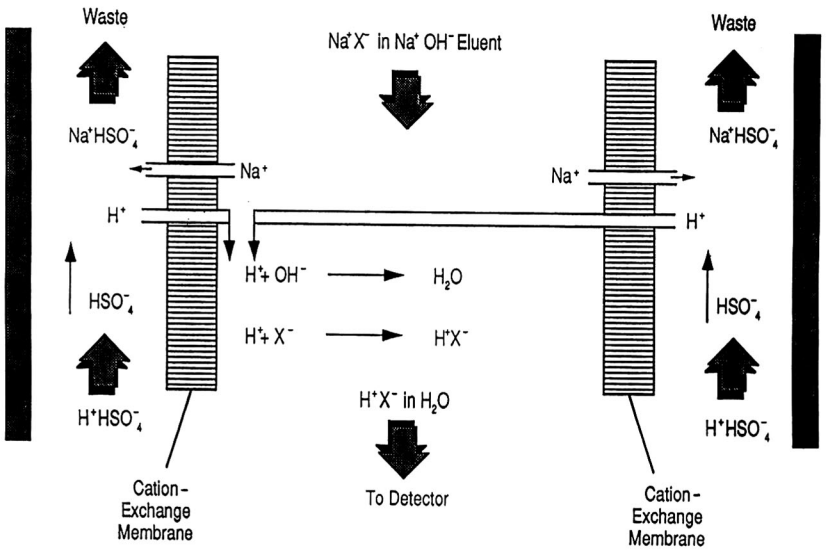

Fig. 3. Suppression mechanism of the Anion MicroMembrane Suppressor.

regenerant chamber to the eluent chamber. The hydronium ions neutralize the hydroxide to its weakly ionized form (water). The sodium counterions transport from the eluent to regenerant chamber to maintain electronic neutrality in the regenerant solution. These are then swept out with the regenerant solution waste. Conductivity enhancement of the analyte ions occur in much the same fashion. The counterions to the analyte exchange through the cation-exchange membrane with hydronium ions, thus creating a significantly higher conductometric signal.

Fig. 4 represents the cation suppressor case. Mineral acids, strong organic acids, and amino acids are commonly used as eluents. In this example, HCl is the eluent. The regenerant flowing counter-current

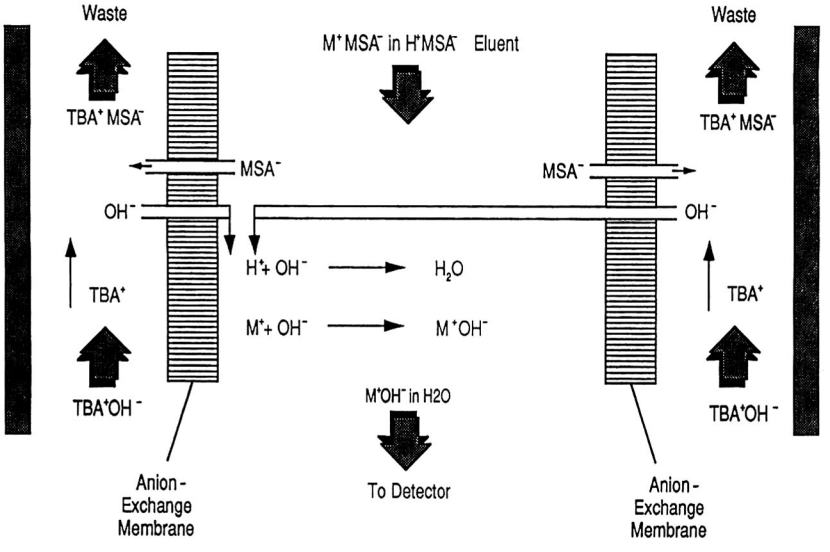

Fig. 4. Suppression mechanism of the Cation MicroMembrane Suppressor.

to the eluent is a strong base such as tetrabutylammonium hydroxide (TBAOH). Anion-exchange membranes permit the exchange of hydroxide from the regenerant chambers with the eluent counterions. Hydroxide ions traverse the membrane and neutralize the hydronium ions from the eluent. Simultaneously, chloride ions leave the eluent chamber to the regenerant chambers to maintain charge balance, which are removed by the liquid flow. For the analyte, the anions are exchanged with hydroxide ions to enhance the conductivity of the analyte.

The design of the MicroMembrane Suppressor addresses many of the problems of the previous suppressors. Eluent passes through a chamber that is defined by an ion-exchange screen sandwiched between two membranes, thus the dead volume is very low, on the order of 50 μl, roughly 1/6th that of the fiber suppressors and more than an order of magnitude smaller than the packed beds. This allows very efficient peaks, greater than 8000 theoretical plates per column.

Membrane suppressors have much greater suppression capacity as well. Suppression capacity is defined as the number of equivalents of eluent ion that is suppressible per unit time. Due to the low dead volume, a high linear velocity is maintained inside the suppressors, which allows for efficient transfer of ions through the membranes. This leads to suppression capacities of 200–300 μequiv./min, significantly higher than that for the previous suppression devices.

Concentration gradients are possible with membrane suppressors [6]. This has proved to be a very useful tool for analytical chemists. By changing the eluent concentration over time, one can elute ions that are tightly held on the column. Membrane suppressors can handle steep gradient ramps due to continuous regeneration of the eluent chamber and high dynamic capacity. As a demonstration of the gradient capability of suppressed IC, a standard containing 35 anions can be eluted with a sodium hydroxide gradient in less than 30 min (see Fig. 5). The MicroMembrane suppressor also allows the use of organic modifiers in the eluent to further mediate the analyte retention on the column. Multiphase analytical columns have been developed that have the ability to control ion-exchange and adsorption or ion-pair retention with use of organic solvents [7].

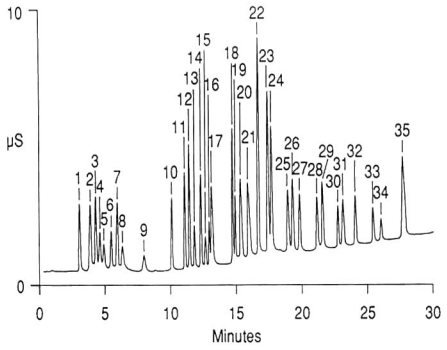

Fig. 5. Gradient separation of inorganic and organic anions. Column: AS5A. Suppression: ASRS, cell effluent recycling. Eluents: (E1) 0.75 m*M* NaOH, (E2) 200 m*M* NaOH. Flow-rate: 1.0 ml/min. Gradient program (E1–E2): 0 min (100:0), 5 min (100:0), 15 min (85:15 min), 30 min (57:43). Peaks: 1 = fluoride; 2 = acetate; 3 = α-hydroxybutyrate; 4 = butyrate; 5 = gluconate; 6 = α-hydroxyvalerate; 7 = formate; 8 = valerate; 9 = pyruvate; 10 = monochloroacetate; 11 = bromate; 12 = chloride; 13 = galacturonate; 14 = nitrite; 15 = glucuronate; 16 = dichloroacetate; 17 = trifluoroacetate; 18 = phosphite; 19 = selenite; 20 = bromide; 21 = nitrate; 22 = sulfate; 23 = oxalate; 24 = selenate; 25 = α-ketoglutarate; 26 = fumarate; 27 = phthalate; 28 = oxalacetate; 29 = phosphate; 30 = arsenate; 31 = chromate; 32 = citrate; 33 = isocitrate; 34 = *cis*-aconitate; 35 = *trans*-aconitate.

One of the major drawbacks of the membrane suppressors was that they required a constant flow of regenerant to provide continuous suppression. This could consume large volumes (up to 10 ml/min) of regenerant, necessitating large reservoirs of the chemicals needed for suppression. A device introduced in 1987 circumvents this problem. The AutoRegen accessory developed by Dionex allows for continuous regenerant recycling. A large ion-exchange cartridge is used to remove the suppression waste products such as eluent counterions and replace it with fresh regenerating ions. A pump recirculates the regenerant through the suppressor and the cartridge. This requires only a small reservoir of regenerant for effective operation. For example, in anion suppression, sulfuric acid is used for regeneration. The suppression product is sodium hydrogensulfate. Sodium ion is caught on a cation-exchange bed in the hydronium form and exchanged for hydronium ion. This serves to insure a fresh supply of regenerant solution for the suppressor. This device allows full around the clock oper-

ations as the cartridges can last several weeks before replacement. On-line IC systems in particular benefit from regenerant recycling [8].

Microbore membrane suppressors for IC were introduced in 1991. Microbore HPLC (column internal diameters up to 2 mm) has been around since the inception of HPLC [9]. One problem with microbore HPLC and UV–Vis detection is the loss of mass sensitivity with conventional detector cells [10]. Microbore IC with 2 mm I.D. columns and suppressed conductivity detection has no loss of sensitivity because conductivity is not mass dependent. Microbore IC has the other advantages of low sample volume, low flow-rate and reduced waste.

One important advantage of the microbore membrane suppressor is greatly enhanced suppression capacity. The microbore MicroMembrane suppressor has been scaled down to reduce dispersion relative to its larger cousin, the original suppressor designed for 4 mm I.D. columns. As shown in Fig. 6, the overall internal volume has been decreased by a factor of 3 to 4 to maintain the same linear velocity as found in the 4 mm versions. If the regenerating solution flow-rate is maintained at the same 3–10 ml/min, a greater eluent counterion concentration gradient is maintained between the eluent and regenerant chambers, leading to higher suppression capacity. Suppression capacity for microbore systems are 2–3 times greater than the 4 mm analogues. This allows greater concentration eluents to be used, which in turn expands the types of analyses that can be performed, such as the analysis of a number of polyphosphates ions in polyphosphoric acid (see Fig. 7).

Alternative modes of chemical suppression

There have been some other suppression schemes mentioned in the literature. Chelation by a transition metal form ion-exchange resin of a chelating agent has been suggested as an effective form of chemical suppression [11]. For this system, the potassium salt of ethylenediamine diacetic acid (EDDA) was used as the eluent, and a cation-exchange bed in the copper form was the suppressor. As eluent entered the suppressor, EDDA chelated with Cu(II) ions, forming a neutral species that was trapped in the resin matrix. Analyte counterions passing through the suppressor would also exchange for copper. This device gave relatively low backgrounds on the order of 5 μS/cm, however due to the counterion exchange for the rather weakly conducting Cu(II) ion, sensitivities would not be as

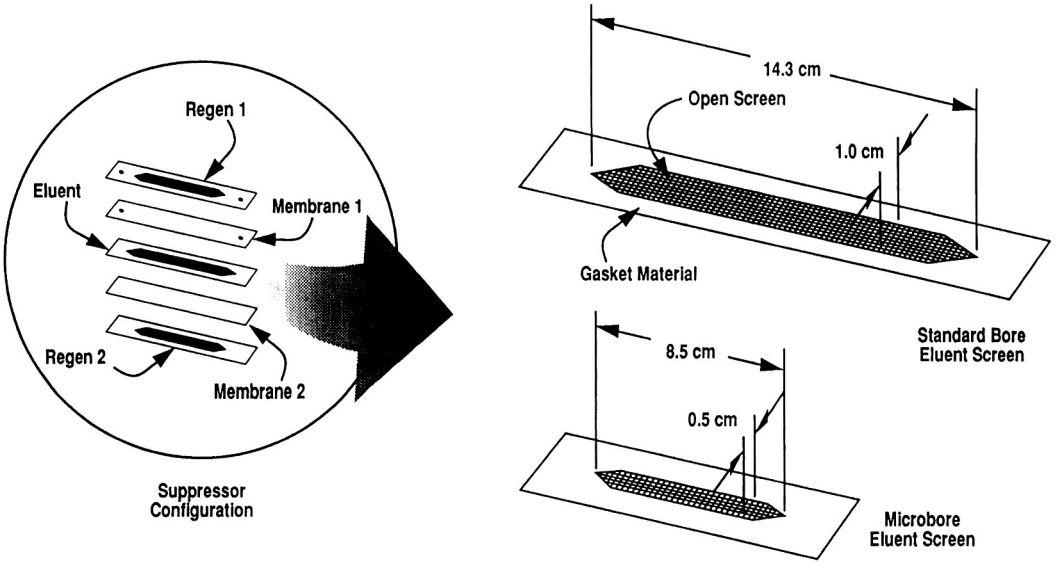

Fig. 6. Internal dimensions of microbore *vs.* standard bore MicroMembrane Suppressors.

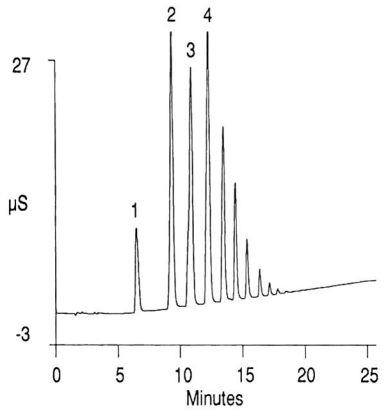

Fig. 7. Separation of polyphosphates in polyphosphoric acid. Column: PAX-100. Eluent: 40–300 m*M* NaOH in 20 min with 5% methanol at 0.25 ml/min. Suppression: ASRS with chemical regeneration. Peaks: 1 = orthophosphate; 2 = pyrophosphate; 3 = tripolyphosphate; 4 = tetrapolyphosphate.

good as for suppressors that use neutralization chemistry which exchange for highly conducting hydronium ion.

Electrochemical suppression

Since the early days of chemical suppression, attempts have been made to use an electric field to improve ion transport through ion-exchange membranes with electrodialysis. The logic for using an electric field would be to provide an extra "push" for the ions in the suppression reaction by driving the neutralizing ions (such as hydronium in a suppressor for anion chromatography) with an electrode of the same charge, and attracting the counterions to an oppositely charged electrode to facilitate removal.

Tian *et al.* [12] have constructed a suppressor that uses electrodes separated from a resin-packed eluent chamber by cation-exchange membranes. The authors claim the main feature of this device is the use of a static regenerant solution of 100 m*M* sulfuric acid using a current of 50 mA and a cell voltage of 4 V. The contention is that application of the electric field helps remove sodium ions from the eluent chamber. It is not mentioned, however, if the device would work in the absence of electrical current. With a high concentration of sulfuric acid on one side of a cation-exchange membrane, it is quite likely that a simple concentration gradient would allow diffusion of hydronium ions in the manner of the membrane based suppressors. Also unclear is the fate of the sodium ion buildup in the regenerant chamber —if a static regeneration solution is used, then eventually this suppressor would become expended when the sodium ions in the regenerant chamber approach equilibrium with those in the flowing eluent stream.

The patent literature teaches of a similar device using flat membranes with electrodes [13]. Similar to the device of Tian *et al.*, flowing sulfuric acid is used as electrolyte in the regeneration chambers, in this instance separated from an open eluent chamber by two cation-exchange membranes. Typical operating conditions were a current of 120 mA at a voltage of 200 V. A similar device was developed by Ban *et al.* [14], using a tubular design with HCl as the regenerant solution. In each of these suppressors, it is claimed that the electric field is used merely as a "pusher", that is, an aid to ion mobility through the ion-exchange membrane. However, one cannot have charged electrodes with no current passing between them; ions can conduct the current between the electrodes, but redox chemistry must be occurring at the electrode surfaces to complete the circuit. This suggests that electrochemistry, not electrodialysis, is the main driving force of electrolytic-type suppressors. In fact, it has been shown that the presence of sulfuric acid in the regenerant chambers of an electrolytic suppressor has a deleterious effect on overall suppression [15]. Electrochemical suppressors which operated without the presence of external acid or base will be discussed in the next section.

The well-known electrolysis of water produces the chemical reactions as outlined in eqns. 1 and 2.

$$\text{Anode:} \quad 3\,H_2O \rightarrow 2\,H_3O^+ + 1/2\,O_2 + 2\,e^- \quad (1)$$

$$\text{Cathode:} \quad 2\,H_2O + 2\,e^- \rightarrow 2\,OH^- + H_2 \quad (2)$$

These reactions are quite facile, especially at metal surfaces with low overpotentials such as platinum [16]. Since hydronium and hydroxide ions are generated in these reaction, it is possible that with the correct ion-exchange membranes, one can utilize the ions for suppression [17]. Thus, a suppressor for anion analysis uses generated hydronium ion with cation-exchange media to neutralize a basic eluent,

and a cation version uses hydroxide ion with anion-exchange sites.

Strong and Dasgupta [15] designed the first practical suppressors to use water electrolysis. They used single-membrane and double-membrane helical designs for their units. A peristaltic pump was used to deliver water as the regenerant source. They were able to suppress up to 200 m*M* sodium hydroxide eluents, and demonstrated good gradient chromatography for anions.

New electrolytic suppressor for IC

In 1992, Dionex introduced the first commercial electrochemical suppressor, which they named the "Self Regenerating Suppressor", or SRS [18]. A flat membrane design similar to their membrane suppressor was used as the suppression means, with two platinum electrodes incorporated into the design that allow electrolysis of water to occur. A constant current power controller generates the electric field for the electrolytic reaction. One significant feature of this design is that it allows the use of very low flow-rates for the regenerant water, to the point where the suppressor can use the deionized eluent after suppression from the detector cell waste as its water source, greatly simplifying the plumbing scheme and reducing waste (see below). Since water electrolysis is utilized as the regenerant ion source, no independent chemical feed is necessary as was needed for past suppression devices.

The internal design of the suppressor is shown in Fig. 8. Functionalized ion-exchange screens are present in the regenerant chambers to facilitate electric current passage, with permselective ion-exchange membranes defining an eluent chamber containing another functionlized ion-exchange screen to minimize dead volume. Two platinum electrodes are placed in the regenerant chambers, one between a regenerant screen and the hardware shell, and another between the membrane and the other regenerant screen. This electrode placement proved optimal for current efficiency and removal of the waste gases.

The neutralization reactions occurring in the SRS are similar to those of the membrane-based suppressors. For anion-exchange chromatography, using the Anion Self Regenerating Suppressor (ASRS), hydronium ions generated at the anode

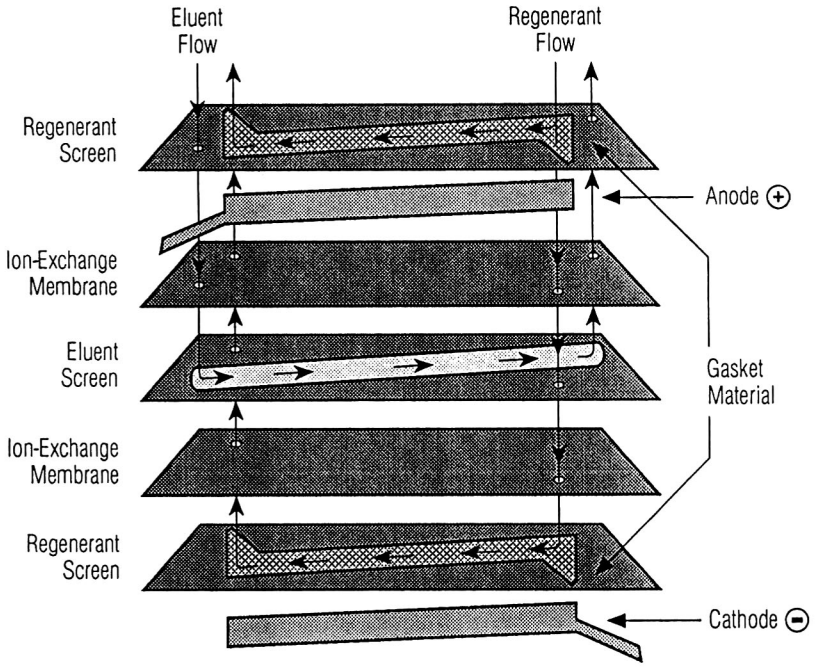

Fig. 8. Internal schematic of the Self Regenerating Suppressor.

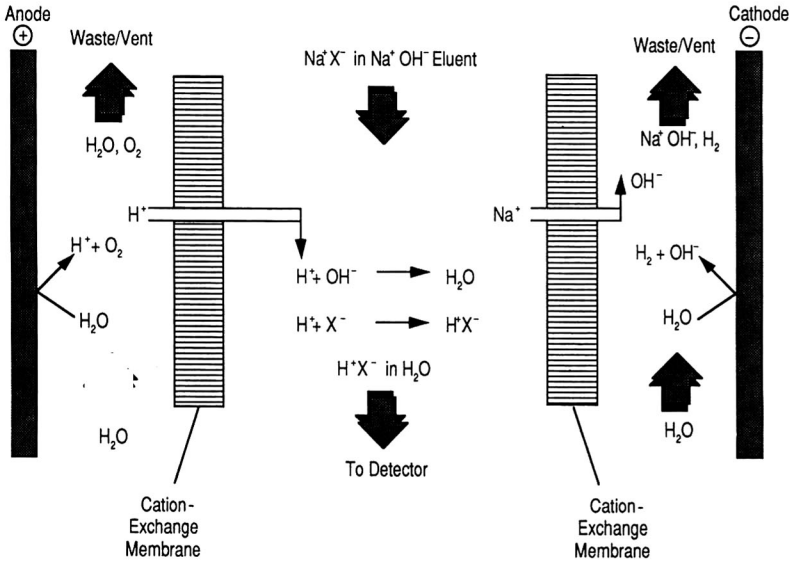

Fig. 9. Mechanism of suppression for the Anion Self Regenerating Suppressor.

traverse the cation-exchange membrane to neutralize the basic eluent, in this example, sodium hydroxide as shown in Fig. 9. The neutralized eluent proceeds to the detector cell. Sodium counterions are attracted to the negatively charged cathode, where they permeate the membrane in the cathode chamber and pair off with electrogenerated hydroxide ions to maintain electronic neutrality. Waste gases of hydrogen (from the cathode) and oxygen (from the anode) are vented with the liquid waste of aqueous sodium hydroxide. As with other suppressors, analyte signals are enhanced by exchange of their counterions with hydronium ions.

For cation analysis, the Cation Self Regenerating

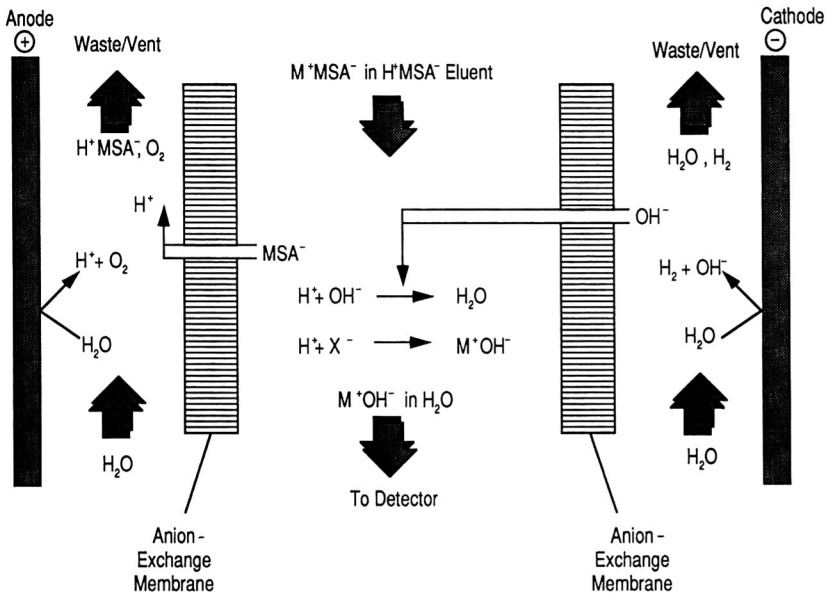

Fig. 10. Mechanism of suppression for the Cation Self Regenerating Suppressor. H^+MSA^- = Methanesulfonic acid.

Suppressor (CSRS) chemistry is shown in Fig. 10. Hydroxide ions generated at the cathode traverse the anion-exchange membrane to neutralize the acidic eluent, methanesulfonic acid in this demonstration, forming water, which continues to the detector cell. Methanesulfonate ions attracted to the anode traverse the opposing membrane, associating with hydronium ions produced at this electrode to maintain electronic neutrality. Analyte counterions are also attracted to the anode, exchanging for hydroxide ions generated at the cathode which serves to enhance the conductivity signal. As in the anion case, by-product gases and methanesulfonic acid proceed to waste and vent.

In contrast with other chemical suppressors, the SRS exhibits an overall directionality with respect to the suppression chemistry. A membrane suppressor with chemical regenerant bathing both regenerant chambers can have the regenerant ions coming from either membrane. In contrast, the ASRS generates hydronium for suppression only at the anode, so the only membrane containing and passing hydronium ions is the one in the anodic chamber. Counterion removal occurs only in the cathodic chamber and the associated membrane, where the counterion can associate with a generated hydroxide ion. The net result is that the anodic membrane is partially in the hydronium ion form, and the cathodic membrane is partially in the sodium form. CSRS chemistry is completely analogous, with one membrane in the hydroxide ion form, and the other in the methanesulfonate form.

An important concept for suppressors that use water electrolysis is the need for intimate electrical contact of the electrode with the membrane, either through direct contact or by use of an intermediate ion-exchange medium, such as functionalized screens. The electrical circuit inside the suppressor itself is conducted by ion passage through ion-ex change sites. When a regenerant ion is generated a one electrode, it sets off a cascade of ions pushin others off of ion-exchange sites until one is used fo neutralization. Simultaneously, the counterion t the eluent does likewise, setting off another cascad until one leaves with the waste electrogenerated ior The key to the function of an electrolytic suppresso is that ions have a low-resistance pathway usin ion-exchange sites to flow between the electrodes t allow conductance of the electrical current.

The new suppressors have three possible oper ational modes. Each is designed to work for a par ticular set of determinations.

(1) Cell effluent recycling. The easiest operationa mode utilizes the cell effluent as its deionized wate source for electrolysis as shown in the schematic i Fig. 11. The eluent passes through the separatio column, then proceeds to the suppressor. In th suppressor, the eluent is neutralized and the coun terions removed. At this point, the suppresse eluent is largely deionized water containing a fe analyte ions. This stream proceeds to the detecto cell, then is routed back to the suppressor to flo through the regenerant chambers.

Recycling the cell effluent has many advantages Beside creating a simple plumbing scheme, waste i greatly reduced. Waste volumes of an SRS equipped IC system are now no more than that o the eluent itself while giving all of the advantages o chemical suppression. Also, there is no need fo chemical regenerants such as sulfuric acid or tet rabutylammonium hydroxide as with past suppres sion devices. Operational costs are also greatly re duced, particularly for TBAOH which is somewha expensive. Labor costs are also reduced as no main tenance is required.

This mode covers the vast majority of applica

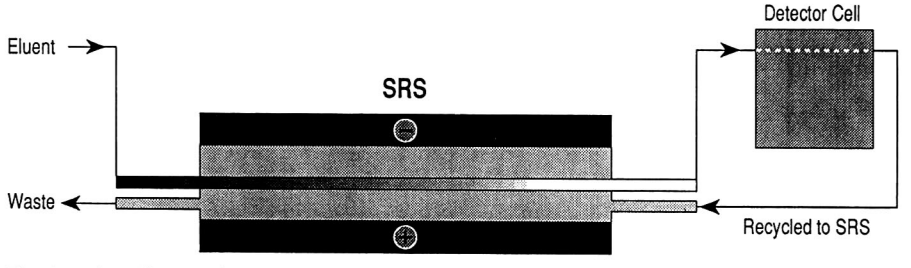

Fig. 11. Flow diagram for the Self Regenerating Suppressor using cell effluent recycling.

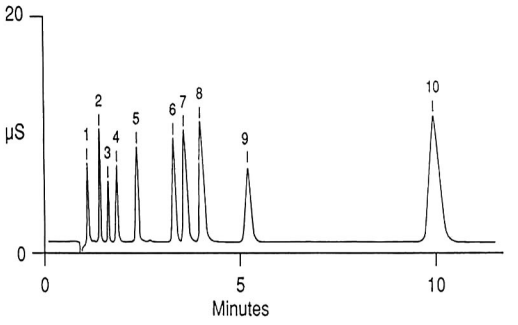

Fig. 12. Separation of common inorganic anions including oxyanions. Column: AS9-SC. Eluent: 1.8 m*M* sodium carbonate, 1.7 m*M* sodium hydrogencarbonate at 2.0 ml/min. Suppression: ASRS, cell effluent recycling. Peaks: 1 = fluoride (1 mg/l); 2 = chlorite (5 mg/l); 3 = bromate (5 mg/ml); 4 = chloride (1.5 mg/l); 5 = nitrite (6 mg/l); 6 = bromide (10 mg/l); 7 = chlorate (15 mg/l); 8 = nitrate (15 mg/l); 9 = phosphate (20 mg/l); 10 = sulfate (25 mg/l).

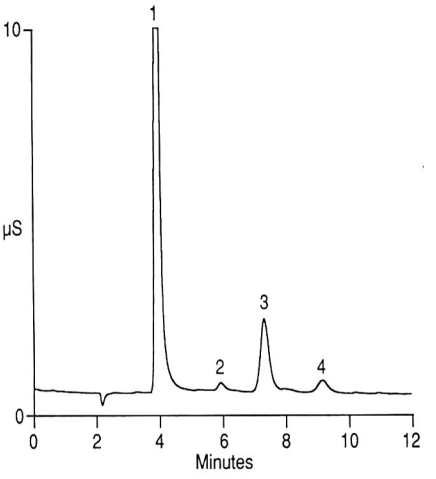

Fig. 13. Determination of cations in sea water. Column: CS12 2 mm. Eluent: 20 m*M* MSA at 0.25 ml/min. Sample diluted 1/1000, injection volume of 2.5 μl. Suppression: CSRS 2 mm, cell effluent recycling. Peaks: 1 = sodium (13.0 mg/l); 2 = potassium (0.3 mg/l); 3 = magnesium (1.2 mg/l); 4 = calcium (0.4 mg/l).

tions extant for IC today. Typical IC separations such as common inorganic anions and oxyhalides (Fig. 12) and cations in sea water on an IonPac CS12 (Fig. 13) are performed easily. Other, more difficult separations such as a steep NaOH gradient (Fig. 5) can also be done with this suppressor with a small baseline deflection.

(2) External water source. When lower system noise or higher suppression capacity is required, an external deionized water source may be used to increase the flow-rate through the regenerant chambers. This provides better sweep out of the eluent counterions, which leads to lower noise and thus more sensitivity. A pressurized bottle or pump is used to deliver water to the suppressor for the electrolytic reaction up to a flow-rate of 10 ml/min. After electrolysis, the stream containing the counterions, electrolytic side product and gases proceed to waste. The eluent stream proceeds to the detector cell as in the cell recycle model, then is also routed to waste. This mode is specialized and would only be used in a few cases.

(3) Chemical regeneration mode. The new suppressors are similar to the membrane suppressors, thus can be used with chemical regenerants as well. There are some limitations to electrolytic operation which would necessitate use of chemical regenerant.

Organic solvents, methanol in particular, are not well tolerated in the electrolytic modes. This is due to oxidation of the solvent to form ionic by-products, which create noise and high backgrounds in the chromatography. Eluents containing organic solvents can be used with chemical regenerant, such as the polyphosphoric acid run on an OmniPac PAX-100 as shown in Fig. 7.

Chloride-containing eluents also present a problem for cation determinations in the electrolytic modes. Chloride ion can oxidize to form hypochlorite which is injurious to the ion-exchange membrane. Hydrochloric acid and hydrochloride salts of amino acids are common eluents for cations. If HCl is used alone in the eluent system, however, electrolytic modes can be used by replacing the HCl with methanesulfonic acid (MSA) which is electrochemically inert. MSA is a direct replacement for HCl by using the same hydronium concentration. Samples containing chloride are not a problem since the volume injected is so small that it is highly diluted by the time it reaches the regenerant chamber and the electrode.

The new suppressors give very quiet baselines when working electrolytically, particularly when using external water as the regenerant source. When recycling the eluent as regenerant, the amount of water available is limited to the eluent flow-rate. Consequently counterion sweep out is not as facile,

TABLE I

LIMITS OF DETECTION (LOD) WITH SRS

Species	LOD, cell effluent recycle (μg/l)	LOD, external water (μg/l)
Anions[a]		
Chloride	4	2
Nitrate	12	5
Phosphate	44	17.5
Sulfate	18	8
Cations[b]		
Lithium	1	0.7
Sodium	4	2
Ammonium	5	3
Potassium	4	3
Magnesium	5	3
Calcium	8	4

[a] Conditions: column: AS4A-SC; suppressor: ASRS; eluent: 1.8 m*M* carbonate, 1.7 m*M* hydrogencarbonate; flow-rate: 2 ml/min; injection volume: 50 μl.

[b] Conditions: column: CS12; suppressor: CSRS; eluent: 20 m*M* MSA; flow-rate: 1 ml/min; injection volume: 25 μl.

leading to somewhat greater noise than when using external water, which is run typically at flow-rates at 3–10 ml/min. This does not preclude the use of recycling for most applications, however, as the increase in performance is for the most part outweighed by the convenience offered by recycling.

Detection limits (as defined as three times the baseline noise) for anions and cations by direct injection are shown in Table I. As is evident, the recycle mode gives somewhat higher detection limits than when using external water, however it is quite reasonable for most applications. Cell effluent recycling has the advantage of greater ease of use, so the somewhat elevated detection limits relative to the use of external water makes it much more desirable for routine use.

CONCLUSIONS

Suppressed IC has undergone many improvements since its early days. Suppressors have advanced from a column that required considerable user intervention to the latest, an electrolytic suppressor that is essentially invisible in operation. Analysts are always looking for greater ease of use, better performance, improved signal-to-noise ratio, and lower cost of operation. The new electrolytic suppressors described in this paper accomplish all of these while making suppression less like a post-column treatment system as has been the case in the past and more like an integral part of the overall detection scheme.

ACKNOWLEDGEMENTS

The authors gratefully acknowledge the help of the many people involved in this project. They include Maria Rey, Dew Siriraks, Lori Takahashi, Harpreet Dhillon, Jill Jekot, Mike Harrold, John Statler, Chris Pohl, David Hsia and Ruthann Kiser of Dionex for helpful discussions and data collection.

REFERENCES

1 H. Small, T. S. Stevens and W. C. Bauman, *Anal. Chem.*, 47 (1975) 1801.
2 T. S. Stevens, J. C. Davis and H. Small, *Anal. Chem.*, 53 (1981) 1488.
3 J. Stillian, *LC Mag.*, 3 (1985) 802.
4 J. Weiss, *Handbook of Ion Chromatography*, Dionex, Sunnyvale, CA, 1986.
5 R. A. Wetzel, C. A. Pohl, J. M. Riviello and J. C. MacDonald, in J. C. MacDonald (Editor), *Inorganic Chromatographic Analysis*, Wiley, New York, 1985, Ch. 9.
6 R. D. Rocklin, C. A. Pohl and J. A. Schibler, *J. Chromatogr.*, 411 (1987) 107.
7 J. R. Stillian and C. A. Pohl, *J. Chromatogr.*, 499 (1990) 249.
8 G. J. Lynch, *Process Qualit. Control*, 1 (1991) 249.
9 R. P. W. Scott and P. Kucera, *J. Chromatogr.*, 169 (1979) 51.
10 A. Y. Tehrani, *LC Mag.*, 3 (1985) 42.
11 H. Sato and A. Miyanaga, *Anal. Chem.*, 61 (1989) 122.
12 Z. W. Tian, R. Z. Hu, H. S. Lin and J. T. Wu, *J. Chromatogr.*, 439 (1988) 159.
13 K.-H. Jansen, K.-H. Fischer and B. Wolf, *US Pat.*, 4 459 357 (1984).
14 T. Ban, T. Murayama, S. Muramoto and Y. Hanaoka, *US Pat.*, 4 403 039 (1983).
15 D. L. Strong and P. K. Dasgupta, *Anal. Chem.*, 61 (1989) 939.
16 P. W. Atkins, *Physical Chemistry*, W. H. Freeman, San Francisco, CA, 1978.
17 C. Pohl, R. W. Slingsby, J. R. Stillian and R. Gajek, *US Pat.*, 4 999 098 (1991).
18 A. Henshall, S. Rabin, J. Statler and J. Stillian, *Am. Lab.*, 24 (1992) 20R

Journal of Chromatography, 640 (1993) 111–125
Elsevier Science Publishers B.V., Amsterdam

CHROMSYMP. 2674

Simultaneous determination of sub-mg/l levels of sulphur and chlorine in liquid hydrocarbons by a coupled combustion–ion chromatography technique

M. Andrew*, I. M. V. Burholt, N. J. Kernoghan, T. P. Lynch, R. Mackison, D. Mealor, J. A. Price and P. Schofield

BP Research Centre, BP International Ltd., Sunbury Research Centre, Analytical Division, Building 100, Room 110, Chertsey Road, Sunbury-on-Thames, Middlesex TW16 7LN (UK)

ABSTRACT

A method for elemental analysis that employs a novel coupled combustion–ion chromatography (C–IC) apparatus is described in detail. The samples are combusted and the products collected in a dilute peroxide solution. This solution is loaded onto a concentrator column which is then introduced into the injection position of a suppressed conductivity anion chromatography system. The method is rapid, reliable, free from interferences and has the capacity for simultaneous determination of sulphur and chlorine in organic liquids at concentrations down to 0.03 mg/l. Provided that the capacity of the concentrator column is not exceeded, the recovery for organic standards of both chlorine and sulphur in a variety of organic solvents is greater than 93%, irrespective of the solvent and the sample volume and concentration. Repeatability is only slightly worse than that observed for conventional direct IC analysis of aqueous solutions. At concentrations of 0.4 mg/l Cl and 0.5 mg/l S, the % standard deviations (n = 10) were found to be 2.9 and 3.5% respectively. The results obtained with the C–IC analyser for both standards and petroleum-based samples are in good agreement with those obtained by microcoulometry.

INTRODUCTION

Organo-sulphur and organo-chlorine are well documented poisons of catalysts [1–3]. Since catalysts are used in a wide variety of applications in the petroleum industry [4], close monitoring of these species in feeds and products from various petroleum and petrochemical processes is essential in order to meet modern process specifications and to avoid loss of catalyst activity. At BP, microcoulometry (oxidative) [5–8] had been used since the early 1970s for such monitoring and had become the established technique within the petroleum industry for both sulphur [9] and chlorine [10]. However, these methods had several inherent problems associated with them:

(i) As separate electrolytic cells are required for sulphur and chlorine analysis, simultaneous determination of sulphur and chlorine is not possible. Thus, analysis for both elements by microcoulometric techniques involves two calibration procedures and changing the cell configuration. Furthermore, the stabilisation time between the changing of cells had been found to be excessive (average 3–4 h), particularly when changing from sulphur to chlorine.

(ii) Day-to-day variation in cell performance, particularly the chlorine cell, required the full-time attention of an experienced analyst to balance the settings for amplifier gain and bias in order to obtain the optimum peak response to facilitate accurate quantification.

(iii) Both organic bromine and organic iodine species interfered with the chlorine analysis since they form entities which are titrated in the cell.

(iv) In the combustion of organo-sulphur species,

* Corresponding author.

0021-9673/93/$06.00

sulphur trioxide as well as sulphur dioxide is produced because of the strongly oxidative nature of the conditions used. Since only sulphur dioxide is titrated in the cell, accurate quantification relies on samples and standards combusting to give the same dioxide:trioxide ratio. In practice, depending on the combustion temperature and oxygen concentration, this ratio may vary for different organo-sulphur species [8]. SO_2 conversion is normally above 90% but, within the terms of the IP methods [9,10] can be as low as 75% and still be acceptable.

These problems, coupled to sensitivity limitations, led to the requirement for an alternative method that could determine, simultaneously, trace levels of organo-sulphur and organo-chlorine compounds in organic media.

In 1988 a brief overview of ion chromatography (IC) in the oil industry [11] highlighted its potential for simultaneous multi-elemental analysis. To accommodate elemental analysis in organic materials a combustion stage prior to IC analysis may be applied [12]. Combustion of the sample followed by IC analysis had been used to determine the halogens, sulphur, phosphorus and selenium and had been applied successfully to coal and oil shale [13] using a Parr oxygen bomb, fuel oils [14] and other organic materials [15,16] employing Schöniger oxygen flask combustion, and to silicate rocks [17] with a furnace combustion set-up. However, all these analyses involved a distinctly separate combustion stage, followed by IC analysis of the combustion products after absorption into a suitable media. Mealor [11] suggested that a combination of combustion and IC in one instrument would greatly enhance the technique, making it simple and rapid to operate, and rendering it more suitable to automation. Furthermore, with the introduction of a concentrator column [18] the method would permit analysis of chlorine and sulphur at sub ppm levels, and thus provide a more sensitive alternative to microcoulometry. This paper describes the development between 1987–1988 of such an analyser. It concludes a detailed description of the coupling of the tube furnace combustion stage to the ion chromatography module with a suitable "small volume" bubbler, and compares the results obtained with microcoulometric determinations.

Since this work, further combustion–ion chromatography (C–IC) studies have been reported, covering applications in the pharmaceuticals [19], paper [20], edible oil [21,22] and oil and petrochemicals [23–25] industries. However, these studies have continued to use a separate combustion stage, either by Schöniger oxygen flask [19,20,26,27], Parr oxygen bomb [21,22], PTFE Parr bomb [23] or tube furnace [24,25,28]. Due to the limitations on combustion mass, the volumes of absorber required, and the absence of a concentration stage, studies reported in the literature invariably have higher limits of detection (LODs) than that reported in this study. Only Assenmacher and Frigge [24] have described a combination of combustion followed by IC capable of measurement at sub-ppm levels, using large sample masses and absorber volumes of 50 ml. Thus, with respect to both sensitivity and the elegant combination of the combustion and IC stages, the work described here compares favourably with the C–IC studies published to date.

EXPERIMENTAL

Instrumentation

C–IC analyses were carried out on the C–IC analyser developed during this study. A schematic diagram and photograph of the C–IC analyser are shown in Figs. 1 and 2, respectively. Essentially the analyser consists of three modules as detailed below.

Sample combustion module. This consists of a twin-tube furnace (Carbolite CFM 12/2) set at 900°C. Gas flows (helium and oxygen) through the system are controlled by needle valves and measured by 0–250 ml/min Gap meters. The furnace houses two silica combustion tubes —one single-chamber tube (used for oxygen purification) and one two-chamber tube (used for sample combustion).

The oxygen used for sample combustion is passed through the first (single-chamber) combustion tube (length, 300 mm; diameter, 22 mm) where any trace organic impurities present are converted to the corresponding acidic combustion products, hydrogen chloride, sulphur dioxide and sulphur trioxide. The hot oxygen then passes through an absorber train comprising three 125-ml Dreschel bottles, the first two of which contain 50 ml of 50% sodium hydroxide to remove both the acidic combustion products of organic impurities and any trace inorganic impu-

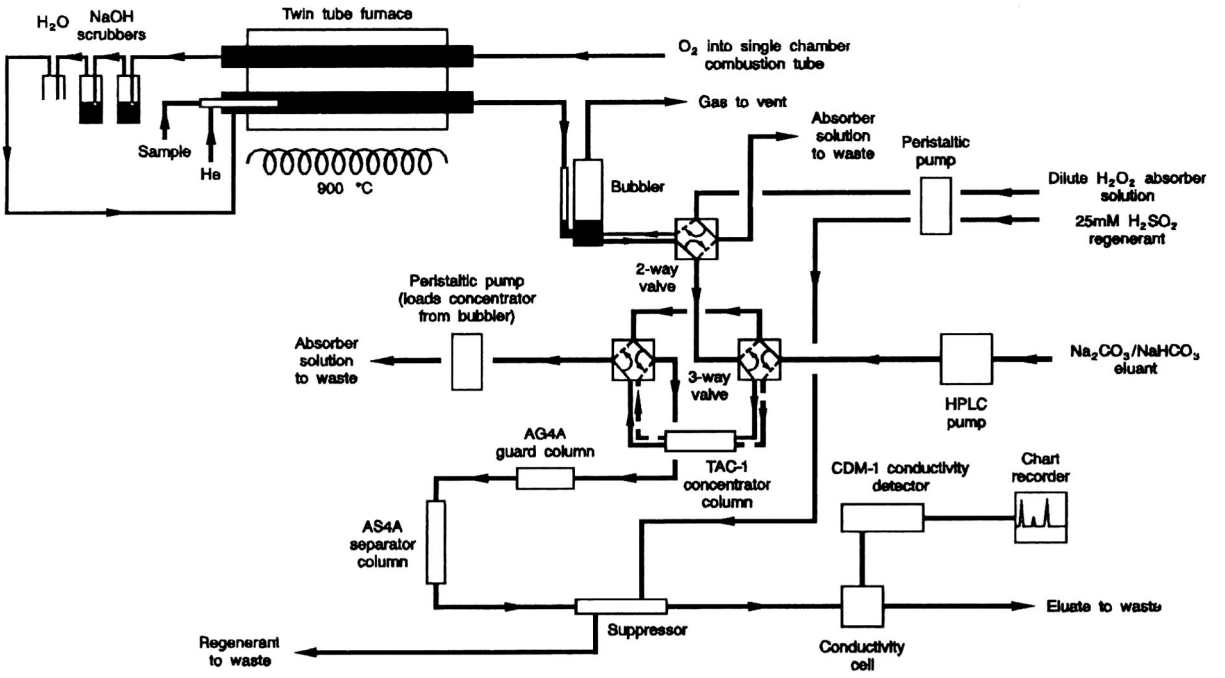

Fig. 1. Schematic diagram of the C–IC aparatus. Not drawn to scale. See Experimental section for details.

rities that may be present. The last Dreschel bottle contains 50 ml of conductivity water to remove any residual NaOH carried over from the first two scrubbers. This purification stage is essential in order to reduce the gas blanks to a manageable level.

The purified oxygen is then fed into the outer chamber of the second combustion tube (H. Baumbach Ltd.). This tube consists of inner and outer silica sleeves (see Fig. 3). The sample is injected through a rubber septum into a helium gas carrier stream in the inner chamber of this combustion tube. Sample introduction is carried out via a syringe (Hamilton, 100 μl, fitted with a 71 mm needle), mounted on a constant rate injector (Sage Instruments Model 341). The sample is volatilised in the helium stream and carried down the inner chamber where it passes through four slits. At this point the sample–helium mixture meets the purified oxygen in the outer chamber and combustion takes place. The combustion products are then swept into the interface module.

Interface module. This module links the combustion furnace to the ion chromatograph (see Fig. 3). It consists of a glass bubbler containing a fixed volume of dilute hydrogen peroxide absorber solution through which the exit gases from the combustion tube are vented to atmosphere. The peroxide solution is introduced into the bubbler by a peristaltic pump (Ismatec MP13) fitted with 2.79 mm purple/white silicon tubing, via a PTFE two-way rotary valve (Rheodyne Type 50). Whilst the sample is being combusted the bubbler is connected to the back end of the sample combustion tube by a ball and socket joint and held in place by a spring clip. A low-voltage heating tape (Electrothermal Engineering), maintained at 60°C via a variable voltage transformer (Zenith Instruments), is wound around the delivery arm of the bubbler to avoid "cold spots" and consequent condensation problems.

The chromatography module. This module is essentially made of components manufactured by Dionex (see Figs. 1 and 2) and plumbed with 1/16 in. I.D. tubing (1 in. = 2.54 cm) throughout. A three-way, air-activated valve (Dionex P/N 035913) is used to control the flow of sample and eluent during the loading and injection operations. When

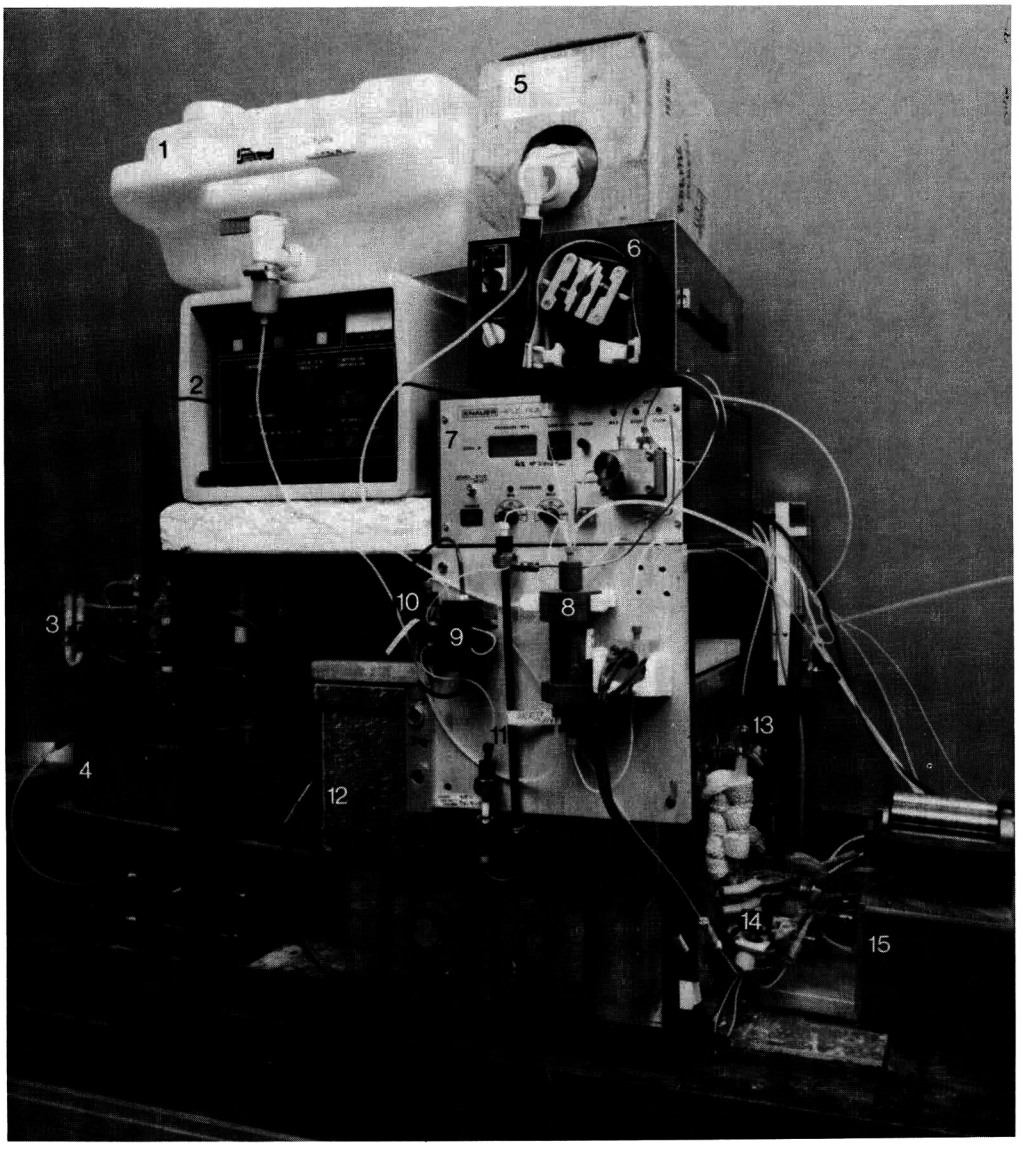

Fig. 2. Photograph of the C–IC analyser Mk I. 1 = Regenerant housing; 2 = conductivity detector; 3 = NaOH and solid scrubbers (the solid scrubbers were later removed); 4 = syringe drive; 5 = eluent housing; 6 = peristaltic pump (Watson-Marlow); 7 = HPLC pump; 8 = fibre suppressor; 9 = 3-way valve; 10 = concentrator column; 11 = IC columns; 12 = twin combustion furnace, housing the two combustion tubes; 13 = bubbler; 14 = 2-way valve; 15 = peristaltic pump (Ismatec). For further details see Experimental section.

the valve is switched to the "load" position the absorber solution containing the acidic combustion products is drawn, by a peristaltic pump (Watson-Marlow 202U) fitted with marprene tubing, through a Dionex TAC-1 concentrator column. When switched to the "inject" position, the concentrator column is flushed with eluent pumped through the system by an HPLC pump (Knauer Type 64). The anions of interest are separated from each other and interfering species by ion (exchange) chromatography using Dionex AG4A and AS4A guard and separator columns, and detected by con-

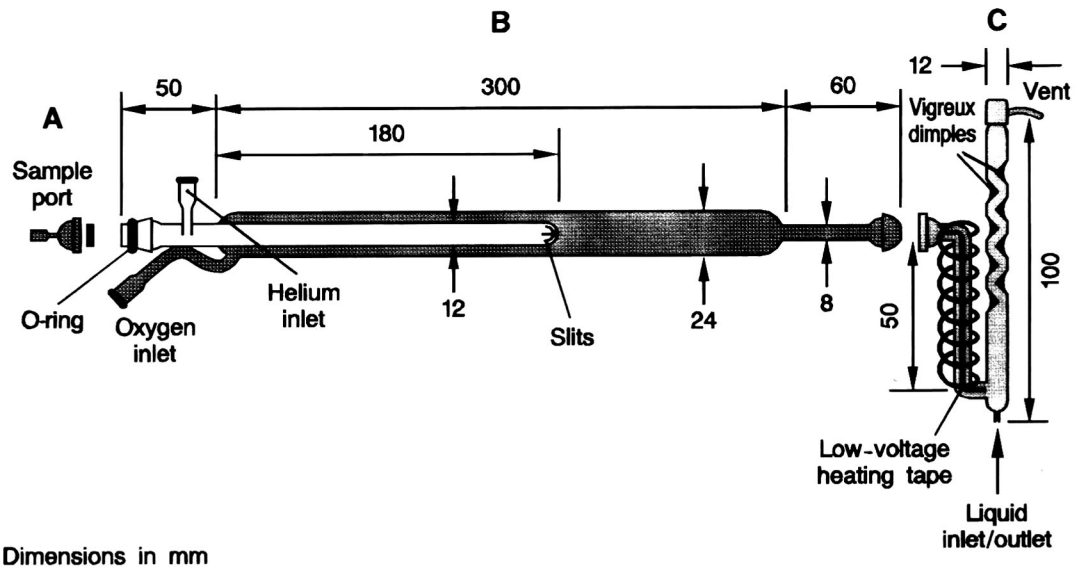

Fig. 3. (A) Injection port, (B) combustion tube and (C) bubbler used in the C–IC analysis. Individual units are drawn to scale, but the bubbler scale is different to that of the combustion tube.

ductivity using a Dionex CDM-1 conductivity detector and cell after chemical suppression of the eluent [29] using a Dionex Fibre Suppressor (P/N 035691). Dilute sulphuric acid regenerant is pumped through the suppressor column at a constant rate via the Ismatec MP13 peristaltic pump. The chromatograms are recorded on a chart recorder (Servogor 120) and the heights measured manually.

Reagents

All reagents were AnalaR grade purchased from BDH and used as received, unless otherwise stated.

Conductivity water, <0.06 μS/cm. Freshly distilled and deionised using a water purifier (Millipore, Milli-Q system).

Organic solvents. Xylene, low in sulphur (SLR grade, Fisons), decalin (decahydronaphthalene) (GPR grade), isooctane (2,2,4-trimethylpentane) (ASTM reference grade, Hatterman Fuels), *n*-hexadecane (GPR grade), propan-2-ol(IPA), acetone and toluene.

Standard materials. Dibutyl sulphide, ($[CH_3(CH_2)_3]_2S$), (Aldrich), chlorobenzene (C_6H_5Cl), 1-chloro-2,4-dinitrobenzene [$C_6H_3Cl(NO_2)_2$], (Microanalytical reagent, Hopkin & Williams), S-benzyl-thiuronium chloride [$C_6H_5CH_2$–S–C(:NH)–NH_2 · HCl], (Microanalytical reagent grade), sodium chloride, (Aristar grade) and sodium sulphate, anhydrous powder.

C–IC reagents. Sodium hydroxide solution (50%, w/v), sulphuric acid (sp. gr. 1.84), hydrogen peroxide, 100 vol (Aristar grade), sodium carbonate, (Aristar grade) and sodium hydrogen carbonate.

Gases. Oxygen (BOC), helium, ultrapure grade (G & E Union Carbide).

Preparation of reagent and standard solutions

Conductivity water was used in the preparation of all eluents and aqueous reagents and standards.

IC Eluent. 2.0 m*M* Na_2CO_3, 0.75 m*M* $NaHCO_3$ was prepared in 4-l batches by dilution of eluent concentrates of 1 *M* Na_2CO_3 and 1 *M* $NaHCO_3$.

Regenerant. 12.5 m*M* H_2SO_4, prepared by diluting 5.6 ml of the conc. acid to 8 l.

Absorber solution. 0.02 vol H_2O_2, prepared in 4-l batches by dilution of the 100 vol H_2O_2.

Scrubber solution. 50% NaOH solution, as purchased.

Inorganic standards. Stock solutions (100 ml) of Cl^- and SO_4^{2-} (1000 mg/l) were prepared after drying the NaCl at 150°C for 2 h, and the Na_2SO_4 at 105°C for 1 h.

Organic standards. Stock solutions (100 ml) con-

taining *ca.* 600 mg/l Cl were prepared accurately by dissolving known masses of chlorobenzene and 1-chloro-2,4-dinitrobenzene in toluene. Similarly a stock solution containing *ca.* 600 mg/l S was prepared by dissolving dibutyl sulphide in isooctane, and a mixed standard containg *ca.* 300 mg/l of Cl and S by dissolving S-benzyl-thiuronium chloride in propan-2-ol. Calibration standards were freshly prepared as required by dilution of the stock solutions with the appropriate solvent, and discarded after five days.

All organic standards, the eluent concentrates and the 100 vol H_2O_2 were stored in a refridgerator at 4 ± 1°C.

Analytical conditions

Sample injection volume, 50–100 μl; sample injection rate, *ca.* 20 μl/min; helium flow-rate, 40 ml/min; oxygen flow-rate, 160 ml/min; absorber solution volume, *ca.* 1.5 ml (wash volume, *ca.* 1.5 ml); eluent flow-rate, 2 ml/min; suppressor regenerant flow-rate, 2 ml/min.

Operation of the C–IC analyser

The sample is injected into the inner sleeve of the combustion tube via a syringe held in a constant-rate injector. The syringe is positioned so that the needle tip protrudes approximately 60 mm into the inner chamber of the combustion tube, *i.e.* approximately 10 mm past the furnace entrance. The sample volatilises in a helium carrier stream and passes through four slits into the outer chamber where it combusts on contact with purified oxygen. The combustion products (H_2O, CO_2, HCl, SO_2, SO_3, NO, HBr, etc.) are carried into the bubbler where the water-soluble compounds are scrubbed from the gas stream by the dilute peroxide. The dilute peroxide ensures that all the combustion products of organic sulphur are converted to sulphate.

When all the sample has been combusted (normally 2.5–5 min), the bubbler is disconnected from the combustion tube (by removing the spring clip), and its contents loaded into the concentrator column by turning on the second (Watson-Marlow) peristaltic pump, with the Dionex valve switched to the load position. Provided its capacity is not exceeded, the concentrator column collects all the anionic species whilst the excess peroxide solution is pumped through the concentrator to waste. When this operation is complete a further aliquot of peroxide solution is pumped into the bubbler via the Rheodyne two-way switching valve. The bubbler is then reconnected to the combustion tube for 15 s so that the gas flow through the absorber solution effectively "washes" the walls of the bubbler. This aliquot is also pumped onto the concentrator column.

Once loading of the second aliquot (wash) of peroxide has been completed, the air-activated valve is switched to the "inject" position in order to direct eluent through the concentrator column. The eluent displaces the anions from the concentrator onto the main column where the ions of interest are separated from each other and interfering species, and detected as the acids by conductivity after chemical suppression of the eluent. The chromatograms are recorded on a chart recorder and the peak heights used for quantification. Correction for any contribution from the gases and absorber solution is made by repeating the above operations but without injecting any sample, *i.e.* allowing the gases to bubble through the absorber solution for the same time as that for the samples.

The total analysis time using typical sample injection volumes of 50 μl and an injection rate of 20 μl/min can be calculated from the formula $12n - 3$, where n (the number of analyses) is greater than 1. Each analysis takes approximately 12 min, but loading of each subsequent sample onto the concentrator column may be performed whilst the preceding sample is still eluting from the main column, since the time for combustion is never shorter than the time required for a sample to elute from the concentrator. For analysis at levels below 0.1 mg/l where larger volumes of sample may be combusted, total analysis time will increase in accordance with the time taken for combustion.

Microcoulometry

Sulphur determinations were carried on a Dohrmann MCTS-130 using conditions laid down in ref. 9. Chlorine determinations were carried out on a Dohrmann MCTS-120 using conditions laid down in ref. 10.

TABLE I

CHARACTERISTICS OF VARIOUS COMBUSTION METHODS FOR ELEMENTAL ANALYSIS BY IC

	Oxygen flask	Oxygen bomb	Wickbold
Sample size	20 mg	0.5 g	30 g
Final absorber volume (ml)	5	10	100
Sample type	Solids	Solids	Liquids
	Non-volatile liquids	Liquids	Gases
Detection limit (mg/kg), Cl	100	10	<0.5
S	50	5	<0.5

DEVELOPMENT OF THE C–IC ANALYSER

Previous studies [11] had indicated that C–IC had the potential for analyses at sub ppm (w/w) level provided the sample combustion products could be collected in a volume of absorber solution small enough to be loaded onto a concentrator column. Oxygen flask [30,31] and oxygen bomb [32] methods were limited by either the sample mass combusted or the volume of absorber required. Wickbold combustions employing an oxyhydrogen burner [33] were compatible with sub-ppm (w/w) analysis (Table I) but required a large sample mass (*ca.* 30 g). From these studies it was concluded that none of these combustion methods was suitable for interfacing with an IC module and that a tube furnace combustion would be both compatible with interfacing and the safest way of burning the samples.

The development of the C–IC analyser from the initial concept to the point at which it could be used routinely for "real" samples (Mk I Model, Fig. 2) occurred over a two-year period. A number of significant changes and refinements to the original designs and procedures were made.

Purification of the oxygen supply

The success of the analyser is critically dependent on establishing a consistent, low blank. The blank is made up of any entities which ultimately contribute to the species of interest *i.e.* chloride and sulphate ions. In the early development stages, it was apparent that the chloride blank was extremely variable and significant in analyses at levels of *ca.* 5 mg/l. A very small sulphate blank was also observed at these levels but was found to be consistent. The extent of the chloride blank was a source of concern because it had the potential to limit both the LOD and repeatability of the method. The principal source of the chloride blank was found to be the oxygen supply, probably due to contamination from traces of chlorinated solvent associated with degreasing agents used to clean the hard-plumbed gas lines from the cylinder bays outside the building. For this reason, a clean-up procedure for the oxygen supply was implemented. Thus, the original single furnace was replaced by a twin furnace to allow the oxygen to be purified as described earlier. Solid scrubbers containing soda lime and charcoal (situated between the combustion tube and NaOH scrubbers) were also tried, but these were discarded since, when saturated, they were found to contribute to the blank. The ultrapure helium was found to be free of organo-chlorine and organo-sulphur so this was used without further purification.

Bubbler design

Another key area of development for the analyser was the design of the glass bubbler. Original feasibility studies were carried out using a bubbler fitted with a tap (Fig. 4a). This allowed the absorber solution to be drained from the bubbler and manually injected onto the concentrator column. Once suitable combustion conditions were established, a bubbler design was required that had the capacity to be disconnected from the combustion tube after each analysis (to keep the blanks down to a minimum), and an end fitting that would accommodate loading of the concentrator column directly. Early prototypes had straight internal surfaces, no capillary feed and were open to the atmosphere (Fig. 4b). The side arm was fitted with a heating tape (controlled at 60°C) to avoid any problems with

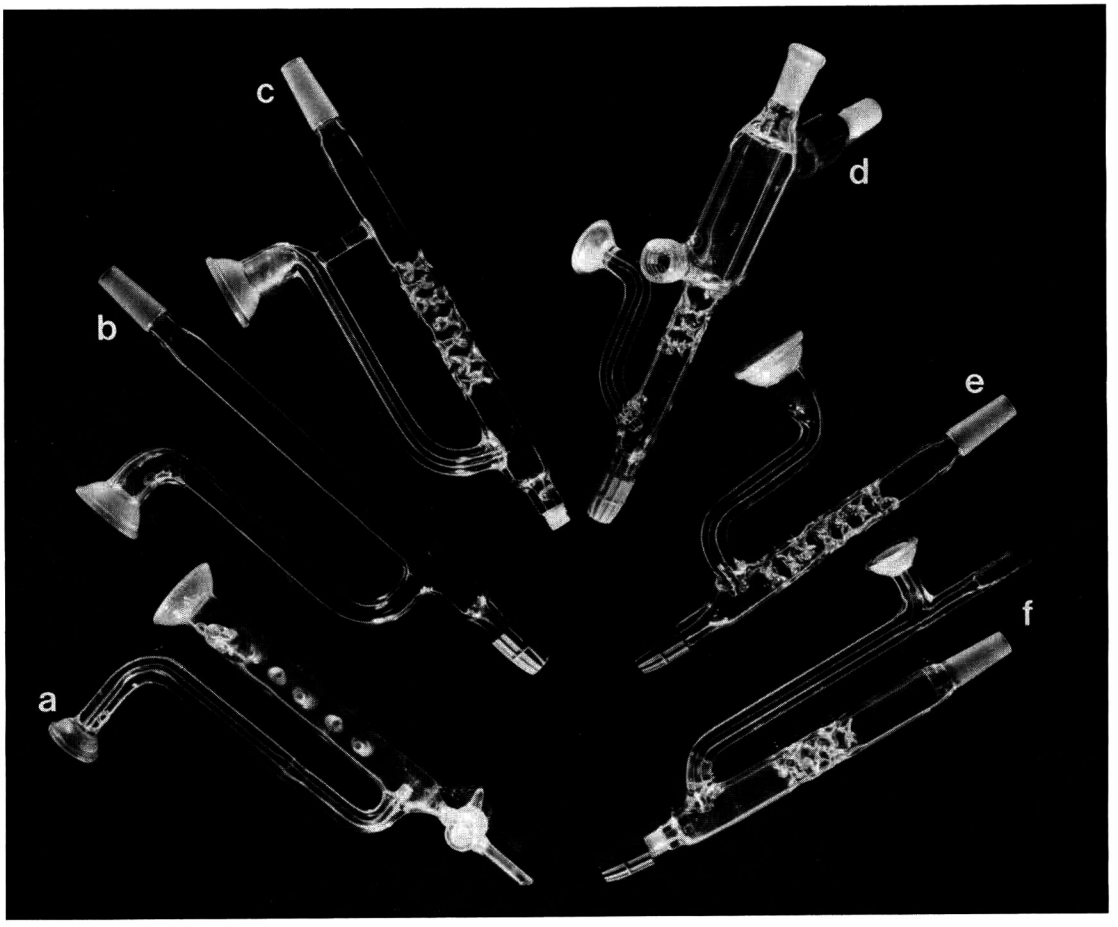

Fig. 4. Development of the bubbler. (a) Original bubbler with tap fitting; (b) straight bubbler, no capillary; (c) long sidearm, capillary and vigreux-type dimples; (d) short sidearm and condenser; (e) short sidearm, extra vigreux dimples, no condenser; (f) bubbler with metal attachment on the sidearm to accommodate an ozone stream for simultaneous Cl, S and N analysis.

condensation of combustion products. Although these prototypes worked fairly well, recoveries were variable due to loss of absorber through the top of the bubbler. This was overcome by introducing a capillary into the sidearm, and adding "Vigreux-type dimples" to the internal walls to break up the bubbles (Fig. 4c). At one stage a condenser was also fitted onto the bubbler (Fig. 4d) but this was found to have no advantage. Finally the size of the bubbler was reduced, extra Vigreux dimples introduced and the length of the sidearm reduced in proportion to the bubbler (Fig. 4e).

On-line absorber supply

During the original studies the H_2O_2 solution was added manually via pipette. The new designs allowed the bubbler to be filled via a valve and peristaltic pump. This reduced the possibility of contaminating the absorber solution.

Procedural changes

Apart from the oxygen supply, other possible sources of sulphur and chlorine contaminants are the solvents used in the preparation of standards (ASTM-grade isooctane was found to contain < 0.03 μg/ml chlorine), the absorber solution and the operator. The use of a regimented procedure in making up standards and operating the instrument, including taking care to dispense the same volume of absorber (and wash) for each analysis, discon-

necting the bubbler from the column as soon as each combustion was complete, and wearing gloves to prevent post-combustion contamination with inorganic salts (Cl^- in skin), resulted in consistent, low blanks.

It was also noticed that at the start of the day, the initial blanks from washing the bubbler were very high and contained up to six peaks. This was thought to be due to contamination from the laboratory atmosphere. This contamination was greatly reduced by adding a cap (with vent) (Fig. 3) to the bubbler, and leaving the bubbler full of deionised water when not in use.

RESULTS AND DISCUSSION

Operating conditions

The combustion conditions were optimised by setting the helium flow-rate as recommended in [10] and adjusting the oxygen flow-rate so that no loss from the bubbler was evident and complete combustion of standards in isooctane was observed when the sample injection rate was set at 20 μl/min. This optimum flow-rate, based on observation rather than experimental data, was found to be 160 ml/min. At lower oxygen flow-rates, incomplete combustion could be observed by the deposition of carbon in the bubbler. At higher flow-rates, loss of the absorber solution from the top of the bubbler was observed. Volatilising the sample in a carrier stream of helium rather than injecting directly into a stream of oxygen allows a faster injection rate, which is a critical factor in determining both the analysis time and, more importantly, the blank level.

Since standard IC conditions recommended by the manufacturer were used, further optimisation experiments were deemed unnecessary.

Blank values

High, inconsistent blanks render the analyser inoperable at trace levels. However, using the purification stages and procedures described earlier, consistent, low blanks were attained (Table II), enabling trace analysis at levels down to 0.03 mg/l.

Concentrator column capacity

The capacity of the concentrator column is important when traces of one element are to be determined in the presence of much higher concentrations of another element.

Using inorganic standards made up in absorber solution, the capacity of the TAC-1 concentrator column was found to be in excess of 100 μg for sulphate (33 μg sulphur) and 50 μg for chloride. These capacities were found to decrease by just over 50% over a period of 6 months.

For a mixture containing sulphate and chloride ions, the column capacity for chloride is limited by the sulphate concentration, since sulphate has a greater affinity for the resin and displaces chloride if no free sites are available. At the loading rate used in the C–IC analyser, loss of chloride at the 0.05 μg level was observed when the sulphate exceeded 75 μg. Studies of capacity with organic standards in isooctane (injection volume 50 μl) were in good agreement with the inorganic studies. It was shown that no loss of organic chlorine at the 1 mg/l level (0.05 μg Cl) was observed until the concentration of sulphur exceeded 520 mg/l (26 μg S, equivalent to 78 μg sulphate). These studies showed that chloride was displaced by sulphate prior to complete saturation, indicating that another factor is involved. It was thought that a lower loading rate may increase the level of sulphate at which chloride is lost, but this was not tried since this would increase the time of analysis and was not particularly relevant since the analyser was being developed for trace level applications.

TABLE II

TYPICAL BLANK DATA

Peak heights obtained after the combustion of 50 μl isooctane combusted under the normal CIC conditions listed in the Experimental section. Sensitivity set at a full scale detection (FSD) of 3 μS.

	Chlorine	Sulphur
$\bar{x}$	35.3	7.6
σ_{n-1}	3.30	1.6
$2\sigma_{n-1}$	6.60	3.30
Detection limit (mg/l)[a]	0.022	0.030

[a] Detection limits calculated from $2\sigma_{n-1}$ and the heights obtained for standard calibrations of 1-chloro-2,4-dinitrobenzene and dibutyl sulphide in isooctane, using 50-μl injection volumes.

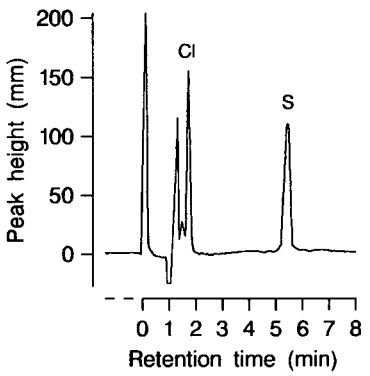

Fig. 5. IC separation of elemental chlorine and sulphur after combustion and conversion to chloride and sulphate. Standard concentrations, 0.4 mg/l Cl (chlorobenzene) and 1.0 mg/l S (dibutyl sulphide) in isooctane. Injection volume, 50 μl at 20 μl/min. Other conditions as described under analytical conditions in the Experimental section.

These studies showed that the absolute capacity of the concentrator column depends on its age and condition, whilst the efficiency of the retention process for a particular species is dependent on both the interference effects of other ions and the loading rate.

Recoveries

The recovery of chlorine and sulphur is effectively a measure of the efficiency of the sample combustion, the trapping of the combustion products in the absorber solution and the retention of the subsequent anions on the concentrator column. As all the sulphur and chlorine species formed in combustion are converted in the peroxide absorber solution to sulphate and chloride respectively, it was possible to directly compare peak heights (blank corrected) from combustion of organic standards with those associated with direct injection of inorganic standards onto the concentrator column. A typical chromatogram obtained for a mixed organic standard after combustion is shown in Fig. 5. This chromatogram differs from that obtained by direct injection of inorganic standards, in that formate and acetate peaks, directly between the water dip and chloride peaks, are often observed. These peaks are due to incomplete combustion of the organic matrix. However, this does not appear to affect adversely the recovery of chlorine and sulphur.

From the data shown in Table III it can be seen that at the 2 mg/l level the recoveries for Cl and S were greater than 94% for injection volumes ranging from 10–50 μl (0.02–0.1 μg). The matrix and sample type appeared to have little or no effect on recovery. Table IV shows that at the 2 mg/l level, recoveries for various standards of chlorobenzene, 1-chloro-2,4-dinitrobenzene, benzyl-thiuronium chloride and dibutyl sulphide in a range of solvents, were always greater than 93%.

TABLE III

RECOVERY OF S AND Cl AT THE 2 mg/l LEVEL FOR VARIOUS SAMPLE INJECTION VOLUMES

Various volumes of organic standards of chlorobenzene (Cl = 2 mg/l) and dibutyl sulphide (S = 2 mg/l) in isooctane were analysed by C–IC (using the analytical conditions described in the Experimental section) and the peak heights (blank corrected) directly compared to those obtained for inorganic standards prepared from NaCl (Cl = 2 mg/l) and Na_2SO_4 (SO_4^{2-} = 6 mg/l) and analysed directly by IC by injecting onto the concentrator column. All peak heights are means of three analyses and quoted in mm. FSD for Cl heights = 10 μS, FSD for S heights = 3 μS.

Injection volume (ml)	Chlorine			Sulphur		
	Inorganic	Organic	Recovery (%)	Inorganic	Organic	Recovery (%)
10	33	31	94	40	38	95
20	67	64	96	86	84	98
30	103	100	97	130	127	98
40	139	136	98	176	172	98
50	175	177	101	223	226	101

TABLE IV

RECOVERY OF ORGANIC Cl AND S IN VARIOUS SOLVENT MATRICES

Organic standards with Cl and S concentrations of 2 mg/l were prepared by dissolving chlorobenzene and butyl sulphide in toluene, xylene, decalin and hexadecane; 1-chloro-2,4-dinitrobenzene and butyl sulphide in isooctane, and S-benzyl-thiuronium chloride in propan-2-ol (Cl = 2 mg/l, S = 1.8 mg/l). Recoveries calculated by direct comparison of the peak heights (blank corrected) obtained from C–IC analysis (using analytical conditions described in Experimental section) with those obtained from direct IC analysis of inorganic standards (Cl^- = 2 mg/l, SO_4^{2-} = 6 mg/l).

Solvent	Recovery (%)	
	Chlorine	Sulphur
Toluene	98.4	–
Isooctane	101.0	101.0
Xylene	100.8	96.3
Decalin	95.1	99.1
Hexadecane	93.1	98.0
Propan-2-ol	99.2	98.7

Linearity and repeatability

Calibrations with mixed standards of 1-chloro-2,4-dinitrobenzene and dibutyl sulphide in isooctane showed that over the trace level range (0–3 mg/l) the detector response expressed as peak height was rectilinear for both chlorine (r = 0.9997, n = 8) and sulphur (r = 0.9994, n = 9) (Fig. 6). Similar linearity (Cl, r = 0.9996, n = 5; S, r = 0.9995, n = 6) was observed using individual standards of chlorobenzene (Cl conc. range, 0–0.6 mg/l) and dibutyl sulphide (S conc. range 0–1.0 mg/l) in xylene (Fig. 7).

It was noticed that for the C–IC analyses the day-to-day variation in peak heights and the peak height ratios Cl^-:SO_4^{2-} varied much more than in aqueous IC using a sample loop injection. This may have been caused by small changes in eluent composition and the condition of the concentrator, guard and separator columns. However, this variation did not affect recoveries or repeatability. The practice of preparing the eluent by dilution of eluent concentrates reduced this variation but a daily calibration was still required.

Repeatability studies were carried out for both Cl and S using standards of chlorobenzene and dibutyl sulphide in isooctane. From Table V it can be seen that for Cl at the 0.4 mg/l and 0.05 mg/l levels the standard deviation (n = 10) was found to be 2.9 and 9.9%, respectively. For S, the % standard deviation was found to be 3.5 and 6.9%, at the 0.5 mg/l and 0.1 mg/l levels, respectively.

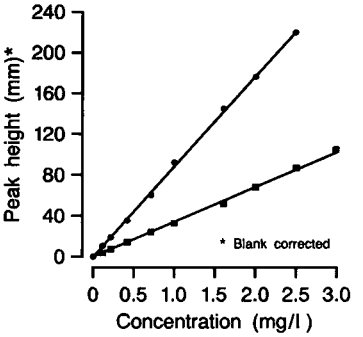

Fig. 6. Calibration curves for Cl (●) and S (■) in the range 0–3 mg/l after combusting mixed standards of 1-chloro-2,4-dinitrobenzene and dibutyl sulphide in isooctane. Sensitivity set at an FSD of 10 μS.

Comparison with microcoulometry

Good agreement between the C–IC method and the established technique of microcoulometry [34] was obtained for Cl and S standards in isooctane (conc. range 0.5–50 mg/l) (Table VI), and samples of crude oil distillates and reformer feedstocks (Table VII). However, the repeatability of the C–IC method was found to be superior to that of microcoulometry, especially at levels of less than 0.4 mg/l.

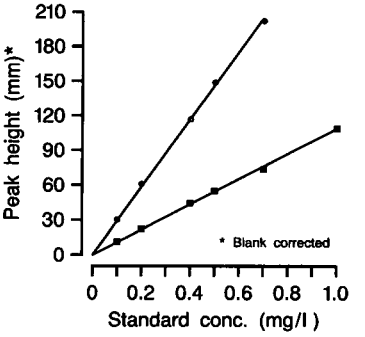

Fig. 7. Calibration curves for Cl (0–0.6 mg/l) (●) and S (0–1.0 mg/l) (■) obtained from the combustion of individual standards of chlorobenzene and dibutyl sulphide in xylene. Sensitivity set at an FSD of 3 μS.

TABLE V

REPEATABILITY DATA (n = 10) FOR THE DETERMINATION OF SULPHUR AND CHLORINE BY C–IC

Standards of chlorobenzene and dibutyl sulphide in isooctane, injection volume 50 μl. Analytical conditions as described in Experimental section.

	Chlorine		Sulphur	
	0.40 mg/l	0.05 mg/l	0.50 mg/l	0.10 mg/l
Sensitivity setting (μS)	3	1	3	1
Peak heights (mm)	120	49	54	33
(blank corrected)	126	53	51	37
	118	48	57	35
	124	41	56	41
	123	41	55	39
	128	44	59	34
	124	43	55	36
	124	40	60	35
	126	41	57	34
	117	48	55	35
$\bar{x}$ (mean height, mm)	123	44.8	56.6	35.9
σ_{n-1}	3.6	4.42	1.96	2.47
$2\sigma_{n-1}$	7.2	8.84	3.92	4.94
$\bar{x}$ (mg/l)[a]	0.41	0.050	0.51	0.109
$2\sigma_{n-1}$ (mg/l)	±0.024	±0.010	±0.036	±0.015

[a] Calculated from calibration curve obtained for inorganic standards.

A comparison of S results by C–IC with those obtained by inductively coupled plasma–optical emission (ICP) for a series of catalyst samples in different solvents is shown in Table VIII. As most of these samples contained much higher levels of S, dilution with the appropriate solvent prior to analysis was carried out. With one exception all the results agreed to within 6.4%.

TABLE VI

COMPARATIVE DATA: C–IC *VERSUS* MICROCOULOMETRY —STANDARDS

A series of standards of chlorobenzene in xylene and dibutyl sulphide in isooctane were analysed by C–IC (using the analytical conditions in the Experimental section) and microcoulometry (using the analytical conditions and procedures laid down in refs. 9 and 10).

Standard concentration	Chlorine (mg/l)		Sulphur (mg/l)	
	C–IC	Microcoulometry	C–IC	Microcoulometry
0.5	0.48	0.6	0.51	0.6
1.0	1.05	1.1	0.98	1.0
2.0	2.05	2.1	1.99	2.1
5.0	5.1	5.1	5.0	5.1
10.0	9.8	9.6	9.8	10.2
50.0	51	48	48	48

TABLE VII

COMPARATIVE DATA: C–IC *VERSUS* MICROCOULOMETRY —SAMPLES

Crude oil distillates and reformer feedstocks were analysed by C–IC (using the analytical conditions described in the Experimental section) and microcoulometry (using the analytical conditions and procedure laid down in refs. 9 and 10). Quantification was carried out by reference to an external calibration with chlorobenzene and dibutyl sulphide in isooctane. Errors: At levels below 0.4 mg/l the error bar for microcoulometric results is ±0.05 compared to ±0.02 for C–IC results.

Sample	Chlorine (mg/l)		Sulphur (mg/l)	
	C–IC	Microcoulometry	C–IC	Microcoulometry
Crude oil distillates (15–149°C)				
Tapis blend	0.68	0.6		
Labuan	1.03	1.1		
Iranian heavy	0.42	0.5		
Iranian light	0.59	0.6		
Reformer feeds				
A	0.12	0.13		
B	0.29	0.25		
C	0.37	0.35		
D	0.41	0.40		
E			0.48	0.54
F			0.25	0.19
G			0.10	0.09

Applications and scope

Between 1988–1992, the C–IC analyser has been used to analyse over 900 samples. Originally the analyser was developed to analyse for Cl and S at sub-mg/l levels in reformer feeds and naphthas. However, due to demand and the lack of other suitable instrumentation the analyser was used to analyse other sample types. Crude oil distillates, C_4–C_{10} aromatics, gasolines, dimates and ethyl benzene have all been analysed for chlorine, whilst sulphur in toluene, C_5/C_6 hydrocarbons, reformate aromatics, North Sea condensates, decane, methanol, hexane, jet fuel, 2-ethylhexanol and propan-2-ol has been determined. Such analyses have not been achieved without problems. Firstly, the more refractory samples can block the syringe. Secondly, whilst the analysis of samples with high levels (< 50 mg/l) of S and/or Cl is operationally very simple, since blank contributions at this level are negligible, subsequent trace level determinations can sometimes prove difficult, due to carry over from the combustion tube. Analysis at ultra-trace levels is best performed with a dedicated combustion tube and bubbler.

RECENT DEVELOPMENTS AND FUTURE WORK

The Mk I Analyser has also been successfully used to determine nitrogen and bromine in organic

TABLE VIII

COMPARATIVE DATA. C–IC *VERSUS* ICP FOR S IN CATALYST SOLUTIONS

A series of catalyst solutions in various solvents were analysed for S by C–IC, using the analytical conditions described in the Experimental section, and diluting with the appropriate solvent where necessary (to give S concentrations in the range 20–30 mg/l). ICP analyses were carried out using a Spectroflame Model P optical emission spectrometer (Spectro Analytical Instruments) set at 182.04 nm, calibrated with matrix-matched standards. C–IC quantification was by reference to an external calibration of dibutyl sulphide in isooctane.

Solvent	C–IC (mg/l)	ICP (mg/l)
Water	25.3 ± 0.3	25
Water	128 ± 5	120
Water	185 ± 5	185
2-Ethylhexanol	317 ± 10	374
2-Ethylhexanol	530 ± 25	566
Hexane	147 ± 5	155

and aqueous media. For simultaneous nitrogen, sulphur and chlorine determinations a modified bubbler (Fig. 4f) was required to facilitate the introduction of ozone into the sidearm. As the combustion product of nitrogen under these conditions is nitrogen monoxide (NO) which is insoluble in water, an oxidation stage with ozone to form soluble nitrogen dioxide (NO_2) was required. Recoveries for nitrogen were found to be 35% at best. If sulphur and chlorine are not required, nitrogen recovery could theoretically be improved to 100% by bubbling the combustion products through an acidic $KMnO_4$ solution and absorbing in dilute peroxide. However, this was not tried since trace nitrogen is more conveniently determined by a combustion–chemiluminescence method using commercially available equipment.

The determination of bromide has also been investigated briefly. Bromide recoveries, determined by combusting standards of cetyl pyridinium bromide in xylene under the same analytical conditions as for Cl and S and comparing the peak heights with those obtained for aqueous KBr standards analysed directly, were found to be greater than 98% at the 1 mg/l level. Excellent agreement with X-ray fluorescence (XRF) was obtained for a series of Br^--containing catalyst solutions in various solvents (Table IX). Obviously these analyses could now be carried out directly on the newly developed solvent compatible IC columns, but the same method could be applied to the determination of bromine.

Since the development of the Mk I Analyser, IC technology has improved and these advances have been incorporated into the C–IC analyser. Thus, the fibre suppressor has been replaced with an AMMS-II membrane suppressor, with the regenerant being supplied by a pressurised vessel, the columns have been updated and the chromatograms recorded by an AI-450 data collection station. Furthermore, a UV–Vis detector has been introduced in-line to accommodate analysis of UV-absorbing species and to help in the identification of unknown peaks.

The most recent work has been the development of a new "flow cell" interface which allows a constant flow of fresh absorber solution into the bubbler and continual loading of combustion products onto the concentrator. This flow cell is still being evaluated. Future studies will include the application of post column reactions to improve sensitivity and include other elements (*e.g.* thorium and xylenol orange to determine fluorine), extending the scope of the analyser to facilitate the analysis of solid samples, and the automation of the analyser.

TABLE IX

COMPARATIVE DATA: C–IC *VERSUS* XRF FOR Br^- IN CATALYST SOLUTIONS

A series of catalyst solutions in various solvents were analysed for Br^- by C–IC, using the analytical conditions described in the Experimental section, and diluting with the appropriate solvent where necessary (to give Br^- concentrations in the range 1–10 mg/l). XRF analyses were carried out using a Philips PW1404 wavelength dispersive X-ray spectrophotometer, using standard analytical conditions. C–IC quantification was by reference to an external calibration of cetyl pyridinium bromide in xylene.

Solvent	C–IC (mg/l)	XRF (mg/l)
m-Xylene	< 0.6	< 2
Hexane	90 ± 5	80 ± 1
Propan-2-ol	1260 ± 15	1375 ± 5
Water	2.5 ± 0.2	4 ± 0.5
	66 ± 2	64 ± 1
	246 ± 5	238 ± 1
	246 ± 5	246 ± 1
	253 ± 5	250 ± 1
	245 ± 5	244 ± 1

CONCLUSIONS

The C–IC analyser described here can be used to determine sulphur and chlorine in liquid hydrocarbons at levels down to 0.03 mg/l, with the potential for measurements at single ng/ml levels. Results obtained are in good agreement with those obtained by conventional microcoulometric techniques. The simultaneous nature, speed and sensitivity of the analysis, gives the C–IC method several advantages over microcoulometry. The analyser has the potential for multi-elemental analysis and has the scope for adaptation to accommodate solid sample analysis.

ACKNOWLEDGEMENTS

The authors wish to thank Dr. H. W. Handley for permission to discuss the new flow cell, Mr. M.

S. Jones for carrying out the ICP analysis, and Mr. T. Jervis and Mr. M. Townsend for making the bubblers and other specialised glassware.

REFERENCES

1 J. M. deMan, E. Pogorzelska and L. Deman, *J. Am. Oil Chem. Soc.*, 60 (1983) 558.
2 J. B. Butt and E. E. Petersen, in *Activation, Deactivation and Poisoning of Catalysts*, Academic Press, London, 1984, Ch. 4.
3 L. L. Hegedus and R. W. McCabe, in *Catalyst Poisoning (Chemical Industries*, Vol. 17), Marcel Dekker, New York, 1984.
4 J. G. Speight, in H. Heinemann (Consulting Editor), *The Chemistry and Technology of Petroleum*, Marcel Dekker, New York, 1980.
5 F. C. A. Killer and K. E. Underhill, *Analyst*, 95 (1970) 505.
6 A. Cedergren, *Talanta*, 20 (1973) 621.
7 D. C. White, *Anal. Chem.*, 49 (1977) 1615.
8 M. C. van Grondelle, P. J. Zeen and F. van de Craats, *Anal. Chim. Acta*, 100 (1978) 439.
9 *IP373/86, Sulphur in Liquid Petroleum Products by Microcoulometry (Oxidative Method)*, Institute of Petroleum, London, Wiley, Chichester, 1986.
10 *Chlorine in Liquid Petroleum Products by Microcoulometry (Oxidative Method)*, IP Proposed Method, Designation AK, Institute of Petroleum, London.
11 D. Mealor, in G. B. Crump (Editor), *Petroanalysis'87: Developments in Analytical Chemistry in the Petroleum Industry*, Wiley, Chichester, 1988, p. 221.
12 P. R. Haddad and P. E. Jackson, *Ion Chromatography, Principles and Applications (Journal of Chromatography Library*, Vol. 46), Elsevier, Amsterdam, 1990, Ch. 14.
13 R. A. Nadkarni and D. M. Pond, *Anal. Chim. Acta*, 146 (1983) 261.
14 M. J. McCormick, *Anal. Chim. Acta*, 121 (1983) 233.
15 J. R. Kreling, F. Block, G. T. Louthan and J. DeZwaan, *Microchem. J.*, 34 (1986) 158.
16 J. F. Colaruotolo and R. S. Eddy, *Anal. Chem.*, 49 (1977) 884.
17 K. L. Evans and C. B. Moore, *Anal. Chem.*, 52 (1980) 1908.
18 R. A. Wetzel, C. L. Anderson, H. Schleicher and G. D. Crook, *Anal. Chem.*, 51 (1979) 1532.
19 J. P. Senior, *Anal. Proc.*, 27 (1990) 116.
20 M. Douek and J. Ing, *J. Pulp Pap. Sci.*, 15 (1989) J72.
21 R. C. Wijesundera, R. G. Ackman, V. Abraham and J. M. deMan, *J. Am. Oil Chem. Soc.*, 65 (1988) 1526.
22 R. C. Wijesundera and R. G. Ackman, *J. Am. Oil Chem. Soc.*, 65 (1988) 1531.
23 R. P. Singh, K. Alam, D. S. Redwan and N. M. Abbas, *Anal. Chem.*, 61 (1989) 1924.
24 H. Assenmacher and J. Frigge, *Fresenius' Z. Anal. Chem.*, 332 (1988) 41.
25 M. Feige, J. Schafer and D. Frahne, *GIT. Fachz. Lab.*, 35 (1991) 443.
26 H. Nagashima, S. Orita and K. Kuboyama, *Bunseki Kagaku*, 38 (1989) 378.
27 T. Kitagawa, S. Koda and Y. Morimoto, *Iyakuhin Kenkyu*, 20 (1989) 975.
28 G. E. M. Hall and J. A. Vaive, *Geostand. Newsl.*, 13 (1989) 1.
29 J. S. Fritz, D. T. Gjerde and C. Pohlandt, in W. Bertsch, W. G. Jennings and R. E. Kaiser (Editors), *Ion Chromatography*, Hüthig, Heidelberg, 1982, p. 52.
30 *IP242/83, Sulphur in Petroleum Products: Flask Combustion Method*, Institute of Petroleum, London, Wiley, Chichester, 1983.
31 *IP244/71, Chlorine in Petroleum Products: Flask Combustion Method*, Institute of Petroleum, London, Wiley, Chichester, 1971.
32 *IP61/84 (ASTM D129-83), Standard Test Method For Sulphur in Petroleum Products by Bomb Method*, Institute of Petroleum, London, Wiley, Chichester, 1984.
33 *IP243/83. Sulphur in Petroleum Products: Wickbold Oxy–Hydrogen Method*, Institute of Petroleum, London, Wiley, Chichester, 1983.
34 *Dohrmann MCTS-130/120-Automated Sulfur and Chlorine Analysers Operations Manual*, Rosemount Analytical, Santa Clara, CA, 2nd ed., 1988.

Journal of Chromatography, 640 (1993) 127–134
Elsevier Science Publishers B.V., Amsterdam

CHROMSYMP. 2751

Ion-pair reversed-phase high-performance liquid chromatography for trace metal preconcentration followed by ion-interaction chromatography

Corrado Sarzanini*, Giovanni Sacchero, Maurizio Aceto, Ornella Abollino and Edoardo Mentasti

Department of Analytical Chemistry, Via P. Giuria 5, 10125 Turin (Italy)

ABSTRACT

Ion-interaction chromatography of Plasmocorinth B (a disulphonated azo dye) complexes of Co(III), Cu(II), Fe(III), Ga(III), In(III), Ni(II), V(V) and Zr(IV) was studied. The behaviour of two different reversed-phase C_{18} columns (5 and 10 μm) was compared and an on-line enrichment procedure was developed following the optimization of eluent (pH, ligand concentration, ionic strength and organic modifier). The described technique, applied to the analysis of metal ions at μg/l levels in natural waters, gave satisfactory precision and accuracy in comparison with inductively coupled plasma atomic emission spectroscopic results.

INTRODUCTION

Direct and reversed-phase high-performance liquid chromatography (HPLC) procedures have been developed for the determination of metal ions [1–3]. Complex formation followed by extraction [4,5] or by sorption on coated or uncoated columns and pre-column or on-column on-line formation of chelates [6–10] are the commonest methods of achieving preconcentration and separation of metals.

The objective of this study was to investigate the feasibility of using metal complexes, obtained by reaction with a sulphonato azo dye (Plasmocorinth B) in ion-pairing reactions for metal preconcentration and separation by HPLC. The effect of different parameters, namely pH, ligand and ion-pairing concentration, ionic strength and stationary phase size, was assessed.

The optimization of the method enabled analyte metals to be separated from alkaline and alkaline earth elements and the interfering matrix ions that are not complexed and which pass through the column unretained. The preconcentration procedure furnished enrichment factors of up to 900, and the technique has been applied successfully to samples of river water. Detection limits are in the range 15–90 ng/l.

EXPERIMENTAL

Apparatus and materials

The liquid chromatograph used for this work was a Varian Model LC 5000 equipped with a Rheodyne injection valve (100-μl sample loop inserted), a Vista 401 Data Station, gradient programmer and a Varian UV-100 detector (Varian, Walnut Creek, CA, USA). The analytical columns were reversed-phase LiChrospher 100 RP-18 5 μm and 10 μm (250 × 4 mm I.D.) columns. The operating conditions (at 25°C) were: mobile phase flow-rate 1.0 ml/min, complex detection at $\lambda = 270$ nm. For trace enrichment, a chemically inert Model DQP-1 pump (Dionex, Sunnyvale, CA, USA) was used.

High-purity acids were obtained with a sub-boil-

* Corresponding author.

0021-9673/93/$06.00

ing quartz still (K. Kurner, Rosenheim, Germany).

An Orion EA 920 pH-meter equipped with a glass-calomel electrode was used for pH measurements.

Plasmocorinth B was obtained from Aldrich, and tetrabutylammonium hydroxide was a Fluka product (Buchs, Switzerland); all other chemicals were of analytical–reagent grade (Merck, Darmstadt, Germany).

Standard metal solutions, 1000 mg/l (Merck), were diluted daily to obtain reference and working solutions. The chelates were obtained by mixing the aqueous analyte solution with the reagent at the appropriate concentrations (see below). All solutions were prepared with high-purity water (HPW; Milli-Q water system, Millipore). Analytical reagent-grade methanol and HPW were filtered through a 0.45-μm filter and used as mobile phase solvents.

All glass and polyethylene or polypropylene labware were cleaned with nitric acid in a microwave oven (2450 MHz) for 4 min, power 540 W, and then repeatly rinsed with HPW.

Chelates preparation

The method is based on the formation of metal complexes by reaction with the ligand Plasmocorinth B. The chelating agent 3-(5-chloro-2-hydroxyphenylazo)-4,5-dihydroxynaphthalene-2,7-disulphonic acid, acts like tridentate planar ligand [11] and is characterized by the presence of two hydroxy substituents in the *ortho* position relative to the azo group and two sulphonato groups not involved in the complexation. Plasmocorinth B was selected because of its ability to form thermodynamically stable metal ion complexes [12] and to form ion pair with proper ion-interaction reagents, *i.e.*, the tetrabutylammonium (TBA) cation. Fig. 1 shows schematically the rections between Plasmocorinth B and metal ions and ion-pairing reactions involved in the considered system. In order to achieve metal complex formation, samples containing 1–10 mg/l of metals or mixtures of metals containing 0.80 m*M* Plasmocorinth B were prepared, buffering (acetic acid, sodium hydroxide) the solution to eluent pH. In preliminary experiments the samples (100 μl) were introduced into the chromatographic system as such.

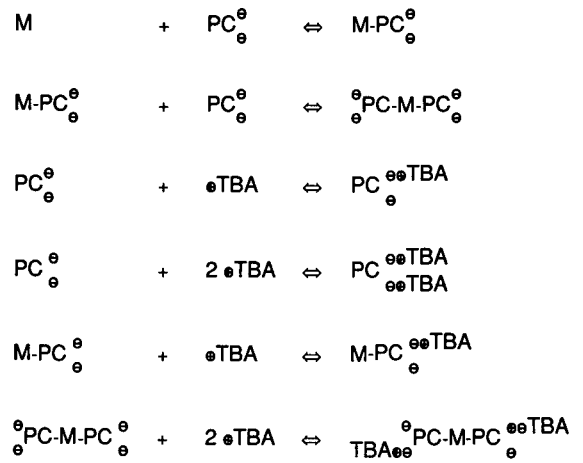

Fig. 1. Complexation and ion-pairing reactions involved in the system (M = metal ion, PC = Plasmocorinth B, TBA = tetrabutylammonium ion; metal charges and functional groups omitted).

Chromatographic study

A chromatographic study was developed to optimize the solvent system, enabling the separation of all metal–Plasmocorinth B complexes. For these studies analyte samples were prepared as mentioned above. Metal mixtures, Al(III), Co(III), Cu(II), Fe(III), Ga(III), In(III), Ni(II), V(V) and Zr(IV), and individual metal samples were prepared to verify specific peaks in each chromatogram.

The eluents investigated were methanol–water solutions. Methanol–water was used as the ionic strength (sodium nitrate), ion-pairing (TBA hydroxide) and pH (acetic acid, sodium hydroxide) adjusting solvent. Different concentrations of Plasmocorinth B in the eluent were also investigated.

The behaviour of two kinds of column, 5-μm and 10-μm LiChrospher 100 RP-18 (250 × 4 mm I.D.) columns, was evaluated.

RESULTS AND DISCUSSION

The reactions involved in the proposed method, shown schematically in Fig. 1, involve bi- and trivalent metal ions, their complexes with Plasmocorinth B and related ion pairs with TBA. Considering the nature of these compounds, the chromatographic mechanisms operating could be modified by varying the methanol (organic modifier) and TBA concentration as well as the ionic strength and pH.

The first experiments evaluated the effect of the methanol concentration in the eluent. Dramatic fluctuations in the capacity factor for metal–Plasmocorinth B complexes were found when the methanol concentration was reduced below 48% (v/v). In addition, methanol concentrations greater than 50% decreased the retention times of trivalent metal ions too much. A concentration of 50% (v/v) resulted the optimum compromise between good resolution and capacity factors.

The effect of Plasmocorinth B concentration in the eluent was investigated. Concentrations of 0–40 μM did not affect the capacity factors of metal chelates (see Fig. 2), but the presence of Plasmocorinth B, even at low concentrations, optimized the system performance. In fact, the baseline was also stabilized for injection of samples at high Plasmocorinth B concentrations and peak reproducibility improved as a result. Taking into account these considerations and to avoid an unfavourable increase in eluent absorbance owing to high Plasmocorinth B concentration, 2.0 μM PC was selected for eluent composition.

In ion-interaction chromatography an important role is usually played by the ion-pairing agent. Fig. 3

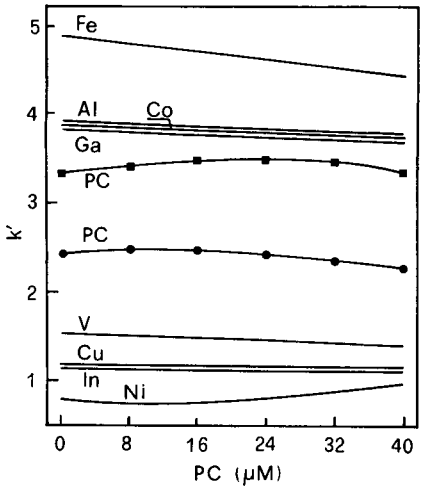

Fig. 2. Effect of Plasmocorinth B (PC) concentration on capacity factor (k') of metal chelates. Chromatographic conditions: mobile phase, methanol–water (50:50, v/v) containing 10 mM acetic acid, 15 mM sodium nitrate, 1.6 mM TBA hydroxide, PC as shown and sodium hydroxide up to pH 6.3; flow-rate, 1.0 ml/min. Sample volume, 100 μl; 0.80 mM Plasmocorinth B, 2–6 mg/l metals.

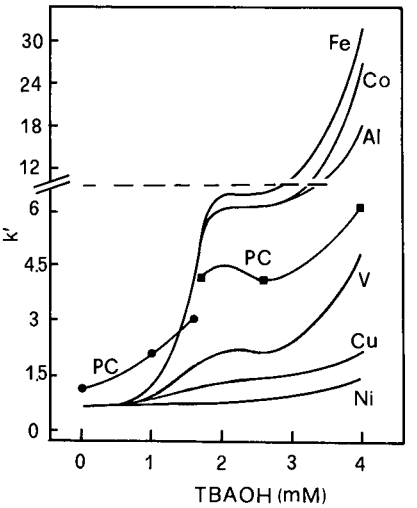

Fig. 3. Effect of TBA concentration on capacity factor (k') of metal chelates. Chromatographic conditions: mobile phase, methanol–water (50:50, v/v) containing 10 mM acetic acid, 15 mM sodium nitrate, 2.0 μM Plasmocorinth B (PC), TBA hydroxide (TBAOH) as shown and sodium hydroxide up to pH 6.3; flow-rate, 1.0 ml/min. Sample volume, 100 μl; 0.80 mM Plasmocorinth B, 2–6 mg/l metals.

shows the effect of different concentrations of TBA on the capacity factor of considered complexes. Concentrations below 1.6 mM result in peak overlapping, while higher concentrations give too large capacity factors. Thus 1.6 mM was selected as the working concentration. In the eluent optimization, to evaluate the ionic strength effectiveness, 0–250 mM sodium nitrate was investigated. The results in Fig. 4 show that low concentrations gave too high retention times, but poor resolution was obtained at concentrations higher than 25 mM. It seems remarkable that the complexes most affected by ionic strength modification were complexes of trivalent metal ions. This may be explained by considering that Plasmocorinth B complexes of these metals exhibit a 2:1 (ligand to metal) molar ratio, which could result in ion pairs containing one (metal-Plasmocorinth B–TBA) or more, usually two (metal-Plasmocorinth B–TBA_2), molecules of TBA. The ionic strength enhancement improves the competition of NO_3^- for TBA, and probably only metal-Plasmocorinth B–TBA is formed, which shows reduced retention times. In the subsequent experiments 10.0 mM sodium nitrate, which gave good separations, was used unless stated otherwise.

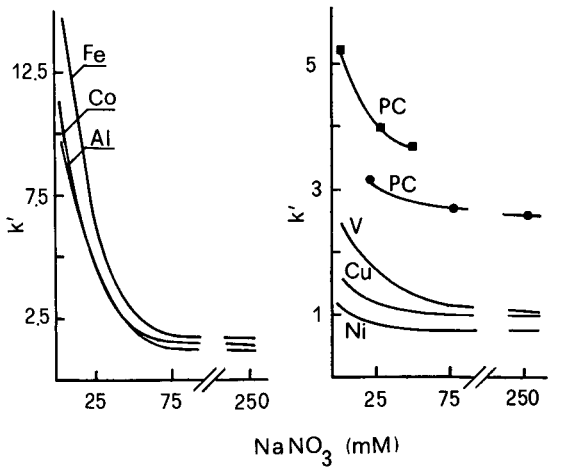

Fig. 4. Dependence of the capacity factor (k') of metal chelates on ionic strength (sodium nitrate). Chromatographic conditions: mobile phase, methanol–water (50:50, v/v) containing 10 mM acetic acid, 2.0 μM Plasmocorinth B (PC), 1.6 mM TBA hydroxide, sodium nitrate as shown and sodium hydroxide up to pH 6.3; flow-rate, 1.0 ml/min. Sample volume, 100 μl; 0.80 mM Plasmocorinth B, 2–6 mg/l metals.

It should be pointed out that Figs. 2, 3 and 4 show two different lines for Plasmocorinth B ion pairs. This is because, as a function of eluent composition, two peaks can be ascribed to the ligand. The structure of Plasmocorinth B suggests that the two sulphonato groups present on the ligand can form 1:1 or 1:2 (ligand to ion-pairing ratio) ion pairs. In particular (Fig. 4), when high concentrations of Na^+ and NO_3^- are present the competition for SO_3^- and TBA^+ ions reduces the capacity of ion-pairing available to form Plasmocorinth B–TBA_2 (1:2 stoichiometry) ion pairs and only the peak of Plasmocorinth B–TBA (1:1 stoichiometry) appears at lower retention time.

The behaviour of capacity factors for some of the considered metal–Plasmocorinth B complexes (Fig. 5) showed that low pH values affect the separation performance, with great fluctuations in retention times resulting from small variations in pH. In the next experiments a pH value of 6.3 was adopted to ensure good separation of peaks, a reduced chromatographic time and better reproducibility of data.

The concentration of ligand in the sample solutions was also investigated. Fig. 6 shows the behaviour of peak area as a function of Plasmocorinth B concentration, from which a good reproducibility could be expected for Plasmocorinth B concentrations of 0.4 mM or more. Also of interest (Fig. 7) is the behaviour of the asymmetry factor (AF10) as a function of the ratio of ligand to stoichiometric ligand concentration (L/L_s), where the stoichiometric term is related to metal concentration.

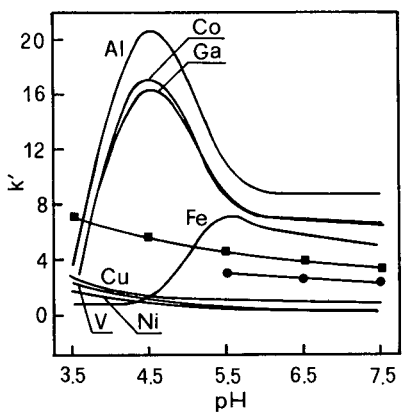

Fig. 5. Effect of pH on capacity factor (k') of metal chelates. Chromatographic conditions: mobile phase, methanol–water (50:50, v/v) containing 2.0 μM Plasmocorinth B (PC), 1.6 mM TBA hydroxide, pH as shown; flow-rate, 1.0 ml/min. Sample volume. 100 μl; 0.80 mM Plasmocorinth B, 2–6 mg/l metals.

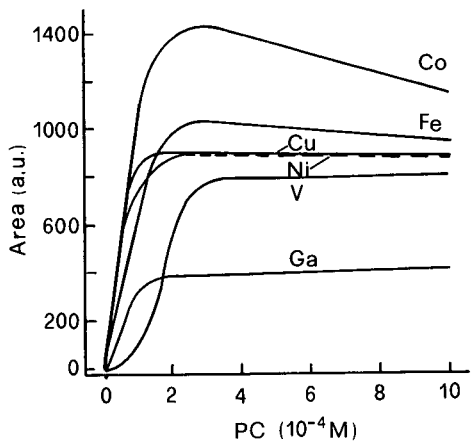

Fig. 6. Dependence of peaks area on Plasmocorinth B (PC) concentration of the sample. Chromatographic conditions: mobile phase, methanol–water (50:50, v/v) containing 10 mM acetic acid, 2.0 μM Plasmocorinth B, 1.6 mM TBA hydroxide, 10 mM sodium nitrate and sodium hydroxide up to pH 6.3; flow-rate, 1.0 ml/min. Sample volume, 100 μl; 2–6 mg/l metals, Plasmocorinth B as shown.

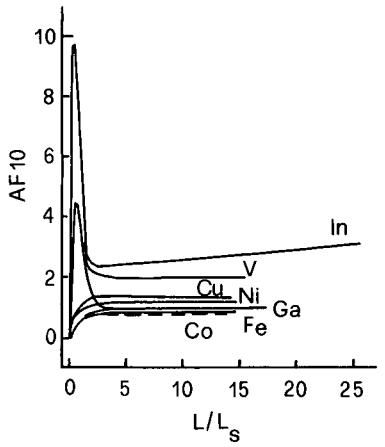

Fig. 7. Effect of the ratio of the ligand to stoichiometric ligand concentration (L/L_s) on asymmetry factor (AF10). Chromatographic conditions as in Fig. 6.

Taking into account these data and the fact that the method will used exclusively for the preconcentration of metal ions at trace levels, a 0.8 m*M* Plasmocorinth B concentration was chosen, which corresponds to values of the L/L_s ratio of 10–22.5, enabling the determination of total metal ions from ng/l up to mg/l concentration levels.

Standard metal ion solutions containing Ca^{2+}, Mg^{2+}, Na^+ and K^+ (30, 2, 2 and 2 mg/l, respectively), usually present in mineral waters, or 0.5 *M* sodium chloride (which simulates seawater), were analysed with the developed method. The agreement between chromatograms, and the results (peak area) confirm that the method is reproducible in the same standard deviation range (see below).

Columns and gradient elutions

The isocratic procedure optimized on a 10-μm LiChrospher RP-18 column was also tested on a 5-μm column of the same type. The chromatograms of a mixture of metals, *i.e.*, Ni(II), Cu(II), V(V), Co(III) and Fe(III) at 0.40, 0.50, 0.80, 0.70 and 0.80 mg/l, respectively, were compared (see Fig. 8). The 10-μm column shows a better performance in terms of resolution of peaks at shorter retention times; however, separation with the 5-μm column is

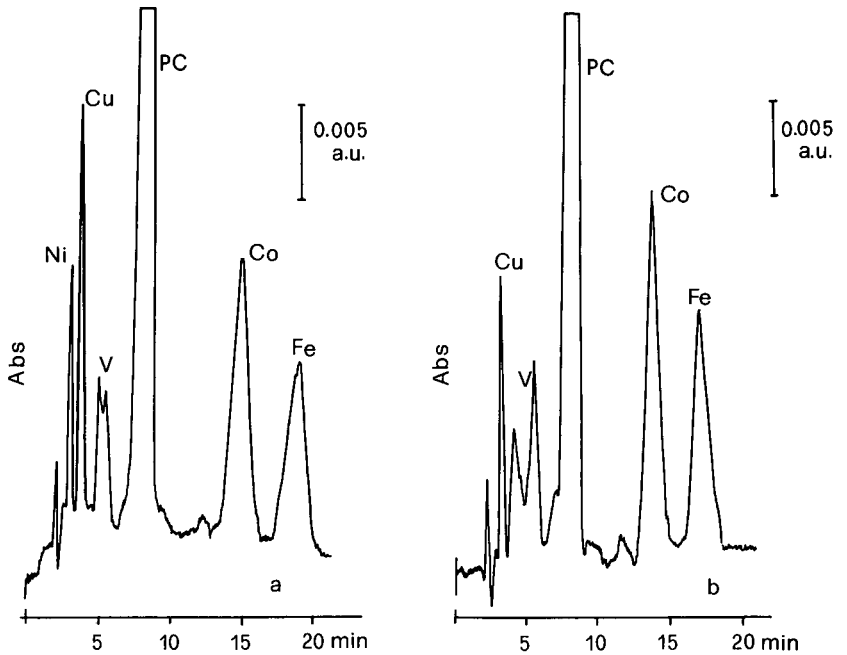

Fig. 8. Comparison of columns performance: (a) 10 μm and (b) 5 μm. Chromatographic conditions: mobile phase, methanol–water (50:50, v/v) containing 10 m*M* acetic acid, 2.0 μ*M* Plasmocorinth B (PC), 1.6 m*M* TBA hydroxide, 12.5 m*M* sodium nitrate and sodium hydroxide up to pH 6.3; flow-rate, 1.0 ml/min. Sample volume, 100 μl; 0.80 m*M* Plasmocorinth B, metals 0.40 mg/l Ni, 0.50 mg/l Cu, 0.80 mg/l V and Fe, 0.70 mg/l Co. Detection 270 nm.

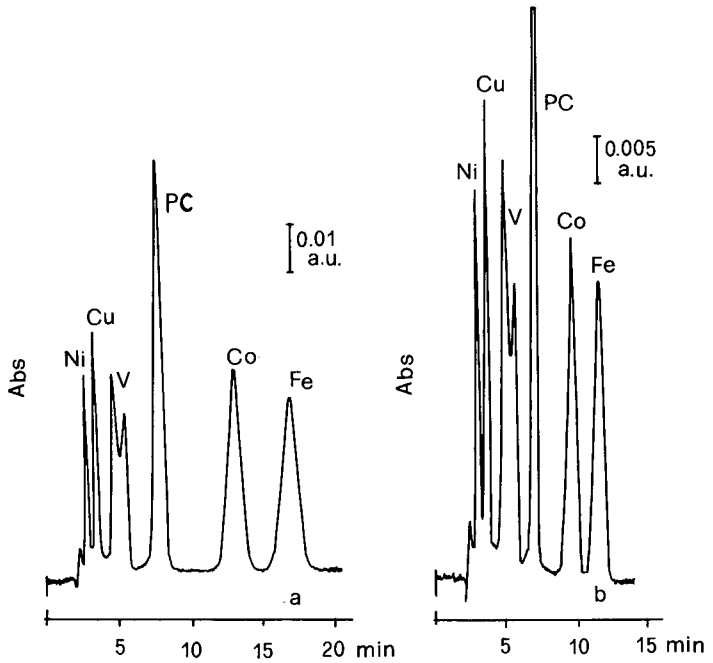

Fig. 9. Comparison of isocratic and flow-rate gradient elution. Chromatographic conditions: mobile phase, methanol–water (50:50, v/v) containing 10 m*M* acetic acid, 2.0 μM Plasmocorinth B (PC), 1.6 m*M* TBA hydroxide, 8.75 m*M* sodium nitrate and sodium hydroxide up to pH 6.3. (a) Isocratic flow-rate, 1.0 ml/min. (b) Gradient flow-rate (time: 0–5, 5–6, 6–12, 12–13 min; flow: 1, 1–2 linear; 2, 2–1 linear ml/min). Sample volume, 100 μl; 0.80 m*M* Plasmocorinth B, metals 1.0 mg/l Ni, 1.5 mg/l Cu, 3.5 mg/l V, 2.0 mg/l Co, 3.0 mg/l Fe. Detection 270 nm.

more sensitive for trivalent metals with longer retention times.

Taking into account the mechanism involved in the separation, the effectiveness of gradient elutions, namely flow-rate, ionic strength and organic modifier, were also evaluated. Flow-rate gradient elutions resulted in unchanging baseline, good resolution and shorter retention time. Chromatograms for the same sample obtained by isocratic and flow-rate gradient elution are shown in Fig. 9.

An equilibration period is not required to restore the starting conditions between consecutive injections. Similar results, good separation and reduced retention times were obtained with organic modifier and ionic strength gradient elutions. But, in these cases, 30 min are required to restore the starting conditions and the whole procedure was more time-consuming than isocratic elution.

Preconcentration procedure

The microcolumns used for preconcentration based on the developed precomplexation and ion-pairing method were evaluated. The 100-μl loop on the Rheodyne valve was replaced by a 5-μm or 10-μm LiChrospher 100 RP-18 (4 × 4 mm I.D.) microcolumn. Samples of 100 ml were fluxed through the microcolumn with the aid of a Dionex pump (Model DQP-1). A flow-rate of 4.0 ml/min was selected for the loading procedure because recovery yields were unchanged up to this value and higher rates resulted in counterpressure phenomena.

Preconcentration recoveries were evaluated by comparing the peak areas obtained by direct injection (100-μl loop) of samples (Co, Cu, Fe, Ga, Ni concentration: 3 mg/l each) with those obtained by loading the cartridge with 100.0-ml aliquots of mixtures (3 μg/l of each metal ion).

Because preliminary investigations showed that metal–Plasmocorinth B complexes are not retained by the microcolumn, an alternative procedure was adopted. Taking into account the hydrophobic nature of cartridges and the lower charge of ion pairs

compared with metal chelates, the ion-pairing reaction was carried out directly on the samples. An investigation was also made on the efficiency of Plasmocorinth B and TBA sample concentrations. L/L_s values (see above) of 10 or more and 0.32 m*M* TBA produced the best concentrations. This TBA concentration, which seems very high in comparison with eluent composition taking into account the preconcentration step, is required to enable the formation of ion pairs of all metal complexes in the microcolumn. The preconcentration procedure involved a washing step after the sample loading. A 10.0-ml volume of water removed the matrix and excess TBA. The washing volume must be well defined and taken into account when evaluating blanks.

Table I compares the recovery yields obtained for 5-μm and 10-μm microcolumns, before the optimization of Plasmocorinth B concentration, with the enrichment on a 10-μm column after optimization at lower metal ion concentration. Fig. 10 shows a representative chromatogram obtained using preconcentration and flow-rate gradient elution procedures.

Linear range and detection limits

The optimized procedure was used to determine the linear range: samples of increasing concentration were prepared until the chromatographic peak areas exhibited non-linearity. Calibration ranges within

TABLE I

PRECONCENTRATION RECOVERY YIELD (%) WITH DIFFERENT COLUMNS AND AFTER OPTIMIZATION

Chromatographic conditions: mobile phase, methanol–water (50:50, v/v) containing 10.0 m*M* acetic acid, 2.0 μ*M* Plasmocorinth B, 1.6 m*M* TBA hydroxide, 12.5 m*M* sodium nitrate and sodium hydroxide up to pH 6.3; flow-rate, 1.0 ml/min; sample, 100 ml; pH 6.3; 0.8 μ*M* Plasmocorinth B; 0.32 m*M* TBA; loading flow-rate 4.0 ml/min; detection 270 nm. Preconcentrators: LiChroCART 100 RP-18 (4 × 4 mm I.D.).

Element	Recovery yield (%)		
	5 μm[a]	10 μm[a]	10 μm[b]
Co	26.2	47.9	95.7
Cu	28.5	83.0	95.8
Fe	26.8	40.7	94.9
Ga	10.0	15.0	94.8
Ni	–	38.2	72.0

[a] $L/L_s = 2.5$; metals 3.0 μg/l.
[b] $L/L_s = 10.0$; metals 0.8 μg/l Cu, Ga and Ni, 0.5 μg/l Co and Fe.

TABLE II

CALIBRATION RANGE AND DETECTION LIMITS FOR METAL DETERMINATION

Element	Linearity range (mg/l)	R^a	Detection limit (μg/l)[b]
Al	0.1 –2.0	0.991	50
Co	0.1 –10	0.999	30
Cu	0.2 –10	0.990	60
Fe	0.05–10	0.999	15
Ga	0.2 –10	0.998	60
Ni	0.2 –10	0.999	65
V	0.5 –10	0.994	30
Zr	0.2 –4	0.998	150

[a] R = Linear regression coefficient.
[b] Detection limits of procedure defined as three times absolute blank.

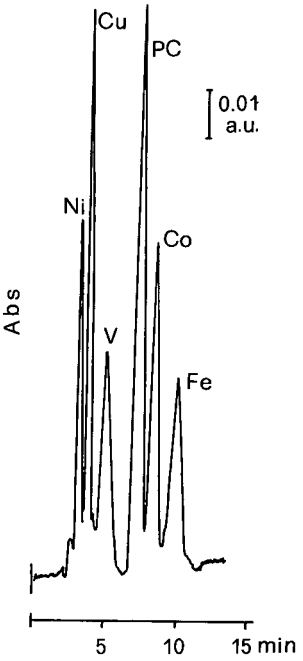

Fig. 10. Preconcentration followed by gradient (flow-rate) elution. Chromatographic conditions as in Fig. 9. Sample volume 100 ml; pH 6.3; 0.32 m*M* TBA; 0.80 μ*M* Plasmocorinth B (PC); Ni, Cu, V, Co and Fe 3 μg/l; preconcentration flow-rate, 4.0 ml/min; 10-μm column.

TABLE III

RETENTION TIME AND PEAK AREA REPRODUCIBILITY FOR METAL IONS BY OPTIMIZED PROCEDURE

Metals 3 μg/l.

Element	Retention time (min)[a]	Area (μV s)[a]
Co	8.5 ± 1.7	1252 ± 1
Cu	3.8 ± 0.7	939 ± 7
Fe	10.2 ± 2.1	868 ± 6
Ni	3.2 ± 1.1	363 ± 11
V	5.2 ± 3.1	784 ± 9

[a] Mean ± standard deviation (%).

the coefficient of linear regression and detection limits (DL) are listed in Table II. Obviously, the developed preconcentration procedure resulted in a greater reduction of DL, and the resulting values ranged between 15 and 90 ng/l. Reproducibilities achieved for retention times and peak areas are summarized in Table III.

Real sample

The results of the analysis of Po river water samples are given in Table IV. The river water data can be compared with the results of direct analysis by graphite furnace atomic absorption spectrometry with Zeeman-effect background correction, and with those obtained with a different on-line preconcentration method using an XAD-2 microcolumn functionalized with 1-(2-thiazolylazo)-2-naphthol and inductively coupled plasma [13]. The good agreement between the results confirms that the method is suitable for the analysis of natural samples.

ACKNOWLEDGEMENTS

Financial support from Ministero dell'Università e della Ricerca Scientifica e Tecnologica (MURST, Rome) and from the Italian National Research Council (CNR, Rome) is gratefully acknowledged.

TABLE IV

ANALYTICAL DATA FOR THE ANALYSIS OF A RIVER WATER SAMPLE

HPLC–ion-interaction chromatography: developed method; ion-exchange chromatography–inductively coupled plasma atomic emission spectroscopy; see ref. 13; GF Zeeman AAS: graphite furnace atomic absorption spectrometer Zeeman-effect background correction. Standard deviations within 10%.

Element	Concentration (μg/l)		
	HPLC–ion-interaction chromatography	Ion-exchange chromatography–inductively coupled plasma atomic emission spectroscopy	GF Zeeman AAS
Co	<DL	–	<DL
Cu	1.5	1.3	1.5
Fe	5.7	5.9	5.4
Ni	5.6	5.5	5.4

REFERENCES

1 S. Dilli, P. R. Haddad and A. K. Htoon, *J. Chromatogr.*, 500 (1990) 313.
2 A. R. Timerbaev, O. M. Petrukhin, I. P. Alimarin and T. A. Bol'shova, *Talanta*, 38 (1991) 467.
3 K. Robards, P. Starr and E. Patsalides, *Analyst*, 116 (1991) 1247.
4 H. Osashi, N. Vehara and Y. Shijo, *J. Chromatogr.*, 539 (1991) 225.
5 H. Shofstahl and J. K. Hardy, *J. Chromatogr. Sci.*, 28 (1990) 225.
6 Y. Shito, K. Tanaka and N. Nehara, *Anal. Sci.*, 7 (1991) 507.
7 C. Lin, X. Zhang and X. Liu, *Analyst*, 116 (1991) 277.
8 E. A. Jones, H. S. Bezuidenhout and J. F. Van Staden, *J. Chromatogr.*, 537 (1991) 277.
9 G. Sacchero, O. Abollino, V. Porta, C. Sarzanini and E. Mentasti, *Chromatographia*, 31 (1991) 539.
10 M. V. Main and J. S. Fritz, *Talanta*, 38 (1991) 253.
11 H. Hoshino, K. Nakano and T. Yotsuyanagi, *Analyst*, 115 (1990) 33.
12 C. Sarzanini, O. Abollino, M. De Luca and E. Mentasti, *Anal. Sci.*, 8 (1992) 201.
13 V. Porta, C. Sarzanini, O. Abollino, E. Mentasti and E. Carlini, *J. Anal. Atom. Spectrom.*, 7 (1992) 19.

Journal of Chromatography, 640 (1993) 135–143
Elsevier Science Publishers B.V., Amsterdam

CHROMSYMP. 2754

Electrodialysis for clean-up of strongly alkaline samples in ion chromatography

Paul R. Haddad* and Soehendra Laksana

Department of Chemistry, University of Tasmania, GPO Box 252C, Hobart, Tasmania 7001 (Australia)

Ray G. Simons

School of Physics, University of New South Wales, P.O. Box 1, Kensington, N.S.W. 2033 (Australia)

ABSTRACT

An electrodialysis method is described for the off-line neutralization of strongly alkaline samples containing trace levels of common inorganic anions. This method uses an electrodialysis cell comprising three compartments separated from each other by cation-exchange membranes. These compartments comprise an anode compartment housing, a platinum wire anode and 10 ml of a suitable hydrogen ion donating medium, a sample compartment which contains 1 ml of the alkaline sample, and a cathode compartment housing a platinum wire cathode and a dilute solution of sodium hydroxide. During electrodialysis at either constant applied current or constant applied power, hydrogen ions from the anode compartment displace sodium ions from the sample, thereby effecting neutralization.

Experimental parameters, such as the magnitude of the applied current or power, the type of cation-exchange membrane used and the design of the cell have been studied and optimum results were obtained using a Neosepta CM-2 membrane, of area 616 mm^2 supported between two perspex discs, with an applied current of 150 mA or applied power of 3 W. Under these conditions, a 1 ml sample of 1 *M* sodium hydroxide could be neutralized in 11 min. The most effective hydrogen ion donating medium consisted of a 2:1 (w/v) slurry of BioRad AG 50W-X8 (200–400 mesh, H^+ form) cation-exchange resin in 1 m*M* octanesulfonic acid. Recoveries of solute anions (3–10 μg/ml) from the dialysed solution were close to quantitative, except for fluoride and nitrite, which gave recoveries of less than 60%. It is suggested that low recoveries for these ions are due to formation of neutral, protonated species within the membrane with subsequent loss by diffusion.

INTRODUCTION

Dialysis is a technique based on a diffusion process in which selected sample components are transferred across a membrane. The technique can be divided into passive dialysis and active (or Donnan) dialysis. Passive dialysis involves the diffusion of particles of a specified molecular mass range through a neutral membrane and is a slow process that often requires a large volume of sample and normally results in severe sample dilution. On the other hand active or Donnan dialysis involves the transfer of ions of a specified charge through an ion-exchange membrane. It is a much faster and more reliable process than passive dialysis. Active dialysis has been used to achieve both matrix normalization and sample preconcentration when used for sample clean-up in ion chromatography (IC) [1,2]. In previous work, we have successfully employed active dialysis with a membrane fibre device for the treatment of strongly alkaline samples prior to IC analysis [3].

Further refinement to active dialysis methods can be achieved by coupling electric fields with membranes; this process is known as electrodialysis. The electrodialytic process has been used for many years in industry for water purification, wastewater treat-

* Corresponding author.

0021-9673/93/$06.00

ment and desalination procedures [4–7]. On the analytical scale, the method has been used as an extraction method in drug analysis [8,9] and has been reported for the treatment of strongly acidic samples prior to the determination by IC of magnesium(II) and calcium(II), using a dual anion-exchange membrane tube device [10]. In this work, concentric anion-exchange membrane tubes were used to form the sample and electrolyte compartments and migration of anions was induced under conditions of constant current. Cations were prevented from movement between compartments as a result of the permselectivity of the membranes. These authors have also suggested the potential applicability of electrodialysis using the same experimental arrangement for the pre-treatment of alkaline samples prior to analysis using IC. Electrodialysis coupled on-line with HPLC has also been described for the determination of basic and acidic compounds in environmental samples [11,12], but no study has been reported on the use of this technique for inorganic anions determination by IC.

In the present work electrodialysis is used for the off-line pre-treatment of alkaline solutions prior to their analysis by anion-exchange IC. Such samples are traditionally difficult to analyze by IC because of the severe baseline disturbances generally caused when the sample is injected onto the column. Simple neutralization with acid is not practicable because of the resultant high concentration of the acid anion introduced into the sample. Electrodialysis can be achieved by arranging two sheets of cation-exchange membrane in a stack to form a three-compartment cell comprising compartments for anode, cathode and sample. The anode compartment contains a hydrogen ion donating medium, the cathode compartment contains a dilute alkaline solution (which acts as a receiver) and the sample compartment is filled with a mixture of inorganic anions in a sodium hydroxide solution. Application of a dc electrical field causes cations (especially sodium ions) to move from the sample compartment towards the cathode, and to be replaced by hydrogen ions from the anode compartment. Anions do not move between compartments. The net effect of this process is the neutralization of the alkaline sample solution. During the electrodialysis, water will be oxidized at the anode to produce O_2 and H_3O^+ and will be reduced at the cathode to form H_2 and OH^-. The concentration of OH^- in the cathode compartment therefore increases, whilst the amount of water in the anode compartment decreases at the end of the process.

The stability of the membrane to changes in pH and temperature during electrodialysis is an important factor for the ultimate success of the process, as are the changes in shape of the membrane which will directly affect the electrodialysis time. Chemical stability and high permselectivity of the membrane also play a significant role in the recovery of inorganic ions present in the sample. In this work, the electrodialysis technique is applied to the neutralization of alkaline samples, with particular attention to the design of a cell suitable to minimize the electrodialysis time and to optimize the electrodialysis conditions.

EXPERIMENTAL

Instrumentation

The ion chromatograph consisted of a Millipore-Waters (Milford, MA, USA) Model 510 pump, Model U6K injector and Model 430 conductivity detector, operated in both the suppressed and non-suppressed modes. The column used for non-suppressed IC was a Millipore-Waters IC Pak A anion column, 50 × 4.6 mm I.D., packed with polymethacrylate anion-exchange resin. The column used for suppressed IC was a Dionex HPIC AS-4A anion separator with AG-4A guard column, connected with an AMMS membrane suppressor. A Waters reagent delivery module was used to pass the regenerant of 12.5 m*M* H_2SO_4 through the suppressor. Sodium ion was determined using a Millipore-Waters IC Pak C cation column, 50 × 4.6 mm I.D., packed with styrene–divinylbenzene resin. Chromatography was carried out at room temperature with an eluent flow-rate of 1.2 ml/min.

The electrodialysis cell used is shown schematically in Fig. 1. The cell was constructed as a series of cylindrical perspex components held together by two plates compressed with longitudinal threaded rods (Fig. 2). Electrodes were constructed from platinum wires (60 × 0.25 mm O.D.), clipped to the cell and connected to the power supply. The cation-exchange membranes (see Table II for thickness) were supported on each side with perspex discs (not shown in Fig. 2), 0.9 mm in thickness, through

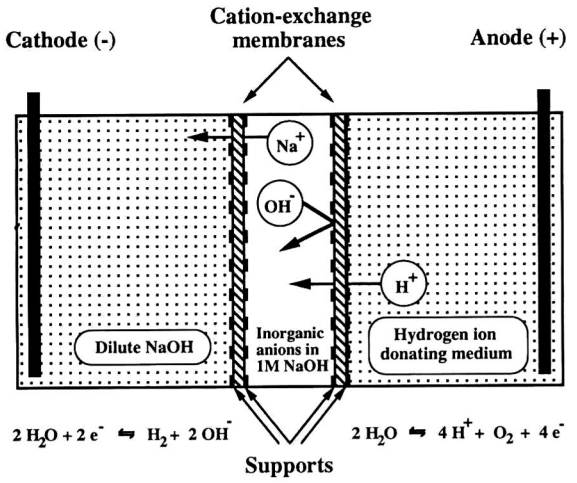

Fig. 1. Schematic diagram of the electrodialysis process.

which had been drilled closely spaced 3.2 mm diameter holes covering a circular area 28 mm in diameter. Under these conditions, the surface area of the membrane in contact with the sample and electrode solutions was 616 mm^2. The perspex disc supports added no significant increase to the electrodialysis time and their use virtually eliminated buckling of the membrane due to heat production. The volume of both the anode and cathode compartments was 10 ml, whilst the sample compartment contained 1 ml. Samples were introduced into the sample compartment by means of a 500-μl glass microsyringe.

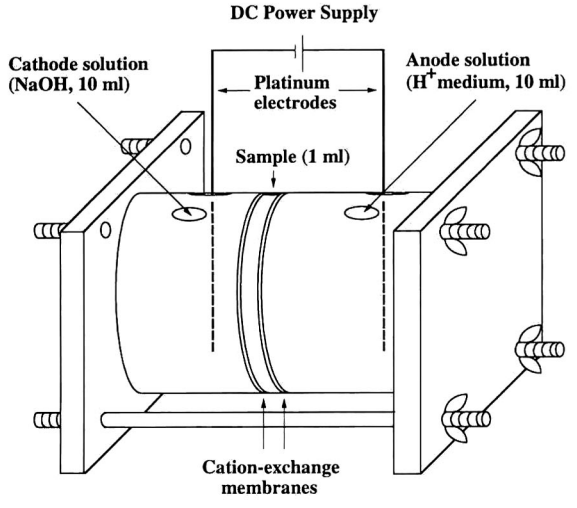

Fig. 2. Electrodialysis cell.

A Bio-Rad (Richmond, CA, USA) microprocessor-controlled electrophoresis power supply (Model 3000 Xi) was used in the fixed potential, fixed current and fixed power modes. When an applied current in excess of 300 mA was required, a GoodWill (Taiwan) laboratory dc power supply (Model GPR-7530D) was used.

Reagents

All chemicals used were of analytical reagent grade and the water employed for the preparation of standard solutions and eluents was purified on a Millipore (Bedford, MA, USA) Milli-Q water treatment system. Samples and eluents were filtered through a Millipore 0.45 μm membrane filter and degassed in an ultrasonic bath prior to use. The eluent used for non-suppressed IC analysis of the treated samples contained 1.3 m*M* sodium tetraborate, 5.8 m*M* boric acid and 1.4 m*M* potassium gluconate adjusted to pH 8.5 and made up in water–acetonitrile (88:12, v/v). The eluent for the suppressed system contained 2 m*M* sodium bicarbonate and 2 m*M* sodium carbonate. The eluent for sodium determination contained 0.5 m*M* EDTA and 2 m*M* nitric acid.

Standard stock solutions of inorganic anions were prepared by dissolving appropriate amounts of the sodium salts in water. Working solutions of these ions were obtained by diluting the stock solutions with sodium hydroxide to give final concentration of 1 *M* NaOH. The concentration of inorganic anions in these solutions was in the range 30–100 μg/ml for the non-suppressed system and in the range of 3–10 μg/ml for the suppressed system.

Hydrogen ion donating solutions for use in the anode compartment of the electrodialysis cell were prepared using 0.0005–0.05 *M* sulfuric acid, methanesulfonic acid (MSA), octanesulfonic acid (OSA), camphorsulfonic acid (CSA) and *p*-toluenesulfonic acid (TSA). All were obtained from Sigma (St. Louis, USA) with the exception of octanesulfonic acid which was prepared by passing a solution of sodium octanesulfonate through a glass column packed with 100 g Bio-Rad AG 50W-X8 hydrogen form cation-exchange resin, 200–400 mesh. This same cation-exchange resin was also used as hydrogen-ion donating medium and prior to its use for this purpose, was washed thoroughly with Milli-Q water.

The cation-exchange membranes used in this work were obtained from Asahi Glass, Japan (CMV), Du Pont (Wilmington, DE, USA) (Nafion 324, Nafion 901), Ionics Incorp., USA (CZL-386, AZL-389), Tokuyama Soda, Japan (Neosepta CM-2, CMS, C66-10F, CLE-E), Pall RAI, USA (Raipore R-5010-M) and Asahi Chemical Company, Japan (K-101).

Procedures

The determination of co-ion concentrations present in a particular membrane was carried out by first soaking the membrane in Milli-Q water for 24 h to remove any residual ions, after which it was equilibrated in 100 ml of 0.1 *M* sodium salt solutions (*e.g.*, NaF, NaCl, NaBr, $NaNO_3$, Na_3PO_4, Na_2SO_4) for a further 24 h period and then blotted to dryness. The co-ions present in the membrane were displaced by soaking the membrane for 24 h in 20 ml of 0.3 *M* potassium chloride for sulfate ion or in 20 ml of 0.2 *M* potassium sulfate for other anions. The displaced anions were determined by suppressed IC and the displaced sodium ion (which is a measure of the cation-exchange capacity of the membrane) was measured by non-suppressed IC.

RESULTS AND DISCUSSION

Selection of electrodialysis conditions

Preliminary tests showed that the mechanical stability of the membranes was a major consideration in that distortion of the membrane as a result of the heat generated in the cell was the most common source of failure. Since the electrodialysis can be performed by applying the electrical field in three ways, namely constant potential, constant current or constant power, these methods were evaluated with respect to heat evolution in the cell.

The constant potential mode was found to give rapid temperature rises, even at the start of the electrodialysis. For example a constant potential of 30 V applied to a sample of 20 ml of 1 *M* NaOH caused the temperature of the sample solution to reach 80°C within the first few min of electrodialysis. Lowering the applied potential reduced heat production but neutralization of the sample could not be achieved. For these reasons, dialysis at constant potential was not performed further.

Dialysis at constant current proved to be suitable in that both the current and voltage (and hence the temperature) could be held fairly constant over most of the dialysis, with significant changes occurring only as neutralization was approached and the conductance of the sample decreased. The time required for a particular dialysis was found to be inversely proportional to the current density, which in turn was dependent on the surface area of the membrane and the magnitude of the applied current. Currents in the range 100–200 mA were found to give effective dialysis without excessive heat production under the experimental conditions used. Similarly, dialysis at constant power was also suitable, provided that the applied power did not produce currents outside the working range indicated above. For this reason, the applied power was restricted to about 3 W. More aggressive conditions always caused pronounced buckling of the membrane (even when mechanical supports were used) and loss of sample through volatilization.

Cell design

The cell was designed to optimize the dialysis of a sample solution containing up to 1 *M* sodium hydroxide since most samples occurring in practice should be dilutable to this level. Varying volumes of sample were dialysed under differing applied currents until neutralization was reached. This point was indicated by either a rapid increase of applied potential or by the change in colour from blue to yellow of bromothymol blue indicator (pK_a = 7.0) added to the sample compartment. Tests indicated that there was no penetration of the indicator through the cation-exchange membrane nor did the presence of the indicator interfere in the analysis of the inorganic anions by non-suppressed or suppressed IC. The cathode compartment of the cell was filled with 20 ml of 0.1 *M* sodium hydroxide and the anode compartment was filled with 10 ml of 0.05 *M* sulfuric acid. The membrane used in this experiment was Asahi CMV, a cation-exchange membrane with an ion-exchange capacity of 2.1 mequiv./g.

Table I shows the dialysis time required under different experimental conditions and indicates that this time was directly proportional to the moles of hydroxide in the sample and inversely proportional to the applied current (note that the membrane area was constant for all experiments). Moreover, the

TABLE I

ELECTRODIALYSIS TIMES AT CONSTANT APPLIED CURRENT FOR NEUTRALIZATION OF SAMPLES TO pH 6

Sample volume (ml)	[NaOH] (*M*)	Current (mA)	Voltage (V)	Time (min)
20.0	0.1	15	6–50	220
20.0	0.1	150	10–50	25
10.0	0.1	15	6–50	115
10.0	0.1	150	10–50	12
10.0	1.0	150	10–100	90
10.0	1.0	450	17–100	30
10.0	1.0	750	26–100	15.3
1.0	1.0	150	10–100	11.1
1.0	1.0	450	18–100	3.9
1.0	1.0	750	24–100	2.1

dialysis times obtained were in close agreement with those calculated using the current density and the known number of moles of hydroxide in the sample, showing that the cell was performing efficiently. In practical terms, an electrodialysis time of 11 min could be achieved in the neutralization of 1 ml of 1 *M* NaOH solution by applying a constant current of 150 mA, without the production of excessive heat and resultant distortion of the membrane. Electrodialysis could be performed on two samples simultaneously by coupling two identical cells in parallel to the same power supply. The applied total current was distributed evenly to both cells and each sample reached the neutralization point at the same time. For example, the electrodialysis time for a single sample containing 1 ml of 1 *M* NaOH with a current of 150 mA was 11 min, whilst 22 min was required for two parallel cells, each containing 1 ml of the same sample. Increasing the current to 300 mA for the parallel cells reduced the dialysis time to 11 min.

Selection of the membrane

The cation-exchange membranes used in the construction of the cell must show a high permselectivity towards cations and be able to withstand the heat generated in the cell. A range of membranes was evaluated and the important properties of each are listed in Table II. These membranes were soaked in water for at least 24 h prior to use, except for Nafion 901 which was soaked in 2% NaOH so-

TABLE II

PROPERTIES OF THE COMMERCIAL CATION-EXCHANGE MEMBRANES USED IN THIS STUDY

Supplier	Type	Electrical resistance (Ω cm^2)	Total cation transport number	Burst strength (kg/cm^2)	Exchange capacity (mequiv./g)	Thickness (mm)
Asahi Glass	CMV	2.0–3.5	>0.92	3–5	2.1[a]	0.13
Du Pont	Nafion 901	2.8	n.a.[b]	n.a.	n.a.	0.45
Du Pont	Nafion 324	4.5	n.a.	n.a.	o.6[a]	0.32
Ionics	CZL-386	13	n.a.	8	2.7	0.60
Ionics	ZAL-389	28	n.a.	27	2.6	1.20
Tokuyama Soda	Neosepta CM-2	2.0–3.0	>0.98	3–5	2.2[a]	0.14
Tokuyama	Neosepta	1.5–2.5	>0.98	3–4	2.4[a]	0.16
Tokuyama Soda	Neosepta C66.10F	5.0–8.0	>0.98	6–8	1.7–2.2	0.30
Tokuyama Soda	Neosepta CLE-E	15–25	>0.98	8–10	1.3–1.8	1.10
Pall RAI	R-5010-M	4–8	0.92	n.a.	n.a	0.17
Asahi Chemical	K-101	n.a.	n.a.	n.a.	n.a.	0.20

[a] Value determined experimentally.
[b] n.a. = Data not available.

TABLE III

PERCENTAGE RECOVERY OF ANIONS (3–10 μg/ml) FROM 1 *M* NaOH SOLUTION AFTER ELECTRODIALYSIS AT 3 W USING VARIOUS CATION-EXCHANGE MEMBRANES

The range derived from 5 replicates is shown in parentheses.

Membrane	F^-	Cl^-	Br^-	NO_3^-	HPO_4^{2-}	SO_4^{2-}
Neosepta CM-2	4.4 (2.1)	96.1 (4.2)	94.1 (4.4)	97.3 (3.2)	98.5 (1.4)	89.5 (5.4)
Asahi CMV	30.0 (4.3)	87.2 (6.5)	85.7 (6.9)	87.4 (6.2)	85.6 (3.6)	66.5 (7.8)
Asahi K-101	55.0 (5.0)	79.4 (8.1)	75.6 (3.8)	80.9 (3.4)	80.6 (4.2)	80.7 (6.3)
Neosepta CMS	9.2 (3.6)	86.8 (8.7)	88.9 (7.3)	87.5 (6.3)	83.6 (3.6)	78.7 (2.4)
Raipore R-5010-M	19.4 (6.0)	78.8 (2.5)	83.2 (4.3)	83.8 (4.8)	82.8 (2.6)	80.3 (6.8)
Nafion 324	35.0 (2.0)	73.0 (5.2)	86.8 (4.1)	90.4 (3.5)	85.3 (3.6)	76.8 (3.8)
Nafion 901	33.3 (4.5)	69.2 (7.0)	83.6 (6.5)	91.2 (5.6)	83.2 (4.2)	76.6 (3.4)

lution as suggested by the manufacturer. When the membranes were supported with the porous perspex discs (as described under Experimental), all showed adequate mechanical stability with the exception of the Neosepta CMS membrane. The Neosepta CM-2 membrane was tested by repeated usage for the neutralization of 1 *M* NaOH sample solutions and showed minimal distortion even after 20 h use.

The permselectivities of the membranes were assessed by determining the recoveries for a range of inorganic anions initially added to 1 *M* NaOH before the samples were subjected to electrodialysis at 3 W constant power until neutralized. Some of the thicker membranes (*e.g.*, Ionics AZL-389 and CZL-386, Neosepta CLE-E and Nafion 901) showed insufficient permselectivity, leading to low recoveries. The results for some of the more successful membranes are given in Table III, which shows that with the exception of fluoride, the Neosepta CM-2 membrane gave recoveries which were close to quantitative. Recovery data of the type determined here are governed by the degree to which the anionic solutes (*i.e.*, solutes having the same charge as the membrane, or "co-ions") can diffuse into the negatively charged membrane. This diffusion for any specified co-ion can be measured by equilibrating the membrane with a solution of that anion (generally by soaking for 24 h), drying the membrane by blotting and then displacing any co-ion from the membrane using a relatively concentrated solution of another anion. For example, the diffusion of fluoride into the membrane could be measured by first soaking the membrane in 0.1 *M* sodium fluoride and then displacing with 0.2 *M* potassium sulfate. The displaced fluoride can be measured by IC, as can the concentration of sodium displaced, which is a measure of the ion-exchange capacity of the membrane.

Table IV shows the co-ion concentrations found in some of the membranes shown earlier to have promise for electrodialysis. It can be seen that these

TABLE IV

CO-ION CONCENTRATIONS FOR DIFFERENT CATION-EXCHANGE MEMBRANES

Anion	Co-ion concentration (mequiv./g)			
	Neosepta CM-2	Neosepta CMS	Asahi CMV	Nafion 324
F^-	0.13	0.07	0.05	0.02
Cl^-	0.002	0.003	0.007	0.002
Br^-	0.001	0.001	0.008	0.006
NO_3^-	0.001	0.002	0.009	0.009
SO_4^{2-}	0.001	0.003	0.009	0.004
HPO_4^{2-}	0.022	0.022	0.020	0.025

concentrations vary significantly, illustrating that there are substantial differences in the permselectivities of the membranes. Comparison of Tables III and IV highlights the fact that an elevated co-ion concentration for a particular membrane is reflected by a reduced recovery for that ion after electrodialysis. For example, the Neosepta CM-2 membrane gave the highest concentration of fluoride and the lowest recovery for this ion. Despite this, the CM-2 membrane gave the best overall performance and, with some supplementation by the Asahi CMV membrane, was used in further studies.

The consistently low recoveries obtained for fluoride for all membranes merits comment. The most plausible explanation for the low recoveries is that partial protonation leads to the formation of neutral hydrofluoric acid which can then diffuse through the membrane. The electrodialysis was terminated when the sample solution reached pH 6, so it would not be expected that there would be any significant formation of hydrofluoric acid (pK_a = 3.17). However, it must be remembered that the pH inside the membrane is likely to be much lower than that existing in the bulk external solution because under the Donnan effect, there is an accumulation of cationic species inside the membrane compared to the bulk solution. This accumulation ratio is often very high [13], so that protonation of fluoride is therefore quite probable. In a similar manner, losses of nitrite can be predicted due to the formation of nitrous acid (pK_a = 3.14). Recovery studies obtained from electrodialysis of alkaline nitrite solutions with the Neosepta CM-2 membrane gave an average recovery of 20.9%, in accordance with this prediction. A further complication observed in this particular experiment was the appearance of a small nitrate peak in the final chromatogram (equivalent to 5.4% of the original nitrite), presumably from oxidation of nitrite. Losses of both fluoride and nitrite during electrodialysis could be reduced by terminating the electrodialysis at a higher pH value (*e.g.* pH 10), but in all cases the recoveries for these two ions were less than 60%. These results suggest that under the conditions used in this paper, electrodialysis is unsuitable for samples containing fluoride and nitrite, and perhaps also for other anions of weak acids.

Selection of hydrogen ion donating medium

After design of a suitable cell and selection of the optimal electrodialysis mode and membrane type, the next step was to determine the best composition of the hydrogen ion donating medium used to fill the anode compartment. Important factors to be considered in the choice of the hydrogen ion donating medium are the degree of sample contamination resulting from penetration of the acid anion through the cation-exchange membrane, and the effect on performance parameters such as the time of dialysis and the amount of heat produced. As in our previous studies on treatment of alkaline samples using Donnan dialysis, a range of aliphatic and aromatic sulfonic acids was compared with sulfuric acid and with slurries of cation-exchange resin in acid solution.

All of the hydrogen ion donating media gave similar performance (with the CMV membrane) in terms of dialysis time and heat production, but significant differences were observed in the degree of the incursion of acid anion into the sample. Table V shows the penetration of acid anions from solutions of hydrogen ion donating media into the sample after electrodialysis at different fixed currents. The degree of incursion increased with concentration of the hydrogen ion donating solution and with the applied current. The concentration of the acid anions found in the sample solution after dialysis is expressed as a percentage of the initial concentration of this anion in the solution of hydrogen ion donating medium. Surprisingly, sulfate showed less penetration than the larger sulfonate anions.

One possible means to reduce penetration of the acid anion is to use a cation-exchange resin in the hydrogen form as the hydrogen ion donating medium [14]. This approach has been utilized successfully in our previous studies on Donnan dialysis [3]. However, these studies also showed that resin beads can act as effective hydrogen ion donating media only when they are used as a slurry with a suitable acid solution. The interstitial acid solution is necessary for site-to-site transport of hydrogen ion from the bulk slurry to the membrane surface. Some penetration of the anion of the slurrying acid is therefore possible, but this can be minimized by keeping the concentration of this acid as low as practicable. Studies showed that Bio-Rad AG 50W-X8 (200–400 mesh, H^+ form) slurried in a 2:1 (w/v) ratio

TABLE V

PENETRATION OF ANION FROM THE HYDROGEN ION DONATING MEDIUM (ANODE COMPARTMENT) INTO THE SAMPLE, EXPRESSED AS A PERCENTAGE OF THAT INITIALLY PRESENT IN THE ANODE COMPARTMENT

The CMV Membrane was used.

H^+-donating medium	0.05 *M*			0.025 *M*		
	150 mA	300 mA	450 mA	150 mA	300 mA	450 mA
Sulfuric acid	0.06	0.06	0.09	0.09	0.03	0.03
Methanesulfonic acid	2.7	4.3	4.6	2.1	2.3	2.5
Toluenesulfonic acid	2.7	3.6	8.6	0.1	0.2	0.2
Camphorsulfonic acid	1.0	1.7	2.5	0.3	0.5	0.5
Octanesulfonic acid	1.7	2.5	6.7	0.05	0.1	0.1

with 1 m*M* toluenesulfonic acid, octanesulfonic acid or camphorsulfonic acid acted as a suitable hydrogen ion donating medium, without any measurable penetration of the acid anion into the sample solution during electrodialysis. Dialysis times were increased marginally (approximately 5-10%) over those obtained with the solutions of hydrogen ion donating media of higher concentration used for Table V, but this was considered to be a minor drawback. Therefore 1 m*M* octanesulfonic acid was used as the slurrying solvent in further work.

Application

A chromatogram showing the application of the electrodialysis system to the treatment of a 1 *M* sodium hydroxide solution containing fluoride, chlo-

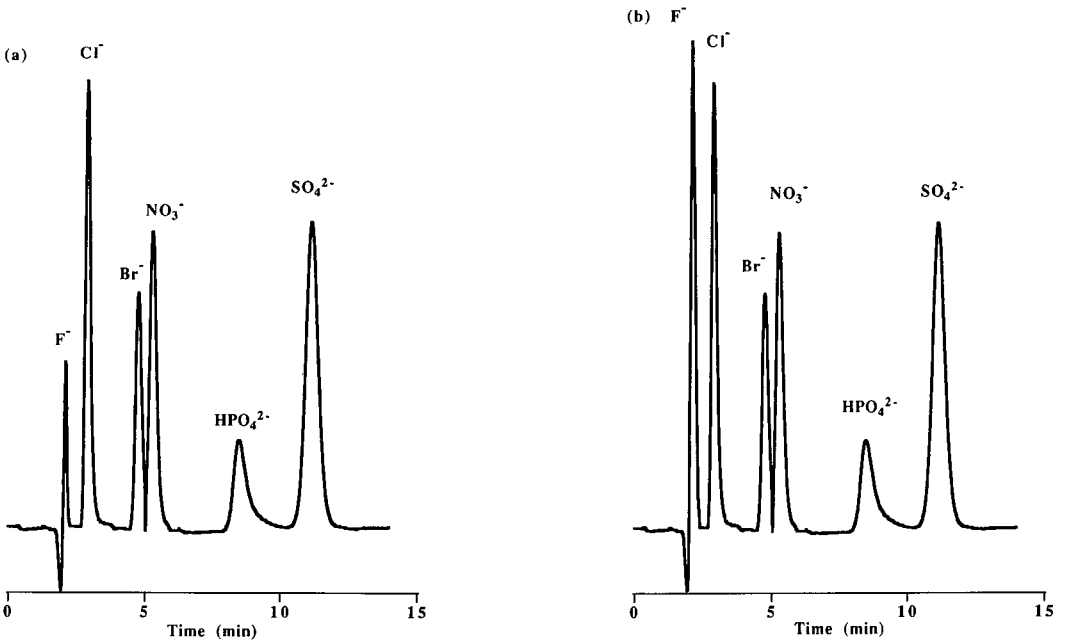

Fig. 3. Chromatogram of inorganic anions (3–10 μg/ml) in (a) 1 *M* NaOH after electrodialytic treatment and (b) Milli-Q water. Injection volume: 10 μl; eluent: 2.0 m*M* Na_2CO_3–1.8 m*M* $NaHCO_3$; column: Dionex HPIC-AS4A with AG4A guard column and AMMS suppressor.

ride, bromide, nitrate, phosphate and sulfate in the concentration range 3–10 μg/ml is given in Fig. 3. Fig. 3a shows the treated sample, whilst Fig. 3b shows a chromatogram for the same initial concentrations of anions in Milli-Q water. The two chromatograms are virtually identical, except for the low recovery of fluoride in the treated sample. By contrast, the chromatogram obtained for the original sample before electrodialysis showed no solute peaks whatsoever, but rather only a single, large solvent peak which obscured the entire chromatogram.

CONCLUSIONS

Provided correct attention is paid to the design of the cell and the manner in which the current (or power) is applied, electrodialysis can be used for the rapid neutralization of strongly alkaline samples as a clean-up step for IC. A 1 ml sample of 1 *M* sodium hydroxide could be neutralized in about 10 min, without loss of strong acid anions present in trace amounts in the sample. Weak acid anions, such as fluoride and nitrite, gave poor recoveries probably due to protonation reactions occurring within the membrane leading to the formation of neutral species which could diffuse from the sample compartment. Electrodialysis under the conditions used in this study is therefore not recommended for these ions. Multiple samples can be treated simultaneously without extending the dialysis time by using several cells arranged in parallel.

REFERENCES

1 J. A. Cox and Z. Twardowski, *Anal. Chim. Acta*, 119 (1980) 39.
2 J. A. Cox, E. Dabek-Zlotorzynska, R. Saari and N. Tanaka, *Analyst (London)*, 113 (1988) 1401.
3 S. Laksana and P. R. Haddad, *J. Chromatogr.*, 602 (1992) 57.
4 T. Kawara, K. Asada and T. Ishida, *Desalination*, 23 (1977) 213.
5 B. R. Nott, *Ind. Eng. Chem. Prod. Res. Dev.*, 20 (1981) 170.
6 M. H. Lopez Leiva, *Lebensm.-Wiss. Technol.*, 21 (1988) 119.
7 M. H. Lopez Leiva, *Lebensm.-Wiss. Technol.*, 21 (1988) 177.
8 N. Tsukanawa, *Chem. Pharm. Bull.*, 19 (1971) 1164.
9 J. A. Cox and R. Carlson, *Anal. Chim. Acta*, 130 (1981) 313.
10 Y. Okamoto, N. Sakamoto, M. Yamamoto and T. Kumamaru, *J. Chromatogr.*, 539 (1991) 221.
11 A. J. J. Debets, W. Th. Kok, K. -P. Hupe and U. A. Th. Brinkman, *Chromatographia*, 30 (1990) 361.
12 A. J. J. Debets, K. -P. Hupe, W. Th. Kok and U. A. Th. Brinkman, *J. Chromatogr.*, 600 (1992) 163.
13 D. C. Spanner, *Introduction to Thermodynamics*, Academic Press, London, New York, 1964, Ch. 12.
14 J. A. Cox and N. Tanaka, *Anal. Chem.*, 57 (1985) 385.

Journal of Chromatography, 640 (1993) 145–149
Elsevier Science Publishers B.V., Amsterdam

CHROMSYMP. 2739

Ion-exchange preconcentration and group separation of ionic and neutral organic compounds

Luther Schmidt and James S. Fritz*

Department of Chemistry, Iowa State University and Ames Laboratory, US Dept. of Energy, Ames, IA 50011 (USA)

ABSTRACT

In many cases sample pretreatment continues to be the most time-consuming and costly step in the analytical process. In the present work it is shown that macroporous ion-exchange resins of low exchange capacity can be used both to preconcentrate organic solutes from aqueous samples and to separate these solutes into groups. Thus, neutral and basic organic compounds are both taken up from aqueous solution by a very short column packed with a special cation-exchange resin. The neutral group of compounds is subsequently eluted with an organic solvent. The bases are then eluted by 2 *M* methylamine in methanol. In a similar manner organic acids are concentrated on a special anion-exchange column. Extensive data are shown to demonstrate the efficiency of the preconcentration and group separation of neutral and basic compounds.

INTRODUCTION

Solid-phase extraction (SPE) is fast becoming the preferred technique for analytical preconcentration [1]. It uses much smaller amounts of organic solvents than liquid–liquid extraction. SPE is easily automated and is capable of obtaining very high concentration factors.

SPE is usually carried out with a very small tube (or column) packed with a spherical solid of small particle size and high surface area. It can be thought of as low-performance liquid chromatography. Maximum retention is desired for the substances of interest with minimum retention of the other sample materials. The adsorbed substance can be subsequently eluted by a very small volume of an organic solvent or other suitable solvent.

The use of a short ion-exchange precolumn is well established to concentrate anions or cations prior to their separation and determination by ion chromatography. In the present work an ion-exchange resin with suitable properties is used to preconcentrate organic substances from aqueous samples and then separate them into two fractions: neutral and basic compounds. The basis for this separation is that neutral organic compounds are readily eluted from the SPE column by an organic solvent while basic compounds remain on the ion-exchange resin as protonated cations. The latter can then be eluted by an organic solvent containing a base to neutralize the protonated solute cations. This same principle has been used previously [2–4], but not to any extent for simultaneous preconcentration and group separation.

EXPERIMENTAL

Reagents and chemicals

The reagents used for the derivatization of the ion-exchange resins were of analytical grade. Reagents used and analytes studied in SPE were >99% pure and used as obtained from Aldrich, Fisher and Kodak. Laboratory distilled water was further purified using a Barnstead Nanopure II system (Sybron Barnstead, Boston, MA, USA).

The resins were prepared using a highly porous, cross-linked polystyrene resin, Amberchrome 161

* Corresponding author.

0021-9673/93/$06.00

(Supelco, Bellefonte, PA, USA). This spherical resin has an average particle size of about 40 μm and a surface area of about 720 m^2/g.

The procedure for the preparation of the sulfonated cation-exchange resin is as follows. In an ice bath, 1 g of resin was wetted with 1 ml of glacial acetic acid and stirred to form a slurry. To this slurry 25 ml of concentrated sulfuric acid was added. After 90 s, the reaction was stopped by adding an excess of ice water. The final product was then rinsed with methanol, water and acetone. The cation-exchange capacity was then determined by first passing 5 ml of 1 *M* HCl through a known mass of resin to assure the resin was all in the protonated form. The resin was then rinsed with deionized water and tested with litmus paper to assure that any excess acid was washed from the reservoir. Then 5 ml of a standardized NaOH solution was passed through the column. This was followed by another rinse with deionized water. The NaOH solution and water rinse was collected and titrated with a standard HCl solution. The capacity of the sulfonated resin was determined to be approx. 1.1 mequiv./g.

The apparatus used for SPE consists of a 30-ml glass reservoir connected by a small adapter to the SPE column itself. The SPE columns were obtained from Varian (Harbor City, CA, USA). Approximately 100 mg of the resin was packed into the 55 × 6.5 mm I.D. columns. The resin was held in place above and below by 20 μm polyethylene frits. The resin bed height was approximately 12–15 mm. The top of the reservoir has a ground glass joint which may be connected to a source of constant adjustable air pressure. The columns were connected to the laboratory-made reservoir by an adapter (Alltech Assoc., Deerfield, IL, USA). The flow-rate was controlled by the air pressure applied to the reservoir.

The concentrated samples collected were analyzed using an HP 5880A gas chromatograph with a flame ionization detector, an HP 5880A Series level 4 integrator, and an HP 7637A automatic sample injector (Hewlett-Packard, Avondale, PA, USA). The capillary column used was a Supelco (Bellefonte, PA, USA) SPB-1.

Procedure for SPE

Prior to initial use, the sulfonated columns were cleaned by passing through *ca.* 2 ml of methanol and acetonitrile. This was followed by approximately 5 ml of a 2-*M* solution of HCl in methanol in order to ensure the sulfonic acid groups on the resin would be protonated. The columns were then "wetted" with approximately 1 ml of methanol. The resin was not allowed to dry before passing the sample solution through the column.

The sample solutions were then prepared by adding a dilute methanol solution of several basic and neutral compounds to 10 ml of deionized water so that the final concentration of each compound was 5 ppm (v/v). In the base-neutral group separation, the pH of this solution was then lowered to *ca.* 2 with HCl. In the separation of strong bases from weak bases and neutrals a 0.1-*M* buffer solution of sodium phosphate was used to adjust the pH to 7. The sample was then added to the reservoir and the air pressure adjusted to give a sample flow-rate of approximately 1 ml/min. The column and reservoir were then rinsed with about 5 ml of water and air dried for several seconds.

The column was then rinsed with 1 ml of methylene chloride to elute the neutral fraction. This was collected in a GC vial. An internal standard of 0.1 ml of 500 ppm quinoxaline in methanol was then added to the vial. The vial was capped, mixed with an orbital stirrer, and then analyzed by GC. A 1-μl aliquot was injected with a split ratio of 1:40. Helium carrier gas was used at a flow-rate of 15 ml/min. The oven temperature was held initially at 65°C for 2 min, then ramped at 15°C/min to a final temperature of 225°C. The basic fraction was then eluted with 1 ml of either 2 *M* methylamine or 2 *M* NH_3 in methanol. Quinoxaline was also added as an internal standard as before. The vial was then capped, mixed, and analyzed by GC under the previously given conditions. Recoveries were calculated by comparing the relative peak heights of collected samples to those not subjected to SPE. All results are an average of multiple trials ($n \geqslant 3$).

RESULTS AND DISCUSSION

Group separation of neutral and basic compounds

Previous work has shown that polystyrene–divinyl benzene (PS–DVB) beads of high surface area (typically *ca.* 400–750 m^2/g) are very efficient for SPE of low concentrations of organic solutes in aqueous samples [5,6]. These resin beads still retain organic solutes when the beads are sulfonated pro-

vided that the degree of sulfonation is rather low. The sulfonated beads are able to retain protonated amine cations by an ion-exchange mechanism. So long as the amines are present as cations, they are not washed off the resin by an organic solvent.

The extent of sulfonation, as indicated by the exchange capacity of the sulfonated resin, can be kept low by sulfonation at 0°C for only a short period of time. To a first approximation over short time periods, the capacity of the resin *vs.* the reaction time is linear. A reaction time of 40 s yielded an exchange capacity of 0.45 mequiv./g, a time of 60 s gave an exchange capacity of 0.8 mequiv./g, and 90 s 1.1 mequiv./g. A sulfonated resin with an exchange capacity of 1.1 mequiv./g was used for SPE.

The scheme for preconcentration of low concentrations of organic solutes and their separation into groups was as follows. The sample was adjusted to an acidic pH with hydrochloric acid. This converted the basic compounds to the protonated cations. Then the sample was passed through a small column containing sulfonated resin in the H^+ form at a flow-rate of approximately 1 ml/min. The neutral organic solutes were eluted as a group with a small volume of metnhylene chloride. Then the basic fraction was eluted with a small volume of methylamine or ammonia in methanol.

TABLE I

RECOVERIES OF NEUTRAL ORGANIC SOLUTES (5 ppm) ELUTED WITH METHYLENE CHLORIDE

Conditions: 10 ml aqueous solution, pH = 1.8, lowered with H_2SO_4, cation-exchange resin (1.1 mequiv./g). All samples 5 ppm.

Compound	Recovery (%)
4-Nitroacetophenone	98
Nitrobenzene	99
Benzothiazole	92
Octyl alcohol	94
o-Hydroxyacetophenone	99
Benzonitrile	95
Toluene	98
trans-2-Hexenylacetate	96
Butyl benzene	95
Anisole	90
Octyl aldehyde	97
Ethyl crotonate	88
Propyl benzene	94
1-Octanol	94
Benzonitrile	95
Nitrobenzene	99

Table I shows excellent recovery of neutral organic solutes in water at 5 ppm. In each case essentially complete elution is obtained with methylene chloride. The recoveries of some basic organic solutes studied are summarized in Table II. None of these compounds was eluted with methylene chloride except 2,3-dimethyl quinoxaline which is an extremely weak base and therefore behaves almost like a neutral compound. Some of the basic compounds were eluted well with methanol containing aqueous ammonia, but stronger bases like butylamine and *n*-octylamine were not eluted. However, methylamine in methanol eluted all of the bases efficiently. Methylamine (pK_b in water = 3.1) is a stronger base than ammonia (pK_b = 4.8). In the gas chromatographic step methylamine is quite volatile and elutes well before any of the sample solutes.

An aqueous mixture containing 5 ppm each of five neutral compounds and six basic compounds was preconcentrated and the groups separated by our scheme. Fig. 1 shows the gas chromatogram obtained for the neutral group. Fig. 2 shows the gas chromatogram of the compounds in the basic group.

The effect of pH on the group separation was investigated. Results were compared for samples buffered at pH 2.0 with 0.1 *M* sodium dihydrogenphosphate and at pH 7.0 using disodium hydrogenphosphate. The results in Table III show that at pH 2.0 neutral compounds were eluted with methylene chloride and basic compounds with methylamine in methanol, as expected. Recoveries averaged lower with the pH 2.0 phosphate buffer than when the sample was acidified with HCl. At pH 7.0 the weaker bases (aniline, quinoline, etc.) were not protonated, and therefore were eluted with the neutral group. The stronger bases (hexylamine, ocytalmine, etc.) remained protonated at this pH, and therefore are not eluted until the methylamine in methanol wash step. Thus an additional group separation of aliphatic amines from aromatic amines and nitrogen heterocyclic compounds appears to be feasible.

Group separation of neutral and acidic compounds

The same principle used to preconcentrate and separate neutral and acidic groups should be appli-

TABLE II

RECOVERIES OF BASIC ORGANIC SOLUTES (5 ppm) ELUTED WITH AMMONIA OR METHYLAMINE IN METHANOL

Conditions 10 ml aqueous solution, pH = 1.8, lowered with H_2SO_4, cation exchange resin (1.1 mequiv./g). All samples 5 ppm.

Compound	Recovery (%)	
	Ammonia in methanol	Methylamine in methanol
Pyridine	91	91
Aniline	95	99
N,N'-dimethyl aniline	61	92
Quinoline	92	96
Butyl amine	0	103
Octyl amine	0	97
Quinaldine	92	95
Ethyl pyridine	–	93
Isopropyl pyridine	–	101
N-methyl aniline	–	92
sym-Collidin	–	95
Phenethyl amine	–	98
2,3-Dimethyl quinoxaline	63[a]	63[a]
Hexyl amine	0	95
Cyclohexyl amine	–	98
2,4-Lutidine	–	101

[a] Eluted with 37% methylene chloride.

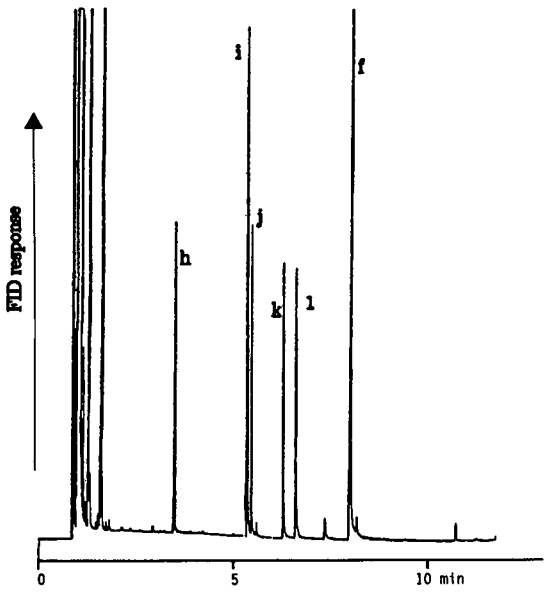

Fig. 1. Gas chromatogram of neutral compounds concentrated from aqueous solution with ion-exchange resin and eluted with methylene chloride. Peaks: h = ethyl crotonate; i = propyl benzene; j = 1-octanol; k = benzonitrile; l = nitrobenzene; and f = quinoxaline (internal standard).

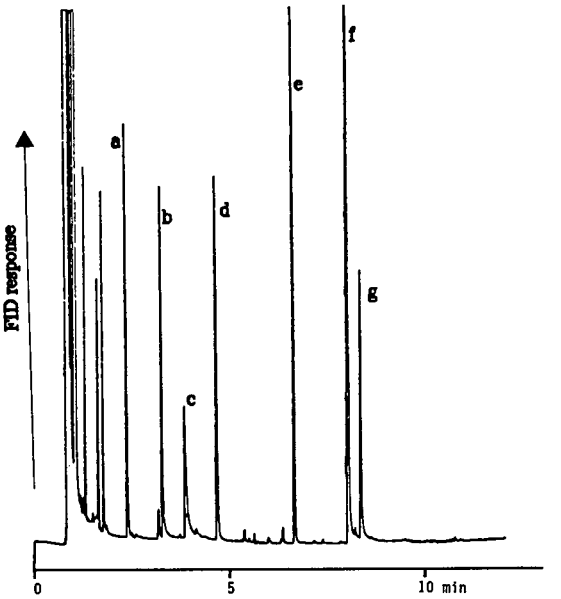

Fig. 2. Gas chromatogram of basic compounds concentrated from aqueous solution with ion-exchange resin from aqueous solution and eluted with methyl amine in methanol. Peaks: a = pyridine; b = hexyl amine; c = cyclohexyl amine; d = 2,4-lutidine; e = N,N'-dimethyl aniline; f = quinoxaline (internal standard); and g = quinoline.

TABLE III

RECOVERIES OF SOLUTES (5 ppm) FROM 10 ml OF AQUEOUS SOLUTION BUFFERED AT pH 2.0 AND pH 7.0

Compound	Recovery (%)			
	pH 2.0		pH 7.0	
	Methylene chloride	Methylamine	Methylene chloride	Methylamine
Pyridine	0	44	43	0
Toluene	95	0	101	0
Cyclohexyl amine	0	76	0	76
Aniline	0	88	81	0
Benzyl alcohol	93	0	98	0
Benzonitrile	98	0	90	0
Octyl alcohol	93	0	99	0
Nitrobenzene	101	0	–	0
N,N'-Dimethyl aniline	0	96	–	0
p-Ethanol	92	0	91	0
o-Hydroxyacetophenone	95	0	94	0
Benzothiazole	94	0	100	0
Quinoline	0	90	93	0
Quinaldine	0	90	88	0
2,3-Dimethyl quinoxaline	85	0	94	0
4-Nitroacetophenone	75	0	86	0
Hexyl amine	0	91	0	90
Octyl amine	0	91	0	90

cable for the separation of neutral and acidic groups of organic solutes. In this case the resin used would be a porous polymeric material functionalized with a quaternary ammonium group. Neutral organic compounds would be eluted from such a resin by an organic solvent, while acidic compounds would be retained as anions (when loaded at an alkaline pH). These organic anions could then be eluted by an organic solvent containing an acid (such as HCl) to convert the solute anions of the molecular organic acid.

Preliminary results indicate that this scheme does indeed work. Research on this project is continuing.

ACKNOWLEDGEMENTS

This research was supported by a grant from the 3M Co., St. Paul, MN, USA. The work was performed in the Ames Laboratory at Iowa State University. Ames Laboratory is operated for the US Department of Energy under Contract No. W-7405-Eng-82.

REFERENCES

1 I. Liska, J. Krupcik and P. A. Leclercq, *J. High Resolut. Chromatogr.*, 12 (1989) 577–590.
2 J. R. Kaczvinsky, Jr., K. Saitoh and J. S. Fritz, *Anal. Chem.*, 55 (1983) 1210–1215.
3 J. J. Richard and G. A. Junk, *Water Qual. Bull.*, No. 2 (1981) 40–42, 54–55.
4 M. Moors and D. L. Massart, *Trends Anal. Chem.*, 9 (1990) 164–169.
5 G. A. Junk, J. J. Richard, M. D. Grieser, D. Witiak, J. L. Witiak, M. D. Arguello, R. Vick, H. J. Svec, J. S. Fritz and C. V. Calder, *J. Chromatogr.*, 99 (1974) 745.
6 J. J. Sun and J. S. Fritz, *J. Chromatogr.*, 590 (1992) 197–202.

Journal of Chromatography, 640 (1993) 151–160
Elsevier Science Publishers B.V., Amsterdam

CHROMSYMP. 2827

Determination of anions and cations in concentrated bases and acids by ion chromatography

Electrolytic sample pretreatment

Archava Siriraks* and John Stillian

Dionex Corporation, 1228 Titan Way, Sunnyvale, CA 94088 (USA)

ABSTRACT

The development of a high-capacity electrochemical membrane suppressor has resulted in new ion chromatographic methods for the determination of trace ions in concentrated acids and bases. Unlike previous membrane suppressors, the new one does not require chemical regeneration, thus eliminating regenerant leakage across the membranes. The new suppressor electrolyses water to create the acid or base required for neutralization and thus permits contamination-free acid–base neutralizations of concentrated reagents. This makes the new suppressor ideal for sample pretreatment of acids or bases prior to analysis by ion chromatography. This technique has been applied to trace anion determination in concentrated bases (*e.g.* 50% NaOH and concentrated NH_4OH) and trace cation determination in concentrated acids (*e.g.* 48% H_2SO_4, 43% H_3PO_4 and 33% methane sulfonic acid). The detection limits for most ions are 1 to 10 ng/ml.

INTRODUCTION

The determination of trace inorganic constituents in concentrated acids and bases has been important in a variety of chemical and semiconductor processes. Although ion chromatography (IC) has successfully determined trace ionic impurities in a wide range of matrices, it has been limited by matrix concentration [1,2]. Generally, an ionic matrix concentration of more than 10 times the eluent concentration interferes with the analytical separation and detection. Specifically, analyte peaks are obscured by the large interfering peak of the sample matrix. Also, the separation is severely changed because the ionic sample matrix is of such high concentration that it becomes the major eluting ion, temporarily overriding the eluent.

In order to determine trace anions in concentrated bases or trace cations in concentrated acids, the sample is usually diluted to the level at which the sample matrix does not interfere with the analytical separation. Another method commonly used is sample pretreatment with ion-exchange resin to remove the interfering sample matrix ion. Although high-capacity resin can be used to neutralize the concentrated sample matrices, the inherent blank associated with the resin usually contaminates the sample. Moreover, the resin requires periodic regeneration. Other forms of sample pretreatment devices include fiber suppressor [3], MicroMembrane Suppressor (MMS) [4] and dialysis membrane-based devices (see ref. 2 and references therein). The fiber suppressor is comprised of approximately 2 m of Nafion hollow fiber. Because of the need to maintain a relatively thick membrane wall (*e.g.* 0.075 cm) to minimize bursting from down stream backpressure, the fiber suppressor has low suppression capacity and is not useful for sample pretreatment. The MMS uses flat ion-exchange membranes ap-

* Corresponding author.

0021-9673/93/$06.00

proximately 0.005 cm thick and consequently has higher suppression capacity than the fiber suppressor. The dialysis device utilizing a length of ion-exchange hallow fiber bathed in a suitable regenerating solution has also been used for sample neutralization (see ref. 2 and references therein). The only advantage of these devices over packed bed resin is that they do not require periodic regeneration. However, these techniques can only be applied to < 0.2 *M* NaOH samples due to their limited neutralization capacities. Also, they produce a significant blank from the acid anion used for sample neutralization.

Recently, an electrolytic micromembrane suppressor device (Self Regenerating Suppressor, SRS) was introduced for suppressed conductivity detection after ion-exchange analytical separation [5,6]. The SRS takes advantage of the design of the MMS, allowing high suppression capacity with the use of thin ion-exchange membranes and ion-exchange screen filling the chambers, and adds the advantages of electrolysis and electrodialysis. The SRS makes the requisite acid or base required for neutralization electrolytically by splitting water at the electrodes in the regenerant chambers. Fig. 1 shows the internal construction of the SRS for anion determination (ASRS) including cation-exchange membranes and cation-exchange screens. The SRS operates in a constant current mode between 50 mA to 500 mA and in the voltage range of 1 to 7 V, typically 3.5 to 4 V. Fig. 2 indicates the neutralization chemistry in an ASRS. An SRS for cation separations (CSRS) works analogously to the ASRS. For cation determinations the eluent anion is removed and replaced with hydroxide, neutralizing the strong acid eluent. The CSRS is composed of anion-exchange membranes and anion-exchange screens. The SRS device is capable of suppressing the high-conductance acidic or basic eluent to produce very-low-conducting water in a contamination-free neutralization process. This is an ideal sample pretreatment process for reducing the high concentration of acid or base matrices prior to ion analysis by IC.

This paper demonstrates the use of the SRS as sample pretreatment for trace anion determination

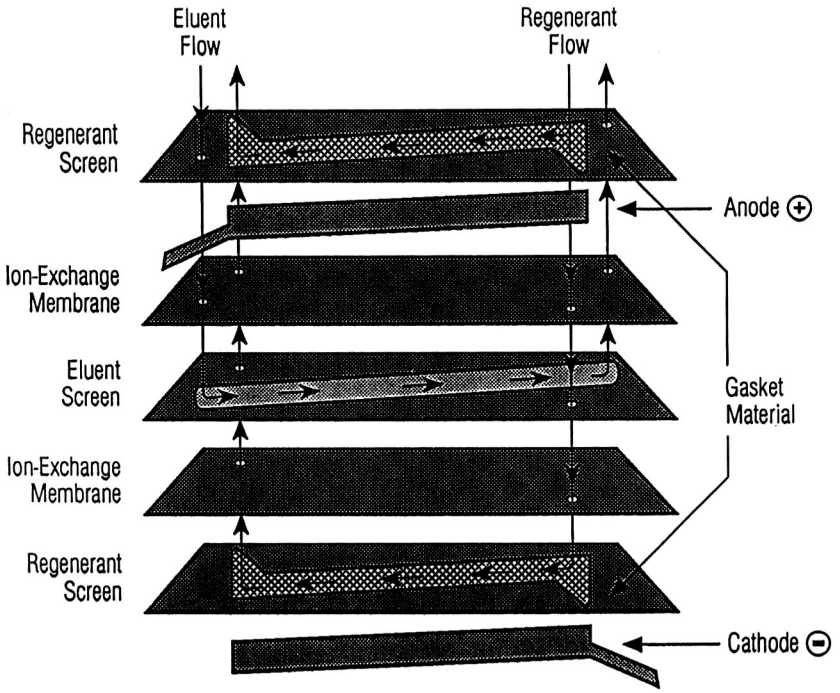

Fig. 1. Internal construction of a Self Regenerating Suppressor (SRS).

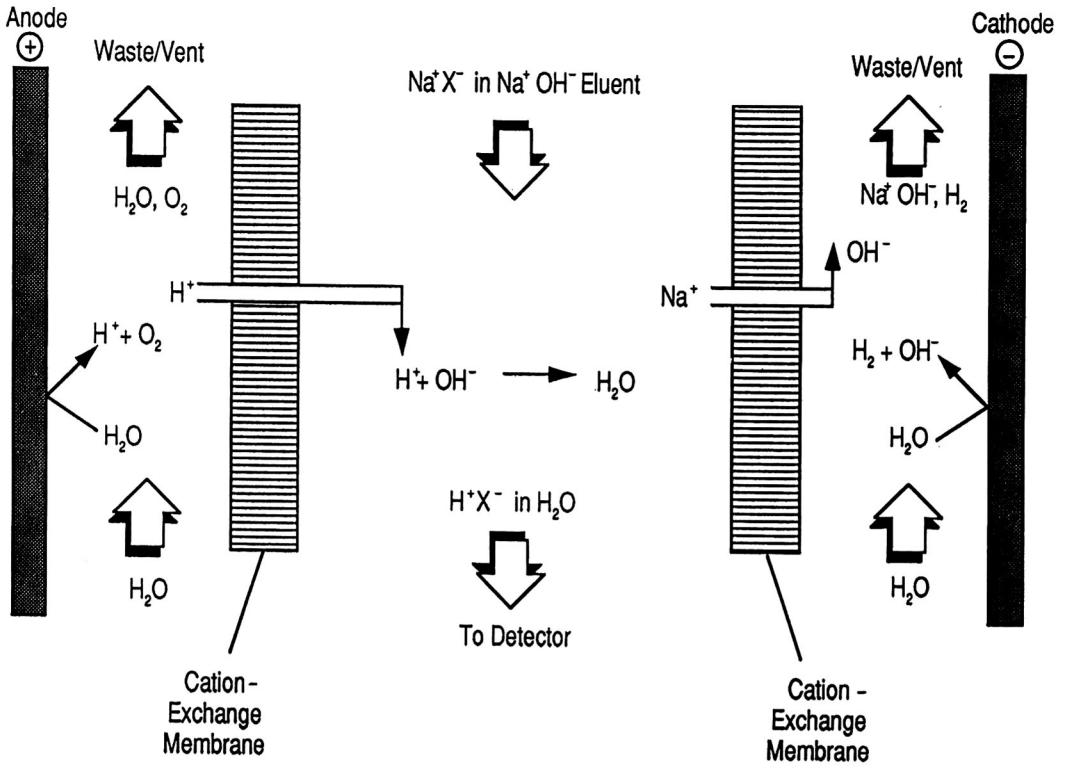

Fig. 2. Suppression chemistry in the Anion Self Regenerating Suppressor (ASRS).

in concentrated bases and trace cation analysis in concentrated acids. The method development, integration of the sample pretreatment to the analytical system, and analytical data are presented.

EXPERIMENTAL

Sample recycling method

Although the SRS is capable of continuous neutralization of up to approximately 0.2 *M* acid or base at 1 ml/min, it does not have adequate capacity to neutralize the concentrated acid or base. The required capacity can be improved by recycling the sample through the suppressor several times until it is completely neutralized. This concept is simple, but it requires careful system design. Sample contamination by the system components (*e.g.* pump, injector, valve) must be avoided.

Fig. 3 shows a recycle device consisting of a double stack, 4-way, low-pressure valve, SRS and conductivity cell. The 4-way valve is used to recycle the sample into the SRS by alternating valve ON and OFF. The conductivity cell positioned immediately after the SRS allows monitoring of the sample con-

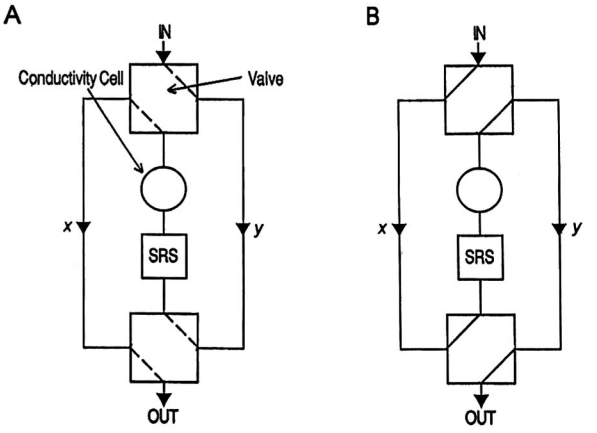

Fig. 3. Sample recycling method. (A) Recycle valve ON, sample flows from *y* to *x*. (B) Recycle valve OFF, sample flows from *x* to *y*.

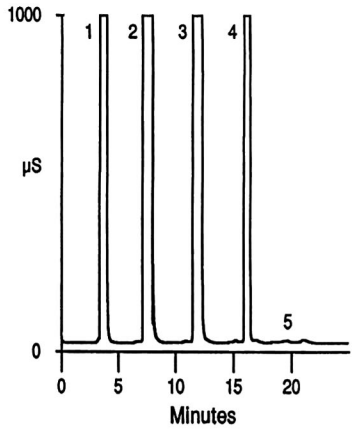

Fig. 4. Monitoring sample conductivity during ASRS sample pretreatment. Sample: 50% NaOH (50 μl), sample flow: 1.0 ml/min, current setting: 100 mA. Cycle 1, 3 and 5 valve B in ON position. Cycle 2 and 4 valve B in OFF position.

ductance to determine when the sample is adequately neutralized. The conductivity signal also serves as a marker for when to actuate the valve. Deionized water delivered by an external pump is used to "push" the sample from the sample loop to the recycle device and the rest of the system. The concentrated acid or base sample never passes through the pump and sample contamination is avoided. A typical sample volume of 5–50 μl is first passed through the SRS when valve is in ON position (Fig. 3A). The sample band passes from the top right of the valve (*y*), SRS and conductivity cell to the left side of the valve. As soon as the sample band has passed through the left side of the valve and before it exits the bottom stack (*x*), the valve is switched to OFF position (Fig. 3B). At this point the sample band passes from the left (*x*), through the SRS and conductivity cell a second time, to the right side of the valve . Before the sample band exits the bottom stack (*y*), the valve is switched back to ON position and the same process as described in Fig. 3A is initiated. When the sample conductivity has been significantly lowered (*e.g.*: less than 20 μS/cm for NaOH) it can be sent from the recycle device to the analytical system. To illustrate the overall process, Fig. 4 shows the recycling of 50% NaOH sample using the recycle valve alternating OFF and ON. The valve switching sequence shown in Fig. 4 is constant as long as the external pump flow-rate is unchanged.

Chomatographic system

The system configuration is shown in Fig. 5. All chromatography was performed on a Dionex (Sunnyvale, CA, USA) DX-300 system. The anion system consisted of a sample concentration module

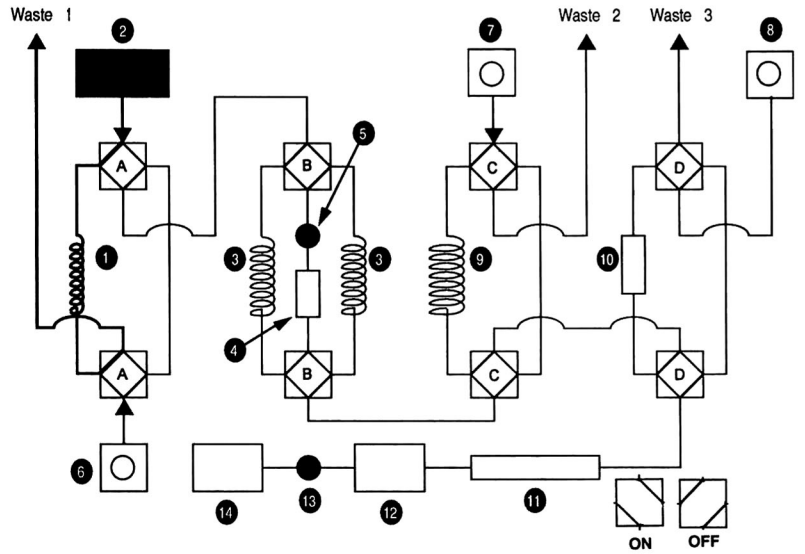

Fig. 5. System configuration. 1 = Sample loop; 2 = autosampler; 3 = recycle loop; 4 = sample pretreatment device; 5 = conductivity cell; 6 = pump 1; 7 = pump 2; 8 = pump 3; 9 = collection loop; 10 = concentrator column; 11 = separator column; 12 = eluent suppressor; 13 = conductivity cell; 14 = data processor.

(SCM), an advanced gradient pump (AGP) and a conductivity detector (CDM-II). The SCM contains two single-piston pumps designated pump 1 and pump 2, three low-pressure, double-stack, 4-way slider valves (valves A, B and C), and one high-pressure, double-stack, 4-way slider valve (valve D). The AGP, pump 3, was used as an analytical pump. The cation system hardware was identical to the anion system except for the columns and the SRSs. The power supply for the CSRS and ASRS was a Dionex SRS Controller capable of supplying constant current power with four settings, 50, 100, 300 and 500 mA and with a voltage range of 1 to 7 V.

Two sets of columns and sample pretreatment devices were used in the anion and cations systems. For the anion system, the Dionex ASRS, a Dionex IonPac AC10 (50 mm × 2 mm) and a Dionex IonPac AS4ASC (250 mm × 2 mm) were used. A Dionex CSRS, a Dionex IonPac TCC-2 (35 mm × 4mm), a Dionex MetPac CC-1 (50 mm × 4 mm) and a Dionex IonPac CS12 (250 × 4 mm) were employed for the cation system. The eluent suppression devices were the Dionex Anion MicroMembrane Suppressor (AMMS-II) and Cation MicroMembrane Suppressor (CMMS-II) for anion and cation systems, respectively. The sulfuric acid and tetrabutyl ammonium hydroxide regenerants were delivered to the AMMS-II and CMMS-II by two Dionex AutoRegen systems. The chromatographic conditions for the anion and cation systems are listed in Table I.

TABLE I

CHROMATOGRAPHIC CONDITIONS

Sample pretreatment	
Pretreatment device	ASRS (anion system)
	CSRS (cationic system)
Sample loop	50 μl
Recycle loop	3.0 ml
Collection loop	8.0 ml
Pump 1 flow	1.0 ml/min
Pump 2 flow	1.0 ml/min
Analytical system	
Anion system	
Column	IonPac AC10 (2 mm)
	IonPac AS4A SC (2 mm)
Eluent	1.7 m*M* $NaHCO_3$–1.8 m*M* Na_2CO_3
Flow	0.5 ml/min
Detection	Suppressed conductivity
Cation system	
Column	MetPac CC-1, TCC-2
	IonPac CS12
Eluent	22 m*M* Hydrochloric acid
Flow	1.0 ml/min
Detection	Suppressed conductivity

System operation and method development

The valve configuration shown in Fig. 5 was used to automate the overall process. Valves A, B, C and D are designated as injection valve, recycle valve, collection valve and concentration valve, respectively. Valves A, B and C were controlled by valve 5 on the AGP. This single-valve control processed the sample pretreatment steps. Valve D was controlled by valve 6 on the AGP. The sample travels from the left to the right of the diagram. The typical valve sequencing program used for 3-cycle pretreatment is summarized in Table II.

Reagents

The high purity sodium hydroxide, 30% Supra-Pur grade (VWR Scientific) and 50% NaOH (Fisher Scientific) were used as samples for the anion system. For cation analysis, concentrated sulfuric acid (Fisher Scientific), phosphoric acid (Fisher Scientific) and methane sulfonic acid (Aldrich) samples were employed. The sodium bicarbonate–carbonate eluent was prepared from a dilution of Dionex AS4A eluent concentrate solution with 18 Ω cm water. The HCl eluent was prepared from dilution of ultrapure concentrated hydrochloric acid (SeaStar Chemicals) with 18 Ω cm water.

RESULTS AND DISCUSSION

ASRS sample pretreatment: trace anions in concentrated bases

Electrochemical reaction and neutralization. Increasing the current increases the electrolytic reaction. The amount of electrolytic products, hydronium and hydroxide, determine the neutralization capacity. Hence, the number of sample cycles through the SRS can be minimized at high current. The typical sample conductivity response at various ASRS current settings is shown in Fig. 6. The 50% NaOH sample was neutralized as described in the experimental section. The sample conductivity in the recy-

TABLE II

SAMPLE PRETREATMENT STEPS

Time (min)	Event	Valve A, B, C	Valve D	Comments
0.0	Sample loading	Off	On	Sample is injected into the 50-μl loop (valve A)
0.5	Recycling 1	On	On	Sample is flushed from the sample loop (valve A) and passed through valve B for sample neutralization. At the end of this step (time 5.0 min), the sample band is located in the left recycle loop.
0.5	Recycling 2	Off	On	The sample band is passed through the bottom stack of valve B upward through the SRS and the conductivity cell for the second time. At the end of this step (time 8.0 min), the sample band is located in the right recycle loop.
8.0	Recycling 3	On	On	The sample flow path is identical to that of recycle 1. After the sample band has been passed through the SRS for the third time, valve B remains ON for 5 min. The sample band is passed through valve B through valve C. At the end of this step (time 16.0 min), sample band is completely transfered into the collection loop.
16.0	Concentration	Off	Off	Sample band in the collection loop is flushed to the concentrator on valve D. The sample is concentrated on the concentrator column at the end of the step (time 24.0 min).
24.0	Analytical separation	Off	On	Eluent from the AGP removes the concentrated analytes from the concentrator to the analytical system, where they are separated and detected.

cle valve was monitored each time it passed through the ASRS. The sample flow-rate was maintained at 1.0 ml/min. The sample band splitting seen in Fig. 6 is due to the change in sample viscosity and ionic strength during the neutralization process. As the front end of the peak is neutralized, its viscosity is reduced therefore dispersing faster than the rest of the sample band. The peak splitting was not observed when the dilute NaOH sample was injected.

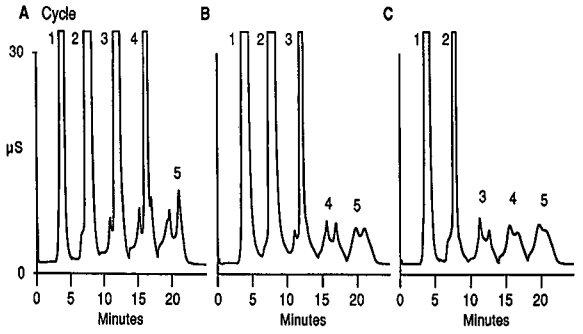

Fig. 6. Increasing the current increases the electrolytic and electrodialytic rates. The ASRS neutralization of 50% NaOH using (A) 100 mA, (B) 300 mA and (C) 500 mA.

It was found that a minimum of 5 cycles was required at 100 mA current setting (Fig. 6A). At higher current settings, 300 mA, 500 mA and 600 mA, the minimum of 4 cycles (Fig. 6B), 3 cycles (Fig. 6C) and 3 cycles (not shown), was observed. The results of these experiments conclude the 3-cycle pretreatment with a current setting of 500 mA is sufficient to reliably neutralize the concentrated NaOH sample.

Coupling to the analytical system. After the sample is completely neutralized, the treated sample composed of acid-form anions in a water matrix can be directly coupled to any standard concentrator column for subsequent analytical separation and detection. Since the SRS maximum operating backpressure is 150 p.s.i. (1 p.s.i. = 6894.76 Pa), a collection loop (Fig. 5) of 8 ml was used to isolate the low-pressure SRS device from the relatively high-pressure concentrator column.

A microbore system, the IonPac AC10 concentrator, and the IonPac AS4ASC analytical column with the AMMS-II (2 mm format), was used for anion separation and detection. Fig. 7 shows the the simultaneous conductivity responses of the 50% NaOH sample during the neutralization and sub-

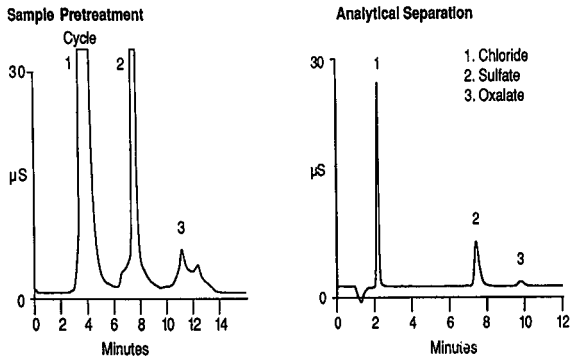

Fig. 7. Trace anions in 50% NaOH.

sequent analytical separation. Pretreatment conductivity monitoring is only necessary as a method development or troubleshooting aid. Once the method is developed, it can be used for several days without any significant changes in the analytical peak response unless the external pump flow-rate changes.

Dynamic range of sample pretreatment and spike/recovery. The linearity of anions detected in varying concentrations of the same NaOH sample reflects the dynamic range of the sample pretreatment. Varying the matrix concentration not only identifies the degree of matrix interference, if there is any, it also indicates the limitation of the sample pretreatment process. The spike/recovery experiment of varying analyte concentrations in a fixed matrix concentration alone does not isolate the degree of matrix interference from dynamic range of the method. In many instances, similar methods fail when applied to the real samples of varying matrix concentrations without matrix matching (identical matrix concentration used in standard calibration). To validate any method for highly complex matrices, the linearity study of analytes as a function of matrix concentration experiment is performed, followed by an evaluation of the spike/recovery of analytes in matrix concentration within the linear range.

To determine the linearity of anions in various NaOH concentrations, the 50% NaOH was spiked with anions to make a 49.9% spiked NaOH sample. This sample was then diluted with deionized water to make up 6.08, 12.2, 24.4 and 48.4% NaOH samples. To avoid the density differences in various NaOH concentrations the sample was prepared volumetrically instead of gravimetrically. Since various amounts of water were used for sample dilution, the water was analyzed for trace ion contamination and the result was used for blank correction. The five samples containing 6 to 49.9% NaOH were analyzed; typical chromatograms are shown in Fig. 8. The corresponding linearity of Cl^-, NO_2^-, HPO_4^{2-}, SO_4^{2-}, Br^-, NO_3^- and oxalate as a function of

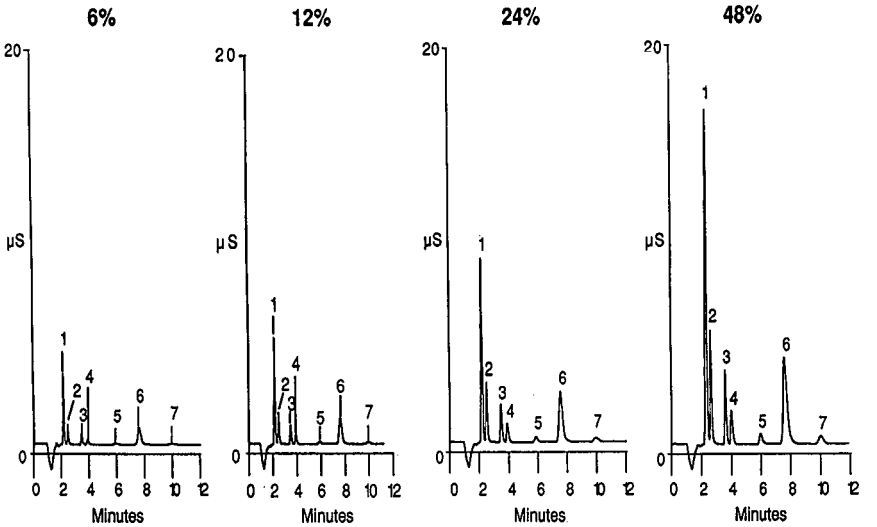

Fig. 8. Dynamic range of ASRS sample pretreatment (%NaOH). Peaks: 1 = chloride; 2 = nitrite; 3 = bromide; 4 = nitrate; 5 = phosphate; 6 = sulfate; 7 = oxalate.

NaOH matrix concentration is 0.9999, 0.9996, 0.9955, 0.9995, 0.9994, 0.9997 and 0.9995, respectively.

The spike/recovery study was performed using ultrapure 30% NaOH, which was found to contain 0.2 μg/ml chloride and 0.3 μg/ml sulfate. The results shown in Table III are blank corrected for these chloride and sulfate concentrations. Good recovery was observed for all anions studied. Recovery of fluoride was not studied because it partially coelutes with an unknown peak in the 30% NaOH sample. The ASRS sample pretreatment is limited to strong anions. For weak acid analytes with pK_a greater than about 3 (such as fluoride, formate and acetate) the non-ionized weak acids pass through the membrane resulting in low recoveries. This observation perhaps also explains the high R.S.D. for phosphate shown in Table III.

Although ASRS sample pretreatment is virtually a contamination-free neutralization process, it was determined that some of the blank was due to the device. The high-capacity sulfonated membranes release sulfate, especially in a newly installed ASRS. It was found that the level of sulfate blank declined to a constant level after 10 to 15 h of operation. The sulfate blank does not effect the quantification of the sulfate analyte since it is consistent; however, it does decrease the calculated detection limit of this method for sulfate.

TABLE III

SPIKE/RECOVERY OF TRACE ANIONS IN 30% SODIUM HYDROXIDE

The results are blank corrected. Measured chloride and sulfate concentrations in unspiked 30% NaOH are 0.24 μg/ml and 0.32 μg/ml, respectively.

Anion	Spike (μg/ml)	Recovery (μg/ml)	R.S.D. (%) (n = 7)
Chloride	0.06	0.07	3.2
Nitrite	0.50	0.58	1.1
Bromide	0.50	0.55	2.3
Nitrate	0.30	0.27	1.2
Phosphate	0.45	0.51	12
Sulfate	0.45	0.55	3.3

CSRS sample pretreatment: trace cations in concentrated acids

Electrochemical reaction and neutralization. The study of acid neutralization as a function of the CSRS current setting was performed identically to that of the ASRS neutralization. The acid concentration used was a 1:1 dilution of the concentrated acids. Three acids were studied: methanesulfonic acid sulfuric acid, and phosphoric acid representing mono-, di- and trivalent acid samples, respectively. The heat generated by mixing the 1:1 diluted acid sample with water during recycling made it difficult to monitor sample conductivity due to baseline shift. Method development for valve sequencing was accomplished using 1:4 dilution acid sample or calcium or sodium salts of the acid. It was determined that three cycles of a 1:1 dilution of the acid being studied and 500 mA current, was sufficient for neutralization of all three acids studied.

Coupling to the analytical system. After the sample is completely neutralized, the treated sample composed of hydroxide-form cations in a water matrix can be directly concentrated onto any standard concentrator column for subsequent analytical separation and detection. In this case, the combination of the MetPac CC-1 and the TCC-2 was used to concentrate mono- and divalent cations prior to analytical separation on the IonPac CS12. The unique combination of chelating resin and cation-exchange allows the use of dilute acid eluent without any complexing agents making the method compatible with the CS12 analytical column. The sample flows through the MetPac CC-1 where the divalent cations are retained, then through the TCC-2 where the monovalent cations are concentrated. The acid eluent flow was in reverse direction so that the monovalent cations were removed first, followed by the divalent cations.

Dynamic range of sample pretreatment and spike recovery. To determine the linearity of cations in various sulfuric acid concentrations, the 1:1 sulfuric acid was spiked with cations to make a 48% spiked sulfuric acid. The sample of 6, 12, 24, 36 and 48% sulfuric acid were prepared in a similar manner to that of NaOH samples. These samples were analyzed and the chromatograms are shown in Fig. 9. The corresponding linearity of Li^+, Na^+, NH_4^+, K^+, Mg^{2+} and Ca^{2+} as a function of sulfuric acid matrix concentration is 0.9995, 0.9997, 0.9986, 0.9998, 0.9998 and 0.9986, respectively.

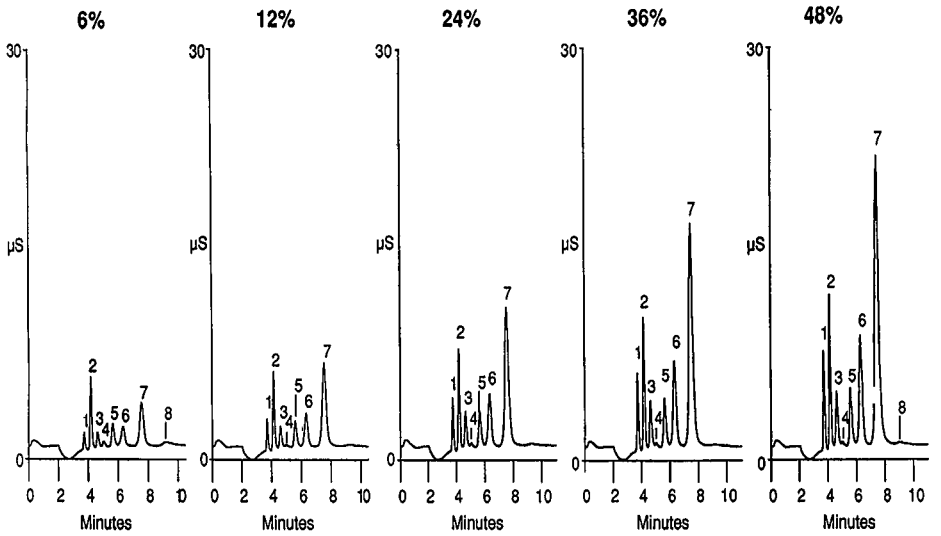

Fig. 9. Dynamic range of CSRS sample pretreatment (%H_2SO_4). Peaks: 1 = lithium; 2 = sodium; 3 = ammonium; 4 = unknown; 5 = potassium; 6 = magnesium; 7 = calcium; 8 = unknown.

The spike/recovery studies were performed using 48% sulfuric acid, 43% phosphoric acid, and 33% methane sulfonic acid (MSA). The spike/recovery data for those matrices are shown in Table IV. Good recovery was observed for all strong-base cations studied. The CSRS sample pretreatment is limited to relatively strong-base analyte cations (pK_a > 10). For weak-base analytes, such as ammonium and amines, the non-ionized weak base formed during matrix neutralization passes through the membrane and out of the sample stream, resulting in low recoveries. This observation explains the low recovery of ammonium as shown in Table IV.

Although the CSRS pretreatment is essentially a contamination-free neutralization process, some of the inherent blank released from the device was observed. The high-capacity aminated materials release alkylamines, especially in a newly installed CSRS. The example of this blank is shown in Fig. 9, peaks 4 and 8. It was found that the level of these blanks declined over time to a constant level after 10 to 15 h of operation. The amine blanks do not

TABLE IV

SPIKE/RECOVERY OF TRACE CATIONS IN CONCENTRATED ACIDS

Cation	48% Sulfuric acid		43% Phosphoric acid		33% Methanesulfonic acid	
	Expected (μg/ml)	Found (μg/ml)[a]	Expected (μg/ml)	Found (μg/ml)[a]	Expected (μg/ml)	Found (μg/ml)[b]
Li^+	0.064	0.063 ± 0.001	0.063	0.066 ± 0.001	0.064	0.064 ± 0.001
Na^+	0.401	0.42 ± 0.04	0.499	0.445 ± 0.006	0.261	0.229 ± 0.005
NH_4^+	0.610	0.314 ± 0.006	0.729	0.570 ± 0.001	0.494	0.383 ± 0.009
K^+	0.276	0.256 ± 0.005	0.358	0.340 ± 0.006	0.191	0.202 ± 0.005
Mg^{2+}	0.299	0.30 ± 0.02	0.332	0.35 ± 0.02	0.190	0.194 ± 0.006
Ca^{2+}	1.415	1.51 ± 0.06	1.846	2.14 ± 0.05	1.01	1.00 ± 0.09

[a] n = 8.
[b] n = 6.

TABLE V

DETECTION LIMITS BY SRS SAMPLE PRETREATMENT COUPLED IC FOR CONCENTRATED REAGENTS

Anion	Detection limit (ng/ml)	Cation	Detection limit (ng/ml)
Chloride	3.0	Lithium	0.1
Nitrite	8.0	Sodium	0.8
Bromide	8.0	Ammonium	5.0
Nitrate	6.0	Potassium	0.8
Phosphate	30	Magnesium	0.6
Sulfate	20	Calcium	1.0

affect the quantification of cations since they are consistent and separated from the rest of the cations studied.

Concentrated hydrochloric and concentrated nitric acid matrices were also evaluated, and it was found that even with a three-fold dilution of these concentrated acids the process of neutralization eventually damaged the ion-exchange components of the SRS. In the case of concentrated HCl, this is probably due to the electrochemical formation of hypochlorite at the anode, followed by concentration of the hypochlorite in the adjacent anion-exchange screens and membranes, which caused oxidative decomposition of the ion-exchange media by the concentrated hypochlorite. Concentrated nitric acid is probably also oxidatively decomposing the ion-exchange media since molar concentrations of nitric acid are present in the anode chamber during neutralization of this matrix. Therefore, this technique is not applicable with matrices that are strong oxidizers. We are currently studying if larger dilutions (1:10 to 1:100) of the matrix, followed by sample re-concentration of a larger volume (5 to 50 ml) will provide an acceptable life for the SRS with these matrices.

Detection limits by SRS sample pretreatment coupled IC

Table V summarizes the detection limits obtained by the anion and cation system for base and acid samples, respectively. The detection limits are based on three times signal to noise. The reported detection limits are comparable to those obtained by direct injection of ions in H_2O matrix. Since the sample volume injected into the pretreatment system is comparable to sample volumes used for direct injection, this indicates that the pretreatment process is relatively efficient and that sample dispersion is minimized.

CONCLUSIONS

New methods for trace anions in concentrated bases and trace cations in concentrated acids have been developed. The methods use the electrolytic sample pretreatment devices to neutralize acid and base matrices to produce water. The recycling method has been introduced to overcome the limited capacity of the electrolytic ion-exchange membrane devices. These methods have been applied to trace anion determination in 50% sodium hydroxide and trace cation analysis in several concentrated acids. The detection limits obtained by this technique are comparable to those obtained by analysis for the same analyte is deionized water, using direct injection.

REFERENCES

1 A. Siriraks, C. A. Pohl and M. Toofan, *J. Chromatogr.*, 602 (1992) 89.
2 S. Laksana and P. R. Haddad, *J. Chromatogr.*, 602 (1992) 57
3 T. S. Stevens, J. C. Davis and H. Small, *Anal. Chem.*, 53 (1981) 1488
4 J. Stillian, *LC Mag.*, 3 (1985) 802.
5 A. Henshall, S. Rabin, J. Statler and J. Stillian, *Am. Lab.*, Nov. (1992) 20R.
6 S. Rabin, J. Stillian, V. Barreto, K. Friedman and M. Toofan, *J. Chromatogr.*, 640 (1993) 97.

Journal of Chromatography, 640 (1993) 161–165
Elsevier Science Publishers B.V., Amsterdam

CHROMSYMP. 2663

Simultaneous determination of the three main inorganic forms of nitrogen by ion chromatography

Shifen Mou*, Huitong Wang and Qun Sun

Research Centre for Eco-Environmental Sciences, Academia Sinica, P.O. Box 2871, Beijing 100085 (China)

ABSTRACT

An ion chromatographic method for the determination of nitrite, nitrate and ammonium simultaneously is described. An appropriate eluent–column–detector combination for separating and detecting these ions is discussed. On a bifunctional ion-exchange column, nitrite and nitrate anions were separated by anion exchange and ammonium cation by cation exchange. Nitrite and nitrate were detected by UV spectrometry and ammonium using a chemically suppressed conductivity detector. The detection limits for the three ions were all below 0.02 ppm (w/w) and the relative standard deviations for the three ions were all less than 0.5%. Several samples such as water, soil and acid rain were analysed with this method and the recoveries of the three ions were all within 100 ± 5%. The results agreed well with those obtained by a standard method.

INTRODUCTION

The simultaneous determination of cations and anions in one sample injection has the potential to increase the efficiency of a laboratory engaged in ion chromatographic analyses. As the selection of the eluent–column–detector combination is crucial to the success of the simultaneous determination of anions and cations, few methods have been reported in this field. One of these methods used a cation-exchange column, an anion-exchange column and a switching valve, and ions were detected with a conductivity detector [1]. Other methods used a bifunctional column, ions being detected by conductimetric detection [2–4], by indirect photometric detection [5,6] or using a UV and a fluorescence detector in series [7]. However, the sensitivity and selectivity of these methods were not very good.

This paper reports a system consisting of dilute hydrochloric acid–glycine as eluent, a bifunctional ion-exchange column and a UV spectrophotometric–conductivity detector that can simultaneously determine nitrite, nitrate and ammonium ions. The methods is very sensitive and selective, and few species interfere.

EXPERIMENTAL

Apparatus and reagents

All chromatography was performed on a Dionex Model 2000i ion chromatograph equipped with a UV–Vis detector and a CDM-I conductivity detector. Output data were recorded on a Dionex dual-pen recorder. A Dionex HPIC-GC5 guard column, a Dionex HPIC-CS5 separation column and a Dionex CMMS suppressor were used. The sample loop volume was 50 μl. The eluent was a mixture of 5 m*M* hydrochloric acid and 8 m*M* glycine solution. The regenerant was 10 m*M* potassium hydroxide solution. Glycine was of biochemical reagent grade and other chemicals were of analytical-reagent grade.

Analytical procedure

The samples which were eluted from the separation column first flowed into a UV spectrophotometric cell where nitrite and nitrate were detected,

* Corresponding author.

0021-9673/93/$06.00

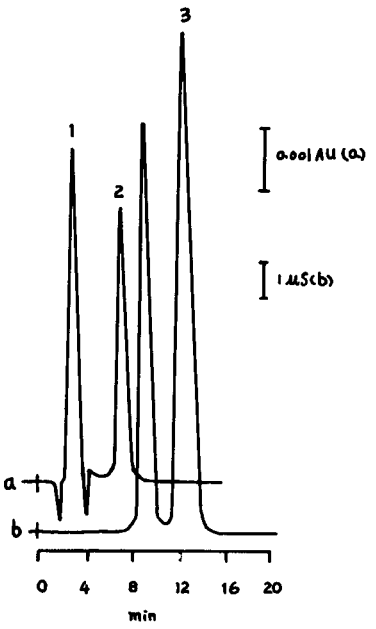

Fig. 1. Simultaneous separationof the nitrite, nitrate and ammonium ions. (a) UV detection; (b) conductivity detection. Peaks: 1 = NO_2^- (10 ppm, w/w); 2 = NO_3^- (5 ppm); 3 = NH_4^+ (5 ppm).

then through the cation suppressor and conductivity detector cell where ammonium was detected. The eluent flow-rate was 2.0 ml/min and the regenerant flow-rate 1.0 ml/min. The recorder chart paper speed was 0.25 cm/min. The UV–Vis detector was set at 215 nm. The samples were injected directly after the baseline was stable. The peak-height methods was used for quantative analysis. Fig. 1 shows the separation of nitrite, nitrate and ammonium.

RESULTS AND DISCUSSION

Selection of instrumentation

UV and conductivity detectors were chosen for two reasons. First, nitrite and nitrate absorbed well at 215 nm whereas other common anions and cations did not, and the conductivity detector was sensitive to ammonium ions without a postcolumn derivatization reaction. Second, these detectors are the most commonly used type and are available in many laboratories. The UV and conductivity detectors were connected is series.

To separate nitrite, nitrate and ammonium ions simultaneously without chemical pretreatment, an appropriate column would contain two kinds of ion-exchange function. The HPIC-CS5 separation column has a resin core of polystyrene cross-linked with divinylbenzene which is surface sulphonated for cations exchange and aminated latex with quaternary ammonium groups for anion exchange, *i.e.*, it is a bifunctional column. The experiments showed that it could separate anions and cations simultaneously, so it was chosen as the separation column in this work.

Selection of eluent

There were several important factors for consideration in the selection of the eluent for the simultaneous determination of anions and cations. (a) The eluent should be capable of separating and eluting the analyte ions effectively, and contain both efficient cation- and anion-eluting ions for separating anions and cations simultaneously on one column. (b) The eluent must not produce a high response to the detector. When a UV detector is used, the eluents should be chosen to be non-absorptive or slightly absorptive at the UV wavelength used. When a chemically suppressed conductivity detector is used, the conductivity of the eluent should be suppressed easily. (c) A highly acidic eluent could cause partial protonation of weakly acidic nitrite anions. As a result, the effective ionic concentration and hence the sensitivity would decrease. It is clear that the concentration of hydrogen ions in the eluent should be low.

Based on the above considerations, a mixture of dilute hydrochloric acid and glycine (NH_2CH_2COOH) was chosen as eluent. The hydrogen ions in dilute hydrochloric acid could elute cations, whereas the chloride ion elute anions without oxidation or reduction reaction with nitrite or nitrate. Glycine is the simplest amino acid, its pK_{a_1} = 2.34 (K_{a_1} = 0.00457), pK_{a_2} = 9.60 and the pH of the isoelectric point is 5.97. If the concentration of hydrogen ions is above 4.6 m*M*, glycine exists mainly in the form of the protonated ion $HGly^+$. As the pH is increased, glycine passes through being a neutral molecular at its isoelectric point and finally becomes a monovalent anion at basic pH. Protonated ion $HGly^+$ is much more powerful for eluting cations than an eluent containing only hydrogen ions,

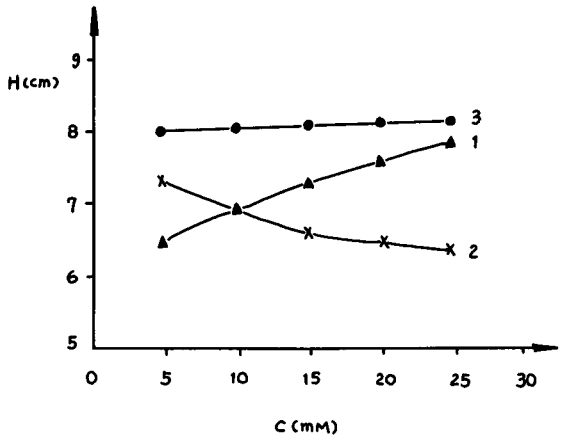

Fig. 2. Effect of HCl concentration on the peak heights of the three ions. 1 = NH_4^+; 2 = NO_2^-; 3 = NO_3^-.

so the elution of ammonia was accelerated. In addition to being powerful, eluents containing glycine have very low background conductivity after suppression [8], because glucine is either removed from the dynamic suppressor through the anion-exchange membrane into the regenerant stream, or is eluted from the suppressor as a neutral molecule as its isoelectric point is close to the effluent pH of the suppressor. This behaviour of glycine increased the sensitivity of ammonium detection.The presence of $HGly^+$ decreased the concentration of free hydrogen ions, hence the protonation of nitrite was decreased and the sensitivity of nitrite detection was increased.

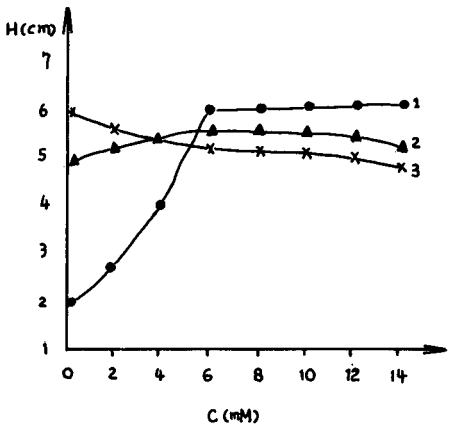

Fig. 3. Effect of glycine concentration on the peak heights of the three ions. 1 = NH_4^+; 2 = NO_2^-; 3 = NO_3^-.

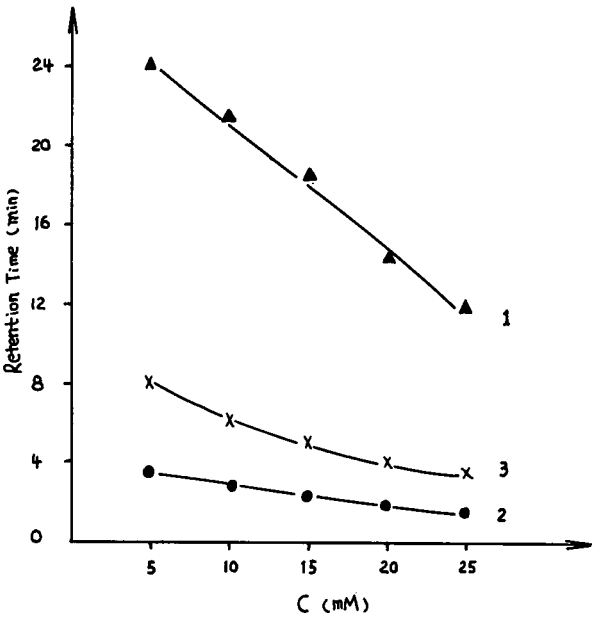

Fig. 4. Effect of the HCl concentration on the retention times of the three ions. 1 = NH_4^+; 2 = NO_2^-; 3 = NO_3^-.

The effect of the eluent concentration on the peak height and retention time is shown in Figs. 2–5. It was found that the concentration of glycine exerted

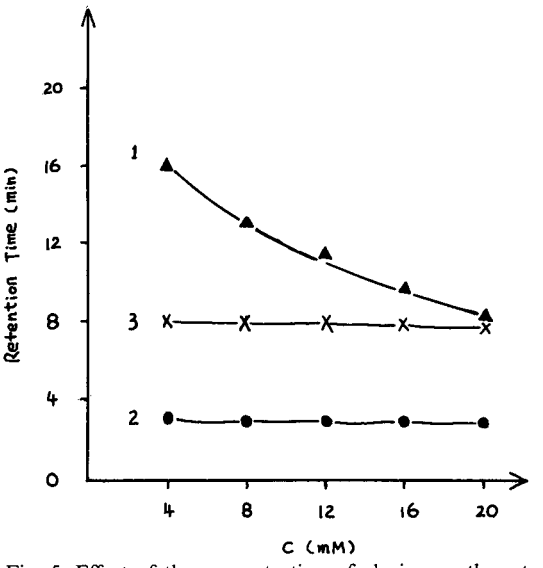

Fig. 5. Effect of the concentration of glycine on the retention times of the three ions at a constant concentration of 5 m*M* HCl. 1 = NH_4^+; 2 = NO_2^-; 3 = NO_3^-.

TABLE I

EFFECT OF FLOW-RATE ON PEAK HEIGHT, RETENTION TIME AND SYSTEM PRESSURE

Parameter	Ion	Flow-rate (ml/min)					
		3.3	3.0	2.5	2.0	1.5	1.0
Peak height (cm)	NO_2^-	7.6	7.5	7.2	7.0	6.5	5.8
	NH_4^+	8.9	8.7	8.5	8.2	7.8	6.5
	NO_3^-	6.8	6.6	6.4	6.1	5.8	5.0
Retention time (min)	NO_2^-	1.3	1.8	2.0	2.5	3.0	4.0
	NH_4^+	8.0	9.0	10.5	12.0	14.5	16.5
	NO_3^-	5.4	6.0	6.8	7.5	8.2	10.0
System pressure (p.s.i.)[a]		1700	1580	1420	1200	860	680

[a] 1 ps.i. = 6894.76 Pa.

TABLE II

LINEARITY, RELATIVE STANDARD DEVIATIONS (R.S.D.) AND DETECTION LIMITS FOR NITRITE, NITRATE AND AMMONIUM IONS

Ions	Linearity correlation coefficient	R.S.D. (%) (n = 9)	Detection limit (μg/l)
NH_4^+	0.9999 (0–20 ppm)	0.27	8
NO_2^-	0.9999 (0–40 ppm)	0.36	10
NO_3^-	0.9991 (0–20 ppm)	0.38	20

TABLE III

RECOVERIES OF NITRITE, NITRATE AND AMMONIUM IN REAL SAMPLES

Sample	Ion	Result (ppm)	Added	Recovery (%)
Acid rain	NH_4^+	2.7	2.50	101.48
	NO_3^-	3.55	2.50	102.40
	NO_2^-	0.05	5.00	99.00
Tap water	NH_4^+	0.36	2.50	103.60
	NO_3^-	13.73	2.50	104.60
	NO_2^-	0.0	5.00	98.43
Soil extraction solution	NH_4^+	0.42	2.50	99.60
	NO_3^-	7.85	2.50	101.72
	NO_2^-	1.36	5.00	97.45

a much greater influence on the peak height and retention time of ammonium than on those of nitrite and nitrate ions, as glycine was a powerful eluting cation for ammonium. When the hydrochloric acid concentration increased, the retention times of the three ions decreased; however, the peak height of nitrite became lower. In view of all the factors discussed, including the low pH of the eluent, large peak height, short retention time and good separation of the three ions, the optimum eluent composition selected was a mixture of 5 mM hydrochloric acid and 8 mM glycine.

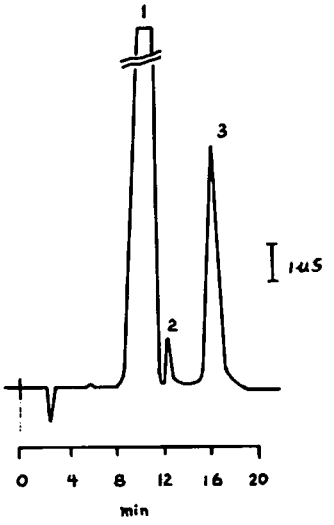

Fig. 6. Determination of ammonium ions in drinking water. Peaks: 1 = Na^+; 2 = NH_4^+; 3 = K^+.

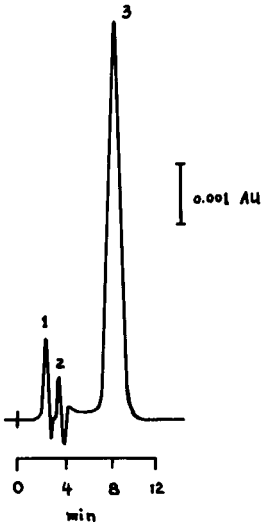

Fig. 7. Determination of nitrite and nitrate in soil. Peaks: 1 = Cl^-; 2 = NO_2^-; 3 = NO_3^-.

Table I shows the effect of the eluent flow-rate on peak height, retention time and system pressure. Considering the resolution and the pressure that the whole analytical system could withstand, 2.0 ml/min was chosen as the optimum eluent flow-rate.

Selectivity and detection limit

Although the method presented here has a high sensitivity towards alkali metals, there was no interference in the determination of ammonium when the concentrations of sodium and potassium ions were 100 times higher than that of ammonium ions. Divalent cations are very strongly retained on the HPIC-CS5 column and cannot be eluted by the eluent. They occupied the cation-exchange functional sites and shortened the retention time of ammonium ions. When the retention time of ammonium ions has halved, the divalent cations should be removed from the column with 0.2 *M* hydrochloric acid.

Because of the good resolution and non-absorption at 215 nm, common anions did not interfere with the detection of nitrite and nitrate.

In order to detect nitrite at low concentrations (< 0.05 ppm), the UV–Vis detector was set at a high sensitivity. Because glycine had a weak absorption at 215 nm, the water dip was large and interfered with the detection of nitrite at a high sensitivity setting. The watere dip, which elutes near the nitrite peak and interferes with this peak, can be eliminated by the addition of the equivalent of 0.1 ml of concentrated (100-fold) eluent to 10 ml of each standard and sample.

TABLE IV

COMPARISON OF THE RESULTS OBTAINED BY THE PROPOSED METHOD AND THE EPA METHOD [9]

Analyte	Concentration in synthetic sample (ppm)	Concentration found (ppm)	
		This method	EPA method
NH_4^+	5.00	5.15	5.10
NO_3^-	2.50	2.45	2.30
NO_2	2.00	2.00	2.10

Sample analysis

Table II shows the linearity, relative standard deviations and detection limits for the determination of the three ions. The results and recoveries for the analyses of water, acid rain and soil are given in Table III. Two typical chromatograms for sample analyses are shows in Figs. 6 and 7. A synthetic sample was analysed by the proposed method and an EPA standard method [9] and the results agreed well (Table IV).

REFERENCES

1 R. S. Nordhaus and J. M. Anderson, *J. Chromatogr.*, 549 (1991) 257.
2 V. K. Jones and J. G. Tarter, *J. Chromatogr.*, 312, (1984) 456.
3 D. M. Brown and D. J. Pietriyk, *J. Chromatogr.*, 466 (1991) 291.
4 J. G. Tarter, *J. Chromatogr. Sci.*, 27 (1989) 462.
5 P. J. Pietriyk, S. M. Senne and D. M. Brown, *J. Chromatogr.*, 101 (1991) 546.
6 C. Erkelens, H. A. H. Billiet, L. de Galan and E. W. B. de Leer, *J. Chromatogr.*, 404 (1987) 67.
7 *Application Note 118*, Dionex, Sunnyvale, CA, 1987.
8 R. D. Rocklin, *J. Chromatogr. Sci.*, 27 (1989) 474.
9 J. W. O'Dell, J. D. Pfaff, M. E. Gales and G. D. McKee, *Determination of Inorganic Anions in Water by Ion Chromatography, Method 300.0, EPA-600/4-84-017*, Environmental Protection Agency, Environmental Monitoring and Support Laboratory, Cincinnati, OH, 1984.

Journal of Chromatography, 640 (1993) 167–178
Elsevier Science Publishers B.V., Amsterdam

CHROMSYMP. 2733

Comparison of silica-based and polymer-based cation exchangers for the ion chromatographic separation of transition metals

Andreas Klingenberg and Andreas Seubert*

Institute of Inorganic Chemistry, University of Hannover, Callinstrasse 9, W-3000 Hannover 1 (Germany)

ABSTRACT

Silica gel- and polymer-based exchangers differ not only in the substrate but usually also in the structure of their sulphonic acid exchange group. The performance and chromatographic behaviour of modern macroporous poly(styrene–divinylbenzene) polymers of 5-μm particle size after surface sulphonation were examined. Further, two commercially available silica gel cation exchangers were investigated as references for what is now possible and how the chromatographic performance is influenced by the substrate and the structure of the exchange site. The influence of the capacity of surface-sulphonated exchangers for acid and complexing eluents, which are necessary when transition metals are to be separated, was studied. The interaction of polarizable metal cations with the π-system of the polymer depends on the resin capacity, and a comparable dependence for H^+ and complexing eluents was found. The distance of the functional group from the core influences the adsorption effects dramatically. Lowering the non-specific interaction increases the chromatographic efficiency rapidly. The performance of silica gel-based exchangers is nearly one order of magnitude better than that of surface-sulphonated exchangers. The selectivity of the exchangers investigated is strongly dependent on the structure of the exchange site and on the resin capacity.

INTRODUCTION

The application of cation chromatography (CIC) is routinely limited to the determination of alkali and alkaline earth metal ions in drinking water or high-purity water for microelectronic purposes [1–4]. The analysis of heavy and transition metals is normally done by atomic spectrometry, but CIC offers some unique advantages, namely non-destructive separation [1], speciation analysis [1,5–7], low absolute detection limits and low costs [8]. A specific advantage in comparison with atomic spectrometry is the ability to determine molecular ions such as ammonium compounds or alkyl–metal cations [1–4,9].

The combination of trace-matrix separation (TMS) via cation exchange and the preconcentration capabilities of ion exchangers allows ultratracé analyses in complex matrices such as refractory metals using CIC [8].

Modern powerfull HPLC cation exchangers are based on silica gel. The advantage of silica gel over polymers is their narrow particle size distribution, which is about half that for polymers. The functionalization is strictly held on the surface, which dominates for the observed rapid mass transfer [10,11].

A disadvantage for the routinely use of silica-based cation exchangers is the solubility of silica gel in all aqueous solvents, which leads to a continuous decrease in exchange capacity and also a decrease in chromatographic performance. This effect must be continuously compensated for by adjusting the elution system. Every elution system described in the literature in strongly dependent on the lifetime of the column used and therefore exactly reproducible only with substantial expertise. Drawbacks of silica gels for combined TMS and CIC separation is the

* Corresponding author.

0021-9673/93/$06.00

limited pH range of 2–7 and the incompatibility with fluoride-containing samples. These points are extremely important if trace separation and preconcentration are necessary [8].

The advantage of porous poly(styrene–divinylbenzene) (PS–DVB) packings is their high chemical stability. Nevertheless, PS–DVB materials show often a slow mass transfer through the chromatographic bead that leads to poor chromatographic efficiency [11]. An attempt to overcome this shortcoming was made by chemical modification of commercially available PS–DVB resins of 5 μm diameter, a narrow size distribution and extremely high cross-linking. The pore size of these resins is comparable to that of the most powerful cation exchangers based on silica gel. The resins were sulphonated with concentrated sulphuric acid and silver sulphate as catalyst. The exchange capacity, Q_g, of the resins was determined under different sulphonation conditions (reaction time and temperature) and varied in the range $Q(H^+)$ = 0.3–1.9 mmol/g.

A popular elution system for the analysis of the most common di- and trivalent ions is the tartaric acid–base system, where the base can be an alkali metal hydroxide or ammonium derivatives [8]. The analytical power of this elution system in combination with the chromatographic efficiency of the HPLC cation exchanger Nucleosil 5SA permits the simultaneous analysis of up to twelve ions in a single isocratic run (Fig. 1).

The most common silica based HPLC-exchangers, Nucleosil SA, RoSil CAT (now BioSil CAT) and a dynamically coated cation exchanger based on RoGel, were compared with laboratory-modified polymer exchangers for a better understanding of the separation processes.

For division of the elution behaviour of the tartaric acid–base system into a complexation-dominated part and a counter ion elution part, the selectivity coefficients for the polymer exchangers were evaluated with nitric acid as a protic eluent. This allows a comparison of the selectivity coefficients in acid and in complexing eluents.

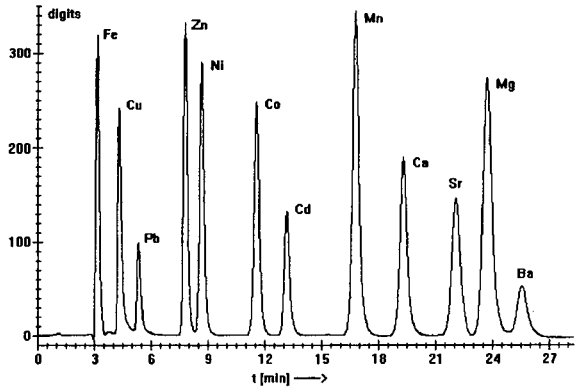

Fig. 1. Separation of twelve ions on a 300 mm × 4 mm I.D. Nucleosil 5SA column under optimized operating conditions [0.1 *M* tartrate (pH 3.3, adjusted with NH_3), flow-rate 1.0 ml/min].

EXPERIMENTAL

Column packings

The macroporous PS–DVB copolymers used in this work for the preparation of partially sulphonated ion exchangers were commercially available beads (RoGel SEC and RP) distributed by Bio-Rad Labs. (Munich, Germany). Their common application is in organic size-exclusion or reversed-phase chromatography. The degree of cross-linking is very high in order to guarantee HPLC conformity. The silica-based cation exchanger RoSil CAT was also obtained from Bio-Rad Labs. The widely used silica-based cation exchanger Nucleosil 5SA was supplied by Macherey–Nagel (Düren, Germany). All materials have an average core diameter of 5 μm and their general physical properties are given in Table I.

Sulphonation of polystyrene

The sulphonation of PS–DVB beads has been widely described [12–20]. The following procedure was finally used to produce homogeneous cation-exchange resins.

A 20-ml volume of concentrated sulphuric acid (96%) was placed in a 50-ml reaction vessel. After the addition of 0.1 g of silver sulphate as sulphonation catalyst the mixture was warmed to the desired reaction temperature. The catalyst was dissolved only by mechanical shaking. A portion of 1 g of dry resin was transferred to the reaction vessel and ultrasonically dispersed. The colour of the reaction mixture immediately turned from slightly yellow to dark brown. The beads were sulphonated for various reaction times (30 min–3 h) and at temperatures ranging from 0 to 87°C (see Table II). The reaction was quenched by removal of the liquid by filtration.

TABLE I

PHYSICAL PROPERTIES OF THE UNMODIFIED RESINS

Physical properties	RoGel SEC	RoGel SEC	RoGel RP	Nucleosil	RoSil
Particle size (μm)	5	5	5	5	5
Cross-linking	Very high	Very high	Very high	–	–
Maximum pressure (MPa)	20	20	20	60	80
Mean pore size, d_{p50} (nm)	3	7	7	10	9
Maximum pore size, d_{p10} (nm)	11	40	No specification	No specification	No specification
Surface area (m^2/g)	500	450	450	350	250
Pore volume (ml/g)	0.67	1.30	1.30	1.0	0.65
Maximum diameter, d_{p10} (nm)	No specification	7	7	6.5	6
Minimum diameter, d_{p10} (nm)	No specification	3	3	3.5	4

The resin was then suspended in 9 *M* H_2SO_4 to prevent breakage of the cores by sudden contact with aqueous solutions. After removal of the excess of sulphuric acid, the beads were washed in sequence with 3 *M* HCl, water, ethanol, water, 2 *M* ammonia solution, water and 1 *M* HCl. Subsequently the materials were refluxed with water for complete removal of residual acid. The grey to slightly brown products were filtered, dried and characterized [15,16,19,21]. A slurry technique was used for column packing of polymeric and silica-based materials.

TABLE II

SULPHONATION CONDITIONS AND OBSERVED CAPACITIES FOR DIFFERENT PS–DVB COPOLYMERS

Material	Reaction time (h)	Reaction temperature (°C)	Specific capacity (H^+) (mmol/g)
RoGel SEC (3 nm)	1	65	1.55
	1	30	0.72
	1	10	0.61
	1/2	0	0.34
RoGel RP (7 nm)	1	87	1.95
	1	0	0.45
	1/2	0	0.36
RoGel SEC (7 nm)	3	67	1.76
	1/2	0	0.34

Evaluation of the selectivity coefficient against H^+

The selectivity coefficients for several sample ions were determined with 4, 3, 2, 1, 0.5, 0.25 and 0.125 *M* nitric acid as eluents and inductively coupled plasma spectrometry (ICP-AES) for element-specific detection (simultaneous working type from Spectro A.I., Kleve, Germany). The instrumentation has been described in detail elsewhere [22].

Instrumentation

The HPLC system consisted of a Type 64 HPLC-pump (Knauer, Berlin, Germany), a pneumatic injection valve (Knauer) with a 20-μl sample loop, a Type 87.00 variable-wavelength detector and 100 mm × 4 mm I.D. stainless-steel columns (Vertex) as analytical column. Postcolumn detection of the ions was effected by reaction with 4-(2-pyridylazo) resorcinol (PAR), Zn–EDTA ($0.25 \cdot 10^{-4}$ *M* Zn–EDTA, $1 \cdot 10^{-4}$ *M* PAR, 2 *M* NH_3). The postcolumn reagent was added to the eluate in the postcolumn reactor by a single-piston HPLC pump (LDC Analytical). The absorbance of the eluate was monitored at 495 nm. The overall system control and the readout of the detector were processed by a computer system.

Reagents

All reagents were of high purity and standard solutions of the inorganic cations were prepared using 1000 mg/l stock standard solutions. Aliquots of

these stock standard solutions were used to prepare cation mixtures containing the ions to be investigated in a range 2–60 mg/l.

Eluent preparation

All eluents were prepared with tartaric acid (Fluka, microselect quality) and water purified with a Milli-Q system (Millipore) with a minimum resistivity of 18 MΩ. The pH was adjusted with 4 *M* NaOH (Merck, analytical-reagent grade, maximum 0.0002% K^+). The concentration of the eluents ranged from 0.1 to 0.25 *M* tartaric acid and their pH from 2.7 to 3.96.

To prepare a dynamically coated ion exchanger from the unmodified PS–DVB resins, 0.005 *M* dodecyl sulphonate solution was passed through the column until equilibration was achieved. The mobile phase was then changed to tartrate containing 0.002 *M* dodecyl sulphate to maintain the coating [23].

RESULTS AND DISCUSSION

Table III shows an overview of the exchangers investigated. The prepared polymer exchangers have volume capacities comparable to those of commercial silica gel-based exchangers.

Sulphonation behaviour of RoGel

The capacities of the sulphonated beads are given in Table II as function of reaction time and temperature. The capacities of the sulphonated resins are easily adjustable in the range 0.3–0.7 mmol/g and increase with increasing reaction temperature and time. The temperature is more important than the reaction time for the observed capacity, hence the temperature should be selected very carefully. The capacity $Q(H^+)$ of 2 mmol/g seems to be the maximum sulphonation grade possible with 96% sulphuric acid for these resins. Attempts to obtain higher capacities resulted in increasing breakage of the beads (Fig. 2).

No differences in the sulphonation behaviour could be determined for RoGel SEC and RoGel RP. The capacities reported [13,17] under similar sulphonation conditions as chosen are not comparable for low-cross-linked PS–DVB. The large surface area of the macroporous RoGel results in faster sulphonation of the core. Therefore, it can be assumed that the sulphonation is controlled by the surface area of the beads.

Selectivity coefficients in nitric acid

The fundamental exchange characteristics of a cation exchanger could be investigated with a

TABLE III

DESCRIPTION OF THE COLUMNS USED

Column	Short name	Surface sulphonated	Volume capacity (H^+) (mmol/ml)	Specific capacity per gram of resin (H^+) (mmol/g)
RoGel SEC (7 nm)	RoS7-34	Yes	0.135	0.34
RoGel RP (7 nm)	RoR7-36	Yes	0.142	0.36
RoGel SEC (3 nm)	RoS3-34	Yes	0.183	0.34
RoGel SEC (3 nm)	RoS3-61	Yes	0.301	0.61
RoGel SEC (7 nm)	RoS3-72	Yes	0.366	0.72
RoGel RP dodecyl sulphate	RoR7-Do			–
Nucleosil 5SA	Nucl-SA		0.151	
RoSil CAT (5 μm)	Rosil		0.374	
Only for H^+ measurements:				
RoGel RP (7 nm)	RoR7-45	Yes	0.117	0.45
RoGel SEC (3 nm)	RoS3-155	Yes	0.678	1.55
RoGel SEC (7 nm)	RoS7-176	Yes	0.701	1.76
RoGel RP (7 nm)	RoR7-195	Yes	0.838	1.95
AG 50W-X8 (< 400 mesh)	50W-X8	Yes	1.86	5.1
AG 50W-X16 (200–400 mesh)	50W-X16	Yes	2.02	5.1

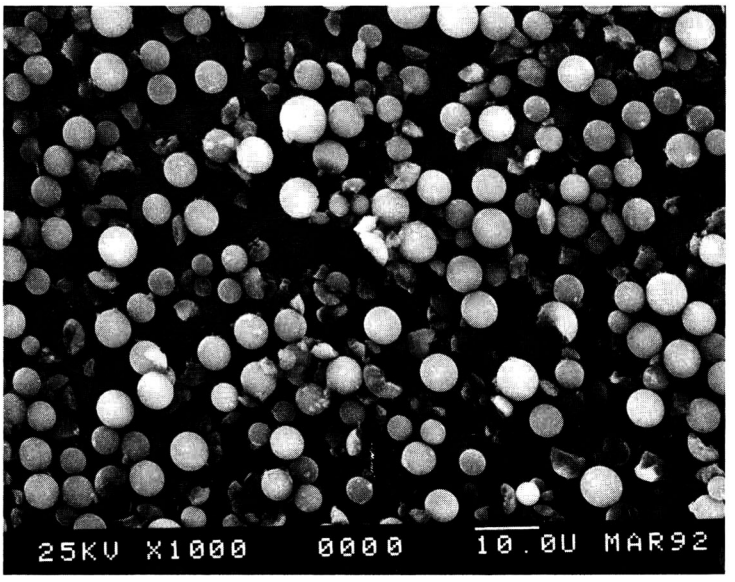

Fig. 2. Breakage of the RoGel PS–DVB cores obtained for high sulphonation grades.

strong acid as protic eluent. In this work nitric acid was used because of its low complexation tendency.

The affinity of a cation to a cation exchanger is normally described by the selectivity coefficient K_M^E, which is defined as the equilibrium constant of the ion-exchange reaction

$$n\,E^+R + M^{n+} \rightleftharpoons M^{n+}R_n + n\,E^+ \quad (1)$$

where E^+ is usually a monovalent eluent cation (in this study hydrogen or sodium), M^{n+} is the sample metal ion and R represents the cation exchanger. The term $[M^{n+}R_n]$ means the concentration of the analyte fixed at the exchange group. The selectivity coefficient for this reaction is

$$K_M^E = \frac{[M^{n+}R_n]\,[E^+]^n}{[E^+R]^n\,[M^{n+}]} \quad (2)$$

At low loading of sample ions, the term $[E^+R]$ is approximately equal to the resin capacity Q_v. The ratio $[M^{n+}R_n]\,/\,[M^{n+}]$ is given by the capacity factor k'. All terms in square brackets are volume concentrations. A plot of the product of the capacity factor and the reciprocal of resin capacity (volume capacity) *versus* the reciprocal of the square or cube (depending on the sample ion charge) of the eluent cation concentration gives as the slope the selectivity coefficient:

$$k'\,[Q_v]^{-n} = K_M^E \cdot [E^+]^{-n} \quad (3)$$

The selectivity coefficients for a number of ion-exchange resins are given in Table IV. The classical ion exchangers AG 50W-X8 and -X16 were investigated as references. Those resins are fully sulphonated and the observed selectivity coefficients are taken as a standard value for the selectivity caused only by ion exchange. The other exchangers are based on macroporous PS–DVB and have an increasing exchange capacity from 0.1 to 0.85 mmol/ml.

For ions with a high exchange density such as Mg^{2+}, Zn^{2+}, Ni^{2+} and Co^{2+} the selectivity coefficient is nearly independent of both the resin capacity and porosity. This behaviour is more evident for trivalent cations. Copper shows no dependence on resin capacity. More polarizable cations such as Cd^{2+}, Mn^{2+} and the alkaline earth metals Ca^{2+} and Ba^{2+} show a increasing selectivity coefficient with increasing capacity. The univalent K^+ ion shows a similar behaviour. The increase in the selectivity coefficient could be explained by adsorption.

TABLE IV

SELECTIVITY COEFFICIENT FOR VARIOUS CATION EXCHANGERS OBTAINED WITH NITRIC ACID ELUENTS

Element	Charge	Selectivity coefficient (K_M^E) for H^+						
		RoR7-45 (0.117)[a]	RoS3-61 (0.301)[a]	RoS3-155 (0.678)[a]	RoS7-176 (0.701)[a]	RoR7-195 (0.838)[a]	AG 50W-X8 (1.86)[a]	AG 50W-X16 (2.02)[a]
Al	3	27	15	9.6	8.9	7.5	10	10
Fe	3	60	54	36			14	13
Cr	3	28	19	11	12	9.6	11	11
Mg	2	2.6	2.0	1.9	2.2	1.9	2.6	2.7
Ca	2	4.4	11	15	25	28	5.1	7.4
Ba	2	12	25	38	67	78	13	14
Cu	2	3.6	3.7	3.9	4.6	4.0	3.0	3.4
Zn	2	2.9	2.6	2.65	3.1	2.7	2.9	2.3
Ni	2	2.9	2.5	2.5	2.8	2.4	3.0	2.1
Co	2	2.9	2.6	2.6	3.1	2.6	3.1	2.2
Cd	2	3.8	5.4	5.7	6.8	8.8	2.8	3.3
Mn	2	3.3	3.8	4.4	6.0	5.7	3.4	4.0
Pb	2	21	63	26	65	42	7.2	7.7
K	1	0.7	1.5	4.1	4.8	8.4	2.8	4.5
Na	1	0.5	0.5	1.13	1.5	2.1	1.3	1.6

[a] Volume capacity (mequiv./ml).

It should be noted that the extent of this non-specific interaction is correlated with the capacity of the resin.

Pb^{2+} always shows a higher selectivity coefficient on partially sulphonated macroporous resins than on the classical fully sulphonated microporous resins. The exchange group $-SO_3^-$ seems to be necessary to lower the distance between the sample ion and the residual hydrophobic surface of a partially sulphonated macroporous resin and therefore permits adsorption.

The selectivity coefficients for Al^{3+}, Fe^{3+} and Cr^{3+} ions are decrease strongly with increasing resin capacity. The values for high-capacity macroporous resins are similar to the values obtained for the microporous AG 50W exchangers. The extremely high selectivity coefficients at low capacities are probably caused by the large distance between the exchange sites, which does not allow interaction with the stochiometrically needed three $-SO_3^-$ groups.

Tartaric acid–base elution system

Elution systems for heavy and transition metals consists of a complexing reagent and a singly or doubly charged cation, which is normally delivered from the pH-adjusting base. The complexing reagent must be weak for a cation exchanger, otherwise the sample ion is fully complexed and no longer retained by cation exchangers. Most common complexing reagents are hydroxycarboxylic acids such as tartaric or citric acid. The elution mechanism is a combination of the mass action effect of the eluent cation and complexation of the sample ion, which lowers the actual sample ion concentration that interacts with the exchange sites.

Tartaric acid is a dibasic acid with close pK values. For a total ion strength of 0.1, $pK_{a_1} = 2.92$ and $pK_{a_2} = 4.09$ [26]. The greatest changes in the complexation behaviour should be obtained at pH values below pK_{a_1}; smaller changes should be obtained between pK_{a_1} and pK_{a_2}. The pH range between pK_{a_1} and pK_{a_2} was investigated in this work.

For a theoretical description of a complexing eluent, a factor α_M is defined [24,25], which represents the ratio between non-complexed and complexed sample ions in the solution:

$$[M'^{n+}] = \frac{[M^{n+}]}{\alpha_M} \quad (4)$$

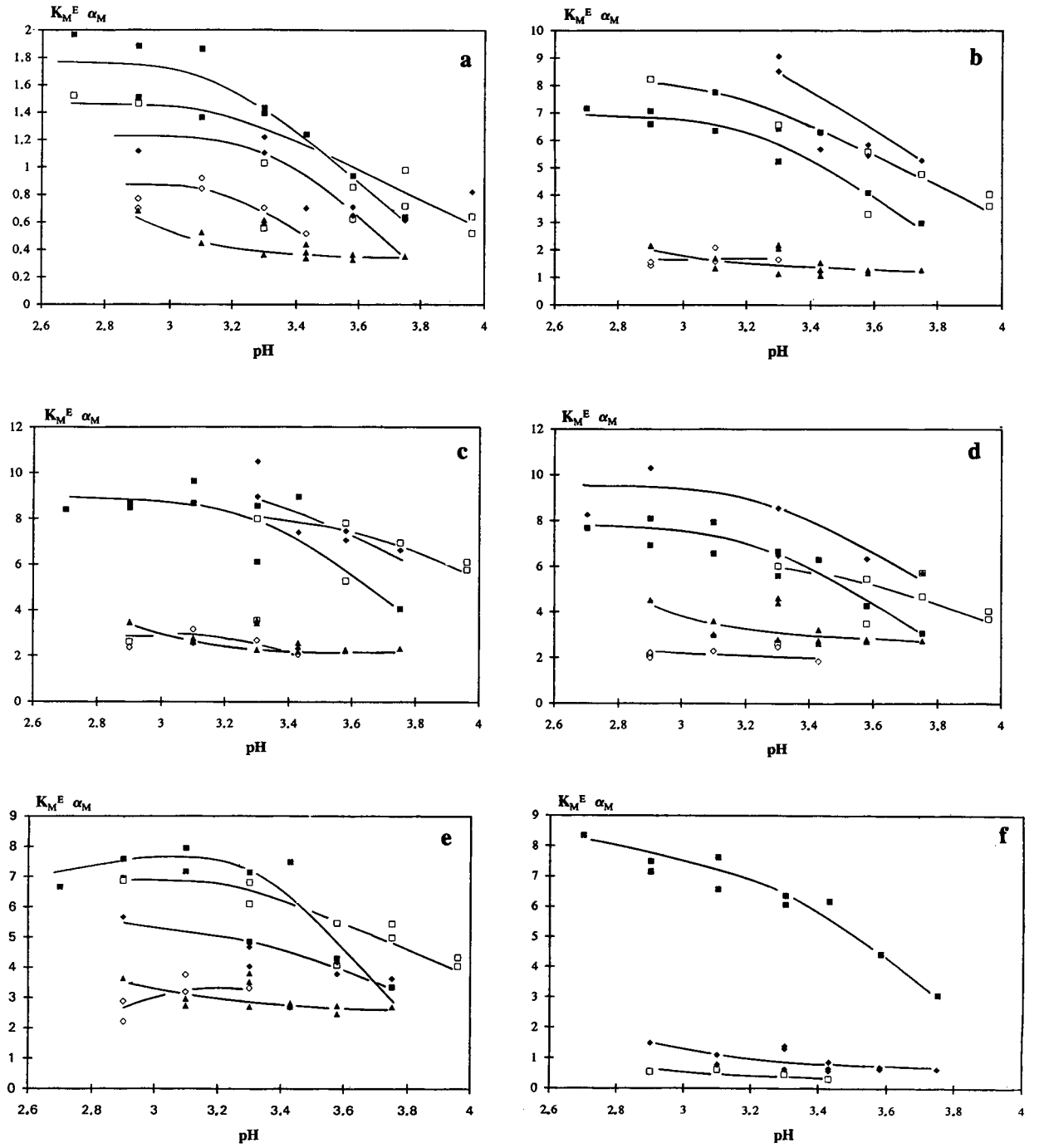

Fig. 3. Plot of the product of the selectivity coefficient, K_M^E, and the fraction of the uncomplexed sample ions in the solution, α_M, *versus* the pH of the tartrate eluent for (a) Zn, (b) Cd, (c) Mn, (d) Ca, (e) Mg and (f) Pb. (a–e) ■ = RoR7-34; □ = RoS3-61; ◆ = RoS3-72; ◇ = Nucl SA; ▲ = RoSil. (f) ■ = RoR7-34; □ = Nucl SA; ◇ = RoSil.

The modified eqn. 2 is now

$$K_M^E = \frac{[M^{n+}R_n]\,[E^+]^n}{[E^+R]^n\,[M'^{n+}]\alpha_M} \quad (5)$$

or, with $k' = [M^{n+}R_n] / [M^{n+}]$,

$$k'Q_v^{-n}\,[E^+]^n = K_M^E\,\alpha_M \quad (6)$$

A plot of $k'\,[Q_v]^{-n}\,[E^+]^n$ *versus* the pH of the eluent allows the product of the selectivity coefficient and α_M to be obtained. The α_M value should be constant for a given pH value, whereas differences between the K_M^E values are obtained. On the other hand, the K_M^E value should be constant for a given exchanger and a change in α_M caused by as pH change is obtained.

Fig. 3a–f show such diagrams for selected sample ions. Some ions such as the less polarizable Zn^{2+}, Ni^{2+},Co^{2+} and Mg^{2+} show only small differences between silica gel and polymeric exchangers. The polymeric exchangers generally have higher selectivity coefficients with an increasing tendency towards lower exchange capacities. This agrees with the behaviour of these ions against protic eluents.

The less polarizable Mn^{2+} ion shows a smaller increase in the selectivity coefficient with increasing resin capacity for surface-sulphonated exchangers than Cd^{2+}, Ca^{2+} and Pb^{2+} ions. This behaviour is not obvious for dynamically coated exchangers and for silica gel-based exchangers with their different exchange site structure. A detailed discussion of the effects is given later.

Comparison of polymer- and silica gel-based exchangers

Significant differences between silica gel and polymeric exchangers are the hydrophobicity of the substrate and the position of the functional group. The silica gel exchangers Nucleosil SA ($n = 3$) and RoSil CAT ($n = 1$) have an $R(CH_2)_nC_6H_4SO_3H$ group, whereas the sulphonic acid group of the polymeric exchangers is directly attached to the PS–DVB substrate. The HETP values (Table V) show the variation in performance with the sulphonic acid group location. The HETP values for silica gel exchangers are lower than those obtained for the polymer-based exchangers.

Division of the performance difference between surface-sulphonated exchangers and those with a distance between the exchange site and substrate into particle size distribution-dominated and exchange site structure-dominated parts is possible be generation of a dynamically coated exchanger based on the same substrate as the surface-sulphonated exchangers. The even lower HETP values for silica gel exchangers than observed for the dynamically coated exchanger are caused by the narrower particle size distribution, which is a typical advantage of silica gel substrates. It is not possible to produce PS–DVB exchangers at this quality level.

The observed changes in HETP for Mg as a late-eluting ion with no adsorption tendency are caused only by the slower mass transfer at the exchange site. Other elements such as Pb, Cd and Mn show

TABLE V

HETP VALUES (mm) FOR VARIOUS IONS UNDER THE SAME CHROMATOGRAPHIC CONDITIONS (0.175*M* TARTARIC ACID, pH 3.3 WITH NaOH) FOR DIFFERENT EXCHANGERS

Column	Zn^{2+}	Ni^{2+}	Co^{2+}	Cd^{2+}	Mn^{2+}	Ca^{2+}	Mg^{2+}	Pb^{2+}
RoGel SEC (7 nm, 0.34 mmol H^+/g)	0.20	0.23	0.14	0.24	0.20	0.16	0.14	1.47
RoGel RP (7 nm, 0.36 mmol H^+/g)	0.17	0.23	0.14	0.23	0.17	0.15	0.14	1.28
RoGel SEC (3 nm, 0.34 mmol H^+/g)	0.28	0.32	0.29	0.34	0.28	0.28	0.20	1.36
RoGel SEC (3 nm, 0.61 mmol H^+/g)	0.30	0.35	0.28	0.28	0.25	0.27	0.15	2.62
RoGel SEC (7 nm, 0.72 mmol H^+/g)	0.34	0.42	0.23	0.28	0.44	0.21	0.19	>3
RoGel RP dodecyl sulphate	0.12	0.14	0.11	0.11	0.11	0.16	0.084	0.315
Nucleosil 5SA	0.095	0.085	0.065	0.063	0.051	0.044	0.048	0.12
RoSil CAT (5 μm)	0.04	0.045	0.026	0.025	0.017	0.015	0.017	0.25

increased HETP values for the surface-sulphonated exchangers caused by an increase in the non-specific interaction with the polymer surface. The differences between the HETP values of elements with comparable retention times on surface-sulphonated exchangers such as Mg and Pb cannot be explained by different locations of the exchange groups such as *ortho-* and *para*-sulphonic acid groups [2]. For Pb the non-specific interaction seems to be an important part of the separation process.

The performance of RoSil CAT is nearly one order of magnitude better than those of surface-sulphonated resins; compared with Nucleosil SA there is a 2–4-fold better performance. On the one hand the chromatographic performance of RoSil CAT is excellent, but on the other the selectivity is not sufficient for the separation of Pb and Co or of Mn and Mg using the tartaric acid elution system (Fig. 4).

Resolution of selected sample ion pairs

The resolution of selected ion pairs is discussed with the help of the separation factor α as defined by

$$\alpha_{A/B} = k'_A / k'_B \quad (7)$$

Zn–Ni. These ions are normally not completely separated with surface-sulphonated polymeric exchangers using the tartaric acid elution system. Only silica gel-based exchangers and the dynamically coated exchangers are able to separate these ions. The selectivity data obtained are given in Table VI.

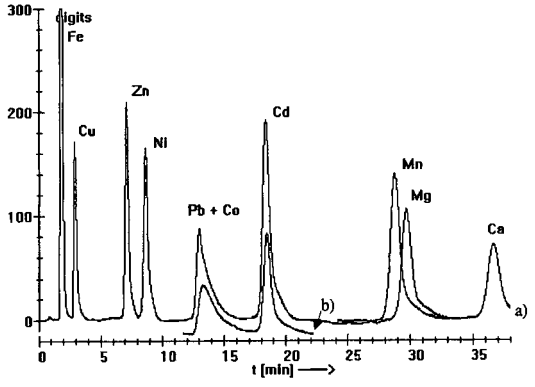

Fig. 4. Typical chromatogram obtained with RoSil CAT for a 100 × 4 mm I.D. column with 0.25 *M* tartrate (pH 2.9, adjusted with NaOH) and with a flow-rate of 1.0 ml/min. The overlaid chromatogram (b) shows the Pb peak without Co overlap.

TABLE VI

SELECTIVITY OBSERVED FOR Zn–Ni FOR DIFFERENT EXCHANGERS OBTAINED WITH 0.1–0.25 *M* TARTARIC ACID WITH pH RANGING FROM 2.7 TO 3.96 (ADJUSTED WITH NaOH) AND FOR THE PAIR Ni–Co AT A FIXED pH OF 3.3 AND 0.175 *M* TARTARIC ACID

Column	$\alpha_{Zn/Ni}$		$\alpha_{Ni/Co}$
	Value	R.S.D.[a] (%)	
RoGel SEC (7 nm, 0.34 mmol H^+/g)	1.11	2.6	1.88
RoGel RP (7 nm, 0.34 mmol H^+/g)	1.09	5.8	1.85
RoGel SEC (3 nm, 0.34 mmol H^+/g)	1.08	3.5	2.03
RoGel SEC (3 nm, 0.61 mmol H^+/g)	1.03	4.8	1.98
RoGel SEC (7 nm, 0.72 mmol H^+/g)	0.93	3.1	2.06
RoGel RP dodecyl sulphate	1.25	2.3	1.71
Nucleosil 5SA	1.19	2.4	1.45
RoSil CAT (5 μm)	1.28	3.7	1.70

[a] $n = 10$.

The low relative standard deviation (R.S.D.) of the observed selectivity over a wide pH range and for three different tartrate concentrations suggests that the resolution is independent of pH and eluent concentration. This is caused by the similar selectivity coefficients (Table IV) and the similar complexation behaviour of the two ions. For polymeric resins the selectivity is dependent on the resin capacity with an inversion point near 0.3 mmol/ml resin capacity (Table VI).

Ni–Co. These ions have very similar selectivity coefficients (Table IV); their separation is mainly caused by differences in their complexation behaviour. The selectivity generally increases with increasing pH; Fig. 5a displays two typical graphs for $\alpha_{Ni/Co}$ *vs.* pH. The offset between the different tartaric acid concentrations is probably caused by small differences in the selectivity coefficients against the sodium ion. This explains the tendency shown in Table VI for the different packing materials. $\alpha_{Ni/Co}$ is generally higher for surface-sulphonated PS–DVB packings than for modified silica gel or the dynamically coated exchanger.

Co–Cd. The selectivity coefficient for Cd increases strongly with increasing resin capacity. This dependence is similar for H^+ (Table IV) and Na^+ (Fig. 3b) as eluent cation. This is not evident for silica gel-based exchangers, whereas the selectivity

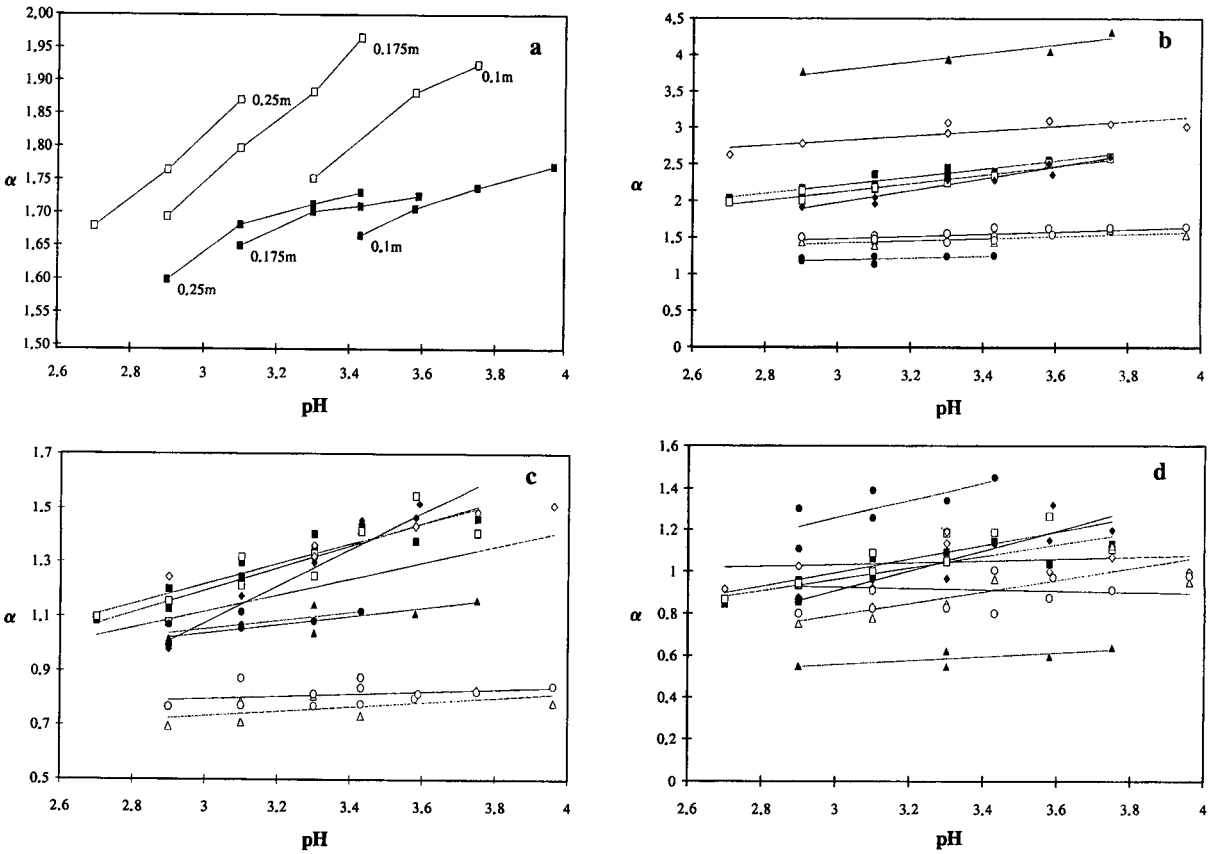

Fig. 5. Plot of the separation factor, α, *versus* pH for the ion pars (a) Ni–Co, (b) Co–Cd, (c) Ca–Mn and (d) Ca–Mg. (a) ■ = Rosil; □ = RoS7-34. (b–d) ■ = RoS7-34; □ = RoR7-36; ◆ = RoS3-34; ◇ = RoS3-61; ▲ = RoS3-72; △ = RoR7-Dodec; ● = Nucl SA; □ = Rosil.

coefficients are nearly independent of resin capacity (Fig. 3b). The Co^{2+} ion shows only a small dependence of the selectivity coefficient with an increase with decreasing capacity. The separation of the two ions is difficult only with silica gel-based exchangers; in comparison, the surface-sulphonated exchangers show selectivities ranging from 2 to 4 with an increase with increasing resin capacity (Fig. 5b). This is caused by the dominating increase of the selectivity coefficient for Cd. It should be noted that the behaviour of both ions is very similar on RoSil CAT and on the dynamically coated exchanger.

Ca–Mn. The separation of Ca and Mn is a difficult task with Nucleosil SA. Fig. 5c shows that both the higher capacity RoSil CAT and the dynamically coated exchanger with a similar capacity to RoSil CAT and also the surface-sulphonated exchangers permit a better separation of these ions RoSil CAT and the dynamically coated exchanger show an inverse elution order, Mn being eluted before Ca. This behaviour is caused by the different selectivity coefficients for Ca and Mn. This is the main effect which leads to the better separation observed for surface-sulphonated exchangers. Table IV and Fig. 3e and f show a small difference between the selectivity coefficients at low functionalization grades and a rapid increase for Ca with increasing capacity. For Mn only a small increase in the selectivity coefficient is observed. When the selectivity coefficients are nearly equal, the more stable Ca–tartaric acid complex {log β_1 (Ca–tart) = 1.7 [26]; log β_1 (Mn–tart) = 1.44 [27]} is dominant for the good

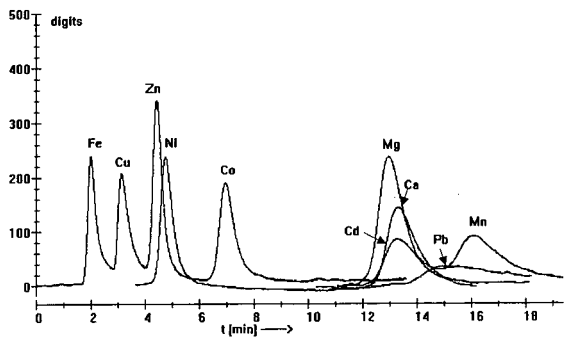

Fig. 6. Overlay of several chromatograms obtained with RoS7-34 for a 100 × 4 mm I.D. column with 0.175 *M* tartrate (pH 3.1, adjusted with NaOH) with a flow-rate of 1.0 ml/min.

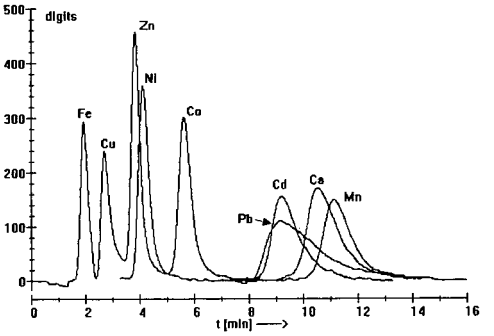

Fig. 7. Overlay of several chromatograms obtained with RoS3-61 for a 100 × 4 mm I.D. column with 0.25 *M* tartrate (pH 2.9, adjusted with NaOH) with a flow-rate of 1.0 ml/min.

separation of these ions. At higher resin capacities this different complexation behaviour is compensated for by the rapidly increasing selectivity coefficient for Ca.

Ca–Mg. Between these ions large differences in the complexation behaviour and in the selectivity coefficients are observed. Mg is only slightly complexed by tartrate, the elution being dominated by the mass action of the eluent cation. On the other hand, Ca forms stable tartrate complexes similarly to the Mn^{2+} ion.

Fig. 3e shows the dependence of the α_M value on pH for Mg and Fig. 3d that for Ca. The tendency is the same for both ions, but only for Ca is a significant difference between the two silica gel exchangers observable, which means that a dependence of the selectivity coefficient on the capacity of the exchanger is evident. This is in good agreement with the results of selectivity coefficient evaluations in nitric acid solutions (Table IV). The selectivity coefficients observed for surface-sulphonated resins increase with sodium as eluent cation for Mg with decreasing resin capacity; the behaviour of Ca is the opposite. This agrees with the selectivity coefficients obtained for H^+ as eluent cation.

The separation of Ca and Mg is strongly dependent on eluent pH, the separation factor increases for all resins with increasing pH. Only for the high-capacity surface-sulphonated resins and RoSil CAT does the separation factor for Ca and Mg decrease with increasing pH. On the other hand, the separation factor increases for low-capacity polymeric exchangers and for Nucleosil SA. Between these capacities the separation factor for Ca / Mg is very close to one and their separation is possible only with a high-performance column.

This tendency is also shown in Fig. 5d; the increasing separation factor is caused by an increase in complexation of the Ca^{2+} ion. The best resolution is obtained for the low-capacity Nucleosil SA with elution of Ca before Mg and for the highest capacity surface-sulphonated exchanger with an inverse elution order.

Pb. Lead is the sample ion with the greatest difference between the behaviour on silica gel- and polymer-based exchangers. It forms a relatively stable tartaric acid complex and has an extremly high selectivity coefficient. The higher the exchange capacity of the resin, the higher is the selectivity coefficient for lead. On surface-sulphonated polymeric resins an extremely high degree of adsorption is observed. At pH values higher than 3.1 Pb is eluted directly after Cd; below pH 3.1 Pb is eluted after Mg.

On Nucleosil SA Pb is eluted early between Cu and Zn. On RoSil CAT Pb is eluted closely after Co and on the dynamically coated exchanger just before Co. A sulphonic exchange group at a distance from the substrate lowers the selectivity coefficient for Pb. In addition, the HETP value decreases by nearly one order of magnitude.

CONCLUSIONS

The chromatographic performance of surface-sulphonated exchangers is in all instances well be-

low the performance obtained with silica gel exchangers (Figs. 1 and 4 compared with Figs. 6 and 7; Table 5). The use of modern PS–DVB substrates leads to a performance one order of magnitude below the standard set by the RoSil CAT exchanger. With elimination of the influence of different particle size distributions by generation of a dynamically coated exchanger, the performance is approximately five fold below that of Rosil CAT. This leads to the conclusion that the structure of the exchange site is extremely important for the chromatographic performance. Only a sulphonic acid group that is not directly attached to the substrate permits optimum performance.

The surface-sulphonated resins show substantial non-specific interaction for polarizable ions. This results for lead, for example, in poor performance with HETP values of 1.2–3 mm. The influence of adsorptive interactions on the selectivity coefficient increases with increasing resin capacity. This could be explained with help of the hydrophobic character of the substrate, which is only lowered at locations with a sulphonic acid group. A cation with a hydrophilic water cloud in the wider coordination sphere will only interact with the π-system of the core if the distance between the core and the polarizable cation is lowered by ion attraction of the exchange group.

In general, the selectivity coefficients increase at low capacities, which probably arise when the distance between the stochiometrically needed exchange sites becomes to great. This point is reached for trivalent cations at even higher volume capacities than for divalent cations.

The dynamically coated exchanger shows an exchange behaviour very similar to that of the silica gel-based RoSil CAT exchanger. The two silica gel-based exchangers show different selectivities owing to their different capacities, whereas the capacity of Nucleosil SA seems to be the optimum for the separation system investigated. The higher chromatographic performance of RoSil CAT is insufficient to solve separation problems caused by poorer selectivity characteristics for this elution system.

ACKNOWLEDGEMENTS

The authors thank G. Wünsch for his support of this work and R. Krismer of Metallwerk Plansee for the SEM pictures.

REFERENCES

1 J. Weiss, *Ionenchromatographie*, VCH, Weinheim, 2nd ed., 1991.
2 K. Dorfner, Ion Exchangers, Walter de Gruyter, Berlin, New York, 4th ed., 1991.
3 P. R. Haddad and P. E. Jackson, *Ion chromatography (Journal of Chromatography Library*, Vol. 46), Elsevier, Amsterdam, 1990.
4 D. T. Gjerde and J. S. Fritz, *Ion Chromatography*, Hüthig, Heidelberg, 2nd ed., 1987.
5 L. Dunemann and G. Schwedt, in *Trace Element Analytical Chemistry in Medicine and Biology —Proceedings of the 5th internatonal Workshop*, Walter de Gruyter, Berlin, New York, 1988, p. 99.
6 P. M. Bertsch and M. A. Anderson, *Anal. Chem.*, 61 (1989) 535.
7 F. Laborda, M. T. C. de Loos-Vollebregt and L. de Galan, *Spectrochim. Acta, Part B*, 46 (1991) 1089.
8 A. Seubert and G. Wünsch, *Anal. Chim. Acta*, 256 (1992) 331.
9 K. L. Jewett and F. E. Brinckman, *J. Chromatogr. Sci.*, 19 (1983) 583.
10 J. Gawdzik, B. Gawdzik and U. Czerwinska-Bil *Chromatographia*, 26 (1988) 399.
11 R. Wood, L. Cummings and T. Jupille, *J. Chromatogr. Sci.*, 18 (1980) 551.
12 J. S. Fritz and J. N. Story, *Anal. Chem.*, 46 (1974) 825.
13 J. S. Fritz and J. N. Story, *J. Chromatogr.*, 90 (1974) 267.
14 D. H. Freemen, S. Goldstein and G. Schmuckler, *Isr. J. Chem.*, 7 (1969) 741.
15 P. Hajos and J. Inczedy, *J. Chromatogr.*, 201 (1980) 253.
16 L. C. Hansen and T. W. Gilbert, *J. Chromatogr. Sci.*, 12 (1974) 458.
17 K. H. Lieser, *Radiochem. Radioanal. Lett.*, 18,5 (1974) 323.
18 K. W. Pepper, *J. Appl. Chem.*, 3 (1951) 124.
19 F. Schoebrechts, E. Mercing and G. Daylkaerts, *J. Chromatogr.*, 174 (1979) 351.
20 G. J. Sevenich and J. S. Fritz, *React. Polym.*, 4 (1986) 195.
21 P. Hajos and J. Inczedy, *J. Chromatogr.*, 201 (1980) 193.
22 A. Seubert, *Fresenius' J. Anal. Chem.*, 345 (1993) 547.
23 R. M. Cassidy and S. Elchuk, *Anal. Chem.*, 54 (1982) 1558.
24 G. J. Sevenich and J. S. Fritz, *J. Chromatogr.*, 371 (1986) 361.
25 G. J. Sevenich and J. S. Fritz, *Anal. Chem.*, 55 (1983) 12.
26 A. Ringbom, *Complexation in Analytical Chemistry*, Wiley-Interscience, New York, 1963.
27 J. Kragten, *Atlas of Metal–Ligand Equilibria in Aqueous Solution*, Ellis Horwood, Chichester, 1978.

Journal of Chromatography, 640 (1993) 179–185
Elsevier Science Publishers B.V., Amsterdam

CHROMSYMP. 2752

Ion-interaction chromatographic studies on metal ions complexed with Plasmocorinth B dye

Corrado Sarzanini*, Giovanni Sacchero, Maurizio Aceto, Ornella Abollino and Edoardo Mentasti

Department of Analytical Chemistry, Via P. Giuria 5, 10125 Turin (Italy)

ABSTRACT

The ion-interaction chromatographic behaviour of Plasmocorinth B (a disulphonated azo dye) and of its complexes formed with metal ions in oxidation states +2 and +3 (Cu^{2+}, Ni^{2+}, Al^{3+}, Co^{3+}, Fe^{3+}, Ga^{3+}) was investigated. The effect of cationic ion-pairing agents (tetramethyl-, benzyltrimethyl- and tetrabutylammonium) was also evaluated in the presence of alkali metal ions competitors (Li^+ and Na^+). The effects of organic modifier and of pH were also considered. The remarkably different behaviour of the ligand and the complexes suggests the formation of $M(II)L^-$ and $M(III)L_2^{2-}$. The stoichiometry of complexes was confirmed by applying the electrostatic theory derived from Gouy–Chapman and a modified Langmuir adsorption isotherm to the experimental data.

INTRODUCTION

Ion-interaction chromatography is an efficient and sensitive technique for the separation of heavy and transition metal ions [1–5]. These species may be separated as simple, hydrated ions or as anionic complexes, using suitable ligands. The ion-interaction reagent added to the eluent mixture is usually a strong base cation, such as the tetraalkylammonium ion, which is considered to give a dynamic equilibrium between the eluent and the stationary phase surface [6,7]. An increase in the organic solvent in the eluent decreases the interaction with the stationary phase [8], but pH and ionic strength also affect the equilibria involved in the separation [9–11]. Many studies have examined the retention mechanism [12–18] and, for a quantitative evaluation of the proposed models, the Gouy-Chapman theory associated with a modified Langmuir isotherm is a useful tool [17].

In this work the chromatographic behaviour of 3-(5-chloro-2-hydroxyphenylazo)-4,5-dihydroxynaphthalene-2,7-disulphonic acid (Plasmocorinth B, a disulphonated azo dye) and its metal ion complexes has been studied. PC acts as a planar tridentate ligand with a metal, forming five- and six-membered or two six-membered ring systems [18,19]. The evaluation of capacity factors (k') for Plasmocorinth B and its chelates with metal ions in different oxidation states (*e.g.* Cu^{2+} and Fe^{3+}), for different concentrations of ion interaction reagent, enabled us to determine or confirm the charge and the stoichiometry of the metal chelates.

The efficiency of different eluent compositions was also evaluated in order to optimize the separation of considered metal ions.

EXPERIMENTAL

Apparatus and reagents

The chromatographic system was a Varian LC 5000 liquid chromatograph (Varian, Walnut Creek, CA,USA) equipped with a Reodyne injection valve, a Varian spectrophotometric detector and a Vista 401 Data System. The analytical column was a LiChrospher 100 RP-18 (10 μm) (250 × 4 mm I.D.) column, coupled with a LiChroCART

* Corresponding author.

0021-9673/93/$06.00

100 RP-18 (5 μm) guard column (4 × 4 mm I.D.), both obtained from Merck (Darmstadt, Germany). Columns and tubings were cleaned daily with a methanol–water (50:50, v/v) solution for 1 h at a flow-rate of 1.0 ml/min. Absorption measurements and spectra were performed with a Hitachi 150-200 double-beam spectrophotometer. An Orion digital pH-meter (Orion, Cambridge, MA, USA) was used for pH measurements.

All solutions were prepared with high-purity water obtained from a Milli-Q System (Millipore, Bedford, MA, USA). Acetic acid, sodium hydroxide, methanol for chromatography and standard metal solutions (Cu^{2+}, Ni^{2+}, Al^{3+}, Co^{3+}, Fe^{3+} and Ga^{3+} chlorides at 1000 mg/l) were Merck analytical–grade products. Lithium nitrate, Plasmocorinth B (see Fig. 1), tetramethylammonium hydroxide (TMAOH), tetrabutylammonium hydroxide (TBAOH) and benzyltrimethylammonium hydroxide (BTMAOH) were obtained from Aldrich (Milwaukee, WI, USA).

Mobile phase

The mobile phases were methanol–water (50:50, v/v) mixtures unless otherwise stated. The optimized eluent composition was: 2.0 μ*M* Plasmocorinth B (ligand), 1.6 m*M* TBAOH (ion-interaction reagent), 6.2 m*M* sodium nitrate (ionic strength modifier), 10 m*M* acetic acid and sodium hydroxide up to pH 6.3. During the optimization the concentrations of TMAOH, TBAOH and BTMAOH ranged from 0 to 25.0 m*M*. The concentrations of sodium nitrate or lithium nitrate were from 0 to 0.25 *M* for studying the influence of ionic strength on capacity factors. The eluents were prepared daily, filtered on a 0.45-μm filter (Millipore HAWP 04700) and degassed under vacuum. In all experiments the flow-rate was 1.0 ml/min. The void volume of the chromatographic system was measured for every composition of mobile phase (without ion-interaction reagent present) by injection of a 100-μl sample of 0.5 m*M* sodium nitrate.

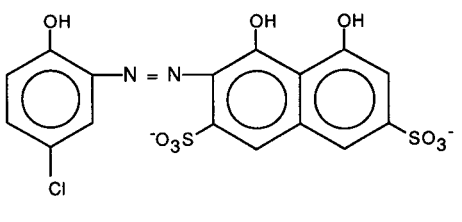

PLASMOCORINTH B

Fig. 1. Structure of Plasmocorinth B.

Samples

Appropriate quantities of metal stock solution (1000 mg/l) were added to an aqueous solution of 0.80 m*M* Plasmocorinth B (pH 5.3) to obtain the metal chelates in concentrations from 1 to 6 mg/l. pH was adjusted (1.0 *M* sodium hydroxide or lithium hydroxide) up to pH 6.3 in order to match that of the eluent; 100-μl sample volumes were analysed.

Detection

Before the chromatographic studies a detailed spectrophotometric study was performed on metal chelates. Plasmocorinth B exhibits two analytical peaks with maximum absorbance values at 270 and 527 nm. The wavelength of detection for chromatographic determinations of metal chelates was 270 nm because at this wavelength the maximum absorbance difference between metal complexes and Plasmocorinth B occurs.

RESULTS AND DISCUSSION

The parameters governing the separation of anion metal complexes by ion-interaction chromatography can be summarized as follows.

The pH affects the complex stability as well as the chromatographic separation. In this study the eluent was buffered to pH 6.3 with acetic acid and sodium or lithium hydroxide.

The ligand, added to the eluent, improves the complex stability. Experiments (0–4 μ*M* Plasmocorinth B) also showed that there is an improvement in the stability of the chromatographic baseline when the ligand is added. A concentration of 2.0 μ*M* Plasmocorinth B resulted in the best compromise, and this concentration was therefore used since an increase of ligand concentration results in higher background adsorbance.

The optimization of ion-interaction reagent and organic modifier concentrations such as ionic strength are detailed below.

Effect of ion-interaction reagents

The dependence of capacity factors (k') on the

concentration and type of ion-interaction reagent was evaluated for Plasmocorinth B and its complexes with Cu^{2+} and Fe^{3+}, chosen as reference metal ions. The effect of TMAOH, TBAOH and BTMAOH on the chromatographic elutions is shown in Fig. 2. It is shown that only TBA enables metal separation through a partition equilibrium between the solid and the mobile phase. The TBAOH was selected as the hydrophobic ion-interaction reagent. A more detailed study and a large number of experiments were performed to determine the difference in retention times, for Plasmocorinth B, Cu and Fe, as a function of TBAOH concentration. Fig. 3 shows that the magnitude of the retention increases with increasing TBAOH ion concentration. Each anion after a maximum shows a dramatic decrease in k', for TBAOH concentrations between 10 and 15 mM, followed by a subsequent increase until a plateau is reached. Increasing amounts of TBAOH in the mobile phase result in increased competition between the counter ion (*e.g.* nitrate) and the sample ion, as well as competition between free TBAOH and ion pairs for the surface of the stationary phase. Micelle formation could be advanced as an explanation for the reduced capacity factors at high TBAOH concentrations, but light-scattering experiments did not provide evidence of any detectable micelle formation.

It seems of interest to point out that divalent cations (Cu^{2+}, Ni^{2+}) have, at all TBAOH concentra-

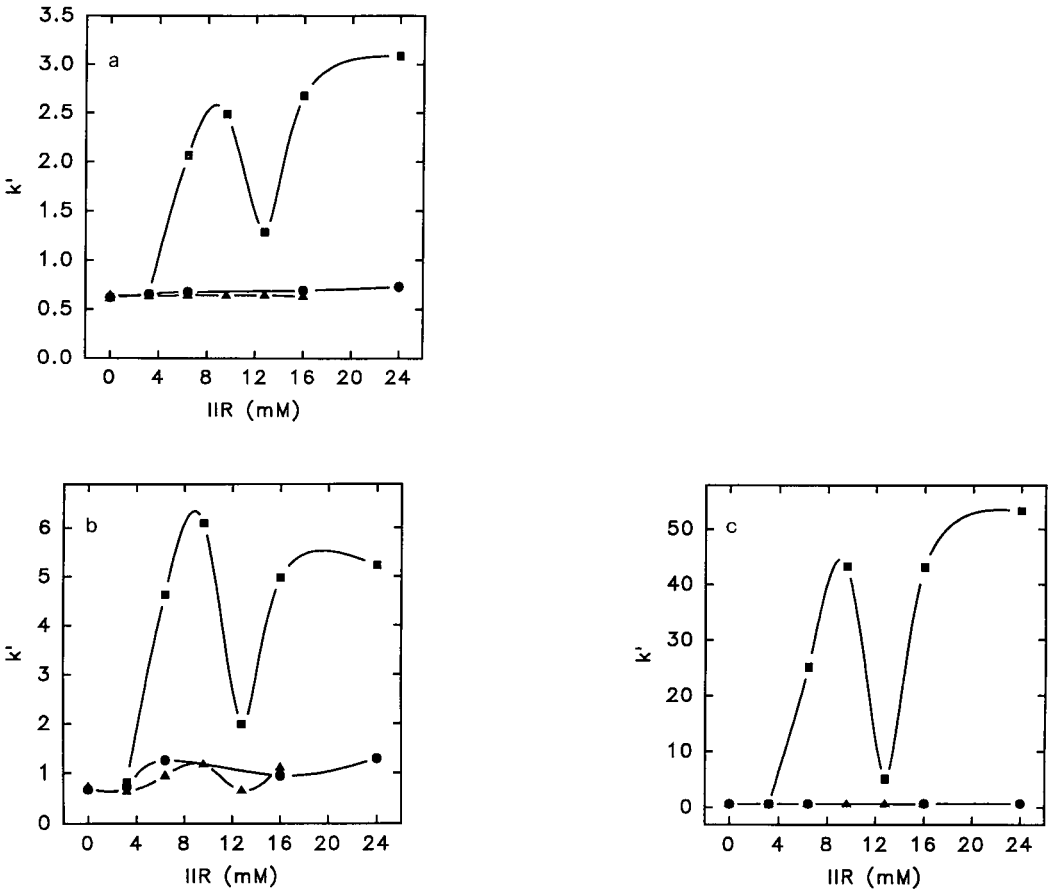

Fig. 2. Effect of ion-interaction reagents (IIR) on capacity factor (k') of (a) Cu, (b) Plasmocorinth B and (c) Fe. Chromatographic conditions: mobile phase, methanol–water (60:40, v/v) containing 19 mM acetic acid, 2.0 μM Plasmocorinth B, 15 mM sodium nitrate, sodium hydroxide up to pH 6.3; IIR: ■ = Tetrabutylammonium; ▲ = tetramethylammonium; ● = benzyltrimethylammonium, as shown. Injection volume, 100 μl; 2.0 mg/l Cu, 0.80 mM Plasmocorinth B, 6.0 mg/l Fe.

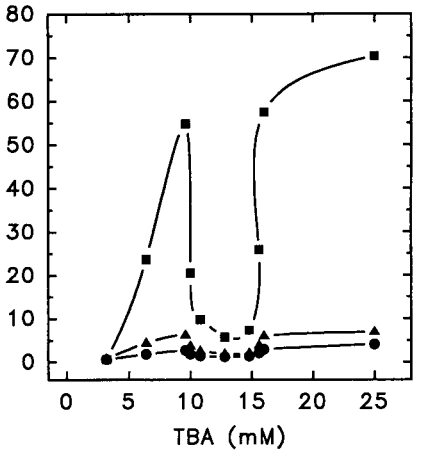

Fig. 3. Dependence of capacity factor (k') on tetrabutylammonium (TBA) concentration. Chromatographic conditions: mobile phase, methanol–water (60:40, v/v) containing 17 mM acetic acid, 2.0 μM Plasmocorinth B, 15 mM sodium nitrate, sodium hydroxide up to pH 6.3; TBA as shown. Injection volume, 100 μl; ● = 2.0 mg/l Cu; ▲ = 0.80 mM Plasmocorinth B; ■ = 6.0 mg/l Fe.

TABLE I

EFFECT OF IONIC STRENGTH (SODIUM NITRATE) ON CAPACITY FACTOR (k')

Chromatographic conditions: mobile phase, methanol–water (50:50, v/v) containing 10.0 mM acetic acid, 2.0 μM Plasmocorinth B (PC), 1.6 mM TBAOH, sodium hydroxide up to pH 6.3; flow-rate 1.0 ml/min; injection volume 100 μl; 0.80 mM Plasmocorinth B; 2.0 mg/l Cu; 6.0 mg/l Fe.

Sodium nitrate conc. (mM)	Capacity factor (k')			
	PC1	PC2	Cu(PC)	$Fe(PC)_2$
0	–	4.12	1.32	11.7
5	–	5.18	1.54	14.8
25	3.10	4.17	1.29	6.73
50	2.79	3.64	1.11	2.38
75	2.75	–	1.04	1.85
100	2.74	–	1.01	1.57
175	2.62	–	1.03	1.39
250	2.30	–	1.05	1.05

TABLE II

EFFECT OF IONIC STRENGTH (LITHIUM NITRATE) ON CAPACITY FACTOR (k')

Chromatographic conditions: mobile phase, methanol–water (50:50, v/v) containing 10.0 mM acetic acid, 2.0 μM Plasmocorinth B (PC), 1.6 mM TBA, lithium hydroxide up to pH 6.3; flow-rate 1.0 ml/min; injection volume 100 μl; 0.80 mM Plasmocorinth B; 2.0 mg/l Cu; 6.0 mg/l Fe.

Lithium nitrate conc. (mM)	Capacity factor (k')			
	PC1	PC2	Cu(PC)	$Fe(PC)_2$
0	–	4.12	1.32	11.7
5	–	4.65	1.44	14.6
25	2.93	3.89	1.28	9.23
50	2.54	3.61	1.27	3.96
75	2.51	–	1.25	1.65
100	2.43	–	1.22	1.40
175	2.59	–	1.18	1.38
250	2.46	–	1.11	1.11

tions, a capacity factor lower than Plasmocorinth B, and trivalent cations (Al^{3+}, Co^{3+}, Fe^{3+}, Ga^{3+}) show the opposite behavour. This may be explained by considering that trivalent cations are coordinated by two molecules of ligand, and the complexes have four sulphonato groups able to form ion pairs. This situation enables the formation of 1:2:2 (metal–ligand–ion-interaction reagent molar ratio) metal complex ion pairs, which show greater adsorption onto the stationary phase than 1:1:1 metal complex ion pairs of divalent metal ions. This explanation is supported also by the variation in k' with Plasmocorinth B concentration as a function of ionic strength (see below).

Effect of ionic strength

In order to evaluate the effect of ionic strength (I) and the counter cation of analytes, I was modified by using salts with the same anion and different cations (sodium nitrate or lithium nitrate). Tables I and II show the capacity factors for Plasmocorinth B and its complexes with Cu^{2+} and Fe^{3+} as a function of the ionic strength of eluent expressed as sodium nitrate or lithium nitrate molarity. The variation in k' is not affected by the presence of different cations, and this confirms that there is great competition between the nitrate counter anion and the analytes for ion-pairing TBA. Tables I and II include two species (PC1 and PC2) corresponding to two peaks that can be ascribed to the ligand. Fig. 4 shows the disappearance of one species and the ap-

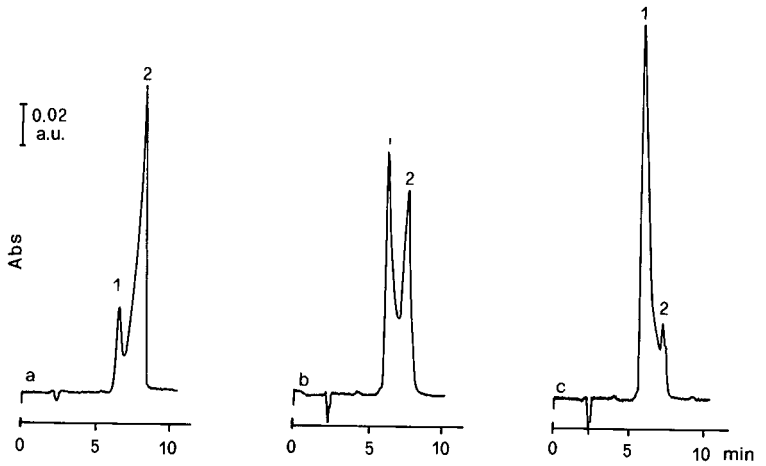

Fig. 4. Effect of sodium nitrate concentration on Plasmocorinth B (PC) chromatographic behaviour: 1 = PC(TBA); 2 = $PC(TBA)_2$. Chromatographic conditions: mobile phase, methanol–water (50:50, v/v) containing 10 m*M* acetic acid, 2.0 μM Plasmocorinth B, 1.6 m*M* TBA and sodium hydroxide up to pH 6.3; (a) 25 m*M* sodium nitrate; (b) 40 m*M* sodium nitrate; (3) 50 m*M* sodium nitrate; flow-rate 1.0 ml/min. Injection volume, 100 μl; 0.80 m*M* Plasmocorinth B; detection 270 nm.

pearance of another at lower retenton times by increasing *I*. This fact agrees with the point made above about the formation of two species with different stoichiometry, the first, 1:2 (Plasmocorinth B–TBA molar ratio), existing at low concentrations of anion competitor and the second, 1:1, due to the competition of nitrate for TBA counter ion.

Effect of organic modifier

The effect of organic modifier (methanol) concentrations was studied with reference to the chromatographic performance. Fig. 5 shows the behaviour of k' for Plasmocorinth B and metal complexes as a function of methanol concentration (v/v) in the eluent. In order to obtain reduced retention times with well resolved peaks as well as to reduce W/2 (width of the peak at half height), the best compromise for the next experiments required the use of a 50% methanol (v/v) concentrations.

Evaluation of complex stoichiometry

Experimental k' values obtained as a function of ion-interaction reagent concentration can give useful information on the charge of the complexes and on their stoichiometry.

An electrostatic theory for ion-pair chromatography has been formulated from the Gouy–Chapman equation coupled with a modified Langmuir adsorption isotherm [17,20]. This theory is summarized by the general expression:

$$\left(\frac{k'_c}{k'_{0c}}\right)^{-z_i/z} = f(C) \qquad (1)$$

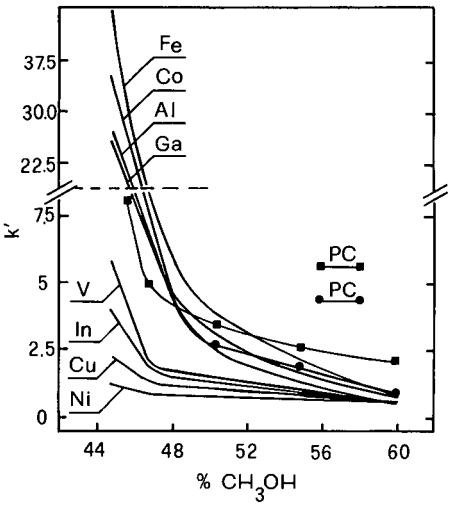

Fig. 5. Effect of methanol on capacity factor (k'). Chromatographic conditions: mobile phase, methanol–water, as shown, containing 10 m*M* acetic acid, 2.0 μM Plasmocorinth B (PC), 15 m*M* sodium nitrate 1.6 m*M* TBA and sodium hydroxide up to pH 6.3; methanol as shown. Injection volume, 100 μl; 0.80 m*M* Plasmocorinth B, 2–6 mg/l metals. ● = PC(TBA); ■ = $PC(TBA)_2$.

where k'_c and k'_{0c} are the capacity factors for an analyte at the concentrations c and zero of ion-interaction reagent; z_i is the charge of the ion-interaction reagent and z is the charge of the analyte. It must be pointed out that when no amphiphilic modifer is present in the mobile phase the electrostatic potential is set to zero. In addition, eqn. 1 is the same for different analytes and it is a function of the ion-interaction reagent concentration [20].

The higher retention time for complexes of trivalent metals in comparison with Plasmocorinth B is attributed to the 1:2 (metal to ligand ratio) stoichiometry of the complexes. We will consider now, for example, the iron–Plasmocorinth B (PC) complex: if the charge, z, for PC is -2, for $Fe(PC)_2$ it will be -4, and we can write:

$$\left(\frac{k'_{Fe}}{k'_{0Fe}}\right)^{1/4} = \left(\frac{k'_{PC}}{k'_{0PC}}\right)^{1/2} \quad (2)$$

by squaring the eqn. 2 and by collecting the constant terms in a, one obtains

$$k'_{Fe} = a(k'_{PC})^2 \quad (3)$$

Eqn. 3 becomes for 1:1 metal chelates [metal (M) to ligand ratio], *i.e.* Cu^{2+}:

$$k'_{Cu} = a(k'_{PC}) \quad (4)$$

Linear regression coefficients (R) for plots of k'_M *vs.* (k'_{PC}) or $(k'_{PC})^2$ were within 1.00 and 0.994 (three replicates for six points for each element). Copper and nickel complexes have a 1:1 metal to ligand molar ratio and a molecule of water is also coordinated [3,21]. This fact explains their reduced affinity for the stationary phase and their lower retention times compared with Plasmocorinth B molecules.

In conclusion, Fig. 6 shows the chromatogram, after optimization of the method, of a sample containing Co^{3+}, Cu^{2+}, Fe^{3+} and Ni^{2+} (2.0, 1.5, 3.0 and 1.0 mg/l, respectively). The metal ions are well separated and behaviour typical of divalent metals, ligand and tervalent metals is shown by their retention times. The procedure has been optimized in terms of preconcentration, separation and determination of metal ions at trace levels [22].

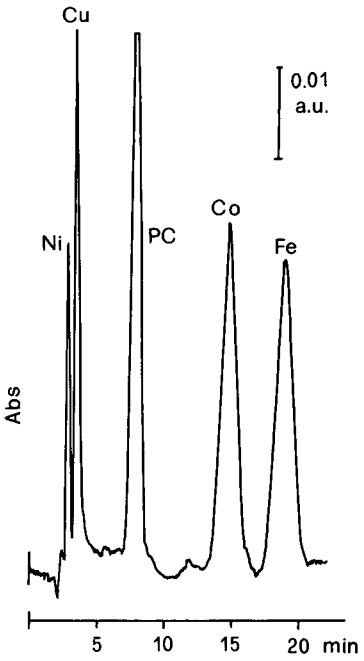

Fig. 6. Chromatogram of metal complexes. Chromatographic conditions: mobile phase, methanol–water (50:50, v/v) containing 10 mM acetic acid, 2.0 μM Plasmocorinth B (PC), 6.2 mM sodium nitrate, 1.6 mM TBA and sodium hydroxide up to pH 6.3; flow-rate 1.0 ml/min; injection volume, 100 μl; detection 270 nm. Peaks: 1.0 mg/l Ni; 1.5 mg/l Cu; 0.8 mM PC, 2.0 mg/l Co; 3.0 mg/l Fe.

ACKNOWLEDGEMENTS

Financial support from Ministero dell'Università a della Ricerca Scientifica e Tecnologica (MURST, Rome) and from the Italian National Research Council (CNR, Rome) is gratefully acknowledged.

REFERENCES

1 M. L. Marina, J. C. Diez-Masa and M. V. Dabrio, *J. High Resolut. Chromatogr. Chromatogr. Commun.*, 9 (1986) 300.
2 H. Siren, *Chromatographia*, 29 (1990) 144.
3 H. Hoshino, K. Nakano and T. Yotsuyanagi, *Analyst*, 115 (1990) 133.
4 G. Sacchero, O. Abollino, V. Porta, C. Sarzanini, E. Mentasti, *Chromatographia*, 31 (1991) 539.
5 A. R. Timerbaev, O. M. Petrukin, V. I. Orlov and A. A. Aratskova, *J. Liq. Chromatogr.*, 15 (1992) 1443.
6 A. Bartha and Gy. Vigh, *J. Chromatogr.*, 260 (1983) 337.
7 M. E. Del Rey and L. E. Vera-Avila, *J. Liq. Chromatogr.*, 10 (1987) 2911.

8 H. Zou, Y. Zhang and P. Lu, *J. Chromatogr.*, 545 (1991) 59.
9 W. E. Rudzinski, D. Bennet, V. Garcia and M. Seymour, *J. Chromatogr. Sci.*, 21 (1983) 57.
10 P. R. Haddad and P. E. Jackson, *Ion Chromatography, —Principles and Applications (Journal of Chromatography Library*, Vol. 46), Elsevier, Amsterdam, New York 1990, Ch. 6, p. 165.
11 Y. K. Zhang, H. F. Zou, M. F. Hong and P. C. Lu, *Chromatographia*, 32 (1991) 538.
12 B. A. Bidlingmeyer, S. N. Deming, W. P. Price Jr., B. Sachok and M. Petrusek, *J. Chromatogr.*, 186 (1979) 419.
13 A. Bartha and Gy. Vigh, *J. Chromatogr.*, 265 (1983) 171.
14 A. Bartha, H. A. H. Billiet, L. De Galan and Gy. Vigh, *J. Chromatogr.*, 291 (1984) 91.
15 Q. Xianren and W. Baeyens, *J. Chromatogr.*, 456 (1988) 267.
16 C. Petterson and G. Schill, *Chromatographia*, 28 (1989) 437.
17 J. Ståhlberg, *J. Chromatogr.*, 356 (1986) 231.
18 G. W. Latimer, Jr., *Talanta*, 15 (1968) 1.
19 R. G. Anderson and G. Nickless, *Talanta*, 14 (1967) 1221.
20 J. Ståhlberg and A. Furangen, *Chromatographia*, 24 (1987) 783.
21 C. Sarzanini, O. Abollino, M. De Luca and E. Mentasti, *Anal. Sci.*, 8 (1992) 210.
22 C. Sarzanini, G. Sacchero, M. Aceto, O. Abollino and E. Mentasti, *J. Chromatogr.*, 640 (1993) 127.

Journal of Chromatography, 640 (1993) 187–194
Elsevier Science Publishers B.V., Amsterdam

CHROMSYMP. 2670

Studies on the retention behaviour of α-hydroxyisobutyric acid complexes of thorium(IV) and uranyl ion in reversed-phase high-performance liquid chromatography

Hao Fuping and Paul R. Haddad*

Department of Chemistry, University of Tasmania, G.P.O. Box 252C, Hobart, Tasmania 7001 (Australia)

Peter E. Jackson and Joe Carnevale

Millipore Australia, Waters Chromatography Division, Private Bag 18, Lane Cove, N.S.W. 2066 (Australia)

ABSTRACT

The retention behaviour of complexes of thorium(IV) and uranyl ion with α-hydroxyisobutyric acid (HIBA) on a C_{18} reversed-phase column is investigated. Using a mobile phase comprising 400 m*M* HIBA at pH 4.0 in 10:90 (v/v) methanol–water, the thorium(IV) peak was eluted before the uranyl peak, despite the fact that calculations based on formation constants suggested that the thorium(IV) was present as the neutral tetra(HIBA) complex, whilst uranyl was present as the anionic tris(HIBA) complex. Hydrolysis of the thorium-(IV) complex (with subsequent inclusion of hydroxyl in the coordination sphere of the metal ion and formation of an overall negative charge) is proposed as a likely explanation for the early elution of this complex. When the percentage of methanol in the mobile phase was varied, both thorium(IV) and uranyl complexes exhibited reversed-phase behaviour. The retention times of both complexes decreased when the concentration of HIBA in the mobile phase was increased over the range 50–600 m*M*, despite the fact that increased complexation should be favoured. This effect was attributed to competition for the adsorption sites on the stationary phase by neutral, protonated HIBA in the mobile phase. A retention mechanism based on hydrophobic adsorption (rather than cation-exchange) is suggested.

INTRODUCTION

Ion-interaction chromatography using dynamically coated columns has been applied widely to the separation of lanthanides [1–3]. In this method, a C_{18} column is generally used and is coated with sodium *n*-octanesulphonate (OSA) as the ion-interaction reagent (IIR) to convert it into a dynamically coated cation-exchange column. A suitable ligand, usually α-hydroxyisobutyric acid (HIBA), is added to the mobile phase and serves the purpose of reducing the effective charge on the injected metal ions and so enabling them to be eluted within a reasonable time. Detection has generally been performed by spectrophotometry after post-column reaction with a suitable dye, usually 3,6-bis[(*o*-arsenophenyl)azo]-4,5-dihydroxy-2,7-naphthalenedisulfonic acid (Arsenazo III) or 4-(2-pyridylazo)resorcinol (PAR). The advantage of ion-interaction chromatography is the ease with which the column ion-exchange capacity and selectivity can be altered. Several studies have confirmed that the lanthanide ions are separated predominantly by a cation-exchange mechanism with retention being moderated by the complexing effects of the eluent ligand. Gradient elution may be effected in these systems by progressively increasing the concentration of HIBA in the mobile phase [1].

In the course of these studies it has been noted that thorium(IV) and uranium(VI) (as uranyl ion) were eluted in the early part of the chromatogram

* Corresponding author.

0021-9673/93/$06.00

and showed similar retention times to some of the lanthanides. However, when eluent parameters were varied, the behaviour of thorium(IV) and uranyl showed some differences to that of the lanthanides, suggesting that a different retention mechanism could be operating. Thorium(IV) and uranyl could either be eluted amongst the lanthanides or after them by varying the OSA concentration in the mobile phase. Retention of thorium(IV) and uranyl as HIBA complexes on a C_{18} column was then demonstrated without the presence of an anionic IIR (such as OSA) in the mobile phase and this effect was used subsequently as a means to preconcentrate these species [4,5]. When the eluent ligand was changed to mandelic acid, thorium(IV) and uranyl showed greater retention than the lanthanides and again could be retained without the use of an anionic IIR in the mobile phase [6].

Whilst some of the factors influencing retention of HIBA complexes of thorium(IV) and uranyl have been reported, the mechanism of their retention on a reversed-phase column remains unclear. In the present study we have examined in detail the factors which affect retention and have related the trends observed to the nature of the complexes which exist under the chromatographic conditions used. A coherent retention mechanism is then described and used to derive chromatographic conditions suitable for the determination of thorium(IV) and uranyl using a solid-phase preconcentration procedure.

EXPERIMENTAL

Instrumentation

The HPLC system consisted of a Millipore–Waters (Milford, MA, USA) Model 590 programmable pump, a Model U6K injector and a Model 481 UV–Vis spectrophotometric detector couped to a Waters 820 chromatography data station. The detector was operated at 658 nm. The analytical column was a Waters μBondapak C_{18} reversed-phase column (300 × 3.9 mm I.D.), fitted with a C_{18} guard column housed in a Waters Guard-Pak precolumn module. The post-column reagent solution was delivered with a Waters reagent delivery module.

Reagents and procedures

The mobile phase was prepared using HIBA (Sigma, St. Louis, MO, USA), HPLC-grade methanol (Millipore–Waters) and water treated with a Millipore (Bedford, MA, USA) Milli-Q water purification system. The most commonly used mobile phase comprised 400 m*M* HIBA and 10% methanol, adjusted to pH 4.0 with sodium hydroxide. The post-column reagent solution contained 0.13 m*M* Arsenazo III (BDH Laboratory Chemical Division, UK), 10 m*M* urea (May & Baker, Dagenham, UK) and 62 m*M* acetic acid in Milli-Q water. Both the mobile phase and the post-column regent solution were filtered through a Millipore 0.45-μm membrane and degassed in a ultrasonic bath prior to use.

Thorium and uranium standards were prepared from thorium(IV) nitrate (May & Baker) and uranyl nitrate (Ajax Chemicals, Sydney, Australia), respectively. Stock solutions of 1000 mg/l were prepared initially and were further diluted as required.

The column was re-equilibrated with each new mobile phase for at least 20 min prior to injections being made. All experiments were carried out at room temperature, except in the studies on the effect of temperature on retention, in which case a Waters temperature control module was used. Each data point throughout this research was obtained at least in duplicate.

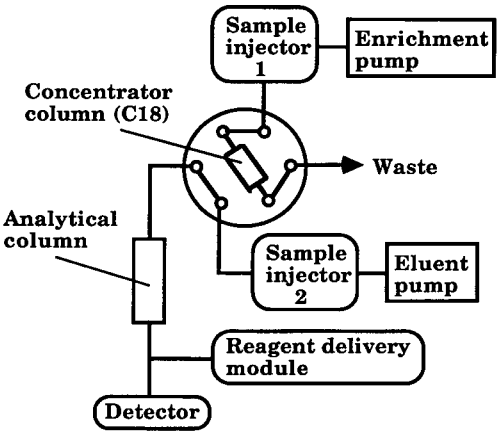

Fig 1. Schematic representation of the preconcentration system used. Note that two injectors were used so that samples could be applied either by direct injection (injector 2) or using preconcentration (injector 1).

Preconcentration studies

For the preconcentration procedure the apparatus was configured as shown in Fig. 1, in which a six-port high-pressure switching valve was added between the injector and the analytical column. The sample was prepared in 20 m*M* HIBA solution at pH 4.0 and a 1.0-ml portion was loaded into injector 1 (which was fitted with a 2-ml loop) and pumped through a Waters μBondapak C_{18} guard column, using 40 m*M* acetic acid (pH 4.0) as the driving solvent, using the enrichment pump. The valve was then rotated and the adsorbed complexes back-flushed onto the analytical column using the normal eluent. The switching sequence used to control the valves was performed through the Waters 820 chromatography data station. Direct injection of samples was possible using sample injector 2 in Fig. 1.

RESULTS AND DISCUSSION

Selection of eluent ligand

Polyvalent cations, such as UO_2^{2+} and Th^{4+}, are not suited to direct cation-exchange methods because the magnitude of the electrostatic interaction of these species with the functional groups on the ion exchanger is such that these cations are very strongly retained. They are best separated chromatographically as complexes with a suitable ligand and these complexes can be formed either prior to the separation step or *in situ* by adding the ligand to the mobile phase. In general, the latter approach is the more convenient and was pursued in this work.

Thorium(IV) and uranyl are known to form complexes with a wide range of ligands, with the most stable complexes being with hydroxycarboxylic acids, such as glycolic, mandelic, lactic and hydroxybutyric acids [7]. The overall formation constants observed for HIBA are amongst the highest and are given in Table I. The distribution of the various complexes of HIBA with thorium(IV) and uranyl as a function of HIBA concentration in the range 0–200 m*M* is given in Figs. 2 and 3, respectively. These distributions were calculated using a pH of 4.0, at which point the HIBA (pK_a = 3.77) is 63% ionised.

TABLE I

OVERALL FORMATION CONSTANTS FOR THORIUM(IV) AND URANYL COMPLEXES WITH HIBA IN AQUEOUS SOLUTION

Measured in 1 *M* $NaClO_4$ at 20°C. Data from refs. 7 and 8.

Species	log β_1	log β_2	log β_3	log β_4
Thorium(IV)	4.43	8.15	11.06	13.60
Uranyl	3.18	5.13	6.67	–

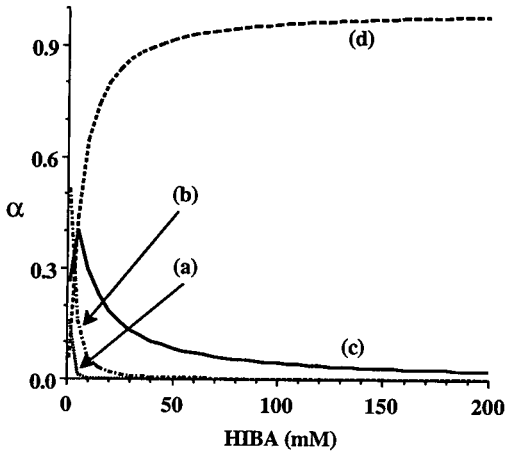

Fig. 2. Fraction (α) of each thorium(IV)–HIBA complex present at various concentrations of HIBA at pH 4.0. (a) $Th(HIBA)^{3+}$; (b) $Th(HIBA)_2^{2+}$; (c) $Th(HIBA)_3^{+}$; (d) $Th(HIBA)_4$. Calculated using the formation constants given in Table I.

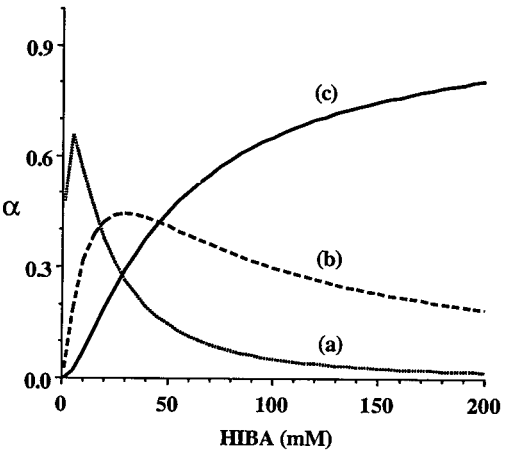

Fig. 3. Fraction (α) of each uranyl–HIBA complex present at various concentrations of HIBA at pH 4.0. (a) $UO_2(HIBA)^+$; (b) $UO_2(HIBA)_2$; (c) $UO_2(HIBA)_3^-$. Calculated using the formation constants given in Table I.

This pH was chosen because it is near to that of the maximum buffer capacity for HIBA. These figures may be used to select experimental conditions under which only one type of complex with each metal ion is present in solution so that the resultant chromatography can be simplified. Fig. 2 shows that the tetra(HIBA) complex of thorium(IV) dominates at most HIBA concentrations. This species does not become the sole complex present until the HIBA concentration reaches at least 400 m*M* (not shown in Fig. 2). On the other hand Fig. 3 shows that the distribution of HIBA complexes with uranyl varies markedly with HIBA concentration. Even at 400 m*M* HIBA, the uranyl ion is distributed chiefly as the tris(HIBA) complex (89.4%) and the bis(HIBA) complex (10.1%). If thorium(IV) and uranyl were injected into a 400 m*M* HIBA solution buffered at pH 4.0, it would therefore be expected that the thorium would be present solely as the tetra(HIBA) complex, whilst the uranyl would be present predominantly as the tris(HIBA) complex. Since HIBA can be expected to be present in its deprotonated form in metal complexes, the thorium complex should be neutral, whilst the uranyl complex should be anionic.

Selection of a suitable chromatographic method can be based on these predictions, and reversed-phase chromatography should be appropriate for thorium and anion-exchange chromatography (or ion-interaction chromatography using a cationic IIR) for uranyl. When reversed-phase chromatography was examined using a C_{18} column with a mobile phase comprising 10% methanol and 400 m*M* HIBA at pH 4, the chromatogram shown in Fig. 4 resulted. The observed elution order was opposite to that expected from Figs. 2 and 3 in that the uranyl complex [presumed to be anionic and containing fewer ligand molecules than the thorium(IV) complex] was the more strongly retained. Further studies were therefore undertaken to determine the factors affecting retention and to elucidate the retention mechanism.

Factors affecting retention

The influence of the percentage of organic modifier in the mobile phase is shown in Fig. 5, using methanol as the modifier. Retention changes were measured over the range 0–20% methanol at 400 m*M* HIBA for both thorium(IV) and uranyl, and at

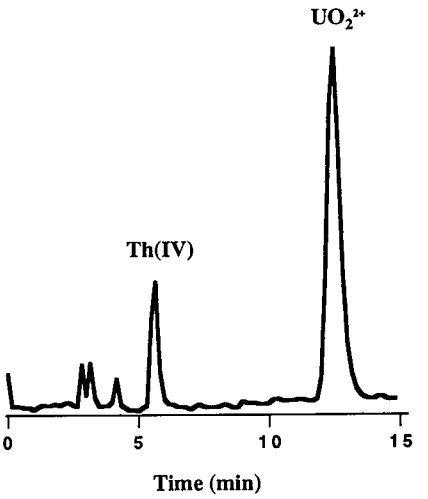

Fig. 4. Chromatogram of thorium(IV) (1.0 ppm) and uranyl (4.0 mg/l). Conditions: Waters μBondapak C_{18} column, mobile phase of 400 m*M* HIBA at pH 4.0 in 10:90 (v/v) methanol–water at a flow-rate of 1 ml/min. Detection by absorbance at 658 nm after post-column reaction with Arsenazo III.

20 m*M* HIBA for thorium(IV). For comparison, the retention of a neutral reference compound (in this case, phenol) was also measured and is included in Fig. 5. In all cases, linear plots of log *k'* *versus* the percentage of methanol were obtained, indicating that these solutes were being retained by a reversed-phase mechanism. It will be noted that this conclusion applies for the thorium(IV) complex even when

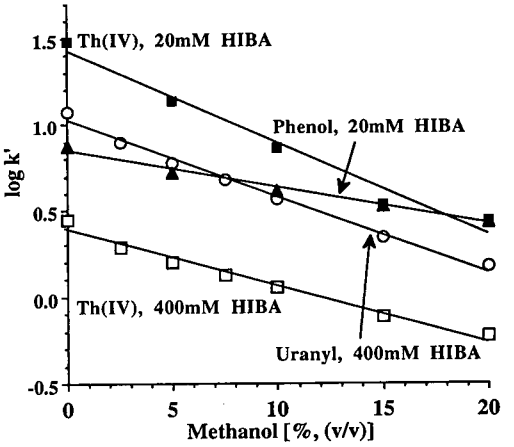

Fig. 5. Effect on retention of varying percentages of methanol in the mobile phase. With the exception of the methanol concentration, chromatographic conditions were as for Fig. 4.

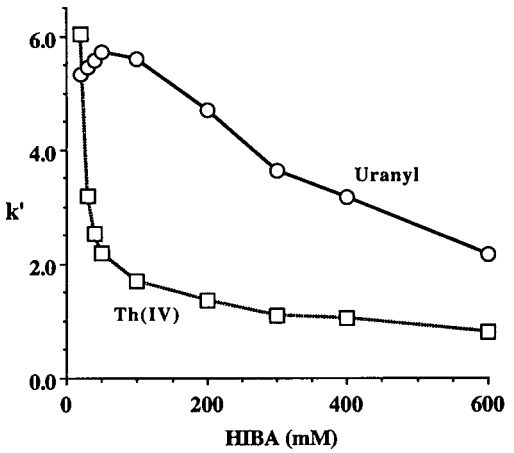

Fig. 6. Dependence of capacity factors for thorium(IV) and uranyl on the concentration of HIBA in the mobile phase. With the exception of the HIBA concentration, chromatographic conditions were as for Fig. 4.

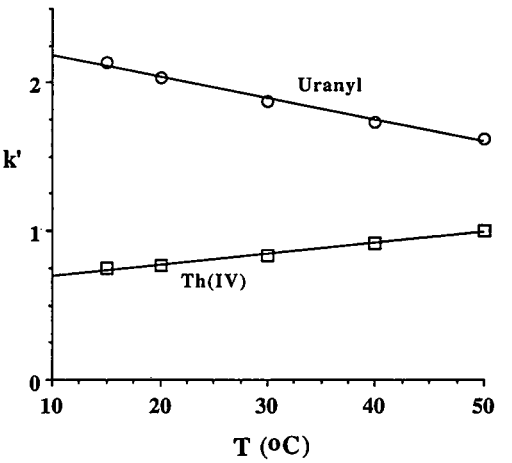

Fig. 7. Effect of temperature on capacity factors of thorium(IV) and uranyl. With the exception of the temperature, chromatographic conditions were as for Fig. 3.

the HIBA concentration is as low as 20 m*M*. Results similar to those shown for methanol were also obtained using acetonitrile (over the range 0–15%) as the organic modifier.

The effect of the concentration of HIBA on retention is shown in Fig. 6, which indicates that the capacity factors for both thorium(IV) and uranyl decreased overall with increasing HIBA concentration, with the most rapid changes being observed for thorium(IV) at HIBA concentrations of less than 50 m*M*. It should be possible to compare these observations with the predicted forms of the metals complexes shown in Figs. 2 and 3, however, contradictions emerge. In the range 0–50 m*M* HIBA, Fig. 2 suggests that there is an increasing proportion of the neutral thorium(IV) tetra(HIBA) complex present, so that one would expect retention to increase progressively as the HIBA concentration is raised. The opposite trend occurs in Fig. 5. Similarly, the proportion of the uranyl tris(HIBA) complex rises progressively over the range 100–200 m*M* HIBA, but retention decreases.

TABLE II

EFFECTS OF MOBILE PHASE pH ON RETENTION

The mobile phase comprised 50 m*M* HIBA (pH 4.0) and 20% methanol. The retention time of phenol was unaltered over the pH range studied.

pH	Retention time (min)	
	Thorium(IV)	Uranyl
2.5	4.5	4.1
3.0	4.9	5.3
3.5	5.2	6.7
4.0	5.9	9.5
4.5	8.8	16.0

The mobile phase pH was varied over the range 2.5–4.5 and the retention times of both thorium(IV) and uranyl were found to increase, as shown in Table II. The effect of variation of the temperature of the mobile phase on capacity factor was also studied and the results are shown in Fig. 7. The progressive decrease in capacity factor for uranyl with increasing temperature is in accordance with typical reversed-phase behaviour [9], but anomalous effects were observed for thorium(IV), which showed an increase in capacity factor with temperature. Similar effects for thorium(IV) and uranyl have been reported for eluents containing mandelic acid [6].

Studies were undertaken in which both cationic and anionic IIRs were added to the mobile phase as a means of determining whether the eluted metal ions were present as anionic, neutral or cationic spe-

TABLE III

EFFECTS OF ANIONIC AND CATIONIC ION-INTERACTION REAGENTS ON RETENTION

Mobile phase[a]	Retention time (min)			Relative retention time	
	Phenol	Thorium(IV)	Uranyl	Thorium(IV)	Uranyl
80 m*M* HIBA, 5 m*M* TBA^+	11.0	4.6	8.2	0.42	0.74
400 m*M* HIBA, 5 m*M* TBA^+	9.7	3.7	7.4	0.38	0.76
80 m*M* HIBA	11.0	5.3	8.1	0.48	0.74
400 m*M* HIBA	9.3	4.3	6.1	0.46	0.66
80 m*M* HIBA, 5 m*M* OSA^-	11.0	4.2	5.1	0.38	0.46
400 m*M* HIBA, 5 m*M* OSA^-	9.5	3.5	4.0	0.37	0.42

[a] TBA^+ = Tetrabutylammonium; OSA^- = octanesulfate.

cies. In each case, the column was equilibrated with the desired mobile phase, thorium(IV), uranyl and phenol (as a neutral marker compound) were injected and the relative retention time (comparative to that of phenol) of each metal was calculated. The results are given in Table III, which shows that at the higher HIBA concentrations, the only significant change observed was a reduction in the relative retention time for uranyl in the presence of octanesulfonate as the IIR. This suggests that the uranyl complex may be anionic under these conditions, but the observed increase in relative retention time in the presence of tetrabutylammonium as the IIR was only slight. The conclusions reached from these studies are two-fold. First, any charge present on the complexes is sufficiently diffuse that it does not exert a great effect on retention. Second, there is a consistent trend for all solutes, including the neutral marker, for retention time to decrease as the concentration of HIBA is increased. This suggests that HIBA itself is adsorbed onto the stationary phase and at the high concentrations used, probably precludes any appreciable adsorption of the IIR (which is present at much lower concentrations than HIBA), thereby preventing the IIR from significantly influencing retention. Decreases in relative retention times for thorium(IV) in the presence of octanesulfonate also suggest an anionic complex, but corresponding increases in retention when tetrabutylammonium was added to the mobile phase were not observed.

Mechanism of retention

Evaluation of the above factors affecting retention of the HIBA complexes of thorium(IV) and uranyl on a reversed-phase column was undertaken in order to suggest a retention mechanism which explains all of the observed trends. The behaviour of the uranyl complex is perhaps the more straightforward. The effect of increasing the percentage of organic modifier (Fig. 5) and the temperature effect (Fig. 7) are consistent with reversed-phase adsorption. Despite the fact that complete complexation leads to the formation of the anionic tris(HIBA) complex, the resultant charge distribution must be sufficiently diffuse that the complex exhibits a degree of hydrophobicity that permits reversed-phase adsorption. The decreased retention noted when the concentration of HIBA in the mobile phase is increased above 80 m*M* can be considered to result from increasing competition for the stationary phase adsorption sites by the considerable amount of unionized HIBA in the mobile phase. This effect has been suggested previously to explain a similar retention trend for mandelic acid complexes of uranyl on a reversed-phase column. Evidence in support of this hypothesis can be seen from the retention behaviour of phenol at the two different HIBA concentrations given in Table III. Here, a decrease in the retention time of phenol was noted with increasing HIBA concentration. This factor will contribute to the behaviour shown in Fig. 5 in addition to the effect that increased formation of the anionic tris(HIBA) complex of uranyl would be expected to favour decreased retention. The retention maximum observed for uranyl at about 50 m*M* HIBA in Fig. 6 corresponds closely to the point where maximum formation of the neutral bis(HIBA) uranyl

complex occurs (Fig. 3). Finally, the increased retention observed with increasing pH (Table II) can be attributed to increased complexation of uranyl and a concomitant decrease in the concentration of neutral HIBA in the mobile phase.

The retention behaviour of the thorium(IV) complex is somewhat anomalous in that under most of the conditions examined, it is eluted prior to the uranyl complex, despite the fact that it is expected to be a neutral complex with four ligand molecules, compared to a maximum of three for uranyl. Fig. 5 confirms that reversed-phase retention applies even at low concentrations of HIBA, but the temperature effect shown in Fig. 7 is the opposite to that normally encountered in reversed-phase chromatography. Further anomalies are evident in Fig. 6, where the retention of the thorium(IV) complex is seen to decrease rapidy as the HIBA concentration is increased from 15 to 50 m*M* and to then show a modest decrease with higher concentrations of HIBA. Fig. 2 would suggest the opposite trends of a rapid increase in retention followed by a plateau region as formation of the neutral tetra(HIBA) complex dominates. Allowing for competition for the stationary phase adsorption sites by unreacted HIBA in the mobile phase could result in decreased retention at high HIBA concentrations, so that a maximum might be expected in the plot for thorium(IV) in Fig. 6. The effect of pH on retention of thorium(IV) is similar to that observed for uranyl and can again be attributed to increased complex formation and reduced levels of neutral HIBA in the mobile phase.

One possible explanation for these results lies by considering the known propensity for thorium(IV) to hydrolyse in aqueous solution, even at acidic pH values [10], in juxtaposition with the fact that thorium(IV) often exhibits very high coordination numbers when complexed [11]. It is therefore likely that one or more hydroxyl ligands are incorporated into the coordination sphere of the thorium(IV), thereby reducing the overall charge on the complex. This would lead to the bis- or tris(HIBA) complexes being neutral, whilst the tetra(HIBA) complex would be anionic. Comparison of the retention times of the thorium(IV) and uranyl complexes in a mobile phase containing 400 m*M* HIBA and considering the higher stoichiometry of the former complex suggests that the negative charge on the thorium(IV) complex should be greater than than for the uranyl complex. This indicates the presence of at least two hydroxyls in the thorium(IV) complex. Some evidence for this is the rapid decline in retention observed for thorium(IV) in Fig. 6 over the HIBA concentration range in which there is conversion of the bis(HIBA) complex (presumably neutral if two hydroxyls are present) into the tris(HIBA) complex (presumably anionic). Decreasing stability of the mixed ligand species at higher temperatures may account for the anomalous increase in retention observed with increasing temperature.

Calibration data and preconcentration studies

Linear calibration plots (correlation coefficient >0.99) were obtained for both thorium(IV) and uranyl over the concentration range 0–10 mg/l, however, it is likely that linearity extends beyond these upper concentration limits. Detection limits for a 100-μl injection volume were 22 μg/l for thorium(IV) and 53 μg/l for uranyl.

The behaviour of the HIBA complexes of thorium(IV) and uranyl suggests that sample preconcentration techniques could be applied to these solutes. A sample comprising thorium(IV) and uranyl in the presence of 20 m*M* HIBA at pH 4.0 should permit preconcentration of both species on a C_{18} concentrator column, with subsequent elution and separation using 400 m*M* HIBA in 10% methanol. A somewhat similar approach has been used by Kerr *et al.* [4], except that 110 m*M* HIBA at pH 5.5 was used for enrichment and a mobile phase comprising 220 m*M* HIBA at pH 3.5 and 25 m*M* pentanesulfonate was employed for analysis. Our results suggest that these conditions are not optimal. A preconcentration system was configured according to the schematic diagram shown in Fig. 1 and was shown to be applicable to the preconcentration of sample volumes up to 1 ml. Fig. 8 shows a chromatogram of a preconcentrated sample. Under these conditions linear calibration plots over the range 0–300 μg/l of both thorium(IV) and uranyl were constructed, giving detection limits of 2.2 and 5.8 μg/l, respectively, for a 1.0-ml sample volume. Recovery studies showed that adsorption of the complexes on the concentrator column was very close to quantitative.

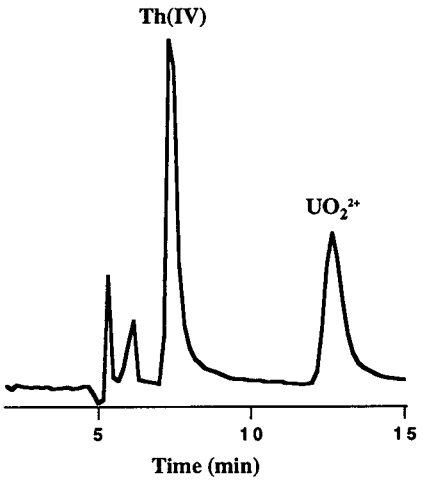

Fig. 8. Preconcentrated sample (1 ml) containing 300 μg/l of both thorium(IV) and uranyl in 20 m*M* HIBA at pH 4.0. The separation conditions were as for Fig. 4.

CONCLUSIONS

The elution characteristics of HIBA complexes of thorium(IV) and uranyl are dependent on the particular complexes existing in solution under the chromatographic conditions used. In the case of uranyl, the anionic tris(HIBA) compex dominates at 400 m*M* HIBA (pH 4.0) and is retained on a reversed-phase column by hydrophobic adsorption, despite its anionic nature. On the other hand, thorium(IV) forms a neutral tetra(HIBA) complex, which hydrolyses readily to produce an anionic complex probably containing at least two coordinated hydroxyl ions. This complex is also retained by hydrophobic adsorption, but to a lesser extent than the uranyl complex. The behaviour of thorium(IV) and uranyl in mobile phases containing HIBA is quite different to that exhibited by lanthanide ions, which are retained by a cation-exchange mechanism. This difference can be explained by the smaller formation constants and lower ligand/metal ratios of these species in comparison to thorium(IV) and uranyl.

ACKNOWLEDGEMENT

Helpful discussions with Mr. Ian Gough of AMC Mineral Sands Pty. Ltd. are gratefully acknowledged.

REFERENCES

1 C. H. Knight, R. M. Cassidy, B. M. Recoskie and L. W. Green, *Anal. Chem.*, 56 (1984) 474.
2 D. J. Barkley, M. Blanchette, R. M. Cassidy and S. Elchuk, *Anal. Chem.*, 58 (1986) 2222.
3 R. M. Cassidy, S. Elchuk, N. L. Elliot, L. W. Green, C. H. Knight and B. M. Recoskie, *Anal. Chem.*, 58 (1986) 1181.
4 A. Kerr, W. Kupferschmidt and M. Attas, *Anal. Chem.*, 60 (1988) 2729.
5 R. M. Cassidy, S. Elchuk, L. W. Green, C. H. Knight, F. C. Miller and B. M. Recoskie, *J. Radioanal. Nucl. Chem.*, 139 (1990) 55.
6 S. Elchuk, K. I. Burns, R. M. Cassidy and C. A. Lucy, *J. Chromatogr.*, 558 (1991) 197.
7 L. Magon, A. Bismondo, L. Maresca, G. Tomat and R. Portanova, *J. Inorg. Nucl. Chem.*, 35 (1973) 4237.
8 L. Magon, G. Tomat, A. Bismondo, R. Portanova and U. Croatto, *Gazz. Chim. Ital.*, 104 (1974) 967.
9 P. J. Schoenmakers, *Optimization of Chromatographic Selectivity*, Elsevier, Amsterdam, 1986, p. 67.
10 S. Hietanen and L. G. Sillen, *Acta Chem. Scand.*, 22 (1968) 265.
11 F. A. Cotton and G. W. Wilkinson, *Advanced Inorganic Chemistry*, Wiley Interescience, New York, 2nd ed., 1967, p. 1090.

Journal of Chromatography, 640 (1993) 195–206
Elsevier Science Publishers B.V., Amsterdam

CHROMSYMP. 2665

Review

Complexation ion chromatography —an overview of developments and trends in trace metal analysis☆

A. R. Timerbaev*

Department of Analytical Chemistry, Mendeleev University of Chemical Technology, 125190 Moscow (Russian Federation)

G. K. Bonn

Department of Analytical Chemistry, Johannes Kepler University, A-4040 Linz (Austria)

ABSTRACT

Complexation ion chromatography (IC), including all ion chromatographic modes in which complexation is exploited for the separation and detection of metal ions in different ways, is now a widely accepted method of trace metal analysis. Some of the significant advances in the theoretical aspects and practical applications of complexation IC modifications (non-suppressed cation chromatography with complex-forming mobile phases, coordination chromatography with chelate-forming bonded phases, ion-exchange and ion-pair chromatography of anionic metal chelates) recently developed in the authors' laboratories are reviewed. The retention behaviour and separation mechanism of non-complexed and complexed metal analytes are discussed from the point of view of basic coordination chemistry (stability of metal complexes, effective charge of metal atom, ligand complexing ability, etc.). Comparisons and contrasts between various metal complexation IC techniques and their common features and advantages relative to other methods used in analyses for transition and heavy metal ions are evaluated.

CONTENTS

* Corresponding author. Present address: Department of Analytical Chemistry, Johannes Kepler University, A-4040 Linz, Austria.

☆ Dedicated to Professor Oleg M. Petrukhin on the occasion of his 60th birthday.

0021-9673/93/$06.00

1. INTRODUCTION

The development and substantial practical achievements of ion chromatography (IC) in the analysis of metal ions in the last decade have been achieved mainly by the exploitation of metal complexation (*e.g.*, refs. 1–7 among many others recently published). The complexation reactions can take place in either the mobile or stationary phase and sometimes simultaneously in both. Chromatographic separations of metal complexes formed before chromatography and detection by postcolumn complex-forming reactions are also within the scope of complexation IC. Hence it appears that a major advantage of the chromatographic determination of metals in the form of various complexes is that a variety of separation modes and detection methods can be utilized.

In general, complexation IC is considered to include all metal ion chromatographic separation techniques based on or dependent on complexation processes [5]. Among the diverse possible chromatographic variants, cation chromatography with complex-forming mobile phases and coordination chromatography of metal ions on chelate-forming bonded stationary phases, ion-exchange and ion-pair chromatography of anionic metal chelates with direct conductivity or spectrophotometric detection, including postcolumn complexation derivatization, has been the focus of our recent interest.

This review is devoted to a critical evaluation of separations recently obtained in the authors' laboratories and some recently published literature data on this subject. Fundamentals of coordination chemistry related to the consideration for the retention behaviour of metal chelates and complexed metal ions are discussed. Comparisons and contrasts are discussed between the various metal ion chromatographic techniques. The resolution and detection parameters are also compared and illustrated by some applications of practical relevance, mainly in trace metal determinations.

2. RESULTS AND DISCUSSION

2.1. Chromatographic methods

In our research on the determination of transition and heavy metals, we have relied mainly on the four IC methods summarized in Table 1.

Cation-exchange IC is the most obvious and therefore the most common chromatographic method for the determination of metal ion. When using silica- [8,9] or polymer-based [10] sulphonated ion-exchange stationary phases, selective and efficient separations of bivalent metal ions require the addition of a complexing ligand (*e.g.*, di- or tribasic carboxylic acids) to the eluent, which is able to decrease differentially via complexation the effective charge of the metal cation and, hence, the retention. When chelating chemically bonded phases (such as an iminodiacetic acid functional silica-bonded material [11,12]) are used instead of cation exchangers, complexation reactions in the stationary phase are responsible for the separation (sometimes together with complexation in the eluent and the ion-exchange mechanism due to free or protonated chelating groups, which act as ion-exchange sites) and offer a number of advantages in terms of selectivity.

Another promising approach to the ion chromatographic determination of metal ions is their precolumn conversion into the negatively charged chelates, followed by anion-exchange chromatographic separation [13]. The separation of the same type of metal chelates {mostly of heterocyclic azo dyes, such as 4-(2-pyridylazo) resorcinol (PAR) [14,15]}, on dynamicaly coated anion-exchange columns, *i.e.*, in the ion-pairing mode, introduces addi-

TABLE 1

COMPLEXATION ION CHROMATOGRAPHY OF METAL IONS

Chromatographic technique	Metal forms separated[a]	Chelating ligand (L)	Metal ions determined
Cation-exchange IC	M^{n+} ... $ML_m^{(n-m)\pm}$	Carboxylic acids (citric, tartaric, oxalic)	Cd(II), Co(II), Cu(II), Fe(II), Fe(III), Mn(II), Ni(II), Pb(II), Zn(II), alkaline earths
Coordination IC	M^{n+} ... $ML_m^{(n-m)\pm}$	Carboxylic acids, pyridine-2,6-dicarboxylic acid, nitrilotriacetic acid	Cd(II), Co(II), Fe(II), Mn(II), Pb(II), Zn(II), alkaline earths
Anion-exchange IC	ML_n^{n-}	4-(2-Pyridylazo)-resorcinol (PAR), EDTA	Cd(II), Co(II), Cu(II), Fe(III), Ni(II), Pb(II), Zn(II)
Ion-pair chromatography	ML_n^{n-} ... ML_nB_n	PAR	Co(II), Cu(II), Fe(III), Ni(II)

[a] B = Quaternary ammonium ion.

tional possibilities for improving the resolution [16,17].

2.2. Retention behaviour and separation mechanism

2.2.1. Cation-exchange IC

To overcome the strong electrostatic interactions of transition metal ions with the column, ethylenediamine (EDA) has been used in the eluent as a competing ion. EDA is highly protonated at the pH level used (usually between 3 and 5) and loses its ability to act as a ligand. A schematic representation of the cation-exchange interactions between EDA and the bivalent sample ion, M^{2+}, on a stationary phase, R, with complexing eluents (H_2L) is shown by the following equilibria:

$$\begin{aligned} &R\text{–}M + EDAH_2^{2+} + L^{2-} \\ &\quad \rightleftharpoons R\text{–}EDAH_2 + M^{2+} + L^{2-} \\ &\quad \rightleftharpoons R\text{–}EDAH_2 + ML \end{aligned}$$

In the absence of a complexing ligand, L^{2-}, transition metal ions are bound firmly to the sulphonic acid groups, and elution by the ethylenediammonium cation is ruled only by the EDA concentration. If a complexing agent is added to the eluent, its anionic carboxylate groups compete for the metal ion, thus favouring release from the stationary phase by EDA, resulting in a decrease in retention time.

Under conditions where the same solute cation, M^{2+}, is eluted from the same column with varying concentrations of competing cation, En^{2+}, in the eluent, a plot of log k' *versus* log $[En^{2+}]$ will be a straight line with a slope equal to -1 [18]. The slopes of the experimentally observed dependences shown in Fig. 1 are in a good agreement with the

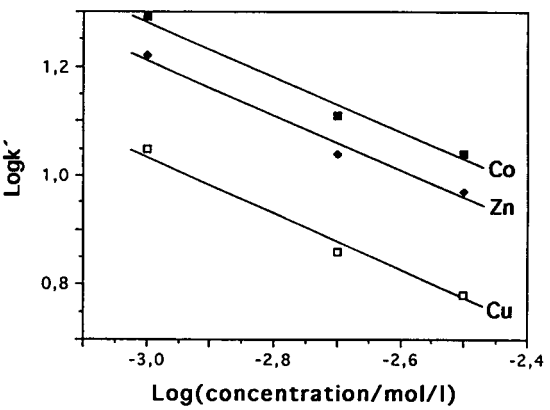

Fig. 1. Dependence of log k' values of metal ions on the concentration of ethylenediamine in the mobile phase. Stationary phase, G-253 macroporous methacrylate ion exchanger; column, 100 × 6 mm I.D.; mobile phase, EDA–2 mmol/l tartaric acid, flow-rate, 2.0 ml/min.

theoretical value. This suggests that in the presence of complex-forming ligands cation exchange remains the operating retention mechanism.

The effect of the eluent complexing agent on retention behaviour is equivalent to reducing the effective charge of the metal ion. This results in a decrease in the retention times of all bivalent cation studied with increase in the concentration of a carboxylic acid [10]. The selectivity of the separation is also changed owing to complexing effects. This is attributable to the fact that the distribution coefficients of transition metals (K_D) with a charge and size of the same magnitude differ only slightly in the absence of complexing acids. On the other hand, when complexation becomes a part of the separation mechanism the relative retention of two metal ions is determined by

$$K_D^{compl}(1)/K_D^{compl}(2) = [K_D(1) / K_D(2)]\,[\beta_n(1) / \beta_n(2)]$$

where β_n is the stability constant of the corresponding complex [10,19]. The differences between the values of the stability constants of transition metal complexes with carboxylic acids are usually larger than the variations in the distribution coefficients. The dominant impact of complexation effects on the selectivity of separation can be confirmed by the linear correlation between the log k' and log β_n values observed in different chromatographic systems (Fig. 2). The more stable the metal ion–carboxylate complex, the more rapidly it will be eluted.

The dependence of the resolution on the pH of the mobile phase must also be carefully controlled to optimize the separation. Increasing the pH increases the complex-forming ability of hydroxy acids and the effective constant of complex formation, resulting in decreased retention times and better separations. On the other hand, the pH of the eluent influences the degree of protonation of the amino groups of EDA and thereby interactions between the stationary phase and the metal ions. The result of optimizing the pH of the EDA–citrate mobile phase is illustrated by the separation of a number of transition metal ions of environmental importance (and also some mono- and bivalent cations) with a baseline resolution within 20 min (Fig. 3).

Obviously, the separation of transition metal ions in cation-exchange IC is based on the combined effects of ion-exchange elution with the eluent cation and complexation with the eluent ligand, followed by the formation of complexes of different stability in the mobile phase.

2.2.2. Coordination IC

Among many combinations of immobilized chelating ligand and base material examined [5], we

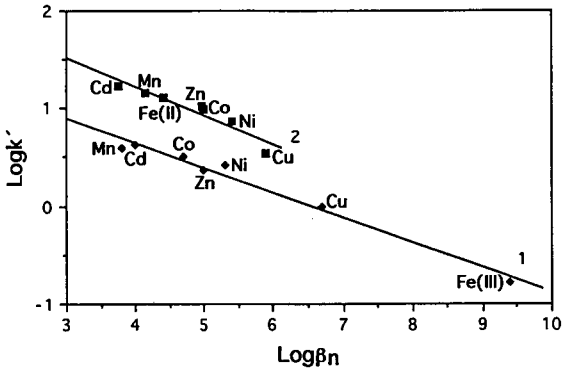

Fig. 2. Log k' *vs.* log β_n plots. 1 = G-253 column with 2 mmol/l EDA–2 mmol/l oxalic acid (pH 4.0) mobile phase; 2 = TSK IC cation SW column with 3.5 mmol/l EDA–10 mmol/l citric acid (pH 2.8) mobile phase.

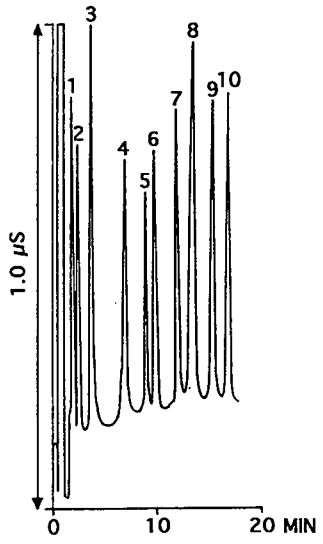

Fig. 3. Simultaneous separation of alkali, alkaline earth and transition metal ions. Column, TSK IC cation SW; mobile phase, 3.5 mmol/l EDA–10 mmol/l citric acid (pH 2.8); flow-rate, 1.0 ml/min; detection, conductivity. Peaks: 1 = Na; 2 = K; 3 = Cu; 4 = Ni; 5 = Co; 6 = Zn; 7 = Fe^{2+}; 8 = Mn; 9 = Cd; 10 = Ca. From ref. 9.

considered a stationary phase with silica-bound iminodiacetic acid (IDA) functions to be one of the most favourable from the point of view of the kinetics and specificity of chelate formation [11,12]. IDA exhibits different complexing abilities for different transition metals, most of the complexes being kinetically labile and moderately stable. These properties ensure the reversible sorption of metal ions.

The most important parameters controlling the retention of cations in coordination chromatography are the concentration of a complexing agent and the pH of the mobile phase. All eluents can be classified into two main types, depending on their complexing ability.

2.2.2.1. Weak complexing eluents. The basic function of these eluents (*e.g.*, citric or tartaric acid) is to regulate the dissociation of free carboxylate groups acting as ion-exchange sites, owing to the pH variations with the changes in eluent concentration (Fig. 4). Nevertheless, although in the pH range investigated (2.5–4.0) there is evidence for ion-exchange processes taking place additionally (also with partially protonated IDA moieties), the retention behaviour reflects the affinity of metal ions to IDA as a complexing ligand. The elution order of metal ions is consistent with the stability constants of metal–IDA complexes and confirms the dominating contribution of complexation reactions within the IDA column to the elution mechanism. Therefore, both citric and tartaric acid can elute only certain transition metal ions from the column, whereas other ions, which form more stable IDA complexes (*e.g.*, Cu^{2+}, Ni^{2+} and Pb^{2+}), remain irreversibly retained.

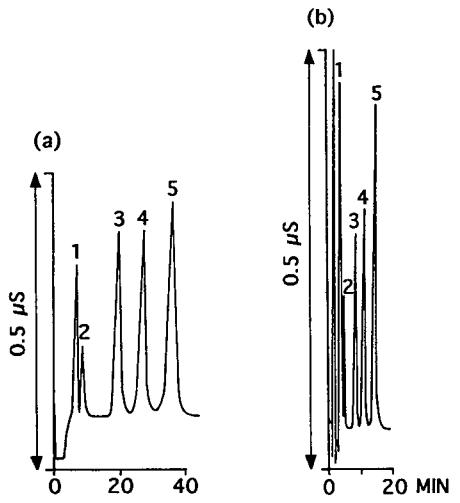

Fig. 4. Chromatograms of metal ions with different concentrations of citric acid: (a) 10 and (b) 25 m*M*. Stationary phase, 7-μm porous silica coupled with IDA; column, 100 × 4.6 I.D.; flow-rate, 1.0 ml/min; detection, conductivity. Peaks: 1 = Mg; 2 = Fe^{2+}; 3 = Co; 4 = Cd; 5 = Zn. From ref. 12.

2.2.2.2. Strong complexing eluents. A high complexing ability of the IDA phase requires the use of sufficiently strong complexing agents in the mobile phase, such as pyridine-2,6-dicarboxylic acid (DPA) or nitrilotriacetic acid (NTA). Both DPA and NTA have the same three coordination centres in complexation as IDA (*i.e.*, the two carboxylate groups and the nitrogen atom), which are apparently very similarly arranged within the molecules. Consequently, under these conditions, complex formation in the IDA phase becomes comparable to that in the eluent.

DPA proved to be a particularly useful eluent for the IDA column [11,20]. Its anion shows a unique degree of complexation owing to the following steric effect. The nitrogen atom of the DPA anion is part of an aromatic system, which rigidly holds the carboxylate groups in a position coplanar to the pyridine ring, thus favouring complex formation (whereas IDA and NTA molecules have a flexible structure).

However, at low DPA concentrations, even transition metals of high complex stability exhibit a retention behaviour similar to that of alkaline earth metal ions, being eluted mainly through an ion-exchange mechanism. Only if higher concentrations of DPA are incorporated in the eluent, complexation processes are favoured. The log k' values plotted against the logarithm of the DPA concentration give straight lines, and the slopes of these dependences are proportional to the formation constants of the metal–DPA complexes (Fig. 5). The $\Delta\log k'/\Delta\log$ [DPA] values increase with increaisng pH, reflecting the increasing dissociation and complexing ability of the ligand. Calculations of conditional stability constants in the pH range studied (2.5–5.0) show that the stability of metal–DPA complexes is fairly high, confirming the ability of this complexing agent to accelerate the elution of transition metal ions under acidic conditions.

Thus, two complexation reactions can take place

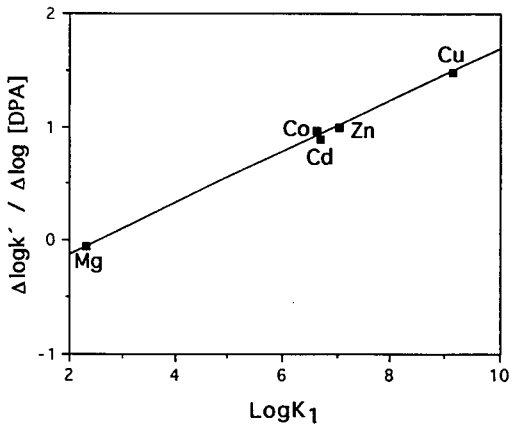

Fig. 5. Correlation between the slope of log k' *vs.* log [DPA] dependences for metal ions and the first formation constant of metal–DPA complexes. Stationary phase, 7-μm porous silica coupled with IDA; column, 100 × 4.6 mm I.D.; flow-rate, 1.0 ml/min; detection, conductivity.

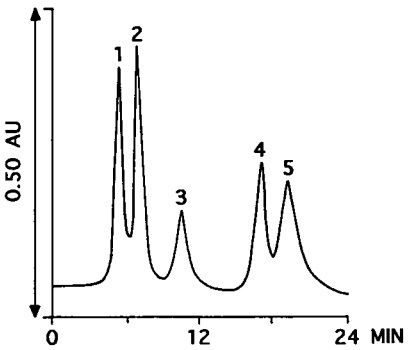

Fig. 6. Chromatogram of metal pyridylazoresorcinolates. Stationary phase, HIKS-1 resin-based anion-exchanger; column, 200 × 6 mm I.D.; mobile phase, 50 mmol/l sodium carbonate–acetone (60:40, v/v) (pH 11.8); flow-rate, 1.0 ml/min; detection, 500 nm. Peaks: 1 = Co; 2 = Cu; 3 = Zn; 4 = Fe^{3+}; 5 = Ni. From ref. 17.

in coordination IC, and the retention and separation of metal ions are governed predominately by the ratio of the stability constants of their complexes with the chelating groups immobilized on the stationary phase and with the complexing agent incorporated in the eluent.

2.2.3. *Anion-exchange IC*

Anion-exchange chromatography of transition metals as previously formed, stable, anionic chelates is a comparatively new chromatographic method. This method has decided advantages, such as a stable baseline and simple instrumentation (see also below). This chromatographic mode can also be achieved by using the on-column complexation technique where the complexing agent is added to the mobile phase [21] or injected into the column before the separation [22,23].

When light-absorbing chelating reagents, such as PAR, are used, the main problem of optimizing the elution conditions is that the metal complexes are strongly retained because of non-ion-exchange sorption, especially on polymer-based ion exchangers [13,17]. We have overcome this problem by adding organic solvents (up to 40 vol. % of 2-propanol or acetone) to the mobile phase. The complete dissociation of the complexes under these conditions requires the use of strongly alkaline eluents, *e.g.*, sodium carbonate. A typical chromatogram is presented in Fig. 6. It should be emphasized that a sufficiently high chromatographic stability of transition metal–PAR chelates in these eluents is provided by their extremely high thermodynamic stability.

Fig. 7 shows the effect of sodium carbonate concentration on the retention. As the eluent concentration increases, the retention time decreases. The linear character of these dependences is indicative of the ion-exchange mechanism of separation, although the slope (−0.4 to −0.7) is less than the theoretical value of −1 [24] (most of the complexes

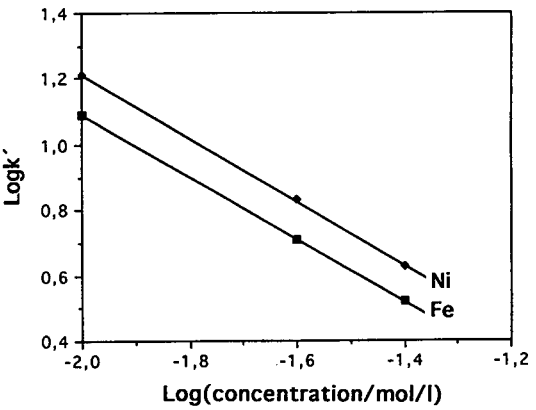

Fig. 7. Dependences of the capacity factors of Fe–PAR and Ni–PAR on the concentration of sodium carbonate in the mobile phase. Mobile phase, sodium carbonate–2-propanol (60:40, v/v). Other conditions as in Fig. 6.

studied have a charge of −2, and the eluent competing ion is also doubly charged in this pH range). The pH increase also considerably decreases the retention time of complexes; the Na_2CO_3 concentration is less and the influence of pH is stronger.

Hence the retention of metal pyridylazoresorcinolates in anion-exchange IC is obviously due to both ion-exchange and adsorption mechanisms. This peculiarity of their chromatographic behaviour allows one to regulate the selectivity of separation by varying independently the eluent competing ion and organic modifier concentration. The metal complexes of aminopolycarbonic acids (*e.g.*, EDTA), on the other hand, experience a comparatively low hydrophobic sorption effect and can be separated by elution with standard carbonate–hydrogencarbonate eluents [13,17].

2.2.4. *Ion-pair chromatography (IPC)*

This HPLC mode, in which mobile phases containing an ion-pairing reagent are used along with a reversed-phase stationary phase, can be considered as a more promising alternative to anion-exchange IC on fixed-site ion-exchange columns. According to the abundant literature on the use of IPC for the separation of metal ions recently reviewed [15–17], two main retention models, the ion-interaction and the ion-partition model, may serve to explain the retention behaviour of metal chelates. Normally, the real retention mechanism is a mixed one, but under certain conditions, ion exchange or adsorption may occur preferentially. The relative contributions of these mechanisms depend on the mobile phase composition and, as we have shown on the example of metal–PAR chelates [16,17], the eluting strength and concentration of the organic modifier are the most important parameters in controlling elution and selectivity in IPC.

When water–organic eluents with comparatively low eluting ability are used, the adsorption of the ion-pairing counter ion on a non-polar stationary phase and the ion-exchange sorption of anionic solutes dominate. This is why the retention of metal complexes is greatly affected by the basicity of an appropriate ionized group of the ligand, participating in ion-exchange interactions, and, thereby, by the electron-acceptor ability of the metal atom. Hence, the higher the effective charge of the metal atom, the stronger is the retention (Fig. 8a). An increase in organic modifier concentration or hydrophobicity transfers the ion-pair formation from the stationary phase to the mobile phase. Consequently, the absorption of ion pairs becomes the predominant separation mechanism and, as in reversed-phase HPLC systems [25,26], the complexes of more electronegative metals have the longer retention times (Fig. 8b). Fig. 9 shows that the stability constant as a universal structure-dependent characteristic of the metal complex can also be suitable for the *a priori* evaluation of the retention values in IPC.

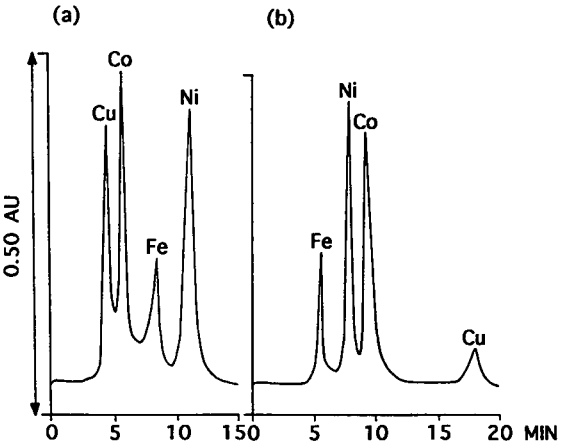

Fig. 8. Effect of the nature of the organic modifier on the retention mechanism of metal–PAR complexes. (a) Ethanol; (b) acetone. Stationary phase, Silasorb C_8 (10 μm); column, 200 × 6 mm I.D.; mobile phase, organic solvent–water (20:80, v/v) containing 8 mmol/l of tetrabutylammonium hydroxide (pH 11.8); flow-rate, 1 ml/min; detection, 500 nm.

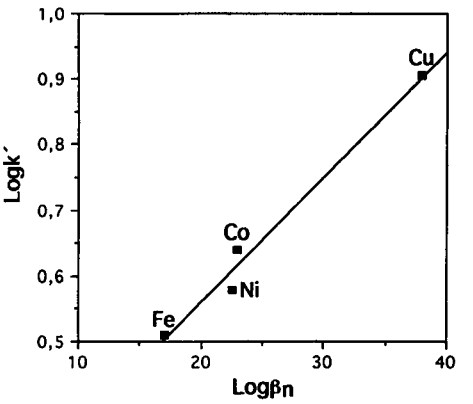

Fig. 9. Plot of log k' *versus* log β_n values for metal–PAR complexes. Chromatographic conditions as in Fig. 8b.

TABLE 2

RESULTS FOR METAL DETERMINATION IN DIFFERENT SAMPLES

Sample	Metals determined	Found (ppm ± S.D.)[a]	Certified value (ppm)
Waste water from electroplating plant	Cu	12.8 ± 0.4	12.0
	Zn	8.8 ± 0.3	9.0
Drinking water	Fe	2.0 ± 0.1	2.1
Wine	Cu	1.4 ± 0.1	1.3
	Fe	8.4 ± 0.3	8.2
Apple–grape juice	Cu	2.0 ± 0.1	1.9
	Fe	13.4 ± 0.5	13.6

[a] n = 3–4.

Thus, changing of the retention mechanism leads to changes in the elution order of metal complexes and, moreover, can result in a complete reversal of the retention. The other numerous parameters of the mobile phase (nature and concentration of the ion-pairing agent, pH, concentration of the eluent co-ion) govern the IPC separation at the same time and with different effects [16,17]. Therefore, this complexation chromatographic technique is characterized by distinct possibilities for regulating the separation due to both multi-component eluent composition and complex retention mechanism.

2.3. Analytical applications

2.3.1. Cation-exchange IC

Post-column reaction detection is now the most commonly applied detection mode for the determination of trace amounts of transition metals by non-suppressed cation chromatography [27,28]. In practical applications we also prefer spectrophotometric detection to direct conductivity measurements. PAR was used as a postcolumn derivatizing reagent [10] and the method was successfully applied to the analysis of waste waters, drinking water, food and beverage products, fertilizers and other matrices. Analytical data for some of these samples are given in Table 2. Further, the potential of the method in the differential analysis of iron species in real samples is demonstrated in Fig. 10.

2.3.2. Coordination IC

The affinity of the IDA stationary phase towards transition metal ions is of great advantage for the determination of trace metals in samples containing high levels of alkali and alkaline earth metal ions. Fig. 11 gives a chromatogram of a sea-water sample, spiked with transition metals, as an example of alkali and alkaline earth metal-rich matrices (*e.g.*, sodium and magnesium are present in more than a 10^4-fold excess over sub-ppm concentrations of transition metals).

A further advantage of coordination IC is the possibility of simultaneous preconcentration and separation on the same column [29]. In this way, zinc was determined in a pretreated urine sample [30]. Using a fully automatic chromatographic system, including a separate concentrator IDA column [12], matrix interferences can also be eliminated. As a result, the detection limits were improved by about three orders of magnitude, reaching the 0.1–

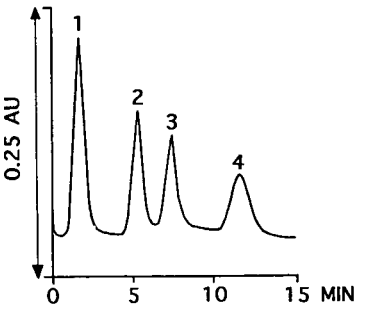

Fig. 10. Cation-exchange IC analysis of waste water. Stationary phase, G-953; column, 100 × 6 mm I.D.; mobile phase, 2 mmol/l EDA–2 mmol/l tartaric acid (pH 4.5); flow-rate, 2.0 ml/min; postcolumn reagent, PAR, 0.001% in 0.5% ammonia solution, flow-rate 1.5 ml/min; detection, 500 nm. Peaks: 1 = Fe^{3+} (18 ppm); 2 = Cu (13 ppm); 3 = Zn (9 ppm); 4 = Fe^{2+} (16 ppm).

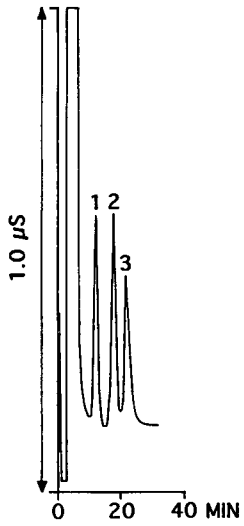

Fig. 11. Separation of transition metals in sea water by coordination IC. Stationary phase, IDA-silica; mobile phase, 10 mmol/l tartaric acid (pH 2.5); flow-rate, 1.0 ml/min; detection, conductivity. Sample: sea water spiked with (1) 5 ppm of Co, (2) 5 ppm of Zn and (3) 10 ppm of Cd. From ref. 11.

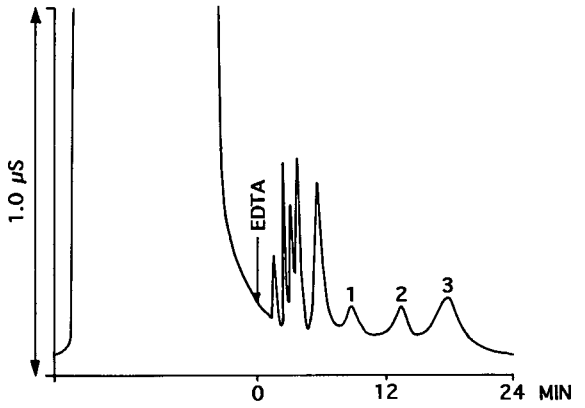

Fig. 12. Chromatogram of the determination of heavy metals in sea water. Stationary phase, KanK-Ast (15 μm); column, 100 × 3 mm I.D.; mobile phase, 2 mmol/l sodium carbonate–0.5 mmol/l ammonium hydrogencarbonate; flow-rate, 0.9 ml/min; detection, conductivity. Peaks: 1 = Cd + Pb ($2 \cdot 10^{-6}$ *M*); 2 = Zn ($\leqslant 5 \cdot 10^{-6}$ *M*); 3 = Cu ($4 \cdot 10^{-6}$ *M*). The first eluted overscaled peak corresponds to the anions. The arrow shows the time of EDTA injection.

0.2 ppb level for zinc, cadmiun, and cobalt with conductivity detection.

2.3.3. Anion-exchange IC

Owing to the high sensitivity with respect to intensely coloured metal–PAR chelates, this method can be used in combination with spectrophotometric detection to analyse some real samples without preconcentration, *e.g.*, waste waters from electroplating wash tanks [13,17]. When the iron content was high [*e.g.*, in the purification of effluents by coprecipitation of metals with hydrous iron(III) oxide], a modification by on-column complexation proved to be effective [26]. In contrast to other metals, iron(III) does not form a complex under these conditions, probably for kinetic reasons, and does not interfere.

The simultaneous ion chromatographic determinations of transition metal cations and inorganic anions on a central ion exchanger (KanK-Ast) possessing both anion- and cation-exchange capacity, proposed by Dolgonosov [31], using conductivity detection were recently described [22,23]. The successive separation of anions and metal cations retained on the column during the elution of anions is achieved by the subsequent injection of EDTA and anion-exchange separation of the metal–EDTA complexes formed. The method was applied to the analysis of natural samples. Fig. 12 shows the chromatogram of a sea-water sample. The bifunctional ion-exchange properties of the proposed ion-exchange material permit a multi-step on-column preconcentration of metal ions and, as a result, the detection limits were lowered to the mid-ppb level.

2.3.4. Ion-pair chromatography

In comparison with anion-exchange IC, the limits of detection provided by IPC are lower by about one order of magnitude and, therefore, sufficiently low to analyse directly samples containing low levels of transition metals, such as purified waste waters, drinking water and beverages. An example of the application of IPC to water and beverage quality control is presented in Fig. 13. As for anion-exchange IC, the use of the simplest and fastest pre-column complex formation by direct mixing of the sample and reagent solution does not adversely affect the analysis time (the sample pretreatment is usually less than 15 min).

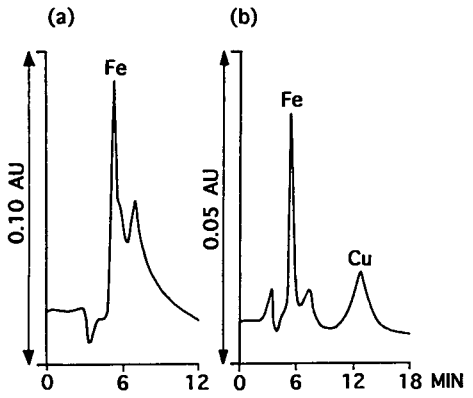

Fig. 13. Analysis of real samples by IPC. (a) Tap water; (b) apple–grape juice. Mobile phase, acetone–water (20:80, v/v) containing 6 mmol/l of tetrabutylammonium hydroxide (pH 12.0). Other conditions as in Fig. 8. Peaks: Fe^{3+}, (a) 8.6 ppm, (b) 13.5 ppm; Cu, 2.1 ppm. From ref. 17.

2.4. Comparison of different complexation IC methods

The complexation IC methods described above are distinguished by a complicated retention behaviour of metal ions and their complexed forms in a chromatographic system. This common feature is related to a number of complexation reactions, accompanying the chromatographic process, and/or a complex retention mechanism. As a consequence, the enormous possibilities of varying the separation selectivity within wide limits by changing the mobile phase composition are apparent. One more distinguishing feature, confirming a relationship between all IC methods based on complexation reactions, is that the main elution regularities and separation mechanisms are determined by the stability of metal complexes. This basic characteristic is of great importance in regulating interactions between the metal ion or complex and the mobile and stationary phases. The stability constants play an important role in the prediction of retention and in the theoretical analysis of chromatographic behaviour in HPLC of metal chelates based on one-dimensional retention models [25,32] and, as shown above, they can also be widely applied for these purposes in complexation IC. Naturally, each of the complexation IC variants considered also has its own peculiarities, accounting for their advantages and disadvantages.

Cation-exchange IC allows the separation and subsequent detection of a large number of transition metals in one analysis step, simultaneously with some alkali and alkaline earth cations. Tedious sample clean-up procedures may be omitted in many instances to shorten analysis times. Additionally, in comparison with precolumn complexation IC techniques, cation-exchange IC has the advantage of avoiding the preliminary complex formation, and this also saves analysis time. However, only metals that undergo complexation rapidly enough can be determined. Such benefits as the ability to separate interferents from peaks of interest, multi-element capability, minimum sample pretreatment and low detection levels are valuable assets that make this chromatographic method very attractive for the speciation of trace elements.

Coordination IC has practically the same merits as cation-exchange IC. Further, the use of stationary phases with higher selectivities for transition metal ions facilitates the solution of an important problem often encountered in the IC of environmental or biological samples, *i.e.*, matrix interferences due to other constituents. However, the gain in selectivity is achieved at the cost of increased analysis times, and this is an adverse aspect of the high affinity of chelating stationary phases towards transition metal ions. The lack of commercially available chelating columns also hinders the application of coordination IC to routine analyse for transition metals.

Both ion-exchange an ion-pair IC are distinguished by the application of metal complexes formed before introduction into the column, so that there is no need for a postcolumn derivatization system. As a result, the solvent-delivery system and handling are simpler, and the analytical precision is better. Further, selective precolumn complexation reactions can largely eliminate interferences from environmental sample matrices, while by varying the complex-forming conditions the selectivity of metal determination can be increased.

The ability to use light-absorbing reagents to form highly coloured and stable chelates with numerous transition metals often makes the preconcentration stage unnecessary, and this speeds up and simplifies the analysis. In addition, the detection limits are low, because an extra dispersion of the chromatographic zones is not introduced by the

mixing procedure. The lower sensitivity of ion-exchange IC (because of the lower efficiency) can be compensated for by the higher sample volumes that can be used (*i.e.*, due to the preconcentration directly on the analytical column). IPC has the advantage of possessing a larger number of parameters that can control the retention and regulate the selectivity of the separation. Finally, the separation of transition metals as anionic species by these chromatographic techniques opens up new possibilities for the determination of metal ions and various anions in one run.

Summarizing, the four possibilities for separating and detecting metal ions presented in this review represent a good potential of complexation IC as a versatile tool for the monitoring and routine determination of transition and heavy metals. The versatility of complexation IC is due to the vast range of different metal-complexing forms and complex cation equilibria that can be utilized to control the resolution. Depending on the particular analytes and samples, different chromatographic techniques can be chosen and applied in order to obtain the greatest selectivity. Therefore, it may be concluded that at present complexation IC modifications do not compete but complement each other well.

Limits of detection of a few nanograms are typical in complexation IC, but after preconcentration limits as low as the parts per billion level can be obtained. For many metals these detection limits are comparable to those of instrumental methods such as atomic absorption, X-ray fluorescence or X-ray emission spectrometry. Further, in many instances the chromatographic separations achieved are difficult to obtain by other analytical methods. In comparison with multi-element techniques, such as inductively coupled plasma, atomic emission, and atomic fluorescence spectrometry, HPLC instrumentation is much less expensive and more accessible for many laboratories. The possibility of determining several elements without large-scale decomposition operations is one of the advantages of chromatographic methods over atomic absorption spectrometry. Electrochemical methods demand careful control over all experimental parameters and are more susceptible to matrix interferences than is complexation IC.

With regard to the relative merits of complexation IC and the tranditional techniques used in the determination of metal ions, it should be noted that complexation IC (i) is easily adapted to a variety of analytical problems and (ii) to the consecutive determination of metals in different oxidation states and non-metals in different chemicals forms; (iii) it can be combined with metal preconcentration methods; (iv) the analytical results hardly depend on sample treatment; (v) handling and maintenance are simple; and (vi) good technical equipment is available at comparatively low cost.

In fairness, some disadvantages of complexation IC should also be enumerated: the analysis times are comparatively long, ultrapure chemicals (reagents, buffers, solvents) and even metal-free HPLC systems must be used for ultra-trace analyses and considerable chemical expertise and knowledge are required for method development [5]. These are the major objectives of future improvements.

3. CONCLUSIONS

The HPLC determination of metal ions was first developed in the mid-1970s, the earliest achievements being largely attributable to normal- and reversed-phase HPLC of metal chelates. More recently, a shift has occurred towards the use of ion-pair reversed-phase HPLC of charged chelates, and subsequently IC methods, in which complex formation is also utilized to a greater or lesser extent. These are principally cation-exchange IC with postcolumn reaction detection, IC of metal complexes of chelate or non-chelate nature and coordination IC on chelating bonded phases. These chromatographic variants have rapidly gained importance owing to the growing demand for rapid methods for the determination of transition and heavy metals in complex matrices. The intense development of complexation IC seen recently is related to its main field of practical application, namely the analysis of environmental water samples [26,33,34], where this method is becoming the technique of choice.

An analysis of basic trends in the chromatographic determination of trace metals by complexation techniques suggests that adsorption HPLC of neutral metal chelates is gradually declining in popularity, although its modern modifications (supercritical fluid chromatography, chromatography with micellar mobile phases) look very promising. Among the complexation chromatographic meth-

ods considered here, non-suppressed cation chromatography already holds (or will soon take) the key positions. Ion-interaction IC on dynamically coated columns undoubtedly occupies a worthy place in the rank of complexation IC techniques. Nevertheless, at this stage it is difficult to evaluate the prospects of these methods, as they are highly developed technically and methodologically. The present situation with several powerful chromatographic methods competing in the practice of metal ion determinations may last for a long time, and only the future can tell which method will become the favourite, and when.

4. ACKNOWLEDGEMENTS

The authors thank all their colleagues for their assistance and personally Professor Oleg M. Petrukhin, Mendeleev University of Chemical Technology, Moscow (to whom this paper is dedicated on the occasion of his 60th birthday) and Dr. Petr Jandik, Waters Chromatography, Millipore Corporation, Milford, MA, USA.

REFERENCES

1 G. G. Wallace and J. M. Rivello (Editors), *Complexation Chromatography*, Royal Society of Chemistry, Cambridge, 1990.
2 H. Small, *Ion Chromatography*, Plenum Press, New York, London, 1990.
3 P. R. Haddad and P. E. Jackson, *Ion Chromatography. Principles and Applications (Journal of Chromatography Library*, Vol. 46), Elsevier, Amsterdam, 1990.
4 I. S. Krull (Editor), *Trace Metal Analysis and Speciation (Journal of Chromatography Library*, Vol. 47), Elsevier, Amsterdam, 1991.
5 K. Robards, P. Starr and E. Patsalides, *Analyst*, 166 (1991) 1247.
6 P. K. Dasgupta, *Anal. Chem.*, 64 (1992) 775A.
7 L. Nondek, in D. Cagniant (Editor), *Complexation Chromatography (Chromatographic Science Series*, Vol. 57), Marcell Dekker, New York, 1992, p. 1.
8 S. Reiffenstuhl and G. Bonn, *Fresenius' Z. Anal. Chem.*, 332 (1988) 130.
9 S. Reiffenstuhl and G. Bonn, *J. Chromatogr.*, 482 (1989) 289.
10 V. I. Orlov, A. A. Aratskova, A. R. Timerbaev and O. M. Petrukhin, *Zh. Anal. Khim.*, 47 (1992) 686.
11 G. Bonn, S. Reiffenstuhl and P. Jandik, *J. Chromatogr.*, 499 (1990) 669.
12 G. Bonn, S. Nathakarnkitkool and P. Jandik, in P. Jandik and R. M. Cassidy (Editors), *Advances in Ion Chromatography*, Vol. 1, Century International, Medfield, MA, 1991, p. 197.
13 V. I. Orlov, A. A. Aratskova, A. R. Timerbaev and O. M. Petrukhin, *Zh. Anal. Khim.*, 44 (1989) 2060.
14 M. L. Marina, J. C. Diez-Masa and M. V. Dabrio, *J. Liq. Chromatogr.*, 12 (1989) 1973.
15 I. P. Alimarin, E. M. Basova, T. A. Bol'shova and V. M. Ivanov, *Zh. Anal. Khim.*, 45 (1990) 1478.
16 A. R. Timerbaev and O. M. Petrukhin, *Zh. Anal. Khim.*, 46 (1991) 213.
17 A. R. Timerbaev, O. M. Petrukhin, V. I. Orlov and A. A. Aratskova, *J. Liq. Chromatogr.*, 15 (1992) 1443.
18 P. R. Haddad and R. C. Foley, *J. Chromatogr.*, 500 (1990) 301).
19 J. Hradil, F. Svec, A. A. Aratskova, L. D. Belyakova and V. I. Orlov, *J. Chromatogr.*, 509 (1990) 369.
20 P. N. Nesterenko and T. A. Bol'shova, *Vestn. Mosk. Univ., Ser. Khim.*, 31 (1990) 167.
21 J.-I. Toei, *Chromatographia*, 23 (1987) 355.
22 A. M. Dolgonosov, T. V. Grishinova and A. R. Timerbaev, *International Ion Chromatography Symposium 1991, Denver, CO, October 1991*, Abstract No. 16.
23 A. M. Dolgonosov, *React. Polym.*, 17 (1992) 95.
24 P. R. Haddad and A. D. Sosimenko, *J. Chromatogr. Sci.*, 27 (1989) 456.
25 A. R. Timerbaev, I. G. Tsoi and O. M. Petrukhin, *J. Chromatogr.*, 498 (1990) 337.
26 A. R. Timerbaev, O. M. Petrukhin, I. P. Alimarin and T. A. Bol'shova, *Talanta*, 38 (1991) 467.
27 R. M. Cassidy and B. D. Karcher, in I. S. Krull (Editor), *Reaction Detection in Liquid Chromatography*, Marcel Dekker, New York, 1986, p. 129.
28 P. K. Dasgupta, *J. Chromatogr. Sci.*, 27 (1989) 422.
29 P. R. Haddad and P. E. Jackson, in Z. B. Alfassi and C. M. Wai (Editors), *Preconcentration Techniques for Trace Elements*, CRC Press, Boca Raton, FL, 1992, p. 243.
30 G. K. Bonn, S. Nathakarnkitkool, J. F. Rankl and P. Jandik, presented at *10 Königsteiner Chromatographic-Tage 1989, Nürnberg, October 1989*.
31 A. M. Dolgonosov, *Ph. D. Thesis*, Moscow, 1988.
32 A. R. Timerbaev and O. M. Petrukhin, *Zh. Anal. Khim.*, 44 (1989) 1424.
33 R. E. Smith, *Ion Chromatography Applications*, CRC Press, Baco Raton, FL, 1988.
34 O. A. Shpigun and Yu. A. Zolotov, *Ion Chromatography in Water Analysis*, Ellis Horwood, Chichester, 1988.

Journal of Chromatography, 640 (1993) 207–216
Elsevier Science Publishers B.V., Amsterdam

CHROMSYMP. 2784

Determination of cadmium and lead at μg/l levels in aqueous matrices by chelation ion chromatography

N. Cardellicchio*

CNR — Istituto Sperimentale Talassografico, Via Roma 3, 74100 Taranto (Italy)

S. Cavalli

Dionex srl, Via Grigna 9, 20155 Milan (Italy)

J. M. Riviello

Dionex Corporation, Sunnyvale, CA 94086 (USA)

ABSTRACT

A method for the simultaneous determination of μg/l or sub-μg/l levels of cadmium and lead in sea water by chelation ion chromatography is demonstrated. The method consists in the preconcentration of a sea-water sample containing cadmium and lead on an iminodiacetate chelating resin; alkali and alkaline earth metals are removed from the resin with an ammonium acetate buffer, the metals are eluted and separated by cation-exchange chromatography, followed by postcolumn derivatization with 4-(2-pyridylazo)resorcinol and spectrophotometric detection at 520 nm. The concentration and separation steps are automated. The detection limit, when concentrating 200 ml of sea water, was found to be 2 ng for cadmium and 6 ng for lead. Relative standard deviations of 4.5% and 6.8% for 10 μg/l of cadmium and lead, respectively, were obtained. Transition metals (Fe, Co, Ni, Zn, Cu, Mn) do not interfere in the analysis. An application of the method to the determination of cadmium and lead in sea-water samples collected in the Taranto gulf (Italy) is presented.

INTRODUCTION

The determination of trace elements, particularly heavy metals, in real matrices has received increasing attention in recent years. The use of fertilizers, pesticides, coal and oil in combustion processes and, most significantly, the wide use of metals in a variety of industries has resulted in a significant increase of their concentration in the environment.

Among heavy metals, cadmium and lead have special importance from the ecotoxicological point of view, both for the high toxicity of their compounds and their accumulation in various organisms [1–4]. The concentrations of both metals in sea water are usually in the range of μg/l or less. Different techniques have been developed for trace level determinations of cadmium and lead in sea water; in particular, anodic stripping voltammetry (ASV) [5,6], also coupled to flow-injection analysis [7], HPLC [8] and preconcentration techniques coupled to flow-injection atomic absorption spectrometry (AAS) [9] or to inductively coupled plasma mass spectrometry (ICP-MS) [10] have been used.

Direct determination of metals is highly desirable as it entails minimum sample handling and pretreatment, thereby minimizing the risk of contamination and, more important, eliminating the reagent blank common to all chemical pretreatment methods. In sea water low concentration levels of cadmium and

* Corresponding author.

0021-9673/93/$06.00

lead are associated with high concentrations of alkali and alkaline earth metals, whose presence produces interferences due to matrix effects, making direct analysis difficult. For the determination of trace metals in complex matrices it is therefore necessary to implement preconcentration followed by a separation step. This procedure is useful in order to obtain both an increase in detectability of analytes and to minimize matrix interferences.

In the preconcentration step, metals are generally complexed by chelating agents; metal complex separation can be effected by solvent extraction [11] or by precipitation [12]. The chelating agent could be in an immobilized form in a resin and packed in a chromatographic column. Metals can be released eiher by digesting the resin with acid [13] or by changing the ionic form of the resin.

The properties of iminodiacetate chelating resins such as Chelex-100 are well known [14–28]. Kingston *et al.* [24] studied the use of Chelex-100 in sea-water analysis, introducing a preliminary separation of alkali and alkaline earth elements collected on the column by stripping with 1 *M* ammonium acetate at pH 5.2. Cadmium and lead recoveries from sea water were higher than 90% at μg/l levels; the recovery values are influenced by pH and they are quantitative only in the narrow pH range 4.7–5.5. Using these resins, preconcentration methods and the separation of the saline matrix were reliable [29–31] and allowed enrichment factors of >100 [32].

Chelex-100 resin has been used in the batch mode for preconcentration and matrix elimination prior to graphite furnace AAS [24,29], ICP atomic emission spectrometry (AES) [32,33] and neutron activation analysis [31]. Recently, different workers have implemented an automated on-line column preconcentration for flow-injection AAS [34–36]. Many attempts to improve metal retention on Chelex-100 chelating resin have been made by decreasing the flow-rate [15], adjusting the resin size and packing in different acidic and basic solutions [24] and lowering the ammonium acetate concentration to avoid metal loss during the matrix elimination step [35]. The slight improvements observed were not considered adequate to enhance the accuracy of analysis. Characteristically, the resin volume changes substantially in acidic and basic solutions owing to its low cross-linked (gel-type) microporous poly(styrene–divinylbenzene) (PS–DVB) supporting polymer. It was concluded that the low recovery of metal ions from Chelex-100 resin [36,37] was caused by physical degradation of the resin under pressures greater than 0.69 MPa. This causes a series of problems in the use of these columns in automatic preconcentration systems.

Recently, such problems have been solved with the development of a highly cross-linked macroporous PS–DVB-based resin with iminodiacetate functional groups [38]. This resin was used to prepare a MetPac-CC1 column, which gave the best results in automatic preconcentration systems from aqueous matrices coupled on-line to ion chromatography, ICP-AES and ICP-MS. In recent years ion-exchange chromatographic techniques have been developed for environmental application [39] and in particular in the separation and detection of metals [38,40]. Ion chromatographic techniques with spectrophotometric detection after postcolumn derivatization with a chromogenic ligand, coupled on-line with preconcentration by chelation, allowed the determination of trace levels of transition metal and lanthanides in complex matrices. For transition metals the metallochromic indicator most often used is 4-(2-pyridylazo)resorcinol (PAR) [41–43]. PAR–metal complexes show relatively high molar absortivities ($>20\ 000$) in the range 500–540 nm and a relatively low background absorbance at the same wavelengths.

This paper describes an automated chelation ion-exchange chromatographic system followed by postcolumn derivatization and spectrophotometric detection for the simultaneous determination of trace levels of cadmium and lead in sea water. In particular, we discuss the preconcentration of cadmium and lead present in sea water on highly cross-linked iminodiacetate chelating resin and the use of cation-exchange chromatography for the separation of the metals. Selectivity, interferences, linear dynamic range and detection limits of the technique are also discussed.

EXPERIMENTAL

Instrumentation

A metal-free high-pressure ion chromatographic (IC) system including one gradient pump (GPM, 4500i series), two single reciprocating piston pumps

(DQP) and a pressurized postcolumn reagent delivery module (RDM) (Dionex, Sunnyvale, CA, USA) was used. The gradient pump was employed for delivering different reagents during the matrix elimination, metal elution and chelating column reconditioning steps. One DQP pump was used for sample preconcentration on a MetPac CC-1 column, and the other DQP pump, equipped with a pulse damper, was used to deliver eluent through the analytical column. Two air-activated metal-free slider valves were used for switching reagents, sample, pumps and columns. The eluent and postcolumn reagent solution were mixed with the aid of a low-dead-volume T-piece, positioned at the exit of the analytical column, followed by a packed-bed reaction coil. A VDM UV–Vis detector (Dionex) was used for metal detection. Traces of metals in the chromatographic system were removed by flushing all flow paths, pumps, valves and columns with 0.2 *M* oxalic acid for 3 h at 1 ml/min, followed by rinsing with deionized water. After column removal, the flow path was washed with 6 *M* HNO_3 for 3 h at 1 ml/min, followed by rinsing with deionized water. Data manipulation and the operation of all components in the system were controlled by AI-450 chromatographic software (Dionex) interfaced via an Advanced Controller Interface (ACI; Dionex) to a Model 80386-based computer (Olivetti, Ivrea, Italy).

Fig. 1 shows a flow diagram of the automated chelation ion chromatographic system. The programming of time and events for columns, valves and reagent switching is outlined in Table I.

A PAR 384 B polarographic analyser (Princeton Applied Research, Princeton, NJ, USA) equipped with a mercury electrode (Model 303 SMDE) was used for cadmium and lead determination in seawater samples by differential-pulse anodic stripping voltammetry (DPASV).

Reagents and standards

Potassium chloride, potassium sulphate, potassium nitrate and oxalic acid were of analytical-reagent grade (Novachimica, Milan, Italy) and hydrochloric acid, sulphuric acid, nitric acid, ammonia solution and acetic acid were of Ultrex grade (J. T. Baker, Phillipsburg, NJ, USA). 4-(2-Pyridylazo)resorcinol (PAR) of analytical-reagent grade was obtained from Aldrich (Milwaukee, WI, USA). A 2 *M* ammonium acetate solution (pH 5.5 ± 0.1) was prepared from ultrapure acetic acid and ammonia solution. All reagents and standards were prepared daily with ultra-pure deionized water (<0.1 μS at 25°C) obtained by treating doubly distilled water in a Milli-Q system (Millipore, Milford, MA, USA). Working standard solutions were prepared by serial dilution of a stock standard solution containing 1000 mg/l of Cd(II), Pb(II), Fe(II), Mn(II), Co(II), Ni(II), Zn (II) and Cu(II) (BDH, Poole, UK).

All standard, samples and reagents were stored in polyethylene bottles cleaned and conditioned fol-

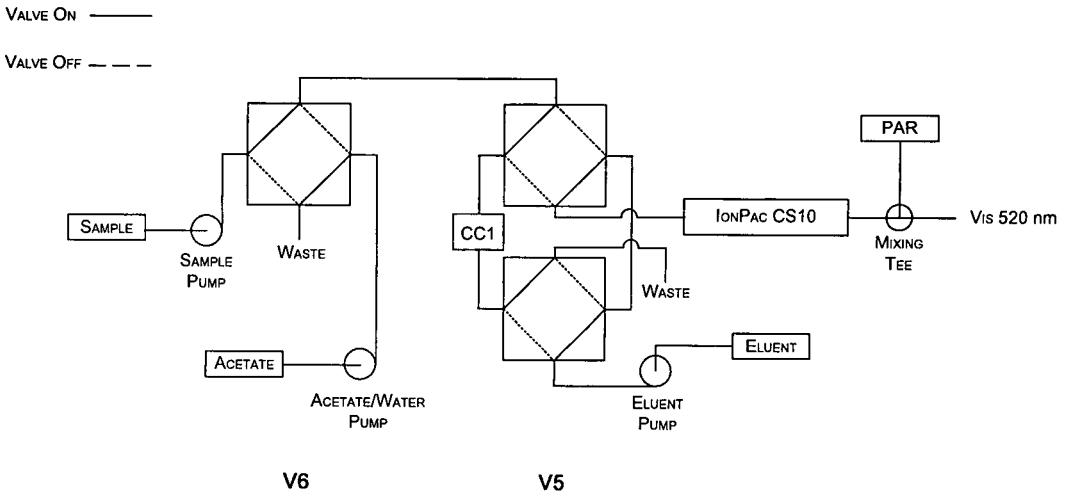

Fig. 1. Schematic flow diagram of automated chelation IC.

TABLE I

CHELATION IC PROGRAMME FOR CONCENTRATING 20-ml SEA-WATER SAMPLES

Time (min)	Sample[a]	Acetate[b]	Water[b]	Eluent[c]	V5[d]	V6[d]	Event
0.0	0	1	0	1	0	1	Start MetPac conditioning
2.0	0	1	0	1	0	1	End MetPac conditioning
2.1	0	0	1	1	0	1	Start acetate elimination
2.9	0	0	1	1	0	1	End acetate elimination
3.0	1	0	0	1	0	0	Load sample on MetPac
11.0	1	0	0	1	0	0	Sample loaded
11.1	0	1	0	1	0	1	Start matrix elimination
11.4	0	1	0	1	0	1	Matrix eliminated
11.5	0	0	0	1	1	1	Injection

[a] Flow-rate 2.5 ml/min.
[b] Flow-rate 3 ml/min.
[c] Flow-rate 1 ml/min.
[d] 1 = On; 0 = off.

lowing suggested procedures for trace element determination [44,45].

Eluent

The final choice for the chromatographic eluent was 0.075 *M* H_2SO_4–0.1 *M* HCl–0.1 *M* KCl. The eluent flow-rate was 1 ml/min.

Postcolumn reagent

The postcolumn reagent (PCR) solution consisted of 0.3 m*M* PAR in 1.0 *M* 2-dimethylaminoethanol–0.5 *M* ammonia solution–0.5 *M* sodium hydrogencarbonate buffer. The solution was filtered through a 0.45-μm filter before use. The chromatographic response (peak area) was found to be dependent on the PAR flow-rate. Excellent linearity was obtained in the range 0.2–0.5 ml/min. The PCR flow-rate was finally set to 0.5 ml/min. The detector wavelength was set at 520 nm.

Columns

Preconcentration and matrix elimination were carried out on a MetPac-CC1 (Dionex) column (50 mm × 4 mm I.D.) packed with a styrene-based macroporous 12% cross-linked iminodiacetate-functionalized chelating resin. The particle size was 20 μm and the capacity of the resin was about 0.9 mequiv. Cu(II)/g. The separations were carried out on a IonPac CS10 (Dionex) column (250 mm × 4 mm I.D.) packed with 8.5-μm solvent-compatible PS–DVB substrate agglomerated with 175-nm cation-exchange latex for a total ion-exchange capacity of 80 μequiv. per column.

Sea-water sampling

Surface sea-water samples (1–2 m depth) were collected using a Niskin bottle from the Taranto gulf (Ionian Sea, Italy). Samples were filtered immediately after collection by vacuum filtration through glass-fibre filters (GF/F grade, diameter 47 mm, nominal pore size 0.7 μm) and preserved by the addition of ultra-clean concentrated hydrochloric acid (1 ml/l). The samples were immediately frozen at −4°C using polypropylene bottles for storage. Before analysis, acidified samples were buffered with 2 *M* ammonium acetate (pH 5.5).

RESULTS AND DISCUSSION

Chelation ion chromatography

The complete chromatographic procedure for sample preconcentration, matrix elimination and separation can be described as follows: (1) the MetPac-CC1 column was activated with 2 *M* ammonium acetate; (2) sample buffered at pH 5.5 was loaded on to the MetPac-CC1 column; (3) alkali and alkaline-earth metals in the sample were washed off the MetPac-CC1 column with ammonium acetate;

(4) ammonium acetate remaining on the chelating column was washed off with deionized water; (5) the MetPac-CC1 column was switched to the eluent line and metals concentrated on the resin was then injected into the chromatographic system for separation; (6) after separation, PAR, added postcolumn, formed derivatives of metals that were detected by a spectrophotometric detector. A schematic diagram for automated chelation IC is shown in Fig. 1 and the chelation IC programme is described in Table I.

Preconcentration on MetPac-CC1 column

MetPac-CC1 has a highly cross-linked polymeric backbone compared with the Chelex-100 resin type [38]. Because of this characteristic, both the physical and mechanical properties remain stable over a wide range of pH values and ionic strengths.

In the preconcentration of transition metals it has been demonstrated that the recovery is independent of both the flow-rate used for sample loading on to the resin and 2 *M* ammonium acetate flow-rate [38]. Usually the complete elution of Cd(II) and Pb(II) from an iminodiacetate resin such as Chelex-100 was obtained by using a strong acid (HNO_3) or a complexing agents such as 0.0025 *M* EDTA at pH 8 [46].

In this work the same eluent as used for the ion chromatographic separation of metals was used to elute them from chelating resin. With these restrictions it was necessary to evaluate how the acidic eluent used for separation could be used for the quantitative elution of metals from the iminodiacetate resin. The types of acids and counter ions chosen must be compatible with the following chromatographic separation.

In Fig. 2 are shown the different elution profiles of cadmium and lead from the MetPac-CC1 column obtained with different acidic solutions. The resulting chromatograms show that elution is more efficient at higher acidity. The best results, corresponding to complete elution of metals in a smaller volume, can be achieved with 0.5 *M* HNO_3, which was found not to be useful for the desired ion chromatographic separation. Different mixtures of sulphuric and hydrochloric acid and potassium

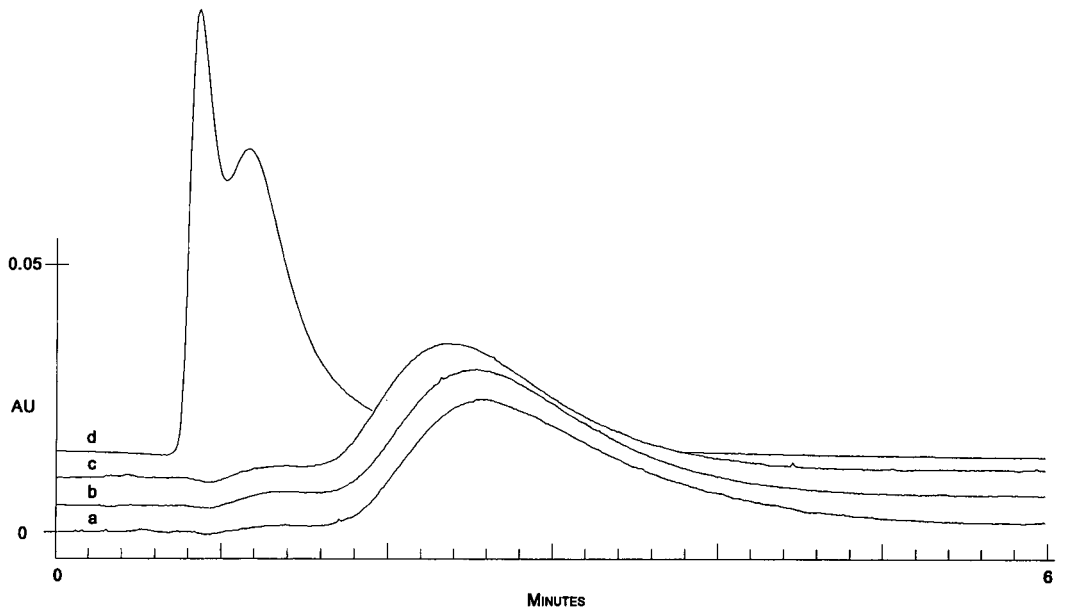

Fig. 2. Elution profile of Cd (500 ng) and Pb (500 ng) from MetPac-CC1 column using different eluents. Flow-rate, 1 ml/min; detection, absorbance (520 nm) after postcolumn derivatization with 0.3 m*M* PAR in 1.0 *M* 2-dimethylaminoethanol–0.5 *M* ammonia solution–0.5 *M* sodium hydrogencarbonate buffer. (a) 0.075 *M* H_2SO_4–0.05 *M* HCl–0.1 *M* KCl; (b) 0.075 *M* H_2SO_4–0.05 *M* HCl–0.15 *M* KCl; (c) 0.075 *M* H_2SO_4–0.1 *M* HCl–0.1 *M* KCl; (d) 0.5 *M* HNO_3–0.1 *M* KCl.

chloride elute metals in a larger volume than nitric acid, but in a volume small enough for our purposes. The elution volume for 500 ng of Cd and Pb, concentrated on the MetPac-CC1 column, using the same eluent of chromatographic separation at a flow-rate of 1 ml/min was 2.5 ml, as shown in Fig. 2.

In addition to the acidity effect, the effects of complexing agents such as chloride must also be considered. The formation of chloro–metal complexes contributes to decreasing the elution volume of cadmium and lead from the chelating resin. For the choice of the eluting solution and the successive chromatography all these effects were considered together with PAR postcolumn derivatization compatibility.

Matrix elimination

It has been demonstrated previously that iminodiacetate resins can efficiently eliminate alkali and alkaline-earth metals, resulting in a great advantage in sea-water analysis. Elimination of Na, K, Mg and Ca is necessary because of interferences in chromatography and in determination by postcolumn derivatization with PAR. For the experiment, 50 ml of synthetic sea water with concentrations of 1.30 g/l of Mg and 0.41 g/l of Ca were preconcentrated on the MetPac-CC1 column, then the resin was eluted with 2 *M* ammonium acetate buffered at pH 5.5. The elution volume of alkali and alkaline-earth metals was only 1.5 ml. Changes in the flow-rate from 1 to 3 ml/min did not influence the recoveries of retained metals. With Chelex-100 a decrease in recoveries, as a function of acetate flow-rate, was observed [32].

Ion chromatography

Separation of transition metals can usually be accomplished via complexation with eluent and anion or cation exchange [40]. The main problem with strong complexing eluents such as pyridine-2,6-dicarboxylic acid or oxalate is that they interfere with the metallochromic indicator used for postcolumn reaction. Also, the pH can interfere in the PAR complexation process; a higher pH increases the ionization of PAR, thus exploiting its complexing capabilities, but hydrolysis of metals could be observed along with the simultaneous disappearance of the signal, whereas on the other hand using very low pH can result in precipitation of PAR. The separation of selected groups of transition metals can be readily accomplished using cation-exchange resins. As a result of the differences in the hydrated radii of aquated metal ions within a group (*e.g.*, zinc, cadmium and mercury) and/or different rows of the Periodic Table, sulphonated cation-exchange resins have sufficient selectivity for these separations. Separations of transition metals that are in different rows or columns of the Periodic Table can usually be accomplished by cation exchange without the addition of complexing agents. A secondary equilibrium (complexation) is not required if the metal ions have different valences or different charge densities, which is often the case when the metal ions are well separated in the Periodic Table. Chromatographic separations of Cd and Pb from other transition metals performed on an IonPac CS10 cation exchanger are shown in Fig. 3. An increase in acidity lowers the retention time of the considered metals, while the separation of Cd and Pb from Fe(II) and other transition metals is sufficient.

The effect of the counter ion was investigated, because in general most transition metals show lower retention on cation exchangers as the chloride concentration increases owing to the formation of neutral or anionic complexes. Selectivity generally increases as the chloride concentration increases. For effective separation using IonPac CS10 cation-exchange resin, chloride concentrations of 0.05 *M* and above are required; in instance case cadmium and lead are separated by cation exchange while most of first-row transition elements co-elute under these conditions. Fig. 4 shows chromatograms of a standard solution containing Cd, Pb and Fe(II) analysed with different eluents; the importance of Cl^- as a complexing ion on the separation of different metals can be observed. Sulphate also acts as a ligand and probably contributes to the separation.

The best compromise between total run time and selectivity was achieved with 75 m*M* H_2SO_4–100 m*M* HCl–100 m*M* KCl as eluent.

Recovery

For the calculation of recoveries, the MetPac-CC1 column was washed with 6 ml of 0.5 *M* HNO_3 at 1 ml/min to eliminate any traces of metals, then rinsed with deionized water. The resin was then converted into the ammonium form by pumping 2 *M* ammonium acetate solution followed by 3 ml of

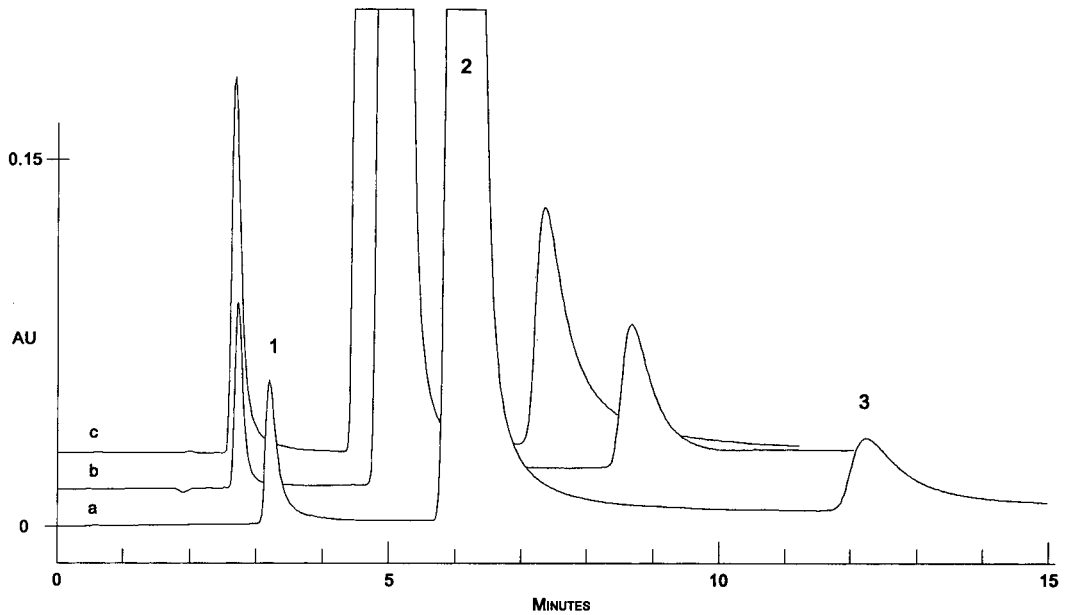

Fig. 3. Chromatogram of a standard solution (500 ng each) of metals with different eluents. Peaks: 1 = Cd; 2 = Fe(II), Ni, Cu, Zn, Co, Mn; 3 = Pb. Column, IonPac CS10; flow-rate, 1 ml/min; detection, as in Fig. 2. (a) 0.075 *M* H_2SO_4–0.05 *M* HCl–0.1 *M* KCl; (b) 0.075 *M* H_2SO_4–0.1 *M* HCl–0.1 *M* KCl; (c) 0.075 *M* H_2SO_4–0.125 *M* HCl–0.1 *M* KCl.

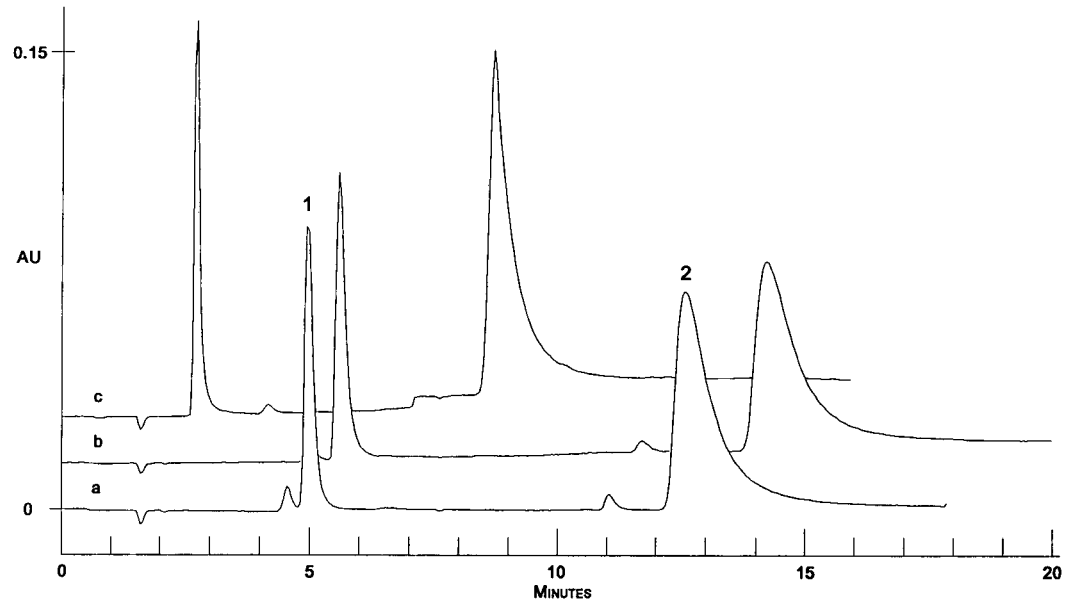

Fig. 4. Chromatogram of a standard solution (1 μg each) of metals with different counter ions in the eluent. Peaks: 1 = Cd; 2 = Pb. Column, IonPac CS10; flow-rate, 1 ml/min; detection, as in Fig. 2. (a) 0.15 *M* H_2SO_4–0.05 *M* K_2SO_4; (b) 0.15 *M* H_2SO_4–0.1 *M* KNO_3; (c) 0.15 *M* H_2SO_4–0.1 *M* KCl.

TABLE II

RECOVERIES OF METALS ADDED TO DEIONIZED AND SEA-WATER MATRICES

Element	Recovery (%)[a]		R.S.D. (%)
	Deionized water	Sea water	
Cd	100	91	4.8
Pb	100	89	5.2

[a] Average recoveries ($n = 5$); sample size = 50 ml, concentrated.

deionized water for washing off the residual acetate. A sea-water sample adjusted to pH 5.5 with 2 *M* ammonium acetate was spiked with 10 μg/l each of Cd and Pb. The content of Cd and Pb was then confirmed by DPASV [47]. The preconcentration and matrix elimination procedure was then effected on-line by the following procedure. First 50 ml of sample were pumped through the MetPac-CC1 column at 1 ml/min. The resin was then washed by pumping 10 ml of 2 *M* ammonium acetate to eliminate alkaline-earth metals; 6 ml of eluent were pumped through the MetPac-CC1 column for elution of metals.

Table II gives the recoveries of cadmium and lead from 50 ml of sea water spiked with 5 μg/l of each metal.

Linearity and detection limit

The method shows good linearity for both cadmium ($r = 0.997$) and lead ($r = 0.998$) up to 500 ng, which means that is possible to preconcentrate, *e.g.*, 20 ml of sea water with Cd and Pb concentrations ranging from 1 to 50 μg/l within the linearity of the system. Volumes of sea water up to 200 ml were preconcentrated with good linearity of response at lower metal concentrations. The detection limit (twice the standard deviation of the blank sample) was 2 ng for cadmium and 6 ng for lead.

Reproducibility

The reproducibilities of the peak area and retention time were calculated by performing five replicate analyses of sea-water samples collected far from the coast of Taranto. This sea water, which usually has concentrations of Cd and Pb in the ng/l range, was fortified with 10 μg/l each of Cd and Pb.

The relative standard deviations (R.S.D.) for peak area were 4.5% and 6.8% for Cd and Pb, respectively. The R.S.D.s for retention time were

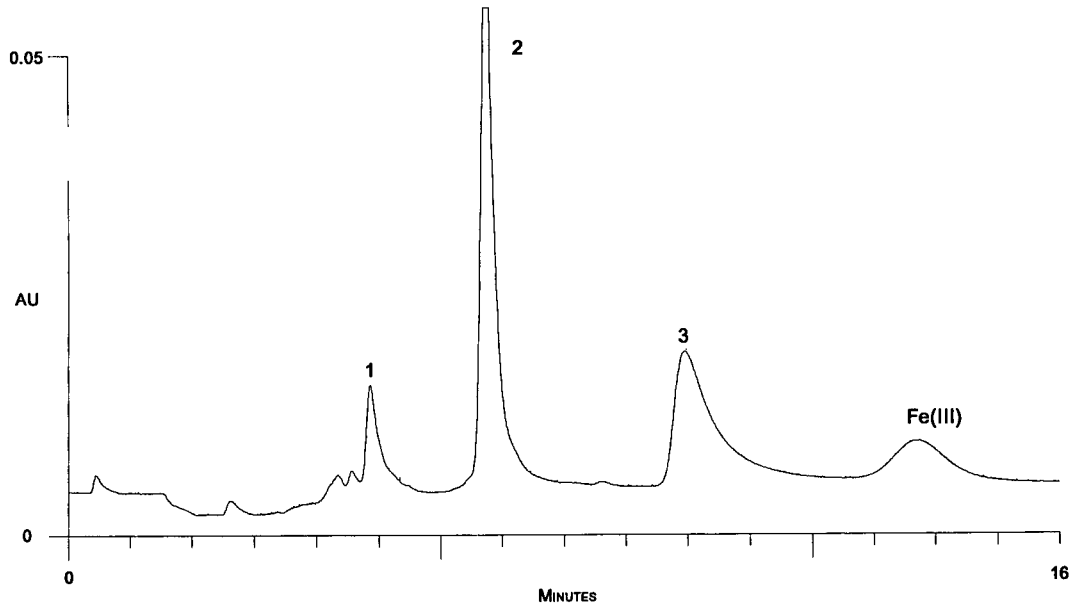

Fig. 5. Chromatogram of a standard solution. Peaks: 1 = Cd (500 ng); 2 = Fe(II), Ni, Cu, Zn, Co, Mn (50 ng each); 3 = Pb (500 ng). Column, IonPac CS10; eluent, 0.075 *M* H_2SO_4–0.1 *M* HCl–0.1 *M* KCl; flow-rate, 1 ml/min; detection, as in Fig. 2.

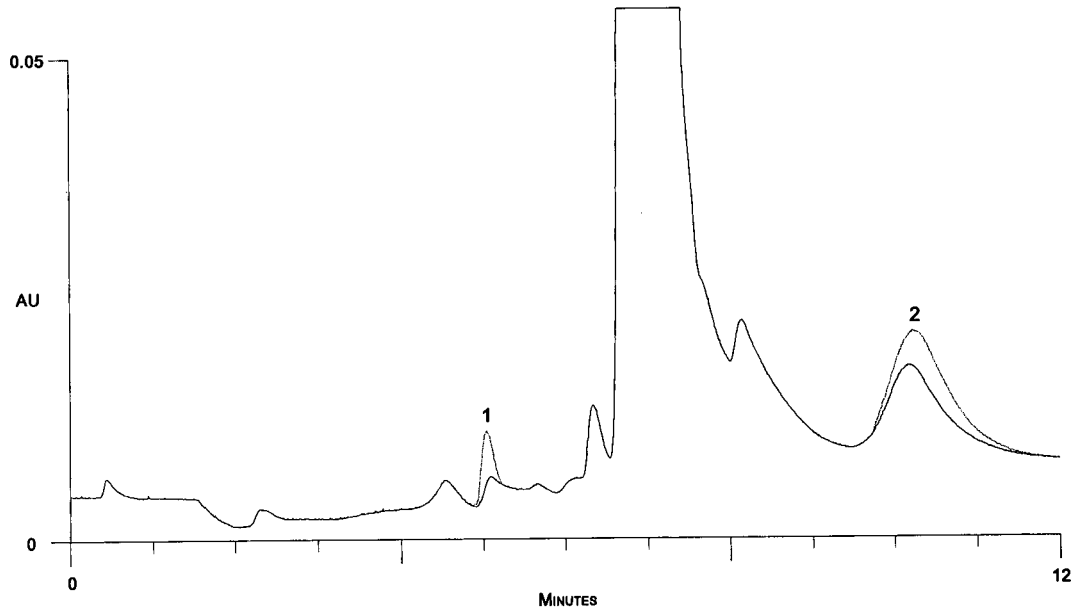

Fig. 6. Determination of metals in Taranto gulf sea water (80 ml, preconcentrated). Peaks: 1 = Cd (0.33 μg/l); 2 = Pb (2.06 μg/l). Dotted line = same sample spiked with 5 μg/l each of Cd and Pb (80 ml, preconcentrated); Cd, 5.50 μg/l; Pb, 7.46 μg/l. Conditions as in Fig. 5.

1.2% and 2.5% for Cd and Pb, respectively.

The reliability of the method was tested by analysing Taranto gulf sea-water samples, usually containing Cd and Pb in the low μg/l range, with both chelation ion chromatography and DPASV. In all instances the results were in good agreement.

Sea-water analysis

Blank. Reagents (particularly ammonium acetate) and water were the main source of blank contamination. Major contributions to contamination arise from iron, copper and zinc. This kind of contamination can be reduced by using ultrapure reagents and water. Also, washing the flow paths with nitric and oxalic acid as described elsewhere can reduce the contamination. In any case the eventual contamination due to first-row transition metals does not interfere with cadmium and lead determination, as shown in Fig. 5.

Sea-water samples. For sea-water analysis it must be noted that most of the dissolved Cd and Pb can be associated with inorganic colloidal species, such as oxides, silicates, sulphides and organic materials such as humic acids [47]. Colloidal particles were not retained by the chelating resin, hence the values obtained are relative only to the "dissolved fraction" metals concentration, which is lower than the total content. A UV photo-oxidation treatment in acid, which destroys the organic matter, allows bonded metals also to be detected [29].

Fig. 6 shows the chromatogram of a sea-water sample from the Taranto gulf with trace levels of cadmium and lead; the dotted line shows the same sample spiked with 5 μg/l each of Cd and Pb. The pH of both samples was adjusted to 5.5 with 2 *M* ammonium acetate, then 80 ml of each sample were analysed. The R.S.D. for peak area were 6.4% and 7.2% for Cd and Pb, respectively. Good agreement was obtained in comparison with DPASV using the method of Batley and Florence [47].

CONCLUSION

A simple, automated method for the determination of low concentrations of cadmium and lead in complex matrices, such as sea water, has been developed. The higher cross-linked resin used for preconcentration and matrix elimination provides reliable and reproducible analyses. The chromatographic separation of Cd and Pb by cation-exchange chromatography does not suffer from interferences from transition metals and of postcolumn derivati-

zation with PAR is suitable for detection, without competition in complexation.

ACKNOWLEDGEMENTS

The authors express their gratitude to Filippi Maria, Marra Claudio and Ragone Pietro for their assistance with the chelation ion chromatographic and DPASV measurements.

REFERENCES

1 G. W. Bryan, in R. Johnston (Editor), *Marine Pollution —Heavy Metal Contamination in the Sea*, Academic Press, London, 1976, p. 185.
2 D. F. Flick, H. F. Kraybill and J. M. Dimitroff, *Environ. Res.*, 4 (1971) 71.
3 O. Ravera, *Experientia*, 40 (1984) 2.
4 B. Scaule and C. C. Paterson, presented at the *Conference on Trace Metals in Sea Water, Nato Advanced Research Institute, Erice, Sicily, March 30–April 1, 1981.*
5 T. M. Florence, *Talanta*, 29 (1982) 345.
6 A. R. Fernando and J. A. Plambeck, *Anal. Chem.*, 61 (1989) 2609.
7 P. Jayaweera and L. Ramaley, *Anal. Chem.*, 61 (1989) 2102.
8 J. H. Shofstahl and J. K. Handy, *J. Chromatogr. Sci.*, 28 (1990) 220.
9 S. Hirata, K. Honda and T. Kumamaru, *Anal. Chim. Acta*, 221 (1989) 65.
10 E. M. Heithmar, T. A. Hinners, J. T. Rowan and J. M. Riviello, *Anal. Chem.*, 62 (1990) 857.
11 J. C. Van Loon, *Selected Methods of Trace Metal Analysis*, Wiley-Interscience, New York, 1985, p. 104.
12 X.-Q. Shan, T. Jun and G.-G. Xie, *J. Anal. At. Spectrom.*, 3 (1988) 259.
13 Y. S. Chung and R. M. Barnes, *J. Anal. At. Spectrom.*, 3 (1988) 1079.
14 H. Loewenschuss and G. Schmuckler, *Talanta*, 11 (1964) 1399.
15 J. P. Riley and D. Taylor, *Anal. Chim. Acta*, 40 (1968) 479.
16 J. P. Riley and D. Taylor, *Deep-Sea Res.*, 19 (1972) 727.
17 M. J. Abdullah, O. A. El-Rayis and J. P. Riley, *Anal. Chim. Acta*, 84 (1974) 363.
18 T. M. Florence and G. E. Batley, *Talanta*, 22 (1975) 201.
19 T. M. Florence and G. E. Batley, *Talanta*, 23 (1976) 179.
20 P. Figura and B. McDuffie, *Anal. Chem.*, 51 (1979) 120.
21 P. Figura and B. McDuffie, *Anal. Chem.*, 52 (1980) 1433.
22 L. L. Hendrikson, M. A. Turner and R. B. Corey, *Anal. Chem.*, 54 (1982) 1633.
23 P. Figura and B. McDuffie, *Anal. Chem.*, 49 (1977) 1959.
24 H. M. Kingston, I. L. Barnes, T. J. Brady, T. C. Rains and M. A. Champ, *Anal. Chem.*, 50 (1978) 2064.
25 J. A. Buckley, *Anal. Chem.*, 57 (1985) 1488.
26 M. G. Rao, A. K. Gupta, E. S. Williams and A. A. Aguwa, *AIChE Symp. Ser.*, 78 (1982) 103.
27 S. C. Pai, P. Y. Whung and R. L. Lai, *Anal. Chim. Acta*, 211 (1988) 257.
28 S. C. Pai, *Anal. Chim. Acta*, 211 (1988) 271.
29 R. E. Sturgeon, S. S. Bernan, A. Desaulniers and D. S. Russel, *Talanta*, 27 (1980) 85.
30 R. E. Sturgeon, S. S. Bernan, A. Desaulniers, A. P. Mykytluk, J. W. McLaren and D. S. Russel, *Anal. Chem.*, 52 (1980) 1588.
31 R. R. Greenberg and H. M. Kingston, *Anal. Chem.*, 55 (1983) 1160.
32 C. J. Cheng, T. Akagi and H. Haraguchi, *Anal. Chim. Acta*, 198 (1987) 173.
33 K. Vermeiren, C. Vandecasteele and R. Dams, *Analyst*, 115 (1987) 17.
34 S. Olsen, L. C. R. Pessenda, J. Ruzicka and E. H. Hansen, *Analyst*, 108 (1983) 905.
35 R. R. Greenberg and H. M. Kingston, *J. Radioanal. Chem.*, 71 (1982) 147.
36 W. Van Berkel Werefridus, A. W. Overbosch, G. Feensha and J. M. Maessent, *J. Anal. At. Spectrom.*, 3 (1988) 249.
37 S. C. Pai, P. Whung and R. L. Lai, *Anal. Chim. Acta*, 211 (1988) 257.
38 A. Siriraks, H. M. Kingston and J. M. Riviello, *Anal. Chem.*, 62 (1990) 1185.
39 W. T. Frankenberger, H. C. Mehra and D. T. Gjeerde, *J. Chromatogr.*, 504 (1990) 211.
40 J. M. Riviello and C. A. Pohl, presented at the *35th Pittsburgh Conference, 1984.*
41 A. Siriraks and H. M. Kingston, *Anal. Chem.*, 62 (1990) 1185.
42 R. M. Cassidy, S. Elchuk and J. O. McHugh, *Anal. Chem.*, 54 (1982) 727.
43 J. R. Jezorek and H. Freiser, *Anal. Chem.*, 51 (1979) 373.
44 M. Betti, M. P. Colombini, R. Fuoco and P. Papoff, *Mar. Chem.*, 17 (1985) 313.
45 A. W. Struempler, *Anal. Chem.*, 45 (1973) 2251.
46 Y. Lu and J. D. Ingle, Jr., *Anal. Chem.*, 61 (1989) 520.
47 G. E. Batley and T. M. Florence, *Mar. Chem.*, 4 (1976) 347.

Journal of Chromatography, 640 (1993) 217–226
Elsevier Science Publishers B.V., Amsterdam

CHROMSYMP. 2725

Automatic simultaneous determination of anions and cations in atmospheric aerosols by ion chromatography

Ewa Dabek-Zlotorzynska* and Joseph F. Dlouhy

Chemistry Division, River Road Environmental Technology Centre, Environment Canada, 3439 River Road, Ottawa, Ontario K1A 0H3 (Canada)

ABSTRACT

The application of an automatic quadruple ion chromatography system for the simultaneous determination of inorganic and organic anions, and inorganic cations in atmospheric aerosol extracts using a total volume of 5 ml is described. The automation of the analysis via a single loading system and analysis by anion isocratic, anion gradient (with and without preconcentration) and cation gradient methods with chemical suppression and conductometric detection is presented. Comparison of anion results obtained by the respective methods is shown.

INTRODUCTION

The measurement of the chemical, or at least elemental, composition of atmospheric aerosols is of great importance for better understanding of the nature of air pollution. Energy dispersive X-ray fluorescence spectroscopy (EDXRF) is a recognized method for analysis of elements in atmospheric aerosols collected on thin PTFE filters with virtual dichotomous samplers [1–3]. Ion chromatography (IC) is used to characterize the chemical form of compounds [2–4], because EDXRF measures only elemental composition.

IC has become the standard method of analysis for inorganic anions in many types of environmental samples. Common examples include river water, precipitation and atmospheric aerosols [5]. The value of IC for the analysis of atmospheric aerosols was first demonstrated by Mulik *et al.* [6] and was discussed in several papers presented at the 2nd Symposium on Ion Chromatography [7]. IC coupled with a concentration step is a powerful technique for trace and ultra-trace analysis [8].

Simultaneous analysis of inorganic and organic anions and cations is of particular interest to an environmental analytical laboratory, because this approach is potentially more effective than the existing methods, where the samples are analyzed separately.

Several different chromatographic strategies have been used for the simultaneous separation of anions and cations. One of these procedures converts the cations into anions by using suitable complexing agents and then separates and detects all species as anions [9]. In another approach a mixed bed ion-exchange column containing both cation- and anion-exchanger particles was used for simultaneous separation of inorganic mono- and di-valent anions and cations using a single sample injection [10]. Dual anion and cation columns with a single conductometric detection with synchronal sample injection [11] and anion and cation columns connected in series with indirect UV detection [12,13] have been used. A general method developed by Jones *et al.* [14–17] uses a serial placement of cation and anion columns followed by conductometric detection to effect separation and measurement. Cheam and Chau [18] determined major inorganic anions and cations using a double IC system. However, none of the procedures can analyze inorganic and organic anions and inorganic cations simultaneously.

* Corresponding author.

0021-9673/93/$06.00

The object of the research reported here was to develop a procedure whereby it would be possible to perform the routine separation and detection of inorganic and organic anions, and inorganic cations in a simultaneous system. Such system greatly increases the reliability and overall efficiency of the ion chromatographic procedures. This study describes the fully automated system for the simultaneous analysis of ten inorganic and organic anions and ten cations by IC in the aqueous extracts of atmospheric aerosols. The automation of the analysis via a single loading system and analysis by anion isocratic, anion gradient (with and without preconcentration) and cation gradient methods is presented. Comparison of anion results obtained by the three methods was performed.

EXPERIMENTAL

Chromatographic system

All IC equipment, columns and software used in this study were from one manufacturer (Dionex). Two personal computers (IBM, Model PS2/70) contained the operating and processing software (Model AutoIon 450). They were connected through interface modules (Model ACI). Two computerized advanced chromatography modules (Model CHA-6) were used for all anions and cations analyses. The system contained three ion chromatographs (Model 4500i) with gradient pumps (Model GPM), an ion chromatograph (Model 2110i) with an isocratic pump (Model APM), an automated sample changer (Model ASM), four micromembrane chemical suppressors (Models AMMS-II and CMMS-II), four micro conductivity detectors (Model CDM-2), four autoregeneration accessories (Model AutoRegen), four guard columns and four analytical columns.

The flow scheme of the single sample loading and injection configuration for analysis of inorganic and organic anions and inorganic cations is shown in Fig. 1. The first loading valve (V1) was connected to the anion gradient GB and cation gradient CAT channels (loading valves V2 and V3); the waste line of V3 valve was connected to valve V4 (anion gradient GA channel) and finally to valve V5 (anion isocratic IA channel) with the smallest possible dead volume between all valves.

Separation of anions and cations was carried out on the columns and under conditions listed in Table I.

Two anion trap columns (ATC-1) were used to minimize background contamination in each anion gradient system. One cation trap column (CTC-1) was installed in the cation system in a weak eluent line.

Anion and cation suppressors were continuously regenerated with 25 m*M* sulfuric acid and 100 m*M* tetrabutylammonium hydroxide (TBAOH), respectively. All regeneration solutions were continuously regenerated by autoregeneration accessories. The chromatograms and the results were printed on two printers (Epson, Model FX-850).

Operational procedure. The quadruple IC system is simultaneously loaded and samples are injected onto the separation columns at the same time. The speed of the system is determined by the speed of the slowest method (cation gradient method). The system can operate unattended for 48 h. Stability of aqueous extracts of atmospheric aerosols is the limiting time factor. At the present time, a 24-h period of unattended operation is used.

The pumps and the valves are under computer control, as indicated in Fig. 1. Loading–injection processes are automatically achieved in a timed sequence. By monitoring the programmable controller unit (1), the valve V1 is switched to bring analyzed samples from autosampler vials into the sample loops (valves V3–V5). Next, the valve V1 is switched to load concentrator column (valve V2) with the residue of the sample (2 ml). After the sample has been loaded onto the concentrator column, it is backflushed with eluent onto the guard and the analytical columns. At the same time, the analyte from sample loops is injected onto columns for separation.

Methods

Aqueous extracts of atmospheric aerosols collected on thin PTFE filters were analyzed for inorganic and organic anions, and inorganic cations. Four methods were applied:

Anion isocratic method (IA). The separation of inorganic anions (chloride, nitrite, bromide, nitrate, phosphate and sulphate) and oxalate was carried out isocratically on an IonPac-AS4A column with an IonPac-AG4A guard column. An eluent consisting of 1.7 m*M* $NaHCO_3$ and 1.8 m*M* Na_2CO_3 at

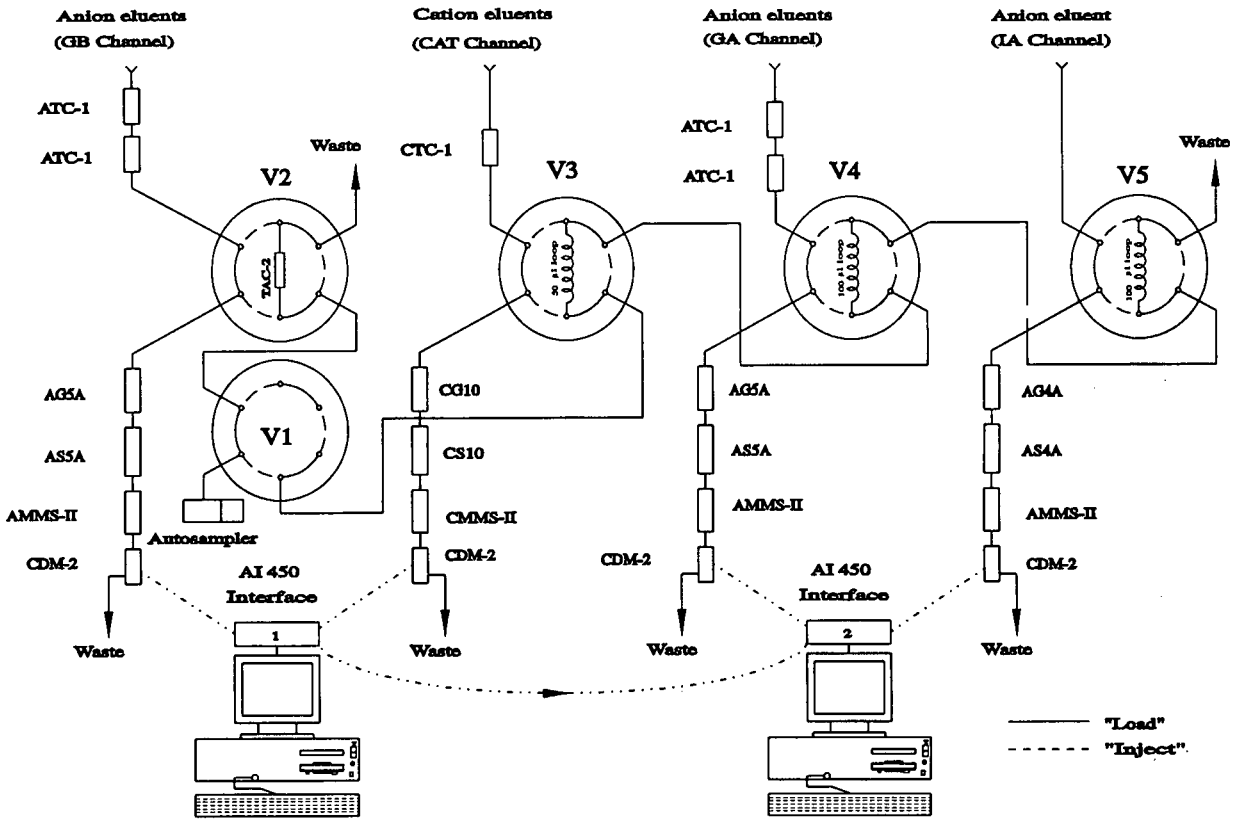

Fig. 1. The flow diagram of the single sample loading and injection configuration for simultaneous determination of anions and cations by ion chromatography.

TABLE I

EXPERIMENTAL CONDITIONS FOR ION CHROMATOGRAPHIC ANALYSIS

Parameter	IA method	GA/GB method	CAT method
Ions determined	Cl^-, NO_2^-, Br^-, NO_3^-, PO_4^{3-}, SO_4^{2-}, oxalate	F^-, acetate, formate, Cl^-, NO_2^-, Br^-, NO_3^-, PO_4^{3-}, SO_4^{2-}, oxalate	Li^+, Na^+, NH_4^+, K^+, Rb^+, Cs^+, Mg^{2+}, Ca^{2+}, Sr^{2+}, Ba^{2+}
Separation column	IonPac-AS4A (250 × 4 mm I.D.)	IonPac-AS5A (250 × 4 mm I.D.)	IonPac-CS10 (250 × 4 mm I.D.)
Guard column	IonPac-AG4A (50 × 4 mm I.D.)	IonPac-AG5A (50 × 4 mm I.D.)	IonPac-CG10 (50 × 4 mm I.D.)
Micromembrane suppressor	AMMS-II	AMMS-II	CMMS-II
Eluent	1.7 m*M* $NaHCO_3$–1.8 m*M* Na_2CO_3	E_1 = 0.75 m*M* NaOH E_2 = 200 m*M* NaOH	E_1 = 40 m*M* HCl E_2 = 40 m*M* HCl–20 m*M* DAP[a]
Regenerant	25 m*M* H_2SO_4	25 m*M* H_2SO_4	100 m*M* TBAOH [b]
Eluent flow-rate	2.0 ml/min	1.0 ml/min	1.0 ml/min
Regenerant flow-rate	10 ml/min	10 ml/min	10 ml/min
Sample loop	100 µl	100 µl/2 ml	50 µl

[a] Diaminopropionic acid.
[b] Tetrabutylammonium hydroxide.

flow-rate 2.0 ml/min was used for separation of these anions. The ions are separated in approximately 11 min. Fluoride, acetate and formate are eluting in the water dip. A chromatogram of a standard solution of these anions is presented in Fig. 2a. Other operating conditions are given in Table I.

Anion gradient method (GA). The former method gives a good separation of inorganic anions but it does not separate fluoride and some organic anions such as acetate and formate. At present, organic compounds are arousing increased interest. Formic and acetic acids have been found to be the most abundant atmospheric organic acids [19].

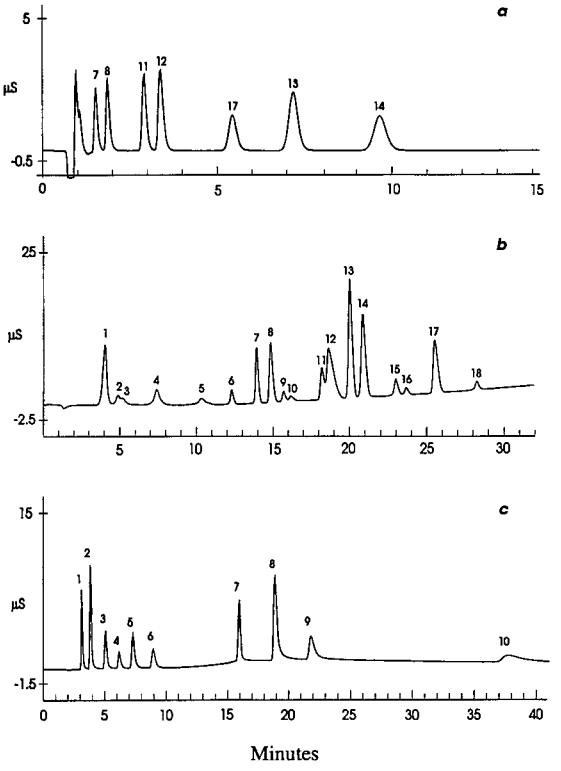

Fig. 2. Typical chromatograms of standard solutions obtained by (a) anion isocratic IA (b) anion gradient GB and (c) cation gradient CAT methods. Peaks (a): 7 = Cl^-, 0.50 μg/ml; 8 = NO_2^-, 1.0 μg/ml; 11 = Br^-, 2.0 μg/ml; 12 = NO_3^-, 2.0 μg/ml; 13 = SO_4^{2-}, 2.0 μg/ml; 14 = oxalate, 2.0 μg/ml and 17 = PO_4^{3-}, 2.5 μg/ml. (b): 1 = F^-, 0.05 μg/ml; 2 = acetate, 0.05 μg/ml; 3 = propionate, 0.05 μg/ml; 4 = formate, 0.05 μg/ml; 5 = methanesulfonate, 0.05 μg/ml; 6 = chloroacetate, 0.05 μg/ml; 7 = Cl^-, 0.05 μg/ml; 8 = NO_2^-, 0.10 μg/ml; 9 = dichloroacetate, 0.05 μg/ml; 10 = benzoate, 0.05 μg/ml; 11 = Br^-, 0.20 μg/ml; 12 = NO_3^-, 0.20 μg/ml; 13 = SO_4^{2-}, 0.20 μg/ml; 14 = oxalate, 0.20 μg/ml; 15 = fumarate, 0.05 μg/ml; 16 = phthalate, 0.05 μg/ml; 17 = PO_4^{3-}, 0.25 μg/ml and 18 = citrate, 0.05 μg/ml. (c): 1 = Li^+, 0.50 μg/ml; 2 = Na^+, 2.5 μg/ml; 3 = NH_4^+, 2.0 μg/ml; 4 = K^+, 1.0 μg/ml; 5 = Rb^+, 5.0 μg/ml; 6 = Cs^+, 5.0 μg/ml; 7 = Mg^{2+}, 1.0 μg/ml; 8 Ca^{2+}, 5.0 μg/ml; 9 = Sr^{2+}, 5.0 μg/ml and 10 = Ba^{2+}, 10.0 μg/ml.

Separation of major organic and inorganic anions (fluoride, acetate, formate, chloride, nitrite, bromide, nitrate, sulphate, oxalate and phosphate) was performed on an IonPac-AS5A column with an IonPac-AG5A guard column at flow-rate of 1.0 ml/min. Gradient elution is accomplished by changing from a weak eluent (0.75 m*M* NaOH) to a strong eluent (200 m*M* NaOH) during the run using gradient program described by Rocklin *et al.* [20]. Operating conditions are presented in Table I.

Anion gradient method with concentrator column (GB). To increase sensitivity of analysis of inorganic and organic anions, the anion trace concentrator column (Model TAC-2) was used. Anions contained in aqueous extracts of atmospheric particulates are trapped on the concentrator column and are then eluted onto a guard (Model IonPac-AG5A) and analytical (Model IonPac-AS5A) columns for separation. Only 2.0 ml of analyte extract due to limited volume of the autosampler vials (5 ml Polyvial) were available for concentrator loading. Conditions for separation of anions were the same as for the anion gradient method without preconcentration. A typical chromatogram of standard mixture of anions is shown in Fig. 2b. Operating conditions are given in Table I.

As expected, no problem was observed with separation of samples of low ionic strength. However, most fine atmospheric aerosol extracts contained sulphate at high level, which interfered in the determination of nitrate, oxalate and other anions. On column elimination of high level of sulphate will be the subject of future research project.

Cation gradient (CAT) method. Ammonium and, alkali and alkaline-earth metal cations were separated on an analytical column (Model IonPac-CS10) with a guard column (Model IonPac-CG10) under conditions described previously [4]. This method is the slowest method in the quadruple IC system. The analysis time and the equilibration of the column are about 55 min. Operating conditions are presented in Table I. A chromatogram of standard solution of these cations is shown in Fig. 2c.

Quantitation procedure

Identification of individual ions is based on the

comparison of elution times of analytes with those of standard solutions.

Four standard calibrations were used with linear least-squares regression analysis. Calibrations were performed over the range of concentrations expected in the samples. Peak areas in gradient elution were found to have better linearity and better reproducibility for most anions and cations. Peak heights were used in isocratic elution.

Detection limits were calculated by analyzing dilute solutions. They were taken as three times the standard deviation of twenty replicate analyses of samples containing analytes with concentrations of ten times the expected detection limit.

Quality control. Principles of quality assurance were an integral part of the laboratory investigations. Three control reagent blanks to monitor contamination and recovery of one control standard were routinely analyzed in the same manner as samples. The recovery data of control standard for quadruple IC system are presented in Table II. Quadruple IC system performance was monitored daily.

Reagents

Ultra pure water (18 MΩ cm resistivity at 25°C) was obtained by treating the tap water using reverse osmosis and ion-exchange columns (Millipore, modified Model RO 20 and Model Super Q).

Hydrochloric and sulfuric acids (J. T. Baker), 50% aqueous sodium hydroxide, methanol (Fisher Scientific), 2,3-diaminopropionic acid hydrochloride (DAP, Fluka), 50% aqueous solution of tetrabutylammonium hydroxide (Sachem, Austin, TX, USA) and other chemicals used were of analytical reagent-grade purity. Acetic, oxalic, citric, fumaric and phthalic acids and sodium formate (Fisher Scientific) and propionic, methanesulfonic, chloroacetic and benzoic acids and sodium dichloroacetate (Aldrich) were of highest available purity.

Anion stock standard solution was prepared from high purity salts (Fisher Scientific) and standardized *versus* NIST standard solutions (fluoride, chloride, bromide, nitrate, sulphate and phosphate). Stock solution of all nine cations was prepared from NIST standards. Ammonium standard solution was prepared from ammonium chloride (Fisher Scientific).

All eluents were prepared using helium degassed water. To avoid CO_2 pickup by sodium hydroxide eluents, eluents were prepared from 50% NaOH, which was pipetted from the middle of the bottle. He atmosphere was constantly applied over eluents. Composition of all eluents used in this work is presented in Table I.

TABLE II

RECOVERY DATA FOR CONTROL STANDARD

Reported results are the mean and standard deviation of 20 measurements of anion standard (F^-, acetate, formate, Cl^- 0.2 μg/ml; NO_2^- 0.4 μg/ml; Br^-, NO_3^-, SO_4^{2-}, oxalate 0.8 μg/ml and PO_4^{3-} 1.0 μg/ml), and cation standard (Li^+ 0.2 μg/ml; Na^+ 1.0 μg/ml; NH_4^+ 0.8 μg/ml; K^+, Mg^{2+} 0.4 μg/ml; Rb^+, Cs^+, Ca^{2+}, Sr^{2+} 2.0 μg/ml and Ba^{2+} 4.0 μg/ml).

Ion	Recovery ± S.D. (%)			Ion	Recovery ± S.D. (%)
	IA Method	GA Method	GB Method		CAT Method
F^-	N/A[a]	98.8 ± 3.2	97.6 ± 3.7	Li^+	95.9 ± 5.8
Acetate	N/A	102.4 ± 10.5	99.5 ± 14.0	Na^+	93.6 ± 6.4
Formate	N/A	95.8 ± 8.1	94.4 ± 7.6	NH_4^+	92.4 ± 6.8
Cl^-	100.6 ± 6.0	98.7 ± 7.8	94.5 ± 7.6	K^+	96.6 ± 7.1
NO_2^-	100.8 ± 4.5	97.1 ± 3.0	94.4 ± 6.4	Rb^+	96.5 ± 4.7
Br^-	99.2 ± 4.5	97.1 ± 4.3	95.0 ± 4.5	Cs^+	96.5 ± 6.2
NO_3^-	98.3 ± 3.6	98.1 ± 4.5	97.9 ± 5.5	Mg^{2+}	99.6 ± 7.0
SO_4^{2-}	102.2 ± 3.7	97.6 ± 3.8	98.3 ± 4.1	Ca^{2+}	100.6 ± 7.0
Oxalate	99.7 ± 3.3	97.9 ± 2.7	97.5 ± 4.2	Sr^{2+}	96.7 ± 7.1
PO_4^{3-}	98.8 ± 5.5	95.1 ± 6.8	99.4 ± 6.0	Ba^{2+}	93.4 ± 11.5

[a] N/A = not analyzed.

Filter extraction

Atmospheric aerosols collected on thin PTFE filters using virtual dichotomous samplers were obtained from the Pollution Measurement Division, River Road Environmental Technology Centre, Environment Canada. The samplers fractionated the aerosol into two aerodynamic size ranges yielding "fine" (<2 μm) and "coarse" (<10 μm) samples.

The elemental composition of collected atmospheric aerosols was nondestructively determined for forty elements using X-ray fluorescence (XRF). Then, the filters were placed in glass bottles for extraction. Particulates were extracted using water (19 ml) by sonication in an ultrasonic bath (Branson & Smithkline, Model Bransonic 42) for 30 min. Because some atmospheric aerosols and the PTFE are hydrophobic, the filters were wetted before addition of water with methanol (1 ml). The extracts were transferred to autosampler vials, which after prewashing had contamination levels below 10 ng/ml for all ions determined. Analysis was carried out as soon as possible after extraction (within less than 24 h). The residue of extracts was stored at 4°C.

Stability of samples. Stability of aqueous extracts of atmospheric aerosols is one of important factors for correct analysis.

The preliminary study indicates that the extracts are relatively unstable. Some ions undergo chemical reactions (*e.g.* partial or complete oxidation of NO_2^- to NO_3^- and SO_3^{2-} to SO_4^{2-} in dependence on the pH of the extracts and other factors). Other ions are used up or generated in biochemical processes caused by the presence of microbiota (*e.g.* NO_3^-, NH_4^+). Biological activity in the samples containing carboxylic acids has been reported by Keene and Galloway [21]. Losses of formate and acetate were found in the extracts that were not treated with the biocide (chloroform). The extracts were therefore analyzed within less than 24 h after extraction.

The diluted working standard solutions are less sensitive to changes of concentration due to controlled pH and the absence of microbiota. They were nevertheless prepared freshly for each daily run. The effects of various preservation methods on stability of aqueous extracts of atmospheric aerosols will be reported in another paper [22].

RESULTS AND DISCUSSION

Analytical performance

The system stability was verified by constructing calibration curves from freshly prepared standard solutions every day that samples were analyzed. Within a six months period during which some 500 samples were analyzed, the relative standard deviations (R.S.D.) of slopes of the calibration curves were in the range 6–20%. Early eluting anions and cations in gradient elution (fluoride, acetate, formate, lithium and sodium) had an R.S.D. of retention time less than 5%. The R.S.D. of retention time was less than 2% for other cations and anions. The overall variability reflects uncertainties in preparation of standard solutions (gravimetric and volumetric errors), in standard stability (organic acids), in eluent variations from one batch to the next, and in instrument fluctuations (*e.g.* autoregeneration cartridge and/or suppressor exhaustion).

The long-term performance of the quadruple IC system was monitored by periodical re-analysis of standard solutions (as a rule one quality control standard solution was analyzed with each daily run). Recovery data of quality control standards are presented in Table II. The results indicate good system stability over the six months period.

Another measure of analytical performance involves interlaboratory comparison of water samples analyzed according to a "blind" protocol [23]. The data agree with interlaboratory median (Table III). The range of recovery was 96–106%. The analytical results were also precise as shown by the standard deviation of ten replicates.

The detection limits of the ten anions and ten cations studied using described system are listed in Table IV. It can be seen that all anions and cations have detection limit in the low ng/ml range. The concentrator column used in anion analysis improved the detection limits by about an order.

Filter results

Typical chromatograms of an extract of a fine and coarse atmospheric aerosol samples are shown in Fig 3. Chloride, sulphate, sodium and calcium are the major ions of coarse atmospheric aerosol extracts. All samples of fine atmospheric aerosol extracts contain sulphate and ammonium as major ions. Nitrate concentration was almost always only

TABLE III

DETERMINATION OF MAJOR ANIONS AND CATIONS IN WATER SAMPLE

Reported results are the mean and standard deviation of 10 replicates.

Ion	Inter-laboratory median (μg/ml) [23]	Found ± S.D. (μg/ml)		
		IA Method	GA Method	GB Method
Cl^-	0.835	0.810 ± 0.021	0.850 ± 0.004	0.813 ± 0.016
NO_2^-	1.386	1.449 ± 0.029	1.443 ± 0.006	1.402 ± 0.037
NO_3^-	12.954	12.916 ± 0.182	12.733 ± 0.293	
SO_4^{2-}	22.740	24.052 ± 0.423	23.115 ± 0.201	
		CAT Method		
Na^+	0.207	0.199 ± 0.005		
NH_4^+	2.186	2.229 ± 0.019		
K^+	0.326	0.339 ± 0.011		
Mg^{2+}	2.640	2.624 ± 0.038		
Ca^{2+}	8.678	8.596 ± 0.296		

a small fraction of the sulphate concentration. It is possible to detect minor peaks in fine and coarse atmospheric aerosol extracts attributable to other cations [4] and anions. Some of the regularly reported anions are below the detection limits even after the concentration step.

Along with inorganic anions such as chloride, nitrite, nitrate and sulphate, organic anions were found in the extracts of atmospheric aerosols. Formate and acetate were usually present in higher concentration than other organic anions. They are mainly produced by anthropogenic (gas phase oxidation) and/or biogenic activity. They are often present in similar concentrations as sulphate and nitrate in urban areas on clear summer days [19]. As can be seen in Fig. 3 (chromatograms obtained after concentration of sample), fine and coarse atmospheric aerosol extracts contain other organic anions. Propionate, methanesulfonate and benzoate that have not yet been identified by other techniques were found in very low concentrations after preconcentration in some samples. The identification of other peaks will be the subject of future research.

TABLE IV

DETECTION LIMITS

Ion	Detection limit (μg/ml)				
	IA Method	GA Method	GB Method	Ion	CAT Method [4]
F^-	N/A	0.01	0.001	Li^+	0.005
Acetate	N/A	0.04	0.005	Na^+	0.025
Formate	N/A	0.03	0.002	NH_4^+	0.040
Cl^-	0.04	0.04	0.005	K^+	0.010
NO_2^-	0.02	0.01	0.002	Rb^+	0.040
Br^-	0.03	0.06	0.006	Cs^+	0.050
NO_3^-	0.03	0.01	0.006	Mg^{2+}	0.050
SO_4^{2-}	0.02	0.02	0.004	Ca^{2+}	0.050
Oxalate	0.04	0.02	0.002	Sr^{2+}	0.040
PO_4^{3-}	0.06	0.03	0.009	Ba^{2+}	0.400

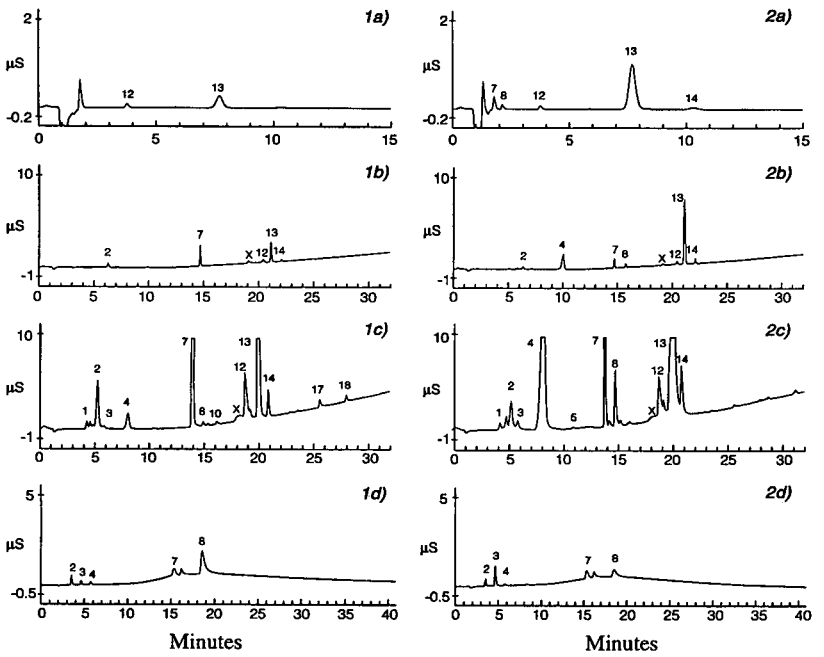

Fig. 3. Chromatograms of (1) coarse and (2) fine atmospheric aerosol extracts obtained by automatic quadruple ion chromatography system (a = anion isocratic IA; b = anion gradient GA; c = anion gradient with preconcentration GB and d = cation gradient CAT methods). Conditions are the same as those reported in Table I. Peaks: × = carbonate; others are the same as in Fig. 2.

Anion methods comparison study

The anions for which different elution methods can be compared are sulphate, chloride, nitrate and formate. Only these anions were present in sufficient amount to permit a quantitative anion methods comparison. The comparison of results obtained by isocratic and gradient (with and without preconcentration) elution is given in Table V. The results are expressed as mean ratio of concentrations of analyte obtained by above mentioned elution methods. There was a close agreement (the range of the ratios was 0.94–1.03) between values obtained by the respective methods. Nitrate is the only exception caused by the sulphate interference. Sulphate was usually present in the samples at much higher concentration level than nitrate. Relative standard de-

TABLE V

ANION METHODS COMPARISON

All ratios are calculated from data where both concentrations were over quantitation limit.

Ion	IA *vs.* GA			GB *vs.* GA		
	Concentration range (µg/ml)	n^a	Ratio ± S.D.	Concentration range (µg/ml)	n^a	Ratio ± S.D.
Formate			N/A	0.1–1	82	1.02 ± 0.04
Cl^-	0.1–4	191	1.03 ± 0.08	0.1–2	137	0.94 ± 0.15
NO_3^-	0.1–6	255	0.97 ± 0.18	0.04–3	298	0.82 ± 0.14
SO_4^{2-}	0.07–8	460	1.03 ± 0.10	0.07–4	411	1.00 ± 0.10

[a] n = Number of samples.

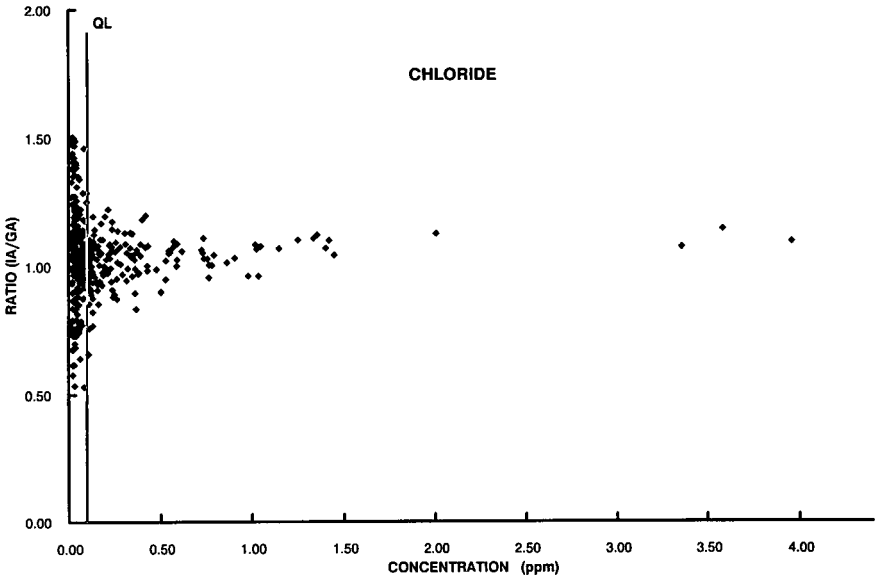

Fig. 4. Comparison of chloride determined by isocratic IA *vs.* gradient GA elution (QL = quantitation limit).

viations are better than 20%. Figs. 4 and 5 show the comparison of chloride and formate results obtained by isocratic and gradient (with preconcentration) methods *vs.* gradient method, respectively.

CONCLUSIONS

The described fully automated IC system is suitable for routine analysis of aqueous extracts of at-

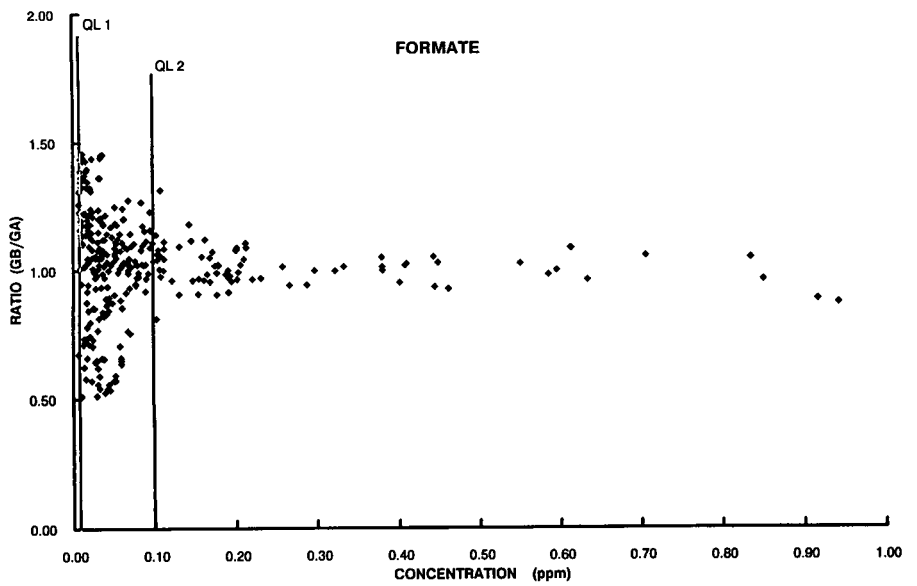

Fig. 5. Comparison of formate determined by gradient GB *vs.* gradient GA elution (QL1, QL2 = quantitation limits of GB and GA methods, respectively).

mospheric aerosols. It provides accurate and precise simultaneous multi-anion and multication determination capability. Other advantages of described IC system are the small sample volume required and the reduction of the probability of differential contamination of each sample. The stability of aqueous extracts of atmospheric aerosols is the limiting factor of time operation. Anion methods comparison has shown that there is good agreement between values obtained by the respective methods. Different approaches and changes, which will improve the method were found.

REFERENCES

1 T. G. Dzubay, R. K. Stevens and C. M. Peterson, *X-ray Fluorescence Analysis of Environmental Samples*, Ann Arbor Sci. Publ., Ann Arbor, MI, 1977, p.95.
2 R. K. Stevens and T. G. Dzubay, *Atmos. Environ.*, 12 (1978) 35.
3 Ch. W. Lewis and E. S. Macius, *Atmos. Environ.*, 14 (1980) 185.
4 E. Dabek-Zlotorzynska and J. F. Dlouhy, *J. Chromatogr.*, in press.
5 W. T. Frankenberger, Jr., H. C. Mehra and D. T. Gjerde, *J. Chromatogr.*, 504 (1990) 211.
6 J. D. Mulik, R. Puckett, D. Williams and E. Sawicki, *Anal. Lett.*, 9 (1976) 653.
7 E. Sawicki, J. D. Mulik and E. Wittgenstein (Editors), *Ion Chromatographic Analysis of Environmental Pollutants, Vol. 1*, Ann Arbor Science Publishers, Ann Arbor, MI, 1978
8 P. I. Jackson and P. R. Haddad, *J. Chromatogr.*, 439 (1988) 37.
9 D. Yan and G. Schwedt, *J. Chromatogr.*, 516 (1990) 383.
10 D. M. Brown and D. J. Pietrzyk, *J. Chromatogr.*, 466 (1989) 300.
11 N. P. Barkley, G. L. Contner and M. Malanchuck, in J. D. Mulik and E. Sawicki (Editors), *Ion Chromatographic Analysis of Environmental Pollutants, Vol. 2*, Ann Arbor Sci. Publ., Ann Arbor, MI, 1979, p.115.
12 H. Small and T. E. Miller, *Anal. Chem.*, 54 (1982) 462.
13 Z. Iskandarani and T. E. Miller, *Anal. Chem.*, 57 (1985) 1591.
14 V. K. Jones and J. G. Tarter, *J. Chromatogr.*, 312 (1984) 456.
15 V. K. Jones and J. G. Tarter, *Am. Lab.*, 17, No. 7 (1985) 48.
16 V. K. Jones, S. F. Frost and J. G. Tarter, *J. Chromatogr. Sci.*, 23 (1985) 442.
17 V. K. Jones and J. G. Tarter, *Analyst*, 113 (1988) 183.
18 V. Cheam and A. S. Y. Chau, *Analyst*, 112 (1987) 993.
19 W. C. Keene, J. N. Galloway and J. D. Holden Jr., *J. Geophys. Res.*, 88 (1983) 5122.
20 R. D. Rocklin, Ch. A. Pohl and J. A. Schibler, *J. Chromatogr.*, 411 (1987) 107.
21 W. C. Keene and J. N. Galloway, *Atmos. Environ.*, 11 (1984) 2491.
22 J. F. Dlouhy, E. Dabek-Zlotorzynska and D. Mathieu, *Ion Chromatographic Determination of the Effects of Some Preservation Methods on the Stability of Aqueous Extracts of Ambient Air Particulates*, River Road Environmental Technology Center, Ottawa, 1993.
23 N. Arafat and K. I. Aspila, *LRTAP Intercomparison Study L-29: Major Ions, Nutrients and Physical Properties in Water*, National Water Research Institute, Burlington, 1992.

Journal of Chromatography, 640 (1993) 227–230
Elsevier Science Publishers B.V., Amsterdam

CHROMSYMP. 2741

Ion chromatographic investigations of leachates from a hazardous-waste landfill

Beate Gade

Forschungs- und Entwicklungszentrum Sondermüll, Siemensstrasse 3–5, D-8540 Schwabach (Germany)

ABSTRACT

Leachates from different areas of a modern hazardous-waste landfill were investigated. In addition, samples of the waste to be buried were taken, and leachability tests in accordance with German standards were performed. The composition of the leachates from the landfill and the leachates produced by the leachability tests varied over a wide range, depending on the kind and volume of hazardous waste buried and the weather conditions. High concentrations of some anions were often found in combination with low concentrations of other anions. In the leachates the following concentration ranges were found: Cl^-, 30–6000 mg/l; NO_2^-, 0–150 mg/l; NO_3^-, 0–150 mg/l; SO_2^{2-}, 100–6000 mg/l. Therefore, several dilutions of one sample often had to be measured. The complex matrix often also requires several sample preparation steps for the elimination of interfering effects. Experience to date has shown that ion chromatography in this application field is efficient.

INTRODUCTION

The control of landfills, especially of hazardous waste landfills, is becoming increasingly important. Depending on the industrial structure of the region where the landfill is located, most of the hazardous wastes to be buried are electroplating sludges and wastewater treatment sludges. For environmental control purposes, the leachates from hazardous waste landfills and leachability test samples have to be analysed regularly. For this reason, a research project to investigate the input and the output of a modern hazardous waste landfill was carried out. Many parameters of leachates from different parts of the landfill were analysed. Ion chromatography (IC) was used for the analysis of the most important anions (Cl^-, NO_2^-, NO_3^-, SO_4^{2-}) in these samples.

EXPERIMENTAL

Apparatus

An isocratic ion chromatograph with a Waters 510 pump, a Waters 431 conductivity detector and a Waters 712 WISP autosampler were used. The analyses were carried out with a Waters IC PAK-Anion column (50 × 4.6 mm I.D.) and a Waters RP C_{18} precolumn.

Chemicals

Gluconic acid [50% (w/w) solution] and lithium hydroxide monohydrate (analytical-reagent grade) were purchased from Fluka (Buchs, Switzerland). Boric acid (analytical-reagent grade) and glycerine [87% (w/w) solution, analytical-reagent grade) were obtained from Merck (Darmstadt, Germany); acetonitrile (Chromasolv) was from Riedel-de Haen (Seelze, Germany).

Procedure

A single-column separation with subsequent direct conductivity detection was carried out [1]. A borate–gluconate eluent was used [2–5]. The borate–gluconate eluent concentrate was prepared with 17.0 g of boric acid, 11.75 ml of gluconic acid [50% (w/w) solution), 4.3 g of lithium hydroxide monohydrate and 62.5 ml glycerine and made up with purified water (Milli-Q, Millipore) to 500 ml. The eluent was prepared by adding 14 ml of eluent concentrate to 120 ml of acetonitrile and made up to 1000 ml with purified water. The mobile phase was

0021-9673/93/$06.00

TABLE I

CONCENTRATION RANGE AND ANALYTICAL CONDITIONS

Samples to be measured	Concentration range (ml/l)		Dilution	Measures to be taken against interferences
Leachability test samples of different hazardous wastes, mainly electroplating sludges	Cl^-	30–4500	1:10	Sample preparation filtration 45 μm cation exchanger standard addition
	NO_3^-	10–150	1:100	
	SO_4^{2-}	300–5500	1:500	
	NO_2^-	10–150	1:1000	
Leachates from the hazardous waste landfill	Cl^-	1200–6000	1:10	Sample preparation filtration 45 μm, cation exchanger standard addition
	NO_3^-	30–300	1:100	
	SO_4^{2-}	300–1600	1:500	
	NO_2^-	10–150	1:1000	
Leachates from the hazardous waste landfill; monodisposal	Cl^-	0–60	1:10	Sample preparation filtration 45 μm, cation exchanger; after IC run, cleaning column with eluent concentrate
	NO_3^-	0–30	1:100	
	SO_4^{2-}	100–2500	1:500	

degassed by vacuum filtration through a Nuclepore filter of 0.45 μm pore size.

The chromatographic separation was carried out at a flow-rate of 1 ml/min isocratically. The run time of the first runs was 20 min; later the run time was shortened to 15 min. Overlapping of the peaks of chloride and/or sulphate with the peaks of anions with lower concentrations often occurred at shorter run times. Therefore, further optimization of the run time was not possible. The injection volume was 50 μl. In general, the analyses were done twice. If necessary, the measurements were repeated. The analytical conditions are shown in Table I.

Sample preparation

The leachability test samples were produced by adding 1 l of purified water to an amount of a (wet) hazardous waste sample equivalent to 100 g of dry substance. The sample and the water were placed in a 2-l polyethylene bottle. The bottles were rotated at a speed of 1 rpm in a rotation apparatus for a period of 24 h [6]. After filtration, the leachability test samples were analysed.

For sampling the leachate, computer-controlled automatic samplers are installed at the landfill site. Random samples and weekly average samples were taken. The samples were filtered through a filter of 45 μm pore size and diluted. For the sample preparation of some leachates, especially leachates produced in a monodisposal area of the landfill, a Millitrap H^+ cation exchanger was used.

Standards

The standards were made using sodium chloride, sodium bromide, sodium nitrite, sodium nitrate, potassium dihydrogenphosphate and sodium sulphate, all analytical-reagent grade. Prior to the preparation of the standard solutions, sodium nitrate, potassium dihydrogenphosphate and sodium sulphate were dried at 105°C; sodium chloride, sodium bromide and sodium nitrite were dried at 150°C in accordance with German Industrial Standards [7].

The standard solutions for the calibrations were prepared in the concentration range 2–20 mg/l. The linearity range of the calibration curves was tested with a variance homogeneity test. The calibration curves were found to be linear in the above-mentioned range.

RESULTS AND DISCUSSION

Different leachates are produced in different areas of the hazardous waste landfill. Most of the leachate is produced in an area where various kinds of hazardous waste are buried. These leachates can generally be treated like the leachability test samples, although the concentrations of the anions in

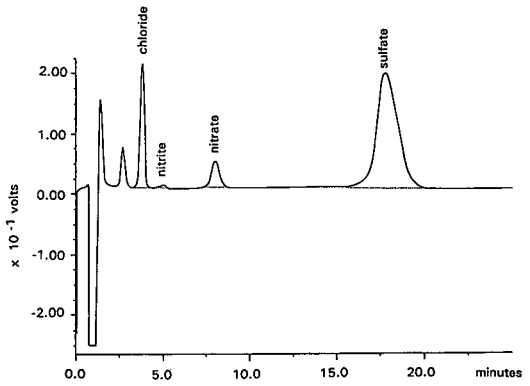

Fig. 1. Ion chromatogram of a leachability test sample of an electroplating sludge. Concentrations in the undiluted sample: Cl^-, 63.1 mg/l; NO_2^-, 3.2 mg/l; NO_3^-, 54.0 mg/l; SO_4^{2-}, 421 mg/l.

the leachate are often higher than in the leachability test samples.

Owing to the diversitiy of hazardous wastes to be buried, there is a wide range of concentrations of the main anions Cl^-, NO_2^-, NO_3^- and SO_4^{2-}. Fig. 1 shows a typical ion chromatogram of a leachability test sample. In most cases, large amounts of chloride and sulphate and minor amounts of nitrate and sometimes nitrite are present.

Fig. 2 shows two typical chromatograms of a random and a weekly average sample. The most difficult to measure leachates were collected from a monodisposal area where special iron oxide sinters are buried. These leachates contain large amounts of metals and ammonium. It is necessary to use a cation exchanger for sample preparation for every sample. Fig. 3 shows an example of this leachate

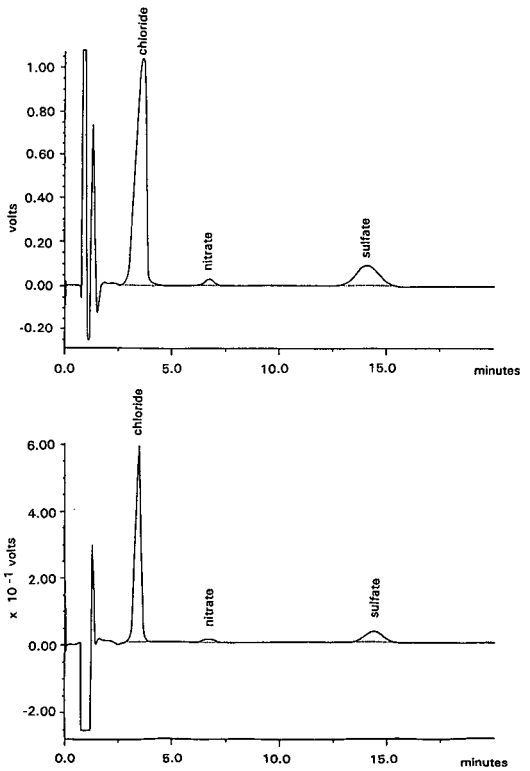

Fig. 2. Two examples of the concentration range in leachates from a hazardous waste landfill. Top: weekly average sample: dilution 1:10. Concentrations in the undiluted sample: Cl^-, 1365 mg/l (not quantified in this chromatogram but in a 1:100 dilution); NO_3^-, 66.6 mg/l; SO_4^{2-}, 355 mg/l. Bottom: random sample: dilution 1:100. Concentrations in the undiluted sample: Cl^-, 4280 mg/l; NO_3^-, 201 mg/l; SO_4^{2-}, 1057 mg/l.

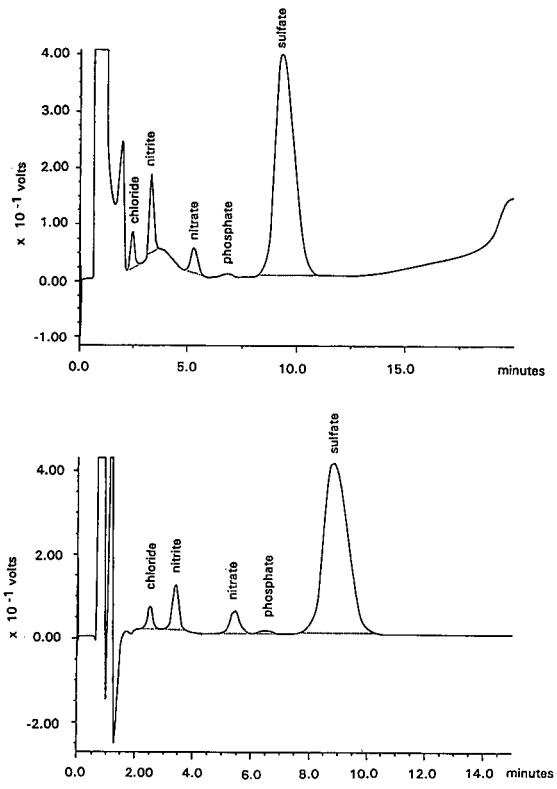

Fig. 3. Chromatograms of a leachate from a monodisposal area of the landfill. Top: without using a cation exchanger. Bottom: with using a cation exchanger. Concentration of the undiluted sample: Cl^-, 16.7 mg/l; NO_2^-, 59 mg/l; NO_3^-, 60.6 mg/l; PO_4^{3-}, 17.1 mg/l; SO_4^{2-}, 735 mg/l.

measured with and without the use of a cation exchanger for sample preparation.

Chromate contents can also cause interferences. To avoid drastic changes in pH, no other pretreatment measures were taken. If these samples are measured, runs are integrated in the automatically worked sample queue for cleaning the chromatographic system, *e.g.* by injecting eluent concentrate and purging for a sufficient time to avoid the delayed elution of interfering substances in the chromatogram of the following sample.

Because of the diversity of the hazardous wastes, it is necessary in many cases to check whether the chromatograms show the signals of the anions to be measured or interferences. In addition to the measures already mentioned, such as the use of ion exchangers and standard addition, other measurements such as photometry sometimes have to be carried out also to confirm the results of ion chromatography. Depending on the different kinds of samples, purging runs of differing lengths are integrated in the automatic measurements.

In addition, plausibility checks should be performed whenever possible. A direct correlation between the concentration of the anions and the amount of precipitation and leachate production can be found. High concentrations of the anions are associated with low amounts of leachate and *vice versa*. These results, provided by ion chromatography, are plausible because of the diluting effect of the rainwater on the leachate.

The results obtained so far can be summarized as follows:

Fluoride can in principle be measured by the method described above. As a result of a period of testing, the fluoride measurements are executed with a fluoride-sensitive electrode because of frequent interferences in this retention range that could not be removed completely.

Like fluoride, bromide and phosphate can be determined by this method. However, because of the composition of the hazardous wastes and the leachates of the landfill, they have rarely been found until now. Because of this, a final evaluation of the suitability of the analytical method for these ions cannot be given.

CONCLUSIONS

Ion chromatography has proved to be a useful analytical method for the analysis of hazardous waste samples, especially eluates and leachates from a hazardous waste landfill. Nevertheless, it was necessary during the establishment of the analytical facilities to check the quality of the analyses of these samples with partially complex matrices using other analytical methods.

Special steps for the analysis of the different kinds of samples have been developed. Now a routine analysis of the ions Cl^-, NO_2^-, NO_3^- and SO_4^{2-} is done in a wide concentration range.

REFERENCES

1 D. T. Gjerde and J. S. Fritz, *Ion Chromatography*, Hütig, Heidelberg, Basel, New York, 2nd ed., 1987.
2 C. Erkelens, H. A. H. Billiet, L. de Galan and E. W. B. De Leer, *J. Chromatogr.*, 404 (1987) 67.
3 *Environmental Application Note, WB0927*, Waters, Milford, MA, 1987.
4 A. A. Hafez, S. S. Goyal and D. W. Rains, *J. Chromatogr.*, 546 (1991) 387.
5 M. Roman, R. Dovi, R. Yoder, F. Dias and B. Warden, *J. Chromatogr.*, 546 (1991) 341.
6 *Deutsche Industrienorm (DIN) 38405*, Teil 19, VCH, Weinheim, 1988.
7 *Deutsche Industrienorm (DIN) 38414*, Teil 5, VCH, Weinheim, 1984.

Journal of Chromatography, 640 (1993) 231–240
Elsevier Science Publishers B.V., Amsterdam

CHROMSYMP. 2675

Determination and identification by high-performance liquid chromatography and spectrofluorimetry of twenty-three aromatic sulphonates in natural waters

Orfeo Zerbinati*, Giorgio Ostacoli, Daniela Gastaldi and Vincenzo Zelano

Dipartimento di Chimica Analitica, Università di Torino, v. Giuria 5, I-10125 Turin (Italy)

ABSTRACT

A method for detecting and identifying 23 aromatic sulphonates in natural waters was optimized. Samples were pretreated by solid-phase extraction in order to eliminate interferents and to preconcentrate the analytes. Separation of the extracted analytes was accomplished by ion-pair HPLC with fluorimetric detection; the eluent composition and pH were optimized. The detection limits lie in the low $\mu g\ l^{-1}$ range. Some of the investigated compounds were found in the water of the river Bormida (N.W. Italy). Unknown components were identified from their fluorescence spectra.

INTRODUCTION

Aromatic sulphonates and their hydroxy and amino derivatives are used for many purposes, especially as intermediates in dyes manufacture. Their production and use can lead to very pollutant wastes for superficial and underground waters.

These substances are surface active and they can be modified by microorganisms. In fact, it has been observed that a green alga can use 1-naphthalenesulphonic acid as a sulphur source, even in the presence of sulphate ion, leaving the naphthalene ring undegraded [1]. Other bacteria can produce 5-sulphosalicylic and gentisic acid as intermediates in the biodegradation of 1,6- and 2,6-naphthalenedisulphonic acid [2,3]. Little is known about the possible environmental effects of these substances.

To study these effects adequately, a sensitive and selective method of analysis is required. Further, an ancillary technique for confirmation of unknown components, even at low concentrations, is necessary. In fact, owing to the large number of possible positional isomers of the investigated class of compounds, chromatographic retention time alone cannot support qualitative analysis.

Underground and river waters can contain relatively large amounts of interferents of natural origin (*e.g.*, humic acids) or industrial origin (*e.g.*, nonpolar or slightly polar organic substances). Hence there is also a need for pretreatment of the sample in order to remove such interferents.

In previous work, the separation of a limited numbers of isomers was achieved by several techniques: low-pressure ion-exchange chromatography [4], TLC [5], ion-exchange electrokinetic chromatography [6] and ion-pair chromatography [7–9]. All these studies dealt with limited numbers of compounds and the identification of the unknowns was based on the retention times only.

The GC or GC–MS analysis of some aromatic sulphonic acids has been also carried out, after their conversion into volatile derivatives, by means of thionyl chloride and further amidation with an aliphatic amine [10] or by means of phosphorus pentachloride and further esterification with trifluoroethanol [11]. Unfortunately, the substances investigated in this study contain also amino and hydroxy

* Corresponding author.

0021-9673/93/$06.00

groups, which can react with the reactants used for halogenating the sulphonic group. Further, derivatization processes are complex and time consuming.

Anion-exchange liquid chromatography, coupled with UV and particle beam MS detection, has also been proposed for the determination of eight aromatic sulphonic acids [12]. This method seems more suitable for mono- than disulphonic acids; further, the detection limits lie in the nanogram range using UV detection or in the microgram range using particle beam MS detection.

Ion-pair chromatography seemed more promising for the separation of mixtures of large numbers of isomers in the presence of interfering substances. Owing to the intense fluorescence properties of the substances investigated in this study, spectrofluorimetry seemed the most sensitive detection technique, and it also seemed suitable for performing qualitative analysis, even at very low concentrations, owing to the specificity of the shapes of the fluorescence spectra. In this work, the chromatographic technique and the pretreatment of real samples were optimized; the identification of unknown components on the basis of their fluorescence spectra is proposed.

EXPERIMENTAL

Reagents

All aqueous solutions were prepared with ultra-high-quality (UHQ) water obtained by passing deionized water through an Elga-Stat water-purification apparatus. Methanol and acetonitrile, both of HPLC grade with low UV absorption, tetrabutylammonium (TBA) hydroxide and cetyltrimethylammonium bromide (CTMABr) were obtained from Aldrich. The compounds listed in Table I were obtained from Aldrich or Kodak. Citric acid, ammonia solution and magnesium sulphate were obtained from Carlo Erba. Solid-phase extraction (SPE) columns were obtained from Baker and Merck.

Stock solutions of the investigated sulphonates were prepared with UHQ water, kept in dark-glass flasks, stored in a refrigerator (4°C) and were used within 1 week, except those of 4-amino-3-hydroxy-1-naphthalenesulphonate, which were prepared immediately before use.

Apparatus

The HPLC system consisted of a Pye Unicam PU 4015 pump, a Rheodyne valve fitted with a 20-μl loop and a 250 × 4.6 mm I.D. Alltech Adsorbosphere C_8 (5 μm) column. The eluent was degassed by means of a stream of helium.

The detector was an Hitachi F-4000 computerized spectrofluorimeter, equipped with an 18-μl flow cell and an analogue output. The same instrument was used to run and memorize the fluorescence spectra. Quantitative calculations were performed with a Shimadzu C-R3A data processor.

RESULTS

Optimization of chromatographic conditions

After some preliminary chromatograms, five substances were chosen to test the influence on capacity factors of pH, organic content of mobile phase, ion-pair reagent and buffer concentration. Unless specified otherwise, the composition of the mobile phase was acetonitrile–water (58:42) containing 5 g l^{-1} of CTMABr and 1 g l^{-1} of citric acid (pH 7.0).

Effect of pH. Fig. 1A shows the influence of the pH of the mobile phase on the capacity factors of the five compounds. The ratio of acetonitrile to water in the mobile phase was 60:40 for 1,5- and 2,7-naphthalenedisulphonate and 46:54 for 6-amino-4-hydroxy-2-naphthalenesulphonate and 4-amino-1- and 5-amino-2-naphthalenesulphonate.

The pH of the eluent had a great effect on the capacity factors. Those of 1,5- and 2,7-naphthalenedisulphonate decreased as the pH of the eluent was increased, whereas those of the amino and/or hydroxy derivatives exhibited a more complex trend. Some of them showed a maximum around pH 4.

Ion-pairing reagent concentration. The results for the five selected compounds are shown in Fig. 1B. Their chromatographic behaviour is typical of a reversed-phase system in that an increase in ion-pairing reagent concentration increased the retention times. TBA phosphate was also tried as an ion-pairing reagent, but its performance did not seem better than that of CTMABr, so the development of the chromatographic method was done using the latter reagent.

Organic content of the mobile phase. Fig. 1C shows the results obtained with eluents whose with acetonitrile to water ratios ranging from 50:50 to 58:42.

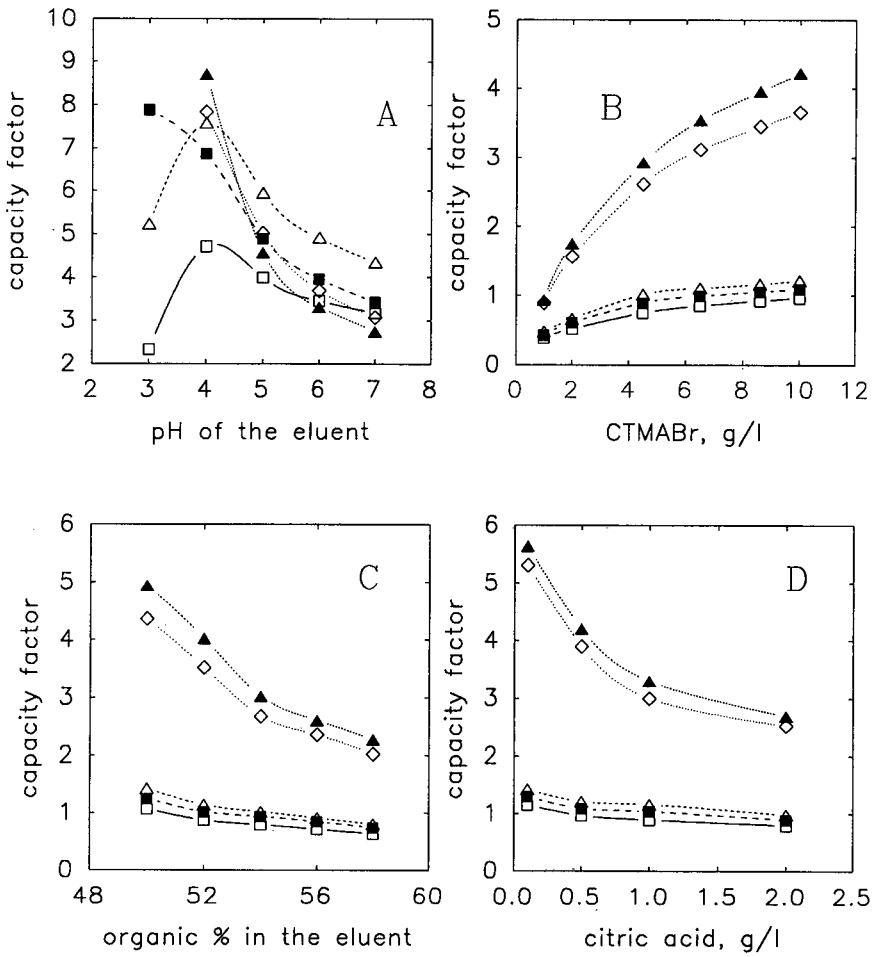

Fig. 1. Effects on capacity factors of (A) pH, (B) CTMABr concentration, (C) percentage of organic component and (D) citric acid concentration in the eluent. □ = 6-Amino-4-hydroxy-2-naphthalenesulphonate; ■ = 4-amino-1-naphthalenesulphonate; △ = 5-amino-2-naphthalenesulphonate; ◇ = 2,7-naphthalenedisulphonate; ▲ = 1,5-naphthalenedisulphonate.

Beyond these limits, the retention times became unacceptably long or short. As expected, an increased acetonitrile content reduced the capacity factors of the analyte compounds.

Buffer concentration. Citric acid was chosen to buffer the pH of the eluent, as it is readily soluble and does not increase the background fluorescence. The results for the investigated compounds are shown in Fig. 1D.

Detector conditions. A computerized spectrofluorimeter was used as a detector, giving high sensitivity, good selectivity and the possibility of characterizing eluted compounds by means of their excitation and emission spectra. The fluorescence emission and excitation spectra of the 23 compounds investigated were examined in the range 220–800 nm; some typical examples are shown in Fig. 2. Spectra were not corrected for the influence of the instrumental system, because the automatic correction range of the spectrofluorimeter covered only wavelengths shorter than 600 nm, whereas the investigated compounds showed characteristic emission also in the range 600–800 nm. The spectrofluorimeter was found to be very stable, and even spectra recorded 3 months apart coincided perfectly.

Amino and hydroxy substituents on the naph-

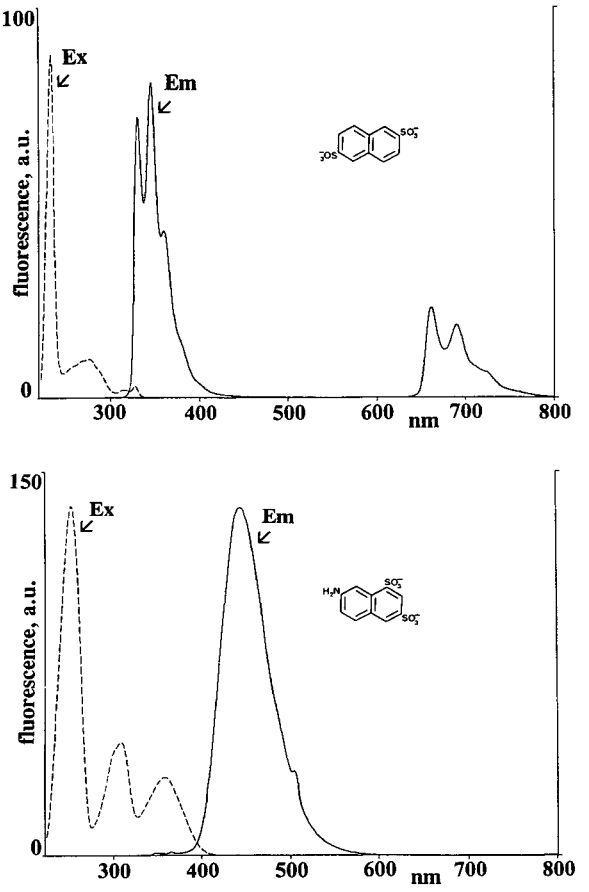

Fig. 2. Typical fluorescence spectra of excitation (dashed line) and emission (solid line) of two investigated compounds.

thalenesulphonate moiety produce a red shift in the excitation and emission maxima with respect to the unsubstituted naphthalenesulphonate. These last compounds and the three positional isomers of aminobenzenesulphonate and of 1-hydroxy-2-naphthalenesulphonate showed a second emission maximum around 660 nm, whereas the other compounds investigated showed no relevant fluorescence between 600 and 800 nm. Therefore, it was possible to separate the 23 compounds investigated into two groups, by detecting chromatograms with excitation and emission wavelengths of 250 and 455 or 240 and 660 nm, respectively. None of the investigated compounds is detected at both pairs of wavelengths. Two injections per sample are required to monitor all the investigated compounds but, with the optimized chromatographic conditions, only 30 min are needed to perform the double chromatographic run.

Quantitative analysis. Quantification was performed by measuring peak heights. The reproducibility of the chromatographic analysis alone (without preconcentration) was tested. Four replicate injections of a standard solution containing nine compounds gave an average relative standard deviation of 8%. Standard solutions of the 23 compounds were progressively diluted with ultrapure water and analysed. The detection limits (without preconcentration, signal-to-noise ratio >6), together with the wavelengths used for their detection, are reported in Table I. The peak heights were found to be linearly proportional to concentration up to the third order of magnitude over the individual detection limits.

Optimization of pretreatment conditions

Sample clean-up. River water samples were eluted on a C_{18} SPE cartridge with the aim of removing non-polar substances potentially dangerous for the chromatographic column. Under the same experimental conditions, the analytes studied were not retained from an aqueous solution. A small volume (5 ml) of aqueous solutions of the compounds listed in Table I, at concentrations 50 times higher than the individual detection limits, were analysed before and after elution through the C_{18} cartridge. No effect on the concentrations of the solutes was observed.

Stationary phase for SPE. The extraction of the 23 analytes from aqueous solutions was tried with various types of solid-phase sorbents. The following procedure was used: 20 ml of standard test mixtures whose components, at the same concentrations as the solutions used for testing the sample clean-up, were eluted through quaternary amine, amino and diamino Baker SPE cartridges. Further tests were conducted using C_8 and C_{18} cartridges, previously loaded with CTMABr.

Chromatographic analysis of the eluted solutions indicated that all the cartridges retained 100% of the solutes. The cartridges were also examined visually by illuminating them with a UV lamp. The adsorbed compounds produced a single and narrow fluorescent band at the top of the stationary phase column.

Elution of the adsorbed aromatic sulphonates. Although the solutes were quantitatively retained, many of them were not quantitatively recovered by elution. Extraction from ion-exchange cartridges

TABLE I

RESULTS OF THE CHROMATOGRAPHIC ANALYSIS AND SOLID-PHASE EXTRACTION OF AROMATIC SULPHONATES

NS = naphthalenesulphonate; NDS = naphthalenedisulphonate; BZS = benzenesulphonate; A = excitation maximum (nm); B = emission maximum (nm); C = retention time (min); D = detector wavelength, ex/em (1 = 240/660 nm, 2 = 250/455 nm); E = detection limit of the chromatographic analysis (ppb); F = mean recovery ± S.D. ($n = 6$) (%); G = concentration in the solution to be extracted (ppb).

Substance	Chromatography					SPE	
	A	B	C	D	E	F	G
1-NS	230	338	7.25	1	25	85 ± 5	1.9
2-NS	230	339	6.97	1	25	87 ± 10	1
1.5-NDS	230	336	11.29	1	100	81 ± 7	4
2,6-NDS	234	345	8.49	1	12	88 ± 15	0.5
2,7-NDS	234	342	10.37	1	50	92 ± 13	2
1-OH-2-NS	240	350	14.64	1	15	96 ± 17	0.6
1-OH-4-NS	237	436	5.06	2	10	87 ± 16	0.3
1-OH-3,6-NDS	245	475	9.76	2	100	94 ± 23	3
2-OH-3,6-NDS	240	462	17.30	2	8	107 ± 19	0.3
2-OH-6,8-NDS	239	468	15.95	2	5	103 ± 16	0.2
2-NH_2-1-NS	246	406	7.53	2	20	86 ± 11	0.1
4-NH_2-1-NS	247	415	4.03	2	5	84 ± 3	0.2
5-NH_2-2-NS	249	455	4.33	2	4	89 ± 3	0.15
8-NS_2-2-NS	249	464	5.41	2	4	88 ± 4	0.15
3-NH_2-2,7-NDS	251	440	10.21	2	1	92 ± 7	0.05
7-NH_2-1,3-NDS	251	444	12.71	2	1	92 ± 5	0.05
4-NH_2-3-OH-1-NS	248	442	4.51	2	2	78 ± 3	0.3
4-NH_2-5-OH-1-NS	346	400	3.64	2	60	77 ± 11	4
6-NH_2-4-OH-2-NS	253	407	3.73	2	10	78 ± 3	0.4
8-NH_2-1-OH-3,6-NDS	240	408	9.03	2	25	79 ± 11	1
2-NH_2-1-BZS	245	366	4.18	1	150	87 ± 12	6
3-NH_2-1-BZS	245	366	3.24	1	120	97 ± 9	5
4-NH_2-1-BZS	253	347	2.95	1	25	98 ± 3	1

was tried with aqueous solutions of pH 1–13, saturated solutions of LiCl and $MgSO_4$, pure methanol, pyridine and 5% HCl in methanol. All these eluents, except the last, gave very poor results. The recoveries obtained with 5% HCl in methanol were only partially satisfactory, because the recovered amounts of six substances were below 50%. Further, in the chromatographic analysis, some closely eluted compounds were resolved worse, even if the HCl was neutralized with NH_3 prior to injection.

More satisfactory results were obtained with reversed-phase SPE cartridges loaded with CTMABr. C_8 and C_{18} stationary phases furnished by Merck and Baker were tested. As the Adsorbex C_{18} type gave slightly better results than the others, it was adopted in subsequent studies.

Methanol gave satisfactory results for the extraction of the substances adsorbed on the C_{18} SPE cartridge. In order to find the optimum overall volume of eluent, during elution fractions of 0.5 ml were collected and analysed. Those corresponding to an overall volume larger than 2 ml contained negligible amounts of the analytes, hence that volume was adopted to elute the SPE cartridge.

Recoveries from standard solutions of the analytes, at the reported concentrations, are given in Table I, together with the standard deviations calculated, for a 95% confidence interval, from the data for six replicate extractions.

Influence of pH and inorganic salts. The influence of inorganic salts and pH on the extraction yields was also investigated. The pH of the standard

solutions was adjusted from 4 to 9 with either HCl or NaOH. Further tests were conducted with solutions with 30 g l^{-1} NaCl or 2 g l^{-1} Na_2SO_4 added.

The recoveries of all the compounds decreased; in particular 30 g l^{-1} of NaCl reduced the recoveries of orthanilic, methanilic and sulphanilic acid below 30%, whereas 2 g l^{-1} of Na_2SO_4 and an acidic pH reduced the recoveries of methanilic and sulphanilic acid below 50%. A basic pH had only a slight influence on the extraction yields. The recoveries of the other substances listed in Table I were always >70%.

Conditioning of the SPE cartridges. Conditioning of the cartridges was found to be very useful in increasing the recoveries; it consisted of eluting with 2 ml of methanol, two aliquots of UHQ water, 2 ml of 1% CTMABr solution and two aliquots of 5 ml of UHQ water. This procedure was carried out three times before passing the water sample through the cartridge. A pretreatment consisting of a single series of elutions resulted in poorer recoveries, particularly for those compounds that have longer retention times. No increase in recoveries was observed if the cartridge were pretreated with more than three series of elutions.

DISCUSSION

The chromatographic separation of the analytes was performed with an isocratic eluent delivered at a flow-rate of 1.5 ml min^{-1}. Gradient elution was tried, but isocratic conditions were preferred in order to increase the sensitivity (due to the better stability of the baseline), to obtain more reproducible retention times and to shorten the analysis time (because no column conditioning was required after each analysis). Further, isocratic conditions allowed the background fluorescence to be subtracted efficiently from the spectra of the analytes; therefore, it was also possible to characterize unknown analytes by means of their fluorescence spectra even at very low concentrations.

The optimized mobile phase had a pH of 7.0, an acetonitrile–water ratio of 58:42 and contained 7 g l^{-1} of CTMABr and 1 g l^{-1} of citric acid. The pH was buffered to 7.0, as lower pH values produced poorer peak shapes for many compounds and lengthened the retention times; at that pH, all the compounds were eluted within 18 min with acceptable resolution. An acetonitrile-to-water ratio of 58:42 was considered to be the most favourable because none of the 23 compounds investigated was non-retained and they were all eluted within 18 min with good resolution of adjacent peaks. A 7 g l^{-1} concentration of CTMABr seemed the most favourable, as lower concentrations resulted in poorer peak shapes for some compounds, and all the peaks were well resolved in an acceptable time.

The excitation/emission monochromators of the detector were set alternatively at 250/455 or 240/660 nm and their band widths were 20/40 nm, respectively. Two replicate injections of each sample were made. Good separations of the analytes and short analysis times were obtained. Typical chromatograms are shown in Fig. 3.

Before the analysis, the water samples were filtered through a 0.45-μm cellulose acetate filter and then eluted through a 400-mg C_{18} Merck SPE column in order to retain non-polar interferents.

Analytes were extracted from water by passing a suitable amount of sample through another C_{18} SPE cartridge at a flow-rate of 8 ml/min. That cartridge was previously conditioned as described above. Volumes of sample exceeding 100 ml resulted in an excessive increase in the flow resistance across the cartridge, and consequently in an increase in the analysis time. The retained compounds were further eluted with 2 ml of methanol and analysed by HPLC.

A further injection was done in order to obtain fluorescence spectra of the eluted substances. A few seconds before a peak appeared, the eluent flow was gradually slowed and then stopped on the top of the peak. The band widths of the excitation and emission monochromators were set at 5 nm and a first pair of spectra of unknown analyte were obtained and memorized. The flow of the eluent was then started again, and it was subsequently re-stopped on the decreasing portion of chromatographic peak; a second pair of spectra were memorized, under the same instrumental conditions. The latter spectra were subtracted from the corresponding former spectra, in order to avoid eluent and matrix disturbances, and the resultants were compared with those of the standards. It was observed that the spectra of the unknown peaks were identifiable if their maximum intensity was greater than twice the background fluorescence.

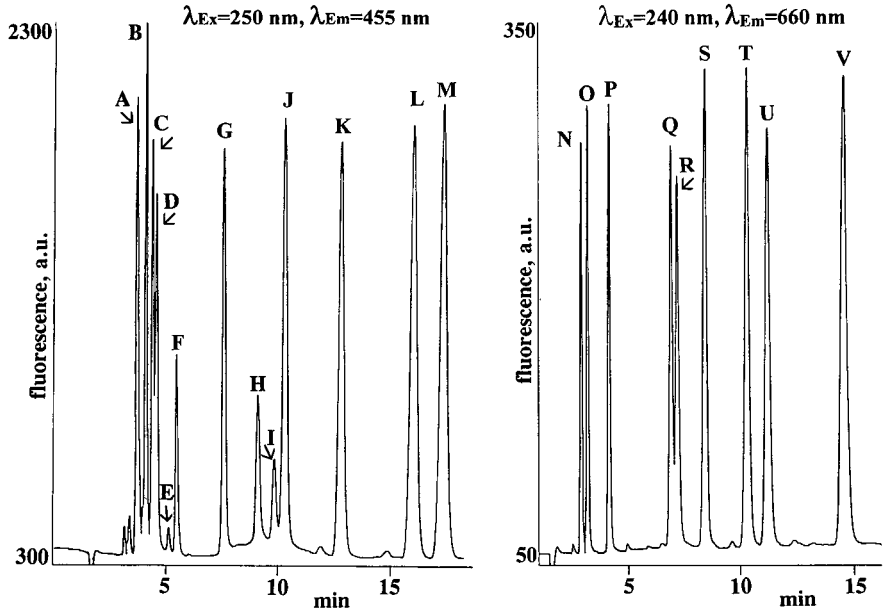

Fig. 3. Chromatograms of a standard mixture of 22 compounds (NS = naphthalenesulphonate, NDS = naphthalenedisulphonate, BZS = benzenesulphonate). A = 4-amino-5-hydroxy-1-NS, 4 ppm; B = 4-amino-1-NS, 0.25 ppm; C = 5-amino-2-NS, 0.15 ppm; D = 4-amino-3-hydroxy-1-NS, 0.3 ppm; E = 1-hydroxy-4-NS, 0.3 ppm; F = 8-amino-2-NS, 0.06 ppm; G = 2-amino-1-NS, 1.2 ppm; H = 8-amino-1-hydroxy-3,6-NDS, 2 ppm; I = 1-hydroxy-3,6-NDS, 5 ppm; J = 3-amino-2,7-NDS, 0.1 ppm; K = 7-amino-1,3-NDS, 0.12 ppm; L = 2-hydroxy-6,8-NDS, 0.8 ppm; M = 2-hydroxy-3,6-NDS, 1.2 ppm; N = 4-amino-1-BZS (sulphanilate), 0.5 ppm; O = 3-amino-1-BZS (methanilate), 3 ppm; P = 2-amino-1-BZS (orthanilate), 3 ppm; Q = 2-NS, 1 ppm; R = 1-NS, 1.9 ppm; S = 2,6-NDS, 0.5 ppm; T = 2,7-NDS, 1.5 ppm; U = 1,5-NDS, 5 ppm; V = 1-hydroxy-2-NS, 1 ppm.

The analyte concentration changes with time, due to diffusion inside or outside the flow cell, were examined by observing the drift of the fluorescence after stopping the flow. The variation in fluorescence intensity was $<1\%$ min^{-1}; distortion of the shape of the spectra was avoided by using the fastest scan speed available (600 nm min^{-1}).

Reference spectra were measured using standard sulphonic acids dissolved in the optimized chromatographic eluent, and were memorized on a floppy disk, with the aim of comparing them with the spectra of unknown components. Standard solutions had a concentration of 1 mg l^{-1}, and no influence of concentration on spectral shapes was observed in the range 0.01–1 mg l^{-1}.

To take into account possible variations of the recoveries of the SPE, an internal standard was added to real samples prior to preconcentration. After the analysis, a factor was calculated by dividing the expected concentration (accounting for the yield in Table I) by the observed value. The yields in Table I for the remaining analytes were multiplied by this factor. Orthanilic acid was found to be absent in all the real samples analysed, hence it was used as the internal standard.

Analysis of river water

The method described was used to analyse water samples from the Bormida, a river situated in the N.W. Italy. The chromatograms of the extract of a sample are reported in Fig. 4; Table II gives the data for the analytes identified in four different samples. As can be seen, their concentrations range from fractions of 1 $\mu g\, l^{-1}$ to several thousand mg l^{-1}. The concentration factors adopted for the analysis are given in Table II; the most concentrated sample was diluted 400-fold prior to the analysis.

As an example of qualitative identification, Fig. 5 reports the four spectra (excitation and emission) obtained for the unknown peak F, together with those of 2,7-naphthalenedisulphonic acid; as can be seen, they coincide well. Good agreement was also

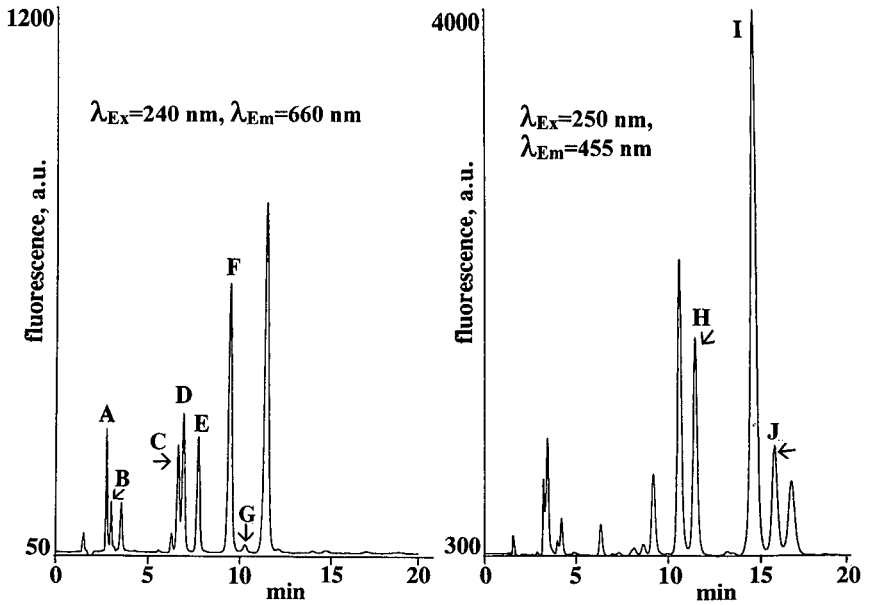

Fig. 4. Chromatograms obtained from the sample D in Table II. The spectra of the unidentified peaks did not coincide with any of those of the standards. A = 4-amino-1-BZS; B = 3-amino-1-BZS; C = 2-NS; D = 1-NS; E = 2,6-NDS; F = 2,7-NDS; G = 1,5-NDS; H = 7-amino-1,3-NDS; I = 2-hydroxy-6,8-NDS; J = 2-hydroxy-3,6-NDS (abbreviations as in Fig. 3).

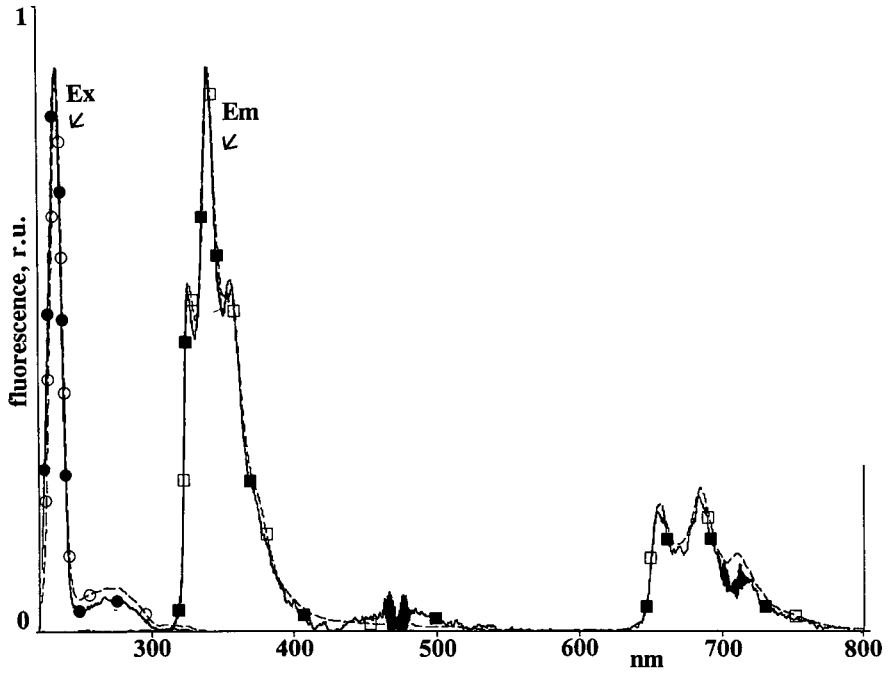

Fig. 5. Superimposed excitation and emission spectra of the unknown peak F (● = excitation, ■ = emission) and of 2,7-naphthalenedisulphonate (○ = excitation, □ = emission). The bands of stronger noise around 470 and 700 nm are due to the Rayleigh scattering of the incident light; r.u. = relative units.

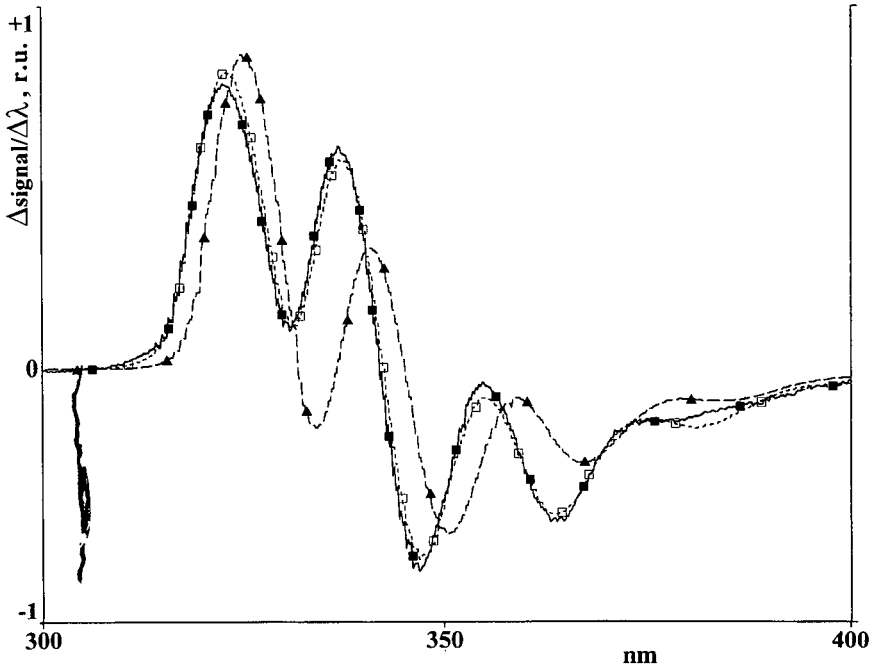

Fig. 6. First-order derivative of the emission spectra in the range 300–400 nm. ■ = Unknown peak F; □ = 2,7-naphthalenedisulphonate; ▲ = 2,6-naphthalenedisulphonate; r.u. = relative units.

TABLE II

CONCENTRATIONS OF THE IDENTIFIED COMPOUNDS IN FOUR RIVER WATER SAMPLES

NS = naphthalenesulphonate; NDS = naphthalenedisulphonate; BZS = benzenesulphonate.

Substance	Concentration (mg l^{-1})			
	A[a]	B[a]	C[a]	D[b]
7-NH_2-1,3-NDS	0.0002	0.0017	0.0027	76
2-OH-6,8-NDS	0.0015	0.0092	0.0065	1667
2-OH-3,6-NDS	0.0011	0.024	0.035	371
4-NH_2-1-BZS	0.0045	0.0026	0.0015	408
3-NH_2-1-BZS	NF[c]	0.015	0.0076	943
2-NS	NF[c]	0.0083	0.0017	558
1-NS	0.0065	0.016	0.031	1569
2,6-NDS	0.0016	0.0030	0.0013	245
2,7-NDS	0.010	0.015	0.0093	1658
1,5-NDS	NF[c]	0.16	0.27	195

[a] The concentration factor of the pretreatment was 30:1.
[b] The sample was diluted 400-fold with UHQ water; the analysis was performed on 2 ml of the diluted solution.
[c] NF = Not found.

observed with the spectra of the 2,6-isomer, which precedes the 2,7-isomer in the elution order. In order to discriminate between these standards, the first-order derivatives of the emission spectra were also taken into account. Fig. 6 shows the first-order derivatives, in the range 300–400 nm, of the emission spectra of the unknown analyte F and of the two cited isomers. It can be seen that the derivative of the spectrum of the 2,7-isomer coincides very well with that of the unknown, whereas that of the 2,6-isomer not. Similar conclusions were reached also for the other compounds identified. It was observed that the retention times, together with the fluorescene excitation and emission spectra, can furnish specific indications about the nature of the unknown analytes found in river water.

CONCLUSIONS

An HPLC separation and a characterization method based on spectrofluorimetry was optimized for the identification of aromatic sulphonic acids

derivatives in natural waters. The method is very sensitive, it allows the spectroscopic identification of unknown compounds and it is able to discriminate even positional isomers having very similar chromatographic and spectroscopic characteristics.

In the future, further investigations will be carried out in order to study whether the compounds considered in this work can be modified in the aquatic environment.

REFERENCES

1 M. Luther, *Ber. Kernforschungsanlage Jülich*, Jül-2236, 1988.
2 T. Ohe and Y. Watanabe, *Agric. Biol. Chem.*, 52 (1988) 2409.
3 R. M. Wittich, M. G. Rast and H. J. Knackmuss, *Appl. Environ. Microbiol.*, 54 (1988) 1842.
4 R. H. Stehl, *Anal. Chem.*, 42 (1970) 1802.
5 H. S. Freeman, Z. Hao and W.-N. Hsu, *J. Liq. Chromatogr.*, 12 (1989) 919.
6 S. Terabe and T. Isemura, *Anal. Chem.*, 62 (1990) 652.
7 H. Miyoshi, T. Nagai and M. Ishikawa, *Bull. Shizuoka Pref. Inst. Publ. Health Environ. Sci.*, 27 (1984) 45.
8 C. Pettersson and G. Schill, *Chromatographia*, 28 (1989) 473.
9 E. Arviddson, L. Hackzell, G. Schill and D. Westerlund, *Chromatographia*, 25 (1988) 430.
10 H. Kataoka, T. Okazaki and M. Makita, *J. Chromatogr.*, 473 (1989) 276.
11 M. L. Trehy, W. E. Gledhill and R. G. Orth, *Anal. Chem.*, 62 (1990) 2581.
12 I. S. Kim, F. I. Sasinos, D. K. Rishi, R. D. Stephens and M. A. Brown, *J. Chromatogr.*, 589 (1992) 177.

Journal of Chromatography, 640 (1993) 241–249
Elsevier Science Publishers B.V., Amsterdam

CHROMSYMP. 2832

Monitoring of ionic concentrations in airborne particles and rain water in an urban area of central Germany

H. Schumann* and M. Ernst

Landesamt für Umweltschutz Sachsen-Anhalt, PF 681, 4020 Halle/Saale (Germany)

ABSTRACT

The primary objective of this investigation was to document fluctuations of levels of ions in airborne particles and in rain water with the help of ion chromatography. The environmental emission situation in the investigated geographic area is characterized by a widespread use of domestic coal-burning furnaces. The use of a parallel impactor for particulate sampling permits the results to be interpreted additionally in terms of particle size. The anions and cations were extracted from the filters in the sampling devices into ethanol–water mixtures by sonication. Rain water samples were analysed after a simple dilution step. The data obtained on ionic fluctuations are compared with similar data sets published by other laboratories.

INTRODUCTION

Frequent analyses of air contaminants in rain water and airborne and settled dust particles are essential for any reliable estimates of damage caused by air pollution. After polyaromatic and halogenated hydrocarbons, inorganic anions and cations represent the most important information that needs to be provided by any air monitoring programme. Especially a knowledge of the levels of anionic components in aerosols is desirable in view of the increasing acidity of natural precipitation. It is well known that the main causes of this effect are the high emission levels of sulphur and nitrogen oxides, which are converted under atmospheric conditions into detectable amounts of sulphuric and nitric acid. Additional anionic contributions to atmospheric pollution in the form of fluoride and chloride come from power-generating processes. Determined cation levels are used in mass balance calculations to verify the completeness of the analytical information obtained with regard to total ion contamination.

Apart from these chemical properties, the physical properties, in particular the particle size distribution, are important for the toxicity of airborne dust. Airborne dust particles from aerosols and are taken up by humans chiefly by inhalation. Coarse dust particles (>3.5 μm) are retained largely in the rhynopharynx and discharged relatively quickly via the gastro-intestinal tract. In contrast, fine dust particles (<3.5 μm) may enter the alveolar system. Therefore, the resorption rate and hence the toxicity are significantly higher. Irrespective of the toxicity aspect, published investigations on acid aerosols include, in most instances, determinations of pollutants without regard to particle size.

The results presented in this paper were obtained in a highly industrialized area characterized by the widespread use of relatively obsolete, emission-prone processes. The problem of high levels of air pollution has been ongoing, despite the large number of industrial stoppages and the drastic decrease in production output that have occurred in the last 2 years. Even with such decreased levels of industrial production, the Leipzig–Halle–Bitterfeld industrial area is currently (1990–91) still showing levels of air pollution that are distinctively higher than those found elsewhere in Germany [1,2]. Our lab-

* Corresponding author.

0021-9673/93/$06.00

oratory participates in air monitoring as a member of an extensive network, which on completion will provide a complete coverage of the local geographical area. Some of the recent results indicate a clear trend towards a general improvement in the environmental situation.

EXPERIMENTAL

Sampling techniques

The sampling of dust was carried out at a location in Halle characterized by a high traffic volume and a high density of housing utilizing predominantly brown coal for heating. Two different designs of dust sampling devices were utilized during the air monitoring experiments.

The first investigations carried out from February to June 1991 dealt with the time dependence of the pollutants absorbed by the airborne dust particles on their surface and its distribution according to the particle size. The sampling device, an ICP 5 parallel impactor developed by the Frauenhofer Institute for Environmental Studies in Hannover (Germany), was a prototype. The function of this sampler is that a defined volume of aerosol sucked in is split into six equal flows and fed via prefilters in such a manner that only defined particle fractions can reach the analytical filter arranged beneath. The fractions obtained are as follows: (I) 0–3.5 μm; (II) 0–6 μm; (III) 0–10 μm; (IV) 0–17 μm; (V) 0–25 μm; (VI) total dust. According to Puxbaum [3], such fractionation allows one to discriminate reliably between very fine particles (accumulation maximum at 0.7 μm) and coarser particles (accumulation maximum at 10 μm). The sampling period was 48 h and the air volume was *ca.* 28 m^3.

The filtration material tested was compressed glass-wool beds owing to the limited pump capacity of the device. This filter material makes it possible only to determine anions because it has a high sodium blank level. On the other hand, it is sufficient to determine the anion values for assessment of pollutants.

For ion balance studies a second experimental series was started in June 1992, using another sampling device, a GS 050/3, obtained from Derenta (Berlin, Germany). Here we used PTFE filters (diameter 50 mm, pore size 1.2 μm, from Sartorius, (Göttingen, Germany). The sampling period was usually 24 h and the collected dust volume was 35–40 m^3.

The sample preparation for both types of filter merely involved the extraction of inorganic ions from the particles accumulated on the filters during the sampling. To achieve this, each of the filters was placed in a polyethylene beaker containing 10 ml of ethanol–water (1:9). The extraction of water-soluble sample components with ethanol–water mixtures is a widely used standard procedure [4]. The filters were kept immersed in the extraction liquid overnight and then subjected to ultrasonication. After filtration through a 0.45-μm filter (Type HV; Millipore, Bedford, MA, USA), the extraction liquid containing water-soluble ions from the collected dust particles was subjected to ion chromatographic analysis. A check on this dissolution step by performing a second one under identical conditions confirmed a better than 95% efficiency for the single-step extraction procedure.

The sampling of rain water was carried out in an industrial park located in the eastern part of Halle. During the period poor in rain between February and July 1992 (only sixteen "rain events" occurred), the samples were collected with the help of a "wet-only collector".

The collector obtained from the Institute of Energetics in Leipzig (Germany) possesses an electrode sensor that opens a polyethylene funnel after coming into contact with wet precipitation. The rain water runs into a 2-l polyethylene flask that is positioned in a sampling carousel. At programmable intervals (standard condition = 24 h) another polyethylene bottle will be positioned below the reception funnel. When the heatable sensor at the end of deposition becomes dry, the reception funnel is closed. A temperature sensor controls a three-level heating system, the function of which is to prevent the pyramid setting sensor becoming moistened by dew or hoar frost. This device also guarantees the melting of snow and the opening of the collector to collect water from snow. Each of the sixteen samples was divided into a number of aliquots that were utilized for pH and conductivity measurements and finally also for ion chromatographic (IC) analyses for anions and cations.

The IC runs were carried out immediately, if possible. When an immediate analysis of samples was not possible, the samples were preserved by storage

at freezing temperature until the time of their injection into the IC system.

Ion chromatography

Non-suppressed IC was utilized exclusively. The IC system consisted of a Model 510 pump, a U6K injector and a Model 431 conductivity detector. All hardware components and the data acquisition and data reduction system were obtained from Waters Chromatography Division of Millipore (Milford, MA, USA).

The separations of anions (fluoride, chloride, nitrate, sulphate) were performed on an IC Pak A HC column (Waters) with a gluoconic acid–boric acid (1.3 m*M* each, pH = 8.5) aqueous solution as the eluent. The flow-rate was maintained at 2 ml/min. An IC Pak C M/D column (Waters) was used for all cation separations (sodium, ammonium, potassium, magnesium, calcium) with 3.0 m*M* nitric acid–EDTA 0.1 m*M* solution as the eluent. The flow-rate was 1.0 ml/min. Quantitative analysis was based on calibration graphs obtained with five different standard concentrations in suitable ranges for each application. Peak areas rather than heights were plotted against standard concentrations to construct the calibration graphs.

To determine the blank levels, five unexposed PTFE filters were extracted with ethanol–water as described above. The extracts were filtered and injected into the IC system for the measurement of anions and cations. The background levels in the analysis of rain water were evaluated by rinsing the "wet-only collector" with a volume of deionized water corresponding to the collected sample volume of 400 ml (median value). The blank rinse was collected in presoaked polyethylene containers and analysed for anions and cations by IC.

The detection limits listed in Table I were estimated according to VDI 2449/1 [5] from the blank levels and three times the standard deviation for deionized water in eight determinations:

$$x = x_0 + 3\,s_{x_0}$$

where x = detection limit, x_0 = middle background level and s_{x_0} = standard deviation from n determinations. For the airborne dust particles from an average sampling volume of 40 m^3 the relative detection limit obtained are also given in Table I. The accuracy of the quantitative results for anions and cations was verified by analysis of artificial rain samples prepared according to procedures specified by VDI [6] and also with standard reference material (SRM 2694, NIST, Gaithersburg, MD, USA). The ranges of analyte recoveries were 88–125% and 88–94% for anions and cations, respectively.

TABLE I

DETECTION LIMITS FOR IONS MONITORED IN AIRBORNE DUST AND RAIN WATER

Ion	Dust ($\mu g/m^3$)	Rain water ($\mu g/l$)
Fluoride	0.005	200
Chloride	0.01	50
Nitrate	0.01	400
Bromide	0.01	400
Phosphate	0.02	750
Sulphate	0.02	750
Sodium	0.025	50
Ammonium	0.008	30
Potassium	0.02	40
Magnesium	0.005	20
Calcium	0.02	50

RESULTS AND DISCUSSION

Analysis of airborne dust particles

A typical chromatogram from anions, obtained after ethanol–water extraction of dust particles collected on filters inside the dust samplers, is shown in Fig. 1. The chromatogram illustrates a satisfactory separation of all analytes of interest within 18 min. The separation results for cations are shown in Fig. 2. The peaks for the two main components, ammonium and sodium, were not completely resolved. We found, however, that this did not affect the precision of peak area determination. The precision of the results for these two cations was the same as for the other cations. The separation of ammonium, alkali metal and alkaline earth metal cations was accomplished in only 12 min.

The results of anion monitoring during 1991 will be discussed first. Fig. 3 illustrates the time dependence of the sulphate concentrations found in total dust particles during the winter months. During the summer only a few measurements were carried out

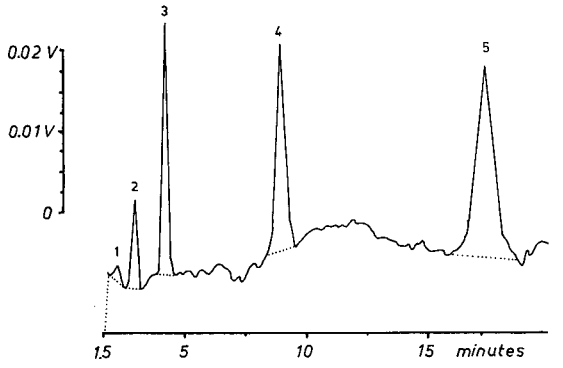

Fig. 1. Ion chromatographic separation obtained from a dust sample. Column, IC Pak A HC (10 μm); eluent, 1.3 m*M* gluconate–borate; pH, 8.5; flow-rate, 2.0 ml/min; detection, non-suppressed conductivity; sample, 50 μl dust ethanol–water extract. Peak identities and concentrations: 1 = fluoride, 0.33 ppm; 2 = hydrogencarbonate; 3 = chloride, 3.03 ppm; 4 = nitrate, 7.93 ppm; 5 = sulphate, 12.42 ppm.

for comparison with the winter period. The summer levels of sulphate are not shown in Fig. 3. One bar represents the sulphate content absorbed by non-fractionated airborne dust particles during 48 h (during February 20–28th the sampling device was faulty).

The range of fluctuations of sulphate concentrations illustrated in Fig. 3 is similar to those of the

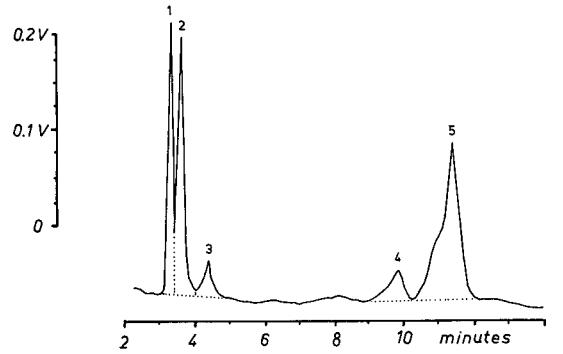

Fig. 2. Typical separation of cations extracted from a dust sample. Column, IC Pak C M/D (5 μm); eluent, 3.0 m*M* HNO_3–0.1 m*M* EDTA; flow-rate, 1.0 ml/min; detection, non-suppressed conductivity; injection volume, 10 μl. Peak identities and concentrations: 1 = sodium, 4.5 ppm; 2 = ammonium, 3.87 ppm; 3 = potassium, 0.47 ppm; 4 = magnesium, 0.58 ppm; 5 = calcium, 8.8 ppm.

TABLE II

MEAN MONTHLY TOTAL DUST LOAD AND ITS WATER-SOLUBLE ANION CONTENT COLLECTED IN HALLE IN 1991, USING THE ICP 5

Month (1991)	*n*	Total dust ($\mu g/m^3$)	Water-soluble ion content ($\mu g/m^3$)		
			Chloride	Nitrate	Sulphate
January	6	243.5	8.1	10.8	47.6
February	10	272.2	7.8	13.8	42.9
March	15	214.9	4.7	14.4	29.9
April	15	168	3.6	8.5	33.1
June	8	54.7	1.3	4.1	9.9

total mass content of dust particles in the air and to the magnitude of changes in heavy metal cations found in the same dust particles. The uneven distributions of levels of dust particles and of the corresponding ion concentrations are caused by meteorological factors on the one hand and by changes in the industrial emission on the other.

A comparison of montly average concentrations of anions is presented in Table II. As expected, the anion concentrations and dust load are higher during the winter months than in summer. This represents clear evidence of the contributing role of domestic coal-burning furnaces to the pollution of air by dust and inorganic contaminants.

In the following we discuss the dust fractions collected using the ICP 5. Fig. 4 and Table III illustrate the distribution of three anions among the collected

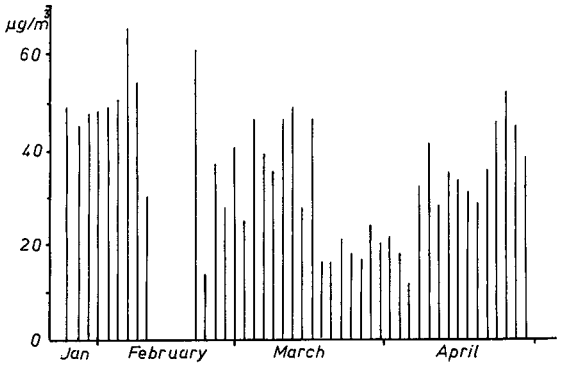

Fig. 3. Sulphate content in unfractionated dust samples collected using the ICP 5 in 1991 in Halle.

TABLE III

TWO TYPICAL EXAMPLES (WINTER AND SUMMER) OF ANION DISTRIBUTIONS (mg/l) IN DIFFERENT PARTICLE SIZE FRACTIONS OF AIRBORNE DUST

Period	Ion	Particle size (μm)					
		0–3.5	0–6	0–10	0–17	0–25	Total dust
Winter (2–3 Feb. 1991)	Chloride	9.1	10.2	10.3	10.2	10.4	10.4
	Nitrate	8.4	9.3	9.5	10.9	10.9	11.2
	Sulfate	46.9	49.0	49.2	49.0	49.0	49.2
Summer (18–20 June 1991)	Chloride	0.3	0.4	0.5	0.4	0.4	0.4
	Nitrate	2.7	2.9	2.9	3.2	3.5	3.6
	Sulfate	4.0	4.6	4.6	4.7	4.7	6.2

particle size fractions. It is shown that in winter 95% of sulphate, 87% of chloride and 75% of nitrate are found in particles having diameters smaller than 3.5 μm. This is in a good agreement with the results of monitoring heavy metal levels in dust [7]. The very small size of the dust particles carrying the largest portion of ionic contaminants facilitates deep deposition of toxic substances in the alveolic system of the lungs.

The simultaneous assays of anions and cations were performed in June 1992. These values were utilized for, among other things, calculations of the ionic mass balance in the dust samples obtained. The montly averages (n = 29) and the minimum and maximum values found for each of the ions measured are presented in Table IV. The ion ratio $\varepsilon_{cations}$:ε_{anions}, calculated from the equivalent concentrations listed in Table IV, is 1.17. This imbalance is not surprising, as the method employed for anions does not provide a complete value for silicates, carbonates and organic acids. Also not included in our mass balance calculations is the concentration of hydronium ions.

Table IV shows sulphate and ammonium ions to exhibit the highest concentration in airborne particles at the sampling sites. In view of the additional results presented in Fig. 5 and in Table V, it is possible to conclude that ammonium sulphate is followed by calcium sulphate as the main components

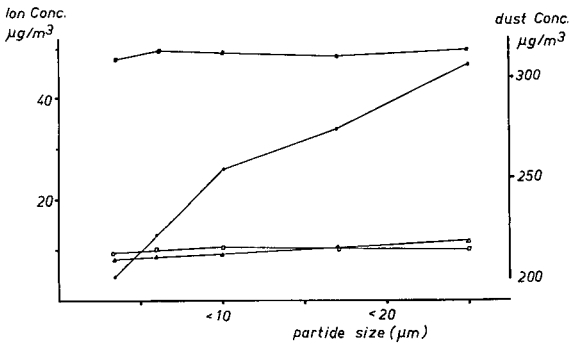

Fig. 4. Distribution of anion concentrations in different particle size fractions of dust. ● = Dust; ■ = sulphate; △ = nitrate; □ = chloride.

TABLE IV

AVERAGE MASS AND EQUIVALENT CONCENTRATIONS OF IONS IN DUST COLLECTED IN HALLE IN JUNE 1992 USING THE GS 50/3

Ion	Monthly average		Minimum (μg/m³)	Maximum (μg/m³)
	(μg/m³)	(nmol/m³)		
Fluoride	<0.05			
Chloride	0.33	9.3	0.10	0.97
Nitrate	2.72	43.6	0.74	9.83
Sulphate	9.37	195.1	3.14	19.80
ε_{anions}		248.0		
Sodium	0.32	13.9	0.03	1.27
Ammonium	2.67	146.7	0.69	5.17
Potassium	0.33	8.4	0.02	1.11
Calcium	2.17	108.2	0.88	4.43
Magnesium	0.13	10.7	0.01	0.33
$\varepsilon_{cations}$		287.9		

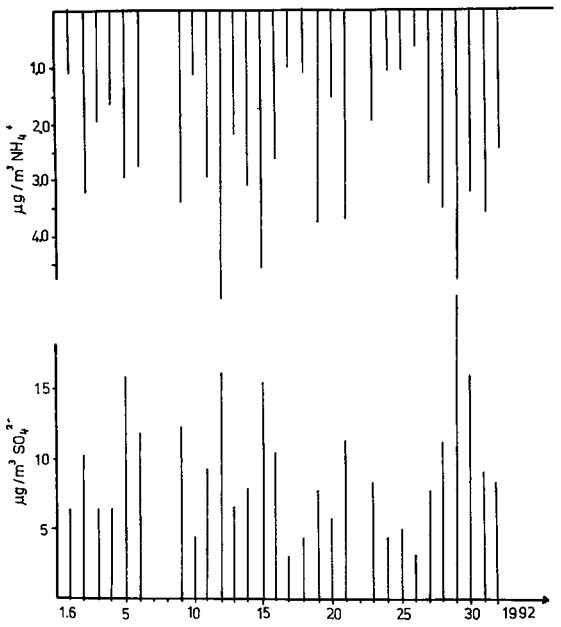

Fig. 5. Mutual dependence of sulphate and ammonium concentrations in airborne dust particles collected in 1991 in Halle.

of the airborne dust in this area. These conclusions agree also with some previously published data [9,10].

Comparisons enable us to identify the source of ammonium sulphate-containing dust. During the winter, there is a clear dependence between the mass of total dust load on the one hand and the ammonium, sulphate and chloride concentrations on the other (see also Table V). These observations help to identify the individual household furnaces, using salt- and sulphur-rich coal for fuel, as the source of inorganic ions in dust particles.

TABLE V

CORRELATIONS BETWEEN COMPONENTS IN WINTER AEROSOLS

Correlation factor		Parameters		
X	*Y*	*f*	*r*	*P*
Dust	Sulphate	42	0.53	0.99
	Ammonium	27	0.42	0.95
	Chloride	40	0.34	0.95
	Calcium	27	0.24	
	Sodium	27	0.10	
Sulphate	Ammonium	27	0.89	0.99
	Calcium	27	0.58	0.99
Chloride	Sodium	27	0.64	0.99

Table VI shows a comparison of ion concentrations in airborne dust determined in several German cities. A comparison of the ion concentrations that we determined with values published by other workers is difficult because the sampling periods were rarely identical. The concentration levels determined by us in Halle can probably be considered similar to those obtained in Berlin. In comparison with cities in southern Germany, Halle is burdened by air pollution having clearly higher levels of anthropogenic air components, such as total dust, chloride, nitrate and sulphate. The same is also true for cations in dust, *i.e.*, ammonium and calcium.

TABLE VI

COMPARISON OF ION CONCENTRATIONS IN DUST FROM SEVERAL GERMAN CITIES

City	Year	Sampling period	Ref.	Dust ($\mu g/m^3$)	Mean ion concentration ($\mu g/m^3$)							
					Na^+	NH_4^+	K^+	Ca^{2+}	Mg^{2+}	Cl^-	NO_3^-	SO_4^{2-}
Berlin	1987	Jan.–Dec.	8	98	1.0	4.7	0.6	3.1	0.3	2.1	7.5	16.5
Berlin	1988	Jan.–Dec.	9	79	0.8	3.8	0.4	2.3	0.2	1.4	5.5	11.7
Mannheim	1988	Jan.–Dec.	10	36	0.5	2.0	0.3	0.4	0.1	<0.2	1.3	6.7
Stuttgart	1988	Jan.–Dec.	10	33	0.4	1.4	0.2	0.8	0.1	<0.2	1.0	4.8
Halle	1991	Jan.–July	This work	211						5.3	11.7	35.5
Halle	1991	June–July	This work	55						1.3	4.1	9.9
Halle	1992	June–July	This work	66	0.3	2.6	0.3	2.2	0.1	0.3	2.7	9.4

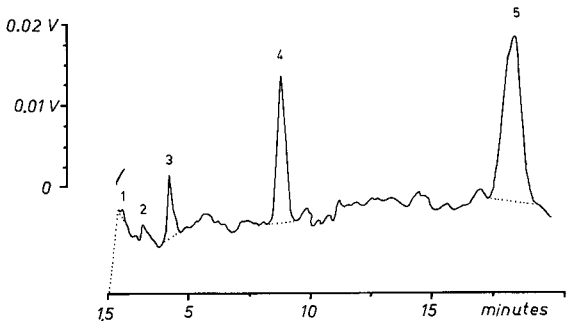

Fig. 6. Anion chromatogram of rain water sample. Conditions as in Fig. 1. Peak identities and concentrations: 1 = fluoride; 2 = hydrogencarbonate; 3 = chloride, 0.42 ppm; 4 = nitrate, 3.09 ppm; 5 = sulphate, 6.65 ppm.

Analysis of rain water

The chromatograms in Figs. 6 and 7 are typical for our results obtained with rain samples. They were obtained by injecting a sample of rain from June 1992 into the ion chromatograph. Both chromatograms show sufficient sensitivity and separation for all rain water samples, including the only lightly contaminated samples collected during the summer months. The most important results from the rain water monitoring are summarized in Table VII.

In a similar fashion to the dust samples, the rain water samples show differences in the levels of ions during the water and summer periods. The time dependence of ion levels in rain water is presented in Table VIII.

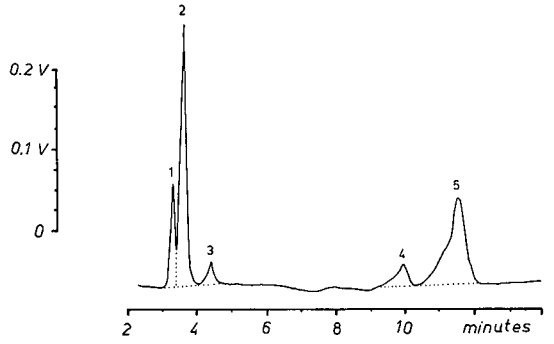

Fig. 7. Typical separation of cations found in rain water samples. Conditions as in Fig. 2. Peak identities and concentrations: 1 = sodium, 0.27 ppm; 2 = ammonium, 0.97 ppm; 3 = potassium, 0.08 ppm; 4 = magnesium, 0.13 ppm; 5 = calcium, 0.83 ppm.

TABLE VII

SUMMARY OF RESULS FROM MONITORING RAIN WATER SAMPLES COLLECTED BETWEEN FEBRUARY AND JUNE 1992

Parameter	Average	Minimum	Maximum
Rain volume (ml)	715	184	2100
Conductivity (μS/cm)	44.1	25	105
pH	4.7	4.2	6.5
Ion concntrations (mg/l):			
Chloride	0.8	<0.2	3.4
Nitrate	3.8	1.7	9.3
Sulphate	9.2	3.4	29.7
Sodium	0.4	0.2	2.4
Ammonium	1.4	0.6	3.3
Potassium	0.14	0.02	0.53
Magnesium	0.24	0.11	0.74
Calcium	2.38	0.74	7.30

Another similarity between the dust and rain water samples is the predominance of ammonium, calcium and sulphate ions. As with dust, ammonium sulphate and calcium sulphate seem to be the main components also in rain water (see Fig. 8). For comparison, Fig. 8 includes not only the values obtained from rain water, but also the data from the dust monitoring discussed in the preceding section. The similarity of the dust and rain water results is not surprising and represents a strong indication of the contribution of individual coal-burning furnaces not only to dust pollution but also to ionic contamination of airborne aerosols.

The ionic mass calculations for rain water yielded well balanced cation to anion ratios ($\varepsilon_{cations}:\varepsilon_{anions} \approx 1$) over the entire monitoring period. The relatively small number of measurements, however, do not allow further interpretation. We also feel that a comparative interpretation of the analytical results for rain water and dust obtained in this study is still problematic owing to differences in sampling techniques and atmospheric conditions.

The air pollution situation can be further illustrated by comparing the results of our monitoring study with those obtained by other workers in different regions of Germany (see Table IX). As already mentioned in the discussion about dust, the

TABLE VIII

TIME-DEPENDENT CHANGES IN ION CONCENTRATIONS IN RAIN WATER COLLECTED IN HALLE BETWEEN FEBRUARY AND JUNE 1992

Month	*n*	Cl^-	NO_3^-	SO_4^{2-}	Na^+	NH_4^+	K^+	Mg^{2+}	Ca^{2+}
February	2	2.4	7.3	17.4	1.35	2.12	0.36	3.95	0.5
March	1	2.5	7.1	11.3	0.67	1.83	0.36	2.66	0.34
April	5	0.3	3.2	9.2	0.23	1.35	0.11	3.18	0.22
May	5	0.3	3.1	6.4	0.28	1.11	0.06	1.72	0.2
June	3	0.3	2.7	7.1	0.32	1.25	0.12	1.02	0.16

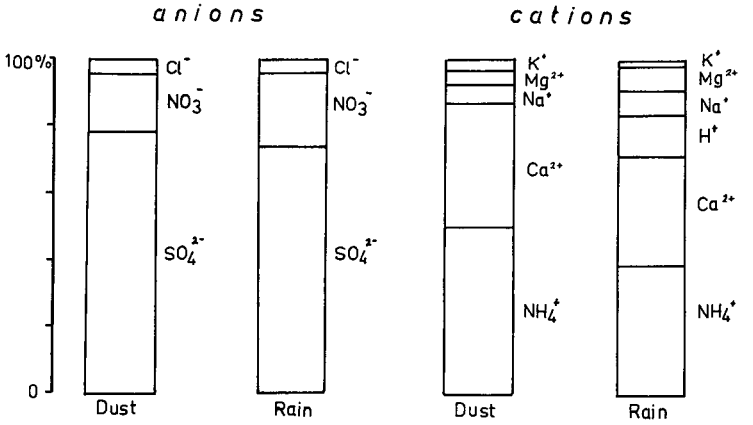

Fig. 8. Distributions of the most important anions and cations in dust and rain water.

TABLE IX

COMPARISON OF ION CONCENTRATIONS IN PRECIPITATIONS IN DIFFERENT GERMAN REGIONS

Region	Sampling period	Ref.	Ion concentration (mg/l)					
			Cl^-	NO_3^-	SO_4^{2-}	NH_4^+	Na^+	K^+
Germany (ranges)	Aug. 79–July 81	11	0.6–5.0	1.8–3.5	3.0–6.6			
Stollberg (Jülich)	Jan.–Dec. 83	12	1.5–1.7	3.1	5.1–6.0			
Kolmberg/Odenwald	May 88	13	1.2	9.0	9.5	2.7	1.0	1.17
Halle	Feb.–June 92	This work	0.8	3.8	9.2	0.4	1.4	0.14
Winter levels								
Jülich	Jan. 89	14	2.1	4.4	6.6	2.6	1.0	0.16
Essen	Jan. 89	14	1.9	4.1	5.2	1.2	0.7	0.2
Dortmund	Dec. 88	14	3.1	2.1	3.3	0.7	1.3	0.12
Hamburg	Jan. 89	14	6.8	4.3	7.1	1.0	2.9	2.09
Halle	Febr. 92	This work	2.4	7.3	17.4	2.1	1.4	0.36

values obtained in this work cannot be compared in detail with those published elsewhere. The 6-month averages obtained in Halle appear to be in general agreement with 12-month ionic averages obtained in other parts of Germany. A more differentiating comparison, however, shows distinctly higher levels of anthropogenic pollution in Halle, especially in February and other winter sampling periods. The anthropogenic contamination is especially recognizable by elevated levels of SO_x and NO_x emissions during the household heating periods. This leads to an acidic pH (*ca.* 4.2) and to an increased sulphate and nitrate load in natural precipitation.

ACKNOWLEDGEMENTS

The authors are grateful to C. Schiller for allowing them to use aliquots of his rain water samples. They also acknowledge the help of B. Fritzsch during the analytical processing of rain water and dust samples.

REFERENCES

1 *Immissionsschutzbericht des Landes Sachsen-Anhalt*, Ministerium für Umweltschutz, Magdeburg, 1990.
2 *Limes-Jahresbericht 1990, Reihe B-Schwebstaub und Inhaltsstoffe, Kohlenwasserstoffe*, Landesanstalt für Immissionsschutz Nordrhein-Westfalen, Essen, 1991.
3 H. Puxbaum, *Fresenius' Z. Anal. Chem.*, 298 (1979) 110–122.
4 *VDI-Richtlinie 3497/4 (Entwurf); Messen partikelgebundener Anionen in der Aussenluft*, VDI-Verlag, Düsseldorf, 1989.
5 *VDI-Richtlinie 2449/1; Prüfkriterien von Messverfahren*; VDI-Verlag, Düsseldorf, 1970.
6 *VDI-Richtlinie 3870/10 (Entwurf); Messen von Regeninhaltsstoffen*, VDI-Verlag, Düsseldorf, 1988.
7 K. Dannecker, K. Naumann and J. Bergmann, *Staub-Reinhalt. Luft*, 42 (1982) 176–182.
8 *Staubbericht 1987 für Berlin (West)*, Berliner Institut für Analytik und Umweltforschung, Berlin, 1988.
9 *Technisches Bericht D-89/185; Messungen der Luftqualität in Berlin (West) 1988*, Technischer Überwachungsverein, Berlin, 1989.
10 J. Iburg, U. Fritsche and H. Marfels, *Forschungsbericht der PEF Ausgewählte anorganisch-chemische Komponenten in Luftstäuben Baden-Württembergs*, Schmallenberg, 1990.
11 H. W. Georgii, C. Perseke and E. Rohbock, *Forschungsprojekt 10402600 des Umweltbundesambt Berlin*, Berlin, 1982.
12 F. Wagner, P. Valenta and H. W. Nürnberg, *Fresenius' Z. Anal. Chem.*, 320 (1985) 470–476.
13 K. Bächmann, K.-H. Blaskowitz, H. Bukatsch, S. Pohl and U. Sprenger, *J. Chromatogr.*, 482 (1989) 307–316.
14 V. D. Nguyen, *J. Chromatogr.*, 482 (1989) 413–421.

Journal of Chromatography, 640 (1993) 251–258
Elsevier Science Publishers B.V., Amsterdam

CHROMSYMP. 2743

Field investigation of major and minor ions along Summit (Central Greenland) ice cores by ion chromatography

M. Legrand*, M. De Angelis and F. Maupetit

Laboratoire de Glaciologie et Géophysique de l'Environnement du CNRS, B.P. 96, 38402 St. Martin d'Hères (France)

ABSTRACT

As a part of the European EUROCORE and GRIP (Greenland Ice Core Project) operations aimed at recovering deep ice cores at Summit (Central Greenland), we have for the first time successfully performed ion chromatography measurements in the field and investigated in detail the soluble impurities, including Na^+, NH_4^+, K^+, Mg^{2+}, Ca^{2+}, F^-, CH_3COO^-, CH_2OHCOO^-, $HCOO^-$, $CH_3SO_3^-$, Cl^-, NO_2^-, SO_4^{2-} and $C_2O_4^{2-}$, trapped in ice deposited over some 200 000 years in Greenland.

INTRODUCTION

Over the last decades, scientific studies have increasingly focused on the chemical composition of the Earth's atmosphere. The major objective of such studies is to understand the preindustrial environmental system and to anticipate its future evolution (chemical composition of the atmosphere and climate) in response to human activities. Owing to the lack of data for the past, most of these studies are limited to our present atmosphere. However, polar ice cores provide precipitation samples in which the atmospheric chemical composition at the time of deposition is recorded, offering a unique possibility of reconstructing the chemical composition of the atmosphere back to the preindustrial time period.

Among a wide variety of chemical species trapped in snow layers (insoluble particles, trace metals and ionic species), the ionic species appear to be the most useful in tracing major natural and anthropogenic sources of impurities which lead to the final composition of our atmosphere [1–6]. Such studies of the composition of soluble species trapped in snow deposits have clearly opened up an important new scientific field. As discussed by Legrand [7], it is very important in such work to perform a comprehensive study of the soluble species present in the ice in order to check the equilibrium between anions and cations. It is then possible to reconstruct the initial association between the ions and discuss such data in terms of origins and sources. Ion chromatography (IC) is a multispecies technique, as opposed to others such as neutron activation, atomic absorption spectrometry and ionometric and colorimetric methods, and it is well suited to such comprehensive studies of all soluble impurities in ice, except for H^+, which can be measured using an acid titration method such as the one developed by Legrand *et al.* [8].

Nevertheless, such studies have been relatively slow to come into use because of technical difficulties linked with the required low detection limit and with contamination control, both of which are important when working with the low levels of impurities characterizing polar precipitations. Studies were initially dedicated to major anions and cations [9, 10], namely Na^+, NH_4^+, K^+, Ca^{2+}, Mg^{2+}, Cl^-, NO_3^- and SO_4^{2-}, and more recently have been extended to include some minor anions, such as fluoride [11] and some light carboxylates [12,13].

In this paper, we describe an ion chromatography method for determining mineral as well as some or-

* Corresponding author.

0021-9673/93/$06.00

ganic ions (Na^+, NH_4^+, K^+, Ca^{2+}, Mg^{2+}, F^-, CH_3COO^-, CH_2OHCOO^-, $HCOO^-$, $CH_3SO_3^-$, Cl^-, NO_2^-, NO_3^-, SO_4^{2-} and $C_2O_4^{2-}$) that we have successfully applied in the field over the four successive summer seasons, 1989–1992, in Central Greenland as a part of the European EUROCORE and GRIP projects. Excellent sensitivity is achieved for all species, and with a 5-ml sample volume it is possible to measure down to a few tenths of an nanogram per gram. We will discuss numerous advantages provided by such field measurements compared with the tedious sample preparation methods used in laboratories to avoid contamination of the samples.

EXPERIMENTAL

A heated laboratory equipped with two IC set-ups on the Greenland ice cap

At the beginning of the 1989 summer season (EUROCORE operation) at Summit, Central Greenland (72° 34′ N, 37° 38′ W, elevation 3240 m above sea level, mean annual temperature −32.5°C), a shelter was equipped to conduct ion chromatography measurements. The equipment in this heated laboratory included a Milli-Q ultrapure water production unit (Millipore), an uninterruptible power system (416 Leroy-Somer), a class 100 horizontal laminar flow clean hood (Flufrance) and a data capture system (Epson PC AX2) connected to two integrators (4270 Spectra-Physics and Chromjet) and to two Dionex Series (4000i and 4500i) ion chromatographs.

A production of 30–90 l per day of ultrapure water is required to prepare eluents and regenerants, to clean sample containers and to process all equipment that comes into contact with ice samples (see section *Sample preparation*). This ultrapure water is obtained by melting snow collected outside the camp and pumping the meltwater through four Milli-Q cartridges (one Super-C, two Ion-ex and one Organex-Q) and a final filter (0.4 μm).

Owing to rather frequent failures of the main power supply of the camp, we used a battery back-up system (1 kW) to supply the PC and the two ion chromatographs (total consumption of 250 W), allowing us to continue running measurements for almost 45 min in the event of a power problem.

The two chromatographic systems were carefully rinsed with methanol prior to packing and transport to Greenland.

All chromatographic columns were handled with care in the field by workers, taking special precautions to avoid damage by the low temperature. In spite of this, during the first operation (1989), the cation micromembrane suppressor (CMMS) was damaged before arriving at Summit and the tetrabutylammonium hydroxide (TBAOH) solution (40%) used to prepare the regenerant for cation measurements reached Greenland completely frozen.

During the winters of 1989–1990, 1990–1991 and 1991–1992 the laminar flow hood, the battery back-up system and the Millipore system stayed in Greenland and survived in spite of very low temperatures (−65°C). Other equipment (ion chromatographs, PC and chromatographic columns) was sent back to France at the end of each summer.

Sample preparation

The outer part of firn and ice cores extracted from ice caps were generally significantly contaminated during the drilling procedure. When the entire core was available, the outer part of the core was removed using an ice core lathe designed in our Grenoble laboratory (Fig. 1). The efficiency of such a procedure was tested with an ice core section from a depth of 159 m at Dome C (Antarctica), on which successive shaving fractions were recovered and measured (Fig. 2). The results clearly show that there was very significant superficial contamination of the ice, except for $CH_3SO_3^-$. Then concentrations decrease rapidly from the outside to the inside of the ice core, the inner part exhibiting a plateau corresponding to the part of the core that is free of contamination. Fig. 2 also suggests that the contamination remains restricted mainly to the first outer centimetre of the core. Such a procedure was used along the upper 70 m of the Eurocore core for which the entire core was available.

Along the GRIP core, numerous experiments have been carried out by various workers, and only small lamella (2.5 × 3.5 cm section) were available to perform our study of soluble species. The use of the lathe was therefore not possible. However, considering the limited penetration of the contamination inside a piece of ice (Fig . 2), we proceeded in the field with mechanical decontamination by shav-

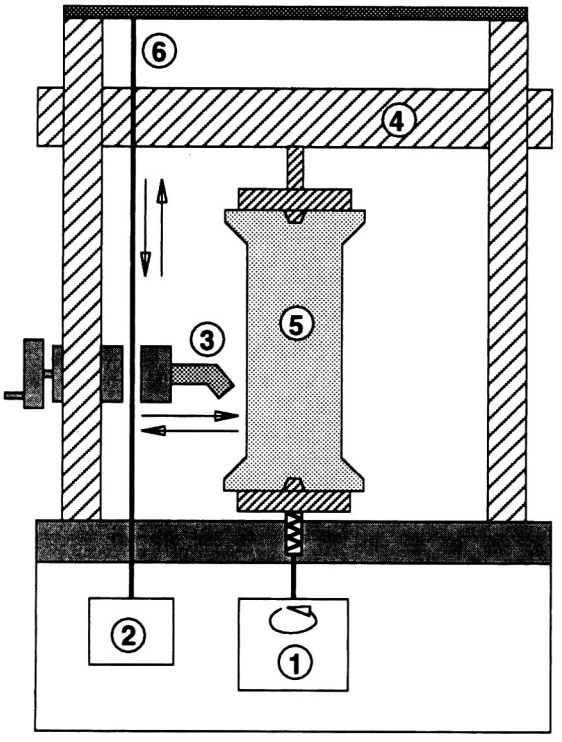

Fig. 1. Ice core lathe equipped with a stainless-steel knife (3) used to remove the outer part of ice core sections. 1 = Motor; 2 = reducer; 4 = mobile plateau; 5 = ice core section; 6 = threaded rod.

ing off approximately 50% of the ice lamella with scalpels previously rinsed with ultrapure water. Such a procedure performed in the field presents two major advantages. First, performed immediately after core recovery, such a procedure does not require ice sections to be stored in sealed plastic bags, a process that leads to organic acid contamination [11]. Second, such field work prevents us from breaking these small and fragile pieces of ice during the transport.

Because the species we are concerned with may be present in the atmosphere of the heated laboratory as aerosols or in the gas phase, special precautions have to be taken during the melting step. A clean air hood prevents our samples from contamination by aerosols but not from contamination by trace gases such as nitric acid or ammonia and some volatile organic acids.

To investigate this problem, several vials filled with 10 ml of ultrapure water were left open over increasing time periods within a clean air bench located in our Grenoble laboratory. As reported in Table I, rapid contamination occurs for NH_4^+, $HCOO^-$ and CH_3COO^-, as previously pointed out by Legrand *et al.* [9] and Saigne *et al.* [11], corresponding to the dissolution of ammonia and carboxylic acid traces present in the atmosphere:

$$NH_3 + H_2O \rightleftharpoons NH_4^+ + OH^-$$

$$HCOOH + H_2O \rightleftharpoons HCOO^- + H_3O^+$$

$$CH_3COOH + H_2O \rightleftharpoons CH_3COO^- + H_3O^+$$

TABLE I

CONCENTRATIONS OF VARIOUS IONS IN VIALS FILLED WITH 10 ml OF ULTRAPURE WATER AND LEFT OPEN OVER INCREASING TIME PERIODS WITHIN A CLEAN AIR HOOD IN OUR GRENOBLE LABORATORY

Species	Concentration after 90 min (ng g^{-1})	Mean rate (ng g^{-1} h^{-1}) of contamination over 8 h
NH_4^+	12	9
$HCOO^-$	7	5
CH_3COO^-	22	18
NO_2^-	2	2.5

Furthermore, the observation of NO_2^- contamination (Table I) is probably due to the presence of nitric acid in the atmosphere of our laboratory following:

$$HNO_2 + H_2O \rightleftharpoons NO_2^- + H_3O^+$$

To prevent our samples from such rapid contamination during the melting step, we put the decontaminated pieces of ice in air-tight bottles kept frozen until the analyses.

Ion chromatography

For the anion chromatographic system, we used AS5A and Pax-500 separator columns with AG5 and CG10 guard columns, respectively. Two anion trap columns (ATC1) were placed in series before the injection valve. A Dionex anion micromembrane suppressor (AMMS1 and later on AMMS2)

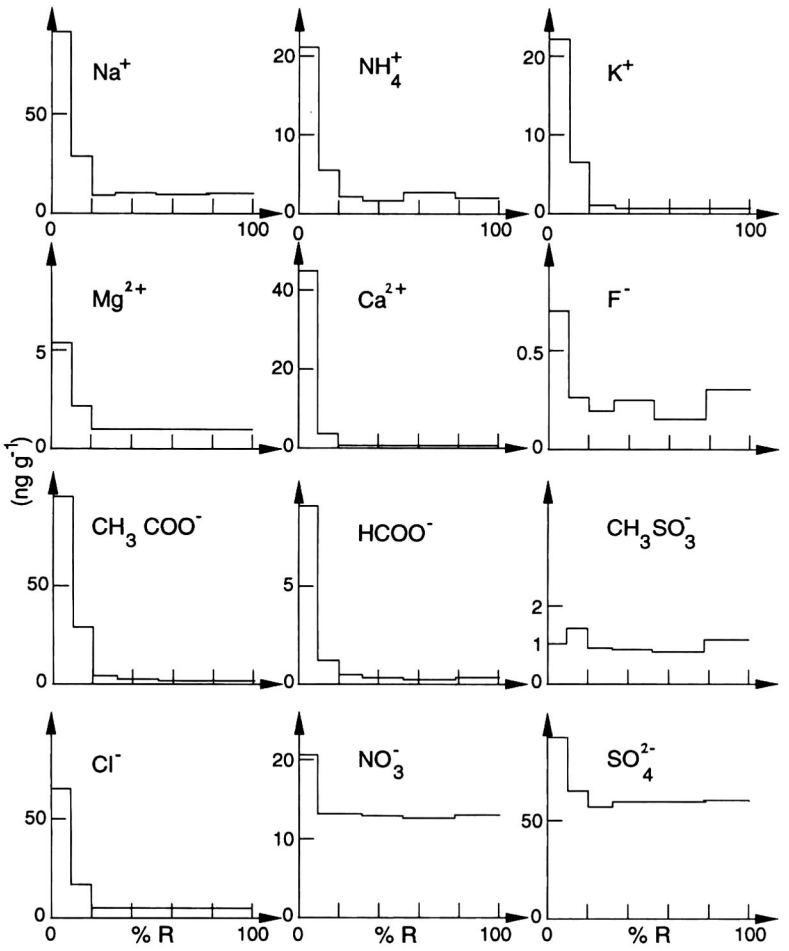

Fig. 2. Decontamination of a piece of ice from a depth of 159 m at Dome C (Antarctica) using the lathe. Concentrations (in ng g^{-1}) are given as a function of the shaved fraction of the ice core section (percentage of the initial radius, R).

TABLE II

WORKING GRADIENT CONDITIONS USED FOR ANION DETERMINATIONS WITH THE AS5 SEPARATOR COLUMN

Time (min)	Eluent 1, 200 m*M* sodium hydroxide (%)	Eluent 2, water (%)	Eluent 3, 1 m*M* sodium hydroxide (%)	Injection valve	Flow-rate (ml/min)	Eluent (m*M* sodium hydroxide)
0.1	0	50	50	Inject	1.8	0.5
2.5	0	50	50	Inject	1.8	0.5
11.5	15	35	50	Inject	1.8	30.5
12.0	15	35	50	Inject	1.8	30.5
12.2	0	50	50	Inject	1.8	0.5
14.2	0	50	50	Load	1.8	0.5

TABLE III

WORKING GRADIENT CONDITIONS USED FOR ANION DETERMINATIONS WITH THE PAX-500 SEPARATOR COLUMN

Time (min)	Eluent 1, 200 m*M* sodium hydroxide (%)	Eluent 2, water (%)	Eluent 3, 4 m*M* sodium hydroxide (5% methanol) (%)	Injection valve	Flow-rate (ml/min)	Eluent (m*M* sodium hydroxide) (1.25% methanol)
0.1	0	75	25	Inject	1.0	1.0
0.5	0	75	25	Inject	1.0	1.0
8.0	14	61	25	Inject	1.0	29.0
14.0	14	61	25	Inject	1.0	29.0
14.1	0	75	25	Inject	1.0	1.0
18.5	0	75	25	Load	1.0	1.0

was used with a mobile phase (0.025 *M* sulfuric acid) at a flow-rate of 1.6 ml/min. A 5-ml sample volume was preconcentrated on an TAC1 column. Using the gradient pump system, the mobile phase is a mixture of three different liquids (water, sodium hydroxide solutions at two different concentrations and methanol continuously degassed by flowing helium; see Tables II and III) at a flow-rate of 1.8 and 1.0 ml/min for the AS5 and Pax-500, respectively. With the AS5 column and using the working gradient conditions reported in Table II, we obtained a background conductivity of approximately 1.8–2.5 μS and 0.8–1.3 μS with the AMMS1 and AMMS2, respectively, for the weak eluent. Using an AMMS2 and the working conditions reported in Table II and Table III, we observed an increase in the background conductivity of 0.3 and 0.5 μS for AS5 and Pax-500, respectively, along the run.

For the cation chromatographic system, we first used Fast Cation I and Cation II to perform two runs, one for monovalent cations, the other for divalent cations. Later on, a CS10 separator column, which allows a separation of mono- and divalent cations in a single isocratic run, was used. Rejecting the use of TBAOH, we first prepared regenerant using a 25% tetramethylammoniumhydroxide (TMAOH) solution, but later on we preferred the use of TMAOH pentahydrate at 97% (Janssen), which provides more stable and lower background conductivity (3–5 μS). The mobile phase was 50 m*M* hydrochloric acid–5.1 m*M* 2,3-diaminopropionic acid monohydrochloride (DAP), and the regenerant was 70 m*M* tetramethylammonium hydroxide (TMAOH), with flow-rates of 1.0 and 4–5 ml/min, respectively. The background conductivity of the cation system ranges between 3 and 4.5 μS with a new CMMS but then increases slowly. We found that this increase in the background conductivity with time was highly dependent on the quality of the TMAOH.

RESULTS AND DISCUSSION

The ion chromatographic procedures were calibrated with artificial samples of various concentrations using a pipette to dilute the required volume of the parent solutions in ultrapure water. Parent solutions were prepared by dilution of individual standard solutions at 1000 mg l^{-1} with concentration ratios chosen to be similar to those in Greenland ice. Because of the observed decrease (up to 50% after 2 weeks) in the formic and acetic contents in these parent solutions with time (probably due to biological activity), it was necessary to make new parent solutions for anions at regular intervals (once a week). The different standard solutions used for calibration were prepared just a few min before they were needed.

Calculated regression lines, estimated errors, correlation coefficients and detection limits are given in Table IV and Table V. Significant (twice the detection limit) positive *y*-intercepts are observed for CH_3COO^- (*ca.* 1 ng g^{-1}) and NH_4^+ (*ca.* 1 ng g^{-1}). Such blank values probably reflect weak contam-

TABLE IV

CALIBRATION PARAMETERS FOR ANION (USING AN AS5 SEPARATOR COLUMN) AND CATION DETERMINATIONS

c represents the concentration (in ng g^{-1}) and S the peak area expressed in relative units. DL denotes the detection limit defined as the amount of solute producing a signal to noise ratio of 5. r is the correlation coefficient.

	F^-	CH_3COO^-	CH_2OHCOO^-	HCOO	$CH_3SO_3^-$
Range	0.1–1.8	1.2–22.5	0.25–4.5	1.0–16.0	0.5–9.0
Regression line	$S = -0.03 + 2.76c$	$S = 0.42 + 0.35c$	$S = -0.03 + 0.4c$[a]	$S = 0.26 + 0.958c$	$S = 0.03 + 0.565c$
Error	± 0.03	± 0.5[a]	See text	± 0.15	± 0.1
r	0.9997	0.9988	0.9955	0.9998	0.9997
DL	0.05	0.6	0.25	0.2	0.25
	Cl^-	NO_2^-	NO_3^-	SO_4^{2-}	$C_2O_4^{2-}$
Range	2.5–45.0	0.5–9.0	7.5–135.0	10–180	0.5–4.5
Regression line	$S = 0.003+0.135c$	$S = -0.02+0.113c$	$S = -0.01+0.082c$	$S = -0.26+0.108c$	$S = -0.02+0.1c$[a]
Error	± 0.3	± 0.2	± 1.0	± 3.0	see text
r	0.9999	0.9997	0.9999	0.9998	0.998
DL	0.5	0.5	1.5	1.5	0.5
	Na^+	NH_4^+	K^+	Mg^{2+}	Ca^{2+}
Range	0.5–40	0.5–40	0.125–10	0.25–20	0.5–40
Regression line	$S = 0.03+0.282c$	$S = 0.22+0.198c$	$S = -0.03+0.221c$	$S = -0.1+0.538c$	$S = -0.1 + 0.34c$
Error	± 0.6	± 0.6	± 0.4	± 0.3	± 0.8
r	0.9997	0.993	0.998	0.9996	0.9995
DL	0.2	0.3	0.25	0.2	0.5

[a] See text.

ination during the preparation of the standard solutions in relation to the above-mentioned rapid contamination by trace gases present in the atmosphere of the laboratory, especially for NH_4^+ and CH_3COO^- (Table I).

In two cases we calculated a negative y-intercept, one for SO_4^{2-} when using an AS5 column (Table IV), the other for NO_3^- when using a Pax-500 column (Table V). Such negative blank values (2.5 and 3 ng g^{-1} for SO_4^{2-} and NO_3^-, respectively) appear when the peak (sulphate with AS5 and nitrate with Pax-500) overlaps the wide hydrogencarbonate peak (Fig. 3) that corresponds to the carbon dioxide dissolution in our sample. Areas calculated using a linear baseline on the tail of the bicarbonate peak are slightly underestimated, leading to errors for nitrate and sulphate when present at low levels.

Determinations of CH_2OHCOO^- and $C_2O_4^{2-}$ using an AS5 column can lead to major errors because of a large overlapping of their peaks with acetate and sulphate peaks respectively (see Fig. 3a). Indeed, depending on the ratios CH_3COO^-/CH_2OHCOO^- and $SO_4^{2-}/C_2O_4^{2-}$, the peak areas have to be calculated in different ways (baseline at valley or resolved rider peak on the tail of the preceding peak). More accurate determinations of these two organic acids were obtained using a Pax-500 separator column, even using a minimal amount of methanol (1.25%), which significantly increases the separation between these species and acetate and sulphate species.

For all species, excellent sensitivity was achieved with detection limits sometimes one order of magnitude lower than the mean content of Greenland precipitation (see Table VI).

The IC method described has been used for investigation in various glaciochemical studies. Among the results, the discovery of the important

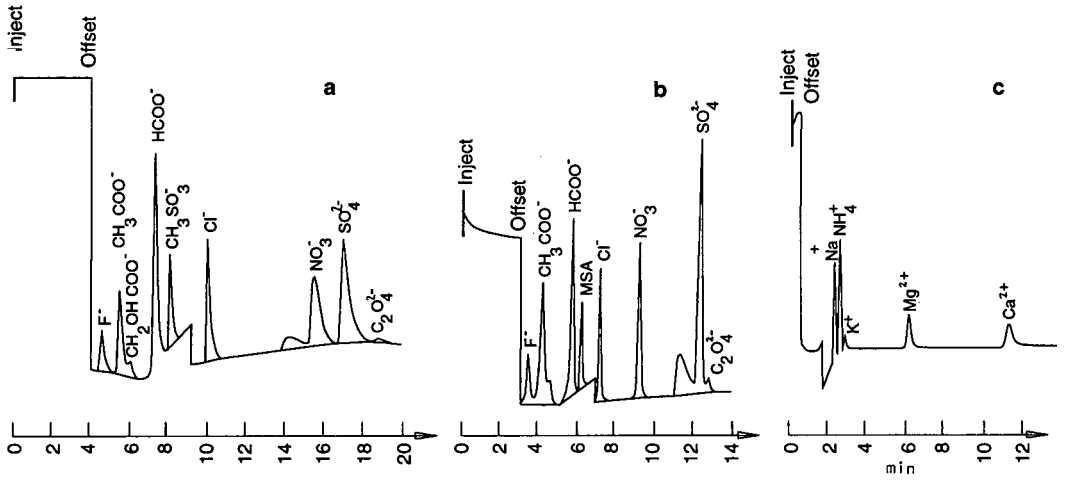

Fig. 3. (a) Anion Pax-500 chromatogram: F^- (0.4 ng g^{-1}), CH_3COO^- (5 ng g^{-1}), CH_2OHCOO^- (1 ng g^{-1}), $HCOO^-$ (5 ng g^{-1}), $CH_3SO_3^-$ (4 ng g^{-1}), Cl^- (20 ng g^{-1}), NO_3^- (40 ng g^{-1}), SO_4^{2-} (60 ng g^{-1}), $C_2O_4^{2-}$ (4 ng g^{-1}). (b) Anion AS5 chromatogram: F^- (0.8 ng g^{-1}), CH_3COO^- (10 ng g^{-1}), CH_2OHCOO^- (2 ng g^{-1}), $HCOO^-$ (6 ng g^{-1}), $CH_3SO_3^-$ (4 ng g^{-1}), Cl^- (20 ng g^{-1}), NO_3^- (60 ng g^{-1}), SO_4^{2-} (80 ng g^{-1}), $C_2O_4^{2-}$ (2 ng g^{-1}). (c) Cation CS10 chromatogram: Na^+ (4 ng g^{-1}), NH_4^+ (4 ng g^{-1}), K^+ (1 ng g^{-1}), Mg^{2+} (2 ng g^{-1}), Ca^{2+} (4 ng g^{-1}). The sample volume was 5 ml. The detector sensitivity was 3 μS at the beginning of the run and 30 μS later on (change between the $CH_3SO_3^-$ and the Cl^- peaks) for anions (a and b), and is unchanged (c) for cations (10 μS).

role played by organic acids in the chemical composition of the past atmosphere has been discussed by Legrand *et al.* [6]. This study of organic species, which are particularly sensitive to severe contamination, has shown the great advantage of performing IC measurements in the field.

TABLE V

CALIBRATION PARAMETERS FOR ANION DETERMINATIONS USING A PAX-500 SEPARATOR COLUMN

	F^-	CH_3COO^-	CH_2OHCOO^-	$HCOO^-$	$CH_3SO_3^-$
Range	0.1–1.8	1.2–22.5	0.25–4.5	1.0–18.0	0.5–9.0
Regression line	$S = 0.03 + 4.77c$	$S = 0.59 + 0.543c$	$S = -0.03 + 1.071c$	$S = -1.1 + 1.9c$	$S = 0.01 + 0.9995c$
Error	± 0.02	± 0.5	± 0.2	± 0.3	± 0.2
r	0.9998	0.998	0.998	0.993	0.9995
DL	0.02	0.6	0.2	0.2	0.25
	Cl^-	NO_2^-	NO_3^-	SO_4^{2-}	$C_2O_4^{2-}$
Range	2.5–45.0	0.5–9.0	7.5–135.0	10–180	0.5–4.5
Regression line	$S = -0.05 + 0.267c$	$S = -0.004 + 0.157c$	$S = -0.44 + 0.145c$	$S = -0.27 + 0.201c$	$S = -0.025 + 0.146c$
Error	± 0.3	± 0.25	± 2	± 0.2	± 0.15
r	0.9998	0.998	0.9996	0.9998	0.997
DL	0.5	0.5	1.5	1.5	0.5

TABLE VI

MEAN IONIC COMPOSITION OF GREENLAND PRECIPITATION OBSERVED BY LEGRAND *et al.* [9]

Values followed by asterisks denote large disturbances of the background level of NH_4^+ and of some organic species in relation to inputs from forest fires, as discussed in ref. 9.

	Ionic composition (ng g^{-1})				
	F^-	CH_3COO^-	CH_2OHCOO^-	$HCOO^-$	$CH_3SO_3^-$
Range	0.05–0.3	10–35*	0.5–15*	10–1000*	0.5–5.0
Mean	0.15	13	1	12	3
	Cl^-	NO_3^-	SO_4^{2-}	$C_2O_4^{2-}$	Na^+
Range	2–30	25–100	10–40	0.5–20.0*	1–20
Mean	15	80	30	1	8
	NH_4^+	K^+	Mg^{2+}	Ca^{2+}	
Range	3–400*	0.5–3	0.5–4.0	0.5–10	
Mean	5	1.0	2.0	8	

ACKNOWLEDGMENTS

We thank M. Ricard, who designed the ice core lathe used for subsampling. We thank C. Rado for his assistance in equipping the shelter. The field work was supported by the ESF associate programme (EUROCORE and GRIP). The laboratory work was supported by the CNRS (Programme "Atmosphere Polaire" du Pirenvironnement).

REFERENCES

1 M. Legrand, C. Lorius, N. I. Barkov and V. N. Petrov, *Atmos. Environ.*, 22 (1988) 317.
2 P. Mayewski, W. B. Lyons, M. J. Spencer, M. S. Twickler, C. F. Buck and S. Whitlow, *Nature*, 346 (1990) 554.
3 M. Legrand and R. Delmas, *Nature*, 328 (1987) 671.
4 M. Legrand, C. Feniet-Saigne, E. S. Saltzman, C. Germain, N. I. Barkov and V. N. Petrov, *Nature*, 350 (1991) 144.
5 P. Mayewski and M. Legrand, *Nature*, 346 (1990) 258.
6 M. Legrand, M. De Angelis, T. Staffelbach, A. Neftel and B. Stauffer, *Geophys. Res. Lett.*, 19 (1992) 473.
7 M. Legrand, *J. Phys.*, 48 (1987) 77.
8 M. Legrand, A. Aristarain and R. Delmas, *Anal. Chem.*, 54 (1982) 1336.
9 M. Legrand, M. De Angelis and R. Delmas, *Anal. Chim. Acta*, 156 (1984) 181.
10 C. F. Buck, P. Mayewski, M. J. Spencer, S. Whitlow, M. S. Twickler and D. Barrett, *J. Chromatogr.*, 594 (1992) 225.
11 C. Saigne, S. Kirchner and M. Legrand, *Anal. Chim. Acta*, 203 (1987) 11.
12 M. Legrand and C. Saigne, *Atmos. Environ.*, 22 (1988) 1011.
13 R. Udisti, E. Barbolani and G. Piccardi, *Ann. Chim. Ital.*, 81 (1991) 325.

Journal of Chromatography, 640 (1993) 259–270
Elsevier Science Publishers B.V., Amsterdam

CHROMSYMP. 2657

Ion-exchange high-performance liquid chromatography in the brewing industry

H. Klein*

Quality Assurance and Development, Österreichische Brau AG, Poschacherstrasse 35, A-4020 Linz (Austria)

R. Leubolt

Austrian Beverage Institute, Michaelerstrasse 25, A-1182 Vienna (Austria)

ABSTRACT

Isocratic HPLC methods using an ion-exchange column (Aminex HPX) for the determination of carbohydrates, organic acids, alcohols (methanol, ethanol, glycerol), 5-hydroxymethylfurfural and purines in wort, beer, wine and soft drinks are presented. The strategy for selecting the best column geometry, the appropriate counter ion and specific detection systems is discussed.

INTRODUCTION

Beverages such as beer, wine, fruit juice, carbonated soft drinks and their raw materials are complex mixtures of several natural compounds Table I [1]. Because of their different concentrations, chemical behaviour and molecular mass ranges, the isolation, enrichment and determination of distinct compounds may cause serious problems. Isocratic HPLC methods using ion-exchange materials based on polystyrene–divinylbenzene resins in combination with a suitable eluent and specific detection may overcome these problems.

This paper reports a strategy for selecting the best separation system for particular analytical problems in the food and beverage industry. One major advantage of ion-exchange resins is that normally no organic modifier such as methanol or acetonitrile need be used, only pure water or dilute salt solutions being required. Another advantage is that large molecules such as proteins or polysaccharides are excluded from the pores and elute with the void volume. Therefore, a minimum of sample preparation (filtration and dilution) is needed before analysing a sample.

TABLE I

NATURAL COMPOUNDS IN BEVERAGES

Proteins	Carbohydrates (mono-, di-, tri-, oligo- and polysaccharides, sugar alcohols)
Peptides	Glycerol
Amino acids	Polyphenols
Organic acids	Diols
Alcohols	Aldehydes
Phenolic acids	Ketones
Vitamins	Bitter substances
Preservatives	Antioxidants

EXPERIMENTAL AND RESULTS

Reagents

Water for the preparation of the mobile phase must be distilled freshly and degassed with helium. Sulphuric acid, potassium sulphate and ammonium sulphate were of analytical-reagent grade from

* Corresponding author.

0021-9673/93/$06.00

Merck (Darmstadt, Germany). Calcium oxides have been prepared in the laboratory. All reference standard solutions were prepared from analytical-reagent grade chemicals (Sigma, Deisenhofen, and Aldrich, Steinheim, Germany).

Instrumentation

System A. This system consisted of Model 1350 HPLC pump (Bio-Rad Labs., Richmond, CA, USA), and SPD-2AS UV spectrophotometric detector (Shimadzu, Kyoto, Japan), a CTO-2AS column oven unit (Shimadzu), a Model 1755 refractive index (RI) detector (Bio-Rad Labs., and a Model 7125 sample injection valve (Rheodyne, Cotati, CA, USA).

System B. This system consisted of a Model 64.00 HPLC pump (Knauer, Berlin, Germany), a Model 89.00 column oven unit (Knauer), a Model 87.00 UV spectrophotometric (Knauer), a Chromascope high-speed scanning UV detector (Barspec, Rehovot, Israel); a Model 98.00 RI detector (Knauer) and a Model 7110 sample injection valve (Rheodyne).

Resin-based ion-exchange columns

The following columns were obtained from Bio-Rad Labs.: Aminex HPX 42A (300 × 7.8 mm I.D.) with de-ashing system; Aminex HPX 87H (300 × 7.8 mm I.D.); "Fast-Acid" (100 × 7.9 mm I.D.); Aminex HPX 87C (300 × 7.8 mm I.D.); Aminex HPX 87K (300 × 7.8 mm I.D.); Aminex HPX 72S (300 × 7.8 mm I.D.); Cation H (30 × 4.6 mm I.D.) and Carbo C (30 × 4.6 mm I.D.). All column materials were packed in stainless-steel tubes and refilling by Bio-Rad Labs. was not possible.

The following columns were obtained from Inovex (Vienna, Austria): Inores S259H (250 × 7.5 mm I.D.); Inores S259C (250 × 7.5 mm I.D.) and Ino-Pre (25 × 4.6 mm I.D.). These materials were introduced in 1992. They are comparable to Aminex and gives similar separation patterns. All column materials were packed in PEEK tubes and can be refilled by Inovex.

Strategy for column selection

Resin-based ion-exchange materials offer several possibilities for the selection of suitable separation systems [2]: (a) cation (for neutral or acidic compounds) or anion exchanger (for basic compounds); (b) column geometry (length); short columns for compounds with long retention times (*e.g.*, phenolic acids, aldehydes) or for high-speed separations with specific detection systems (*e.g.*, total sulphite in beer or wine); (c) cross-linkage; separation of oligosaccharides (4%, 6% or 8% divinylbenzene); lower cross-linkage gives greater interstitial pores for separating oligosaccharides up to a degree of polymerization (DP) of 11; (d) counter ion; H^+, Ca^{2+}, K^+, Ag^+, OH^- or SO_4^{2-}; these ions effect the separation of mono- and disaccharides and of sugar alcohols; (e) eluent strength (pH); strong effect on organic acids, but no effect on sugars, diols or alcohols; (f) column temperature; higher temperatures give better separations and resolutions (normally 65–85°C); (g) specific detection; RI for carbohydrates, sugar alcohols, alcohols, diols and glycerol, UV for organic acids, aldehydes and ketones and electrochemical detection for phenols, vitamins and sulphite; (h) sample preparation; for co-eluting compounds with similar detector response; a powerful tool for the extraction of anionic compounds (organic acids) is to use solid-phase extraction (SPE) with quaternary amines.

Determination of carbohydrates in wort, beer, fruit juice and carbonated beverages

The only sample preparation necessary for all of the following examples is degassing, dilution and filtration of the samples.

Matrix wort. Mono-, di-, tri- and oligosaccharides appear along with bitter substances, proteins and phenolic compounds. For controlling the degradation of the polysaccharides during the mash procedure, the best separation is achieved by isocratic HPLC with RI detection using the Aminex HPX 42A column and de-ashing system. The guard column removes both anions and cations. Chloride and sulphate have to be removed before analysis because they give a precipitate with silver counter ions of the column and this may clog the analytical column [3–6]. This system separates carbohydrates up to DP 11 and monosaccharides. No interference from other compounds can be seen. Proteins are eluted with the void volume and the other constituents are not detected by the RI detector.

The HPLC conditions are as follows: column Aminex HPX 42A (300 × 7.8 mm I.D.) with de-ashing system; eluent, doubly distilled water; flow-

rate, 0.5 ml/min; temperature, ambient; detector, RI.

For the determination of fermentable sugars in pitching wort, another separation system is used because only maltotriose, maltose, glucose and fructose can be fermented by brewers yeast. In this system determination up to DP 11 is not necessary. It is possible to decrease the analysing time by using the Aminex HPX 87H or the Inores S259H column. Maltooligosaccharides up to DP 4 and monosaccharides are separated by using dilute sulphuric acid. Chloride or sulphate do not cause problems in this system. Nevertheless, appropriate guard columns should be used to protect analytical columns against contamination.

The HPLC conditions are as follows: column, Aminex HPX 87H (300 × 7.8 mm I.D.) or Inores S259H (250 × 7.5 mm I.D.); guard column, Cation H or Ino-Pre (25 × 4.6 mm I.D.); eluent, 0.005 *M* sulphuric acid; flow-rate, 0.6 ml/min; temperature, 65°C; detector, RI.

This method is accepted by the European Brewery Convention (EBC) for the determination of fermentable sugars in wort [7]. The flow-rate described in the *EBC-Analytica* [7] is set to 0.2 ml/min and the separation therefore takes about 40 min. This very low flow-rate is not necessary because 0.6 ml/min gives a similar resolution and shorter analysis times (< 10 min).

Matrix beer. Beer contains mono-, di- and trisaccharides in addition to bitter substances, organic acids, proteins, fermentation by-products (glycerol, sulphite, alcohols and phenolic compounds). Using the Aminex HPX 87H or the Inores S259H column with RI detection, carbohydrates, glycerol and ethanol can be determined simultaneously [8,9]. Fig. 1 shows an alternative method for the determination of ethanol in alcohol-free beer. Sample preparation includes degassing and dilution (1:10 with the eluent).

The HPLC conditions are as follows: column, Aminex HPX 87H (300 × 7.8 mm I.D.) or Inores S259H (250 × 7.5 mm I.D.); guard column, Cation H or Ino-Pre (25 × 4.6 mm I.D.); eluent, 0.005 *M* sulphuric acid; flow-rate, 0.6 ml/min; temperature, 65°C; detector, RI.

Matrix fruit juice and concentrates. This matrix consists of glucose, fructose and sugar alcohols (*e.g.*, sorbitol) in addition to organic acids. The resin is in the H^+ form and does not separate fructose from sorbitol. Therefore, a column with another counter ion (Ca^{2+}) must be used. Generally the res-

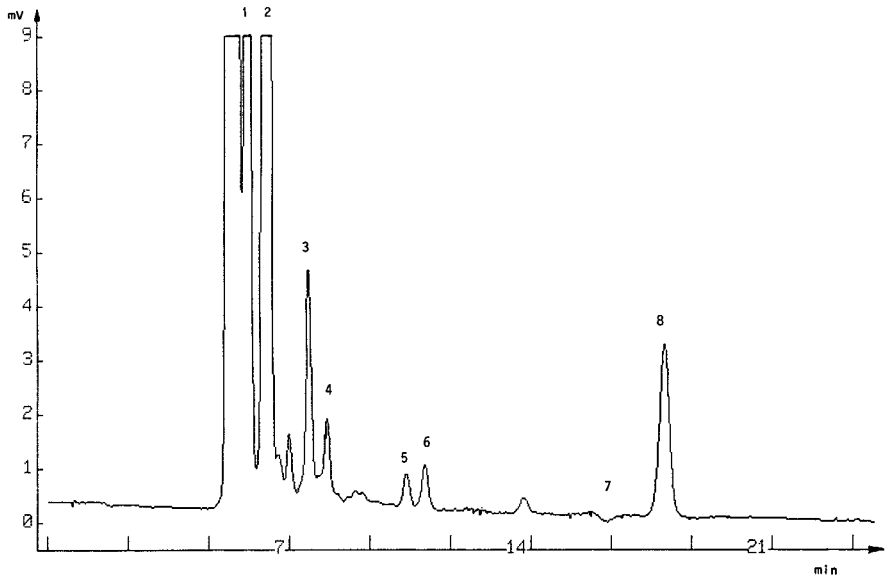

Fig. 1. Determination of ethanol in non-alcoholic beer. Chromatographic conditions as described in text. Peaks: 1 = maltotriose; 2 = maltose + sucrose; 3 = glucose; 4 = fructose; 5 = lactic acid; 6 = glycerol; 7 = carbonate (negative); 8 = ethanol.

in in the Ca^{2+} form separates the sugar alcohols from mono- and disaccharides [9].

The HPLC conditions are as follows: column, Aminex HPX 87C (300 × 7.8 mm I.D.) or Inores S259C (250 × 7.5 mm I.D.); guard column, Cation H or Ino-Pre (25 × 4.6 mm I.D.); eluent, 0.02% Ca azides; flow-rate, 0.6 ml/min; temperature, 85°C; detector, RI.

Sugars in carbonated beverages. Carbonated beverages consist mainly of sucrose (up to 100 g/l), glucose, fructose and organic acids (mainly citric acid). For separating these four compounds, two different columns can be used, either the H^+ or the Ca^{2+} form. Both columns have a similar retention behaviour for sugars. The important difference between this methods is the column temperature. Using the Aminex HPX 87H or the Inores 259H column, the analysis must be done at room temperature because sucrose inverts quickly to glucose and fructose under acidic solutions at higher temperatures. This problem does not occur when using the Ca^{2+} form because the eluent is pure water. High temperatures (up to 85°C) can be applied.

The HPLC conditions are as follows: (I) column, Aminex HPX 87H (300 × 7.8 mm I.D.) or Inores S259H (250 × 7.5 mm I.D.); guard column, Cation H or Ino-Pre (25 × 4.6 mm I.D.); eluent, 0.005 *M* sulphuric acid; flow-rate,0.6 ml/min; temperature, ambient; detector, RI; and (II) column, Aminex HPX 87C (300 × 7.8 mm I.D.) or Inores S259C (250 × 7.5 mm I.D.); guard column, Carbo C; eluent, distilled water or 0.02% Ca azides; flow-rate, 0.6 ml/min; temperature, 85°C; detector, RI.

Separation of sucrose and maltose in dark beer. Sometimes malt is partially substituted by sucrose for brewing dark beers. Neither the H^+ nor the Ca^{2+} form of resin can separate carbohydrates of DP 2 (sucrose, maltose). To solve this problem one must use the K^+ form of the Aminex resin (Fig. 2).

The HPLC conditions are as follows: column, Aminex HPX 87K (300 × 7.8 mm I.D.); eluent, 0.005 *M* K_2SO_4; flow-rate 0.6 ml/min; temperature, 85°C; detector, RI.

Table II gives a compilation of methods for the determination of carbohydrates using ion-exchange chromatography.

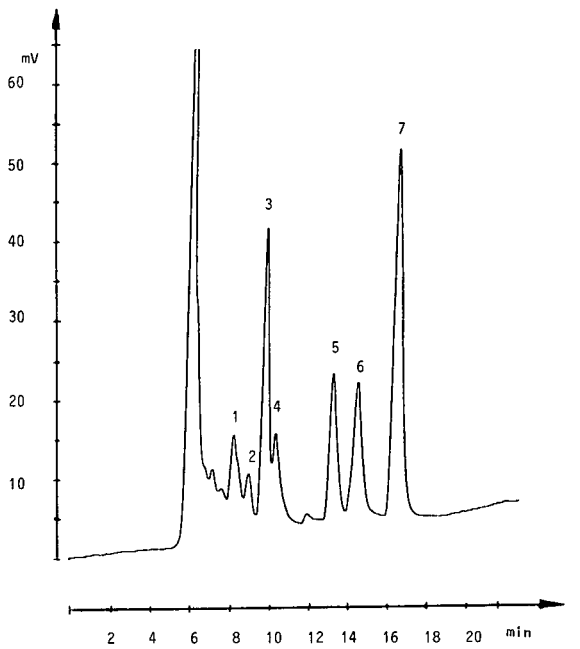

Fig. 2. Separation of maltose and sucrose in dark beer on an Aminex HPX 87K column. Chromatographic conditions as described in text. Peaks: 1 = DP 4; 2 = DP 3; 3 = sucrose; 4 = maltose; 5 = glucose; 6 = fructose + glycerol; 7 = ethanol.

Organic acids

Beer. Organic acids can also be separated by ion-exchange chromatography with UV detection [8,10,11]. It is possible to check the peak purity with a diode-array system. The main problem with UV detection is that not only organic acids are detected, as can be seen in the UV spectra. Phenolic compounds, bitter substances and fructose exhibit a significant response at 210 mm. This problem cannot be solved be changing the columns or chromatographic conditions, and sample clean-up with SPE is necessary (Analytichem SAX; quaternary amine mini-column).

A 10-ml volume of diluted beer sample (1:10 with NaOH, pH 10) was applied to the SPE column. The organic acids were retarded on the strong anion exchanger. The column was washed with 5 ml of NaOH (pH 10), then the organic acids were eluted three times with 1 ml of 1 *M* HCl. The eluates were diluted about 1:20 with eluent (0.005 *M* sulphuric acid). These chromatograms can be seen in Fig. 3a–c. The recovery of the organic acids was 92–97%.

TABLE II

SEPARATION OF CARBOHYDRATES USING DIFFERENT RESIN-BASED CATION-EXCHANGE COLUMNS

Carbohydrates	Aminex HPX column			
	87H	87C	87K	42A
Oligo- and monosaccharides	<DP	<DP5	<DP6	<DP11
Maltose and sucrose	No	No	Yes	No
Fructose and sugar alcohols	No	Yes	No	–
Invert of sucrose at high temperature	Yes	No	No	No
α- and β-glucose	No	Yes	No	No

All co-eluting peaks which are non-organic acids were now present in the primary eluate and in the wash solution, as they passed through the SPE column. Organic acids were in the HCl eluate. The spectra of one specific organic acid peak are shown in Fig. 4.

The retention behaviour of organic acids on this column is sensitive to the eluent concentration and temperature (Tables III and IV). Higher temperatures and lower eluent concentrations give better resolutions of organic acids. For sugar separation, the eluent concentration has no influence on the retention time. One advantage of this type of ion-exchange chromatography for organic acids is the possibility of separating the optical isomers of lactic acid and malic acid (Fig. 5).

The HPLC conditions are as follows: column, Aminex HPX 87H (300 × 7.8 mm I.D.) or Inores S259S (250 × 7.5 mm I.D.); guard column, Cation H or Ino-Res (25 × 4.6 mm I.D.); eluent, 0.005 *M* sulphuric acid; flow-rate, 0.6 ml/min; temperature, 65°C; detector, UV at 210 nm or diode array.

Fruit juice (concentrates). A similar problem occurs in the determination of organic acids in fruit juice. Co-eluting compounds are quinic acid and fructose, which, in contrast to glucose, are also UV-active at 210 nm. Because of the low concentration of quinic acid depending on the other constituents, SPE is not only a cleaning but also a concentration step.

The HPLC conditions are the same as those given above under *Beer*.

Diols and glycerol in wine

Wine contains residual sugars, alcohols, fermentation by-products (glycerol), organic acids, proteins and phenolic compounds. The conditions for the determination of sugars and alcohols are similar to those described for beer [12,13]. The determination of diols by ion-exchange HPLC is not common [11]; they are mostly analysed by GC.

These compounds play an important part in wine adulteration. Well known diols are diethylene glycol, which is added for simulating higher extract, and 1,3-propanediol. The determination of these two substances can be achieved with the H^+ form of the columns. Moreover, acetic acid, methanol and ethanol can be determined in one run (without sample preparation). One example is shown in Fig. 6 (Austrian white wine without diols).

The HPLC conditions are as follows: column, Aminex HPX 87H (300 × 7.8 mm I.D.) or Inores S259H (250 × 7.5 mm I.D.); guard column, Cation H or Ino-Pre (25 × 4.6 mm I.D.); eluent 0.005 *M* sulphuric acid; flow-rate 0.6 ml/min; temperature, 65°C; detector, RI.

With little sample preparation and using ion-exchange SPE, it is possible to determine sugars, diols and alcohols in addition to organic acids [11,14].

Aldehydes in beer: 5-hydroxymethylfurfural (HMF) and furfural

HMF is an indicator for thermal treatment of solutions that contain proteins and carbohydrates. Furfural is an aldehyde which appears during the storage of beer under certain conditions. Therefore, the determination of these two substances is impor-

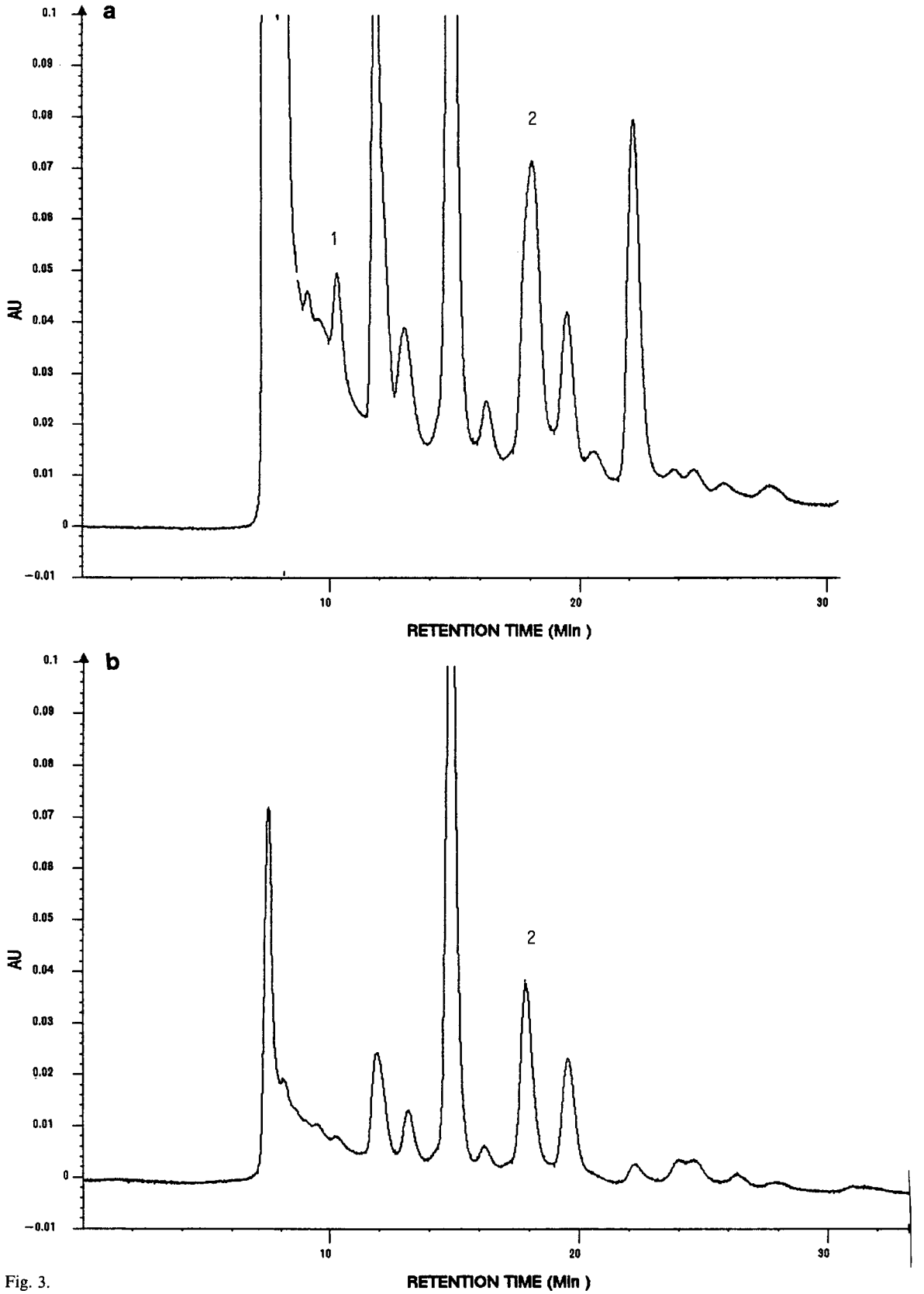
a
b
AU
RETENTION TIME (Min)
1
2
0.1
0.09
0.08
0.07
0.06
0.05
0.04
0.03
0.02
0.01
0
−0.01
10
20
30

Fig. 3.

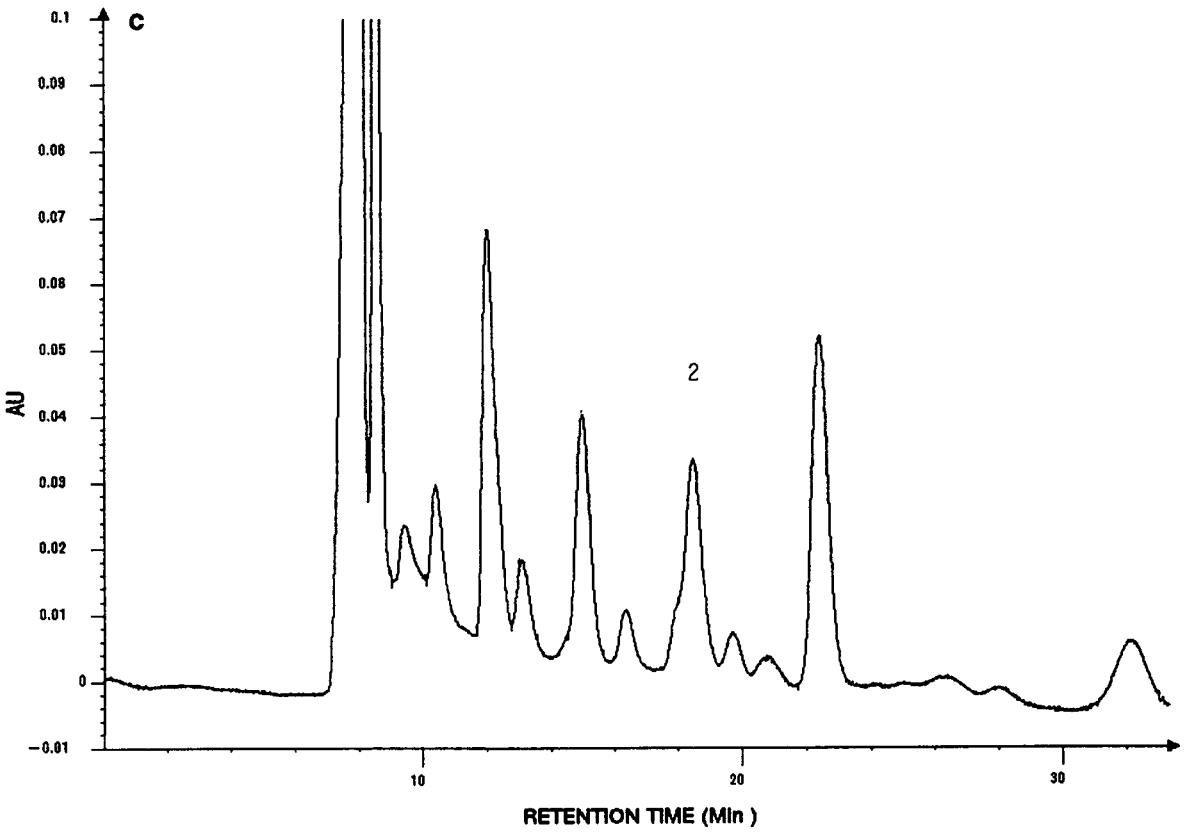

Fig. 3. Chromatograms of (a) beer sample diluted 1:10 with eluent, (b) unretarded compounds and (c) HCl eluate. Chromatographic conditions as described in text.

tant for controlling the storage conditions of bottled beverages [15].

Because of strong interactions between aldehydes and the ion exchangers, it is preferable to use shorter columns for this kind of separation. The analysis takes only about 10 min on the "Fast Acid" column, which is only a third of that with the Aminex HPX 87H column. There are no interferences from other compounds because UV detection is effected at 283 nm. Details of this method can be found elsewhere [16].

The HPLC conditions are as follows: column, "Fast Acid" (100 × 7.8 mm I.D.), with guard column, Cation H; eluent, 0.005 *M* sulphuric acid; flow-rate, 1.2 ml/min; temperature, 65°C; detector, UV (283 nm).

Preservatives and antioxidants

Substances such as ascorbic acid, sulphite, propionic acid, benzoic acid or sorbic acid are often added to beverages. By using different columns and different detection systems it is possible to optimize the analytical parameters for rapid and accurate analysis.

Determination of ascorbic acid and free and total sulphite in beer, wine and soft drinks. Details of these methods are given in the accompanying paper [17].

Determination of preservatives in soft drinks. Because of the very strong interaction of propionic acid, benzoic acid and sorbic acid with the aromatic backbone of the resin, the guard column (Cation H) is used as an analytical column. Only degassing and dilution of the materials to be analysed are neces-

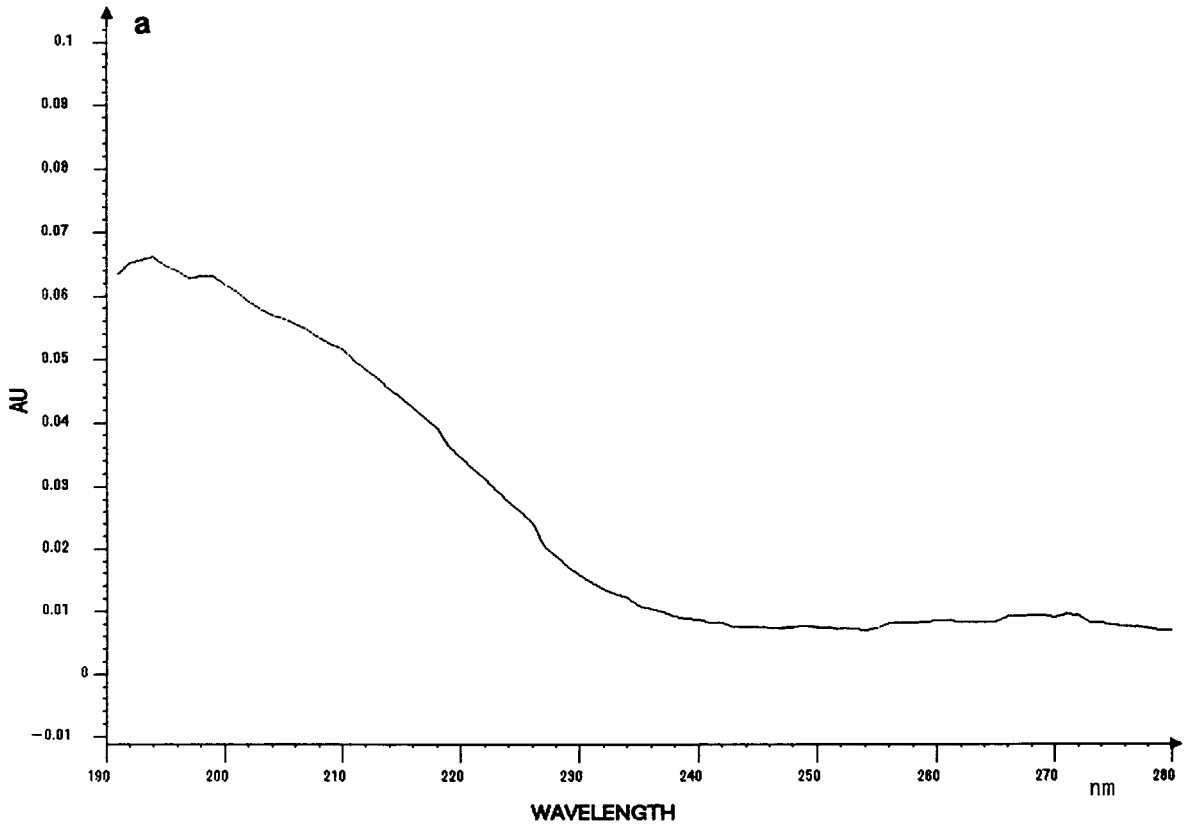
a
AU
0.1
0.09
0.08
0.07
0.06
0.05
0.04
0.03
0.02
0.01
0
−0.01
190
200
210
220
230
240
250
260
270
280
nm
WAVELENGTH

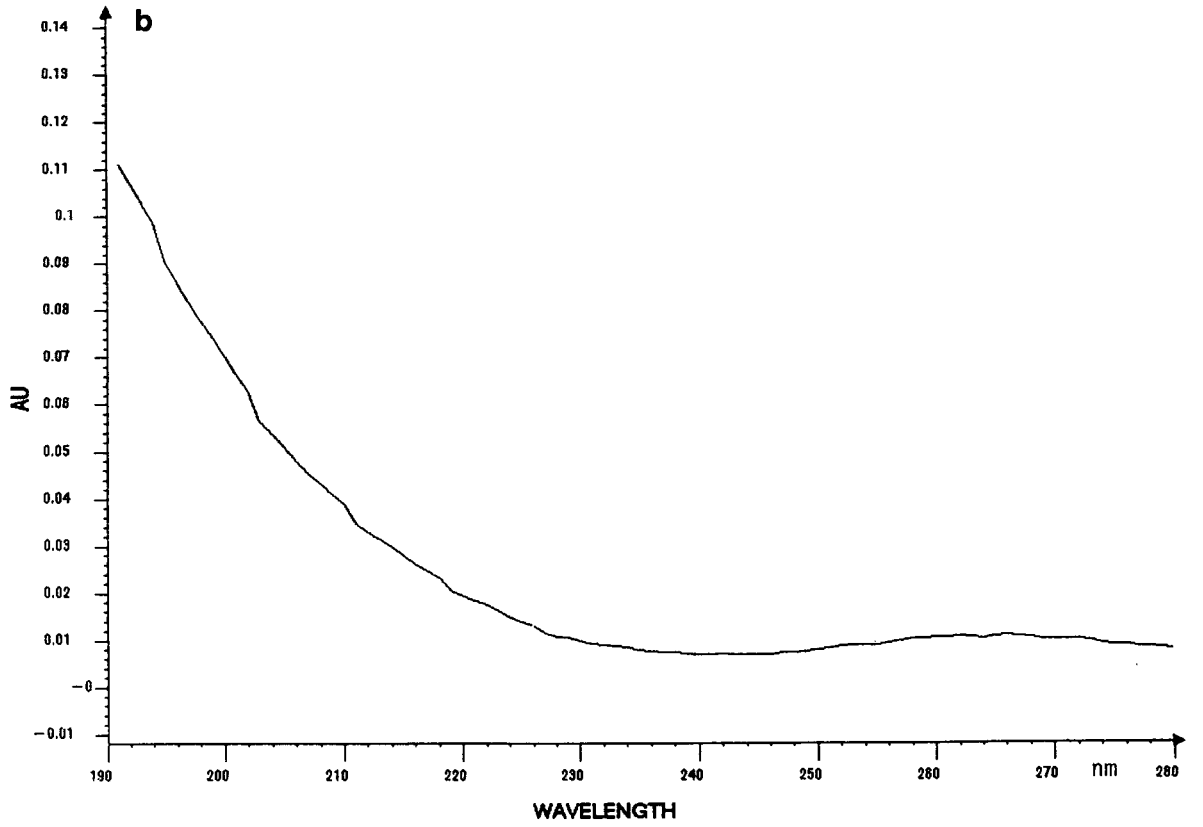
b
AU
0.14
0.13
0.12
0.11
0.1
0.09
0.08
0.07
0.06
0.05
0.04
0.03
0.02
0.01
−0
−0.01
190
200
210
220
230
240
250
260
270
280
nm
WAVELENGTH

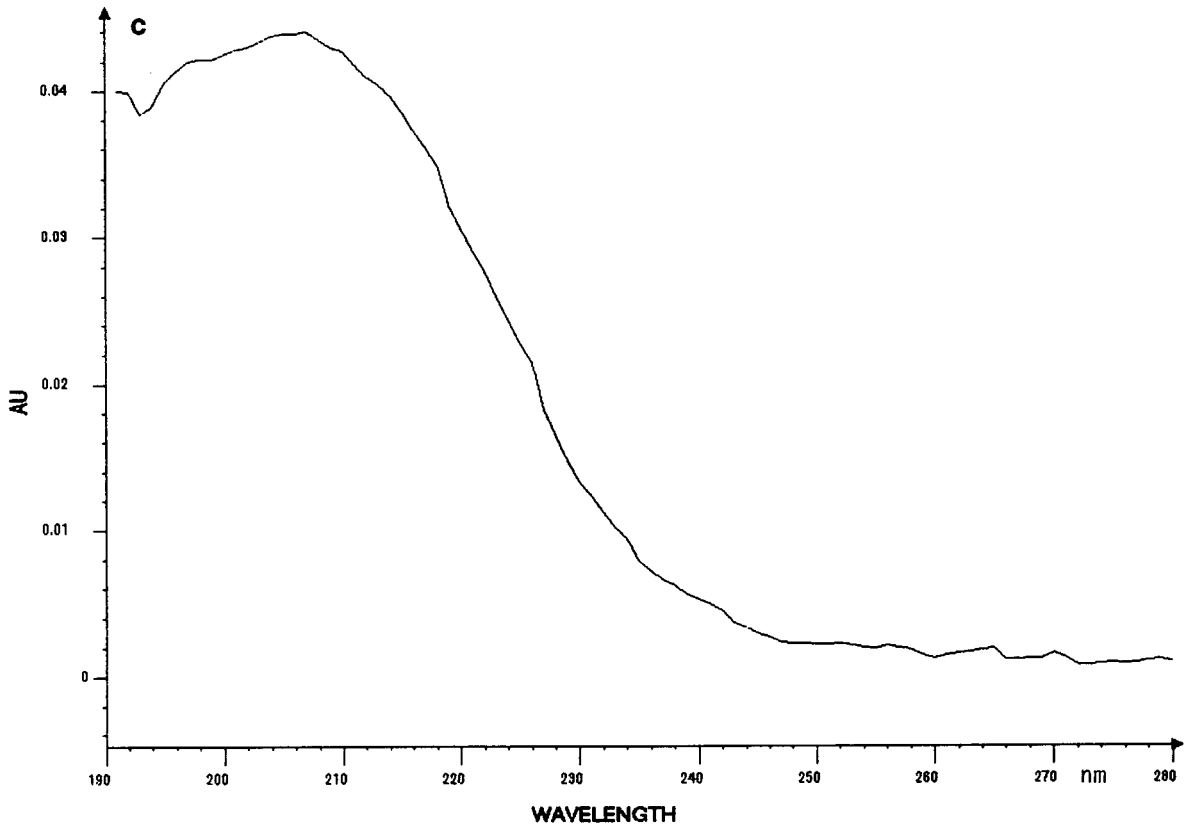

Fig. 4. Spectra from peak 2 in the chromatograms in (a) Fig. 3a, (b) Fig. 3b and (c) Fig. 3c (succinic acid).

sary and the analysis takes about 5 min. The advantage over to reversed-phase HPLC is that no organic modifier (methanol or acetonitrile) need be used.

The HPLC conditions are as follows: column, Cation H (30 × 4.6 mm I.D.) eluent, 0.005 *M* sulphuric acid; flow-rate 0.6 ml/min; temperature, 65°C; detector, UV (240 nm) (benzoic acid, sorbic acid).

For the determination of propionic acid it is better to use the "Fast Acid" column because of the higher retention. With the Cation H column this compound elutes close to the void volume. The best sensitivity is obtained at 210 nm.

Purines in beer

The determination of purines which are fermentation by-products, in beer, causes problems because of their low concentrations and the complex sample matrix. Therefore, clean-up and concentration are necessary [18,19]. The clean-up was done by gel filtration chromatography (Bio-Gel P-2; Bio-Rad Labs.) and three fractions were obtained. These fractions were concentrated by evaporation to dryness under reduced pressure and the residues were dissolved in the eluent. Each fraction was then analysed by ion chromatography.

Purines are basic compounds and can be separated on Aminex-type anion exchangers with UV detection. Table V shows the retention times of these substances.

The HPLC conditions are as follows: Aminex HPX 72S (300 × 7.8 mm I.D.); eluent, 0.13 *M* $(NH_4)_2SO_4$; flow-rate, 1 ml/min; temperature, 65°C; detector, UV (260 nm).

TABLE III

INFLUENCE OF ELUENT CONCENTRATION ON RETENTION BEHAVIOUR OF ORGANIC ACID

Analytical column: Aminex HPX 87H (300 × 7.8 mm I.D.).

Parameter	Conditions		
pH	3.02	2.00	1.24
Temperature (°C)	45	45	45
H_2SO_4 concentration (*M*)	0.0005	0.005	0.05
Acid	Retention time (min)		
Oxalic acid	5.85	6.66	8.44
Citric acid	6.89	7.91	8.21
Isocitric acid	7.24	8.00	8.23
D-Gluconic acid	8.17	9.16	10.88
L-Malic acid	8.50	9.48	9.73
Quinic acid	8.96	9.86	10.12
L-Lactic acid	9.11	11.91	12.77
Glycolic acid	11.26	12.06	12.25
D-Lactic acid	11.71	12.50	12.77
Acetic acid	14.80	14.98	15.15
D-Malic acid	10.76	14.73	15.93
Fumaric acid	10.76	14.73	15.85
Succinic acid	11.40	14.73	15.84
Formic acid	12.51	13.67	13.93

CONCLUSIONS

With consideration of some basic rules, ion chromatography with resin-based materials is a powerful analytical technique in the food and beverage industries: knowledge of the sample matrix; separation behaviour of the different ion-exchange columns (eluent concentration, temperature, flow-rate, counter ion); chemical properties of analyte substances; simultaneously eluted compounds under distinct conditions; chemical reactions during analysis (sucrose); detection systems for specific identification; and sample preparation for special problems. In most instances the sample preparation is reduced to a minimum (degassing, filtration, dilution). Acidic, neutral and basic compounds can be determined in alcoholic or non-alcoholic beverages.

The following applications are possible with resin-based ion-exchange columns: carbohydrates in fermentation broth (wort), beer, wine, fruit juice (appel juice) and soft drinks; diols and glycerol in wine and beer; alcohols in fermentation broth, beer and soft drinks; organic acids in wine, beer and soft drinks; aldehydes (HMF, furfural) in beer, fruit

TABLE IV

INFLUENCE OF TEMPERATURE ON RETENTION BEHAVIOUR OF ORGANIC ACIDS

Analytical column: Aminex HPX 87H (300 × 7.8 mm I.D.).

Parameter	Conditions				
pH	3.02	3.02	3.02	3.02	3.02
Temperature (°C)	25	35	45	55	65
H_2SO_4 concentration (*M*)	0.0005	0.0005	0.0005	0.0005	0.0005
Acid	Retention time (min)				
Oxalic	5.7	5.78	5.85	5.74	5.70
Citric acid	7.01	6.95	6.89	6.82	6.82
Isocitric acid	7.74	7.37	7.24	7.21	7.13
D-Gluconic acid	8.08	8.21	8.17	8.21	8.27
L-Malic acid	8.59	8.64	8.50	8.45	8.36
D-Malic acid	11.55	11.36	10.76	10.52	10.17
Quinic acid	8.99	8.99	8.96	9.12	8.90
L-Lactic acid	8.92	9.20	9.11	9.31	9.34
D-Lactic acid	12.24	11.80	11.71	11.75	11.74
Glycolic acid	11.31	11.40	11.26	11.24	11.19
Acetic acid	14.92	14.99	14.80	14.72	14.61
Fumaric acid	11.56	11.37	10.76	10.53	10.16
Succinic acid	11.70	11.67	11.40	11.21	11.02
Formic acid	12.57	12.70	12.51	12.49	12.42

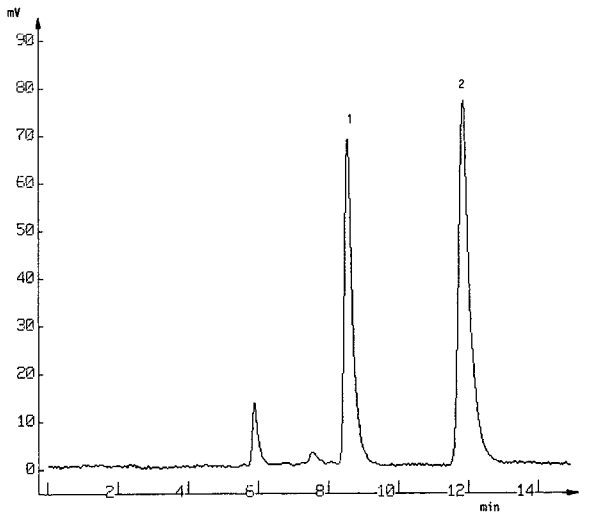

Fig. 5. Separation of optical isomers of malic acid. Chromatographic conditions as described in text. Peaks: 1 = L-malic acid; 2 = D-malic acid.

TABLE V

RETENTION TIMES OF PURINES IN BEER

Fraction	Retention time (min)	Compound
I	11.4	Cytidine
I	13.7	Uridine
I	27.0	Adenosine
I	37.1	Guanosine
II	13.1	Thymidine
II	18.5	Hypoxanthine
II	19.4	Xanthine
III	9.8	Cytosine
III	12.6	Uracil
III	15.9	Thymine
III	35.7	Adenine + guanine

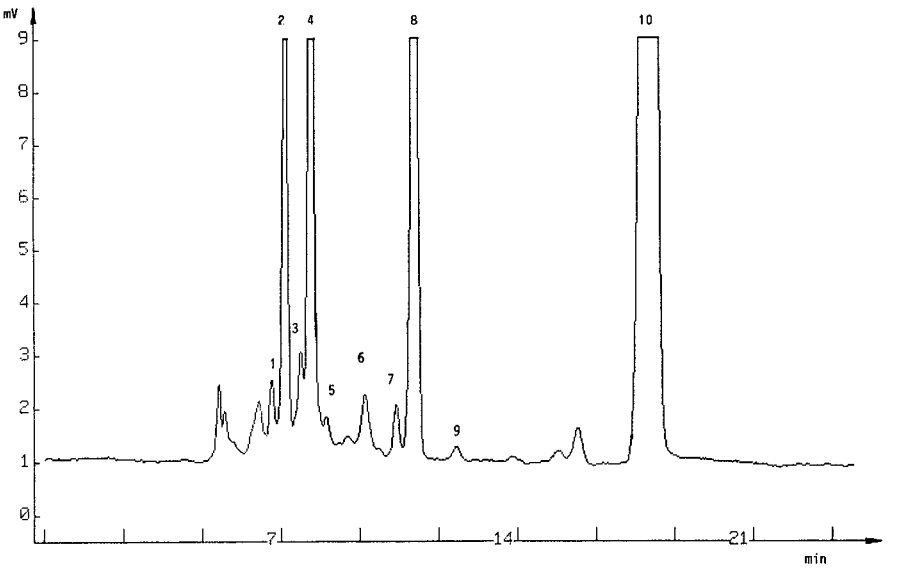

Fig. 6. Separation of Austrian white wine on an Inores S 259H column. Chromatographic conditions as described in text. Peaks: 1 = citric acid; 2 = tartaric acid; 3 = glucose; 4 = malic acid; 5 = fructose; 6 = succinic acid; 7 = lactic acid; 8 = glycerol; 9 = acetic acid; 10 = ethanol.

juice concentrates and brandy; purines in beer; sorbic acid and benzoic acid preservatives in beer and soft drinks; and ascorbic acid, dehydroascorbic acid antioxidants in beer and soft drinks.

REFERENCES

1 J. R. A. Polluk, *Brewing Science*, Vol. 2, Academic Press, London, Ch. 3, 4 and 5.
2 *Guide to Aminex HPLC Columns for Biochemical Applications*, Bio-Rad Laboratories, Richmond, CA, 1987.
3 M. Dadic and G. Belleau, *J. Am. Soc. Brew. Chem.*, 40 (1982) 141–146.
4 J. Schmidt, M. John, H-J. Niefind and H. Moonen, *Monatsschr. Brauwiss.*, 14 (1981) 114–117.
5 K. M. Brobst and H. D. Scobell, *Starch*, 34 (1982) 117–121.
6 G. Bonn, *J. Chromatogr.*, 322 (1985) 411–424.
7 *EBC-Analytica*, European Brewery Convention, Brauerei u. Getränkerundschau, Zürich, 4th ed., 1987, Method 8.5.
8 R. Pecina, G. Bonn, E. Burtscher and O. Bobleter, *J. Chromatogr.*, 287 (1984) 245–258.
9 G. Belleau and M. Datic, *J. Am. Soc. Brew. Chem.*, 43 (1985) 47–53.
10 S. H. Ashoor and J. Welty, *J. Chromatogr.*, 287 (1984) 452–456.
11 *Bio-Rad Bulletin 7035D*, Bio-Rad Laboratories, Richmond, CA, 1987.
12 P. Pfeiffer and F. Radler, *Z. Lebensm.-Unters.-Forsch.*, 181 (1985) 24–27.
13 C. Santa Maria, A. Olano and M. Tejedor, *Chromatographia*, 20 (1985) 197–200.
14 U. Hämmann, *Schweiz. Z.Obst- Weinbau*, 126 (1990) 613–617.
15 M. Natter, R. Leubolt, H. Klein and J. Püspök, in *Proceedings of the 22nd Congress of the European Brewery Convention, Zürich, 1989*, Oxford University Press, New York, 1989, pp. 461–468.
16 R. Leubolt and H. Klein, *Brauwissenschaften*, 42 (1989) 207–210.
17 R. Leubolt and H. Klein, *J. Chromatogr.*, 640 (1993) 271.
18 H. Kieninger, N. Hums and M. Tavera, *Monatsschr. Brauwiss.*, 29 (1976) 71–75.
19 D. Boeck and H. Kieninger, *Monatsschr. Brauwiss.*, 32 (1979) 160–166.

Journal of Chromatography, 640 (1993) 271–277
Elsevier Science Publishers B.V., Amsterdam

CHROMSYMP. 2658

Determination of sulphite and ascorbic acid by high-performance liquid chromatography with electrochemical detection

R. Leubolt

Austrian Beverage Institute, Michaelerstrasse 25, A-1182 Vienna (Austria)

H. Klein*

Quality Assurance and Development, Österreichische Brau AG, Poschacherstrasse 35, A-4020 Linz (Austria)

ABSTRACT

A rapid HPLC method with electrochemical detection for the determination of free and total sulphite and ascorbic acid in beer and other beverages is presented. Interferences of these compounds are discussed, in addition to the behaviour in buffer solutions of different pH. Only a dilution step is required before injecting the sample into the chromatographic system. To obtain better specificity for these compounds, two different working electrodes (platinum for sulphite and carbon glass for ascorbic acid) with distinct potentials are used.

INTRODUCTION

Sulphur compounds such as cysteine and glutathione and disulphide bridges in peptides and proteins, occurring naturally in the raw materials used during the brewing process, may be oxidized to sulphite [1]. Yeast such as *Saccharomyces carlsbergenis* could reduce sulphate to sulphite. These redox processes lead to sulphite contents up to 30 mg/l in finished beers. Ascorbic acid is a powerful antioxidant in beer, preventing colour changes and alterations of aroma and flavour and extending the storage time of the bottled beverage. Normally between 30 and 50 mg/l of ascorbic acid are incorporated in the product.

The sulphite content in foods is often analysed determined the Monier-Williams method [2], which is time consuming and subject to interferences at low sulphite levels. Some alternative techniques for the measurement of sulphite in food were summarized by Kim *et al.* [3]; their paper was concerned with a method using ion-exclusion chromatography with electrochemical detection. Other workers have reported comparison studies for the determination of sulphite in food [4]. Most published methods are time consuming because of the sample preparation required [1,5]. Official methods for the European brewing industry are published by the European Brewery Convention (EBC) [6] and the Mitteleuropäische Brautechnische Analysenkommission (MEBAK) [7].

The accepted method of the AOAC for the determination of ascorbic acid is visual titration using 2,6-dichloroindophenol [8], which works poorly with foods because of an ill-defined end-point. Other methods using isotachophoresis [9], differential-pulse polarography [10] and HPLC with fluorimetric [11], electrochemical [12–15] and UV detection [16–18] have been reported. Chromatographic

* Corresponding author.

0021-9673/93/$06.00

methods with derivatization steps have also been published [19,20]. None of the reported HPLC methods considered that sulphite and ascorbic acid elute close together from the column and that this tends to cause serious problems in the subsequent determination of these two compounds even when specific detectors such as electrochemical systems are used (see Fig. 1a and b). Using a pulsed amperometric detector combined with another ion-exclusion column, some negative effects can be avoided [21].

In this paper, the conditions for the determination of free and total sulphite and ascorbic acid in beer by HPLC with electrochemical detection (ED) are discussed.

EXPERIMENTAL

Reagents

Water for the preparation of the mobile phase and the standards of sulphite and ascorbic acid must be freshly distilled and degassed with helium to prevent oxidation. Before use, oxygen and carbon dioxide were removed in an ultrasonic bath. Ascorbic acid, sodium metabisulphite, metaphosphoric acid and sulphuric acid were of analytical-reagent grade from Merck (Darmstadt, Germany) and mannitol was obtained from Sigma (St. Louis, MO, USA). Standard solutions were prepared freshly before use.

Apparatus

The chromatographic system consisted of a Model 64 HPLC pump from Knauer (Berlin, Germany), a Rheodyne (Cotati, CA, USA) Model 7110 injection valve and an Amor electrochemical detector from Spark (Emmen, Netherlands) with a glassy carbon and a platinum electrode. The column used for ion-exchange chromatography was a "Fast Acid" (100 × 7.8 mm I.D.) with a Cation H guard column (30 × 4.6 mm I.D.) or Aminex HPX 87H (300 × 7.8 mm I.D.), from Bio-Rad Labs. (Richmond, CA, USA).

Chromatographic conditions

The eluent was 0.005 *M* sulphuric acid containing 0.001 *M* chloride (NaCl as used) at a flow-rate of 1 ml/min. The temperature was ambient and the sample volume was 20 μl.

The detector conditions were as follows: for sulphite, platinum working electrode, Ag/AgCl reference electrode, potential +0.4 V; and for ascorbic acid, glassy carbon working electrode, Ag/AgCl reference electrode, potential +0.6 V.

Procedure

Buffer and stock standard solutions for the determination of sulphite. Buffer 1 for free sulphite was 0.005 *M* sulphuric acid–0.01 *M* mannitol (pH 2.3) and buffer 2 for total sulphite was 0.02 *M* Na_2HPO_4–0.01 *M* mannitol, (pH 8.9). A stock standard solution containing 7.4 g of $Na_2S_2O_5$ + 37.5 mg of EDTA in 1 l of degassed water was prepared. A working standard solution (5 ppm) was prepared by dilution of the stock standard solution 1:1000 with distilled water and adding 37.5 mg/l of EDTA. The latter solution must be prepared freshly every day.

Stock standard solution of ascorbic acid. A 15-g amount of metaphosphoric acid was dissolved in 1 l of cold, degassed water in a volumetric flask (stabilizing the ascorbic acid), then 50 mg of ascorbic acid were weighed and dissolved in the acidic solution. This solution must be prepared freshly every day.

Sample preparation for free sulphite. A 2-ml volume of a cold beer sample (2°C) was transferred into a 25-ml volumetric flask containing about 20 ml of buffer 1 and diluted to volume with buffer 1.

Sample preparation for total sulphite. The same procedure as for the determination of free sulphite was used except that buffer 2 was used instead of buffer 1.

Sample preparation for ascorbic acid. A 2-ml of a cold beer sample (2°C) was transfered into a 25-ml volumetric flask containing 20 ml of 1.5% metaphosphoric acid. The air above the solution was removed by flushing with helium. The solution was then diluted to volume with 1.5% metaphosphoric acid. This solution must be analysed immediately.

Enzymatic reactions. For sulphite, Boehringer Mannheim Sulfite-Kit, Order No. 725854, and, for ascorbic acid, Boehringer Mannheim L-Ascorbic-Kit, Order No. 409677, were employed.

Samples. The following were used: 1 = lager beer; 2 = export beer 1; 3 = export beer 2; 4 = dark beer; 5 = pilsner 1; 6 = pilsner 2; 7 = pilsner 3; 8 = light beer; 9 = non-alcoholic beer; 10 = "weizen" beer.

RESULTS AND DISCUSSION

Different pH values allow the measurement of free and total sulphite using HPLC with electrochemical detection. At pH 8 sulphite, which is bound to various aldehydes, is set free and then measured as free sulphite. At pH 2 it is possible to detect only free sulphite. For stabilizing sulphite it is essential to add mannitol [3] to the buffers.

If both ascorbic acid and sulphite are present in the beer sample, difficulties arise when using the "Fast Acid" column. Both have very similar retention times (Fig. 1a and b), and they are electrochemically active. Fig. 2a–c show the detector response for sulphite and ascorbic acid for various pH values and different working electrodes of the electrochemical detector. The dilutions in pH 2 buffer show considerable responses at all potentials for free sulphite and ascorbic acid using the platinum working electrode (Fig. 2a). This means that it is impossible to determine free sulphite in the presence of ascorbic acid in the same run, because ascorbic acid is fairly stable at this pH (see Fig. 3a). At pH 8 ascorbic acid is destroyed within a short time (15 min), whereas sulphite is relatively stable. There is no interference by ascorbic acid (Fig. 3b). For the determination of free sulphite in food and beverages the content of ascorbic acid must be known and the integrator counts corrected, otherwise too high results are obtained.

The calibration graphs obtained using external standards (correlation coefficient 0.999) are linear within a wide range up to 50 mg/l, but the slopes are different. Separate calibrations for free and total sulphite must be used. The highest response for sulphite was found at +0.4 V. This is the potential for the lowest response for ascorbic acid. The detection limit for sulphite is about 0.1 mg/l.

To show the efficiency and the recovery of the method, different amount of sodium metabisulphite were added to a beer containing ascorbic acid. Table I shows the results of these experiments. The determination of ascorbic acid suffers minor problems, because sulphite shows no response at the carbon glass electrode below +0.6 V. Above this potential, *e.g.*, +0.8 V, as described in the literature [13], a higher response for ascorbic acid may be founds because of interference by sulphite. As ascorbic acid is also unstable in acidic solution, it

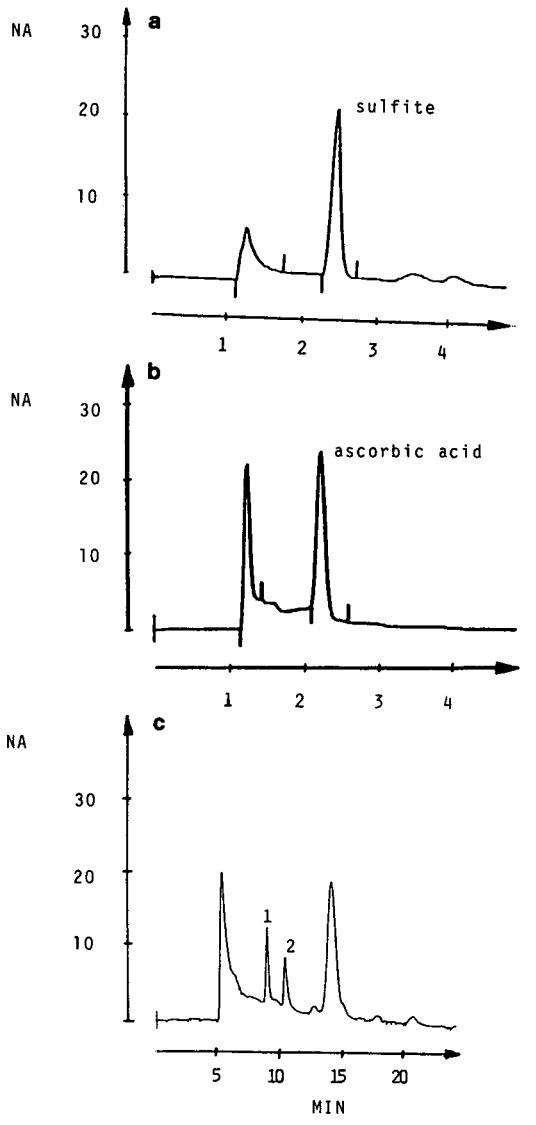

Fig. 1. (a) Chromatogram of a beer sample containing 1.5 mg/l SO_2. Column, "Fast Acid"; eluent, 0.005 *M* sulphuric acid–0.001 *M* chloride (NaCl); flow-rate, 1 ml/min; temperature, ambient; sample volume, 20 µl, detector conditions, Pt working electrode, Ag/AgCl reference electrode, potential +0.4 V; sample preparation, beer was diluted 2:25 in buffer (0.02 *M* Na_2HPO_4–0.01 *M* mannitol, pH 8.9). (b) Chromatogram of a beer sample containing 20 mg/l ascorbic acid. HPLC conditions as in (a); detector conditions, glassy carbon working electrode, Ag/AgCl reference electrode, potential +0.6 V; sample preparation, beer was diluted 2:25 with 1.5% metaphosphoric acid. (c) Chromatogram of a beer sample spiked with ascorbic acid and SO_2. Column, Aminex HPX 87H (300 × 7.8 mm I.D.), other HPLC conditions as in (a); detector conditions, Pt working electrode, Ag/AgCl reference electrode, potential +0.56 V; sample preparation, beer was diluted 2:25 in buffer (0.005 *M* sulphuric acid–0.01 *M* mannitol, pH 2.3). Peaks: 1 = ascorbic acid; 2 = SO_2.

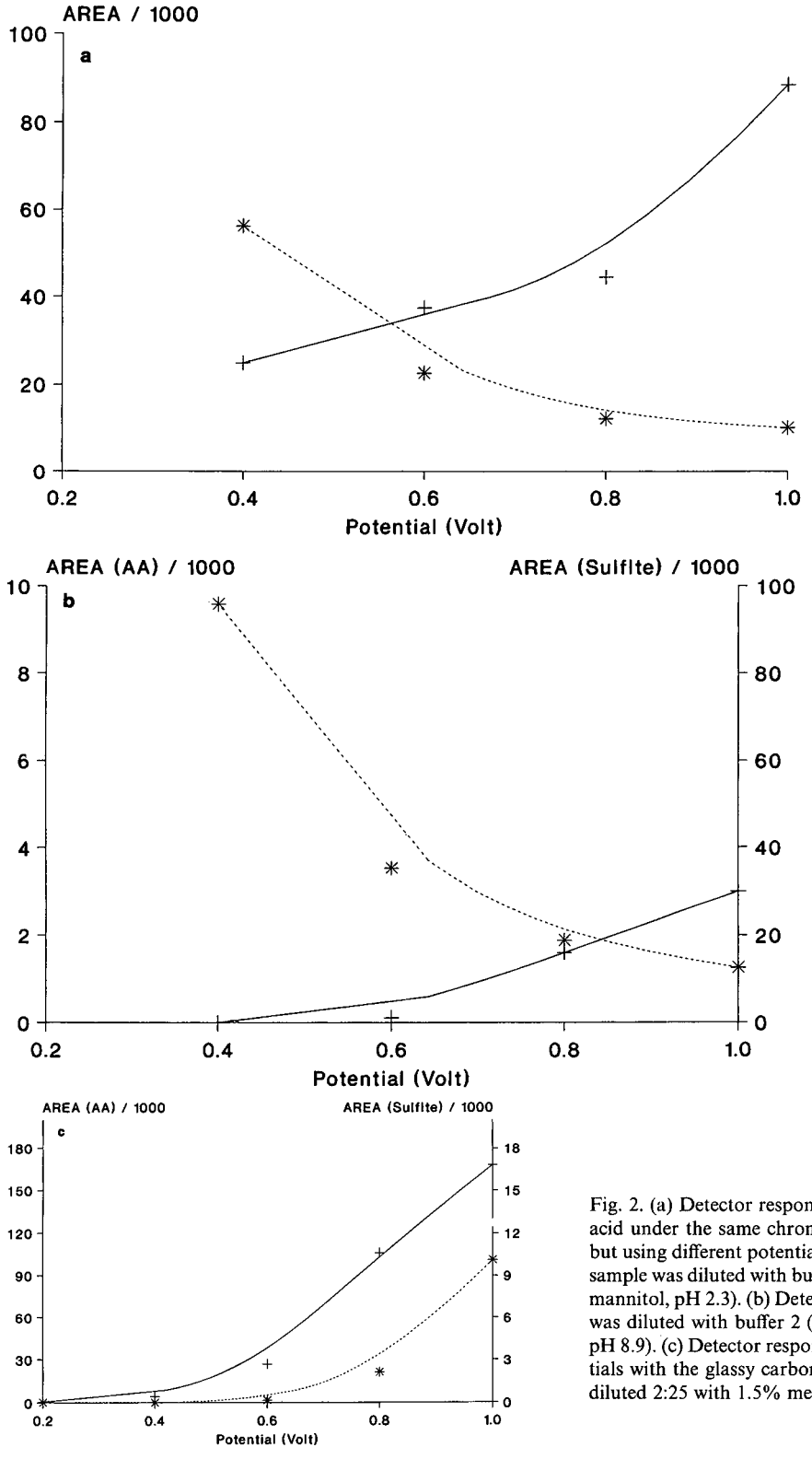

Fig. 2. (a) Detector response for (*) sulphite and (+) ascorbic acid under the same chromatographic conditions as in Fig. 1a, but using different potentials with the Pt working electrode. The sample was diluted with buffer 1 (0.005 *M* sulphuric acid–0.01 *M* mannitol, pH 2.3). (b) Detector response as in (a), but the sample was diluted with buffer 2 (0.02 *M* Na_2HPO_4–0.01 *M* mannitol, pH 8.9). (c) Detector response as in (b) but using different potentials with the glassy carbon working electrode. The sample was diluted 2:25 with 1.5% metaphosphoric acid.

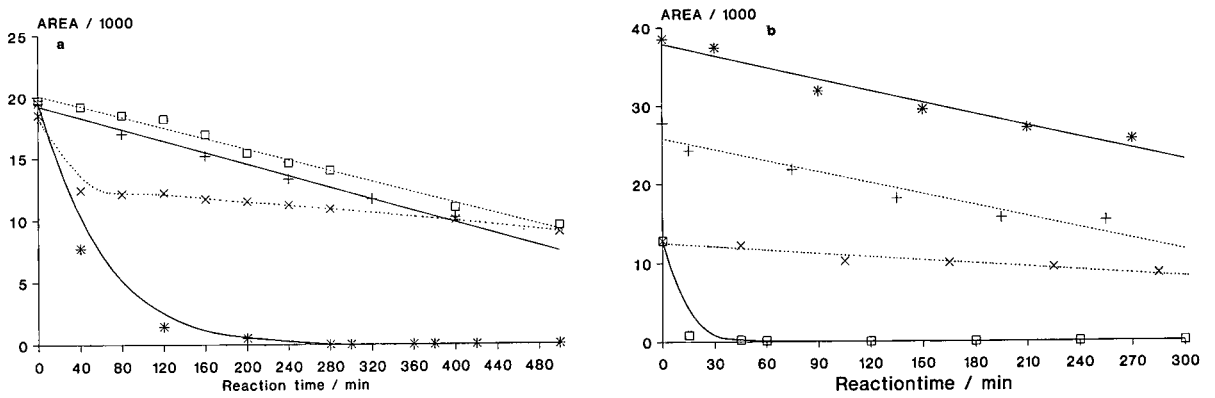

Fig. 3. (a) Different responses of ascorbic acid with the glassy carbon electrode with a potential of +0.6 V. The sample was prepared in different buffer solutions: ✳ = buffer 2 (0.02 *M* Na_2HPO_4–0.01 *M* mannitol, pH 8.9); + = buffer 1 (0.005 *M* sulphuric acid–0.01 *M* mannitol, pH 2.3); × = 0.1% metaphosphoric acid; □ = 1.5% metaphosphoric acid. (b) Different responses of ascorbic acid and sulphite under the same chromatographic conditions as in (a). □ = Response for ascorbic acid in buffer 2; × = response for ascorbic acid in buffer 1; + = response for sulphite in buffer 1; ✳ = response for sulphite in buffer 2.

should be determined immediately. The detection limit for ascorbic acid is about 0.5 mg/l.

Fig. 3a shows the decrease in ascorbic acid in various solutions. This should be kept in mind when working with automatic sample devices. The calibration graph with external standards is linear up to 50 mg/l (correlation coefficient 0.998). The recovery for this measurement is 97–100%. The results obtained with the developed method for ascorbic acid are in good agreement with those given by another HPLC method [12] and with the enzymatic test. The values correspond within ± 1 mg/l at a level of 20 mg/l (see Table II).

The separation of ascorbic acid and sulphite can be achieved under similar chromatographic conditions by using a longer ion-exchange column filled with the same resin as "Fast Acid" [*e.g*, Aminex HPX 87H (300 × 7.8 mm I.D.); Fig. 1c]. The main differences are the flow-rate (0.6 ml/min) and the detector voltage (0.56 V for a Pt working electrode or 0.8 V for a glassy carbon working electrode). Details can be seen in Fig. 2a and b. These condi-

TABLE I

RECOVERY FOR MEASUREMENT OF TOTAL AND FREE SULPHITE AND ASCORBIC ACID

Sample	Total sulphite		Free sulphite		Ascorbic acid	
	Found (ppm)	Recovery (%)	Found (ppm)	Recovery (%)	Found (ppm)	Recovery (%)
Beer	6.6	–	1.0	–		
Beer + 10 ppm sulphite	18.2	110	12.0	111		
Beer + 20 ppm sulphite	28.6	108	22.0	105		
Beer + 30 ppm sulphite	37.4	102	31.5	102		
Beer					18.0	–
Beer + 2 ppm ascorbic acid					19.6	98
Beer + 4 ppm ascorbic acid					22.0	100
Beer + 10 ppm ascorbic acid					27.6	99
Beer + 20 ppm ascorbic acid					36.8	97
Beer + 40 ppm ascorbic acid					58.1	100

TABLE II

COMPARISON OF DIFFERENT METHODS FOR THE DETERMINATION OF ASCORBIC ACID IN DIFFERENT TYPES OF BEER

Beer No.	Ascorbic acid (mg/ml)		
	HPLC–ED on HPX column 87H	HPLC–ED on RP-18 column [12]	Enzymatic test
1	21	19	20
2	20	21	18
3	19	20	19
4	17	15	17
5	43	33	34
6	17	19	32
7	28	25	24
8	10	12	–
9	33	33	–
10	21	21	19

tions give the best sensitivity for both compounds.

The application of this column is limited to the simultanous determination of ascorbic acid and free sulphite. Because of the degradation of ascorbic acid under basic conditions the determination of total sulphite and ascorbic acid is not possible (Fig. 3b). For total sulphite the "Fast Acid" column (100 × 7.8 mm I.D.) is the best choice, giving a short analysis time and a high detector response (0.4 V, Pt working electrode, no interferences by ascorbic acid).

TABLE III

COMPARISON OF DIFFERENT METHODS FOR THE DETERMINATION OF SULPHITE IN DIFFERENT TYPES OF BEER

Beer No.	Sulphite (mg/l)			
	HPLC–ED	EBC titrimetric [6]	MEBAK photometric [7]	Enzymatic
1	3.0	1	8	7
2	3.5	1	12	7
3	4.0	1	10	7
4	2.5	1	–	9
5	3.0	1	7	5
6	5.5	1	8	8
7	4.0	1	5	7
8	5.5	1	11	5
9	1.0	1	2	2
10	7.0	1	7	7

The reference methods for the European brewing industry [6,7] measure only the content of total sulphite in beer. Table III gives the results for the EBC distillation–titrimetric method No. 9.12.1 [6], the MEBAK photometric rosaniline method No. 7.24.1 [7] and the enzymatic test from Boehringer (Mannheim, Germany), which also detects only total sulphite. These results indicate that the levels obtained depend on the method used. The highest values are obtained with the photometric rosaniline method. Compared with the other methods, it seems that some other compounds react in addition to sulphite. The problems with the enzymatic test are the high absorbance (2.0), the low absorbance difference (0.1) and non-specific reactions so that extrapolation is necessary.

Comparing our results with established data in the literature [5,21] we found general agreement for the range of values of free and total sulphite in beers. The values for free sulphite are between 0.5 and 1.5 mg/l and those for total sulphite between 1 and 15 mg/l.

REFERENCES

1 C. Borchert, K. Jorge-Nothaft and E. Krüger, *Monatsschr. Brauwiss.*, (1988) 464.
2 *Official Methods of Analysis of the Association of Official Analytical Chemists*, AOAC, Arlington, VA, 14th ed., 1984, Sec. 20.123.
3 H.-J. Kim, G. Y. Park and Y.-K. Kim, *Food Technol.*, 41 (1987) 85.
4 G. Schwedt and A. Bäurle, *Fresenius' Z. Anal. Chem.*, 322 (1985) 350.
5 L. R. Moreno and P. I. de la Vega, *J. Am. Soc. Brew. Chem.*, 47 (1989) 6.
6 *EBC-Analytica*, Brauerei u. Getränkerundschau, Zürich, 4th ed., 1987, Sec. 9.12.1.
7 *Brautechnische Analysenmethoden*, Vol. II, Mitteleuropäische Brautechnische Analysenkommission, MEBAK Verlag, Freising-Weihenstephan, 1979, Sec. 7.24.1.
8 *Official Methods of Analysis of the Association of Official Analytical Chemists*, AOAC, Arlington, VA, 14th ed., 1984, Sec. 43.064.
9 H. Roben, H. Evers, E. Krüger and K. Rubach, *Monatsschr. Brauwiss.*, 1984 425.
10 A. G. Fogg and A. M. Summam, *Analyst*, 108 (1983) 691.
11 A. J. Speek, J. Schrijver and W. H. P. Schreurs, *J. Agric. Food Chem.*, 32 (1983) 352.

12 E. J. Knudsen and K. H. Siebert, *J. Am. Soc. Brew. Chem.*, 45 (1987) 33.
13 B. Luckas, *Fresenius' Z. Anal. Chem.*, 323 (1986) 496.
14 L. A. Pachla and P. T. Kissinger, *Methods Enzymol.*, 62 (1979) 15.
15 N. Moll and J. P. Joly, *J. Chromatogr.*, 405 (1987) 347.
16 R. C. Rose and D. L. Nahrwold, *Anal. Biochem.*, 114 (1989) 140.
17 S. H. Ashoor, W. C. Monte and J. Welty, *J. Assoc. Off. Anal. Chem.*, 67 (1984) 78.
18 A. Floridi, R. Coli, A. A. Fidanza, C. F. Burgeois and R. A. Wiggins, *Int. J. Vitam. Nutr. Res.*, 52 (1982) 193.
19 J. A. J. S. van Boeckel and C. A. J. M. Meeuwissen, *J. Chromatogr.*, 261 (1983) 176.
20 B. Kacem, M. R. Marshall, R. F. Matthews and J. F. Gregory, *J. Agric. Food Chem.*, 34 (1986) 271.
21 H. P. Wagner, M. J. McGarrity, *J. Chromatogr.*, 546 (1991) 119.

Journal of Chromatography, 640 (1993) 279–286
Elsevier Science Publishers B.V., Amsterdam

CHROMSYMP. 2768

Quantitative analysis of fluid inclusions in evaporites by ion chromatography

Bernhard Knipping* and Fred Türck

Institute for Mineralogy and Mineral Resources, Department of Salt Deposits and Underground Repositories, Technical University of Clausthal, Adolph Roemer Strasse 2a, 38678 Clausthal-Zellerfeld (Germany)

ABSTRACT

Natural salt minerals often contain inclusions of saturated salt solutions with diameters from 1 to >100 μm. With the quantification of the composition of the fluid inclusions, the origin and metamorphism of the salt rocks can be interpreted. Hence, these data are important concerning the long-term safety of underground repositories in salt rocks [1]: For the extraction of the solutions in fluid inclusions with diameters $\geqslant 300$ μm, an optical precision instrument was developed. For the simultaneous determination of Cl^-, Br^-, SO_4^{2-}, Li^+, Na^+, K^+, Mg^{2+} and Ca^{2+} two ion chromatographic systems with conductivity detection for cations and anions and additional photometric detection for Br^- were used. To prevent column overload, the Cl concentration must be less than 50 μg/ml in the measuring solution. The extracted samples (volumes >0.1 μl) are diluted with demineralized water by a factor of $1 \cdot 10^4$ (20-μl sample loops). The practical limit of determination for the measured elements is 0.01–0.3 μg/ml in the measuring solutions. By calculation of the anion and cation charge balance (molar equivalence), a relative error of $<5\%$ for the analysis of fluid inclusions was found.

INTRODUCTION

Natural salt rocks (evaporites) always contain saturated aqueous solutions (brines). Often with gases the solutions are stored in cracks, joints and cavernous voids (volumes ranging from ml to >1000 m^3) and in so-called fluid inclusions (with diameters ranging from 1 to >100 μm) of salt minerals such as halite (NaCl), sylvite (KCl), carnallite ($KMgCl_3 \cdot 6H_2O$) and others.

In our department, extensive research on salt solutions has been directed at quantifying geochemical processes involved in the formation and metamorphism of marine evaporites and the long-term safety of underground repositories for anthropogenic wastes in evaporites (*e.g.*, ref. 1).

Although the chemical compositions of the solutions found in cracks, joints and caverns are well known, there have been no systematic studies on the quantitative composition of individual fluid inclusions in the minerals of marine evaporites regarding their origin and metamorphism.

The composition of the saturated solutions in fluid inclusions in salt minerals can be characterized by quaternary and quinary systems for marine evaporites. The chloride type of marine evaporites is characterized by the systems $NaCl–KCl–MgCl_2–H_2O$ and $NaCl–KCl–MgCl_2–CaCl_2–H_2O$ and the sulphate type of marine evaporites by the system $NaCl–KCl–MgCl_2–Na_2SO_4–H_2O$ [2]. Both the major constituents Na, K, Mg, Ca, Cl and SO_4 and the minor components Li and Br have to be determined in order to characterize the composition and interpret the genesis of the fluid inclusions (*e.g.*, refs. 2 and 3).

The composition of salt solutions in fluid inclusions can only be quantified by direct methods. For the extraction of the solutions in fluid inclusions with diameters $\geqslant 300$ μm, an optical precision instrument was developed [4]. This allowed systematic studies and the consideration of the inclusion

* Corresponding author.

0021-9673/93/$06.00

composition in salt minerals for the quantitative interpretation of evaporite-forming processes. Ion chromatography is necessary for chemical analysis of the extracted solutions because of their usually small volumes of about 0.5 μl.

EXTRACTION OF FLUID INCLUSIONS AND SAMPLE PREPARATION

In addition to other methods, the direct analysis of individual inclusions is possible by opening the fluid inclusions with a needle or micro-drill followed by extraction of the solutions (*e.g.*, refs. 5–8). The best-developed method for the determination of the major and minor chemical components of individual fluid inclusions (diameters >250 μm) in salt minerals was the extraction method optimized by Lazar and Holland [8].

For our studies, a new extraction apparatus was developed [4]. This instrument can be used for extracting aqueous salt solutions from fluid inclusions with diameters ⩾300 μm (for explanation, see Fig. 1). A video system is used for documentation of the

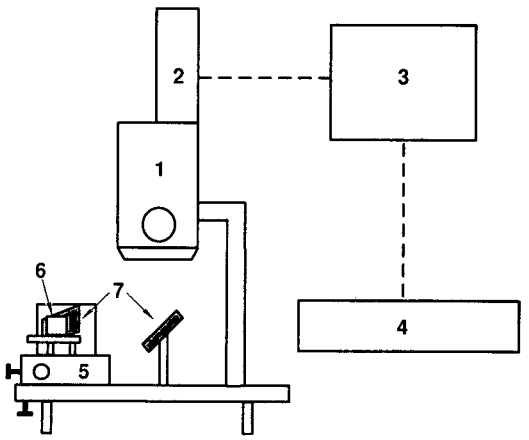

Fig. 1. Schematic diagram of equipment for extracting salt solutions from fluid inclusions >300 μm. 1 = Stereo microscope with (2) a colour video camera, (3) monitor, and (4) video recorder. (5) Universal stage attached to the built-on stage of the stereo microscope. The stage in front of the microscope is used for securing the mineral or rock sample containing the inclusions (6) to work with the tungsten-carbide micro-drill and micro-pipette for penetration and extraction of the inclusion. Since the universal stage is in front of the stereo microscope, the image must be projected by two flat mirrors (7) into the optical system of the microscope and the videocamera for observation and monitoring of the work. The mirror system allows a simultaneous view of the sample from two directions.

processes occurring within the inclusion upon penetration, *e.g.*, enlargement of pressurized gas bubbles when the inclusions are opened. Thus, the pressure experienced by a gas bubble in an inclusion can be calculated by measuring its diameter before and after penetration of the inclusion (Boyle–Mariotte law).

After the inclusion has been penetrated with a tungsten micro-drill, a micro-pipette (a capillary tube made of borosilicate glass) is used for extraction of the saturated salt solutions if the inclusions have diameters of 300–400 μm; for diameters >400 μm a microlitre syringe is used. The projecting end of the capillary is about 0.01 mm thick. The steel cannula of the microlitre syringe has a diameter of 0.18 mm.

The capillary is inserted in the fluid inclusion and the salt solution is drawn from the inclusion into the glass capillary with a plastic syringe. To prevent water from evaporating during this procedure (causing a change in the concentration of the solution and crystallization of salt), a small volume of oil is first drawn into the empty capillary. After the aqueous solution has been extracted, oil is again drawn into the capillary so that both ends are protected from evaporation.

Depending on the size of the fluid inclusion, 0.1–1 μl of saturated salt solution is extracted with the glass capillary. The volume of this solution is calculated based on the geometry of the liquid column in the capillary. Subsequently the organic (oil) and inorganic (salt solution) phases in the capillary are carefully separated as they are pushed out, to prevent contamination of the columns with organic phases.

The embedding of the inclusion solution in oil is not necessary if a microlitre syringe is used. Hence, there is no risk of contaminating the columns with organic phases. The cannula has to be filled with membrane-filtered demineralized water before extraction. Thus the volume of the solution is directly given by the graduation marks on the syringe. For a detailed description of the extraction procedure, see ref. 3.

The salt solutions are diluted by a factor of about 10^4 with deionized water (see Table I) and frozen in plastic flasks until analysis.

It should be emphasized that all measuring solutions should be membrane filtered and the tools

TABLE I

COMPOSITION OF ANIONS AND CATIONS IN TWO FLUID INCLUSION SAMPLES AFTER DILUTION

See Figs. 3–5; data after ref. 3 and L. E. von Borstel (personal communication). For measuring conditions see Table II.

Parameter	Sample GO-K		Sample WI-5	
	Diluted sample	Extracted solution	Diluted sample	Extracted solution
Volume	1.8 ml	0.16 μl	2.99 ml	0.31 μl
Calculated density[a]	–	1.297 g/cm^3	–	1.226 g/cm^3
Dilution factor	11 250.00	–	9354.84	–
Cl^-	26.4 μg/g	22.9%	21.1 μg/g	16.1%
Br^-	0.38 μg/g	3353 μg/g	0.06 μg/g	486 μg/g
SO_4^{2-}	0.71 μg/g	0.62%	2.36 μg/g	1.8%
Li^+	0.022 μg/g	191 μg/g	n.d.[b]	–
Na^+	0.98 μg/g	0.85%	12.1 μg/g	9.2%
K^+	0.55 μg/g	0.48%	1.31 μg/g	1.0%
Mg^{2+}	8.53 μg/g	7.4%	0.96 μg/g	0.73%
Ca^{2+}	0.01 μg/g	0.009%	n.d.[b]	–
Molar equivalents, anions	0.6584		0.4914	
Molar equivalents, cations	0.6583		0.4862	
Molar equivalents, relative error referred to the anions	0.01%		0.7%	

[a] Calculated after ref. 9.
[b] Not detected.

should be repeatedly cleaned with hot deionized water before use. This is necessary because of the small volumes of the concentrated solutions. For example the microlitre syringe has to be cleaned about 20 times after use until there are no residues of the extracted solutions.

SET-UP OF THE USED ION CHROMATOGRAPHIC SYSTEM

The anions and cations in the fluid inclusions are determined by ion chromatography with chemical suppression of the background conductivity. We used two 2000iSp systems from Dionex. Fig. 2 shows a scheme of the instrumental set-up and Table II gives a summary of the measurement conditions.

At the beginning of the studies the samples were injected manually, but for flushing and proportionally filling the two 20-μl sample loops for measurement of anions and cations usually just 1–3 ml of measuring solution are available (see Table I). Because of these small volumes the arrangement of the chromatographic modules was carefully optimized to minimize the dead volume by shorting the lines as far as possible. The manual injection still gave no reproducibility of the measured values. An acceptable relative standard deviation (R.S.D.) of $<5\%$ could only be achieved by using an automatic sample changer.

A knowledge of the concentrations of Br^- and Li^+ is necessary for the interpretation of the data, but the concentrations of the major components are up to 1000 times higher than the concentrations of Br^- and Li^+ (see Table I). A decrease in the background conductivity and an increase in the detection limits could be achieved by using the suppressor technique. From experience a Cl^- concentration of >50 μg/ml in the measuring solutions leads to values that are not reproducible. This is an effect of overloading the separation column with Cl^-. Overloading of the columns causes longer rinsing

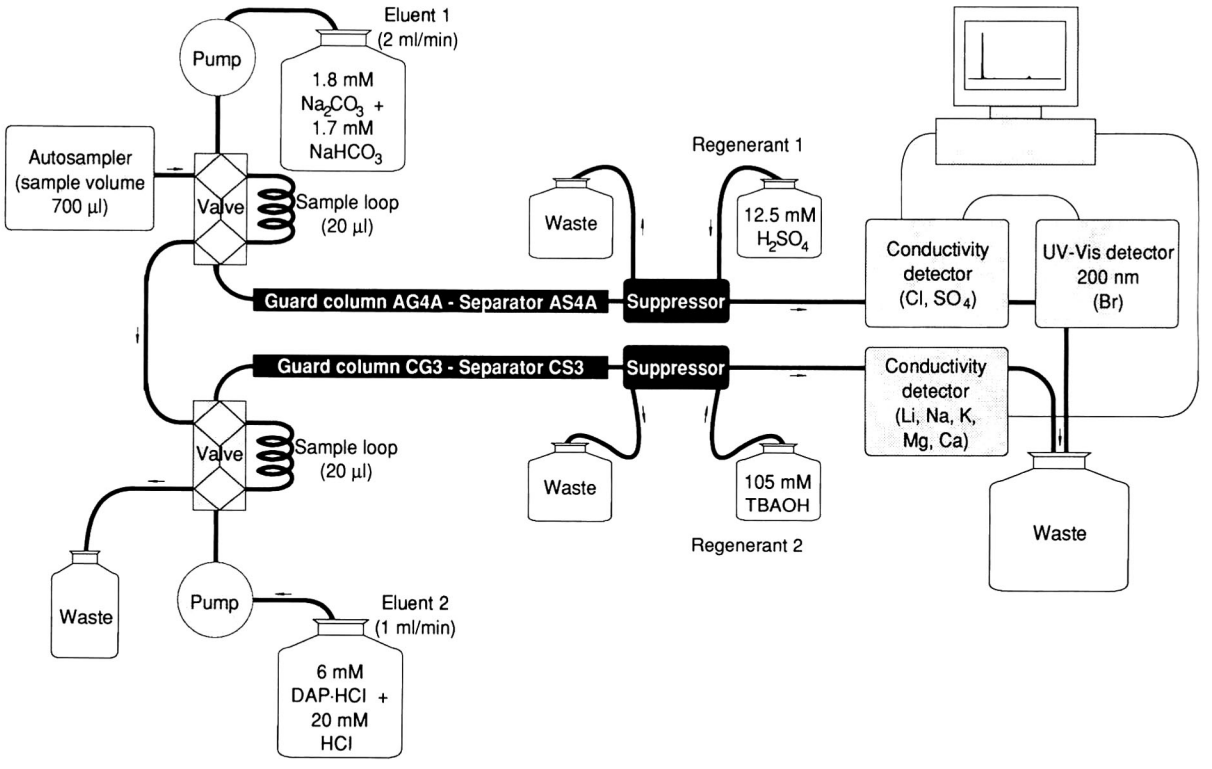

Fig. 2. Scheme of the chromatographic system used for the simultaneous determination of anions and cations in fluid inclusions. For experimental conditions see Table II.

TABLE II

MEASUREMENT CONDITIONS FOR SIMULTANEOUS DETERMINATION OF ANIONS AND CATIONS IN FLUID INCLUSIONS WITH TWO ISOCRATIC DIONEX 2000iSp CHROMATOGRAPHIC SYSTEMS

Cf., Fig. 2. Total injected volume of measuring solution, 700 µl.

Parameter	Anions (Cl^-, Br^-, SO_4^{2-})	Cations (Li^+, Na^+, K^+, Mg^{2+}, Ca^{2+})
Guard column	AG4A	CG3
Separation column	AS4A	CS3
Eluent	1.8 m*M* Na_2CO_3 + 1.7 m*M* $NaHCO_3$	6 m*M* 2,3-diaminopropionic acid (DAP · HCl) + 20 m*M* HCl
Flow-rate	2 ml/min	1 ml/min
Pressure	8.3 MPa (1200 p.s.i.)	5.5 MPa (800 p.s.i.)
Sample loop	20 µl	20 µl
Suppressor	AMMS-1	CMMS-1
Regenerant	12.5 m*M* H_2SO_4	105 m*M* tetrabutylammonium hydroxide (TBAOH)
Flow-rate	4–5 ml/min	4–5 ml/min
Detection	(a) Conductivity (Cl^-, SO_4^{2-}) (b) Photometry, UV detection at 200 nm (Br^-)	Conductivity
Background	(a) 19.9 µS (b) Set to 0 automatically	3.4 µS

times. In addition, often the volumes of the extracted solutions are too small to work with different dilution steps because we try to carry out at least two measurements per sample.

The AS4A separation column and the AMMS suppressor are suitable for the determination of the anions Cl^-, Br^-, and SO_4^{2-}. The anions are determined by using two different detection systems, a conductivity detector and a UV detector. Two systems are necessary as the amount of Cl^- is up to 300 times higher than that of Br^-. In addition, the retention times of Cl^- and Br^- are similar. Hence a measurement of the signals for Cl^- and Br^- using conductivity detection alone is not possible when there are large differences in concentration (*e.g.*, ref. 10, p. 320). Br^- is determined by direct UV absorption as Cl^- is significantly less photoactive than Br^-. This means that the Cl^- peak in the UV detector is substantially smaller, and thus the Br^- signal is clearly separated from that of Cl^- (Fig. 3). The conductivity detector is used for measuring Cl^- and SO_4^{2-} (Fig. 4).

The CS3 separation column and the CMMS suppressor are used for determining the cations Li^+, Na^+, K^+, Mg^{2+}, and Ca^{2+} with a conductivity detector. The monovalent alkali metal ions Li^+, Na^+ and K^+ and the divalent alkaline earth metal ions Mg^{2+} and Ca^{2+} are determined in a single run (Fig. 5).

For filtration of the TBAOH, the common acetate and nitrate filters were first used, but these materials are not completely resistant to the regenerant. It should be emphasized that the background conductivity of the cation system could be decreased from about 9 to 3.4 μS by using nylon filters.

Table III gives an overview of the retention times of anions and cations. For the evaluation of the results a three- to six-point calibration is required. Complete measurement of anions and cations takes about 15 min. A drift correction can be carried out by using the blank and one calibration solution.

When measuring near the detection limit manual reintegration of the peaks is often necessary in order to obtain reliable analytical data. The Windows software used makes possible a convenient and clear optimization of the results. In combination with spreadsheet software a rapid statistical evaluation of the results or, for example, the calculation of the mole equivalents for examination of the quality of the results (*cf.*, Table I) is possible.

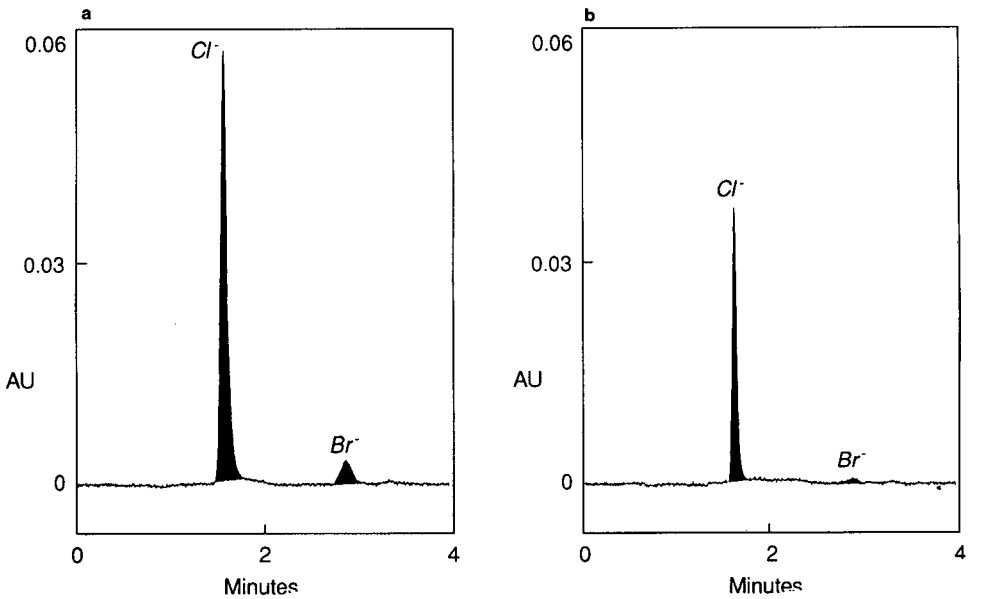

Fig. 3. Determination of Br^- in fluid inclusion samples in natural NaCl crystals with direct UV detection. (a) Sample GO-K; (b) sample WI-5. For concentration data see Table I and for experimental conditions see Table II.

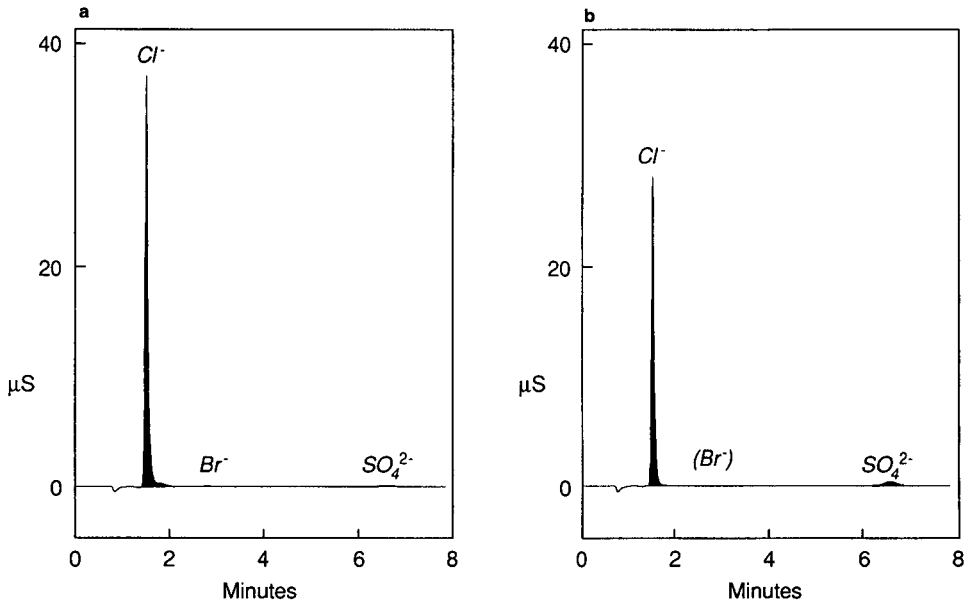

Fig. 4. Determination of anions in fluid inclusion samples in natural NaCl crystals with conductometric detection. (a) Sample GO-K; (b) sample WI-5. For concentration data see Table I and for experimental conditions see Table II.

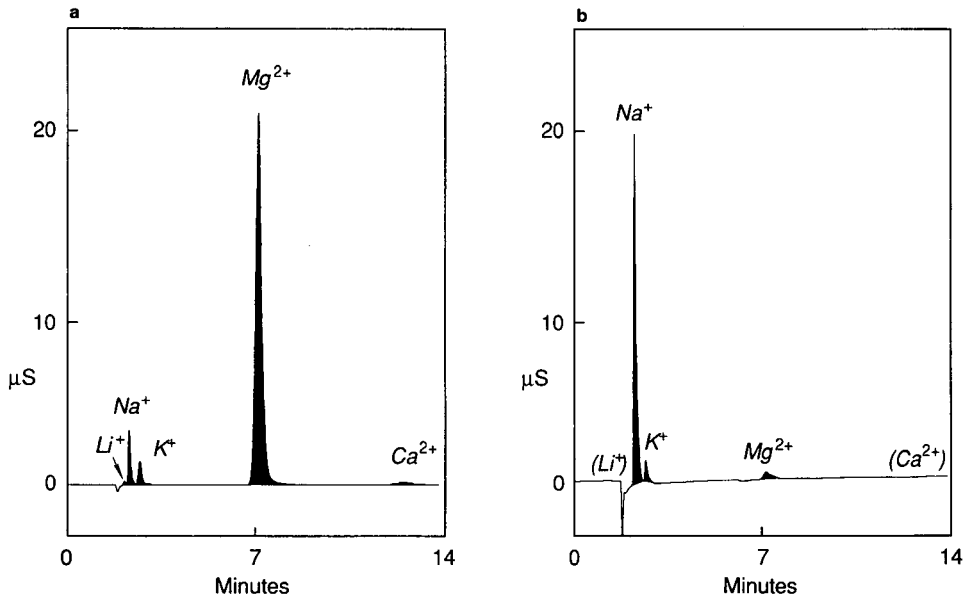

Fig. 5. Determination of cations in fluid inclusion samples in natural NaCl crystals with conductimetric detection. (a) Sample GO-K; (b) sample WI-5. For concentration data see Table I and for experimental conditions see Table II.

TABLE III

RETENTION TIMES FOR SIMULTANEOUS DETERMINATION OF ANIONS AND CATIONS IN FLUID INCLUSIONS

For measuring conditions see Table II. Retention times ± threshold values for peak detection.

Component	Retention time (min)	Component	Retention time (min)
Cl^-	1.54 ± 0.023	Na^+	2.29 ± 0.034
Br^-	2.89 ± 0.043	K^+	2.69 ± 0.040
SO_4^{2-}	6.74 ± 0.169	Mg^{2+}	7.06 ± 0.177
Li^+	2.14 ± 0.032	Ca^{2+}	12.21 ± 0.305

Calculation of the analytical data

Table I shows the composition of two typical solutions from fluid inclusions. For calculation of the analytical results in other common units (*e.g.*, g/l or mol per 1000 mol of water), a knowledge of the density of the extracted solutions is necessary. Because of the small volumes this cannot be measured directly. Therefore, the density is calculated based on the volume and quantitative composition of the solution using a computer program [4] based on the method of D'Ans *et al.* [9].

The mean composition of the measuring solutions is Cl^- 20, Br^- 0.3, SO_4^{2-} 10, Li^+ 0.1, Na^+ 10, K^+ 3, Mg^{2+} 10 and Ca^{2+} 1 μg/g. A mean error (R.S.D., $n = 30$) of <0.5% was calculated for this composition. The R.S.D. of the complete method including extraction by using a glass capillary and dilution is 10–13%, which is about ten times higher than for extraction of the solutions from the fluid inclusions with a microlitre syringe (*ca.* 1–3%).

The detection limits in one-component solutions are about 0.01–0.04 μg/g for Br^-, 0.1 μg/g for Li^+, Mg^{2+} and Ca^{2+} and about 0.1–0.3 μg/g for Cl^-, SO_4^{2-}, Na^+ and K^+. It should be emphasized that these are theoretical values. For example the empirical determination limit for Li^+ depends strongly on the Na^+ content of the solutions (*cf.*, Fig. 5).

Interpretation of analytical data

The geochemical interpretation of the data involves the formation and origin of the fluid inclusions in the evaporite minerals. Two important questions should be answered: are the inclusions residues of concentrated brines (sea water) from former basins in which the salts were deposited million years ago, or do the fluid inclusions contain solutions that are products of mineral reactions and material transports after the evaporite deposition? The mathematical calculations necessary to answer these questions are based on physical chemistry and experimental data of solution equilibria (*e.g.*, refs. 1, 2, 3 and 11).

In conclusion, these investigations, in connection with geological and other geochemical studies [1], enable one to state whether and where a salt rock body suffered metamorphism in the geological past. These results are important contributions to statements about the long-term safety of underground repositories in salt rocks [1].

ACKNOWLEDGEMENTS

This work was made possible by financial support of the Bundesamt für Strahlenschutz, to whom we are particularly grateful. We sincerely thank Professor Dr. A. G. Herrmann for initiating these studies and for his continuous support. Dr. L. E. von Borstel kindly provided the analytical data for the examples.

REFERENCES

1 A. G. Herrmann and B. Knipping, *Waste Disposal and Evaporites —Contributions to Long-Term Safety* (*Lecture Notes in Earth Sciences*, Vol. 45), Springer, Berlin, 1993.
2 A. G. Herrmann and L. E. von Borstel, *Neues Jahrb. Mineral., Monatsh.*, H6 (1991) 263.
3 L. E. von Borstel, *BfS Schriften*, Vol. 10, Bundesamt für Strahlenschutz, Salzgitter, 1993.
4 A. G. Herrmann, B. Knipping, K. Schröder and L. E. von Borstel, *Neues Jahrb. Mineral., Monatsh.*, H1 (1991) 39.

5 W. T. Holser, in A. C. Bersticker (Editor), *Proceedings of the Symposium on Salt*, Northern Ohio Geological Society, Cleveland, OH, 1963, pp. 86–95.
6 W. T. Holser, *Geol. Soc. Am. Spec. Pap.*, No. 88 (1968).
7 O. I. Petrichenko, in E. Roedder and A. Kozlowski (Editors), *Fluid Inclusions Research, Proceedings of COFFI*, Vol. 12, University of Michigan Press, 1979, pp. 214–274.
8 B. Lazar and H. D. Holland, *Geochim. Cosmochim. Acta*, 52 (1988) 485.
9 J. D'Ans, P. Höfer and H. Tollert, *Kali Verw. Salze Erdöl*, 34 (1940) 99–105.
10 J. Weiss, *Ionenchromatographie*, VCH, Weinheim, 1991.
11 O. Braitsch, *Salt Deposits, Their Origin and Composition*, Springer, Berlin, 1971.

Journal of Chromatography, 640 (1993) 287–292
Elsevier Science Publishers B.V., Amsterdam

CHROMSYMP. 2673

Improved analysis of process liquors for the pulp and paper industry by ion chromatography

Steve Utzman

Boise Cascade Research and Development, 4435 N. Channel Avenue, Portland, OR 97217 (USA)

ABSTRACT

In this paper, techniques are presented to overcome interferences from caustic matrices and neighboring ions found in process solutions. Column switching and the use of low-capacity columns to characterize strongly retained analytes are described. Oxalate, sulfide, sulfite, sulfate and thiosulfate are characterized on one set of separator columns. High-capacity cation-exchange resins are shown to be an effective pre-treatment tool for neutralizing a caustic chlorine dioxide scrubbing liquor, enabling baseline resolution of chlorate.

INTRODUCTION

Wood is converted into fibers for papermaking by a number of pulping processes [1,2]. Chemical pulping is a process that dissolves lignin, leaving the cellulose and hemicellulose components of the fibers for papermaking [3]. In the kraft process, wood chips are delignified by digesting at high temperature with a cooking liquor consisting of an aqueous solution of sodium hydroxide and sodium sulfide. The cooking solution is called a white liquor.

The white liquor becomes black after the pulp is digested, due to dissolved and degraded wood constituents. The black liquor is then washed from the pulp and transferred to a storage tank where sodium sulfate is added to make-up for losses of inorganic elements during the digestion. The mixture from the storage tank is evaporated to a solids content of 60–70% and fed to a recovery furnace where the organic components are burned to evolve heat. A molten mass of sodium carbonate and sodium sulfide remain. It contains impurities in small quantities of sodium sulfate, sulfite, and thiosulfate [4]. A green liquor is produced by dissolving the molten mass in water. The mixture is treated with a suspension of calcium hydroxide to convert the sodium carbonate back into sodium hydroxide, thereby producing white liquor for reuse in the cooking process.

Some pulp mills employ the use of an on-site bleach plant to manufacture chlorine dioxide as an additional method of delignifying the pulp. Concerns about chemicals released to the atmosphere from a bleach plant have resulted in the establishment of state and federal programs, limiting the emissions of chlorine and chlorine dioxide. To combat these emissions, studies have shown that white liquor is among the more effective process solutions used as a scrubbing agent [5]. This scrubbing action (by the white liquor) becomes another process that is tied into the recovery liquor cycle. It is also a point in the process where corrosive ions are introduced.

Pulp mill process engineers are very concerned about corrosion, and how efficient the recovery cycle is working. The ion chromatographer plays an important role in monitoring and troubleshooting the process chemistry involved in the recovery cycle.

Corrosion is best understood by focusing on chloride, chlorite and chlorate. Sulfite, sulfate and thiosulfate have already been mentioned as by-products of the recovery process. The presence of oxalate can cause the formation of insoluble salts. The relative abundance of all these anions provide a

0021-9673/93/$06.00

method of monitoring the reduction–oxidation environment at various points in the recovery cycle.

One of the goals of this paper is to present an analysis of anions in pulping and scrubbing solutions, with an emphasis on minimizing system modifications. All too often, the analyst incorporates numerous methods —each developed for a specific family of anions— in an effort to obtain a comprehensive anion characterization. This is often tedious and time-consuming: columns are changed and equilibrated, eluents are modified or replaced, all requiring a period of time to re-equilibrate. The methods presented in this paper will reduce column changes, improve the baseline resolution of chlorate and improve the resolution of oxalate from sulfate using a carbonate eluent.

Previous work has described a fast analysis of sulfite, sulfate and thiosulfate in pulping liquors using column switching [6]. The switching technique was originally designed for white liquors and other process solutions. This paper will expand upon that work to consider the more complex black liquor. Sulfide analysis will also be presented using the same column configuration for oxalate, sulfite, sulfate and thiosulfate analysis. Improved chlorate resolution is achieved through sample matrix neutralization, using a high-capacity cation-exchange resin.

EXPERIMENTAL

Instrumentation

Method development was performed isocratically on a gradient ion chromatograph (Model 4000, Dionex, Sunnyvale, CA, USA). The sample loop size was 50 μl and the eluent flow-rate was 1.0 ml/min. The chromatograph module was equipped with two eight-port slider valves. The first valve is used for injection; the other for column switching to redirect the flow of anions. The column switching, or slider valve is placed in series after the injector valve. The OmniPax-100 guard (50 × 4 mm) and analytical (250 × 4 mm) columns were placed on either side of the switching valve. These columns were used for the separation of oxylate, sulfide, sulfite, sulfate and thiosulfate. AS9-SC guard (50 × 4 mm) and analytical (250 × 4 mm) columns were used to resolve chlorate.

Sulfite, sulfate, thiosulfate and oxalate were resolved using an eluent composed of 1.3 m*M* Na_2CO_3, 6 m*M* NaOH and 1.58 m*M* *p*-cyanophenol. For sulfide, an eluent of 10 m*M* boric acid, 15 m*M* ethylenediamine, 10 m*M* NaOH, 1 m*M* $NaNO_3$ in 2% methanol was used. The chlorate eluent was composed of 2 m*M* Na_2CO_3 and 0.75 m*M* $NaHCO_3$.

Chemical suppression was achieved with an anion micromembrane suppressor (Dionex), using 10 m*M* sulfuric acid regenerant at a flow-rate of 5 ml/min.

Oxalate, chlorate, sulfite, sulfate and thiosulfate were detected by conductivity (Model CDM, Dionex) in the 30 μS range. Sulfide was detected electrochemically using amperometry (Model PAD-2, Dionex), at an applied potential of 0 V. The detector cell is solvent compatible, three-electrode thin-layer design with a silver working electrode and an Ag/AgCl reference electrode. The working electrode was cleaned as needed, with fine polishing compound.

Detector output was directed to a Waters LAC/E interface and 845 workstation. Data processing was performed with Waters ExpertEase chromatography software, version 3.0.

Reagents

Sulfite, sulfate, thiosulfate, oxalate and chlorate standards were prepared from 1000 mg/l stock solutions using analytical-grade EM-Science reagents. The sulfite working standard was prepared in 10% isopropanol to prevent oxidation. The use of formaldehyde as an anti-oxidant was avoided. Formaldehyde will influence the peak height and retention characteristics, based on the amount of formaldehyde added [7,8].

Working sulfide standards were prepared from a 1000 mg/l stock solution containing 1 ml/l anti-oxidant buffer (17.6 g of ascorbic acid, 8 g of 50% NaOH and 1.0 ml of ethylenediamine in 100 ml of water). The stock solution was standardized by potentiometric titration with cadmium nitrate using a sulfide ion-selective electrode.

Working standard solutions of sulfite and sulfide were prepared fresh daily. Degassed, high-purity 18 MΩ cm water was used for all eluent and standard solution preparations.

Dealkalization of white liquor samples was achieved with Duolite C-433 weak-acid cation-ex-

change resin. The resin was pre-wetted and rinsed with high-purity deionized water. The resin slurry was poured into a glass, gravity flow column (30 × 0.9 cm, Spectrum Industries, Los Angeles, CA, USA). The resin bed was washed with 3–5 bed volumes of distilled, deionized water. Sample loading volumes were 5 ml; bed volume was 18.9 ml, with a void volume of 6 ml. Samples collected for chlorate analysis were made at 8 ml, using a 2-ml aliquot. The resin was returned to its fully regenerated form with 1% H_2SO_4. The acid dosage was set at 105% of the resin operating capacity (4 equiv./l).

RESULTS AND DISCUSSION

Fig. 1 is a chromatogram of a diluted black liquor and shows the resolution of oxylate from sulfate. A column-switching technique was used to shorten the analysis time and maximize the resolution of the divalent species. Initially, the switching valve is in the off position, allowing chloride, sulfite, sulfate and oxalate to pass through the guard column and on to the analytical column in less than 3 min. Thiosulfate remains on the guard column. At 3.1 min, the switching valve is activated, redirecting the flow of anions. For the remainder of the analysis, chloride, sulfite, sulfate and oxalate all flow from the analytical column back to the guard column where they elute with thiosulfate. Thiosulfate only passes through the guard column and is eluted after chloride. The time saved by using column switching for thiosulfate analysis is approximately 60% [6]. The reduction in retention time also improved the peak symmetry of this strongly retained analyte.

Polymeric multi-mode columns, like the OMNIPAX columns used in Fig. 1, are ideal for process liquor analysis. They allow ion exchange in a solvent compatible matrix [9]. And most importantly, they can be cleaned with pure solvent, washing off strongly retained hydrophobic compounds (like humic acids) and other contaminants found in process liquors. The manufacturing of the multimode columns (Dionex), requires the use of at least 1% organic solvent to hydrate the hydrophobic regions of the resin.

Poor resolution of oxalate from sulfate was found, using a carbonate eluent with the minimum amount of recommended organic solvent. Resolution was improved (over direct injection) using column switching. However, this technique alone did not supply baseline resolution of these two analytes.

It was found by *eliminating* the organic solvent entirely, complete resolution of oxalate from sulfate was achieved, as shown in Fig. 1. When the solvent was removed, system back-pressure increased by a

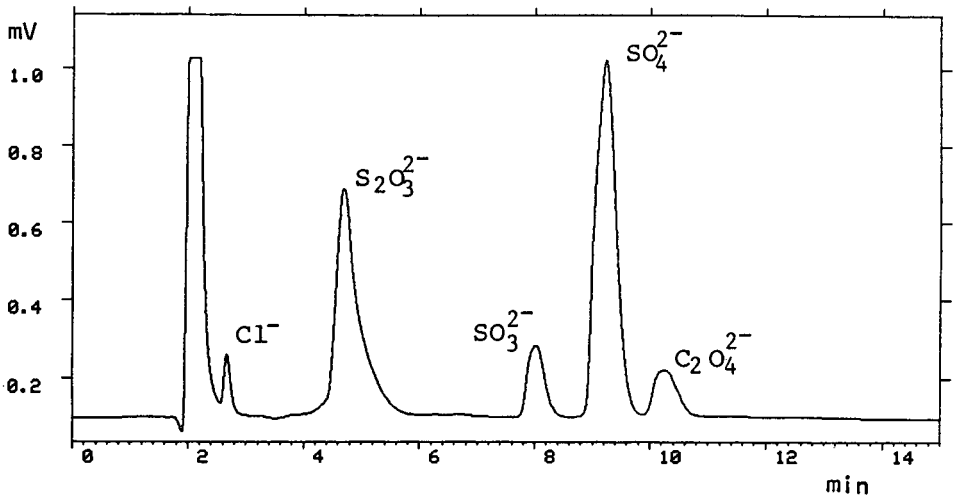

Fig. 1. Chromatogram of a diluted (1:500) black liquor using the column-switching technique. The switching valve was activated at 3.1 min. The eluent was composed of 1.3 m*M* Na_2CO_3, 6 m*M* NaOH and 1.58 m*M* *p*-cyanophenol. All other conditions are described in text.

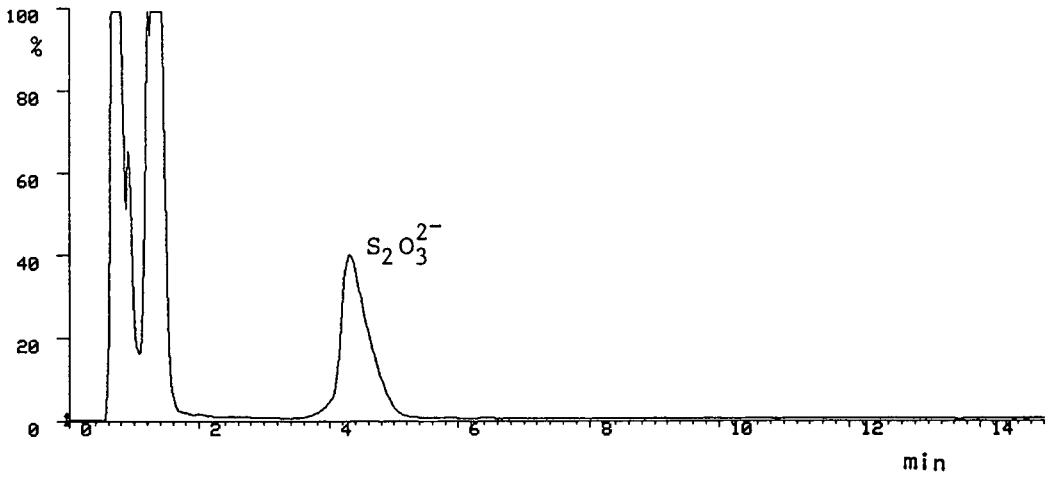

Fig. 2. Chromatogram of the same black liquor sample used in Fig. 1. The column switching method was optimized for thiosulfate by activating the switching valve at 0.3 min. The sample passes only the switching valve and guard column at this activation time. All other conditions the same as in Fig. 1.

modest 100 p.s.i. Perhaps in the absence of organic solvent, the *p*-cyanophenol component of the eluent is sufficient to condition the hydrophobic regions of the column. No reduction in column performance was observed in six months of using eluent without organic solvent (in the presence of *p*-cyanophenol), or other separations and cleaning methods requiring high solvent concentrations.

Caution should be exercised when quantifying thiosulfate in the presence of significant levels of nitrate or phosphate, using the column-switching technique. Simultaneous elution was found with all three of these anions using a column-switching time of 3.1 min.

This problem was avoided by directing all the anions through the guard column alone. This was accomplished by advancing the switching time to 0.3 min. This was the minimum time necessary for the sample to clear the switching valve. Fig. 2 is a chromatogram showing the use of the shorter

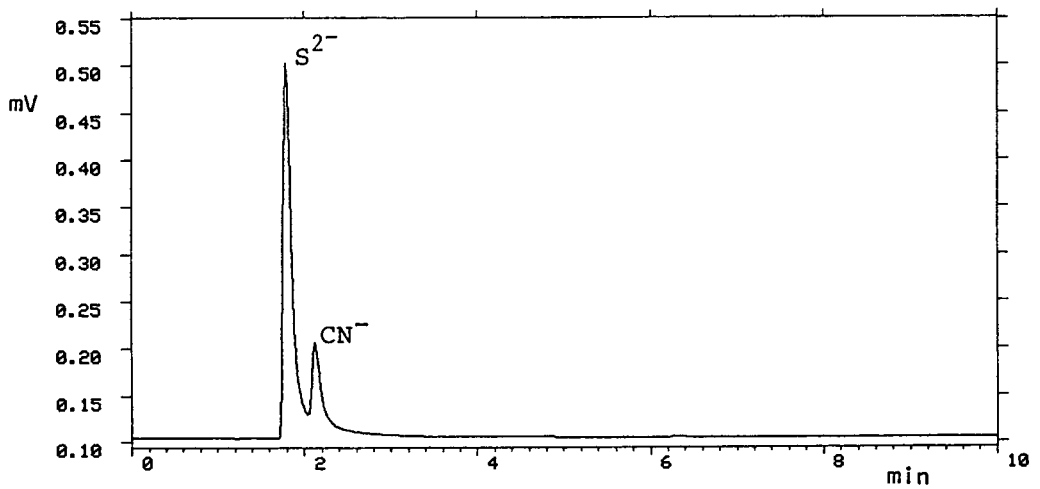

Fig. 3. Chromatogram of a diluted (1:2000) white liquor and a 1 mg/l cyanide spike, direct injection. The spike was added to show the resolution of sulfide from other anions using the PAX-100 columns. An eluent of 10 m*M* boric acid, 15 m*M* ethylenediamine, 10 m*M* NaOH and 1 m*M* $NaNO_3$ in 2% methanol was used.

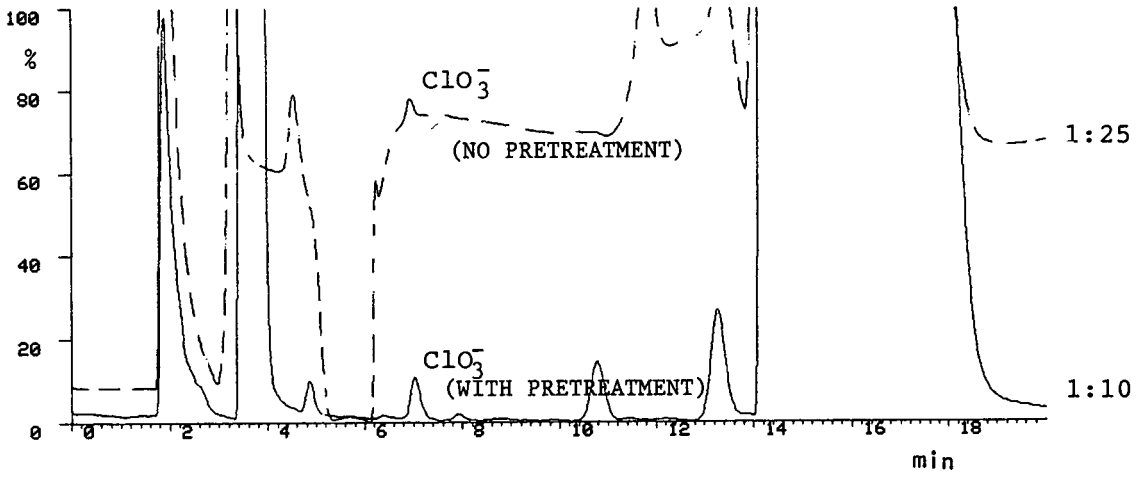

Fig. 4. Chromatograms of diluted white liquors showing the dealkalization of the sample matrix by pretreating the diluted sample with cation-exchange resin. The upper chromatogram is a diluted (1:25) white liquor with no pretreatment. The lower chromatogram is the same sample, diluted 1:10, after pretreatment with Duolite C-433 cation-exchange resin. Conditions for chlorate analysis were: Dionex AS9-SC guard and analytical columns, with an eluent of 2 m*M* Na_2CO_3 and 0.75 m*M* $NaHCO_3$. Injection volume was 50 μl. Chlorate was detected by conductivity in the 30 μS range.

switching time, with the same diluted black liquor used in Fig. 1. The chromatogram in Fig. 2 shows thiosulfate eluting in less than 5 min, with good peak symmetry. One of the simultaneously eluting anions in Fig. 1, nitrate, is now eluted much earlier with the weakly retained anions and does not interfere. It was found that a low-capacity guard column cannot resolve thiosulfate from phosphate. However, black liquors (the most complex process solution) contain low levels of phosphate, and errors from contamination are minimal.

In an effort to reduce system modifications, columns used for oxylate, sulfite, sulfate and thiosulfate determinations were also tested for sulfide analysis. A linear calibration plot for sulfide was obtained using these columns. Fig. 3 is a chromatogram of a diluted white liquor, showing the resolution of sulfide from a 1 mg/l cyanide spike. The OMNI-PAX multi-mode columns are not optimized for weakly retained analytes such as sulfide. The added cyanide spike was included to demonstrate the resolving power of these columns for weakly retained species, under the conditions described. Fortunately, a column with more selectivity for weakly retained anions is not necessary for sulfide analysis in process liquors. Large dilutions (*i.e.* 1:2000) are necessary to bring sulfide concentrations within the working range of the electrochemical cell. Hence, all possible contaminants are eliminated by dilution.

Chlorate analysis in caustic white liquors was improved with sample dealkalization. Fig. 4 shows chromatograms of a white liquor diluted 1:25 without pretreatment, and the same liquor sample at 1:10, treated with ion-exchange resin. When alkaline earth metals are removed by the resin, hydroxide levels are also reduced. This pretreatment process has a great effect on improving the baseline stability of a conductivity detector. Little to no baseline upset was observed in the more concentrated sample. The weak-acid resin, with a capacity of 4 equiv./l, neutralized the pH 14 liquors to pH 5. This process had little if any effect on chlorate stability: recoveries were between 94 and 104%. Chlorate is a stable analyte, resisting degradation from reductions in pH [10].

Attempting to neutralize caustic liquor samples more concentrated than 1:10 generated visible amounts of dangerous hydrogen sulfide in the pretreatment column resin. This was due to the acidification of sulfide and polysulfide species present in the sample. During the neutralization of the more concentrated samples, air pockets formed and channeling occurred. This is not a problem for low

level chlorate determinations in scrubbing liquors. At a 1:10 dilution, chlorate levels were found to be at or above 0.5 mg/l.

CONCLUSIONS

Previous work has demonstrated the effectiveness of column switching in reducing the analysis time of white liquors and dilute recirculated process solutions. A more complete characterization of process liquors is now achieved. Oxalate and sulfide can be characterized using the same multi-phase columns used for sulfite, sulfate and thiosulfate analysis. Low levels of chlorate can be determined in chlorine dioxide scrubbing liquors via pre-treatment with cation-exchange resin.

REFERENCES

1 R. G. MacDonald (Editor), *The Pulping of Wood*, Vol. I, McGraw-Hill, New York, 2nd ed., 1969.
2 C. E. Libby (Editor), *Pulp and Paper Science and Technology*, Vol. 1, McGraw-Hill, New York, 1962.
3 S. Rydholm, *Pulping Processes*, Wiley, New York, 1965.
4 J. P. Casey (Editor), *Pulp and Paper, Chemistry and Chemical Technology*, Vol. 1, Wiley, New York, 3rd ed., 1980.
5 *Technical Bulletin No. 616*, National Council of the Paper Industry for Air and Stream Improvement, New York, September 1991.
6 S. Utzman and D. Campbell, *LC · GC*, 9 (1991) 300.
7 D. B. Easty and J. E. Johnson, *Tappi J.*, 70 (1987), 109.
8 M. Lindgren and A. Cedergren, *Anal. Chim. Acta*, 141 (1982) 279.
9 *OmniPac Guidebook*, Dionex, Sunnyvale, CA, 1991.
10 F. A. Cotton and G. Wilkinson, *Advanced Inorganic Chemistry*, Interscience, 3rd ed., 1972.

Journal of Chromatography, 640 (1993) 293–297
Elsevier Science Publishers B.V., Amsterdam

CHROMSYMP. 2664

Analysis of multiple sugar probes in urine and plasma by high-performance anion-exchange chromatography with pulsed electrochemical detection

Application in the assessment of intestinal permeability in human immunodeficiency virus infection

Simon C. Fleming*

Department of Clinical Biochemistry and Metabolic Medicine, The Medical School, University of Newcastle upon Tyne, Framlington Place, Newcastle upon Tyne NE2 4HH (UK)

J. A. Kynaston

Department of Child Health, University of Newcastle upon Tyne, Newcastle upon Tyne NE2 4HH (UK)

M. F. Laker

Department of Clinical Biochemistry and Metabolic Medicine, University of Newcastle upon Tyne, Newcastle upon Tyne NE2 4HH (UK)

A. D. J. Pearson

Department of Child Health, University of Newcastle upon Tyne, Newcastle upon Tyne NE2 4HH (UK)

M. S. Kapembwa and G. E. Griffin

Division of Communicable Disease, St. George's Hospital Medical School, London (UK)

ABSTRACT

Mannitol, 3-O-methylglucose and lactulose administered orally are used to investigate small intestinal absorption pathways and mucosal integrity. Current methods of analysis include thin-layer chromatography, gas chromatography (GC) and enzymatic analysis, which require separate estimation of mono- and disaccharides and for GC, prior derivatization. We describe a high-pressure anion-exchange chromatographic method coupled with pulsed electrochemical detection allowing simultaneous measurement of all three sugars and its clinical application in monitoring intestinal damage in human immunodeficiency virus (HIV) infection. Sample preparation is simple and fast. All sugars are resolved within 10 min. Mean recovery is 93.3% for all sugars and the overall relative standard deviation is 4.2%. Intestinal permeability (lactulose/mannitol ratio) rises with disease progression to AIDS, indicating mucosal damage. The greatest increase in permeability is associated with chronic diarrhoea. The method is an ideal non-invasive test to assess gut mucosal damage in HIV infection.

* Corresponding author.

0021-9673/93/$06.00

INTRODUCTION

The measurement of the urinary excretion of orally administered non-metabolized sugar probe molecules has been used to assess the permeability of small bowel mucosa in a variety of intestinal diseases [1–3]. Several probe molecules, including mannitol, 3-O-methylglucose and lactulose, have been used to assess active and passive transport in the small intestine.

Mannitol, a low-molecular-weight sugar alcohol, is thought to diffuse through water-filled pores in the enterocyte membrane. Lactulose, a synthetic disaccharide, crosses the mucosa via the intercellular tight junctions. 3-O-Methylglucose is transported in a similar manner to glucose and, therefore, acts as a marker of active intestinal transport [4]. Expressing the ratio of these sugars in a timed urine sample provides an index of intestinal permeability [1].

The difficulty in quantifying urinary and plasma sugars has limited the widespread use of these tests. The introduction of high-performance liquid chromatography (HPLC) with pulsed amperometric detection had enabled the rapid and simultaneous determination of lactulose and mannitol in urine [5]. We have further developed this method to allow simultaneous measurement of mannitol, 3-O-methylglucose and lactulose both in plasma and urine, for use in intestinal permeability studies.

We also report the clinical application of such permeability testing in subjects with human immunodeficiency virus (HIV) infection.

EXPERIMENTAL

Sugars

Lactulose (4-O-D-galactopyranosyl-D-fructofuranose) and 3-O-methylglucose (3-O-methyl-α-D-glucopyranose) were supplied by Sigma (Poole, UK). Mannitol and melibiose (6-O-α-D-galactopyranosyl-D-glycopyranose) were supplied by BDH (Poole, UK).

Chemicals

Sodium hydroxide (50%, w/v), zinc acetate (anhydrous), 5-sulphosalicylic acid, Amberlite resins IR-120 H^+ and IRA-400 Cl^- were obtained from BDH. Deionized water (18 MΩ/cm) was produced with an in-house deionizer (Elga, High Wycombe, UK).

Equipment

A quarternary gradient HPLC system with pulsed electrochemical detector was supplied by Dionex UK (Camberley, UK). A high-performance anion-exchange column (Carbopac PA-1; 250 mm × 40 mm I.D.) with associated guard column was also supplied by Dionex UK.

Eluent preparation

Deionized water (989.4 ml) was degassed with helium for 20 min. A 1-ml volume of 0.5 mol/l zinc acetate solution was added and mixed. A 9.6 ml volume of 50% (w/v) sodium hydroxide was added with degassing for a further 10 min.

Sample preparation

Urine. Depending on collection volume, samples were diluted between 1:10 and 1:40 with deionized water to a volume of 1 ml. This dilution was performed on an aliquot of the neat frozen urine. A 1-ml volume of internal standard (melibiose, 250 mg/l) was added and the mixture de-salted with hydrogen ion-exchange resin (Amberlite IR-120 H^+) occupying up to a third of the total volume.

Plasma. A 200-μl volume of plasma was added to 200 μl of internal standard (melibiose, 250 mg/l) and mixed. To this, 200 μl of ice-cold 5-sulphosalicylic (35 g/l) was added to precipitate plasma proteins, and the samples were left on ice for 20 min. Samples were centrifuged at 9000 *g* for 5 min and the supernatant removed. Supernatant was mixed with ion-exchange resin (IR-120 H^+ and IRA-400 Cl^- in mass ratio 1:1.5) and centrifuged again.

HPLC analysis

Supernatant (25 μl) was injected onto the column. For urine analysis, samples were eluted with 120 mmol/l sodium hydroxide, 0.5 mmol/l zinc acetate at a flow-rate of 1 ml/min at 20°C. For plasma, analysis samples were eluted with 160 mmol/l sodium hydroxide, 0.675 mmol/l zinc acetate. At the end of each plasma sample run a 4-min wash with 1 *M* sodium hydroxide was employed to maintain stability of retention times.

Detection was with a pulsed electrochemical detector, with a detection potential of −0.01 V (0–0.5

s), an oxidation potential of +0.75 V (0.51–0.64 s) and a reduction potential of −0.75 V (0.65–0.75 s) with an integration period of 0.05–0.5 s. Peak heights or peak areas were measured with internal standardization.

Subjects

Controls. Nineteen healthy caucasians (twelve males and seven females), age range 21–39 years, with no history of gastrointestinal disease acted as control subjects.

HIV group. Forty HIV antibody-positive males living in London were recruited prospectively to the study, after giving informed consent. The HIV clinical status was: AIDS, 26; AIDS-related complex (ARC), 7; asymptomatic, 7. Of the 33 subjects with AIDS or ARC 15 had chronic diarrhoea.

Protocol

All subjects were fasted overnight, being allowed only water to drink. On the morning of the test, subjects provided a pre-test urine sample. They then drank a solution containing 10 g of lactulose and 5 g of mannitol dissolved in 50 ml of water (osmolality, 1350 mmol/kg). Urine was collected over 6 h into a container with 1 ml of 20% (w/v) chlorhexidine as preservative.

The total urine volume was recorded on completion of the test, and a 40-ml aliquot was stored at −20°C until analysis. Subjects were encouraged to drink fluids freely after the first hour of the test to maintain an adequate urine output. All subjects avoided ingesting alcohol or non-steroidal anti-inflammatory drugs for at least 12 h prior to the test.

RESULTS

Linearity

The linearity of the method was assessed by adding known amounts of analytes to urine and plasma against a fixed concentration of internal standard. The method was linear for each sugar to the following concentrations: mannitol, 125 mg/l; 3-O-methylglucose, 300 mg/l; and lactulose, 40 mg/l. Standard curves are represented by the following equations: mannitol, $y = 0.0062x + 0.0185$ (standard error of the estimate, S.E.E., 0.035); 3-O-methylglucose, $y = 0.0021x + 0.0001$ (S.E.E., 0.005); and lactulose, $y = 0.0014x + 0.002$ (S.E.E. 0.051).

Detection limit

Lactulose was detectable to levels of 0.4 mg/l in urine and plasma.

Recovery

The analytical recovery was determined by adding known amounts of sugars to urine and plasma and comparing the concentration measured with the amount added. The results are shown in Table I. Recovery ranged between 89 and 105% for all analytes, at various concentrations.

Precision

The imprecision of the method was determined by the repeated measurement of sugars in test urine and plasma samples and the results are summarised in Table II. Overall relative standard deviations ranged from 1.8 to 8.5%.

Interference

No other peaks were found in urine with the same retention times as the probe markers, and all sugars were well resolved within 10 min. In plasma, the eluent conditions had to be changed slightly to avoid interference from an unidentified peak that sometimes co-eluted with lactulose. An increase in eluent concentration from 120 to 160 mmol/l sodium hydroxide resolved the two peaks as shown in Fig. 1.

Subjects infected with HIV

The lactulose/mannitol ratio (mean ± 2 S.D.) was higher in subjects with AIDS (0.064 ± 0.014, $p = 0.03$) and in subjects with ARC (0.042 ± 0.013, $p = 0.03$) than in asymptomatic HIV antibody subjects (0.027 ± 0.004) and control subjects 0.024 ± 0.002). In addition HIV-infected subjects with diarrhoea had a higher lactulose/mannitol ratio (0.072 ± 0.017, $p = 0.001$) than HIV-infected individuals without diarrhoea (0.034 ± 0.006). There was no significant difference between asymptomatic HIV antibody-positive subjects and control subjects. Thus, changes in intestinal permeability were only detected in patients with AIDS and ARC particularly in the presence of diarrhoea. Mannitol absorption in subjects with AIDS (11.33 ± 1.02%) and subjects with ARC (8.84 ± 2.6%) and asymptomatic HIV-positive subjects (9.71 ± 2.34%) was not different from that of control subjects (11.4 ±

TABLE I

ANALYTICAL RECOVERIES OF MANNITOL, 3-O-METHYLGLUCOSE AND LACTULOSE FROM URINE AND PLASMA SAMPLES

Matrix	Amount added (mg/l)	Measured concentration[a] (mg/l)	Recovery[a] (%)
Mannitol			
Urine	31.25	28.5 ± 0.2	91.3 ± 0.7
Plasma	31.25	28.9 ± 0.3	92.3 ± 0.8
Urine	125.0	111.4 ± 1.4	89.1 ± 1.1
Plasma	125.0	118.6 ± 1.5	94.9 ± 1.2
3-O-Methylglucose			
Urine	75.0	66.8 ± 0.7	89.1 ± 0.9
Plasma	75.0	77.6 ± 1.2	103.4 ± 1.5
Urine	150.0	149.21 ± 4.6	99.5 ± 3.1
Plasma	150.0	145.6 ± 5.2	97.1 ± 3.6
Lactulose			
Urine	6.25	6.1 ± 0.4	97.6 ± 6.8
Plasma	6.25	6.6 ± 0.6	105.4 ± 9.1
Urine	12.5	12.1 ± 0.7	97.1 ± 6.0
Plasma	12.5	12.0 ± 0.9	95.7 ± 7.5
Melibiose			
Urine	250.0	244.9 ± 2.7	98.0 ± 1.1
Plasma	250.0	248.6 ± 3.3	99.4 ± 1.3

[a] Mean ± 2 S.D.

0.98%). Similarly, there was no significant difference in lactulose permeation between all the groups. Only the lactulose/mannitol ratio showed significant differences between the groups, and this clearly demonstrates the discriminative value of expressing intestinal permeability as a ratio of two markers.

DISCUSSION

High-performance anion-exchange chromatography coupled with pulsed electrochemical detection overcomes many of the problems previously encountered in the analysis of carbohydrates in low

TABLE II

IMPRECISION OF ESTIMATION OF MANNITOL, 3-O-METHYLGLUCOSE AND LACTULOSE IN URINE AND PLASMA FROM A CONTROL SUBJECT

Analyte	Matrix	Within batch (mean ± S.D., n = 10)		Overall (mean ± S.D., n = 20)	
		Concentration (mg/ml)	R.S.D. (%)	Concentration (mg/ml)	R.S.D. (%)
Mannitol	Urine	104.3 ± 0.42	0.4	107.8 ± 2.7	2.5
	Plasma	28.07 ± 0.193	0.69	29.7 ± 0.95	3.2
3-O-Methylglucose	Urine	226.0 ± 0.90	0.4	222.6 ± 3.9	1.8
	Plasma	29.6 ± 0.13	0.4	30.2 ± 0.8	2.7
Lactulose	Urine	3.08 ± 0.15	4.9	3.23 ± 0.18	5.6
	Plasma	5.35 ± 0.45	8.5	5.25 ± 0.29	6.8

[a] Mean ± S.D. (CV %).

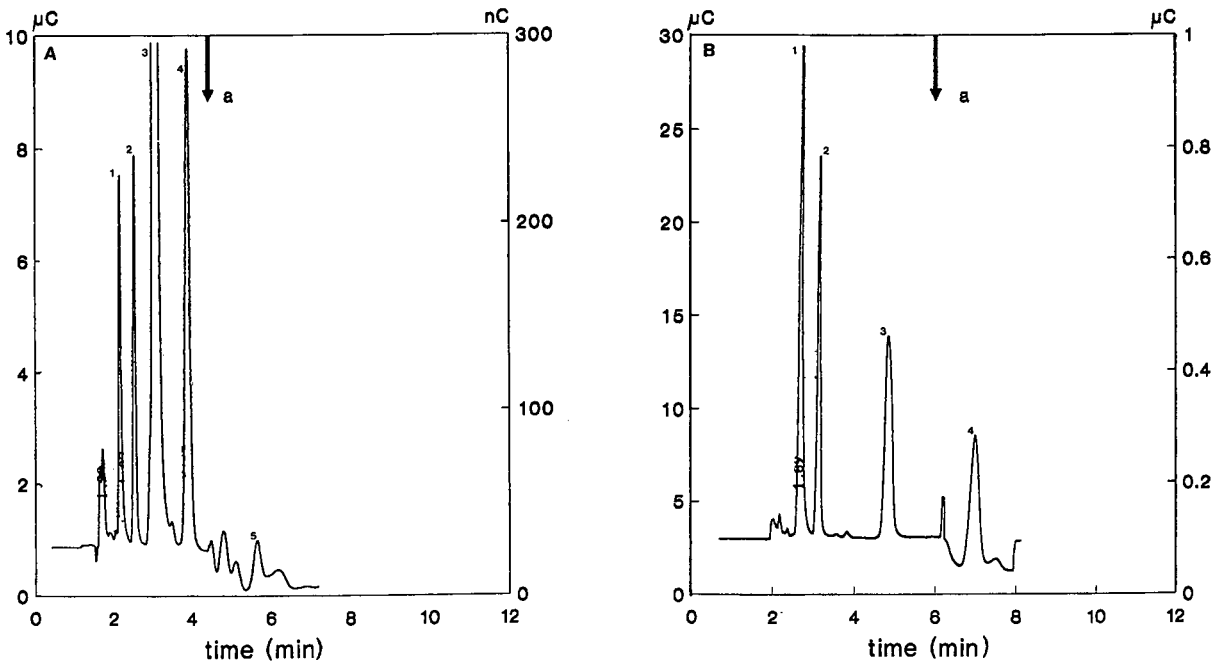

Fig. 1. (A) Chromatographic analysis of a plasma sample 90 min post sugar ingestion in a healthy subject. Eluent: 160 mmol/l sodium hydroxide, 0.675 mmol/l zinc acetate at 1 ml/min. Note sensitivity scale change at a: monosaccharides at 10 μC = disaccharides at 300 nC. Peaks (retention times of sugars in parentheses): 1 = mannitol (2.1 min); 2 = 3-O-methylglucose (2.5 min); 3 = glucose (3.2 min); 4 = melibiose (4.0 min); 5 = lactulose (5.9 min). (B) Chromatographic analysis of a 6-h urine sample post sugar ingestion in a healthy subject. Eluent: 120 mmol/l sodium hydroxide, 0.5 mmol/l zinc acetate at 1 ml/min. Note sensitivity scale change at a: monosaccharides at 30 μC = disaccharides at 1 μC. Peaks (retention times of sugars in parentheses): 1 = mannitol (2.2 min); 2 = 3-O-methylglucose (2.7 min); 3 = melibiose (4.6 min); 4 = lactulose (6.9 min).

concentrations in biological fluids. The method described here is precise, reproducible and highly sensitive. The inclusion of zinc acetate in the eluent effects separation of lactulose and lactose, a potential problem in the paediatric age group. Sample preparation is straightforward and fast for both urine and plasma samples. Analysis time is short with all the sugar probes being resolved within 10 min, enabling a large number of samples to be analyzed within one day.

The use of non-metabolized sugar probes in intestinal permeability testing is well recognized [6]. Such a test is a convenient, non-hazardous method of assessing small intestinal absorption pathways and mucosal integrity in HIV-infected subjects. The results presented here demonstrate altered small intestinal permeability in male subjects infected with HIV. Diarrhoea appears to be the major clinical correlate with intestinal mucosal damage, although an increase in permeability is seen with disease progression to AIDS.

The lactulose/mannitol test has potential application in HIV disease, and its longitudinal use may be helpful in the monitoring of progression of HIV-related intestinal damage.

REFERENCES

1 I. Cobden, R. Dickinson, J. Rothwell and A. Axon, *Br. Med. J.*, ii (1978) 1060.
2 A. Pearson, E. Eastham, M. Laker, A. Craft and R. Nelson, *Br. Med. J.*, 285 (1982) 20–21.
3 L. Juby, J. Rothwell and A. Axon, *Gut*, 30 (1989) 476-480.
4 J. S. Fordtran, P. H. Clodi, K. H. Soergal and F. J. Ingelfinger, *Ann. Intern. Med.*, 57 (1962) 883–891.
5 S. C. Fleming, M. S. Kapembwa, M. F. Laker, G. E. Levin and G. E. Griffin, *Clin. Chem.*, 36 (1990) 797–799.
6 S. Travis and I. Menzies, *Clin. Sci.*, 82 (1992) 471–488.

Journal of Chromatography, 640 (1993) 299–301
Elsevier Science Publishers B.V., Amsterdam

CHROMSYMP. 2662

Comparison of the determination of anions in dissolved organic carbon-loaded water samples by ion chromatography and photometric methods

Volker Schwartz

Bayerische Forstliche Versuchs- und Forschungsanstalt, Hohenbachernstrasse 20, W-8050 Freising (Germany)

ABSTRACT

Dissolved organic carbon (DOC) in water samples can cause strong interferences in photometric detection methods using complexing reactions. Ion chromatography was demonstrated to minimize DOC effects on the determination of anions. Further, it can be used to examine the accuracy of photometric methods by calculating the difference in the ion balance using ion chromatographic values.

INTRODUCTION

Ion chromatographic and photometric methods are often used for the routine laboratory determination of anions in water samples [1,2]. Therefore, the question arises of which method is applicable to reduce matrix effects, especially those caused by dissolved organic carbon (DOC).

EXPERIMENTAL

To answer the above question, 160 samples of seepage water prepared from lysimeters underneath the humus layer and cup lysimeters (ceramic material; installation depth 40 cm) were analysed for sulphate, chloride and nitrate by both methods. Because of the installation depth of the lysimeters, these water samples contain high concentrations of DOC ranging up to 50 ppm whereas samples prepared from cup lysimeters in the mineral soil horizon are nearly free from DOC, generally lower than 0.8 ppm [2].

Ion chromatographic detection was carried out with a Dionex 4010i instrument using micromembrane suppression (AMMS-1) and an HPIC-AS3 analytical column under standard conditions [1].

The following methods for photometric analysis with an automated wet chemistry (AWC) system were used: nitrate at 520 nm after reduction to nitrite as an azo dye [3]; sulphate at 490 nm indirectly by releasing an azo dye [1,8-dihydroxy-2-(4-sulphobenzeneazo)-naphthalene-3,6-disulphonic acid] from the corresponding thorium(IV) complex [4]; and chloride at 480 nm indirectly as iron(III) thiocyanate equivalent after reaction with mercury(II) thiocyanate [5].

RESULTS

Both the ion chromatographic and photometric methods gave accurate results for the determination of sulphate, nitrate and chloride of DOC-free cup lysimeter samples (Fig. 1). On the other hand, DOC had a strong influence on the photometric determination of sulphate and chloride. Both methods are based on complexing reactions with metal cations. As a consequence of the complexing character of DOC, high results for the determination of sulphate and chloride in samples from lysimeters containing high concentrations of DOC were found (Fig. 1).

On account of the detection wavelength (>440 nm), self-absorption of the DOC can be excluded as a reason for these high results. Because a total organic carbon analyser was not available, the DOC

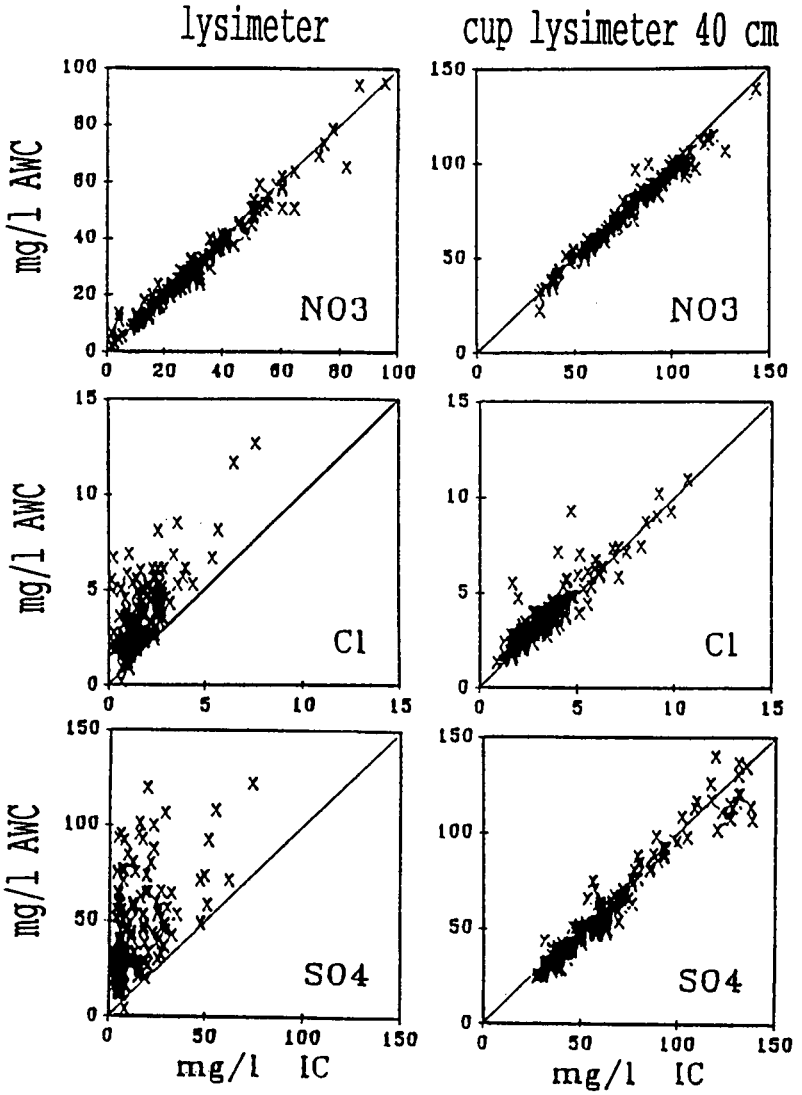

Fig. 1. Comparison of the values obtained using AWC photometric methods (AWC) and ion chromatography (IC).

content of the water samples had to be calculated indirectly as the difference in the ion balance (cations minus anions) using ion chromatographic (IC) values for the anions, inductively coupled plasma values for the cations and the pH (values not given here). The relationship between the DOC content and the overestimation of sulphate and chloride can be seen in Fig. 2.

The effect of DOC on the photometric methods can be reduced but not completely removed by solid-phase extraction with reversed-phase material because polar carbon compounds will not be adsorbed on this material.

DISCUSSION

Ion chromatography is applicable for the specific determination of anions in DOC-loaded water samples using a reversed-phase material for protection of the analytical column. The advantage of ion

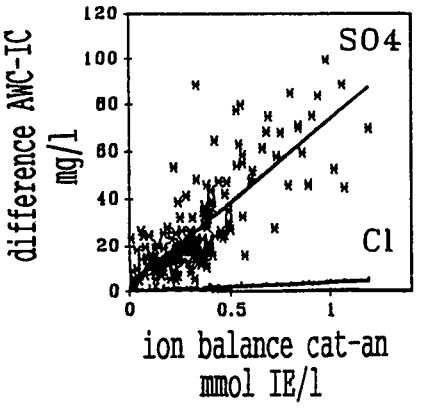

Fig. 2. Influence of DOC on the values obtained by photometric (AWC) methods (DOC calculated as the difference in the ion balance, based on IC values). cat = Cations; an = anions. IE = ion equivalent.

chromatography over photometric methods lies in its insensitivity to DOC interferences. Therefore, it is possible to calculate the relative influence of DOC on photometric methods using IC values. Finally, ion chromatography of anions produces less toxic waste than most photometric methods and is much easier to handle.

REFERENCES

1 *Deutsche Einheitsverfahren zur Wasser-, Abwasser- und Schlammuntersuchung: Anionen*, DIN 38405, Teil 19, 1988.
2 A. Mahr, T. Türck, A. Debrowolski and R. Horn, *Z. Pflanzenernähr. Bodenkd.*, 154 (1991) 369–375.
3 *Industrial Methods AAII 100-70W*, Technicon, 1973.
4 J. A. Cooper and J. M. Vernon, *Anal. Chim. Acta*, 23 (1960) 351–354.
5 K. J. Meiwes, N. König, P. K. Khana, J. Prenzel and B. Ulrich, *Berichte des Forschungszentrums Waldökosysteme/Waldsterben*, Vol. 7, Institut für Bodenkunde und Walderährung, Universität Göttingen, Göttingen, 1984.

Journal of Chromatography, 640 (1993) 303–308
Elsevier Science Publishers B.V., Amsterdam

CHROMSYMP. 2830

The role played by ion chromatography in the assessment of amines for two-phase erosion corrosion control in nuclear electric's steam–water circuits

J. C. Greene* and R. M. Donaldson

Technology Division, Nuclear Electric plc, Timpson Road, Wythenshawe, Manchester M23 9LL (UK)

ABSTRACT

Two-phase erosion corrosion is a world-wide problem and has been experienced in steam-generating plants in both Europe and the USA. In the UK, carbon steel boiler tubes in a number of Magnox Power Stations, operated by Nuclear Electric, have suffered from failures caused by two-phase erosion corrosion. Following a comprehensive investigation of the phenomenon, Nuclear Electric has solved this problem by changing to amine-dosed feedwater in place of the original ammonia treatment. This investigation included laboratory and large-scale rig studies together with a plant trial, which lead to a successful outcome.

This paper describes in detail the important part ion chromatography has played in this project. The analytical procedures are described and calibration curves are included. Examples of practical results obtained in the laboratory, in rig tests and in a plant trial are given. Further examples of cation chromatography will demonstrate application to product purity determination and thermal breakdown behaviour under simulated and real plant conditions.

INTRODUCTION

This paper describes the details of an analytical method for the measurement of amines in aqueous solution based on ion chromatography (IC). The technique was used as part of a major project to investigate a potentially expensive plant problem caused by two-phase erosion corrosion.

Two-phase erosion corrosion is a world-wide problem and has been experienced in steam-generating plants in both Europe and the USA [1,2]. In the UK, carbon steel boiler tubes in a number of Magnox Power Stations operated by Nuclear Electric have suffered failures from this phenomenon. Erosion corrosion occurs when a highly turbulent fluid comes into contact with a mild steel surface interfering with the mechanism of protective oxide film formation by removing soluble iron. It is flow dependent but also solubility dependent and can be retarded by raising the pH of the liquid flowing past the corrosion site. It is also especially prevalent at high steam qualities (*ca.* 70%, w/w) at temperatures of approximately 250°C [3]. Nuclear Electric has considerably reduced this problem by introducing amine-dosed feedwater in place of the original ammonia treatment [4–6].

The study leading to this success was conducted in four successive stages. First, a literature survey identified a large number of possible amines to be considered. The base dissociation constant and the steam–water partition coefficient of each amine were important properties to be considered in judging its suitability. Secondly, laboratory studies were directed at studying the most promising amines. Thirdly, large scale boiler rig investigations tested the effectiveness of a smaller number of the test candidate amines in controlling two-phase erosion corrosion. The boiler rig contains a full scale replication of a singe boiler tube and operates under identical operating conditions of flow, temperature, pressure and heat flux as the plant. Details of the

* Corresponding author.

0021-9673/93/$06.00

facility are available elsewhere [4]. Finally, a plant trial lasting two weeks looked at the acceptability of the chosen amine for long term use on the plant. The chosen amine, 2-amino-2-methyl propan-1-ol (AMP), replaced ammonia in the plant in September 1983. More recently, further work has identified an even better amine, 5-aminopentan-1-ol (5-AP), which has been in use in the plant since November 1992 [7]. This paper describes the role played by IC in the last three stages of this major project and concentrates on the analysis of the two amines used in the plant.

AMINE SELECTION

The required amine needed to display a number of key properties in order to be suitable for this special application. It was necessary to achieve a sufficiently high alkaline pH within the boiler at the potential corrosion sites [7]. The amines ability to achieve this is defined by both its base dissociation constant and the steam–water partition coefficient. Additionally, the amine had to be available economically in commercial quantities, to the required purity, be non-toxic and thermally stable up to the maximum boiler operating temperature of 350°C. The selected amine must also be compatible with the circuit materials including the condensate purification plant ion exchange resins [8,9].

EXPERIMENTAL

The two amines in question are water soluble and sufficiently dissociated to produce protonated amine cations and alkaline solutions. Cation-exchange chromatography, with eluent suppression and conductivity detection, was therefore chosen for the analytical chemistry part of this project.

Equipment

A Model 2000i Dionex chromatograph was used in this work. The major components of this system were a high pressure pump, two matched sample loops, columns, a micromembrane eluent suppressor, conductivity cell and meter and an 8-port sample injection valve. A Spectra-Physics Chromjet computing integrator was used for computing the results and the system operation was controlled using an Autoion 100 controller.

Analytical details

Dilute hydrochloric acid, typically 8 m*M*, was used as eluent at a flow-rate of 1.0 ml/min. Sample was injected alternately by means of two matched sample loops. Sufficient sensitivity was obtained with 0.5 ml loops and for the amine concentrations of interest (typically up to 10 ppm) there was no evidence of overloading the separator column. Satisfactory separation was obtained using a cation separating column of the CS2 type. For most applications, the smaller size guard/concentrator (CG2) columns were sufficient to give the necessary separation. Where greater resolution was required, either two CG2 columns were used in series or a CG2 followed by a CS2 was employed. Tetrabutylammonium hydroxide (TBAOH) regenerant (20 m*M*) was used in the micromembrane suppressor at a flow-rate of 2.0 ml/min. The flow-rate was achieved using a peristaltic pump. In earlier work a reservoir fitted with a CO_2 trap was used for the regenerant. For later work, however, an Autoregeneration system was used, leading to lower consumption of the expensive TBAOH. With both systems a background conductivity of less than 1 μS cm^{-1} was obtained consistently.

RESULTS AND DISCUSSION

The level of amine dosed in the plant is in the concentration range 0 to 10 ppm. Multi-level calibrations were, therefore, carried out covering this concentration range. The results of one such calibration for 5-AP are shown in Fig. 1. The calibration using peak area is linear and goes through the origin. In fitting the experimental results to a straight line equation the linear correlation coefficient was 0.9999. Using peak height, the calibration line is curved and when the experimental results are fitted to a straight line equation the linear correlation coefficient is 0.9948. In all the studies reported here, therefore, peak areas were used to determine cation concentrations.

During calibrations, an opportunity was taken to examine the precision of the method. Five successive measurements were made of a 5.0-ppm standard of AMP. A standard deviation equivalent to 0.003 ppm of AMP was obtained from these results. Further results obtained from 5-AP are given in Table I. The results show that the method is capable of

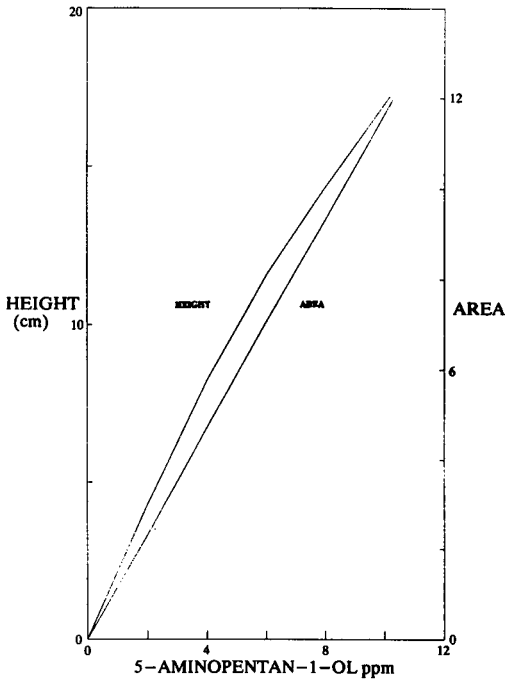

Fig. 1. Calibration for 5-aminopentan-1-ol using peak area and peak height.

good precision. The good chromatographic peak profiles together with the steady baselines obtained by the method contribute significantly to this good reproducibility.

When an analytical method is used continuously it is important to establish the required frequency of calibration. This information can be deduced from the long-term performance of the method obtained during the full scale boiler rig tests. The system was standardised with 0.5 ppm AMP and 0.58 ppm 5-AP prepared from stock 1000 ppm standards at the beginning of the test and the method was run continuously day and night. Standardisations were repeated after four and nine days with freshly prepared standards each time. The fresh 0.5 ppm AMP gave values of 0.480 ppm and 0.472 ppm, based on the original response factor, after four and nine days respectively. The corresponding values for the 5-AP were 0.568 ppm and 0.553 ppm. The causes of this gradual loss in sensitivity were not explored. One possible explanation may lie in the performance of the Autoregeneration system such that the background conductivity may rise slowly leading to a slight change in sensitivity. Nevertheless, it is clear

TABLE I

METHOD STATISTICS

Amine	Concentration (ppm)	Standard deviation (ppm)	Number of measurements
AMP	0.50	±0.003	5
5-AP	0.58	±0.003	5
5-AP	0.19	±0.0026	7

that for the method described, it is appropriate to recalibrate the analytical system at intervals of approximately every two days.

In the laboratory studies several amines were investigated and all of these amines were quantified by the IC method described. An example of the determination of ammonia, AMP and 5-AP is shown in Fig. 2. The concentrations of ammonia, AMP

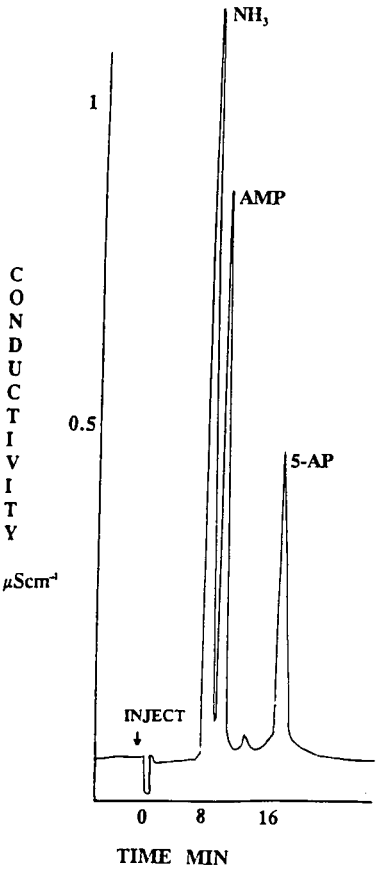

Fig. 2. Separation of ammonia, AMP and 5-AP.

and 5-AP in this example are 0.2, 0.5 and 0.5 ppm respectively. The small peak detected after the AMP has been identified as 2-aminobutan-1-ol. This compound is an impurity found in the AMP and is present in the supplied product at a concentration of approximately 3%. This example demonstrates the ability of the IC method in assess product purity.

The high temperature studies in the laboratory included measurements of the amine dissociation constant, the steam–water partition coefficient and thermal stability. Following these, the most promising candidates were selected to go forward for further evaluation on a large scale boiler rig facility. As described earlier, the boiler rig contains a full scale replication of a singe boiler tube and operates under identical operating conditions of flow, temperature, pressure and heat flux as the plant. The chromatograms shown in Fig. 3 were obtained during the four week full scale boiler rig trial. At the test section inlet, 0.5 ppm AMP was detected together with the trace of 2-aminobutan-1-ol but there was an absence of ammonia. On passing through the heated test section and flowing around the circuit to the polishing plant the fluid is diluted with pure make-up water by approximately 5%. On the basis of this dilution effect, the measured concentration of AMP at the polishing plant inlet would be expected to be 0.475 ppm. The measured concentration was 0.46 ppm AMP and this provides evidence of thermal degradation of AMP in the heated test section. The simultaneous formation of ammonia as one of the breakdown products of AMP is further evidence of this. Although the IC technique was being used primarily to quantify the amine concentration it can be seen that it is sufficiently versatile to simultaneously detect and quantify the ammonia.

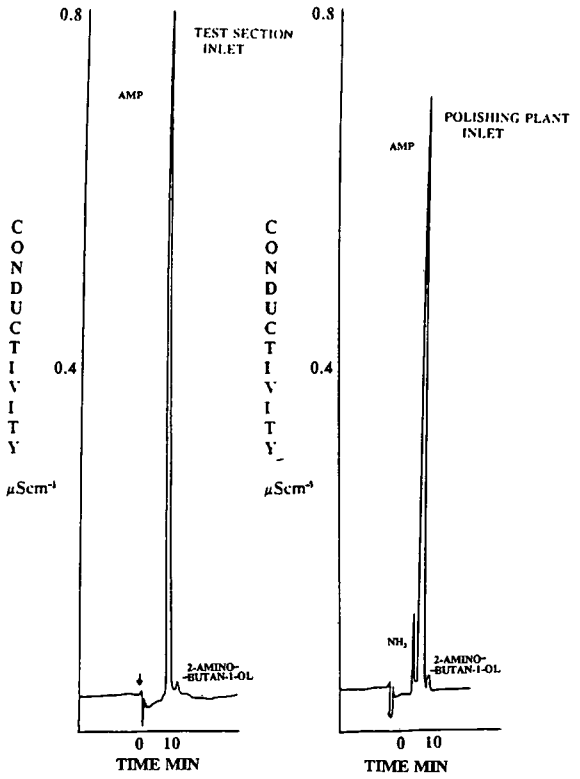

Fig. 3. Measurements of AMP during full-scale rig studies showing thermal breakdown.

Results obtained during the plant trials are shown in Fig. 4. These chromatograms were obtained when amine dosing was changed from AMP to 5-AP during the two week trial. There is good resolution between AMP and 5-AP as shown in Table II.

Further plant measurements were carried out to explore the thermal stability characteristics of the 5-AP (Fig. 5). These chromatograms of boiler inlet and steam, obtained during the 5-AP plant trial, demonstrate the stability of 5-AP. Despite a boiler inlet temperature of 130°C and boiler outlet steam temperature of 350°C and an overall residence time of approximately 5 min, no thermal breakdown products were detected. Boiler inlet and steam concentrations were identical at 6.2 ppm 5-AP.

In normal plant operation the feedwater dosing requirements are controlled and monitored continuously by direct specific conductivity measurement.

TABLE II

RESOLUTION BETWEEN AMP AND 5-AP CHANGE-OVER

Time since change-over (h)	AMP (ppm)	5-AP (ppm)
0	7	0
1	2.5	3.5
2	1	4
4	0.8	7
5	0.6	8

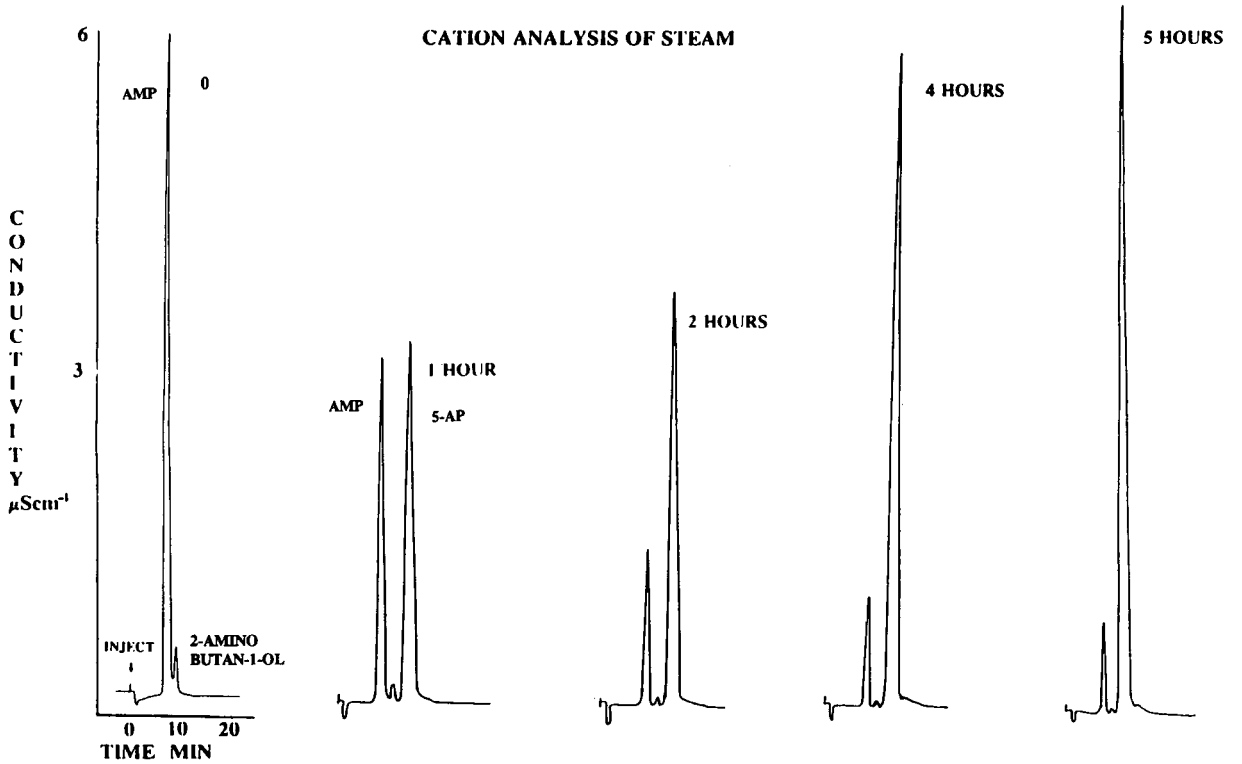

Fig. 4. Measurements taken during plant trial during change-over from AMP to 5-AP.

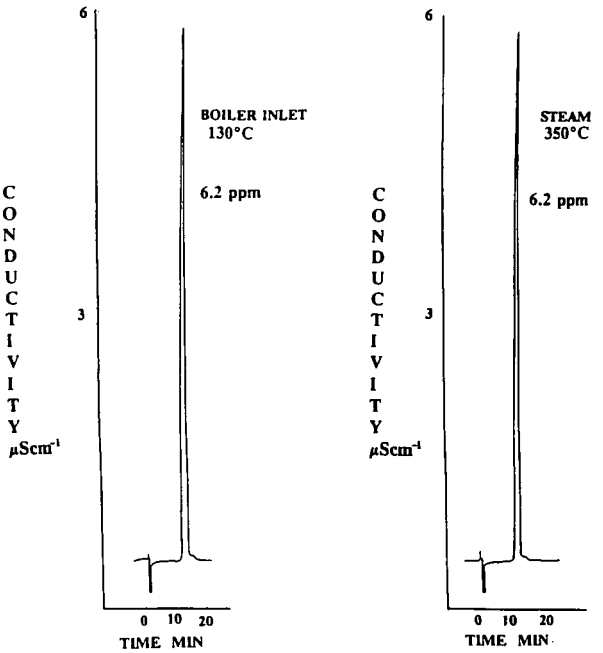

Fig. 5. Measurements made during plant trial of 5-AP to assess thermal stability (residence time *ca.* 5 min).

Experience has shown that this method is robust and reliable. Regular double-checks are made using a separate, independent analytical procedure. Prior to the adoption of continuous AMP dosing in the plan it was necessary to produce a plot relating amine concentration to specific conductivity. One such curve is shown in Fig. 6. This was produced

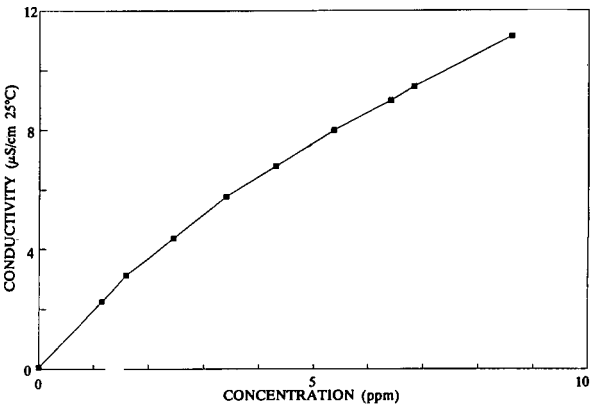

Fig. 6. Relationship between conductivity and concentration of AMP for use in continuous plant monitoring.

during boiler rig trials by dosing AMP into the ultra pure recirculating water at different dosing rates. Samples were drawn continuously, thermostatted to 25°C, through a sensitive, calibrated conductivity cell. Samples from the cell outlet were analysed by IC. More recently, a similar relationship has been established for 5-AP. These curves have been used by plant operators for routine continuous plant monitoring purposes.

CONCLUSIONS

From the foregoing description of the analytical method, it is apparent that it has played a vital role in a successful project. It is suitable for analysing a wide range of water soluble amines. The method has been shown to be sensitive and specific. Tests have been described which measured the precision of the method applied to two amines at two different concentrations. Examples have been given showing its application to the determination of multicomponent mixtures. Its full versatility was displayed in the analysis of amines covering the varied environments of the laboratory, large scale rig and power station plant. The required sensitivity and precision were achieved because of the well resolved peaks and low conductivity, stable baseline. Capable of identifying and quantifying a multicomponent cation mixture in one analysis in about 20 min, the technique was applied to product purity evaluation and thermal stability studies. The long-term performance of the method, extending over 216 h, was demonstrated in the full scale boiler rig studies and from this the calibration frequency requirements were determined.

ACKNOWLEDGEMENTS

This paper is published by permission of the Director of Technology, Nuclear Electric plc. The authors wish to acknowledge the technical contributions of their colleagues within the Company.

REFERENCES

1 C. F. Palomero and K. Garbett, *Workshop on Use of Amines in Conditioning Steam/Water Circuits, Tampa FL*, EPRI, 1991, Paper No. 34.
2 C. F. Palermo, E. Pla and K. Garbett, *BNES Conference on Water Chemistry of Nuclear Reactor Systems 3*, 1983, Vol. 1, pp. 235–242.
3 M. J. Fountain, G. S. Harrison, D. Penfold, J. C. Greene and M. A. Walker, *Proceedings of the 45th International Water Conference, Pittsburgh, PA*, 1984, pp. 393–399.
4 D. Penfold, G. S. Harrison, J. C. Greene and M. A. Walker, *BNES Conference on Water Chemistry of Nuclear Reactor Systems 4*, 1986, Vol. 1, pp. 347–353.
5 M. R. Darvill, A. J. Bates, J. C. Bates, D. J. Gardner and M. A. Sadler, *BNES Conference on Water Chemistry of Nuclear Reactor Systems 4*, 1986, Vol. 2, pp. 175–182.
6 M. J. Fountain, E. A. M. Wetton and G. G. Lewis, *Workshop on Use of Amines in Conditioning Steam/Water Circuits, Tampa, FL*, EPRI, 1991, Paper No. 33.
7 E. A. M. Wetton and G. G. Lewis, *BNES Conference on Water Chemistry of Nuclear Reactor Systems 4*, 1986, Vol. 1, pp. 355–361.
8 R. R. Harries, J. C. Bates and J. C. Greene, *BNES Conference on Water Chemistry of Nuclear Reactor Systems 5*, 1989, Vol. 1, pp. 247–255.
9 M. J. Fountain, J. C. Greene and M. G. Jones, *Workshop on Use of Amines in Conditioning Steam/Water Circuits, Tampa, FL*, EPRI, 1991, Paper No. 39.

Journal of Chromatography, 640 (1993) 309–316
Elsevier Science Publishers B.V., Amsterdam

CHROMSYMP. 2774

Ion chromatography of organic-rich natural waters from peatlands

I. Cl^-, NO_2^-, Br^-, NO_3^-, HPO_4^{2-}, SO_4^{2-} and oxalate

William Shotyk

Geological Institute, University of Berne, Baltzerstrasse 1, CH-3012 Berne (Switzerland)

ABSTRACT

Organic-rich natural waters from peat bogs in continental (Switzerland) and maritime (Shetland Islands, Scotland) areas were analysed for Cl^-, NO_2^-, Br^-, NO_3^-, HPO_4^{2-}, SO_4^{2-} and oxalate using ion chromatography. These anions can be determined simultaneously in the surface and pore water samples from the continental bogs using a 250-μl injection loop. Using this loop, the detection limits were *ca.* 5 ng/g for the monovalent anions and SO_4^{2-} and 10 ng/g for HPO_4^{2-} and oxalate. An organics-removal cartridge (Dionex OnGuard P) was used to remove humic materials. These cartridges did not significantly affect the measured concentrations of anions in blind standards. Analyses of deionized water treated with these cartridges are not significantly different from those for untreated deionized water. For the maritime bogs, the relatively high concentrations of Cl^- (more than 100 μg/g in many samples) and SO_4^{2-} (up to 50 μg/g) require two separate determinations for complete analyses. A 10-μl injection loop was used to determine Cl^-, Br^-, and SO_4^{2-}. A 250-μl injection loop was used to measure NO_2^-, NO_3^-, HPO_4^{2-} and oxalate. In each instance a Dionex OnGuard P cartridge was used to remove humic materials. In addition, a chloride-removal cartridge (Dionex OnGuard AG) was used to remove Cl^- when the larger injection loop was used. This cartridge has no significant effect on the measurement of HPO_4^{2-} at concentrations of 20 ng/g. In each of the bog water chromatograms there were usually a number of unknown peaks. These are probably due mainly to organic anions.

INTRODUCTION

The surface waters of "ombrotrophic" (rain-fed) peat bogs are isolated from the influence of groundwaters and mineral soil waters, and are fed only by atmospheric deposition [1]. Consequently, these waters contain relatively low concentrations of inorganic solids, are rich in dissolved organic matter [of the order of 100 mg/l of dissolved organic carbon (DOC)] and are acidic (pH 4). Nitrogen and especially phosphorus are thought to be the most important nutrients limiting plant growth. However, there have been relatively few reports of the concentrations of inorganic anions such as nitrate and phosphate in bog surface and pore waters [2]. The paucity of quantitative information regarding the abundance of such species in these waters may be partly due to the interference of dissolved organic compounds in the spectrophotometric determination of inorganic anions [3].

Accurate measurement of inorganic nutrient anions such as nitrate, phosphate and sulphate could be extremely helpful in ecological peatland studies. Species such as nitrite, nitrate, and sulphate in pore waters are redox indicators and their determination may be useful to describe the oxidation–reduction status of the peatland system [1]. Chloride and bromide in bog waters may be used as indicators of ionic strength or the extent of marine influence. Finally, quantitative analyses of each of the major anionic species are necessary in order to calculate the electrical charge balance of the waters:

0021-9673/93/$06.00

the total organic anionic charge is calculated as the difference between the sums of the total cationic and total inorganic anionic charges.

Traditionally, the quantitative measurement of each of these anionic species required at least as many different analytical methods as the number of species to be determined [4]. Even in a recent study of diagenesis in anaerobic sediments, the analytical methods employed to determine fluoride, chloride, nitrate, phosphate and sulphate included spectrophotometry, gravimetry, turbidity and ion-selective electrode potentiometry [5]. Clearly, the amount of time and labour required in the laboratory increase with the number of analytical methods employed.

One of the principle advantages of ion chromatography (IC) is the simultaneous determination of each of these inorganic anionic species, in addition to some organic species, in a relatively short time, with minimum sample preparation [6, 7]. The results presented here show that IC is convenient for the determination of chloride, bromide, nitrite, nitrate, phosphate, sulphate and oxalate in less than 10 min with acceptable accuracy and precision. Even in chloride-rich pore waters from bogs at maritime sites, the method can be used without modification for determinations of inorganic anions. To illustrate its applicability and reproducibility, examples of the abundance and distribution of some of the major inorganic anionic species in representative continental and maritime bog pore water profiles are presented.

EXPERIMENTAL

Locations of sites

The two continental bogs studied (Etang de la Gruyère and Tourbière des Veaux) are located in the Franches-Montagnes region of the Jura Mountains in the northwestern part of Switzerland. Lochs o' da Fleck is on the Island of Foula, *ca.* 50 km west of the main island (The Mainland) of Shetland in Scotland.

Sampling of surface waters

Water samples were collected from surface pools in clean polypropylene bottles. They were stored in a refrigerator and analysed as soon as possible after collection.

Sampling of peat pore waters

The pore waters were collected as follows. Using a Wardenaar peat profile sampler [8], a peat core *ca.* 100 × 10 × 10 cm was removed from the bog, wrapped in plastic and brought to the laboratory. The fresh core was immediately sliced using a serrated stainless-steel knife into 3-cm slices. The first slice (+3 cm to 0 cm) corresponds to the living plant material on the bog surface and the subsequent slices (in increments of 3 cm) represent peat samples varying in degree of decomposition. Each slice was placed in a plastic bag and the bag was squeezed by hand to express the pore water. The volume of pore water obtained in this way ranges from 0 to more than 100 ml, depending on the degree of decomposition of the peat.

Pore water filtration

Prior to ion chromatographic analyses, all water samples were filtered to exclude all material larger than 0.2 μm. Filtering raw peat pore waters directly through a 0.2-μm filter without pre-filtering may be extremely slow (up to 2 h for a 50-ml sample, depending on the degree of decomposition of the peats) and require several filters. To speed up this process and to minimize the number of filters required, the pore waters were first centrifuged at 5000 *g* in clean polyethylene centrifuge tubes. This procedure approximately halves the time required for filtration. The centrifuged samples were then filtered under vacuum using the sequence of nominal pore sizes 3.0, 0.8 and 0.2 μm.

All peatland water samples were injected through an organics-removal cartridge (Dionex OnGuard-P) prior to injection. This cartridge consists of polyvinylpyrrolidone and its sole purpose was to remove humic materials which otherwise would progressively damage the separation column. One cartridge was used per sample. Each cartridge was first rinsed with 4 ml of deionized water and 2 ml of sample.

Sample preservation

The measured concentrations of chloride, bromide, phosphate and sulphate are not directly affected by sample oxidation. In order to maintain the integrity of nitrite and oxalate, which are both sensitive to oxidation, however, the peat core would have had to be collected and subsampled under an

inert atmosphere such as nitrogen and the pore waters expressed and filtered under nitrogen. These capabilities were not available at the time of sample collection and preparation. Thus, by the time the samples had been filtered there may have been considerable oxidation of nitrite and oxalate. The measured concentrations of nitrite, nitrate and oxalate are not presented because they may not necessarily reflect their concentrations in the pore waters at the time of sample collection. Although the analytical method described here is suitable for the quantitative measurement of these species, improvements are required in sample collection, preparation and preservation against oxidation.

Ion chromatography

The theoretical basis for the quantitative measurement of anions using ion chromatography has been described in detail [6,7]. All anion analyses were performed using a Dionex 4500i ion chromatographic system with Dionex columns, conductivity detector and computer interface. The entire system was operated using the Dionex AutoIons program (version 3.2). The anions were separated on an AS4A separation column after an AG4A guard column and the background conductivity of the eluent was suppressed using an AMMSII membrane suppressor. The suppressor was continuously regenerated using an anion membrane suppressor regenerant cartridge and 50 m*M* H_2SO_4.

The eluent used was 1.8 m*M* Na_2CO_3–1.7 m*M* $NaHCO_3$, which allows the separation and determination of Cl^-, NO_2^-, Br^-, NO_3^-, HPO_4^{2-}, SO_4^{2-} and oxalate. Analytical-reagent grade Na_2CO_3 and $NaHCO_3$ (Merck) were used to prepare the eluent. All standards were prepared using 18 MΩ deionized water. Merck 1000 mg/l anion standards were used for all of the anion standards except oxalate, which was prepared from oxalic acid dihydrate (Merck). All standards were prepared in clean polypropylene bottles and stored in a refrigerator. Fresh standards were prepared prior to each set of pore water analyses.

For continental bog waters, a 250-μl injection loop was employed and the instrument was calibrated with 20, 50, 250 and 1000 ng/g (ppb) mixed anion standards (Cl^-, NO_2^-, Br^-, NO_3^-, HPO_4^{2-}, SO_4^{2-} and oxalate). The linearity of the standards over this concentration range was excellent (r^2 = 0.999 or better for each species).

For maritime bog waters with Cl^- concentrations up to 100 μg/g (ppm), two separate runs were required. In each instance an OnGuard P cartridge was used to remove humic materials. For Cl^-, Br^- and SO_4^{2-}, a 10-μl injection loop was used and the instrument was calibrated with 10, 50 and 100 μg/g Cl^-, 2, 10 and 50 μg/g SO_4^{2-} and 0.1, 0.5 and 2.5 μg/g Br^-. These standards also contained 0.1, 0.5 and 2.5 μg/g NO_3^- and HPO_4^{2-} because the pore waters closest to the surface (the plant rooting zone) contain elevated concentrations of these species. Thus, in near-surface pore waters all of the anions of interest can be determined in a single run. For NO_2^-, NO_3^-, HPO_4^{2-} and oxalate in deeper pore waters, a 250-μl injection loop was used and the instrument was calibrated with 10, 20, 50, 250 and 1000 ng/g standards. In this instance, a chloride-removal cartridge (Dionex OnGuard AG) was used to remove Cl^-. Again, the linearity of the standards was excellent in each instance (r^2 = 0.999 or better).

RESULTS

Continental bog waters

Typical chromatograms of standards and samples. A typical chromatogram of a 100 ng/g anion standard is shown in Fig. 1a. The first peak is F^-, followed by Cl^-, NO_2^-, Br^-, NO_3^-, HPO_4^{2-}, SO_4^{2-} and oxalate.

A typical chromatogram for a peatland water sample is shown in Fig. 1b. Note that there are more peaks (and therefore more anions) in this chromatogram compared with the standard. These additional peaks are probably due to organic anions and were consistently seen in most of the chromatograms of bog water samples. In general they are clearly separated from the inorganic anions of interest and do not interfere with their measurement. However, the peak at 1.2 min which appears to be F^- (Fig. 1b) is actually F^- plus some organic anions (probably formate plus acetate, propionate, butyrate and lactate, but possibly also some others) which co-elute using the carbonate–hydrogenbicarbonate eluent.

The chemical complexity of these waters can be illustrated using a weaker (borate) eluent. For example, using a gradient elution ranging from 7 to 21 m*M* $Na_2B_4O_7$, as many as 30 anionic species were found in a chromatogram of bog water (Fig. 2).

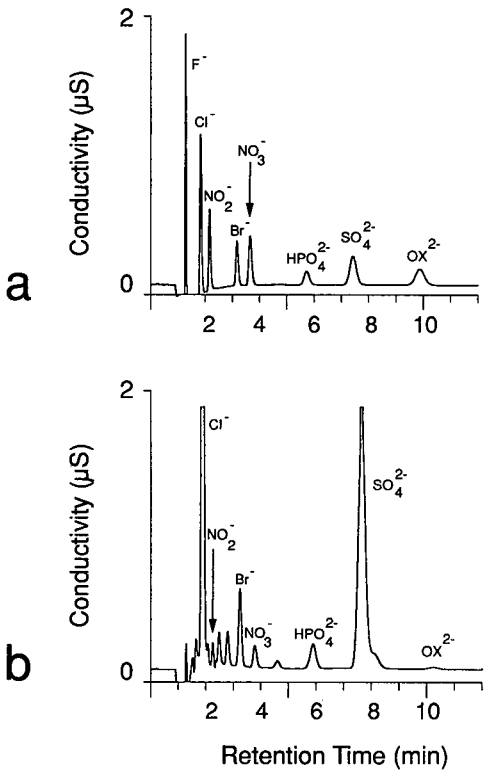

Fig. 1. (a) Chromatogram of a 100 ng/g anion standard using a 250 μl injection loop. (b) Chromatogram of a pore water sample squeezed from peat 6–9 cm below the bog surface of La Tourbière des Veaux. Concentrations (ng/g) were as follows: Cl^-, 1413 ± 37; NO_2^-, not determined; Br^-, 220 ± 15; NO_3^-, 83 ± 1; HPO_4^{2-}, 198 ± 2; SO_4^{2-}, 824 ± 20; oxalate, not determined. The peaks before chloride include fluoride plus some organic anions. No attempt was made to determine fluoride. The other unknown peaks (between NO_2^- and Br^-, between NO_3^- and HPO_4^{2-} and the shoulder on SO_4^{2-}) are probably organic anions.

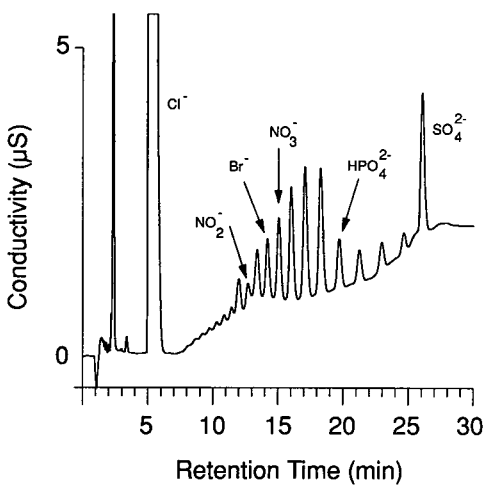

Fig. 2. Chromatogram of bog water using a borate gradient. The two eluents consisted of deionized water (E_1) and 70 m*M* $Na_2B_4O_7 \cdot 10\,H_2O$ (E_2). The gradient was performed as follows: 90% E_1 from 0.0 to 10.0 min; decreased to 80% E_1 from 10.0 to 20.0 min; decreased to 70% E_1 from 20.0 to 25.0 min; held at 70% E_1 from 25.0 to 30.0 min; increased to 90% E_1 from 30.0 to 35.0 min. The chromatogram shown corresponds to a pore water (36–39 cm) from La Tourbière des Veaux. In addition to the species identified in the figure, formate and glycolate were found. The other peaks have not yet been identified.

Approximately ten peaks are seen before Cl^- elutes and another 20 peaks before SO_4^{2-}. Except for the inorganic anions plus glycolate and formate, most of these peaks have not yet been identified.

Changing retention times. During the analyses of peatland waters the retention times of the anions typically decreased slightly with time, compared with those of the standard. This may be due to the presence of dissolved organic material in the peatland water samples adsorbing on the resin of the separation column and slightly changing its anion retention properties. In order to confirm the retention times of the anions, a blind standard was injected in triplicate after every tenth sample injection.

Effect of organics removal cartridge. A 1000 ng/g anion standard was analysed in triplicate before and after filtration through an OnGuard-P humics-removal cartridge and the results are given in Table I. The anion concentrations in the anion standard that had been passed through a rinsed OnGuard-P cartridge were not significantly different from the concentrations in the corresponding standard that had not been filtered through an OnGuard-P cartridge. Hence the OnGuard-P cartridge does not appear to contribute any significant error to the analyses of anions in peatland waters.

Analyses of blanks. The deionized water used in the laboratory was analysed after calibrating the instrument with 1, 2, 5 and 10 ng/g standards. In the deionized water only chloride (*ca.* 3 ng/g) and nitrate (*ca.* 1 ng/g) were measurable. The concentrations of anions in a sample of this water filtered through a rinsed OnGuard-P organics-removal cartridge were not significantly different from those in

TABLE I

EFFECT OF ONGUARD P PRETREATMENT CARTRIDGE ON MEASURED ANION CONCENTRATIONS

Anion	Concentration (ng/g)[a]	
	No filter	OnGuard P
Cl^-	1024 ± 14	1025 ± 19
NO_2^-	1005 ± 19	991 ± 10
Br^-	948 ± 19	935 ± 22
NO_3^-	992 ± 9	981 ± 36
HPO_4^{2-}	985 ± 2	982 ± 4
SO_4^{2-}	992 ± 2	993 ± 4
Ox^{2-}	987 ± 1	986 ± 7

[a] Mean ± S.D. (n = 3).

the unfiltered deionized water. Hence the organics-removal filters used did not contribute significantly to the measured anion concentrations.

Sensitivity and limits of detection. Using the 250-μl injection loop, the anions Cl^-, NO_2^-, Br^-, NO_3^- and SO_4^{2-} can be measured down to *ca.* 1–2 ng/g and HPO_4^{2-} and oxalate down to 5 ng/g. Hence the limits of detection were *ca.* 5 ng/g for the first group of anions and 10 ng/g for phosphate and oxalate. Using this injection volume, each of these anions is easily quantified even in dilute natural waters such as rain water (Fig. 3). Because the concentrations of inorganic anionic species in peatland waters generally are significantly higher than the limits of detection, the sensitivity of the method is not expected to restrict its application. In some deep pore water samples, concentrations of phosphate as low as 10 ng/g were observed. However, a larger injection loop (500 μl or more) may be used in such instances to improve the detection limit for this species further.

Analytical procedure variability. An estimate of the analytical procedure variability was made by analysing a blind working standard (250 ng/g) in triplicate after every tenth injection. These results were pooled to calculate the mean ± one standard deviation for nine analyses: Cl^-, 245 ± 10; Br^-, 281 ± 10; NO_3^-, 249 ± 29; HPO_4^{2-}, 255 ± 8; SO_4^{2-}, 274 ± 11 ng/g.

Precision of pore water analyses. The reproducibility of the analyses is best illustrated by comparing the results of the duplicate pore water analyses.

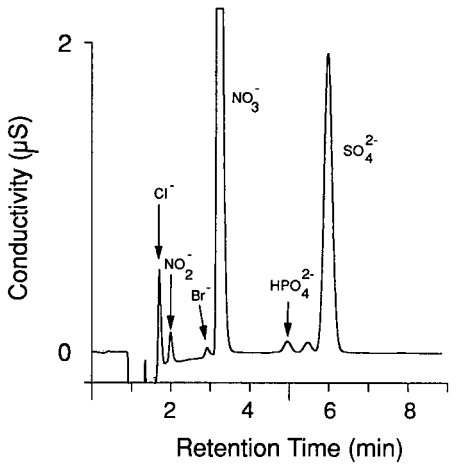

Fig. 3. Chromatogram of rain water collected in Berne on 31.10.91. Concentrations (ng/g) are as follows Cl^-, 17; NO_2^-, 51; Br^-, 5, NO_3^-, 1329; HPO_4^{2-}, 50; and SO_4^{2-}, 519. Cl^-, NO_2^-, Br^- and HPO_4^{2-} were determined using a single-point calibration against a 20 ng/g standard. NO_3^- and SO_4^{2-} were calculated using a three-point linear calibration (50, 250 and 1000 ng/g standards).

The vertical distribution of the four major anions in the pore waters at Etang de la Gruyère are shown in Fig. 4. The average standard deviations of the 35 duplicate pairs were estimated according to ASTM Designation D 4210 [4] and are Cl^-, 40; Br^-, 39; HPO_4^{2-}, 26 and SO_4^{2-}, 13 ng/g.

The reproducibility was generally good except for Br^- at depths between 20 and 30 cm and HPO_4^{2-} in the deeper layers (Fig. 4). The relatively large variation in Br^- in some of the samples may be due to the combined effect of changing retention times and relatively abundant (organic?) anions in the pore waters causing incorrect peak identification. In pore waters expressed from strongly decomposed peats, the position of the Br^- peak should be confirmed regularly with spiked samples. The relatively large variation in HPO_4^{2-} may be due to the instability of phosphate in Fe-rich anoxic water samples exposed to the air [9]. Subsequent studies of these pore waters maintained in an anoxic condition have yielded significantly higher concentrations of HPO_4^{2-} [10].

Maritime bog waters

Effect of chloride-removal filter. A typical chromatogram for a 250-μl injection without a chloride removal cartridge is shown in Fig. 5a. A chromato-

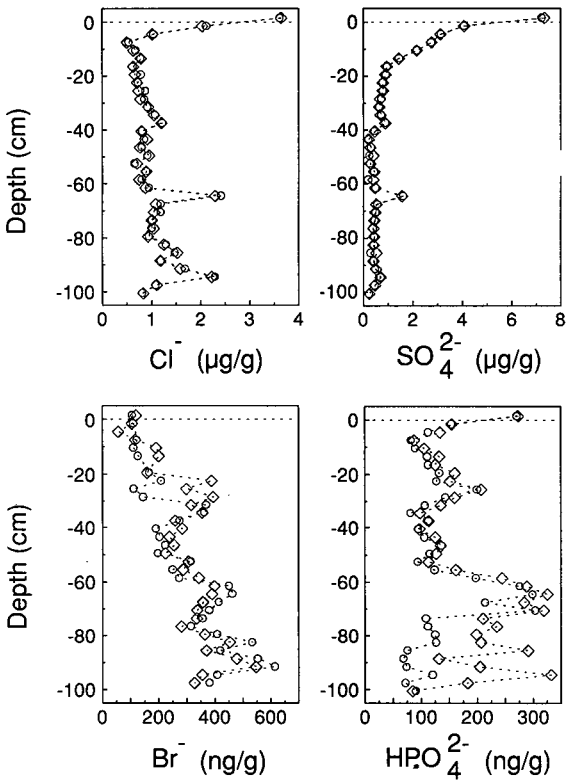

Fig. 4. Major anions (Cl^-, SO_4^{2-}, Br^-, HPO_4^{2-}) in pore waters at Etang de la Gruyère. The circles and squares represent two separate sets of analyses (duplicates). The poor reproducibility for Br^- at a depth of 30 cm may be due to interfering unknown (organic) anions. The poor reproducibility for HPO_4^{2-} from 70 to 100 cm may be due to the oxidation of Fe^{2+} during sample handling (see text).

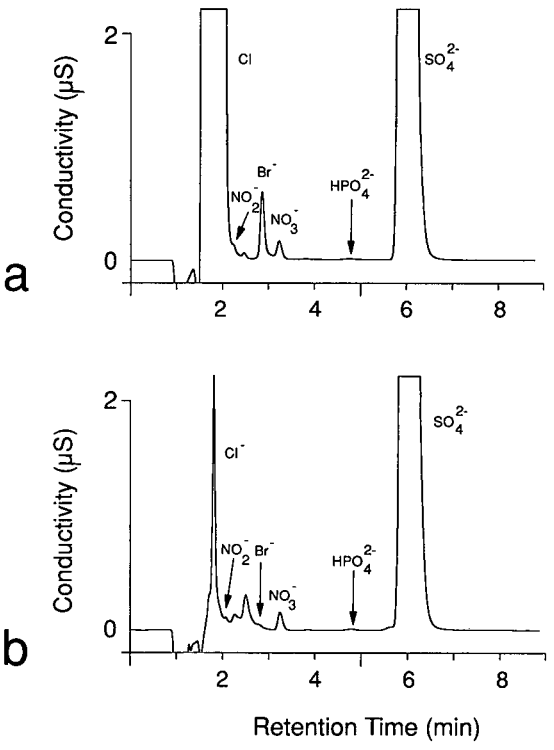

Fig. 5. Effect of chloride-removal cartridge (Dionex OnGuard AG) on maritime bog waters (250-μl injection). (a) No cartridge. Concentrations were *ca.* 95 μg/g Cl^-, 24 ng/g NO_3^-, 16 ng/g HPO_4^{2-} and 16 μg/g SO_4^{2-}. (b) Same sample as in (a), but filtered through an OnGuard AG cartridge. Measured concentrations of nitrate, phosphate and sulphate were not significantly different.

gram of a sample that had been passed through a chloride-removal cartridge prior to injection is shown in Fig. 5b. To evaluate the effect of the cartridge on the measurement of low concentrations of phosphate, a blind standard containing 20 ng/g of phosphate was analysed seven times with and without a cartridge. The measured phosphate concentrations were 22.9 ± 1.6 and 20.8 ± 2.2 ng/g, respectively. Therefore, although this cartridge successfully removes most of the chloride, it has no significant effect on the measurement of phosphate at the concentrations present in the bog pore waters.

A representative chromatogram for a 10-μl injection of a maritime bog water is shown in Fig. 6a. In the near-surface samples, nitrate and phosphate may be measured, in addition to Cl^-, Br^- and SO_4^{2-}. A chromatogram for a 250-μl injection of a maritime bog water filtered through an OnGuard AG chloride-removal cartridge is shown in Fig. 6b. Both nitrate and phosphate were conveniently measured with this method at concentrations down to 10 ng/g.

Analytical procedure variability. After every tenth injection a blind standard containing 50 μg/g Cl^-, 10 μg/g SO_4^{2-} and 250 ng/g Br^- was analysed in triplicate. These results were pooled to calculate the mean ± one standard deviation for the six analyses: Cl^-, 50.6 ± 1.6 μg/g; SO_4^{2-}, 9.6 ± 0.0 μg/g; and Br^-, 270 ± 17 ng/g.

Precision of the pore-water analyses. The reproducibility of the methods is best assessed from duplicate analyses of the four major anions in the pore

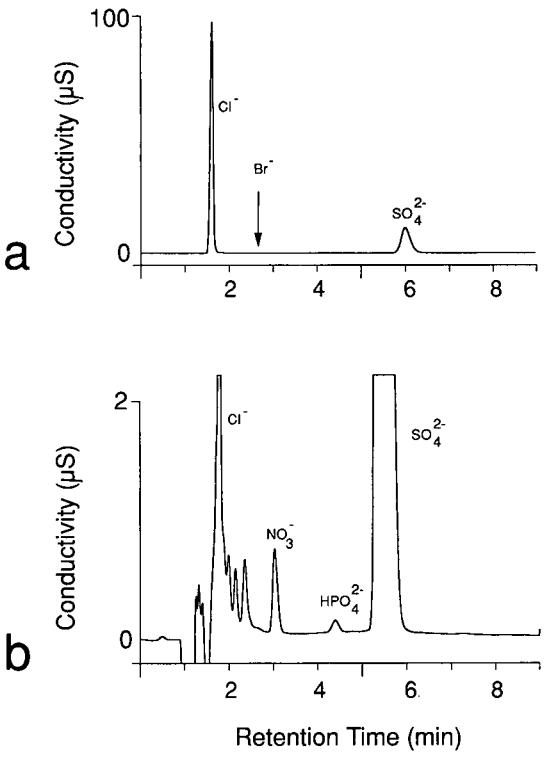

Fig. 6. Chromatograms of surface water from a Lochs o' da Fleck. (a) 10-μl injection for Cl^-, Br^- and SO_4^{2-}. In subsurface samples (plant rooting zone), nitrate and phosphate concentrations are significantly higher than deeper in the profile and can be measured in the same run. (b) 250-μl injection through an On-Guard AG chloride-removal cartridge for the determination of nitrate and phosphate.

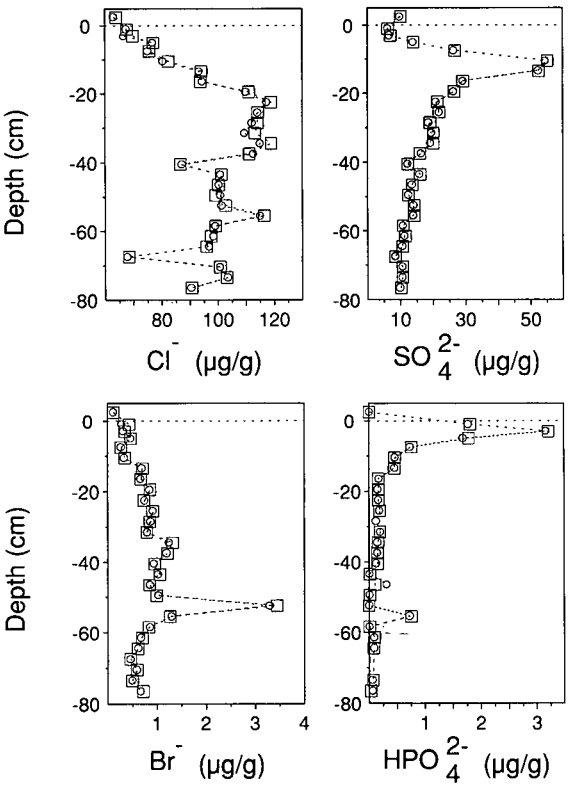

Fig. 7. Major anions (Cl^-, SO_4^{2-}, Br^-, HPO_4^{2-}) in pore waters at Lochs o' da Fleck. The circles and squares represent two separate sets of analyses (duplicates).

waters at the Lochs o' da Fleck (Fig. 7). The average standard deviations of the 27 duplicate pairs estimated according to the ASTM Designation D 4210 [4] are as follows: Cl^-, 0.7 μg/g; SO_4^{2-}, 0.1 μg/g; Br^-, 15 ng/g; and HPO_4^{2-}, 11 ng/g.

The precision of Br^- in these samples was much better than in the continental bog waters because the Br^- concentrations were significantly higher (owing to sea spray).

CONCLUSION

The dominant inorganic anions in peatland waters (Cl^-, Br^-, NO_3^-, HPO_4^{2-} and SO_4^{2-}) plus nitrite and oxalate may be measured rapidly (in less than 10 min) and with adequate sensitivity and precision using ion chromatography. An organics-removal cartridge was used to filter the water prior to injection, but appeared to have no significant effect on the measured anion concentrations. In addition, for nitrate and phosphate determination in chloride-rich bog waters from marine sites, a chloride-removal cartridge was used prior to injection. However, this cartridge has no significant effect on measured phosphate concentrations down to 20 ng/g.

A large number of unknown anionic species in the bog waters eluted when a weak (borate) gradient was used. These are probably organic anions. The size of these peaks compared with those for the inorganic anions suggests that they also may be important constituents of the waters. Further studies are in progress to identify them.

ACKNOWLEDGEMENTS

I am indebted to Professor Albert Matter of this Institute for generously providing all of the required laboratory facilities and equipment. Additional financial support from the Canton of Berne (SEVA Lottofonds) and the Swiss National Science Foundation (Grant 21-30207.90) is also sincerely appreciated. Mr. Philipp Steinmann helped to collect the peat cores and Ms. Jill Engi skillfully prepared all of the samples and standards. Professor Teodoro Miano of the University of Bari performed the borate gradient chromatography shown in Fig. 2. Finally, I thank colleagues at Henry A. Sarasin AG for expert technical support with all aspects of the ion chromatography.

REFERENCES

1 W. Shotyk, *Earth-Sci. Rev.*, 25 (1988) 95.
2 W. Shotyk, *Water Qual. Bull.*, 14 (1989) 47.
3 E. Gorham and N.E. Detenbeck, *J. Ecol.*, 74 (1986) 899.
4 American Society for Testing and Materials, *Annual Book of ASTM Standards*, Vols. 11.01 and 11.02, ASTM, Philadelphia, PA, 1991.
5 P. D. Rude and R. C. Aller, *Geochim. Cosmochim. Acta*, 55 (1991) 2491.
6 H. Small, *Ion Chromatography*, Plenum Press, New York, 1989.
7 J. Weiss, *Handbook of Ion Chromatography*, Dionex, Sunnyvale, CA, 1986.
8 E. C. P. Wardenaar, *Can. J. Bot.*, 65 (1987) 1772.
9 W. B. Lyons, H. E. Gaudette and G. M. Smith, *Nature*, 277 (1979) 48.
10 P. Steinmann, *Ph.D. Thesis*, in preparation.

Journal of Chromatography, 640 (1993) 317–322
Elsevier Science Publishers B.V., Amsterdam

CHROMSYMP. 2669

Ion chromatography of organic-rich natural waters from peatlands

II. Na^+, NH_4^+, K^+, Mg^{2+} and Ca^{2+}

William Shotyk

Geological Institute, University of Berne, Baltzerstrasse 1, CH-3012 Berne (Switzerland)

ABSTRACT

Organic-rich natural waters from peat bogs in continental (Switzerland) and maritime (Shetland Islands, Scotland) environments were analysed for Na^+, NH_4^+, K^+, Mg^{2+} and Ca^{2+} using ion chromatography. These cations were determined simultaneously in surface and pore water samples from the continental bogs using a 250-μl injection loop in an isocratic separation. Using this loop, detection limits of the order of 1 ng/g were achieved. An organics-removal cartridge (Dionex OnGuard P) was used to remove humic materials. Analyses of deionized water filtered through these cartridges showed acceptably low blank values (*e.g.*, *ca.* 5 ng/g) and appeared to have no significant effect on the measured cation concentrations. For the maritime bog waters, the low concentrations of NH_4^+ (*ca.* 1 μg/g) compared with Na^+ (*ca.* 100 μg/g) required improved peak separation. This was accomplished by using a gradient separation beginning with 40 m*M* HCl–1 m*M* D,L-2,3-diaminopropionic acid monochloride (DAP) and switching to 40 m*M* HCl–12 m*M* DAP after 2 min. Using a 25-μl injection loop, Na^+, NH_4^+, K^+, Mg^{2+} and Ca^{2+} were determined simultaneously in less than 25 min. In this instance, even with $Na^+/NH_4^+ > 100$, there was no interference from Na^+ in the determination of NH_4^+ (baseline separated).

INTRODUCTION

The surface waters of "ombrotrophic" (rain-fed) peat bogs are isolated from the influence of groundwaters and mineral soil waters, and are fed only by atmospheric deposition [1]. As a result, Ca concentrations are relatively low, typically of the order of 1 mg/l or less, and sodium is the dominant cation. In "minerotrophic" (groundwater-fed) peatlands such as fens and swamps, Ca concentrations are much higher and Ca is the dominant cation [2]. By measuring the concentration of Ca in peatland surface waters, ombrotrophic bogs may be distinguished from minerotrophic fens and swamps. Thus, the concentration of Ca has become one of the most important criteria for describing the trophic status of peatlands.

Unfortunately, the utility of Ca measurements has given rise to extensive interest in this element at the expense of other major metallic cations. For example, very little is known about the geochemistry of K and Mg in peatland ecosystems. Analyses for each of the major cationic species are necessary in order to calculate the electrical charge balance of the waters; the total cationic charge is needed to calculate the total inorganic anionic and organic anionic charges. Because peatlands are anaerobic below the water table, ammonium may also be a quantitatively important cation. In addition, the determination of ammonium may be helpful for describing the oxidation–reduction status of the peatland system [1].

Today, Na, K, Mg, and Ca are usually determined using either atomic absorption spectrometry

0021-9673/93/$06.00

(AAS) to measure the metal concentrations one at a time, or inductively coupled plasma spectrometry (ICP) to measure the metals simultaneously. Ammonium is typically determined using ion-selective electrode potentiometry, which measures the concentration of free ammonium [3]. One of the principle advantages of ion chromatography (IC) is the possibility of determining each of these cationic species simultaneously, in a relatively short time, with minimum sample preparation [4,5]. The use of IC has already been applied to measurements of Na^+, NH_4^+, K^+, Mg^{2+}, Ca^{2+} in dilute natural waters such as rainwater [6].

The results presented here show that IC is a convenient method for the determination of Na^+, NH_4^+, K^+, Mg^{2+} and Ca^{2+} in organic-rich peatland waters. Even in bog waters in maritime areas with more than 100 ppm of sodium, NH_4^+ can be clearly separated from Na^+, allowing all five cations to be determined in less than 25 min. To illustrate the applicability and reproducibility of the methods, examples of the abundance and distribution of these cations in representative bog pore water profiles are presented.

EXPERIMENTAL

Locations of sites

The two continental bogs studied (Etang de la Gruyere and Tourbière des Veaux) are located in the Franches-Montagnes region of the Jura Mountains in the northwestern part of Switzerland. Fleck o' da Lochs is on the Island of Foula, approximately 50 km west of the main island ("The Mainland") of Shetland in Scotland.

Sampling of waters and sample preparation

The sampling and sample handling procedures have been described elsewhere [7].

Ion chromatography

The theoretical basis for the determination of cations using IC has been described in detailed in several recent books [4,5]. All cation determination were performed using a Dionex 4500i IC system with Dionex columns, conductivity detector and computer interface. The entire system was operated using the Dionex AutoIons program (version 3.2). The cations were separated on a CS10 separation column after a CG10 guard column and the background conductivity of the eluent was suppressed using a CMMSII membrane suppressor. The suppressor was continually regenerated using 100 m*M* tetramethylammonium hydroxide (Fluka, Buchs, Switzerland).

The eluent and all standard solutions were prepared using 18-MΩ deionized water. Merck 1000 mg/l cation stock standard solutions were used to prepare all of the cation working standard solutions. All working standard solutions were prepared in clean polypropylene bottles and stored in a refrigerator. Fresh standard solutions were prepared prior to each set of pore water analyses.

Isocratic separation of cations in continental waters. The eluent was 40 m*M* HCl–12 m*M* D,L-2,3-diaminopropionic acid monochloride (DAP) (Fluka), which allows the separation and determination of Na^+, NH_4^+, K^+, Mg^{2+} and Ca^{2+}. For continental bog waters, a 250-μl injection loop was employed and the instrument was calibrated with 20, 50, 250, and 1000 ng/g (ppb) mixed cation standards (Na^+, NH_4^+, K^+, Mg^{2+} and Ca^{2+}) using linear regression. The linearity of the calibration graph for each of the cations over this concentration range was excellent ($r^2 = 0.999$ or better).

Gradient separation of cations in maritime waters. This was accomplished using a gradient beginning with 40 m*M* HCl–1 m*M* DAP (E_1) and switching to 40 m*M* HCl–12 m*M* DAP (E_2) as follows: 0.0–2.0 min, E_1; 2.0–4.0 min, switching to E_2; 4.0–15.0 min, E_2; 15.0–17.0 min, switching to E_1; 17.0–25.0 min, E_1. The last step (17–25 min) is simply a rinse following the elution of Ca^{2+}. This step was necessary to ensure reproducible separation of the monovalent cations in the following sample. Although 5 m*M* HCl–4 m*M* DAP can also be used as E_1, the difference in background conductivities (E_1 *versus* E_2) was much greater.

Using a 25-μl injection loop, the instrument was calibrated with the following standards: 10, 20, 50, 100 μg/g (ppm) Na^+; 1, 5, 10, 20 μg/g Mg^{2+}; 0.1, 0.5, 2.0, 10.0 μg/g NH_4^+, K^+ and Ca^{2+}. Again, linear regression was used to calculate the calibration graphs and the fit was excellent ($r^2 = 0.999$ or better).

RESULTS

Continental bog waters

Typical chromatograms of standards and samples. A typical chromatogram of a 500 ng/g cation standard is shown in Fig. 1a. The first peak is Na^+, followed by NH_4^+, K^+, Mg^{2+} and Ca^{2+}. A representative chromatogram of a subsurface bog pore water sample is shown in Fig. 1b. Note that NH_4^+ is by far the dominant cation in the bog pore water.

Effect of organics-removal filter. A 1000 ng/g cation working standard was analysed in triplicate before and after filtration through an OnGuard-P humics-removal cartridge and the results are given in Table I. The cation concentrations in the cation standard which has been passed through a rinsed OnGuard-P cartridge are not significantly different from those in the corresponding standard which has not been so filtered. Hence the use of the organics-removal cartridge has no significant effect on the measured cation concentrations.

Analyses of blanks. The deionized water was analysed after calibrating the instrument with 1, 2, 5 and 10 ng/g standards. In the deionized water only Mg^{2+} (<1 ng/g) and Ca^{2+} (<2 ng/g) peaks are visible. Five deionized water samples filtered through a rinsed OnGuard-P organics-removal cartridge yielded concentrations of Na^+ 5.3 ± 0.6, NH_4^+ 5.9 ± 0.5, Mg^{2+} 2.5 ± 1.0 and Ca^{2+} 3.5 ± 1.3 ng/g. These concentrations are well below the lowest concentrations measured in the bog waters and represent acceptable blank values.

TABLE I

EFFECT OF ONGUARD P PRE-TREATMENT CARTRIDGE ON MEASURED CATION CONCENTRATIONS

A 1000 ng/g working standard was analysed in triplicate with and without an OnGuard P cartridge.

Cation	Concentration (ng/g)	
	No filter	OnGuard P
Na^+	999 ± 12	1028 ± 47
NH_4^+	947 ± 35	992 ± 7
K^+	1009 ± 9	1010 ± 14
Mg^{2+}	1000 ± 9	1003 ± 5
Ca^{2+}	991 ± 12	1013 ± 8

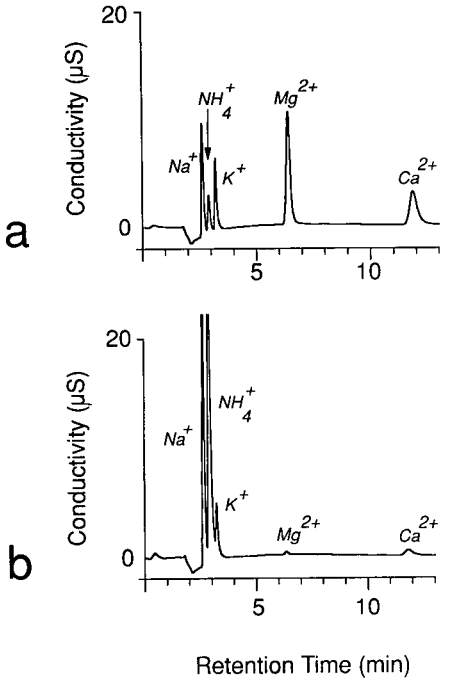

Fig. 1. Chromatograms of (a) a 500 ng/g cation standard using a 250-μl injection and (b) a pore water sample (90–93 cm) from Etang de la Gruyère.

Sensitivity and limits of detection. Under ideal operating conditions and using the 250-μl injection loop, the limit of detection of each of the cations is *ca.* 1 ng/g. Hence, the limits of determination are *ca.* 2 ng/g. One example of the sensitivity of the method is the measurement of each of the cations in dilute natural waters such as rainwater (Fig. 2). However,

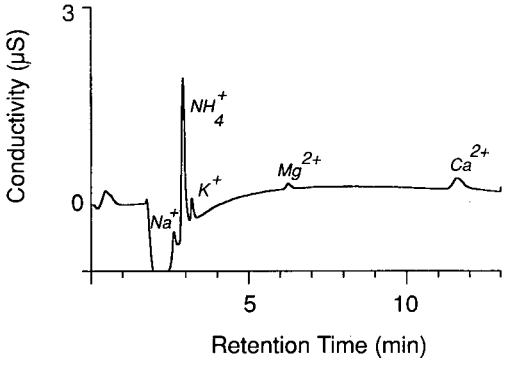

Fig. 2. Chromatogram of rainwater collected in Berne on 31.10.91. The average measured concentrations ± one standard deviation of the water analysed in triplicate are Na^+ 7 ± 1, NH_4^+ 265 ± 3, K^+ 24 ± 1, Mg^{2+} 5 ± 1 and Ca^{2+} 25 ± 0 ng/g.

the concentrations of inorganic cationic species in peatland waters are generally much higher than the limits of detection. Hence, the sensitivity of the method is certainly adequate for measurements of cations in bog waters.

Variability of analytical procedure. An estimate of the variability of the analytical procedure was made by analysing a blind working standard (500 ng/g) in triplicate after every tenth injection. These results were pooled to calculate the mean ± one standard deviation for fifteen analyses of the 500 ng/g working standard: Na^+, 511 ± 19; NH_4^+, 518 ± 37; K^+, 489 ± 21; Mg^{2+}, 508 ± 12; Ca^{2+}, 496 ± 7 ng/g.

Precision of pore water analyses. The precision of the pore water analyses is most clearly illustrated by examining the reproducibility of duplicate analyses of the dominant cations in the pore waters (Fig. 3). The average standard deviations of the 35 duplicate pairs were estimated according to ASTM Designation D 4210 [3] and are Na^+ 17.3, NH_4^+ 71.1, K^+ 9.5, Mg^{2+} 4.3 and Ca^{2+} 8.8 ng/g.

Maritime bog waters

Typical chromatograms of standards and samples. A sample of bog surface water from an Irish bog analysed using the isocratic separation of cations is shown in Fig. 4a. In this instance, the NH_4^+ peak (*ca.* 5 μg/g) is masked by that of Na^+ (*ca.* 27 μg/g). At higher Na^+/NH_4^+ ratios the separation becomes increasingly poor.

Examples of chromatograms obtained using the gradient method are shown in Fig. 4b and c. A chromatogram of a standard containing 100 μg/g of Na^+ and 10 μg/g of NH_4^+ shows that the two peaks are clearly separated (Fig. 4b). In this instance, with $Na^+/NH_4^+ > 10$, there is no interference of Na^+ (3.1 min) in the determination of NH_4^+ (3.9 min). Even when $Na^+/NH_4^+ > 100$, these two peaks are

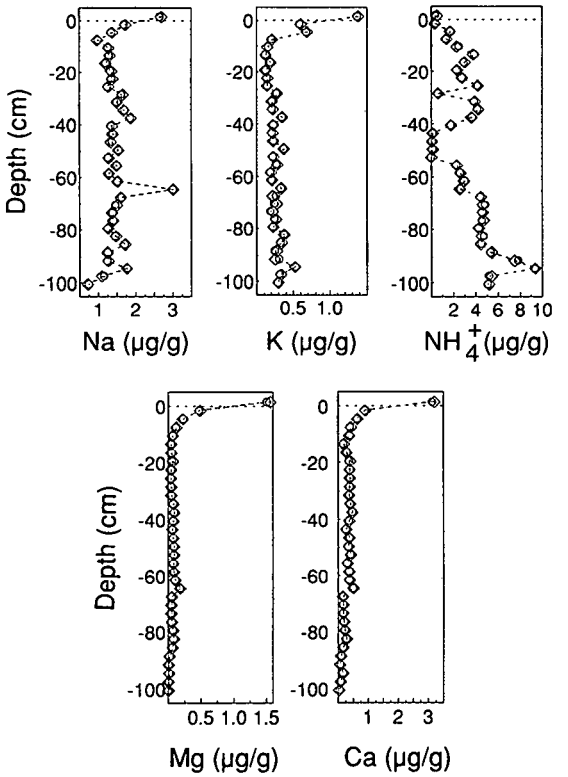

Fig. 3. Cations in pore waters at Etang de la Gruyère. The circles and diamonds represent two separate sets of analyses (duplicates).

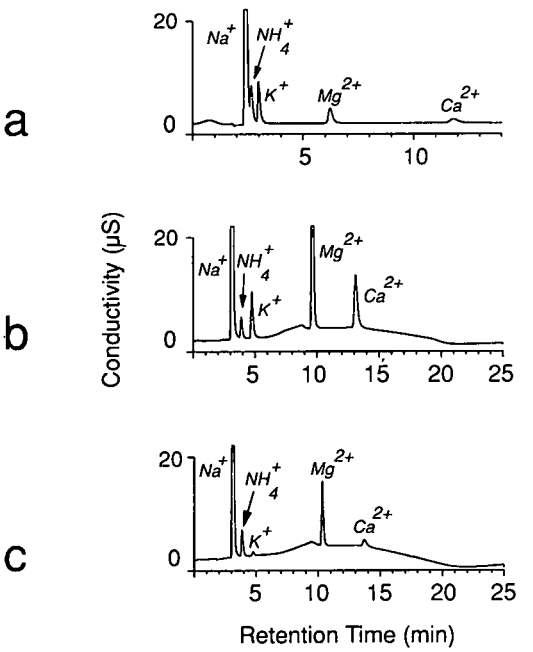

Fig. 4. (a) Isocratic separation of cations in surface water from an Irish bog. Note that NH_4^+ (*ca.* 5 μg/g) is masked by Na^+ (*ca.* 27 μg/g). With increasing Na^+/NH_4^+ ratio the separation becomes increasingly poor. (b) Gradient separation of cations in a standard containing: 100 μg/g of Na^+, 10 μg/g each of NH_4^+, K^+ and Ca^{2+} and 20 μg/g of Mg^{2+}. (c) Gradient separation of cations in pore water (63–66 cm) from Lochs o' da Fleck. Note that NH_4^+ is clearly separated from Na^+.

still baseline separated. A pore water sample from Lochs o' da Fleck is shown in Fig. 4c. The sample contains 53.4 μg/g of Na^+ and 11.3 μg/g of NH_4^+, but the two peaks are clearly separated.

The isocratic and gradient methods for cation separations were compared by analysing a sample of water from Tourbière des Veaux using both methods. The results of the analyses are not significantly different (Table II). The main advantage of the isocratic method is the shorter time required for analysis (15 min *versus* 25 min for the gradient method). The isocratic method provides adequate separation of sodium and ammonium when the Na^+ to NH_4^+ ratio is relatively low (continental bog waters). The main advantage of the gradient method is the improved separation of Na^+ and NH_4^+ in waters with a high Na^+ to NH_4^+ ratio (maritime bog waters).

Variability of analytical procedure. After every tenth injection a blind standard containing 50 μg/g of Na^+, 10 μg/g of Mg^{2+} and 2 μg/g each of NH_4^+, K^+ and Ca^{2+} was analysed in triplicate. These results were pooled to calculate the mean ± one standard deviation for twelve analyses of the working standard: Na^+, 55.2 ± 4.3; NH_4^+, 2.1 ± 0.1; K^+, 2.2 ± 0.1; Mg^{2+}, 10.6 ± 0.5; Ca^{2+}, 2.3 ± 0.3 μg/g.

Precision of the water analyses. Again, the precision is best illustrated by comparing duplicate sets of analyses of the dominant cations in a maritime bog (Fig. 5). The average standard deviations of the 27 duplicate pairs estimated according to ASTM Designation D 4210 [3] are Na^+ 1.8, NH_4^+ 0.2, K^+ 0.1, Mg^{2+} 0.2 and Ca^{2+} 0.2 μg/g.

TABLE II

COMPARISON OF ISOCRATIC AND GRADIENT METHODS OF CATION DETERMINATION

A sample of surface water from Tourbière des Veaux was analysed six times using each method.

Cation	Concentration (ng/g)	
	Isocratic separation	Gradient separation
Na^+	505 ± 1	485 ± 22
NH_4^+	1605 ± 30	1507 ± 50
K^+	1126 ± 47	1191 ± 44
Mg^{2+}	173 ± 7	171 ± 6
Ca^{2+}	763 ± 12	723 ± 26

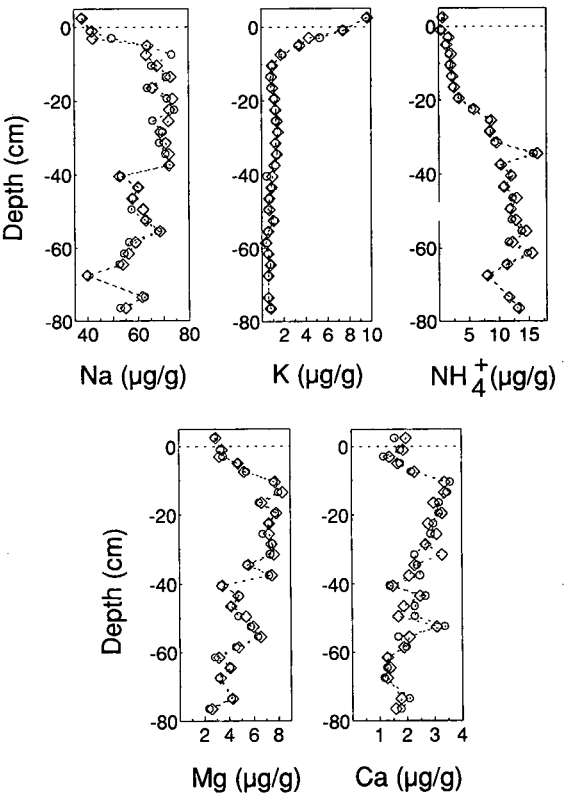

Fig 5. Cations in pore waters at Lochs o' da Fleck. The circles and diamonds represent two separate sets of analyses (duplicates).

Comparison of the determination of Na, K, Mg and Ca by IC versus ICP

Na, K, Mg and Ca were determined by both IC and ICP methods in one complete set of pore waters from Etang de la Gruyere. The relationship between the two sets of values is illustrated in Fig. 6. The results obtained by ICP are 20–40% higher than the corresponding data obtained using the IC. The concentrations of dissolved organic carbon (DOC) in the pore water samples were also measured and found to vary from 50 to 120 mg/l. The ratios of measured metal concentrations (ICP/IC), however, are independent of DOC concentration. The ratios of measured metal concentrations (ICP/IC) were also compared with the pH values of the pore waters, which range from 3.8 to 4.2. The measured differences between the ICP and the methods IC are also independent of the pH values of the

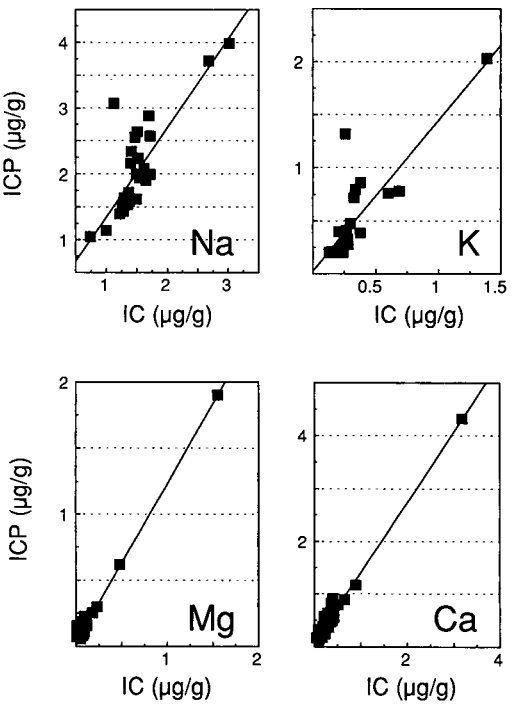

Fig. 6. Comparison of measured metal concentrations using ICP *versus* IC. The data represent a complete set of pore waters (32 samples) from Etang de la Gruyère in which the metal cations were measured by both methods. The detection limits using ICP are Na 30, K 200, Mg 40 and Ca 10 ng/g. The linear regression equations are as follows: Na, ICP = 1.35 IC − 0.07 (r^2 = 0.664); K, ICP = 1.42 IC + 0.02 (r^2 = 0.708); Mg, ICP = 1.21 IC + 0.03 (r^2 = 0.986); Ca, ICP = 1.33 IC + 0.08 (r^2 = 0.975). All of the correlation coefficients are significant at the 0.01 level of probability.

solutions analysed. Additional studies are needed to explain the differences in measured metal concentrations between the two methods.

CONCLUSIONS

The dominant cations in peatland waters (Na^+, NH_4^+, K^+, Mg^{2+} and Ca^{2+}) can be measured simultaneously in less than 15 min and with adequate sensitivity and precision using IC. The principle advantage of IC over AAS and ICP is the measurement of NH_4^+, in addition to the metallic cations. This may be especially valuable with pore waters from continental bogs because NH_4^+ may be the dominant cation. An organics-removal cartridge is used with each injection, but this has no significant effect on the measured cation concentrations.

In waters from continental bogs with relatively low Na^+ to NH_4^+ ratios, the isocratic method allows adequate separation of these two cations. In waters from maritime bogs with large Na^+ to NH_4^+ ratios, a gradient method must be used to separate these two peaks clearly.

ACKNOWLEDGEMENTS

The author is indebted to Professor Albert Matter of this Institute for generously providing all of the required laboratory facilities and equipment. Additional financial support from the Canton of Berne (SEVA Lottofonds) and the Swiss National Science Foundation (Grant 21-30207.90) is also sincerely appreciated. Philipp Steinmann helped to collect the peat cores and Jill Engi skillfully prepared all of the samples and standards. Dr. Peter Blaser at the Swiss Federal Forestry Research Institute provided the ICP analyses of the pore waters. Finally, the author thanks colleagues at Henry A. Sarasin AG (Basle) for expert technical support with all aspects of the ion chromatography.

REFERENCES

1 W. Shotyk, *Earth-Sci. Rev.*, 25 (1988) 95.
2 W. Shotyk, *Water Qual. Bull.*, 14 (1989) 47.
3 American Society for Testing and Materials, *Annual Book of ASTM Standards*, Vols. 11.01 and 11.02. ASTM, Philadelphia, PA, 1991.
4 H. Small, *Ion Chromatography*, Plenum Press, New York, 1989.
5 J. Weiss, *Handbook of Ion Chromatography*, Dionex, Sunnyvale, CA, 1986.
6 S. R. Bachman, J. E. Rothert, B. Kaiser, C. J. Brennan and M. E. Peden, *Method 300.7*, United States Environmental Protection Agency, Cincinnati, OH, 1986.
7 W. Shotyk, *J. Chromatogr.*, 640 (1993) 309.

Journal of Chromatography, 640 (1993) 323–333
Elsevier Science Publishers B.V., Amsterdam

CHROMSYMP. 2726

Application and development of ion chromatography for the analysis of transition metal cations in the primary coolants of light water reactors

M. D. H. Amey* and D. A. Bridle

AEA Technology, Winfrith Technology Centre, Dorset, DT2 8DH (UK)

ABSTRACT

This paper provides an overview of the application of ion chromatography for the analysis of nuclear power reactor coolants. It covers the development of sampling and on-line chromatography on operating plants in Europe for measuring soluble transition metals and, in particular, cobalt at part-per-trillion (ng/kg) levels. The results of the plant investigations are highlighted with respect to their importance in understanding factors influencing the minimisation of Occupational Radiation Exposure. Development of chemiluminescence as a post-column detection technique is also reported which has resulted in the ability to detect and measure one picogram of cobalt.

INTRODUCTION

An understanding of the behaviour of soluble transition metal ions, particularly cobalt, in the high-temperature coolant (310°C) of light water reactors is very important to identify the transport mechanisms, materials and chemistry issues responsible for the build-up of out-of-core radiation fields. Limiting such radiation fields results in lower radiation doses to operators (termed Occupational Radiation Exposure, ORE) during maintenance periods. Cobalt behaviour is particularly important, since naturally occurring cobalt-59 provides the source for its activated daughter product, cobalt-60. This radionuclide is a major contributor to out-of-core radiation fields in water-cooled power reactor plants. The transport and activation process in the primary system of a water reactor is shown in Fig. 1. The coolant provides the transport medium for corrosion and activation products both as soluble and particulate species.

Transition metal ion chromatography (IC) has been used to determine both soluble and insoluble elemental species in reactor coolants, and the use of γ-spectrometry on post-column separated fractions has permitted radiochemical information to be obtained. It has been necessary to give particular attention to the determination of soluble elemental

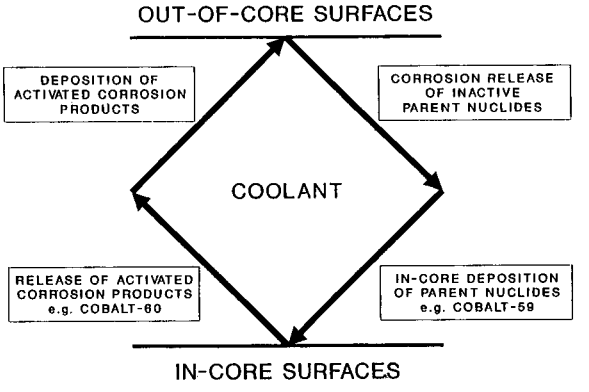

Fig. 1. Transport cycle for corrosion and activation products.

* Corresponding author.

0021-9673/93/$06.00

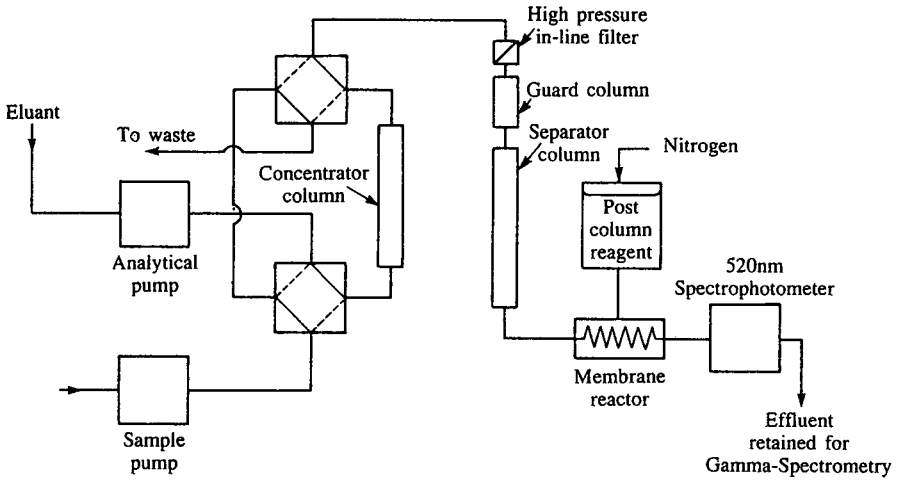

Fig. 2. Flow diagram for ion chromatography system.

cobalt at levels as low as 1 ng/kg (1 part-per-trillion). Soluble species have been determined directly following their on-line concentration from up to one litre of reactor coolant using spectrophotometric post-column detection. Much of the work reported here has been carried out using a Dionex 2003i series ion chromatograph coupled to a suitable microprocessor for data collection and processing (Fig. 2). Post-column detection based upon chemiluminescence has been pursued to elim-

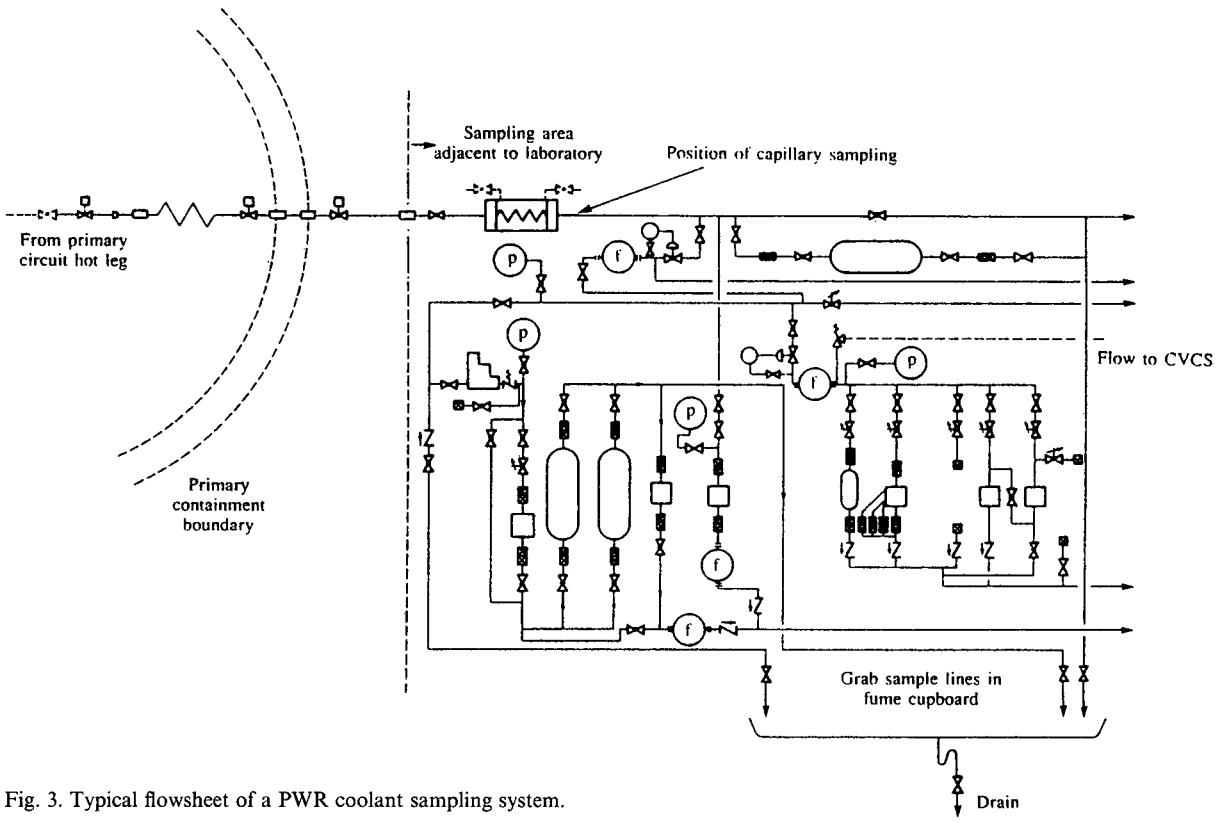

Fig. 3. Typical flowsheet of a PWR coolant sampling system.

inate the need for sample preconcentration. Insoluble species collected on filter membranes following filtration of up to 1500 l of coolant have been solubilised by potassium hydrogensulphate fusion prior to ion chromatography.

AEA Technology (UK Atomic Energy Authority) has collaborated for many years with a number of pressurised water reactor (PWR) utilities in Europe, and more recently with certain Eastern European water reactor utilities of the VVER design. Collaboration in fundamental chromatography research (*e.g.* chemiluminescence detection) has been undertaken with the University of Plymouth in the UK.

REACTOR SAMPLING

Conventional sampling systems for primary circuit coolant installed on commercial PWRs are essentially similar in design. Fig. 3 shows a typical flowsheet for a primary coolant sampling line at a Westinghouse plant. Routine grab sampling is carried out from a continuously flowing sampling line of 6 to 12 mm diameter by operation of relatively large valves. This can introduce pressure and flow perturbations in the system which can influence the measured values.

While generally satisfactory for the measurement of major soluble species required for reactor control, such as the boron and lithium concentrations, these basic systems have been shown to be unsatisfactory for both the representative sampling of particulate material and the continuous on-line determination of very low concentrations of soluble transition metal species such as cobalt and nickel. Capillary sampling has been employed to obtain better representation of particulate species and to provide unperturbed, continuous, low volume sam-

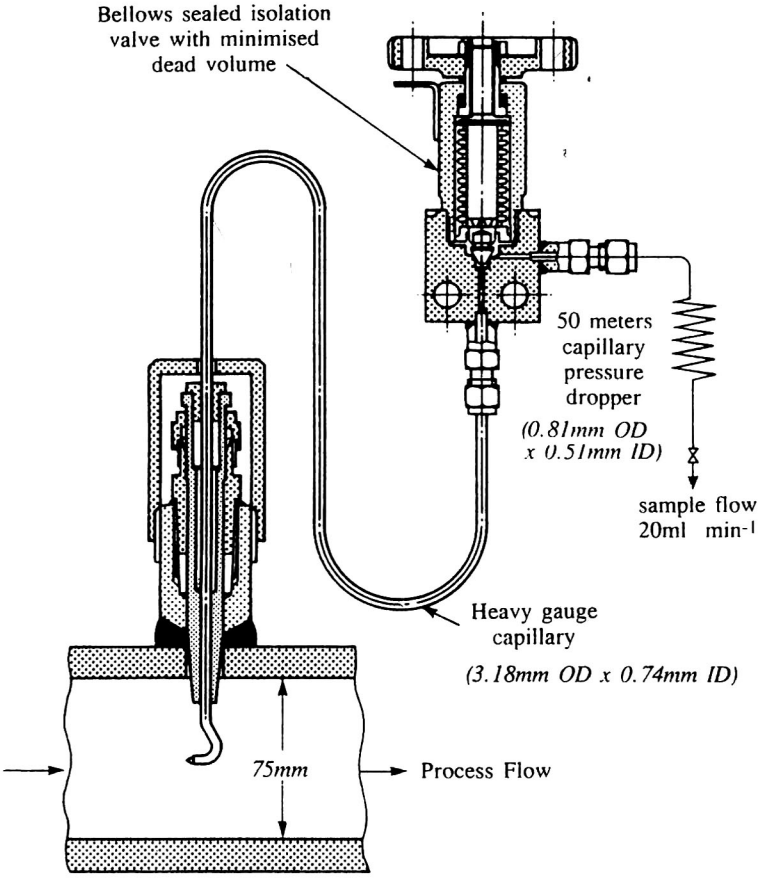

Fig. 4. Direct capillary installation in process line.

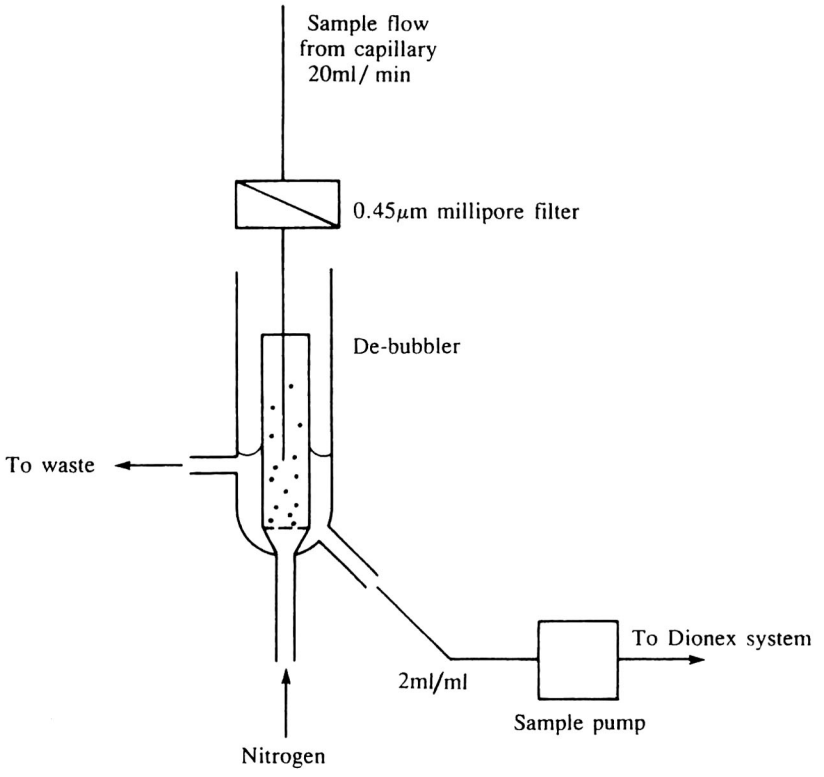

Fig. 5. Arrangement for hydrogen degassing of samples.

pling for the determination of soluble species. An example of a capillary sampling system installed on a high pressure (190 bar) reactor line is shown in Fig. 4. As far as possible, the fluid velocity in the capillary system is matched to that in the primary line from which the sample is being extracted in order to achieve iso-kinetic conditions.

Hydrogen, dissolved in the primary circuit coolant at pressure to prevent water radiolysis in the reactor core, is released in the form of very small bubbles following depressurisation within the sampling capillary. It is essential that these bubbles are removed before the sample is fed to the preconcentration pumping system of the ion chromatograph. The apparatus used on plant to achieve degassing of the coolant sample is shown in Fig. 5. Flow from the capillary passes through a 0.45-μm membrane filter to remove particulate matter. Hydrogen in the coolant is degassed using nitrogen and the coolant overflows into a constant head device which allows sampling by the IC pump.

Insoluble species, collected on the filter membranes after the passage of at least 200 l and up to 1500 l of reactor coolant, required some treatment prior to chromatographic analysis. The filter membranes were moistened with acetone and warmed gently in a silica flask to assist decomposition. The residues were fused with potassium hydrogensulphate until a clear melt was achieved. The "melts" were dissolved in ultra-pure water, and aliquots taken for IC analysis.

DEVELOPMENT OF CHROMATOGRAPHIC METHOD

A variety of methods for the separation and quantification of transition metal, lanthanide, and heavy metal ions have been reported based upon standard HPLC ion-exchange resins [1–3]. Cassidy and Elchuck [4] were able to modify reversed-phase material to act as a cation exchanger, a technique which allowed some control of the ionic capacity of the stationary phase. Organic acids, such as oxalic,

citric and lactic, have been mainly used in transition metal ion separation, whilst spectrophotometry has been widely utilised for post-column detection. The use of mineral acids for the mobile phase can cause problems with transition metal analysis at ultra-trace levels, particularly if conventional steel HPLC systems are used. Indeed, at ultra-trace levels, even the use of organic acids can cause problems. Thus, either totally inert systems made from polymers or all-titanium systems are to be preferred for ultra-trace level work.

Jones *et al.* [5] demonstrated the separation and detection of cadmium, cobalt, copper, iron, lead, manganese, magnesium, nickel and zinc in about 45 min using an inverse photometric detector based upon Eriochrome Black T. This method was the first applied to the measurement of soluble transition metals in PWR primary circuit coolant [6]. Subsequently, Dionex transition metal IC has been extensively used in research studies into the behaviour of soluble transition metals in the primary circuit of a PWR both in out-of-pile research loops and operating power reactors and it has been adapted for on-line analysis [7,8]

Initially, cationic IC was employed for transition metal analysis, but this was changed to anionic separation with the development of improved ion-exchange material based upon anionic latex coating of surface sulphonated cation resins. Transition metal separation has been achieved by chromatography of metal–ligand anionic complexes. Organic chelating agents such as tartrate, citrate and oxalate form anionic complexes which are too stable for post-column derivatisation with spectrophotometric reagents such as 4-(2-pyridylazo)-resorcinol (PAR). Pyridine-2, 6-dicarboxylic acid (PDCA) forms stable complexes with all the transition metal ions of importance in primary circuit waters and allows their chromatographic separation. It also allows coloured complexes to be formed between the transition metal ions and the PAR used as the post-column reagent. Modifications to an original mobile phase reagent (6 m*M* PDCA adjusted to pH 4.8) were required to allow sequential analysis of the important trace elements. Determination of manganese required the addition of sodium sulphate and sodium chloride to the mobile phase.

Reliable quantification of the soluble iron content of coolant samples required a second modification to the PDCA-based reagent. Whilst technically possible to separate and quantify ferrous and ferric ions, in practice problems were experienced with erratic results due to changes in the oxidation state of iron during analysis. Reduction of all soluble iron species to the ferrous state was adopted for all reactor coolant analysis and this has allowed reliable and reproducible results to be obtained on the total soluble iron concentrations in the coolant. Additions of ascorbic acid, sodium sulphite and methanol were required to reduce any ferric to ferrous and prevent the development of damaging bacterial growths in the reagent. Such growths severely limit the shelf-life of the reagent to less than one day and could lead to deterioration in column performance and blockages.

The eluent and post-column reagents used in the reactor coolant studies were prepared as follows. For the eluant, 2.0 g of PDCA, 5.84 g of sodium chloride, 0.72 g lithium hydroxide monohydrate, 0.50 g of sodium sulphite and 0.57 g of sodium sulphate were dissolved in high purity water followed by the addition of 0.7 g ascorbic acid and 40 ml of methanol and the resultant solution diluted to 4 l with high purity water. The eluant was filtered through a 0.45-μm filter membrane. The post-column reagent was prepared by dissolving 0.1 g of PAR in 700 ml of deionized water followed by the addition of 180 ml of ammonium hydroxide solution (sp.gr. 0.880) and 67 ml of glacial acetic acid. This solution was diluted to 1 litre with further deionized water and filtered through a 0.45-μm membrane.

Pulse free addition of the post-column reagent was found to be particularly important for the trace level measurement to ensure minimum baseline noise. This was achieved using a Dionex membrane reactor where the PAR reagent diffuses under nitrogen gas pressure into the column eluent through a permeable fibre membrane.

Elution of the transition metal ions was typically achieved in 20 min and a representative chromatogram from a reactor coolant sample is shown in Fig. 6A with peak data shown in Table I. The same chromatogram is shown in Fig. 6B with five times expansion and baseline correction. Limits of detection, based upon 4.65 standard deviations of the background/blank noise, were 1 ng for nickel and 0.5 ng cobalt. In practice, the limit of detection is

influenced by the resolution from and the magnitude of the peaks eluting before and after the element of interest. The maximum volume of coolant which was practical to preconcentrate was one litre which gave a limit of detection of 0.5 ng/kg cobalt (or 0.5 ppt).

REACTOR MEASUREMENTS

Using the sampling and analytical techniques described, measurements of soluble transition metals, and in some cases insoluble and radiochemical species, have been made on a number of European PWRs [9]. Analytical measurement campaigns for transition metal ions have been made on five Westinghouse designed plants, four Kraftwerk Union (KWU) and four Soviet designed VVER-440. Measurements have been made during steady full power operation close to mid-cycle, and at some reactor start-ups and shutdowns. Table II summarises the results of a number of the measurements made during steady operation at mid-cycle for each plant. As far as possible the plants are arranged in descending order of soluble elemental cobalt concentration measured in the primary coolant whilst retaining the plant groupings.

Both the Westinghouse plants and the earlier KWU plant (C) have high cobalt alloys (Stellites) within the primary coolant circuit, including significant in-core components and, apart from plant B, show the highest concentrations of soluble elemental cobalt. In the later KWU stations, represented by plants D, E and F, a policy of progressive replacement of Stellites and control of cobalt in structural materials has been pursued, and the benefits of this are clearly reflected in the soluble concentrations of cobalt in the coolant. Plant G, the Soviet designed VVER-440 unit, gave the lowest soluble elemental cobalt values of any plant monitored. Such measurements have been confirmed in further analyses carried out at two additional VVER-440 units in Eastern Europe. High cobalt containing

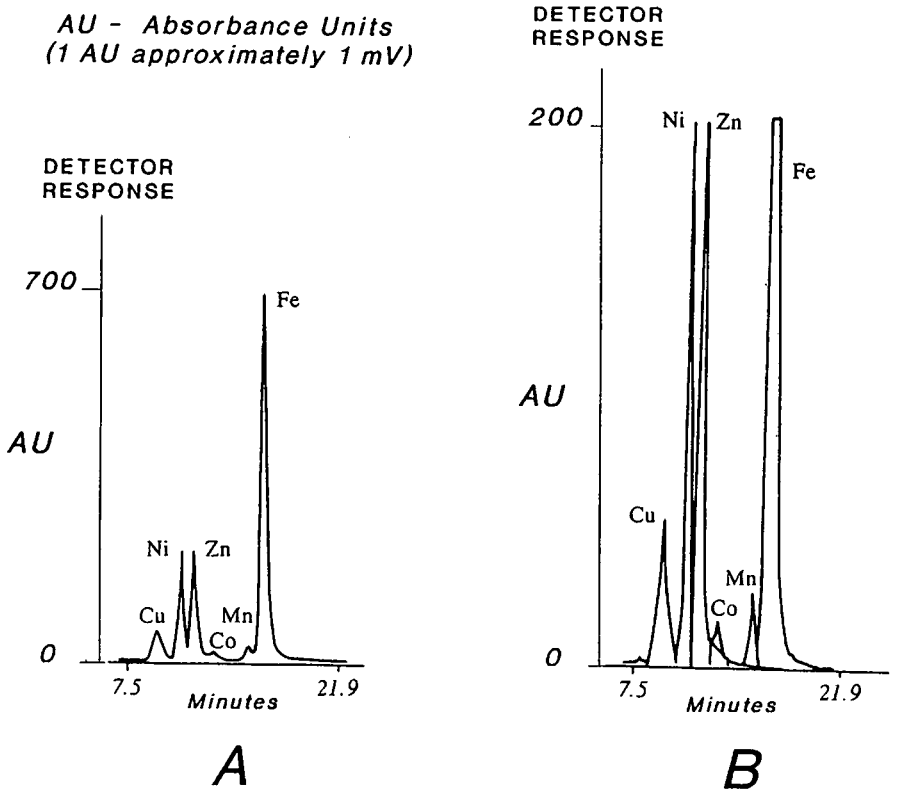

Fig. 6. Typical chromatogram from a PWR primary coolant.

TABLE I

PEAK DATA FOR TYPICAL PWR COOLANT CHROMATOGRAM SHOWN IN FIG. 6

Element	Loading (ng)	Retention time (min)	Peak height	Peak area
Cu	22.5	8.50	55	1059
Ni	90	9.40	211	4499
Zn	180	10.27	210	5329
Co	4.5	11.47	10.9	253
Mn	18	13.73	27	815
Fe	675	14.70	760	29 982

Stellite alloys have not been used in the VVER design of plants and other differences from Westinghouse and KWU plants can be found in the primary circuit chemistry and heat exchanger surfaces. Heat exchanger surfaces are stainless steel in VVERs compared with nickel-based alloys in Westinghouse and KWU plants, also the primary circuit chemistry operates with ammonia–potassium hydroxide–boric acid as opposed to a lithium hydroxide–boric acid regime. The relationship between measured levels of soluble elemental cobalt circulating in the primary circuit coolant and the observed out-of-core radiation dose rate (as measured at the channel head of the steam generator) appears to be independent of reactor type (Fig. 7). The most important factor would appear to be the cobalt inventory of the circuit, an indication of which is provided by the transition metal IC measurement.

POST-COLUMN DETECTION BY CHEMILUMINESCENCE

Greater sensitivity for cobalt determination was desirable for the unambiguous resolution of the cobalt peak from the chromatographic background, as a confirmatory detection system for cobalt peak identification, and to avoid long preconcentration times associated with collecting one litre of reactor primary coolant. Whilst alternative spectrophotometric reagents might be identified which had greater selectivity and/or sensitivity for cobalt, it was unlikely that any reagent would have the necessary "orders of magnitude" increase in its molar extinction coefficient compared with PAR. A different approach was considered necessary for any significant increase in sensitivity, since, within a small factor, the ultimate potential of molecular absorption would appear to have been reached.

Luminescence methods were thought to offer considerable scope for development and of all the

TABLE II

PRIMARY CIRCUIT COOLANT MEASUREMENTS ON EUROPEAN PWRs

Plant	Boron (mg/kg)	pH 300°C	Elemental Co (ng/kg)		Co-60 (Bq/kg)		Specific activity (GBq/g)		Elemental Ni ng/kg)	
			Sol.	Insol.	Sol.	Insol.	Sol.	Insol.	Sol.	Insol.
(A) Westinghouse (Cycle 3)	840	7.23	10.0	–	430	–	43	–	280	–
(B) Westinghouse (Cycle 13)	489	7.00	4.0	0.52	78	50	20	96	334	135
(C) KWU (Cycle 13)	450	7.29	9.0	–	730	–	81	–	87	–
(D) KWU (Cycle 4)	380	7.35	7.9	–	1670	–	211	–	39	–
(E) KWU (Cycle 4)	300	7.42	2.0	0.19	180	24	90	126	32	58
(F) KWU (Cycle 1)	440	7.30	1.8	0.20	59	5	33	25	21	26
(G) VVER 440 (Cycle 13)	594	7.32	1.1	0.14	6	1.14	5.5	8.1	83	13

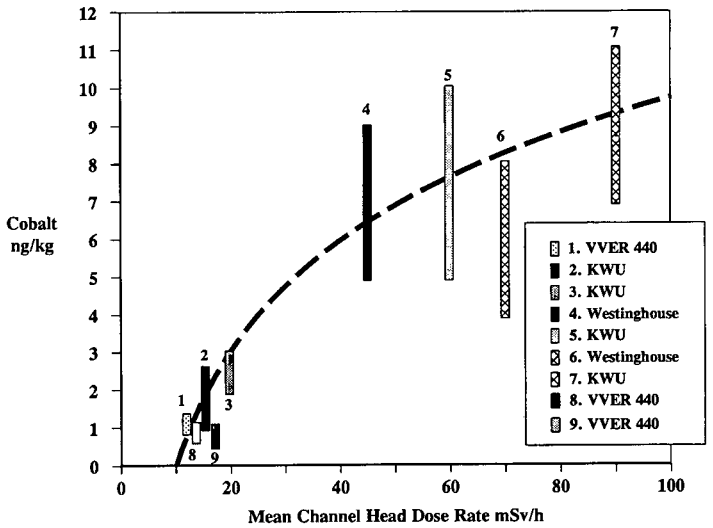

Fig. 7. Comparison of soluble elemental cobalt in the primary coolant with channel head dose rate.

techniques, chemiluminescence was considered to be the most suitable for ultra-trace cobalt analysis. The earliest reported use of chemiluminescence for the analysis of transition metal ion was for cobalt by Babko and Lukovskaya in 1963 [10]. Despite the limitations of photographic plate detection, an absolute detection limit of 2 ng cobalt was obtained. Development of flowcell systems in the early 1970s led to a method for the separation and quantification of cobalt and copper based upon HPLC and chemiluminescence [11]. However, high-efficiency ion-exchange materials were not available at that time, so the chromatographic separation was relatively poor.

Boyle *et al.* [12] used a luminol post-column reaction system with HPLC to determine cobalt, but this method required elaborate sample handling and a multiple-valve chromatographic system. More recently the technique has been used to measure cobalt in seawater at trace levels using a relatively simple flow injection system [13]. Whilst the absolute amount of cobalt detected in this case was only comparable with the existing HPIC–spectrophotometric detection (0.5 ng cobalt), further potential of the detection system was considered possible. Preliminary studies undertaken at the University of Plymouth (previously Plymouth Polytechnic) indicated that very high sensitivity could be achieved using luminol–hydrogen peroxide chemiluminescence.

Luminol chemiluminescence

Certain metal ions catalyse the reaction between luminol (5-amino-2,3-dihydro-1,4-phthalazinedione) and hydrogen peroxide. In excess of the reagents, the degree of chemiluminescence observed is directly proportional to the metal ion concentration over several orders of magnitude [14]. Catalysis of the luminol reaction is inherently non-selective, but certain metal ions have a greater effect than others. Cobalt is second only to chromium in its sensitivity as a result of its ability to catalyse the luminol–peroxide reaction.

Catalysis of the chemiluminescence reaction by cobalt would be affected by other competing reactions such as the strength of the cobalt-eluent ligand bonds. Thus, application of chemiluminescence as a post-column detection technique for HPIC required changes to the chromatographic separation conditions and eluent used to prevent interference.

Chemiluminescence detector

Detectors for chemiluminescence detection can be characterised by their simplicity. A suitable detector was constructed in a light proof housing (Fig. 8) which contained a photoreceptor. Cables and re-

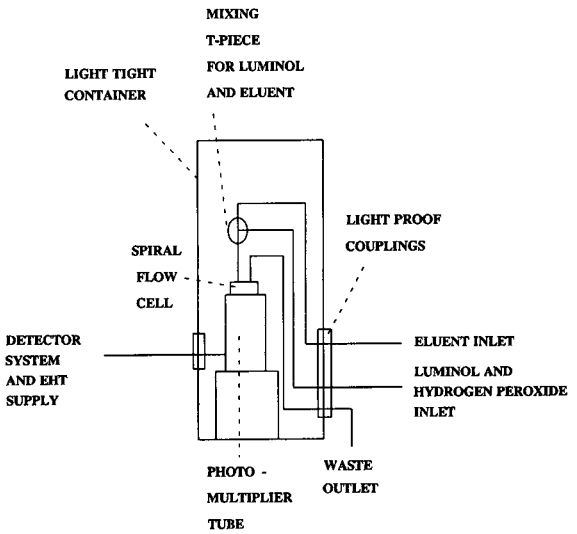

Fig. 8. Chemiluminescence detector.

agent lines passed through light-proof couplings into the container to minimise the amount of adventitious light reaching the photoreceptor. The photoreceptor used was a flat-faced photomultiplier tube (Thorn EMI type 6097) having a spectral range of 330–680 nm, and a maximum sensitivity at 450 nm.

An optical coil flowcell was constructed from narrow bore transparent PTFE tubing as a 45-mm diameter flat spiral. The coil was wound from the centre outwards, returning again to the centre. This shape of coil flowcell maximised the area/volume of the eluent in contact with the detector. The total volume of the flowcell was 200 μl, giving a residence time of about 5 seconds. A matt black backing disc was mounted behind the flowcell to reduce any stray incident light.

Chromatographic conditions for chemiluminescence detection

Spectrophotometric detection utilised in the measurements made on power stations relied upon the anionic separation of transition metal–PDCA complexes. However, it was necessary to revert to the use of cation-exchange material for chemiluminescence post-column detection because of effects of ligand complexation. PDCA complexes were considered to be too stable to permit release of cobalt ions to catalyse the luminol–peroxide reaction.

Early attempts at cobalt determination using high-capacity cation-exchange material with a tartrate-based eluent gave poor results in terms of sensitivity [15]. Strong suppression of the chemiluminescence response was observed as a result of the presence of tartrate. Low capacity ion-exchange material was required with the use of an eluent with a lower chelating ability than tartrate. Dionex cation ion-exchanger C2, having high efficiency and low ion-exchange capacity, had already been shown to give good separation of transition metals in reactor plant applications with a lactate-based eluent and spectrophotometric detection [7].

A suitable HPIC system was established with a chemiluminescence detector and most of the work carried out using a 5-cm long Dionex C2 resin column. Optimum pH for the 0.12 *M* lactic acid eluent was found to be 3.8 with ammonium hydroxide being used for pH adjustment [16]. Elution order determined by spectrophotometric detection was iron(III), copper, zinc, nickel, cobalt, iron(II), and manganese. At a lactate eluent flow-rate of 1.2 ml/min, cobalt was eluted after approximately 13 min.

Following optimization of the chromatography conditions, attention turned to optimization of the chemiluminescence detection. Copper was found to give a large response, but the response was strongly dependent upon the alkalinity of the luminol–peroxide reagent [16]. Post-column reagent conditions were selected such that the resultant pH of the combined column eluent–luminol–peroxide solution was greater than pH 10. The post-column reagent was prepared by dissolving 0.1 g luminol and 3 g boric acid in 500 ml of ultra-pure water containing 5 ml of hydrogen peroxide. This solution was adjusted to pH 12 using potassium hydroxide.

A typical response trace of the chemiluminescence determination of cobalt in a PWR coolant sample is shown in Fig. 9 which can be compared with spectrophotometric detection shown in Fig. 6B. The specificity of the method is demonstrated by the absence of other peaks in the chromatogram (Fig. 9) and the stability of the baseline is particularly notable. Sensitivity of the detection systems was found to be good with more than a thousand-fold increase when compared with spectrophotometric detection. The limit of detection was found to be 0.3 pg cobalt compared with 0.5 ng cobalt for spectrophotometric detection.

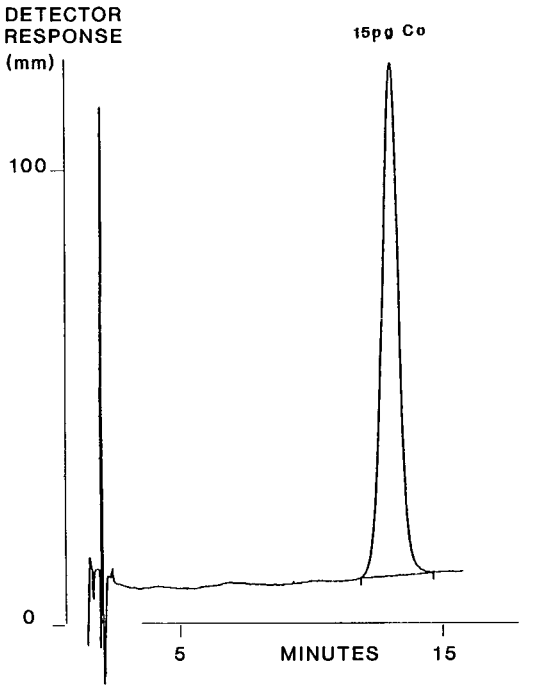

Fig. 9. Chemiluminescence detection of cobalt in PWR coolant samples.

COMPARISON OF DETECTION TECHNIQUES

One inherent weakness in all chromatographic analysis is the unambiguous identification of peaks, but the use of more than one detection system is able to resolve such uncertainties. Conclusive evidence of the validity of the cobalt determinations on PWR primary circuit coolants by the spectrophotometric detection technique was achieved by the application of chemiluminescence detection.

There was a marked contrast in the sensitivity and clarity of the specific chemiluminescent determination of cobalt and the standard multi-element technique based upon anion-exchange and spectrophotometric detection. A peak of only 15 pg cobalt measured by chemiluminescence detection (Fig. 9) can be compared with the peak produced by 4500 pg cobalt using the PAR spectrophotometric approach (Fig. 6B).

Typically, the maximum volume for direct injection in chromatographic procedures is 500 μl, and this enables cobalt concentrations in PWR coolants to be measured when present at *ca.* 0.5 ng/kg (0.5 ppt) using chemiluminescence detection. Spectrophotometric detection requires the preconcentration of one litre of coolant for such ultra-trace levels. Thus, more convincing results are likely to be obtained from the former technique when cobalt concentration are at or below the 1 ng/kg level. However, such sensitivity may only be required for specific applications or investigations, and at other times a multi-element capability will be more important that high sensitivity/specificity.

CONCLUSIONS

Ion chromatography has been successfully demonstrated and used for the on-line determination of soluble transition metals in PWR primary coolant, with a detection limit of less than 1 ng/kg achieved for cobalt.

Determination of cobalt in the primary coolant of PWRs has led to observations concerning important factors influencing the build-up of out-of-core radiation fields. In particular, the relationship between soluble cobalt levels in the coolant of a water-cooled power reactor and the out-of-core radiation field appears to follow a trend irrespective of reactor type. There is evidence of a correlation between the soluble cobalt levels in reactor coolant with the progressive removal of high cobalt containing alloys and the control of cobalt levels in structural materials of the primary circuit. Data obtained by ion chromatography measurements remain a diagnostic tool with respect to systems materials effects.

Capillary modifications to existing sampling systems have proved an excellent means of providing a continuous, representative, low volume sample flow to analytical instrumentation, eliminating problems associated with the perturbations caused by grab sampling.

Chemiluminescence has been shown to have potential as a highly specific and sensitive post-column detection system for the ion chromatographic determination of cobalt. Absolute detection of 0.3 pg cobalt has been achieved which allows direct injection of samples of PWR coolant when the cobalt concentration is only at the 1 ng/kg (1 part-per-trillion) level.

ACKNOWLEDGEMENTS

The authors would like to thank Dr. P. Jones and Mr. T. Williams of the University of Plymouth for their work concerning the development of chemiluminescence, and the various station chemists on the different reactor plants for their help in making the measurements. Work associated with reactor plant measurements referred to in this paper were originally funded by Nuclear Electric plc and/or the UK Health and Safety Executive.

REFERENCES

1 J. S. Fritz and J. N. Story, *Anal. Chem.*, 46 (1974) 825–829.
2 Y. Takata and K. Fujita, *J. Chromatogr.*, 108 (1975) 255–263.
3 J. E. Girard, *Anal. Chem.*, 51 (1979) 836–839.
4 R. M. Cassidy and S. Elchuk, *Anal. Chem.*, 51 (1979) 1534–1538.
5 P. Jones, P. J. Hobbs and L. Ebdon, *Analyst*, 109 (1984) 703.
6 P. Jones, K. Barron, and L. Ebdon, *J. Chromatogr.*, 354 (1986) 407–415.
7 M. D. H. Amey and G. R. Brown, *Recent Developments in Ion Exchange*, Elsevier Applied Science, Barking, 1987, pp. 180–187.
8 E. J. Bird, D. A. Bridle and M. D. H. Amey, presented at the *4th BNES Conference on Water Chemistry, Bournemouth, October, 1986*, British Nuclear Energy Society, 1986, pp. 21–27, Paper No. 7.
9 D. A. Bridle and P. Cake, presented at the *6th BNES Conference on Water Chemistry of Nuclear Reactor Systems, Bournemouth, October 1992*, British Nuclear Energy Society, Paper No. 12, in press.
10 A. K. Babko and M. M. Lukovskaya, *Zavod. Lab.*, 29 (4) (1963) 404–407.
11 M. P. Neary, W. R. Seitz and D. M. Hercules, *Anal. Lett.*, 7, (1974) 583–590.
12 G. Boyle, B. Handy and A. van Geen, *Anal. Chem.*, 59 (1982) 1499.
13 C. M. Sakamoto-Arnold and K. S. Johnson, *Anal. Chem.*, 59 (1987) 1789–1894.
14 W. R. Seitz and D. M. Hercules, *Chemiluminescence and Bioluminescence*, Plenum Press, New York, 1973, pp. 427–449.
15 P. Jones, T. Williams and L. Ebdon, *Anal. Chim. Acta*, 217 (1989) 157.
16 P. Jones, T. Williams and L. Ebdon, *Anal. Chim. Acta*, 237 (1990) 291.

Journal of Chromatography, 640 (1993) 335–343
Elsevier Science Publishers B.V., Amsterdam

CHROMSYMP. 2704

Analysis of cellulose and kraft pulp ozonolysis products by anion-exchange chromatography with pulsed amperometric detection

L. Van Nifterik, J. Xu, J. L. Laurent* and J. Mathieu

Ecole Nationale Supérieure de Chimie de Toulouse, Laboratoire de Chimie des Procédés, 118 Route de Narbonne, 31077 Toulouse Cedex (France)

C. Rakoto

Degrémont, 183 Avenue de 18 juin 1940, 92508 Rueil-Malmaison Cedex (France)

ABSTRACT

Efforts to reduce the level of chlorinated organics discharged into the environment have led to interest in ozone bleaching of kraft pulp. In the course of this operation the transformation of cellulose has to be reduced to the minimum. With this aim, the investigation of the cellulose–ozone reaction was carried out from a mechanistic point of view. The initial interest was in the composition of kraft pulp and cellulose ozonation effluents. High-performance anion-exchange chromatography with pulsed amperometric detection was used to separate and partially identify the soluble modified or unmodified carbohydrates of kraft pulp and cellulose ozonolysis. The main results indicate that after ozonation at 0, 25 and 65°C, cellulose gives oligosaccharides, monosaccharides and probably oxidized forms of those products. Formaldehyde was also directly determined under the same conditions as for carbohydrates.

INTRODUCTION

The traditional methods of bleaching involving chlorine and chlorine dioxide followed by an alkaline extraction stage result in excessive waste water and pollution. The worldwide concern over environmental control has motivated a search for new processes of bleaching that will eliminate the problem of pollution caused by chlorinated organic materials [1,2]. One attractive candidate in the development stage is ozone because of its delignifying and brightening abilities [3]. However, while lignin, a phenolic-type high-molecular-mass material, is readily attacked by ozone [4,5], the cellulose is simultaneously modified, which more or less leads to a loss of pulp properties. This problem still awaits solutions in terms of selectivity and remains a great challenge in the pulp and paper industry. Thus, the aim of this work was the elucidation of the action of ozone on cellulose and the reduction of its effect.

Although there is considerable information regarding the by-products from chlorinating pulp [6,7], much less is known about the by-products from ozone bleaching, especially the carbohydrates. Sonnenberg *et al.* [8] recently determined the identities of low-molecular mass pulp ozonolysis products from lignin degradation by gas chromatography coupled with mass spectrometry but they did not consider possible cellulose degradation products. The ozonation of glucose and cellobiose has been reported and some ozonation by-products have been identified [9]. However, so far no analysis of carbohydrates from ozonation effluents of cellulose or kraft pulp has appeared in the literature.

Hence we decided to analyse the soluble ozona-

* Corresponding author.

0021-9673/93/$06.00

tion products of cellulose and kraft pulp. A preliminary study on the liquid part of poplar sawdust ozonation showed [10] that carbohydrate analysis was possible by high-performance anion-exchange chromatography (HPAEC) with pulsed amperometric detection. Carbohydrates, whether present as monosaccharides, disaccharides or oligosaccharides, can be directly injected in aqueous solution without derivatization and pretreatment [11–13]. HPAEC–pulsed amperometric detection provides a simple, selective and sensitive method [14]. For these reasons, this method was applied here to separate and partially identify the soluble, modified or unmodified carbohydrates that originate from the cellulose, transformation of cellulose and kraft pulp ozonation.

Further identification work by nuclear magnetic resonance (NMR) spectrometry, on separated products with preparative chromatography could help to elucidate the prevalent reaction pathways for the modification of the cellulose by ozone. In addition, the knowledge of ozonation by-products is also of interest from an environmental point of view.

EXPERIMENTAL

Ozonation system

Ozone for the experiments was produced from pure oxygen in a laboratory cold plasma ozone generator. The gas flow was 60 l/h (under normal conditions) and the concentration of ozone in the gas mixture leaving the generator was about 30 mg/l (under normal conditions), which was measured with a BMT 961 ozone analyser (BMT Messtechnik). The residual ozone leaving the reactor was measured by the iodimetric method [15]. The carbohydrate–ozone reactions were carried out in a constantly stirred and thermostated glass reactor.

Substrates

Cellulose and softwood kraft pulp were used for the experiments. Cellulose of analytical-reagent grade was obtained from Merck (Darmstadt, Germany) and softwood kraft pulp was provided by the Centre Technique du Papier (Grenoble, France). A 12-g amount of oven-dry kraft pulp or 12 g of oven-dry cellulose were ozonated at a consistency of 1.2% (on oven-dry pulp or cellulose). Kraft pulp was also ozonated at a consistency of 3% (on oven-dry pulp) in the case of ozonation at 65C and ozone charge 4%. The charges of ozone were calculated in relation to the oven-dry substrates.

Instrumentation

The HPLC system was a Dionex (Sunnyvale, CA, USA) 4500i series chromatograph equipped with a pulsed electrochemical detector. Injection was performed using a Dionex inert high-pressure valve. Data acquisition from the detector and determinations of retention times and peak heights and areas were performed on a Compaq IBM-compatible computer using a Model 1 ACI interface and AI-450 software version 3.2 (Dionex).

Column

A (Dionex) CarboPac PA1 column (250 mm × 4 mm I.D.) with polystyrene–divinylbenzene pellicular resin (particle size 10 μm) and a 1700 p.s.i. pressure limit was used (1 p.s.i. = 6894.76 Pa). The degree of cross-linking of the resin was 5%. A Dionex CarboPac PA1 guard column was used.

Reagents

Purified water (18 MΩ) obtained with a Millipore (Bedford, MA, USA) Milli-Q Plus water purification system was used for preparing all solutions (ozonation solutions, mobile phases and standard solutions).

All the chemicals used for standards were of analytical-reagent grade. L-Fucose, D-glucose, cellobiose and D-glucuronic acid were obtained from Fluka (Buchs, Switzerland), L-rhamnose, L-arabinose, gluconic acid, D-xylose, D-mannose, 5-(hydroxymethyl)-2-furaldehyde (HMF), 1,6-anhydro-D-glucose and cellodextrins from Merck, glucaric acid from Sigma (St. Louis, MO, USA), formaldehyde as a 35% aqueous solution and. Anhydrous sodium acetate from Merck and sodium hydroxide solution (50%, w/w) from J.T. Baker (Deventer, Netherlands).

Operating conditions for oligosaccharide analysis

Eluent 1 was 150 m*M* NaOH, eluent 2 was 500 m*M* CH_3COONa–150 m*M* NaOH and eluent 3 was deionized water. The eluent flow-rate was 1.0 ml/min.

A 50-μl sample loop was used. The detector was

operated in the amperometric mode using a gold working electrode and an Ag/AgCl pH-reference electrode. The applied potentials were as follows: E_1 = 0.40 V, t_1 = 500 ms; E_2 = 0.90 V, t_2 = 80 ms; and E_3 = −0.30 V, t_3 = 50 ms.

The gradient programme was as follows:

Time (min)	1 (%)	2 (%)	3 (%)	
0.00	70	0	30	Equilibration
10.00	70	0	30	Injection of sample, start of gradient ramp 1
20.00	60	10	30	Start of gradient ramp 2
35.00	40	30	30	
50.00	40	30	30	End of Analysis

Operating conditions of monosaccharides and formaldehyde analysis

The analysis was performed with the same analytical column. Eluent 1 was 150 m*M* NaOH and Eluent 2 was deionized water. The eluent flow-rate was 1.0 ml/min.

A 100-μl sample loop was used. The detector was operated in the amperometric mode using a gold working electrode and an Ag/AgCl, pH-reference electrode with post-column addition of 500 m*M* NaOH (flow-rate 0.6 ml/min). The applied potentials were as follows: E_1 = 0.40 V, t_1 = 500 ms; E_2 = 0.90 V, t_2 = 80 ms; and E_3 = −0.30 V, t_3 = 50 ms.

The gradient programme was as follows:

Time (min)	1 (%)	2 (%)	
0.00	6	94	Equilibration, start of isocratic elution 1
15.00	6	94	Injection of sample
33.00	6	94	Step gradient
34.00	0	100	Start of isocratic elution 2
45.00	0	100	End of analysis

Sample preparation

Before injection, the samples were passed through a polyvinylpyrrolidone (PVP) filter cartridge (Dionex On-Guard P cartridge), in order to eliminate the phenolic fraction originating from the lignin in the pulp.

Identification of peaks

All peaks were identified by systematic addition of standard solutions to the samples.

RESULTS AND DISCUSSION

Preliminary investigations

Earlier studies [9] have shown that ozonation of D-glucose produced gluconic and D-glucuronic acids, which were confirmed by both amperometric and conductimetric detection (chromatograms and data are not shown here) [16]. In addition, glucaric acid was also produced after a heavy ozone charge (26%). It was not detected by amperometry but was found with conductimetric detection [16].

Ozonation of cellobiose afforded mainly D-glucose together with the same oxidized products such as gluconic and D-glucuronic acids [9]. Moreover, formaldehyde has been identified in both instances *i.e.*, ozonation of D-glucose and cellobiose by HPAEC-pulsed amperometric detection [16].

Also, the ozonation of MαG (methyl α-D-glucopyranoside) has been studied [17]. The results indicated D-glucose to be the major ozonation by-product.

Ozonation of cellulose and softwood kraft pulp

Figs. 1 and 2 illustrate the gradient elution (see Experimental) of ozonation products of cellulose and softwood kraft pulp, respectively, at 0, 25 and 65°C. All chromatograms were allowed to run for over 40 min and no peaks appeared at later times. A chromatogram of a standard solution of a mixture of cellodextrins in water is shown in Fig. 3. Cellotriose is the oligosaccharide found with the highest concentration in the case of ozonation of cellulose at 0°C (about 0.01% of initial cellulose).

It is found that the chromatograms of each substrate have a similar pattern of oligosaccharides but different degrees of intensity, which might indicate the dependence of cellulose degradation on temperature. Apparently the degradation of cellulose is minimized at 0°C. The reason might be the lower decomposition rate of ozone and consequently less attack on cellulose by hydroxyl radicals. The differences between the chromatograms of cellulose and those of kraft pulp can be explained by the presence of hemicelluloses and lignin in the kraft pulp (limited accessibility of cellulose).

Figs. 4 and 5 show the separation by a step gradient of ionic strength (see Experimental) of monosaccharides respectively after ozonation of cellulose and softwood kraft pulp, respectively, (ozone

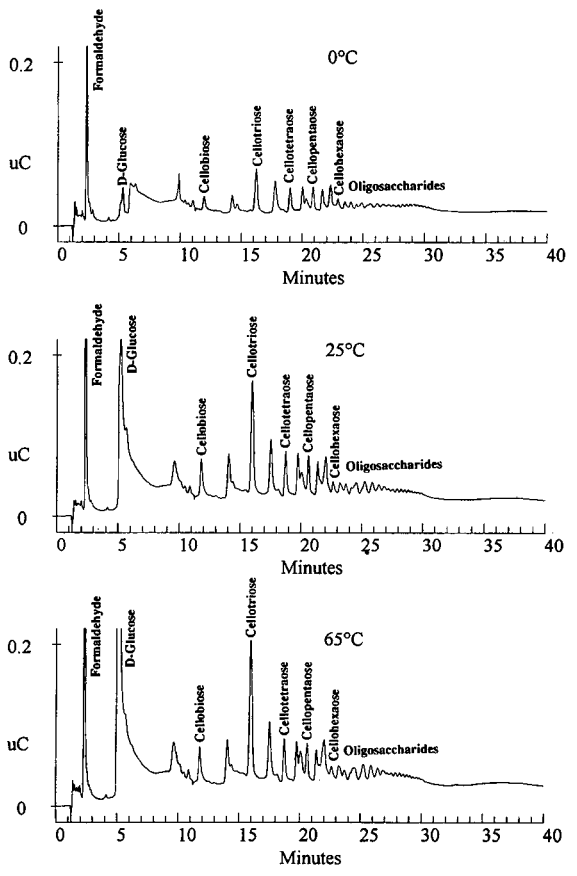

Fig. 1. Separation of ozonation products on an anion-exchange resin using gradient elution and pulsed amperometric detection. Influence of temperature on the degradation of cellulose by ozone (ozone charge 0.92%).

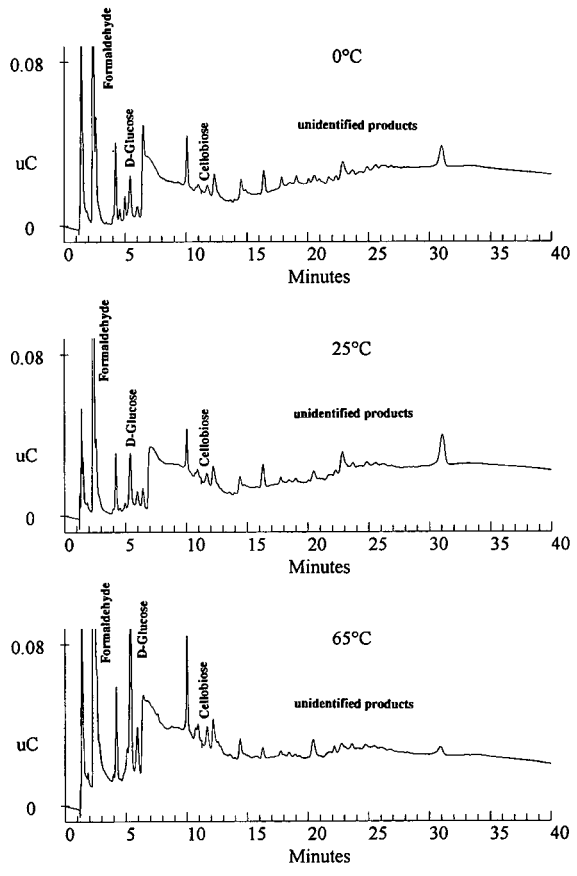

Fig. 2. Separation of ozonation products on an anion-exchange resin using gradient elution and pulsed amperometric detection. Influence of temperature on the degradation of softwood kraft pulp by ozone (ozone charge 0.92%).

charge 2% and 4%, respectively; temperature 65°C). Fig. 6 shows a standard chromatogram of a mixture of monosaccharides with formaldehyde and HMF at ppm (w/w) levels under the same conditions. The chromatograms obtained after ozonation of cellulose indicate the presence of D-glucose after splitting of glycosidic linkages and of L-arabinose in the ozonation solution, probably produced via Ruff degradation [18]. Traces of HMF (very unstable) are obtained at very high charge in ozone, *e.g.* 26% (chromatogram not shown). D-Xylose is the most monosaccharide obtained (about 0.01% of initial cellulose). However, an explanation for why ozonation of cellulose gives relatively more D-xylose than D-glucose remains to be found.

Similar chromatograms are obtained for softwood kraft pulp, where L-arabinose, D-galactose, D-xylose could be contributed to by the cleavage of hemicelluloses contained in pulp. The low concentration of D-glucose relative to the other monosaccharides remains to be explained.

Formaldehyde is obtained in all chromatograms. This presence was predictable, because ozonation of D-glucose [16] and phenol [9] leads to the formation of formaldehyde by oxidative cleavage. Formaldehyde can be detected in HPAEC–pulsed amperometric detection because it is a *gem*-diol in aqueous solution and contains two hydroxyl groups [19]. The analyte has a very high sensitivity for pulsed amperometric detection. The minimum detection

Pk. Num	Ret Time	Component Name	Concentration ppm	Height	Area	Bl. Code
1	2.32	Formaldehyde	0.528	203532	1421367	1
2	5.08	Glucose	0.033	2265	21343	1
3	11.27	Cellobiose	0.528	23929	276046	1
4	14.95	Cellotriose	0.942	37366	488028	1
5	18.15	Cellotetraose	1.115	32546	419327	1
6	20.60	Cellopentaose	0.602	14599	186591	1
7	22.62	Cellohexaose	0.144	2524	32842	1
		Totals	3.892	316761	2845545	

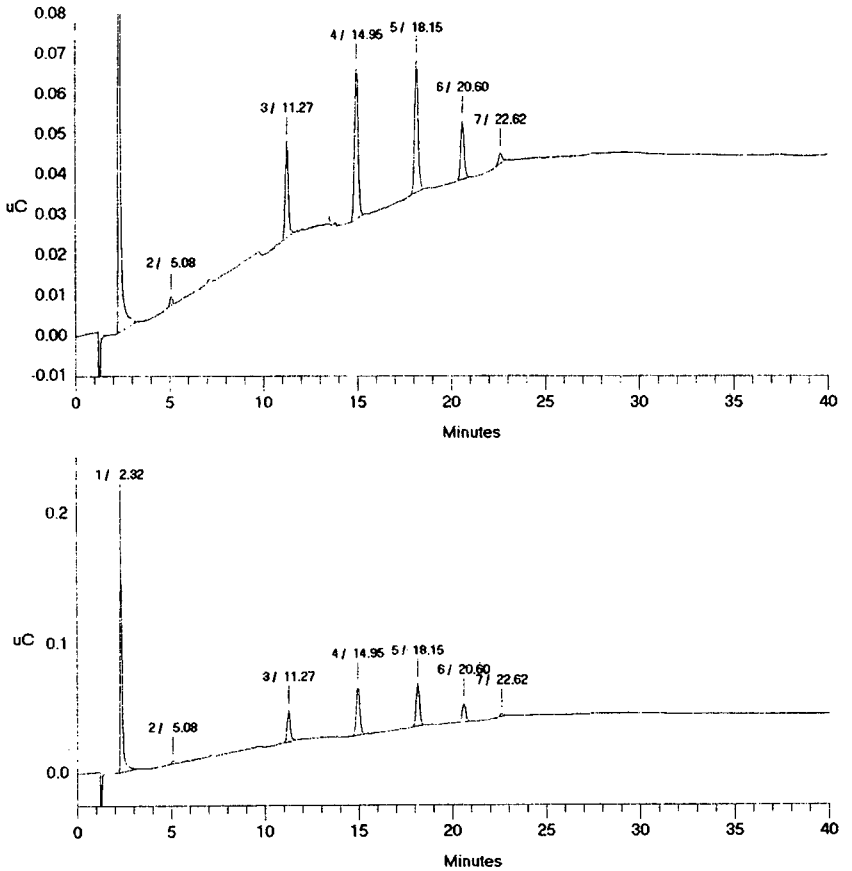

Fig. 3. Typical chromatogram of a standard mixture of formaldehyde and cellodextrines on an anion-exchange resin using gradient elution and pulsed amperometric detection.

limit is about 10 ppb. A better separation of formaldehyde is obtained at lower sodium hydroxide concentrations, *e.g.*, 3 m*M* NaOH, where the retention time was 3.5 min in isocratic elution with post-column addition of strong base (500 m*M* NaOH) in order to optimize the pulsed amperometric detector sensitivity with a Dionex postcolumn pneumatic controller. However, this postcolumn addition can lead to an increase the baseline drift. In the future, the new (Dionex) CarboPac MA1 high-efficiency anion-exchange column will be particularly suited to the analysis and separation of weakly ionizable

********** Component Report: Components Found **********

Pk. Num	Ret Time	Component Name	Concentration ppm	Height	Area	Bl. Code
2	3.47	Formaldehyde	0.718	242015	3129429	3
5	13.85	Arabinose	0.084	4046	173374	1
6	20.62	Glucose	0.171	9758	419355	1
7	23.78	Xylose	1.350	64176	3737340	1
		Totals	2.323	319995	7459497	

********** Peak Report: Unknown Peaks **********

Pk. Num	Ret Time	Component Name	Concentration ppm	Height	Area	Bl. Code
1	1.97		0.000	169305	4194483	2
3	4.30		0.000	3037	38621	4
4	4.73		0.000	5926	68876	2
		Totals	0.000	178268	4301980	

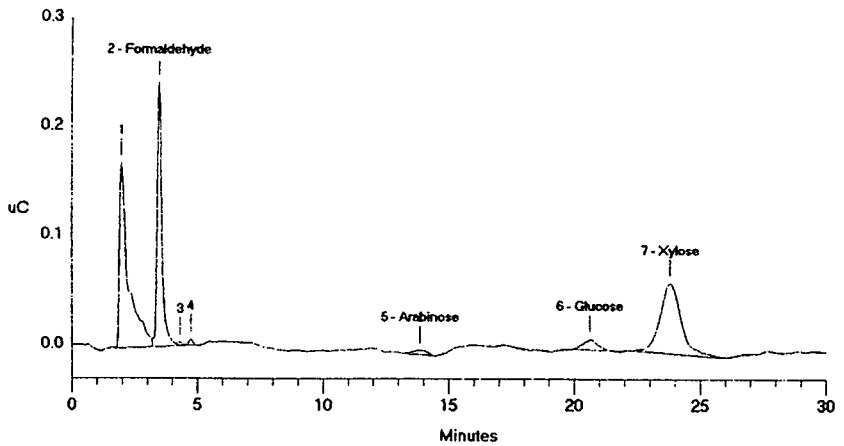

Fig. 4. Separation of monosaccharides on an anion-exchange resin using a step gradient of ionic strength and pulsed amperometric detection after ozonation of cellulose (ozone charge 2%, temperature 65C).

carbohydrates such as the peaks at the beginning of all chromatograms and specifically formaldehyde.

In all the chromatograms obtained by application of a step gradient of ionic strength, an oxygen dip in the baseline with a retention time of 14 min is observed [20]. This dip only appears on the higher sensitivity current scales, and it effectively limits the detection limit by obscuring the arabinose peak when low concentrations are determined.

To give a clearer view of ozone–carbohydrate reactions, Table I summarizes the identified soluble by-products after ozonation of cellulose and softwood kraft pulp using HPAEC–pulsed amperometric detection.

Reactions of ozone with carbohydrates

Based on the chromatograms from ozonation of cellulose and kraft pulp, the increase in the oligosaccharides is evidence for cellulose degradation. To account for this observation, *i.e.*, the splitting of glycosidic linkages, a free-radical chain mechanism involving oxygen in the propagation step was pro-

********** Component Report: Components Found **********

Pk. Num	Ret Time	Component Name	Concentration ppm	Height	Area	Bl. Code
3	3.42	Formaldehyde	1.401	547405	6106486	2
5	13.82	Arabinose	1.454	99655	2998262	1
6	18.25	Galactose	0.054	3486	137240	1
7	19.87	Glucose	0.032	1924	79213	1
8	23.28	Xylose	0.153	7548	422343	1
		Totals	3.094	660018	9743544	

********** Peak Report: Unknown Peaks **********

Pk. Num	Ret Time	Component Name	Concentration ppm	Height	Area	Bl. Code
1	1.93		0.000	28516	393874	2
2	2.50		0.000	24887	435043	2
4	4.65		0.000	6575	77502	2
		Totals	0.000	59978	906419	

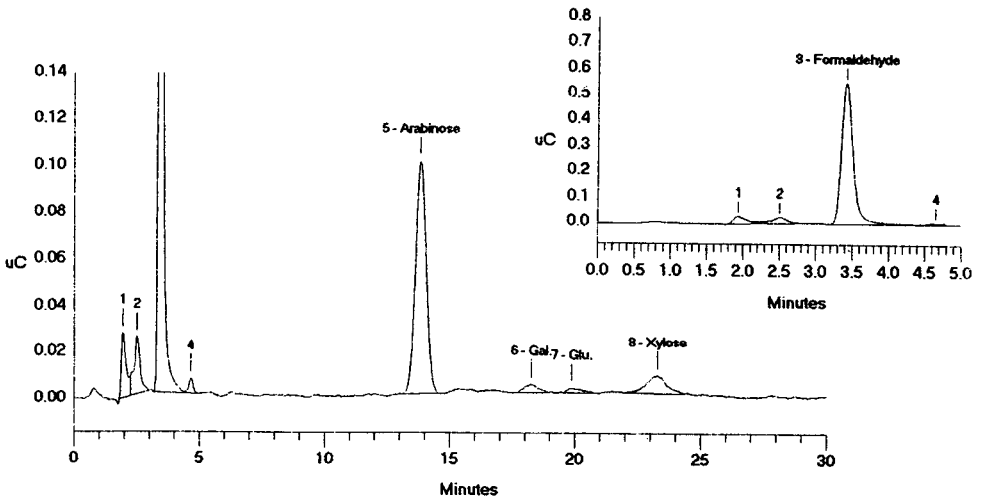

Fig. 5. Separation of monosaccharides on an anion-exchange resin using a step gradient of ionic strength and pulsed amperometric detection after ozonation of softwood kraft pulp (ozone charge 4%, temperature 65C).

posed [21]. However, an electrophilic attack of ozone on carbohydrates to liberate the anomeric carbon via an ozone-catalysed hydrolysis of glycosidic bonds would be also possible [21].

CONCLUSIONS

HPAEC–pulsed amperometric detection is a very versatile approach for the analysis of complex ozonation samples, in particular the separation of carbohydrate ozonation by-products in aqueous solution. The chromatograms reported in this paper show the applicability of this technique to follow the degradation of cellulose by ozone. The results demonstrate clearly the relatively higher concentrations of D-xylose and L-arabinose compared with D-glucose, which are not explicable by the random attack of ozone with scission on the macromolecules mainly formed by D-glucose.

Cellulose degradation, which gives oxidized and/

Pk. Num	Ret Time	Component Name	Concentration ppm	Height	Area	Bl. Code
1	2.78	1,6-Anhydro-glu	0.595	111445	1192136	2
2	3.45	Formaldehyde	0.621	233352	2707116	2
3	5.08	HMF	0.483	89815	1201634	1
4	6.30	Fucose	0.738	120641	1924180	1
5	12.65	Rhamnose	0.797	56794	1871400	1
6	13.93	Arabinose	1.025	79798	2113285	1
7	18.38	Galactose	1.036	63946	2641459	1
8	20.42	Glucose	1.567	89072	3851115	1
9	23.53	Xylose	1.752	92195	4849087	2
10	24.62	Mannose	1.876	34273	2138969	2
		Totals	10.490	971332	24490378	

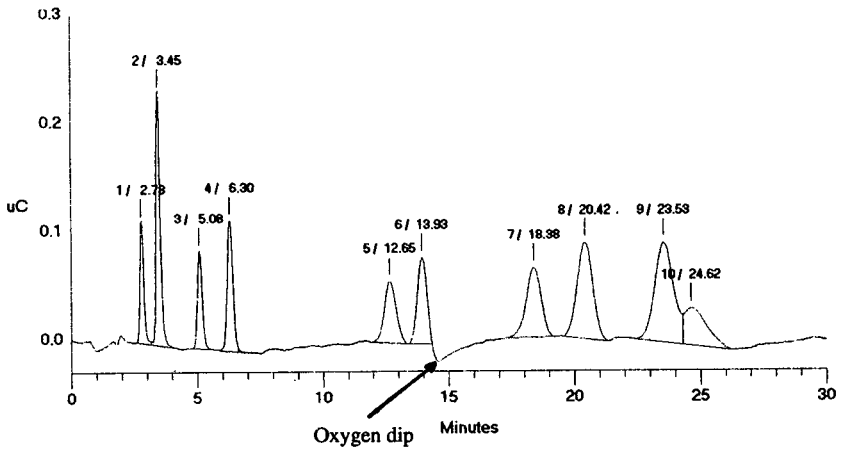

Fig. 6. Typical chromatogram of a standard mixture of formaldehyde, HMF and monosaccharides on an anion-exchange resin using a step gradient of ionic strength and pulsed amperometric detection.

TABLE I

IDENTIFIED SOLUBLE BY-PRODUCTS AFTER OZONATION OF CELLULOSE AND SOFTWOOD KRAFT PULP USING HPAEC

Original data obtained using different conditions of ozonation (ozone charge, temperature, pH). Absence of L-fucose, L-rhamnose and D-mannose.

Cellulose	Softwood kraft pulp
Formaldehyde	Formaldehyde
HMF	HMF
L-Arabinose	L-Arabinose
D-Glucose	D-Glucose
D-Xylose	D-Xylose
	D-Galactose
Cellobiose	Cellobiose
Cellotriose	
Cellotetraose	
Cellopentaose	
Cellohexaose	

or non-oxidized monosaccharides and oligosaccharides, might be caused by a free-radical attack and ozone electrophilic attack on carbohydrates. Anyway, cellulose seems less degraded at lower temperatures.

In addition, formaldehyde in aqueous solution can also be directly determined down to sub-parts per million levels by HPAEC separation with pulsed amperometric detection.

In further work, the purification and identification of unknown carbohydrate ozonolysis products by preparative chromatography and methods such as nuclear magnetic resonance and mass spectrometry will be carried out.

ACKNOWLEDGEMENTS

Financial support from the Société Degrémont–L'Air Liquide and the French Ministry of Industry

(Contrat MIAT "Amélioration des procédés de blanchiment des fibres papetieres") is gratefully acknowledged.

REFERENCES

1 N. Liebergott, B. Van Lierop and A. Skothos, *Tappi J.*, 75, No. 1 (1992) 145.
2 N. Liebergott, B. Van Lierop and A. Skothos, *Tappi J.*, 75, No. 2 (1992) 117.
3 M.V. Byrd, Jr., J.S. Gratzl and R.P. Singh, *Tappi J.*, 75, No. 3 (1992) 207.
4 S. C. Puri and S. M. Anand, *Cellulose Chem. Technol.*, 20 (1986) 535.
5 H. Kaneko, S. Hosoya, K. Iiyama and J. Nakano, *J. Wood Chem. Technol.*, 3 (1983) 399.
6 B. Holmbolm, *Paperi Puu Papper Tra*, 9 (1980) 523.
7 L. R. Suntio, W. Y. Shiu and D. Mackay, *Chemosphere*, 17 (1988) 1249.
8 L. B. Sonnenberg, K. M. Poll, R. M. Le Lacheur and R. G. Murphy, in *Proceedings of the Environmental Conference, Richmond, VA, April 1992*, 1992, book 1, p. 353.
9 W. J. Masschelein, *Ozone et Ozonation des Eaux*, Lavoisier-Technique et Documentation, Paris, 1991, Ch. 14, p. 121.
10 T. Lasry, J. L. Laurent, V. Euphrosine-Moy, R. S. Bes, J. Molinier and J. Mathieu, *Analusis*, 18 (1990) 192.
11 R. D. Rocklin, C. A. Pohl, *J. Liq. Chromatogr.*, 6 (1983) 1577.
12 H. Small, *Ion Chromatography*, Plenum Press, New York, 1989, p. 242.
13 B. Herbreteau, *Analusis*, 20 (1992) 355.
14 J. D. Olechno, S. R. Carter, W. T. Edwards and D. G. Gillen, *Anal. Biotechnol. Lab.*, 5 (1987) 38.
15 Official Method 001/87, International Ozone Association, Standardisation Committee–Europe, Brussels, 1987.
16 L. Van Nifterik, J. Xu, C. Rakoto, J. L. Laurent, J. Mathieu, J. Molinier, C. Coste and Ph. Kalek, in *Proceedings of the 2nd European Workshop on Lignocellulosics and Pulp, September 1992, Centre Technique du Papier, Grenoble, 1992*, p. 165.
17 G.Y.Y. Pan, *Ph. D. Thesis*, North Carolina State University, Raleigh, NC, 1982.
18 T. W. G. Solomons, *Organic Chemistry*, Wiley, New York, 1988, p. 1018.
19 J. F. Walker, *Formaldehyde*, Robert E. Krieger Huntington, NY, 1975.
20 *Technical Note*, Vol. 3, No. 2, Dionex, Sunnyvale, CA, 1992.
21 A. A. Katai and C. Schuerch, *J. Polym. Sci., Part A1*, 4 (1966) 2683.

Journal of Chromatography, 640 (1993) 345–350
Elsevier Science Publishers B.V., Amsterdam

CHROMSYMP. 2634

Chromatographic studies of corrosion sites in metallic materials

H. S. Scully, L. C. Brumback and R. G. Kelly*

Center for Electrochemical Science and Engineering, Department of Materials Science and Engineering, University of Virginia, Charlottesville, VA 22903 (USA)

ABSTRACT

Many types of corrosion phenomena are controlled by the ionic composition of a small volume of solution at the surface. Localized corrosion and atmospheric corrosion are two examples in which < 1 μl of solution can cause dramatic damage. Ion chromatographic (IC) techniques have been used to analyze these solutions in order to gain a better understanding of the mechanisms which govern them. Two examples are presented. The presence of minor alloying elements at localized corrosion sites in two aluminum alloys has been demonstrated, indicating non-stoichiometric dissolution of the alloy during localized corrosion. In addition, IC analysis allowed the determination of the species responsible for the atmospheric corrosion failure of electrical connectors, including their likely origin.

INTRODUCTION

The corrosion of metals is intimately tied to the composition of the solution layer next to the material surface. This solution not only affects the metal dissolution rate and mechanism, but the solution composition is also affected by the chemical and electrochemical processes involved with metal dissolution. In cases where there is restricted mass transport, the composition of the solution adjacent to the metal surface can change dramatically [1–3]. Two corrosion phenomena in which severe mass transport restrictions normally occur are localized corrosion and atmospheric corrosion. Both of these types of corrosion are inherently difficult to study due to the small volumes of solution associated with the corrosive action. In both cases, typically volumes of < 1 μl contain the species of interest. In most cases, the elemental composition of the solution is of limited use; it is the ionic composition that determines the nature and severity of the corrosion that occurs. Recently, the utility of ion chromatography (IC) to the study of corrosion problems was demonstrated [4–6]. In this paper, after giving background information on the two types of corrosion phenomena, the application of IC to the localized corrosion of aluminum alloys and to the failure analysis of electrical components which had undergone atmospheric corrosion is presented.

Localized corrosion

Localized corrosion describes attack that occurs at discrete sites on a material surface rather than uniformly over the entire surface. If often occurs at physical or chemical inhomogeneities on the surface. Such inhomogeneities can result from (a) deposits that develop during service, (b) areas enclosed between two materials (crevices), or (c) the formation of additional phases in the alloy. During the propagation of this attack, the chemical composition of the surface site and/or local solution volume is altered due a combination of the restricted mass transport and hydrolysis reactions of the dissolution products [1–3]. This altered solution is much more aggressive than the bulk solution, leading to accelerated, localized attack. The mechanism(s) which lead to this behavior are still the sub-

* Corresponding author.

0021-9673/93/$06.00

ject of debate [7–9]. Unfortunately, due to the limited volumes of solution in such localized sites (typically < 1 μl), little detail is known about their composition or the effects of important experimental variables such as alloy composition and electrochemical potential. These and other variables can have large effects on the observed localized corrosion behavior. Thus, in order to test present models rigorously and develop more accurate ones, a better understanding of the chemical composition of these sites is required.

Failure analysis of meter socket

Atmospheric corrosion can lead to the failure of electronic components. This type of attack takes place in electrolyte layers that are between 10 monolayers and 10 μm thick which form on surfaces due to the dissolution of pollutant gases into the adsorbed water layers present under ambient conditions (near room temperature, relative humidity above 60%). The absolute rates of attack can be small, but due to the low corrosion tolerances allowed for electrical connectors, even low rates are unacceptable if they produce resistive films. Often, traditional post-exposure analysis of failed components does not reveal the nature or origin of the aggressive specie(s). In such cases, it is difficult to prevent future failures.

One example of such a case follows. In 1989, a production run of galvanized steel meter sockets (galvanized steel cases used to encase household electric or gas meters) were manufactured and packaged along with their fastener kits in cardboard boxes before being inventoried in a warehouse. In 1992, severe corrosive attack of a number of the sockets was discovered. The following observations were made:

(1) Attack was not a function of storage location either within the storehouse or within a given pallet of packaged meter sockets.

(2) Attack occurred on the exterior and interior of socket casings, as well as within polymer bags containing fasteners, and thus did not require direct contact with the cardboard packing material.

(3) Galvanized steel components were especially attacked producing red rust and a white (presumably zinc-containing) corrosion product.

(4) The problem was not typical and appeared to be limited to a single manufacturing lot.

While the portion of the surfaces exposed to the air space showed attack, those portions of the surfaces in contact with each other were not attacked. The consistent observation of such a corrosion morphology indicates that the corrosion did not occur due to condensation of a large water layer. These facts implied that the corrosive agent was in the vapor form and was especially aggressive towards iron and zinc. In addition, only some packages contained sockets that were attacked. However, inside a package that contained corroded components, all components were attacked, including parts enclosed in (unsealed) plastic bags. Identification of the specie(s) responsible for the attack, as well as their origin, was required in order to prevent future failures.

This paper will discuss the application of IC to studies of localized corrosion as well as vapor-phase corrosion. In both cases, the technique's mass sensitivity, ability to ionically speciate and ability to use small injection volumes were critical to developing a better understanding of these processes.

EXPERIMENTAL

Localized corrosion testing

Two commercial aluminum alloys were studied. Alloy 2024 contains 4.4% (w/w) Cu, 0.6% (w/w) Mn, and 1.5% (w/w) Mg. Alloy 8090 contains 2.4% (w/w) Li, 1.2% (w/w) Cu, 0.7% (w/w) Mg and 0.12% (w/w) Zr. Both are important materials in the aerospace industry due to their low density and excellent mechanical properties. Crevices were formed by clamping an alloy specimen between two cylinders of PTFE (1 cm diameter) via the device shown in Fig. 1. This simulates the type of crevice corrosion testing used [10], as well as the crevice formed by a gasket, for example. The electrical connection to the specimen was insulated from the solution. This arrangement allowed the application of a known torque of 0.23 Nm. This pressure corresponded to a total crevice volume of 2.4 μl. This volume was checked by placing 1.2 μl of water onto one side of the alloy surface and pressing PTFE crevice former onto the surface with 0.23 Nm torque. The 1.2 μl just covered the surface to the edge of the crevice former. A Princeton Applied Research Model 173 Potentiostat was used to apply a set potential between the aluminum alloy surface

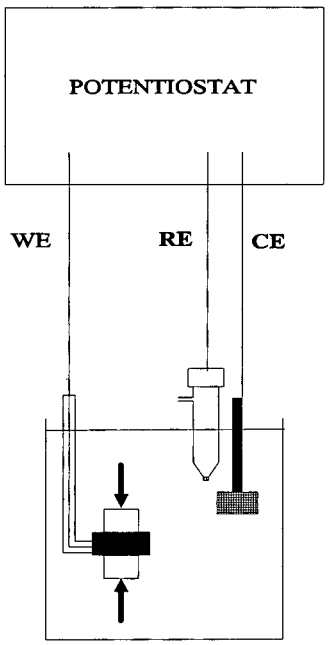

Fig. 1. Experimental schematic of crevice former. The potentiostat is used to control the potential between the working electrode (WE) (aluminum alloy specimen) and the reference electrode (RE). The PTFE crevice formers are clamped to the surface with a variable pressure apparatus (not shown). CE = Counter electrode.

and a saturated calomel (SCE) reference electrode in a test solution of 0.35% (w/w) KCl. A platinized niobium counter electrode was also connected to the potentiostat, and the apparatus was placed in a vessel containing the test solution. The potential of the sample was then scanned at 0.5 mV/s first in the anodic direction from 100 mV below the specimen's corrosion potential to a potential at which the applied current was 1 mA/cm^2. The direction of the scan was then reversed and the potential was scanned in the cathodic direction until the intial potential was reached. All potentials cited are *versus* SCE. After the scan complete, the clamped sample was removed from the solution, the clamp carefully loosened, and the sample as well as the crevice formers were soaked in 5 ml of 18 MΩ cm water in a PTFE beaker. A sample of this solution was then analyzed chromatographically.

Atmospheric corrosion

A similar approach was used for the meter socket analysis. Samples of both corroded and uncorroded components were selected. In order to investigate the source of species found, samples of cardboard packaging material were cut from the accompanying boxes. In each case, the samples were immersed and soaked for 45 min in approximately 10 ml of 18 MΩ cm water from a Barnstead purification unit. Samples of each solution were analyzed chromatographically.

Chromatography

For all experiments, a Waters Action Analyzer and a Rheodyne injector with a 100-μl fixed loop were used. For the localized corrosion experiments, the dissolution of the minor alkali and alkali earth elements was of interst. A Waters Mono-di column (150 mm × 3.9 mm I.D.) was used. The eluent consisted of 3 m*M* HNO_3 with 0.1 m*M* EDTA [11]. The flow-rate was 1 ml/min, and indirect conductivity detection was accomplished via a Waters Model 431 conductivity detector. The eluent for this method has a high background conductivity (1150 μS) and thus indirect conductivity was used. In such detection, a decrease in the conductivity of the solution passing through the detector (*e.g.*, due to the passage of the void volume) will be observed as a positive peak in the chromatogram. Standards were made from reagent grade salts, except for Al^{3+} which was made from a 1000 mg/l atomic absorption standard. All water used was 18 MΩ cm from a Barnstead purification unit.

For the atmospheric corrosion work, inorganic acid anions were separated and analyzed with a Waters IC Pak-A column and a borate-gluconate eluent. Organic acid anions were separated and analyzed with a Waters ion exclusion column (300 mm × 7.8 mm I.D.) and an octane sulfonic acid eluent [12]. In both cases, conductivity detection with a Model 431 conductivity detector was used.

RESULTS

Localized corrosion

Fig. 2 shows the chromatogram obtained when a mixture of Li^+, Al^{3+}, K^+, and Mg^{2+} is injected. The dip in the chromatogram following the Li^+ is due to the presence of the Al^{3+} as discussed below.

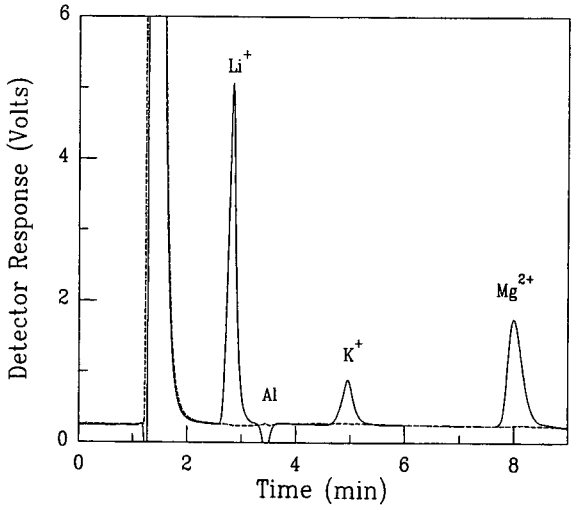

Fig. 2. Chromatogram of standard containing Li^+, K^+, Mg^{2+} and Al^{3+} using indirect conductivity detection. Also included is a water injection. The presence of aluminum does not compromise the analysis of the other components. ——— = Standard; --- = water.

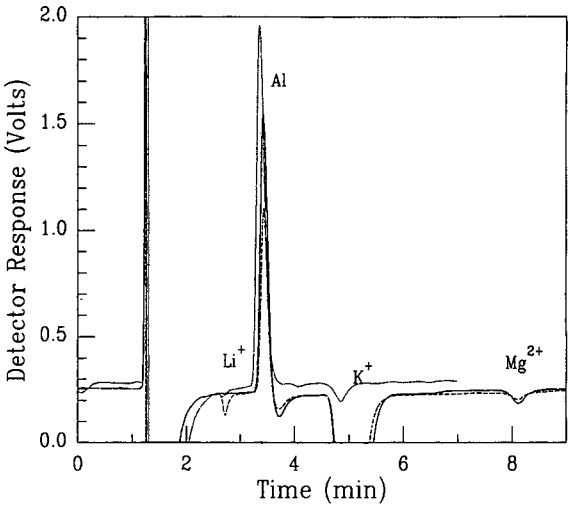

Fig. 4. Chromatogram of solutions from Fig. 3 using direct conductivity detection. The alkali and alkali earth metals now appear as negative peaks, while the presence of aluminum causes a positive peak to appear. ——— = Alloy 2024; --- = alloy 8090; ····· = 5 ppm standard.

An injection of pure water is included for comparison. Note the small Na^+ peak at t = 3.4 min. Fig. 3 shows the chromatograms resulting from the injection of the rinse solutions from the crevice sites of the two alloys, as well as from an injection of the deionized water. The detection of the minor alloying elements (Li and Mg) from the two alloys is clear. The large K^+ peak is due to the KCl used in the test solution. Fig. 4 shows chromatograms resulting from injections of the same solutions as used in Fig. 3 as well as the Al^{3+}-containing standard of Fig. 2, but with direct, rather than indirect, conductivity detection. It appears that the presence of Al^{3+} in the sample causes a positive peak during direct detection. It elutes at the same time as Na^+, but with the opposite effect on conductivity. Determination of the origin of this peak is presently underway.

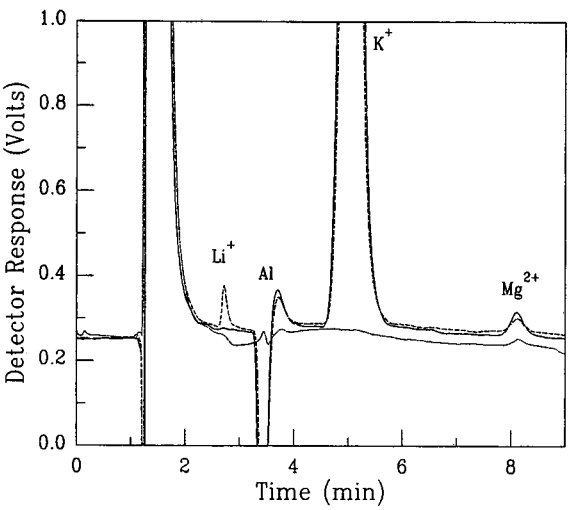

Fig. 3. Chromatogram of solutions extracted from aluminum alloy crevices. In both cases, Mg is detected, while from the Alloy 8090 crevice, Li^+ is detected as well. Also included is a water injection. ——— = Alloy 2024; --- = aloy 8090; ····· = water blank.

Failure of meter socket

In order to determine the cause of the failure, a series of analyses were performed, including analysis for organic acids. Fig. 5 shows two chromatograms from the organic acid analyses: the rinse solution from an attacked bolt; and the rinse solution from an identical, but unattacked, bolt. The presence of large amounts of formate and acetate on the attacked bolt and their absence on the unattacked bolt is clearly shown. Fig. 6 shows an overlay of two chromatograms: the soak solution from a piece of

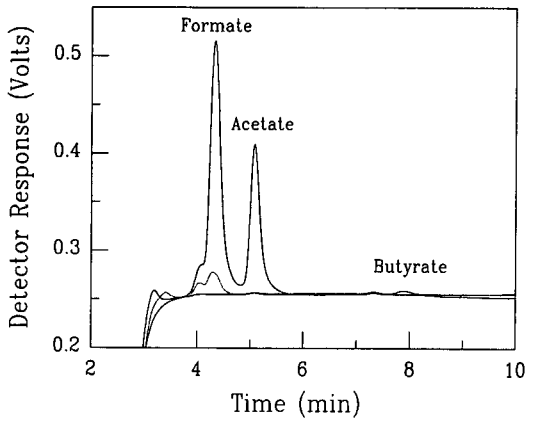

Fig. 5. Chromatogram of rinse solutions from a corroded component (———), and an uncorroded component (····). Also included is a water injection.

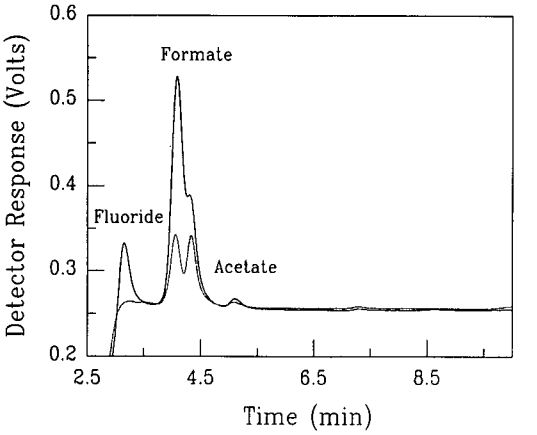

Fig. 6. Chromatogram of soak solutions from cardboard packaging material that contained corroded components (———), and uncorroded components (····).

the cardboard packaging that contained attacked components; and the soak solution from an identical piece of the cardboard packaging that contained unattacked components. The correlation between the presence of organic acids and corrosive attack is maintained.

DISCUSSION

Localized corrosion

Recently, the use of IC for the speciation of the chemical composition of solutions extracted from localized corrosion sites in stainless steel was demonstrated [4–6]. The present work extends that approach to another alloy system, precipitation hardened aluminum alloys. Aluminum alloys are fairly dilute with the sum of all alloying elements comprising approximately 10% (w/w) of the alloy. These alloying elements provide the means by which aluminum alloys are made technologically useful by increasing both the material's strength and stiffness [13,14]. However, they also decrease the localized corrosion resistance [14], though the operational mechanisms are uncertain. The present work demonstrates that IC is capable of detecting the minor alloying elements even in the presence of large amounts of Al^{3+}. Clearly, the minor alloying elements are preferentially dissolving, though quantitation of the degree of non-stoichiometric dissolution remains to be done. In addition, the presence of the Al^{3+} leads to a peak coincident with Na^{+}, but with an opposite polarity. Present work is aimed at determining the correspondence of this peak with the presence of an aluminum specie.

Failure of meter socket

The results of the IC analysis of the rinse/soak solutions from the meter socket bolts provided the critical information necessary to determine: (a) the cause of failure, (b) the identity of the aggressive species as well as (c) the source of the aggressive species. Both iron and zinc are quite susceptible to vapor-phase attack by organic acids [15]. The comparative IC analysis demonstrates that such attack took place inside the packages in which corroded components were found (Fig. 5). Conventional analyses of the corrosion products using X-ray diffraction and energy dispersive spectroscopy revealed little except for the presence of a sodium zinc sulfite on some corroded parts. The most likely source of the organic acids is the cardboard packaging material (Fig. 6). One possible scenario as to the origin and progression of the corrosion is as follows. Incomplete washing of the pulp used to make the cardboard allowed retention of organic acids (and inorganic ions such as sulfite) in the finished product. During the long (3 years) storage time, some of the acids vaporized and attacked the metallic surfaces. Further investigation revealed that all of the attacked components were packaged in card-

board manufactured in a single lot, while the unattacked sockets were packaged in cardboard manufactured in a different lot. This lends additional credence to the suspected source of the aggressive species.

This example clearly shows the utility of IC for corrosion failure analysis. Its ability to ionically speciate small volumes of solution with high mass sensitivity makes it especially attractive for corrosion analyses in which small volumes of solution at the metal/solution interface often control the nature and rate of the important processes.

At the present time, the application of capillary electrophoresis is also being pursued as a tool for corrosion failure analysis as well as both applied and fundamental studies of corrosion phenomena. With its combination of excellent detection limits and very small sample solution volumes required, capillary electrophoresis appears to be an ideal technique for such work.

ACKNOWLEDGEMENTS

This work was supported in part by a grant from the National Science Foundation (DMR-9119304). Additional financial support was provided by the Virginia Center for Innovative Technology. The assistance of Ray Kilmer (University of Virginia) in performing the X-ray diffraction and EDS analyses is also gratefully acknowledged.

REFERENCES

1 M. G. Fontana and N. D. Greene, *Corrosion Engineering*, McGraw Hill, New York, 1967, p. 41.
2 B. F. Brown, C. T. Fujii and E. P. Dahlberg, *J. Electrochem. Soc.*, 116 (1969) 218.
3 T. Suzuki, M. Yamabe and Y. Kitamura, *Corrosion*, 29 (1973) 18.
4 B. K. Nash and R. G. Kelly, *J. Electrochem. Soc.*, 139 (1992) L48.
5 B. K. Nash and R. G. Kelly, *J. Chromatogr.*, 602 (1992) 135.
6 B. K. Nash and R. G. Kelly, *Corros. Sci.*, (1993) in press.
7 S. E. Lott and R. C. Alkire, *Corros. Sci.*, 28 (1988) 479.
8 R. C. Newman, *Corros. Sci.*, 25 (1985) 341.
9 J. Mankowski and Z. Szklarska-Smialowska, *Corros. Sci.*, 15 (1975) 493.
10 *1985 Annual Book of ASTM Standards*, Vol. 3.02, American Society for Testing and Materials, Philadelphia, PA, 1985, ASTM G-48.
11 Waters Assoc., *Waters Innovative Methods for Ion Analysis*, Millipore, Milford, MA, July 1990, Method C-207.
12 Waters Assoc., *Waters Innovative Methods for Ion Analysis*, Millipore, Milford, MA, July 1990, Method A-109.
13 J. E. Hatch (Editor), *Aluminum: Properties and Physical Metallurgy*, American Society for Metals, Metals Park, OH, 1984.
14 M. G. Fontana and N. D. Greene, *Corrosion Engineering*, McGraw-Hill, New York, 1967, p. 169.
15 *Metals Handbook, Vol. 13, Corrosion*, ASM International, Metals Park, OH, 1987 p. 545.

Journal of Chromatography, 640 (1993) 351–353
Elsevier Science Publishers B.V., Amsterdam

CHROMSYMP. 2769

Highly selective ion chromatographic determination of ammonium ions in waters with a suppressor as postcolumn reactor

A. M. Dolgonosov* and A. N. Krachak

V. I. Vernadsky Institute of Geochemistry and Analytical Chemistry, Kosygin str. 19, 117975 Moscow (Russian Federation)

ABSTRACT

A highly selective ion chromatographic method for the determination of ammonium ions using an anion-exchange separation column with a bipolar ion exchanger was developed. The method is based on the reaction in a suppressor column between ammonium ions and nitrous acid formed from the eluent components followed by the negative conductimetric signal. The determination of more than 0.1 ppm of NH_4^+ in water is possible in the presence of 100-fold amounts of alkali metals and inorganic anions.

INTRODUCTION

Ammonium ion is one of the components that need to be monitored in natural and waste waters. For this purpose a number of methods have been applied, including ion chromatographic methods in the cation-exchange separation mode [1–3]. To increase the selectivity and sensitivity of the determination of ammonium ions we have developed an ion chromatographic method with conductivity detection based on the highly selective reaction of ammonium ions with nitrous acid in the suppressor column.

PRINCIPLE OF IC DETERMINATION OF AMMONIUM IONS

In an acidic medium, the reaction between ammonium ions and nitrous acid occurs as follows:

$$NO_2^- + NH_4^+ \rightarrow N_2 + 2H_2O \quad (1)$$

Hence the reaction results in the formation of neutral molecules from the electroconductive starting compounds, which is reflected in conductimetric measurements in a large decrease in the conductivity signal. This is an essential prerequisite for increasing the sensitivity of the determination of ammonium ions.

As nitrous acid is very unstable, it is impossible to use it as an eluent, so sodium nitrite solution is used. To obtain the nitrous acid necessary for reaction 1, we have used a suppressor column with a cation exchanger in the H^+ form. To avoid the retention of ammonium ions in the part of the suppressor column present in the Na^+ form, an alkaline eluent was used, which converts ammonium ions into ammonia molecules according to the reaction

$$NH_4^+ + OH^- \leftrightharpoons NH_3 + H_2O \quad (2)$$

The pressure in the chromatographic system is always sufficient for the complete dissolution of ammonia in the eluent (several bar). The suppressor column can exchange all the eluent cations with H^+ ions, hence these cations (with the exception of amides participating in a reaction similar to reaction 2) do not influence the determination of ammonium ions.

The separation column should possess an anion-exchange capacity in order to separate ammonium

* Corresponding author.

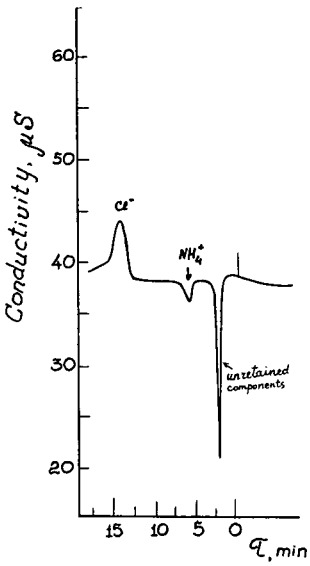

Fig. 1. Typical chromatogram for the IC determination of ammonium ions. For chromatographic conditions, see text. Concentration of ammonium ions, 0.2 mmol/l.

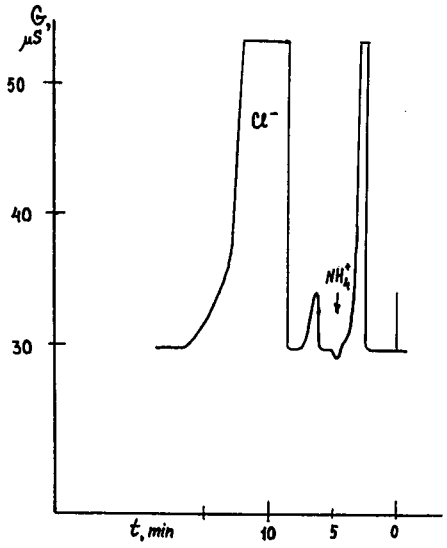

Fig. 2. IC analysis of sea water. For chromatographic conditions and sample preparation, see text.

ions from anions. On the other hand, the ammonium ion zone should move more slowly than the liquid phase in order to avoid superposition of the ammonium ion peak and peaks of unretained substances (*e.g.*, water). The anion exchanger is capable of retaining ammonia according to the ion-exclusion mechanism, but this effect is not sufficient for separating the ammonium ion peak from the water peak. To increase the ammonia retention, the stationary phase should act as a bipolar ion exchanger having both anion- and cation-exchange active sites.

By varying the eluent pH and the ratio between the cation- and anion-exchange capacities one can achieve a low concentration of ammonium ions (several percent), being in equilibrium with ammonia and, thereby, providing complete separation of ammonium ions from anions and unretained components.

EXPERIMENTAL

A ZVET-3006 ion chromatograph (DOKBA, Dzerzhinsk, Russian Federation) with a BIE-03 conductimeter (DOKBA) was used. A separation column (100 × 3 mm I.D.) was filled with KanK-BP bipolar central-localized sorbent (15 μm) [4] (GEOHI, Moscow, Russian Federation). Both the anion- and cation-exchange capacities of the packing were 0.2 mequiv./ml. A suppressor column (120 × 5 mm I.D.) was filled with Dowex-50X8 (50 μm) in the H^+ form. A 30-μl sampling loop was used. The eluent flow-rate was 1.7 ml/min.

The eluent and all solutions were prepared by dissolution of analytical-reagent grade chemicals (Reakhim, Moscow, Russian Federation) in doubly distilled water. An aqueous solution of sodium nitrite (0.5 mmol/l) and sodium hydroxide (3.0 mmol/l) was used as the eluent. An artificial sea-water sample was prepared by mixing sodium chloride (0.5 mol/l), sodium sulphate (0.02 mol/l) and potassium bromide (0.8 mmol/l), and 1.0 mmol/l ammonium chloride was added.

RESULTS AND DISCUSSION

Fig. 1 shows a typical chromatogram for the IC determination of ammonium ions. The height of the negative peak corresponding to ammonium ions is proportional to the amount of ammonium ions in the sample, as established by the correlation between the amounts of ammonium ions in various mixtures

and the detector response at the position of the ammonium ion peak. This correlation can be expressed by the equation

$$\Delta G = -A[NH_4^+]$$

where $A = 13.20 \pm 0.39$. The retention time of ammonium ions is 370 ± 10 s. The determination of ammonium ions is possible down to a concentration of 5 μmol/l (90 ng/ml; detection limit). Under the above conditions 100-fold molar excesses of alkali metal ions (Na^+, K^+) and inorganic anions (Cl^-, Br^-, SO_4^{2-}, etc.) do not interfere.

The proposed method can be applied to the determination of ammonium ions in natural waters, as shown in Fig. 2. The determination of ammonium ions in sea water is possible down to the level of a few parts per million.

REFERENCES

1 H. Small, T. S. Stevens and W. S. Bauman, *Anal. Chem.*, 47 (1975) 1801.
2 C. A. Pohl and E. L. Johnson, *J. Chromatogr. Sci.*, 18 (1980) 442.
3 S. Bouyoucos, *Anal. Chem.*, 49 (1977) 401.
4 A. M. Dolgonosov, *React. Polym.*, 17 (1992) 95.

Journal of Chromatography, 640 (1993) 355–358
Elsevier Science Publishers B.V., Amsterdam

CHROMSYMP. 2776

Determination of anions in an epoxy curing agent by ion chromatography

Homer L. Tucker*, Terri K. Smith and Stonewall J. Van Hook, III

Analytical Services Organization, Oak Ridge Y-12 Plant, Martin Marietta Energy Systems, Inc., Oak Ridge, TN 37831-8189 (USA)*

ABSTRACT

Within Martin Marietta's Analytical Services Organization (ASO), epoxy samples have traditionally been analyzed by high-performance ion chromatography (HPIC) using a bomb-prep method. Erratic sulfate results prompted an experimental 10% methanol preparation dissolution method to be used with subsequent analysis by HPIC. An HPIC method with isocratic separation and micromembrane suppression is discussed in this paper. This method is specifically for the determination of sulfur as sulfate and fluoride in an epoxy curing agent. The new method will be used as a replacement for a current production laboratory bomb-prep HPIC method. Matrix interferences caused by Parr bomb (see *Oxygen Combustion Bombs, Bulletin 1100*, Parr Instrument, Moline, IL, USA) combustion products were eliminated using this method. A precision and bias study was done to document the effectiveness of the new method.

INTRODUCTION

In the past, plant processes have used adhesives that contain methylenedianiline (MDA). The Occupational Safety and Health Administration is in the process of setting new standards for the regulation of MDA, which has shown carcinogenic characteristics in laboratory tests on animals. Dr. G. F. Dorsey, a scientist in the Development Division of Martin Marietta Energy Systems, Oak Ridge Y-12 Plant (Oak Ridge, TN, USA), has invented a new curing agent. Tests conducted on this curing agent thus far have shown it to be non-mutagenic. The new agent may be suitable as a replacement for MDA, and it yields a product for polyurethane and epoxy resins used in adhesives, encapsulants, coatings, filament windings, and binders [1].

During the development of this epoxy curing agent, samples were submitted for ion chromatography (IC) characterization. Boron trifluoride etherate, sulfuric acid, and sodium sulfate were used in the development process, and residual sulfur (analyzed as sulfate and calculated as sulfur) and fluoride were the anions of interest. IC analysis of the as-submitted epoxy product required a sample preparation step. The Parr-bomb preparation process is currently used for this type of matrix [2], but the procedure is technique-intensive and often gives erratic results (Table I). A preparation meth-

TABLE I

SAMPLE PREPARATION COMPARISON

Parr-bomb method		Methanol method	
Aliquot No.	Sulfur (μg/g)	Aliquot No.	Sulfur (μg/g)
Intitial preparation			
1	610	1	53
2	< 50	2	63
		3	63
		4	63
Rerun			
3	52		
4	20		
5	< 20		

* Corresponding author.

* Managed by Martin Marietta Energy Systems, Inc., for the US Department of Energy under contract DE-AC05-84OR21400.

0021-9673/93/$06.00

od that is simple, fast and efficient was developed as a replacement. This method eliminates the problem of interfering ions in the sulfate analysis, which is caused by combustion products generated in the Parr-bomb preparation (Figs. 1 and 2). The desired fluoride anion analyses were also determined by this method.

EXPERIMENTAL

Apparatus

All chromatography was performed using a Model 2320i series Dionex ion chromatograph, with a 50-μl sample loop. The system components consisted of one anion HPIC-AG-4A guard column (250 × 2 mm I.D.), one anion HPIC-AS-4A separator column (250 × 4 mm I.D.), an anion micromembrane eluent suppressor (AMMS), a conductivity detector (CDM-1), and a gradient pump (GP). A concentration of 0.0125 *M* sulfuric acid regenerant was delivered to the AMMS by plumbing the "B" valve in conjunction with a pressurized 24-l container. The eluents were delivered to the columns by a Dionex eluent degas module (EDM).

Materials

Deionized ultrapure distilled water with a minimum conductivity of 15 MΩ · cm was used to make the eluents and regenerant. Reagent-grade sulfuric acid, sodium hydrogencarbonate, and sodium carbonate were used. The standard solutions were made using ultrapurity-grade sodium sulfate and sodium fluoride. Methanol, HPLC/spectro grade, was used as the initial solvent.

Eluent preparation

The eluent for fluoride analysis (0.0001 *M* $NaHCO_3$) was made by dissolving 21.0025 g of sodium hydrogencarbonate in 1 l of ultrapure water (stock eluent) and making a secondary dilution of 0.4 ml of stock solution to each liter of working eluent. The stock eluent for the sulfate analysis was made by dissolving 47.0456 g of sodium hydrogencarbonate and 47.6955 g of sodium carbonate in 1 l of ultrapure water. The secondary eluent (0.0028 *M* $NaHCO_3$–0.00225 *M* Na_2CO_3) was made by diluting 5 ml of the stock solution to each liter of working eluent [3].

Regenerant and standard preparation

The regenerant (0.0125 *M*) was made from reagent-grade sulfuric acid. The standards were prepared by diluting a 1000-ppm stock solution of sulfate and fluoride to make the working concentrations shown in Table III.

Flow-rates

The regenerant flow-rate was 2.5 to 3.0 ml/min. The eluent flow-rate was 2.0 ml/min.

Sample preparation

The unbombed samples were prepared by dissolving *ca.* 1 g of sample in 10 ml of methyl alcohol and diluting to 100 ml with ultrapure water. The final dilutions were made after filtering the emulsion through a 0.45-μm Millex-HV filter.

RESULTS AND DISCUSSION

The initial step in the new preparation method is to dissolve *ca.* 1 g of the epoxy product in 10 ml of methanol. Boron trifluoride–methanol is a boron trifluoride soluble [4]. The residual sulfur in the epoxy products, as received for analysis, is present as a contaminant and is readily soluble. One aliquot is spiked, and deionized water is added to make 100-ml volume. After mixing, the solution is filtered through a Millipore Millex-HV 0.45 μm filter unit, which is methanol compatible. This breaks up the emulsion and produces a clear solution that can be diluted and injected into the chromatograph. Spiked samples are taken through this preparation method to measure the recovery rates of fluoride and sulfate and to measure the precision of the method (Tables II and III). Parr-bombed samples are prepared as recommended [5]. The sulfate analysis scans obtained using the methanol preparation method were easier to interpret due to the absence of interfering peaks that are generated during the oxygen combustion Parr-bomb preparation method (Figs. 1 and 2). Fluoride results are acceptable when using either preparation method. Preparation time for the Parr-bomb method is *ca.* 1 h. Sample backlog delays of 1 or more weeks are common. The methanol preparation method is typically <15 min. In both cases, the sample analysis time is <10 min (not including preparation time).

TABLE II

PRECISION OF STANDARD ADDITION ANALYSIS OF EPOXY CURING AGENT

Concentration of spike (mg/l)	Calculated sample concentration (mg/l)[a]	Mean	S.D.	R.S.D. (%)
Fluoride				
0.00	6010			
0.20	6270	6010	334	5.6
0.40	5740			
1.00	6050			
Sulfate				
0.00	195			
0.20	172	190	12	6.4
0.40	186			
1.00	205			

[a] All samples were diluted in order to match linearity range of standards at 3 μs using an AS-4A column (Dionex).

TABLE III

STANDARD LINEARITY IN EPOXY MATRIX (METHANOL DISSOLUTION)

Fluoride		Sulfate	
Added (mg/l)	Recovered (mg/l)	Added (mg/l)	Recovered (mg/l)
0.20	0.17	0.50	0.55
0.40	0.37	1.00	1.00
1.00	0.95	1.50	1.40
2.00	1.80	2.00	1.72

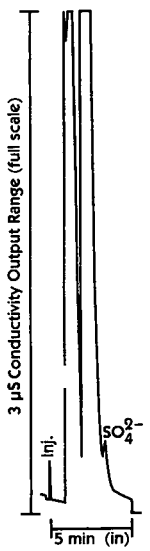

Fig. 1. Sulfate analysis with combustion product interferences. Conditions: Parr-bomb preparation sample, 2:1 diluted; columns, AG-4A and AS-4A; eluent: 0.0028 *M* $NaHCO_3$–0.00225 *M* Na_2CO_3; flow-rate, 2 ml/min.

CONCLUSIONS

IC analysis of an epoxy product, specifically boron trifluoride etherate, is possible after either Parr-bomb or 10% methanol–water preparation. The methanol preparation method is quicker and more efficient. The solution–filtration method relies less on the proficiency of the technician's technique than the Parr-bomb method. When using the methanol preparation method and the AS-4A column and eluent, IC analysis is straightforward, and the

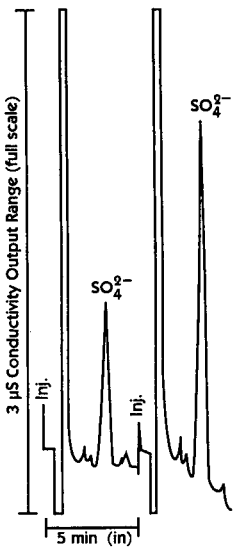

Fig. 2. Sulfate analysis after methanol preparation. Conditions: methanol preparation sample, 2:1 diluted + 0.50 mg/l sulfate spike; columns, AG-4A and AS-4A; eluent: 0.0028 *M* $NaHCO_3$–0.00225 *M* Na_2CO_3; flow-rate, 2 ml/min.

problem of interfering ions from the Parr-bomb combustion products is eliminated. Additionally, the cost of sample preparation associated with using the platinum-lined Parr-bomb is negated.

ACKNOWLEDGEMENTS

The authors wish to express their appreciation for the valuable help of R. E. Carroll, R. A. Dyer and Dr. G. F. Dorsey, Martin Marietta Energy Systems, Inc., Oak Ridge Y-12 Plant, for their valuable contribution to this manuscript.

REFERENCES

1 G. F. Dorsey, personal communications, Martin Marietta Energy Systems, Oak Ridge, TN.
2 *Oxygen Combustion Bombs, Bulletin 1100*, Parr Instrument, Moline, IL.
3 *The Dionex Ion Chromatography Cookbook*, Dionex, Sunnyvale, CA.
4 N. I. Sax, *Hawley's Condensed Chemical Dictionary*, Van Nostrand Reinhold, New York, 11 ed., p. 165 and 1987.
5 *Analytical Methods for Oxygen Bombs, Bulletin 207M*, Parr Instrument, Moline, IL.

Journal of Chromatography, 640 (1993) 359–364
Elsevier Science Publishers B.V., Amsterdam

CHROMSYMP. 2753

Analysis of cationic nutrients from foods by ion chromatography

John Morawski*, Peter Alden and Art Sims

Millipore Corp. Waters Chromatography, 34 Maple Street, Milford, MA 01757 (USA)

ABSTRACT

This paper describes the feasibility of combining two relatively new technologies to generate data on the cationic nutrient content of foods. Single-column ion chromatography was used to monitor several analytes following the use of a microwave digestion scheme aimed at rapid, multiple sample digestion. The result is a more streamline and productive approach to multi-sample preparation and multi-analyte determination when investigating the cation content of foods.

Linearity and limits of detection for the chromatographic procedure were established. Sample size as well as digestion acid type and amount were investigated during the microwave process. The method was applied to a variety of food matrices to evaluate its scope. Results generated with this method compare favorably to those from atomic absorption.

Finally, capillary ion electrophoresis (Waters' trade name: Capillary Ion Analysis), a subset of capillary electrophoresis which has been optimized for ion analysis, was applied to the sample digests to investigate the usefulness of this technology to the analysis of mono-/divalent cations from foods.

INTRODUCTION

Currently, the analysis of cationic nutrients in foods is a routine procedure using atomic absorption spectroscopy (AAS) or inductively coupled plasma spectroscopy (ICP). The former is a tedious process allowing only single analyte determination and the latter represents a significant investment in instrumentation. In both cases, microwave or hotplate acid digestion as well as combustion oven ashing are used for sample preparation. These techniques are lengthy and require time consuming hands on manipulation of the samples.

The development of new ion chromatography (IC) chemistries has provided the ability to separate mono- and divalent cations in a single analysis. Coordination IC performed on a poly(butadiene–malic acid)-coated silica column with an EDTA–nitric acid isocratic eluent and conductimetric detection allows the separation and detection of nutritionally relevant cations such as sodium, potassium, magnesium and calcium [1,2].

Microwave technology has made a broad entry into the analytical laboratory for a variety of sample preparation procedures. Microwave acid digestion of food matrices has been shown to be useful prior to cationic nutrient determination by AAS for more rapid sample preparation [3]. Complete digestion of multiple samples (10 plus a standard and blank) in less than 1.5 h, as well as the ability to automate the process, positions microwave technology as a desirable sample preparation alternative, especially when used in conjunction with a multiple analyte technique such as IC.

This study incorporates both of these unique technologies. The microwave digestion procedure was optimized relative to sample size and which acids to use in order to provide a digest which was compatible with the ion chromatographic process. Sample concentrations and dilutions were optimized relative to the sensitivity/mass load capabilities of the chromatography. A variety of food samples were chosen to be representative of the diversi-

* Corresponding author.

0021-9673/93/$06.00

ty of matrices which could potentially challenge a food analysis method.

A preliminary evaluation of the application of capillary ion electrophoresis (CIE) (Waters' trade name: Capillary Ion Analysis, CIA) to this analysis was also conducted. All sample digests were introduced into a capillary electrophoresis system in which the chemistry was optimized for cation separation [4]. Good separations of the analytes of interest with no sample induced baseline upsets were observed with this technology and the results were compared to AAS.

EXPERIMENTAL

Instrumentation

The microwave digestion apparatus was a CEM MDS 2000 equipped with lined digestion vessels and the pressure-control option from CEM Corp., Matthews, NC, USA. The liquid chromatograph consisted of an Action Analyzer, a WISP 712 autoinjector, a Model 431 conductivity detector, a Waters IC-Pak C M/D column, and a Model 860 Expert Ease chromatography and data management system, all from Millipore, Waters Chromatography, Milford, MA, USA. A Quanta 4000 capillary electrophoresis unit and AccuPure fused-silica capillaries, also from Millipore, Waters Chromatography, were used for the CIE portion of the study.

Eluents and electrolytes

The eluent used for the IC was a solution of 0.1 m*M* ethylenediaminetetraacetic acid (EDTA free acid) and 3.0 m*M* nitric acid.

The electrolyte used for the CIE separations was a 1.2 m*M* UV-Cat-2 and 3.0 m*M* Tropolone solution.

Reagents

EDTA free acid was analytical-reagent grade from J. T. Baker, Phillipsburg, NJ, USA. Nitric acid was Ultrex grade and hydrogen peroxide (30%) was analytical-reagent grade both from J. T. Baker. Sodium, potassium, magnesium and calcium standards were prepared from sodium chloride, potassium chloride, magnesium nitrate hexahydrate and calcium nitrate tetrahydrate, respectively, and all were Sigma grade, Sigma, St. Louis, MO, USA. Tropolone was reagent grade from Aldrich, Milwaukee, WI, USA. UV-Cat 2 was from Millipore, Waters Chromatography. Water purified (18 MΩ) using a Millipore Milli-Q water purification system (Millipore Corporation, Bedford, MA, USA) was used for all solutions.

RESULTS AND DISCUSSION

All samples were prepared using the procedure outlined in Fig. 1 prior to analysis by IC, AAS and CIE. The amount of nitric acid used for the digestion process was minimized to 3 ml. Through experimentation this proved to be enough acid to complete the digestion without challenging the chromatographic equilibrium during a 100-μl injection.

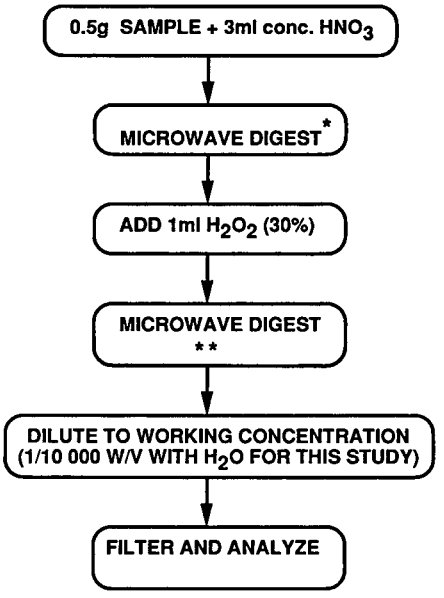

Fig. 1. Schematic of samples preparation used for all three (AAS, IC and CIE) methods of analysis. Notes: * CEM MDS 2000 microwave with lined digestion vessels and pressure control; 1 p.s.i. = 6894.76 Pa.

	Stage				
	1	2	3	4	5
% Power (varies with wattage of system and No. of samples)	30	30	30	30	30
Pressure (p.s.i.)	20	40	85	125	170
Time (min)	15	15	15	15	15
Time at pressure (min)	5	5	5	5	5

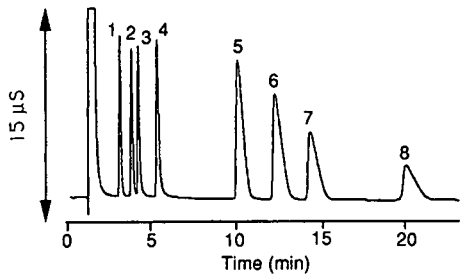

Fig. 2. Standard separation of eight mono- and divalent cations with coordination chromatography. Conditions, column: Waters IC-Pak C M/D; eluent: 0.1 m*M* EDTA–3.0 m*M* nitric acid, flow-rate: 1.0 ml/min; detection: conductivity; injection 100 µl. Peaks: 1 = lithium (0.25 mg/l); 2 = sodium (1.0 mg/l); 3 = ammonium (1.0 mg/l); 4 = potassium (3.0 mg/l); 5 = magnesium (2.0 mg/l); 6 = calcium (3.0 mg/l); 7 = strontium (5.0 mg/l); 8 = barium (5.0 mg/l).

Using more than 3 ml of nitric acid for the digestion procedure produced a large negative response just prior to the sodium peak which restricted integration routines. However, since only 3 ml of nitric acid could be used, the samples had to be submitted to a secondary microwave step involving H_2O_2, and sample size had to be limited to 0.5 g in order for the digestion procedure to produce water clear digests suitable for the subsequent dilutions prior to injection.

The IC used for this experiment had the ability to separate more than just the mono- and divalent cations of nutritional importance. Fig. 2 exemplifies this with an eight-cation separation. Using this chromatography and a series of standard solutions, linearity statements for both the mono- and divalent cations lithium, sodium, potassium, magnesium, calcium, strontium and barium were generated. For these cations the correlation coefficients are better than 0.9996 over a range of 0 to 10 mg/l for monovalent cations and 0 to 20 mg/l for divalent cations. This represents the range of these analytes typically found in the final injection solution of food digests. Table I lists the detection limits of this IC technique as determined with low level standard injections and based on a 3:1 signal-to-noise ratio.

TABLE I

DETECTION LIMITS FOR MONO- AND DIVALENT CATIONS USING COORDINATION CHROMATOGRAPHY WITH CONDUCTIMETRIC DETECTION AS IN FIG. 2

Calculated based on a 3:1 signal-to-noise ratio of standards.

Analyte	Concentration (µg/l)
Lithium	1
Sodium	5
Ammonium	5
Potassium	20
Magnesium	5
Calcium	10
Strontium	50
Barium	100

The samples chosen for this study were intended to represent a wide range of the cations of interest and also a diversity of sample matrices. Pretzels (salted), parsley (dried), bread crumbs, parmesan cheese and peanut butter all present different opportunities for matrix related excipients to potentially interfere with the chromatography. However, as can be supported by the examples of Figs. 3–7, the combination of the acid–peroxide microwave digestion and coordination IC produce an interference free chromatogram.

Pretzels, representing a high sodium (salt added) content sample generated the chromatogram seen in Fig. 3. The sodium peak rises out of the negative response created by the digestion solution residues. This digestion solution response creates a challenge for peak integration. The lift-off point for the sodi-

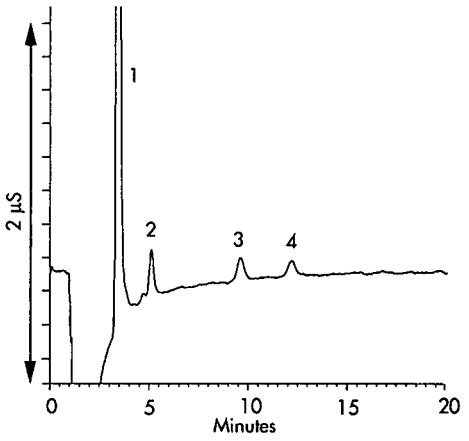

Fig. 3. Cation analysis from pretzels with coordination chromatography following microwave digestion. Conditions as in Fig. 2. Sample diluted 1/10 000. Peaks and amounts in original sample: 1 = sodium (1.47%); 2 = potassium (0.106%); 3 = magnesium (0.0224%); 4 = calcium (0.0214%).

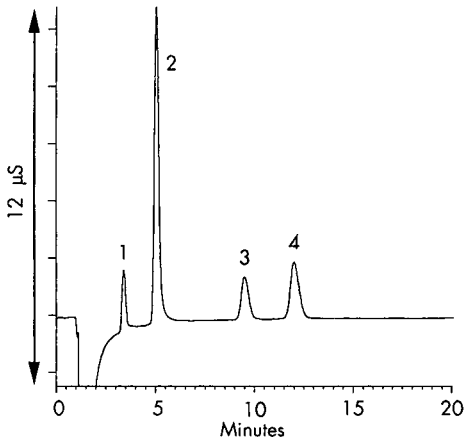

Fig. 4. Cation analysis from parsley with coordination chromatography following microwave digestion. Conditions as in Fig. 2. Sample diluted 1/10 000. Peaks and amounts in original sample: 1 = sodium (0.405%); 2 = potassium (4.78%); 3 = magnesium (0.27%); 4 = calcium (0.579%).

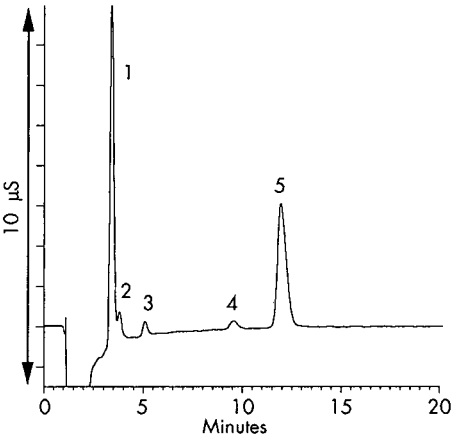

Fig. 6. Cation analysis from parmesan cheese with coordination chromatography following microwave digestion. Conditions as in Fig. 2. Sample diluted 1/10 000. Peaks and amounts in original concentration: 1 = sodium (1.72%); 2 = ammonium (not determined); 3 = potassium (0.15%); 4 = magnesium (0.040%); 5 = calcium (0.944%).

um peak had to be carefully determined with manual integration techniques. Fig. 4 depicts a natural sodium level food example using parsley as the sample. This matrix contained much less sodium which provides a chromatogram where integration of this analyte is much more easily defined because the sodium peak is not rapidly rising out of the negative response of the digestion solution. Also of interest in this example is the high level of magnesium present (0.27%) relative to the other samples. It should be noted that this is a sample high in chlorophyll, a magnesium-containing compound.

Figs. 5–7 demonstrate the presence of ammonium in the chromatogram as well as the other cations

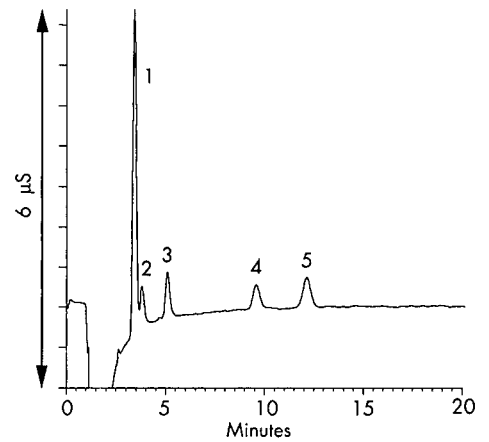

Fig. 5. Cation analysis from bread crumbs with coordination chromatography following microwave digestion. Conditions as in Fig. 2. Sample diluted 1/10 000. Peaks and amounts in original sample: 1 = sodium (0.766%); 2 = ammonium (not determined); 3 = potassium (0.219%); 4 = magnesium (0.0485%); 5 = calcium (0.104%).

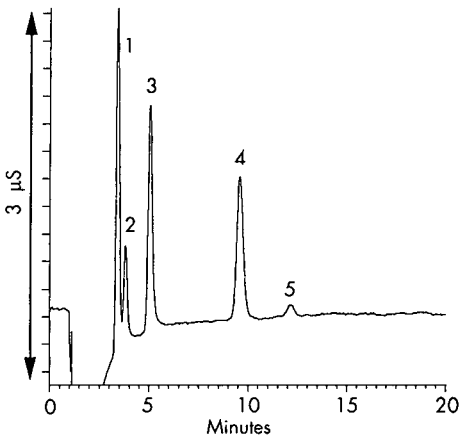

Fig. 7. Cation analysis from peanut butter with coordination chromatography following microwave digestion. Conditions as in Fig. 2. Sample diluted 1/10 000. Peaks and amounts in original sample: 1 = sodium (0.456%); 2 = ammonium (not determined); 3 = potassium (0.673%); 4 = magnesium (0.166%); 5 = calcium (0.021%).

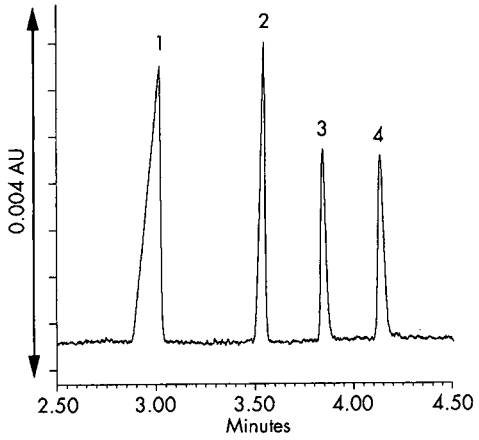

Fig. 8. Cation analysis from parsley with CIE following microwave digestion. Conditions, capillary: 60 cm × 75 μm fused silica; electrolyte: 1.2 m*M* UV Cat-2–3.0 m*M* tropolone; potential: 20 kV positive; detection: indirect UV at 185 nm; injection: hydrostatic, 10 cm for 30 s. Sample diluted 1/10 000. Peaks and amounts in original sample: 1 = potassium (4.90%); 2 = calcium (1.23%); 3 = sodium (0.448%); 4 = magnesium (0.39%).

of interest. Since the system had not been calibrated for this analyte, it was not quantified. The latter two of these examples, parmesan cheese and peanut butter, represent this methods ability to deal with relatively high fat matrices.

Figs. 8 and 9 are electropherograms generated by subjecting the microwave digests of parsley and bread crumbs to a CIE system optimized for cations. All four of the cations of interest were readily resolved with a different selectivity than the IC separation and with no intereferences observed. It is known, however, that with the UV Cat-2–tropolone electrolyte used for this feasibility evaluation, there is a comigration of potassium and ammonium. This is reflected in the elevated CIE potassium results of the three samples (Figs. 5–7) where IC showed the presence of ammonium.

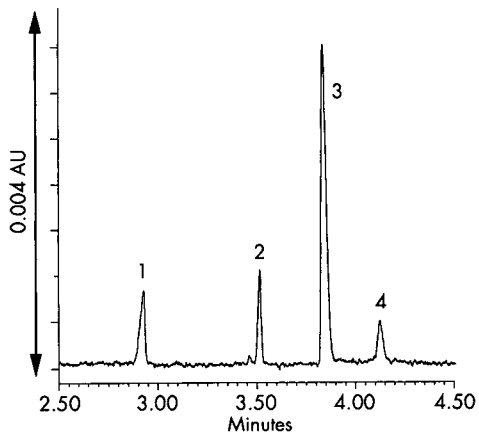

Fig. 9. Cation analysis from bread crumbs with CIE following microwave digestion. Conditions as in Fig. 8. Sample diluted 1/10 000. Peaks and amounts in original sample: 1 = potassium (0.489%); 2 = calcium (0.241%); 3 = sodium (0.752%); 4 = magnesium (0.063%).

TABLE II

MONO- AND DIVALENT CATION RESULTS FOR AAS, IC AND CIE WHEN APPLIED TO THE SAME SAMPLE DIGESTS

	Sodium (%)	Potassium (%)	Magnesium (%)	Calcium (%)
Pretzels				
AAS	1.49	0.25	0.019	0.09
IC	1.47	0.11	0.022	0.02
CIE	1.38	0.26	0.037	0.10
Parsley				
AAS	0.63	5.20	0.22	0.82
IC	0.40	4.79	0.27	0.58
CIE	0.45	4.90	0.39	1.23
Bread crumbs				
AAS	0.82	0.34	0.057	0.20
IC	0.77	0.22	0.049	0.10
CIE	0.75	0.49	0.063	0.24
Parmesan				
AAS	2.00	0.32	0.043	1.28
IC	1.72	0.15	0.040	0.94
CIE	1.63	0.51	0.058	1.96
Peanut butter				
AAS	0.51	0.70	0.140	0.05
IC	0.46	0.67	0.166	0.02
CIE	0.46	1.02	0.246	0.09

Table II presents the data results from the three analytical methods applied in this study. With the exception of calcium for IC and potassium for CIE, the results compare favorably to AAS. In the case of the calcium results by IC, it is known that with coordination chromatography, the calcium is chelated off of the column by the EDTA portion of the eluent. It could be speculated that an increase in this component of the eluent may provide better chelating capabilities for higher IC results for calcium and better correlation to the other data. As previously

mentioned, the elevated potassium results for the CIE data are caused by a comigration of potassium and ammonium. These analytes can be resolved with this technique through the use of complexing agent such as 2.0 m*M* 18-crown-6 ether in the electrolyte [5].

CONCLUSIONS

Microwave digestion and coordination IC can be used in series to provide advantages to current methods of analysis for cation determinations from food. Multi-sample, multi-analyte capabilities offered by this approach can decrease analysis time and increase throughput while minimizing sample handling. Initial studies generated results which are acceptable relative to atomic absorption. Further investigation with respect to low calcium results need to be conducted as do method validation parameters such as precision (reproducibility) and accuracy (spike recoveries). CIE can also be applied to the sample digests as either a substitute for or in addition to IC with good results. This technique offers the advantage of speed with run times of 4.5 min *versus* 20 min for IC. This speed provides a better compliment to the microwave digestion scheme since a batch of 10 samples can now be analyzed in a shorter time than is required to digest another batch of 10 samples. So in this example, an analytical laboratory incorporating microwave digestion followed by CIE determination can process 50 samples times 4 analytes or 200 cation analysis per day.

REFERENCES

1 P. G. Alden and J. Krol, *The Waters Column*, Winter (1992) 3.
2 P. E. Jackson, T. Bowser and P. G. Alden, *LC · GC*, 10 (1992) 786.
3 P. J. Oles and W. M. Graham, *J. Assoc. Off. Anal. Chem.*, 74 (1991) 812.
4 A. Weston, P. R. Brown, A. L. Heckenberg, P. Jandik and W. R. Jones, *J. Chromatogr.*, 602 (1992) 249.
5 F. Stover, *Electrophoresis*, 11 (1990) 750.

Journal of Chromatography, 640 (1993) 365–369
Elsevier Science Publishers B.V., Amsterdam

CHROMSYMP. 2760

Determination of copper, nickel, zinc, cobalt and manganese in seawater by chelation ion chromatography

Raffaela Caprioli and Sandro Torcini*

Italian National Agency for New Technology, Energy and the Environment, Environmental Geochemistry Division, Via Anguillarese 301, 00100 Rome (Italy)

ABSTRACT

Preconcentration and determination of trace elements in seawater by chelation ion chromatography (CIC) was studied. For the retention of metal ions (0.25–0.30 *M*), ammonium acetate (at pH 4.8–5.1) and macroporous iminodiacetate chelating resin were used. This system (CIC) permits trace and ultra-trace determination of metals in a variety of complex matrices, in particular those with a high content of alkali and alkaline earth metals. Detection limits range from 0.1 to 0.5 ng. Satisfactory results are obtained in the range 0.05–0.5 μg/l when 60 ml of sample are preconcentrated. In this work the contents of zinc, copper, nickel, cobalt and manganese in seawater from the Venice lagoon are presented. The results obtained by chelation ion chromatography are compared with those obtained using preconcentration of metals with dithizone and ammonium pyrrolidinedithiocarbamate in chloroform and analysed by graphite furnace atomic absorption spectrometry.

INTRODUCTION

The determination of trace metals at μg/l levels in seawater is hampered by the matrix effect due to the high alkali and alkaline earth metal concentration. This high cation concentration makes it impossible to concentrate metal cations by conventional cation-exchange methods. Unlike conventional ion-exchange concentration methods that are typically not selective for ions of the same valency [1], chelation concentration is a selective concentration method.

Chelation ion chromatography (CIC) is a new method that combines analyte concentration and matrix elimination with analytical separations and selective detection for transition metals [2].

In recent years ion-exchange resin has been used for trace metal determinations in combination with on-line chromatographic detection. For this reason, iminodiacetate chelating resin (Chelex-100), which for many years has been used with success in batch analysis for the determination of many metals in complex matrices [3,4], was packed in a column and eluent forced through at 1–2 ml/min. The results showed that in these conditions only partial recovery of some trace metals is achieved. After many attempts to improve the metal retention on Chelex-100 chelating resin, it was concluded that the low recovery of metal ions was caused by a physical degradation of the resin under pressure because of low degree of cross-linking of microporous polystyrene–divinylbenzene (PS–DVB) supporting polymer. For this reason, Dionex has developed a more highly cross-linked macroporous PS–DVB containing the iminodiacetate functional group that allows operation at high pressure without physical degradation (Met Pac CC-1 column) [2]. Using this resin high recoveries of several metals has been obtained with complex matrices.

In the present work a chelating column (Met Pac CC-1) was used to preconcentrate trace elements starting from a sample volume ranging from 5 to 60 ml.

* Corresponding author.

0021-9673/93/$06.00

Alkali metals and anions are not retained by the chelating column during the sample loading. Alkaline earth metals are removed by the chelating column and selectively eluted to waste by a 2 *M* ammonium acetate pH 5.5 buffer.

The concentrated transition metals are then eluted with 0.5 *M* nitric acid and sent to a second concentrator column. The concentrated metals are then separated in an analytical column by pyridine-2,6-dicarboxylic acid (PDCA).

Detection is accomplished by visible absorbance after post-column derivatization with a metallochromic indicator, 4(2-pyridylazo) resorcinol mono sodium salt hydrate (PAR) [5,6].

EXPERIMENTAL

Materials

Chromatographic equipment. The ion chromatography (IC) system consisted of a Model 2020i chromatograph with eluent degas module (EDM) and reagent-delivery module (RDM), a gradient pump module (GPM), a DQP-1 sample pump and a variable-wavelength detector module (VDM).

An advanced computer interface (ACI) was in series with a 386 Uni Bit PC.

Columns. The column used for chelation, containing a macroporous PS–DVB iminodiacetate chelating resin, was from Dionex (Met-Pac CC-1). The column has a capacity of 0.45 mequiv.

A second concentrating column, TMC-1 (sulphonated PS–DVB cation-exchange resin), with high capacity (2.2 mequiv./ml), a CS5 separation column, a CG5 precolumn (packed with a mixed-bed ion-exchange resin) and GPM programme (for CIC) were from Dionex [7].

Reagents. Ammonium acetate 2 *M*, pH 5.4 ± 0.1, PDCA, PAR and ammonium nitrate 0.1 *M*, pH 3.5 ± 0.1, were purchased from Dionex.

Nitric acid was Aristar grade (BDH); bidistilled water was obtained using a Milli-Q Plus system from Millipore.

Chloroform was GPR grade (BDH); ammonium pyrrolidinedithiocarbamate (APDC) and dithizone were, respectively, Spectrasol and AnalaR grade (BDH).

Analytical conditions.

Fig. 1 shows a scheme of the chelation concentration chromatography system.

Ammonium acetate 2 *M* was used for chelation on the CC-1 column.

In order to stabilize the samples for storage, both samples and standards were acidified to pH 2 with nitric acid. Before concentration, to ensure the complete recoveries of trace metals, the solutions were buffered with 2 *M* ammonium acetate pH 5.4.

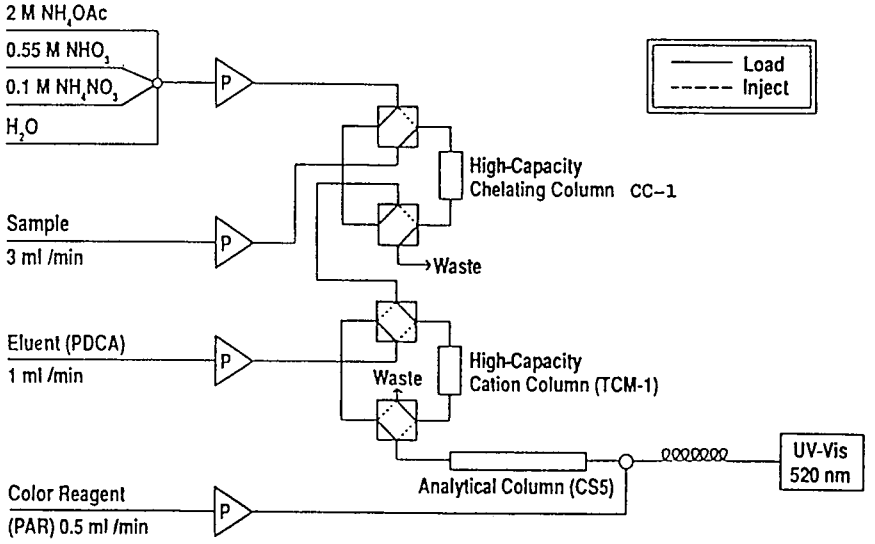

Fig. 1. Scheme of the chelation concentration method for the determination of transition metals.

The recommended analytical conditions were as follows: ammonium acetate final concentration between 0.25 and 1 *M* and final pH 5.4 ± 1 [7].

Variation of the pH, by addition of 2 *M* ammonium acetate was followed in bidistilled water and seawater acidified to pH 2.2 and in seawater that had not been acidified. The recommended pH for 100 ml of seawater is achieved by addition of 90–100 ml of ammonium acetate, resulting in a solution of about 1 *M* ammonium acetate. However, dilution of the sample and the high cost of the large amount of ammonium acetate used preclude the application of the method in these conditions. For this reason the final ammonium acetate concentration was 0.25–0.30 *M* (final pH 4.8–5.1), depending on whether standard or seawater solution was used. This was achieved by addition of 10–20 ml of ammonium acetate for every 100 ml of standard or sample solution.

Nitric acid 0.35 *M* was used to elute metals in the preconcentration column (TMC-1). Before the metals preconcentrated in the TMC-1 column [7] can be injected into the analytical stream, the TMC-1 must be converted from the acid (H^+) form to the ammonium (NH_4^+) form. This is accomplished by pumping 0.1 *M* ammonium nitrate (at pH 3.5) into the TMC-1 column.

RESULTS AND DISCUSSION

Fig. 2 shows a typical chromatogram of a standard solution of trace metals analysed by chelation concentration when 6 m*M* pyridine-2,6-dicarboxylic acid (PDCA) was used.

We also studied the variation in the retention time of copper, nickel, zinc, cobalt and manganese and noted a very low variation when many analyses were performed.

To assure the validity of the analytical data, the evaluation of analytical blanks using chelation concentration was performed.

To minimize the influence of the metals on the blank, analytical-grade reagents and glassware were used and all parts of the system were thoroughly washed with 0.1 *M* oxalic acid. Care was taken to minimize reagent and sample contamination during preparation and handling.

Generally, iron and zinc are the most common metal contaminants, while a small amount of copper may also be observed. Fig. 3 shows a typical level of background contaminant in a blank run.

The average values of the blank, when 60 ml of bidistilled water were preconcentrated, were 0.1, 0.05 and 0.30 ppb for copper, nickel and zinc, respectively. When several blanks (n = 8) were analysed, the observed R.S.D.s were 1.1, 0.7, and 2.1% for copper, nickel and zinc, respectively. Cobalt and manganese peaks do not occur on blank chromatograms.

To verify the linearity of the CIC method in relation to the volume of lagoon water used (after purification with Chelex 100 resin [4]), copper, nickel, zinc, cobalt and manganese at 1, 2, 2, 2, 2 μg/l, respectively, were added and 5, 10, 20 and 40 ml of sample were preconcentrated.

To evaluate the linearity with the increase in metal concentrations in saline matrix, the method of additions was carried out on Venice lagoon water. In the both cases the excellent linearity of the method was confirmed.

To evaluate the precision of the method at ppb levels, analysis of standards was repeated a number

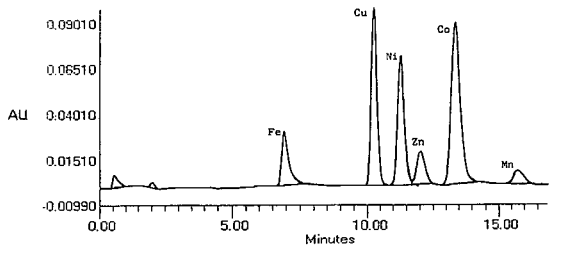

Fig. 2. Typical chromatogram of a standard solution of copper, nickel, cobalt (1 μg/l), zinc and magnanese (2 μg/l) by chelation concentration when 60 ml of solution were preconcentrated and 6 m*M* pyridine-2,6 dicarboxylic acid (PDCA) was used.

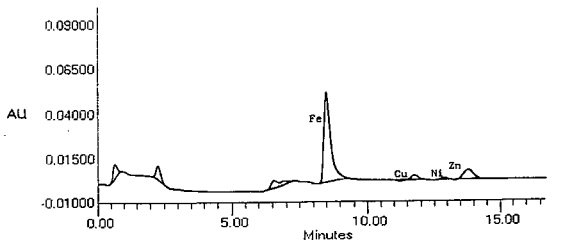

Fig. 3. Typical level of background using chelation concentration. Copper, nickel and zinc are 0.060, 0.040 and 0.20 μg/l, respectively. In this case we did not calculate the blank of iron.

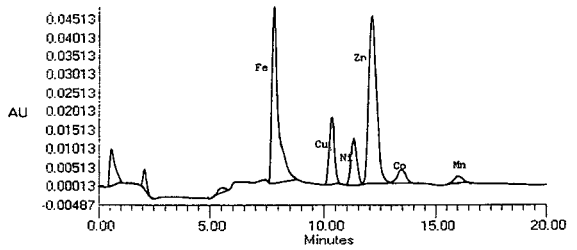

Fig. 4. Typical chromatogram of Venice lagoon seawater when 60 ml of sample were preconcentrated. Copper, nickel, zinc, cobalt and manganese levels are 0.3, 0.35, 4.2, 0.09 and 0.36 μg/l respectively. In this case we did not calculate the iron level.

of times and R.S.D.s calculated. When 60 ml of copper, nickel, zinc, cobalt and manganese standard samples were preconcentrated R.S.D.s of 0.26, 2.3, 16.2, 0.41 and 4.6%, respectively, were obtained. The data confirm that the precision of the method at the ppb level is good.

Finally, analysis of Venice lagoon seawater was performed to control the level of trace metals in the channel connecting the lagoon with the sea. A 60-ml sample of the lagoon seawater was sampled at 3.5 m depth, filtered through a 0.45-μm cellulose filter, immediately loaded on the preconcentrating column and analysed. Fig. 4 shows a typical chromatogram of Venice lagoon seawater.

The results obtained by chelation ion chromatography are compared with those acquired using preconcentration of metals with dithizone (diphenylthiocarbazone) and APDC absorption spectrometry in chloroform and analysed by graphite furnace atomic absorption spectrometry (AAS) after re-extraction in acid solution [8]. The data obtained with the two methods are very similar; only the manganese concentration is different because during the loading phase a part of it is not quantitatively retained on the preconcentrating column. It has been verified that, during the washing phase with ammonium acetate, about 15% of manganese is lost when the rate of sample loading is 3 ml/min. This is not a problem since the percentage of manganese eluted during this elution process is constant.

The linear range calculated for the system using a seawater matrix was from 0.1 ng (detection limit) to at least 250 ng for the metals studied. The detection limits for copper, nickel, zinc, cobalt and manganese in seawater, when 60 ml of sample were preconcentrated, were 0.05, 0.05, 0.15, 0.05 and 0.1 μg/l, respectively.

The data obtained from many successive analyses of Venice lagoon seawater show low variations of copper, nickel and cobalt, while zinc is a highly variable because of the changes of the chemical composition of water flowing in the channel. A higher degree of uncertainty was found for manganese, which in some analyses was below the detection limit.

Regarding the iron concentration, this was not determined because of the high levels of iron found in the blank during the analytical procedure.

CONCLUSIONS

The CIC method shows high validity. This technique allows the analysis of many metals at trace levels in a few minutes and it is possible to eliminate completely the salty matrix interferences.

Alkali metals and anions are not retained by the chelating column. Alkaline earth metals are selectively eluted to the waste when 2 *M* ammonium acetate is pumped through the chelating column.

Up to 100 ml of seawater were concentrated on the chelating column without significant loss of the transition metals.

The precision of CIC at the low-ppb level is very good. Zinc typically shows a higher relative standard deviation. This mainly results from the higher blank value. The reliability of the method is very high.

Table I shows the comparison between the CIC method and a preconcentration method by APDC

TABLE I

CHARACTERIZATION OF VENICE LAGOON WATER BY GRAPHITE FURNACE AAS AND CIC

Element	AAS	CIC
Copper	0.55	0.58
Nickel	0.73	0.71
Zinc	2.0	1.93
Cobalt	0.04	0.08
Manganese[a]	1.90	1.15

[a] During the elution process with ammonium acetate some manganese (15%) is eluted.

or dithizone extraction and graphite furnace AAS analysis.

The analysis of Venice lagoon water in the zone examined shows rather low heavy metal values. Only for zinc are the values higher as a result of both different environmental conditions and a greater probability of contamination by this element. Analysis of heavy metals for environmental monitoring in Venice lagoon, utilizing the CIC technique, was also taken in account. Some problems related to the filtration equipment and the automatic sample treatment present (particularly for zinc), at this moment, a limitation to the application of the monitoring system.

REFERENCES

1 J. P. Riley and D. Taylor, *Anal. Chim. Acta*, 40 (1968) 479.
2 A. Siriraks, H. M. Kingston and J. M. Riviello, *Anal. Chem.*, 62 (1990) 1185.
3 Su-Cheng Pai, Pai-Yee Whung and Ruei-Lung Lai, *Anal. Chim. Acta*, 211 (1988) 257.
4 R. Boniforti, R. Ferraroli, P. Frigeri, D. Heltai and G. Queirazza, *Anal. Chim. Acta*, 33 (1984) 162.
5 J. A. Cox and N. Tanaka, *Anal. Chem.*, 57 (1985) 385.
6 J. R. Jezorek, H. Freiser, *Anal. Chem.*, 51 (1979) 373.
7 *Technical Note*, No. 25, Dionex, Sunnyvale, CA, February, 1990.
8 M. Brondi, M. Dall'Aglio, E. Ghiara and R. Gragnani, *Chemistry in Ecology*, 2 (1986) 289.

Journal of Chromatography, 640 (1993) 371–378
Elsevier Science Publishers B.V., Amsterdam

CHROMSYMP. 2828

Improved method for the determination of manganese in nuclear power plant waters

Archava Siriraks* and John Stillian

Dionex Corporation, 1228 Titan Way, Sunnyvale, CA 94088-3603 (USA)

Dennis Bostic

Virginia Electric and Power Company, Surry Power Station, Surry, VA 23883 (USA)

ABSTRACT

An improved method for manganese determination in nuclear power plant waters has been developed. This method combines a selective chelation concentration method with a unique analytical separation for manganese from the interfering matrix using a weak acid cation exchange column. The detection sensitivity by conventional post-column derivatization is improved with the combination of chemical eluent suppression and subsequent post-column derivatization. The detection limit for manganese in ammonium matrix is approximately 2 pg/ml and the limit of quantitation 10 pg/ml with 100 ml sample volume.

INTRODUCTION

During the past decade, ion chromatography (IC) has been the primary analytical method for monitoring trace ionic impurities in power plant waters such as chloride, sulfate, organic acids and recently, manganese [1,2]. It has been reported that on-line monitoring of soluble manganese could be used effectively as an indicator of feed water corrosion product transport in nuclear power plants [2]. This report has brought attention to the existing corrosion monitoring techniques which are semi-quantitative and time consuming. The Electric Power Research Institute, ERI, has recommended the monitoring of iron in power plant waters [3]; however, only 40% of total iron (pH > 7) is soluble. On the other hand, more than 90% of manganese is soluble and real-time corrosion monitoring is possible. As the new concept has received significant attention, an improved method for on-line manganese monitoring is being explored. Due to the fact that manganese concentration can be as low as 40 pg/ml in feedwater containing ammonia or morpholine, an improved method for manganese monitoring is required. It has been suggested that the required manganese detection limit and limit of quantitation must be 5 pg/ml and 50 pg/ml, respectively. The current IC suppressed conductivity method [2] for manganese shows detection limits of 50 pg/ml.

This paper will describe the development of a method for the determination of manganese in power plant waters. Sample concentration makes use of a chelating resin to more selectively concentrate manganese. Separation is accomplished on a carboxylate ion-exchange stationary phase which allows elution of manganese and other alkali metal and alkaline earth cations with a simple acid eluent. The detection mode involves a post column derivatization followed by visible detection to obtain pg/ml Mn detection limits. The use of a cation suppressor after the separator column and before the post-column system allowed the use of a weak com-

* Corresponding author.

0021-9673/93/$06.00

plexing agent to improve manganese separation from other interfering transition metals.

BACKGROUND

The existing analytical chromatographic methods for manganese combine cation-exchange separation with suppressed conductivity, or mixed-bed ion-exchange chromatography with post-column derivatization [1]. The sample concentration mode commonly used is cation-exchange concentration. Most of the cation concentrator columns are made of low capacity, sulfonic acid, ion-exchange materials which are not particularly selective for manganese over other common cations. Concentration methods with this type of resin have been limited to a maximum of only 50 ml of sample due to high concentrations of ammonium and/or morpholinium relative to the manganese concentration. The limitation on concentration volume directly affects method detection limits. In addition, the elution of concentrated divalent cations from the cation concentrator to the analytical system requires divalent eluent components such as diaminopropionic acid (DAP) or ethylenediamine, or chelating eluent components such as oxalic acid, tartaric acid or pyridine 2,6-dicarboxylic acid [4]. These complexing agents degrade detection limits for manganese by suppressed conductivity or post-column derivatization.

In order to improve upon the manganese detection limit obtained by the existing IC method, the following factors must be considered. A selective concentration method for manganese is required in order to concentrate manganese from a large amount of sample containing interferences such as ammonium and morpholinium ions. The kinetics of divalent cation-exchange reaction should be relatively fast and column capacity should be relatively high so that a high sample flow-rate can be used to minimize sample loading time. It is very important that the concentration chemistry does not require resin regeneration or a chemical matrix elimination step, which normally leads to a high analytical blank. Also, the choice of the analytical column is very important. The elution chemistry of the concentrator column must be compatible with the analytical column such that the eluent used for removing the concentrated manganese from the concentrator is also useful for analytical separation. Finally, the detection method must be sensitive so that a relatively small sample preconcentration volume is needed to meet the detection limit requirements.

Sample concentration method

The choice for the ion-exchange concentration method usually depends upon the sample matrix complexity, ion-exchange selectivity and ion-exchange capacity. Generally, a low-capacity, non-selective cation-exchange concentrator column (*e.g.* sulfonate type) is commonly used for analyte concentration from relatively clean matrices [1,2]. As the sample matrices become more complex, a selective concentration method is required [5].

Although a sulfonate-type cation-exchange concentrator column has been used successfully to concentrate manganese [2], the combination of the ammoniated or morpholinated matrix of the power plant water combined with the detection limit requirements suggest that the sulfonated concentrator wil not be satisfactory. The ammonium or morpholinium in the matrix acts as an eluent during concentration causing breakthrough of the manganese and limits the maximum volume of sample that can be concentrated. Since the imminodiacetate concentrator is highly selective for manganese as compared with ammonium and morpholinium, there should be no matrix limitation on the concentration volume.

Analytical separation system

Three types of ion-exchange stationary phases are available for cation separations, strong acid cation-exchange sulfonate type, weak acid cation exchange carboxylate type and mixed cation and anion exchange. Strong acid cation exchange requires either a divalent component in the eluent which limits the maximum concentration volume on the concentrator column, or requires a chelating component in the eluent which compromises the detection system. Mixed-bed ion-exchange systems are used with an eluent containing chelating components to improve the separation of divalent cations. In this way divalent cations are separated both as free cations and as anionic complexes. This system gives the most control over selectivity for multicomponent cation separations but compromises detection sensitivity due to a competition between the eluent–cation complex and the detection reagent–

cation complex. The most promising ion-exchange stationary phase for cation separation allowing the detection limits required for manganese is the weak acid carboxylate ion exchanger. It is possible to separate and elute monovalent and divalent cations from this type of resin with just a simple acid eluent due to its high selectivity for hydronium ion. Although it does not afford the selectivity control of mixed-bed ion-exchange systems it does offer the potential for the necessary separation selectivity for manganese from other transition metals and the simple acid eluent should not interfere with the post-column detection system.

Detection method

Suppressed conductivity detection is currently used for divalent detection including manganese [1,2]. This detection method provides only low to moderate sensitivity for manganese, thus, a large sample preconcentration is required. A benefit, however, is that some of the co-eluting metals, such as Zn and Ni, are hydrolyzed and removed by the suppressor due to the high pH environment of the suppression reaction and these elements do not interfere with manganese detection.

Currently, at least 60–80 ml of sample are concentrated to obtain quantitation limits of 150 pg/ml (9–12 ng total) Mn by suppressed conductivity. With this detection system, lowering the limits of quantitation from 150 pg/ml to 10 pg/ml Mn would require at least 900 ml of sample to be concentrated. The analysis time using this method would be at least 2 h per sample.

A post-column derivatization method can be used to lower the detection limits of manganese. Many colorimetric reagents used for manganese determination are very selective and sensitive; however, the reaction rates are too slow for a dynamic post-column derivatization system. Most of these reagents form neutral, water-insoluble complexes with manganese. The well known water-soluble fluorimetric reagent for manganese determination, 8-hydroxyquinoline-5-sulfonic acid, does not give the required sensitivity for Mn because the kinetics are too slow. Formaldoxime has been reported as a useful colorimetric reagent for manganese determination using flow injection analysis [6]; however the sensitivity reported by this method is only 100 ng/ml for Mn. Another candidate is pyridylazoresorcinol (PAR) which has been commonly used for trace transition metal detection [7]. This method provides an excellent selective and sensitive detection method for Mn in high ammonium or morpholine matrix. Our preliminary experiments showed that only 500 pg of Mn are required to obtain the same detection sensitivity as 9000 pg by suppressed conductivity detection. Therefore, the sample volume required to obtain identical levels of quantification can be reduced by at least 18 times. The maximum absorption ratio of the Mn–PAR complex is found at 530 nm.

EXPERIMENTAL

All chromatography was performed on a Dionex (Sunnyvale, CA, USA) DX-300 chromatographic system equipped with two quaternary gradient pumps (AGP), a reagent-delivery module (RDM), a conductivity detector module (CDM-II), a variable-wavelength detector module (VDM-II) and a basic chromatography module. One of the gradient pumps was used to deliver eluents to the system. The other gradient pump was used as a sample pump. The on-line ion chromatograph series 8100 was used at Virginia Electric and Power Company (Surry, VA, USA). The Dionex columns used include the MetPac CC-1 concentrators (25 mm × 3 mm, 35 mm × 4 mm and 50 mm × 4 mm) and IonPac CS 12. For simultaneous detection of alkali, alkaline earth and Mn, the post-column system was replaced by Cation Micromembrane Suppressor (CMMS-II) and CDM-II. The eluent suppression with subsequent post-column derivatization detection used to improve Mn detection was accomplished by placing the CMMS-II between analytical column and post-column system. Data was collected and processed using Dionex AI-300 (8100 on-line system) or AI-450 software (DX-300 system).

The separation was accomplished on a Dionex IonPac CS12 column. Chromatographic conditions are listed in Table I. The HCl and pyrophosphoric acid eluents were prepared with ultrapure grade concentrated HCl (SeaStar Chemicals, B.C., Canada) and 97% pyrophosphoric acid (Aldrich, WI, USA). The standard solutions were prepared by dilution from stock 1000-mg/l atomic absorption grade with 18 MΩ cm deionized water.

TABLE I

CHROMATOGRAPHIC CONDITIONS

Concentrator	MetPac CC-1
Sample flow	5–10 ml/min
Eluent	10 m*M* HCl—8 m*M* pyrophosphoric acid
Eluent Flow	1.0 ml/min
Detection	
(1) Suppressed conductivity	
Eluent suppressor	Cation MicroMembrane Suppressor (CMMS)
Regenerant	100 m*M* Tetrabutylammonium hydroxide
Regenerant flow	5–10 ml/min
Detector	CDM-II
(2) Post-column derivatization	
Post-column reagent	0.4 m*M* Pyridylazoresorcinol 1.0 *M* Dimethylethanolamine 0.3 *M* Sodium hydrogencarbonate
Post-column device	Membrane reactor
Post-column flow	0.5 ml/min
Detector	VDM-II, 530 nm

RESULTS AND DISCUSSION

Chelation concentration

Iminodiacetate (IDA) chelating resin is known for its high selectivity for transition and post transition metals *vs.* alkali and alkaline earth metal cations [8,9]. At pH between 4.0 and 6.0, most of the transition metals are strongly retained by the resin, while the alkali and alkaline earth metals are only partially retained. The rate of exchange of metal cations and IDA is not diffusion-controlled, but governed by the rate of the chelation reaction itself [10]. Many reports have concluded that most divalent metal ions exhibit maximum distribution coefficients at pH 4.5 [11]. The selectivity coefficients for this resin relative to calcium are 4.9 for Mn, 20.5 for Co, 19.8 for Zn, 52 for Ni and 500 for Cu [12]. It has also been demonstrated that the resin acts as a tridentate ligand, forming a very stable metal complex which coordinates through the imino nitrogen atom and bonds through the two carboxylic oxygen atoms. This chelate formation involves the deprotonation process of carboxylic oxygen atoms [13–16].

The IDA resin has been used for several applications, particularly the separation/matrix elimination of transition metals from alkali and alkaline earth metals as a function of pH [5,8,9]. Only a few reports indicate metal uptake by the IDA in acid form since the conventional IDA-resins, Dowex A-1 (Dow Chemicals), and Chelex-100 (Bio-Rad Labs.) shrink considerably at low pH, and the exchange rates are subsequently limited by diffusion processes rather than chelation reaction [17].

A unique IDA resin prepared by incorporating IDA on 20-μm macroporous polystyrene–divinylbenzene substrate showed a behavior similar to that of the conventional chelating resins. The exchange rate of this material is controlled by the chelation reaction, and because of its structural rigidity, it is not limited by diffusion processes at low pH. This fully functionalized, high-capacity resin was used to pack the MetPac CC-1 metal concentrator column. The MetPac CC-1 was used to concentrate samples at up to 10.0 ml/min. The selective concentration of manganese from high concentrations of alkali–alkaline earth metals, ammonium, and morpholine was accomplished by acidifying the sample with 0.1 to 1.0 m*M* of an ultrapure acid. It was found that the presence of a low concentration of hydronium ion reduced the distribution coefficients of the matrix components; however, it did not significantly affect the manganese retention. The concentrated manganese was efficiently removed from the column in a tight band with as little as 20 m*M* HCl, enabling the column to be easily coupled directly to a low capacity cation separator column.

In an effort to maintain the maximum sensitivity, the effect of the concentration step on chromatographic efficiency for manganese was determined by comparing peak widths and heights obtained from the separation following preconcentration with those following direct injection. In the concentration mode, 100 ml of 20 pg/ml Mn (2.0 ng total) in 0.5 m*M* acetic acid were concentrated at a flow-rate of 9.9 ml/min, eluted from the MetPac CC-1 to the IonPac CS12 and then to the post column system. In the direct injection mode, 50 μl of 4.0 μg/ml Mn standard (2.0 ng total) were injected directly into the system and the peak width and heights were compared with that of the concentration mode. It was found that peak widths and heights were comparable in both modes.

The column capacity and dynamic range of sample concentration were evaluated by concentrating various amounts of sample containing fixed amount of manganese. Overloading the column capacity with a large amount of sample would result in non-linear response. In this experiment, various volumes of sample containing 10 pg/ml Mn in 6.0 μg/ml ammonium (ammonium hydroxide) were employed. This sample represents a 1:60 000 mass ratio of Mn to ammonium ion. The sample was acidified with 1.0 *M* ultrapure acetic acid to make 0.1 m*M* concentration of acetic acid in the sample. Sample volumes ranging from 50 to 400 ml were concentrated on 25 mm × 3 mm and 35 mm × 4 mm MetPac CC-1 columns. Good linearity was observed. In addition, the *x*-intercepts in both cases are almost equivalent. Both sets of data indicate the minimum preconcentration volumes required by the two column dimensions are 7.9 ml for 25 mm × 3 mm and 9.0 ml for 35 mm × 4 mm. The slightly higher sample volume required by the 4 mm × 35 mm column is probably due to the higher dead volume producing band dispersion in the column. Also, this set of data may be used to estimate the detection limits of the two systems at 79 pg and 90 pg for 25 mm × 3 mm and 4 mm × 35 mm, respectively. The higher-capacity MetPac CC-1, 50 mm × 4 mm column, also gave excellent linearity and was used extensively in power plant as discussed later in this text.

Analytical separation

The IonPac CS12 column was used to separate manganese from ammonium and interfering transition metals that may present in the power plant samples. The CS12 is composed of an ethylvinylbenzene–divinylbenzene substrate polymer of very high cross-linking, onto which is grafted a weak acid carboxylate ion-exchange polymer active layer [18]. The highly cross-linked substrate core provides good mechanical stability for changes in ion-exchange form and compatibility with common HPLC eluent solvents.

Using HCl as an eluent on the CS12, manganese was only partially separated from Zn and Ni. Although Zn and Ni are present in very low level in these samples, the peak integration for manganese becomes difficult. The eluted Zn can be eliminated before the post-column system by inserting a CMMS between the IonPac CS12 and the post-column system. The CMMS hydrolyzes zinc and the hydrolysis products are either removed in the suppressor or do not react with the post column reagent.

The selectivity of the IonPac CS12 column can be altered by using a weak complexing agent such as pyrophosphoric acid (PPA). The combination of HCl and PPA eluent cleanly separate Mn from Zn and Ni. Although the PPA is not available in ultrapure grade, it was found that manganese contamination in this reagent is very low. The combination of HCl and PPA eluent with post-column derivatization has been used extensively at Virginia Electric and Power. Typical system blank and detection of 10 pg/ml Mn are shown in Fig. 1.

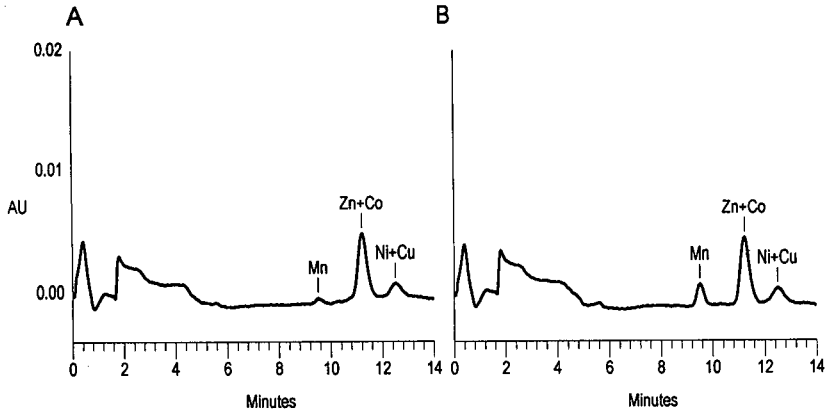

Fig. 1. Separation of Mn and other transition metals. (A) System blank, (B) 100 ml of 10 pg/ml Mn. Eluent: 10 m*M* HCl–8 m*M* PPA. Chromatographic conditions are listed in Table I.

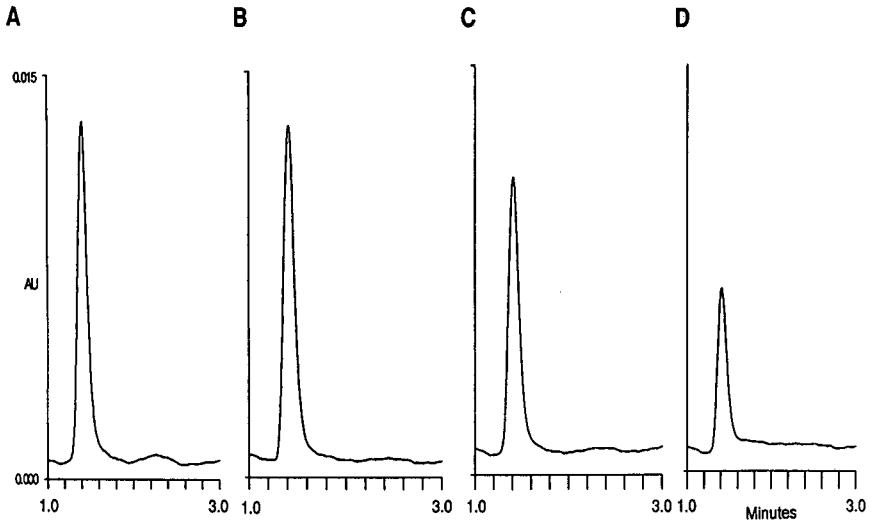

Fig. 2. Detectability of Mn in various eluents by PAR post-column derivitization. (A) 20 m*M* HCl, (B) 40 m*M* HCl–10 m*M* diaminopropionic acid, (C) 10 m*M* HCl–8 m*M* PPA and (D) 6 m*M* pyridine-2,6-dicarboxylic acid.

Detection method

Using complexing eluent modifiers such as pyrophosphoric acid, oxalic acid or pyridine-2,6-dicarboxylic acid normally result in loss in sensitivity by post-column detection as discussed earlier. The results from flow injection analysis for Mn, using PAR reagent, to determine the loss of sensitivity using different eluents is shown in Fig. 2. The experiment was performed by preparing 100 ng/ml Mn in various complexing eluents. A 50-μl volume of these solutions was injected into the eluent stream followed by post-column and visible detection at 530 nm. The order, from left to right, follows the increase in formation constant of Mn with complexing eluent (*i.e.* HCl < acid < pyrophosphoric acid < pyridine-2,6-dicarboxylic acid) indicated by the trend of decreasing sensitivity. An additional experiment was performed to confirm the competition reaction between the eluent and PAR by placing a CMMS-II between the separator column and the post column system. The eluent used was 10 m*M* HCl–8 m*M* PPA. The CMMS-II served as an eluent suppressor, removing the pyrophosphate anion and replacing it with hydroxide, forming water. Once pyrophosphate was removed, the sensitivity loss due to a competition reaction with PAR did not occur and essentially most of the manganese reacted with PAR. Fig. 3 shows the 50-μl direct injection of Mn and comparison of Mn detection response with and without eluent suppression before post-column derivatization. The elution order is slightly changed as compared with that of Fig. 1 because the MetPac CC-1 was not used. Interestingly, many metals were hydrolyzed in the basic environment of the suppressor and the hydrolysis prod-

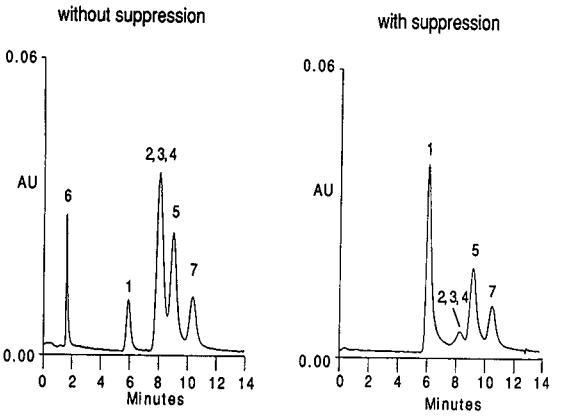

Fig. 3. Improved PAR post-column detection by eluent suppression. (A) Without eluent suppression and (B) with eluent suppression. Peaks: 1 = Mn (2.0 μg/ml); 2 = Cu (0.5 μg/ml); 3 = Cd (0.5 μg/ml); 4 = Zn (2.0 μg/ml); 5 = Co (2.0 μg/ml); 6 = Fe(III) (10 μg/ml); 7 = Ni (2.0 μg/ml).

ucts were removed by the suppressor or not detected by the post-column detection. This observation may be useful for using the suppressor as a sample preparation device.

The new improved method for Mn was installed at Virginia Electric and Power (Surry, VA, USA) and has been currently used for Mn monitoring. The chromatographic conditions was identical to that shown in Table I. The detection method used was eluent suppression with subsequent post-column derivatization. Typical detection limits obtained by this system is approximately 3 pg/ml (240 pg total) for 80 ml sample concentration.

Analytical precision and detection limits

The precision of the analysis was determined to establish the detection limits and limits of quantitation of this method. Deionized water (18.2 MΩ cm) was first purified to remove trace manganese, if present, by passing it through the MetPac CC-1 (50 mm × 4 mm, two columns in series), and the column effluent was collected in acid-cleaned PTFE bottles. The purified water was then analyzed for a manganese blank before it was used for standard preparation. Next, the standard 6 μg/ml ammonium was prepared from ultrapure ammonium hydroxide solution by dilution with the purified water and the solution was analyzed for manganese contamination. Finally, the 100-ml sample containing spiked with 10 pg/ml manganese in 6 μg/ml ammonium (1:60 000 mass ratio) was concentrated on the 35 mm × 4 mm MetPac CC-1, and separated using the chromatographic conditions listed in Table I. Statistical evaluation of three times standard deviation was used to obtain the detection limits of 1.2 pg/ml (120 pg total) for Mn. These data agrees well with the estimated detection limits by dynamic range study indicating 90 pg.

Application

Manganese mass transport. In a mass transport study conducted at Surry Power Station, the goal was to employ the new manganese method to monitor key sample points to identify corrosion rates. Fig. 4 shows the Mn mass transport of the feedwater (FW), main steam (MS), high-pressure heater drain (HPHD), condensate (COND) and polisher effluent (PE). The detail discussion of these components and mass transport rate can be found in the previous report [2].

The FW consists of 64% PE and 28% HPHD, with the remaining 8% from various drips from the MS. The total FW flow is $4.9 \cdot 10^6$ kg/h. The HPHD originates from MS that is used to reheat steam directed to the high-pressure turbine. The "spent" steam condenses to a collection tank then being pumped forwarded in the FW train. The HPHD flow is $1.4 \cdot 10^6$ kg/h which is 28% of the generated MS. The remaining portion of MS is the motive force used to turn the turbines to generate the pro-

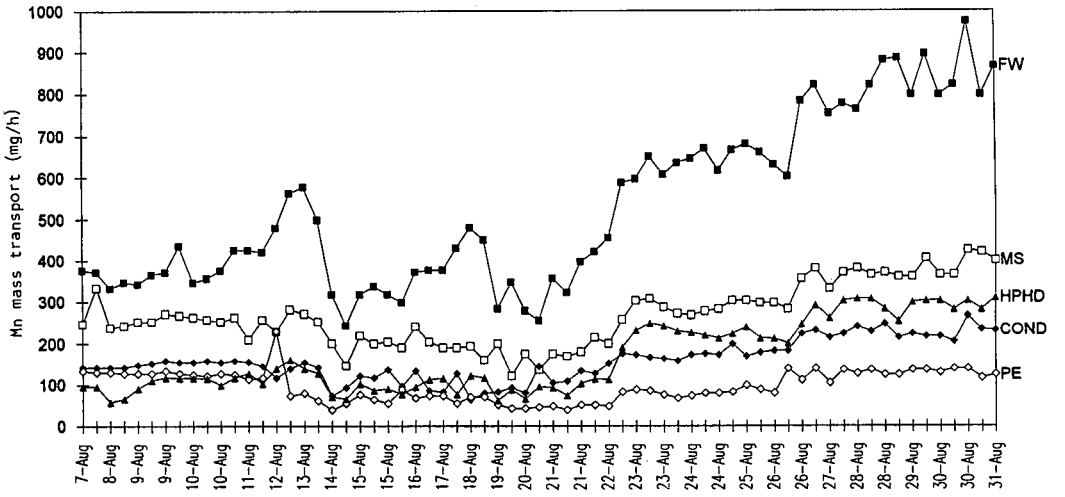

Fig. 4. Manganese mass transport data (mg/h). See text for abbreviations.

duced electricity. The "spent" steam then condenses back to liquid form (COND), and then "polished" as it passed through a series of mixed bed demineralizers (PE) to be used again as FW.

Understanding this relationship, specific areas of corrosion are identified. Fig. 4 clearly shows how changes in FW Mn mass transport has an effect on the other process streams, and how these data can be used to identify corrosion rates. Using the data from August 31, the following information is obtained. The PE has a Mn mass transport of 100 mg/h, while the HPHD Mn transport is 290 mg/h. Therefore, the FW Mn transport should be 390 mg/h. In actuality, the FW Mn transport rate is 850 mg/h, which indicates a Mn production rate of 460 mg/h.

The second area of corrosion concern is with the HPHD system. Again using the data of August 31, a similar correlation is shown. The MS Mn Mass transport rate of 400 mg/h minus the COND Mn mass transport of 200 mg/h equals 200 mg/h, the calculated value of the HPHD. However, the measured value of 290 mg/h Mn indicates Mn production occurring at the rate of 90 mg/h.

These results may appear relatively low. However, considering the manganese content of carbon steel which may range from 0.6% to 1.0% [19] and correlation constant using the total manganese-to-iron ratio [2], these corrosion rates equate to over 200 pounds of iron per year.

CONCLUSIONS

An improved method for ultra-trace (pg/ml) determination of manganese in power plant waters has been developed. The method uses a selective concentration chemistry, a unique carboxylated ion exchange separation and a sensitive post-column detection for picogram levels of manganese in high concentrations of ammonium matrix. The detection limits of this method were found to be 1 to 3 pg/ml Mn for 80 to 100 ml sample concentration.

REFERENCES

1 D. L. Campbell, J. Stillian, S. Carson, R. Joyce and S. Heberling, *J. Chromatogr.*, 546 (1991) 229.
2 D. Bostic, G. Burns and S. Harvey, *J. Chromatogr.*, 602 (1992) 163.
3 *Steam Generator Reference Book: Corrosion Product Control*, Steam Generators Owners Group and Electric Power Research Institute, Palo Alto, CA, May 1988.
4 P. R. Haddad and P. Jackson, *Ion Chromatography—Principles and Applications*, Elsevier, Amsterdam, 1990, Ch. 4.
5 A. Siriraks, H. M. Kingston and J. M. Riviello, *Anal. Chem.*, 62 (1990) 1185.
6 M. F. Gin'e, E. A. G. Zagatto and H. Bergamin, *Analyst*, 104 (1979) 371.
7 J. A. Cox and N. Tanaka, *Anal. Chem.*, 57 (1985) 385.
8 J. P. Riley and D. Taylor, *Anal. Chim. Acta*, 40 (1968) 479.
9 H. M. Kingston, I. L. Barns, T. J. Brady, M. A. Champ and T. C. Rain, *Anal. Chem.*, 50 (1978)14.
10 R. Turse and W. Rieman, III, *J. Phys. Chem.*, 65 (1961) 1821.
11 D. E. Leyden and A. L. Underwood, *J. Phys. Chem.*, 68 (1964) 2093.
12 R. Rrosset, *Bull. Soc. Chim. Fr.*, (1966) 59.
13 A. Nakashima, T. Isobe and T. Tarutani, *Bull. Chem. Soc. Jpn.*, 55 (1982) 1811.
14 P. J. Hoek and J. Reedijk, *J. Inorg. Nucl. Chem.*, 41 (1979) 401.
15 K. Umezawa and T. Yamabe, *Bull. Chem. Soc. Jpn.*, 45 (1972) 56.
16 C. Heitner-Wirguin and N. Ben-Zwi, *Israel J. Chem.*, 8 (1970) 913.
17 S. C. Chatterjee and A. Chatterjee, *J. Indian Chem. Soc.*, 49 (1972) 681.
18 M. A. Rey, C. A. Pohl and M. P. Harrold, presented at the *43rd Pittsburgh Conference, New Orleans, LA, March 9, 1992*, Paper No. 237.
19 *Specification for Seamless Carbon Steel Pipe for High Temperature Service, SA-106, Annual Book of Standards*, American Society for Testing and Materials, Philadelphia, PA, 1978.

Journal of Chromatography, 640 (1993) 379–385
Elsevier Science Publishers B.V., Amsterdam

CHROMSYMP. 2822

Separation of acetylated amino acids

Philip G. Simonson☆ and Donald J. Pietrzyk*

Department of Chemistry, University of Iowa, Iowa City, IA 52242 (USA)

ABSTRACT

Acetylated amino acids (NAc-AA) are separated as anions on a reversed stationary phase from a mobile phase containing a quaternary ammonium (R_4N^+) salt as a mobile phase additive. If the counteranion accompanying the R_4N^+ or ionic strength salt is detector active than the separated NAc-AA derivatives can be detected by an indirect detection strategy. Variables influencing the separation are NAc-AA side chain structure and the mobile phase parameters such as hydrophobicity of the alkyl groups in the R_4N^+ salt, R_4N^+ salt concentration, counteranion eluent strength, counteranion concentration, solvent composition, and pH. Indirect detection is influenced by these same mobile phase parameters as well as the properties of the detector active counteranion. The detection limit for indirect photometric detection at 287 nm using a tetrapentylammonium salt with a disodium 1,5-naphthalenedisulfonate–sodium benzoate counteranion mixture was about 70 pmol of NAc-AA depending on the amino acid injected as a 10-μl sample.

INTRODUCTION

The separation and determination of N-acyl amino acid (N-acyl-AA) derivatives in biological systems is of growing interest. Many of these derivatives, which have been identified as metabolites in urine, blood plasma, and other biological fluids and materials as well as in plant matter, have been correlated to exposure, dietary, and health disorders. For example, excretion of aromatic carboxylic acids that are produced endogenously or derived from exogenous sources such as drugs in normal human metabolism undergo reaction with glycine to yield an N-acyl glycine derivative, exposure to toluene leads to formation of N-*p*- and *m*-benzoylglycine [1,2], and the presence of aliphatic and aromatic N-acyl-AA have been correlated to organic acidurias and other disorders [3–6]. Other studies suggest N-acetylation is a pathway in the metabolism of amino acids and accounts for the presence of several different aliphatic N-acyl-AA in normal urine [7]. Typical N-acyl-AA that have been detected in physiological and plant samples, which is reviewed elsewhere [7,8], include N-benzoyl-, substituted N-benzoyl-, N-hydroxybenzoyl-, N-vanilloyl-, N-phenyl-, aliphatic-N-acyl, and N-acetyl-AA derivatives.

The N-acyl-AA derivatives have been separated by thin-layer chromatography [8–11], gas–liquid chromatography [3,4,6–8,10,12,13], and by high-performance liquid chromatography (HPLC) [1,2,5,8,14–19]. In general, HPLC separations have been carried out on either reversed stationary phases [1,2,5,8,14,16–19] or ion exchangers [15]. UV detection of N-acyl-AA derivatives is possible for derivatives that contain an aromatic ring attached to the acyl group. Aliphatic-N-acyl- and N-acetyl-amino acid (NAc-AA) derivatives, however, are not readily detected except at a very low wavelength where the acyl group absorbs. At this wavelength absorption interferences due to solvent, mobile phase components, and sample matrix can be significant.

It was recently demonstrated that NAc-AA mixtures are resolved on a reversed stationary phase using an iron(II)-1,10-phenanthroline, $Fe(phen)_3^{2+}$, salt as a mobile phase ion interaction reagent [19]. The additive enhances retention of the NAc-AA de-

* Corresponding author.
☆ Present address: Parke-Davis, Pharmaceutical Research Division, Ann Arbor, MI 48106, USA.

0021-9673/93/$06.00

rivatives and allows an indirect detection of the derivatives with a detection limit of about 0.5 nmol in a 10-μl injection. It was also shown that free amino acids could be separated and detected at 0.5 nmol by first derivatizing the amino acids through an acetylation reaction.

This paper describes a procedure for the separation of NAc-AA derivatives on a reversed stationary phase by using a tetrapentylammonium ($TPeA^+$) salt and a detector active counteranion as mobile phase additives. The $TPeA^+$ salt is an ion interaction reagent that enhances retention of the anionic form of the NAc-AA derivatives while the counteranion provides eluting power and a means for indirect detection. Since the indirect detection is based on an anion-exchange equilibrium between the detector active counteranion and the NAc-AA anion, the mobile phase parameters influencing retention, elution, and indirect detection are fewer and more easily controlled than when using a Fe $(phen)_3^{2+}$ salt as the additive where the indirect detection is due to the shift of the equilibrium involving interactions between the $Fe(phen)_3^{2+}$ salt, counteranion, and stationary phase surface [19].

EXPERIMENTAL

Materials

Tetraalkylammonium chloride or bromide salts were obtained from Eastman Kodak while the sodium sulfonates and carboxylates or free acids were obtained from Eastman Kodak, Fisher Scientific, and Sigma. NAc-AA derivatives of L-AA were purchased from Sigma. Ionic strength salts were analytical reagent grade, organic solvents were LC quality, and LC water was obtained by passing in-house distilled water through a Millipore Milli-Q Water System. PRP-1 (Hamilton) polystyrenedivinylbenzene (10 μm, 150 mm × 4.1 mm I.D.), Zorbax-ODS (Mac Mod Anal.) (5 μm, 150 mm × 4.6 mm I.D.), and Supelco ODS (Supelco Sep. Tech.) (250 mm × 4.6 mm I.D.) columns were used. LC instrumentation consisted of a Spectra Physics 8800 gradient pump, a Waters U6K or Rheodyne 7125 fixed loop injector, and a Spectra-Physics 770 variable-wavelength, Kratos 900 fluorescence, or a EG and G Princeton Applied Research 400 electrochemical detector. Column temperature was controlled with a Bioanalytical LC-22A controller and data analysis was done on a Spectra-Physics 4270 recording integrator and manipulated with an Epson Equity I+ computer equipped with Spectra-Physics WINner software.

Procedures

R_4N^+ salts were converted into a specific counteranion form by anion exchange (Amberlite IRA-400). Mobile phases were prepared by combining aliquots of standard solutions of R_4N^+, ionic strength, and buffer salts that provided the desired counteranion, solvent, and pH. The pH was adjusted with dilute NaOH prior to dilution to volume when necessary. Solvent mixtures were percent by volume and basic mobile phases were protected from atmospheric CO_2. Column peformance was monitored during the study and compared to manufacture certification using a phenol, benzene, toluene mixture and an acetonitrile–water (85:15) mobile phase.

Columns were conditioned by passing the R_4N^+ salt mobile phase through the column beyond the column breakthrough until the detector background signal remained constant. Column breakthrough volume was determined by monitoring column effluent at a detector setting that responds to the appearance of the counteranion. The equilibrium amount of R_4N^+ salt maintained on the column for a given mobile phase condition was calculated from the breakthrough volume and the R_4N^+ mobile phase concentration. The R_4N^+ salt was removed from the column by elution with acetonitrile–water (4:1). Aqueous solutions of NAc-AA (0.1 to 1.0 mg/ml) derivatives were prepared and injected by syringe in 1–10 μl aliquots. NAc-AA derivatives were detected by indirect detection at detector settings where the counteranion benzoate (228 nm), 1,5-naphthalenedisulfonate (NDS) (287 nm), naphthalenesulfonate (NS) (287 nm), and salicylate (298 nm) absorb, where salicylate (λ_{ex} 300 nm, λ_{em} 410 nm) and NDS (λ_{ex} 320 nm, λ_{em} 450 nm) fluoresces, or where I^- (500–800 mV *versus* SCE) and salicylate (850–1050 mV *versus* SCE) are oxidized. The background absorbance, fluorescence, or electrochemical signal due to the counteranion was compensated for by the detector offset capability. For indirect photometric detection the background absorbance should not exceed about 0.7 AU. Mobile phase flow was usually 1.0 ml/min, in-

let pressure was under $6.9 \cdot 10^6$ Pa, column temperature was 25°C, and column void volume was 1.1–1.3 ml. Usually, three or more measurements were made to establish the effects of mobile phase and indirect detection parameters, while for the determination of the calibration curve, data points were established with five or more measurements.

RESULTS AND DISCUSSION

Retention and detection of NAc-AA derivatives

Acetylation of the amino group in an amino acid reduces its basic property and dissociation occurs only at the carboxyl group according to eqn. 1.

$$CH_3C(O)NHCHRCO_2H + H_2O \rightleftarrows CH_3C(O)NHCHRCO_2^- + H_3O^+ \quad (1)$$

Thus, NAc-AA derivatives are anions at an intermediate pH and should be retained on a reversed stationary phase, S, when the mobile phase contains a quaternary ammonium (R_4N^+) salt additive. This occurs because an equilibrium amount of the R_4N^+ salt, assuming the R groups are hydrophobic and micelle formation is absent, is maintained on the stationary phase's surface for a given mobile phase condition as shown in eqn. 2.

$$S + R_4N^+ + C^- \rightleftarrows S \cdots R_4N^+C^- \quad (2)$$

The formation of the double layer on the surface provides the sites for interaction with the NAc-AA anions as shown in eqn. 3.

$$S \cdots R_4N^+C^- + \text{NAc-AA}^- \rightleftarrows S \cdots R_4N^+\text{NAc-AA}^- + C^- \quad (3)$$

The number of sites is determined by the R_4N^+, its concentration, solvent composition, the counteranion C^-, and the reversed stationary phase [20–22]. For a given R_4N^+ salt and concentration manipulation of the other variables, for example C^- concentration, allows the elution of the NAc-AA as shown in the reverse of eqn. 3. If C^- is also detector active then indirect detection is possible when the detector is adjusted to respond to C^-. If C^- absorbs, fluoresces, or is electrochemically active indirect photometric (IPD), indirect fluorescence (IFD), and indirect electrochemical (IED) detection is possible. Because of the equilibrium in eqn. 3 and the detector's response to the detector active counteranion, the chromatographic peak for the eluted NAc-AA derivatives will be negative.

Column optimization

Two reversed stationary phases, PRP-1, which is more stable in a basic mobile phase, and Zorbax ODS, were compared. The amount of R_4N^+ salt maintained on the PRP-1 was found to be higher than on the Zorbax column of the same dimensions. For example, breakthrough measurements indicated 210 μequiv. of TPeA salicylate is maintained on the PRP-1 for an aqueous 0.25 m*M* tetrapentylammonium ($TPeA^+$) salicylate, pH 7.5 mobile phase while for the Zorbax column the equilibrium amount is 150 μequiv./column. If the R chain length or the R_4N^+ salt concentration is increased the equilibrium amount on the stationary phase is increased. Adding organic modifier or switching to a counteranion that is weaker in eluent power (see eqn. 3) decreases the equilibrium amount of R_4N^+ salt on the stationary phase surface.

Table I compares the retention of several NAc-AA derivatives on the PRP-1 and Zorbax columns for a given TPeA salicylate mobile phase. Even though retention is higher on the PRP-1 the Zorbax column was used in additional studies because resolution on the latter column is greater due to a higher column efficiency (by a factor of 1.5–2 depending on the NAc-AA) and a modest enhancement in se-

TABLE I

RETENTION OF NAc-AA DERIVATIVES ON TWO REVERSED STATIONARY PHASES

Amino acid derivative	Capacity factor, k'[a]	
	PRP-1	Zorbax ODS
NAc-L-Asn	6.91	4.39
NAc-L-Ser	7.04	4.55
NAc-Gly	7.65	4.75
NAc-L-Glu	7.72	4.70
NAc-L-His	8.39	
NAc-L-Ala	8.43	5.34
NAc-L-Pro[b]	10.6/12.7	6.55/7.67
NAc-L-Val	16.4	14.1
NAc-L-Met		15.2
NAc-L-Ile	34	34
NAc-L-Leu	39	41

[a] Mobile phase, aqueous 0.25 m*M* TPeA salicylate, pH 7.5; column, Zorbax ODS; detection, IPD at 298 nm.

[b] Double peak is probably due to acetylation at both N in proline.

lectivity. Table I also demonstrates that retention, which is significant, correlates to the structural properties of the AA side chain group; the more hydrophobic or acidic the side chain is, the higher the retention becomes. Furthermore, indirect detection is sensitive since each NAc-AA derivative was readily located by monitoring column effluent at a wavelength where the salicylate counteranion absorbs.

Mobile phase and indirect detection optimization

Several mobile phase parameters influence retention of the NAc-AA derivatives and their optimization requires a compromise. As the R_4N^+ salt concentration increases the equilibrium amount of R_4N^+ salt on the stationary phase surface increases (see eqn. 2) which increases the number of ion interaction sites. However, NAc-AA retention does not continue to increase but eventually decreases [21,22] because of the increase in the counteranion concentration that accompanies the R_4N^+ salt, thus, reducing retention according to eqn. 3. Elution of NAc-AA derivatives requires a strong eluent counteranion or one that has a large anion-exchange selectivity to elute the NAc-AA derivatives in a reasonable time. This type of counteranion also produces a system peak that does not interfere with the analyte peaks [19,23]. In addition, the counteranion should be detector active. Several counteranions, which have favorable molar absorptivities, were evaluated and their effect on IPD and NAc-AA retention is shown in Table II. Increasing counteranion concentration decreases NAc-AA retention. The eluent strength for several counteranions on Zorbax ODS follows the order: I^- < benzoate < salicylate < naphthalenesulfonate (NS) < naphthalene disulfonate (NDS), which is consistent with their anion-exchange selectivities towards strong base quaternary ammonium type anion exchangers. In each case IPD was used at a wavelength where the counteranion absorbs. IFD is an option since salicylate fluoresces while IED is possible by using I^- as the counteranion. However, I^- is not a strong enough eluent counteranion to resolve NAc-AA derivatives particularly those with very non-polar or acidic amino acid side chains. Thus, if I^- is used, eluent power must be increased through an additional factor. Decreasing counteranion concentration, for example NDS, sharply decreases NAc-AA retention as shown in Fig. 1. In the absence of NDS in Fig. 1 eluent strength is due solely to benzoate.

TABLE II

EFFECT OF COUNTERANION ON RETENTION

Amino acid	Capacity factor, k'		
	Counteranion[a]		
	Benzoate	NMS	NDS
NAc-L-Ser	8.23	3.68	1.69
NAc-L-Ala	11.5	5.05	2.25
NAc-L-Pro	16.6	8.90	3.60
NAc-L-Val	23	13.4	6.86
NAc-L-Met	29	16.2	7.91
NAc-L-Ile	81	45	18.5
NAc-L-Leu	95	52	21
NAc-L-Phe			47

[a] Mobile phase, aqueous 0.10 m*M* TPeA benzoate–0.10 m*M* Na salt of benzoate (NMS) or NDS, pH 7.5; column, Zorbax ODS; detection, IPD at 287 nm.

For a given counteranion NAc-AA retention decreases as organic modifier is increased with aceto-

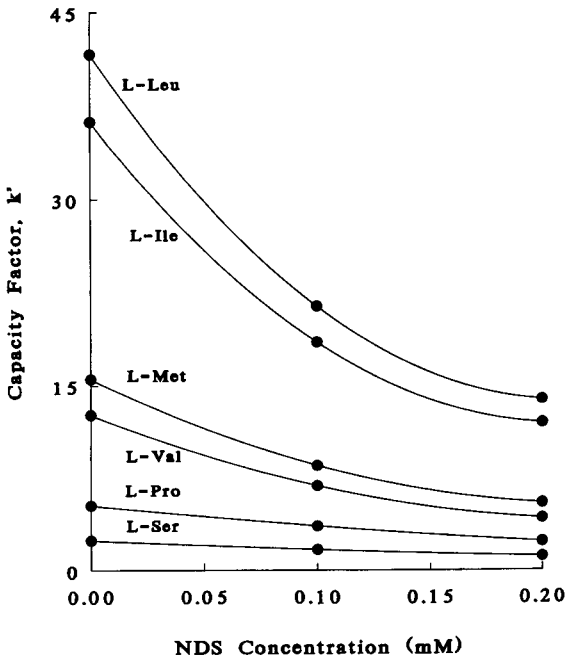

Fig. 1. Effect of NDS mobile phase concentration on the retention of NAc-AA derivatives. Conditions are the same as in Table II with varying NDS concentration.

nitrile being more effective than ethanol at comparable percent water–solvent mixtures. Retention of the more polar NAc-AA is already low for benzoate, NS, or NDS counteranion and adding organic modifier is required only when separating the more highly retained non-polar and acidic side chain NAc-AA. Mobile phase pH influences retention as shown in Fig. 2. Over the pH range studied the non-polar side chain NAc-AA are dissociated (see eqn. 1) and retention gradually increases as pH increases. For derivatives with acidic side chains retention increases significantly as pH increases because of additional dissociation at the acidic side chain. Thus, the elution order of L-Glu and L-Asp derivatives is more dependent on pH relative to the other NAc-AA. For low pH dissociation is suppressed and retention is sharply reduced. A mobile phase pH >8.0 is not recommended because this contributes to the formation of OH^- and HCO_3^-/CO_3^{2-} system peaks [19,23] both of which will interfere with several of of the NAc-AA chromatographic peaks. As hydroxide concentration increases the OH^- system peak area increases and shifts to a lower retention time while at the same time preventing CO_2 absorption in the mobile phase becomes more difficult. Also, the higher mobile phase pH limits the use of the silica based ODS column.

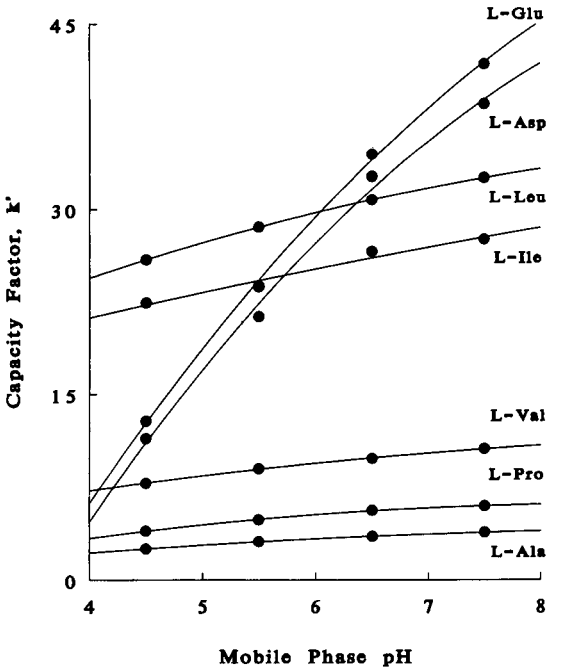

Fig. 2. Effect of mobile phase pH on the retention of NAc-AA derivatives. Mobile phase: 0.10 m*M* TPeA salicylate–0.10 m*M* Na salicylate, pH 4.5–7.5; column, Zorbax ODS; detection, IPD at 298 nm.

Separations

Fig. 3 illustrates a typical separation of several NAc-AA derivatives using IPD where salicylate absorbs. Chromatographic peaks, which are negative and inverted in Fig. 3 for convenience, are well defined, free of tailing, and yield a favorable detection limit. A double peak was observed for the NAc-L-Pro standard and is probably due to derivatization at both Pro nitrogens. If salicylate or organic modifier concentration in Fig. 3 is increased retention decreases. While both conditions favor elution of the highly retained NAc-AA resolution is significantly reduced for the low retained, polar derivatives. A salicylate system peak occurs at a high retention time and does not interfere with the NAc-AA peaks. If the pH is lowered from pH 7.5 (Fig. 3) to pH 4.5 with all other conditions being the same, NAc-AA retention decreases and resolution of the early eluting derivatives is still maintained. The major advantage of the lower pH is that elution times for the acidic side chain L-Asp and L-Glu derivatives are reduced significantly; their peaks at the lower pH follow L-Val (about 10 min) at 12 and 14.5 min, respectively. At pH 4.5 the L-Phe derivative is eluted at about 60 min in contrast to >100 min at pH 7.5. Elution of the L-Tyr derivative is also pH sensitive because of the acidic side chain and its peak occurs between the L-Glu and L-Ile at lower pH and greater than L-Glu at higher pH (see Fig. 3). The L-Trp derivative, which contains a non-polar side chain, elutes in the L-Phe derivative region. Although not shown peaks in Fig. 3 can be detected by IFD since salicylate fluoresces.

Fig. 4 illustrates the separation of NAc-AA derivatives using a longer ODS column (250 mm) and a stronger eluent. Detection is by IPD at 287 nm where NDS absorbs. IFD is also possible since NDS fluoresces. Since the pH is 5.0 the L-Asp and L-Glu peaks elute early following the L-Val peak. The weakly retained NAc-AA are still well resolved because of the column length while the more highly retained peaks are eluted as sharp, well resolved peaks at a reasonable time because the mobile phase

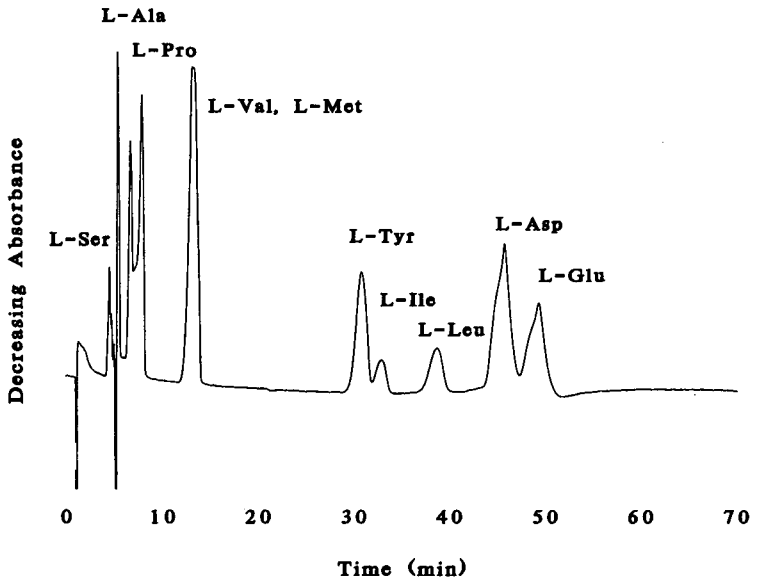

Fig. 3. Separation of NAc-AA derivatives. Conditions are the same as in Fig. 2 with pH = 7.5.

contains the strong eluent counteranion NDS. The benzoate system peak is due to the TPeA benzoate which was employed as the ion interaction reagent.

Detection limits

The IPD detection limit for NAc-AA derivatives depending on the mobile phase and detector was about 70 pmol injected as a 10-μl sample for a signal to noise ratio of 3:1. The calibration curve linear range covered about three orders of magnitude. For example, for IPD of NAc-L-Ser the calibration curve using the conditions in Fig. 4 was shown to follow the equation peak area = 673 (ng NAc-L-Ser) + 58.8 with a correlation coefficient of

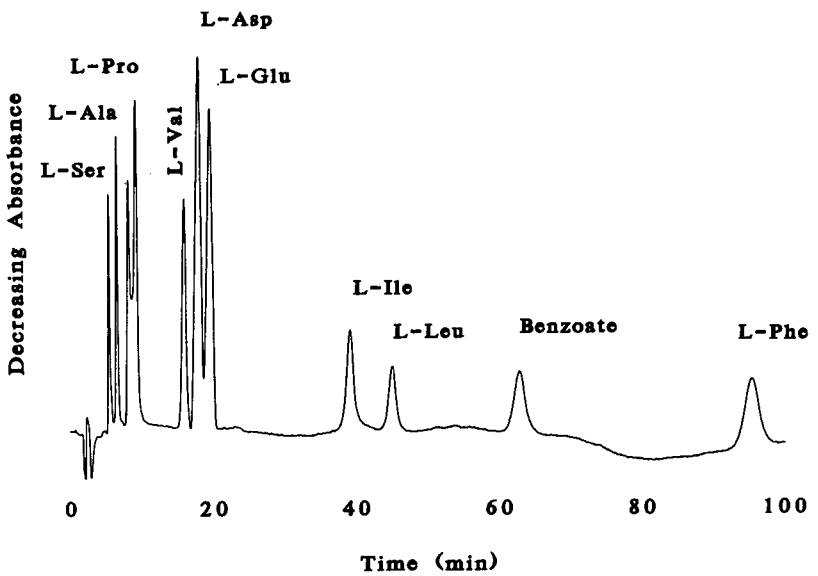

Fig. 4. Separation of NAc-AA derivatives on a longer column. Mobile phase: aqueous 0.10 m*M* TPeA benzoate, 0.10 m*M* Na_2NDS, pH 5.0; column, Supelco ODS; detection, IPD at 287 nm.

> 0.995. Three replicate injections of seven different standards were used to establish the calibration curve. In general, the more weakly retained NAc-AA have lower detection limits than the more highly retained NAc-AA derivatives, because of sharper chromatographic peaks. IPD sensitivity and detection limits are directly related to molar absorptivity of the counteranion [19,23] and detection limits by IPD can be lowered by using a counteranion with a higher absorptivity. While IFD and IED are also options by using counteranions that fluoresce or are electrochemically active (salicylate and NDS and iodide, respectively, were studied), IPD is more versatile because more counteranions are readily available that have both high absorptivity values and suitable counteranion elution characteristics. Also, measurement of a fluorescence or electrochemical change on a significant fluorescent or electrochemical background signal, respectively, is more susceptible to background noise depending on the detector and the quality of its offset capabilities [19].

CONCLUSIONS

NAc-AA are quantitatively separated using a R_4N^+ salt and a chromophoric anion in the mobile phase to enhance retention and provide indirect detection, respectively. The detection limit is about 70 pmol depending on the NAc-AA. Retention and resolution are altered by adjusting mobile phase solvent composition, R_4N^+ and counteranion concentration, and pH. IPD, which is sensitive to these parameters, is largely affected by counteranion absorptivity. Free AA can also be separated and determined by this procedure following an acetylation derivatization step [19].

REFERENCES

1 M. Matsui, M. Kasao and S. Imamura, *Br. J. Ind. Med.*, 34 (1977) 310–313.
2 R. Tardif, J. Brodeur and G. L. Plaa, *J. Anal. Toxicol.*, 13 (1989) 313–316.
3 E. C. Horning and M. J. Horning, *Clin. Chem.*, 17 (1971) 802–809.
4 O. Stokke, L. Eldjam, E. Jellum, H. Pande and P. E. Waller, *Pediatrics*, 49 (1972) 726–735.
5 L. Zimmerman, H. Jörnvall and J. Bergström, *Nephron*, 55 (1990) 265–271.
6 H. M. Liebich and C. Först, *J. Chromatogr.*, 338 (1985) 187–191.
7 H. S. Ramsdell and K. Tanaka, *J. Chromatogr.*, 181 (1980) 90–94.
8 C. F. Van Sumere, K. Vande Casteele, R. Hanselaer, M. Martens, H. Geiger and L. Van Rompaey, *J. Chromatogr.*, 234 (1982) 141–155.
9 H. Van Den Berg and F. A. Hommes, *J. Chromatogr.*, 104 (1975) 219–222.
10 J. Gärtzke and H. J. Weigmann, *J. Chromatogr.*, 162 (1979) 234–236.
11 M. S. Dubra, D. M. Alperin, A. Sagedahl, V. P. Idoyaga-Vargas, and H. Carminatti, *J. Chromatogr.*, 250 (1982) 124–128.
12 J. P. Kamerling, M. Brouwer, D. Ketting and S. K. Wadman, *J. Chromatogr.*, 164 (1979) 217–221.
13 H. S. Ramsdell and K. Tanaka, *Clin. Chim. Acta*, 74 (1977) 109–114.
14 S. Tsunasawa and K. Narita, *J. Biochem. (Tokyo)*, 92 (1982) 607–613.
15 K. Narita, *Methods Enzymol.*, 91 (1983) 84–92.
16 E. Busker and J. Martens, *Fresenius' Z. Anal. Chem.*, 559 (1986) 325–326.
17 A. Astier and A. M. Deutsch, *J. Chromtogr.*, 182 (1980) 88–93.
18 H. J. C. F. Nelis, M. C. Lefevere, E. Baert, W. D'Hoore and A. P. De Leenheer, *J. Chromatogr.*, 333 (1985) 381–387.
19 D. Yuan and D. J. Pietrzyk, *J. Chromatogr.*, 557 (1991) 315–324.
20 Z. Iskandarani and D. J. Pietrzyk, *Anal. Chem.*, 54 (1982) 1065–1071.
21 Z. Iskandarani and D. J. Pietrzyk, *Anal. Chem.*, 54 (1982) 2427–2431.
22 R. H. A. Sorel and A. Hulshoff, *Adv. Chromatogr.*, 21 (1983) 87–129.
23 P. G. Rigas and D. J. Pietrzyk, *Anal. Chem.*, 60 (1988) 454–459.

Journal of Chromatography, 640 (1993) 387–395
Elsevier Science Publishers B.V., Amsterdam

CHROMSYMP. 2792

Method development approaches for capillary ion electrophoresis

William R. Jones

Applied Technology Group, Waters Chromatography Division of Millipore, 34 Maple St., Milford, MA 01757 (USA)

ABSTRACT

Capillary ion electrophoresis (CIE) is a capillary electrophoretic technique optimized for rapid determination of low-molecular-mass inorganic and organic ions. CIE predominantly employs indirect UV detection since the majority of the analytes lack specific chromophores. Described are three methods for detection and electrolyte optimization. The first method discussed approaches for optimizing sensitivity, selectivity and peak confirmation using a chromate electrolyte and selected detection wavelengths. Peak confirmation is aided by using both direct and indirect detection of analytes. The second and third methods involve an unattended electrolyte development approach for instruments that only provide fresh electrolyte on the injection side of the capillary. The electrolyte composition is changed in both the injection side vial and in the capillary before each sample injection while leaving the receiving side electrolyte vial constant at the initial electrolyte composition. In one mode, the concentration of the electroosmotic flow (EOF) modifier used to induce anodic flow is varied while keeping the background electrolyte composition constant. In a second experiment, the background electrolyte co-ion is sequentially changed from high mobility to low mobility while keeping the EOF modifier concentration constant. The end effect is to achieve a broad range of controlled peak symmetry for analytes in a sample matrix. The results are compared to separations obtained when the injection side and receiving side electrolytes are manually matched.

INTRODUCTION

Capillary ion electrophoresis (CIE) (Water's tradename: Capillary Ion Analysis, CIA), introduced in the beginning of this decade, is finding solutions to a number of difficult and challenging problems ranging from sulfur specification of Kraft black liquors in the pulp and paper industry to determining trace impurities in the presence of percent level of ionic material to routine analysis of parts per billion (ppb) level contaminants in high purity water [1–11]. The rapid growth of this technique is due to the inherent simplicity of the hardware and because the nature of the fused-silica capillary's inner wall surface can be altered by the choice of electrolyte. In essence the electrolyte and the polarity of the applied voltage programs the capillary to separate anionic, cationic or neutral species. This represents a substantial economy over established ion analysis techniques such as ion chromatography where separations are wholly dependent on dedicated specialized analytical columns that cost as much as 100 times more than the fused-silica capillaries.

To date, photometric detection in CIE has been dominated by the indirect ultraviolet mode [12,13] as an "universal" detection approach, with some applications of direct UV having been reported. Other reported detection modes include indirect fluorometry [14], direct conductometry [15,16] and suppressed conductometry [17,18]. However, UV detection, offers more versatility over bulk property detectors such as conductivity; there is more flexibility in optimizing sensitivity through a proper selection of the electrolyte co-ions and measurement wavelength. This is especially important when analyzing samples containing disparate concentration levels of the analyte [9]. Also, there is a greater selection of UV absorbing co-ions with mobilities similar to the inorganic anions of interest than there are fluorescent or suppressible co-ions.

In CIE separations of anions, a quaternary amine EOF modifier is used in the electrolyte. This dy-

0021-9673/93/$06.00

namically coats the inner wall of the fused-silica capillary. The modifier imparts a positive charge on the wall and changes the EOF towards the anode hence augmenting the mobility of the anions. Since the analysis time is short (3 to 5 min), high sample throughput is achievable through automation. Electrolytes containing the EOF modifier equilibrate rapidly in the capillary. An unused 60 cm × 75 μm fused-silica capillary is stabilized in less than 2 min by drawing electrolyte into the capillary via a 15 p.s.i. (1 p.s.i. = 6894.76 Pa) vacuum. Generally 2 capillary volumes (less than 6 μl) of electrolyte is adequate when varying electrolyte parameters such as pH or ionic strength. To minimize electrolyte solubility incompatibilities and baseline drift, extra steps involving flushing with water and then with the next electrolyte are required when changing the electrolyte co-ion.

With such short periods needed for analysis and electrolyte interchange, several electrolyte compositions can be evaluated in less than an hour. Due to the constraint of having the receiving side electrolyte stationary, automated methods development typically requires leaving the receiving electrolyte unchanged throughout the experiments. Recent work by Bocek and co-workers [19,20] showed that analyte selectivity can be changed through careful selection of the receiving side electrolyte composition (anodic chamber) as delivered by either a step-change or a transient pulse during the analysis. CIE anion separations are not sensitive to receiving side composition unless the electrolyte is substantially different in composition. The anodic EOF prevents large cationic species from reaching the cathodic electrolyte and even impedes the migration of the faster alkali metal ions to the injection side. However, baseline perturbations and drift were observed when the receiving electrolyte was very dilute or when the pH was highly acidic. In these situations, it is recommended that the electrolyte injection and receiving side electrolytes are the same.

EXPERIMENTAL

Instrumentation

The CE system employed was the Quanta 4000 (Waters Chromatography Division of Millipore Corporation, Milford, MA, USA) with a negative power supply. A Hg lamp was used for 185, 254, 313, 365, 405, 436 and 546 nm detection. A Zn lamp and a Cd lamp were used for 214 and 229 nm detection respectively. Waters AccuSep polyimide coated fused-silica capillaries was used throughout this work. The capillary dimensions are 75 μm I.D. × 375 μm O.D. with the detection window placed 8 cm from the receiving electrolyte end to the detector cell. Capillary lengths used were 40 and 60 cm.

Data acquisition was carried out with a Waters 860 data station with SAT/IN and LAC/E modules connecting the CE system to the data station with signal polarity inverted. Detector time constant was set at 0.1 s and data acquisition rate was 20 Hz. Collection of electropherographic data was initiated by a signal cable connection between the Quanta 4000 and the SAT/IN module.

UV spectra was generated using a Waters Model 990 photodiode-array detector in a flow-injection analysis made using a Rheodyne (Colati, CA, USA) Model 7010 injector.

Preparation of electrolytes

Background electrolyte solutions were prepared from various salts: sodium chromate tetrahydrate (99+%, Aldrich, Milwaukee, WI, USA), potassium hydrogenphthalate, *p*-hydroxybenzoic acid and potassium sorbate (all 99%, Sigma, St. Louis, MO, USA). The electroosmotic flow modifier was prepared from Waters CIA-Pak OFM Anion-BT [21] obtained as a 20 m*M* concentrate. Adjustment of electrolyte pH was done with either sulfuric acid (J. T. Baker, Phillipsburg, NJ, USA) or lithium hydroxide monohydrate (Aldrich). Solutions of 100 m*M* of the acid or base were used for the adjustment of electrolyte pH. The 100 m*M* lithium hydroxide solution was also used in the first of a three-stage capillary conditioning rinse cycle. Milli-Q reagent grade water (Millipore, Bedford, MA, USA) was used throughout.

Standard analyte solutions

All standard solutions were prepared by a dilution of 1000 ppm stock solutions containing a single anion. The stock solutions were prepared fresh every six months and were stored in 2000 ml polycarbonate tissue culture flasks (Corning Glass Works, Corning, NY, USA). All mixed anion standards were prepared freshly for each of the experiments. Milli-Q water and polymethylpentene containers

(Nalgene, Rochester, NY, USA) were used throughout.

System operation

Two sample carousel configurations were employed for the CE system. The 20 sample carousel used 600 μl polypropylene centrifuge tubes (Waters) for sample vials and 20 ml high density poly-ethylene (HDPE) sample side electrolyte vials (Waters). The six-sample carousel used 4 ml (15 × 45 mm) polypropylene Sunvials (Sunbrokers, Wilmington, NC, USA) for electrolytes and samples. Receiving side electrolyte vials were 20 ml glass scintillation vials (Waters) for both carousels. All vials were rinsed with Milli-Q water and dried prior to use.

RESULTS AND DISCUSSION

Indirect UV detection optimization for chromate background electrolyte

The use of chromate as a co-ion was first reported by Jones and Jandik in 1990 [22] and has been used extensively for anion analysis due to its unique combination of UV absorbtion characteristics and high electrophoretic mobility [1–10,22–26]. Fig. 1 shows a UV absorption spectra of chromate from 200 to 400 nm superimposed with lines indicating the measurement wavelengths commonly available

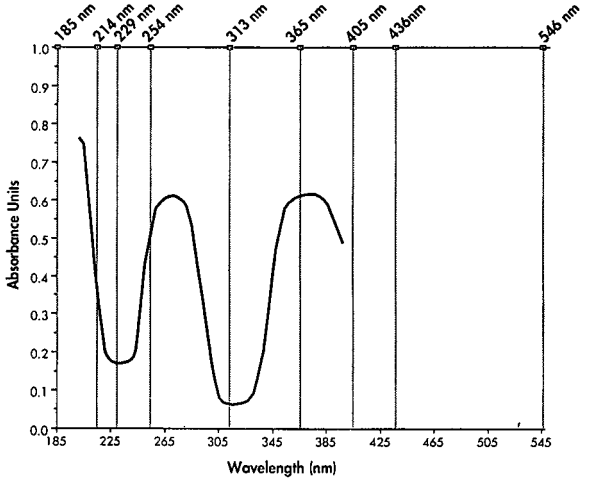

Fig. 1. Typical UV spectra obtained for chromate (sodium salt) using a photodiode-array detector in the range 200–400 nm. Superimposed on UV spectra are lines representing the wavelengths used for detection of analytes on a chomate electrolyte described in Table I.

from Hg, Zn and Cd light sources. There are three UV maxima for chromate at 200, 272 and 370 nm. The largest signal generated for indirect UV detection is found where chromate absorbs most strongly and the analytes absorbs least. From Fig. 1, the strongest background signal for chromate is 185 nm, assuming that chromate continues to absorb strongly below 200 nm. The next strongest signal is found at 365 nm which is near chromate's third UV maxima. Finally another convenient monitoring wavelength is 254 nm, near the second UV maxima. Table I shows peak height ratios of 11 inorganic anions with respect to 254 nm for nine wavelengths using a 5-m*M* chromate–0.5 m*M* OFM Anion-BT electrolyte. Consistent with the UV spectra, 185 nm produced the largest signal for 9 of the 11 anions while 365 nm and 254 nm had the second and third largest signal for 7 anions respectively. Large detector signals alone do not always provide the most sensitivity, lamp energy effects detector performance since the higher lamp energies provides more photons per unit time resulting in reduced short noise [27,28]. The measured lamp output defined as the difference between the sample and reference side photodiode currents is 0.40, 1.55 and 0.08 nA for 185, 254 and 365 nm respectively. The high Hg lamp current found at 254 nm provides the best detection limits for the 11 analytes. Using the fluoride anion for comparison, the detection limit (defined here as 3 times the baseline noise) is 80 ppb for 254 nm compared to 190 ppb at 185 nm and 220 ppb at 365 nm. Table I also lists the detection limits for the 11 anions at the various wavelengths. In all three wavelengths discussed, Fig. 2, the peaks are detected indirectly except for bromide at 185 nm which absorbs sligthly more than chromate. The poor sensitivity for bromide is ideal for samples where excessive bromide is a matrix intererence masking proper identification and quantitation of adjacent peaks. The 185 nm wavelength has also been shown to be suited for the detection of sulfide which absorbs similarly to chromate at 254 nm [5].

Direct UV detection for chromate background electrolyte

At 214 and 229 nm, the UV absorption of chromate is at a minimum: this does not permit universal indirect detection. However, these wave-

TABLE I

PEAK HEIGHT RATIO WITH RESPECT TO 254 nm FOR EIGHT DIFFERENT WAVELENGTHS USING AN ELEVEN INORGANIC ANION MIXTURE AND DETECTION LIMITS DEFINED AS 3 × NOISE IN ppm

Negative numbers indicate the analyte is more absorbing than the background electrolyte. The terms dl and np stand for detection limit and no peak respectively. Concentrations (ppm): All anions are at 4 ppm except for chloride (2); molybdate and tungstate (10); fluoride (1). The electrolyte is 5 m*M* 0.5 m*M* OFM Anion-BT adjusted to pH 8.0. Applied potential is 20 kV (negative polarity). Capillary dimensions are 60 cm (52 cm to detector) × 75 μm I.D. fused-silica. UV detection (wavelengths listed in table). Injection is hydrostatic (10 cm for 30 s). Capillary flushed with fresh electrolyte for 2 min prior to loading of sample.

No.	Anion	Wavelength (nm)								
		185	214	229	254	313	365	405	436	546
Peak height ratio (with respect to 254 nm)										
1	Thiosulfate	3.55	−0.58	−0.61	1.00	dl	1.67	0.57	0.14	np
2	Bromide	−0.18	−0.08	0.21	1.00	dl	1.56	0.54	0.14	np
3	Chloride	2.71	0.51	0.20	1.00	dl	1.52	0.52	0.12	np
4	Sulfate	4.04	0.53	0.20	1.00	dl	1.51	0.52	0.13	np
5	Nitrite	2.87	−2.29	−0.92	1.00	dl	1.55	0.53	0.11	np
6	Nitrate	2.26	−2.94	−0.38	1.00	dl	1.49	0.53	0.14	np
7	Molybdate	5.10	−2.44	−1.74	1.00	dl	2.19	0.75	0.19	np
8	Tungstate	2.64	0.12	0.16	1.00	dl	1.53	0.54	0.12	np
9	Fluoride	4.03	0.52	0.21	1.00	dl	1.57	0.51	0.15	np
10	Phosphate	3.79	0.60	0.25	1.00	dl	1.44	0.49	0.12	np
11	Carbonate	3.93	0.49	0.17	1.00	dl	1.55	0.58	0.12	np
Detection limit (3 × noise in ppm)										
1	Thiosulfate	0.71	−1.32	−1.39	0.25	6.00	0.70	2.68	3.05	np
2	Bromide	−10.17	−6.84	2.62	0.18	6.00	0.55	2.05	2.21	np
3	Chloride	0.38	0.60	1.52	0.10	3.00	0.31	1.17	1.40	np
4	Sulfate	0.30	0.69	1.84	0.12	6.00	0.38	1.42	1.63	np
5	Nitrite	0.51	−0.19	−0.48	0.15	6.00	0.44	1.65	2.15	np
6	Nitrate	0.95	−0.22	−1.72	0.22	6.00	0.67	2.42	2.48	np
7	Molybdate	1.13	−0.71	−1.00	0.58	15.00	1.23	4.64	5.15	np
8	Tungstate	2.31	15.61	11.25	0.61	15.00	1.85	6.74	8.52	np
9	Fluoride	0.19	0.43	1.09	0.08	1.50	0.22	0.88	0.86	np
10	Phosphate	0.78	1.49	3.55	0.30	6.00	0.96	3.63	4.29	np
11	Carbonate	0.84	2.02	5.74	0.33	6.00	1.00	3.41	4.72	np

lengths are aids for confirming peak identity for UV absorbing anions such as thiosulfate, nitrite, nitrate and molybdate as shown in Fig. 3. Good candidates for background electrolytes for indirect UV detection at 214 nm are the strongly absorbing nitrite, nitrate and molybdate ions while only nitrite and molybdate are optimal as background electrolytes at 229 nm. Selection of a UV absorbing analyte as the electrolyte co-ion for purposes of indirect UV detection is optimal if it has a similar mobility to the analytes of interest for best peak symmetry and also if the sample matrix has an excess of the ion used as the electrolyte co-ion, which is therefore not necessary to quantitate. In the experiments that follow, 254 nm detection provides the best overall performance and is the wavelength used throughout the rest of this paper.

Successive increase in EOF modifier concentration

In earlier work, a linear correlation was obtained with adjusted ionic equivalent conductance values from the literature for individual analytes plotted against reciprocal migration times of 27 inorganic and organic anions [24]. Three anions did not fit the linear relationship, iodide, thiocyanate and perchlorate which all had significantly longer migration times than predicted. It was suspected that the mobility difference was due to hydrophobic interac-

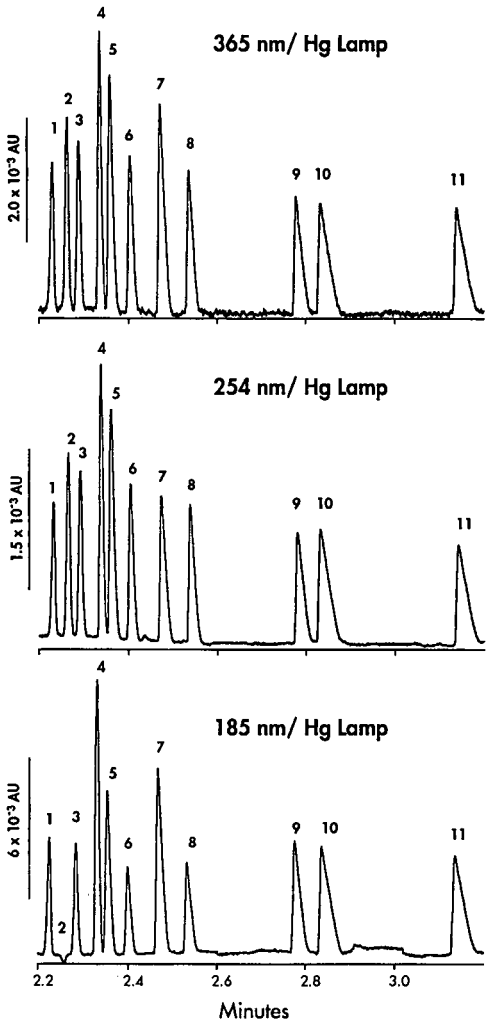

Fig. 2. Separations of 11 inorganic anions listed in Table I using Hg lamp detection at or near chromate UV maxima. Electrolyte and running conditions described in Table I. All peaks are visualized indirectly except for negative bromide (peak 2) at 185 nm.

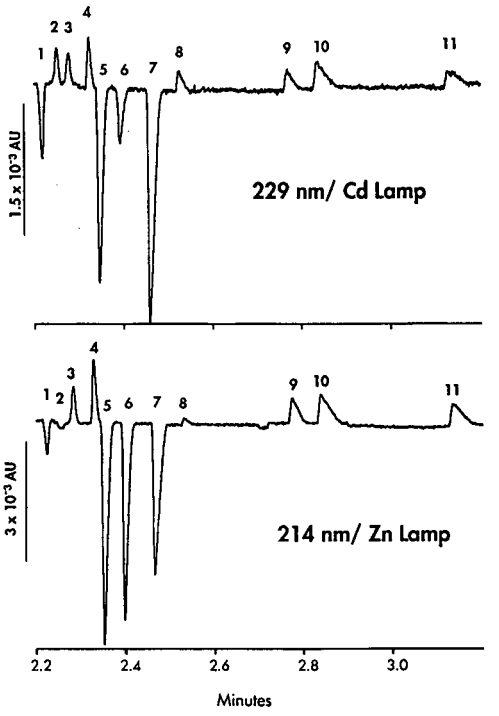

Fig. 3. Separations of 11 inorganic anions listed in Table I using a Cd lamp for 229 nm and a Zn lamp for 214 nm detection. Chromate is at a UV minima at two of these wavelengths, all positive peaks are visualized indirectly. Running conditions listed in Table I.

tion of the analytes with 0.5 m*M* EOF modifier in a 5-m*M* chromate electrolyte. These 3 anomalous analytes included in a 13 anion test mixture were evaluated for effects on selectivity in a 5-m*M* chromate electrolyte with respect to the EOF modifier ranging from 0.25 m*M* to 1.5 m*M*. A six-electrolyte carousel was used for the evaluation. Each electrolyte vial is used with a specific sample vial. Therefore each sample vial was filled with the same test mixture. The receiving side electrolyte is not automated and remains constant with the initial electrolyte composition unless manually changed. To reduce running time a 60-cm capillary was shortened by 20 cm from the injection end. The applied field strength (kV/cm) was kept constant by reducing the applied voltage to prevent overheating conditions in the capillary. This permitted a proportional reduction in the programmed running parameters consisting of data acquisition, injection and capillary flush times. The result was 5.7 min per sample with a total experiment time of less than 35 min for the evaluation of 6 electrolytes. The migration time data was normalized with respect to nitrite for improved visualization in changes in selectivity. The graph generated from the automated sequence of unmatched electrolytes is shown in Fig. 4A. The 3 polarizable anions are highlighted with bold lines. As evident from the increasing migration time ra-

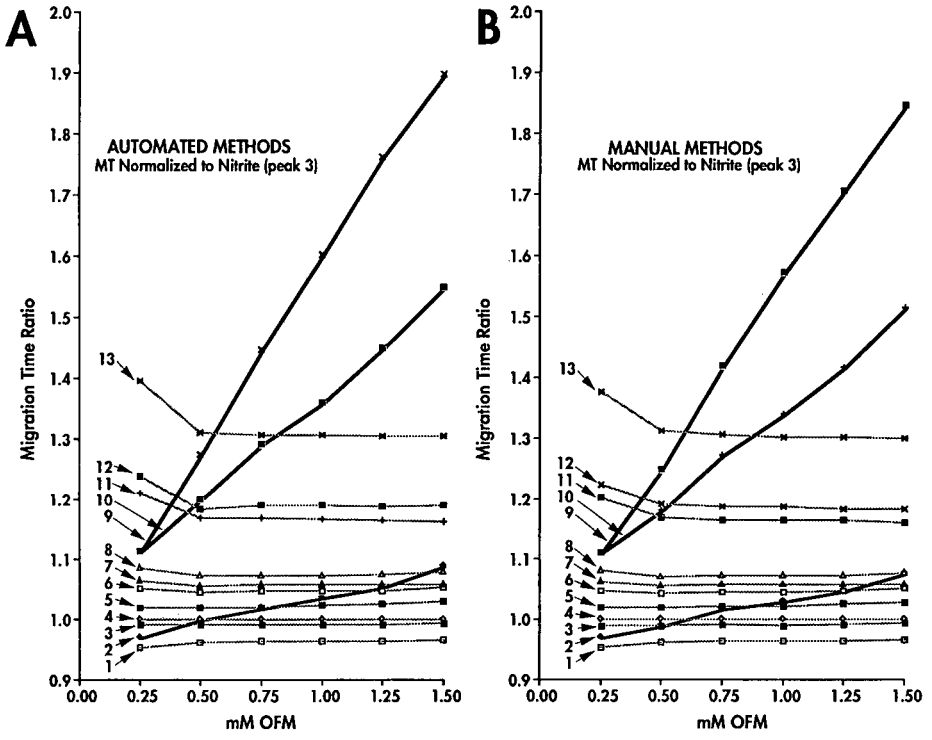

Fig. 4. Selectivity changes obtained from automated electrolyte changing where the receiving side electrolyte remains constant with the first electrolyte composition. Selectivity changes obtained from manual electrolyte changing where the receiving side electrolyte matches the injection side. Concentrations (ppm): 1 = bromide (4); 2 = iodide (5); 3 = sulfate (4); 4 = nitrite (4); 5 = nitrate (4); 6 = molybdate (10); 7 = azide (4); 8 = tungstate (10);9 = perchlorate (4); 10 = thiocyanate (4); 11 = fluoride (1); 12 = phosphate (4); 13 = carbonate (4). The EOF modifier, OFM Anion-BT, concentration is increased from 0.25 m*M* to 1.5 m*M* in 6 discrete electrolytes all containing 5 m*M* sodium chromate adjusted to pH 8.0. Applied potential is 13.3 kV (negative polarity). Capillary dimensions are 40 cm (32 cm to detector) × 75 μm I.D. fused-silica. UV detection at 254 nm. Injection is hydrostatic (10 cm for 20 s). Capillary flushed with fresh electrolyte for 1.4 min prior to loading of sample.

tios, these anions show a high sensitivity to minor changes in EOF modifier concentration. Further experiments have to date placed iodide after peak 13 (bicarbonate) using 3 m*M* EOF modifier.

The same experiment was repeated using a fresh capillary except this time the receiving electrolyte is identical to the injection side electrolyte (Fig. 4B). Comparing the graphs in Fig. 4A and B we see that the data is virtually identical. Since migration times are inversely related to the ionic equivalent conductance Fig. 5 shows the data from Fig. 4A as reciprocal normalized migration times for each analyte under the different electrolyte conditions. The ionic equivalent conductance (IEC) obtained from the literature [29] are adjusted (IEC_{adj}) according to reference [24]. A linear curve fit is obtained for the 0.5 m*M* OFM Anion-BT data with iodide, thiocyanate and perchlorate data points omitted. A correlation coefficient of $r^2 = 0.982$ is obtained. From this graph it can be seen that as the EOF modifier concentration approaches zero, the observed mobility of polarizable anions approach the value calculated from IEC_{adj}. Deviations from the line for the 0.25 m*M* data for the slower anions carbonate, phosphate and fluoride is not due to interaction with the EOF modifier but due to a slower EOF obtained using less modifier. An improved curve fit for this data is obtained when the normalized migration times reflect the electrophoretic mobilities rather than the apparent mobility. To do this correctly it is necessary to subtract the contribution due to the EOF, *e.g.* as measured with a neutral

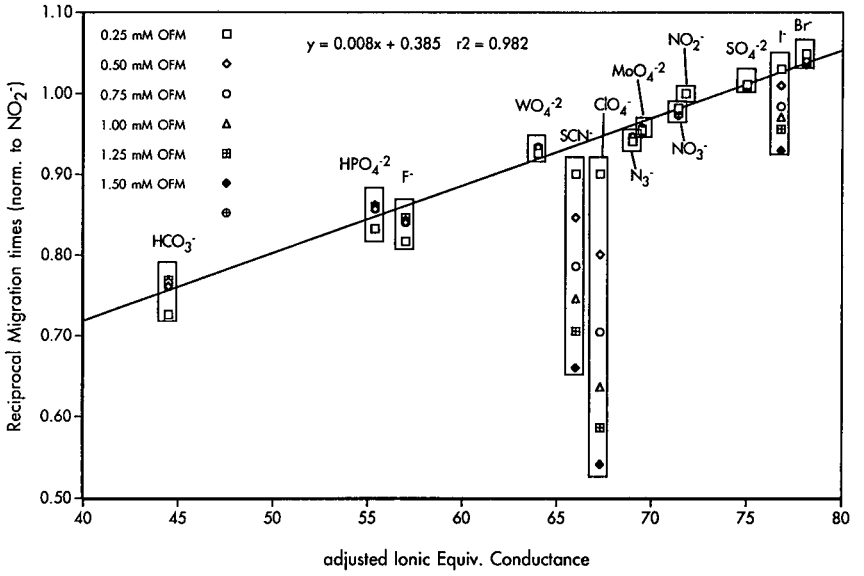

Fig. 5. Plot of reciprocal migration times normalized to nitrite anion from data obtained in Fig. 4A. This graph illustrates the deviation from predicted mobility IEC_{adj} due to EOF modifier concentration. See text for details.

marker. In order to accurately predict the mobility of the polarizable anions in the electrolyte, a hydrophobic factor (defined as a function of the EOF modifier concentration) must be included to the adjustments.

Successive change in electrolyte co-ion mobility

In situations where different electrolytes offer improved sensitivity and peak symmetry for specific analytes, it may be advantageous to analyze a sample under different electrolyte conditions. Three background electrolytes were selected with strong UV absorbtion around 254 nm, chromate, *p*-hydroxybenzoate and sorbate. Chromate is optimum for highly mobile inorganic anions through fluoride and phosphate. At an elevated pH *p*-hydroxybenzoate becomes a moderately mobile divalent anion through ionization of the hydroxyl group. The sorbate anion absorbs more strongly than *p*-hydroxybenzoate and is a low mobility electrolyte optimized for anions migrating after the bicarbonate ion. A four-quadrant electrolyte carousel with two sample vials that alternate as capillary conditioning rinse vials was used in the experiment. Again, the receiving side electrolyte is not automated and remains constant with the initial electrolyte composition unless manually changed. A three-stage rinse cycle consisting of a dilute base, water rinse and the next electrolyte composition described elsewhere [9] was used to simulate a situation where removal of sample excipients retained on the inner wall necessitates on-line clean-up of the capillary. A 15 anion mixture was injected with the three different mobility electrolyte systems. All electrolytes were 5 m*M* in co-ion concentration and 0.5 m*M* in EOF modifier. The automated and manual sequence of electrolyte changing all included a three-cycle capillary conditioning step described earlier. The manually balanced injection and receiving side electrolyte was run after the automated sequence using the same capillary. Fig. 6A shows the three electropherograms obtrained with the 15 anion mixture injected and the three different electrolytes, using the automated method. The chromate electrolyte (top) separation shows all the anions fully resolved with increased tailing for the later peaks. The *p*-hydroxybenzoate electrolyte shows improved peak symmetry for the 8 through 11 but fails to resolve peaks 1 through 5. The sorbate electrolyte shows best sensitivity and selectivity for peaks 11 through 15 but does not resolve peaks 1 through 7. In terms of the standard, the chromate electrolyte is sufficient for

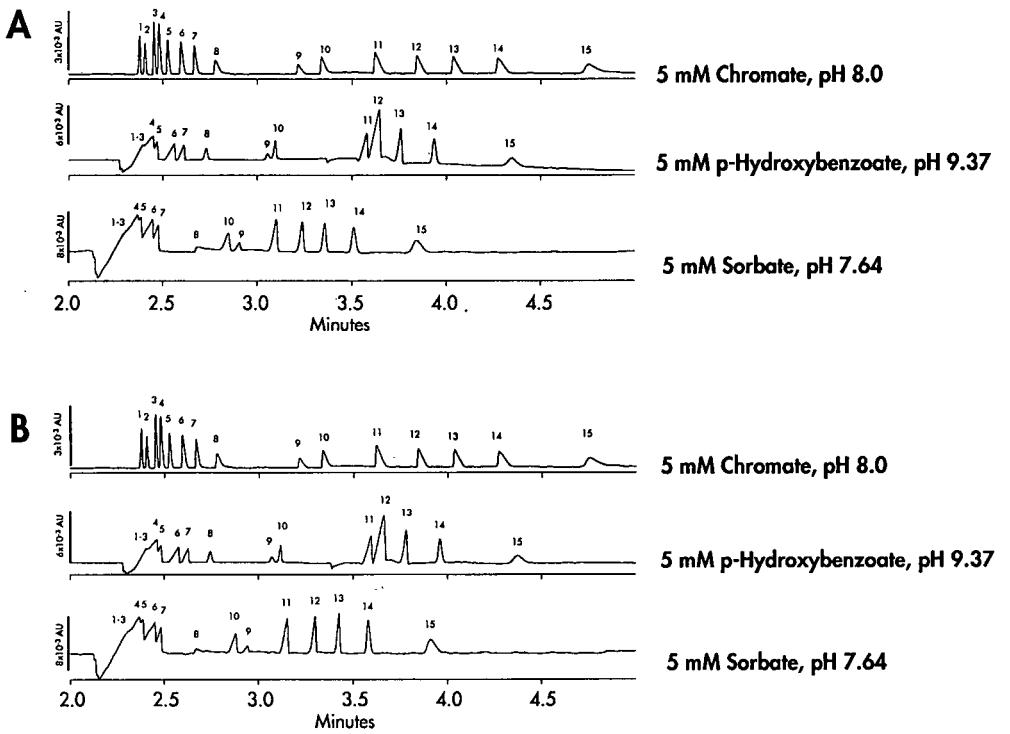

Fig. 6. Selectivity changes obtained from automated electrolyte changing where the receiving side electrolyte remains constant with the first electrolyte composition. Selectivity changes obtained from manual electrolyte changing where the receiving side electrolyte matches the injection side. Concentrations (ppm): 1 = bromide (4); 2 = chloride (2); 3 = sulfate (4); 4 = nitrite (4); 5 = nitrate (4); 6 = molybdate (10); 7 = tungstate (10); 8 = citrate (4); 9 = phthalate (4); 10 = carbonate (4); 11 = ethanesulfonate (5); 12 = propanesulfonate (5); 13 = butanesulfonate (5); 14 = pentanesulfonate (5); 15 = hexanesulfonate (5). All electrolyte contain 0.5 m*M* OFM Anion-BT. Applied potential is 20 kV (negative polarity). Capillary dimensions are 60 cm (52 cm to detector) × 75 μm I.D. fused-silica. UV detection at 254 nm. Injection is hydrostatic (10 cm for 30 s). Capillary flushed with fresh electrolyte for 2 min with dilute base, 1 min with Milli-Q water and 2 min with next electrolyte composition prior to loading of sample.

separating all 15 components. In real world situations the late migrators may contain more complex mixtures which the chromate electrolyte may not fully resolve due to peak assymmetry [1,9].

The manually matched electrolyte separations found in Fig. 6B show that the results are again virtually identical to those obtained with the automated method.

CONCLUSIONS

CIE provides a rapid and highly efficient analysis approach for small ions that extends into facilitating methods development. In this paper the versatility of UV detection using properly selected wavelengths with respect to electrolyte chemistry was demonstrated. This technique offers means for universal, selective or confirmational determination of analytes. The simplicity of using an open tubular fused-silica capillary permits rapid conversion from one electrolyte composition to another in 1–2 min and less than 5 minutes if on-line capillary clean-up is required. The data obtained for a selectivity chart which maps the changes in analyte mobility with respect to six discrete changes of a single electrolyte parameter was accomplished automatically under 35 min. In a second variation, rapid electrolyte conversion in the capillary permitted full optimization of peak symmetry and sensitivity for highly mobile inorganic anions to less mobile organic acids.

REFERENCES

1 J. Romano, P. Jandik, W. R. Jones and P. Jackson, *J. Chromatogr.*, 546 (1991) 411.
2 B. J. Wildman, P. Jackson, W. R. Jones and P. G. Alden, *J. Chromatogr.*, 546 (1991) 459.
3 W. R. Jones, P. Jandik and R. Pfeifer, *Am. Lab.*, 23 (8) (1991) 40.
4 G. Bondoux, P. Jandik and W. R. Jones, *J. Chromatogr.*, 602 (1992) 79.
5 D. R. Salomon and J. Romano, *J. Chromatogr.*, 602 (1992) 219.
6 S. C. Grocott, L. P. Jefferies, T. Bowser, J. Carnevale and P. E. Jackson, *J. Chromatogr.*, 602 (1992) 257.
7 P. D. Mudgett, J. R. Shultz and R. L. Sauer, *22nd Inter. Conf. Environ. Sys*, (1992) 1.
8 K. A. Hargadon and B. R. McCord, *J. Chromatogr.*, 602 (1992) 241.
9 W. R. Jones and P. Jandik, *J. Chromatogr.*, 608 (1992) 385.
10 R. A. Carpio and R. Mariscal and J. Welch, *Anal. Chem.*, 64 (1992) 2123.
11 M. Koberda, M. Konkowski, P. Youngberg, W. R. Jones and A. Weston, *J. Chromatogr.*, 602 (1992) 235.
12 E. S. Yeung, *Acc. Chem. Res.*, 22 (1989) 125.
13 F. Foret, S. Fanali, L. Ossicini and P. Bocek, *J. Chromatogr.*, 470 (1989) 299.
14 L. Gross and E. S. Yeung, *Anal. Chem.*, 62 (1990) 427.
15 F. Foret, M. Deml, V. Kahle and P. Bocek, *Electrophoresis*, 7 (1986) 430.
16 X. Huang, J. A. Luckey, M. J. Gordon and R. N. Zare, *Anal. Chem.*, 61 (1989) 766.
17 P. Dasgupta, presented at the *International Ion Chromatography Symposium, Denver, CO, October 6–9, 1991*, plenary lecture 1.
18 P. Dasgupta, presented at the *International Ion Chromatography Symposium, Linz, Austria, September 21–24, 1992*, poster 129.
19 J. Sudor, Z. Stransky, J. Posichal, M. Deml and P. Bocek, *Electrophoresis*, 10 (1989) 802.
20 P. Bocke, M. Deml and J. Pospichal, *J. Chromatogr.*, 500 (1990) 673.
21 *US Pat.*, 5 104 506, 5 128 055 and 5 166 724 (1992).
22 W. R. Jones and P. Jandik, *Amer. Lab.*, 22 (9) (1990) 51.
23 P. Jandik, W. R. Jones, A. Weston and P. R. Brown, *LC · GC*, 9 (1991) 634.
24 W. R. Jones and P. Jandik, *J. Chromatogr.*, 546 (1991) 445.
25 P. Jandik and W. R. Jones, *J. Chromatogr.*, 546 (1991) 431.
26 W. Buchberger and P. R. Haddad, *J. Chromatogr..*, 608 (1992) 59.
27 W. Baumann, *Fresenius' Z. Anal. Chem.*, 284 (1977) 31.
28 J. B. Li, *LC · GC*, 10 (1992) 856.
29 R. C. Weast (Editor), *Handbook of Chemistry and Physics*, CRC Press, Boca Ration, FL, 66th ed., 1985, Section 6, pp. 30–31.

Journal of Chromatography, 640 (1993) 397–402
Elsevier Science Publishers B.V., Amsterdam

CHROMSYMP. 2667

Increased selectivity for electrochromatography by dynamic ion exchange

Tommy W. Garner and Edward S. Yeung*

Ames Laboratory–US Department of Energy and Department of Chemistry, Iowa State University, Ames, IA 50011 (USA)

ABSTRACT

The separation of compounds with similar mobilities is expected to be difficult with capillary zone electrophoresis. Increased selectivity is shown for compounds of this type when other modes of separation are added to the system. A capillary coated with a hydrophobic stationary phase is shown to be a dynamic ion exchanger when a quaternary ammonium compound is added to the running buffer. Compounds are shown to have a decrease in retention when the concentration of the buffer ion is increased. The effect of adding an organic modifier and the influence of the concentration of the surface active reagent are also studied.

INTRODUCTION

Capillary zone electrophoresis (CZE) has been demonstrated to provide highly efficient separations of many charged species including small organic molecules, amino acids, peptides and nucleic acids [1–5]. Because CZE separates compounds based on their differential migration rates, compounds with similar mobilities pose resolution problems, however [6,7]. The most common optimization techniques for CZE are changing the pH of the running buffer, coating the column with a hydrophobic stationary phase, and using additives to decrease the electroosmotic flow.

The addition of hydrophobic ion-interaction reagents (IIR) to the mobile phase to enhance retention and resolution has been widely used in the liquid chromatographic (LC) separation of charged species on reversed-phase columns [8–13]. The ion-pair model presumes that an ion pair between the IIR and the sample ion is formed in the mobile phase. The ion-piar then partitions into the stationary phase. Alternatively, retention can be explained by a dynamic ion-exchanged model [14]. This model presumes that the IIR is adsorptively bound to the column where it behaves as an ion-exchanger. The retention and separation in this mode are very similar to those in ion-exchange chromatography. There is, however, added flexibility in dynamic ion-exchange due to the many parameters that affect the retention of a species. Another variation is the ion-interaction model where the IIR is dynamically adsorbed to the column forming a charged double layer. Sample ion are then retained due to their coulombic attraction to the double layer. The actual mechanism of ion-pair chromatography is probably a mixture of these models depending upon the specific conditions.

In this paper, separation of compounds with similar electrophoretic mobilities is performed using a reversed-phase coated capillary with dynamic ion-exchange sites. An IIR, cetyltrimethylammonium bromide (CTAB), is added to the running buffer and is sorptively bound to the hydrophobic stationary phase to allow ion-exchange. The results of these experiments support the dynamic ion-exchange model for retention and separation.

EXPERIMENTAL

The buffers used in these experiments were prepared in deionized water (Millipore, Bedford, MA,

* Corresponding author.

0021-9673/93/$06.00

USA; Milli-Q system). CTAB solutions were prepared by diluting with buffer solution and adjusting to pH 7 with a 0.1 *M* solution of NaOH. The anions, 4-amino-1-naphthalenesulphonic acid (4A1N) and 5-amino-2-naphthalenesulphonic acid (5A2N) (both from Aldrich, Milwaukee, WI, USA), were prepared in running buffer prior to injection.

The fused-silica capillaries (Polymicro Technologies, Phoenix, AZ, USA) were 50 cm long and nominally 10 μm in I.D. These capillaries were used as supplied or coated, and the coating later cross-linked with 10.0% (w/w) OV-17v (Alltech Assoc., Deerfield, IL, USA) as described in ref. 15. The polyimide coating was removed with hot sulphuric acid 40 cm from the injection end of the capillary to facilitate on-column detection. The CZE–electrochromatographic system is similar to the one described previously [16]. The electric field is supplied by either a positive or a negative high-voltage supply (0–30 kV, Glassman High Voltage, Whitehouse Station, NJ, USA; Model MJ30P0400-11 or MJ30N0400-11).

Sample introduction was accomplished by using electromigration in all cases. Detection was accomplished by UV absorption (240 nm, ISCO Model 3850, Omaha, NE, USA) or by using a laser-based fluorescence detector similar to one described previously [16] with the exception being that the laser line used was the 325-nm line of a He–Cd laser (Liconix, Sunnyvale, CA, USA; Model 4240NB).

All data were either collected on a strip chart recorder or subjected to analog-to-digital conversion (Data Translation, Marlborough, MA, USA; Model DT 2827, 5–10 Hz) and later stored on a personal computer (IBM PC-AT).

DISCUSSION

The resolution of compounds separated by CZE is given by

$$R = \frac{1}{4\sqrt{2}} (\mu_{e,1} - \mu_{e,2}) \sqrt{\frac{V}{D(\bar{\mu}_e + \mu_{eo})}} \quad (1)$$

where $\mu_{e,1}$ and $\mu_{e,2}$ are the electrophoretic mobilities of the solutes, $\bar{\mu}_e$ is the average electrophoretic mobility, μ_{eo} is the electroosmotic flow coefficient, V is the applied potential and D is the diffusion coefficient. As can be seen from this equation, resolution is directly proportional to the difference in mobilities of the two species of interest.

The separation of compounds with similar mobilities is therefore expected to be difficult with CZE [7]. This can be demonstrated by the attempted separation of positional isomers, which would be expected to have similar mobilities. When 4A1N and 5A2N are injected into the commercial capillary electrophoresis system at pH 7 (10 m*M* sodium phosphate buffer), no separation is achieved. One way to enhance the selectivity of this separation would be to change the pH of the buffer which may change the charge, and therefore the mobility, of each species to different degrees. This, however, would not be expected to work in all cases due to a small range of pK values for the components in the mixture. Compounds with very similar but distinct mobilities will not separate unless $\mu_{eo} \approx -\mu_e$, which can be achieved through the addition of modifiers to the buffer. This condition leads to analysis times that approach infinity, however.

Selectivity can also be enhanced by adding another mode of separation to the system. One way to do this for the compounds we have selected is to add anion-exchange sites to the column. Compounds with larger affinities for the ion-exchange sites would be impeded and would have longer migration times. This can be accomplished by first coating the column with polymeric stationary phase [17]. This will have two effects on the column. First, the charged silanol groups on the surface of the column would be shielded, thus drastically reducing electroosmotic flow. Second, the surface of the column would be changed from a polar to a relatively non-polar, hydrophobic surface. Compounds with a hydrophobic character can therefore partition into the stationary phase and can be separated based on retention [18].

For the separation of anions, the dynamic ion-exchange sites are added to the column by the addition of a surface-active quaternary ammonium compound to the buffer. The hydrophobic end of this molecule is expected to adsorb to the hydrophobic surface of the coated capillary, allowing the charged end of the molecule to be exposed to the polar (aqueous) mobile phase. The surface of the capillary would therefore be expected to carry a positive charge with a corresponding association of anions in the double-layer region that extends to the diffuse layer. This is in contrast to a bare fused-silica column, where under normal (aqueous) conditions

the solid surface has an excess anionic charge resulting from ionization of surface silanol groups. The counter-ions in the diffuse layer in that case would therefore be positive. The migration of hydrated counter-ions in the diffuse layer is the propulsive force behind electroosmotic flow [19]. In the case of a bare fused-silica capillary we would expect the flow to be towards the cathode while in the case of the dynamic exchange mode the flow would be in the direction of the anode.

The fact that the electroosmotic flow is reversed when a surface-active quaternary ammonium compound is added to the buffer supports the dynamic ion-exchange model for ion-pair chromatography. This is the process where the surface-active agent is first adsorbed to the surface of the column, and the sample ion is then retained by an ion-exchange mechanism. The mechanism is more complex than ion-exchange, however, because the ion-exchange site is sorptively bound, while in an ion chromatography column the ion-exchange site is covalently bound.

The C_{18} chain of the CTAB molecule is expected to be readily adsorbed onto the surface of a reversed-phase column by hydrophobic attraction and would tend to behave as an ion-exchange site. Since conductance data indicate that R_4N^+ salts are highly dissociated under similar conditions it can be assumed that ion-pair formation is negligible [12]. The adsorption of the CTAB to the column was confirmed by washing the column with acetonitrile and the observation that the electroosmotic flow changes back to its original direction, *i.e.*, towards the cathode.

The retention of a compound by dynamic ion-exchange, as discussed above, is complex. Some of the parameters that can influence the dynamic ion-exchange retention of compounds in HPLC are the size of the surface-active agent, pH, type and concentration of the organic modifier and the stationary phase characteristics [13,14]. These parameters would be expected to have similar effects in electrochromatography.

In Fig. 1, the two compounds, 4A1N and 5A2N, are separated on a column coated with 2% OV-17v. The buffer consists of potassium phthalate, a common eluent used in ion-exchange chromatography, and 400 μM CTAB. The column was equilibrated with the buffer for 2 h to increase the stability of the

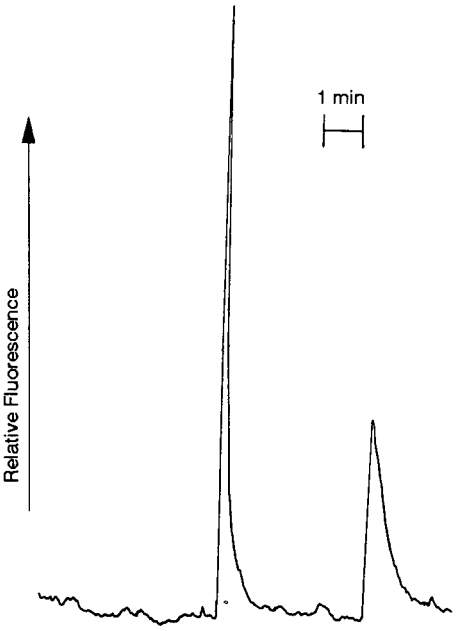

Fig. 1. Elution profile for (left) 4A1N and (right) 5A2N. Buffer conditions: 32 mM potassium phthalate, 400 μM CTAB, pH 7.0.

migration times. There is a reduction in efficiency compared to CZE in this system based on the observed number of theoretical plates in each peak. This would be expected due to the increased contribution of mass transfer in the stationary phase to the plate height.

The equilibrium describing the exchange of an anion A and the buffer ion E is

$$A_{aq} + nE_s \rightleftarrows A_s + nE_{aq} \quad (2)$$

where the subscripts s and aq refer to the stationary and mobile phases, respectively.

Models for dynamic ion-exchange based on HPLC experiments predict that increased buffer ion concentration will have two effects on the retention of sample ions. The increased concentration of the counter ion increases the amount of the surface-active agent adsorbed to the surface of the capillary [11]. This is greatly offset, however, by the increased competition for the exchange sites as can be seen from eqn. 2. Pfeffer and Yeung [18] and Tsuda [20] have shown that the addition of a surface-active reagent, such as CTAB, to the hydrophobic surface of a coated capillary column has the effect of

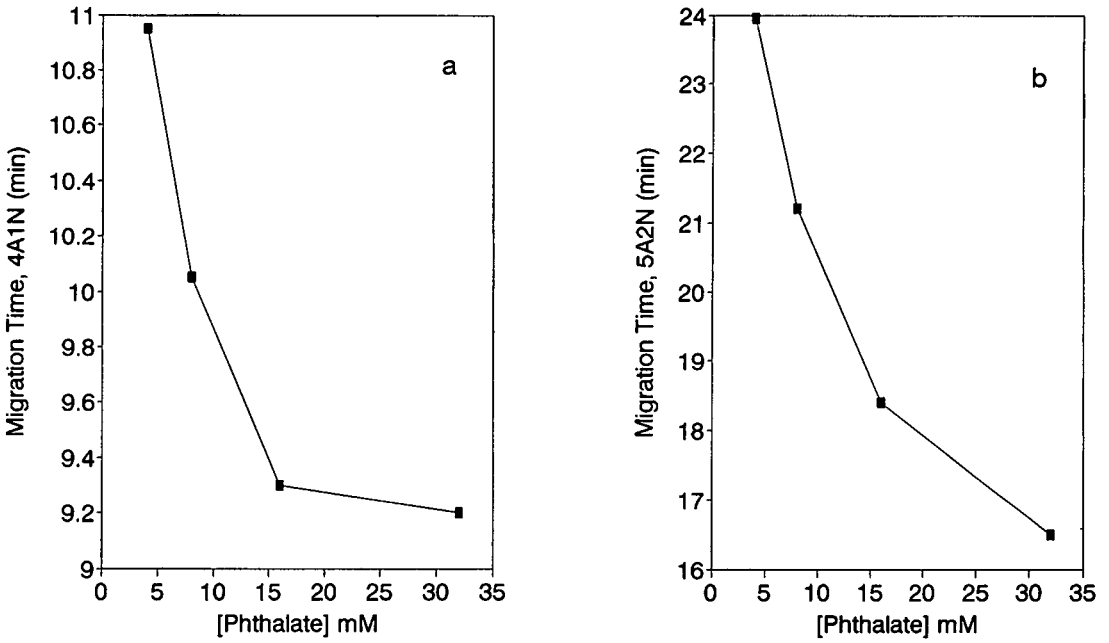

Fig. 2. Dependence of migration times on buffer ion concentration for (a) 4A1N and (b) 5A2N. Buffer conditions are the same as in Fig. 1.

increasing electroosmotic flow. A maximum in flow-rate is reached when charge repulsion prevents additional CTAB adsorption and the hydrophobic phase is essentially saturated. With a 10 m*M* phosphate and 10% acetonitrile buffer this maximum was reached in the range of 20 μM CTAB. With no organic solvent in the mobile phase the saturation point would be expected to be even lower.

In our system we used a CTAB concentration of 400 μM to ensure that the walls of the capillary were saturated. The net effect, therefore, of an increase in buffer ion concentration should be a decrease in migration time of the sample ions. This was confirmed in our experiments as shown in Fig. 2. Another interesting result is that 4A1N, the least retained compound, showed very little change in retention at the highest concentration of buffer ion. This is because this compound is only slightly retained at the high buffer ion concentrations. Therefore, its migration time depends almost entirely upon its mobility as in zone electrophoresis. 5A2N, on the other hand, showed a decrease in retention at all buffer ion concentrations.

In addition to the cation-exchange sites, there will also be reversed-phase character to this column due to the hydrophobic nature of the polymeric-film coating. This reversed-phase character can be examined by adding an organic component, acetonitrile, to the mobile phase and observing its effect on the migration times in the absence of CTAB.

Fujiwara and Honda [21] have shown that the addition of acetonitrile to a CZE buffer can increase the velocity of electroosmotic flow by almost 30%. We expect that the addition of acetonitrile will decrease the migration times of non-retained compounds by the increase in flow-rate, and decrease the migration times of retained compounds by an even larger amount, due to the decrease in retention. As seen from Fig. 3, the addition of acetonitrile to our system did have the predicted effect on the migration times of these species. In our experiment the retention time of 4A1N decreased about 40%, indicating that there is some reversed-phase retention of this compound. The 5A2N migration time decreased about 200%, indicating that this compound has a strong reversed-phase component.

Because the amount of organic modifier added to the system also affects the adsorption of CTAB to

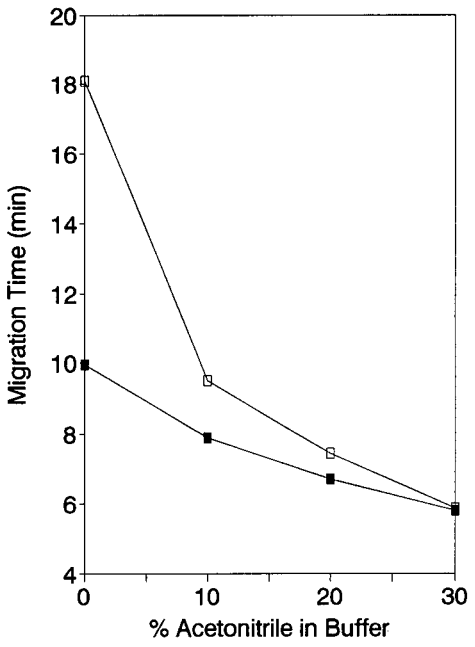

Fig. 3. Dependence of migration times on the concentration of organic modifier. Buffer conditions: 32 m*M* potassium phthalate, pH 7.0, no CTAB. (□) 4A1N; (■) 5A2N.

the surface of the capillary, this could be an additional way to adjust retention in this system. The contribution of these two retention mechanisms to the separation can be estimated by noting the dependence of migration times on the concentration of the ion-exchange sites on the surface of the column. As noted before, as the CTAB concentration increases the velocity of electroosmotic flow also increases, up to the point of saturation of the column wall with the CTAB molecules. The addition of CTAB would, therefore, shield reversed-phase sites on the column up to the point of saturation. A compound with a stronger reversed-phase component would have a decreased migration time with an increase in CTAB concentration, while a compound with a stronger ion-exchange component would be expected to have an increased migration time as the number of ion-exchange sites increased.

Fig. 4 shows the effect of CTAB concentration on the migration times of 4A1N and 5A2N. The compound with the strongest reversed-phase component, 5A2N, did show a decrease in retention as the CTAB was increased. The 4A1N migration time, however, shows a sharp increase between 50 and 100 μM CTAB, and then slowly increases as the CTAB concentration is increased further. The diminished effect of further addition of CTAB can be explained by the saturation of CTAB on the walls of the column. 4A1N, therefore, has a stronger ion-exchange component, while 5A2N has a stronger reversed-phase component.

In summary, we have shown that manipulation of the surface of a capillary electrophoresis column can add selectivity to separations. The retention of the sample ions can be varied in this system by changing the concentration of the buffer ion, the addition of an organic modifier, and by changing the concentration of the IIR. The mechanism described here is complementary to that of ion pairing [7] in our

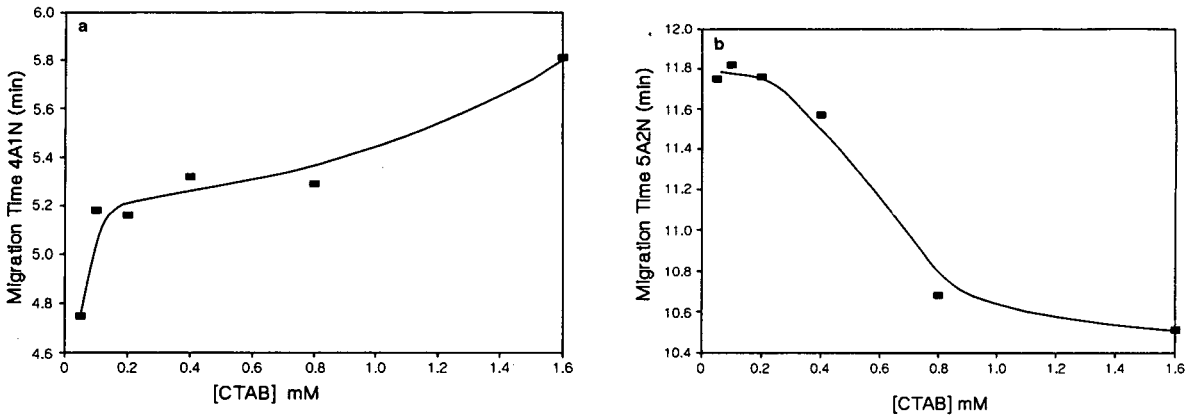

Fig. 4. Dependence of migration times on the CTAB concentration for (a) 4A1N and (b) 5A2N. Buffer conditions: 8 m*M* potassium phthalate, CTAB as noted, pH 7.0.

earlier work for the same analytes. The addition of the dynamic ion-exchange mode to electrochromatography extends it use while adding flexibility. The system can be converted back to the reversed-phase mode by simply washing the column with a less polar mobile phase, which removes the IIR adsorbed to the hydrobic surface.

ACKNOWLEDGEMENTS

Ames Laboratory is operated for the US Department of Energy by Iowa State University under Contract No. W-7405-Eng-82. This work was supported by the Director of Energy Research, Office of Basic Energy Sciences, Division of Chemical Sciences.

REFERENCES

1 J. W. Jorgenson and K. D. Lukacs, *J. Chromatogr.*, 218 (1981) 209.
2 W. G. Kuhr and E. S. Yeung, *Anal. Chem.*, 60 (1988) 1832.
3 Y. Cheng and N. J. Dovichi, *Science*, 242 (1988) 562.
4 X. Huang, J. A. Luckey, M. J. Gordon and R. N. Zare, *Anal. Chem.*, 61 (1989) 66.
5 R. Takigiku and R. E. Schneider, *J. Chromatogr.*, 559 (1991) 247.
6 S. Terabe and T. Isemura, *Anal. Chem.*, 62 (1990) 650.
7 W. D. Pfeffer and E. S. Yeung, *J. Chromatogr.*, 557 (1991) 125.
8 M. L. Bieganowska, A. Petruczynik and M. Gadzikowska, *J. Chromatogr.*, 520 (1990) 403.
9 I. Molnar, H. Knauer and D. Wilk, *J. Chromatogr.*, 201 (1980) 225.
10 T. Takeuchi and E. S. Yeung, *J. Chromatogr.*, 370 (1986) 83.
11 F. F. Cantwell and S. Puon, *Anal. Chem.*, 51 (1979) 623.
12 Z. Iskandarani and D. J. Pietrzyk, *Anal. Chem.*, 54 (1982) 1065.
13 J. Inczedy and F. Szokoli. *J. Chromatogr.*, 508 (1990) 309.
14 H. Small, *Ion Chromatography*, Plenum Press, New York, 1989.
15 W. D. Pfeffer and E. S. Yeung, *J. Chromatogr.*, 506 (1990) 401.
16 T. W. Garner and E. S. Yeung, *Anal. Chem.*, 62 (1990) 2193.
17 P. R. Dluzenski and J. W. Jorgenson, *J. High Resolut. Chromatogr. Chromatogr. Commun.*, 11 (1988) 332.
18 W. D. Pfeffer and E. S. Yeung, *Anal. Chem.*, 62 (1990) 2178.
19 P. C. Hiemenz, *Principles of Colloid and Surface Chemistry*, Marcel Dekker, New York, 1986.
20 T. Tsuda, *J. High Resolut. Chromatogr. Chromatogr. Commun.*, 10 (1987) 622.
21 S. Fujiwara and S. Honda, *Anal. Chem.*, 59 (1987) 487.

Journal of Chromatography, 640 (1993) 403–412
Elsevier Science Publishers B.V., Amsterdam

CHROMSYMP. 2727

Capillary ion electrophoresis, an environmental method for the determination of anions in water

Joseph P. Romano* and Jim Krol

Waters Chromatography Division of Millipore, 34 Maple Street, Milford, MA 01757 (USA)

ABSTRACT

Capillary ion electrophoresis has recently been introduced as a new separations technique for the analysis of inorganic anions. Among its many attributes are rapid, highly efficient separations with different selectivities (compared to ion chromatography), simplicity, and economy.

This paper demonstrates the ability of capillary ion electrophoresis to analyze primary and secondary anionic contaminants as well as other ions of environmental concern in drinking water, groundwater, and wastewater. Analysis time is less than five minutes. A comparison of the data to ion chromatography shows excellent correlation.

INTRODUCTION

The United States Environmental Protection Agency (EPA) has established analytical methods for inorganic contaminants using ion chromatography (IC) [1]. However, there is an emerging technology that offers considerable advantages. Capillary ion electrophoresis (CIE) (Waters' trade name: Capillary Ion Analysis, CIA) offers significant improvement over IC in efficiency and analysis time. The unique selectivity of CIE provides an alternative solution to coelution problems that occur with IC in real samples [2].

CIE has recently been introduced as a new separation technique for the analysis of inorganic and organic ions [3]. CIE is a branch of capillary electrophoresis (CE) which is optimized for the rapid analysis of low-molecular-mass anions and cations. It separates ions according to their mobility in electrolytic solutions [4–7]. The technique has been successfully applied to the analysis of a variety of anionic solutes in several complex sample matrices [8,9].

CE instrumentation has few moving parts and uses a low cost, easily replaceable open tubular capillary instead of packed chromatography column. No equilibration time is required for the capillary. Simply fill the capillary with electrolyte and run. Sample preparation is minimal because there is no chromatography column to be protected from extraneous materials in the sample. Analyses are completed in less than five minutes.

The scale of electrolyte consumption is at least an order of magnitude smaller than liquid or ion chromatography eluent consumption. High sensitivity is achieved while analyzing only nanoliters of sample, using only a few microliters of electrolyte in the capillary. This ability to analyze complex samples without producing any significant volume of additional waste has caught the attention of analysts who are becoming involved in the mixed waste program.

In this paper a test method using CIE has been developed for the analysis of anions in aqueous matrices. The test method was applied to samples of drinking water, groundwater, and wastewater for the analysis of bromide, chloride, fluoride, nitrate, nitrite, phosphate, and sulfate. The results obtained are compared to data from the same samples analyzed by IC.

* Corresponding author.

0021-9673/93/$06.00

EXPERIMENTAL

Instrumentation

The capillary electrophoresis system employed was the Waters (Waters Chromatography Division of Millipore, Milford, MA, USA) Quanta 4000. The configuration for performing anion analysis included a negative power supply (0–30 kV), a mercury lamp for indirect UV detection at 254 nm, and a Waters Accu-Sep polyimide-coated fused-silica capillary (60 cm × 75 μm I.D.). A hydrostatic sample injection mode (10 cm for 30 s) was used in this work. Data acquisition was performed with a Waters 860 data station. Detector time constant was set at 0.1 s and data acquisition rate was 20 points/s.

The ion chromatograph used in this study was a Waters Action Analyzer with a 700 WISP Satelite auto sampler and a Model 431 conductivity detector. The Waters 860 data station was also employed for data acquisition. The data acquisition rate was 1 point/s. The analytical column used was a Waters IC-Pak Anion HC (150 × 4.6 mm I.D.) methacrylate-based anion exchanger.

Reagents

Water (18 MΩ) (Millipore, Bedford, MA, USA) was used to prepare all solutions. The chromate electrolyte was prepared from a concentrate containing 100 m*M* sodium chromate tetrahydrate (Malinkrodt, Paris, KY, USA; analytical-reagent grade) and 0.0056 m*M* sulfuric acid (J. T. Baker, Phillipsburg, NJ, USA; Ultrex grade) Electroosmotic flow (EOF) modifer for reversal of the direction of EOF was a 20 m*M* concentrate (CIA-Pak OFM anion BT) obtained from Waters. The working electrolyte consisted of 4 m*M* chromate–0.3 m*M* OFM anion BT, pH 8.1. CIA methods are covered under U.S. Patents: 5 104 506 and 5 128 055.

When using the Waters MilliTrap H^+ membrane cartridge the modified borate–gluconate eluent is recommended [10]. The eluent was prepared from analytical-grade chemicals, boric acid, gluconic acid, and lithium hydroxide monohydrate obtained from Aldrich, Milwaukee, WI, USA. Glycerin and HPLC-grade acetonitrile were of obtained from J. T. Baker. Eluents and working electrolytes were prepared fresh daily, filtered and degassed with a Millipore solvent clarification kit prior to use.

The standard mixtures were prepared by diluting 1000 ppm stock solutions containing a single anion. Particulates from samples were removed with disposable prerinsed Millex-GV 0.22 μm filters (Millipore). The samples were diluted with water or run neat.

RESULTS AND DISCUSSION

Anion analysis

In CIE, a free zone separation occurs as the ions migrate according to their mobility in the carrier electrolyte when an electric field is applied through the capillary. The electrolyte co-ion is selected to have a different UV absorbance but similar mobility to the analytes of interest to permit differential UV detection with optimal peak symmetry. Detection sensitivity can be maximized by selecting a background ion that has both maximum molar absorptivity and matching ionic mobility [6]. For anion analysis an electroosmotic flow modifier (OFM) is added to the electrolyte to ensure the bulk flow of the electrolyte, electroosmotic flow (EOF), is directed towards the detector. Anions move in the same direction as the EOF towards the anode or co-EOF. This increases the net velocity of the anions through the capillary and creates a fast separation. Water from the sample has no net charge and therefore migrates in the same direction at the rate of the EOF. Note that cations such as those found in groundwater samples (sodium, potassium, calcium, and magnesium) migrate in the opposite direction (counter-EOF) towards the cathode.

Electropherogram is the proper name to describe the chart generated by CIE although the separation does resemble a chromatogram. The analytes each have a migration time which is the time it takes the analyte to migrate from the point of injection to the detector portion of the capillary. Identification and quantitation is performed by an external standard. Fig. 1 shows the separation of a seven-anion standard by CIE consisting of inorganic anions commonly monitored in water. The concentration of each anion in the standard is in the low ppm range. Due to the different separation mechanism of CIE, bromide is the first to migrate followed by chloride, sulfate, nitrite, nitrate, fluoride, and phosphate. The analysis time is under 5 min.

Peak shape is optimized by closely matching the mobility of the carrier electrolyte ions with that of

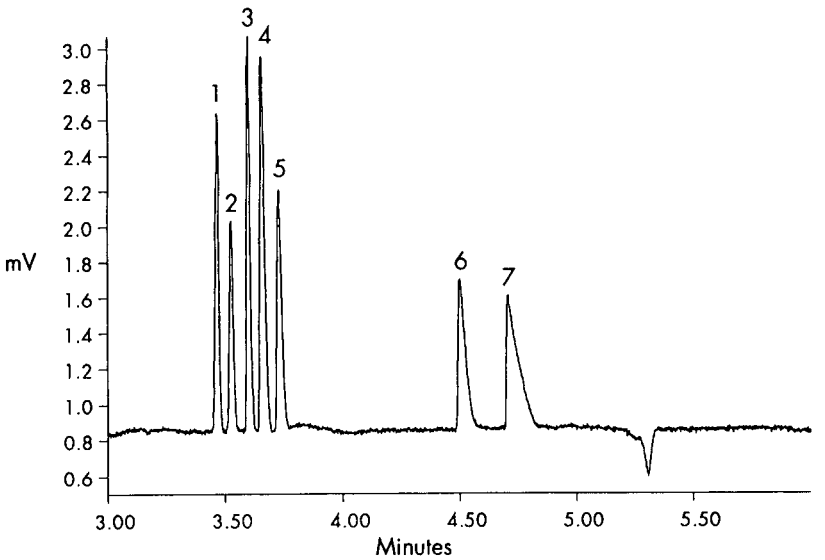

Fig. 1. Electropherogram of seven-anion standard. CIE test method conditions: Fused-silica 60 cm × 75 μm I.D. capillary; voltage 15 kV (negative); 4 m*M* chromate–0.3 m*M* CIA-Pak OFM Anion BT (patented) at pH 8.1; indirect UV detection at 254 nm; hydrostatic injection (30 s at 10 cm). Peaks: 1 = bromide (4 ppm); 2 = chloride (2 ppm); 3 = sulfate; (4 ppm); 4 = nitrite (4 ppm); 5 = nitrate (4 ppm); 6 = fluoride (1 ppm); 7 = phosphate (4 ppm).

the analyte ions. When analyte anions have lower mobility than the electrolyte co-ion , the peaks will tail; when the analyte ion mobility is higher, the peaks will front [11]. For any set of ionic mobilities, peak asymmetry increases with increasing concentration of the analyte ion in the migrating zone [12].

Selectivity is based on the charge and size of the ion. The greater the charge to mass ratio (more conductive) the faster the analyte migrates. The inherent speed of CIE enables high peak capacity in a very short time frame with separation efficiencies reaching over 500 000 theoretical plates. Electrolyte parameters that can change or optimize selectivity include pH, ionic strength, EOF modifiers, complexing agents, and organic solvents.

Drinking water analysis

The CIE test method was first successfully applied to drinking water Fig. 2 shows the electrophoretic separations of two drinking water samples.The upper electropherogram contains a separation of chloride, sulfate, nitrate, and carbonate of a sample taken from a well. The first three components are well resolved for easy identification and quantitation. Carbonate, a weak acid, exhibits low mobility at the electrolyte pH 8.1 and elutes well after the strong acid anions. At pH 8.1, carbonate exists as bicarbonate (HCO_3^-) and exhibits a gradually increasing mobility (shorter migration time) as the pH of the electrolyte increases. As it converts to its dibasic form (CO_3^{2-}) at pH 12 it migrates just after nitrate [4].

The peak shape of carbonate can be attributed to the electrostacking condition [6,13]. According to the electrostacking condition, the samples zones in hydrostatic injections must have lower ionic strength than the carrier electrolyte. The net effect is an accumulation of sample ions inside a very narrow zone at the sample-carrier electrolyte boundary. This electrostacking occurs before the migration of the analyte ion zone through the bulk of the carrier electrolyte solution. The result is narrow, symmetrical peaks. The excessive amount of carbonate contained in the water samples creates the adverse effect; a broad, asymmetrical peak. A simple solution is to dilute the sample in water (18 MΩ).

The lower electropherogram in Fig. 2 displays a drinking water sample obtained from a household

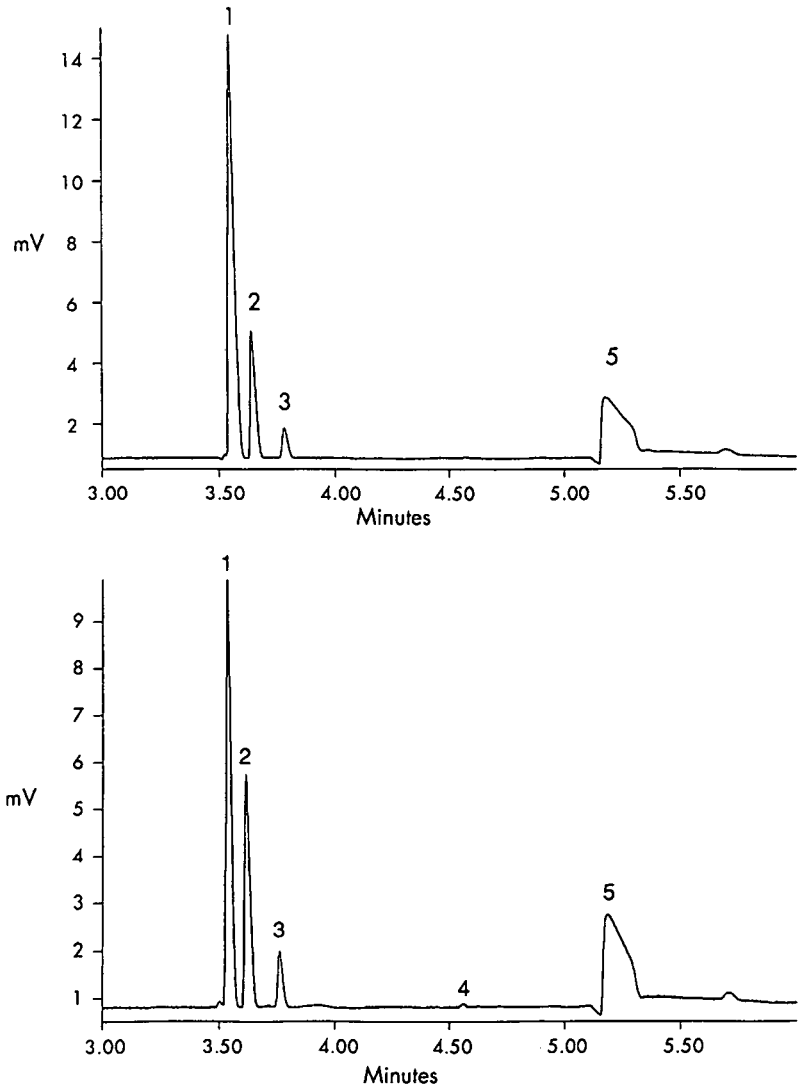

Fig. 2. Analysis of anions in drinking water. Same CIE test method conditions as in Fig. 1. Upper electropherogram: Wellwater neat sample. Peaks: 1 = chloride (36.5 ppm); 2 = sulfate (11.4 ppm); 3 = nitrate (3.2 ppm); 5 = carbonate (not quantitated). Lower electropherogram: Tapwater neat sample. Peaks: 1 = chloride (20.0 ppm); 2 = sulfate (14.1 ppm); 3 = nitrate (3.5 ppm); 4 = fluoride (0.06 ppm); 5 = carbonate (not quantitated).

tap. Four components of interest were found along with ubiquitous carbonate. Note the high sensitivity for fluoride and its migration time. Using an IC anion-exchange column, early eluting fluoride is found close to the void volume that contains cations, neutral species and the classic water dip. This can make detection and quantitation of fluoride difficult. With CIE, fluoride migrates in the latter portion of the electropherogram well resolved from any other components. High sensitivity for fluoride is achieved due to the "lightness" of the ion. Principles of differential UV detection revolve around displacement of the electrolyte co-ion in this case chromate. when the analyte ions are UV transparent. It

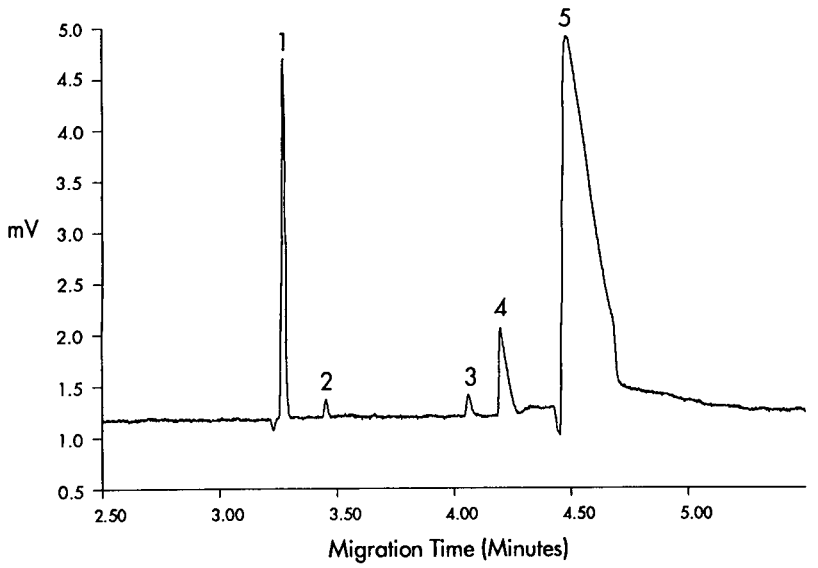

Fig. 3. Electropherogram of EPA groundwater sample No. 1. Same CIE test method conditions. The sample was diluted 1:10 with water. Original sample concentrations reported. Peaks: 1 = chloride (50.3 ppm); 2 = nitrate (4.4 ppm); 3 = fluoride (1.8 ppm); 4 = phosphate (26.1 ppm); 5 = carbonate (not quantitated).

takes two monovalent fluoride (F^-) ions to displace one divalent chromate (CrO_4^{2-}) ion. Since fluoride is a "light" ion there are more molecules per unit of concentration placed into the capillary. For example using the atomic masses of fluoride (18.9) and chloride (35.5), 1 ppm of fluoride = 0.05 mequiv./l and 1 ppm of chloride = 0.03 mequiv./l. Therefore mass to mass, fluoride generates a greater response than chloride.

Groundwater analysis

The characteristics of CIE are extremely advantageous for the analysis of anions in groundwater. An example of the power of this technique is demonstrated by the analysis of groundwater samples taken by the EPA from a hazardous waste site. Figs. 3–5 show electropherograms of groundwater samples taken from different locations at the site.

EPA groundwater sample No. 1 (Fig. 3) displays the separation of four anions of interest, chloride, nitrate, fluoride, and phosphate, in the presence of an excessive level of carbonate. Due to the unique selectivity of CIE, the large amount of carbonate does not interfere with the analysis. Cations contained in the sample do not participate in the separation. The water peak is not seen in the separation because it does not reach the detector until 8 min. These features make identification and quantitation of anions in groundwater easy and simple. Sample preparation simply involved diluting the sample in deionized water and filtration to remove particules.

The electropherogram of EPA groundwater sample No. 2 (Fig. 4) shows an expanded view of a separation of anions in a high carbonate sample matrix. Three components of interest, chloride, sulfate, and fluoride, were identified and quantitated. By taking a closer look at the electropherogram, a fluoride peak can easily be distinguished. It is an example of the high sensitivity of CIE in real samples. The solution concentration of fluoride detected is 60 ppb based on a 1:10 dilution of the sample. This amount of fluoride would be impossible to detect in the analysis of this groundwater sample by IC. It is a classic example of coelution problems that exist under normal isocratic IC conditions as described earlier.

Fig. 5 demonstrates the ability of CIE to detect anions of interest in EPA groundwater sample No. 3 in the presence of high sulfate. The sample was

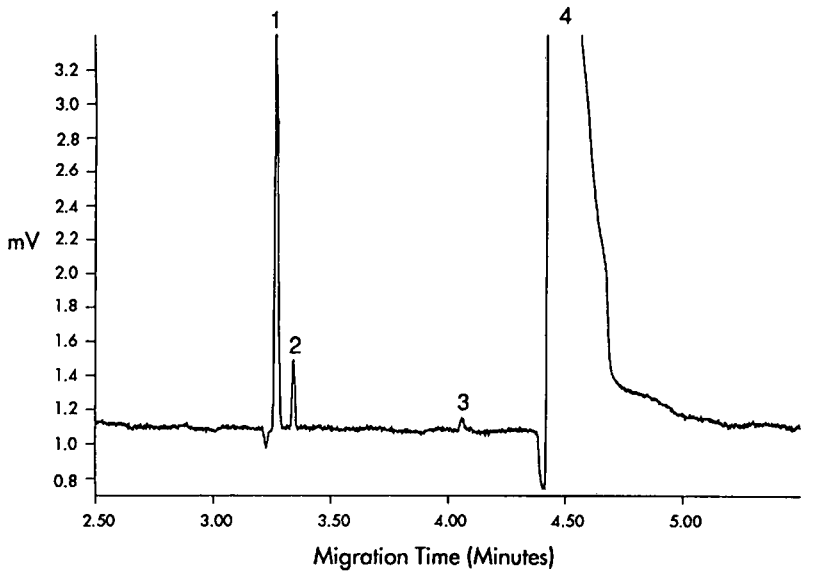

Fig. 4. Expanded view of the electropherogram of EPA groundwater sample No. 2. Same CIE test method conditions. The sample was diltued 1:10, with water. Original sample concentrations reported. Peaks: 1 = chloride (32.8 ppm); 2 = sulfate (6.1 ppm); 3 = fluoride (0.6 ppm); 4 = carbonate (not quantitated).

diluted 1:1000 to maintain optimum peak shape. A small amount of chloride is separated and detected from a large amount of sulfate. Phosphate was also identified in the sample. The solution concentrations displayed in the electropherogram for chloride and phosphate are 271 ppb and 330 ppb, respectively.

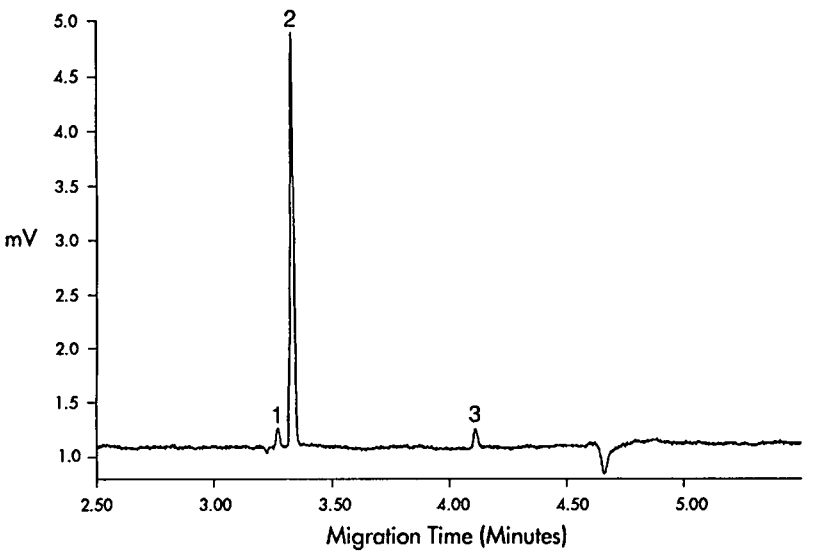

Fig. 5. Electropherogram of EPA groundwater sample No. 3. Same CIE test method conditions. The sample was diluted 1:1000 with water. Original sample concentrations reported. Peaks: 1 = chloride (271.0 ppm); 2 = sulfate (8165.8 ppm); 3 = phosphate (330.3 ppm).

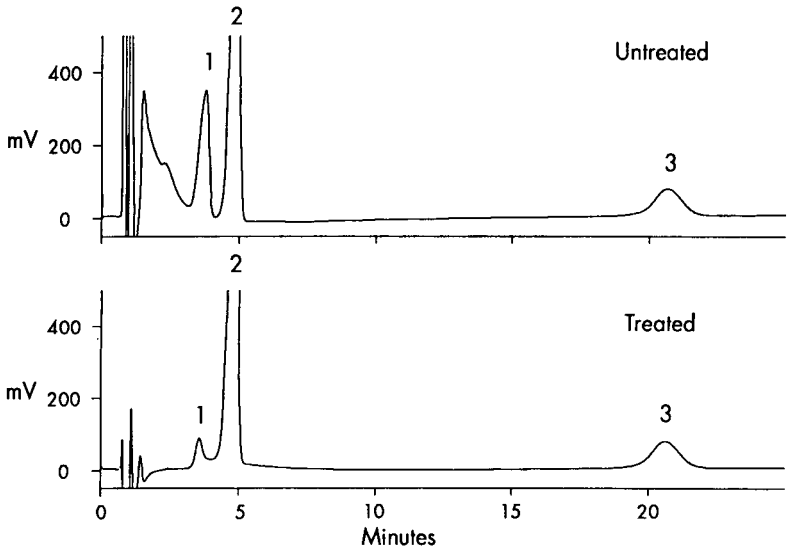

Fig. 6. Anion analysis of industrial wastewater by ion chromatography using Waters Method A-1000. Conditions, column: Waters IC-Pak Anion HC, eluent: modified borate–gluconate, flow-rate: 2.0 ml/min, detection: conductivity. Upper chromatogram; untreated wastewater sample. Lower chromatogram; same wastewater sample after treatment with Waters Millitrap H^+ membrane cartridge. Peaks: 1 = carbonate (not quantitated); 2 = chloride (83.2 ppm); 3 = sulfate (23.8 ppm).

Wastewater analysis

The selectivity for anion separations using CIE differs significantly from that obtained using conventional anion-exchange columns in IC, where retention is largely a function of valence state or affinity to the anion-exchange sites. In IC, fluoride elutes first followed by the monovalents chloride, nitrite, bromide and nitrate, then the divalents hydrogenphosphate and sulfate. Analysis time typically ranges from 10 to 20 min. An example of the selectivity of IC is demonstrated by the analysis of an industrial wastewater sample using Waters Method A-1000: conductivity detection of anions using single column ion chromatography [10]. The upper chromatogram in Fig. 6 contains the separation of the untreated wastewater sample. With an anion-exchange separation; cations, neutral organic species, and water; all elute at the void volume of the column. Short-chained monocarboxylic acids and weakly retained anions, such as fluoride and methanesulfonate, are all eluted early and tend to be poorly resolved in many instances. The presence of elevated carbonate and/or high levels of sample cations may further complicate the early portion of the chromatogram. The use of gradient or coupled IC systems can often overcome these resolution problems. However, both of these approaches are more complex than simple isocratic methods.

Another possible solution is sample pre-treatment, that is removal of interferences before analysis. The lower chromatogram in Fig. 6 represents the separation of the same wastewater sample after passing it through a Millitrap H^+ membrane cartridge. The sample preparation device removes cations, reduces the amount of carbonate and neutralizes high pH samples. This "cleans up" the early portion of the chromatogram allowing better detection and quantitation of the anions of interest. In this sample chloride and sulfate were identified.

Anion analysis of wastewater using CIE exhibits several significant advantages. First, the cations migrate in the opposite direction so they do not interfere in the separation. Second, the strong acid anions (inorganics) *i.e.*, bromide, chloride, sulfate, nitrite, nitrate, fluoride, and phosphate, have high charge-to-ionic radii ratios so they are the first to migrate through the capillary. Third, organic acids commonly found in wastewater such as formate, ace-

tate, and propionate migrate later and are significanly removed form their migration time band. Since their pK_a values range from 3 to 5, they are fully ionized at pH 8.1. However, the organic acids have a smaller charge to mass ratio (less conductive) and therefore lower mobility. Fourth, carbonate also a weak acid, migrates among the short chain carboxylic acids. Fifth, neutral components like water, are carried along by the EOF and have appreciably longer migration times. Since the capillary is an open tube, the analysis is complete when the last peak of interest passes through the detector. The remaining slower migrating anions and neutral species can be simply purged from the capillary with an automated vacuum purge once the desired separation is obtained. This also refills the capillary with fresh electrolyte for the next sample. Thus analysis times are typically less than five minutes.

These attributes are confirmed from the analysis of the same "untreated" industrial wastewater sample by CIE. Fig. 7 contains an expanded view of the electrophoretic separation identifying chloride and sulfate at the same concentrations determined by IC in Fig. 6. Taking a closer look at the electropherogram, a fluoride peak is easily detected and quantitated. Fluoride was not detected in the wastewater sample by IC even after sample pre-treatment with a Millitrap membrane cartridge.

Analysis of a power plant wastewater effluent by CIE is described in Fig. 8. Chloride, sulfate, and nitrate were detected in the presence of carbonate. Based on a 1:10 dilution of the sample the nitrate peak represents a solution concentration of 220 ppb.

Under the electrophoretic conditions described in his study, the capillary electrophoresis system displays linearity over three orders of magnitude. The reproducibility of the system is excellent. The % relative standard deviation (R.S.D.) of migration times from 15 consecutive hydrostatic injections of a seven-anion standard is less than 0.5%. The R.S.D. of peak areas from 4 consecutive hydrostatic injections of a seven-anion standard is less than 1.4%.

Comparison of the data

Four water samples were analyzed by both IC and CIE. The results are summarized in Table I. Columns 2 and 3 contain the original concentrations in ppm of each anion detected in the samples by IC and CIE, respectively. The concentrations for

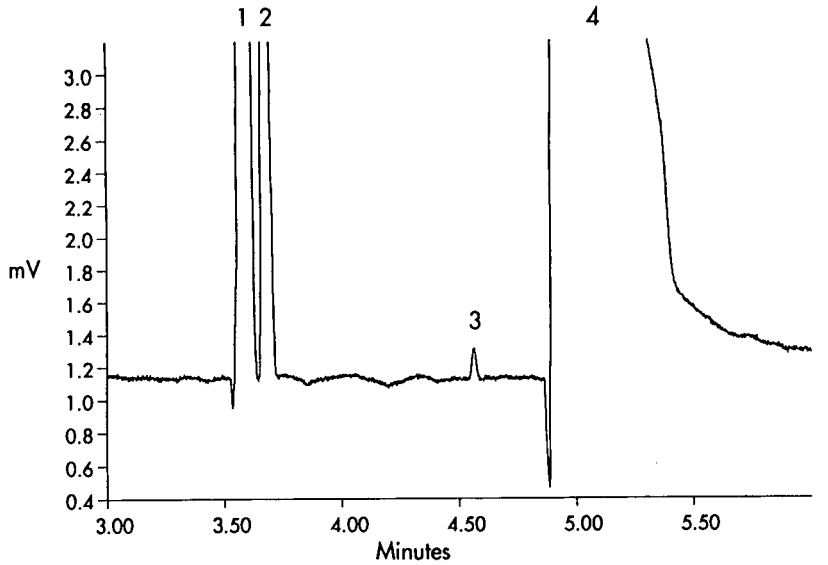

Fig. 7. Anion analysis of industrial wastewater by CIE. Same CIE test method conditions. Electropherogram of the same untreated wastewater sample described in Fig. 6. Peaks: 1 = chloride (83.0 ppm); 2 = sulfate (23.1 ppm); 3 = fluoride (0.13 ppm); 4 = carbonate (not quantitated).

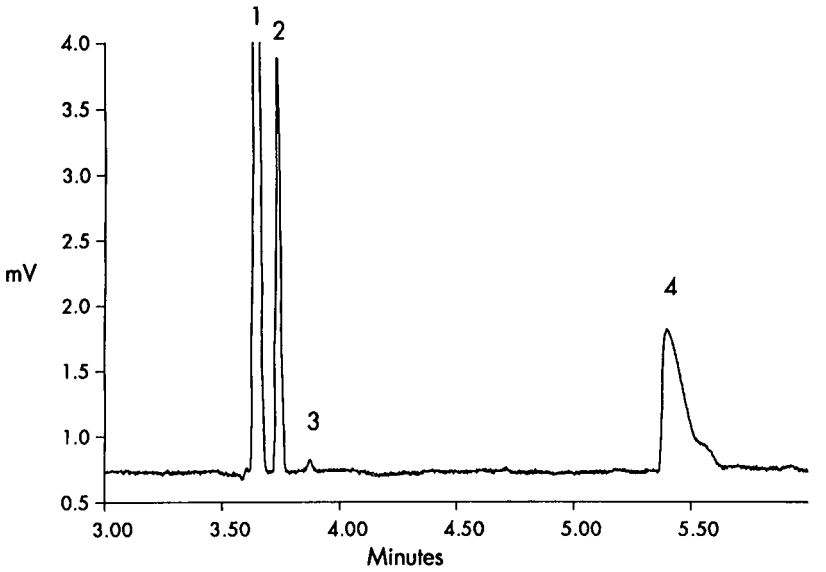

Fig. 8. Electropherogram of power plant wastewater effluent. Same CIE test method conditions. Sample was diluted 1:10 with water. Original sample concentrations reported. Peaks: 1 = chloride (199.8 ppm); 2 = sulfate (76.8 ppm); 3 = nitrate (2.2 ppm); 4 = carbonate (not quantitated).

chloride, sulfate, and nitrate determined by both analytical techniques show excellent correlation. Column 4 displays a simple ratio calculated by taking the CIE concentration in column 2 and dividing it by the corresponding IC concentration in column 2. A value of 1.000 is the ideal number. The actual ratios ranged from 0.937 to 1.041. Note that fluoride detected in two of the samples by CIE was not detected by the IC method.

TABLE I

DATA COMPARISON OF 4 WATER SAMPLES

	IC (ppm)	CIE (ppm)	CIE/IC
Tapwater			
Chloride	20.222	20.035	0.991
Sulfate	14.772	14.044	0.951
Nitrate	3.551	3.531	0.994
Fluoride	Not detected	0.062	–
Wellwater			
Chloride	37.650	36.476	0.969
Sulfate	11.951	11.432	0.956
Nitrate	3.165	3.179	1.004
Industrial wastewater			
Chloride	83.148	83.025	0.998
Sulfate	23.831	23.065	0.967
Fluoride	Not detected	0.132	–
Power plant wastewater			
Chloride	191.834	199.768	1.041
Sulfate	79.882	76.748	0.961
Nitrate	2.384	2.231	0.937

CONCLUSIONS

Capillary ion electrophoresis is a powerful separation technique which offers many advantages for the analysis of inorganic and organic acid anions in aqueous matrices. Rapid, highly efficient separations with different selectivities compared to ion chromatography are obtained. The matrix independent separation requires minimal sample preparation. Only nanoliters of sample volume and small amounts of electrolyte are needed to perform the analysis. This low reagent consumption minimizes the waste that is produced. The instrumentation is simple with low maintenance and very economical to operate. More important the capillary is not a chemical product and is a fraction of the cost of an IC column.

Due to these attributes, this new environmental method has been submitted to the ASTM committee D-19 on Water and subcommittee D19.05 on Inorganics in Water for review. Further investiga-

tion of CIE for environmental analysis is proceeding.

REFERENCES

1 J. P. Romano and J. Krol, *J. Chromatogr.*, 602 (1992) 205.
2 J. P. Romano, P. Jandik, W. R. Jones and P. E. Jackson, *J. Chromatogr.*, 546 (1991 411.
3 W. R. Jones and P. Jandik, *Am. Lab*, 22 No. 9 (1990) 51.
4 W. R. Jones and P. Jandik, *J. Chromatogr.*, 546 (1991) 445.
5 W. R. Jones and P. Jandik and R. Pfeifer, Am. Lab, 23, No. 8 (1991) 40.
6 P. Jandik, W. R. Jones, A. Weston and P. R. Brown, *LC · GC*, 9 (1991) 634.
7 A. Weston, P. R. Brown, P. Jandik, W. R. Jones and A. Heckenberg, *J. Chromatogr.*, 593 (1992) 289.
8 D. R. Salomon and J. Romano, *J. Chromatogr.*, 602 (1992) 219.
9 W. R. Jones and P. Jandik, *J. Chromatogr.*, 608 (1992) 385.
10 A. L. Heckenberg, P. G. Alden, B. J. Wildman, J. Krol, J. P. Romano, P. E. Jackson, P. Jandik and W. R. Jones, *Waters Innovavtive Methods for Ion Analysis, Rev. 2.0*, Millipore Corp., Milford, MA, 1991.
11 F. E. P. Mikkers, F. M. Everaerts and T. P. M. Verheggen, *J. Chromatogr.*, 169 (1979) 1.
12 S. Hjérten, *Electrophoresis*, 11 (1990) 665.
13 P. Gebauer, W. Thormann and P. Boček, *J. Chromatogr.*, 608 (1992) 47.

Journal of Chromatography, 640 (1993) 413–417
Elsevier Science Publishers B.V., Amsterdam

CHROMSYMP. 2740

Capillary zone electrophoresis in the analysis of dyes and other compounds employed in the dye-manufacturing and dye-using industries

Stephen M. Burkinshaw, David Hinks* and David M. Lewis

Department of Colour Chemistry and Dyeing, University of Leeds, Leeds LS2 9JT (UK)

ABSTRACT

High-resolution separation of several dyes and related intermediates, as well as other compounds employed in the dye-manufacturing and dye-using industries, has been achieved using capillary zone electrophoresis (CZE).

The analysis of anionic dyes and some non-coloured anionic intermediates has been achieved using 10 m*M* $Na_2B_4O_7$–40 m*M* sodium dodecyl sulphate (SDS) buffer; high-resolution separations of water soluble anionic, neutral and cationic intermediates were also achieved using this micellar buffer. Micellar electrokinetic capillary chromatography (MECC) has also been developed for the analysis of aqueous insoluble, electrically neutral compounds by incorporating a co-solvent, acetonitrile, into a micellar buffer. In addition, MECC has been used successfully for following all the major steps involved in the synthesis of a disperse dye.

INTRODUCTION

Previous work on the analysis of dyes by capillary electrophoresis (CE) has largely involved separations using conventional aqueous buffers such as phosphate, borate or citrate [1–3]. Although, in general, efficient separations have been achieved, the range of compounds which could be successfully analysed have been limited to charged simple anionic and cationic dyes and some related intermediates. The analysis of most aqueous soluble neutral analytes and all aqueous insoluble compounds is beyond the scope of conventional capillary zone electrophoresis (CZE). Terabe's introduction of micellar electrokinetic capillary chromatography (MECC) [4] enabled aqueous soluble, electrically neutral species to be separated. Only recently has MECC been used for the analysis of dyes [5] and their intermediates.

This paper demonstrates the range of compounds which can be separated using MECC with only two micellar buffer systems. A conventional MECC buffer has been used for the separation of anionic, cationic and neutral species, and also an MECC buffer containing acetonitrile as co-solvent has been used for the separation of aqueous insoluble, neutral compounds.

EXPERIMENTAL

Materials

p-Phenylenediaminesulphonic acid, *m*-phenylenediaminesulphonic acid, orthanilic acid, *m*-nitrobenzenesulphonic acid and *p*-sulphinic acid-phenylacetanilide were supplied by ICI Specialties (Blackley, UK). *m*-Trimethylammoniumaniline and 2-(aminoethyl)pyridinium chloride were prepared by the method described by Evans *et al.* [7]. HPLC-grade acetonitrile was supplied by BDH Chemicals (Poole, UK). All other reagents were analytical grade supplied by BDH Chemicals. All samples were filtered and degassed.

* Corresponding author.

0021-9673/93/$06.00

Analysis

A Dionex capillary electrophoresis system CES1 (Dionex, Sunnyvale, CA, USA) was used for all analyses. Uncoated silica capillaries were used of internal diameter 75 μm and 60 cm length; the capillary was activated by pressure injection of 0.5 *M* sodium hydroxide solution for 10 min followed by rinsing with deionised water. Sample injection was by gravity: the samples were elevated by 100 mm for 12 s. A voltage of 25 kV was applied for each run with the detector positioned at the cathode and detection was by on-line UV absorbance at 254 nm. Deionised water was used throughout.

RESULTS

Use of MECC in following dye synthesis reactions involving aqueous insoluble compounds

It is important for the dye synthetic chemist to be able to accurately follow how a particular reaction is proceeding. This is often achieved using either high-performance liquid chromatography (HPLC) or thin-layer chromatography (TLC). HPLC is perhaps most commonly used for the separation of charged dyes and intermediates whilst TLC is suited to the analysis of water insoluble dyes such as disperse dyes; TLC, however, generally only provides qualitative information.

CE has been shown to offer higher resolution separations, compared to HPLC, for some dyes and intermediates [2,3], but so far it has only been achieved with charged samples. MECC enables efficient separations of water soluble neutral compounds to be achieved but water insoluble compounds cannot be analysed by conventional MECC. However, by incorporating a co-solvent into the buffer system aqueous insoluble, neutral species have been separated thus enabling the analysis of uncharged water insoluble (disperse) dyes.

The synthesis of a disperse dye (Fig. 1) was followed using MECC; the buffer used was 10 m*M* $Na_2B_4O_7$–50 m*M* H_3BO_3–20 m*M* SDS and 50% (v/v) acetonitrile as co-solvent. All the main reagents used in the reactions were detected (Fig. 2).

This MECC buffer system was unsuitable for the separation of anionically charged dyes as the electro-osmotic flow of buffer was insufficient, due to the presence of acetonitrile, to force the dyes to elute at the cathode. Also, due to the alkaline pH of the buffer (pH 10), the analysis of cationic dyes using this system was also found to be unsuccessful. The separation of cationic dyes usually requires acidic buffer conditions in order to prevent the dyes interacting with the capillary wall [3]; at high pH values the capillary wall is highly dissociated and positively charged dyes appear to have affinity for the negatively charged silanol groups on the interior surface of the capillary wall. Consequently, cationic dyes often exhibit low electrophoretic mobility and poorly resolved separations under alkaline buffer conditions and, due to the alkaline nature of this

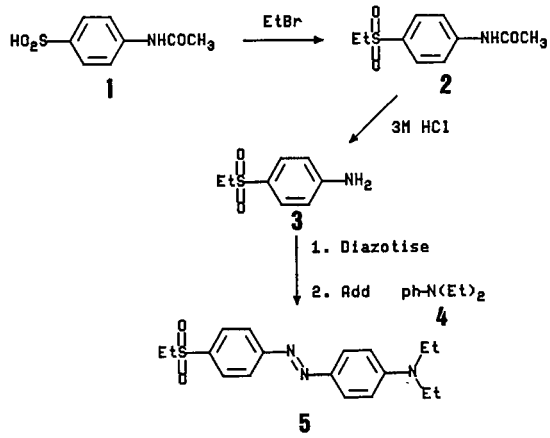

Fig. 1. The synthesis of a disperse dye (**5**).

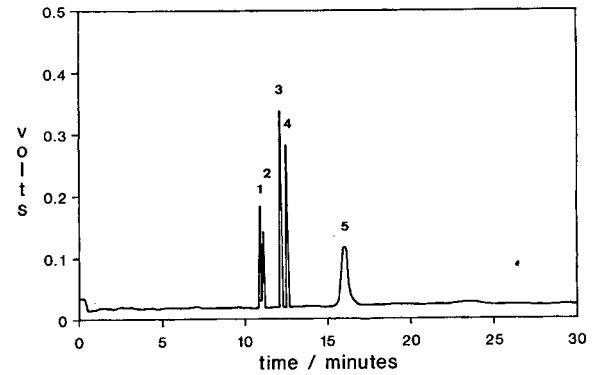

Fig. 2. Separation of the major reagents involved in the synthesis of **5** (shown in Fig. 1) using the following conditions. Buffer: 10 m*M* $Na_2B_4O_7 \cdot 10H_2O$–50 m*M* H_3BO_3–20 m*M* SDS (pH 10) and 50% (v/v) acetonitrile; sample concentration: 10–40 mg dm^{-3}; sample injection: gravity (100 mm for 12 s); voltage: 25 kV; detection (at the cathode): 254 nm; capillary: glass silica 60 cm × 75 μm I.D.

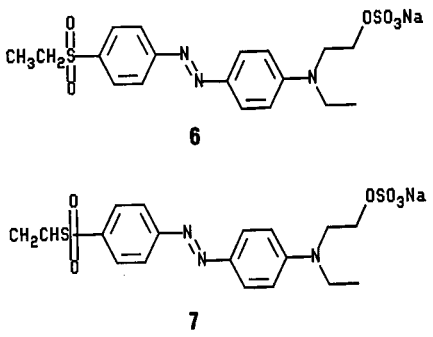

Fig. 3. Molecular structure of two acid dyes.

buffer, no satisfactory separations of cationic dyes were achieved using this system.

Analysis of acid dyes by MECC

Two acid dyes were analysed with similar molecular structure and relative molecular mass (Fig. 3). When a mixture of the dyes was analysed by a conventional buffer (10 m*M* KH_2PO_4, pH 9) the two dyes did not separate (Fig. 4). A micellar buffer system, however, (10 m*M* $Na_2B_4O_7$–40 m*M* SDS) separated the compounds very well (Fig. 5). This improved separation efficiency when using MECC indicates strongly that the technique has potential to be an excellent method of analysis for the dye chemist.

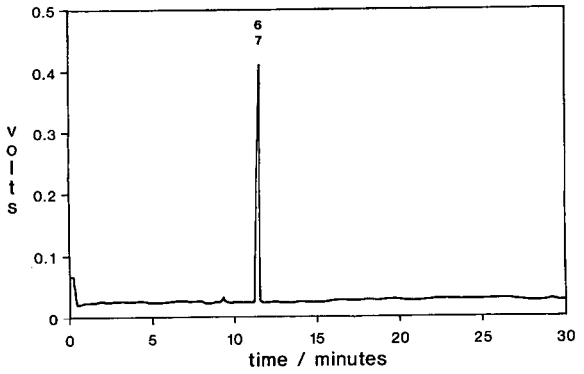

Fig. 4. Separation of two acid dyes (shown in Fig. 3) using conventional CE. The following conditions were employed. Buffer: 10 m*M* KH_2PO_4 (pH 9); sample concentration: 20–50 mg dm^{-3}; sample injection: gravity (100 mm for 12 s); voltage: 25 kV; detection (at the cathode): 254 nm; capillary: glass silica 60 cm × 75 μm I.D.

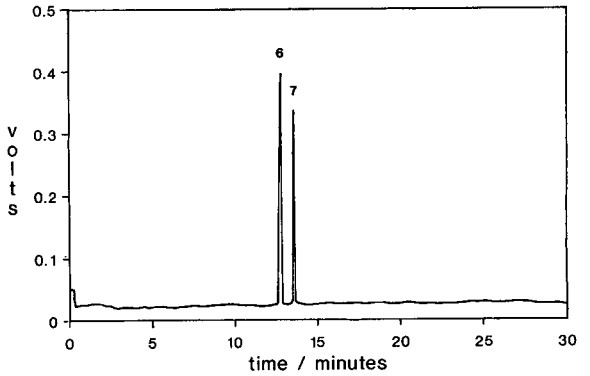

Fig. 5. Separation of two acid dyes (shown in Fig. 3) using MECC. The following conditions were employed. Buffer: 10 m*M* $Na_2B_4O_7 \cdot 10H_2O$–40 m*M* SDS; sample concentration: 30–40 mg dm^{-3}; sample injection: gravity (100 mm for 12 s); voltage: 25 kV; detection (at the cathode): 254 nm; capillary: glass silica 60 cm × 75 μm I.D.

Analysis of dye intermediates by MECC

MECC has been used for the analysis of a number of charged and uncharged, water soluble and water insoluble compounds commonly used in dye synthesis.

Anionic intermediates. Several anionic dye intermediates (Fig. 6) were analysed using 10 m*M* $Na_2B_4O_7$–40 m*M* SDS as buffer (Fig. 7). The two isomers, **8** and **10**, separated exceptionally well.

Cationic intermediates. Four fully cationic compounds (Fig. 8) were separated using 10 m*M* $Na_2B_4O_7$–40 m*M* SDS. Excellent separation was achieved (Fig. 9). The analysis of cationic *dyes*, however, was unsuccessful using this buffer due to

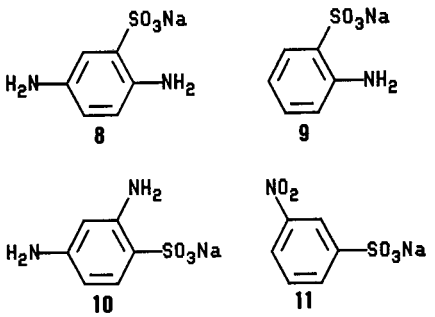

Fig. 6. Molecular structure of four sulphonated dye intermediates.

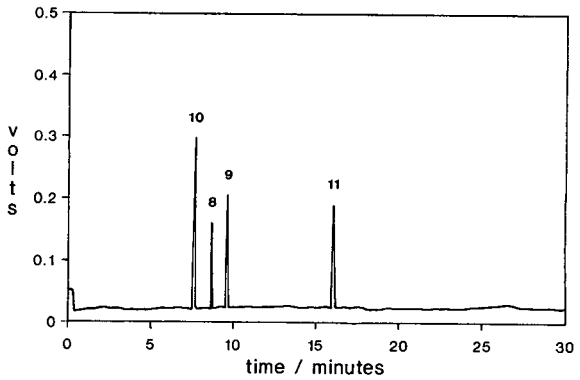

Fig. 7. Separation of anionic dye intermediates (shown in Fig. 6) using MECC. The following conditions were used. Buffer: 10 m*M* $Na_2B_4O_7 \cdot 10H_2O$–40 m*M* SDS; sample concentration: 20–40 mg dm^{-3}; sample injection: gravity (100 mm for 12 s); voltage: 25 kV; detection (at the cathode): 254 nm; capillary: glass silica 60 cm × 75 μm I.D.

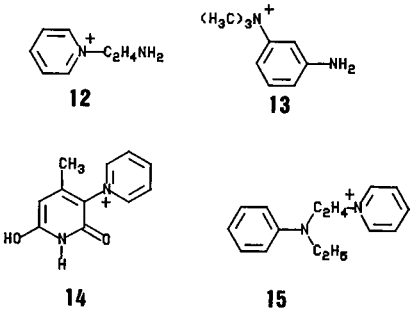

Fig. 8. Molecular structure of four cationic dye intermediates.

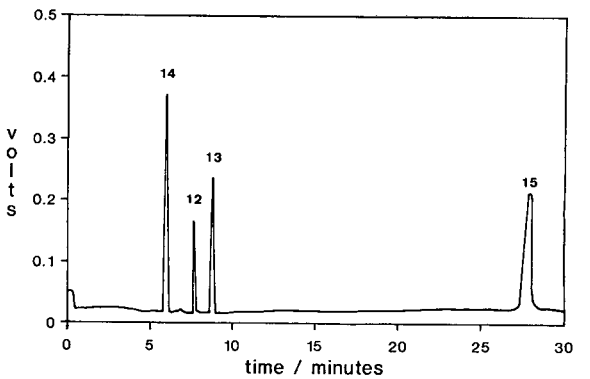

Fig. 9. Separation of cationic dye intermediates (shown in Fig. 8) using MECC. The following conditions were used. Buffer: 10 m*M* $Na_2B_4O_7 \cdot 10H_2O$–40 m*M* SDS; sample concentration: 80–100 mg dm^{-3}; sample injection: gravity (100 mm for 12 s); voltage: 25 kV; detection (at the cathode): 254 nm; capillary: glass silica 60 cm × 75 μm I.D.

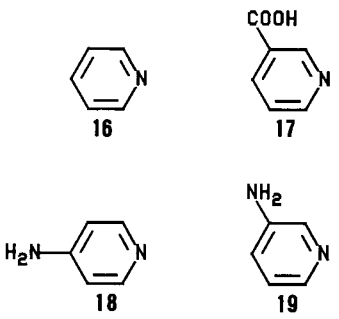

Fig. 10. Molecular structure of four pyridine based, water soluble intermediates.

the alkaline conditions employed (the reasons for this are discussed above).

Neutral, water soluble intermediates. Four pyridine based compounds with no full cationic charge (Fig. 10) were separated by MECC using an identical buffer to that above. Excellent separation was achieved (Fig. 11).

Neutral, water insoluble intermediates. Three aqueous insoluble compounds (Fig. 2) commonly used for the synthesis of disperse dyes were successfully analysed by MECC using 10 m*M* $Na_2B_4O_7 \cdot 10H_2O$–50 m*M* H_3BO_3–20 m*M* SDS and 50% (v/v) acetonitrile. Acetonitrile was required to aid dissolution of the analytes and surfactant was included in the buffer to facilitate separation of the neutral

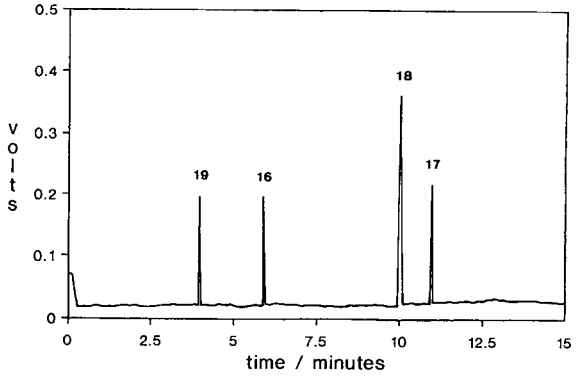

Fig. 11. Separation of four water soluble pyridine based compounds (shown in Fig. 10) using MECC. The following conditions were used. Buffer: 10 m*M* $Na_2B_4O_7 \cdot 10H_2O$–40 m*M* SDS; sample concentration: 50–100 mg dm^{-3}; sample injection: gravity (100 mm for 12 s); voltage: 25 kV; detection (at the cathode): 254 nm; capillary: glass silica 60 cm × 75 μm I.D.

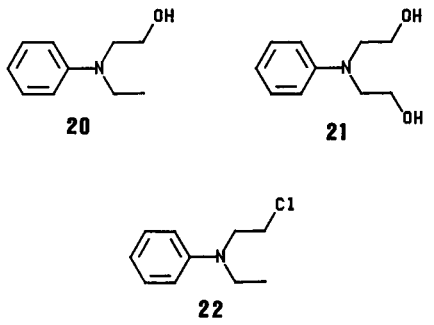

Fig. 12. Molecular structure of four neutral, water insoluble dye intermediates.

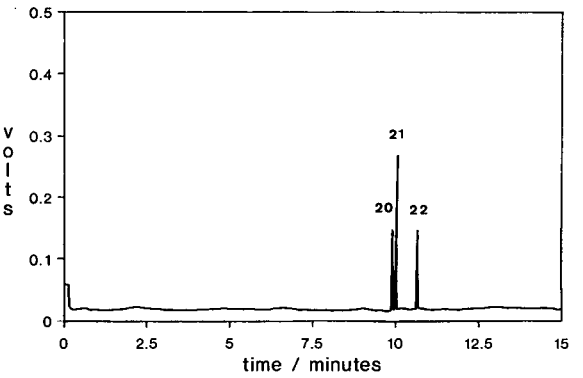

Fig. 13. Separation of three water insoluble dye intermediates (shown in Fig. 12) by MECC. The following conditions were used. Buffer: 10 mM $Na_2B_4O_7 \cdot 10H_2O$–50 mM H_3BO_3–20 mM SDS; sample concentration: 20–30 mg dm^{-3}; sample injection: gravity (100 mm for 12 s); voltage: 25 kV; detection (at the cathode): 254 nm; capillary: glass silica 60 cm × 75 μm I.D.

samples by micellar electrophoresis. The separation, shown in Fig. 13, strongly indicates that this technique can be used for the analysis of water insoluble anilino derivatives used for the synthesis of disperse dyes. Presently these compounds are usually analysed by conventional TLC or HPLC methods.

CONCLUSIONS

Micellar electrokinetic capillary electrophoresis has been used to analyse non-ionic aqueous insoluble compounds by incorporating a co-solvent into a micelle buffer. The synthesis of a non-ionic disperse dye was followed using this technique. MECC has also been used for the successful analysis of a number of charged and uncharged, water soluble and water insoluble dye intermediates. In addition, two almost identical acid dyes, which could not be separated by conventional CE methods, were successfully separated using MECC.

By utilising the various modes of capillary electrophoresis, this technique clearly has potential to be a powerful and diverse analytical method for both the dye-using and dye-manufacturing industries alike.

ACKNOWLEDGEMENTS

The authors would like to acknowledge the financial support of Zeneca Specialties and the Science and Engineering Research Council.

REFERENCES

1 E. D. Lee, W. Mück, J. D. Henion and T. R. Covey, *Biomed. Environm. Mass Spec.*, 18 (1989) 209.
2 S. N. Croft and D. M. Lewis, *Dyes Pigm.*, 18 (1992) 309.
3 S. N. Croft and D. Hinks, *J. Soc. Dyers Colour.*, in press.
4 S. Terabe, *Anal. Chem.*, 56 (1984) 111.
5 G. L. Beaumont and K. P. Evans, *J. Chromatogr.*, 636 (1993) in press.
6 G. E. Evans, J. Shore and C. V. Stead, *J. Soc. Dyers Colour.*, 100 (1984) 285.

Journal of Chromatography, 640 (1993) 419–424
Elsevier Science Publishers B.V., Amsterdam

CHROMSYMP. 2672

Effect of temperature on the salt balance of milk studied by capillary ion electrophoresis

Marc Schmitt*, Franck Saulnier, Luc Malhautier and Guy Linden

Laboratoire de Biochimie Appliquée, Associé à l'Institut National de la Recherche Agronomique, Université de Nancy I, Boulevard des Aiguillettes, BP 239, 54506 Vandoeuvre-les-Nancy Cedex (France)

ABSTRACT

Many inorganic species, such as calcium, phosphate and magnesium, are in equilibrium between the liquid and colloidal phases of milk and hence are of importance with respect to the coagulation properties of milk. Capillary ion electrophoresis makes possible the determination of anions and cations in less than 6 min. The soluble phase of milk was obtained by ultrafiltration and samples had to be diluted 250-fold before analysis. Cold storage increased soluble calcium and phosphate concentrations, and warm-up of the milk restored the initial ionic equilibria. More drastic heat treatments (80–90°C) caused precipitation of tricalcium phosphate and calcium citrate.

INTRODUCTION

The saline components of milk (5–9.5 g/l) consist of many different species which are present as ions, salts or undissociated complexes [1]. The inorganic species are mainly calcium, potassium, magnesium, sodium, chloride and phosphate; citrate is the most important of the organic anions.

Many components, such as chloride, sodium and potassium, are completely soluble whereas others, such as calcium, magnesium, inorganic phosphorus and citrate, are in equilibrium between the liquid and colloidal phases. They take part in the formation of casein micelles and hence can be considered as part of the proteinic structure of milk. Studies on the distribution of mineral species between the liquid and colloidal phases have already been published [2]. Physico-chemical parameters (ionic strength, pH and temperature) influence the equilibrium of milk [3,4].

The saline equilibrium has a direct impact on the coagulation aptitude and cheese-making from milk. For this reason, it is important to study and to control the concentrations of these ions. The dairy industries needs to know the saline equilibria of milk in order to determine the optimum time for starting the production of cheese.

Conventional methods of ion analysis are not convenient; they suffer from many limitations and are materials and/or time consuming. Moreover, milks are now standardized in proteins, calcium and fats.

The recently introduced technique of capillary ion electrophoresis (CIE; Waters trade name Capillary Ion Analysis, CIA) is advantageous for ion analyses. Speed of analysis, reliability and the low cost of use of this method are especially attractive. It allows improvements in the determination of inorganic ions.

The development and evaluation of an effective sample preparation procedure are the first step in the study of the effect of temperature on milk equilibrium, and were the main aim of this work.

EXPERIMENTAL

Materials and reagents

The CIE system used was a Waters–Millipore (Milford, MA, USA) Quanta 4000 with a fused-silica capillary (60 cm × 75 μm) I.D.

* Corresponding author.

0021-9673/93/$06.00

A Model M14011 centrifuge was obtained from Jouan (St. Herblin, France). Ultrafiltration was performed with Millipore (Milford, MA USA) Ultrafee-MC filters with a molecular mass cut-off (MMCO) of 10 000.

CIA-PAK UV Cat-1 reagent and OFM Anion-BT were obtained from Waters-Millipore and sodium chromate tetrahydrate from Aldrich (Milwaukee, WI, USA).

Milk samples

Milk was obtained from a farm near Nancy (France) from the morning milking of a Holstein breed herd. Samples were stored in a cold room at 4°C and heated quickly to the appropriate temperature when required.

Sample preparation

The soluble phase was obtained as follows: 0.5 ml of raw milk was placed in an Ultrafree-MC filter with an MMCO of 10 000 and centrifuged at 3000 *g* for 15 min. The ultrafiltrates obtained were diluted 250-fold with 18-MΩ water.

Ion determination

Ion determinations were performed according to Jandik *et al.* [5]. Injection was hydrostatic (injection volume 10 nl for 30 s) for both anions and cations. For cations, indirect UV detection at 214 nm was used, the electrolyte was 5 m*M* UV-Cat-1–6.5 m*M* α-hydroxyisobutyric acid (HIBA) (a metal ion complexant which improves the separation of cations) (pH 4.4) and the applied voltage was 20 kV. For anions, indirect UV detection at 254 nm was used, the electrolyte was chromate containing OFM Anion-BT and the applied voltage was 20 kV.

RESULTS AND DISCUSSION

Evaluation of the technique

The sample preparation method was optimized to make it simple, rapid and reliable. Three different methods to obtain the soluble phase of milk were tested: dialysis, ultracentrifugation and ultrafiltration [2]. We selected ultrafiltration as it is faster and requires only a centrifuge.

Several commercial filtration systems were tested (Sartorius Centrisart I with MMCO 5000 and 10 000, Millipore Ultrafree-MC with MMCO 5000 and 10 000 and Filtron Microsep with MMCO 3000 and 5000). Ease of use, cost and repeatability of results were the criteria for selection. The Millipore Ultrafree-MC with MMCO 10 000 appeared to be the best compromise for our purposes.

Cations in the ultrafiltrates obtained by centrifugation at different speeds (1000 and 3000 *g*) and for various times (5, 7, 10 and 15 min) were determined by CIE (results not presented). The quality of the ultrafiltrate was not affected by time or speed; its composition remains constant (for a concentration factor lower than fivefold) according to the work of Brulé *et al.* [6]. A sufficient volume of ultrafiltrate (50 μl) was obtained by centrifugation at 3000 *g* for 15 min. Before injection, a 250-fold dilution with 18-mΩ water was made for both anions and cations.

CIE results for calcium (nine samples) were confirmed by atomic absorption spectrometry. The correlation between the two techniques was excellent ($y = -0.1077 + 0.9761x$ with $r = 0.99$; where y is the calcium concentration given by AAS and x by CIE).

Complete sample preparation requires about 20 min. The determination of cations analysis is not affected by anions, and *vice versa*. Moreover, a complete analysis for anions or cations is achieved with just one injection. Conventional methods of ion analysis do not have this advantage.

The electropherograms of milk ultrafiltrates show peaks for potassium, sodium, calcium and magnesium for cations and chloride, sulphate, phosphate and citrate for anions (Fig. 1). Both were obtained in less than 6 min. The flexibility, speed of analysis and efficiency of CIA make it the best method for the determination of ions in milk.

A repeatability study of the CIE method gave relative standard deviations (R.S.D.s) of 5.2%, 6% and 6.9% for sodium, calcium and magnesium respectively. The relatively high values could be improved by a larger dilution of the samples.

The 250-fold dilution leads to slight asymmetry of the peaks owing to an overloading of the capillary. This asymmetry results in a decrease in precision. R.S.D.s better than 3% can be obtained with a larger dilution (results not presented). Concerning anions, the R.S.D.s are good for chlorides (2.7%), owing to the good symmetry of the peak, but the determination of citrate (R.S.D. = 5.7%) and phosphate (R.S.D. = 4.5%) is less precise owing to

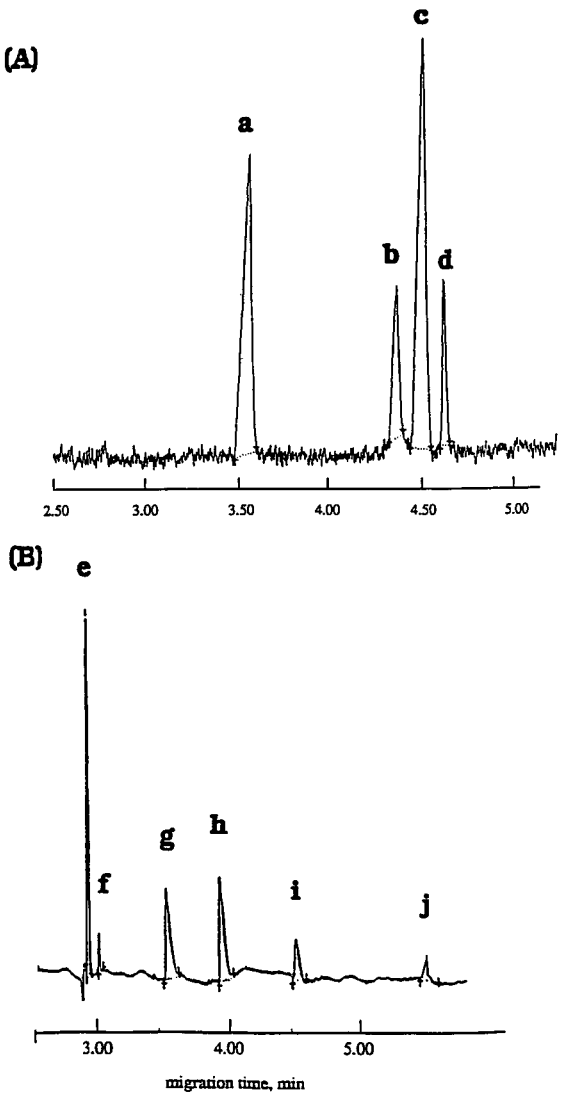

Fig. 1. CIE of (A) cations and (B) anions in the soluble phase of milk. The ultrafiltrate was diluted 250-fold with 18-mΩ water. The applied voltage was 20 kV. Peaks: a = potassium; b = calcium; c = sodium; d = magnesium; e = chloride; f = sulphate; g = citrate; h = phosphate; i = carbonate; j = lactate.

the high mobility of the electrolyte and the too large dilution. The use of an electrolyte optimized for phosphate and citrate (*i.e.*, *p*-hydroxybenzoate) would certainly improve the precision.

The optimum dilution was found to be 1:500 for cations and 1:1000 for anions. Sufficient precision was obtained with a common dilution of 1:250 for both anions and cations, hence we chose this simplified sample preparation procedure.

Effect of temperature on ionic equilibria

Among the different factors having an influence on the saline equilibria of milk, temperature is certainly the most important. The cooling of milk at the farm and storage at 2–4°C for 48–72 h are common practice in the dairy industry.

Inorganic species in raw milk cooled and stored at 4°C for several days were determined by CIE (Fig. 2). The soluble calcium concentration increased during the first day of cooling and remained constant thereafter. This demonstrates, in accordance with the works of Brulé and Fauquant [7], that part of the colloidal calcium migrates to the liquid phase. We have observed the same effect for phosphate, while sodium and chloride are not affected

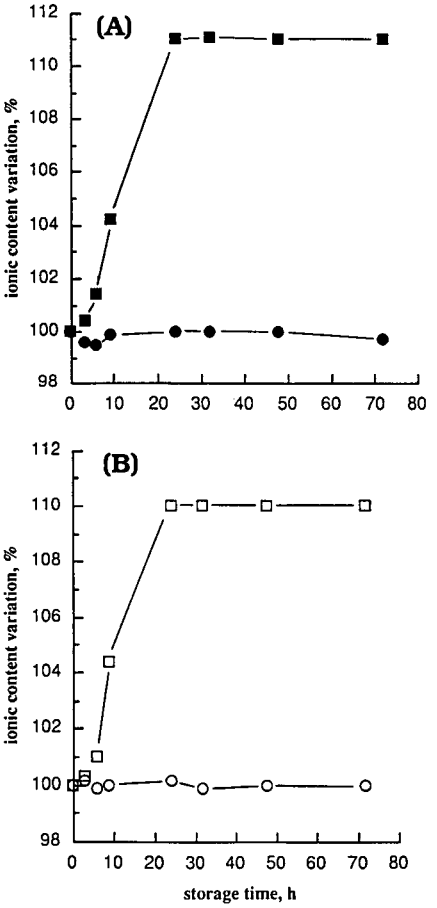

Fig. 2. Effect of cooling of milk on the concentrations of (A) (■) calcium and (●) sodium and (B) (□) phosphate and (○) chloride in the soluble phase of milk.

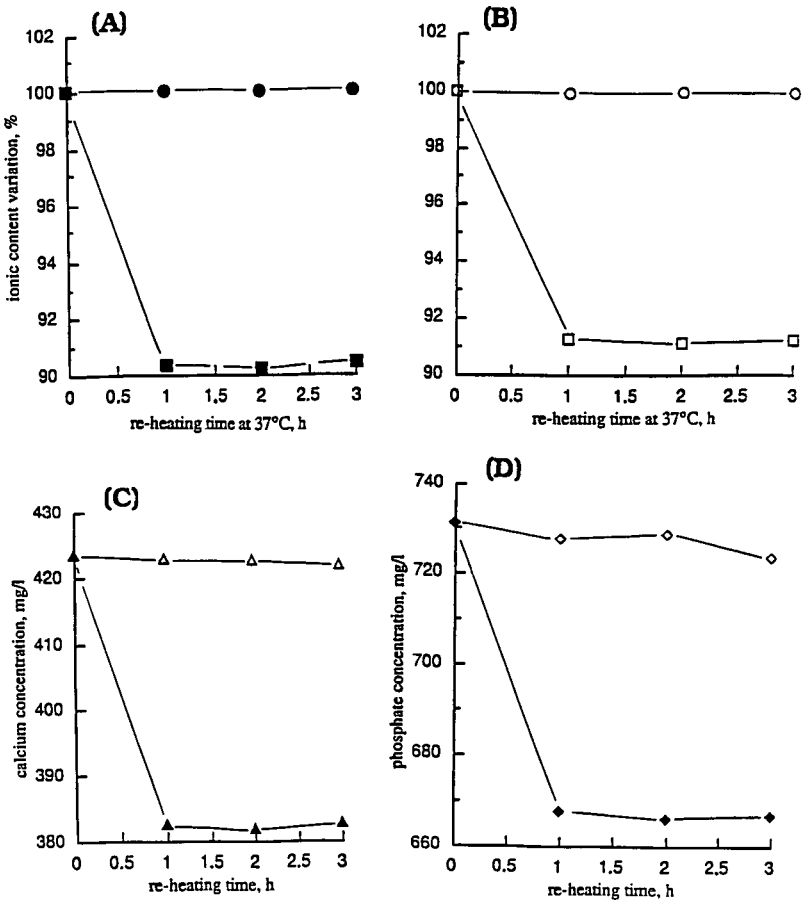

Fig. 3. (A,B) Influence of warming of milk after cold storage on the minerals in the soluble phase: ■ = calcium; ● = sodium; □ = phosphate; ○ = chloride. (C,D) Influence of warming temperature on the concentrations of (C) soluble calcium and (D) soluble phosphate. Measurements were performed at (△,◇) and (▲,◆) 37°C.

by cooling. These results are in good agreement with those of other workers [8–10]. The concentration of calcium phosphate in the liquid phase was increased by cooling [11], which induced a decrease in the mineral charge of the casein micelles.

After several days of cold storage, the milk must be re-equilibrated to allow processing; the removal of the soluble phase modifies the rennet coagulation properties of milk [12,13].

Cooled samples were warmed to 20 or 37°C (Fig. 3). Treatment at 20°C for 3 h did not restore the initial ionic equilibria. At this temperature, re-equilibration takes a very long time [2,9]. At 37°C, the soluble calcium content decreased quickly during the first hour, nearly reaching its initial concentration in raw milk. The same results could be obtained for soluble phosphate, according to other workers [3,4].

These results demonstrate the reversibility of the ionic equilibria and the need for a re-equilibration time before the beginning of cheese manufacture.

More drastic heat treatments were also evaluated. Cooled milk was warmed at 50, 60 or 70°C for 2 min (Table I). This treatment restored the concentration of soluble calcium and phosphate to the levels observed in fresh milk before cooling. Hence the re-equilibration could be performed in 1 hour at 37°C or in 2 min at 60°C.

TABLE I

EFFECT OF HEATING MILK AT SEVERAL TEMPERATURES ON THE CONCENTRATIONS OF SOLUBLE PHOSPHATE AND CALCIUM.

Control: milk stored at 4°C (= 100%) Conditions: applied voltage, 20 kV; injection, 10 nl. For phosphate: electrolyte, chromate with OFM Anion-BT; indirect UV detection at 254 nm. For calcium: electrolyte, 5 m*M* UV Cat-1–6.5 m*M* HIBA (pH 4.4); indirect UV detection at 214 nm.

Ion	Thermal treatment			
	Control	50°C, 2 min	60°C, 2 min	70°C, 2 min
Soluble phosphate	100	91.0	89.6	89.3
Soluble calcium	100	88.7	86	86.2

TABLE III

EFFECT OF INDUSTRIAL UHT TREATMENT ON THE SOLUBLE PHASE OF MILK

Control: raw sample (= 100%). Conditions: applied voltage, 20 kV; injection, 10 nl. For calcium: electrolyte, 5 mM UV Cat-1–6.5 mM HIBA (pH 4.4); indirect UV detection at 214 nm. For anions: electrolyte, chromate with OFM Anion-BT; indirect UV detection at 254 nm.

Ion	Thermal treatment		
	Raw	Pasteurized	Sterilized
Calcium	100	99	92.0
Phosphate	100	94.5	90.1
Citrate	100	97.9	89.7

Drastic heat treatments of milk are frequently used in the dairy industry. Thus, for the study of an industrial UHT treatment, several experiments on the laboratory scale were performed at 80 and 90°C (Table II). We observed an important decrease in soluble calcium and phosphate contents, whereas the contents of soluble sodium and chloride were unchanged. The former decrease was greater than that observed during the re-equilibration after cold storage. The soluble citrate also decreased, but less significantly. This can be explained by the fact that the solubility of calcium phosphate decreases when a drastic thermal treatment is used; the colloidal calcium phosphate reaches saturation and precipitates as tricalcium phosphate [1]. Precipitation of calcium citrate could be the reason for the decrease in soluble citrate [14].

This study was completed by collection of samples in an industrial UHT installation at three different stages: raw milk (stored at 4°C), milk after pasteurization at 88°C for 20 s and UHT milk (indirect sterilization for 2 s at 143°C) (Table III). As expected, the soluble calcium, phosphate and citrate contents decreased slowly after pasteurization, and slightly more after sterilization, but the decrease was smaller than expected. The short dura-

TABLE II

EFFECT OF THERMAL TREATMENT ON IONS IN THE SOLUBLE PHASE OF MILK

Control: milk stored at 4°C (= 100%). Conditions: applied voltage, 20 kV; injection, 10 nl. For cations: electrolyte, 5 m*M* UV Cat-1–6.5 m*M* HIBA (pH 4.4); indirect UV detection at 214 nm. For anions: electrolyte, chromate with OFM Anion-BT; indirect UV detection at 254 nm.

Ion	Thermal treatment					
	Control	80°C, 2 min	90°C, 2 min	90°C, 5 min	90°C, 10 min	90°C, 15 min
Calcium	100	82.9	77.2	75.9	74.5	73.2
Sodium	100	100.5	100	100.8	100	100
Chloride	100	100	100	99.9	99.7	99.8
Phosphate	100	86.5	84.4	83.5	81.2	78.7
Citrate	100	94.8	92.6	90.7	89.8	88.3

tion of the thermal treatment could explain this. It appears that not only temperature, but also its duration, are of importance for the study of these ionic equilibria.

CONCLUSIONS

CIE is a very convenient technique for estabilishing the modifications of ionic equilibria in milk under the influence of temperature changes. Sample preparation is minimal and the run time is less than 6 min. CIE is a very powerful tool and can be used for analysis in control laboratories in the dairy industry and in other food and beverage industries.

ACKNOWLEDGEMENTS

We thank Miss Sylvie Malarbet for her contribution to this study and Mr. Gérard Bondoux (Waters-Millepore, Saint-Quentin-en-Yvelines, France) for useful advice. This work was supported by grants from the Mission Recherche de la Région Lorraine.

REFERENCES

1 C. Holt, in P. F. Fox (Editor), *The Milk Salts: Their Secretion, Concentrations and Physical Chemistry Development in Dairy Industry*, Elsevier Applied Science, Barking, 1985, pp. 143–181.
2 D. T. Davies and J. C. D. White, *J. Dairy Res.*, 27 (1960) 171–190.
3 D. Rose and H. Tessier, *J. Dairy Sci.*, 42 (1959) 969–977.
4 G. Brulé, E. Real del Sol, J. Fauquant and C. Fiaud, *J. Dairy Sci.*, 61 (1978) 1225–1232.
5 P. Jandik, W. R. Jones, A. Weston and P. R., *LC · GC Int.*, 5, No. 1 (1992) 20–27.
6 G. Brulé, J. L. Maubois and J. Fauquant, *Lait*, LIV (1974) 600–615.
7 G. Brulé and J. Fauquant, *J. Dairy Res.*, 48 (1981) 91–97.
8 A. E. Ali, A. T. Andrews and G. C. Cheeseman, *J. Dairy Res.*, 47 (1980) 371–382.
9 J. Ichilczyk-Leone, Y. Amram, M. Schneid and J. Lenoir, *Rev. Lait. Fr.*, 401 (1981) 7–18.
10 J. Lenoir, in *Le Lait, Matière Première de l'Industrie Laitière*, CEPIL-INRA, 1987, pp. 269–274.
11 A. Pierre and G. Brulé, *J. Dairy Res.*, 48 (1981) 417—428.
12 A. Kannan and R. Jenness, *J. Dairy Sci.*, 44 (1961) 808–822.
13 P. A. Morissey, *J. Dairy Res.*, 36 (1989) 333–341.
14 Y. Pouliot, M. Boulet and P. Paquin, *J. Dairy Res.*, 56 (1988) 185–192.

Journal of Chromatography, 640 (1993) 425–431
Elsevier Science Publishers B.V., Amsterdam

CHROMSYMP. 2668

Separation of metal ions by capillary electrophoresis

Min Chen and Richard M. Cassidy*

Department of Chemistry, University of Saskatchewan, Saskatoon, Saskatchewan S7N 0W0 (Canada)

ABSTRACT

A number of experimental parameters have been optimized for the separation of 26 metal ions, including alkali, alkaline earth, transition and lanthanide metal ions. Experimental parameters that were evaluated included nature of indirect-detection reagent, pH of electrolyte, concentration of complexing agent and nature of the surface of the capillary; unbonded and C_1 and C_{18} bonded phases were studied. In addition the effect of internal diameter on linearity and signal-to-noise ratio was examined, and separation efficiency was determined for a variety of experimental conditions. Detecton limits (signal-to-noise ratio = 3) were *ca.* 1 μg/ml for the lanthanides, *ca.* 0.6 μg/ml for transition and alkaline earth ions and *ca.* 0.1–0.8 μg/ml for alkali metal ions. The average relative standard deviations of were 3.7, 5.1 and 2.5% on unbonded, C_1 and C_{18} capillaries, respectively. Whereas conventional regression analysis suggested that the calibration curves were linear over the range of $1 \cdot 10^{-5}$ to $4 \cdot 10^{-4}$ mol/l, sensitivity plots showed that the results were actually linear to within 6% only over the range of $2.5 \cdot 10^{-5}$ to $4 \cdot 10^{-4}$ mol/l.

INTRODUCTION

Metal ions are important in a variety of research and industrial areas, and for many analysis situations ion chromatography (IC) has been used to determine these ions [1–5]. Recently, capillary electrophoresis (CE) has attracted considerably attention as an alternative to traditional chromatographic techniques, particulary in the biological sciences. To date relatively few papers have been published on the CE separation of metal ions [6–21]. Metal ions that have been separated include the alkali, alkaline earth, transition and lanthanide ions. The high resolution of CE suggests that it should be possible to simultaneously separate a mixture containing metal ions from all of these classes, but to do so would require optimization of a number of experimental parameters. In this paper the simultaneous separation 26 metal ions including 3 alkaline, 3 alkaline earth, 6 transition metal ions and 14 lanthanides has been optimized in terms of indirect-detection reagent, pH, concentration of complexing agent and nature of the surface of the capillary. In addition the effect of internal diameter on linearity and signal-to-noise ratios was examined, and separation efficiency was determined for a variety of experimental conditions.

EXPERIMENTAL

Apparatus and electrophoresis

A Waters Quanta 4000 CE system (Millipore Waters, Milford, MA, USA) equipped with a high-voltage power supply (30 kV) was used for all separations; a positive power supply was used except when cetyltrimethylammonium chloride (CTAC) was used. Polyimide-coated (outer surface) fused-silica capillaries, 50–60 cm in length (350 μm O.D.) with inside diameters of 75, 50 and 25 μm were obtained from Polymicro Technology (Phoenix, AZ, USA). The window of the on-column detector cell was created by burning a small section (*ca.* 0.5 cm) of the polyimide coating off with a match, and excess residue was then wiped off with methanol or acetone. The unbonded capillaries were washed with 0.1 mol/l HCl for 1 h, rinsed with water, then equilibrated overnight with the electrolyte. The bonded-phase capillaries were prepared as described previously [19]. The sample was injected hy-

* Corresponding author.

0021-9673/93/$06.00

drostatically with the capillary inlet placed 9.8 cm above the capillary outlet for 1 s per each 10 cm length of capillary, sample volumes were in the range of 7 nl for a 60 cm × 75 μm capillary. The electrolyte was monitored at 214 nm, and the electric field was 500 V/cm. The electropherogram was recorded and evaluated on a PC computer with a Waters SIM interface and Waters Baseline 820 software.

Chemicals

All solutions were prepared from distilled, deionized and redistilled water (Mega-Pure system, MP-6A and D2, Corning, New York, NY, USA). The electrolyte buffer was prepared by dissolving the desired amount of an indirect-detection reagent and α-hydroxyisobutyric acid (HIBA) in water; the pH was adjusted with acetic acid [British Drug Houses (BDH), Toronto, Canada] to the desired value. The pH was measured with a combination glass electrode calibrated with pH 4.00 ± 0.02 and 7.00 ± 0.02 buffers (hydrion dry buffers, Aldrich, Milwaukee, WI, USA). The electrolytes containing surfactants were obtained by diluting a 0.01 mol/kg surfactant stock solution with the buffer. The concentration of all surfactants was below the critical micelle concentration. Triton X-100 (TX-100, Aldrich) was used without further purification. CTAC [Aldrich, 25% (w/w) aqueous solution] was freeze-dried, recrystallized twice in acetone–ethanol (1:9, v/v) and dried in a vacuum oven at 60°C overnight. All electrolyte solutions were filtered through a 0.2-μm nylon-66 membrane syringe filters (Cole-Parmer Instrument, Chicago, IL, USA) prior to use. The N,N-dimethylbenzylamine (DBA), benzylamine and naphthenemethylamine (all from Aldrich) were purified by distillation under vacuum. Benzyltrimethylammonium chloride (Aldrich) was recrystallized from methanol–diethyl ether, and N-1-naphthylethylenediamine dihydrochloride (Eastman, Rochester, NY, USA) was recrystallized from water. Creatinine (Sigma, Louis, MO, USA) was used without further purification.

Lanthanide samples were obtained from Alfa (Danvers, MA, USA) as nitrate salts (Dy, Eu, Gd, Ce) chloride salts (La, Pr, Yb) and oxides (Nd, Sm, Lu, Tm, Ho, Eu, Tb). Nitrate and chloride salts were dissolved directly in water. Oxides were dissolved in an excess of 0.5 mol/l nitric acid, evaporated to dryness and redissolved in water to form a 0.01 mol/l stock solution. The stock solutions of other metal ions were prepared from KCl, NaCl, LiCl, $MnCl_2$, $ZnCl_2$, $FeCl_2$, $BaCl_2$, $CoCl_2$ (all from BDH), $Ni(NO_3)_2$ (Fisher Scientific), $Mg(NO_3)_2$ (BDH) and $Ca(NO_3)_2$ (BDH). All stock solutions were filtered through 0.2-μm nylon-66 membrane syringe filters, and samples were prepared by dilution of the stock solution to 2 ml in the electrolyte.

RESULTS AND DISCUSSIONS

Indirect detection reagent

UV absorption is used widely to monitor compounds in CE, but most metal ions do not exhibit appreciable absorption in this range. Therefore indirect detection, where the analyte ions replace a UV-absorbing ion of the same charge (electrolyte coion) [22], has become a commonly used technique to detect metal ions as negative peaks. The equivalents of replaced coion is closely related to the equivalents of analyte injected, and thus the higher the molar absorbance of the coion, the lower the detection limit. The background absorption should be adjusted to be close to maximum value for the linear range of the detector in order to give the maximum linear calibration range. With DBA the range of linearity was below 0.05 A.U. on 75-μm and 50-μm capillaries. Consequently, the concentration of the different indirect-detection reagents that were evaluated was adjusted to give a background absorption of *ca.* 0.05 A.U.

A 0.03 mol/l creatinine–acetic acid buffer has been reported for the detection of metal ions [13], but when this was used in these studies (75-μm capillary) the background absorption was out of linearity range, and a relatively small signal-to-noise (S/N) ratio of 26 was observed for a $1 \cdot 10^{-4}$ mol/l sample of Ce^{3+}. Creatinine was chosen by Foret *et al.* [13] since its pK_a value of 4.8 permits it to act as a good buffer in the desired working range. However, if the pH is 4.8, only half of the creatinine is in the cationic form. The neutral fraction does not contribute to detection, but does affect the linearity range. Therefore, aromatic amines with pK_a values larger than 7 or quaternary ammonium salts should offer advantages for indirect detection. Since the pK_a of aromatic amines with an amino group connected to a benzene ring is around 4, aromatic

TABLE I

MOLAR ABSORBANCE OF INDIRECT-DETECTION REAGENTS AT 214 nm IN A pH 4.6 SOLUTION

Compound	Molar absorbance (cm^{-1} mol^{-1} l)
Creatinine	$9.2 \cdot 10^3$
Benzylamine	$4.3 \cdot 10^3$
N-Methylbenzylamine	$4.8 \cdot 10^3$
N-1-Naphthylethylenediamine dihydrochloride	$4.8 \cdot 10^4$
Benzyltrimethylammonium chloride	$1.3 \cdot 10^4$
N,N-Dimethylbenzylamine	$6.0 \cdot 10^3$
Naphthene methylamine	$4.4 \cdot 10^4$

amines with the amino group connected via an alkyl group (larger pK_a) are preferred. In this study seven different aromatic amines and quaternary ammonium salts were selected based on their acid/base properties and their molar absorbance values (see Table I).

With benzylamine (electrolyte contained 4 mmol/l HIBA, 9 mmol/l benzylamine and acetic acid at pH 4.6) it was possible to detect all 14 lanthanides, but the S/N was only 22 for a sample containing $1 \cdot 10^{-4}$ mol/l Ce^{3+}. It was found that N-methylbenzylamine also gave good detection, but the improvement in S/N was very small. Both benzyltrimethylammonium chloride and N-1-naphthylethylenediamine dihydrogenchloride gave complex electropherograms in which several positive peaks appeared before a series negative peaks when a mixture of 14 lanthanides were injected. When individual lanthanide samples (La^{3+}, Ce^{3+} and Pr^{3+}) were injected separately, both a positive and a negative peak were obtained for each ion, as shown in Fig. 1. This phenomena appeared to be related to the presence of Na^+, which was added as NaOH to adjust the pH of these electrolytes. The change in concentration of Na^+ when the sample is introduced should cause a positive peak, but the reason for its appearance at a different retention time for different metal ions is unclear. Because of these interferences, however, these two reagents were not studied further.

Table I shows that the molar absorbance of naphthenemethylamine is relatively large, and thus should give sensitive detection. Unfortunately this reagent was not stable. After distillation under vacuum, it became pale yellow within a few hours when stored under nitorgen. In an effort to stabilize this compound an acetate salt was prepared and recrystallized three times from methanol–diethyl ether. To maintain the detector reading within the linear range, the concentration of the acetate salt could not be more than 2 mmol/l. However, the pH of solution containing 4.2 mmol/l HIBA and 2 mmol/l salt was 2.8. At this pH value, the baseline noise was high, the S/N was less than 4 and, because of a fast electroosmotic flow (EOF), the separation was poor. Lower concentrations of HIBA could be used to adjust the pH, but this would also degrade the separation.

The best indirect reagent was DBA. This reagent gave S/N values of >100 for a $1 \cdot 10^{-4}$ mol/l Ce^{3+} solution. Detection limits obtained with DBA are given later in this report.

Capillary internal diameter

In principle higher heat dissipation is obtained with smaller-diameter capillaries, and higher column efficiencies should be obtained with smaller capillaries. However, as the ionic strength of the buffer used in these studies was only 6 mmol/l, the current was about 8 μA with 75-μm capillaries, and

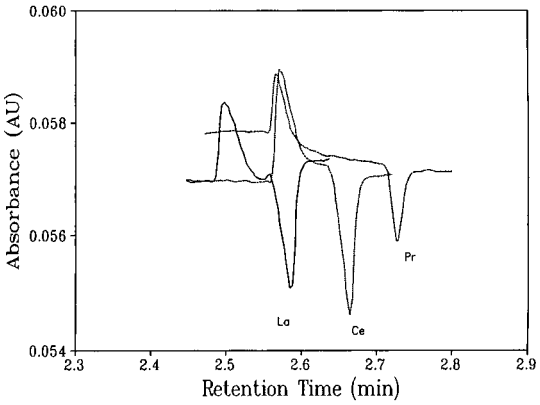

Fig. 1. Electropherogram of La^{3+}, Ce^{3+} and Pr^{3+} on an unbonded capillary. Each sample was injected separately. Electrolyte, 8 mmol/l benzyltrimethylammonium chloride and 4 mmol/l HIBA at pH 4.6 adjusted with sodium hydroxide; capillary, 60 cm × 75 μm fused-silica; electric field, 500 V/cm; injection, 6 s at a differential height of 9.8 cm; indirect detection at 214 nm; concentration of ions, $1 \cdot 10^{-4}$ mol/l.

heat dissipation was not a problem for most of the experimental conditions studied. The results in Table II show that when 25-μm, 50-μm and 75-μm unbonded capillaries were evaluated the 75-μm capillary give the highest S/N value and a low HETP (height equivalent to a theoretical plate) value. With smaller capillaries it is possible to work with higher concentrations of the indirect-detection reagent, which should extend the upper part of the linear working range, but the alignment of the smaller capillaries in the instrument was more difficult. Consequently, 75-μm capillaries were used for the remainder of these studies.

Effect of pH

In the separation of ions the net mobility of an ion is the summation of EOF and electrophoretic mobility. In these studies a weak complexing agent is used to enhance differences in the electrophoretic mobilities, which is the weighted average of the mobility of the free metal ions and its various complexes. Since both the EOF [23] and the speciation of the metal ions is influenced by pH; the pH range from 3.3 to 5.3 (pK_a of HIBA = 3.79 [24]) was studied on unbonded and C_1 and C_{18} bonded-phase capillaries. The S/N ratios and HETP values for Ce^{3+} ($1 \cdot 10^{-4}$ mol/l) at diferent pH values are shown in Table III. The results in Table III show that the S/N values decrease as the pH decreased. This was caused by an increase in the baseline noise which may have been caused by excessive heating due to an increase in the current as a result of the greater mobility of the hydronium ions. At the highest pH value, 5.3, the peaks of lanthanide ions began to broaden on both the unbonded and C_1 capillaries, possibly due to interactions between the cations and the silica surface. The results in Fig. 2 show that the electrophoretic coefficients of the ions decreased as the pH was increased due to complexation. Based on the data shown in Table III and Fig. 2, a pH of 5.0 was chosen to optimize both S/N, HETP values and resolution.

Effect of HIBA concentration

Metal ions belonging to groups such as the transition and lanthanide groups have similar electrophoretic mobilities, and to achieve efficient separations it is necessary to selectively alter the mobilities via some process such as complexation. Complexation reagents such as cyanide [11], 8-hydroxyquinoline-5-sulfonic acid [14], pyridylazoresorcinol [10] and HIBA [13,18–21] have been used. Since HIBA is known to be effective for the selective separation of lanthanides this reagent was chosen for these studies. The net electrophoretic mobility of metal

TABLE II

S/N RATIO AND HETP OF Ce(III) FOR DIFFERENT CAPILLARIES

Electrolyte, 6 mmol/l DBA and 4 mmol/l HIBA; the pH (4.6) was adjusted with acetic acid; Ce^{3+} concentration, $1 \cdot 10^{-4}$ mol/l.

Size of capillary (μm)	S/N	HETP (μm)
75	60	3.2
50	26	3.5
25	3.6	6.4

TABLE III

S/N AND HETP FOR Ce(III) AS A FUNCTION OF pH

Electrolyte, 6 mmol/l DBA and 4 mmol/l HIBA; the pH was adjusted with acetic acid; Ce^{3+} concentration, $1 \cdot 10^{-4}$ mol/l.

pH	Capillary	S/N	HETP (μm)
5.3	Unbonded	65	20
	C_1	30	27
	C_{18}	50	2.6
4.95	Unbonded	105	2.3
	C_1	65	2.7
	C_{18}	105	3.2
4.8	Unbonded	85	2.1
	C_1	82	2.6
	C_{18}	85	2.7
4.3	Unbonded	70	2.5
	C_1	60	3.6
	C_{18}	60	2.6
4.0	Unbonded	40	3.5
	C_1	40	3.8
	C_{18}	60	3.6
3.8	Unbonded	50	4.8
	C_1	20	4.6
	C_{18}	65	4.6
3.3	C_{18}	4	–

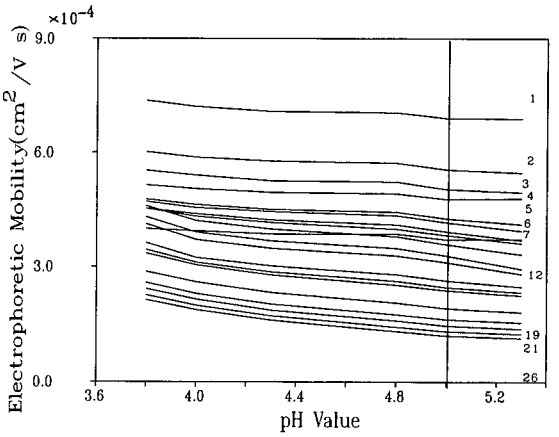

Fig. 2. Electrophoretic coefficients as a function of pH. Electrolyte, 6 mmol/l DBA and 4 mmol/l HIBA, pH adjusted with acetic acid; other conditions as for Fig. 1. Solute identity: 1 = K^+; 2 = Ba^{2+}; 3 = Ca^{2+}; 4 = Na^+; 5 = Mg^{2+}; 6 = Mn^{2+}; 7 = Fe^{2+}; 8 = Co^{2+}; 9 = Ni^{2+}; 10 = Zn^{2+}; 11 = Li^+; 12 = La^{3+}; 13 = Ce^{3+}; 14 = Pr^{3+}; 15 = Nd^{3+}; 16 = Sm^{3+}; 17 = Eu^{3+}; 18 = Gd^{3+}; 19 = Cu^{2+}; 20 = Tb^{3+}; 21 = Dy^{3+}; 22 = Ho^{3+}; 23 = Er^{3+}; 24 = Tm^{3+}; 25 = Yb^{3+}; 26 = Lu^{3+}

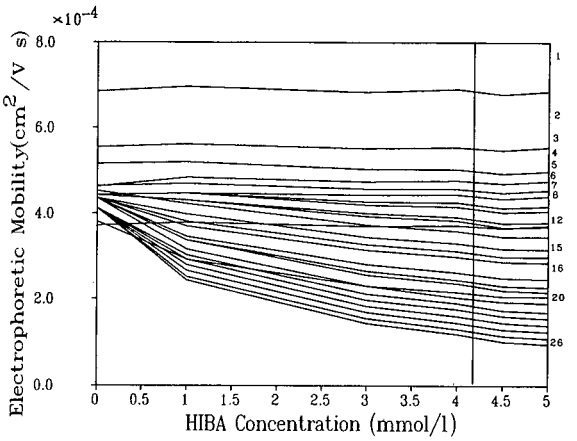

Fig. 3. Electrophoretic coefficients as a function of the concentration of HIBA. Electrolyte, 6 mmol/l DBA at pH 5.0 adjusted with acetic acid; solute identity as for Fig. 2; other conditions as for Fig. 1.

ions is dependent on the degree of complex formation, and thus the separation of the ions is influenced by the concentration of HIBA. Therefore, the concentration of HIBA was studied over the range 0–5 mmol/l at pH 5.0 with an electrolyte containing 6 mmol/l DBA; to maintain the previously determined optimum pH of 5, 5 mmol/l was the upper HIBA concentration that could be used with 6 mmol/l DBA. The electrophoretic coefficients of each ion as a function of the concentration of HIBA are shown in Fig. 3. In the absence of HIBA only group separations were possible. The results in Fig. 3 show that the best separation of the 26 metal ions was obtained when the concentration of HIBA was 4.2 mmol/l, which is in close agreement with similar studies reported previously [18].

Effect of the surfactants

The EOF in bonded-phase and unbonded capillaries can be manipulated by adding small amounts of surfactants [19]. Non-ionic surfactants reduce the EOF to *ca.* 0 and cationic surfactants can both reduce and reverse the EOF. Manipulation of the EOF can be used to optimize resolution as long as column efficiency is not degraded. Consequently, the influence of TX-100 and CTAC was examined.

The column efficiencies and retention times observed for Ce^{3+} on bonded-phase and unbonded capillaries when surfactants were added are shown in Table IV. Good separations were obtained when TX-100 was added, but broad peaks were found with CTAC, except at higher concentrations; the broad peaks may be a result of interactions between the hydrophobic chain of CTAC and the HIBA–metal complexes. Overall, there were only small differences between the performance of the bonded-phase and unbonded capillaries, and the best combination of column efficiency and resolution was obtained when a 0.2 mmol/l solution of TX-100 was used. As expected from EOF effects, the migration times of Ce^{3+} increased with the concentration of TX-100 and reversed with higher concentrations of CTAC. Fig. 4 shows an example of the separation obtained under these optimum conditions; note that the peaks in Fig. 4 are negative due to indirect detection, but could easily be made positive by reversing the polarity of the detector output. The HETP values for the metal ion shown in Fig. 5 were in the range 1–10 μm. The minimum values were observed for Ce^{3+} and Pr^{3+}, which had a mobility that matched that of the electrolyte cation; metal ions with higher mobilities exhibited tailing peaks and slower migrating ion exhibited fronting peaks.

The values of EOF flow for unbonded, C_1 and C_{18} phases with 0.2 mmol/l TX-100 in the electro-

TABLE IV

HETP OF Ce(III) AS A FUNCTION OF SURFACTANT CONCENTRATION

Electrolyte, 6 mmol/l DBA and 4 mmol/l HIBA; the pH was adjusted with acetic acid; Ce^{3+} concentration, $1 \cdot 10^{-4}$ mol/l.

Surfactant	Concentration (mmol/l)	Capillary	HETP (μm)	t_R (min)
TX-100	0.02	Unbonded	2.1	2.50
		C_1	2.9	2.67
		C_{18}	2.2	2.85
	0.05	Unbonded	1.9	2.92
		C_1	2.4	2.81
		C_{18}	2.3	2.90
	0.10	Unbonded	7.9	3.16
		C_1	2.8	3.27
		C_{18}	3.6	2.99
	0.20	Unbonded	1.2	4.33
		C_1	1.4	4.14
		C_{18}	2.0	3.17
CTAC	0.01	Unbonded	4.1	2.49
		C_1	3.7	1.67
		C_{18}	7.7	2.29
	0.05	Unbonded	7.8	2.73
		C_1	7.8	2.08
		C_{18}	20	2.64
	0.20	Unbonded	–	7.40
		C_1	5.2	−4.20[a]
		C_{18}	16	−4.75
	0.40	Unbonded	3.9	−3.77
		C_1	3.2	−2.37
		C_{18}	6.5	−2.61

[a] A negative retention time indicates a reversal in flow.

lyte were $6.0 \cdot 10^{-5}$ $6.8 \cdot 10^{-5}$ and $1.2 \cdot 10^{-4}$ cm^2 V^{-1} s^{-1}, respectively. These results suggest that TX-100 was absorbed more readily on the unbonded capillary surface. The unbonded capillary also gave a higher column efficiency than C_{18} capillaries, possibly due to reduced interactions between the surface and the solute. The HETP values obtained in these studies are a factor of at least 2 better than those reported for a polyamide-coated capillary [13].

Analytical performance parameters

Detection limits (S/N = 3) were *ca.* 1 μg/ml for the lanthanides, *ca.* 0.6 μg/ml for transition and alkaline earth ions and *ca.* 0.1–0.8 μg/ml for alkali metal ions. Relative standard deviations of the areas (four measurements) obtained for each of the lanthanides were determined for the electrolyte not containing a surfactant. The averages (standard deviation given in parentheses) of the relative standard deviations were 3.7 (1.1%), 5.1 (2.2%) and 2.5 (1.1%) on unbonded, C_1 and C_{18} capillaries, respectively. The linearity of the calibration curve was evaluated for the range $1 \cdot 10^{-5}$ to $4 \cdot 10^{-4}$ mol/l for each metal ion; the maximum concentration was chosen to give a concentration that was 100 times less than the concentration of buffer to minimize peak broadening due to differences between the

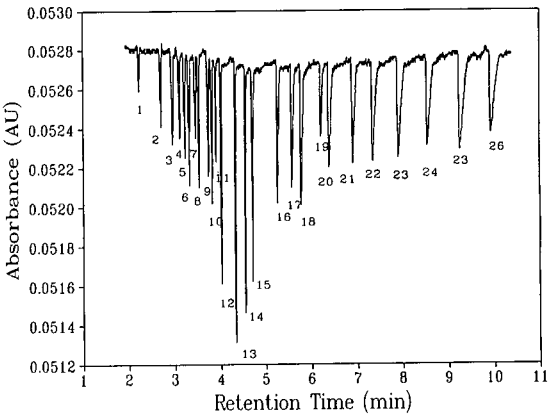

Fig. 4. Electropherogram for the separation 26 metal ions on an unbonded capillary. Electrolyte, 6 mmol/l DBA and 4.2 mmol/l HIBA at pH 5.0 adjusted with acetic acid and 0.2 mmol/l TX-100; peak identity as for Fig. 2; other conditions as Fig. 1.

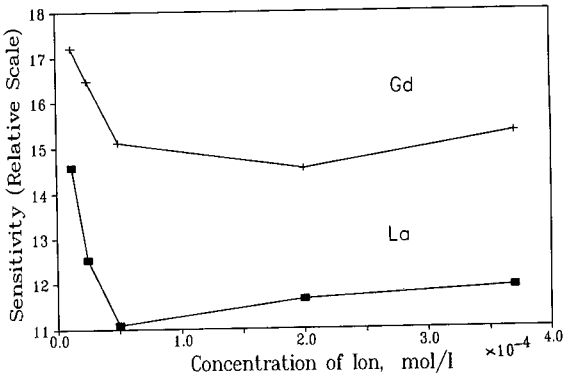

Fig. 5. Corrected sensitivity plots for Gd^{3+} and La^{3+}. Conditions as for Fig. 4 without TX-100.

electrolytes and analyte mobilities [25]. Conventional calibration curves were visually linear over the entire range; regression analysis for two of the test metal ions, La and Gd, gave values of 1.000 for the coefficients of determination (r^2) and the standard error of the slope was *ca.* 1%. However, when the sensitivity values for these two metal ions are corrected for the *y*-axis intercept and plotted *versus* concentration it is obvious that the curves are not linear in the low concentration range (see Fig. 5); perfectly linear data would give a straight-line sensitivity plot with a slope of zero. When the lowest concentration points in Fig. 5 are omitted, the remaining data for La and Gd give average sensitivity values of 11.8 and 15.5, and all of these data points lie within a linearity range of ±6%. Problem associated with the application of conventional regression analysis to the determination of the linearity calibration curves have been discussed in more detail elsewhere [26].

ACKNOWLEDGEMENTS

The authors would like to acknowledge the financial support of the Natural Science and Engineering Research Council of Canada and Waters/Millipore.

REFERENCES

1 C. H. Knight, R. M. Cassidy, B. M. Recoskie and L. W. Green, *Anal. Chem.*, 56 (1984) 474.
2 J. A. Tielrooy, P. H. M. Vleeschhouwer, J. C. Kraak and F. J. M. J. Maessen, *Anal. Chim. Acta*, 207 (1988) 149.
3 R. M. Cassidy and C. Chauvel, *Chem. Geol.*, 74 (1989) 189.
4 R. M. Cassidy, *Chem. Geol.*, 67 (1988) 185.
5 V. Kuban and D. B. Gladilovich, *Collect. Czech. Chem. Commun.*, 53 (1988) 1664.
6 T. Tsuda, K. Kazuhira and G. Nakagawa, *J. Chromatogr.*, 264 (1983) 385.
7 X. Huang, T. J. Pang, M. J. Gordon and R. N. Zare, *Anal. Chem.*, 59 (1987) 2747.
8 X. Huang, M. J. Gordon and R. N. Zare, *J. Chromatogr.*, 425 (1988) 385.
9 J. L. Beckers, Th. P. E. M. Verheggen and F. M. Everaerts, *J. Chromatogr.*, 452 (1988) 591.
10 T. Saitoh, H. Hoshino and T. Yotsuyanagi, *J. Chromatogr.*, 469 (1989) 175.
11 M. Aguilar, X. Huang and R. N. Zare, *J. Chromatogr.*, 480 (1989) 427.
12 L. Gross and E. S. Yeung, *Anal. Chem.*, 62 (1990) 427.
13 F. Foret, S. Fanali, A. Nardi and P. Bocek, *Electrophoresis*, 11 (1990) 780.
14 D. F. Swaile and M. J. Sepaniak, *Anal. Chem.*, 63 (1991) 179.
15 X. Huang and R. N. Zare, *J. Chromatogr.*, 63 (1991) 2193.
16 P. Jandik, W. R. Jones, A. Weston and P. R. Brown, *LC · GC*, 9 (1991) 634.
17 M. Koberda, M. Konkowski, P. Youngberg, W. R. Jones and A. Weston, *J. Chromatogr.*, 602 (1992) 235.
18 A. Weston, P. R. Brown, A. L. Heckenberg, P. Jandik and W. R. Jones, *J. Chromatogr.*, 602 (1992) 247.
19 M. Chen and R. M. Cassidy, *J. Chromatogr.*, 602 (1992) 227.
20 A. Weston, P. R. Brown, P. Jandik, W. R. Jones and A. L. Heckenberg, *J. Chromatogr.*, 593 (1992) 289.
21 A. Weston, P. R. Brown, P. Jandik, W. R. Jones and A. L. Heckenberg, *J. Chromatogr.*, 608 (1992) 395.
22 E. S. Yeung, *Acc. Chem. Res.*, 22 (1989) 125.
23 W. J. Lambert and D. L. Midelleton, *Anal. Chem.*, 62 (1990) 1585.
24 D. D. Perrin, *IUPAC Chemical Data Series No. 22, Stability Constants of Metal–Ion Complexes*, Part B, Pergamon Press, Oxford, 1982, p. 187.
25 R. A. Wallingford and A. G. Ewing, *Adv. Chromatogr.*, 29 (1989) 1.
26 R. Cassidy and M. Janoski, *LC · GC*, 10 (1992) 692.

Journal of Chromatography, 640 (1993) 433–440
Elsevier Science Publishers B.V., Amsterdam

CHROMSYMP. 2671

End-column electrochemical detection for inorganic and organic species in high-voltage capillary electrophoresis

Wenzhe Lu, Richard M. Cassidy* and Andrzej S. Baranski

Chemistry Department, University of Saskatchewan, Saskatoon; Saskatchewan S7N 0W0 (Canada)

ABSTRACT

The electronics and construction are described for an end-column ultramicroelectrode (3–10 μm) detection system that permits the use of medium-sized capillaries (25 μm I.D.) without appreciable effects from the potential field at the end of the capillary. Normal peak-to-peak noise over 10 s was 0.01–0.1 pA. The background noise observed for a 200 × 10 μm carbon-fiber electrode placed either 180 μm within a 25-μm capillary or at a point 500 μm away from the capillary was essentially the same. A study of detector response as a function of the position of the electrode has shown that accurate location of the electrode is important for sensitive and reproducible detection. These studies also showed that differences between the density of the electrolyte exiting the capillary and the electrolyte in the detection cell could cause anomalous electrode response depending on the location of the electrode relative to the end of the capillary. Application of a carbon fiber or an Hg film electrode gave detection limits (twice the peak-to-peak noise over 10 s) of $2 \cdot 10^{-8}$ mol/l for Pb^{2+}, $1 \cdot 10^{-5}$ mol/l for NO_2^- and $5 \cdot 10^{-10}$ mol/l for catechol.

INTRODUCTION

Capillary electrophoresis (CE) has recently attracted considerable attention in many areas of analytical chemistry [1,2]. Due to its uniform flow profile, high separation efficiencies have been obtained for large molecules, such as proteins with small diffusion coefficients (close to $1 \cdot 10^6$ theoretical plates) [3] or for small species, such as inorganic ions (several hundred thousand theoretical plates) [4,5]. Another potential advantage of CE is that very small sample volumes can be analyzed; sample volumes below the attoliter range has been reported [6]. To make full use of these features, sensitive detection techniques are required. UV absorbance is widely employed in CE, but sensitivity is limited by the path length and detection volume, particularly when a small-I.D. capillary is used. Laser-based fluorescence detectors can provide more sensitive detection, but are normally limited to analytes which fluoresce. This is a disadvantage for inorganic species because very few inorganic ions exhibit fluorescence. Electrochemical detection can offer some advantages over these techniques. If ultramicroelectrodes (~10 μm) are used, detector response will not be limited by a small detection volume. Other attractive features of ultramicroelectrodes include high sensitivity, good selectivity and low cost. The first off-column electrochemical detector used in high-voltage CE was developed by Wallingford and Ewing [7,8]. Later similar designs were reported by Huang and Zare [9] and O'Shea *et al.* [10]. In these systems, porous glass or Nafion tubing was used to connect the separation capillary with a short piece of capillary used for detection. In this way the separation current passing through the capillary was separated from the detection cell, and this procedure was reported to be necessary to reduce the background noise. However, even in these systems it was observed that the background noise was proportional to the applied high voltage [7,10]. In spite of this, these systems worked well for the detection of organic compounds, and a detection limit of $6 \cdot 10^{-9}$ mol/l for hydroquinone was reported. The major drawback of these systems was the diffi-

* Corresponding author.

0021-9673/93/$06.00

culty associated with making the porous joint. One alternative, termed 'end-column detection', has been reported [11]. In this technique the electrode is placed outside of the end of the separation capillary, and a porous joint is not used. It was stated that when a small capillary (5 μm) is used, the separation current will be very small and it will not significantly affect the detection current [11]. The use of a very small capillary increases experimental difficulties for routine work, because processes such as washing and drawing electrolyte through the capillary become very difficult. This paper will describe the results obtained for electrochemical detection with 10–25 μm capillaries without a porous-joint system. The detection of inorganic ions and catechol with carbon fiber or Hg-film electrodes was used to illustrate the potential of this electrode system.

Since very small currents (pA range) are produced with ultramicroelectrodes, careful consideration must be given to potential sources of noise. Important aspects that require attention in the design of such systems are discussed briefly, and the relationship between detector performance and positioning of the electrode has been studied. In previous reports it has been suggested that the position and area of the microelectrode relative to the bore of the capillary may be very important in amperometric detection [11,12]. It is expected that poor alignment of electrode with the capillary will significantly affect both column efficiency and detection limits, but to date no quantitative data have been reported on these effects.

EXPERIMENTAL

Apparatus

Polyimide-coated fused-silica capillaries, 10–25 μm I.D., were obtained from Polymicro Technology (Phoenix, AZ, USA). Before use the capillaries were washed with water–acetonitrile (50:50, v/v) and operating electrolyte. The high-voltage power supply, with reversible polarity (0 to *ca.* 30 kV), was obtained from Spellman (Model RHR30PN30, Plainview, NY, USA). The voltage input was housed in a Plexiglas box with an interlock on the access door to protect the operator. The detection cell and detector were housed in a faradaic cage to minimize the interference from external sources of noise. Electrochemical detection was based on a chronoamperometric mode with a three-electrode system. Detection was performed at the end of the separation capillary. The detection process was controlled via a 386DX/40MHz IBM personal computer equipped with PCL-818 or PCL-812 high-performance data acquisition card (B & C Microsystem, Sunnyvale, CA, USA). The computer programs, which controlled the application of potential to the electrode, the collection and display of the data, and the deposition of Hg for Hg-film electrodes, were written locally. In addition, this computer software includes programs for cyclic voltammetry and pulsed electrochemical techniques.

The electronic circuit diagram of the potentiostat for the home-made detector (cost about US$ 100) that was used in this work is shown Fig. 1. All resistors (metal film) had an error of ±1% and the amplifiers were LF353N wide-bandwidth dual-JFET operational amplifiers (Electronics, Toronto, Canada). This circuit is basically composed of a summing inverting amplifier (No. 1) and a differential amplifying circuit with a gain of 100 (Nos. 2, 3 and 4). A high-impedance circuit (amplifiers 5 and 6) was placed in the reference-electrode input circuit to ensure that the current flowing through the capillary did not pass through the reference electrode. This design minimized drift and noise in the reference system, and also helped to eliminate the formation of a ground loop between the reference electrode and ground [13]. To minimize electronic noise, low-pass filters were placed in the output circuit and the working-electrode input circuit. These filters reduced the noise with only a small loss in the separation efficiency (maximum time constant of the filters was 0.1 s). Other strategies used to further decrease background noise included computer software signal averaging, low-noise cables between the potentiostat and electrodes, faradaic cage screening and elimination of possible ground loops. A discussion of some of the factors important in the successful measurement of small currents (pA range) has been given elsewhere [14]. The voltage produced by the signal current was amplified via Nos. 2, 3 and 4 operational amplifiers and sent to the A/D convertor with the minimum step size corresponding to 0.015 pA. The data obtained were monitored in real time on the computer screen, and peak areas were determined as a summation of rectangular peak-area increments over the width of the peak.

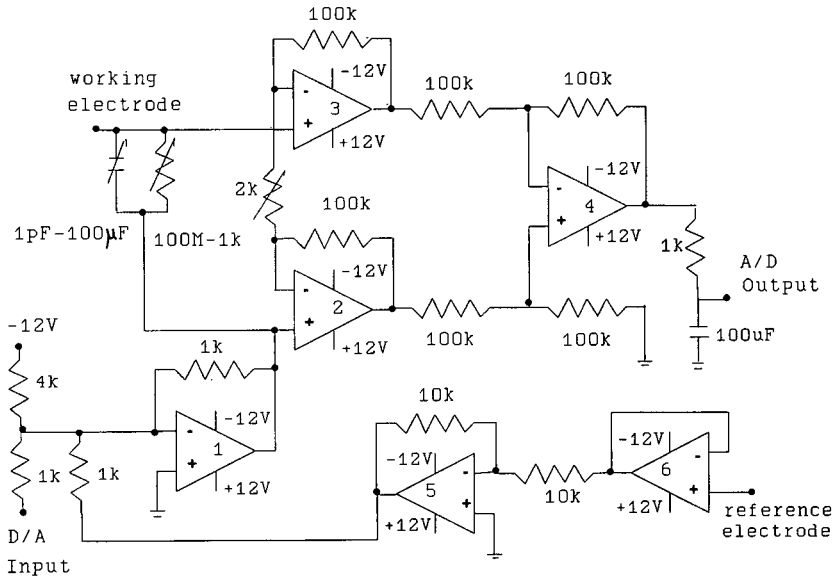

Fig. 1. Electronic circuit diagram for the detector. k = kΩ; M = 10^6 Ω.

Ultramicroelectrodes and detection cell

The ultramicro carbon working electrode was made from a single carbon fiber (10 μm I.D.), which was obtained from Amoco Performance Products (Greenville, USA). A fiber was put into a glass tube with an I.D. of about 0.5 mm at the tip. The tip was sealed with 5-min epoxy glue, and before the glue was dry the carbon fiber was pushed into the tube (under a microscope) until the desired exposed length was left. The length of the exposed fiber was normally in the range 200–400 μm. The carbon fiber was connected to a copper lead via a mercury junction. Ultramicro Hg-film electrodes were made as described elsewhere [15]. The auxiliary electrode was a platinum foil with an exposed surface area of 0.5 cm^2; this electrode also served as the ground for potential drop through the capillary. A saturated calomel electrode (SCE) (Miniature model, Fisher, Ottawa, Canada) was employed as the reference electrode.

To prepare a capillary-electrode detection system a 0.5 ml polyethylene vial was attached to a metal plate that was fastened to the same stand as a XYZ micropositioner (Model MR3, Klinger, Garden City, NY, USA). Fig. 2 shows the arrangement of the electrode cell and the capillary. The microelectrode was fixed above the tube with a small metal bar screwed onto the plate (see Fig. 2) with the exposed carbon fiber 0.2–1.5 mm above the top of the tube. The capillary was mounted on the micropositioner and its position was adjusted (under a microscope) against the end of the capillary. This arrangement allowed one to easily remove and realign both the capillary and the microelectrode. The exact position between the capillary and the electrode was measured with an optical scale under a microscope (to within 1–3 μm) from both a top view and side view direction. Electrolyte, which was added to cover both the capillary and the electrode, was held above the top of the polyethylene tube by surface tension. The reference and auxiliary electrodes were placed into the top of the solution as shown in Fig. 2. This assembly was used in the studies of the effects of alignment on detector performance. For more routine operation the capillary and the ultramicro working electrode were placed on a glass plate; the desired position between the capillary and the electrode was adjusted using the micropositioner (under a microscope), and a wall of epoxy was used to both fix the cell alignment and to function as an electrolyte reservoir for the reference and auxiliary electrodes.

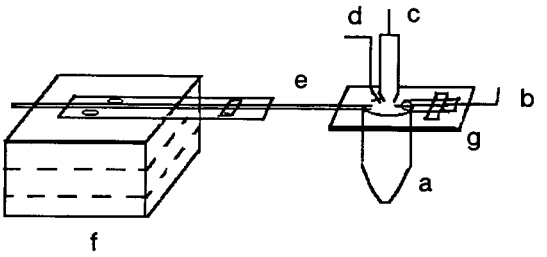

Fig. 2. View of the detection cell assembly. a = Plastic vial; b = carbon-fiber electrode; c = reference electrode; d = counter electrode; e = capillary; f = micropositioner; g = metal plate. The metal plate was fastened to the same heavy stand (not shown in diagram) used to hold the micropositioner.

Chemicals

All solutions were prepared from double-distilled, deionized water (Corning, Mega-Pure system, MP-6A and D2, New York, NY, USA). The background electrolyte for separation and detection of transition metal ions was similar to that used for the CE separation of the lanthanide series of metal ions [4]; this electrolyte was 0.005 mol/l N,N-dimethylbenzylamine, 0.0065 mol/l α-hydroxyisobutyric acid (HIBA) (98%, Aldrich, Milwaukee, WI, USA) and the pH value was adjusted with acetic acid to 4.90. The stock phosphate buffer was prepared by mixing 0.01 mol/l monosodium phosphate, phosphoric acid (BDH, Toronto, Canada) and 0.01 mol/l sodium dodecylsulfate (SDS) (99%, Sigma, St. Louis, MO, USA). The desired pH value (6.95) of the buffer was adjusted with NaOH. This solution was used in the separation and detection of catechol. The electrolyte in the separation reservoir was replaced every day to avoid chemical and pH changes in the electrolyte. The electrolyte used for the separation of NO_2^- was 0.005 mol/l sodium phosphate (BDH) plus 0.005 mol/l cetyltrimethylammonium chloride (CTAC) (Aldrich) at pH 6.52. All pH values were measured with a combination glass electrode calibrated at pH 4.0 and 7.0 (Aldrich, hydrion dry buffers). Thallium chloride, lead acetate, cadmium chloride, copper chloride and sodium nitrite (Aldrich) solutions were prepared as a 0.01 mol/l stock solutions. Catechol (Sigma) stock solutions were 0.01 mol/l, and were made 0.1 mol/l in perchloric acid. Samples were diluted to the desired concentration with operating electrolyte prior to use. All solutions, including electrolytes and samples, were filtered through a 0.2-μm Nylon-66 membrane syringe filter (Cole-Parmer, Chicago, IL, USA).

RESULTS AND DISCUSSION

Effect of electrode alignment

The dependence of the detector response (peak height) on the electrode alignment at the end of a 60 cm × 25 μm capillary was examined. The detector assymbly was arranged as shown in Fig. 2. The starting position of the tip of the carbon fiber (200 μm length) was at the center of the capillary and less than 10 μm from the end; at this position the measured signal current was assigned a value of 1. The error in determining the positions was *ca.* 1–3 μm. The position of the capillary was fixed and the position of carbon electrode was adjusted with the micropositioner. The signal obtained for a migrating sample zone was measured as the electrode was moved up, down, to the side, away in the axial direction and inside the capillary; currents was measured until its value decreased to about 10% of the maximum current. The results of this study are shown in Figs. 3 and 4; each point is the average of at least two measurements and the errors observed for the relative response was ~5%.

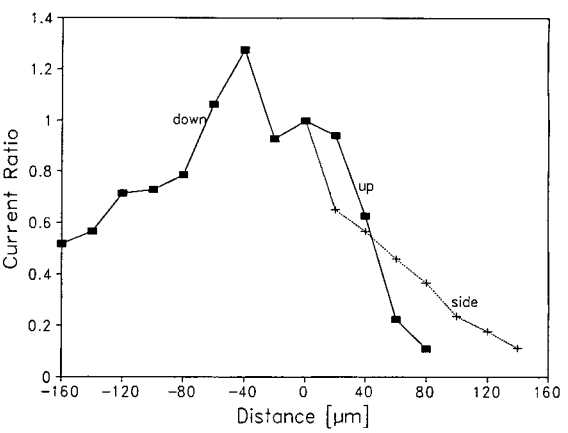

Fig. 3. Dependence of the relative detection sensitivity on the electrode alignment with the bore of a 25 μm I.D. capillary. The current obtained with the electrode at the center position just outside the capillary was given a value of 1.0. Experimental conditions: concentration of analyte, $1 \cdot 10^{-7}$ or $1 \cdot 10^{-5}$ mol/l; separation voltage, 30 kV; electrochemical detection potential, 700 mV; injection, 30 kV for 5 s; 60 cm × 25 μm capillary; electrode, 200 μm × 10 μm carbon fiber.

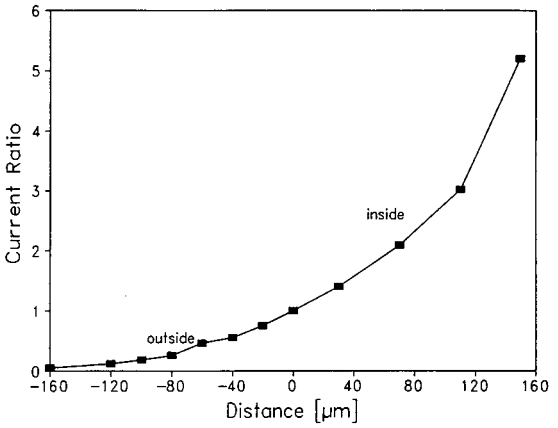

Fig. 4. Dependence of the relative detection sensitivity with axial position of the electrode. Conditions as for Fig. 3.

As expected, as the electrode was moved away upwards or to the side, the detection current decreased with the distance from the center point (see Figs. 3 and 4). When the analyte zone moves out of a capillary the influence of the electroosmotic and electrophoretic forces will stop immediately, and the analyte zone will then be pushed by the electroosmotic flow of the electrolyte still inside the capillary. This action will produce some convection and mixing of the analyte zone as it migrates into the solution in the detection cell. In addition to convection, analyte will diffuse in all directions away from the end of the capillary. When the electrode was positioned in the front of the capillary and then moved into the capillary, the detection sensitivity increased approximately five-fold (Fig. 4), because more electrode surface was exposed to the analyte, which gave improved electrochemical efficiency.

When the electrode was moved down from the center point (Fig. 3), the detection current first passed through a maximum value and then decreased continuously. It was found that the location of this current maximum could be changed to above or below the capillary depending on the density (change in electrolyte concentration) of the solution in the detection cell. The decrease in current past the maximum was slower than that observed in other directions, and was still 10% of the maximum value at a distance of 500 μm. As the analyte zone moves away from the tip of the capillary under the influence of a density difference, its velocity will increase with distance, and thus analyte transfer to the electrode surface will increase with electrode displacement from the center of the capillary. As the distance increases, however, convective mixing begins to dominate, and thus the signal will eventually begin to decrease. The results in Figs. 3 and 4 show that careful alignment of the electrode assembly is important for reproducible results. Once an electrode assembly is aligned it must be fixed firmly in that position.

Under optimum conditions a peak-to-peak noise of 0.01 pA (10 s) was observed when the amplifier was set at its highest sensitivity setting. These noise levels, which are better than or equal to those reported recently elsewhere [1,10], were not obtainable without the high-impedance reference input (see Experimental). These noise levels are of the same order of magnitude as that expected from the thermal noise in resistors, and further reductions in noise levels may require special low-noise circuits. The noise level observed with an electrochemical detection system depends on a number of factors such as electrode material, electrode size, potential applied to the electrode and electrolyte composition. Consequently the normal range observed for noise levels varied from 0.1 to 0.2 pA, depending on experimental conditions. When the effect of electrode position on the signal-to-noise ratio was evaluated with a 200 μm × 10 μm carbon fiber electrode, it was found that there was no obvious trend in the noise level as the electrode was moved down to 360 μm from the center point of a 25-μm capillary. In addition, the background noise observed when the electrode was placed 180 μm inside the end of the capillary was <0.1 pA with and without the application of a 30-kV separation voltage. Smaller capillaries (10 μm) were also used, but no significant decrease in the noise was observed. This is in contrast to other detection systems where the small capillaries (5 μm) were used to reduce background noise [11]. Changes in signal-to-noise ratio within the capillary should follow the same trend as the current ratio shown in Fig. 4. It was observed that for all the electrode positions in this study, the value of the separation voltage had small effects on the absolute level of the background signal, but had no discernable relationship with the value of the peak-to-peak noise.

The effect of electrode alignment on the column

efficiency was also measured. As expected column efficiency decreased as the electrode was moved away from the capillary. For example, when the electrode was moved from the center point downward by 200 μm the efficiency decreased about 80% due to convection and diffusion effects. The same trend was observed for other directions except when the electrode was moved into the capillary; from 0 to 150 μm inside the capillary, the efficiency increased by *ca.* 30%.

The detection sensitivity of a disk-shaped carbon electrode, made by breaking the carbon fiber on a cylindrical electrode, was also determined. Under similar experimental conditions, the sensitivity decreased approximately 40 times with a disk carbon electrode in comparison with cylindrical carbon fiber electrodes (about 250 μm in length). Since the ratio of surface areas of the two electrodes is about 100, this suggests that only about half of the area of the cylindrical electrode is in contact with the analyte. The peak-to-peak background noise observed with the disk electrode was essentially the same as for the cylindrical electrode. The dependence of detection sensitivity and signal-to-noise ratio on the position of the disk-shaped carbon electrode followed the same trend as that for cylindrical electrodes.

Detection of inorganic and organic ions

The performance of the electrode systems was tested for various inorganic ions and catechol; catechol was chosen since this compound was used previously in evaluations of electrochemical detectors for CE, and its use here permits a comparison with previous results [7,8,11]. Fig. 5 shows the electropherogram for the separation and detection of four transition metal ions at an ultramicro Hg-film electrode, 5 μm in radius with a thickness of 3 μm on a gold substrate. Electroreduction was used to detect these metal ions at −1100 mV *versus* SCE. The electrode was placed at the center of the outlet of the capillary. Separations were performed on 60 cm × 25 μm capillaries. A buffer of N,N-dimethylbenzylamine with HIBA was used as the background electrolyte; HIBA was employed as a complexing counter-ion to improve separation selectivity for the metal ions [4,5]. The sample mixture was injected by electromigration at 10 kV for 2 s; the concentrations were $1 \cdot 10^{-6}$ mol/l for Pb^{2+} and $1 \cdot 10^{-5}$ mol/l for other ions. The signal-to-noise ratio for Tl^{+}, Pb^{2+} and Cd^{2+} was larger than 100, and for Cu^{2+} was about 30. The detection limits for these transition metal ions were up to 100 times lower than those reported [16] for UV detection (*ca.* 8 fold for Cd^{2+} and *ca.* 100 fold for Pb^{2+}). The number of theoretical plates (calculated from peak width measured at the half peak height) was approximately $8.5 \cdot 10^{4}$ for Tl^{+}, $1.5 \cdot 10^{5}$ for Pb^{2+}, $3.6 \cdot 10^{5}$ for Cd^{2+} and $7.0 \cdot 10^{4}$ for Cu^{2+}. It should be noted that at the potential used (−1100 mV) oxygen was reduced at the electrode, and consequently high background currents were observed (note background current in Fig. 5 relative to that in Figs. 6 and 7). Thus the detection limits for these elements would be improved if the effects of oxygen were removed. The efficiency for Cd^{2+} is approximately twice that reported previously for end-column conductivity detection with 50-μm capillaries [17].

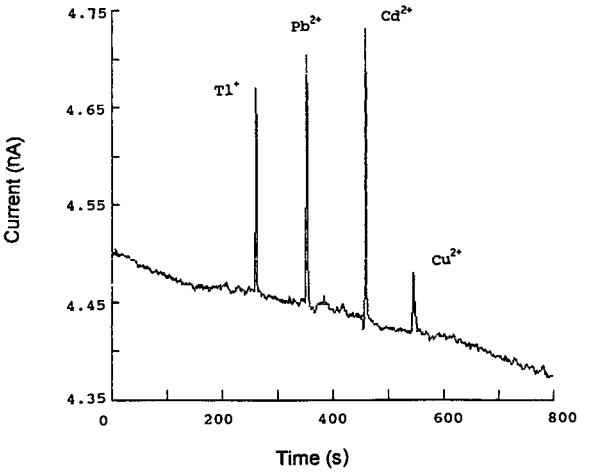

Fig. 5. Electropherogram of transition metal ions with detection at an ultramicro Hg-film electrode (10 × 3 μm). Experimental conditions: concentration of analyte, $1 \cdot 10^{-6}$ mol/l for Pb^{2+} and $1 \cdot 10^{-5}$ mol/l for other ions; separation voltage, 30 kV; electrochemical detection potential, −1100 mV; injection, 10 kV for 2 s.

Separation efficiency was also studied for an inorganic anion, NO_2^-; phosphate with CTAC was used as the operating electrolyte. CTAC was used to modify the internal wall of the capillary and reverse the direction of electroosmotic flow. A cylindrical carbon fiber electrode was held at 700 mV *versus* SCE to detect NO_2^- by electrooxidation. Fig. 6

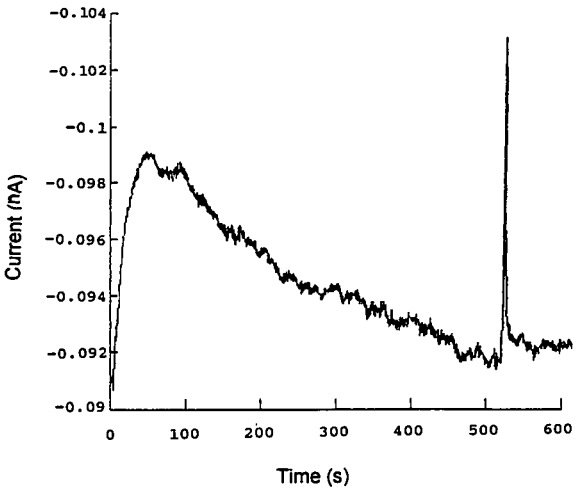

Fig. 6. Electropherogram of NO_2^- with detection at a carbon-fiber electrode. Experimental conditions: concentration of analyte, $1 \cdot 10^{-4}$ mol/l; separation voltage, 8 kV; electrochemical detection potential, 700 mV; injection, 8 kV for 1 s; 55 cm × 25 μm capillary; electrode, 200 × 10 μm carbon fiber.

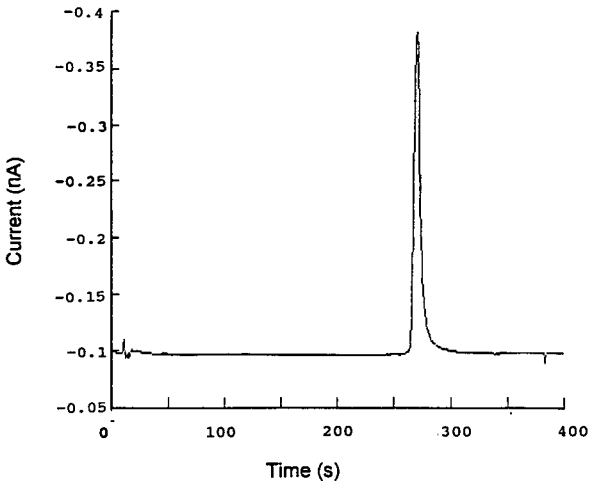

Fig. 7. Electropherogram of catechol with detection at a carbon-fiber electrode. Experimental conditions: concentration of analyte, $1 \cdot 10^{-7}$ mol/l; separation voltage, 30 kV; electrochemical detection potential, 700 mV; injection, 30 kV for 5 s; 60 cm × 25 μm capillary; electrode, 200 × 10 μm carbon fiber.

shows an example of the NO_2^- separation. The signal-to-noise ratio was about 20. The number of theoretical plates was $1.5 \cdot 10^6$, which corresponds to $2.8 \cdot 10^6$ plates per meter. It was observed that the column efficiency increased with a decrease in the separation voltage: plate numbers were $1.9 \cdot 10^5$ at 30 kV, $2.7 \cdot 10^5$ at 20 kV and $6.0 \cdot 10^5$ at 10 kV. This is opposite to the trend expected from longitudinal diffusion effects, and it is unlikely that Joule heating [18] would cause such large effects in a 25-μm capillary. Surface adsorption of the negative charged NO_2^- onto the positively charged surface of the capillary (due to presence of CTAC) may be a factor, but further studies with different concentrations of CTAC would be required to establish if this is the cause of this pattern.

The detection of catechol was tested with a cylindrical carbon-fiber electrode with an electrolyte containing 0.01 mol/l sodium phosphate and 0.01 mol/l SDS at pH 6.95. Fig. 7 shows an electropherogram for catechol with a signal-to-noise ration of ~1000. When a more dilute solution (10^{-8} mol/l) was sampled it was found that the detection limit (twice the peak-to-peak noise) was $5 \cdot 10^{-10}$ mol/l. The sample volume used here was *ca.* 2.2 nl (8 kV for 10 s), which corresponds to a detection limit of 1.1 amol. This compares favourably with a value of 56 amol reported recently for catechol [11] where a 5-μm capillary was used to reduce noise and enhance mass detection limits.

ACKNOWLEDGEMENTS

We acknowledge the financial support of the Natural Science and Engineering Research Council of Canada and Waters–Millipore. The authors also would like to thank John Fisher for his help with the assembly and design modifications of the electronic components, and Amoco Performance Products for donation of the carbon fibers.

REFERENCES

1 P. D. Curry, Jr., C. E. Engstrom-Silverman and A. G. Ewing, *Electroanalysis*, 3 (1991) 587.
2 M. J. Gordon, X. Huang, S. L. Pentoney, Jr. and R. N. Zare, *Science*, 242 (1988) 224.
3 H. H. Lauer and D. McManigill, *Anal. Chem.*, 58 (1986) 165.
4 M. Chen and R. M. Cassidy, *J. Chromatogr.*, 640 (1993) 425.
5 F. Foret, S. Fanali, A. Nardi and P. Bocek, *Electrophoresis*, 11 (1990) 780.
6 T. M. Olefirowicz and A. G. Ewing, *Anal. Chem.*, 62 (1990) 1872.
7 R. A. Wallingford and A. G. Ewing, *Anal. Chem.*, 59 (1987) 1762.

8 R. A. Wallingford and A. G. Ewing, *Anal. Chem.*, 61 (1989) 98.
9 X. Huang and R. N. Zare, *Anal. Chem.*, 62 (1990) 443.
10 T. J. O'Shea, R. D. Greenhagen, S. M. Lunte, C. E. Lunte, M. R. Smyth, D. M. Radzik and N. Watanabe, *J. Chromatogr.*, 593 (1992) 305.
11 X. Huang, R. N. Zare, S. Sloss and A. G. Ewing, *Anal. Chem.*, (1991) 189.
12 R. A. Wallingford and A. G. Ewing, *Anal. Chem.*, 60 (1988) 1972.
13 M. Kaganov, *Am. Lab.*, March (1992) 59.
14 J. F. Keithley, J. R. Yeager and R. J. Erdman, *Low Level Measurements*, Keithley Instruments, Cleveland, OH, 1984.
15 W. Lu and A. S. Baranski, *J. Electroanal. Chem.*, 335 (1992) 105.
16 A. Weston, P. Jandik, W. R. Jones and A. L. Heckenberg, *J. Chromatogr.*, 593 (1992) 289.
17 X. Huang and R. N. Zare *Anal. Chem.*, 63 (1991) 2913.
18 J. W. Jorgenson and K. D. Lukacs, *Science*, 222 (1983) 266.

Journal of Chromatography, 640 (1993) 441–444
Elsevier Science Publishers B.V., Amsterdam

CHROMSYMP. 2709

Capillary electrophoretic determination of inorganic ions in a prenatal vitamin formulation

Michael E. Swartz

Millipore Waters Chromatography, 34 Maple Street, Milford, MA 01757 (USA)

ABSTRACT

Methods for the quantitative analysis of three cations (calcium, iron and zinc), and the qualitative analysis of several anionic species (chloride, sulfate, nitrate, citrate, fumerate, phosphate, carbonate and acetate) from a prenatal vitamin formulation by two different capillary ion electrophoresis methods are reported. The cation method was evaluated for detection and quantitation limits, precision, accuracy and linearity. For standard solutions, detection limits into the ng/ml range, and reproducibility that averaged less than 1% for migration time and 2% for area response were generated. Calibration plots exhibited linearity in excess of three orders of magnitude. In addition, excellent agreement between capillary ion electrophoresis and flame photometry quantitative results for the cation analyses were obtained.

INTRODUCTION

The use of capillary electrophoresis, especially micellar electrokinetic capillary chromatography (MECC), for the analysis of small organic molecules is quickly becoming a valuable analytical tool in the pharmaceutical laboratory [1]. This is due to the fact that these types of compounds, present as active ingredients, often constitute the major proportion of the formulation. Of increasing importance, however, are small-molecular-mass ionic species frequently present in the same formulation. This paper describes the use of an emerging capillary electrophoretic technique called capillary ion electrophoresis (CIE; Waters' trade name Capillary Ion Analysis, CIA) that utilizes indirect ultraviolet (UV) detection to simplify the analysis of small molecular weight ionic species. Reports of the application of electrophoresis to the determination of these types of ions dates back to at least 1967 [2]. More recently, however, reports have appeared in the literature refining the methods and techniques involved for both anionic [3] and cationic [4,5] species. We have adapted the use of these methods for the analysis of these species in a prenatal vitamin formulation. Such species are currently analyzed by ion chromatography (IC), flame photometry (ICP) or atomic absorption (AA). CIE offers several potential advantages including speed, cost, sensitivity and selectivity, as well as offering an alternate to the established methods for the confirmation of results.

EXPERIMENTAL

Apparatus

A Waters Quanta 4000 capillary electrophoresis system was used throughout (Millipore Waters Chromatography, Marlboro, MA, USA). All separations were performed on standard untreated capillaries, 60 cm × 75 μm I.D. Anion analysis was performed using a negative power supply, with indirect UV detection at 254 nm. Cation analyses were performed using a positive power supply, with indirect UV detection at 185 nm. Data were collected and processed on an 845 Chromatographic Data Workstation (Millipore) at 10 points/s. Injections were performed hydrostatically for 30 s (10 cm height). An applied voltage of 20 000 V was used throughout.

0021-9673/93/$06.00

Chemicals and supplies

All chemicals were purchased commercially from either Sigma (St. Louis, MO, USA) or Aldrich (Milwaukee, WI, USA) in the highest purity available, and were used as is without further purification.

Electrolyte solutions

Prepackaged electrolyte solutions for CIE are commercially available and were obtained from Millipore, prepared in Milli-Q water (Millipore), and used as directed without modification. The anion electrolyte was 5 m*M* chromate, 0.4 m*M* CIA-Pak OFM anion BHT, pH 8.0. The electrolyte used for the analysis of cations was 5 m*M* UV-CAT-1, 6.5 m*M* 2-hydroxyisobutyric acid, pH 4.4.

Detection limits and reproducibility

Detection limits were defined as a signal-to-noise ratio (*S/N*) of 3. Quantitation limits were defined as a *S/N* of 10. *S/N* was determined at 1.0 μg/ml, and extrapolated to the appropriate limit. Reproducibility was determined at 1.0 μg/ml, chosen to closely approximate the quantitation limit. All data is an average of three determinations.

Sample preparation and quantitation

For quantitative analysis three tablets of a common commercially available over the counter prenatal vitamin formulation were assayed. Sample preparation consisted of adding a tablet to 500 ml of water adjusted to pH 2.0 with 6 *M* nitric acid. The solution was then sonicated for 30 min, followed by a 5-min stirring. Volumes of 10 ml of the resulting solution were filtered using a Millex HA filter (Millipore), discarding the first ml. The filtrate was then diluted 1:50 with water and injected. Stock standards were prepared in water at the 1000 μg/ml level and diluted to the desired concentration. Quantitation was performed by single point external standard calibration. An aliquot of each sample analyzed by CIE was sent to the laboratory of the Chemistry Department of the University of Vermont (Burlington, UT, USA) for the ICP analyses.

RESULTS AND DISCUSSION

Method validation

According to the United States Pharmacopeia (USP) [6] there are five parameters that need to be adequately investigated and documented to validate a method. These parameters are precision, accuracy, detection and quantitation limits, linearity and selectivity. With the exception of selectivity, which has been adequately documented previously [4,5], each of these parameters was investigated in turn. Linearity was evaluated from 100 μg/ml to the detection limits for a representative sample of inorganic anionic and cationic species. Acceptable linearity of peak area response was obtained over the entire concentration range with correlation coefficients ranging from 0.998 to 1.000. Detection (*S/N* = 3) and quantitation (*S/N* = 10) limits are shown in Table I. Excellent sensitivity with detection limits to the ng/ml level and quantitation limits to the 1.0 μg/ml level are indicated. The precision of peak area response and migration time were evaluated by per-

TABLE I

CIE DETECTION LIMITS, QUANTITATION LIMITS AND REPRODUCIBILITY

Conditions as outlined in Experimental. Data are for ten replicate injections. For reproducibility a 1.0-μg/ml standard solution of each species was evaluated to represent an approximation to the quantitation limit.

Species	Detection limit, *S/N* = 3 (ng/ml)	Quantitation limit, *S/N* = 10 (μg/ml)	Migration time, R.S.D. (%)	Area, R.S.D. (%)
Calcium	274	0.913	0.82	2.23
Zinc	313	1.04	0.84	2.06
Iron	326	1.09	0.86	1.77
Sulfate	157	0.523	0.17	1.90
Nitrate	210	0.700	0.17	1.58

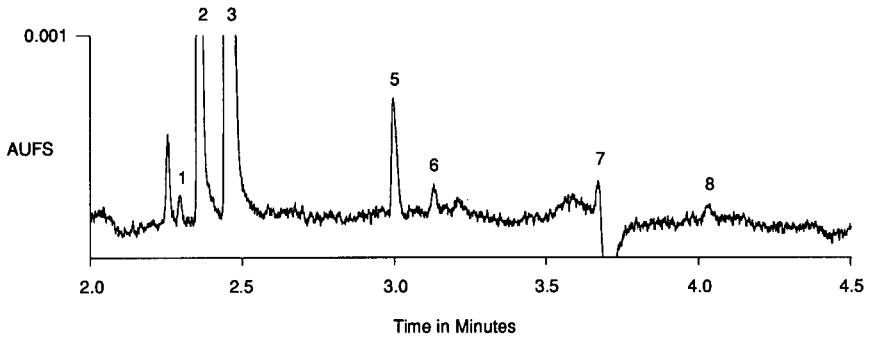

Fig. 1. Electropherogram of prenatal vitamin tablet extract using anion method. Electrolyte: 5 m*M* chromate, 0.4 m*M* CIA-Pak OFM anion BHT, pH 8.0. An untreated capillary, 60 cm × 75 μm I.D., a negative power supply, with indirect UV detection at 254 nm was used. Injections were performed hydrostatically for 30 s (10 cm height). An applied voltage of 20 000 V was used throughout. Peaks: 1 = chloride; 2 = sulfate; 3 = nitrate; 4 = citrate; 5 = fumerate; 6 = phosphate; 7 = carbonate impurity; 8 = acetate. Unlabeled peaks are unknowns.

forming 10 replicate injections, as summarized in Table I. A 1.0-μg/ml standard solution of each species was chosen for this evaluation to represent an approximation to the quantitation limit (Table I).

Prenatal vitamin tablet quantitation

Following sample preparation the vitamin tablet extract was analyzed for both anionic and cationic content. The result of the anion analysis is shown in

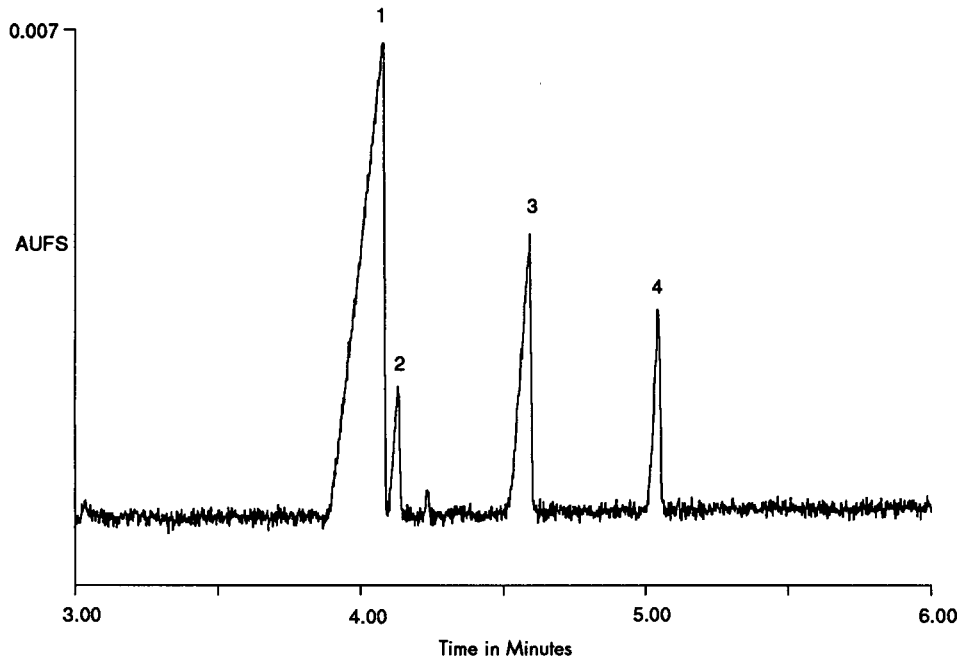

Fig. 2. Electropherogram of prenatal vitamin tablet extract using cation method. Electrolyte: 5 m*M* UV-CAT-1, 6.5 m*M* 2-hydroxyisobutyric acid, pH 4.4. An untreated capillary, 60 cm × 75 μm I.D. and a positive power supply with indirect UV detection at 185 nm was used. Peaks: 1 = calcium; 7.2 μg/ml; 2 = sodium, 0.560 μg/ml; 3 = iron(II), 2.31 μg/ml; 4 = zinc, 0.950 μg/ml.

TABLE II

VITAMIN TABLET CATION QUANTITATION BY CIE

Conditions as detailed in Experimental. Data is the average of triplicate determinations in μg/ml.

Species	Tablet 1		Tablet 2		Tablet 3	
	CIE	ICP	CIE	ICP	CIE	ICP
Calcium	7.20	7.84	7.75	8.60	8.04	9.02
Iron	2.31	2.10	2.66	2.42	2.58	2.46
Zinc	0.95	1.07	0.99	1.15	1.03	1.13

Fig. 1. All of the anionic species identified on the label of the formulation were identified. Quantitation of the levels of each of these species was not performed in this case due to the fact that the levels were not reported on the label. Levels of three of the four cationic species present in the formulation were documented on the label, however, and were used to assess the quantitative accuracy of CIE in comparison with ICP. Fig. 2 presents the results of the cationic analysis on the identical sample used to generate Fig. 1, and submitted for ICP analysis. The comparison of the quantitative results between the two analytical methods (CIE and ICP) for the analysis of three separate tablets is summarized in Table II. Given the 2% error of CIE (Table I) and the 2–9% error obtained from the ICP measurements, these numbers can be shown to overlap within the experimental error and are therefore equivalent. It should also be noted that CIE possess the ability to speciate between iron(II), the species present in the formulation, and iron(III), while ICP does not.

CONCLUSIONS

The results of this work indicate that CIE is a viable alternative to the more traditional methods of analysis for samples of this type, as well as offering significant improvements in efficiency and analysis time. As defined by USP criteria, the reproducibility, linearity, selectivity and sensitivity of this technique are adequate to validate the types of assays used in the pharmaceutical industry. Work continues in our laboratory towards the adoption of these methods to other types of samples of interest in this area.

ACKNOWLEDGEMENTS

The author acknowledges William R. Jones and Joseph Romano for their valuable assistance with this project, and Mathew Swartz of the University of Vermont Chemistry Department for the ICP analyses.

REFERENCES

1 M. E. Swartz, *J. Liq. Chromatogr.*, 14 (1991) 923.
2 S. Hjertén, *Chromatogr. Rev.*, 9 (1967) 122.
3 P. Jandik, W. R. Jones, A. Weston and P. R. Brown, *LC · GC*, 9 (1991) 634.
4 W. R. Jones and P. Jandik, *J. Chromatogr.*, 546 (1991) 445.
5 M. Koberda, M. Konkowski, P. Youngberg, W. R. Jones and A. Weston, *J. Chromatogr.*, 602 (1992) 235.
6 *United States Pharmacopeia XXII, NF XVII*, United States Pharmacopeia Convention, Rockville, MD, 1990.

Journal of Chromatography, 640 (1993) 445–461
Elsevier Science Publishers B.V., Amsterdam

CHROMSYMP. 2810

Anion screening for drugs and intermediates by capillary ion electrophoresis

Jay B. Nair* and Christopher G. Izzo

Analytical Research and Development, Bristol-Myers Squibb Pharmaceutical Research Institute, New Brunswick, NJ 08903-0191 (USA)

ABSTRACT

A method is described to screen bulk pharmaceuticals and their synthetic intermediates for common anions. Capillary electrophoresis (CE) is a rapid separation technique which operates on the basis of the differential migration of charged and uncharged species in an electric field. Capillary ion electrophoresis utilizes the principles of CE in combination with an osmotic flow modifier and indirect UV detection for the rapid determination and quantification of ions. A Waters Quanta 4000 capillary electrophoresis system, equipped with a 60 cm × 75 μm I.D. fused-silica capillary in conjunction with a patented chromate buffer and osmotic flow modifier is used. The detection limit of the assay is 0.5 μg/ml for most anions. Parameters have been optimized so that all analytes migrate within 5.0 min. A number of optimization experiments for parameters such as loading time, voltage, linearity, precision and detection limit of the system are demonstrated. The effects of the presence of organic solvents in the sample diluents on the migration times of anions are examined. Applications of the technique to pravastatin sodium, taxol and iopiperidol are illustrated. Comparison to ion chromatography, advantages and disadvantages, is discussed.

INTRODUCTION

The safety of pharmaceuticals is critically related to their purity, thus the pharmaceutical industry spends a great deal of effort to minimize impurities in bulk drugs and to control degradation of the formulated products [1]. In the past 25 years, impurity analysis has received increasing attention due to the ability of contemporary analytical methodology to yield detailed information on trace impurities.

Impurities typically originate from raw materials, solvents, intermediates, and by-products [2], as well as degradation products and contaminants in the synthetic pathway [2–4]. Thus, there exist many opportunities for impurities to arise in the synthetic process, and despite sample cleanup, many residues remain in the end product in varying amounts.

The present study is useful in screening for anionic impurities in bulk drugs and intermediates. The goal of this screening is the qualitative or the semi-quantitative determination of anionic impurities. Once anions are found using this screening method, individual ion chromatographic (IC) or capillary ion electrophoresis (CIE) (Waters' trade name: Capillary Ion Analysis, CIA) assays are developed for each drug substance specifically for routine monitoring or assay transfer to other labs.

HPLC with refractive index (RI) detection and low-wavelength UV detection have been applied to the analysis of non-chromophoric impurities in pharmaceutical compounds. RI detection has sensitivity problems with polar ionic species, and UV detection is not universally selective. UV detector quality is a critical factor in the success of assays utilizing end absorption, a common feature of many compounds. The separation of ionic species can also be a problem in HPLC since they are usually not well retained. Ion pairing is the most commonly used approach to circumvent this.

IC is the most commonly used method for monitoring ionic species. A gradient suppressed ion

* Corresponding author.

0021-9673/93/$06.00

chromatographic method for screening anions in pharmaceutical compounds is reported [5]. Runtimes are typically more than half an hour for this technique.

Capillary electrophoresis (CE) is an extremely powerful technique with many advantages over gel electrophoresis and fluid chromatographies. An asset of primary importance is the time efficiency of CE separations. Most research using CE in the eighties focused on biomolecules, *i.e.*, proteins, peptides and DNA. Schoots *et al.* [6] analyzed organic anions and quantitated hippuric acid in the blood serum of patients with chronic renal failure. The analysis time for their assay by CE was 8 min, whereas that of the corresponding HPLC assay was 90 min. Furthermore, CE allows smaller sample volumes and greater resolution than other techniques, and no gels, columns, or other complex separation media are required. Upon completion of an analysis, sample residues may be removed from the capillary by purging under vacuum for a few minutes, eliminating the need for more time consuming column washes. Also, minimal sample preparation (filtering through a syringe filter) is required (for an introductory discussion on CE, see ref. 7). The use of CE for the analysis of certain low-molecular-mass ionic species has been documented [8–10].

CIE is a relatively new offshoot of CE. It utilizes the basic principles of CE accompanied by indirect UV or fluorescence detection. An ion with UV absorptive or fluorescent properties in the carrier electrolyte serves as the "visualization agent" which creates a high background signal [11]. Analyte ions are then detected as negative peaks against the constant background. The resolution of complex mixtures is optimized by adding cationic surfactants as osmotic flow modifiers (OFM) [12]. These OFMs control the electroosmotic flow of buffer through the capillary. The Waters Quanta 4000 capillary electrophoresis system combines indirect UV detection, OFM electrolytes, and CE instrumentation to facilitate automated CIE [13] (for a discussion of the theory and range of applications of CIE, see ref. 14).

The effects of various parameters on CE separations have been studied by several investigators [15]. CIE separations can be optimized by varying different parameters such as loading time, run voltage, sample concentration, and sample diluent. In the present study we examined the effects of these parameters. Using optimized parameters, applications of this screening technique are demonstrated in the case of three drug substances.

This anion screening can be helpful in several situations. Such screening method will aid Chemical Process Research departments in determining what assays may be required for characterizing a given drug or intermediate and for setting specifications during the drug development process. Analytical Research and Development can identify potential impurities that are transparent to other chromatographic methods and thereby prevent mass balance concerns before they become issues. In other words, this screening can eliminate the possibility (or establish the presence) of certain anions when mass balance questions arise in certain batches. For synthetic organic chemists and pilot plant chemical engineers, this screening thus give useful information for troubleshooting chemical processes. Finally, it aids in the complete characterization of research reference standards.

The three drug substances illustrated in the present study are pravastatin sodium, taxol and iopiperidol. Pravastatin sodium, a member of the HMG-CoA reductase enzyme inhibitor class, is used to treat primary hypercholesterolemia when diet alone is insufficient. Taxol is a very promising new anticancer agent. Iopiperidol is a new iodinated radiographic contrast imaging agent.

As part of testing the usefulness and efficiency of this screening method, we screend these three compounds, established the absence or the presence of anions in them. If anions were found, individual isocratic IC or sprecific CIE assays were developed to monitor them on a regular basis. Not all the anions detected in this screening had to be quantified at all times. In consultation with the synthetic organic chemists and toxicologists, judgements were made on which anions were important to be monitored routinely.

EXPERIMENTAL

Instrumentation

A Waters Quanta 4000 capillary electrophoresis system (Waters division of Millipore, Milford, MA, USA) equipped with a Waters "AccuSep" 60 cm × 75 μm I.D. fused-silica capillary was used. Data ac-

quisition was performed using a VG Multichrom System on a Microvax computer (Digital Equipment Corporation, Maynard, MA, USA).

Reagents

Sodium chromate AR crystals were obtained from Mallinckrodt (Paris, KY, USA). Sulfuric acid and sodium acetate trihydrate crystals were purchased from J. T. Baker (Phillipsburg, NJ, USA), and sodium nitrite, sodium fluoride, and dibasic sodium phosphate were obtained from Fisher Scientific (Pittsburgh, PA, USA). Sodium bromide, sodium chloride, sodium sulfate, and sodium citrate were obtained from the Aldrich (Milwaukee, WI, USA). Waters Anion-BT electroosmotic flow modifier was obtained from the Waters division of Millipore. Deionized water was from a Waters Milli-Q System. Bulk drug substances were obtained from the Chemical Process Research and Technology Laboratories at the Bristol-Myers Squibb Company (New Brunswick, NJ, USA).

Electrophoretic conditions

Experiments were performed to optimize the CIE system. Unless otherwise specified, the standard conditions used for individual parameters of the system are: 20 kV run voltage, 20 s hydrostatic loading time, and a working electrolyte consisting of a mixture of chromate, dilute sulfuric acid, and Waters Anion-BT OFM [12]. Detection was by UV absorbance at 254 nm. Under these conditions, all the analytes of interest elute wihtin 5.0 min, after which the capillary is purged for 2.0 min under vacuum to remove any remaining drug substance components. Thus, samples can be screened for these anions with a total run time of seven minutes.

Stock standard mixture

The anion screen standard was made by weighing 65.0 ± 2 mg of sodium bromide, 83.0 ± 2 mg of sodium chloride, 75.0 ± 2 mg of sodium sulfate, 75.0 ± 2 mg of sodium nitrite, 78.0 ± 2 mg of sodium citrate, 112.0 ± 2 mg of sodium fluoride, 75.0 ± 2 mg of dibasic sodium phosphate, and 115.0 ± 2 mg of sodium acetate trihydrate crystals into a 100-ml volumetric flask, and diluting to volume with water. This is a concentrated stock solution (approximately 500 μg/ml of each anion) from which appropriate dilutions are made. This stock standard mixture is stable in the refrigerator for up to two months.

Anion screen standard

A fifty-fold dilution of the stock standard mixture gives the 10 μg/ml anion screen standard. Unless otherwise specified, this is the solution used as the standard in all the experiments in this study.

RESULTS AND DISCUSSION

Several parameters can be optimized for CIE. In this study we chose loading time, run voltage, linearity, effect of organic diluents, precision and detection limit. Some of these studies helped us to grasp the nuances of the technique and to test the limits of the system in reality *versus* what was claimed by the manufacturer. Some studies such as the effect of the organic diluent shows the extreme care a user needs to take for preparing standards even for qualitative work with this technique.

Loading time experiment

The purpose of this optimization study is to yield analyte peaks large enough to be quantified reproducibly with baseline separation. The Quanta 4000 is capable of two modes of sample introduction: hydrostatic and electromigration. In this study we used only hydrostatic loading due to the inherent advantages in precision [14]. Loading time is defined as the time in which the inlet end of the capillary is raised to a specific height above the output end. The Quanta 4000 has this height fixed at 10 cm. Loading time is directly proportional to the volume of sample introduced into the capillary in this mode. The effects of different hydrostatic loading times on peak shape and peak area were studied by injecting the anion screen standard at 10, 20, 30, 50, 70 and 90 s loading times. All other parameters were as specified in the experimental section.

The effect of loading time on peak area for some common anions is shown in Fig. 1. The volume of sample loaded was not measured experimentally. Loading time proved to be a good indirect measure of the volume of sample injected for all practical purposes of our study. As expected, peak area increases with increasing loading times. As seen in Fig. 1, for some anions such as bromide, there is a direct linear relationship up to 50 s loading time.

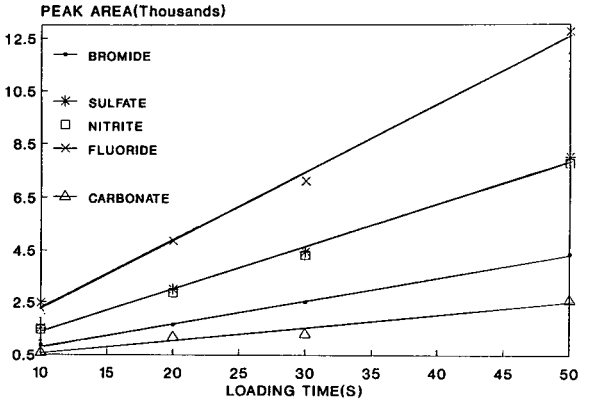

Fig. 1. Effect of loading time on peak areas of some common anions.

Beyond this, the capillary becomes overloaded, resulting in peak overlap. Representative electropherograms are shown in Fig. 2. Fig. 2A shows the electropherogram of the injection at 10 s loading time. Although the peaks are well resolved, the areas are relatively small for these analytes. This is due to the small volume of sample loaded into the capillary relative to longer loading times. This loading time is therefore not acceptable. Fig. 2B–F shows the results of the injections at 20, 30, 50, 70 and 90 s loading time, respectively. From these electropherograms, we arrived at an optimum loading time of 20 s, which, as evidenced in Fig. 2B, results in acceptable peak areas and shapes with little or no peak overlap. We thus confirmed that the default setting on the Waters Quanta 4000 (20 s) is indeed the optimum loading time. In all other optimization experiments in this study, 20 s loading time is used. At 30 s, the overlap between sulfate and nitrite peaks, as well as that between fluoride and phosphate, becomes visibly evident (Fig. 2C). The peaks retain their proper shapes. This loading time can be useful for applications where increased detection limits are required. At 50, 70 and 90 s loading time (Fig. 2D–F), the problems of overlap and skewed peaks become more pronounced. The electropherograms show that 70 and 90 s loading times are clearly unacceptable for this reason.

Run voltage experiment

The purpose of this experiment was to optimize the run voltage. Our objective was to have all the analytes in the standard elute before 5.0 min without peak overlap. The manufacturer-recommended run voltage is 20 kV, therefore we analyzed the range of voltage around this. Samples were loaded at 15, 18, 19, 20, 21, 22, 23, 24 and 25 kV.

A plot of run voltage *vs.* retention rime is shown in Fig. 3. It is evident that each analyte displays a linear, inverse relationship between these parameters. Representative electropherograms of these loadings are shown in Fig. 4. Note that in the 15-kV run, shown in Fig. 4A, the phosphate peak fails to elute within the 5.0-min run time. Running at 25 kV, as evidenced by Fig. 4C, results in shorter elution times, however the resolution suffers. In fact, as the voltage increases, although relative migration times remain the same, the separation deteriorates, as all the analytes migrate sooner. The analytes have less time to be subjected to separatory forces in the capillary, and progressively higher voltages result in poorer resolution.

We determined that 20 kV was indeed the optimum run voltage for our applications, as separation of the analytes of our standard mixture using this voltage are rapid enough to occur within 5.0 min without sacrificing resolution between the peaks (Fig. 4B).

Linearity experiment

The stock standard mixture was diluted to make solutions of the analytes at concentrations of 1, 5, 10, 20, 30, 40, 50, 60, 70, 80, 90 and 100 μg/ml. Each of these solutions were then injected three times on the CIE system using standard conditions. The resulting peak area values were then averaged, and the mean value for each concentration of a single analyte was used in the linear regression calculation for that analyte. Plots of concentration *vs.* peak area for each analyte are shown in Fig. 5. From this figure it can be seen that the dynamic linear range for the analytes in general ranges from 1 μg/ml to 20 or 30 μg/ml. Bromide is an exception, with an upper limit of its linear range at about 80 μg/ml. If the samples have higher anion concentration, they must be diluted to bring down the analyte concentration within the linear dynamic range. This range is rather very narrow as seen from Fig. 5. The coefficient

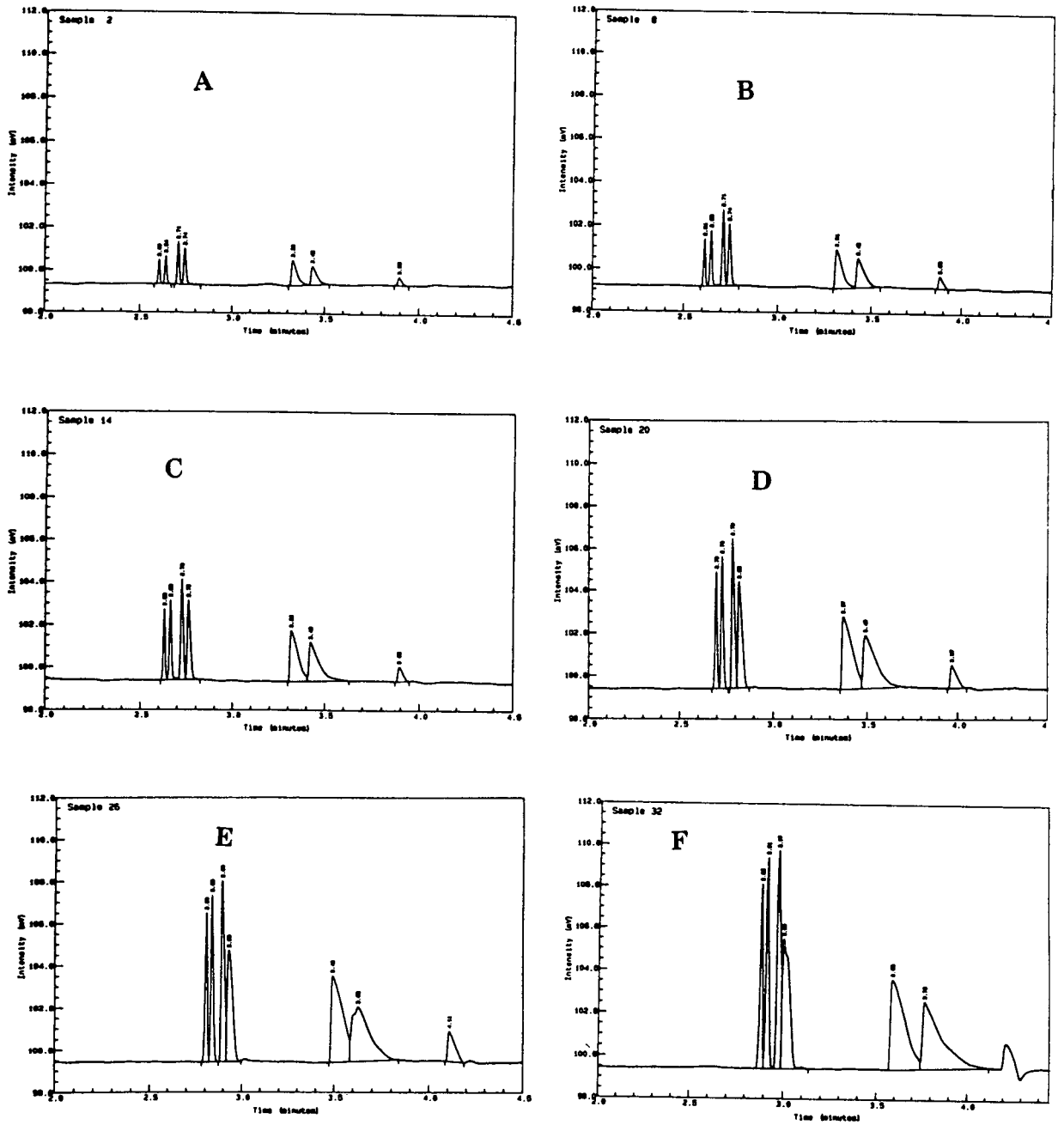

Fig. 2. Anion screen standard (10 μg/ml) at 20 kV run voltage and hydrostatic loading times of (A) 10 s, (B) 20 s, (C) 30 s, (D) 50 s, (E) 70 s and (F) 90 s. The migration order of anions is bromide, chloride, sulfate, nitrite, citrate fluoride and phosphate.

of variation for bromide, chloride and citrate are 0.999 or better. This may be due to their peak symmetry and ease of proper integration at higher concentrations compared to the other anions.

The electropherograms of representative injections at each concentration are shown in Fig. 6. This figure strikingly shows the peak migration time shift with respect to concentration. Thus it is impor-

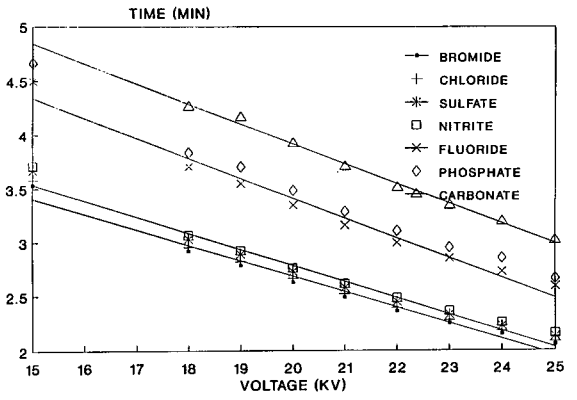

Fig. 3. Effect of run voltage on the migration times of some common annions.

tant to compare unknown samples to standards at similar concentration levels not only for quantitation but also for peak identification. This is particularly important in CIE since peak migration times are very close. Also in Fig. 6, it can be seen that the deviations from linearity at high concentrations for many of the analyte peaks, including fluoride and phosphate, are due to the fact that these concentrations overload the capillary.

The plots of concentrations *vs.* migration time for each analyte are shown graphically in Fig. 7. A "quantitative" picture of the above-mentioned shift in migration times can be seen in Fig. 7. As expected, the anions migrating late are the one most shifted with concentration. The early migrators, bromide, chloride, sulfate and nitrite are less affected by concentration. Calculation of the relative shift in migration times and the correlation with the theoretical prediction of migration times (or their shifts) are beyond the scope of the present study. On the other hand, a good understanding of the extent of this phenomena is essential for useful practical applications of this techniques.

As shown in Fig. 5, the working concentration range (range of interest from 1 to 10 μg/ml) is linear for practical purposes. The results of the linear regression calculations for each analyte in this range showed that all seven anions gave a correlation coefficient of 0.999 or better (Table I). This is a rather narrow linearity range. For qualitative as well as semi-quantitative applications of this technique, up to 30 μg/ml may be acceptable for most anions. If the analyte peaks in the sample fall above this range, then the sample was diluted down to ensure that all anion concentrations fell within this range. It is to be stressed that this is important not only for semi-quantitative work but also for quantitative identification as demonstrated in the above studies.

Effect of organic diluents

Many drugs and intermediates are insoluble in water or other aqueous solutions. Therefore they require organic solvents such as tetrahydrofuran (THF), dimethylacetamide (DMA) etc. to solubilize them. In such cases, anion screening by CIE can be performed by dissolving the samples and anion screen standard in the appropriate solvents. The addition of these solvents to the standard and sample solutions can, however, alter the profile of the analyte peaks and their migration times as shown below.

The effects of differing proportions of organic solvents in the sample diluent on peak shapes, retention times, and baseline stability were studied. The stock anion screen standard was diluted to make several 10 μg/ml solutions, each with 10% (v/v) of the respective organic solvent. The solvents examined were acetonitrile, methanol, isopropanol, THF and DMA. The effects of these organic solvents are shown in Fig. 8A–F. The screens with 10% (v/v) of acetonitrile, methanol, and isopropanol result in peak contamination by co-migration, while those made with THF (Fig. 8E) and DMA (Fig. 8F) result in better separation than the aqueous screen standard (Fig. 8A). The separation between fluoride and phosphate is better in THF and DMA (Fig. 8E and F) than the other solvents. Moreover it was observed that, the screen with 10% (v/v) of DMA increases peak migration times the most without resulting in co-migration or detrimental effects on peak shape (Fig. 8F). Therefore the effect of this solvent on migration times of anions was further investigated. A new set of solutions of anion screen standard (10 μg/ml) at varying proportions (0, 10, 20, 30, 40, 50, 60, and 80%, v/v) of DMA were made from the stock standard mixture. Fig. 9 graphically shows that migration times for all peaks increased with increasing amounts of DMA. The screens consisting of 40% or more DMA resulted in unacceptable baseline disturbances.

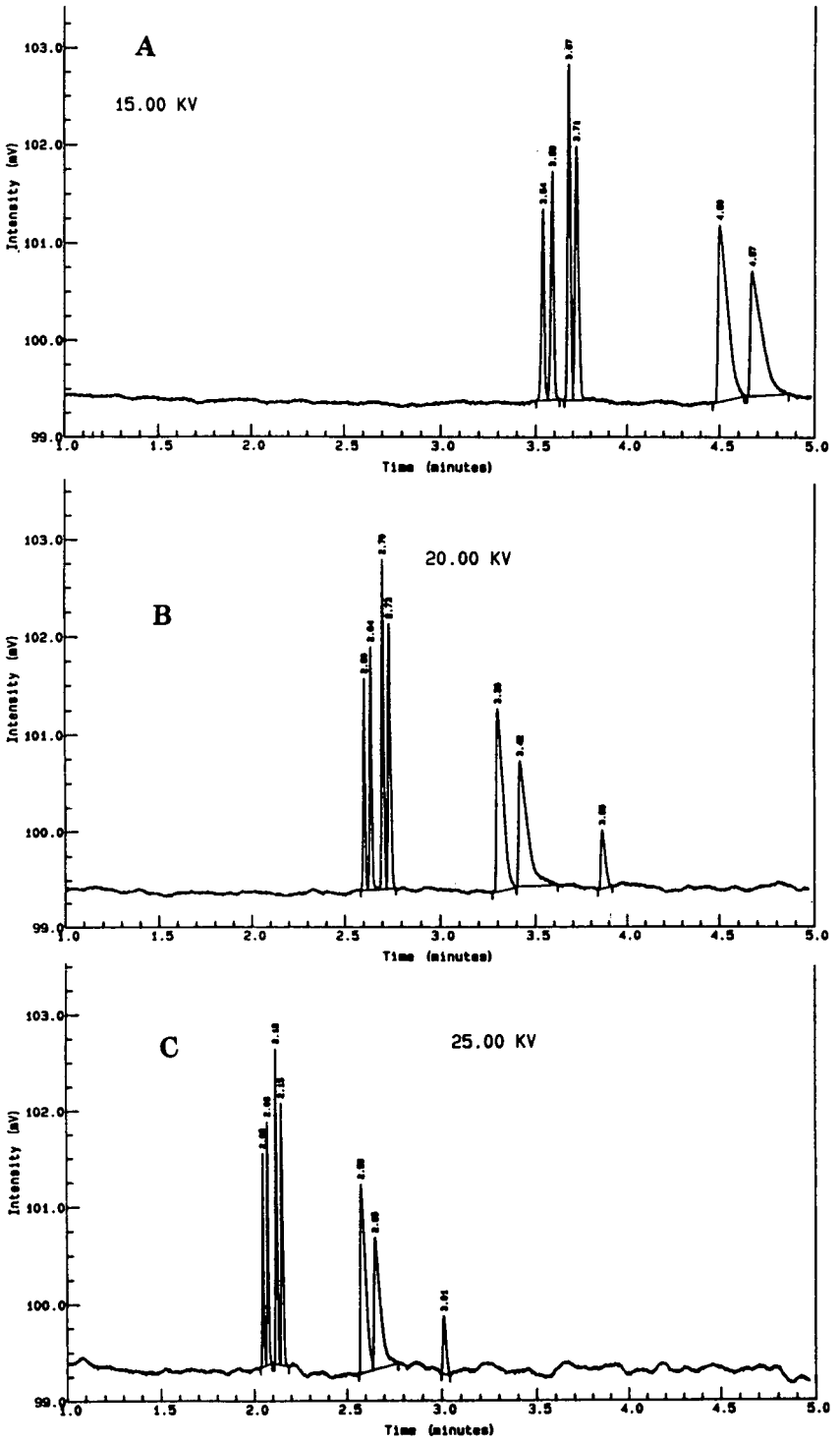

Fig. 4. Anion screen standard (10 μg/ml) at 20 s hydrostatic loading and run voltages of (A) 15 kV, (B) 20 kV and (C) 25 kV. The migration order of anions is bromide, chloride, sulfate, nitrite, citrate, fluoride and phosphate.

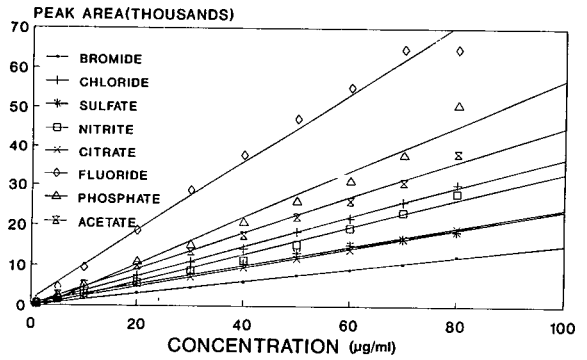

Fig. 5. CIE linearity: the effect of analyte concentration on peak area for eight common anions.

These shifts in migration times may be explained by the established theories of changes in electroosmotic flow when different molecules are introduced into the capillary. They illustrate a very important practical consideration. Even for qualitative identification purposes, it is of extreme importance that the standards are prepared in the exact same diluant as the sample. This may be a slightly unusual consideration for practitioners of HPLC or IC, where usually the retention time changes with sample diluents are minimal. This change in migration time of the anions is exemplified in the case of anion screening of taxol discussed below.

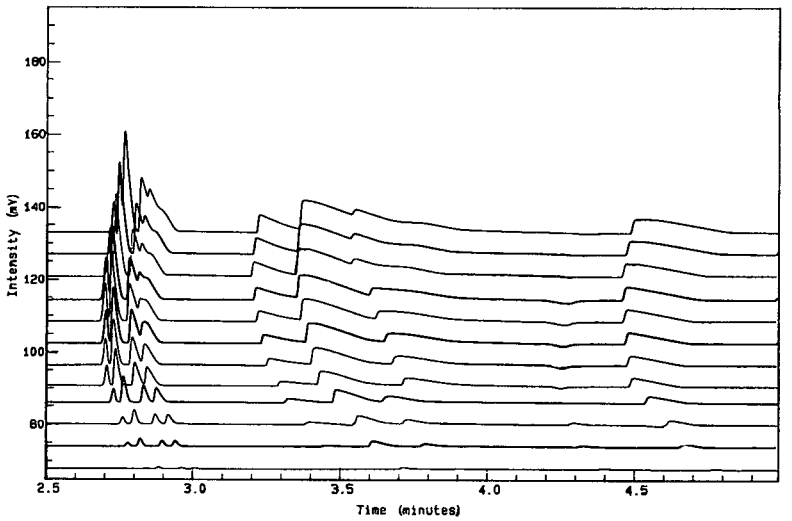

Fig. 6. Electropherogram of the anion screen standard at concentrations of (from bottom to top) 1, 5, 10, 20, 30, 40, 50, 60, 70, 80, 90 and 100 µg/ml. The run was made at 20 kV with a hydrostatic loading time of 20 s. The migration order of anions is bromide, chloride, sulfate, nitrite, citrate, fluoride, phosphate and carbonate.

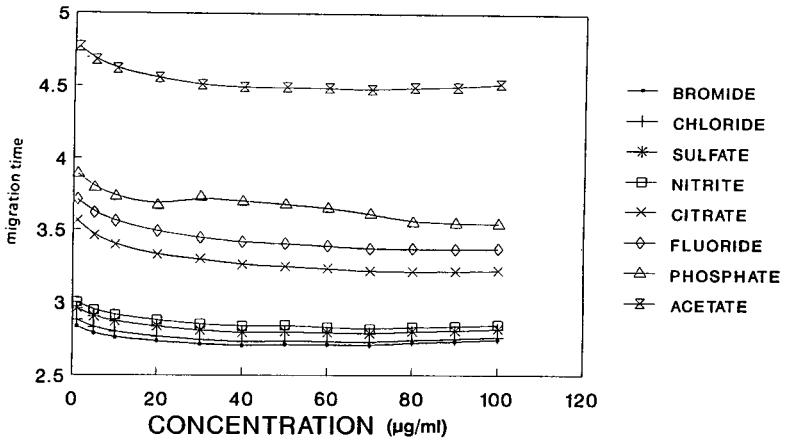

Fig. 7. Effect of analyte concentration on the migration times of common anions.

TABLE I

LINEARITY DATA FOR ANIONS IN THE RANGE 1–100 μg/ml

Concentration (μg/ml)	Mean peak area (n = 2)							
	Bromide	Chloride	Sulfate	Nitrite	Citrate	Fluoride	Phosphate	Acetate
1	140	439	320	344	162	980	456	526
5	868	2037	1496	1583	1165	4561	2377	2655
10	1650	3842	2858	2957	2514	9483	5096	5150
20	3161	7510	5502	5815	5239	18 664	10 981	9895
30	4533	10 938	8119	8793	7054	28 668	15 225	13 474
40	5967	14 320	10 470	11 372	9535	37 880	20 738	17 522
50	7671	18 492	13 244	15 354	11 817	47 343	26 081	22 095
60	9031	21 881	15 242	19 432	13 962	55 187	31 245	26 096
70	10 580	25 865	16 748	23 253	16 781	64 886	37 988	30 830
80	12 454	30 395	18 629	28 113	19 274	64 898	50 849	38 358
90	13 733	33 975	19 573	32 659	21 378	69 989	58 588	43 432
100	15 085	38 114	20 198	38 116	23 551	73 792	67 697	48 141
Intercept	55.5	−180.2	1250.6	−1531.0	84.2	3804.2	−3038.6	−360.4
Slope	151.5	377.6	211.1	370.8	236.4	774.6	654.3	472.1
	0.999	0.999	0.989	0.994	0.999	0.987	0.989	0.997

Precision

The goal of the precision experiment was to assess the peak area reproducibility of the CIE system. Standard conditions were used. Solutions containing 1 mg/ml of lopiperidol spiked with 1 μg/ml of the anion screen were made. The solution was injected eight times. The peak areas were then statistically analyzed. The peak areas of individual injections and the results of the statistical analysis for each analyte are shown in Table II. Standard deviation ranged between 2–7% for the anions. At 1 μg/ml, these standard deviations are acceptable for screening.

Detection limit and minimum quantifiable limit

The electropherogram of the detection limit standard mixture at 0.5 μg/ml of each anion, is shown in Fig. 10. Below 0.5 μg/ml, the signal to noise ratio is often less than acceptable. For drug concentrations of 1 mg/ml, 0.5 μg/ml corresponds to 0.05% (w/w). The detection limit of 0.05% (w/w) is sufficient for monitoring innocuous impurities such as common anions for mass balance purposes. If necessary, this detection limit can be lowered by increasing the drug concentration from 1 to 10 mg/ml or more. Solubility of the drug in a suitable solvent is the only limiting factor to this approach. The minimum quantifiable limit of the common anions is set at 1.0 μg/ml. An electropherogram of anion screen standards at this level is shown in Fig. 11 under optimized conditions.

COMPARISON OF CIE AND IC

The runtime savings in CIE is probably the most significant advantage over IC. CIE runtimes are typically less than 5 or 6 min. When the 2-min vacuum suction of the capillary is added to this time, the total analysis time is still less than 10 min. Standard IC methods may take almost twice as much analysis time for all these anions.

A more significant advantage of CIE over IC is the ease of sample preparation. The drug can be eliminated from the capillary easily by vacuum suction. Vacuum suction works well with most drug compounds or intermediates we have tried. Exceptions may be strong amine containing drugs. They may not be eliminated from the capillary readily by vacuum suction. In IC, either sample preparation to eliminate the drug beforehand or an elution protocol to elute off the drug from the column is necessary. This can be done by different means such as

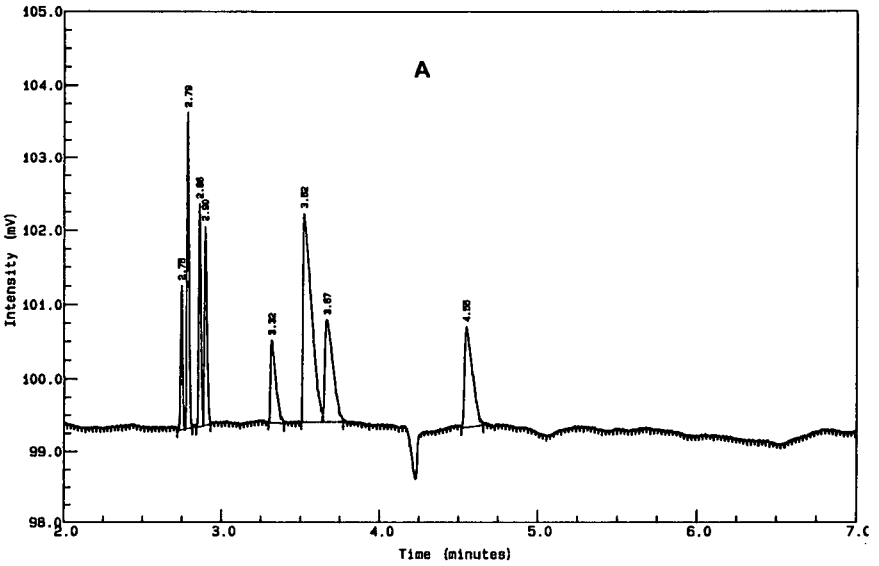
A
Intensity (mV)
Time (minutes)
105.0
104.0
103.0
102.0
101.0
100.0
99.0
98.0
2.0
3.0
4.0
5.0
6.0
2.79
3.32
3.82
3.67
4.89

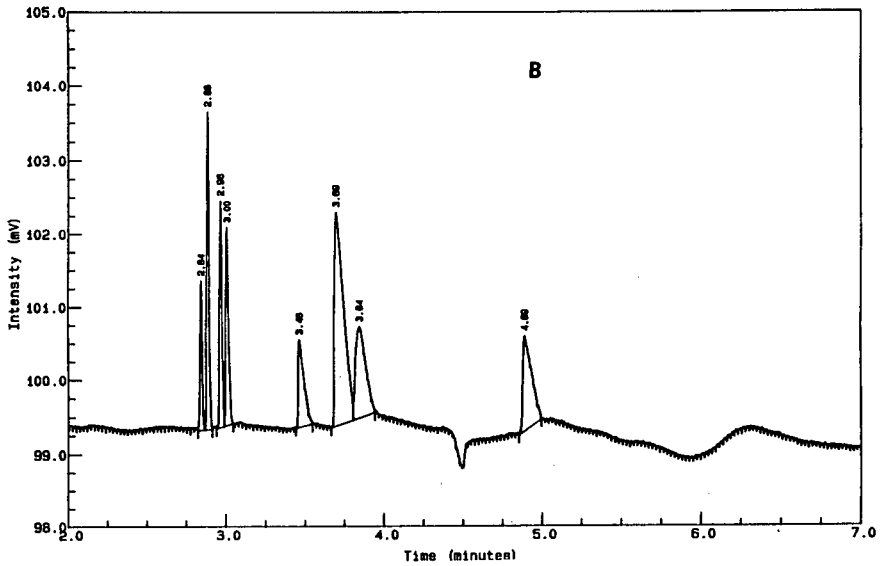
B
Intensity (mV)
Time (minutes)
105.0
104.0
103.0
102.0
101.0
100.0
99.0
98.0
2.0
3.0
4.0
5.0
6.0
7.0
2.88
2.84
2.98
3.00
3.49
3.89
3.84
4.89

Fig. 8.

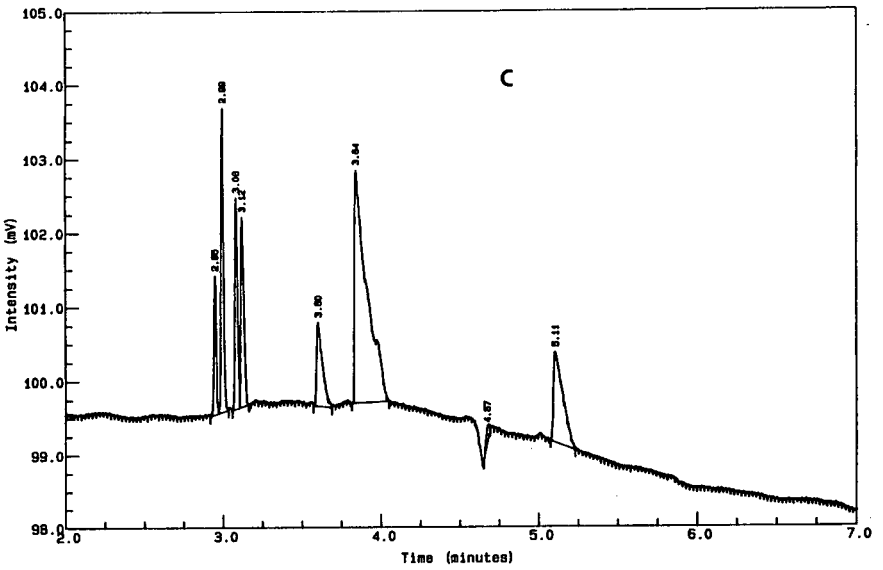

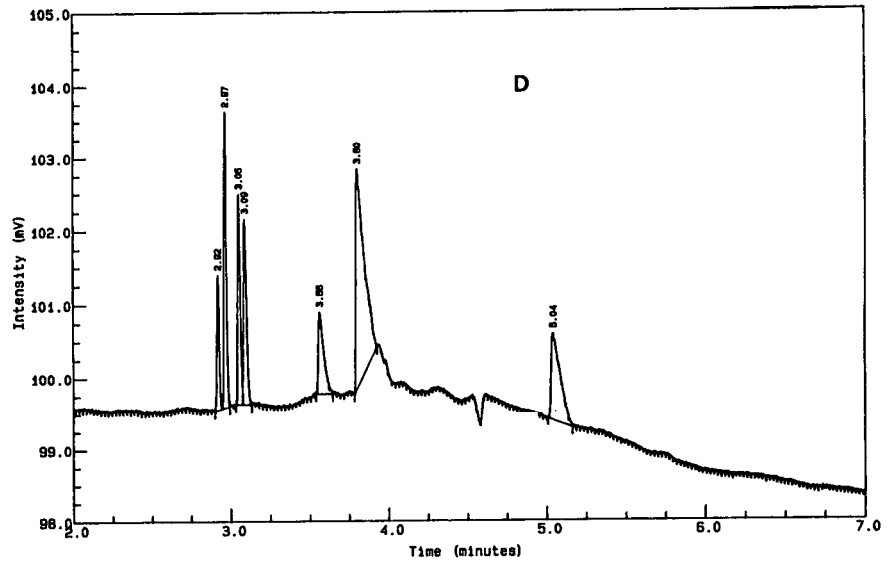

Fig. 8.

(*Continued on p. 456*)

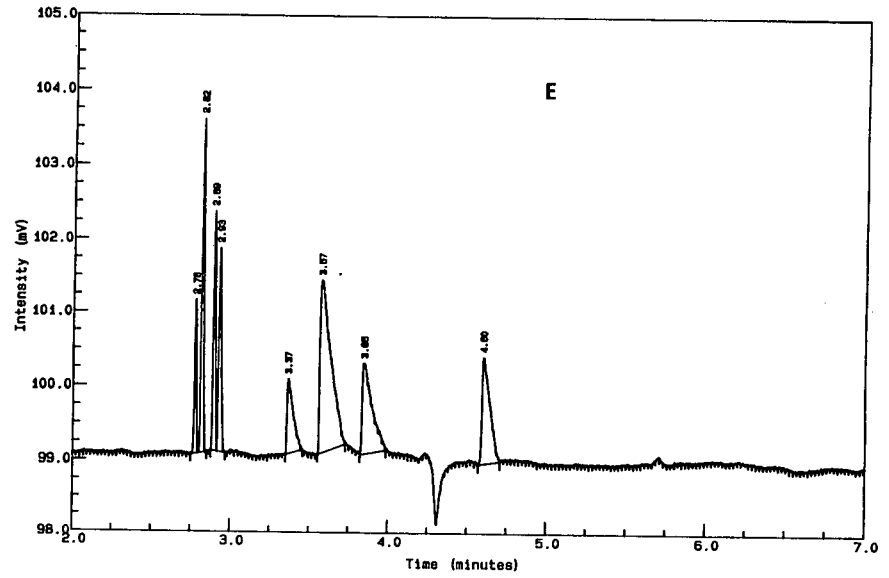

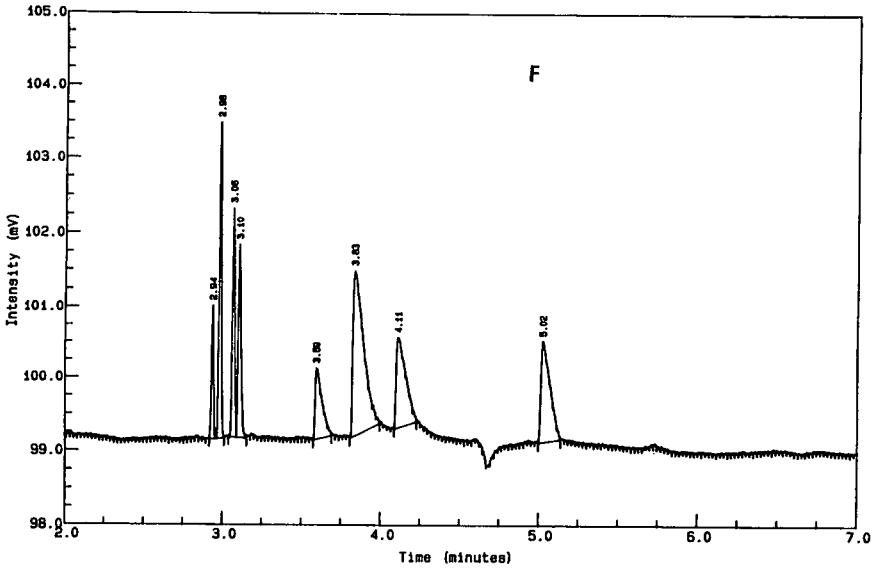

Fig. 8. Electropherograms of 10 μg/ml anion screen standard prepared in: (A) 100% water, (B) 10% acetonitrile, (C) 10% methanol, (D) 10% ispropanol, (E) 10% tetrahydrofuran and (F) 10% dimethylacetamide in water showing the effect of organic solvents in the sample diluent on peak shapes and retention times. The migration order of anions is bromide, chloride, sulfate, nitrite, citrate, fluoride, phosphate and carbonate.

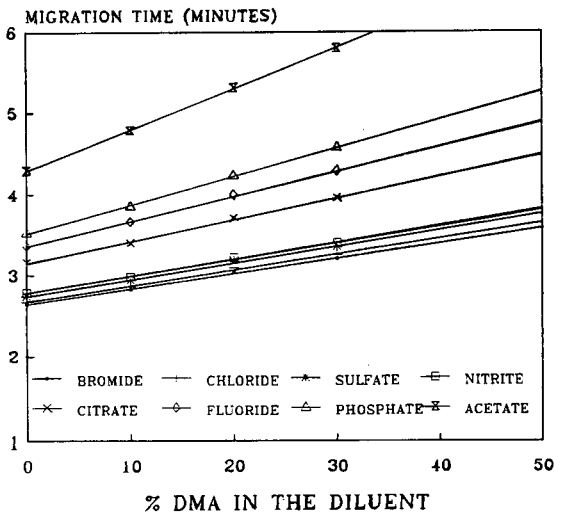

Fig. 9. Effect of amount of dimethylacetamide (DMA) in the sample diluent on peak migration times.

gradient techniques [5]. These procedures increase the time required per analysis. The unavoidable reequilibration time of an ion chromatographic column after any sort of gradient will also contribute to increase in total analysis time.

CIE has the intrinsic baseline noise. As shown in Fig. 12, this can be like a *grass noise*. Changing the buffer and cleaning the capillary can reduce this noise. Fig. 12 shows the worst case scenario for a water loading. This noise can cause lack of absolute sensitivity over suppressed IC. In fact in our experience it was hard to detect below 0.5 μg/ml level for the anions studied. Wherever lower absolute sensitivity is desired, suppressed IC ought to be the method of choice. Integration of the peaks from CIE also took more time and effort from the analyst (because of this inherent baseline noise) than performing the same functions on IC peaks. This extra effort could vary from one data acquisition system to another.

Varying migration times in CIE, necessitates frequent loading of standards. If proper temperature controls are maintained, this is usually not as much of a problem in IC. An example of varying migration times is shown in Fig. 10. In addition, IC methods do not require such stringent equality of sample and standard diluents.

The Quanta 4000 has a carousal with 20 positions for sample vials. Random access to the vials would have increased productivity because three standard concentrations would have needed only three positions. Currently most positions are taken up by the three standard vials bracketing four sample vials.

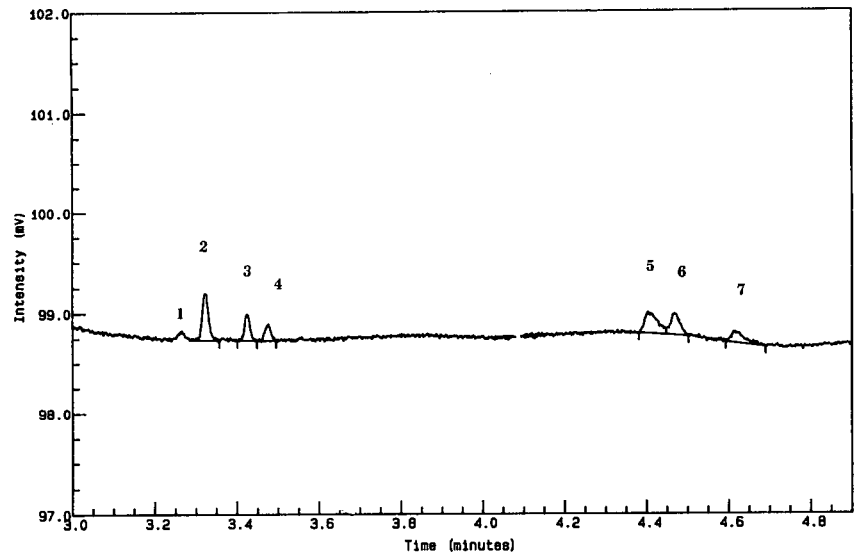

Fig. 10. Detection limit of anions by CIE. All anions at 0.5 μg/ml. The migration order of anions is bromide, chloride, sulfate, nitrite, citrate, fluoride, and phosphate.

TABLE II

PRECISION OF THE CIE SYSTEM FOR IOPIPERIDOL AT 1.0 mg/ml SPIKED WITH ANIONS AT 0.1% (w/w)

Injection	Mean peak area (n = 2)						
	Bromide	Chloride	Sulfate	Nitrite	Fluoride	Phosphate	Acetate
1	131	1467	234	272	801	205	975
2	128	1456	236	261	809	207	1077
3	131	1478	237	273	814	209	985
4	133	1492	236	260	808	209	1039
5	133	1444	262	263	850	212	957
6	127	1447	217	265	808	205	1031
Mean	131	1464	237	266	815	208	1011
S.D.	2.51	18.67	14.39	5.57	17.64	2.71	45.67
R.S.D. (%)	1.9	1.3	6.1	2.1	2.2	1.3	4.5

Applications of CIE anion screening

The CIE screening procedure was utilized for checking mass balance issues on several Bristol-Myers Squibb drugs. Three typical examples are shown. An electropherogram of a batch of deuterated pravastatin sodium at 1 mg/ml in water is shown in Fig. 13. Comparison of this electropherogram with the anion screen standard diluted tenfold (1 μg/ml) allowed us to detect above 0.1% (w/w) each of bromide, fluoride, and acetate. The other peaks in the sample electropherogram were not further investigated.

A batch of taxol was screened using this technique. Taxol is soluble in 100% methanol. A methanol blank gave the CIE trace shown in Fig. 14A. Two solutions were made, one consisting of 1 mg/

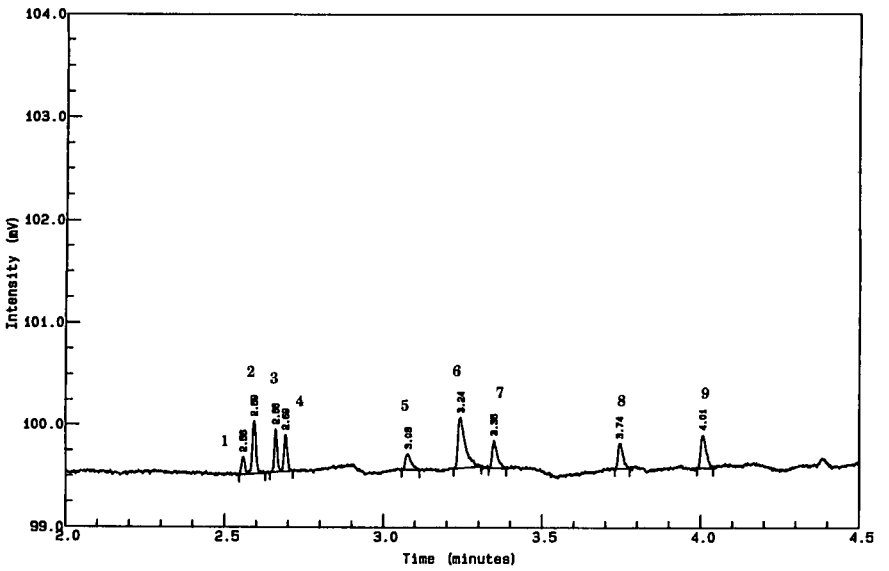

Fig. 11. Minimum quantifiable limit of anions by CIA. All anions at 1.0 μg/ml. The migration order of anions is bromide, chloride, sulfate, nitrite, citrate, fluoride, phosphate, carbonate and acetate. The experimental conditions are the optimized conditions explained in the experimental section.

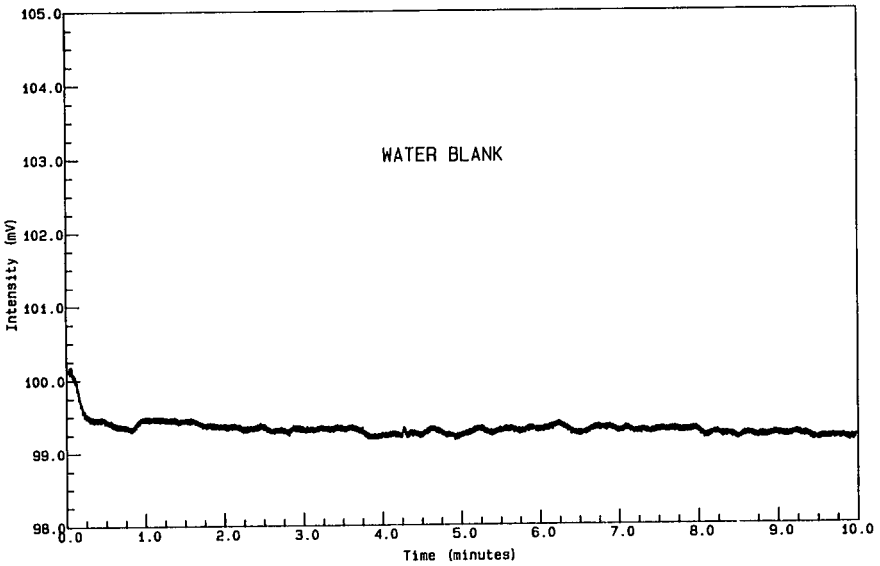

Fig. 12. Electropherogram of water blank under an extreme condition of baseline noise. Standard experimental conditions were used.

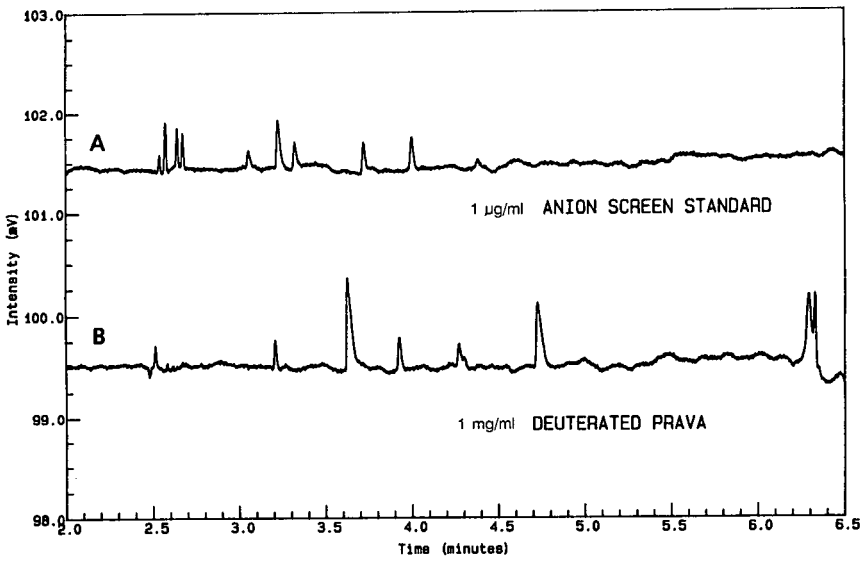

Fig. 13. Electropherograms of (A) 1 μg/ml anion screen standard. The migration order of anions is bromide, chloride, sulfate, nitrite, citrate, fluoride, phosphate, carbonate and acetate. (B) 1 mg/ml deuterated pravachol.

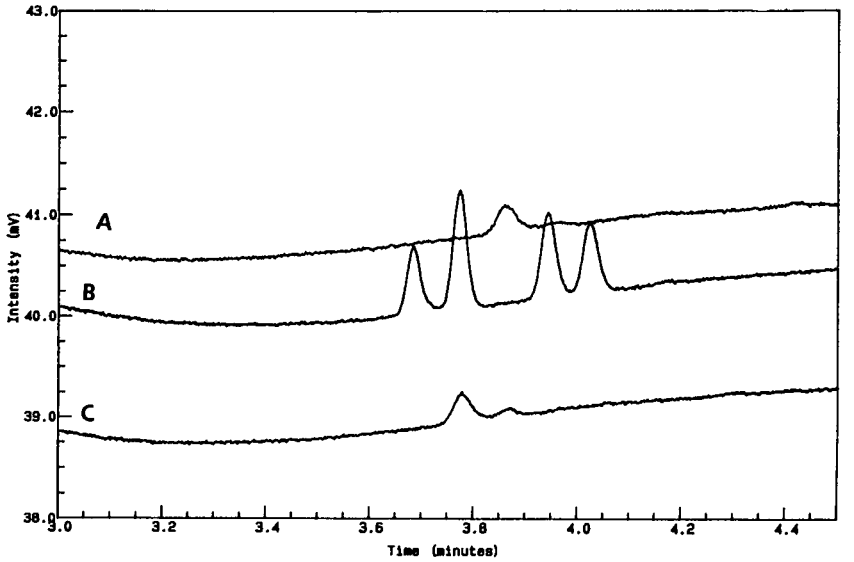

Fig. 14. Electropherograms of (A) a methanol blank (B) 1 mg/ml taxol spiked at 0.5% with bromide, chloride, sulfate and nitrite in methanol, and (C) 1 mg/ml taxol in methanol.

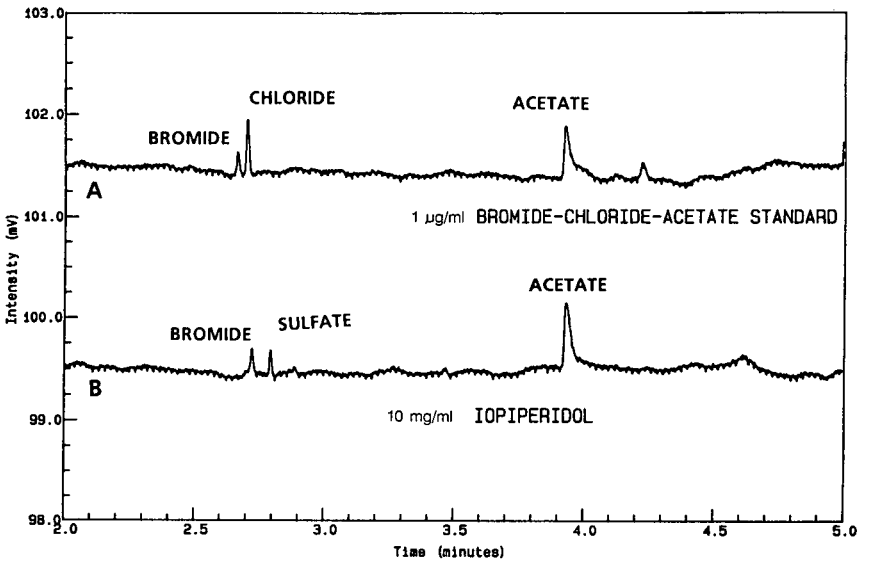

Fig. 15. Electropherograms of (A) 1 µg/ml of bromide, chloride, and acetate standards (B) 10 mg/ml iopiperidol in water.

ml taxol, and another of 1 mg/ml taxol spiked with 5 μg/ml of bromide, chloride, sulfate and nitrite. The electropherograms of these samples are shown in Fig. 14B and C. Note the shift in migration times for all peaks. Bromide, chloride, sulfate, and nitrite migrated within 5.0 min but with later migration times. This experiment demonstrates the profound influence of an organic diluent on analyte migration times. As shown in Fig. 14C, this batch of taxol has no bromide, chloride, sulfate, or nitrite in it. The peak at 3.75 min is seen in the methanol blank too.

Iopiperidol, a novel X-ray contrast agent, is soluble in water. Solutions of the drug were subjected to anion screening by CIE. The electropherogram of one batch is shown in Fig. 15B. Comparison of this sample to anion screen standard at 5 μg/ml (shown in Fig. 15A) enabled us to identify bromide and acetate in the sample solution.

As demonstrated by these examples, this technique facilitates detection of common anions at 0.1% (w/w) level. CIE thus compares favorably with IC for this purpose. In the cases where anions were detected by this screening technique, appropriate specific IC or CIA assays were developed and validated for routine quantitation.

REFERENCES

1 M. W. Dong, P. V. Passalacqua and D. R. Choudhury, *J. Liq. Chromatogr.*, 13 (1990) 2135.
2 S. Ahuja, *Chem. Anal.*, 85 (1986) 195.
3 G. F. Fhillips, *Pharm. Ind.*, 51 (1989) 1282.
4 J. Van Rompay, *J. Pharm. Biomed. Anal.*, 4 (1986) 725.
5 J. Nair, *Pharm. Research*, February (1993) submitted for publication.
6 A. C. Schoots, T. P. E. M. Verheggen, P. M. J. M. De Vries and F. M. Everaerts, *Clin. Chem*, 36 (1990) 435.
7 J. W. Jorgenson and K. D. Lukacs, *Science*, 222 (1983) 266.
8 F. E. P. Mikkers, F. M. Everaerts and T. P. E. M. Verheggen, *J. Chromatogr.*, 169)1979) 11.
9 W. G. Kuhr and E. S. Yeung, *Anal. Chem.*, 60 (1988) 2642.
10 X. Huang, J. A. Luckey, M. J. Gordon and R. N. Zare, *Anal. Chem.*, 61 (1989) 766.
11 T. Wang and R. A. Hartwick, *J. Chromatogr.*, 589 (1992) 307.
12 W. R. Jones, P. Jandik and R. Pfeifer, *Am. Lab.*, 23 (1991) 42.
13 A. L. Heckenberg, P. G. Alden, B. J. Wildman, J. Krol, J. P. Romano, P. E. Jackson, P. Jandik and W. R. Jones, *Waters Innovatie Methods For Ion Analysis*, Millipore Corporation, Milford, MA, 1989.
14 P. Jandik, W. R. Jones, A. Weston and P. R. Brown, *LC · GC*, 9 (1992) 634.
15 G. M. McLaughlin, J. A. Nolan, J. L. Lindahl, R. H. Palmieri, K. W. Anderson, S. C. Morris, J. A. Morrison and T. J. Bronzert, *J. Liq. Chromatogr.*, 15 (1992) 961.

Journal of Chromatography, 640 (1993) 463–471
Elsevier Science Publishers B.V., Amsterdam

CHROMSYMP. 2712

Parameters influencing separation and detection of anions by capillary electrophoresis

Michael P. Harrold*, Mary Jo Wojtusik, John Riviello and Patricia Henson

Dionex Corporation, 1228 Titan Way, Sunnyvale, CA 94086 (USA)

ABSTRACT

Electrolyte composition is critical in optimizing separation and detection of ions by capillary electrophoresis. The parameters which must be considered when designing an electrolyte system for capillary electrophoresis include electrophoretic mobility of electrolyte constituents and analytes, detection mode, and compatibility of electrolyte constituents with one another. An electrolyte system based on pyromellitic acid is well suited for use with indirect photometric detection, and provides excellent separations of anions. The ability to modify the electrophoretic mobility of pyromellitic acid as a function of pH provides flexibility in matching electrophoretic mobilities of analytes. Additionally, the use of alkyl amines as electroosmotic flow modifiers allows the rapid separation of anions by reversing the direction of electroosmotic flow in a fused-silica capillary. The optimization of a capillary electrophoresis electrolyte for anion analysis is also discussed in terms of pH, ionic strength and applied voltage. The effect of organic solvent on separation selectivity is also discussed.

INTRODUCTION

The separation of ionic species by free zone electrophoresis in fused-silica capillaries has attracted considerable attention in recent years. Early work by Mikkers *et al.* [1,2] demonstrated the very high efficiency attainable for separations in inert capillaries and described the fundamental properties of capillary electrophoresis. Jorgenson and Lukacs demonstrated the utility of small diameter glass capillaries for the electrophoretic separation of fluorescent tagged alkyl amines [3] and dansyl amino acids [4]. These authors also described the characteristics of electroosmotic flow in narrow-diameter glass capillaries and derived expressions for resolution and efficiency as a function of many experimental parameters [3,4]. Tsuda *et al.* [5] characterized electroosmotic flow in glass, fused-silica, and polymeric capillaries and demonstrated high-efficiency separations of metal ions, pyridinium ions, and aromatic sulfonates using direct on-capillary UV detection.

The lack of a universal detection scheme for non-chromophoric analytes hampered early development of separations for inorganic anions. Some work has been done adapting on-capillary conductivity detection to capillary electrophoresis [6], but this detection mode has not yet found widespread commercial use. Indirect methods for detection of non-chromophoric ions are attractive because these methods are easily adapted for use with existing instrumentation and they are relatively universal in terms of response. The use of indirect fluorescence detection for HPLC separations has been described [7,8] and this same technique has been shown to be feasible in capillary electrophoresis for the detection of low-molecular-mass anions and nucleotides [9]. Indirect UV methods were described in chromatographic systems [10], as a detection scheme for ion chromatography [11], and their applicability to the capillary electrophoresis format has been documented in several papers [12,13]. Several reports have appeared recently describing the application of capillary electrophoresis for the analysis of organic and inorganic anions with indirect UV detection [14–17]. Jandik and Jones [18] discussed the

* Corresponding author.

0021-9673/93/$06.00

optimization of indirect UV detection schemes and investigated selectivity for inorganic anion analysis using a chromate-based electrolyte system [19]. Applications of capillary electrophoresis with indirect detection for cation and metal analysis have also received attention [20]. Foret *et al.* [21] resolved a variety of alkali, alkaline-earth and lanthanide series metals using capillary electrophoresis with indirect UV detection [21]. The effect of solvent on separations has been explored using isotachophoresis [22–25] and capillary electrophoresis [26], although no systematic study has been performed for solvent effects on anion separations.

The goal of this work was to investigate the parameters that affect the separation of anions using capillary electrophoresis. Analyses were performed using a polycarboxylic acid as the primary electrolyte component. Modification of selectivity and peak shape as a function of pH was investigated. Selectivity changes as a result of organic solvent addition to electrolytes were also explored. As a result of this work, an electrolyte system suitable for the analysis of common inorganic anions was developed. This same electrolyte system, run at different pH values, was also optimized for the analysis of less mobile anions including haloacetates and alkyl sulfonates. Two difficult coelution problems were shown to be resolved by adding organic solvent to capillary electrophoresis electrolytes.

EXPERIMENTAL

Experiment

All electropherograms were generated using a Dionex CES-1 automated capillary electrophoresis system (Dionex, Sunnyvale, CA, USA). Fused-silica capillaries (Polymicro Technologies, Phoenix, AZ, USA) of 50 μm I.D., 375 μm O.D. and various lengths were used. The detection window was located 5 cm from the end of the capillary. Data were collected at five points/s using a Dionex AI-450 data acquisition system. Unless otherwise noted, all injections were hydrostatic and performed by raising the sample vial 100 mm above the level of the destination vial for 30 s. Molar absorptivities were determined using a Hitachi U-2000 UV–Vis spectrophotometer (Hitachi, Danbury, CT, USA) with 1 cm path length quartz cells.

Chemicals

Pyromellitic acid (PMA), 96% was obtained from Sigma (St. Louis, MO, USA). Hexamethonium bromide, monohydrate, 97% was obtained from Aldrich (Milwaukee, WI, USA) and triethanolamine, >99%, from Fluka (Ronkonkoma, NY, USA). Sodium hydroxide, 50% aqueous solution and methanol (Optima grade) were obtained from Fisher Scientific (Pittsburgh, PA, USA). Anion standards were prepared from sodium salts obtained from Fisher Scientific. Deionized water (18 MΩ/cm resistance) was used to prepare all reagents and standards. OnGuard A cartridges containing high-capacity anion-exchange resin for conversion of hexamethonium bromide to hexamethonium hydroxide were from Dionex.

Procedures

The standard electrolyte was 2.25 m*M* pyromellitic acid, 6.5 m*M* sodium hydroxide, 0.75 m*M* hexamethonium hydroxide, 1.6 m*M* triethanolamine at pH 7.7. The electrolyte was made from concentrated stock solutions.

A concentrate of 25 m*M* hexamethonium bromide was prepared and converted to the hydroxide form of the amine during the preparation of the working electrolyte. The conversion of hexamethonium from the bromide form to the hydroxide form was accomplished by first washing an OnGuard A sample preparation cartridge with 10 ml of 1.0 *M* sodium hydroxide followed by 10 ml deionized water.

The pH 3.5 electrolyte was prepared by dissolving 0.156 gram pyromellitic acid in 100 ml deionized water. Hexamethonium hydroxide was added as described above to give a final concentration of 0.75 m*M*. The working electrolyte was titrated to pH 3.5 with dropwise addition of 100 m*M* sodium hydroxide.

RESULTS AND DISCUSSION

Carrier ion

The anion present in the greatest quantity in the electrolyte is termed the carrier ion, and its properties effect the separation of anions by capillary electrophoresis. Perhaps the most important property of the carrier ion is the requirement that the electrophoretic mobility of the primary electrolyte compo-

nent is closely matched to those of the analyte(s) of interest. This condition, the matching of electrophoretic mobility of carrier and analytes, governs the characteristic peak shapes observed in capillary electrophoresis. It has been demonstrated that the asymmetry of peak shapes in capillary electrophoresis is predictable and determined by the boundary anomalies that arise between the sample zone and the bulk carrier electrolyte when the sample contains ions of different ionic mobility than that of the carrier [1]. An electrolyte optimal for common inorganic anions must have a carrier ion with electrophoretic mobility closely matched to that of the anions of interest if a high-resolution separation is to occur.

A second important consideration when choosing a carrier ion for anion analysis is the mode of detection. Present commercial capillary electrophoresis instrumentation is restricted to the use of on-capillary UV–Vis or fluorescence detection. This presents a difficulty in the detection of inorganic anions many of which are UV transparent or absorb only at low UV wavelengths such as nitrite, nitrate and bromide. Using indirect UV detection, the decrease in absorbance observed when an analyte ion displaces a chromophoric ion in the electrolyte is measured. The technique results in a negative peak when a sample band passes through the detector window. Because indirect UV detection relies on displacement of a chromophore, the carrier (or visualizing) ion, should have a large molar absorptivity to maximize the decrease in signal resulting from its displacement. The correlation between peak response and carrier ion molar absorptivity in capillary electrophoresis has been documented by other workers [18]. Additionally, for use in indirect detection, the wavelength at which the chromophore absorbs should be well away from any wavelength at which analyte ions may absorb . This is to prevent an analyte's direct UV absorbance from counteracting the indirect absorbance mechanism.

These conditions, the match of electrophoretic mobility of carrier and analyte ions, and the restrictions arising from the use of indirect UV detection, limit the choice of potential electrolyte components for anion analysis by capillary electrophoresis. In our work, we have chosen pyromellitic acid as the carrier anion for the separation of common inorganic anions. Pyromellitic acid is well suited as an electrolyte because its electrophoretic mobility when fully ionized is closely matched to many common inorganic anions. In addition, pyromellitic acid has the required spectral characteristics, including high molar absorptivity ($7.8 \cdot 10^3$ l mol^{-1} cm^{-1}), and strong UV absorbance at 250 nm, well away from the low UV wavelengths at which several common inorganic anions absorb. The molar absorptivity for pyromellitic acid was measured at pH 7.5, almost 2 pH units above the highest pK_a for pyromellitic acid [27].

The noise in an indirect photometric system is proportional to the magnitude of the background absorbance [11]. This implies that using a very low concentration of carrier ion maximizes the signal-to-noise ratio in such a system. There are however, detection and separation considerations that limit the degree to which the concentration of carrier ion may be decreased. A low concentration of carrier ion results in a decrease of linear dynamic range. Additionally, as the concentration of the carrier ion is decreased, there is a subsequent decrease in loading capacity. A decreased loading capacity results from a decrease in efficiency as a function of sample ion to carrier ion concentration ratio. The optimum concentration of carrier ion is chosen such that desirable detection limits and adequate linear dynamic range are achieved.

Pyromellitic acid is a polycarboxylic acid whose net charge and resulting electrophoretic mobility is pH dependent. The highest pK_a for an acidic proton on pyromellitic acid is 5.6 and thus at pH 7.7, the pyromellitic acid is fully ionized [27]. Fig. 1 demonstrates the high efficiency separation of several inorganic anions using an optimized pyromellitic acid electrolyte at pH 7.7. At lower pH, the pyromellitic acid becomes increasingly protonated and a decrease in its electrophoretic mobility is observed. This pH dependence implies that by using a lower pH electrolyte, the peak symmetry and efficiency can be optimized for lower electrophoretic mobility anions that would display severe peak asymmetry (tailing) with pyromellitic acid electrolyte at higher pH.

Electroosmotic flow modifier

An important feature of capillary electrophoresis separations of anions is the potential for high peak capacity and short analysis time. Under normal

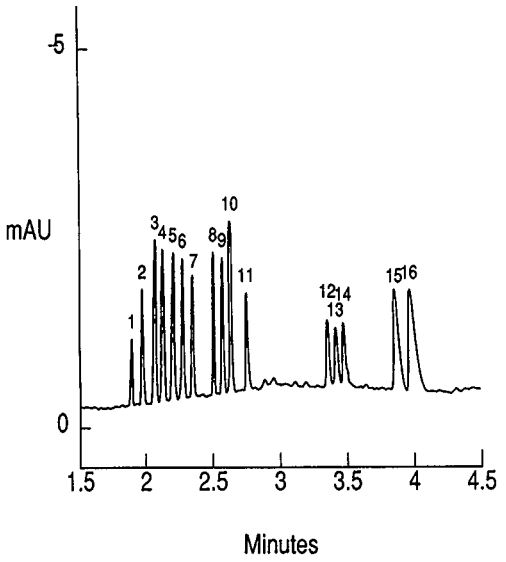

Fig. 1. Anion separation at pH 7.7. Capillary (50 μm), 50 cm length. Electrolyte composed of 2.5 m*M* pyromellitic acid, 6.5 m*M* NaOH, 0.75 m*M* hexamethonium hydroxide, 1.6 m*M* triethanolamine. 30 000 V applied for separation. Indirect UV detection at 250 nm, output polarity reversed to produce positive peaks. Gravity injection, 100 mm for 20 s. Peaks: 1 = dithionate (3 mg/l); 2 = thiosulfate (5 mg/l); 2 = bromide (8 mg/l); 4 = chloride (3 mg/l); 5 = sulfate (3 mg/l); 6 = nitrite (3 mg/l); 7 = nitrate (3 mg/l); 8 = molybdate (5 mg/l); 9 = azide (4 mg/l); 10 = thiocyanate (3 mg/l); 11 = chlorate (3 mg/l); 12 = fluoride (0.5 mg/l); 13 = bromate (3 mg/l); 14 = formate (2 mg/l); 15 = phosphate (3 mg/l); 16 = phthalate (10 mg/l).

electrophoretic conditions using uncoated silica capillaries, the bulk electroosmotic flow is from anode to cathode. This flow arises from the formation of a double layer of electrolyte cations along the surface of the ionized silanol groups of the capillary wall. When an electric field is applied, there is a migration of mobile cations toward the cathode and a resulting bulk solution flow in that direction. In most commercially available capillary electrophoresis instruments, the detector window is fixed near the destination end of the capillary. The natural direction of electroosmotic flow is toward the destination end of the capillary when the destination is cathodic. If the polarity of the applied voltage is reversed, the end of the capillary near the detector is anodic and the electroosmotic flow is away from the detector.

While a normal polarity (detector cathodic) configuration is useful for the determination of cations and neutral compounds, the direction of electroosmotic flow is opposite to the direction of anion migration, and thus detrimental in terms of analysis speed. If anions of very high mobility are being separated, their high intrinsic mobility may cause them to migrate out of the opposite end of the capillary (the anodic end) and not be detected. In order to minimize the time of analysis, it is desirable to produce an electroosmotic flow in the same direction as the migration of the analytes of interest. For the analysis of high mobility anions, the direction of electroosmotic flow should be from cathode to anode, reverse of the direction of a normal bare silica capillary.

Alkyl ammonium salts including cetyltrimethylammonium bromide (CTAB) [28], tetradecyltrimethylammonium bromide (TTAB) [6], and amines such as diethylenetriamine (DETA) [29] have been documented for several applications requiring suppression or reversal of electroosmotic flow. We have investigated a number of alkyl amines for electroosmotic flow reversal. We have found many different mono and poly amines at low to moderate concentrations are useful in controlling electroosmotic flow. Most of these electroosmotic flow modifiers have been found to be compatible with analytes and other electrolyte components. One disadvantage of hydrophobic alkyl ammonium salts, such as CTAB and TTAB is their limited solubility and tendency to form insoluble pairs with some electrolyte components [18,30]. For this reason, we chose 1,6-bis-(trimethylammonium)hexane, a C_6 alkyl diquaternary ammonium salt that does not interact with other electrolyte components. The common name for this compound is hexamethonium bromide. The bromide salt is converted to the hydroxide form to remove bromide ion that can compromise detection. The role of counterions is discussed in the next section. The hexamethonium ion is very effective in reversing electroosmotic flow, is highly soluble, and does not interact with other electrolyte components. In addition, because hexamethonium is a quaternary ammonium, its ability to modify the wall of the capillary is not changed as a function of pH, a phenomenon that could otherwise lead to unstable electroosmotic flow.

Counterion considerations

A phenomenon was observed which places re-

strictions on the types of counterions of electrolyte components. It is desirable to have only one carrier ion in the electrolyte, in this case, the pyromellitate anion. The presence of other anions can lead to baseline aberrations and a decrease in sensitivity. For example, the presence of bromide in the electrolyte causes a dip in the baseline at the migration time corresponding to bromide (a "dip" when using indirect UV is actually an increase in absorbance). This phenomenon has also been observed with sulfate and chloride when these anions are added to the electrolyte. This effect adversely affects accurate determination of an analyte anion that is also present in the electrolyte used for analysis. Additionally, the presence of non-chromophoric anions (at 250 nm) in the electrolyte results in a decrease in sensitivity when using indirect UV detection [11]. Many high purity, commercially available amines which are useful as electroosmotic flow modifiers are available only as the chloride or bromide salts. The addition of a flow modifier with either of these counterions causes disruptions in the baseline and affects quantitation. Chloride and bromide can still be accurately determined by exchanging the chloride or bromide counterion for hydroxide counterion with a sample pretreatment cartridge containing high capacity anion-exchange resin in the hydroxide form. Unlike bromide and chloride counterions, the addition of small amounts of hydroxide to the electrolyte solution has no adverse effect on separation or detection of inorganic anions.

Ionic strength

The ionic strength of the electrolyte is important for two distinct reasons. First, the current observed for a given applied voltage is proportional to the ionic strength of the electrolyte. Generally, effects due to heating increase at higher current resulting from the inability to dissipate heat. These effects, manifested as noise and baseline aberrations, are exacerbated by the use of a highly absorbing carrier ion for indirect UV detection. For this reason, the ionic strength must be minimized to prevent noise resulting from high current. Secondly, efficiency is proportional to electrolyte ionic strength. As ionic strength decreases, lower peak efficiency is observed. This effect is shown in Fig. 2. In both electropherograms, the applied voltage and pH of the electrolyte are identical, only the ionic strength was

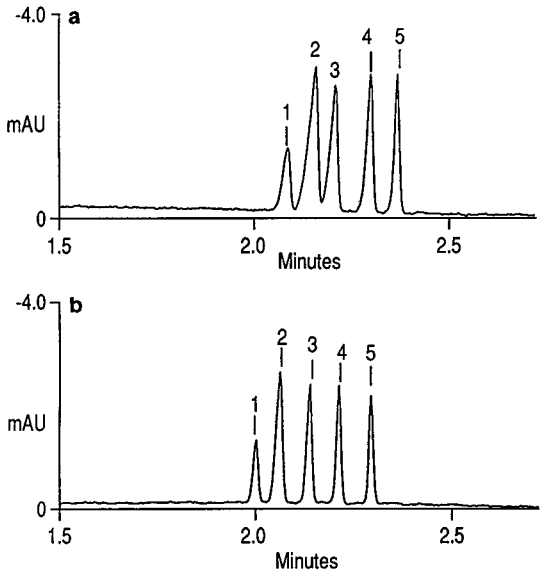

Fig. 2. Effect of ionic strength on peak symmetry. Electrolyte ionic strength: (a) 7.25 m*M*, (b) 11.10 m*M*. Capillary (50 μm), 50 cm length. 30 000 V applied for separaton. Indirect UV detection at 250 nm, output polarity reversed to produce positive peaks. Gravity injection, 100 mm for 30 s. (a) 1.5 m*M* pyromellitic acid, 3.5 m*M* NaOH, 0.75 m*M* hexamethonium hydroxide, 1.6 m*M* triethanolamine, pH 7.8. (b) 2.25 m*M* pyromellitic acid, 6.5 m*M* NaOH, 0.75 m*M* hexamethonium hydroxide, 1.6 m*M* triethanolamine, pH 7.8. Peaks (all 5.0 mg/l): 1 = bromide; 2 = chloride; 3 = sulfate; 4 = nitrite; 5 = nitrate.

different. Clearly, there is an decrease in peak efficiency as the ionic strength is lowered. This effect can be explained in terms of the ratio of sample concentration to carrier electrolyte concentration.

In a system where other sources of dispersion have been minimized, the peak width in capillary electrophoresis has been shown to be proportional to the concentration ratio of sample ions to carrier ions [1]. This implies that in order to obtain a high-resolution separation of closely migrating peaks, the concentration of the injected sample must be kept low relative to the electrolyte. To attain higher efficiency with samples of high concentration, the concentration of the electrolyte must be increased in order to maintain a large ratio of electrolyte concentration to sample band concentration. The other possibility, the dilution of sample to minimize electromigrative dispersion, is generally not desirable

due to the negative impact on peak response. The optimum ionic strength of an anion analysis electrolyte must be a balance which will produce an acceptably low current to minimize noise while maintaining good peak efficiency.

Applied voltage

The electroosmotic flow-rate as well as the velocity of a migrating ion is proportional to the applied voltage used for separation. Therefore, the analysis time can be shortened by increasing the applied voltage. For some separations described in this paper, short analysis times were attained by running the separation at 30 000 V. The relatively low ionic strength of the carrier electrolyte permits the use of such high voltages by producing only a modest current (8–12 μA) at 30 000 V.

pH

The pH of the electrolyte solution used for separation can have a large effect on the separation of anions using capillary electrophoresis. The pH of the electrolyte controls the mobility of anions of weak acids. For the pyromellitic acid based system, the mobility of the pyromellitic acid can be altered by decreasing the pH of the electrolyte. The analytes also display changes in electrophoretic mobility if the pH is changed in the vicinity of their pK. While most low-molecular-mass inorganic anions are unaffected by pH changes in the range 3 to 9, some anions such as phosphate, carbonate and acetate can display large changes in apparent mobility due to small changes in pH. The electrolyte system described here has been optimized at pH 7.7 which provides maximum resolution of phosphate from fluoride and carbonate. The pyromellitic acid–hexamethonium electrolyte system has been buffered at pH 7.7 with triethanolamine. Triethanolamine, with a pK of 7.7 is well suited for this electrolyte system not only because it has the proper pK, but also because it is available in the free base form and thus does not add a counter anion to the electrolyte. The use of a buffered system provides reproducible electrolyte pH as well as stable pH though the course of the run.

The pH of the electrolyte controls the ionization and thus the electrophoretic mobility of the carrier ion. The separation of lower mobility ions can be optimized by decreasing the pH. As the pH of a pyromellitic acid electrolyte is lowered, the pyromellitate ion becomes progressively protonated, decreasing its charge and its electrophoretic mobility. The predictable and controllable degree of ionization of pyromellitate ion is used to control the electrophoretic mobility of the carrier ion. Fig. 3 shows the optimization of the pyromellitic acid electrolyte system for the separation of haloacetates. Lowering the pH of the electrolyte lowers the electrophoretic mobility of pyromellitate so that it more closely matches the mobility of the analyte haloacetates.

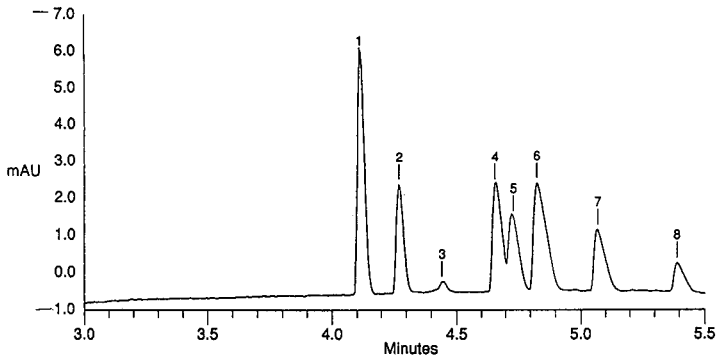

Fig. 3. Separation of haloacetic acids at pH 3.5. Capillary (50 μm), 50 cm length. Electrolyte composed of 2.5 mM pyromellitic acid, 0.75 mM hexamethonium hydroxide, adjusted to pH 3.5 with NaOH. 20 000 V applied for separation. Indirect UV detection at 250 nm, output polarity reversed to produce positive peaks. Gravity injection, 100 mm for 30 s. Peaks (all 5.0 mg/l): 1 = difluoroacetate; 2 = trifluoroacetate; 3 = unknown; = monochloroacetate; 5 = dichloroacetate; 6 = monobromoacetate; 7 = trichloroacetate; 8 = tribromoacetate.

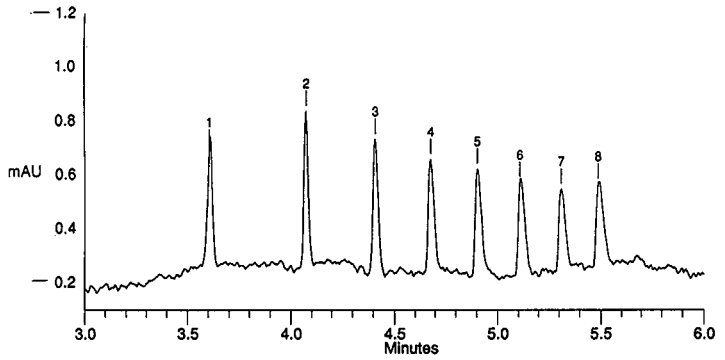

Fig. 4. Separation of alkylsulfonic acids at pH 3.5. Capillary (50 μm), 50 cm length. Electrolyte composed of 2.5 m*M* pyromellitic acid, 0.75 m*M* hexamethonium hydroxide, adjusted to pH 3.5 with NaOH. 20 000 V applied for separation. Indirect UV detection at 250 nm, output polarity reversed to produce positive peaks. Gravitiy injection, 100 mm for 20 s. Peaks (all 2.0 mg/l): 1 = methanesulfonate; 2 = ethanesulfonate; 3 = 1-propanesulfonate; 4 = 1-butanesulfonate; 5 = 1-pentanesulfonate; 6 = 1-hexanesulfonate; 7 = 1-heptanesulfonate; 8 = 1-octanesulfonate.

This results in good peak symmetry for these low mobility anions which have very poor peak shape in a higher pH pyromellitic acid electrolyte.

A low pH method also works well for alkylsulfonates which are shown separated in Fig. 4. In both cases, the charge on the pyromellitate carrier ion is estimated to be approximately −2. With an approximate charge of −2, the pyromellitate ion has a mobility well matched to that of the alkylsulfonates and haloacetates. The match of electrophoretic mobility of carrier and analyte anion results in symmetrical peak shape.

Solvation effects

The effect of solvent addition to a capillary electrophoresis electrolyte has been briefly investigated. Fig. 5 shows the effect of methanol addition to a pyromellitic acid electrolyte system. The conditions for the first electropherogram (standard conditions) are identical to those used for the electropherogram in Fig. 1. Under standard conditions, the migration times of iodide and chloride are identical. Perchlorate and azide also have identical electrophoretic mobility and thus co-migrate under standard conditions. The co-migration of these analytes is consistent with their limiting ionic conductances which are very similar [27]. The second electropherogram in Fig. 5 shows the separation of iodide, chloride, perchlorate, and azide in an electrolyte similar to that used for the first electropherogram, but with the inclusion of 15% (v/v) methanol.

This change in selectivity can be explained on the basis of the relative hydration enthalpies of the anions. The modification of selectivity with the ad-

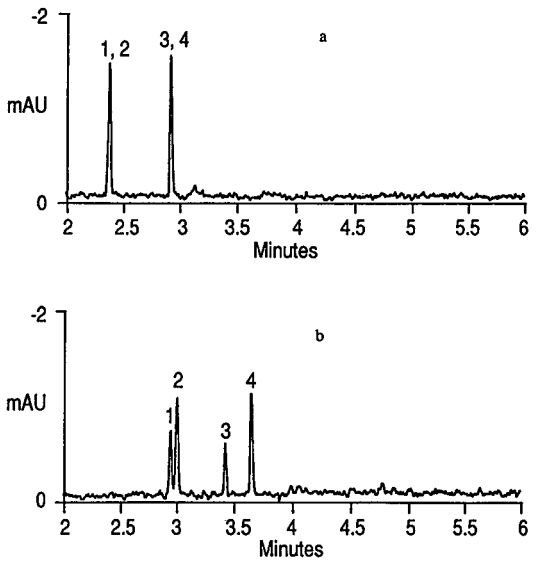

Fig. 5. Effect of solvent on separation of anions using pyromellitic acid electrolyte. Capillary (50 μm), 50 cm length. (a) Electrolyte composed of 2.5 m*M* pyromellitic acid, 6.5 m*M* NaOH, 0.75 m*M* hexamethonium hydroxide, 1.6 m*M* triethanolamine. (b) Electrolyte was same as electrolyte a, but with 15% methanol (v/v), pH = 7.7. 30 000 V applied for separation. Indirect UV detection at 250 nm, output polarity reversed to produce positive peaks. Gravity injection, 100 mm for 20 s. Peaks: 1 = iodide (5.0 mg/l); 2 = chloride (2.5 mg/l); 3 = perchlorate (2.5 mg/l); 4 = azide (2.5 mg/l).

TABLE I

ENTHALPIES OF HYDRATION FOR SELECTED ANIONS

From ref. 32.

Anion	$\Delta H_{hydration}$(kcal/mol)
Iodide	−331
Chloride	−348
Azide	−332
Perchlorate	−317

dition of organic solvent in ion chromatography of metal cations has been demonstrated by Strelow *et al.* [31]. They argued that the observed changes in selectivity are a result of the change in relative hydration of some metal ions in the presence of ethanol. We propose that the mechanism of separation of iodide and chloride as well as azide and perchlorate is similar and due to selective destruction of the hydration cloud which surrounds each ion in aqueous solution. Table 1 lists the standard enthalpies of hydration for several anions [32]. Because the enthalpy of hydration for iodide is less negative than that of chloride, it follows that the waters of hydration are more easily displaced from iodide than from chloride. When these two anions are placed in an electrolyte containing 15% methanol, it is expected that the solvation of iodide will be more pronounced than for chloride. This results in a lesser degree of hydration for iodide relative to chloride and thus an increase in effective mobility due to a decrease in effective mass. The separation shown in Fig. 5 is consistent with this hypothesis in that iodide migrated faster than chloride and the two peaks were fully resolved. The other co-migrating pair, perchlorate and azide, were fully resolved when 15% methanol was added to the electrolyte. The change in selectivity was even more pronounced with azide and perchlorate. Although the mechanism is thought to be the same, there may be an additional mechanism functioning in the case of perchlorate and azide. Perchloric acid is a strong acid whereas azide is a weak acid with $pK = 4.7$ [27]. The use of organic solvent in isotachophoresis has shown that an increase in pK of weak acids occurs in mixed aqueous–organic media and can be used to affect electrophoretic mobility [23]. The change in pK for azide in a 15% methanol solution is not known, however a pK increase of 2–3 units would be sufficient to slow the migration of azide relative to perchlorate. It is possible that resolution of perchlorate and azide in 15% methanol results from a combination of both hydration changes as well as pK changes for the two molecules.

It must also be noted that there is a decrease in electroosmotic flow when methanol is added to the electrolyte. The addition of organic solvent increases the viscosity of the electrolyte and changes the pK of the silanol groups on the wall of the capillary. The result is a decrease in electroosmotic flow when methanol is added to the electrolyte.

The beneficial effect of organic solvent on anion migration time has been demonstrated by Fig. 5. While a tentative mechanism has been proposed, the effect of methanol as well as other solvents must be explored in greater detail. The effect of solvation of anions has the potential to solve many co-migration problems that arise in capillary electrophoresis of ions.

CONCLUSIONS

The separation and detection of ions using capillary electrophoresis can be optimized by considering a number of parameters. To separate anions by capillary electrophoresis with high-efficiency peaks and therefore high resolution, a carrier electrolyte with an electrophoretic mobility matched to that of the analytes is required. If non-chromophoric analytes are to be determined by indirect UV detection, the carrier analyte must also fulfill certain spectral requirements. The speed of analysis is increased by dynamically modifying the surface of the silica capillary using an electroosmotic flow modifier, thereby reversing the direction of electroosmotic flow such that the analyte anions migrate in the same direction as the bulk electroosmotic flow.

An electrolyte for anion analysis using capillary electrophoresis has been systematically developed by modifying the various parameters described in this paper. The electrolyte system uses pyromellitic acid as a carrier ion and hexamethonium hydroxide as the electroosmotic flow modifier. The electrolyte system is buffered at pH 7.7 with triethanolamine so that the pyromellitic acid is in a fully ionized form.

The electrolyte system will separate a variety of common inorganic anions in less than 5 min with very high peak efficiency. The addition of solvent to the standard electrolyte was examined and found to be useful for the resolution of some co-migrating anions.

ACKNOWLEDGEMENTS

The authors would like to thank Dr. John Statler and Michelle Nguyen, both of Dionex Corporation, for their assistance in preparing this manuscript.

REFERENCES

1 F. E. P Mikkers, F. M. Everaerts and Th. P. E. M Verheggen, *J. Chromatogr.*, 169 (1979) 1–10.
2 F. E. P Mikkers , F. M. Everaerts and Th. P. E. M Verheggen, *J. Chromatogr.* , 169 (1979) 11–20.
3 J. W. Jorgenson and K. D. Lukacs, *J. Chromatogr.*, 218 (1981) 209–261.
4 J. W. Jorgenson and K. D. Lukacs, *Anal. Chem.*, 53 (1981) 1298–1302.
5 T. Tsuda, K. Nomura and G. Nakagawa, *J. Chromatogr.*, 264 (1983) 385–392.
6 X. Huang, J. A. Luckey, M. J. Gordon and R. Z. Zare, *Anal. Chem.*, 61 (1989) 766–770.
7 S. Mho and E. S. Yeung, *Anal. Chem.*, 57 (1985) 2253–2256.
8 W. D. Pheffer, T. Takeuchi and E. S. Yeung, *Chromatographia*, 24 (1987) 123–126.
9 L. Gross and E.S. Yeung, *J. Chromatogr.*, 480 (1989) 169–178.
10 R. F. W. Scott, C. G. Scott and P. Kucera, *Anal. Chem.*, 44 (1972) 100–104.
11 H. Small and T. E. Miller, *Anal. Chem.*, 54 (1982) 462–469.
12 E. S. Yeung, *Acc. Chem. Res.*, 22 (1989) 125–130.
13 E. S. Yeung and W. G. Kuhr, *Anal Chem.*, 63 (1991) 275A–282A.
14 F. Foret, S. Fanali, L. Ossicini and P. Bocek, *J. Chromatogr.*, 470 (1989) 299–308.
15 B. J. Wildman, P. E. Jackson, W. R. Jones and P. G. Alden, *J. Chromatogr.*, 546 (1991) 459–466.
16 B. Kenney, *J. Chromatogr.*, 546 (1991) 423–430.
17 A. Nardi, M. Cristalli, C. Desiderio, L. Ossicini, S.K. Shukla and S. Fanali, *J. Microcol. Sep.*, 4 (1992) 9–11.
18 P. Jandik and W. R. Jones, *J. Chromatogr.*, 546 (1991) 431–443.
19 W. R. Jones and P. Jandik, *J. Chromatogr.*, 546 (1991) 445–458.
20 P. Jandik, W. R. Jones, A. Weston and P. R. Brown, *LC–GC*, 9 (1991) 634–645.
21 F. Foret, S. Fanali, A. Nardi and P. Bocek, *Electrophoresis*, 11 (1990) 780–783.
22 T. Hirokawa, T. Tsuyoshi and Y. Kiso, *J. Chromatogr.*, 408 (1987) 27–41.
23 E. Kendler and P. Jenner, *J. Chromatogr.*, 390 (1987) 169–183.
24 E. Kendler and P. Jenner, *J. Chromatogr.*, 390 (1987) 185–197.
25 M. Kovel, D. Kaniansky, M. Hutta and R. Lacko, *J. Chromatogr.*, 325 (1985) 151–160.
26 E. Kendler and B. Gassner, *Anal. Chem.*, 62 (1990) 431–436.
27 J. A. Dean (Editor), *Lange's Handbook of Chemistry*, McGraw Hill, New York, 13th ed., 1985, pp. 5–28.
28 K. Altria and C. Simpson, *Anal. Proc.*, 23 (1986) 453–454.
29 J. Tso, M. Harrold, A. Wainwright, J. Thayer and J. Olechno, presented at the *1991 Pittsburgh Conference, Chicago, IL, 1991*, paper No. 165.
30 E. Jungerman (Editor), *Cationic Surfactants*, Armour-Dial, Chicago, IL, 1969.
31 F. W. E. Strelow, C. R. Van Zyl and C. J. C. Bothma, *Anal. Chim. Acta*, 45 (1969) 81–92.
32 H. F. Halliwell and S. C. Nyburg, *Trans. Faraday Soc.*, 59 (1963) 1126–1140.

Journal of Chromatography, 640 (1993) 473–479
Elsevier Science Publishers B.V., Amsterdam

CHROMSYMP. 2736

Separation of metal ions by capillary electrophoresis with a complexing electrolyte

Youchun Shi and James S. Fritz*

Ames Laboratory, US Department of Energy and Department of Chemistry, Iowa State University, Ames, IA 50011 (USA)

ABSTRACT

Excellent separations of metal ions can be obtained very quickly by capillary electrophoresis provided a weak complexing reagent is incorporated into the electrolyte to alter the effective mobilities of the sample ions. Indirect photometric detection is possible by also adding a UV-sensitive ion to the electrolyte. Separations are described using phthalate, tartrate, lactate or hydroxyisobutyrate as the complexing reagent. A separation of twenty-seven metal ions was achieved in only 6 min using a lactate system. A mechanism for the separation of lanthanides is proposed for the hydroxyisobutyrate system.

INTRODUCTION

Although ion chromatography continues to be the major method used to determine anions and many inorganic cations, capillary zone electrophoresis (CZE) holds the promise of even better separations. It is becoming more and more common to use the term capillary electrophoresis (CE) instead CZE. Some excellent separations of ions have been achieved by CE [1–8]. A complete separation of all thirteen lanthanides has also been obtained [2,8].

Separations by CE are based on differences in the electrophoretic mobilities of the sample ions. In cases where the mobilities of the free cations are very similar, a reagent is often added to partially complex the sample cations and thereby increase the differences in effective mobilities. The separations are affected by the type and concentration of complexing reagent and by other factors such as pH, ionic strength, and viscosity. When indirect photometric detection is used, the separation may also be influenced by the chemical nature and concentration of the UV-active reagent.

In the present work, some new reagents are evaluated for the separation of a number of inorganic metal ions. In the CE of the lanthanides, the distribution of free metal ion and metal–complex species is calculated and a mechanism is proposed for the excellent separation that is obtained.

EXPERIMENTAL

CE was performed with Waters Quanta 4000 capillary electrophoresis system (Millipore waters, Milford, MA, USA), equipped with a positive power supply. Polyamide-coated, fused-silica capillaries (Polymicro Technology, Phoenix, AZ, USA), 60 cm in length with an I.D. of 75 μm, were used. A window for on-column detection was created 7.3 cm from the end of the capillary. Indirect UV detection was employed at 214 nm. The separation voltage applied was 15 or 30 kV.

At the beginning of each experimental day, it was sufficient to rinse the capillary with deionized water for about 15 min. However, in order to keep the capillary clean, the capillary was flushed with 0.5 *M* KOH solution after being used three or four days.

Hydrostatic sample mode was selected for injection and sample time was set at 30 s. Before each run, a 2-min purge of capillary with electrolyte was programmed. A Curken 250-1B plotter (Curken,

* Corresponding author.

0021-9673/93/$06.00

Danbury, CT, USA) was used for recording electropherograms.

All standards and electrolytes were prepared using 18 MΩ deionized waters by a Barnstead Nanopure II system (Sybron Barnstead, Boston, MA, USA). All reagents for preparing electrolytes were of analytical-reagent grade. Hydroxyisobutyric acid (HIBA) and UV-Cat1 were obtained from Waters (Milford, MA, USA). Phthalic acid, *p*-toluidine and phenylethylamine were purchased from Aldrich (Milwaukee, WI, USA). Tartaric acid and 4-methylbenzylamine were supplied by Fisher Scientific (Fair Lawn, NJ, USA) and Fluka (Ronkonkoma, NY, USA), respectively.

RESULTS AND DISCUSSION

General conditions for separation

CE separation of metal ions is based on differences in the mobility of the ions in an electric field. Unfortunately, in some cation groups the individual cations have almost the same mobility. The divalent transition metal cations and the lanthanide cations are examples. In such cases addition of a water-soluble complexing reagent to the capillary electrolyte is used to obtain larger differences in effective mobility. This occurs by complexing the metal ions to differing extents. Ions that are complexed to a greater degree move more slowly through the capillary than those that have a lower fraction of the element in the complexed form. The effects of pH and concentration of complexing reagent have been previously pointed out [2].

The problem of detecting the separated metal ions was solved by indirect photometric detection [3,4]. An organic cation is added to the electrolyte which absorbs in the UV spectral region. A proprietary reagent developed at Waters (UV-Cat1) was found to work well. We also tried a number of aryl derivatives of aliphatic amines, which form cations when protonated. Of those tried, phenylethylamine, benzylamine, *p*-toluidine and 4-methylbenzylamine were the most satisfactory. In order to optimize separation and detection efficiencies, it is important to choose a suitable combination of complexing reagent and UV-sensitive reagent. Some adjustment in the concentration of a UV-sensitive reagent is often required to obtain optimal separation conditions.

Separations using phthalate

Several complexing reagents were tried in connection with the attempted separation of several mono- and divalent metal cations. Only partial complexing of the metal cations is desired because complete complexing is apt to result in species that move at the same rate as the electroosmotic flow. The following complexing reagents were tried initially: HIBA, phthalic acid, malonic acid and succinic acid. Of these, HIBA and phthalic acid were the most promising. HIBA had been used previously for the separation of several mono- and divalent metal ions [3]. However, we obtained even better separations with phthalic acid. A good separation of eight metal ions in about 6 min is shown in Fig. 1.

Separations with phthalic acid were usually better when some methanol was added to the electrolyte. Methanol caused the moving times to be longer and resolution to be better. Elution times of the ions studied increased with added methanol up to about 20% methanol (by volume). With further increases in the proportion of methanol there was a plateau with no further changes in elution times.

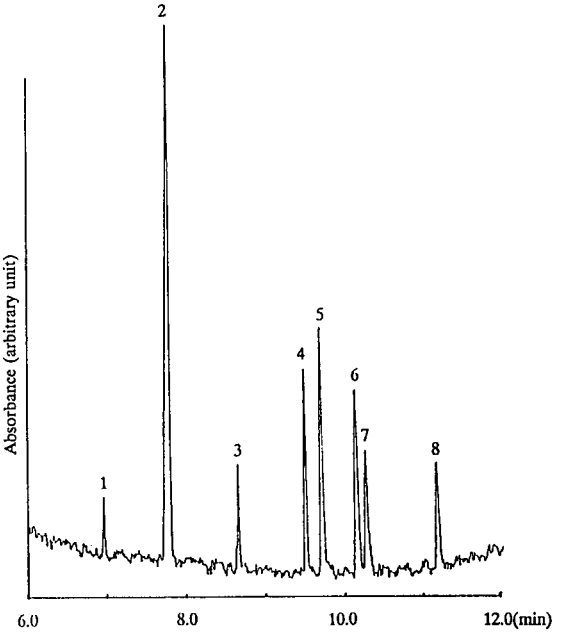

Fig. 1. Separation of metal ions using phthalate. Electrolyte, 2 m*M* phthalic acid, UV-Cat1, 20% methanol, pH 3.3; applied voltage, 15 kV. Peaks: 1 = K^+; 2 = Na^+; 3 = Pb^{2+}; 4 = Mn^{2+}; 5 = Co^{2+}; 6 = Ni^{2+}; 7 = Zn^{2+}; 8 = Cd^{2+}.

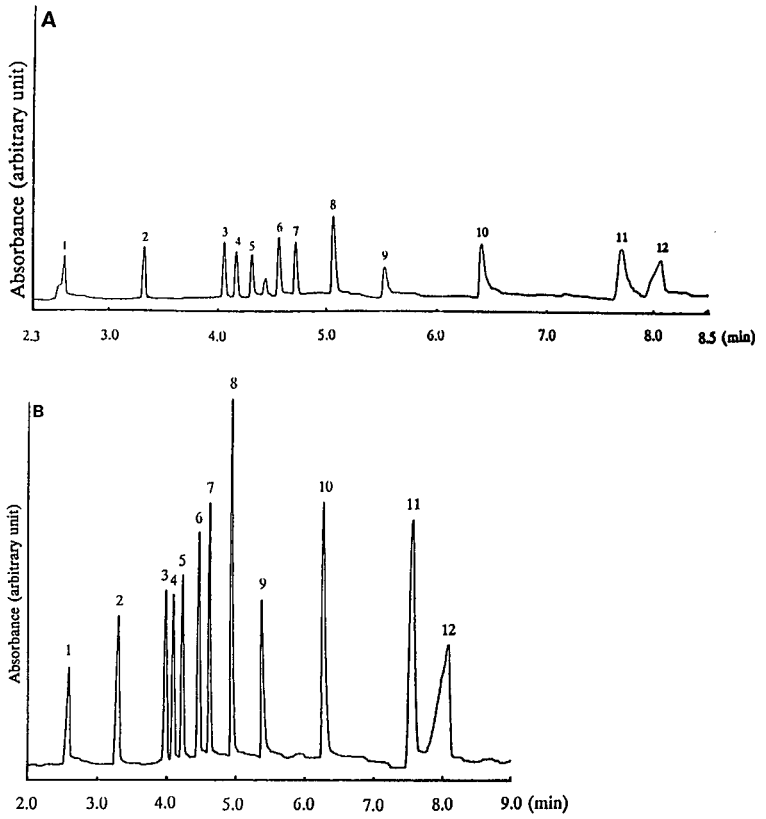

Fig. 2. (A) Separation of 12 alkali, alkaline earth and transition metal ions using tartrate. Electrolyte, 2.5 m*M* tartaric acid, 6 m*M* *p*-toluidine, 20% methanol, pH 4.8; applied voltage, 30 kV. Peaks: 1 = K^+ (1.3 μg/ml); 2 = Na^+ (0.8 μg/ml); 3 = Li^+ (0.2 μg/ml); 4 = Mg^{2+} (0.3 μg/ml); 5 = Ba^{2+} (1.3 μg/ml); 6 = Sr^{2+} (1.3 μg/ml); 7 = Mn^{2+} (0.8 μg/ml); 8 = Ca^{2+} (0.8 μg/ml); 9 = Cd^{2+} (1.3 μg/ml); 10 = Co^{2+} (1.0 μg/ml); 11 = Ni^{2+} (1.0 μg/ml); 12 = Zn^{2+} (1.0 μg/ml). (B) Separation of 12 alkali, alkaline earth and transition metal ions using tartrate. Four times higher concentration of each analyte as in (A). Electrolyte conditions and applied voltage same as described in (A).

Separations using tartrate

After optimizing conditions for CE with a phthalate system, it was found that even better separations of metal cations could be obtained with tartrate as the complexing reagent. Tartrate forms comparatively weak complexes with a number of metal ions and is therefore suitable for capillary ion electrophoresis. However, copper(II) is more strongly complexed and elutes very late or not at all.

An excellent separation of twelve metal ions in a total time of only 8 min is shown in Fig. 2. Resolution is excellent with a steady, flat baseline, as shown in Fig. 2A. At the higher concentration in Fig. 2B, the peaks are very narrow and well shaped.

Some optimization of conditions was required to obtain separations of the quality shown in Fig. 2. The concentration of tartrate and *p*-toluidine used, pH and applied voltage were the most important variables. Methanol (20%) was added to the electrolyte to improve resolution of the divalent metal ions.

Much of the literature on CE does not adequately address the question of the quantitative aspects. We therefore prepared calibration curves for the metal ions studied in the tartrate system. Good linear calibration curves were obtained for the ions studied in the 0.4–10 μg/ml concentration range. The only exception was zinc(II) which gave a relatively poor correlation coefficient for linear regression.

Separations using lactate

Lactate has the same complexing groups as tar-

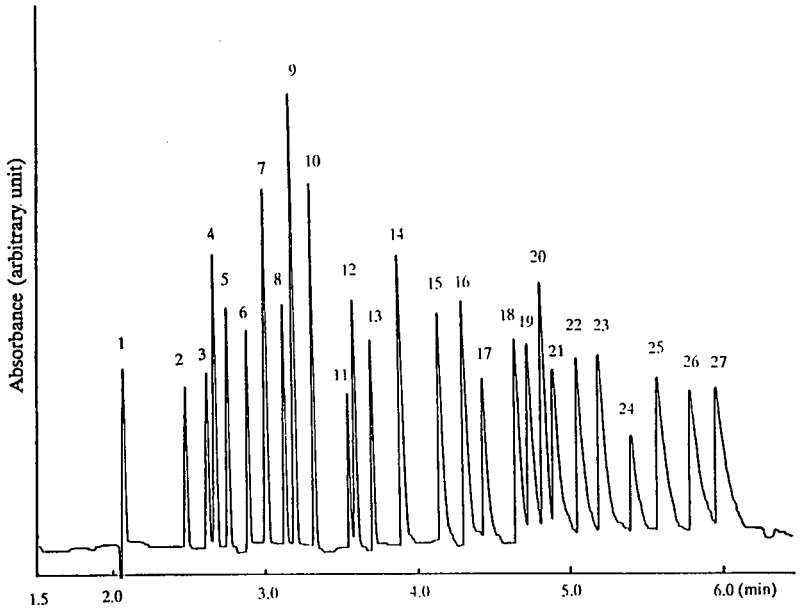

Fig. 3. Separation of 27 alkali, alkaline earth, transition and rare earth metal ions in a single run using lactate. Electrolyte, 15 m*M* lactic acid, 8 m*M* 4-methylbenzylamine, 5% methanol, pH 4.25; applied voltage, 30 kV. Peaks: 1 = K^+; 2 = Ba^{2+}; 3 = Sr^{2+}; 4 = Na^+; 5 = Ca^{2+}; 6 = Mg^{2+}; 7 = Mn^{2+}; 8 = Cd^{2+}; 9 = Li^+; 10 = Co^{2+}; 11 = Pb^{2+}; 12 = Ni^{2+}; 13 = Zn^{2+}; 14 = La^{3+}; 15 = Ce^{3+}; 16 = Pr^{3+}; 17 = Nd^{3+}; 18 = Sm^{3+}; 19 = Gd^{3+}; 20 = Cu^{2+}; 21 = Tb^{3+}; 22 = Dy^{3+}; 23 = Ho^{3+}; 24 = Er^{3+}; 25 = Tm^{3+}; 26 = Yb^{3+}; 27 = Lu^{3+}. The concentration of each lanthanide, Ba^{2+}, Sr^{2+}, and Pb^{2+} was 5 μg/ml; the concentration of transition metals, K^+, Na^+, and Ca^{2+} was 3–4 μg/ml, Mg^{2+} was 2 μg/ml and Li^+ was 1 μg/ml.

trate (carboxyl and hydroxyl) but is a smaller molecule and forms somewhat weaker complexes with most metal ions. Preliminary experiments indicated that a lactate system might give good separations both for divalent metal ions and for trivalent lanthanides.

A brief optimization of major conditions was first carried out for separation of the lanthanides. These conditions included the concentrations of lactate and UV visualization reagent, and pH. A very good separation of the thirteen lanthanides was obtained. It was also found that excellent separations could be obtained under the same conditions for alkali metal ions, magnesium and the alkaline earths, and several divalent transition metal ions. All of these except copper(II) eluted before the lanthanides. An excellent separation of 27 metal ions was obtained in a single run that required only 6 min (Fig. 3).

The detection limit for these metal ions was in the range 0.05–0.5 μg/ml. Light ions are in the low detection limit range, and heavy ions are in the high detection limit range. The average deviation in peak height from one run to another was approximately ± 5% or smaller at the ion concentrations used.

Separations using HIBA

HIBA has been used extensively for CE. Very good separations of magnesium, the alkaline earths and several of the divalent transition metal ions have been reported [3]. Excellent separation of all of the lanthanides have also been obtained [1,3]. In one instance, thirteen lanthanides plus six other metal ions were separated in a single run, although the shapes of some of the earlier peaks were rather poor [1,3].

We experimented with separation of the lanthanides using HIBA as the complexing reagent. A brief optimization was employed to establish pH and suitable concentrations of HIBA and the UV-sensitive reagent. The concentration of HIBA needed was found to be considerably lower than lactic acid in the previous system. A truly excellent separation of the lanthanides was obtained (Fig. 4). The conditions we established are quite similar to those previously reported.

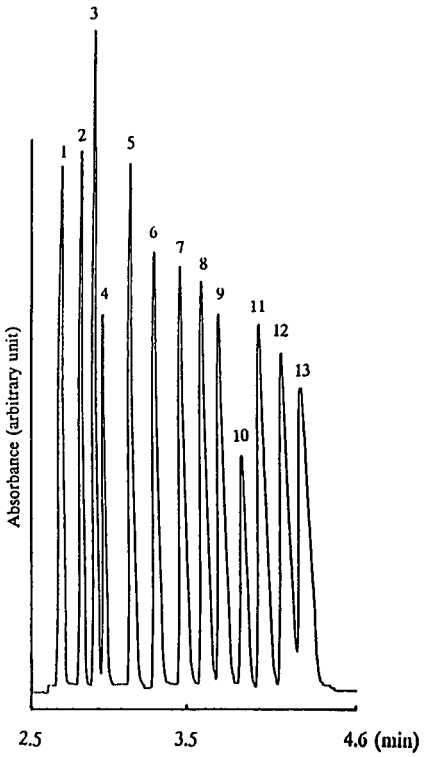

Fig. 4. Separation of 13 lanthanides using HIBA. Electrolyte, 4 m*M* HIBA, 5 m*M* UV Cat1, pH 4.3; applied voltage, 30 kV. Peaks: 1 = La^{3+}; 2 = Ce^{3+}; 3 = Pr^{3+}; 4 = Nd^{3+}; 5 = Sm^{3+}; 6 = Gd^{3+}; 7 = Tb^{3+}; 8 = Dy^{3+}; 9 = Ho^{3+}; 10 = Er^{3+}; 11 = Tm^{3+}; 12 = Yb^{3+}; 13 = Lu^{3+}

The separation mechanism

In CE it is now common to use a reagent to partially complex metal ions and improve the quality of their separation by altering their net flow characteristics. For example, addition of tartrate to a solution containing metal cations (M_1^{2+}, M_2^{2+}, etc.) may convert some fraction of the metal ions to tartrate complexes (M_1–tart, M_2–tart, etc.). The free cations move along the capillary at rates proportional to their ionic mobilities while the *complexed* metal ions move at a slower speed. Continuous equilibration between free and complexed metal ions causes each metal to move through the capillary as a tight zone. Separation occurs because of the different overall rates at which the zones move. The situation is again somewhat analogous to HPLC except that in this case the "stationary phase" (metal tartrate complexes) is not a real phase and is not stationary, but moves at a slower speed than the free metal cations.

The more completely a metal ion is complexed, the slower will be its rate of movement. If the fraction of metal in the free cation is too small, it may take a long time for the metal to emerge from the capillary and no good separation will be obtained. However, if the various metal ions are not sufficiently complexed (too large a fraction of free metal ion), ions of similar ionic mobility may be poorly

TABLE I

FRACTIONS OF FREE (α_M) AND COMPLEXED (α_{ML_n}) RARE EARTH METAL IONS AND AVERAGE NUMBER OF LIGANDS ($\bar{n}$) IN 4 m*M* HIBA ELECTROLYTE SOLUTION AT pH 4.3

Metal	α_M	α_{ML}	α_{ML2}	α_{ML3}	α_{ML4}	$\bar{n}$
La	0.578	0.360	0.612			0.482
Ce	0.448	0.496	0.052	0.004		0.612
Pr	0.407	0.496	0.093	0.005	0.000	0.697
Nd	0.333	0.572	0.085	0.010	0.000	0.772
Sm	0.296	0.520	0.170	0.013	0.001	0.903
Gd	0.250	0.481	0.244	0.024	0.001	1.045
Tb	0.181	0.470	0.307	0.040	0.002	1.212
Dy	0.141	0.384	0.387	0.084	0.004	1.426
Ho	0.122	0.365	0.413	0.093	0.006	1.494
Er	0.097	0.309	0.472	0.112	0.010	1.629
Tm	0.079	0.309	0.473	0.123	0.016	1.686
Yb	0.070	0.296	0.431	0.169	0.033	1.797
Lu	0.047	0.222	0.514	0.172	0.045	1.946

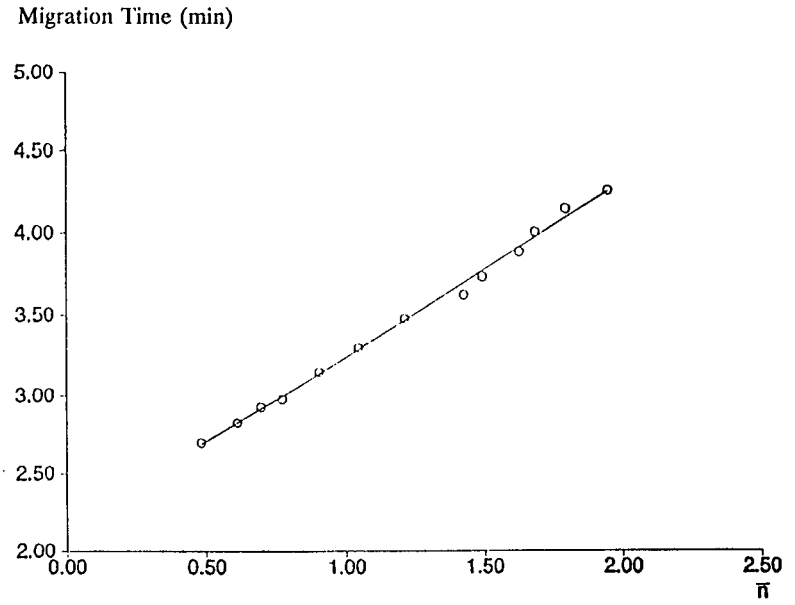

Fig. 5. Plot of moving time *vs.* average number of ligands for 13 lanthanides. Electrolyte conditions and applied voltage same as described for Fig. 4.

separated. Almost nothing has appeared in the literature concerning how strongly metal ions should be complexed for optimal separation by CE. However, Hirokawa *et al.* [9] computed the absolute mobilities of some lanthanide complexes used in isotachophoresis.

We considered the separation of rare earths using 4.0 m*M* HIBA at pH 4.3 as the complexing reagent (see Fig. 4). Using published formation constants [10], the fraction of rare earths present in various chemical forms was calculated by a well-known method [11,12] under the same conditions of pH and HIBA concentration used for the CE separation in Fig. 4. The calculated distribution of chemical species for each rare earth is shown in Table I.

Some interesting conclusions can be drawn from the information in Table I. The predominating species are the free metal ion (M^{3+}), the 1:1 metal–ligand complex (probably ML^{2+}), the 2:1 complex (probably ML_2^+) and the 3:1 complex (probably ML_3). A small fraction of the higher rare earths is also present as the 4:1 complex. Another striking feature is that the average number of ligands associated with a rare earth ($\bar{n}$ increases rapidly with increasing atomic number. This occurs in a fairly regular manner as demonstrated by a plot of $\bar{n}$ against atomic number which has a linear regression correlation coefficient of 0.9958.

In CE the positively charged complexes, as well as the free metal cation, would be expected to move through the capillary by electrophoretic flow as well as by the electroosmotic flow that affects all species. However, the electrophoretic mobility should be slower for ML^{2+} than for M^{3+} and still slower for the larger ML_2^+. Even if the different species move at different rates, rapid equilibrium shifts should keep a tight zone for each of the rare earths. For example, as the faster moving M^{3+} starts to move ahead of the other species, it reequilibrates with the ligand (L) to form a larger fraction of the slower-moving species. At the back edge of the zone, the slower-moving complexes reequilibrate to give a greater fraction of M^{3+}. The average rate of movement should depend on te weighted average of the mobilities of the different species.

This last speculation was tested by plotting the moving time of the various rare earths (from Fig. 4) against the $\bar{n}$ values in Table I. This plot is shown in Fig. 5. It is essentially linear with a correlation coefficient of 0.9978.

ACKNOWLEDGEMENTS

We wish to thank Waters Division of Millipore for their gift of the Waters Quanta 4000 CE system and associated chemicals. We also thank Andrea Weston and Peter Jandik for valuable technical assistance in the initial stages of this research.

Ames Laboratory is operated for the US Department of Energy under Contract No. W-7405-Eng-82. This work was supported by the Director of Energy Research, Office of Basic Energy Sciences.

REFERENCES

1 F. Foret, S. Fanali, A. Nardi and P. Bocek, *Electrophoresis*, 11 (1990) 780.
2 A. Weston, P. R. Brown, A. L. Heckenberg, P. Jandik and W. R. Jones, *J. Chromatogr.*, 602 (1992) 249.
3 A. Weston, P. R. Brown, P. Jandik, W. R. Jones and A. L. Heckenberg, *J. Chromatogr.*, 593 (1992) 289.
4 P. Jandik, W. R. Jones, A. Weston and P. R. Brown, *LC · GC*, 9 (1991) 634.
5 L. Gross and E. S. Yeung, *Anal. Chem.*, 62 (1990) 427.
6 M. Aguilar, X. Huang and R. N. Zare, *J. Chromatogr.*, 480 (1989) 427.
7 X. Huang and R. M. Zare, *Anal. Chem.*, 63 (1991) 2193.
8 M. Chen and R. M. Cassidy, *J. Chromatogr.*, 602 (1992) 227.
9 T. Hirokawa, N. Aoki and Y. Kiso, *J. Chromatogr.*, 312 (1984) 11.
10 *Stability Constants*, Supplement No. 1, Special Publication 25, Chemical Society, London, 1971.
11 A. Ringbom, *Complexation in Analytical Chemistry*, Wiley Interscience, New York, 1963, p. 29.
12 J. S. Fritz and G. H. Schenk, *Quantitative Analytical Chemistry*, Allyn & Bacon, Boston, MA, 5th ed., 1987, p. 197.

Journal of Chromatography, 640 (1993) 481–487
Elsevier Science Publishers B.V., Amsterdam

CHROMSYMP. 2750

Optimization of injection technique in capillary ion electrophoresis for the determination of trace level anions in environmental samples

P. E. Jackson*

Waters Chromatography Division of Millipore, Private Bag 18, Lane Cove, N.S.W. 2066 (Australia)

P. R. Haddad

Department of Chemistry, University of Tasmania, G.P.O. Box 252C, Hobart, Tasmania 7001 (Australia)

ABSTRACT

Capillary ion electrophoresis (Waters' trade name: Capillary Ion Analysis) offers several advantages compared to ion chromatography for the analysis of ionic solutes, primarily simplicity, matrix independence, and a different separation selectivity. The use of electromigration sample introduction leads to on-capillary enrichment of ionic analytes at the sample–buffer interface, permitting the determination of low ng/ml levels of anions in environmental samples of moderate ionic strength. This injection method allows improved sensitivity compared to hydrostatic injection; and is significantly more rapid than precolumn concentration ion chromatography. The analyte enrichment rate, hence peak response, is strongly dependent upon ionic strength and appropriate measures, such as standard addition or internal standard techniques, must be used to account for differences in standard and sample conductance.

INTRODUCTION

Capillary ion electrophoresis (CIE) (Waters' trade name: Capillary Ion Analysis, CIA) is emerging as an alternative analytical technique to ion chromatography (IC) for the determination of inorganic anions, cations and organic acids [1]. There are a number of advantages of using capillary zone electrophoresis (CZE) for ion analysis when compared to IC, primarily simplicity, matrix independence and the fact that the selectivity differs from conventional ion exchange separations [2]. Sample introduction in CZE differs from IC or HPLC in that an injection valve is not typically used. Injection modes in CZE include hydrostatic (or gravity), application of either pressure or vacuum and electromigration injection [3,4]. Electromigration injection involves applying a voltage to the sample in order to force the ions to migrate into the capillary. This injection mode is selectivity biased toward ions of the opposite charge to that of the detection electrode [4], with the bias being proportional to the total mobility of each ion [5]. When electromigration injections of low ionic strength samples are carried out, (electro)stacking of the sample ions occurs [1]. When electromigrating such samples, the voltage drop is not constant over the entire length of the capillary. There is very little voltage drop over the length of the capillary filled with conductive (low resistivity) buffer as almost all of the voltage drop occurs over the low conductance (high resistivity) volume of the sample injection [4]. This effectively leads to on-capillary concentration of the analyte at the sample–buffer interface [6–10].

Applications of on-line sample preconcentration in IC are typically restricted to the analysis of ultratrace (ng/ml) level anions and cations in low ionic

* Corresponding author.

0021-9673/93/$06.00

strength samples, such as boiler, steam condenstate and deionized waters [11–13]. Similarly, electromigration (concentration) injection has been applied to the analysis of ng/ml levels of anions in ultrapure water samples using CIE [10]. It has been demonstrated that quantitative on-column preconcentration of high ionic strength samples is possible in IC for certain anions through appropriate selection of system configuration and operating parameters [14]. In this paper, both qualitative and quantitative aspects of the application of CIE with electromigration concentration injection for the analysis of trace anionic solutes in moderate ionic strength environmental samples, such as estuary waters and soil extracts, are discussed.

EXPERIMENTAL

Instrumentation

The capillary electrophoresis instrument used was a Waters Quanta 4000 with a Waters 820 data station. Data were collected at 20 points per second for CIE. Separations were carried out using a conventional fused-silica capillary (60 cm × 75 μm I.D.) obtained from Waters. Detection was achieved using either indirect spectrophotometry at 254 nm or direct spectrophotometry at 214 nm.

Reagents and procedures

Water (18 MΩ) purified using a Millipore Milli-Q water purification system (Bedford, MA, USA) was used for all solutions. Sodium chromate tetrahydrate was obtained from Aldrich (Milwaukee, WI, USA). Sodium tetraborate [analytical reagent (AR) grade], glycerin [laboratory reagent (LR) grade] and boric acid (AR) were obtained from Ajax Chemicals (Sydney, Australia), as were the analytical grade sodium salts used for the preparation of all the anion standards. Sodium gluconate (LR) was obtained from Fluka (Buchs, Switzerland). Acetonitrile and *n*-butanol (HPLC grade) were obtained from Waters. The electroosmotic flow modifier, CIA-Pak OFM anion-BT is a proprietary chemical obtained from Waters. Eluents and electrolytes were prepared daily, filtered and degassed with a Waters solvent clarification kit. Specific operating conditions are provided as captions to the figures.

RESULTS AND DISCUSSION

Enhancement of sensitivity using electromigration injection

Electromigration injection is frequently used as a sample introduction technique in conventional CZE as it is possible to very accurately control both voltage and time of injection, resulting in good precision. Also, electromigration is the only possible mode of injection when using gel-filled capillaries. However, as this mode is biased toward ions of the opposite charge to that of the detection electrode [4], hydrostatic (or pressure/vacuum) sample introduction is most commonly used in CIE in order to introduce a representative sample into the capillary [2,15]. Fig. 1 shows an electropherogram obtained using CIE with a 30-s hydrostatic injection of a low μg/ml level anion standard using a chromate electrolyte and indirect UV detection at 254 nm and Fig. 2 shows an electropherogram of estuarine water sampled near a sewage effluent outlet obtained using a 15-s hydrostatic injection. Chloride, sulfate, nitrate and carbonate were detected in the water sample at low μg/ml levels. The duration of the hydrostatic injection was then increased in order to introduce more sample into the capillary and investigate the possibility that sub-μg/ml levels of other anions might also be present in this sample. Detection limits improved with longer sampling times, however, sampling times longer than 60 s, which corresponded to the injection of approximately 75 nl on the capillary [4], resulted in poor peak shape due to disturbance of the sample–buffer interface zone; and no additional sensitivity was obtained beyond this point. In this respect, CE is similar to HPLC, where large injection volumes typically lead to distorted peaks [16].

Analysis of the same estuarine water by CIE using a 3-kV electromigration injection for 10 s allowed low ng/ml levels of fluoride (and formate) to be detected in the sample. Increasing the injection time to 30 s further increased the detection sensitivity and allowed phosphate to be detected in the sample, as shown in close-up view in Fig. 3. Using single point, external calibration, the phosphate-P was determined to be present at *ca.* 13 ng/ml in the sample by CIE, compared to *ca.* 8 ng/ml when using a flow injection analysis technique. Table I details the detection limits (2 times the signal-to-noise ra-

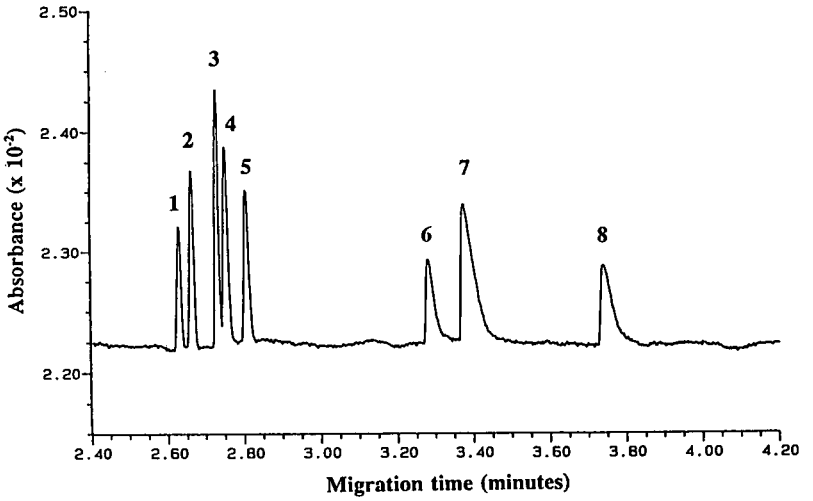

Fig. 1. Electropherogram of standard ions using hydrostatic injection. Conditions: capillary, 60 cm × 75 μm I.D. fused-silica; power supply, negative at 20 kV; electrolyte, 5 m*M* chromate with 0.5 m*M* CIA-Pak OFM Anion-BT at pH 8.0; injection, hydrostatic for 30 s; detection, indirect UV at 254 nm. Solutes: 1 = bromide (4.0 μg/ml); 2 = chloride (2.0 μg/ml); 3 = sulfate-S (1.3 μg/ml); 4 = nitrite-N (1.2 μg/ml); 5 = nitrate-N (0.9 μg/ml); 6 = fluoride (1.0 μg/ml); 7 = phosphate-P (1.9 μg/ml); 8 = carbonate (not quantitated).

tio) obtained using both hydrostatic and electromigration injection modes for the anions present in the estuarine water sample. Overall, CIE with electromigration injection resulted in an approximately 10 times improvement in sensitivity for the common anions for this particular sample when compared to hydrostatic injection. Generally, the lower the ionic strength of the sample, the greater the enhancement of sensitivity and detection limits in the sub-ng/ml range have been achieved for high purity waters with CIE [10], as the electrostacking of the analyte at the sample–buffer interface is very large for high resistivity samples.

Nitrite could not be detected in the estuarine wa-

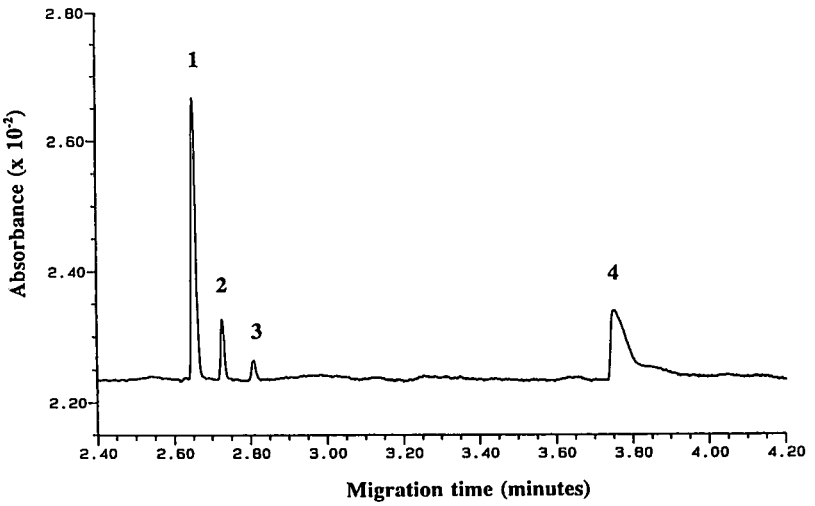

Fig. 2. Electropherogram of estuarine water sample using hydrostatic injection. Conditions as for Fig. 1 except: injection, hydrostatic for 15 s. Solutes: 1 = chloride (12.4 μg/ml); 2 = sulfate-S (1.1 μg/ml); 3 = nitrate-N (0.4 μg/ml); 4 = carbonate.

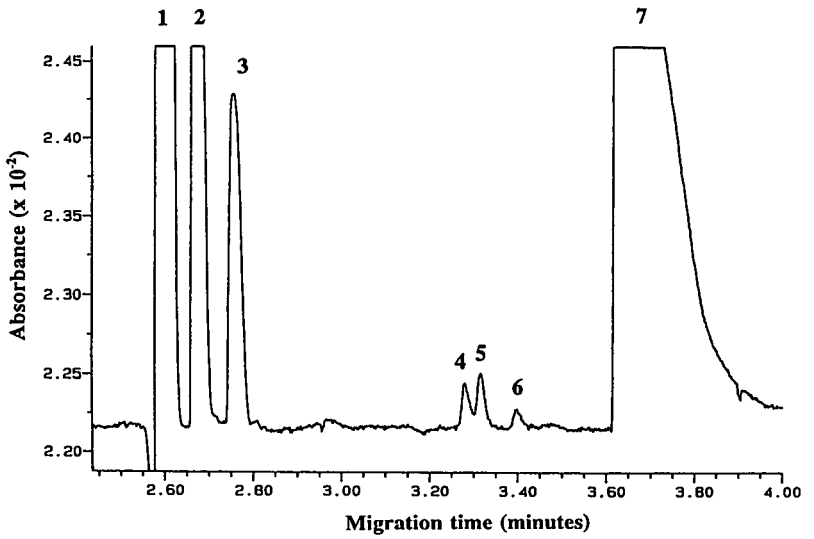

Fig. 3. Electropherogram of estuarine water sample using electromigration injection. Conditions as for Fig. 1 except: injection, electromigration, 3 kV for 30 s. Solutes: 1 = chloride (12.4 μg/ml); 2 = sulfate-S (1.1 μg/ml); 3 = nitrate-N (0.4 μg/ml); 4 = fluoride (0.031 μg/ml); 5 = formate (not quantitated); 6 = phosphate-P (0.013 μg/ml); 7 = carbonate.

ter sample with electromigration injection when using indirect UV detection, as the sulfate peak response increased as higher sampling times (or voltages) and interfered with the detection of nitrite. As is the case with IC [17], increased detection sensitivity and selectivity can be achieved with capillary electrophoresis for UV absorbing anions, such as nitrite and nitrate, by using direct UV detection. Fig. 4 shows an electropherogram of the estuarine water sample obtained with a 3-kV electromigration injection for 3 s using a sulfate electrolyte and direct UV detection at 214 nm. The combination of electromigration injection and direct UV detection allowed the determination of nitrite-N (at a concentration of *ca.* 9 ng/ml) and nitrate-N in the sample. The disturbance in the early portion of the electro-

TABLE I

DETECTION LIMITS (ng/ml) FOR ANIONS IN ESTUARINE WATER SAMPLE BY CIE USING HYDROSTATIC AND ELECTROMIGRATION INJECTION

Anion	Injection method			
	Chromate electrolyte 30 s hydrostatic	Chromate electrolyte 3 kV, 30 s electromigration	Sulfate electrolyte 30 s hydrostatic	Sulfate electrolyte 3 kV, 30 s electromigration
Chloride	157	[b]	[c]	[c]
Sulfate	79	[b]	[c]	[c]
Nitrite-N	31[a]	[b]	19	2.5
Nitrate-N	30	[b]	15	1.6
Fluoride	61[a]	7.1	[c]	[c]
Phosphate-P	74[a]	6.3	[c]	[c]

[a] Detection limit obtained from standard.
[b] Not determined.
[c] Anion not detectable using direct UV absorption at 214 nm.

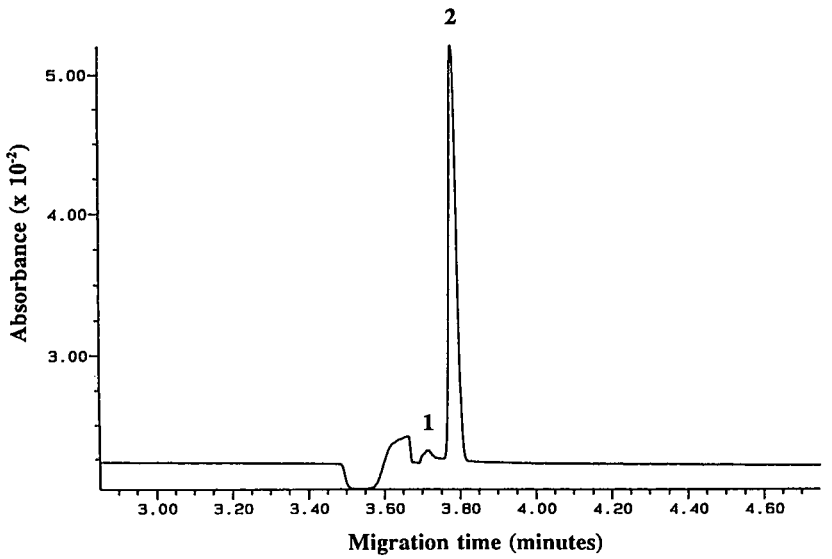

Fig. 4. Electropherogram of estuarine water sample using electromigration injection and direct UV detection. Conditions as for Fig. 2 except: power supply, negative at 14 kV; electrolyte, 10 m*M* sulfate with 0.5 m*M* CIA-Pak OFM Anion-BT; injection, electromigration, 3 kV for 10 s; detection, direct UV at 214 nm. Solutes: 1 = nitrite-N (0.4 μg/ml); 2 = nitrate-N (0.009 μg/ml).

pherogram was due to the migration of the UV transparent chloride and sulfate anions. Table I also details the detection limits obtained by hydrostatic and electromigration injection when using the sulfate electrolyte and direct UV detection at 214 nm.

Quantitation using electromigration injection

CIE offers a distinct advantage over IC for ultratrace analysis in terms of the time taken for the sample 'enrichment' step. In IC, a typical sample volume (10–100 ml) is loaded onto a concentrator column via an HPLC pump at flow-rates of 2–4 ml/min, hence the sample loading step usually takes 5–25 min, or perhaps longer [18]. Large enrichment factors can be achieved in CIE in a matter of seconds using electromigration injection. However, the major disadvantage of using CIE with electromigration injection for ultratrace analysis is that considerable care must be taken in order to achieve accurate quantitation. Initial attempts to use CIE with electromigration injection for the determination of sub-μg/ml levels of fluoride in a low salinity bore water consistently resulted in low values compared to IC when using an anion HR column, a borate–gluconate eluent and conductivity detection [19]. The difference in ionic strength of the standard and sample led to different enrichment factors, resulting in low recoveries for the sample fluoride. This was confirmed by determining the peak response for a fluoride standard prepared containing increasing concentrations of chloride using CIE with both hydrostatic and electromigration injection, shown in Fig. 5. As the ionic strength of the sample increased the fluoride response decreased significantly when using electromigration sample introduction with CIE.

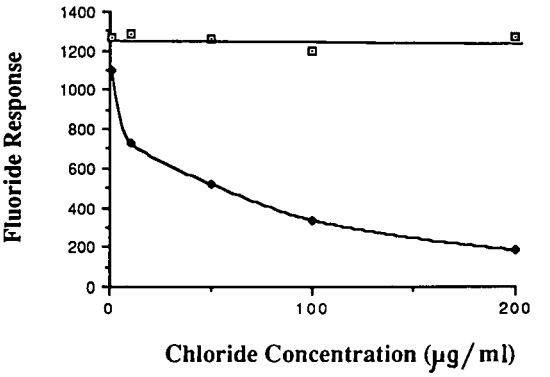

Fig. 5. Effect of chloride concentration on fluoride response using hydrostatic (□) and electromigration (◆) injection. Conditions as for Fig. 1 except: injection, hydrostatic for 30 s and electromigration, 3 kV for 10 s. Solutes: fluoride (1.0 μg/ml); chloride as indicated.

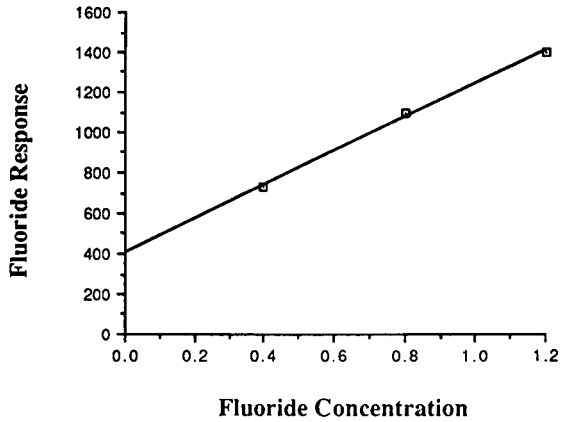

Fig. 6. Standard addition calibration plot for fluoride in bore water using electromigration injection. Conditions as for Fig. 3 except: injection, electromigration, 3 kV for 10 s. Solutes: fluoride spiked at 0.4, 0.8 and 1.2 μg/ml; original fluoride sample concentration calculated to be 0.47 μg/ml.

The use of CIE with electromigration injection has been shown to given accurate quantitation for the analysis of anions in ultrapure waters, after the addition of a constant amount (low μM concentrations) of a non-intefering anion (such as octanesulfonate) to normalize the ionic strength of both standards and samples [10]. This approach is less attractive for samples of higher ionic strength, as the amount of added buffer required to ensure a constant ionic strength would be high, therefore the enrichment factors achieved using electromigration injection would be reduced. When using conventional CZE with electromigration sample introduction, typically, one, or possibly two, internal standards are often added in order to improve quantitation [20]. Another option suggested has been to monitor the current generated during sample introduction and correct for variations, in a similar fashion to the use of an internal standard [20].

Perhaps the simplest approach to achieve accurate quantitation when using electromigration injection is to use standard addition techniques. Fluoride could be accurately determined in the low salinity bore water with electromigration injection and standard addition. The bore water sample was spiked with 0.4, 0.8 and 1.2 μg/ml fluoride and from the calibration plot, shown in Fig. 6, fluoride was calculated to be present at 0.47 μg/ml in the original sample. This compared to a value of 0.45 μg/ml when using IC with an anion HR column, borate–gluconate eluent and conducticity detection. However, there are practical limitations when using standard addition techniques, particularly the accurate preparation and addition of sub-μg/ml standard spikes.

Generally, the use of an internal standard proved to be the most versatile approach for accurate quantitation when performing electromigration sample introduction. A wide range of environmen-

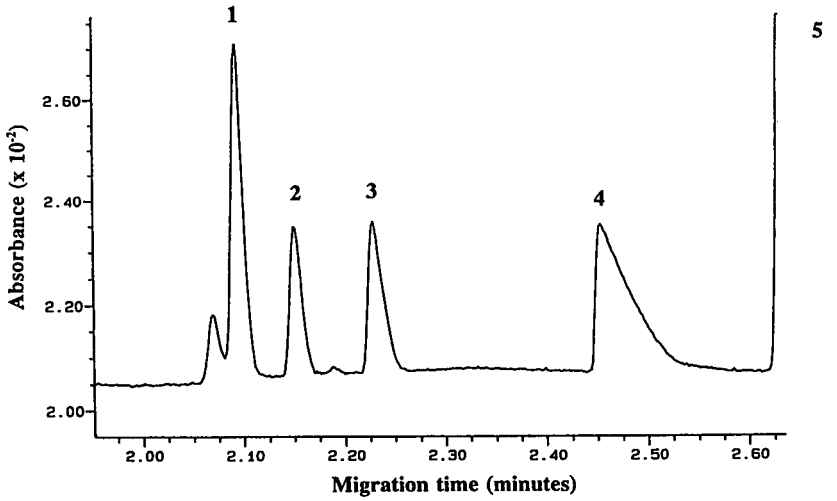

Fig. 7. Electropherogram of sulfate in a phosphate buffer soil extract using electromigration injection. Conditions as for Fig. 3 except: injections, electromigration, 3 kV for 10 s; sample, 4.0 g soil in 20 ml 0.02 M potassium dihydrogenphosphate. Solutes: 1 = chloride; 2 = sulfate-S (3.06 μg/ml); 3 = nitrate; 4 = citrate (internal standard added at 40 μg/ml); 5 = phosphate.

tal samples, including sewage effluents, run-off waters, tailings dam waters, river and lake waters, were successfully analyzed by CIE with electromigration injection. An important example is the determination of sulfate in soil extracts, as this analysis is widely used as an indication of soil fertility. Fig. 7 shows a close-up view of an electropherogram obtained using CIE with a 3-kV, 10-s electromigration injection of a phosphate buffer extract of a soil sample. Citrate was added as the internal standard and sulfate-S was determined to be 3.06 μg/ml in this case, compared to 3.28 μg/ml by IC. A precision of 2.0% R.S.D. was obtained for four consecutive injections of the sample with a detection limit of 21 ng/ml at 2 times the signal-to-noise ratio.

CONCLUSIONS

The use of electromigration sample injection with CIE leads to on-capillary concentration of the analyte at the sample–buffer interface, permitting the determination of low ng/ml levels of anions in samples of moderate ionic strength. This technique allows significantly improved sensitivity compared to hydrostatic injection; and offers a distinct advantage over precolumn concentration IC, as large enrichment factors can be achieved in a matter of seconds. Analyte enrichment rate, hence peak response, is strongly dependent upon ionic strength and appropriate measures, such as the use of standard addition or internal standard techniques, must be used to account for differences in standard and sample conductance.

ACKNOWLEDGEMENTS

The authors wish to thank the Ministery of Agriculture and Fisheries (Hamilton, New Zealand), Auckland Regional Council (Auckland, New Zealand) and Western Australian Water Authority (Perth, Australia) for supplying the various water samples.

REFERENCES

1 P. Jandik, W. R. Jones, A. Weston and P. R. Brown, *LC · GC*, 9 (1991) 634.
2 W. R. Jones and P. Jandik, *J. Chromatogr.*, 546 (1991) 441.
3 W. G. Kuhr, *Anal. Chem.*, 62 (1990) 403R.
4 J. D. Olechno, J. M. Y. Tso, J. Thayer and A. Wainright, *Am. Lab.*, December (1990) 30.
5 X. Huang, M. J. Gordon and R. Zare, *Anal. Chem.*, 60 (1988) 375.
6 S. Hjerten, S. Jerstedt and A. Tiselius, *Anal. Biochem.*, 11 (1965) 219.
7 R.-L. Chien, *Anal. Chem.*, 63 (1991) 2866.
8 R.-L. Chien and D. S. Burgi, *Anal. Chem.*, 64 (1992) 1046.
9 V. Dolnik, K. A. Cobb and M. Novotny, *J. Microcol. Sep.*, 2 (1990) 127.
10 P. Jandik and W. R. Jones, *J. Chromatogr.*, 546 (1991) 431.
11 D. F. Pensenstadler and M. A. Fulmer, *Anal. Chem.*, 53 (1981) 859A.
12 K. M. Roberts, D. T. Gjerde and J. S. Fritz, *Anal. Chem.*, 53 (1981) 1691.
13 R. Gilbert, R. Rioux and S. E. Saheb, *Anal. Chem.*, 56 (1984) 106.
14 P. E. Jackson and P. R. Haddad, *J. Chromatogr.*, 439 (1988) 37.
15 J. Romano, P. Jandik, W. R. Jones and P. E. Jackson, *J. Chromatogr.*, 546 (1991) 411.
16 *Developing HPLC Separations, Book One*, Millipore, Bedford, MA, 1991, p. 2–10.
17 P. R. Haddad and P. E. Jackson, *Ion Chromatography: Principles and Applications* (*Journal of Chromatography Library*, Vol. 46), Elsevier, Amsterdam, 1990, Ch. 12.
18 P. R. Haddad and P. E. Jackson, *J. Chromatogr.*, 367 (1986) 301.
19 *Waters Innovative Methods for Ion Analysis*, Millipore, Bedford, MA, 1989, Method A-103.
20 T. T. Lee and E. S. Yeung, *Anal. Chem.*, 64 (1992) 1226.

Author Index

Vol. 640, Nos. 1 + 2

Journal of Chromatography

NEWS SECTION

INTERNATIONAL ION CHROMATOGRAPHY SYMPOSIUM 1992, LINZ, SEPTEMBER 21–24, 1992

Fig. 1. Professor Josef F.K. Huber (right), University of Vienna, congratulates Joachim Weiss (left), the 1992 Ion Chromatography Achievement Awardee.

Fig. 2. The Scientific Committee (left to right): Doug Gjerde, Sarasep, Inc.; Petr Jandik, Waters Division of Millipore; Paul Haddad, University of Tasmania; John Lamb, Brigham Young University; John Stillian, Dionex Corporation; James Fritz, Iowa State University; Gabriella Schmuckler, Technion; Richard Cassidy, University of Saskatchewan; Donald Pietrzyk, University of Iowa; Günther Bonn, Johannes-Kepler-University.

PUBLICATION SCHEDULE FOR THE 1993 SUBSCRIPTION

Journal of Chromatography and *Journal of Chromatography, Biomedical Applications*

MONTH	1992	J	F	M	A	M	J	J	
Journal of Chromatography	Vols. 623–627	628/1 628/2 629/1 629/2	630/1 + 2 631/1 + 2 632/1 + 2 633/1 + 2	634/1 634/2	635/1 635/2 636/1 636/2	637/1 637/2 638/1 638/2	639/1 639/2 640/1 + 2	641/1 641/2 642/1 + 2 643/1 + 2 644/1	The publication schedule for further issues will be published later
Cumulative Indexes, Vols. 601–650									
Bibliography Section				649/1			649/2		
Biomedical Applications		612/1	612/2	613/1	613/2 614/1	614/2 615/1	615/2 616/1	616/2 617/1	

INFORMATION FOR AUTHORS

(Detailed *Instructions to Authors* were published in Vol. 609, pp. 437–443. A free reprint can be obtained by application to the publisher, Elsevier Science Publishers B.V., P.O. Box 330, 1000 AH Amsterdam, The Netherlands.)

Types of Contributions. The following types of papers are published in the *Journal of Chromatography* and the section on *Biomedical Applications:* Regular research papers (Full-length papers), Review articles, Short Communications and Discussions. Short Communications are usually descriptions of short investigations, or they can report minor technical improvements of previously published procedures; they reflect the same quality of research as Full-length papers, but should preferably not exceed five printed pages. Discussions (one or two pages) should explain, amplify, correct or otherwise comment substantively upon an article recently published in the journal. For Review articles, see inside front cover under Submission of Papers.

Submission. Every paper must be accompanied by a letter from the senior author, stating that he/she is submitting the paper for publication in the *Journal of Chromatography*.

Manuscripts. Manuscripts should be typed in **double spacing** on consecutively numbered pages of uniform size. The manuscript should be preceded by a sheet of manuscript paper carrying the title of the paper and the name and full postal address of the person to whom the proofs are to be sent. As a rule, papers should be divided into sections, headed by a caption (*e.g.*, Abstract, Introduction, Experimental, Results, Discussion, etc.). All illustrations, photographs, tables, etc., should be on separate sheets.

Abstract. All articles should have an abstract of 50–100 words which clearly and briefly indicates what is new, different and significant. No references should be given.

Introduction. Every paper must have a concise introduction mentioning what has been done before on the topic described, and stating clearly what is new in the paper now submitted.

Illustrations. The figures should be submitted in a form suitable for reproduction, drawn in Indian ink on drawing or tracing paper. Each illustration should have a legend, all the *legends* being typed (with double spacing) together on a *separate sheet.* If structures are given in the text, the original drawings should be supplied. Coloured illustrations are reproduced at the author's expense, the cost being determined by the number of pages and by the number of colours needed. The written permission of the author and publisher must be obtained for the use of any figure already published. Its source must be indicated in the legend.

References. References should be numbered in the order in which they are cited in the text, and listed in numerical sequence on a separate sheet at the end of the article. Please check a recent issue for the layout of the reference list. Abbreviations for the titles of journals should follow the system used by *Chemical Abstracts.* Articles not yet published should be given as "in press" (journal should be specified), "submitted for publication" (journal should be specified), "in preparation" or "personal communication".

Dispatch. Before sending the manuscript to the Editor please check that the envelope contains four copies of the paper complete with references, legends and figures. One of the sets of figures must be the originals suitable for direct reproduction. Please also ensure that permission to publish has been obtained from your institute.

Proofs. One set of proofs will be sent to the author to be carefully checked for printer's errors. Corrections must be restricted to instances in which the proof is at variance with the manuscript. "Extra corrections" will be inserted at the author's expense.

Reprints. Fifty reprints will be supplied free of charge. Additional reprints can be ordered by the authors. An order form containing price quotations will be sent to the authors together with the proofs of their article.

The Dawn of a New Era in Ion Analysis

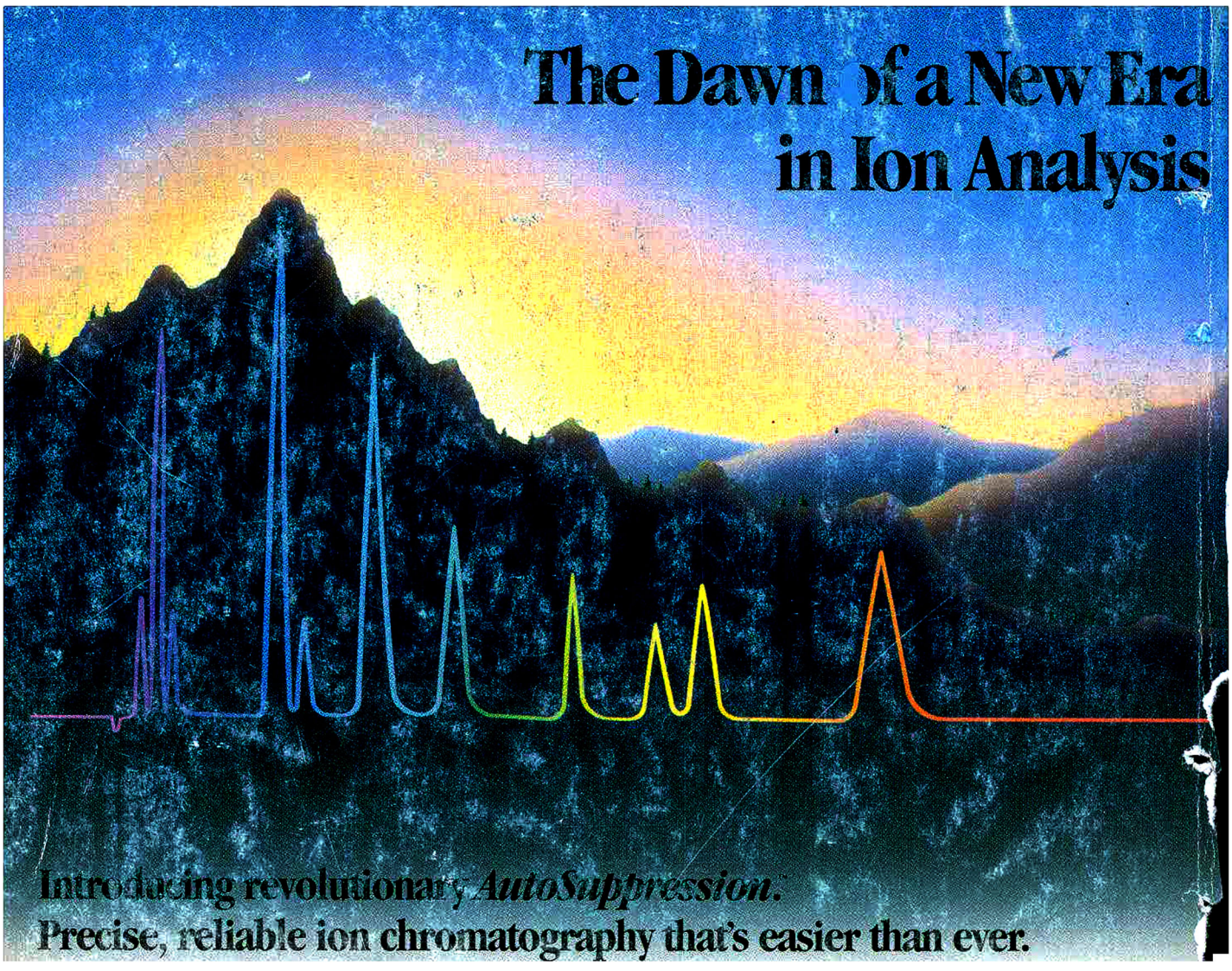

Introducing revolutionary *AutoSuppression*. Precise, reliable ion chromatography that's easier than ever.

Enter a new era in ion analysis, with *AutoSuppression* for ion chromatography.

AutoSuppression increases analyte signal and significantly reduces background noise, giving you detection limits up to *100 times* better than other ion analysis techniques. You get superb detection limits, broad dynamic ranges and ultimate matrix flexibility.

For inorganic anions to organic acids. And for Group I & Group II cations, ammonium and amines.

In short, the most powerful, versatile ion analysis technology available.

And AutoSuppression is effortless. Just plug it in and you're ready.

- No regenerants.
- No maintenance.
- No complicated eluents.

Just a *Self-Regenerating Suppressor* that you can completely forget.

Find out more about the advantages of AutoSuppression and the future of ion chromatography. In the U.S., call **800-227-1817 ext. 440**. Outside the U.S., call the Dionex office nearest you or **408-737-0700 ext. 4223**.

AutoSuppression is provided by our unique Self Regenerating Suppressor (SRS™), available for the entire line of Dionex Systems. Ask about upgrading your existing system with SRS.

29 MAY 96

Dionex Corp. Sunnyvale, CA (408)737-0700 FAX (408)730-9403 **Canada** Dionex Canada Ltd. (416)855-2551 **France** Dionex S.A. (1)39 46 08 40 **Germany** Dionex GmbH (06126)9955-0 **Italy** Dionex S.r.l. (06)30895454 **Japan** Nippon Dionex K.K. (06)885-1213 **Netherlands** Dionex B.V. 076-714800 **United Kingdom** Dionex (UK) Ltd. (0276)691722 SRS and AutoSuppression are trademarks of Dionex Corporation ©1992 Dionex Corp.

DIONEX
A BETTER SOLUTION

2536